Forest Dynamics, Growth and Yield

Hans Pretzsch

Forest Dynamics, Growth and Yield

From Measurement to Model

Springer

Hans Pretzsch
TU München
LS Waldwachstumskunde
Am Hochanger 13
85354 Freising
Germany
hans.pretzsch@lrz.tum.de

ISBN: 978-3-540-88306-7 e-ISBN: 978-3-540-88307-4
DOI: 10.1007/978-3-540-88307-4

Library of Congress Control Number: 2008937496

Cover design: Ulrich Kern and Leonhard Steinacker

Printed on acid-free paper

springer.com

Preface

How do tree crowns, trees or entire forest stands respond to thinning in the long term? What effect do tree species mixture and multi-layering have on the productivity and stability of trees, stands or forest enterprises? How do tree and stand growth respond to stress due to climate change or air pollution? Furthermore, in the event that one has acquired knowledge about the effects of thinning, mixture and stress, how can one make this knowledge applicable to decision making in forestry practice? The experimental designs, analytical methods, general relationships and models for answering questions of this kind are the focal point of this book.

Forest ecosystems can be analysed at very different spatial and temporal levels. This book focuses on a very specific range in scale within which to analyse forest ecosystems, which extends spatially from the plant organ level through to the stand level, and temporally from days or months to the life-time of a forest stand, spanning decades or possibly even centuries. It is this range in scale addressed in the book that gives it its special profile. General rules, relationships and models of tree, and stand growth are introduced at these levels. Whereas plant biology and ecophysiology operate at a higher resolution, forest management and landscape ecology operate at a broader spatial-temporal resolution. The approach to forest dynamics, growth and yield adopted in this book lies in between; it integrates knowledge from these disciplines and, therefore, can contribute to a cross-scale, holistic systems understanding.

The scales selected have practical relevance, as they are identical to those of biological observation and the environment in which people live. As interesting as fragmented details at small temporal or spatial scales obtained through reductionist approaches might be, system management requires rather an integrated, holistic view of the system in question. In this book I outline some ways to draw information of practical relevance from the scientific knowledge acquired.

Why a new book about structural dynamics, growth and yield in central European forests, why this effort when, in any event, very little is read today? The well-known works from Assmann (1970), Kramer (1988) and Mitscherlich (1970) focus on evenaged pure stands, classic silvicultural thinning methods and wood yield at the stand level. However, over time, the structure, dynamics and tending regimes in, and demands on, the forest in central Europe have changed immensely as evident in the

transition from largely evenaged pure stands to structurally diverse mixed stands, from homogenizing thinning regimes to the targeted promotion of individual trees or groups of trees in the stand, from wood production forestry to multipurpose forestry, which is concerned with a broad range of ecological, economic and social functions and services of forest. In short, the forest structure, management activities, and the anticipated effects on the forest in general and forest production in particular have become more complex in the sense that, in a forest ecosystem today, essentially more elements need to be investigated, more relationships among these elements understood, and these need to be taken into account in forest management. In response to this tendency towards increasing complexity, new investigation concepts, analytical methods and model approaches have been developed over the years. They complete the transition from stand-oriented approaches to individual tree approaches, from position independent to functional-structural concepts, from descriptive approaches focussed mainly on the volume growth and yield to interdisciplinary model-oriented ones. As yet these approaches have not been summarised in a textbook.

Given the structures dealt with, which range from plant organs through to the tree, stand and enterprise level, and the processes analysed in a time frame of days or months through to decades or even centuries, this book is directed at all readers interested in trees, forest stands and forest ecosystems. This book has been written especially for readers who are seeking in depth information about individual-based functional-structural approaches for recording, analysing and modelling forest systems. It integrates and imparts essential forest system knowledge to all green-minded natural scientists. The work is compiled for students, scientists, lecturers, forest planners, forest managers, forest experts and consultants.

The book summarises the author's lectures and scientific work between 1994 and 2008 while at the Ludwig Maximilian University, Munich, the Technische Universität München, and at Universities in the Czech Republic, Canada and South Africa. The contents represent the lecture material, the scientific approach and a compilation of the current methods used at the Chair for Forest Growth Science at the Technische Universität München, Germany. This book is dedicated to all students, researchers and colleagues at my Chair who have contributed to the realisation of this book.

For their support in editing specific subject areas, I would like to thank my colleagues Peter Biber (Chap. 8), Rüdiger Grote (Chap. 11), Thomas Rötzer (Chap. 2) and Stefan Seifert (Chap. 11). I also thank Gerhard Schütze and Martin Nickel for their unerring support of the research analysis, Marga Schmid for editing the bibliographical references and Ulrich Kern and Leonhard Steinacker for the cover design. Helen Desmond and Tobias Mette accomplished the overwhelming task of translating and editing the text, Charlotte Pretzsch the compilation of the index, and Ulrich Kern the equally extensive task of preparing the graphic illustrations. I thank you all for the affable and effective collaboration. The willingness to take on the considerable additional workload was founded on the common commitment to all things pertaining to the forest, and it is for all things pertaining to the forest, that is for a better understanding of, and a higher regard for the forest, that this book aims to make a contribution.

Finally, I also extend my thanks to the editors at Springer Publishing, Ursula Gramm and Christine Eckey, for their constructive contribution, and reliable and congenial assistance.

Weihenstephan *Hans Pretzsch*
September 2008

Contents

Chapter 1
Forest Dynamics, Growth, and Yield: A Review, Analysis of the Present State, and Perspective

The study of forest dynamics is concerned with the changes in forest structure and composition over time, including its behaviour in response to anthropogenic and natural disturbances. *Growth* is defined as the biomass (or size) a plant or a stand produces within a defined period (e.g. 1 day, 1 year, 5 years). Yield is the accumulated biomass from the time of stand establishment. Tree growth and disturbances influence and are primary evidence of forest dynamics. They are determined by resources (e.g. radiation, water, nutrients supply) and environmental conditions (e.g. temperature, soil acidity, or air pollution). The first chapter introduces the special characteristics of the forest system. These characteristics are investigated in the study of forest dynamics, of growth and yield science, and of how biological rules are traced systematically and made accessible as practical knowledge. In the course of this chapter, we learn about the past, current, and future challenges to the science of forest growth and yield.

1.1 System Characteristics of Trees and Forest Stands

A system is defined by the system elements that it comprises, the relationships between these elements, and the general rules of the system. The system rules are effective only at the entire system level and not at the individual or subsystem element levels. The functions of the system that are recognized and emphasised depend on the investigator or user's perspective (von Bertalanffy 1951, 1968; Wuketits 1981). The same is true for the system boundaries, which are defined according to specific purposes and seldom correspond to actual natural system boundaries. For instance, in a forest stand, we can distinguish the system elements soil, soil vegetation and trees with roots, stems, branches and needles and/or leaves. The interactions among the system elements create a characteristic system structure, e.g. the shadowing of the trees determines the light conditions for the understory trees and the soil vegetation.

H. Pretzsch, *Forest Dynamics, Growth and Yield: From Measurement to Model*,
DOI: 10.1007/978-3-540-88307-4_1,

In general, except for some wearing out, systems that function independent of time (e.g. a chair, a piano) are termed *static systems*. In dynamic systems (e.g. forest stands, animal populations, scientific working team), the chain of events is time dependent. Past system events decisively influence its future behaviour. Since the specific system characteristics of forest stands ultimately determine the approach and methodology of forest growth and yield research, they are presented below.

1.1.1 Differences in the Temporal and Spatial Scale Between Trees and Humans

One fundamental characteristic of trees and forest stands that has important consequences for their analysis, representation, and modelling is their longevity. The following expresses the life span of various organisms on a power-of-10 scale:

Trees	10^4 years
Humans	10^2 years
Large mammals	10^1 years
Grasses, herbs	10^0 years
Insects	10^{-1} years
Bacteria	10^{-2} years

We see that trees and forest stands live two to six orders of magnitude longer than most animal and plant organisms, including humans. For a bacterium, a tree life is 10^6 times longer, an eternity so to speak. In comparison with the oldest trees in the world ($\sim$6,000 years), the life span of humans ($\sim$100 years) attains only about 100th, or 10^{-2}, that of trees. Consequently, whereas experiments on the growth of bacteria, insects, grain types, herbaceous plants, or mammals can be conducted in hours, days, months, or a few years, experiments on tree growth require continuity over many generations of scientists. Yet, even the oldest thinning experiments from long-term experiments in Bavaria, which date back to the 1870s and continue to be surveyed, cover only a comparably small segment of the potential life span of trees and stands.

The North American tree species Bristlecone pine (*Pinus aristata*) can reach an impressive 5,000–6,000 years of age (Fig. 1.1). Yet even when compared to central European tree species such as Silver birch, European ash, Norway spruce, or Sessile oak, the working, research, or entire life span of a human is comparably short. The entire forest science era, beginning with W. L. Pfeil (1783–1859), H. Cotta (1763–1844), and G. L. Hartig (1764–1837) in the late eighteenth century, an extraordinarily long period, only covers a fraction of the life span of our forest trees (Fig. 1.1).

The longevity of trees and forest stands requires specific approaches, from initial measurements in the field to modelling on the computer, that differ considerably from those adopted for organisms with shorter life expectancies. For example,

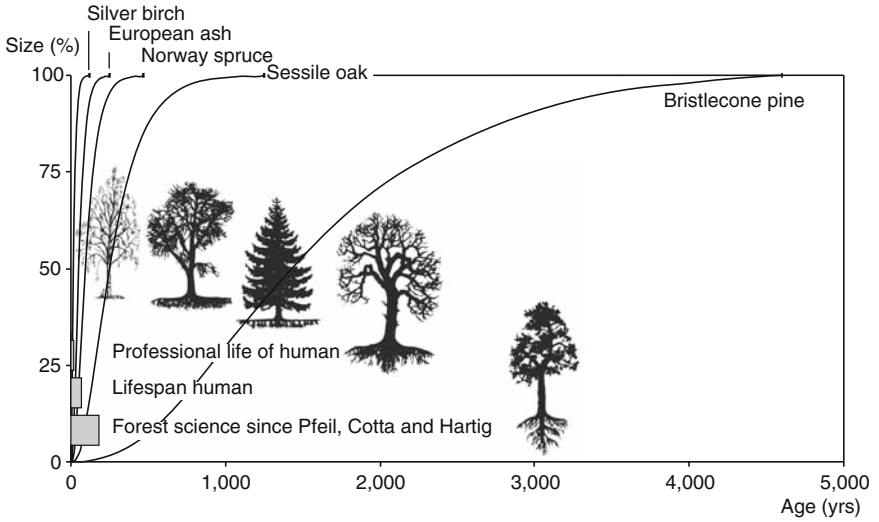

Fig. 1.1 The life span of humans and trees differ by up to two orders of magnitude. The relative size development of individual trees by age is shown for Silver birch (*Betula pendula* Roth), European ash (*Fraxinus excelsior* L.), Norway spruce [*Picea abies* (L.) Karst.], Sessile oak [*Quercus petraea* (Matuschka) Liebl.] and Bristlecone pine (*Pinus aristata* Engelm.). The time bars in the lower part of the graphic point out the superior lifetime of trees are compared to the research time and lifetime of a human, and the entire history of (modern) forest science since its foundation through W. L. Pfeil (1783–1859), H. Cotta (1763–1844), and G. L. Hartig (1764–1837) in the late eighteenth century

investigations of the effect of different thinning regimes on the growth of Norway spruce stands can only be completed after many decades or a century. This is because the long-term effects of the treatments on the growing stock in the final stand are vastly more important than the temporary responses to individual thinning operations. The growth responses after only 5–10 years are, at best, indicative only of tree or stand development over the entire life span.

In the 1860s and 1870s, Franz v. Baur (1830–1897), August v. Ganghofer (1827–1900), Karl Gayer (1822–1907), and Arthur v. Seckendorff-Gudent (1845–1886) outlined a basic approach for the establishment of long-term forestry investigations and initiated a network of widely distributed long-term experimental plots in forest stands in Bavaria. Many of the first experimental plots are being monitored still today, 130 years after their establishment. These long-term experiments are essential in forest science for the derivation of reliable knowledge about forest systems and for the provision of decision support in forestry practice (Fig. 1.2). When no experimental plots are available for observations of forest growth in the long-term (real time series), artificial time series may be established in the form of spatially adjacent stands of different ages (artificial time series). On a suitable site, monitoring plots are set up in stands of different age classes as an artificial time series (Fig. 1.3).

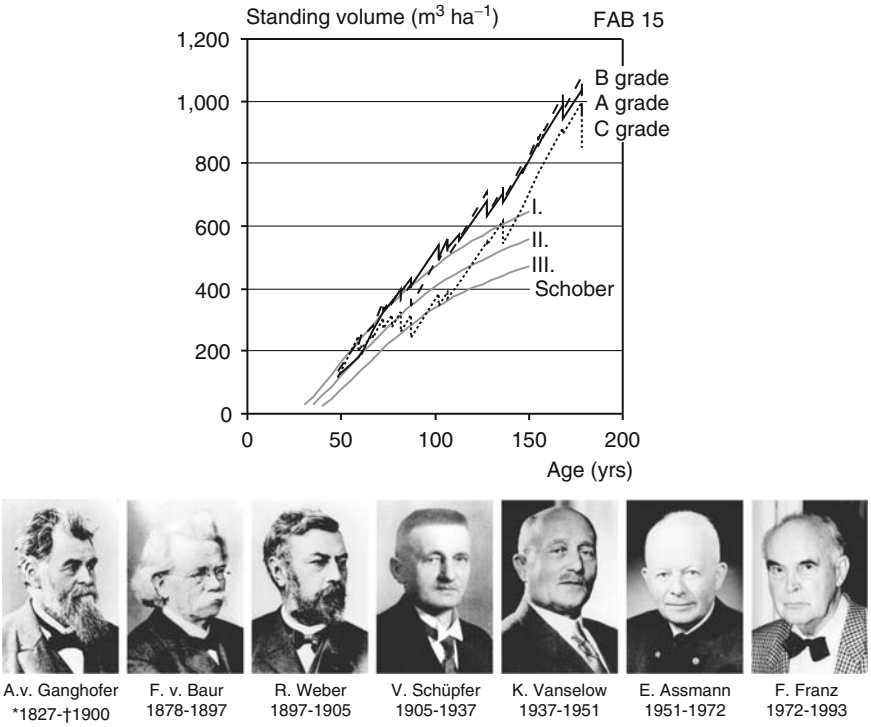

Fig. 1.2 Long-living organisms require long-term research. Development of standing volumes ($m^3\,ha^{-1}$) on the European beech thinning experiment Fabrikschleichach 15 (A, B, and C grade) (*above*) as the result of transgeneration measurements of the forest yield research in Munich (*below*). As one of more than hundred long-term experimental plots in Bavaria, the Fabrikschleichach plots have been surveyed regularly for 130 years

The central thesis of forest growth modelling is directly related to the longevity of trees and stands. Before the large-scale cultivation of new crops such as sunflowers, rape, or corn, their growth and treatment can be tested experimentally in a relatively short time. This approach is possible for organisms with a life expectancy lower that of humans by one or more orders of magnitude. In contrast, a given treatment regime for forest stands cannot be tested in short-term experiments. Long-term experiments on the other hand take too long, and upon conclusion the treatment model in question is presumably already outdated. The longevity of trees and forest stands forces the researcher to use theoretical and experimentally derived relationships and integrate these into growth models. Then, the long-term consequences of given silvicultural prescription or possible disturbances can be simulated with the model and analysed at the stand, enterprise, or landscape level. Consequently, with a reliable model, it is not necessary to respond to each new question by establishing new experiments.

Mature trees and forests are taller than human beings are. Trees reach heights up to 120 m, almost 100 times higher than an adult human does. This makes them difficult to measure. From simple geometrical triangulation methods to modern laser

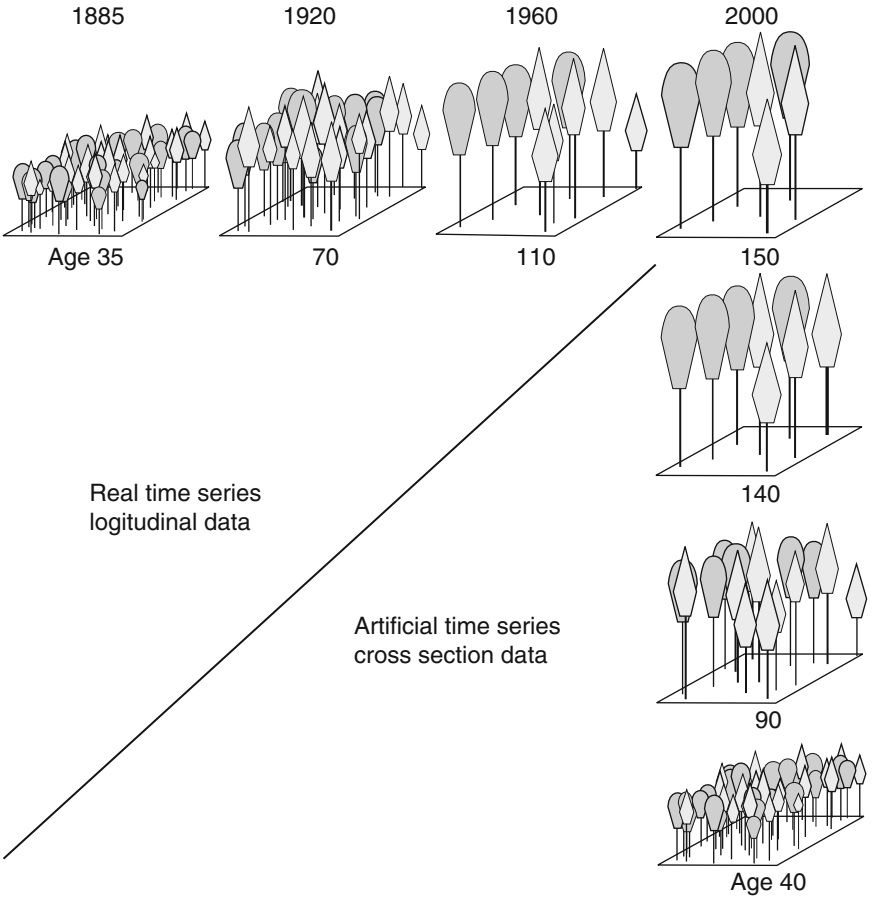

Fig. 1.3 Comparison of the principles of real time series and artificial time series. If stand development is recorded regularly from 1885 to 2000, then the sequence of data produces a real time series with surveys in 1885, 1920, 1960, and 2000 (*row*). In contrast, an artificial time series is constructed from spatially adjacent stands in different development phases (e.g. age 40, 90, 140, and 150) with comparable site conditions (*column*)

techniques that capture the three-dimensional (3D) structure of the stand, many forest mensuration methods with adequate measuring devices have been designed to overcome the size difference. Experiments that directly access the crown space such as cranes, scaffold towers, or gondola systems are elaborate and rare. In the some experiments, however, new species or sometimes species believed extinct have been discovered, the crown architecture analysed with high precision, and growth responses to stress studied in a manner not possible from the ground. Tree size also limits the experimental setup and the assertion of ceteris paribus conditions. Chamber or phytotron experiments for the analysis of cause–effect chains can only be carried out with young trees. Yet, the transferability of such results to old trees or

even entire stands is limited. Field experiments that analyse the response of larger or older trees, for instance, to increased O_3 or CO_2 concentrations are rare and expensive and cannot eliminate the effect of external influences (e.g. weather extremes, biotic calamity).

However, the size difference between humans and trees also offers opportunities. The long life span of trees is documented in their annual ring pattern, which, similar to ice cores, enables conclusions about historical growth conditions, droughts, matter inputs, climate changes, etc., to be drawn. The particular spatial dimension of forests provides a unique opportunity to analyse the history of individual plant growth, competition, and mortality. It also enables growth to be traced from individual plants to the stand level. Comparable insights into herbaceous stands would require a reduction in size of the researcher by factor 10 or 100, like Alice in Wonderland. In grassland systems, it is rarely possible to measure the spatial occupation of individuals and to record losses of individuals and growth of survivors accurately without greatly disturbing them and the stand structure.

1.1.2 Forest Stands are Open Systems

The relationships between elements within a forest ecosystem are closer than relationships between elements outside the system, which makes it easy to distinguish a forest ecosystem from the environment. Nevertheless, relationships between the system and the environment exist in the flow of nutrients, energy, and genetic information. The responses of our forests to environmental influences, ranging from gains in growth to losses in growth and profound destabilisation, have been discussed extensively (Pretzsch 1999c; Spiecker et al. 1996).

Forest stands are open systems and are affected, e.g. by past litter removal in the past or, as in the subsequent example, atmospheric nutrient input that can cause specific growth trends. Since the 1960s, height growth in many Scots pine stands, which are distributed widely across Bavaria in the Upper Palatinate and in Franconia, is significantly higher than would be expected from the yield tables (Pretzsch 1985b; Schmidt 1969). The results for diameter, basal area, and volume growth are similar. Yet the increase in height growth is especially conspicuous because the growth recovery causes Scots pine to develop cone-shaped tips on their otherwise dome-shaped crowns that typically develop upon reaching the early mature and mature phases (Fig. 1.4a). While increases in basal area and volume increment at the stand level are evident in stands of all ages, they are more apparent on sites previously of low fertility than on the better sites. Compared to the yield table, the observed growth rates are 100–150% higher (Fig. 1.4b). Data from forest inventories and long-term experimental plots verify that the diagnosed growth trends are not isolated occurrences but are associated with large-scale changes in growth conditions of our forests. The broad spectrum of sites and disturbances in South Germany is evident in the diversity of growth response patterns of the main tree species (Kenk et al. 1991; Pretzsch 1996a; Röhle 1994; Spiecker et al. 1996). The findings, which

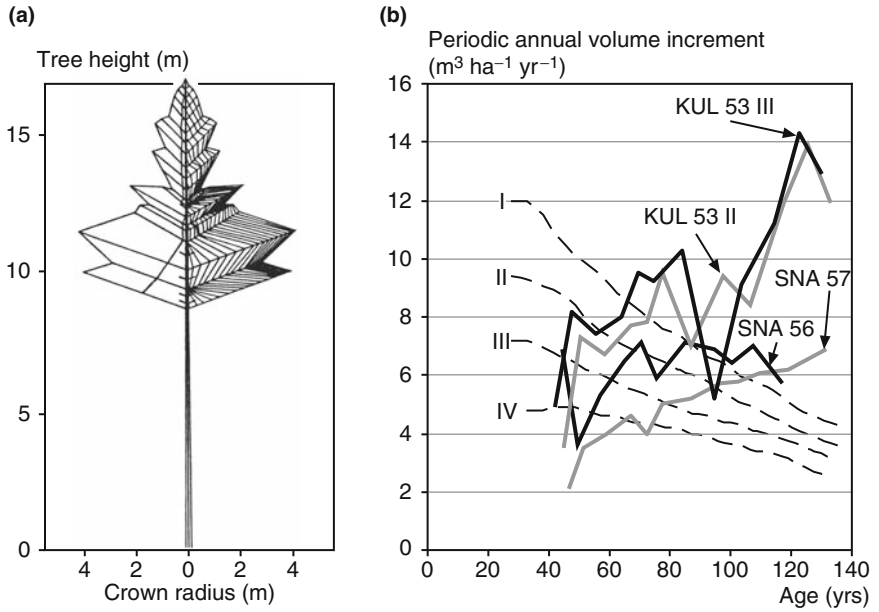

Fig. 1.4 Growth acceleration of Scots pine at the tree and stand level in Northeast Bavaria due to increasing atmospheric nutrient input and gradual recovery from litter raking in the past. (**a**) Crown shape development of Scots pine at Forest District Burglengenfeld, Upper Palatinate and (**b**) periodic annual volume growth on the long-term plots Schnaittenbach 56 and 57, Upper Palatinate and Kulmbach 53, Upper Franconia, compared to the yield table from Wiedemann (1943), moderate thinning

seem paradoxical at times—forest proliferation here, forest decline there—highlight the character of forests as open and heterogeneous systems.

The characteristic of forests as open systems makes experimentation and hence the derivation of causal relationships difficult because the assumption that, except for the factors to be varied, all other conditions remain constant or are controlled is rarely attained. The nitrogen fertilising experiments across Bavaria provide a good example of the interference of experiments by environmental influences. In these experiments the applied nitrogen fertilisation amounts were much lower than the accumulated atmospheric nitrogen input caused by air pollution of up to $50\,\mathrm{kg\,N\,ha^{-1}}$ annually since the experiment began. The derivation of causal relationships between growth and nutrient availability is only possible here if the unintended atmospheric input was also recorded during the observation period and taken into account in the data analysis. When ceteris paribus conditions are not given as in this case, a study provides correlative rather than cause–effect relationships.

Unlike short-lived agricultural crops, forest stands cannot be investigated in climate chambers or phytotrons under controlled and managed environmental conditions. Instead, forest growth research must accept the environmental influences at a given site and record the local conditions as well so that they can be taken into

account in the analysis. If necessary, individual environmental factors may be eliminated, held constant, or measured accurately with considerable effort. Examples of experiments of this kind include the roof experiments in which the precipitation and the deposition of elements contained within is controlled or the field experiments involving gassing with carbon dioxide or ozone, where the effect of the changed air chemistry on tree growth is investigated with considerable effort. However, while one factor is controlled with high accuracy, the possible effect of other environmental conditions, whether constant or changing, must be considered in the assessment. Although the criterion of ceteris paribus conditions, which is needed to derive unequivocal causal relationships, is not fulfilled, it is still possible to determine the correlation between the partly controlled environmental conditions and the forests responses to estimate the influence of the factor analysed in the experiment.

Changes in environmental conditions quickly outdate yield tables, static models, and standard silvicultural prescription measures, which assume a closed system character and constant or steady-state site conditions. Thus, the conventional yield tables for pure stands with their assumption of constant growth conditions are no longer valid in many cases (cf. Fig. 1.4b). When the surrounding influences vary, only models that take into account the exchange of nutrients, energy, and genetic information between forest ecosystems and their surroundings can be expected to predict the behaviour of open systems realistically. The developments from the first experience tables in the eighteenth century to the classical yield tables in the nineteenth and twentieth centuries and, ultimately, the high resolution ecophysiological process models of the last decades reflect the increasing awareness that the understanding and predictions of forest ecosystems must incorporate the variable environmental conditions and resource supplies. The calculation of scenarios, such as those needed to assess the long-term consequences of forest use, nutrient input, and climate change and to develop mitigation strategies, is only possible with open-system approaches and environmentally sensitive models.

1.1.3 Forests are Strongly Structurally Determined Systems

Trees are rooted firmly in the ground, and this ties them inevitably to the given spatial growth arrangement. As they grow, they develop their shape and structure over long periods and thereby they themselves influence the factors essential for their growth, such as access to light and water. The gradual development of tree and stand structures has a major influence on all life processes in forest ecosystems (Pukkala 1988; Pretzsch 1995b). Given that stand structure influences a broad range of ecosystem functions, we concentrate on its effect on structural dynamics, growth, and yield.

The dynamics, growth, and yield of single-layered pure stands can be recorded, modeled, and predicted from stand level data comparably easily, i.e. without taking the spatial stand structure into account. Yet, if we neglect the 3D stand structure in multilayered pure and mixed stands, we ignore the very characteristic of these stands

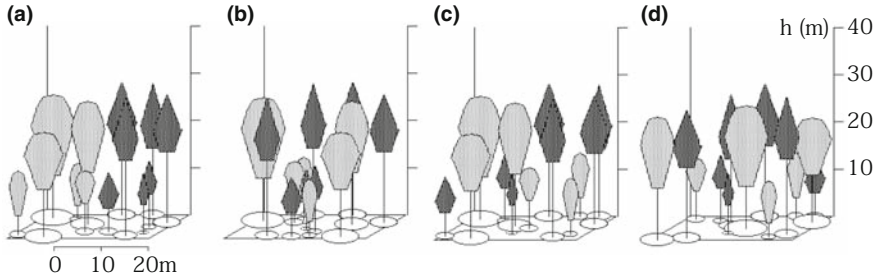

Fig. 1.5 The four Norway spruce–European beech mixed stands have equal mean and cumulative values, diameter, and height distributions but differ in structure: (**a**) group mixtures of Norway spruce and European beech, (**b**) groups of regeneration, two-layered stands with Norway spruce under European beech, (**c**) European beech under Norway spruce, and (**d**) Norway spruce and European beech in single tree mixtures. Their different spatial configuration reflects different pathways of development

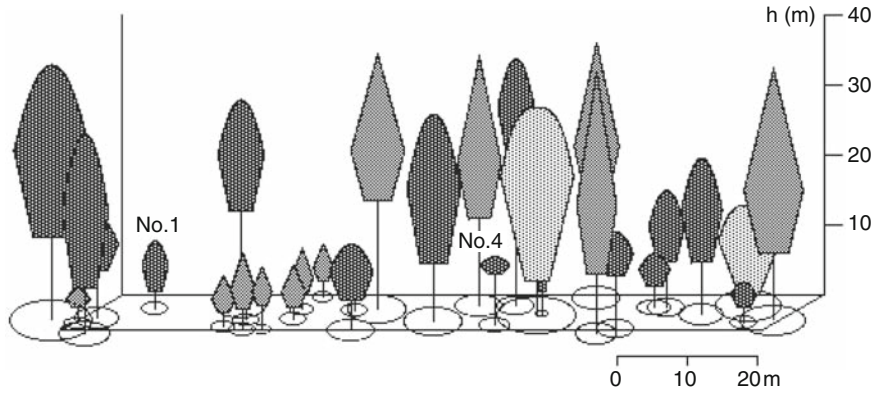

Fig. 1.6 Stand profile for a 5-m-wide strip through the Norway spruce–Silver fir–European beech selection forest experimental plot Freyung 129/2, in the survey year 1980. Norway spruce is *shaded grey*, Silver fir *dark grey*, and European beech *light grey*. Silver fir No. 1 suffers less from competition for light than No. 4 whose crown is already receding

that affects stand dynamics the most. For example, the Norway spruce–European beech mixed stands presented graphically in Fig. 1.5 has similar stand cumulative and mean values as well as similar diameter and height distributions. They only differ in their spatial configuration: the two species (a) are spatially separated, (b) form group mixtures, (c) form two-layered structures, or (d) form single-tree mixtures. This has a major influence on the further development of these stands.

The development of Silver fir in selection forests or in mixed-species mountain forests provides a good example of the long-term effects of structure. Its development depends heavily on the spatial arrangement (Pretzsch 1985a). Figure 1.6 illustrates two different competition scenarios for Silver fir regeneration in a selection forest stand. The free-standing Silver fir No. 1 grows quickly and becomes part of

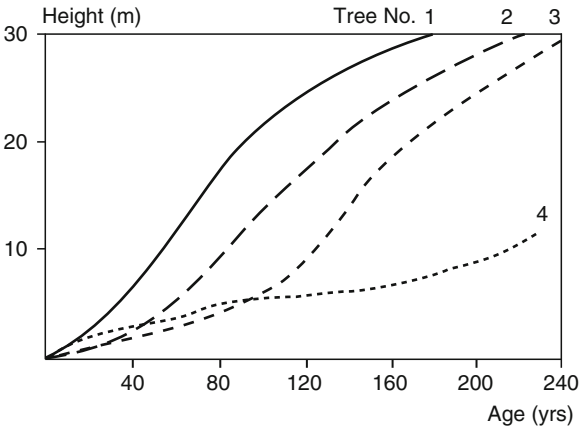

Fig. 1.7 Height development of Silver fir in relation to spatial growth constellation in a multilayered Norway spruce–Silver fir–European beech mixed stand in the Bavarian Alps (after Magin 1959, p. 16). From tree No. 1 (predominant) to No. 4 (suppressed) the competition for growing space aggravates and the delay of height growth increases

the upper storey at an early age, whereas Silver fir No. 4 grows slowly under heavy shade until, eventually, the competitors are removed.

This leads to a differentiated height development as observed by Magin (1959), Pretzsch (1985a), and Preuhsler (1979, 1989) in mixed-species mountain forests in the Bavarian Forest and Bavarian Alps (Fig. 1.7). Here, under similar soil conditions, the height growth varies considerably between favourable and unfavourable spatial arrangements. At 100 years of age, some trees had only reached 5 m and other trees already 25 m height. While Silver fir No. 1 developed as a typically predominant tree, Silver fir No. 4 remained almost solely in the understory. After Silver fir No. 3 spent almost 150 years in the understory, its competitors were removed, and it passed through the height-shoot development phase that its old neighbours had passed through 100–200 years earlier. This example shows that we can understand and predict individual-tree development in heterogeneous mixed-species mountain forests only when we take the spatial stand structure into account (Schütz 1989).

Due to the central importance of forest structure for the understanding and prognosis of forest dynamics, modern physiological and ecological research approaches are based explicitly on the spatial structure of the tree, stand, forest, and landscape. As structure affects a wide range of forest functions, e.g. habitat configuration (Müller et al. 2006; Wiegand 1998), species composition (Ammer and Schubert 1999; Ellenberg et al. 1985), stability and resilience against disturbances (Scherer-Lorenzen 2005; Pretzsch 2003), and landscape aesthetics (Seifert 2006; Sheppard and Harshaw 2001), it has become not only a central element in functional structural modeling but also an output variable of the models (Pretzsch et al. 2008).

1.1.4 Trees, Forest Stands, and Forest Ecosystems are Shaped by History

The processes and structures observed within forests are not determined merely by factors currently affecting it (e.g. site factors, abiotic and biotic stressors) but also by forest history. The condition and function of a nonliving technical system, such as an hourglass, at any given point in time is always pretty much the same (Fig. 1.8a). Unless the hourglass shows wear and tear, the amount of sand that passes through the hole at any time t_1 or t_2 is always the same, and it is independent of the development prior to time t_1 or t_2. In contrast, in living, biological systems both the ontogeny and phylogeny determine its development to a large extent. Thus, at given points of time t_1 or t_2, depending on the history of the tree, variation in height and height increment may occur (Fig. 1.8b).

While the height growth of a Silver fir in a selection forest is largely dependent on the actual growth conditions, the characteristics acquired through the tree's own ontogeny and its inherited traits also have a considerable influence on its ongoing development. Examples of tree characteristics acquired in the past, which may affect future growth include crown size, social position within the stand, extension of the root system, heartwood–sapwood ratio, and past phases of suppression in the lower and middle story of a selection forest.

This ontogenetic variability (phenotype) is embedded within phylogenetically determined limits (genotype) to the growth rate, life span, crown structure, stem

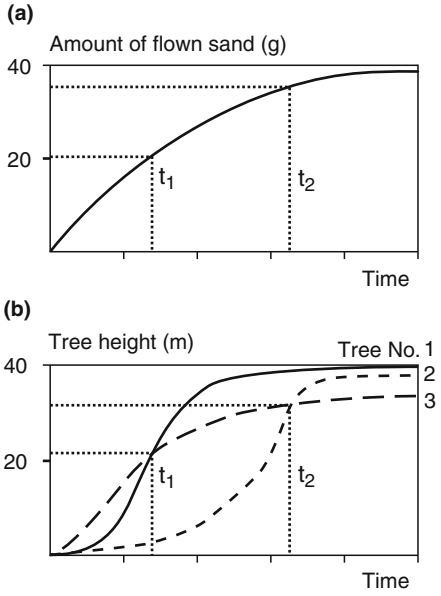

Fig. 1.8 (**a**) For technical systems such as an hourglass, the system parameters are constant and the through flow is similar and predictable at any given point in time. (**b**) In biological systems, the individual genotype and ontogeny result in a less predictable height development with age

form and shoot development and fructification. This influence of ontogenetic and phylogenetic characteristics at the tree, stand, and ecosystem level has far-reaching consequences when recording and modelling the system components and the system. Since a tree or stand may develop significantly differently depending on its genetic resources, stand establishment, or its prior use, such information is crucial for the understanding of the present state and the prognosis of the future development. Information dating further back is generally lacking, even for long-term experimental plots. In ad hoc investigations, historical information may be gathered retrospectively from forestry notes or aerial photographs or obtained from core samples, stem analysis, stocking inventories, or morphological crown characteristics. Stem and crown analyses also reveal the ontogenetic history to a certain degree. Access to the inherited genetic characteristics is possible from marker and isoenzyme investigations, though the integration of these into stand level analyses is still in an early phase. In the long term, such analyses will be useful in identifying the genetic codes and the corresponding growth characteristics.

In classical physics and chemistry, the variation in measured values is essentially caused by error in measurements and in the errors introduced in carrying out the experiment, not by the individual history of the object under investigation. In contrast, the analysis of living systems requires a higher number of replications in the experimental design as knowledge about the prior history of study objects are limited. This way, the differences in growth rates due to stand history or genetic provenances are merged by averaging the results from multiple replications.

Since stand history is equally important for the understanding as well as the prediction of the stand development, models that simulate future development must incorporate stand history as much as possible. This information is included in part already in the spatial tree and stand structure data used to initialise a simulator, since structure largely reflects stand history. Small differences in the initial stand structure can affect further stand development considerably, especially in mixed stands. Consequently, by employing the actual stand structure as the initial condition, "half the prediction" has already been made. As the understanding of the relationship between genetic composition and tree and forest growth is still vague, at present, genetic effects can be dealt with only statistically in models. For this reason, models should also include the residual error, which remains after a regression analysis of the factors known to influence growth (cf. Chap. 10, Sect. 10.6).

1.1.5 Forests are Equipped with and Regulated by Closed Feedback Loops

Forest ecosystems enable a certain degree of self-regulation and maintain a state of equilibrium within a defined range of stability through feedback mechanisms and their closed feedback loops. Feedback loops are a structural abstraction of self-regulating biological, technical, and social systems. Feedback loops are characteristic for systems in which a certain condition produces a specific effect,

which, in turn, affects the condition once again (e.g. nitrogen import stimulates growth, but accelerated growth lowers nitrogen surplus in the soil). Examples include the thermostat, dilation and contraction of the pupil, spatial occupancy patterns, and thinning responses in forest stands. Feedback processes in forests can stabilise them to an extraordinary degree against interventions or disturbances such as thinning, reduction in the ground water table, acid deposition, or nitrogen inputs.

When an ecosystem formation begins, the processes are affected mainly by the abiotic conditions and hydrological factors (geological substrate, debris accumulation, relief, runoff systems, etc.). Subsequently, development factors (advance of herbaceous and woody vegetation) lead to an increasing accumulation of organic substance (flora and fauna) and increasingly participate in shaping the system development. We can distinguish certain phases of ecosystem formation: the rather instable conditions of the abiotic geosystem and hydro-geosystem graduate to an increasingly stable bio-hydro-geosystem (=ecosystem). The stability and resilience against disturbances is due to feedback loops, which guarantee the achievement and maintenance of certain set-point conditions through certain adaptive mechanisms.

If, after disturbance, a system converges back to the same equilibrium, then the system is stable. As the return to equilibrium is brought about by feedback loops, we recognize that feedback loops have a stabilising effect. We distinguish *elasticity* as the ability to keep close to the steady state and *resilience* as the ability to return to steady state after disturbance. Following disturbance, unstable systems do not return to the equilibrium, or they fluctuate unpredictably about the equilibrium state (plasticity). The degree of disturbance up to which a forest ecosystem is still elastic, and when it becomes plastic, is of great interest.

A thermostat is probably the best-known example of a technical cybernetic system where a closed feedback loop keeps temperature in a steady state. It is designed to keep a room temperature x to a predefined desired temperature w (set point value) after a disturbance, such as opening a door or window. To maintain the room temperature close to the desired temperature, the room temperature is measured continuously by a temperature sensor, and this information about the actual temperature is passed on to a regulator. The regulator compares the desired and actual temperatures and increases or reduces the amount of heat accordingly. The feedback between room temperature and heat radiation enables the system to self-regulate the room temperature in a balance about the desired value.

Such compensating feedback loops are responsible for the regulation of body temperature, blood sugar levels, respiration, and transpiration, and they stabilise organisms against internal and external disturbances. Analogous to the technical system of the thermostat, the feedback loop in forest stands, stand structure → growth → tree size and shape → stand structure, enables forest systems to buffer growth losses after a reduction in density (Fig. 1.9). The stand structure determines the growth conditions of individual trees and the stand, the growth conditions determine the growth, and the growth determines the structural changes in the tree and stand. Following a reduction in stand density, the remaining trees may respond to the additional availability of space and resources to a certain extent by increasing growth, thereby partly compensating for the removals. The increase in

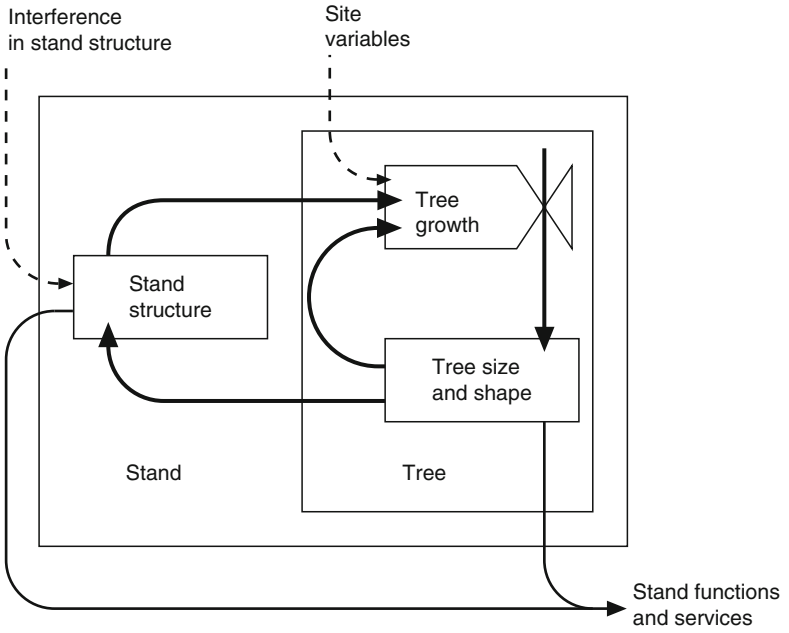

Fig. 1.9 A system with the levels stand and tree, the external variables structural intervention, environmental conditions and resource supply, and the feedback loop stand structure → growth → tree size and shape → stand structure

photosynthesis and, hence, assimilation buffers the effect of the growth disturbance and continues until the site-specific equilibrium, i.e. stand density (ceiling leaf area), is reached once again.

The stabilising effect of this feedback loop (stand structure → growth → tree size and shape → stand structure) is illustrated in Fig. 1.10 for two different stand structural types: Highly structured forests (Fig. 1.10a) are better able to buffer disturbances to stand structure, as shown by the growth performance. Lower stand layers can quickly respond to higher light availability when the canopy is opened by a disturbance. In age-class forests (Fig. 1.10b), where vertical structure is limited, this flexibility is less developed. Consequently, growth decreases quicker and more severely with an increasing degree of canopy opening.

1.1.6 Forest Ecosystems are Organised Hierarchically

The structures and processes in forest ecosystems can be investigated at different temporal and spatial scales, from seconds to thousands of years and from the cellular to the continental level (Ulrich 1993). These processes are either controlled by environmental conditions, such as the day–night rhythm and seasonal periodicity, or

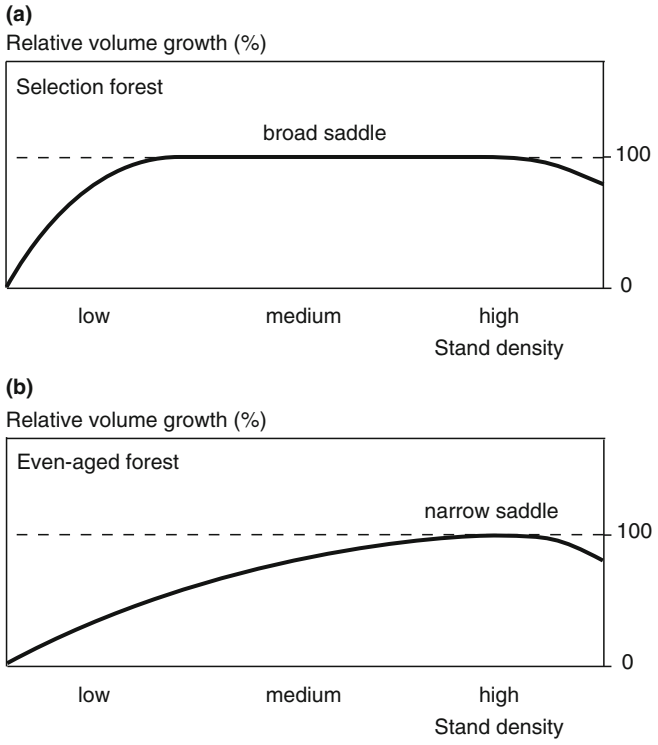

Fig. 1.10 Through the feedback loop, stand structure → growth → tree size and shape → stand structure, (**a**) highly structured mixed stands are better able to buffer growth responses following removals than (**b**) monolayered pure stands

by ontogenetic or ecosystem internal factors such as aging and the regeneration of system elements.

Figure 1.11 shows the process categories discernible in forest ecosystems, classified according to the temporal and spatial scales at which they operate. They range from microprocesses, such as biochemical reactions in cells and in soil compartments, to processes occurring at higher temporal and spatial scales, such as succession and evolution. We denote these different categories by $-3, \ldots, +2, +3, +4$. The reference level 0 was assigned to the most common perspective in forestry. At this level, the growth and competition processes are considered at the individual-tree level (spatial reference) over the course of a year (time reference).

At the lowest scale (i.e. the highest resolution), we consider the biochemical reactions in cells and biochemical reactions in the mineral surface soil (level -3), e.g. photosynthesis or the formation of buffer zones. The second level considers responses such as assimilation and respiration, bind and release certain amounts of carbon dioxide, or the effect of mineralization on the chemical equilibrium of the soil solution (level -2). Examples for the level -1, including the humus structures produced by the decomposers and herbivores, the carbon allocation process, and

	Process	Duration of process	Spatial compartment	Pattern and indicator
+4	Evolution	Millenniums	Continents	Species and genotypes
+3	Succession	Centuries	Landscapes	Plant-animal community
+2	System renewal	Decades-centuries	Ecosystems	Natural regeneration
+1	Stand development (changes of pools in biomass-humus)	Decades	Forest stands (ecosystem section)	Age class-matter budget of the soil
0	Element cycle	Year	Tree-tree groups	Matter budget of the ecosystem
–1	Development of plant organs (leafs, fine roots, fruits, wood)	Weeks-month	Tree+Forest floor vegetation	Tree foliation
–1	Decomposition	Weeks-month	Soil horizon	Humus form
–2	Assimilation-matter uptake	Hours-weeks	Leaf-root	Carbon and ion allocation
–2	Mineralisation	Hours-weeks	Soil aggregate	Soil solution chemistry
–3	Biochemical reaction	Minutes	Cell	Biochemical pattern
–3	Soilchemical reaction	Seconds	Mineral surface	

Fig. 1.11 Processes in forest ecosystems in relation to their temporal and spatial scales, and the patterns and structures they produce (from Ulrich 1993)

the development of plant parts, are revealed by the branching and foliage patterns (level -1). Levels -3 to -1 cover processes and patterns occurring within specific components of the ecosystem. At higher levels, we look at the ecosystem as a whole, beginning with the annual nutrient cycle and growth patterns of trees and their neighbours (level 0). In ecosystems that are in a state of equilibrium, the rate of growth, as well as the input–output balance of nutrients, carbon, and so on, is the same in the long-term. The stand development (level $+1$) can be captured in tree and stand growth patterns and in the development of age classes and stand structures. In an ecosystem in equilibrium, system renewal is a continuous restoration process (level $+2$), whereas after major disturbances, succession forms particular forest communities (level $+3$). Entire forest eras and evolutionary processes result in a specific pattern of species and genotypes (level $+4$). The processes at one level (e.g. assimilation, carbon allocation) are evident in the changes in patterns and structures at the levels above, e.g. in the branching, foliage condition, growth, or, at a level higher still, composition of forest communities (Fig. 1.11, right column). Conversely, the structures at the higher levels provide the framework for processes at lower levels. The interaction of the structures and processes at the different levels is important for forest growth research approaches. As all processes are revealed in the specific patterns and structures, these patterns can be investigated, e.g. forest damage at different levels (Roloff 1989).

The processes at the different levels -3 to $+4$ are characteristically interwoven and obey their own principles: the upper levels exert pressure downwards through regulating parameters, whereas the lower levels influence the upper levels via signals

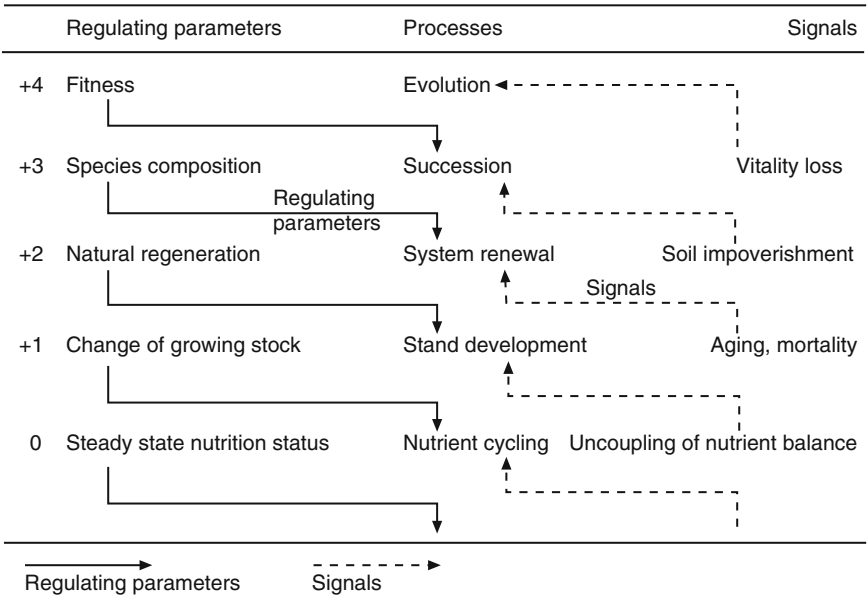

Fig. 1.12 Control and regulation by regulating parameters (*arrows with solid lines*) and signals (*arrows with dashed lines*) influence the processes in forest ecosystems and stabilise them in the event of interventions (from Ulrich 1993)

(Fig. 1.12). For example, tree and stand structure (level +1) regulate radiation, precipitation, and deposition in the stand and determine the initial and limiting conditions for the processes at levels 3, 2, 1, and 0. Processes between trees and the environment or in trees, such as transpiration, interception, assimilation, and allocation, are dominated by the temporal and spatial processes and structures in the levels above. In forest ecosystems, this control and regulation of processes between the levels, through regulating parameters and signals, means that these processes also possess a corresponding hierarchy (Müller 1992; Ulrich 1993).

In stable ecosystems, the slow processes determine those with moderate and high resolution. Signals from the lower levels are processed by the upper levels and are buffered to a certain extent so that the effect on the hierarchical level above is smoothed. We adopt the three processes succession, system renewal, and stand development (levels +3, +2, and +1, respectively) from Fig. 1.12 to provide an example of this type of buffering of bottom-up signals by top-down regulating parameters. As the mature stand is determined by the species composition of the young stand, species composition acts as a regulating parameter. The aging process of the dominant trees represents a signal that initiates system renewal. When old trees die, the regeneration processes are enhanced. This suggests parallels to political organisational structures; democracies are typical systems in which regulating parameters operate from top down and signals from bottom up. As long as the levels above respond to the signals from below (votes, social discontent,

unemployment, participation) with the appropriate activities and processes, such signals are of benefit. Laws, subsidies, or, in a sense, the philosophies conveyed through schools and universities function as regulating parameters from top down. If these means are directed appropriately upon the signals from below, then the system is stable and durable.

In forest ecosystems, if the signals from the lower level cannot be buffered by the process level immediately above, then a disruption in the hierarchy can occur; the system is no longer controlled by regulating parameters from the top down but by signals from the bottom up. In other words, the conditions at one level have changed so quickly and intensively that they cannot be brought into equilibrium by the regulating parameters in the level above. Therefore, a new state of equilibrium is adopted according to a new range of conditions. This is exemplified by forest stands with high nitrogen inputs (cf. Fig. 1.13): The system responds to increased nitrogen inputs by increasing nutrient uptake. Further nitrogen enrichment leads to a reduced formation of fine roots and increased proportion of early wood. This way, the signals from below already affect the next higher level. Further nitrogen input leads to nutrient imbalances, to decrease in humus, to the decline of mycorrhiza,

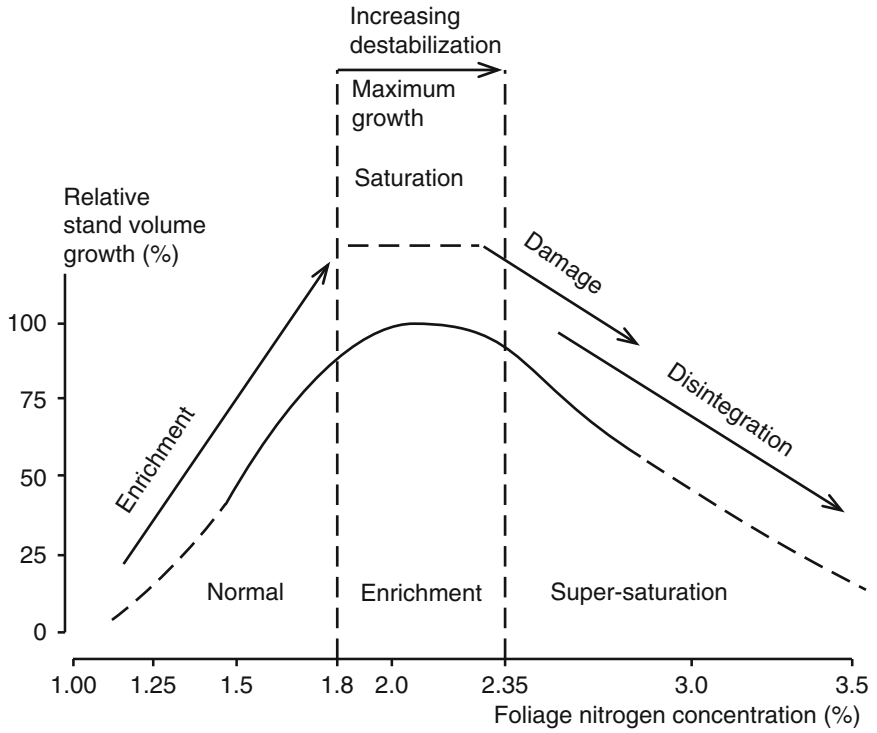

Fig. 1.13 Relationship between nitrogen availability (N concentration in needles) and stand volume increment (volume increment as a per cent of the maximum increment) for Scots pine stands in the East-German lowlands affected by atmospheric nitrogen import (from Hofmann et al. 1990, p. 62)

and it rather impairs stand development. In advanced stages, even system renewal may be endangered because nitrophilic ground vegetation hinders the regeneration process.

A disruption in the hierarchy can also be triggered by management practices. Commencing with a natural forest whose biomass stock is in a steady state, the extent of disturbance increases in the following order: selection forest system, shelterwood system, clear-cut system (Fig. 1.14). After a disturbance, regeneration, and maturation, a forest reaches an oscillating balance; the biomass fluctuates only minimally (Fig. 1.14a). In this phase, the biomass lies only just below the steady-state biomass stock, shown in Fig. 1.14a by the dashed line. The selection forest system approximates the natural processes fairly closely (Fig. 1.14b). In these forests, only the natural mortality of the oldest and biggest trees in the stand is preceded by selection cutting (e.g. at a certain target diameter), so the natural dynamic is emulated. Regulating parameters such as species composition and genetic diversity maintain the system structure. Despite the continuous tree removal, indicated by the

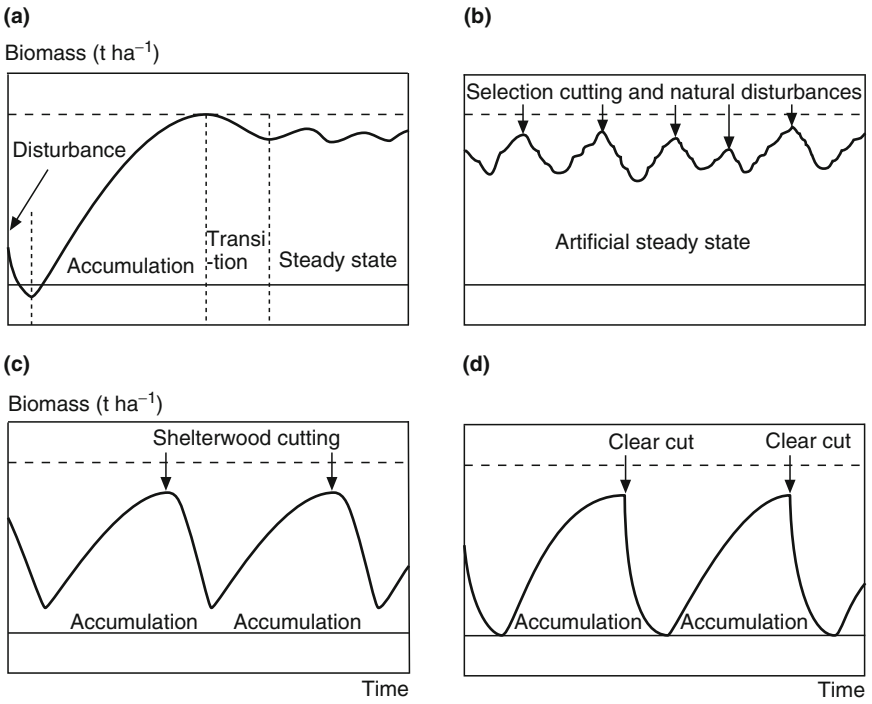

Fig. 1.14 Biomass accumulation during the forest development without disruptions, and with disruptions in hierarchy caused, to a greater or less extent, by management interventions: (**a**) natural development following clear cut or other disturbance, in (**b**) an undisturbed selection forest, (**c**) after a shelterwood felling, and (**d**) in a clear cut system

arrow in Fig. 1.14b, the stand remains in steady state that may last for some time. As for the selection system, the shelterwood system or the group shelterwood system avoids the disruption of the hierarchy by letting the subsequent stand develop from the previous stand. Genetics, species composition, microclimate, macroclimate, soil condition, and so on are maintained to a certain extent by an overlapping phase, which is ecologically very significant (Fig. 1.14c). The strongest disruption in the hierarchy is caused by the clear-cut system, where the stand is harvested before it reaches the maximum biomass accumulation. The newly established stand is not controlled by the regulating parameters of the previous stand (Fig. 1.14d). Sawtooth curves reflect the strong interference of the forest management operations.

The slower processes on a moderate to large spatial scale also possess a higher level of integration and are more than just the sum of the subordinate processes. The feedback mechanisms between processes with the same or different hierarchies shape the characteristic behaviour of biological systems, which cannot be deduced from an isolated view of the underlying process elements. For example, research into and modelling of forest health in relation to isolated soil or plant physiological processes can lead to the prediction of far-reaching destabilisation and stand break-up. The extent to which specific stressors affect stand growth can be overestimated, and the buffering capacity of the cross-scale feedback mechanisms, which stabilise the system, might be underestimated. Dieback scenarios predicted by process models with a high resolution, even in areas under constant biotic and abiotic pressure rarely have occurred yet. This shows that, despite all the experimental accuracy, knowledge about soil chemical, biochemical, or physiological process elements at a high spatial and temporal resolution still cannot replace investigations at the higher levels of integration such as the forest growth research from long-term trial plots.

1.1.7 Forest Stands are Systems with Multiple Output Variables

For almost 300 years, classical forestry has been oriented towards the demands of sustainable wood supply (e.g. von Carlowitz 1713; Hundeshagen 1826). The modern perception of multifunctional silviculture is reflected in the Helsinki Resolution H1 (MCPFE 1993, p.1), in which *sustainable forest management* is defined as "The stewardship and use of forests and forest lands in a way, and at a rate, that maintains their biodiversity, productivity, regeneration capacity, vitality and their potential to fulfil, now and in the future, relevant ecological, economic and social functions, at local, national and global levels, and that does not cause damage to other ecosystems."

In addition to tree and stand attributes, such as volume production assortment yield, and net return, other ecological, economic, and socioeconomic forest functions and services are becoming increasingly important (Constanza et al. 1997). Forest growth research needs to respond to the demand for a broader information base by expanding the list of system output variables recorded, modelled, and reported (Fig. 1.15). In the following chapters, information from the existing and

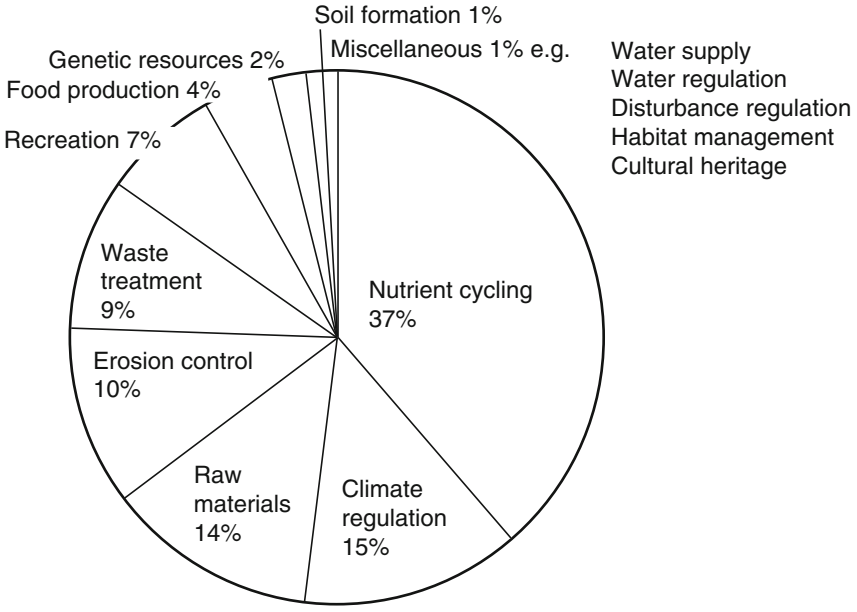

Fig. 1.15 Share (in %) of the worldwide average annual production value of a 1-hectare forest in the categories nutrient cycling, climate regulation, raw material production, erosion protection, waste treatment, recreational value, food production, genetic resources, soil formation, etc. (after Constanza et al. 1997)

continuously expanding database from long-term experimental plots, inventories, and monitoring plots are complemented by information that extends beyond the production function and that may serve to quantify other forest functions and services. This information may assist the implementation of the Pan-European criteria of sustainable forest management, negotiated at the Lisbon Resolution L2: sustainable development of forest resources, vitality and stability, production and regeneration, biological diversity and the fulfilment of additional functions such as protection and the socioeconomic uses (MCPFE 1993).

1.2 From Forest Stand to Gene Level: The Ongoing Spatial and Temporal Refinement in Analysis and Modelling of Tree and Forest Stand Dynamics

As with other realms of science, forest science looks with an ever-increasing spatial and temporal resolution at the functions and structures of woodlands, forest stands, trees, organs, cells, etc. This reductionist trend towards ever more detail is driven mainly by the human fascination and innate thirst for knowledge. We also notice an increasing demand for information for forest ecosystem management (Constanza

et al. 1997; Bundeswaldbericht 2001; State of the World's Forest by FAO 2005). Forest functions, wood and nontimber forest products are valued more and more, refined, exploited commercially, protected, or managed sustainably. This information can only be provided by integrating the known system details and upscaling to the stand or landscape level, where such management decisions are made.

In the following, we sketch the continuing development from classic observations of tree and stand growth to increasingly detailed mechanistic analyses. We discuss concepts for bridging the growing gap between an increasing amount of knowledge about structures and processes at highly resolved temporal and spatial scales on the one hand (chemical, biochemical, molecular biological processes) and the information deficit in the more aggregated lower resolved system levels on the other hand (stand, ecosystem, landscape level). The reconciliation of progressive reductionism and the demand from forest ecosystem management for system knowledge on a stand, enterprise, landscape, or even global scale is a general challenge to forest science and other "green sciences".

1.2.1 Experiments, Inventories, and Measurement of Structures and Rates

Compared with the first attempts to survey forest land by using ell-chains (Stephano and Libalto 1598), today's laser scanner inventories deliver far more detailed information about forests (Fig. 1.16, left, respectively, right). In the seventeenth and eighteenth century, considerable empirical knowledge was accumulated through observations of tree and stand growth. The interest in stand growth was carried out mainly to support forestry practice: the assessment of wood reserves and the potential sustainable annual cut required information about standing volume or volume

Fig. 1.16 Progressive spatial and temporal refinement of measurements in forests. Forest inventory by means of an ell-chain according to Stephano and Libalto (1598, p. 566) (*left*) and 3D image of the experimental plot Freising 813/2 near Kranzberg by terrestrial laser scanning (*right*)

growth per unit area. At the beginning of forest science, towards the end of the eighteenth century, stand growth was measured and conceptualised as standing volume (cubic feet) per unit area (acre). Tree diameter, tree height, and stereometric bodies represented auxiliary variables for models for a rough estimation of standing volume and volume growth of a stand (Cotta 1821). Compared with agriculture, where a crop can be easily mowed and weighed to determine biomass or volume, forest stands require labour-intensive sampling and upscaling. Their sheer size in relation to size of humans requires ingenuity and specialised techniques in forest sampling and measurement (Prodan 1965).

With rising appreciation of quality as well as quantity of wood, stem dimension and form also became relevant. On the early long-term experimental plots, which date back to the 1860s (some are still surveyed today), stem diameter and tree height were measured to calculate mean and cumulative values for the stand, especially for the expected yield (Prodan 1965). Such surveys were repeated at 5- or 10-year intervals to obtain increment and yield information. Already in the late nineteenth, and increasingly in the twentieth century, the stand-oriented approach thus far was refined towards a population approach or even individual-tree approach by distinguishing social tree classes (Kraft 1884), and by the inventory of crown sizes (Assmann 1970), stem quality (Burschel and Huss 1987) and growing space (Oliver and Larson 1990). While such individually based approaches were exceptions before (Reventlow 1879), since 1950, numerous long-term plots were upgraded to incorporate such additional measurements. Successive measurement of, e.g. crown projection, crown base height, or length of the crown receiving direct radiation, transformed former stand-oriented experiments to individual-tree-oriented and spatially explicit experiments (Pretzsch et al. 2002a). Stem analyses and biomass measurements of selected trees on these plots underline the shift from stand to individual-tree research.

In the second half of the twentieth century, studies on how to mitigate soil impoverishment by litter raking, wood exploitation or inappropriate stocking, analyses of the consequences of air pollution by fumes from smelting or steel factories, and assessments of amelioration and fertilisation effects gave rise to a number of very detailed experiments, and the number of recorded variables was raised again (Assmann 1970; Ellenberg et al. 1986). Aboveground tree and stand attributes such as leaf biomass, leaf area, leaf colour, stem quality, crown morphology, or branching and branching anomalies were recorded. Furthermore, in addition to the structural variables measured thus far, a completely new type of variable was introduced, e.g. physiological measures such as assimilation, respiration, transpiration, water and sap flow in phloem and xylem, or more physical measures such as radiation and light absorption in the canopy and flow of water and nutrient solution in plant and soil.

As field experiments aimed at revealing cause–effect relationships between environmental factors and resource supply and physiological processes are always superimposed by a number of uncontrollable disturbances (e.g. weather conditions, pollutants, and insect activities), these were accompanied by green-house and chamber experiments. The latter ensure ceteris paribus conditions as particular factors like CO_2, O_3, temperature, or radiation can be regulated. Soon, scientists

recognized that the results of such chamber experiments could produce very evident and very publishable results. However, they are not always relevant to practical forest management and strategic decisions in the real world. Mature trees under field conditions simply do not behave like juvenile trees of the same species under artificial cover (Matyssek et al. 2005; Ulrich 1999).

1.2.2 From Proxy Variables to "Primary" Factors for Explanations and Estimations of Stand and Tree Growth

The attempt to assess, classify, understand, and even estimate primary productivity, growth, or yield for a given forest stand from causal variables has been investigated in forest research since the first experiments in the eighteenth century (Assmann 1970). However, the approaches have become increasingly mechanistic and more focused on the primary resource and environmental variables.

Initially, in the eighteenth century, the standing stem volume of forest stands was used for the classification of a given stand into a site quality system (Pressler 1877).

$$\text{Site fertility class} = \text{f}\,(\text{standing volume},\ \text{stand age}). \tag{1.1}$$

Then the site fertility class could be applied to estimate growth and yield, e.g.

$$\text{Volume growth} = \text{f}\,(\text{site class, stand age}). \tag{1.2}$$

This classification was somehow circular; the standing volume must be estimated before determining the site fertility class; after which, projections of the future volume productivity could be calculated. This approach only made sense as long as light and moderate thinning were common. With the change to more intensive management concepts in the nineteenth century, the thinning component of total production increased so that standing volume became an increasingly poorer indicator of site fertility class.

As the relationship between stand age and stand height correlates closely with total stand production (Eichhorn 1902) and is less dependent on thinning intensity, it provides an alternative to the former approach. Thus, age and mean height, introduced by v. Baur (1876, 1881) and Perthuis de Laillevault (1803), is used to obtain

$$\text{Site fertility class} = \text{f}\,(\text{mean height, stand age}). \tag{1.3}$$

The classification of stand growth became established despite some reluctance in the beginning (Heyer 1845). Estimates of stand growth and yield result from

$$\text{Stand growth} = \text{f}\,(\text{site fertility class, stand age}). \tag{1.4}$$

With the intensification of thinning from below, which significantly influences calculations of mean height, another change was made in the mid-twentieth century towards the use of top height as an indicator of site fertility (Assmann 1970). The idea of using stand volume or height growth as a "phytometer" for the productivity of a site has continued to the present day. However, this approach is again being questioned as forest practice increasingly implements thinning from above in management regimes to encourage structurally diverse mixed stands. The more a stand deviates from an evenaged, monolayered structure, the greater density and competition influence the relationships between age and height, and the less suitable the age–height relationship becomes as an indicator of site fertility. Especially in highly structured mixed stands, mean and top heights are unsuitable as site fertility indicators.

Heyer (1845) demanded that yield studies not be directed exclusively towards the volume yield, but towards the investigation and measurement of "primary site factors", such as temperature, nutrient supply, radiation. One step into this direction was made by Cajander (1926). He developed a classification system for boreal forests that facilitated the growth and yield estimation from the forest floor vegetation as the indicator (species lichens, mosses, grasses, herbs, shrubs). While this method became standard in the rather uniform and undisturbed boreal forests, the heterogeneity of forest types and human influences makes this approach inadequate for central European forests.

However, the core of Cajander's idea was to combine locally available indicator variables for classifying a particular stand with growth and yield information deduced from site-specific yield tables. The increasing availability of site information and growth and yield data from inventories led to an increased meshing of locally acquired information about site, growth, and yield with general growth and yield relationships deduced from models. Moosmayer and Schöpfer (1972), Wykoff et al. (1982), and Wykoff and Monserud (1988) developed relationships between site conditions and growth at the tree or stand level by regression analysis:

$$\text{Volume growth} = \mathrm{f}\,(\text{stand attributes, site characteristics}). \tag{1.5}$$

For independent variables, they used metric information (e.g. annual precipitation, mean temperature, slope, exposition) and nominal (e.g. levels of nutrition supply, levels of water supply) and ordinal (e.g. growth region, degree of disturbance of topsoil by machines) variables. To estimate the potential height growth, volume growth, and yield in the forest growth simulator SILVA, Kahn (1994) used a set of nine metric site variables (cf. Chap. 13).

Experimental field plots, monitoring plots, and chamber experiments enable the study of metabolic, physiologic, and growth processes as well as the factors affecting growth (environmental conditions, resource supply) at increasingly more refined spatial and temporal resolution. For example, temperature measured per day, hour, or minute and radiation recorded separately for different wavelengths can be used to estimate net primary production, according to the following approach

$$\text{Net primary productivity} = \text{f}\,(\text{leaf area, radiation, temperature, nutrient, water}). \tag{1.6}$$

Simultaneously recorded assimilation rate, respiration, height, and diameter enable a refined estimation also of gross production ($\mathrm{g\,C\,min^{-1}}$, $\mathrm{cm\,day^{-1}}$, $\mathrm{mm\,day^{-1}}$) to be made. The development of inventories monitoring, and innovative regionalisation tools, which deliver all the relevant variables for such primary variable-based approaches Heyer (1845) already had in mind, is in progress. Knowledge about site–growth relationship forms the backbone of forest growth models, and hence the availability of site variables is therefore decisive for the applicability of these models. To overcome the lack of knowledge about the relationships between the primary causes affecting tree and stand development (environmental conditions, resource supply), forest research has gathered much rich experience in the application of "surrogate variables" or "proxy variables" (Oliver and Larson 1990; Zeide 2003). Examples for the application of a surrogate variable or proxy variable include the use of age–height relations for estimations of stand growth, the area available for growth or growing space of a tree for estimations of its resource supply, or the application of competition indices for estimations of height and diameter increment of an individual tree in relation to resource supply. In all cases, the primary factors remain unsolved; however, they are replaced by easy-to-measure auxiliary variables, although they merely reflect the hidden relationships.

1.2.3 From Early Experience Tables to Ecophysiologically Based Computer Models

Before forest scientists understood even some of the basic processes beyond tree growth, considerable empirical knowledge had accumulated from pure observation. The growth relationships derived from observation and not primary causes still made a large contribution to today's understanding of how trees grow and the way they respond under certain growing conditions (in the forest stand). The progression from stand-oriented growth models, such as the pure stand yield tables from Schwappach (1893) and Wiedemann (1932), to stand simulators for management purposes and ecophysiological process models as research tools, as well as the development of succession model, landscape, and biome shift models (Fig. 1.17) reflect the advance in forest ecosystems knowledge, the change in the aims of forest modelling, and the development of theories of forest dynamics.

With a history of over 250 years, yield tables for pure stands may be considered the oldest models in forestry science and forest management. They represent the development of important stand-level parameters (stem number, mean height, mean diameter, basal area, form factor, cumulative annual increment, total production and mean annual increment) in tabular form in 5-year intervals, separately for defined treatments and yield classes (Pretzsch 2001). From the earlier experience tables (Cotta 1821; Paulsen 1795) at the end of the eighteenth century, which were

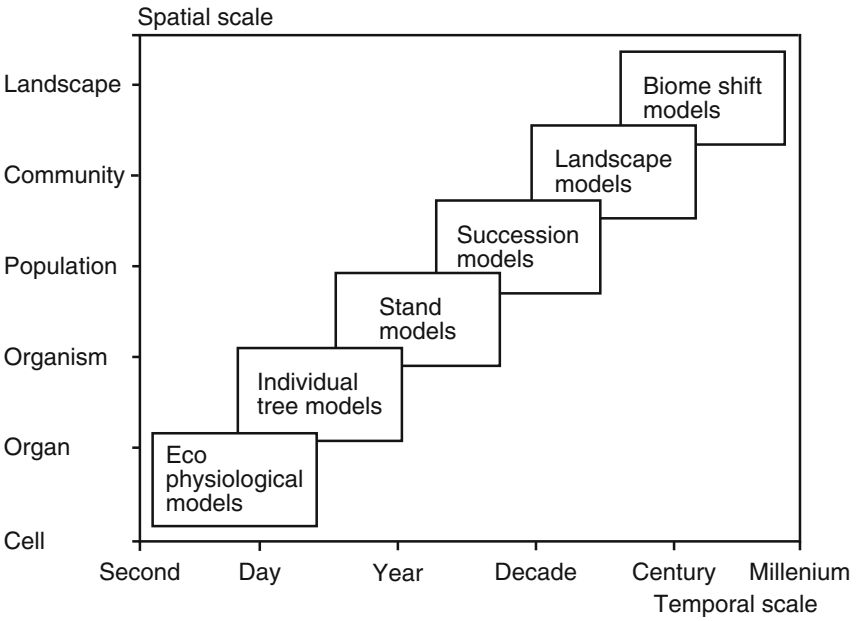

Fig. 1.17 The spatial and temporal aggregation of modelling processes and structures increases from ecophysiological process models to management models to succession, landscape, and biomes shift models

based on estimations or limited measurements, to the first standardised yield tables (Gehrhardt 1909; Schwappach 1893), which were based on long-term observations, and subsequently to the computer-supported yield table models (Assmann and Franz 1963; Schmidt 1971) and yield tables produced by stand simulators (Franz 1968; Hradetzky 1972), models of this generation have become a decisive information base for sustainable volume production. Early experience tables are based on approaches following (1.1) and (1.2). Yield tables that were more developed applied (1.3) and (1.4) for estimation of growth and yield, depending on surrogate variables for site fertility, e.g. site index or vegetation type.

In the 1960s, a second generation of models was initiated, which, in addition to stand level data, also produced stem number frequencies and size classes to enable improved predictions of assortment yield and financial net return. Differential equation models (Moser 1972), distribution extrapolation models (Clutter and Bennett 1965), and stochastic evolution models (Suzuki 1971) served this purpose by abstracting the development dynamics of evenaged homogeneous pure stands by shifting a stem number–diameter distribution along the time axis.

Individual-tree models employ a much higher resolution in the system abstraction and modelling (Newnham 1964; Ek and Monserud 1974; Nagel 1996; Pretzsch et al. 2002a; Wykoff et al. 1982). They divide the stand into a mosaic of individual trees and model their interactions as a spatial temporal system with the computer. The level of description is identical to the level of biological observation,

and the information unit in the model (individual tree) is equally the basic unit of the stand. As individual-tree models contain feedback loops between stand structure and growth, they have greater complexity and flexibility than their precursors. We define position-dependent and position-independent individual-tree models as approaches in which stand competition is modelled with and without consideration of the spatial distribution pattern (stem coordinates, distances between tree pairs, crown parameters), respectively. Pretzsch (2001) reviews the most relevant competition indices, which form the core of such models, as they control individual-tree increment. Stand level data required in forestry can be produced by summarising and aggregating the data of all tree individuals in a stand (Pukkala 1987; Sterba et al. 1995).

Small area or gap models reproduce the growth of single trees in forest patches (e.g. of 100 m^2 area) in relation to the prevailing mean growing conditions at the site (Shugart 1984; Leemans and Prentice 1989). In these models, as the relationships between environmental conditions and growth are described partially statistically and partially ecophysiologically, they adopt an intermediate course between statistically based single-tree models and ecophysiologically oriented process models. They are used to investigate the competition and succession in close-to-nature forests. Individual-tree and gap models estimate increments at the tree or stand level, following (1.5) with a combination of surrogate variables and primary factors as independent variables.

Ecophysiological process models predict tree and stand development from primary processes such as photoproduction, respiration, or carbon allocation (Bossel 1994; Mäkelä and Hari 1986; Mohren 1987). They are based on basic physical, chemical, and ecophysiological relationships as much as possible, and they seek statistical support only to bridge the gap in knowledge where necessary. These models predict the primary production at the individual-tree level (Grote and Pretzsch 2002) or stand level (Landsberg 1986, 2003) and provide information about carbon, nitrogen, and water cycles, thereby supporting a comprehensive understanding and management of ecosystems. Estimations of primary productivity according to (1.6) form the basis of such model approaches. Due to the large demand for initialisation data and to processing of time series of growth determinants by a powerful computer, the ecophysiologically based process models have served primarily as research tools. However, in the future they will become increasingly involved in practical uses; in particular, the integration of structure and function will be of major practical relevance (Kurth 1999; Pretzsch et al. 2008). The increasing demand for information about forest ecosystems and the desire to understand and predict the responses of forest ecosystems to disturbances require a degree of complexity provided only in ecophysiological process or hybrid models.

The search for evidence is important for scientific progress and publication, and it nourishes a large scientific community. This is the reason why experiments move further and further from form and structure to allometry, from allometry to primary and secondary metabolism, to proteome, transcript, and gene level. At best, links to one or two hierarchical levels are made, but the link to a practically relevant level is mostly missing. Relevance of knowledge is something more profane and “merely”

important for the actual real world. For most central European countries, even the application of knowledge at the gene level for genetically engineering improved forest plants plays a minor role so far due to societal resistance against such products. A more detailed analysis of stands and ecosystems is not necessarily a forward movement in the knowledge base relevant to ecosystem management.

1.3 Bridging the Widening Gap Between Scientific Evidence and Practical Relevance

As in many science branches, in forest science we also see a trend from holism towards reductionism. If forest management makes use of any scientific knowledge at all, then it is the integrated knowledge at the stand or landscape level, rather than fragmented details on a small temporal and spatial scale, as interesting as the results of such reductionism are. Contrary to the reductionism in science, system management requires an integrated and a holistic view of the system in question. In the following, we outline some ways of bridging the gap between scientific evidence and practical relevance.

1.3.1 Scale Overlapping Experiments

The investigation of tree and stand growth tends towards higher and higher spatial and temporal resolution and refined causal explanations of structure and functioning. Work is underway to track growth patterns from the morphological or physiological scale down to the metabolic, proteome, and gene level (e.g. Matyssek et al. 2005). Often, however, scientific findings at the gene, cell, or organ level do not necessarily have practical relevance at the tree or stand level. Processes at lower levels (e.g. gene, transcript, organ scale) can be buffered and thus are not apparent in the system behaviour at higher levels (Fig. 1.18). An understanding of forest stand dynamics, for instance, cannot be gained merely by analysing organ or individual-tree growth, as processes like self-thinning or adaptation to density determine stand dynamics only at the stand level (Figs. 1.11 and 1.12).

For example, the research and model approaches used to explain forest decline only from soil processes or plant physiology predicted far-reaching destabilisation and disintegration of forest ecosystems. Mostly, however, the capacity of the stabilising, cross-scale feedback loops to act as a buffer was underestimated, and the effect of specific stressors on stand growth overestimated. Thus, the numerous hypotheses on the causes of forest decline and forecasts of dieback scenarios from high-resolution process experiments and models were largely unfounded (Bossel 1983, 1994).

The knowledge of partial processes with high spatial and temporal resolution cannot replace highly integrated investigations such as those carried out by forest growth research on long-term experimental plots. This is because the slow processes

	H_I	H_{II}	H_{III}	···	H_{XIII}
Stand-population	–	–	**		***
Individual plant	–	*	*		**
Organ	–	*	–		–
Cell	**	**	–		–
Gene-transcript	***	***	–		–

Fig. 1.18 Multiscale falsification of hypotheses H_I to H_{XIII} schematically. Results are traced from gene or transcript level upward to organ, individual plant, stand, and population level. Evidence at lower levels does not necessarily mean relevance at the plant or stand level

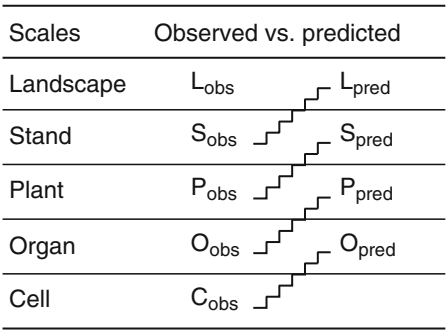

Fig. 1.19 Knowledge gain through scale-overlapping analysis, here from cell to organ, plant, stand, and landscape level (denoted C, O, P, S, and L). The observed system variables at a certain level (C_{obs}, O_{obs}, P_{obs}, S_{obs}, and L_{obs}) can be used to predict the expected behaviour for the next-higher level (O_{pred}, P_{pred}, S_{pred}, and L_{pred}) through linear temporal or spatial upscaling (symbolised by the ladders). Deviations between the observed and predicted values at the next higher level indicate knowledge gaps and the limited relevance of partial processes for the whole. Further explanation is given in the text

on a moderate to large spatial scale and at a higher level of integration are more than just the sum of the smaller scale processes at the level below in the hierarchy. Feedback between processes either between or within the same hierarchies influence the characteristic behaviour of ecosystems, which cannot be understood by considering the subprocesses in isolation. An understanding of forest stand or tree dynamics requires at least measurements from two hierarchical levels, e.g. natural regeneration and mature stand, stand and tree, tree and organs. Explanation means the derivation of a symptom at level n from an integrated interpretation of the details found or measured on level n – 1.

To understand the development of organs, trees, stands, or even landscapes, investigations should be conducted at multiple time and space scales as shown schematically in Fig. 1.19. When the results P_{obs} from observations at the plant level

(e.g. increment or mortality of individual trees in dependence on the growth condition) are upscaled, they predict certain expected patterns at the stand level S_{pred}. The temporal or spatial upscaling time or area units to higher-level (through the ladders in Fig. 1.19) may be carried out through simple addition or multiplication or by modelling. If measurements at the stand level S_{obs} (e.g. long-term records on the stand development through repeated surveys) do not match the expected pattern ($S_{obs} \neq S_{pred}$), this is probably due to a limited relevance of the results at the plant level for explaining the entire system behaviour. Obviously, the transition from tree to stand level introduces new effects, which cannot be deduced from the individual level solely (e.g. adaptation, facilitation, antagonism). We see that scale-overlapping research approaches enable one to estimate the relevance of results at a certain level at the next higher hierarchical level and often reveal knowledge gaps; for forestry practice, it is important to actually trace an observed effect up to the stand level. In general, this approach not only applies to the upscaling from plant to stand level, which is of special importance in forest dynamics, growth, and yield, but analogously to scale overlapping analyses from plant, stand, and landscape level (P_{obs} vs. P_{pred}, S_{obs} vs. S_{pred}, L_{obs} vs. L_{pred}).

1.3.2 Interdisciplinary Links Through Indicator Variables

The design of experiments, which analyse tree and stand growth at high temporal or spatial resolutions often is too discipline specific. Isolated investigations are carried out on soil characteristics, biomass, habitat structure, animal density, etc. This may highlight a certain system characteristic in considerable detail, but often interdisciplinary links to other system aspects are missing. The result is an unconnected patchwork that covers only limited aspects of the functions and productivity of the forest system, providing no knowledge on feedback mechanisms and trade-offs, e.g. between silvicultural prescriptions and nutrient depletion, thinning regimes and species diversity, water balance and stand density.

Still, if at least indicator variables are derived in discipline-specific investigations that provide a link to other forest functions of interest in neighbouring disciplines, the opportunity to obtain statistical links exists. Figure 1.20 gives an example of how tree vitality, stability, habitat and species diversity, or the protective or recreational value of a forest correlate with measures from scales ranging from organ to landscape, e.g. indicator variables such as defoliation, h/d ratio, structural indices, or indices for forest fragmentation. For instance, the diameter distribution, standing volume, and woody debris are comparatively easy to measure and are closely related to the occurrence of rare species of birds, beetles, and butterflies, yet these are much more difficult to record (Gadow 2005).

Scales	Structural indicator		System attribute
Landscape	Fragmentation	~	Recreation value
Stand	Vertical structure	~	Habitat
Plant	h/d-quotient	~	Stability
Organ	Defoliation	~	Vitality

Fig. 1.20 Structural system attributes at the organ, plant, stand, and landscape level play an important role for horizontal knowledge integration. They are relatively easy to estimate or measure and facilitate a link (symbolised by wavy lines) to other relevant system attributes like vitality, stability, habitat and species diversity, or protection and recreation value of a forest

1.3.3 Link Between Experiments, Inventories, and Monitoring by Classification Variables

Results found in one experiment cannot simply be transferred to another site due to divergence of growth behaviour with respect to site conditions, stand structure, species provenance, or genotypes. Thus, in forest science, it is difficult to scale up, even more difficult to generalise, and almost impossible to give site-independent "rules of thumb" for management. Progressing towards improved explanations and modelling of forest dynamics, growth, and yield in relation to primary factors (resource supply and environmental conditions) on a selected number of high-resolution experiments, forest science has gained more and more results outside the very restricted set of site characteristics that are available under normal practical conditions (Gadow 2005). Therefore, we observe a growing gap between the evidence-oriented experiments, which investigate cause-and-effect relationships between growth and underlying primary factors on a few selected sites, and a rather shallow knowledge about site–growth relationships regarding the rest of the forest.

Due to a long history in forest research in Europe, experimental plots, monitoring systems, and grids of inventories have not been designed at the drawing board. So, early long-term experimental plots are distributed rather irregularly, while most inventories follow a systematic grid. Stations for environmental monitoring, again, are not distributed evenly as they were chosen to represent archetypical sites and ecosystems.

To link different types of experimental plots, and inventory and monitoring plots on grids, the concept of ecocoordinates, or bgc-coordinates (variables that characterise the biogeochemical setup of the plot), is helpful. Variables classified in this way form a vector of state and driving variables and typically comprise primary or surrogate variables such as mean annual temperature, precipitation, and length of the growth period; elevation, exposition, and slope; vegetation type; ecoregion; soil water characteristics; nutrient supply; and relevant information about plant material import and export. At the very least, a subset of such classification variables must be recorded to integrate the experimental plot data and its scientific contribution into

existing knowledge, classification systems, or identified growth regions and thus make it useful for teaching, model building, and model evaluation. Without this link, plots deliver fragmented disconnected knowledge, barely useful for understanding or management. Conversely, classification variables can be used to identify experimental plots that are representative of a particular stratum and display archetypical patterns and functioning.

1.3.4 Model Development

As growth models combine detailed system knowledge on forest ecosystems, integrate relevant structures and processes, and enable the user to calculate scenarios and prognoses at the tree, stand, or landscape level, they contribute effectively to bridging the gap between scientific evidence and practical relevance. In the chapter Forest Growth Models, we will get to know empirically based models with rather limited input and output variables. However, they allow useful predictions for those managers who are closely involved in forests managed primarily for wood production. They are based on regression–analytically adapted growth curves between age and height (h) for different site conditions ($h = 20\,m, 25\,m, \ldots, 40\,m$ at age 100). If age a_1 and height h_1 at a given age are known, the height increment in the following period (triangular field) can be read. Analogously, diameter, basal area, and volume increment also can be deduced from the initial variables age and height (Fig. 1.21).

On the other hand, the introduction of mechanistic, ecophysiologically based models, which integrate a broad spectrum of system knowledge at different hierarchical system levels, make this knowledge accessible to forestry practice. They

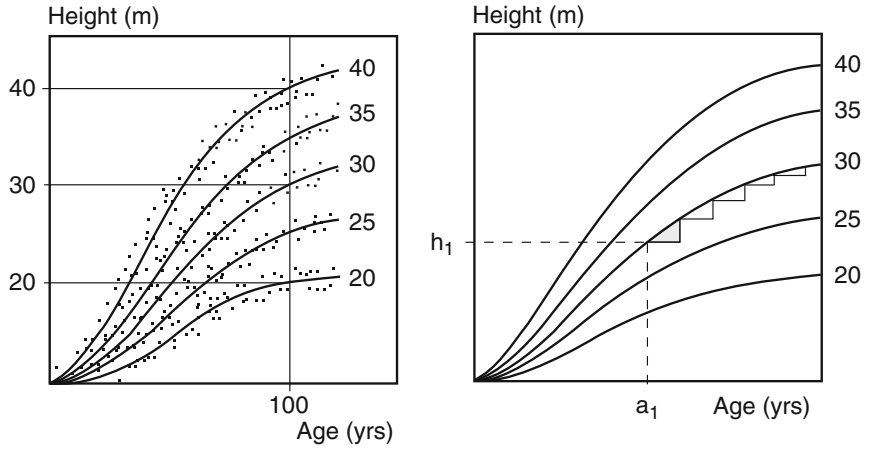

Fig. 1.21 Principle of statistical growth models represented schematically. Explanation in the text

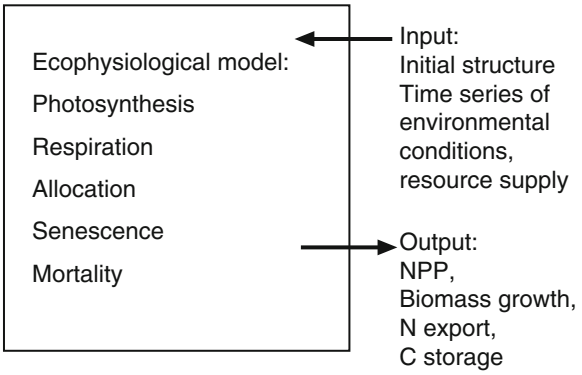

Fig. 1.22 Principle of mechanistic growth models represented schematically. See explanation in the text

describe, among other things, the carbon, nitrogen water cycle and stand growth based on the biological, physical, and/or chemical processes such as incoming radiation, transpiration, photosynthesis, respiration, allocation, aging, and mortality (Fig. 1.22). It requires the input of the initial structure and the differentiated information on environmental conditions and resource supply. However, such models deliver a broad set of output variables that managers need in order to decide the future direction of forest development, long-term planning, and environmental policy. While the empirically based models deliver only a small number of the criteria and indicators needed in forest ecosystem management (forest resources, vitality and stability, production and regeneration, biological diversity, protection, socioeconomic aspects), mechanistic models have at least the potential to providing the remaining information required.

The hybrid models introduced, e.g. by Kimmins (1993), Landsberg (2003), and Pretzsch et al. (2002a, 2008) may present a compromise between empirical models, which provide only limited output variables, and mechanistic models, which are parameterised from intense measurements at only few sites. These models contain functions that estimate the productivity (biomass, wood volume) in relation to primary factors (e.g. precipitation, leaf nitrogen content, temperature, radiation). This can be done based on resource use efficiencies (e.g. nitrogen use efficiency or energy use efficiency) or by assessing the growth curve parameters in relation to the site condition variables (Fig. 1.23). For a sound performance, the initial values and calibration of the internal estimator functions of such models must be backed by a regionally extensive network of inventory data on biomass, soil conditions, climate, and growth.

Figure 1.23 illustrates the principle of hybrid models with the example of the growth simulator SILVA (Kahn 1994; Pretzsch 2002). The model was calibrated from long-term time series of site-specific experimental plots (height and yield development), which have been adjusted by regression analysis and statistically related to the respective site variables $\vec{s}$. The resulting site-specific age–height curve parameters (A, k, p) (right) build an estimation system for growth predictions based

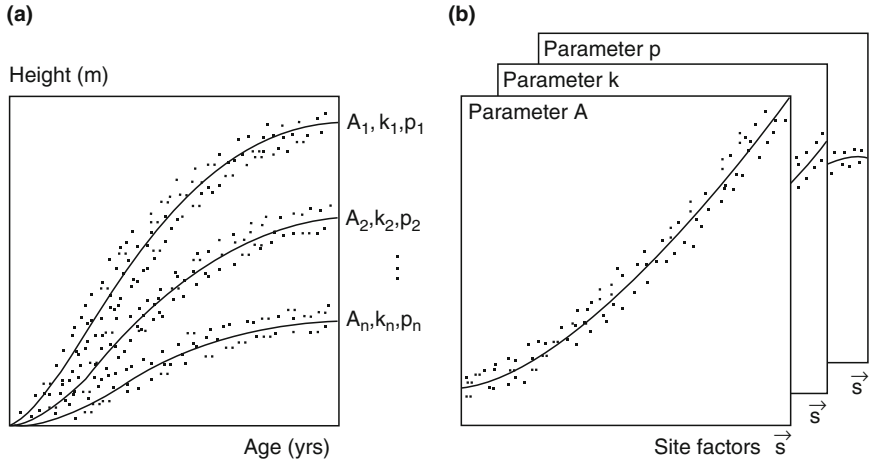

Fig. 1.23 Principle of the site productivity module of the hybrid model SILVA 2.2 represented schematically. See explanation in the text

on regional site conditions. The start-up and control variables of the model are generated from regional-specific inventory data (stand structure, height, site conditions, etc.). Application of hybrid models requires the definition and supply of standardised initial variables (e.g. standing volume, spatial stand structure) and relevant driving variables (e.g. proxy variables like code for the respective ecoregion, elevation over sea level. In the future, more primary information (like temperature, precipitation, radiation, nutrient supply) will indicate the environmental conditions and resource supply. To assure accuracy and acceptance of such models in future, a set of evaluation variables (e.g. biomass growth and yield) needs to be defined, and a standard set of output variables (e.g. indicators for forest resources, vitality and stability, production and regeneration, biological diversity, protection, socioeconomic aspects) needs to be specified to meet the information requirements for sustainable forest ecosystem management.

1.3.5 Link Between Models and Inventories: From Deductive to Inductive Approaches

In particular, two features of modern forest inventories are worth noting as they contribute considerably to bridging the gap between scientific evidence and practical relevance.

Current inventories increasingly need to be used as model input to provide the start or initial variables for simulation runs. While yield tables apply mainly stand height and stand age as the link between inventory and the model, current

inventories provide detailed information about standing volume and diameter distribution and even spatially explicit information about stand structure like stem coordinates, height to crown base, or crown length. As stand dynamics are closely related to the initial stand structure, utilisation of this information can raise the accuracy and precision. Successive inventories on fixed permanent plots provide information about stand and tree growth. When primary information about environmental conditions and resource supply is available, these data can be used to parameterise the relationship between site fertility and productivity or to calibrate models for the ecosystems in question. Such relationships can be used as the basis of hybrid models since they deliver the site-specific potential growth, density, etc. The advantage over conventional model parameterisation based on long-term experimental plots is obvious: inventories cover a much broader range of site conditions and stand structures. Thus, even when plots with unknown history are left out, the remaining datasets are more extensive and representative than the experimental plot data (Gadow 2005).

Repeated surveys of the forest state, increment, environmental conditions, and resource supply make it possible to initialise growth models site specifically and

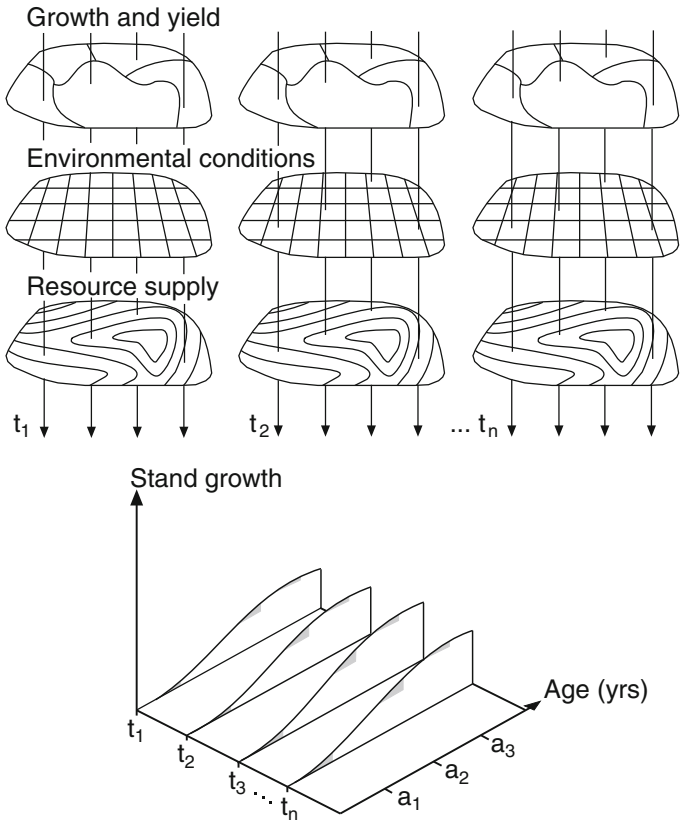

Fig. 1.24 Transition from deductive to inductive model approaches in schematic representation. See explanation in the text

constantly update the parameterisation (Fig. 1.24, time t_1, t_2, t_3, …, t_n). In doing so the initial values and predictions can be adjusted continually to the specific site. The use of inventory data as start values for simulation runs and for the derivation of site–growth relations represents an inductive approach. In this case, information for modelling and simulation are induced from the inventory data itself, while former approaches deduced growth and yield estimations from general models that were based on a small number of long-term experimental plots (Böckmann et al. 1998; Spellmann 1991). By combining general rules for individual tree growth in relation to competition extracted from experimental plots with site-growth relationships extracted from existing inventory data, hybrid models make the best of results from high-resolution experiments and repeated large-scale long-term surveys.

Summary

The introduction points out the very specific system characteristics of trees and forest stands that determine the approach and methods to analyse and model forest stand dynamics, growth, and yield. Like other disciplines, forest science looks with an ever-increasing spatial and temporal resolution on the functions and structures of woodlands, forest stands, trees, tree organs, plant cells, etc. This makes it necessary to discuss concepts for bridging the growing gap between an increasing amount of knowledge on structures and processes on temporarily and spatially highly resolved scales (chemical, biochemical, molecular–biological processes) and an information deficit on more strongly aggregated system levels (stand, ecosystem, landscape scale). The reconciliation between progressing reductionism on the one hand and the demand for holistic system knowledge for forest ecosystem management on the other hand is a general challenge to forest science and other "green sciences".

(1) In terms of lifetime and dimension, trees and forest stands exceed most animal and plant organisms, including humans by several orders of magnitude. Consequently, forest growth experiments extend over many generations of researchers, and special techniques have to be applied to overcome the difference in size. Due to the longevity of forests, models that can predict consequences of new management alternatives or climate changes in time lapse are very important.
(2) Forests are open systems. They exchange matter, energy, and genetic information with their environment. Therefore, to understand the system and to model and predict its responses, one must consider the external determinants of growth (precipitation, temperature, radiation, CO_2 concentrations, atmospheric deposition etc.).
(3) Forests are strongly determined by their spatial stand structure. The consideration of the spatial stand structure is of paramount importance for the understanding and prediction of stand dynamics.
(4) Trees and forests are shaped by their history. In addition to the present factors that act upon them, their development is also determined by their prior use.

Management records, individual allometry, the space occupation pattern of the stand, and the genetic resources of the stand can all be used as indicators of this history.

(5) Forests are cybernetic systems. Feedback mechanisms and systems of closed feedback loops ensure their stability. The closed feedback loop, stand structure → growth constellation of individual trees → growth → stand structure, plays a key role in the recording, representing, and modelling of forest systems.

(6) Forest ecosystems are hierarchical. As higher systems levels (stand) exert force on the subordinate levels (tree, tree component, cells) and lower systems levels, in turn, interact with the higher levels, e.g. by providing the initial conditions, research has developed integrative approaches that incorporate the different levels.

(7) Forest stands are systems with multiple output parameters. In addition to tree and stand attributes such as volume production, assortment yield, and net return, ecological and socioeconomic factors (biodiversity, protection and recreational functions, aesthetic values) are becoming increasingly important.

(8) Since the first attempts to quantify forest productivity in the eighteenth century, experiments drill deeper and deeper from form and structure to allometry, from allometry to primary and secondary metabolism to proteome, transcript, and gene level. A more detailed analysis and modelling of trees, stands, and ecosystems is not necessarily a step forward in terms of the knowledge relevant for ecosystem management.

(9) We observe a shift of forest science from holism towards reductionism. Knowledge and information are often produced on a temporal and spatial scale far from practical relevance. Often, it turns out that scientific findings on the gene, cell, or organ level have no practical relevance on the tree or stand level. If forest management applies any scientific knowledge at all, then it is integrated knowledge about stand level or landscape level rather than fragmented details about system functioning, as interesting as they are. In contrast to the reductionism in science, system management requires integration and a holistic view of the system in question. We see three main approaches to bridge the growing gap. These are listed in items 10 to 12.

(10) Scale overlapping experiments. Integration of knowledge means either to link different system attributes on the same temporal or spatial level or to link investigation results from different levels. When a given question is traced over different levels in order to understand system behaviour over the regarded levels, we speak of vertical knowledge integration. Using horizontal knowledge integration, it is comparatively easy to measure diameter distribution, standing volume, and lying deadwood, while at the same time it is much more difficult to record the closely related occurrence of rare species of birds, beetles, and butterflies.

(11) Link between experiments, inventories, and monitoring. In order to link different types of experimental plots, inventory, and monitoring plots, the concept of ecocoordinates is helpful. At least a subset of such ecocoordinates must be recorded to integrate a certain experimental plot and its scientific contribution

into existing knowledge, classification systems, or identified ecoregions; thus making it useful for teaching, model building, and model evaluation. Without such a link, research plots in forests deliver fragmented unconnected knowledge, hardly usable for understanding or management.

(12) Dynamic models, especially hybrid models, appear suitable for bridging the gap between increasing but more detailed and fragmented system knowledge and missing integrated knowledge for forest ecosystem management. Data from forest inventories can be applied as initial values for simulation runs. In addition, through methods of classification and data mining, site-growth relationships can be "induced" from the inventory data itself and do not have to be "deduced" from general models. Until sufficient data for a mechanistic estimation of growth are available, the calibration of models by inventory-based site-growth relationships can bridge the knowledge gap.

The more diverse the demands on the forest, the more complicated and discouraging become planning and decision making. However, this should not lead to a retreat to basic research; rather it underlines the urgent need for appropriate concepts and tools for decision support.

Chapter 2
From Primary Production to Growth and Harvestable Yield and Vice Versa: Specific Definitions and the Link Between Two Branches of Forest Science

2.1 Link Between Forest Growth and Yield Science and Production Ecology

Forest science and management, which is focussed on wood production, is interested primarily in timber, i.e. the harvestable part of the standing crop. In other words, all growth and management processes are geared to attaining net growth and yield of the commercially viable wood. Net growth is that part of gross primary production that is not respired for maintenance metabolism, is not consumed by animals, is not lost due to physical damage or self-thinning, or remains unused in the forest after the harvest.

Growth and yield are quantified conventionally in terms of stem-wood volume, or merchantable wood volume (>7 cm at the smaller end), in units of m^3 (yield) and $m^3\,yr^{-1}$ (growth) per tree or per hectare. Sometimes these volume units are converted into calorific units (GJ or kWh) for the inventory of fuelwood production, or into tons of biomass or carbon for climate change research. However, the process-oriented research carried out in ecological science is concerned with the magnitude of and the relationships between gross and net primary production; the costs of respiration; the allocation patterns among leaves, seeds, wood, and root production; and the turnover. The principle growth and yield units in ecology are kilograms or tonnes of biomass and biomass production per year, or the energy equivalents Giga Joule (GJ) and GJ yr^{-1}. Such information not only characterises the biomass and energy balance of a system, it is also the key to a more accurate estimation of production potential and to optimising management strategies.

The difference between the approaches in forestry and ecology is also evident in the experimental designs. Forest research looks at the total life span of a tree or stand. Hence, it is usually sufficient to record growth and yield of the wood volume in discrete time intervals, typically 5 or 10 years. Observation series, sometimes of more than 150 years, provide data on growth, yield mortality at the tree and stand level, and thus facilitate the study of long-term growth responses to

H. Pretzsch, *Forest Dynamics, Growth and Yield: From Measurement to Model*,
DOI: 10.1007/978-3-540-88307-4_2,

disturbances. Yet, the 5- to 10-year intervals only partly permit the identification of cause-and-effect relationships, for example the effects of a short drought, cold periods, or fertilisation on growth.

On the other hand, ecophysiological experiments aim to provide an understanding of the relationship between growth and the factors influencing growth, such as resource availability and environmental conditions. The measurements are typically very intensive and may need to be investigated at time resolutions of seconds or minutes. Due to the complex experimental design, often only a part of the system can be studied, e.g. a leaf, a plant organ, or plant, and the experiment can only be run for a limited time period, e.g. a growing season or a few years, but rarely a decade or more. The time series resulting allow a much more differentiated analysis of cause-and-effect chains. However, the results from studies on plant organ level may not necessarily be transferable to the plant or stand level. Therefore, long-term records from forest growth and yield science are needed to support the validation of ecophysiological findings, to scale-up these findings from a plant organ to the plant or stand level, and then to develop applicable generalisations.

We see that both disciplines, forest growth and yield science and production ecology, have their own aims, approaches, and units. Both make complementary contributions to quantifying and understanding tree and stand development. The goal of this chapter is to establish a link between the volume-oriented forestry measures and the biomass measures used in production ecology. Tools and rules of thumb are provided for translating forestry growth and yield values into primary productivity and production efficiencies, and vice versa. The biomass allocation of a tree to needles, leaves, twigs, branches, stem and roots, or the root to shoot ratio, aboveground and belowground turnover, wood density, and carbon content, for example, are dependent on species, provenance, age, site conditions, and the silvicultural treatment. Yet, because exact knowledge about these dependencies is still incomplete and often missing, the factors introduced in this chapter represent estimations based on measurements and literature available to the author. Despite all the uncertainties remaining, the chapter links the measures used in forestry and ecology to bridge the gap between these two disciplines.

2.2 General Definitions and Quantities: Primary Production, Growth and Yield

The following paragraph presents definitions and the relative proportions of primary production, growth, and yield. The term primary *production* is used to address the production process in general, while primary *productivity* means the amount of photoproduction over a given time period for a given area.

Gross primary productivity (GPP, t $ha^{-1}\,yr^{-1}$) refers to the total biomass produced in photosynthesis over a given time period for a given area.

Net primary productivity (NPP, t $ha^{-1}\,yr^{-1}$) is defined as the biomass remaining after subtracting the continuous losses through respiration. The term net primary

productivity equates with gross growth (GG). The choice of either term depends on the focus of the topic. Net growth (NG_{total}, $t\,ha^{-1}\,yr^{-1}$ is obtained by subtracting the continual loss of biomass, i.e. the turnover, as well, which includes the loss of leaves, branches, and roots as a plant grows (short-term or ephemeral turnover of plant organs) and the loss of entire individuals, which die or are removed during stand growth (long-term turnover of whole individual plants). The intermediate state, net growth + turnover of individuals is an important variable in forestry and, therefore, is discussed in this chapter (cf. Sect. 2.3.2).

Net growth of stem wood harvested ($NG_{harvested}$, $t\,ha^{-1}\,yr^{-1}$) reduces the amount of biomass further still as it excludes the volume of roots, tree stumps, the treetops, and brushwood. Merchantable wood volume only refers to the trunk (and branches) above a certain diameter (>7 cm at the smaller end). Here, the net growth (merch) + turnover (merch) of individuals is of special importance.

In forestry, where the general aim is to produce stem wood, the approximate proportion of NPP, net biomass productivity, and net stem growth harvested in relation to 100% GPP is 50%, 25%, and 10%, respectively (Fig. 2.1). This means that 50% of the assimilated carbon is respired, 25% is lost through turnover and recycled, and 15% is unmerchantable or lost through harvesting techniques. Hence, ultimately only 10% of GPP (or 20% of NPP) is commercially viable and measured during the inventory. While this is an important component, it certainly does not represent

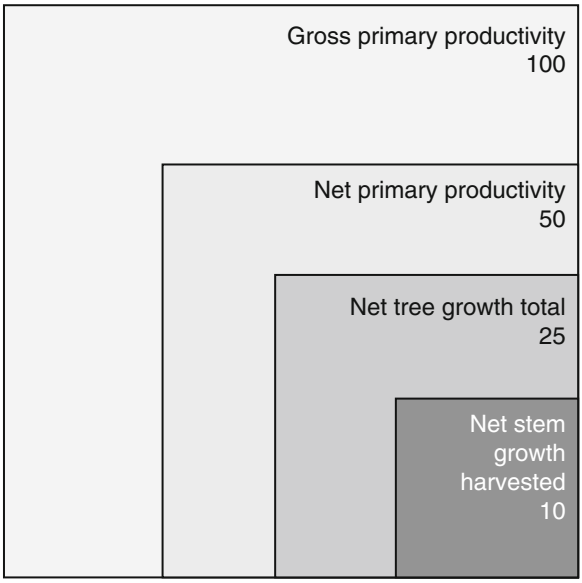

Fig. 2.1 Relative proportions of GPP of biomass, NPP, net tree biomass growth (NG_{total}), and net stem growth harvested ($NG_{harvested}$). Rough guess of the portion for a European beech stand over a 100-year growing period. The relations GPP:NPP:NG_{total}:$NG_{harvested}$ amount to 100:50:25:10. Loss due to respiration, turnover (organs and whole plants), unused root and shoot biomass, and loss due to logging techniques result in a relationship of 10:1 between GPP and $NG_{harvested}$

adequately the elements or energy cycle of the ecosystem. In the following section we refine these proportions.

Figure 2.1 illustrates the relative proportions of the production measures above in a 100-year-old European beech stand under mediocre site conditions. The proportional relationship of 100% GPP to NPP, net biomass growth, and harvested net stem growth is 50%, 25%, and 10%, respectively. This relationship is derived from the long-term means of the production parameters in an evenaged stand. A harvestable net stem growth of $3\,\mathrm{t\,ha^{-1}\,yr^{-1}}$ corresponds to a net biomass production of $7.5\,\mathrm{t\,ha^{-1}\,yr^{-1}}$, a NPP of $15\,\mathrm{t\,ha^{-1}\,yr^{-1}}$, and a GPP of $30\,\mathrm{t\,ha^{-1}\,yr^{-1}}$.

2.2.1 Gross and Net Primary Production

Gross primary productivity includes the production of organic substance (i.e. NPP, or gross growth) plus the respiration losses (R). Gross primary productivity can be determined directly only in chamber experiments. Field experiments estimate NPP directly from energy balances, litter fall, and net yield or indirectly from evapotranspiration measurements (Brünig 1971). The respiration $\sum R$ of stems, roots, and leaves is then added to NPP, or NPP is multiplied as a factor f_r, giving

$$\mathrm{GPP} = \mathrm{NPP} + \sum \mathrm{R} = \mathrm{NPP} \times f_r. \tag{2.1}$$

Herbaceous plants respire 20–50% of their net C-uptake (Larcher 1994, p. 133). Woody plants, especially in forests with a high fraction of photosynthetically inactive biomass (cf. Chap. 2, Sect. 2.5 and Chap. 10, Sect. 10.4), respire 40–60% of the net C-uptake in temperate forests and up to 75% in tropical rainforests (Assmann 1961; Larcher 1994, p. 134; Mar-Möller 1945). In a pure stand, the respiration loss increases from 15% to 30% of GPP in the juvenile stage to 50% in early mature stands to more than 90–100% in old growth stands (Kira and Shidei 1967; Sprugel et al. 1995). In a selection forest with a relatively stable relationship between standing biomass and foliage biomass, the percentage respiration loss relative to GPP should be steady between 30% and 70%. Grier and Logan (1977) describe old grown temperate rainforests along the North American west coast where up to 93% of the C-uptake is used in respiration.

For our purposes, we estimate that a respiration loss of about 50% applies. This corresponds to the respiration factor $f_r = 2$. This reference value holds for temperate regions. Due to the higher temperatures in tropical forests, the percentage respiration loss is higher, and the level of NPP is only slightly higher than in temperate forests. Here GPP, which is higher in tropical forests, is consumed largely in respiration so that NPP is comparable (Kimmins 1996, pp. 46–47). There are still large gaps in knowledge about the absolute magnitude of respiration, the ratio between crown and root respiration, and the dependency of respiration on the factors influencing growth such as site conditions, treatment, and stress.

Net primary productivity quantifies the entire production of organic substances as well as the turnover in a given time period. It is synonymous with gross growth, and we can divide NPP into net growth and turnover.

$$\text{NPP} = \text{net biomass growth} + \text{plant organs and whole plant losses.} \quad (2.2)$$

The net growth of biomass (NG) is still comparably easy to measure although, in forests, some uncertainty still exits about the measurement of wood density and the leaf, brushwood, and root biomass. Moreover, the long-term turnover, affected by the loss of whole trees, can be recorded in repeated surveys at the forest level at least. However, determinations of the turnover of individual plants in herbaceous ecosystems would require an intensive experimental design. The ephemeral turnover in forest and herbaceous vegetation is equally difficult to measure.

According to Brünig (1971, p. 240), the NPP reaches 2–3 t $ha^{-1}\,yr^{-1}$ in boreal conifer forests, 7–17 t $ha^{-1}\,yr^{-1}$ in temperate deciduous broadleaved and evergreen conifer temperate forests, and 18–22 t $ha^{-1}\,yr^{-1}$ in tropical rainforest. Thus, it ranges from 2 to 22 t $ha^{-1}\,yr^{-1}$, or 0.2 to 2.2 kg $m^{-2}\,yr^{-1}$. These values correspond to those from Körner (2002, p. 945) and Larcher (1994, p. 129, Table 2.18). Larcher reports values of 0.1–0.2 t $ha^{-1}\,yr^{-1}$ for tundra, desert and savannah vegetation, 10–15 t $ha^{-1}\,yr^{-1}$ for temperate forests, and 18–30 t $ha^{-1}\,yr^{-1}$ for tropical rainforests. The considerable differences among the vegetation zones are mainly attributable to the length of the growing season. When divided by the length of the growing season, NPP lies between 1.7 and 2.5 t $ha^{-1}\,month^{-1}$ for most vegetation types. The strong dependence of NPP on favourable temperature and precipitation conditions supports the assumption that the increased growth rates in central Europe are at least partly due to the extended growing season (Pretzsch 1999; Spiecker et al. 1996).

The above mentioned NPP values have been averaged over long survey periods and should not be confused with peak values found for a day or a month. Such maxima easily can exceed the average rates by a factor of 10–50, and show the physiological capacity of a plant at a given site. The NPP of plants on sites with superior short-term peak values can be surpassed, in the long run, by plants, which have lower peak values but which maintain constant moderate rates as a consequence of the longer growing season, continuous precipitation, and nutrient availability.

In comparison with the older value of NPP for the world's forests of 67.2 Gt yr^{-1} from Whittaker and Likens (1973), the Intergovernmental Panel of Climate Change IPCC (2001) calculates the current annual NPP at 46.6 Gt yr^{-1} (Gt = 10^9 t). This corresponds to 22–46% of the entire biospheric NPP, including marine ecosystems. For forest cover, the annual NPP is 11.2 and 15.7 t $ha^{-1}\,yr^{-1}$ (1.12–1.57 kg $m^{-2}\,yr^{-1}$) according to IPCC (2001) and Whittaker and Likens (1973), respectively. The global annual NPP of forests of 23.3 and 33.6 Gt C yr^{-1} from IPCC (2001) and Whittaker and Likens (1973), respectively, makes up 3–5% of the total atmospheric C-pool of 750 Gt C yr^{-1}. The annual C-emissions from the combustion of fossil fuels were in the order of 6.3 Gt C yr^{-1} during the 1990s; the C-emissions resulting from land-use change and deforestation, 1.6 Gt C yr^{-1} (IPCC 2001). Given a terrestrial and marine carbon

sink of 5 Gt C yr^{-1}, C-emissions are higher than the ecosystem uptake leading to an annual atmospheric increase in carbon of 3.5 Gt C yr^{-1}, i.e. approximately 0.5%.

Körner (2002, p. 945) points out many sources of uncertainty in the upscaling from biomass increase to NPP. For example, methodological hurdles essentially make it difficult to quantify branch and root turnover. In addition, the estimation of the mycorrhizal assimilate uptake or root exudation is somewhat uncertain. Yet, the current state of research allows us to propose a range in NPP of 10–20 t $ha^{-1}\,yr^{-1}$ or 1–2 kg $m^{-2}\,yr^{-1}$ for central European forests.

As indicated above, this range of NPP values needs to be multiplied by $f_r = 2$ to obtain the total amount of synthesised biomass, and subsequently derive GPP. This produces a GPP of about 20–40 t $ha^{-1}\,yr^{-1}$, or 2–4 kg $m^{-2}\,yr^{-1}$. Given the uncertainties associated with the estimation of respiration losses mentioned above, this range is purely theoretical.

2.2.2 Gross and Net Growth

Growth is defined as the entire biomass produced by a plant or a stand within a defined period (e.g. a day, a year, 5 years). Depending on whether the biomass lost and turned over within this period (i.e. leaves, fine roots, branches, or entire plant individuals) is included or not, we refer to gross or net growth. Whereas GPP and NPP refer to growth including and excluding respiration loss, respectively, gross growth and net growth includes and excludes the turnover of plant organs and individual plants, respectively. The distinction between gross and net growth is of special importance in forests where high levels of mortality and whole trees turnover occur because of their long life spans (Landsberg 1986, p. 172). Thus gross growth, which includes turnover, equals NPP.

$$\text{Gross growth} = \text{net growth} + \text{losses} + \text{mortality} = \text{NPP}. \tag{2.3}$$

The quantity net growth typically is determined from the difference between periodical measurements. For plant biomass w_1 and w_2 at times t_1 and t_2, net growth is

$$NG = (w_2 - w_1)/(t_2 - t_1). \tag{2.4}$$

For an individual plant, net growth (NG) can be expressed as an absolute value in kg yr^{-1}, as a relative growth rate (RGR)

$$RGR = (\ln w_2 - \ln w_1)/(t_2 - t_1) \tag{2.5}$$

in kg $kg^{-1}\,yr^{-1}$ (Harper 1977, pp. 27–28), or as

$$ULR = (w_2 - w_1)/LA/(t_2 - t_1). \tag{2.6}$$

The unit leaf rate (ULR) expresses the biomass growth per leaf area and time in $kg\,m^{-2}\,yr^{-1}$ (Larcher 1994, p. 117). For a stand, the absolute values are given relative to an area unit, e.g. $t\,ha^{-1}\,yr^{-1}$ (Assmann 1961), or as crop growth rate (CGR) in biomass per leaf area and time in $kg\,m^{-2}\,yr^{-1}$ (Larcher 1994, p. 127).

Therefore, NPP is derived from net growth by adding the measured or estimated losses within the measurement period (2.3). The determination of losses and mortality in herbaceous communities such as grasslands is difficult by comparison as one needs to monitor frequently the individual plant losses and the turnover of roots and other plant material. Due to the spatial and temporal scales that apply in forests, the loss of individual trees can be recorded more easily through frequent surveys. In Sect. 2.2 of this chapter, special factors are introduced in the calculation that reduces the gross growth by 40–50% to account for the losses. If NPP = 1–2 $kg\,m^{-2}\,yr^{-1}$ in central European forests, then net growth is about 0.5–1.0 $kg\ m^{-2}\,yr^{-1}$, or 5–10 $t\ ha^{-1}\,yr^{-1}$ when we assume a 50% loss due to turnover and mortality.

2.2.3 Gross and Net Yield

Yield is defined as the entire biomass produced and accumulated from stand establishment onwards. The difference between gross and net yield is analogous to that between gross and net growth. Gross yield includes the entire aboveground and belowground ephemeral biomass such as leaf litter, fine root turnover, and tree mortality. Gross yield can be calculated as the sum or integral of gross growth from stand establishment t_0 up to a specific time t_n:

$$\text{Gross yield} = \int_{t=t_0}^{t_n} \text{gross growth}\,dt \tag{2.7}$$

or, on the basis of the net growth and turnover:

$$\text{Gross yield} = \int_{t=t_0}^{t_n} \text{net growth}\,dt + \int_{t=t_0}^{t_n} \text{turnover}\,dt. \tag{2.8}$$

Net yield only refers to the current, remaining component of biomass production.

$$\text{Net yield} = \text{gross yield} - \int_{t=t_0}^{t_n} \text{turnover}\,dt. \tag{2.9}$$

Yield can be determined at the individual plant level as an absolute value (e.g. kg per plant), or for whole stands for a unit area (e.g. $kg\,m^{-2}$ or $t\ ha^{-1}$). Net yield is

also termed standing crop or standing biomass. It gives the dry weight of a whole plant or a whole stand in both the aboveground and belowground compartments at a given time (Helms 1998, p. 175). Herbaceous plants can be harvested and weighted simply as entire plants. For woody plants, especially in old forest stands, diameter and height dimensions, or other measurements of individual tree size are used to extrapolate the unknown biomass compartments in upscaling functions (cf. Chap. 9).

Net yield or standing crop increases continuously until a threshold biomass stocking, an equilibrium between growth and decline, is reached. On a global perspective, 85% of the vegetation biomass is stored in forests, of which 80% is located aboveground. The range in net yield, or standing crop, is broad: 0.1–1.2 kg m^{-2} in half deserts; 2–6 kg m^{-2} in grasslands, shrublands and agricultural crops; 6–14 kg m^{-2} in seasonal subtropical and tropical forests; 10–22 kg m^{-2} in boreal forests; 10–34 kg m^{-2} in temperate forests; and 14–40 kg m^{-2} in evergreen subtropical and tropical forests.

As 1 kg m^{-2} = 10 t ha^{-1}, the net yield for temperate forests given above translates into 100–340 t ha^{-1}. According to Burschel et al. (1993, p. 42), the net yield in Germany's forests is 260 t ha^{-1} in managed forests, and 310–620 t ha^{-1}, i.e. 31–62 kg m^{-2} in relict primary forests. Clearly, these are average values, which incorporate a broad range of site conditions, age classes and management practices. For old growth coastal rainforest stands in British Columbia, biomass stocks of 1,000 t ha^{-1} (100 kg m^{-2}) or more are found (Grier and Logan 1977). The standing biomass of managed forests in central Europe is estimated roughly at 30 kg m^{-2}, or 300 t ha^{-1}.

About 70% of the earth's surface (510×10^6 km^2) is covered with water. Of the remaining 30% (150×10^6 km^2), forest accounts for only 26% (FAO, 2001, 2005), or 32% (Constanza et al. 1997), i.e. $40–50 \times 10^6$ km^2. Yet, about 77–93% of the entire living biomass of $0.93–1.65 \times 10^{12}$ t (IPCC 2000, 2001; Whittaker et al. 1973) is concentrated in these forests. The global mean value of 6.16–10.94 kg m^{-2} or 61.6–109.4 t ha^{-1} is therefore much lower than the average value for managed forests in central Europe (30 kg m^{-2} or 300 t ha^{-1}) quoted above, which is explained largely by the relative large percentage of open, mainly subtropical forests.

2.3 Specific Terminology and Quantities in Forest Growth and Yield Science

The definition of growth and yield adopted in forest yield science, introduced in Sect. 2.2, essentially relates to stem wood or the merchantable wood, which are quantified in relation to tree height (m), stem diameter at 1.3 m (cm), or volume (m^3 per tree, m^3 ha^{-1}). By growth, we mean the increase in size or weight of a plant or a stand in a given period of time. Depending on whether the plant organs or trees that die in the given time period are included or not, we refer to gross growth or net growth. The same applies for the definitions of gross and net yield.

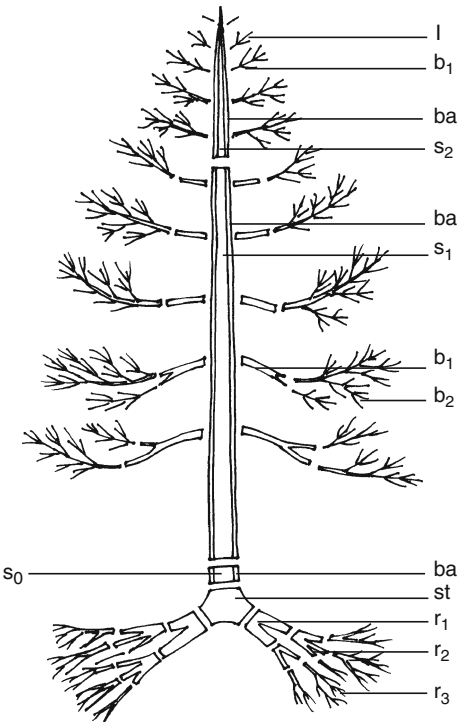

Fig. 2.2 Compartmentalisation of a tree with differentiation of stem volume and merchantable volume <7 cm, standing volume, and harvested volume: l leaves, b_1 branches ≥7 cm at the smaller end, b_2 branches <7 cm, ba bark, s_0, s_1, s_2 stem wood, s_0 trunk base left in the stand due to harvesting techniques, s_1 stem wood ≥7 cm in diameter at the smaller end, s_2 top stem wood <7 cm; st stump wood; r_1, r_2, r_3 root wood of decreasing diameter classes, e.g. >5 mm, 2–5 mm, <2 mm

Figure 2.2 illustrates the partitioning of the woody tree parts into the following compartments: s_t tree stump; s_0 trunk base, which normally is not harvested; s_1 tree trunk of >7 cm diameter between trunk base and tree top; s_2 tree top with <7 cm diameter; b_1 branches with >7 cm diameter; b_2 branches with <7 cm diameter (branch wood); and ba bark. Belowground, we distinguish between coarse, medium, and fine roots (r_1, r_2, r_3).

The standing merchantable wood and stem-wood volume over bark, v(merch) and v(stem), are defined as

$$v(\text{merch}) = s_0 + s_1 + b_1 + ba, \tag{2.10}$$

$$v(\text{stem}) = s_0 + s_1 + s_2 + ba. \tag{2.11}$$

The merchantable wood and stem-wood volume harvested under bark, v(merch harv) and v(stem harv), are

$$v(\text{merch harv}) = s_1 + b_1, \tag{2.12}$$

$$v(\text{stem harv}) = s_1 + s_2. \tag{2.13}$$

Unless explicitly stated, the following discussion always refers to the volume of standing merchantable wood or stem wood over bark because these are the basic forestry units for growth and yield, and also the basic parameters for upscaling to the standing biomass, NPP and GPP. In Sect. 2.4.3, we introduce estimates for the percentage of stump base (s_0) and the percentage of bark (b_a) used to estimate the harvesting losses.

2.3.1 Growth and Yield of Individual Trees

2.3.1.1 Definitions and Examples for Standing Volume, Growth, and Yield

To introduce the most important growth and yield variables, we adopt the 131-year-old Scots pine tree No. 5 from the experimental plot NUE 141/4 near Nürnberg, Southern Germany, by way of example (Figs. 2.3 and 2.4). Figure 2.3 shows the current annual increment in height (CAI_h in $m\,yr^{-1}$), diameter (CAI_d $cm\,yr^{-1}$), and stem volume (CAI_v in $1\,yr^{-1} \hat{=} 10^{-3}\,m^3\,yr^{-1}$) after high-precision stem analysis. Despite the oscillations caused by the factors influencing growth for a brief period, these growth curves conform to unimodal optimum curves with culmination in the early to early-mature stages. Traditionally, the change in volume, as well as the change in diameter and height, at the tree and stand level is referred to as *increment*. Whereas the term *growth* is used to quantify the increase in weight, biomass, and dry weight, the term *increment* is used when referring to structural increases such as height, diameter, basal area, or volume. Essentially growth and increment describe the same thing, i.e. the rate at which the plant or stand increases in weight or size in a given time period. If, instead of annual measurements, periodic surveys at n-year intervals are carried out, then the recorded increment in height, diameter, and volume must be divided by n and is called the periodic annual increment PAI (e.g. PAI_h, PAI_d, PAI_v). Figure 2.3d shows the periodic annual increment of volume in litres per year. Because the stem continually increases in size, and losses in stem or merchantable wood rarely occur, e.g. through crown break or bark loss, the turnover of stem and merchantable wood is minimal to negligible. Thus, at the individual tree level, gross stem growth approximately equals net stem growth. This approximation holds for trees up to 50–150 years at least, the typical harvesting age in central Europe. For old trees with diameters exceeding 50–100 cm, a certain amount of turnover of large branches (b_1) occurs, which affects the merchantable wood volume (but not the stem volume).

By adding the current annual increment CAI over the life span, t_0 to t_n, one obtains the yield,

$$\text{yield} = \int_{t=t_0}^{t_n} \text{growth}\,dt. \tag{2.14}$$

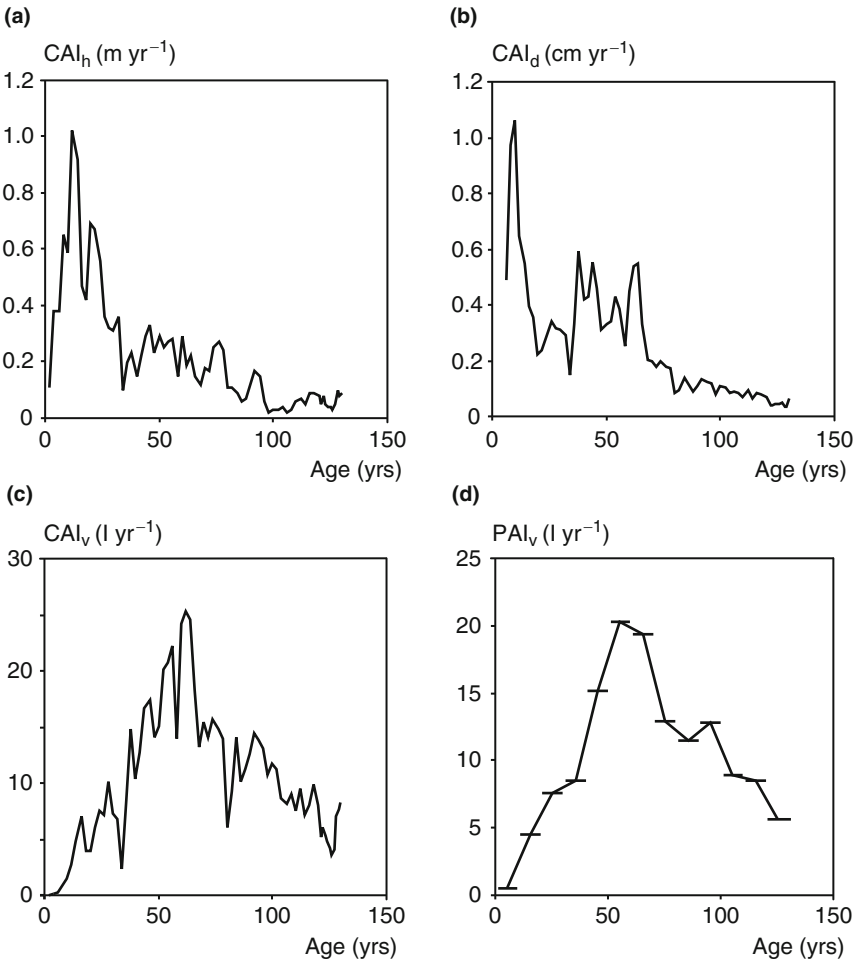

Fig. 2.3 Current annual increment (CAI) and periodic annual increment (PAI) for an individual tree, synonymous with current annual growth and mean periodical annual growth: (**a**) current annual increment of tree height (m yr^{-1}), (**b**) stem diameter at height 1.30 m (cm yr^{-1}), (**c**) stem volume (l yr^{-1}), and (**d**) periodic annual volume increment (l yr^{-1}) over 10-year periods. Results from a stem analysis of the 131-year-old Scots pine No. 5 from long-term plot Nürnberg 141/4

Figure 2.4a–c shows the S-shaped yield curves for height, diameter and volume (Y_h, Y_d, Y_v). The height, diameter, or the volume of the tree stems at a particular point in time represents net yield; and when turnover of stem wood or merchantable wood during ontogenesis is negligible, then

$$\text{Gross yield} \cong \text{net yield} = \int_{t=t_0}^{t_n} \text{net growth}\, dt. \tag{2.15}$$

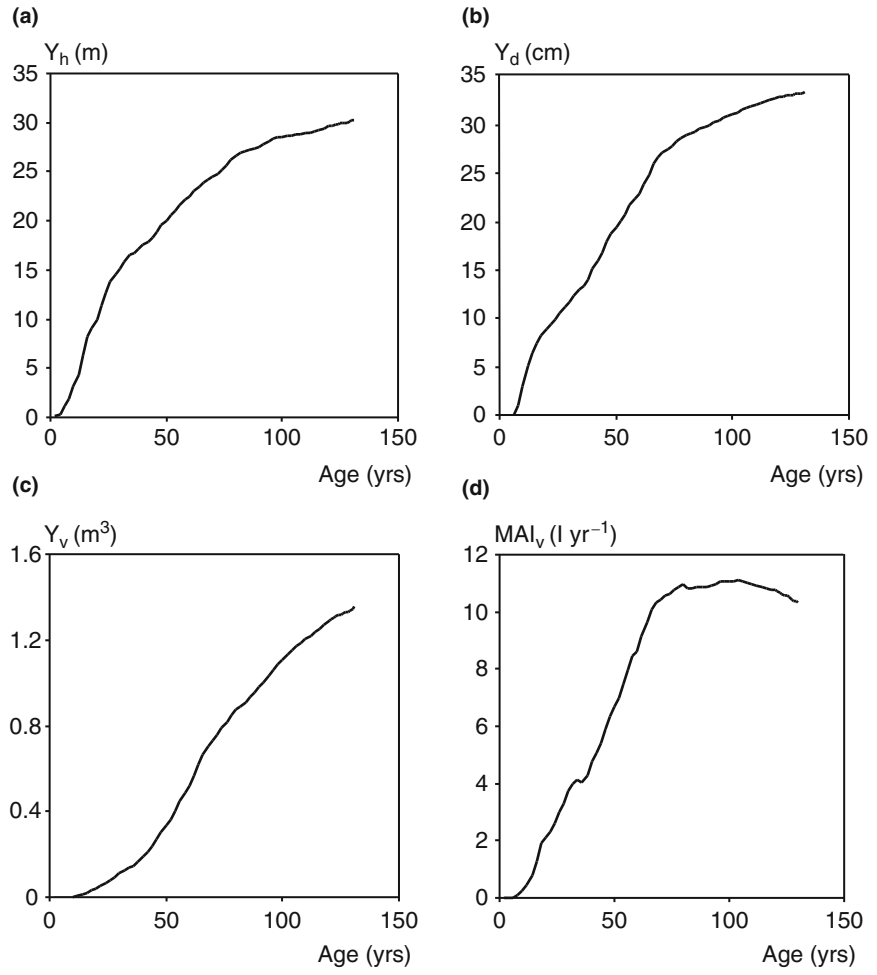

Fig. 2.4 Yield curve for (**a**) tree height (m), (**b**) stem diameter (cm), and (**c**) stem volume (m^3) of Scots pine No. 5 from long-term plot Nürnberg 141/4 (cf. Fig. 2.3). (**d**) Mean annual volume increment (MAI_v) is a synonym for mean annual volume growth

CAI or PAI in selected years or periods are age-dependent, and indicate little about the long-term productivity of a plant or the quality of the site. The long-term productivity is expressed better by the mean annual increment (MAI) (synonymous with mean annual increment); since the time required for woody and herbaceous species to mature differs, it is difficult to make comparisons on the basis of yield data. To overcome this difficulty, the yield at a given time is divided by the age, giving the MAI

$$\text{Mean annual increment (MAI)} = \text{yield}_n/t_n. \tag{2.16}$$

Mean annual increment characterises site quality and delimits the suitable harvesting age. The MAI value resulting reflects the mean long-term productivity level and is an appropriate value for comparisons. Figure 2.4d shows the development of MAI ($l\,yr^{-1}$) for selected Scots pine trees in plot NUE 141/4.

In the literature and in practice, a clear differentiation rarely is made between growth (Fig. 2.3) and yield (Fig. 2.4a–c). In contrast to the strict definitions employed here, all too often yield curves are termed growth curves, e.g. Harper (1977, pp. 5–9). This inconsistency in terminology has led to the misunderstanding and confusion already remarked upon by Bruce and Schumacher (1950, p. 376): "While these curves are commonly called growth curves, it will be noted, that this term is not strictly applicable. [...] The true growth curve is the one showing the relation between the increase in diameter (or height as the case may be) and age. This yearly increase is called the current annual growth." I strongly recommend a more consistent differentiation between the growth curve and its integral, the yield curve.

2.3.1.2 Reference Values for Growth and Yield for Individual Trees

Table 2.1 presents some growth and yield characteristics of a number of 118- to 166-year-old trees after stem analysis (cf. the Chap. 3). The volumes of conifers are given as stem volume and of broadleaves as merchantable wood volume. The final volumes of the selected trees vary between $v = 0.96$–$8.27\,m^3$, the maximum annual increment for diameter $CAI_{d\,max} = 0.37$–$1.37\,cm\,yr^{-1}$, height $CAI_{h\,max} = 0.32$–$0.94\,m\,yr^{-1}$, and volume $CAI_{v\,max} = 13$–$1651\,yr^{-1}$ ($1\,l = 10^{-3}\,m^3$). Usually, diameter growth culminates first (age 8–53), followed by height growth (age 8–68) and, finally, volume growth (age 33–161). Light-demanding species such as Silver birch, Sweet cherry, European ash, and Scots pine reach higher CAI maxima and culminate earlier than shade tolerant species such as European beech, Norway spruce, and Silver fir. The MAI_d, MAI_h, MAI_v at the respective ages 118–166 reach only a half or a third of the maximum CAI_{max} values: $MAI_d = 0.24$–$0.49\,cm\,yr^{-1}$, $MAI_h = 0.16$–$0.32\,m\,yr^{-1}$, and $MAI_v = 7$–$521\,yr^{-1}$. If the turnover of stem wood or merchantable wood is ignored, the standing volume = net yield ≅ gross yield. Then, the net yield and gross yield values of the 118- to 166-year-old trees presented range between 0.96 and $8.27\,m^3$.

Tree size at a given age may vary strongly in the same stand depending on the resource availability of the individual tree. Table 2.2 lists some selected growth and yield values obtained from stem analysis for very slender and very large trees on various experimental plots.

Under favourable site conditions, and with silvicultural promotion, the size difference among the large trees in a stand may be 2–5 times larger in diameter, 1–2 times larger in height, and 5–74 greater in volume than that of the small trees of the same age (cf. lines max : min). The maximum annual increment in diameter, height, and volume in the dominant trees may be as much as 10, 8, and 103 times the suppressed neighbours of the same age, respectively (cf. max:min on the right side of Table 2.2). This demonstrates clearly the potential of thinning to enhance the

Table 2.1 Size (d, h, and v), maximum current annual increment ($CAI_{d\,max}$, $CAI_{h\,max}$, and $CAI_{v\,max}$), and mean annual increment (MAI) of various tree species. The details result from stem analysis and shoot length measurements of individual trees on experimental plots with medium stand density

Tree species	Experiment	Age years	d cm	h m	v m^3	$CAI_{d\,max}$ cm yr^{-1}	Age years	$CAI_{h\,max}$ m yr^{-1}	Age years	$CAI_{v\,max}$ l yr^{-1}	Age years	MAI_d cm yr^{-1}	MAI_h m yr^{-1}	MAI_v l yr^{-1}
Norway spruce	DEN 05	160	77.8	44.6	8.27	0.77	12	0.67	12	125	153	0.49	0.28	52
Scots pine	BAY 51	145	40.9	34.3	2.18	1.37	8	0.94	8	23	33	0.28	0.24	15
Silver fir	RUH110	166	65.6	38.1	5.59	0.58	36	0.65	36	88	161	0.40	0.23	34
European larch	MUE 140	150	69.4	35.5	5.03	0.91	19	0.60	19	75	135	0.46	0.24	34
Sessile oak	KEH 804	118	42.1	31.8	2.30	0.43	15	0.66	10	67	115	0.36	0.27	19
European beech	ROT 634	121	49.1	38.3	3.25	0.59	15	0.60	35	165	125	0.41	0.32	27
White hornbeam	MUE 140	159	40.7	26.2	1.35	0.37	53	0.32	68	30	157	0.26	0.16	8
Silver birch	MUE 140	133	32.3	25.7	0.96	0.41	23	0.78	8	13	113	0.24	0.19	7

d, tree diameter at 1.3 m stem height; h, total tree height; v, tree volume; $CAI_{d\,max}$, $CAI_{h\,max}$, and $CAI_{v\,max}$ and corresponding ages report the maximum annual increment and the tree age when the maximum is achieved; MAI_d, MAI_h, and MAI_v represent mean annual increment of tree diameter, height, and volume.

Table 2.2 Effect of competition on size (d, h, and v), maximum current annual increment ($CAI_{d\,max}$, $CAI_{h\,max}$, and $CAI_{h\,max}$), and mean annual increment of diameter, height, and volume (MAI) of various tree species. The details result from stem analysis of one dominant tree (max) and one suppressed tree (min) on experimental plots with medium stand density. The quotient max:min represents the degree of superiority of dominant trees due to their privileged position and resource supply

Species	d cm	h m	v liter	$CAI_{d\,max}$ cm yr^{-1}	$CAI_{h\,max}$ m yr^{-1}	$CAI_{v\,max}$ l yr^{-1}	MAI_d cm yr^{-1}	MAI_h m yr^{-1}	MAI_v l yr^{-1}
Norway spruce	ZUS 603-3	Age 42							
min	13.4	17.7	139	1.0	0.84	8	0.3	0.42	3
max	28.3	25.2	733	1.3	1.20	42	0.7	0.60	18
max : min	2.1	1.4	5.3	1.3	1.40	5.3	2.1	1.40	5.3
Scots pine	BOD 610-3	Age 50							
min	10.0	12.8	41.1	0.2	0.37	2	0.2	0.26	1
max	29.8	19.7	641	0.8	0.70	31	0.6	0.39	13
max : min	3.0	1.5	15.6	4.0	1.90	20.9	3.0	1.50	16.0
Douglas fir	HEI 608-1	Age 35							
min	15.6	17.5	175	0.6	0.66	13	0.5	0.50	5
max	45.7	25.6	1,729	1.5	1.00	119	1.3	0.73	49
max : min	2.9	1.5	9.9	2.6	1.50	9.5	2.9	1.50	9.9
European beech	STA 91-3	Age 78							
min	9.3	13.3	37	0.1	0.09	1	0.1	0.17	1
max	46.7	29.4	2,727	1.0	0.74	124	0.6	0.38	35
max : min	5.0	2.2	73.7	10.4	8.20	103.3	5.0	2.20	35.0
Sessile oak	ROH 90-3	Age 142							
min	28	25.8	826	0.2	0.11	11	0.2	0.18	6
max	66	33.4	6,098	0.7	0.20	131	0.5	0.24	43
max : min	2.4	1.3	7.4	3.7	1.80	12.0	2.3	1.30	7.4

diameter and volume growth of the remaining trees. Height growth responds less to stand density. Light-demanding tree species (cherry, ash, birch) achieve the highest maximum increment rates ($CAI_{d\,max}$, $CAI_{h\,max}$, $CAI_{v\,max}$). Although the maximum CAI values of the shade-tolerant tree species (Norway spruce, Silver fir, and European beech) are lower, these species achieve high average MAI_d, MAI_h, MAI_v values in the later growth stages.

The values presented in Table 2.2 represent typical tree dimensions in central European forests at harvesting age. They are considered mature for harvest or old growth, even though they are still young in years in relation to their potential maximum age and size. The notable veneer oaks in 350- to 400-year-old stands in the Spessart attain diameters of 2 m and volumes of $>50\,m^3$. Norway spruce, Silver fir, and European beech trees in untouched relict forests in the Bavarian Forest National Park have 1–2 m diameters with $40\,m^3$ merchantable wood volume.

von Carlowitz (1713, p. 138) describes trees in Germany with diameters of almost 4 m and estimated volumes of $>150\,m^3$.

As such giants have been felled systematically in Europe since the Middle Ages, remnants demonstrating the true potential of really old trees here cannot be found. For this, we have to look in Germany at old-growth forests such as the preserved coastal rainforest stands along the Pacific west coast of North America where a single tree can reach 9 m diameter, 100 m height, and $1{,}500\,m^3$ volume at an age that may well exceed 2,000 years. From a list of the largest trees in these forests (Pelt 2001), some of the most impressive tree dimensions were found for the following species: Giant sequoia, *Sequoiadendron giganteum* (General Sherman: $d_{max} = 8.25\,m$, $h_{max} = 83.5\,m$, $v_{max} = 1{,}489\,m^3$); Coast redwood, *Sequoia sempervirens* (Del Norte Titan: $d_{max} = 7.23\,m$, $h_{max} = 93.6\,m$, $v_{max} = 1{,}045\,m^3$); Western red cedar, *Thuja plicata* (Quinault Lake Cedar: $d_{max} = 5.94\,m$, $h_{max} = 53.0\,m$, $v_{max} = 500\,m^3$); Douglas fir, *Pseudotsuga menziesii* (Red Creek tree: $d_{max} = 4.23\,m$, $h_{max} = 73.8\,m$, $v_{max} = 349\,m^3$); and Sitka spruce, *Picea sitchensis* (Queets Spruce: $d_{max} = 4.55\,m$, $h_{max} = 75.6\,m$, $v_{max} = 337\,m^3$).

2.3.2 Growth and Yield at the Stand Level

Growth and yield characteristics at the stand level are derived from periodic inventories, typically at 5- to 10-year intervals. For numerous research plots in Bavaria, time series of >100 years are available (cf. Chap. 3). Unlike on individual tree level on the stand level growth and yield parameters are given relative to a unit area (e.g. hectare, acre), and the tree number per unit area is given as a new separate measure. Tree number decreases with stand development due to self-thinning, silvicultural treatment, or disturbances. In contrast to the tree level, the turnover of merchantable or stem volume at the stand level caused by loss or removal of whole trees is significant.

2.3.2.1 Definitions for Standing Volume, Growth, and Yield

For periodic inventories, the diameter and tree height of all living trees on an area at a point in time t_1 are recorded. From both these parameters and the form factors, the standing volume of the stand $V_{1\,remain}$ at the time of the inventory t_1 can be determined (cf. $V_{1\,remain}$ in Fig. 2.5). In a repeated inventory at time t_2, e.g. 5 or 10 years later, the trees that survived and those that had died or were removed since the previous survey are recorded separately. Consequently, the total volume $V_{2\,total}$ can be divided into the standing volume $V_{2\,remain}$ and the volume turned over $V_{removed}$ ($V_{2\,total} = V_{2\,remain} + V_{removed}$). Although the mortality or removal of trees ($V_{removed}$) is an ongoing process, it is recorded as at the end of an inventory period, resulting in a saw-tooth yield curve of $V_{n\,remain}$ as shown by the solid line in Fig. 2.5. If the inventories were carried out each year, so that the exact time of a tree's death or removal was known, the curve would be much smoother, and the teeth smaller.

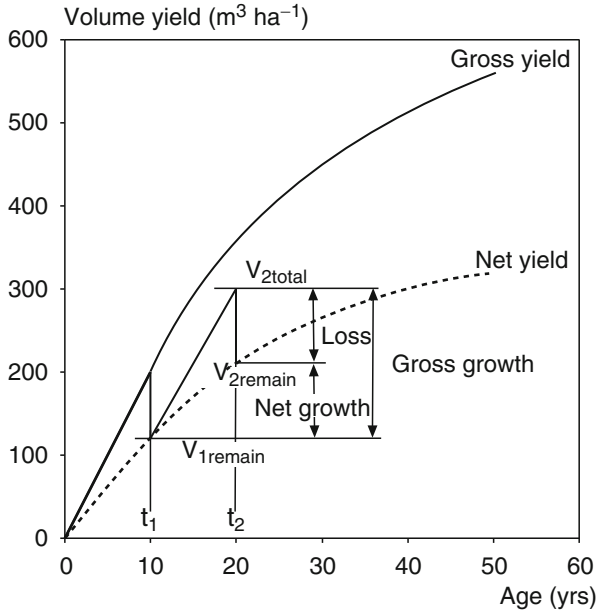

Fig. 2.5 Derivation of growth and yield characteristics by periodical stand inventories presented schematically. Gross and net volume yield (GY_V and NY_V, respectively) are represented by the *upper solid* and the *lower dashed curve*, respectively. $V_{1\,remain}$, $V_{2\,total}$, and $V_{2\,remain}$ represent the live standing volume at time t_1, total standing volume at time t_2, and remaining standing volume at time t_2. Difference $V_{2\,total} - V_{1\,remain}$ = gross growth. Gross growth is based on the two components: $V_{2\,remain} - V_{1\,remain}$ = net growth and $V_{2\,total} - V_{2\,remain}$ = losses due to whole tree turnover

Repeated inventories of whole stands are carried out in a periodic cycle of several years, and produces PAI values rather than CAI values; i.e. the mean annual growth rates over longer time intervals. Between two surveys at time t_1 and t_2, the PAI is

$$\mathrm{PAI} = (V_{2\,remain} - V_{1\,remain} + V_{removed})/(t_2 - t_1). \tag{2.17}$$

The gross yield in volume is calculated from the integral of PAI,

$$\text{Gross volume yield } Y_{V\,gross} = \int_{t=t_0}^{t_n} \mathrm{PAI}\,dt \tag{2.18}$$

and standing volume, equivalent to the net volume yield, is obtained from,

$$\text{Standing volume } Y_{V\,net} = \int_{t=t_0}^{t_n} \mathrm{PAI}\,dt - \int_{t=t_0}^{t_n} V_{removed}\,dt. \tag{2.19}$$

As for individual trees, the mean annual increment MAI is defined as the gross yield at time n divided by the stand age in years,

$$\mathrm{MAI_n} = \text{gross yield}_\mathrm{n}/\mathrm{t_n}. \tag{2.20}$$

Figure 2.6 shows (a) the volume yield curve for individual tree No. 4 at the long-term experimental plot Denklingen 5, trial plot 2 and (b–d) the yield and growth curves at the stand level. The increase in the gross and net stem yield or merchantable volume yield at the tree level is almost identical and monotone because virtually no turnover in stem volume or merchantable volume occurs (Fig. 2.6a). In contrast, tree removals at the stand level (self-thinning, damage, thinning) result in a

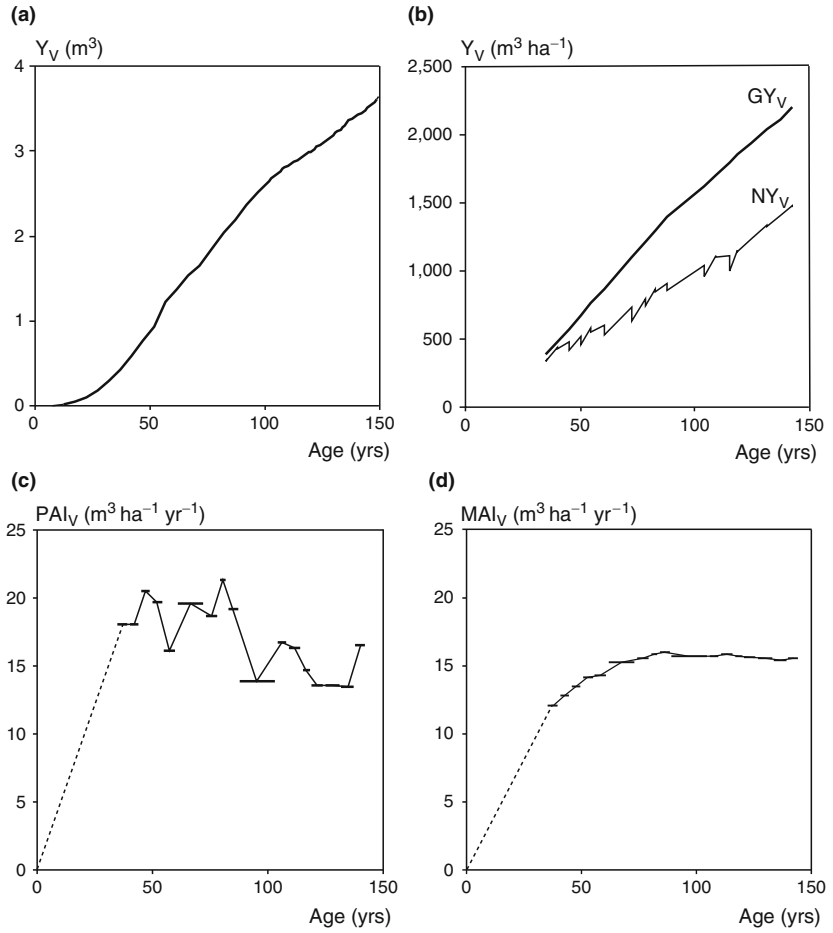

Fig. 2.6 Growth and yield curves of stem volume for long-term experimental plot Denklingen 5, plot 2. (**a**) Net and gross volume yield curve for tree No. 4, derived by stem analysis, (**b**) development of gross volume yield (GY_V) and net volume yield (NY_V) at the stand level, (**c**) periodical annual volume increment PAI_V, and (**d**) mean annual volume increment MAI_V derived from 18 successive surveys since establishment of the experiment in spring 1883

saw-tooth shaped curve for net yield NY_V (Fig. 2.6b, bottom line). One obtains the gross yield (GY_V) by adding the volumes of the remaining and removed trees (Fig. 2.6b, top line). As the stand ages, a continually larger proportion of the gross yield is removed, and hence no longer present. These intermediate yields can be determined from the long-term measurement of removals on long-term experimental plots. Under steady state conditions, the ageing process of PAI and MAI follow a unimodal optimum curve (Fig. 2.6c, d). MAI culminates later and at a lower level than PAI (cf. Chap. 10, Sect. 10.3).

2.3.2.2 Reference Values for Growth and Yield of Pure and Mixed Stands

The following tables present some characteristic growth and yield values for evenaged pure stands (Table 2.3), evenaged mixed stands (Table 2.4) and unevenaged mixed stands (Table 2.5) at experimental sites in Southern Germany. The average growth and yield data collated for up to 130 years, provided for trees and stands, represent moderately thinned and otherwise largely undisturbed stands from experimental research plots with moderate to good site conditions. The volume data refer to merchantable volume (>7 cm at the smaller end) for broadleaved trees and to stem volume for conifers.

In the evenaged pure stands (Table 2.3), the quadratic mean diameter attains 43.3–55.6 cm, stand basal area 28.2–88.4 $m^2\,ha^{-1}$, and standing wood volumes 428–1,480 $m^3\,ha^{-1}$ at age 93–178 years. Norway spruce and Douglas fir rank highest, whereas European larch and Sessile oak rank lowest. Maximum PAI values lie between 10.4 and 33.4 $m^3\,ha^{-1}\,yr^{-1}$, MAI between 5.4 and 17.2 $m^3\,ha^{-1}\,yr^{-1}$ and gross yield between 953 and 2,199 $m^3\,ha^{-1}\,yr^{-1}$. Of this gross yield, 33–55% died or were removed during the stand lifetime (IY_V (%) = intermediate volume yield in percent), giving net yield values of 428–1,480 $m^3\,ha^{-1}$ standing volume.

The values for the evenaged mixed stands (Table 2.4) are based on artificial time series comprising up to ten adjacent plots of different ages, which cover the stand life span (Pretzsch and Schiitze 2005, 2008) (cf. Chap. 9). The stands were inventoried between 1992 and 2008 to derive growth and yield characteristics for the most relevant types of mixed forest in South Germany. The mean height and quadratic mean diameter for the two species present in the stand are listed separately. The first species mentioned generally exceeds the second in height and diameter, introducing a certain horizontal stratification. At 100–146 years of age, the standing volume ranged from 580–921 $m^3\,ha^{-1}$. Evenaged mixed stands, with MAI values of 11.8–18.5 $m^3\,ha^{-1}\,yr^{-1}$ and gross yields of 1,281–2,112 $m^3\,ha^{-1}$ at 100–146 years of age, do not fall behind the pure stands. However, the percentage intermediate yields (IY_V in %) in mixed stands of 50–81% are clearly higher than in pure stands, which means the final standing volume of 580–921 $m^3\,ha^{-1}$, which is equivalent to the net yield, is lower than that of the pure stands.

The unevenaged mixed stands (Table 2.5) represent selection forests and moderately thinned mountain forests, consisting mainly of Norway spruce, Silver fir and European beech. On the research plots, trees range from seedling to almost

Table 2.3 Stand characteristics of evenaged pure stands of various tree species in central Europe after long-term inventory. Several inventories date back to 1870

Tree species	Experiment	Age years	d cm	h m	st. basal area $m^2\,ha^{-1}$	st. volume $m^3\,ha^{-1}$	$PAI_{V\,max}$ $m^3\,ha^{-1}\,yr^{-1}$	MAI_V $m^3\,ha^{-1}\,yr^{-1}$	GY_V $m^3\,ha^{-1}$	IY_V %
Norway spruce	DEN 05	143	54.4	40.3	88.4	1,480	21.3	15.4	2,199	32.7
Scots pine	BAY 52	131	43.3	36.3	44.0	700	12.1	10.5	1,370	48.9
Silver fir	WOL 97	134	53.9	34.0	45.1	637	12.0	9.5	1,268	49.8
European larch	MIS 47	178	55.6	36.7	28.2	428	10.4	5.4	953	55.1
Douglas fir	FRE 85	93	44.6	39.3	61.9	1,012	33.4	17.2	1,603	36.9
Sessile oak	LOH 59	168	50.3	33.0	37.4	605	10.6	7.7	1,301	53.5
European beech	FAB 15	178	51.5	38.0	48.0	950	15.9	8.7	1,551	38.7

d and h mean stand diameter and height; stand basal area; standing stem or merchantable volume, respectively; $PAI_{V\,max}$, maximum periodic annual volume increment since the beginning of the inventory; MAI_V, mean annual volume increment; GY_V, gross volume yield since stand establishment; IY_V, intermediate volume yield [$IY_V = 1 - (\text{standing volume/gross volume yield}) \times 100$].

Table 2.4 Stand characteristics of evenaged mixed stands in Bavaria. The evaluation is based on artificial time series of mixed stands with up to 10 plots per time series and 2–3 successive inventories per plot. Mean annual volume increment (MAI_V), gross yield of volume (GY_V), and percentage of intermediate yield (IY_V) from stand establishment to the age of the oldest plot (age 110, 100, 136, 109, and 146, respectively)

Tree species	Experiment	Age years	d cm	h m	V $m^2\,ha^{-1}$	MAI_V $m^3\,ha^{-1}\,yr^{-1}$	GY_V $m^3\,ha^{-1}$	IY_V %
Norway spruce-	SON 814	110	50.3	38.0	562	11.5	1,267	55.6
European beech			37.4	33.5	359	6.9	764	53.0
Total					921	18.5	2,031	54.8
Scots pine-	NEU 841	100	39.4	30.0	496	9.7	969	48.8
Norway spruce			24.9	25.1	380	7.9	786	51.7
Total					876	17.6	1,755	50.1
Scots pine-	GEI 832	136	59.1	32.3	144	5.4	732	80.3
European beech			23.0	26.1	250	10.1	1,380	81.9
Total					394	15.5	2,112	81.0
European larch-	GEM 871	109	53.6	38.1	197	4.3	467	57.8
European beech			45.9	35.3	383	7.5	814	52.9
Total					580	11.8	1,281	54.7
Sessile oak-	KEH 804	146	48.8	33.6	548	8.8	1,288	57.5
European beech			27.6	26.5	140	3.6	519	73.0
Total					688	12.4	1,807	61.9

300 years old. The quadratic mean diameter of the dominant species (mostly Norway spruce, sometimes Silver fir) attains 39.2–58.1 cm, height 29.4–37.4 m and basal area 29.7–66.9 $m^2\,ha^{-1}$. The standing volume lies between 477 and 1,028 $m^3\,ha^{-1}$. In contrast to the previous, comparably unstratified pure and mixed stands, the standing volumes do not show the final net yield values reached near the end of the rotation cycle, but give continuous averages that vary little due to the periodic removal of individual trees. The mean PAI and maximum PAI attain values of 4.7–15.9 and 5.5–19.6 $m^3\,ha^{-1}\,yr^{-1}$ respectively. In these unevenaged forests, the long-term PAI averages compare best with the MAI values of evenaged rotation forests. A comparison shows that the PAI of unevenaged stands are of the same order as the MAI values in evenaged stands (Table 2.3), and slightly lower than the MAI values in the evenaged mixed stands (Table 2.4), which are highest.

2.3.2.3 Factor for Intermediate Yield or Whole Tree Turnover t_{ind}

At the stand level, the turnover of merchantable wood is considerable due to the loss of entire trees through self-thinning, tree removal and calamities. The spatial and temporal scale of forest stand dynamics makes this turnover easier to measure than in herbaceous communities. We can enter forest stands to measure the living and dead individuals without damaging them conspicuously, or impairing their ongoing development. To undertake similar surveys in herbaceous stands to document whole

Table 2.5 Stand characteristics of unevenaged mixed stands of Norway spruce, Silver fir, and European beech in the temperate mountain forests of Bavaria. Inventories date back to the year 1950

Tree species	Experiment	Age	d_{max}	h_{max}	st. basal area	V	$PAI_{V\,mean}$	$PAI_{V\,max}$
		years	cm	m	$m^2\,ha^{-1}$	$m^2\,ha^{-1}$	$m^3\,ha^{-1}\,yr^{-1}$	$m^3\,ha^{-1}\,yr^{-1}$
N. spruce-Silver fir-European beech	FRY 129/32	2 – 239	42.9	31.0	42.6	663	10.7	13.8
N. spruce-Silver fir-European beech	BOM 130/22	2 – 286	41.2	30.8	44.5	610	10.2	11.3
N. spruce-Silver fir-European beech	PAR 115/1	2 – 203	44.6	32.8	57.2	871	8.1	9.8
N. spruce-Silver fir-European beech	KRE 120/3	2 – 158	39.2	29.4	40.1	502	4.7	5.5
N. spruce-Silver fir-European beech	MAR 108/1	2 – 142	58.1	37.4	66.9	1,028	15.9	19.6
N. spruce-Silver fir-European beech	RUH 110/2	25 – 165	55.3	36.1	29.7	477	7.9	10.4
N. spruce-Silver fir-European beech	RUH 116/1	2 – 183	45.3	33.7	52.6	784	9.8	11.4

d_{max} and h_{max} mean stand diameter and height of the species with maximum size; st., basal area; V, total standing volume; $PAI_{V\,mean}$ and $PAI_{V\,max}$, mean and maximum periodic annual volume growth since start of the survey.

plant turnover, i.e. the mortality of whole plants, the surveyor would need to shrink to one-tenth his size (cf. Chap. 1, Sect. 1.1). Only then could one undertake comparable, spatially explicit measurements of growth and removal of individual plants without damaging the remaining stand, and thereby having an impact on further stand development. Consequently, the amount of turnover of plants in herbaceous stands is largely unknown. Maybe the following values from forests give some idea of the values in herbaceous stands that follow similar self-thinning processes to woody plants (Pretzsch 2002, 2005c).

Table 2.6 shows that, based on yield tables commonly used in Germany, the turnover of merchantable wood volume resulting from whole tree removal (IY (%) = whole tree turnover/total yield $\times 100$) may be as much as 60.7% of the total volume produced (Sessile oak at age 200). For the experimental plots introduced above, the percentage turnover lies between 32.7% and 55.1% in evenaged stands, and 50.1–81.0% in unevenaged stands (cf. Tables 2.3 and 2.4). Hence, a substantial part of the entire stand production is simply absent at the end of the rotation period, and, if not entirely removed, is partially incorporated in the remaining stand in form of carbon, hydrogen and oxygen (C, H, O) or mineral nutrient elements. Long-term experiments on unthinned or lightly thinned (A grade) stands reveal that, during

Table 2.6 Percentage of intermediate yield IY [$IY_V = 1 - (\text{standing volume/gross volume yield}) \times 100$] from age 20 to 200 years according to frequently used yield tables for tree species in Europe. The portion of removed volume decreases from stands with excellent site conditions to poor sites. The values presented apply for moderate thinning, and were derived from the yield tables quoted in the second column. In case of Norway spruce, the values refer to total stem wood; all other values refer to merchantable stem wood >7 cm at the smaller end. The last two columns present the factor t_{ind} for estimation of gross volume yield on the basis of net yield for the stand age 60 and 100 years ($GY_V = NY_V \times t_{ind}$)

Tree species	Yield table	Site class	Intermediate yield IY (%) at stand age							Multiplier t_{ind} at stand age	
			20	40	60	80	100	150	200	60	100
Norway spruce	Assmann and Franz (1965)	O40	15.3	33.2	36.2	37.5	39.4			1.57	1.60
		O20			17.1	21.6	26.2			1.21	1.28
Scots pine	Wiedemann (1943a)	I.		18.4	31.0	39.1	44.9			1.45	1.64
		VI.				7.4	22.0				1.08
Silver fir	Hausser (1956)	I.		16.0	30.0	41.0	47.0	56.0		1.43	1.69
		IV.			4.0	20.0	33.0	48.0		1.04	1.25
European larch	Schober (1946)	I.	7.4	29.2	34.5	37.2	39.7			1.53	1.59
		III.		16.9	27.0	33.1	37.0			1.37	1.49
Douglas fir	Bergel (1969)	I.	9.3	36.5	42.5	43.6				1.74	1.77
		III.		29.4	36.9	39.1				1.58	1.64
Sessile oak	Jüttner (1955)	I.		18.4	32.9	41.1	47.6	56.7	60.7	1.49	1.70
		IV.			6.5	11.3	18.2	32.8		1.07	1.13
European beech	Schober (1967)	I.		5.3	21.5	32.4	39.6	50.1		1.27	1.48
		IV.			7.4	19.5	27.6	41.3		1.08	1.24

the juvenile development phase, i.e. before canopy closure, only little merchantable wood is lost through self-thinning. The main turnover occurs from the early-mature stage onwards, where the percentage of the lost volume amounts to about 30%, a value that is remarkably stable among the tree species (Pretzsch 2005b).

Based on the reported proportions of gross and net yield, we introduce a first-order estimation of the total produced volume (=gross yield GY_V) from the remaining stand volume (=net yield NY_V). We assume a tree loss of 33% between stand establishment and harvesting under light to moderate thinning. This means 67% of the stand volume remains, and the factor for deriving total volume from standing volume, which includes the turnover owing to the removal of individual trees $t_{ind} = 1.5$ at age 100, is:

$$GY_V = NY_V \times t_{ind}, \tag{2.21}$$

with $t_{ind} = 1.5$ (1.04–1.77) at age 100.

The estimate $t_{ind} = 1.5$ is merely an approximation that serves for early-mature and mature stands in rotation forests (Table 2.6). Depending on age, silvicultural treatment and species, this value easily may vary between 1.04 and 1.77 (cf. Table 2.6).

The definitions and datasets introduced so far consider the entire standing stem or merchantable wood volume and do not distinguish dead and living wood. With increasing age and size, heartwood development progresses, and hence the ratio of living: dead tissue decreases. It can be assumed that the net growth of living wood volume in old stands and primary forests is static or even decreases while the total wood volume continues to accumulate. To differentiate living and dead wood volume, we refer to living wood volume as the "true" standing volume, and to the "true" growth and yield. The distinction becomes important when comparing the yield or production of woody and herbaceous stands. Large standing volumes of $>10{,}000\,m^3\,ha^{-1}$, such as found in North American temperate rainforests could never consist entirely of physiologically active tissue (as in herbaceous stands), but mainly of dead, physiologically inactive tissue.

2.4 Stem and Merchantable Volume Growth as a Percentage of Gross Primary Production

The growth and yield measures, stem and merchantable wood volume, are standard forestry variables. In this chapter, we introduce values and rules of thumb for converting this wood volume to wood biomass, to total tree or stand biomass (including leaves, brushwood, and roots), and then into net primary production (NPP, including turnover) and gross primary production (GPP, including respiration). The intention is to bridge the gap between the forestry wood volume standards and the ecological primary productivity standards.

As Kimmins (1996), Landsberg (1986), and Larcher (1994) point out, biomass allocation, turnover, and respiration all depend on the following factors: growing conditions, species, treatment, and age. The quantities and relationships between them express the adaptability of a species to certain growing conditions, and, in this sense, are of major ecological interest. However, to obtain a rough estimate of primary productivity from forestry growth and yield values, the influence of each of these factors is given in relation to their potential deviation from a specific average value.

Despite the broad range in variation in the individual biomass compartments, and the turnover and respiration rates, the conversion from volume-based forestry growth and yield values to biomass, or carbon-based parameters of primary production should become transparent. We provide an insight into the average size of the relative percentages and losses. This insight and this classification of the forestry growth and yield parameters as a part of the whole primary production should not be lost in the plethora of studies about specific elements or new models.

Table 2.7 gives an overview of the descriptions, approximate values and range in variation of the multipliers used in this chapter. R expresses the basic specific wood density; i.e. the wood density defined in relation to green volume (Simpson 1993). The expansion factors e_{br}, e_l and e_r are used in the step-by-step conversion of merchantable volume to aboveground and belowground total volume. The factors e_{br},

Table 2.7 Estimates and range of the specific wood density R, expansion factors e_{br}, e_l, e_r, turnover factors t_{org}, t_{ind}, harvest loss factors l_s, l_b, factor for estimation of sapwood f_{sw}, and respiration f_{re}. The factors provide a rough estimate of standing total biomass, NPP, and GPP in relation to standing merchantable volume and mean annual volume increment. The reciprocal values, 1/R, $1/e_{br}$, etc., assist the estimation of standing merchantable volume from standing total biomass. They can be applied, e.g. for partitioning GPP and NPP into ephemeral and long-lasting components, aboveground and belowground components, stem wood and brushwood biomass. The estimates are based on references mentioned in the text

Conversion from	To	Factor	Thumb value (e.g. R)	Range	Reciprocal thumb value (e.g. 1/R)	Range
tree volume	tree weight	R ($t\,m^{-3}$)	0.50	0.38–0.56	2.00	2.63–1.79
stem volume over bark	tree volume above ground	e_{br}	1.50	1.15–3.00	0.67	0.33–0.87
tree volume above ground	tree volume above ground + leaves	e_l	1.05	1.03–1.12	0.95	0.89–0.97
tree volume above ground + leaves	total tree volume	e_r	1.25	1.11–2.00	0.80	0.50–0.90
stem volume over bark	total tree volume	$e_{br}\,e_l\,e_r$	2.00	1.48–6.72	0.50	0.15–0.68
net biomass growth	net biomass growth + organ turnover	t_{org}	1.30	1.27–9.13	0.77	0.11–0.79
net biomass growth + organ turnover	net biomass growth + organ + tree turnover	t_{ind}	1.50	1.08–1.77	0.67	0.57–0.96
standing stem volume over bark	harvested volume over bark	l_s	0.90	0.90	1.11	1.11
harvested volume over bark	harvested stem volume under bark	l_b	0.91	0.80–0.94	1.10	1.06–1.25
standing stem volume over bark	harvested stem volume under bark	$l_b\,l_s$	0.80		1.25	
total tree biomass	living tree biomass	f_{sw}	–	0.22–1.00	–	1.00–4.55
net primary productivity	net primary productivity + respiration = GPP	f_{re}	2.00	1.18 – 20.00	0.50	0.05–0.85

e_l and e_r are used to determine the proportion of branch wood, the foliage mass and the root biomass respectively. Given net biomass growth, the factors t_{org} and t_{ind}, representing the turnover from the loss of plant organs and whole trees respectively, are used to estimate gross growth. Harvesting losses from leaving the stump in the forest and from bark removal are estimated by l_s and l_b respectively. The factor f_{sw} is used to calculate the proportion of sapwood in the standing volume. Factor f_r is used to extrapolate GPP from NPP, i.e. by increasing the NPP by the respiration amount.

The factors in Table 2.7 facilitate the approximate conversion of known forestry parameters to production ecology measures. As these factors are not closely dependent on age or size, the approximate values (characteristic values) and range in variation are given. The reciprocal values (last column in Table 2.7) are used, when necessary, to derive forestry volume values from GPP or NPP.

2.4.1 From Standing Volume or Stem or Merchantable Wood Volume to Total Biomass

For this, conversion factors or estimate functions are used, which estimate the successive stem and merchantable biomass (in t), the aboveground total biomass and, finally, the total biomass from the volume of the aboveground stem or merchantable wood (in m^3). In particular, the estimate of the belowground components of stem volume, or merchantable volume, is inaccurate because the ratio of aboveground to belowground biomass is heavily dependent on moisture, nutrient and light status, which are determined by site conditions and stand density (Kimmins 1993, p. 13).

2.4.1.1 From Wood Volume to Wood Biomass by Specific Wood Density R

Wood volume v is converted to wood biomass w by the specific wood density R

$$w = v \times R. \tag{2.22}$$

Wood density is a unit of weight per volume and is mostly given in $kg\,m^{-3}$. Wood density R, given in $t\ m^{-3}$, represents the reduction factor from m^3 to t. Of the various possible density measures, we use the specific density, which converts fresh volume, with 100% water saturation and full hydration of cell walls, into dry weight with only 0.5–1% water saturation (Knigge and Schulz 1966, p. 132). In practise, this density is determined by extracting the humidity of the wood in an oven until the point of constant weight. The decomposition and volatilisation of organic compounds must be avoided. Wood density varies between $120.8\,kg\ m^{-3}$ for balsa wood to $1{,}045.5\,kg\ m^{-3}$ for pockwood. The commercial tree species in central Europe have specific densities of $350–550\,kg\ m^{-3}$ (cf. Table 2.8). As specific density varies

Table 2.8 Specific wood density R of selected tree species (R defined on the basis of the green volume). In central Europe tree species with wood densities of 350–550 kg m^{-3}, equivalent to transformation factors of R = 0.35–0.55 (t m^3), dominate (Knigge and Schulz 1966, p. 135)

Tree species		Specific wood density (kg m^{-3})
Balsawood	Ochroma lagopus	120.8
Grand fir	Abies grandis	332.0
White pine	Pinus strobus	338.6
Poplar	Populus spec.	376.8
Norway spruce	Picea abies	377.1
Sitka spruce	Picea sitchensis	401.7
Douglas fir	Pseudotsuga menziesii	412.4
Pine	Pinus spec.	430.7
Larch	Larix spec.	487.3
Maple	Acer spec.	522.2
European beech	Fagus sylvatica	554.3
Elm	Ulmus spec.	555.5
Sessile/Common oak	Quercus petraea/robur	561.1
Ash	Fraxinus spec.	564.2
False acacia	Robinia pseudoacacia	646.8
Bongossi	Lophira procera	890.2
Pockwood	Guaiacum officinale	1,045.5

with stand density (Bues 1984), species composition (Kennel 1965), stand treatment (Seibt 1965) and tree age (Knigge and Schulz 1966), the reference values in Table 2.8 represent average values from Knigge and Schulz (1966, p. 135). It is easiest to calculate a first-order approximation with a density of 500 kg m^{-3}, which is equivalent to the density factor R

$$\mathrm{R(approximate)} = 0.5\,\mathrm{t\,m^{-3}}. \tag{2.23}$$

In their Forest Resource Assessment, the FAO also applies a generalised density factor of 0.5 t m^{-3} for conifer and 0.6–0.7 t m^{-3} for broadleaved forests (FAO 2001; Brown 1997).

2.4.1.2 Brushwood Factor e_{br}: From Stem Volume to Aboveground Wood Volume

In addition to stem wood, the aboveground wood volume also includes brushwood (cf. Fig. 2.2, b_1 and b_2). The yield tables from Grundner and Schwappach (1952) assist the estimation of brushwood volume. Based on more than 70,000 trees, Grundner and Schwappach measured merchantable volume, stem volume, and total volume, including branches, for Silver birch, European beech, Red alder, Norway spruce, Scots pine, European larch, Austrian pine, and Silver fir. Thus, brushwood

volume can be calculated from the difference between total aboveground volume and merchantable volume. Grundner and Schwappach provide brushwood volume values for broadleaved species, and both brushwood and needles for conifers. In the tables, the brushwood percentages (=brushwood volume/merchantable stem volume $\times 100$) are listed in relation to tree age, diameter and height.

Burschel et al. (1993) condensed these tables of brushwood percentages to species-specific, age-dependent brushwood factors e_{br}. For early-mature stands brushwood comprises an estimated 40% of the merchantable wood volume, and in old stands about 20%. Thus, to estimate total aboveground wood volume in relation to merchantable volume, a factor of $e_{br} = 1.4$ and 1.20 needs to be applied for early-mature and mature trees respectively. The factor e_{br} ranges from 2.0 for young trees to 1.20 for old growth trees. For very young stands with virtually no merchantable wood volume, Burschel et al. (1993) propose a constant value be derived from the merchantable wood volume of trees aged from 1–20 years, multiplied by a factor of $e_{br} = 3$ (Table 2.7).

Jacobsen et al. (2003) come to similar results in their biomass study. They employed age-dependent biomass functions for the calculation of aboveground biomass (incl. leaves) from merchantable wood biomass. For comparison, the e_{br} factors at age 20, 50 and 120 for the following species are: Norway spruce $e_{br} =$ 1.84, 1.41, 1.15; Scots pine $e_{br} = 1.71$, 1.44, 1.23; European beech $e_{br} = 1.51$, 1.45, 1.28; and Sessile oak 1.45, 1.45, 1.45.

Thus,

$$\begin{aligned} &\mathrm{v(aboveground\ wood\ volume)} = \mathrm{v(merchantable\ wood\ volume)} \times e_{br} \\ &\text{with } e_{br} = 3.00 - 1.20. \end{aligned} \tag{2.24}$$

For the less frequent extrapolations based on stem volume, the extrapolation factors e_{br} are adjusted variously. For young stands the factors are reduced by a small percentage as the trees in these stands contribute stem volume but little merchantable volume >7 cm. For early-mature and mature conifers with a minimal amount of merchantable branch wood, the extrapolation factor e_{br} is reduced also due to the higher percentage of stem volume compared to merchantable volume. In contrast, in broadleaved stands, the factors increase because the stem-wood volume is smaller than the merchantable volume due to the high proportion of merchantable branch volume >7 cm. The difference between an extrapolation based on stem wood and on merchantable wood declines with age (or the size of the tree), and is ignored here.

For approximate extrapolations in early-mature stands, one can obtain the total volume, or the aboveground biomass by multiplying the merchantable volume, or the merchantable biomass by 1.5 respectively. For a first-order estimation of aboveground volume from merchantable volume, we propose a factor of,

$$e_{br}\,(\mathrm{approximate}) = 1.5. \tag{2.25}$$

For simplicity, we assume that, for all tree organs, $w = v \times R$ applies, so that the expansion factor e_{br} can be used for volume v (2.24) and for biomass weight w.

2.4.1.3 The Leaf Factor e_l: From Aboveground Woody Biomass to Aboveground Total Biomass

The brushwood factor e_{br} derived from the tables by Grundner and Schwappach (1952) already contains the needle biomass for conifers (leaf factor $e_l = 1$). Therefore, a leaf factor needs to be added only for broadleaves:

$$w(\text{total above ground biomass}) = w(\text{above ground wood biomass}) \times e_l. \quad (2.26)$$

In the first approach, leaf biomass is modelled as a function of aboveground woody biomass. The leaf biomass functions from Jacobsen et al. (2003) model the declining leaf fraction of the total aboveground biomass with age. At ages 20, 50 and 120 the percentage of foliage biomass in relation to total aboveground biomass is: 18, 11 and 3% for Norway spruce; 32, 7 and 5% for Scots pine; 3, 3 and 1% for European beech; and 8, 5 and 2% for Sessile oak. This leads, in all cases, to decreasing leaf factors e_l: from $e_l = 1.22$–1.03 for Norway spruce, $e_l = 1.47$–1.05 for Scots pine, $e_l = 1.03$–1.01 for European beech, and $e_l = 1.09$–1.02 for Sessile oak.

In a second approach, the estimate of leaf biomass is independent of wood biomass. Assuming a constant assimilation surface and weight of the leaves in old and uneven-aged stands, the leaf biomass can be estimated from the annual litter fall and the average length of leaf life. For Norway spruce, Ellenberg (1986) measured a constant litter fall of 0.2–0.5 kg $m^{-2}\,yr^{-1}$, or 2–5 t $ha^{-1}\,yr^{-1}$, which corresponds to a needle biomass of 6–15 t ha^{-1} (assuming an average needle life of 3 years). Similarly, Scots pine stands reach 4 t ha^{-1} needle biomass (Ellenberg 1986, average needle life 2.5 years); European larch and Douglas fir stands, a maximum of 12–14 t ha^{-1} (Lyr et al. 1967); European beech stands, 3 t ha^{-1} (Assmann 1961; Ellenberg 1986) to 8 t ha^{-1} (Lyr et al. 1967); Sessile oak and European ash 2–3 t ha^{-1} (Assmann 1961); and Silver birch up to 5 t ha^{-1} (Lyr et al. 1967). For a 50- and 120-year-old European beech stand, a constant leaf biomass of 3–8 t ha^{-1} (mean 5 t ha^{-1}) conforms with the 3% and 1% leaf biomass listed above, when total aboveground biomass is 200 and 600 t ha^{-1}, respectively.

All in all, the orientation value of $e_l = 1.05$ serves as a good estimation of the leaf biomass for broadleaves (early-mature to mature stands), while the needle biomass for conifers is already included in the brushwood factor:

$$\begin{aligned} &e_l\,(\text{thumb, broadleaf}) = 1.05, \\ &e_l\,(\text{conifer}) = 1.00. \end{aligned} \quad (2.27)$$

2.4.1.4 Root Factor e_r: From Aboveground Biomass to Total Plant Biomass

Santantonio et al. (1977) and Fogel (1983) found that the percentage of roots in the total tree biomass ranges from 10–45% approximately depending on the growth conditions, corresponding to a root factor e_r of

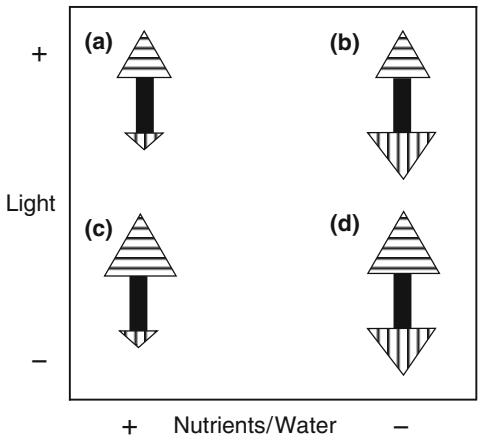

Fig. 2.7 Partitioning of total plant biomass on shoot and root organs in relation to supply of nutrients and water (x-axis) and supply of light (y-axis). Limitation of nutrient and water supply causes a partitioning in favour of roots. Limitation of energy supply raises the investment of biomass into shoots (by courtesy of Kimmins 1993, p. 13.)

$$\begin{aligned} &w(\text{total}) = w(\text{above}) \times e_r, \\ &\text{with } e_r = 1.11\text{–}1.81. \end{aligned} \tag{2.28}$$

Instead of the root factor, the literature mostly refers to the root to shoot ratio, which for the above-mentioned values, lies between 10:90 and 45:55. The large variation in the root to shoot ratio can be explained by the theory that the limitation of a resource leads to the promotion of growth of the plant organ responsible for supplying that critical resource (Comeau and Kimmins 1989; Keyes and Grier 1981).

In Fig. 2.7, four examples indicate the complexity of the root to shoot ratio. In the first example, where light, water and nutrient conditions are favourable (Fig. 2.7a), the tree shown develops a root to shoot ratio of 10:90 ($e_r = 1.11$). Under adequate light conditions, but with a water or a nutrient deficiency (Fig. 2.7b), the tree invests more into root growth, especially fine roots. Thus the root to shoot ratio increases in favour of roots to 45:55, with $e_r = 1.82$. With an adequate water and nutrient supply, yet critical light conditions, e.g. on nutrient-rich soils or for understorey trees (Fig. 2.7c), shoot growth is enhanced, so that the tree root to shoot ratio becomes 30:70, resulting in $e_r = 1.43$. In the case of rich soils, trees in the upper storey tend to allocate growth resources to extensive crown development, whereas trees in the understorey often invest in height growth to escape the shade (Oliver and Larson 1996). If light, water and nutrient supply is limited (Fig. 2.7d), the root to shoot ratio may resemble the example in Fig. 2.7a of 10:90, where $e_r = 1.11$. However, usually, the total biomass comprises a higher proportion of brushwood and fine roots and less stem wood.

Aside from the large variation in the root to shoot ratio caused by different site conditions, Burschel et al. (1993) identified an age-dependent change in root to shoot ratios in several studies from 10:10 for young to 10:30–10:40 for older trees, corresponding to root factors of $e_r = 2.0$–1.25. In the absence of additional information, we recommend an approximate value for e_r of

$$e_r(\text{approximate}) = 1.25. \tag{2.29}$$

When tree biomass is extrapolated from the stem wood, merchantable volume, or the aboveground biomass without taking the site-specific root to shoot ratio into account, the root biomass is underestimated, especially on sites where growth is limited by the soil conditions.

2.4.1.5 Examples for Upscaling Merchantable Wood Volume to Total Plant Biomass

Figure 2.8a shows an example of a European beech stand (site class I, Schober 1971, moderate thinning). The biomass development is divided into the compartments stem wood, bark, brushwood, leaves, coarse and fine roots as derived with the biomass equations from Jacobsen et al. (2003). Similar equations for estimating various biomass components in relation to stem size have been developed, e.g. by Pretzsch (2005c), Pretzsch and Mette (2008), Seifert and Müller-Starck (2008) and Wirth et al. (2004). Based on the yield volume of 28–552 $m^3 ha^{-1}$ at age 30–120 from the tables, the biomass equations and expansion factors predict the biomass of stems, bark, brushwood, leaves, coarse roots and fine roots to be 16–306, 1–8, 6–64, 1–6, 3–53 and 1–4 t ha^{-1} respectively. This produces a total plant biomass of 27–447 t ha^{-1}. The stem wood accounts for 58–68% of the total biomass, which, despite all the uncertainties associated this estimate, is an important percentage for scaling up the total biomass (Fig. 2.8b).

An overall upscaling factor $e_{br,l,r}$ for the direct conversion of merchantable wood volume or biomass into total tree volume or tree biomass can be calculated:

$$e_{br,l,r} = e_{br} \times e_l \times e_r = 1.50 \times 1.05 \times 1.25 \cong 2.0 \tag{2.30}$$

(cf. Table 2.7).

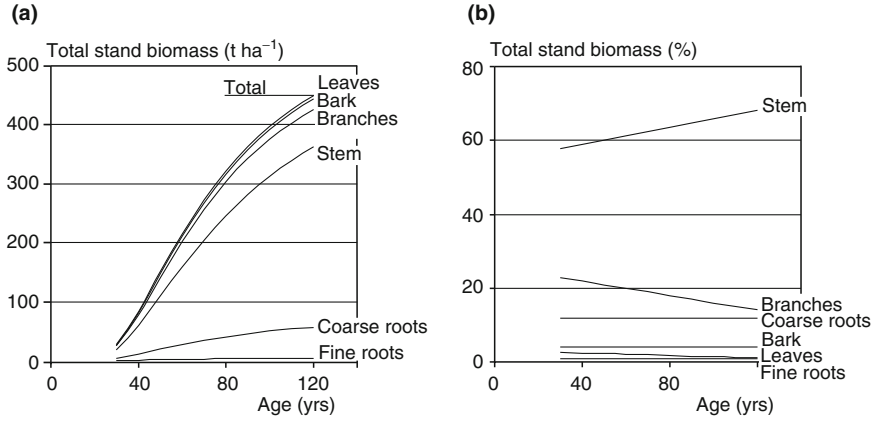

Fig. 2.8 Biomass development of an European beech stand, site index I (Schober 1972, mod. th.), and the fractions of leaves, bark, branches, stem wood, coarse roots, and fine roots: (**a**) stand biomass in t ha^{-1} and (**b**) relative portion of the various tree organs (%)

The second example in Table 2.9 is based on the standing merchantable wood volume in Germany taken from the BWI[2] inventory results (Bundesministerium für Ernährung, Landwirtschaft und Verbraucherschutz, 2005). In 2002, the average standing merchantable volume ranged from 274 $m^3\,ha^{-1}$ in Douglas fir to 480 $m^3\,ha^{-1}$ in Silver fir stands. These values were extrapolated using the specific wood density R and the expansion factors e_{br}, e_l, and e_r to obtain total stand biomass values between 205 and 365 t ha^{-1}. For broadleaved species, the values of merchantable volume in $m^3\,ha^{-1}$ and total plant biomass in $t\,ha^{-1}$ are approximately equal because the reduction factor for wood density R and the expansion factors e_{br}, e_l, and e_r are almost equal. For conifers, the biomass values are 10–30% lower than the merchantable wood volume due to the lower specific wood density.

In Table 2.10 the merchantable wood volume of the long-term experimental plots in Tables 2.3–2.5 are converted into biomass. The range in standing volume of the evenaged pure stands, 428–1,480 $m^3\,ha^{-1}$, is equivalent to a total biomass range of 378 t ha^{-1} (European larch) and 1,012 t ha^{-1} (Norway spruce) (cf. Table 2.10, above). For the evenaged mixed stands, the total biomass calculated from merchantable wood volumes of 394–918 $m^3\,ha^{-1}$ ranges from 371 t ha^{-1} (Scots pine – European beech) to 756 t ha^{-1} (Norway spruce – European beech) (Table 2.10, centre). For the unevenaged mixed stands, the merchantable wood volumes of 477–1,028 $m^3\,ha^{-1}$ correspond to a total biomass of 351–721 t ha^{-1} (Table 2.10, below). In comparison with the wood volume values, the total biomass values of conifers and broadleaved species lie closer together. Often the higher wood density of broadleaved species compensates for the lower packing density of the trees in the stand compared to conifer species.

2.4.2 Ephemeral Turnover Factor t_{org} for Estimation of NPP

Net primary productivity of forest stands is defined as the increase in biomass per unit area over a given time period (e.g. year, decade) plus the turnover of short-lived plant organs (bark, branches, leaves, roots) and entire trees that are lost between inventories. These two components constitute the biomass turnover and are introduced as short-term or ephemeral turnover, which often follows an annual cycle, and the long-term turnover of entire trees through self-thinning, thinning or calamities.

The turnover factor t_{ind} (approximate) = 1.50 (1.08–1.77) was introduced to estimate total merchantable wood volume produced from the volume of the remaining stand (Sect. 2.3.2); in other words the standing volume must be multiplied by $t_{ind} = 1.50$ to obtain the total volume production. The standard variables CAI, PAI, and MAI already include whole tree turnover. Thus, for the calculation of the NPP, only the factor t_{org} for the ephemeral turnover of plant organs (e.g. foliage, roots, branches) is absent. Of course, as with the above factors, the short-term turnover depends on site conditions, stand age, species and stand treatment.

The quantification of ephemeral turnover essentially is accompanied by considerable uncertainty; aboveground litter fall, belowground turnover of fine root biomass,

Table 2.9 Mean standing volume ($m^3\,ha^{-1}$) and mean periodic annual increment ($m^3\,ha^{-1}\,yr^{-1}$) for dominant tree species in Germany according to the Second National Forest Inventory BWI^2 (Bundesministerium für Ernährung, Landwirtschaft und Verbraucherschutz, BWI^2, Der Inventurbericht, pp. 75 and 167), approximate standing biomass ($t\,ha^{-1}$) and NPP ($t\,ha^{-1}\,yr^{-1}$)

Tree species	Mean standing volume $m^3\,ha^{-1}$	PAI $m^3 ha^{-1}\,yr^{-1}$	Specific wood density R $kg\,m^{-3}$	Expansion factor e_{br}	Expansion factor e_l	Expansion factor e_r	Turnover factor t_{org}	Total biomass $t\,ha^{-1}$	NPP $t\,ha^{-1}\,yr^{-1}$	NPP $kg\,m^{-2}\,yr^{-1}$
Norway spruce	404.1	16.37	377.1	1.45	1.00	1.25	1.30	276.2	14.55	1.45
Scots pine	281.7	9.12	430.7	1.45	1.00	1.25	1.30	219.9	9.26	0.93
Silver fir	480.4	15.95	377.1	1.45	1.00	1.25	1.30	328.4	14.17	1.42
European larch	300.7	12.75	487.3	1.45	1.00	1.25	1.30	265.6	14.64	1.46
Douglas fir	273.6	19.41	412.4	1.45	1.00	1.25	1.30	204.5	18.86	1.89
Sessile oak	285.9	8.25	561.1	1.45	1.05	1.25	1.30	305.3	11.45	1.15
European beech	352.4	11.74	554.3	1.45	1.03	1.25	1.30	364.6	15.79	1.58
Total min	273.6	8.25	377.1	1.45	1.00	1.25	1.30	204.5	9.26	0.93
Total max	480.4	19.41	561.1	1.45	1.05	1.25	1.30	364.6	18.86	1.89

Total standing biomass ($t\,ha^{-1}$) was estimated on the basis of standing volume ($m^3\,ha^{-1}$) using specific wood density R and expansion factors e_{br}, e_l, and e_r. Net primary productivity was estimated on the basis of mean PAI ($m^3\,ha^{-1}\,yr^{-1}$) using specific wood density R, expansion factors e_{br}, e_l, and e_r, and turnover factor t_{org}.

Table 2.10 Upscaling from standing merchantable volume to total standing biomass and from mean annual increment of merchantable volume to NPP on selected long-term experimental plots in Southern Germany (cf. Tables 2.2–2.4). Total standing biomass ($t\,ha^{-1}$) was estimated on the basis of standing merchantable volume using specific wood density R and expansion factors e_{br}, e_l, e_r. Net primary productivity was estimated based on MAI ($m^3\,ha^{-1}\,yr^{-1}$) in the case of pure evenaged and mixed evenaged stands and based on PAI ($m^3\,ha^{-1}\,yr^{-1}$) in the case of mixed unevenaged stands. For the upscaling we applied specific wood density R; expansion factors e_{br}, e_l, and e_r; and turnover factor t_{org} (cf. Tables 2.7–2.9)

Tree species	Experimental plot	Standing volume m^3ha^{-1}	Total st. biomass $t\,ha^{-1}$	MAI (PAI) $m^3ha^{-1}yr^{-1}$	NPP $t\,ha^{-1}yr^{-1}$	NPP $kg\,m^{-2}yr^{-1}$
pure even-aged						
Norway spruce	DEN 05	1,480	1,012	15.4	13.7	1.4
Scots pine	BAY 52	700	546	10.5	10.6	1.1
Silver fir	WOL97	637	435	9.5	8.4	0.8
European larch	MIS 47	428	378	5.4	6.1	0.6
Douglas fir	FRE 85	1,012	756	17.2	16.7	1.7
Sessile oak	LOH 59	605	646	7.7	10.8	1.1
European beech	FAB 15	950	983	8.7	11.7	1.2
Total min		428	378	5.4	6.1	0.6
Total max		1,480	1,012	17.2	16.7	1.7
mixed even-aged						
Norway spruce-European beech	SON 814	918	756	18.5	19.7	2.0
Scots pine-Norway spruce	NEU 841	876	647	8.8	8.4	0.8
Scots pine-European beech	GEI 832	394	371	15.5	19.0	1.9
European larch-European beech	GEM 871	580	570	11.8	15.0	1.5
Sessile oak-European beech	KEH 804	688	730	12.4	17.1	1.7
Total min		394	371	8.8	8.4	0.8
Total max		918	756	18.5	19.7	2.0
mixed uneven-aged				PAI		
N. spruce-S. fir-E. beech	FRY 129/32	663	500	10.7	10.5	1.0
N. spruce-S. fir-E. beech	BOM 130/22	610	481	10.2	10.5	1.0
N. spruce-S. fir-E. beech	PAR 115/1	871	626	8.1	7.6	0.8
N. spruce-S. fir-E. beech	KRE 120/3	502	414	4.7	5.0	0.5
N. spruce-S. fir-E. beech	MAR 108/1	1,028	721	15.9	14.5	1.4
N. spruce-S. fir-E. beech	RUH 110/2	477	351	7.9	7.6	0.8
N. spruce-S. fir-E. beech	RUH 116/1	784	591	9.8	9.6	1.0
Total min		477	351	4.7	5.0	0.5
Total max		1,028	721	15.9	14.5	1.4

loss of primary production to microbial symbionts or defoliation by herbivores can account for a very significant, yet rarely quantified proportion of NPP. For example, carbon allocation to mycorrhizal fungi or for symbiontic N-fixation can be an energy demanding process that consumes part of the net primary production. A good estimation of the quantity of ephemeral turnover in relation to site is provided in Comeau and Kimmins (1989) investigation of Lodgepole pine stands (*Pinus contorta*) in the Rocky Mountains, in Southeast British Columbia. The turnover of fine roots is between 50 and 62% of the total NPP on dry soils, yet only between 31 and 40% on soils of medium humidity. On the dry soils, fine and small root production is 3.2–4.9 times as high as needle production, while, on the humid soils, it is only 1.3–2.5 times higher. Obviously, on dry sites, the tree invests in fine root production for the uptake of the more limited resource, water. Keyes and Grier (1981) obtain similar results for Douglas fir stands along the North American west coast. They show that, although stem-wood production was nearly twice as high on good sites as on poor sites, in total, NPP was only 13% higher on the good sites. On the poor sites, 53% of NPP was allocated to the root, primarily to fine root production with a rapid turnover, whereas only 23% of the NPP was invested in belowground biomass growth on good sites. These results confirm that the percentage of ephemeral turnover increases as nutrients and water supply become less favourable. The highest turnover appears to occur for those plant organs that ensure the supply of the most limiting resource.

Keeping in mind site dependency, some typical values for ephemeral turnover from the literature are summarised. These values typically are given as a turnover factor t_{org}, which can be used to estimate mean NPP in relation to volume growth MAI, PAI, or CAI as follows:

$$\text{NPP} = \text{MAI}(\text{total biomass}) \times t_{org}. \tag{2.31}$$

Ellenberg (1986, p. 122–128, 332) found values of $t_{org} = 1.27$–1.45 for Norway spruce, and 1.40–1.83 for European beech, which increased with age. Brünig (1971) obtained values of $t_{org} = 1.69$–2.15, which increased from trees with light–heavy crowns. From von Droste (1969, p. 193), we can derive values of $t_{org} = 1.69$ for Norway spruce only for the aboveground compartments. Assmann (1961, p. 34), who refers to Boysen-Jensen (1932) and Mar-Möller (1945), derives values of $t_{org} = 2.0$–2.17 in European ash stands for the aboveground compartments only. For European beech stands, Mar-Möller (1945) identifies a $t_{org} = 1.40$–1.54, and Larcher (1994, p. 134) a $t_{org} = 1.56$. For tropical rainforests in Thailand, Larcher (1994, p. 134) assumes an ephemeral turnover of $t_{org} = 9.13$, i.e. the turnover exceeds the biomass production by a factor of 9. In the following calculations for temperate forests in central Europe, we assume an ephemeral turnover factor of

$$t_{org}\,(\text{approximate}) = 1.3. \tag{2.32}$$

To reduce age dependency, and attain a long-term average for ephemeral turnover, the MAI should be used to upscale to NPP. By adopting MAI, the long-term average NPP also becomes comparable to the NPP of the annual or periodic cycles of herbaceous stands.

2.4.2.1 Examples for Upscaling from Merchantable Volume Growth or Increment to NPP

Table 2.9 lists, in column 3, the mean periodic annual volume increment ($m^3\,ha^{-1}\,yr^{-1}$) for the most important forestry species in Germany from 1987 to 2002 (Bundesministerium für Ernährung, Landwirtschaft und Verbraucherschutz, 2005). The growth in merchantable wood volume ranges from $8.25\,m^3\,ha^{-1}\,yr^{-1}$ for Sessile oak stands to $19.41\,m^3\,ha^{-1}\,yr^{-1}$ for Douglas fir stands. The values represent the average across all possible site conditions and age classes. Consequently, they represent very stable average PAI values (15 years interval), and provide a good indication of the productivity of central European forests. The conversion to NPP using the appropriate wood density R (t m^3), expansion factors e_{br}, e_l, e_r, and ephemeral turnover factor t_{org} (cf. Table 2.9) results in NPP values between 9.26 t $ha^{-1}\,yr^{-1}$ for Scots pine stands and 18.86 t $ha^{-1}\,yr^{-1}$ for Douglas fir stands, which corresponds to the NPP range of 10–15 t $ha^{-1}\,yr^{-1}$ for woody and herbaceous vegetation in the temperate latitudes given by Körner (2002, p. 945).

The NPP also can be calculated for the long-term experimental plots presented in Tables 2.3–2.5 (Table 2.10). For evenaged pure stands with an MAI of 5.4–17.2 $m^3\,ha^{-1}\,yr^{-1}$, the NPP ranges from 6.1–16.7 t $ha^{-1}\,yr^{-1}$ (maximum for Douglas fir and Norway spruce, minimum for European larch). The evenaged mixed stands, with an MAI of 8.8–18.5 $m^3\,ha^{-1}\,yr^{-1}$, assume an NPP of 8.4–19.7 t $ha^{-1}\,yr^{-1}$. For the unevenaged mixed stands with a PAI of 4.7–15.9 $m^3\,ha^{-1}\,yr^{-1}$, the rough estimate of NPP is 5.0–14.5 t $ha^{-1}\,yr^{-1}$; all these estimates are obtained from the approximate wood density values R (t m^3), expansion factors e_{br}, e_l, e_r, and ephemeral turnover factor t_{org}.

2.4.3 Deriving Harvested Volume Under Bark from Standing Volume over Bark

Standing volume over bark v(standing o.b.) is the volume measure commonly used in forest inventory (stem volume or merchantable volume). It indicates the volume of the standing stem including bark and the later harvesting losses (stump volume). To obtain the harvested volume from this measure of volume over bark, the v(standing o. b.) is reduced by a factor $l_s = 0.90$, which represents the 10% volume of the tree stump (cf. factor l_s, Table 2.11). This factors accounts for the fact that the trunk base s_0 in Fig. 2.2 is not extracted from the forest in conventional harvesting methods.

An additional factor $l_b = 0.80$–0.94 allows for a 6–20% bark volume loss, which is species-dependent (cf. factor l_b, Table 2.11). This result in a harvest loss factor l_s and bark loss factor l_b of:

$$l_s\,(\text{approximate}) = 0.9, \tag{2.33}$$

$$l_b\,(\text{approximate}) = 0.9\,(0.80\ldots0.94). \tag{2.34}$$

Table 2.11 Species-specific relationships between standing stem volume over bark and harvested volume under bark (Bayerisches Staatsministerium für Ernährung, Landwirtschaft und Forsten, 1981, p. 306). For example, in stands of European beech, $1\,m^3$ standing stem volume over bark results in $0.9\,m^3$ harvested volume over bark and $0.85\,m^3$ harvested volume under bark. The losses due to harvest are 10% for all species ($l_s = 0.90$), while the losses due to debarking range from 6% to 20% ($l_b = 0.80$ to $l_b = 0.94$). The last column represents the reciprocal value of the loss factors l_s and l_b, i.e. the expansion factors for converting harvested volume under bark to standing volume over bark (all factors are rounded to two decimal places)

Species resp. Genus	from: standing volume over bark to: harvested volume o. b. l_s	from: harvested volume over bark to: harvested volume u. b. l_b	from: standing volume over bark to: harvested volume u. b. $l_b l_s$	from: harvested volume under bark to: harvested volume o. b. $1/l_b$	from: harvested volume over bark to: standing volume o. b. $1/l_s$	from: harvested volume under bark to: standing volume o. bark $1/(l_b l_s)$
Norway spruce	0.90	0.90	0.81	1.11	1.11	1.23
Scots pine	0.90	0.88	0.79	1.14	1.11	1.27
Silver fir	0.90	0.90	0.81	1.11	1.11	1.23
European larch	0.90	0.80	0.72	1.25	1.11	1.39
Douglas fir	0.90	0.88	0.79	1.14	1.11	1.27
Sessile and Common oak	0.90	0.88	0.79	1.14	1.11	1.27
European beech	0.90	0.94	0.85	1.06	1.11	1.18

Therefore, the actual harvested volume amounts to 72–85% of the standing volume over bark or, conversely, the standing stem volume is 118–139% of the harvested volume under bark (cf. Table 2.11, right column). In Germany, different states, regions and districts use different conversion factors with only minor differences that reflect the various provenances grown, and silvicultural practices and harvesting techniques applied. When wood volume over bark needs to be converted to harvested volume under bark, the reduction factors of 0.72–0.846 are used ($l_s \times l_b$). As an approximate value, $l_s \times l_b$ (approximate) $= 0.8$ can be used:

$$\begin{aligned} &v(\text{harvested u. b.}) = v(\text{standing o. b.}) \times l_s \times l_b, \\ &v(\text{harvested u. b.}) \cong v(\text{standing o. b.}) \times 0.8. \end{aligned} \tag{2.35}$$

Alternatively, if the harvested volume under bark is known, then the corresponding reciprocal multipliers, of $1/(l_b \times l_s) = 1.18$ for European beech, which has a thin bark, to 1.39 for European larch, whose bark is extremely thick, are used (Table 2.11).

Finally, a conversion factor may be needed that converts stacked cubic volume (st. c. m) to solid volume in m^3, since 1 st. c. m $\cong 0.7\,\text{solid}\,m^3$. Conversely, the reciprocal is $1\,m^3$ solid wood $= 1.43$ st. c.m.

$$v(\text{solid } m^3) = v(\text{stacked } m^3) \times 0.7, \tag{2.36}$$

or

$$v(\text{stacked } m^3) = v(\text{solid } m^3) \times 1.43. \tag{2.37}$$

2.4.4 Conversion of Merchantable Wood Volume to GPP

Equipped with the basic specific wood density R and the expansion and conversion factors in Table 2.7, we can estimate roughly the net and gross primary production associated with a given volume growth and yield. Conversely, we can assess how the GPP is partitioned into respiration, turnover and growth of merchantable wood (including harvest losses, if desired). The following two examples summarise the derivation of wood volume from gross primary production.

In the first example, the steps for deriving GPP from the harvested volume (merchantable, under bark) are given in formulae (2.38a)–(2.38g).

Given that the harvest of a 150-year-old European beech stand results in V(merchantable, harvested u. b.) $= 850\,m^3\,ha^{-1}$, which indicates excellent site fertility, this value can be transformed into standing merchantable volume over bark;

$$\begin{aligned} V(\text{merch., standing o. b.}) &= V(\text{merch., harvested u. b.}) \times 1/(l_s \times l_b) \\ &= 850\,m^3\,ha^{-1} \times 1.177 = 1{,}000\,m^3\,ha^{-1}. \end{aligned} \tag{2.38a}$$

(consider that all factors in Table 2.11 are rounded to two decimal places)

In the next step, we determine the total volume of the stand including all above and belowground biomass by applying the expansion factors

$$\begin{aligned} V(\text{standing}) &= V(\text{merch., standing o. b.}) \times e_{br} \times e_l \times e_r \\ &= 1{,}000\,m^3\,ha^{-1} \times 2.00 = 2{,}000\,m^3\,ha^{-1}. \end{aligned} \tag{2.38b}$$

Total volume yield including the intermediate thinnings V(total), i.e. including the turnover of all individual trees is

$$\begin{aligned} V(\text{total}, t_{ind}) &= V(\text{standing}) \times t_{ind} \\ &= 2{,}000\,m^3\,ha^{-1} \times 1.5 = 3{,}000\,m^3\,ha^{-1}. \end{aligned} \tag{2.38c}$$

Total gross volume yield, which includes the intermediate thinnings and plant organ turnover

$$\begin{aligned} V(\text{total}) &= V(\text{total}, t_{ind}) \times t_{org} \\ &= 3{,}000\,m^3\,ha^{-1} \times 1.3 = 3{,}900\,m^3\,ha^{-1}. \end{aligned} \tag{2.38d}$$

By multiplying this value by specific density R, we convert volume to biomass weight

$$W(\text{total}) = V(\text{total}) \times R = 3{,}900\,m^3\,ha^{-1} \times 0.5 = 1{,}950\,t\,ha^{-1}. \tag{2.38e}$$

Mean annual NPP of the 150-year-old European beech stand is obtained when this value is divided by the age of the stand, i.e. by 150 years

$$\begin{aligned} NPP &= W(\text{total})/\text{age} = 1{,}950\,t\,ha^{-1}/150\ \text{years} \\ &= 13.00\,t\,ha^{-1}\,yr^{-1}\ \text{or}\ 1.30\,kg\,m^2\,yr^{-1}. \end{aligned} \tag{2.38f}$$

Finally, we apply $f_{re} = 2.0$ to obtain a rough estimate of GPP

$$\begin{aligned} GPP &= NPP \times f_{re} = 13.00\,t\,ha^{-1}\,yr^{-1} \times 2 \\ &= 26\,t\,ha^{-1}\,yr^{-1}\ \text{or}\ 2.6\,kg\,m^2\,yr^{-1}. \end{aligned} \tag{2.38g}$$

In the reverse calculation, the reciprocal values of the expansion and turnover factors (cf. Table 2.7) enable one to partition the GPP (set 100%) roughly into NPP, total net growth, net growth standing, and net growth harvested (2.39a)–(2.39d). Figure 2.9 shows the reverse calculation of net stem growth harvested from NPP, indicating the various proportional volume losses in percent.

$$NPP = GPP \times (1/f_{re}) = 100\% \times 0.5 \cong 50\%, \tag{2.39a}$$

$$\begin{aligned} \text{Net growth total} &= NPP \times (1/t_{org}) \times (1/t_{ind}) \\ &= 50\% \times 0.77 \times 0.67 \cong 25\%, \end{aligned} \tag{2.39b}$$

$$\begin{aligned} \text{Net growth standing} &= \text{Net total biomass growth} \times (1/e_{br}) \times (1/e_l) \times (1/e_r) \\ &= 25\% \times 0.67 \times 0.95 \times 0.80 \cong 12.5\%, \end{aligned} \tag{2.39c}$$

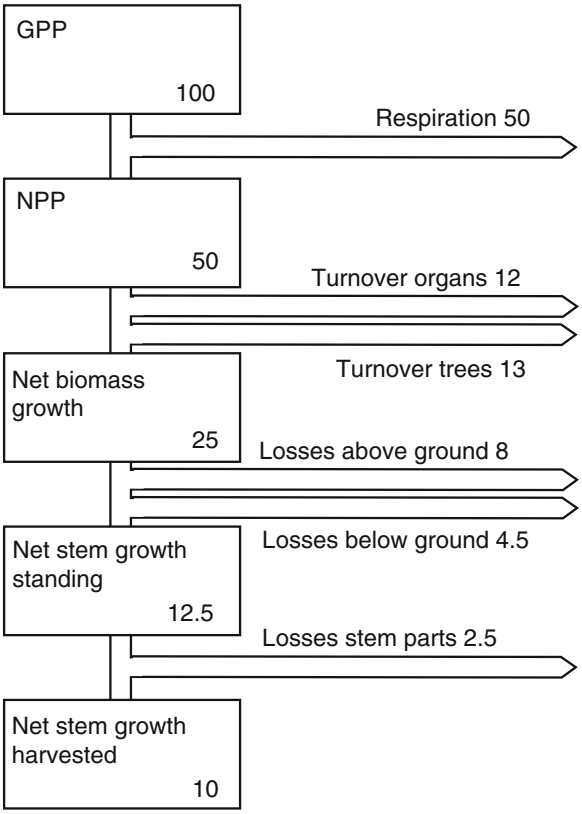

Fig. 2.9 Partitioning of a stand's total synthesised GPP (100%) in respiration, turnover of organs, turnover of whole trees, and losses due to harvest. During a stand development only about one tenth of the GPP and one fifth of the NPP are harvested as merchantable net stem growth

$$\begin{aligned}\text{Net growth harvested} &= \text{Net stem growth standing} \times (1/l_s) \times (1/l_b) \\ &= 12.5\% \times 0.90 \times 0.91 \cong 10\%.\end{aligned} \tag{2.39d}$$

It can be seen that only 10% of the GPP or 20% of the NPP is merchantable and actually harvested in conventional forestry practices. The percentages rise to about 15% and 30% respectively if the trees, which die as a result of self-thinning or which are harvested in intermediate thinnings, are included. Based on these calculations, it is now possible to compare the harvest index HI, commonly applied in agriculture, to the wood harvest in forests. HI is defined as the ratio of harvested biomass to net primary production:

$$\text{HI} = \text{Biomass extracted/NPP}. \tag{2.40}$$

In forestry, the biomass extracted corresponds to the harvested merchantable biomass, which was calculated to be 0.20 of the NPP and 0.30 when the turnover of previous intermediate harvests is included. If the total aboveground biomass

was actually harvested (without harvest loss), the HI may rise to about 0.60 of NPP. Thus, in comparison with the HI of agricultural grass crops (HI up to 0.85), root crops (up to 0.86), or fast growing tree plantations such as willows, poplars or eucalypts (up to 0.70), the harvest index of the conventional wood harvest is much lower (cf. Larcher 1994, p. 128). In agriculture and fuelwood plantations, the high HI also reflects the considerable nutrient removal. As long as the conventional stem-wood harvest in forestry discards the crown in the forest, the majority of the nutrient minerals remain in the ecosystem.

2.5 Dead Inner Xylem

Unlike herbaceous plants, many tree species develop heartwood in the course of ontogenesis (Fig. 2.10, dark grey). For the comparison of growth and yield of woody and herbaceous plants, it is interesting to distinguish the living, or active tree biomass, i.e., the sapwood, from the dead biomass, i.e., the heartwood. We have specified the growth and yield of living, or active biomass as "true" growth and yield. The heartwood falls into the category of turnover, and has to be subtracted from the standing volume or biomass.

In a first approach, the true biomass can be estimated from the total biomass by a simple factor. Of course, the sapwood portion f_{sw} changes with age and size, but for regional or long-term averages, we can say;

$$\text{Biomass (living)} = \text{biomass} \times f_{sw}. \tag{2.41}$$

The heartwood development usually begins when the physiological activity of the inner xylem, i.e. water conduction, has ceased. At a macroscopic scale, the

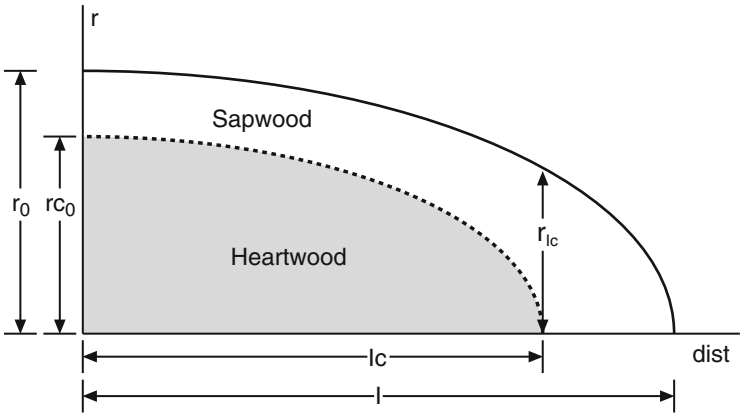

Fig. 2.10 Stem form (*continuous black line*) and border between sapwood and heartwood (*dashed line*) are approximated by a paraboloid. r_0 stem radius at ground level; l stem length; rc_0 radius of dead heartwood at ground level; lc length of core wood zone; r_{lc} stem radius at position lc where sapwood portion is 1.0

heartwood can often be recognised by a transition in colour from the lighter sapwood to the darker heartwood. The heartwood tissue is dead and less permeable to water-based solutions (Knigge and Schulz 1996, p. 104). The sapwood contains the functional, yet dead water-conducting tracheids and xylem vessels, living xylem parenchyma and, towards the outer edge, also the living cambium and phloem tissue. The heartwood development proceeds slowly, and is by no means circular (in year rings), but rather resembles amoeboid proliferations of heartwood into the sapwood (Fig. 2.11).

The proportion of heartwood usually increases with tree size and may be considerable. Trendelenburg and Mayer-Wegelin (1955, pp. 472–474) found

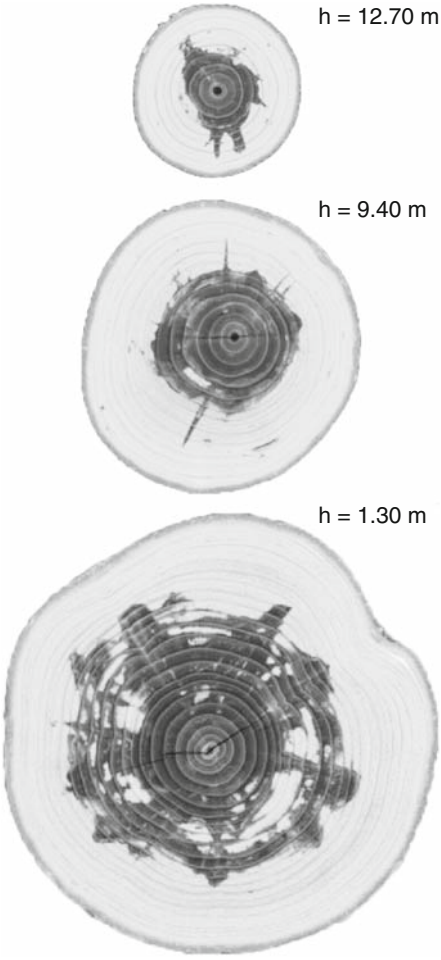

Fig. 2.11 Differentiation between sapwood (*light grey*) and dead heartwood (*dark grey*) via CT scanning. Stem disks of Norway spruce No. 22 from long-term plot TRA 639 near Traunstein/South Bavaria (age 40, $d_{1.3} = 29.1$ cm, h = 18.9 m). In the disks from heights of 1.3 m, 9.4 m, and 12.7 m, the portion of dead heartwood amounts to 39%, 26%, and 25%, respectively

percentage volumes of dead heartwood up to 36, 60, 53 and 74% for European beech, Norway spruce, Scots pine and Sessile oak respectively. Knigge and Schulz (1966, p. 109) report 50 and 75% for Scots pine and Sessile oak. According to Lohmann (1992, p. 46), the inert heartwood can comprise up to 78% in Norway spruce. We summarise the results into f_{sw} values ($f_{sw} = 1 -$ heartwood portion) for Norway spruce $f_{sw} = 0.22$–0.40, Scots pine $f_{sw} = 0.47$–0.50, Sessile oak $f_{sw} = 0.25$–0.26, and European beech $f_{sw} = 0.64$.

An efficient method for distinguishing sapwood and heartwood makes use of computer tomography (CT). In Fig. 2.11, we show the example of a 40 year-old Norway spruce tree from Traunstein (TRA 639) with $d_{1.3} = 29.10\,\text{cm}, h = 18.90\,\text{m}$ and a crown base height of $h_{cb} = 7.20\,\text{m}$. The tree was cut into segments, and three sections at heights of 1.30, 9.40, and 12.70 m were inserted into a computer tomograph type SIEMENS Somatom AR.HP. At each height, three cross-sections 1 mm thick were obtained within close proximity applying an acceleration voltage of 130 kV. With the different intensity in the CT images resulting, the moist sapwood and the dry heartwood can be separated with commercial image software (here: Photoshop^{TM} 7.0). The percentage heartwood in Fig. 2.11 is 39% at 1.30 m height, 26% at 9.40 m height and 25% at 12.70 m height. Unlike conventional staining methods, which react to the starch content or ph-value, the CT method is based on water content, which is closely correlated to physiological activity (Vötter 2005).

Similar analyses of Norway spruce, Scots pine, Sessile oak, and European beech show a species-specific decrease in the proportion of sapwood from $f_{sw} = 1.0$ in the juvenile phase to 0.25–0.50 in the mature phase. The 3D computer tomography model of the proportion of sapwood and heartwood (Fig. 2.10) yields heartwood volume percentages (f_{sw} factors in brackets) of 0% in the juvenile phase of the tree ($f_{sw} = 1$), 1−35% at $d_{1.30} = 10$–$15\,\text{cm}$ ($f_{sw} = 0.99$–0.65) and 3–56% at $d_{1.30} = 30$–$50\,\text{cm}$ ($f_{sw} = 0.97$–0.44) (Pretzsch 2005c). The trees analysed were extracted from pure stands with aboveground biomasses 96–342 t ha^{-1} for Norway spruce, 45–153 t ha^{-1} for Scots pine stands, 109–433 t ha^{-1} for European beech and 93–171 t ha^{-1} for Sessile oak. The corresponding biomass of the dead inner xylem comprised 13–192 t ha^{-1}.

In forest inventories and measures, the differentiation between sapwood and heartwood is of little practical relevance and is disregarded (Oliver and Larson 1996, p. 332). Yet, scientifically, it enables some interesting connections to be made between woody and herbaceous growth and yield behaviour. If the "turnover" in form of increasing heartwood is included in the estimation of net growth, then the actual net growth is smaller than calculated, and turnover would equate with biomass production at a much earlier phase in stand life. Although general correction factors are still lacking, Pretzsch (2005c) outlines a preliminary approach for distinguishing between living sapwood and heartwood where it was possible to link self-thinning and maximum density rules for herbaceous plant communities (Yoda et al. 1963) and forests (Reineke 1933) (cf. Chap. 10, Sect. 10.4). When investigating the ecophysiological capacity or maximum density of an ecosystem, it makes sense to regard only the living, and therefore metabolically active biomass.

2.6 Growth and Yield and Nutrient Content

The immense amount of biomass stored in a forest is composed mainly of carbon, hydrogen and oxygen (C, H, O), but also of the nutrient minerals N, P, S, K, Ca, Mg, K and some trace elements. Unlike herbaceous vegetation with its annual or perennial cycles, this means that a tremendous pool of nutrient minerals is stored in the vegetation and temporarily withdrawn from the soil. These nutrients become available through the decomposition of the organic turnover, which, in some ecosystems such as the tropical rainforests, represents the main source. According to Fink (1969), dry organic biomass from vegetation consists of 90–95% C, H, O in the proportions 44–59% C, 42–46% O and 5–7% H. The remaining 5–10% consists of N, K (1–5%), Ca, Mg, P, S, Cl (0.1–2.0%), Fe, Mn, Zn, Cu, B (5–200 ppm) and Mo (0.2–5 ppm).

Table 2.12 lists the mean percentages of the macronutrients according to Jacobsen et al. (2003). Leaves contain the highest concentration of N, P, K, and Mg, bark the highest Ca concentration. The nutrient store in stems is minimal, on average 5–10% of the leaf concentrations. Broadleaved trees have higher nutrient concentrations than conifers in almost all tree compartments.

Table 2.12 Nutrient concentration in stem wood, bark, branches, leaves and/or needles, coarse roots, and fine roots (results for Norway spruce, Scots pine, Sessile oak and European beech according to Jacobsen et al. (2003))

Tree species	Nutrient	Stem wood mg g^{-1}	Bark mg g^{-1}	Branches mg g^{-1}	Leaves mg g^{-1}	Coarse roots mg g^{-1}	Fine roots mg g^{-1}
Norway spruce	N	0.83	5.17	5.24	13.36	4.14	10.77
	P	0.06	0.65	0.65	1.33	0.37	0.98
	K	0.46	2.83	2.39	5.70	1.38	2.18
	Ca	0.70	8.17	3.33	6.03	1.59	2.61
	Mg	0.11	0.77	0.53	0.79	0.30	0.55
Scots pine	N	0.76	3.85	3.61	14.46	1.77	7.44
	P	0.05	0.46	0.34	1.32	0.21	0.62
	K	0.42	2.08	1.67	5.03	1.08	1.47
	Ca	0.62	5.03	2.07	4.08	0.97	2.83
	Mg	0.18	0.61	0.43	0.87	0.30	0.45
Sessile oak Common oak	N	1.56	5.16	6.19	26.15	3.71	8.94
	P	0.08	0.30	0.43	1.74	0.27	0.74
	K	0.95	2.00	2.00	7.38	2.16	3.40
	Ca	0.46	21.49	4.41	11.43	4.07	6.18
	Mg	0.09	0.65	0.44	2.27	0.40	1.06
European beech	N	1.21	7.35	4.27	26.01	3.03	7.15
	P	0.10	0.50	0.48	1.46	0.35	0.60
	K	0.93	2.34	1.50	8.66	1.34	2.18
	Ca	0.95	20.52	4.02	8.88	2.69	5.29
	Mg	0.25	0.59	0.36	1.25	0.43	0.74

Nitrogen N attains concentrations between 13.36 mg g^{-1} (Norway spruce) and 26.15 mg g^{-1} (Sessile oak). The N concentration in tree compartments decreases in the following order: leaves > fine roots > brushwood ≅ bark > coarse roots > merchantable stem wood.

The amount of phosphorus P stored in the leaves is only approximately one-tenth the N content: between 1.32 mg g^{-1} (Scots pine) and 1.74 mg g^{-1} (Sessile oak). In the tree compartments, the phosphorus concentration decreases in the same order as for nitrogen: leaves > fine roots > brushwood ≅ bark > coarse roots > merchantable stem wood.

Potassium K, with leaf concentrations between 5.03 mg g^{-1} (Scots pine) and 8.66 mg g^{-1} (European beech), and magnesium Mg with leaf concentrations between 0.79 mg g^{-1} (Norway spruce) and 2.27 mg g^{-1} (Sessile oak) show the same distribution pattern as N and P.

Only for Calcium Ca, with bark-concentrations between 5.03 mg g^{-1} (Scots pine) and 21.49 mg g^{-1} (Sessile oak), does the order differ: rough bark > leaves > brushwood ≅ fine roots > coarse roots > merchantable stem wood.

2.6.1 From Total Biomass to the Carbon Pool

The C content is almost similar in all plant organs, and the lower concentration of carbon in leaves is negligible for the tree, so, generally, one can assume that carbon accounts for 50% of the total plant biomass.

$$\text{Biomass(C)} = \text{Biomass(total)} \times 0.5. \tag{2.42}$$

For a more differentiated C allocation pattern in relation to species, position in the stand, and so on, see Körner (2002). Taking the mean values of the standing wood volume from the BWI^2 (Table 2.9, Bundesministerium für Ernährung, Landwirtschaft und Verbraucherschutz, 2005), the carbon pool of the stand biomass ranges from 102 t C ha^{-1} (Douglas fir) to 182 t C ha^{-1} (European beech). The average NPP values calculated range from 4.6 t C ha^{-1} yr^{-1} (Scots pine) to 9.4 t C ha^{-1} yr^{-1} (Douglas fir), and the biomass values for the almost 100-year-old evenaged central European forests in Table 2.10, (upper section) are equivalent to 189 t C ha^{-1} (European larch) to 506 t C ha^{-1} (Norway spruce). The NPP values for the stands in Table 2.10 range from 2.5 t C ha^{-1} yr^{-1} in mixed Norway spruce-Silver fir-European beech mountain forests, to 9.9 t C ha^{-1} yr^{-1} in mixed lowland Norway spruce-European beech forests.

2.6.2 Nutrient Minerals

While the C concentration is relatively stable among the tree compartments, the mineral nutrients N, P, K, Mg, Ca, S and the trace elements are concentrated in the

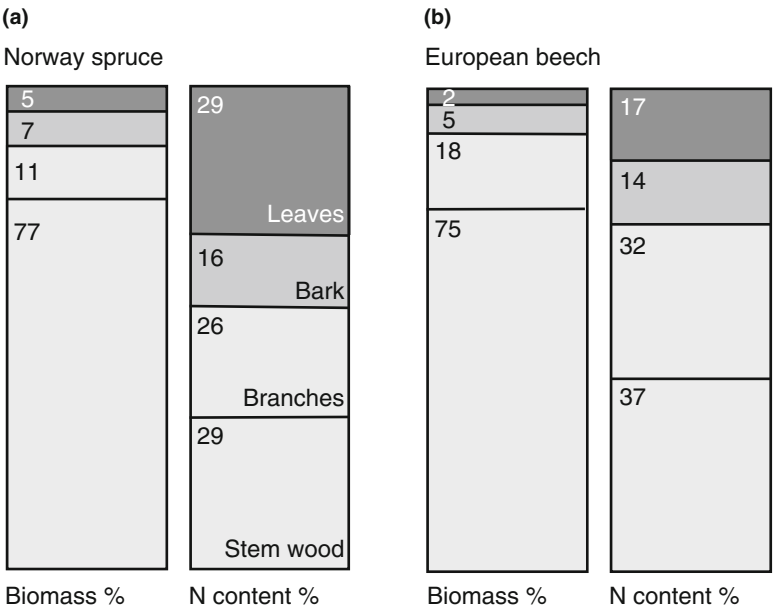

Fig. 2.12 Fraction of aboveground biomass and nitrogen in leaves, bark, branches, and stem wood at age 100 years. (**a**) For Norway spruce, the total above ground biomass at age 100 years amounts to 527 t ha^{-1} and the nitrogen content to 1.2 t ha^{-1}. (**b**) In European beech stands of the same age, the aboveground biomass is 347 t ha^{-1} and the nitrogen content 0.9 t ha^{-1}

leaves and the rough bark. Figure 2.12 depicts the mineral distribution for a 100 year-old (a) Norway spruce stand with 527 t ha^{-1}, and (b) European beech stand with 347 t ha^{-1} aboveground biomass respectively. In each case the left bar shows the distribution of the total aboveground biomass on the different tree organs stem wood, branches, bark and leaves. Although leaves, bark and branches make up only a minor part of the total biomass, they comprise a major portion of the total nitrogen content and other nutrient minerals.

For example, the total amount of nitrogen N stored in the aboveground biomass adds up to 1.2 t ha^{-1} for Norway spruce and 0.9 t ha^{-1} for European beech. Of this amount, 71% and 63% are stored in leaves, bark and branch wood of the Norway spruce and European beech stands, which contribute merely 23% and 25% to the total aboveground biomass respectively. The remaining 29% and 37% in each stand is present in the merchantable wood and is removed in the harvest. Since the distribution of the other macronutrients P, K, Ca, and Mg is more or less equal, it is estimated that the harvest of merchantable wood extracts one third of these minerals as well. Any additional harvesting of the crown, bark or brushwood leads to an over-proportional reduction in the mineral nutrients, which becomes especially critical on nutrient-limited sites.

By applying the biomass equations and the estimations of nutrients contents by Jacobsen et al. (2003) to standard yield table data for Norway spruce and European

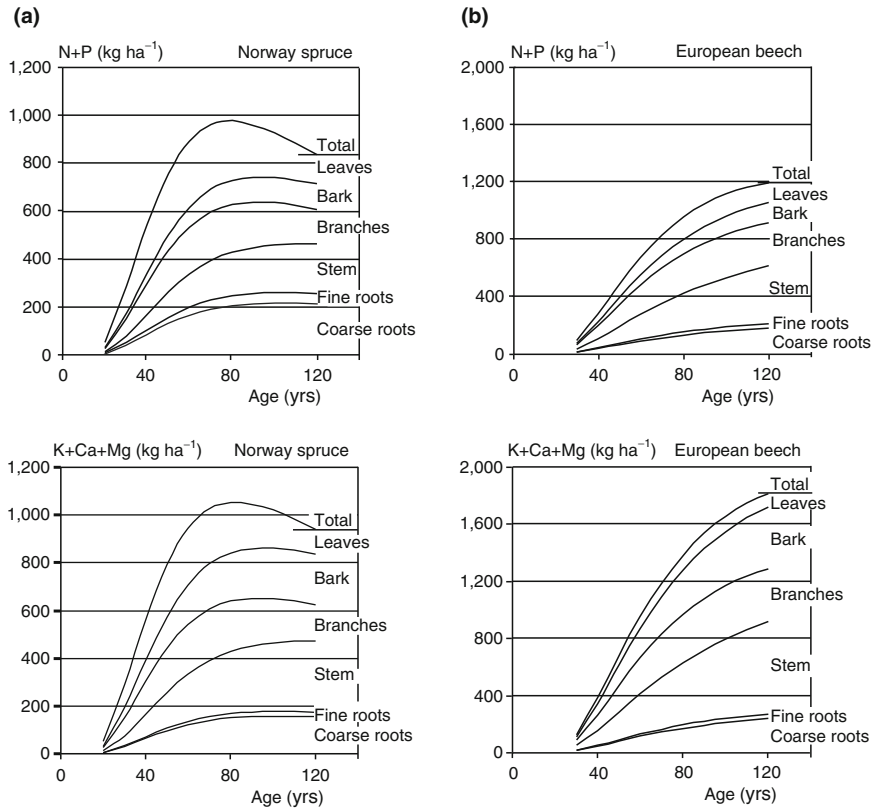

Fig. 2.13 Accumulation of N + P and K + Ca + Mg (kg ha^{-1}) in the total stand biomass, and in the separate compartments leaves, bark, branches, stem wood, fine and coarse roots. (**a**) For Norway spruce, we assumed site index II (Wiedemann, 1936/42, mod. th.). (**b**) For European beech, we applied Schober's yield table and site index I (Schober, 1972, mod. th.). For partitioning of biomass to tree organs and estimations of nutrients contents, we applied functions from Jacobsen et al. (2003)

beech, we now model the mineral nutrient distribution between the tree compartments during stand development. Again, the results are merely approximations. A particular stand may deviate significantly due to its site-specific nutrient constraints. As can be seen in Fig. 2.13, at age 120, Norway spruce stands (left) have accumulated about 1 t ha^{-1} N + P ($\sim$10:1), and an amount of 1 t ha^{-1} K + Ca + Mg. European beech stands accumulate more: 1.2 t ha^{-1} N + P and 1.8 t ha^{-1} K + Ca + Mg. In addition, the figure shows the distribution of N + P and K + Ca + Mg over the different plant organs. Whereas Norway spruce reduces the needle and branch wood biomass after 60–80 years of age, and thus the amount of minerals as well, European beech continues to increase leaf biomass and brushwood, and, consequently, also accumulates more minerals. Of course, in the short-term turnover of these organs, a certain amount of the minerals is constantly recycled and reused.

Table 2.13 Nutrient contents of forest stands of medium site quality at age 100 years. Estimation of standing volume is based on common yield tables from Wiedemann (1936/1942) for Norway spruce, Wiedemann (1943a) for Scots pine, Jüttner (1955) for Sessile oak (1972) for European beech. Nutrients content was estimated according to Jacobsen et al. (2003)

Tree species	Nutrient	Stem wood kg ha^{-1}	Bark kg ha^{-1}	Branches kg ha^{-1}	Leaves-needles kg ha^{-1}	Coarse roots kg ha^{-1}	Fine roots kg ha^{-1}	Total kg ha^{-1}
Norway spruce	N+P	201	106	174	187	218	41	927
Scots pine		125	61	84	98	80	51	498
Sessile/ Common oak		321	136	322	189	260	55	1,283
European beech		343	128	301	155	158	27	1,111
Norway spruce	K+Ca+Mg	287	214	185	159	158	19	1,022
Scots pine		188	108	89	39	60	24	508
Sessile/ Common oak		294	92	333	142	434	61	1,356
European beech		557	381	373	106	208	28	1,654

Table 2.13 summarises the assumed mineral pool, calculated in the same way as in the previous example, in forest stands aged 100 years (medium site quality). Together nitrogen and phosphorus range from 0.498 t ha^{-1} (Scots pine) to 1.283 t ha^{-1} (Sessile/Common oak). The amount of K, Ca and Mg ranges from 0.508 t ha^{-1} (Scots pine) to 1.654 t ha^{-1} (European beech). The N:P ratio is 10:1, and the K:Ca:Mg ratio is 30:60:10. Although thinning measures always recycle part of the minerals in the vegetation, at the end of the rotation period the soils have lost an estimated 1–3 t ha^{-1} minerals to the trees. In selection forests, which typically possess less standing biomass, the minerals stored in the vegetation are probably a little less, and the recycling is more even and not so concentrated at the time of harvest.

Table 2.14, above, gives a range for organic C and the mineral nutrient content stored in forest soils in central Europe (Ziegler 1991; Rehfuess 1981; Burschel et al. 1993). These values do not reflect the actual amount of minerals available to plants, but serve as rough comparisons with organic C and nutrient in the standing biomass (Table 2.14, below). With an organic C content in the soils of 35–362 t ha^{-1} (Ziegler, 1991) or 51–213 t ha^{-1} (Rehfuess 1981), the amount is equal in order of magnitude to the C content in the mean standing biomass in forests in Germany (Bundesministerium für Ernährung, Landwirtschaft und Verbraucherschutz, BWI^2, Der Inventurbericht, p. 75) (cf. Table 2.9). A significant amount of nitrogen also can be stored in the ground vegetation. It can be seen, for instance, that on poor nutrient sites the ground vegetation contains one third of the total ecosystem nitrogen content in extreme cases.

Table 2.14 Range of organic carbon content C_{org} and nutrient content N, P, K, and C in soils in Southern Germany according to Rehfuess (1981) and (Ziegler, 1991), and nutrient content in standing biomass at age 100 years. For the estimation of nutrient content in standing biomass at age 100 years, compare Table 2.13

Compartment	C_{org} $t\,ha^{-1}$	N $kg\,ha^{-1}$	P $kg\,ha^{-1}$	K $t\,ha^{-1}$	Ca $t\,ha^{-1}$
Nutrients in soil					
min	35.00	4,260	2,890	79.0	6.0
max	362.00	21,420	9,895	766.0	578.0
Nutrients in standing biomass at age 100					
Norway spruce	138.10	844	83	0.373	0.568
Scots pine	109.95	456	42	0.150	0.293
Sessile and Common oak	152.65	1,205	78	0.520	0,745
European beech	182.30	1,019	92	0.495	1.031

The 100-year-old Norway spruce and European beech stand (Table 2.14) had accumulated 844, and $1{,}019\,kg\,ha^{-1}$ N respectively, as opposed to the $4{,}260$–$21{,}420\,kg\,ha^{-1}$ in the soil (Rehfuess 1981). The amount of phosphorus in the soil ranges from 2,890 to $9{,}895\,kg\,ha^{-1}$, compared to the $83\,kg\,ha^{-1}$ P in the Norway spruce and $92\,kg\,ha^{-1}$ P in European beech stand. Potassium accumulation amounted to 79–766 t ha^{-1} in the soil compared to $0.373\,t\,ha^{-1}$ in the Norway spruce, and $0.495\,t\,ha^{-1}$ in the European beech stand, and calcium accumulation to 6–578 t ha^{-1} in the soil compared to 0.568 and $1.031\,t\,ha^{-1}$ in each stand.

2.7 Efficiency of Energy, Nitrogen, and Water Use

The energy, nitrogen, and water use efficiency (EUE, NUE, and WUE, respectively) specifies the production per resource demand. In the literature, we find a number of different parameters for the numerator, such as the photosynthetic activity in $\mu mol\,CO_2\,m^{-2}\,s^{-1}$, the NPP in t biomass $ha^{-1}\,yr^{-1}$ or the growth of aboveground dry matter in kg biomass $m^{-2}\,yr^{-1}$ (cf. Kimmins 1993; Landsberg 1986; Larcher 1994). In addition, various parameters are used for the denominator; e.g. for water use efficiency (WUE) can refer to annual precipitation, annual evapotranspiration or annual transpiration. The lack of convention creates difficulties in comparing different studies. Körner (2002) even questions the significance of efficiency quotients in general. Nevertheless, this chapter aims to give a rough idea of the resources needed per unit of wood production. For the production unit (numerator), we distinguish productivity of merchantable wood volume per unit area ($m^3\,ha^{-1}\,yr^{-1}$), annual NPP per unit area (total or aboveground) ($t\,ha^{-1}\,yr^{-1}$) and calorific value of net primary production ($GJ\,ha^{-1}\,yr^{-1}$). For the denominator, we

refer to annual sum of global radiation per unit area ($GJ\,ha^{-1}\,yr^{-1}$) for EUE, average annual content of foliage nitrogen per unit area ($t\,N\,ha^{-1}\,yr^{-1}$) for NUE, and the annual sum of stand transpiration per unit area ($l\,m^{-2}\,yr^{-1}$) for WUE.

Therefore the efficiency quotients resulting are: EUE = productivity unit/global radiation; NUE = productivity unit/foliage nitrogen; and WUE = productivity unit/transpiration. We occasionally apply units such as litres of wood volume, and g or kg of biomass instead of cubic metres or tons to illustrate the relationships more clearly.

These efficiency parameters are especially relevant for forest production and management, and can be used as input for efficiency-driven hybrid growth models (cf. Chaps. 1 and 11). Furthermore, they also may reveal species-specific advantages in certain environments, for example a higher competitiveness under constrained water availability. It is often amazing that, on the one hand, large quantities of water and energy are needed to produce one unit of wood, e.g. approximately 1 J wood per 100–200 J global radiation, or 1 g wood per 500 g H_2O. On the other hand, for nitrogen, the relationship is reversed, e.g. 100–500 g wood per 1 g N. Simply put, if water and energy form the basis of your "soup", nitrogen and other nutrient minerals represent the "salt".

2.7.1 Energy Use Efficiency (EUE)

The calorific value of dry matter for European conifer and broadleaved species is 20.45 and 19.78 $kJ\,g^{-1}$, respectively (Runge, 1973). Ellenberg (1986, p. 331) determined the calorific values of each tree compartment for Norway spruce and European beech. For Norway spruce he obtained values of 20.36–20.79 kJ g^{-1} for wood in stems, branches and roots, 20.34–21.14 kJ g^{-1} in bark, 20.74–20.79 kJ g^{-1} in the needles and fine roots, 21.25 $kJ\,g^{-1}$ in needle litter, and 36.87 kJ g^{-1} in resin. The calorific values for European beech were 19.72–20.10 kJ g^{-1} for stem, branch and root wood, 20.78–23.13 kJ g^{-1} for bark, 20.30–21.63 $kJ\,g^{-1}$ for leaves and fine roots, 21.07 kJ g^{-1} for leaf litter and 23.08 $kJ\,g^{-1}$ for beechnuts. Thus the merchantable wood, which comprises the largest portion of the long-term fixed biomass, has the lowest calorific value. Bark, with its protection and defence functions and its resin content, has a much higher calorific value. In general, the calorific value of herbaceous plants is lower than woody plants, of broadleaves lower than conifers, and of aquatic plants lower than terrestrial plants. Larcher (1994, p. 138) assumes that, in many cases, lower calorific values can be an evolutionary advantage as less energy needs to be invested.

The unit of the calorific value is $1\,J = 2.78 \times 10^{-7}\,kWh = 0.239 \times 10^{-3}\,kcal$. In the following discussion, we use units of kJ, MJ or GJ, which correspond to $J \times 10^3$, $J \times 10^6$ and $J \times 10^9$, respectively. For simplicity, we round the calorific value of broadleaved and conifer wood equally to $20\,kJ\,g^{-1}$ (1 g biomass $\hat{=}$ 20 kJ $\hat{=}$ 0.0056 kWh = 4.78 kcal). The bark and resin, with their protection and defence functions, have higher values, but this does not affect the result significantly because they only

Table 2.15 Calorific value of various tree species per solid cubic metre stem wood (s. c. m, left) and stacked cubic metres (st. c. m, right). We apply the conversion factor st. c. m $\hat{=} 0.7 \times$ s. c. m. R represents the specific wood density defined on the basis of the green volume ($\mathrm{kg\,m^{-3}}$). The biomass is given as $10^6\,\mathrm{g\,m^3}$ (Mega g), calorific value in 10^9 Joule (GJ), and 10^6 Watt hours (Mega Wh)

Tree species	R $\mathrm{kg\,m^{-3}}$	Biomass per $\mathrm{m^3}$ Mega g	Calorific value per $\mathrm{m^3}$ GJ	Calorific value per $\mathrm{m^3}$ Mega Wh	Biomass per st. $\mathrm{m^3}$ Mega g	Calorific value per st. $\mathrm{m^3}$ GJ	Calorific value per st. $\mathrm{m^3}$ Mega Wh
Balsawood	121	0.121	2.416	0.672	0.085	1.691	0.470
Grand fir	332	0.332	6.640	1.846	0.232	4.648	1.292
White pine	339	0.339	6.772	1.883	0.237	4.740	1.318
Poplar	377	0.377	7.536	2.095	0.264	5.275	1.467
Norway spruce	377	0.377	7.542	2.097	0.264	5.279	1.468
Sitka spruce	402	0.402	8.034	2.233	0.281	5.624	1.563
Douglas fir	412	0.412	8.248	2.293	0.289	5.774	1.605
Pine	431	0.431	8.614	2.395	0.301	6.030	1.676
Larch	487	0.487	9.746	2.709	0.341	6.822	1.897
Maple	522	0.522	10.444	2.903	0.366	7.311	2.032
European beech	554	0.554	11.086	3.082	0.388	7.760	2.157
Elm	556	0.556	11.110	3.089	0.389	7.777	2.162
Sessile-Common oak	561	0.561	11.222	3.120	0.393	7.855	2.184
Ash	564	0.564	11.284	3.137	0.395	7.899	2.196
False acacia	647	0.647	12.936	3.596	0.453	9.055	2.517
Bongossi	890	0.890	17.804	4.950	0.623	12.463	3.465
Pockwood	1,046	1.046	20.910	5.813	0.732	14.637	4.069

make up a small portion. By multiplying biomass, in tonnes, by 20, its calorific value can be converted to GJ. Tons of carbon, which makes up 50% of the biomass, must be multiplied by 40 to obtain the calorific value in GJ. The species-specific calorific values for wood volume in $\mathrm{m^3}$ and stacked cubic metres st. c. m ($1\,\mathrm{m^3} \sim 0.7$ st. c. m) are summarised in Table 2.15.

For the denominator in the energy use efficiency quotient, we assume an annual sum of global radiation of $36{,}000\,\mathrm{GJ\,ha^{-1}\,yr^{-1}}$ for central Europe between 47° and 57° N. For the period 1961–1990, the Bavarian climate stations reported the average value of $36{,}719\,\mathrm{GJ\,ha^{-1}\,yr^{-1}}$, the Bavarian climate atlas $35{,}421\,\mathrm{GJ\,ha^{-1}\,yr^{-1}}$ (Rötzer et al. 1997), the German climate atlas $36{,}000\,\mathrm{GJ\,ha^{-1}\,yr^{-1}}$ and long-term climate stations determinations in the different regions in Germany a range between 33,600 and $40{,}799\,\mathrm{GJ\,ha^{-1}\,yr^{-1}}$ (Ellenberg 1986). In the calculation of the energy use efficiency below, we assume an annual global energy sum of $36{,}000\,\mathrm{GJ\,ha^{-1}\,yr^{-1}}$.

Table 2.16 summarises the EUE for the periodic annual merchantable volume increment ($\mathrm{m^3\,ha^{-1}\,yr^{-1}}$) based on the national inventory (BWI^2, Bundesministerium für Ernährung, Landwirtschaft und Verbraucherschutz, 2005). The values for the

periodic annual merchantable volume increment (9.12–16.37 $m^3\,ha^{-1}\,yr^{-1}$) were translated into NPP with the conversion factors introduced in this chapter (9.26–15.80 $t\,ha^{-1}\,yr^{-1}$ = 185–316 $GJ\,ha^{-1}\,yr^{-1}$). The quotient EUE_V relates the growth of merchantable wood volume (volume in litre $ha^{-1}\,yr^{-1}$) to the annual sum of global radiation ($GJ\,ha^{-1}\,yr^{-1}$)

$$EUE_V = \frac{PAI}{\text{Global radiation}}(1GJ^{-1}). \tag{2.43}$$

The EUE_{NPP} uses NPP as a productivity unit ($kg\,ha^{-1}\,yr^{-1}$)

$$EUE_{NPP} = \frac{NPP}{\text{Global radiation}}(kg\,GJ^{-1}). \tag{2.44}$$

Finally, the $EUE_{cal\,NPP}$ is based on the calorific value of the NPP ($GJ\,ha^{-1}\,yr^{-1}$):

$$EUE_{cal\,NPP} = \frac{\text{calorific value NPP}}{\text{Global radiation}}(GJ\,ha^{-1}\,GJ^{-1}\,ha). \tag{2.45}$$

As can be seen in Table 2.16, the energy use efficiency in relation to merchantable wood volume lies between $EUE_V = 0.231GJ^{-1}$ for European oak, and $0.451GJ^{-1}$ for Norway spruce. EUE_{NPP}, the EUE in relation to NPP, amounts to $0.26\,kg\,GJ^{-1}$ for Scots pine and $0.44\,kg\,GJ^{-1}$ for European beech. The $EUE_{cal\,NPP}$ values of 0.005–0.009 reveal, that the efficiency ratio for the conversion of sun energy into biomass production only reaches <1%. Most of the incoming radiation energy

Table 2.16 Energy use efficiency of various tree species in Germany. Estimate of productivity is based on mean periodic annual increment PAI according to Bundesministerium für Ernährung, Landwirtschaft und Verbraucherschutz (2005, p. 167) and expansion and conversion factors reported in Sect. 2.4. Estimate of the corresponding sum of mean global radiation in $GJ\,ha^{-1}\,yr^{-1}$ is based on Rötzer et al. (1997)

Components	Norway spruce	European beech	Scots pine	Sessile and Common oak
Productivity				
PAI merch. volume ($m^3\,ha^{-1}\,yr^{-1}$)	16.37	9.12	11.74	8.25
NPP ($t\,ha^{-1}\,yr^{-1}$)	14.55	9.26	15.80	11.45
Calorific value of NPP ($GJ\,ha^{-1}\,yr^{-1}$)	291.00	185.20	316.00	229.00
Resource				
Global radiation ($GJ\,ha^{-1}\,yr^{-1}$)	36,000	36,000	36,000	36,000
Efficiency				
EUE_V (l merch. volume GJ^{-1})	0.45	0.25	0.33	0.23
EUE_{NPP} ($kg\,GJ^{-1}$)	0.40	0.26	0.44	0.32
$EUE_{cal\,NPP}$ ($GJ\,ha^{-1}\,GJ^{-1}\,ha$)	0.008	0.005	0.009	0.006

EUE_V refers to the litre of merchantable volume per GJ global radiation. EUE_{NPP} represents kg total net primary production per GJ global radiation. $EUE_{cal\,NPP}$ reflects efficiency ratio for the conversion of sun energy into biomass production.

(50–60%) does not fall within the photosynthetically useful spectrum; another 10–20% is reflected or transmitted, and most of the remainder is lost in the process of photosynthesis itself (cf. Larcher 1994, p. 118 and Körner 2002, p. 943).

The energy use efficiency EUE is an important parameter for the estimation of the potential productivity in a certain region, and can be used to initialise simple top-down models (e.g. Landsberg 1986, p. 173; cf. Chap. 11). It is clear that the global radiation solely cannot explain productivity, and to avoid errors caused by such a mono-causal approach, or to obtain a higher spatial resolution, additional limiting factors need to be included in estimation approaches, or in growth models.

2.7.2 Nitrogen Use Efficiency (NUE)

To derive rough estimates for NUE in European forests we apply the productivity values from the BWI^2 (Bundesministerium für Ernährung, Landwirtschaft und Verbraucherschutz, BWI^2, Der Inventurbericht, p. 167). The estimation is based on the species-specific periodic annual volume increments (PAI) of stands in the age class 81–100. The foliage nitrogen content, estimated from the standing volume by using the scaling methods introduced in this chapter, revealed leaf nitrogen pools of 48.9–167.4 kg ha^{-1}. Table 2.17 provides an overview of nitrogen use efficiency values (NUE) in relation to the measures of productivity, stem volume growth in litres, aboveground biomass growth in kg, and NPP in kg. This results in NUE_V values of 108.7–293.51 of merchantable wood volume per kg foliage

Table 2.17 Nitrogen use efficiency of foliage of various tree species in Germany. Estimate of productivity is based on mean periodic annual increment of stands in age class 81–100 years according to Bundesministerium für Ernährung, Landwirtschaft und Verbraucherschutz (2005, p. 167) and expansion and conversion factors reported in Sect. 2.4. The foliage nitrogen content is estimated according to Jacobsen et al. (2003)

Components	Norway spruce	European beech	Scots pine	Sessile and Common oak
Productivity				
PAI merch. volume (m^3 ha^{-1}yr^{-1})	18.2	8.4	14.4	8.6
above g. biomass (t ha^{-1}yr^{-1})	10.0	5.2	11.9	7.4
NPP (t ha^{-1}yr^{-1})	16.2	8.5	19.3	12.0
Resource				
Foliage nitrogen (kg ha^{-1})	167.4	55.1	48.9	74.4
Efficiency				
NUE_V (l stem volume kg^{-1}N)	108.7	151.9	293.5	115.7
NUE_B (kg above g. biomass kg^{-1}N)	59.5	94.8	243.0	98.9
NUE_{NPP} (kg NPP kg^{-1}N)	96.6	154.1	394.9	160.6

NUE_V indicates how many litres of merchantable stem volume are produced in one year per kg foliage nitrogen available during the same year. NUE_B refers to the aboveground biomass in kg per kg foliage nitrogen. NUE_{NPP} stands for kg NPP per kg N.

nitrogen. Related to the aboveground biomass production, the efficiencies assume values of $NUE_B = 59.5–243.0$ kg aboveground biomass per kg leaf N, and, finally, of $NUE_{NPP} = 96.6–394.9$ kg NPP per kg foliage nitrogen (Table 2.17).

The latter nitrogen use efficiencies agree with values from Jørgensen and Schelde (2001) who determined a range of $NUE_{NPP} = 104–370$ kg NPP per kg foliage N from measurements of poplar, willow and pine. Comeau and Kimmins (1986) found a foliage nitrogen efficiency of 35–75 kg NPP per kg foliage N in *Pinus contorta* stands.

2.7.3 Water Use Efficiency (WUE)

The studies by Menzel and Rötzer (2007), Peck (2004), Rötzer et al. (1997), and Wohlrab et al. (1992) provide average transpiration values and an upper and lower limit for the most common tree species in central Europe (Table 2.18). They produce annual transpiration averages of 285–363 mm yr^{-1} ($= 1 m^{-2} yr^{-1}$) and a minimum and maximum of 119 and 765 mm yr^{-1}, respectively.

As for EUE and NUE, the WUE is estimated for the tree species Norway spruce, Scots pine, European beech, and Sessile oak based on the average volume increment data PAI from the BWI[2] (Bundesministerium für Ernährung, Landwirtschaft und Verbraucherschutz, 2005). As shown in Table 2.18, the PAI of 9.1–16.4 $m^3 ha^{-1} yr^{-1}$

Table 2.18 Water use efficiency of various tree species in Germany. Estimate of productivity is based on mean periodic annual increment PAI according to Bundesministerium für Ernährung, Landwirtschaft und Verbraucherschutz (2005, p. 167) and expansion and conversion factors reported in Sect. 2.4. Consumption of water for transpiration is estimated according to Menzel and Rötzer (2007), Rötzer et al. (1997), and Wohlrab et al. (1992)

Components	Norway spruce	Scots pine	European beech	Sessile and Common oak
Productivity				
PAI merch. volume ($m^3 ha^{-1} yr^{-1}$)	16.40	9.10	11.70	8.30
above g. biomass (t $ha^{-1} yr^{-1}$)	8.95	5.70	9.72	7.05
NPP (t $ha^{-1} yr^{-1}$)	14.50	9.30	15.80	11.50
Resource				
Transpiration (l $m^{-2} yr^{-1}$)	287	342	363	285
min	119	173	268	171
max	516	765	601	327
Efficiency				
WUE_V (cm^3 merch. V $kg^{-1} H_2O$)	5.7	2.7	3.2	2.9
WUE_B (g above g. biomass $kg^{-1} H_2O$)	3.1	1.7	2.7	2.5
WUE_{NPP} (g NPP $kg^{-1} H_2O$)	5.1	2.7	4.4	4.0

WUE_V indicates how many cm^3 of merchantable volume can be associated with the transpiration of 1 l of water. WUE_B refers to g of aboveground biomass production per kg water. WUE_{NPP} represents the NPP in g per kg H_2O.

merchantable wood volume and 5.7–9.7 t $ha^{-1}\,yr^{-1}$ aboveground biomass results in water use efficiencies of $WUE_V = 2.7–5.7\,cm^3$ wood volume per kg H_2O and $WUE_B = 1.7–3.1$ g aboveground biomass growth per kg H_2O, respectively. The calculation of the water use efficiency of NPP

$$WUE_{NPP} = \frac{NPP}{transpiration}\,(g\,NPP\,kg^{-1}\,H_2O) \tag{2.46}$$

is based on 9.3–15.8 t $ha^{-1}\,yr^{-1}$ NPP, and yields 2.7–5.1 g NPP per kg H_2O, respectively.

Even though the expansion factors employed in the estimation of aboveground biomass and NPP are only first-order approximations, the water use efficiencies determined correspond well with literature values. Lyr et al. (1967, p. 181) and Assmann (1961, pp. 26–28) report values of 169 and 300 g transpired H_2O needed per 1 g biomass in Douglas fir and Sessile oak stands, respectively. Translated into WUE_B, this means 2.9–5.9 g biomass per kg H_2O. Larcher (1994, p. 107) indicates water use efficiencies in the order of 1.3–3.6 g biomass per kg H_2O for herbaceous plants, 1–2 g $kg^{-1}\,H_2O$ for tropical woody plants, 3–5 g $kg^{-1}\,H_2O$ for temperate conifer and broadleaf trees, and 3–6 g $kg^{-1}\,H_2O$ for sclerophyllous shrubs. Landsberg (1986, p. 158) assigns the WUE a highly indicative value for production prognoses and models. Until now, the WUE is more widely used in agriculture, mainly because transpiration measurements are comparably difficult to obtain in forest vegetation.

2.7.3.1 Efficiency Parameters and Hybrid Models

The translation of traditional wood volume measures from forestry into NPP and the derivation of efficiency parameters, as shown in this chapter, are essential for understanding of hybrid models. Hybrid models are used for the prediction of NPP and stand development (Kimmins 1985; Kimmins et al. 1999). They integrate the knowledge of both forest and ecological sciences in much the same way as was done here. Readily available time series for the development of stand volumes are combined with intensive physiological measurements of biomass allocations available for limited sites and turnover rates to derive site-specific light, water or nutrient use efficiencies. These parameters are applied in hybrid models for estimating NPP, stand dynamics, and yield on a given site, e.g. in relation to silvicultural prescriptions, changing climate conditions, or other disturbance factors (cf. Chaps. 1 and 11).

Summary

This chapter draws a link between the volume-oriented forestry measures and the biomass measures used in production ecology. Tools and rules of thumb will be provided to convert the forestry growth and yield values into primary productivity

and production efficiencies, and vice versa. In ecological studies in the temperate zone of central Europe, direct physiological measurements of the gas exchange in plants and indirect estimations based on energy balances, litter production, or evaporation rates provide approximate values for gross primary production (GPP) of 20–40 t ha^{-1} yr^{-1} or 2–4 kg $m^{-2}yr^{-1}$ and net primary production (NPP) of 10–20 t ha^{-1} yr^{-1} or 1–2 kg m^{-2} yr^{-1}, respectively. Forest inventories and long-term experimental plots, on the other hand, report an average growth of merchantable wood volume of 10–20 m^3 ha^{-1} yr^{-1}. This chapter explains how to convert wood volume growth data to NPP through multiplication with the specific wood density, biomass expansion factors, and turnover rates and to GPP by adding respiration.

(1) The gross primary production (GPP) (in t ha^{-1} yr^{-1}) refers to the total biomass in a certain time period and area synthesised through photosynthesis. The net primary production (NPP) (in t ha^{-1} yr^{-1}) is defined as the biomass that remains after subtraction of the continuous losses through respiration. Growth is defined as the total biomass produced by a plant or a stand within a defined period (e.g. day, year, 5-year period). Depending on whether the biomass that was lost and turned over within this period (i.e. leaves, fine roots, branches or entire plant individuals) is included or not, we refer to gross or net growth. Yield is defined as the entire produced and accumulated biomass since the establishment of a stand. We distinguish gross and net yield, in analogy to the differentiation between gross and net growth. Gross yield includes the entire above and below ground ephemeral biomass losses like leaf litter, fine root turnover, and loss of entire tree individuals through mortality and/or thinning.

(2) In conventional forestry, which aims to produce stem wood, the approximate relative proportions of NPP, net biomass growth, and net stem growth harvested to 100% GPP are 50%, 25%, and 10%, respectively. This means that only 10% of GPP, or 20% of NPP, is merchantable and actually harvested in traditional forestry practice. The harvest index (HI = biomass extracted/NPP) is 0.2, or 0.3 when the intermediate thinning is included. Thus, compared to HI for agricultural grass crops (up to 0.85), root crops (up to 0.86), or fast growing tree plantations such as willows, poplars, and eucalypts (up to 0.60), HI for traditional multifunctional forest management is much lower.

(3) A list of the most important forestry parameters and their values is provided for temperate stands of central Europe. Growth or increment describes the rate at which the volume or coverage of a plant or a stand changes in a given time period current annual increment (CAI) expresses growth over one year, whereas periodic annual increment (PAI) expresses the mean growth over a period of more than one year. Yield is the entire biomass produced and accumulated since the stand establishment. Gross yield includes the accumulated turnover from the time of stand establishment, whereas net yield does not. The long-term productivity of a plant or a stand on a given site is expressed best by the mean annual increment MAI (synonym mean annual growth), obtained by dividing the yield at a given time n by the age t: $MAI = yield_n/t_n$. These terms are equally valid at the tree or stand level. For the main tree species in the temperate forests of central Europe maximum

PAI_V values typically lie in the order of $8-20\,m^3\,ha^{-1}\,yr^{-1}$, MAI_V values $5-19\,m^3\,ha^{-1}\,yr^{-1}$. While old stands on good sites may hold $1000\,m^3\,ha^{-1}$ and more, the German national forest inventory comes up with average stand volumes between 274–480 $m^3\,ha^{-1}$.

(4) To convert standing stem volume or merchantable volume to total biomass, the following factors are applied ("≅" indicates thumb values): wood volume v (m^3) is converted to wood biomass w(t) by the specific wood density R ($w = v \times R$ with $R \cong 0.5\,t\,m^{-3}$); the merchantable volume, or merchantable biomass is multiplied by the brushwood factor $e_{br} \cong 1.5$ to obtain total volume, or aboveground total woody biomass respectively. In general, the reference value $e_l = 1.05$ provides a good estimation of leaf biomass for broadleaves (early mature to mature stands), whereas the conifer needle biomass is already included in the brushwood factor. As roots make up approximately 10–45% of the total tree biomass, we recommend using $e_r \cong 1.25$. The overall scaling factor $e_{br,l,r}$ for the direct conversion of merchantable wood volume, or biomass to total tree volume, or tree biomass, respectively can be calculated by $e_{br,l,r} = e_{br}e_le_r = 1.50 \times 1.05 \times 1.25 \cong 2.0$.

(5) The turnover during stand development incorporates the turnover of short-lived plant organs (bark, branches, leaves, roots), and entire trees that are removed through self-thinning or harvesting. For temperate forests in central Europe, we assume an ephemeral turnover factor of $t_{org} \cong 1.3$; volume or biomass growth MAI, PAI, or CAI is multiplied by t_{org} to obtain total primary production [e.g. NPP = MAI(total biomass) t_{org}]. The turnover factor $t_{ind} \cong 1.50$ (1.08–1.77) estimates the total volume production (i.e. including removed trees) from the volume of the remaining stand; in other words the standing volume is multiplied by $t_{ind} = 1.50$ to obtain total volume production. The turnover depends on site conditions, stand age, species, and stand treatment, and estimated turnover is associated with considerable uncertainty.

(6) To determine harvested volume from the standing volume of stem wood including stump and bark, *v*(standing o.b.), the standing volume is multiplied by a reduction factor $l_s = 0.90$ due to the loss of the tree stump, which remains in the forest in conventional forestry harvesting practices. An additional loss factor $l_b = 0.80$ to $l_b = 0.94$ accounts for 6–20% bark loss, which is species-dependent. Therefore, the actual harvested volume comprises 72–85% of the standing volume over bark.

(7) Many tree species develop dead heartwood during their ontogenesis. In the comparison of growth and yield of woody and herbaceous plants, it makes sense to distinguish the living or active tree biomass, i.e. the sapwood, and the dead biomass, i.e. the heartwood. We specify the growth and yield of the living, or active, biomass as "true" growth and yield, while the dead heartwood falls into the category of the turnover. The true biomass can be estimated from the total biomass with a simple factor f_{sw} [biomass(living) = biomass $\times$ f_{sw}], which presents the proportion of sapwood of the total wood. For Norway spruce, Scots Pine, Sessile oak, and European beech, the factor f_{sw} displays a species-specific decrease from $f_{sw} = 1.0$ in the juvenile phase to 0.25–0.50 in the mature phase.

(8) The biomass stored in a forest consists of 90–95% carbon, hydrogen, and oxygen (44–59% C, 42–46% O, 5–7% H) and the remaining 5–10% is comprised of N (1–5%), K, Ca, Mg, P, S, Cl (0.1–2.0%), Fe, Mn, Zn, Cu, B (5–200 ppm), and Mo (0.2–5 ppm). The C content is almost similar in all plant organs and lower in leaves. Since this difference is negligible at the whole-tree level, carbon is generally assumed to make up 50% of total plant biomass. The total biomass of evenaged central European forests about 100 years old ranges from $189\,\mathrm{t\,C\,ha^{-1}}$ (European larch) to $506\,\mathrm{t\,C\,ha^{-1}}$ (Norway spruce). A biomass value of $300\,\mathrm{t\ ha^{-1}}$ or $30\,\mathrm{kg\ m^{-2}}$, equivalent to $150\,\mathrm{t\,C\,ha^{-1}}$ or $15\,\mathrm{kg\,C\,m^{-2}}$, serves as an approximation of the average standing biomass of managed forests in central Europe.

(9) While leaves, bark, and branches constitute only a minor part of the total biomass, they contain a major fraction of the total nitrogen and other nutrient minerals. Although nutrients in the vegetation are always recycled, at the end of the rotation period, the forests have temporarily stored an estimated $1–3\,\mathrm{t\ ha^{-1}}$ minerals in the vegetation. In a sample calculation for different stands at age 100 (medium site quality), the sum of nitrogen and phosphorus ranged from $0.498\,\mathrm{t\,ha^{-1}}$ (Scots pine) to $1.283\,\mathrm{t\ ha^{-1}}$ (Sessile oak) and the amount of K, Ca, and Mg from $0.508\,\mathrm{t\,ha^{-1}}$ (Scots pine) to $1.654\,\mathrm{t\ ha^{-1}}$ (European beech). On nutrient-poor sites, in extreme cases, the vegetation may contain one third of the total ecosystem nitrogen. Harvesting crown, bark, or brushwood significantly enhances the loss of mineral nutrients, which becomes especially critical on sites with limited nutrient availability.

(10) Energy, nitrogen, and water use efficiency (EUE, NUE, and WUE) specify productivity per resource demand (e.g. EUE = productivity/global radiation). For EUE, we assume an annual sum of global radiation in the denominator of $36{,}000\,\mathrm{GJ\,ha^{-1}\,yr^{-1}}$ for central Europe between 47° and 57° N. The $\mathrm{EUE_V}$ relates the growth of merchantable wood volume ($\mathrm{m^3\,ha^{-1}\,yr^{-1}}$) to the annual sum of global radiation ($\mathrm{GJ\,ha^{-1}\,yr^{-1}}$) and ranges from $0.23\ \mathrm{l\ GJ^{-1}}$ for European oak to $0.46\ \mathrm{l\ GJ^{-1}}$ for Norway spruce. Using NPP as the productivity measure, the $\mathrm{EUE_{NPP}}$ amounts to $0.26\,\mathrm{kg\,GJ^{-1}}$ for Scots pine and $0.44\,\mathrm{kg\,GJ^{-1}}$ for European beech. When measuring productivity in terms of calorific value, $\mathrm{EUE_{cal\ NPP}}$, we assume an equal calorific value for broadleaved and conifer wood of $20\,\mathrm{kJ\,g^{-1}}$ ($1\,\mathrm{g\,biomass} \mathrel{\hat{=}} 20\,\mathrm{kJ} \mathrel{\hat{=}} 0.0056\,\mathrm{kWh} = 4.78\,\mathrm{kcal}$). Relating the calorific value to the global radiation, the resulting $\mathrm{EUE_{cal\,NPP}}$ values of 0.005–0.009 reveal that the efficiency of the conversion of sun energy to biomass production is only $<1\%$.

(11) Nitrogen use efficiency (NUE) relates the stand productivity to the foliage nitrogen content, which was estimated to vary between 48.9 and $167.4\,\mathrm{kg\,ha^{-1}}$ in temperate forests (calculated from averages of species-specific stand volumes for the class of 81–100 years of age). This results in $\mathrm{NUE_V}$ values of 108.7–293.5 litres of merchantable wood volume per kg foliage nitrogen. When related to the aboveground biomass production, the efficiencies assume values of $\mathrm{NUE_B}$ as 59.5–243 kg aboveground biomass per kg leaf N and $\mathrm{NUE_{NPP}}$ as 96.6–394.9 kg NPP per kg foliage nitrogen.

(12) Water use efficiency (WUE) relates stand productivity to annual stand transpiration. The latter lies between 285 and 363 mm yr^{-1} (= litres m^{-2} yr^{-1}) in temperate forests. In relation to the annual growth of merchantable wood volume, WUE_V amounts to 2.7–5.7 cm^3 wood volume per kg H_2O; for aboveground biomass growth, WUE_B is 1.5–3.3 g per kg H_2O and for NPP is 2.7–5.1 g per kg H_2O, respectively.

(13) Hence, large quantities of water and energy are necessary to produce one unit of wood, e.g. approximately 1 J of energy fixed in wood for 100–200 J global radiation, 1 g wood for 500 g H_2O transpirated. In contrast, for nitrogen, the relation is reversed, e.g. 100–400 g wood production for 1 g N stored in the leaves. In simple words, when water and energy form the basis of your "soup", nitrogen and other nutrient minerals constitute the "salt".

Chapter 3
Brief History and Profile of Long-Term Growth and Yield Research

3.1 From Rules of Thumb to Sound Knowledge

Forests have a life span extending well beyond the duration of the working life of an individual researcher. The variation in site conditions, and the resulting diversity in forest growth development, prohibits a generalisation of results from individual local investigations. These forest characteristics make experimentation difficult and require specific investigation methods with temporal and spatial scales extending beyond those adopted in physics, medicine, or agriculture. Therefore, the experimental planning and analysis methods elaborated in standard texts from Cochran and Cox (1957), Jeffers (1960), Linder (1953), Mudra (1958), Munzert (1992), Rasch et al. (1992), and Weber (1980), among others, have only limited transferability to forest growth and yield research.

Visionary researchers such as Franz v. Baur, Bernhard Danckelmann, Ernst Ebermeyer, August v. Ganghofer, Karl Gayer, Carl Heyer, Gustav Heyer, Friedrich Judeich, and Arthur v. Seckendorff-Gudent conceptualised the technical and organisational guidelines for long-term forest yield research across a broad spectrum of research sites during the 1860s and 1870s. The observation and experience of the earlier school of thought needed to be supplemented or replaced by comprehensive measurements on long-term experimental plots. From 1870 onwards, the first Forest Experimental Stations were established in forest regions in Baden, Bavaria, Prussia, Saxony, and Württemberg under the jurisdiction of the above-named founding fathers. These Experimental Stations and those established afterwards lead to the foundation of the Association of German Forest Research Stations (Verein Deutscher Forstlicher Versuchsanstalten) in subsequent years to promote experimental forestry through the development of standardised working plans and methods, the allocation of tasks, and the coordination of analyses and publications. In 1892, the Association of German Forest Research Stations initiated the Association of International Forest Research Stations (Internationaler Verband Forstlicher Versuchsanstalten). The forestry research identities mentioned above paved the

H. Pretzsch, *Forest Dynamics, Growth and Yield: From Measurement to Model*,
DOI: 10.1007/978-3-540-88307-4_3,

way for the foundation of the International Union of Forest Research Organisations (IUFRO) in 1929 and the German Union of Forest Research Organisations (Deutscher Verband Forstlicher Forschungsanstalten) in 1951.

Commencing with the establishment of the first long-term experimental plots in the 1860s and 1870s, forest research organisations have developed a range of specific methods for research design, establishment, and management over the ensuing 140 years without which forest growth and yield research, and hence the provision of reliable information to forestry management, would not be possible. Many of the following examples relate back to the network of long-term experimental plots in Bavaria, currently comprising 162 experimental plots with 1,095 trial plots and an area of 175.2 ha (at 01.01.2008). Yield science traditionally formed, and continues to form, the central division in many forest research stations and centres and thus is frequently perceived to be synonymous with long-term experimental research. Its origin is rooted in the historical development of experimental forestry, which began with the organisation of experimentation on the long-term experimental plots in the middle of the nineteenth century.

Already in the nineteenth century, the long life span and ecological diversity of forests often led to the adoption and application of "supposed" knowledge without circumspection. A forest's long response times to management practices, e.g. to the selection of initial spacing or thinning regimes, meant that a forester rarely gained an overview of the long-term consequences of his/her practices in their entirety. The temporal scale also prohibited testing observations and hypotheses. Moreover, the local observations of forest growth could not be related to other sites due to regional orientation of forestry management. Therefore, the forester tended to make unwarranted generalisations based on his or her local knowledge. The cliché that claims if 10 silviculturalists were confronted with a forest and a silvicultural task, they would come up with at least 10 different optimal solutions is due to the rigid adherence to supposed experiential knowledge. Furthermore August v. Ganghofer, Officer of the Royal Bavarian Forest Department and founder of the yield science research in Bavaria (Fig. 3.3), noted that (1877, pp. I–II) "... the critical forester looked at anyone sceptically who dared to promote his own views as substantiated knowledge, and challenged the dogmatic regulations passed on from generation to generation every now and then. Many an old grumbler turned up their noses as Hartig, in his text book for foresters published in 1791, attempted a systematic presentation of silvicultural rules that were acknowledged as established at the time but, more realistically, were merely believed" (translation by the author). In this text, August v. Ganghofer called for a systematic investigation of forest growth based on measurements made over long time periods on widely distributed experimental sites. At the same time he promoted the establishment of research institutions able to conduct research of this kind. In his work, *Das Forstliche Versuchswesen* (author's translation: *Forestry Research*) published in 1877, he outlined a procedure for the systematic expansion of growth and yield science knowledge from long-term scientific investigations, convinced that conclusions drawn from investigations limited to short periods of stand development under specific site conditions were in danger of being premature and leading to unreliable generalisations (Ganghofer, 1877).

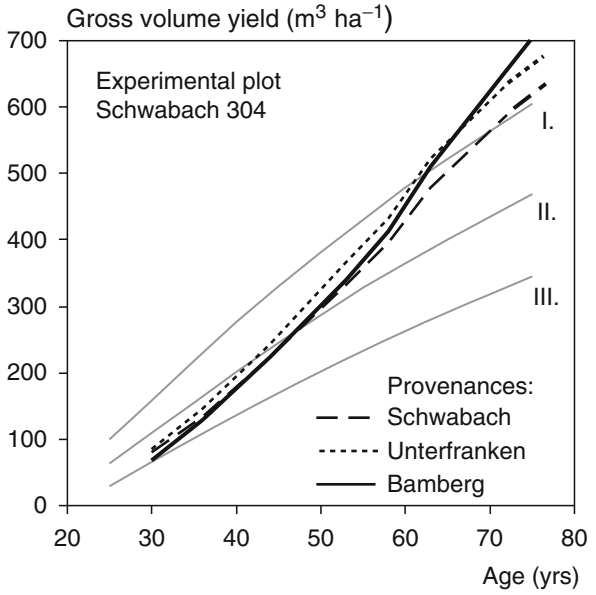

Fig. 3.1 The relevance of long-term experimental plots for sound knowledge exemplified by the Scots pine provenance trial at Schwabach 304 (first survey 1927, latest survey 2003). The final ranking in gross volume yield among the provenances Bamberg, Schwabach, and Unterfranken is only apparent after decades of research. The expected gross volume yield according to the yield tables from Wiedemann (1943a) for moderately thinned Scots pine stands, provides a reference

The provenance experiment Schwabach 304, established in 1927 for the tree species Scots pine, provides an example. This long-term experimental plot showed the production of the provenance Bamberg to be inferior up to an age of 50 years (Fig. 3.1, solid line) compared to the Schwabach and Unterfranken provenances (dashed and dotted lines, respectively). Only the continuation of observations to the present has revealed the superiority of the Bamberg provenance as the stands matured. If the investigation had been closed before the trees were 50 years old, neither the marked superiority of all provenances compared to the Scots pine yield tables by Wiedemann (1943a) for moderate thinning nor the late change in ranking of provenances would have been identified. Yet, even with an observation period extending beyond the typical rotation age, only the results of investigations that are part of a series of widely spread experimental plots permit generalisations about the suitability of the pine provenances. As was common at the time experimental forestry was established, each of the different provenances were replicated only once on Schwabach 304, and consequently the results cannot be backed by statistics.

3.2 Foundation and Development of Experimental Forestry

In the mid-nineteenth century, when other natural science disciplines also experienced a transition to more systematic experimental research approaches, visionary forestry personalities such as Franz v. Baur (1830–1897), Bernhard Danckelmann (1831–1901), Ernst Ebermayer (1829–1909), August v. Ganghofer (1827–1900), Karl Gayer (1822–1907), Gustav Friedrich Heyer (1826–1883), Johann Friedrich Judeich (1828–1894), and Arthur v. Seckendorff-Gudent (1845–1886) devised a concept for long-term investigations in forest science with extensive research sites. Franz v. Baur, professor at the School of Agriculture and Forestry in Hohenheim, Ernst Ebermayer, professor at the Bavarian Central Forestry Training Centre for Agricultural Chemistry and Soil Science in Aschaffenburg, Gustav Friedrich Heyer, Director of the Royal Prussian Forestry Academy in Münden, Johann Friedrich Judeich, Director of the Royal Saxon Forestry School in Tharandt, and Johann Oser (1833–1912), professor at the Forestry School in Mariabrunn, met in Regensburg in 1868 to develop recommendations for the advancement of experimental forestry. Teachings that, until then, were primarily derived from observations and experiential knowledge, were to be supplemented or replaced by replicable measurements on long-term experimental plots. The participants recommended the creation of forest experimental stations with responsibilities for the planning, establishment, technical survey, analysis, and management of long-term experimental plots. From 1870 onwards, the first experimental stations were established in these regions under the influence of the founding fathers, including in Baden, Bavaria, Hessen, Prussia, Saxon, and Württemberg.

Franz v. Baur, the first Head of the Württemberg Forestry Experimental Station and later head of experimentation in forest yield science as professor of Forest Yield Science in Munich from 1878 to 1897, believed that the cross-regional research, essential for silvicultural and yield science research, would be achieved best through cooperation among the experimental stations in the different states. Upon his suggestion the Association of German Forest Research Stations was founded in 1872 in Braunschweig. At this meeting Bernhard Danckelmann, representing Prussia, Karl Gayer from Bavaria, Ludwig Bose (1812–1905) from Hessen, Theodor Hartig (1805–1880) and Ludwig Wilhelm Horn (1829–1897) from Braunschweig, Karl Schuberg (1827–1899) and Friedrich Krutina (1829–1904) from Baden, Max Kunze (1838–1929) from Saxony, and Franz v. Baur from Württemberg drafted the mission of the Association of German Forest Research Stations. This aimed to promote experimental forestry by the standardisation of working plans, development of uniform investigation methods for survey and analysis, division of tasks, and joint analysis and publication of results. Bernhard Danckelmann and later Adam Schwappach (1851–1932) were responsible for the direction of the Association of German Forest Research Stations located at the main centre of experimental forestry in Eberswalde, Prussia, from 1872 to 1898 and from 1899 to 1925, respectively. In close cooperation with the representatives of the other states, they produced effective working plans, e.g. for the design and coordination of thinning and species mix experiments and for the development of form factor, tree volume, and yield tables (see the Chap. 11 Forest Growth Models).

3.3 From the Association of German Forest Research Stations to the International Union of Forest Research Organizations (IUFRO)

Following the success of the cooperation between states the Association of German Forest Research Stations founded the Association of International Forest Research Stations at the annual meeting in Eberswalde in 1892 to extend cooperation beyond the national boundaries.

Participants at this meeting included Friedrich Krutina (1829–1904) from the Baden Forestry Experimental Station, Karl Kast (1859–1943) from the Bavarian Forestry Experimental Station, Ludwig Wilhelm Horn (1829–1897) from the Experimental Station at Braunschweig, Carl Eduard Ney (1842–1916) from the Experimental Station at Alsace-Lorraine, Karl Wimmenauer (1844–1923) from the Hessian Experimental Station, Bernhard Danckelmann and Adam Schwappach from the Central Forestry Experimental Station in Prussia at Eberswalde, Carl Julius Tuisko Lorey (1845–1901) from the Württemberg Experimental Station, Joseph Friedrich (1845–1908) and Roman Lorenz Ritter v. Liburnau (1825–1911) from the Austrian Experimental Station, and Anton v. Bühler (1848–1920) from the Swiss Experimental Station (IUFRO 1993).

Although the Association of International Forest Research Stations initially comprised central European countries, it quickly expanded to include representatives from Scandinavia, Southern and Eastern Europe, Asia, and the Americas so that 25 nations were incorporated already by 1910. At the time it was founded, the aims of this association were to promote the development and standardisation of methods of experimental design, inventory, and analysis of long-term experiments (Killian 1974). After World War I, the composition and aims of the Association of International Forest Research Stations were reviewed at a conference in Stockholm in 1929. Then, not only the Forestry Experimental Stations but all forestry research institutions were included in the union, which became known as the International Union of Forest Research Organisations (IUFRO). The Association of International Forest Research Stations, and later the IUFRO, stem from the Association of German Forest Research Stations, established in 1872 to ensure the continuity in and the standardisation of long-term forest growth and yield experiments.

3.4 Growth and Yield Science Section of the German Union of Forest Research Organisations

Eilhard Wiedemann (1891–1950), Schwappach's successor as the Director of the Prussian Forestry Experimental Station in Eberswalde from 1927 to 1934, was the first to put the newly formulated ideas for experimental forestry into practice and develop them further (Fig. 3.2). Thus the research direction adopted by Schwappach, Wiedemann, and then Schober provides a prime example of scientific continuity.

Fig. 3.2 Founders, pioneers, and driving forces behind long-term growth and yield research in North Germany. (Photos: Archives of Niedersächsische Forstliche Versuchsanstalt in Göttingen and Landesforstanstalt in Eberswalde)

The effect of Wiedemann's work can still be seen today in the large-scale and long-term cross-sectional analysis established for the main tree species in pure stands, resulting in a series of monographs and yield tables for different treatments (see the Chap. 11 Forest Growth Models). In the 1930s, these investigations were expanded to mixed stands, where he analysed the relationships between site conditions and stand dynamics. Despite political resistance, he persevered with the

supervision and systematic expansion of the Prussian growth and yield experimental plots during World War II and thereafter. As the Russian army advanced, he saved his unique database from Northern and Eastern German experimental plots by moving it from Eberswalde to Sarstedt, near Hannover, where he worked towards the establishment of the Lower Saxony Forest Research Station in Göttingen in 1950 (Spellmann et al. 1996). Such long-term cross-generation observations, scientific effort, and further development of a network of experimental plots require creative will and determination from scientists, who perceive themselves to be the guarantors of research continuity.

Schober (1906–1998), one of Baader's students—also professor of Forest Management and Yield Science at the University of Göttingen and Wiedemann's successor as Director of Lower Saxony Forest Research Station—secured the continued existence of the national research organisation by initiating the establishment of the German Union of Forest Research Organisations (Deutscher Verband Forstlicher Forschungsanstalten) in Bad Homburg in 1951. As a counterpart to the International Union of Forest Research Organisations, and as the institution succeeding the Association of German Forest Research Stations, this Union still unites the forestry research institutions in Germany today. In the German Union of Forest Research Organisations, experiments in growth and yield science have been of particular importance since the beginning. Since 1951, the Growth and Yield Science Section (Sektion Ertragskunde im Deutschen Verband Forstlicher Forschungsanstalten) has continued to develop the research direction of the Association of German Forest Research Stations. Between 1951 and 2008, 58 annual conferences were held, the establishment, survey, and analysis of research data coordinated, and recommendations made for the planning, establishment, management, and analysis of investigations (Weihe 1979). While initial working plans and recommendations related primarily to the planning, establishment, and survey of monitoring plots, later recommendations also were carried forward for the evaluation of investigations and the development of models. Examples include the recommendations for the management of foreign tree species (Deutscher Verband Forstlicher Forschungsanstalten 1954), fertilisation and amelioration experiments (Hausser et al. 1969), thinning and release experiments (Deutscher Verband Forstlicher Forschungsanstalten 1986a, b), forest decline and growth (Deutscher Verband Forstlicher Forschungsanstalten 1988), standardised evaluation of long-term growth and yield experiments (Johann 1993), and the standardisation and evaluation of forest growth simulators (Deutscher Verband Forstlicher Forschungsanstalten 2000).

3.5 Continuity in Management of Long-Term Experiment Plots in Bavaria as a Model of Success

Identities in forest research are characterised by their recognition of the need for long-term and large-scale investigations in naturally developed forests or silviculturally managed forests. They are convinced that the advance of knowledge about

forest growth requires long-term investigations (Wiedemann 1928, 1948, 1951). They measured forest dynamics in long time series, often without immediate benefit, in recognition of the usefulness of resulting datasets in 100 years, just as we base our computer models today on the data our great-grandfathers measured. The forest science approach is long-term, large-scale, and thus, in some respects, contrary to the "zeitgeist". The maintenance and expansion of a network of long-term experimental plots assumes that forestry management and development institutions perceive the need for the promotion of long-term research projects to gain knowledge about long-term development processes.

In Bavaria, August v. Ganghofer, head Public Servant of the Royal Forest Department, and Franz v. Baur, the first Director of Yield Science at the University of Munich, are credited for the initiation of systematic forestry research (Fig. 3.3). In the 1870s, the systematic development of a network of experimental plots for growth and yield science research commenced in Bavaria as well as in other states, which all employed the same methods. More than 130 years after their establishment, many of the first experimental sites are still being monitored today, e.g. the European beech thinning experiments Fabrikschleichach 15, Mittelsinn 25 and Hain 27, established in autumn 1870 and spring 1871 in the traditional system of three thinning grades (A, B, and C grade), have been inventoried about 20 times since then. Currently about 170 years old, these experimental plots are impressive examples of experiments managed under leadership spanning generations. As the oldest experiments, they are one of the very few sources of information on long-term stand development under different thinning regimes. They have proven invaluable in forestry assessment, yield table compilation, and decision support and in the identification of growth trends, the derivation of site-production relationships, climate change research, or as examples in teaching and further education. These experimental plots still may serve to answer questions yet to be asked.

After Franz v. Baur occupied the Chair of Growth and Yield Science in Munich, which, at that time, also encompassed the discipline Forest Management, from 1878 to 1897, he was succeeded by Rudolf Weber from 1897 to 1905 and Vincenz Schüpfer from 1905 to 1937. Both Weber and Schüpfer used the database from the Bavarian monitoring plots to develop technical principles for forest management, such as the form-factor tables, volume tables, and assortment tables. They also expanded the range of tree species in the network of experimental plots. With the exception of Rudolf Weber, v. Baur's successors held the position for long periods of time—Vincenz Schüpfer was active for 32 years—so that individual researchers were able to provide continuity in forestry research through long-term observation and analysis.

Karl Vanselow, representative of the Forest Growth and Yield Science in Munich from 1937 to 1951, was first and foremost a silviculturalist and forest manager. The yield tables he developed for Norway spruce in South Bavaria and his investigations into the effects of plant spacing and thinning on the growth of Norway spruce and Silver fir were based largely on the Southern Bavarian Norway spruce experiments in Denklingen, Egelharting, Ottobeuren, Sachsenried, and Wessling—experiments his successors also could access to a large degree.

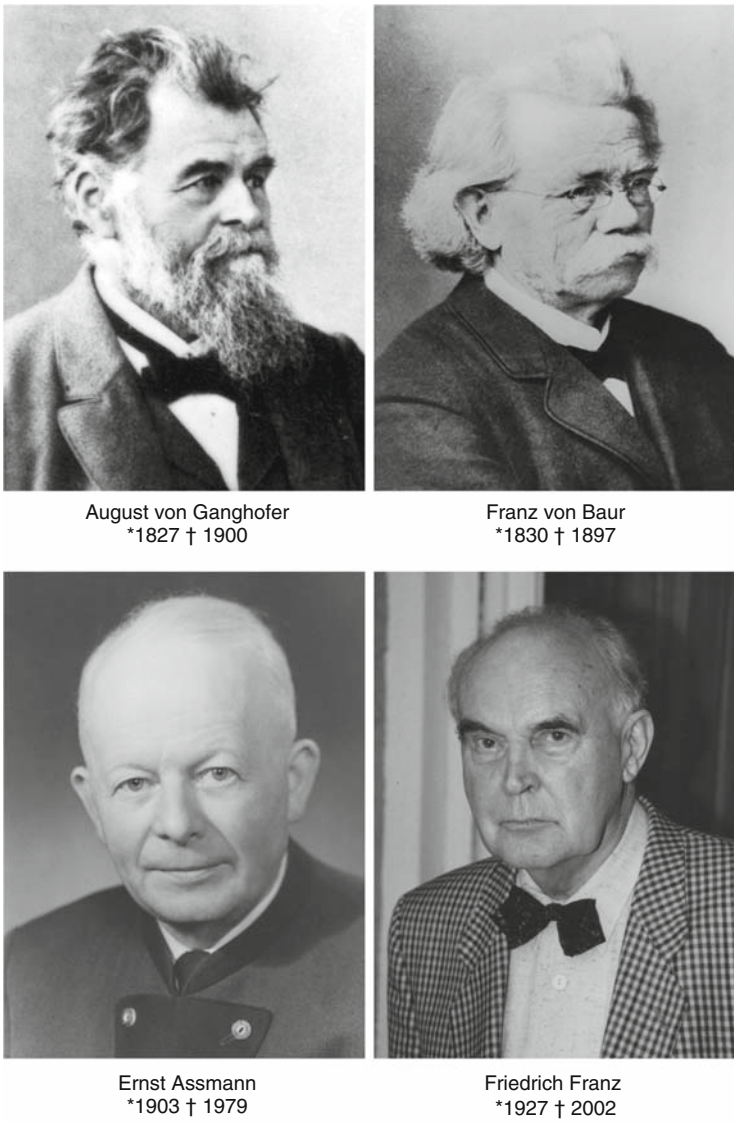

Fig. 3.3 Founders, pioneers, and driving forces behind long-term growth and yield research in Bavaria. (Photos: Archives of Chair for Forest Growth and Yield Science, Technische Universität München)

Ernst Assmann, Director of the Munich Yield Science Institute for 21 years from 1951 to 1972, contributed to the major advancement of forest growth research with the discovery of new relationships and the development of growth models, which still assist assessments and decisions confronting forestry practice today (Fig. 3.3). Through long-term observation of experimental plots, he found a clear relationship

between stocking density and growth performance. Assmann also introduced site-specific, subdivided special yield levels in his yield tables, developed the basal area density as a measure of stand density and stand management, and analysed growth acceleration resulting from early forestry operations (Assmann 1970). He maintained that neither the investigation of these relationships nor the development of regional and site-specific yield tables would have been possible without direct access to the network of long-term experimental plots in Bavaria. Ernst Assmann expanded this network by including fertilisation experiments and mountainous mixed forests experiments. Through his thorough investigations of forest growth, ecology, and physiology, he enabled a causal analysis of individual tree and stand growth behaviour. In the forest ecosystem project Ebersberg, he brought together forest growth, ecophysiological, soil, and meteorological investigative approaches in an older Norway spruce experimental plot to understand and explain the observed forest growth structures and processes at different levels of spatial and temporal resolution.

The introduction of data processing and biometry in experimental forestry and forest growth and yield research, an important stimulus for German forestry in the 1960s in general, is closely associated with Friedrich Franz, a leading figure at the University of Munich from 1973 to 1993 (Fig. 3.3). The opportunities provided by electronic data processing facilitated a more thorough analysis of data from experimental plots and better utilisation of this information in forestry practice. This innovation enhanced the value of long-term experimental plots further still as the potential of the information stored in the database could be accessed more readily. The further development of methods of inventory and modelling, particularly prediction and simulation methods, leading to the development of yield tables, site production tables used frequently for wood supply scenarios and predictions were important outcomes during his 20 years as head of the Institute of Forest Growth and Yield Science in Bavaria.

In retrospect, the long-term network of experimental plots established by v. Ganghofer provides the continuum for forest growth and yield research at Munich. Franz v. Baur and the five subsequent directors of the forest growth discipline, Rudolf Weber, Vincenz Schüpfer, Karl Vanselow, Ernst Assmann, and Friedrich Franz, were able to gain much knowledge and practical benefit for forestry from the long-term experimental plots. The author, who has been responsible for the network of growth and yield long-term experimental plots in Bavaria since 1994, is deeply indebted to his predecessors as most of the data referred to in this textbook originates from their perseverance and commitment to long-term growth and yield experiments.

3.6 Scientific and Practical Experiments

In experiments, planned treatments are carried out on the object under investigation to identify and quantify cause–effect relationships. Long-term growth and yield experiments aim to obtain information about the growth behaviour of individual trees

and stands, e.g. in relation to stand density. Yet, to support decisions in forestry, the information from individual experiments must be brought together to form a picture of the entire system. For this, forest growth models ultimately merge the investigation results (see the Chap. 11 Forest Growth Models).

Once the research question has been formulated, a plan for the investigation is devised. The design, management, and analysis of an investigation is planned to obtain the best possible answer to the research question asked. As statistical considerations in the design of the investigation layout determine the analysis options, and as the treatments carried out in the investigation (e.g. thinning, fertilisation, or pruning) continue over decades, the design, management, and analysis of experimental plots essentially are interconnected. The large areas needed for multifactor designs, the variability in natural conditions, and the limited control over site factors in the field mean that the question needs to be confined to selected relationships in the system.

For example, if one wishes to investigate stand growth for Scots pine in relation to the main site factors water availability, temperature, atmospheric CO_2 concentrations, radiation, nitrogen availability, and thinning and, furthermore, to apply each factor at five different levels (e.g. water regime: dry, mesic, temporarily dry, temporarily moist, moist), one would require $n = 5^6$ trial plots to record all possible factor combinations. If we were to replicate each factor combination five times for statistical confidence, we would need $n = 5^6 \times 5 = 78{,}125$ trial plots, an impossible number. Therefore, in investigations certain factors are held as constant as possible (constant factors) and others are varied deliberately (treatments). Thus, only a small number of factors may introduce uncontrolled effects (external disturbance factors). In this approach, in which only part of the system is investigated, there is always the danger that the influence of other factors that are not considered in the experiment design is ignored. Due to the large area and the long observation periods required to investigate stand growth, laboratory and greenhouse experiments, which would allow climate, weather, radiation, or CO_2 concentrations to be controlled, rarely are realistic. Due to the space requirements, laboratory experiments are usually restricted to the earlier growth phases and certain factors combinations. They are carried out mostly for individual plants, not for stands.

The traditional approaches in forest growth and yield science encompass scientific and practical field experiments:

In scientific experiments the leading investigator manages the treatments in the investigation. Depending on the question, we can differentiate planting experiments, provenance experiments, planting and plant spacing experiments, thinning experiments, fertiliser experiments, regeneration experiments, mixed stand experiments and experiments for the determination of disturbance factors.

Practical experiments are investigations in the broadest sense in which local foresters manage the treatments. The role of the leading investigator is confined to documenting the treatments in the investigation and inventorying them. Examples are investigations of new regeneration methods, conversion trials, and practical investigations for close-to-nature forest management.

The disadvantage of scientific and practical field experiments is that the factors influencing growth, such as climate, weather, radiation, and CO_2 concentrations,

cannot be controlled. These effects can only be studied by setting up plots in different regions where the factor in question varies. In this case, no active treatment of the plots is undertaken, as the treatment variant results from the selection of sites with the desired factor combination when designing the experiment. The ability to control environmental conditions and to explain system behaviour decreases progressively from laboratory experiments to practical experiments. However, typically, the conclusions drawn from field experiments are more relevant to forestry practice because the transferability of laboratory results to field conditions is limited.

Depending on the degree of accuracy desired, data obtained from inventories (representative forest inventories at the enterprise, state, or national level) or monitoring plots (detailed, continuously repeated surveys of long-term changes: monitoring is commonly not area representative due to the resource-intensive measurements) can be used to test hypotheses, to parameterise growth models, or for the statistical analysis of growth responses. Inventory and monitoring cannot replace long-term experiments because they lack the causal relationships between defined treatments variants and growth responses required for the derivation of growth relationships for individual trees and stands. Rather, the surveys of experimental plots over long time periods complement effectively inventory or monitoring data. For the development of growth models and information systems in forestry, data from long-term experimental plots are essential for understanding cause–effect relationships and inventory data for upscaling on landscape level (cf. Chap. 1, Sect. 1.3).

3.7 Establishment and Survey of Long-Term Experimental Plots

This section provides a brief introduction to the standard methods for the establishment and inventory of long-term growth and yield plots as a basis for our understanding of the principles of forest growth research presented in this book. Since the foundation of the Association of German Forest Research Stations, an international standard for the survey, management and analysis of investigations has been defined to ensure the ready exchange of databases, the comparability of experimental results, and comprehensive analyses [see also Bachmann et al. (2001), Johann (1976), Pretzsch (1996a), and Wiedemann (1931)]. A more detailed introduction to forest mensuration may be gained from textbooks by Akça (1997), Avery and Burkhardt (1975), Bruce and Schumacher (1950), Kramer and Akça (1995), Loetsch and Haller (1964), Loetsch (1973), Meyer (1953), and Prodan (1951, 1961, 1965).

3.7.1 Establishment of Experimental Plots and Trial Plots

Although experimental plots may be established at any time of the year, the measurement of diameter, height, crown size, and growth should be carried out either

before or after the growing season, i.e. in spring or autumn. This ensures that the stand growth characteristics derived from measurements such as tree diameter and height include growth increment for the entire year. It also ensures that the variables are interpreted correctly, that comparisons with other research findings are meaningful, and that the data can be used readily for the parameterisation of models (Chap. 11) or the identification of growth disturbances (see Chap. 15).

3.7.1.1 Permanent Marking of Experimental Plots, Trial Plots, and Plot Surroundings

To facilitate site survey and data evaluation, experimental plots and the trial plots set up within them should be square or rectangular if possible. The entire experimental plot and the individual trial plots are surrounded by a buffer strip to protect them from edge effects or potential influences from other treatments on neighbouring trial plots. The width of the buffer strip should be at least 7.5 m or, when the area is sufficiently large, equal to the length of a mature tree. The trees outside the trial plot whose crowns reach inside the trial plots are called surrounding trees. While the trees on the trial plot are numbered consecutively commencing with 1, the surrounding trees are also sprayed with a number in white, which belongs to a separate number series (usually 900 onwards). A yellow ring painted around the trees along the perimeter of the plot boundary ensures the boundary is clearly visible from outside, identifying the experimental plot and protecting it from accidental forest operations (Fig. 3.4). At the corners of the trial plots, ditches are dug in the direction of the adjacent corners, to permanently mark and secure their location. Durable posts from oak or larch are used to identify the corner points permanently. The trial plot corners are measured in relation to a defined map point (boundary stone, path intersection). The trial plot number should be written on distinct trees at all four corners.

3.7.1.2 Enumeration of Trees

It is advisable to number all trees independently of $d_{1.3}$. Tree numbering begins at the starting point defined for the trial plot, and continues in strips running parallel to the x-axis. On slopes it is advisable to number the trees across the slope to ease the process (Fig. 3.5). The null point for a trial plot corresponds to the origin of the coordinate system; it is also the reference point for recording the stem coordinates. One corner of the trial plot is usually chosen as the null point so that the trees inside the trial plot can be displayed in a single quadrant of a Cartesian coordinate system. Normally, the numbering starts at the null point and follows a continuous serpentine path, continuing along the x-axis to the trial plot boundary, and then returning to the former boundary, each new turn covering a strip further inside the trial plot. The tree number of each individual tree is recorded always during measurements conducted in the first and in repeated surveys.

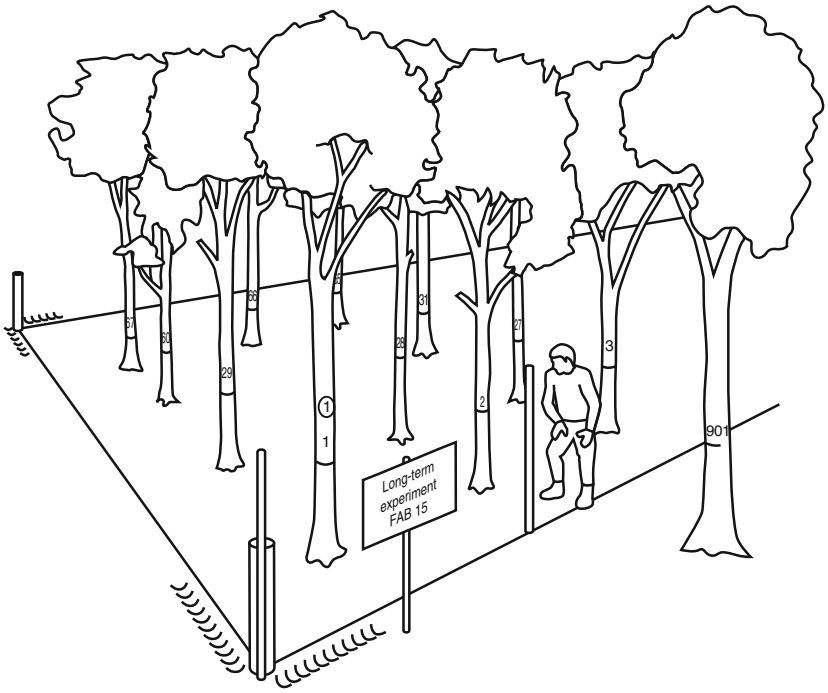

Fig. 3.4 Layout of a long-term experimental plot. The tree numbers assigned and the $d_{1.3}$ measuring position are painted onto all trees. Rectangular trial plots are preferred to assist orientation and reduce the area used when setting up multiple trial plots. Signposts, corner posts, and ditches serve as permanent markers of trial plot boundaries. The surrounding trees reaching inside the trial plot are marked with a separate number sequence

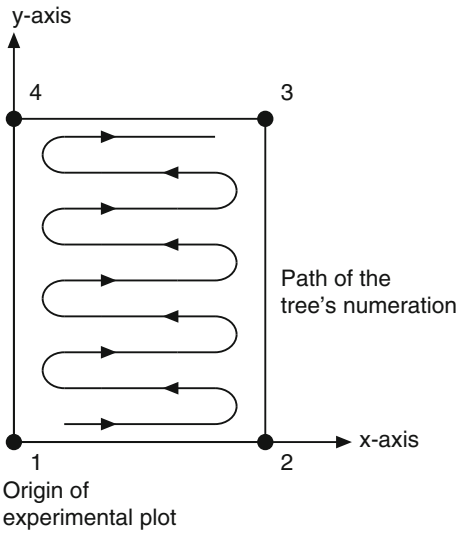

Fig. 3.5 Standard enumeration of trees on long-term experimental plots. The enumeration begins with the tree closest to the origin of the trial plot (corner post 1) and continues to and fro along a serpentine path until corner post 3 is reached

3.7.1.3 Marking the Measuring Position at 1.30 m Height

The $d_{1.3}$ measuring position is permanently marked by painting a white horizontal line on the tree at a height of 1.30 m. As all repeated measurements are carried out at exactly this position, the accuracy of the growth determinations, in particular, can be increased. On a slope, the $d_{1.3}$ position is marked on the uphill side of a tree. On experimental plots located in the vicinity of paths frequently used by the public, tree numbers and measuring positions are marked on the nonvisible side of the trees to preserve the forest aesthetic.

3.7.1.4 Stem Coordinates

On the one hand, stem coordinates are recorded so that individual trees can be identified permanently on long-term experimental plots, but it is also important for the description, analysis, modelling, and evaluation of the spatial structure in forest stands. One method of measurement involves setting up a coordinate system by laying measuring tapes on the forest floor from which to read off the x and y coordinates for the tree position. A second method records the tree positions in polar coordinates with a theodolite or terrestrial laser scanner placed at a few central points with known positions relative to the null point. In this way it is possible to calculate the absolute position of each trial plot and each tree in a regional coordinate system, such as the Gauss–Krüger or the Universal-Transversal-Mercator-System (UTM).

3.7.2 Measuring Standing and Lying Trees

3.7.2.1 Essential Measurements on Standing Trees

The mature stand is recorded to determine the wood volume from individual trees. Due to the greater precision required in repeated inventories of long-term experimental plots, the girth tape is widely used instead of callipers for measuring tree diameter. In all repeated inventories, the diameter at breast height is measured at exactly the same height as in the first survey, on the mark at 1.30 m height (Fig. 3.6a, b). Height measurements are taken from a few representative sample trees mostly using measuring instruments based on the trigonometric principle (Fig. 3.6c). A telescopic height yardstick may be used to measure trees with a height up to 8 m (Fig. 3.6d). It is held perpendicular by one person at the tree to be measured, and it is extended until a second person standing an appropriate distance away indicates that the stick has reached the tip of the tree. The first person then reads off the tree height. The height to the crown base is defined as the height of the lowest green primary branch. It is measured similarly to tree height. To estimate tree volume from diameter and height, the form factor is obtained from standard volume tables or form-factor functions. In the inventory of mature stands, remaining and

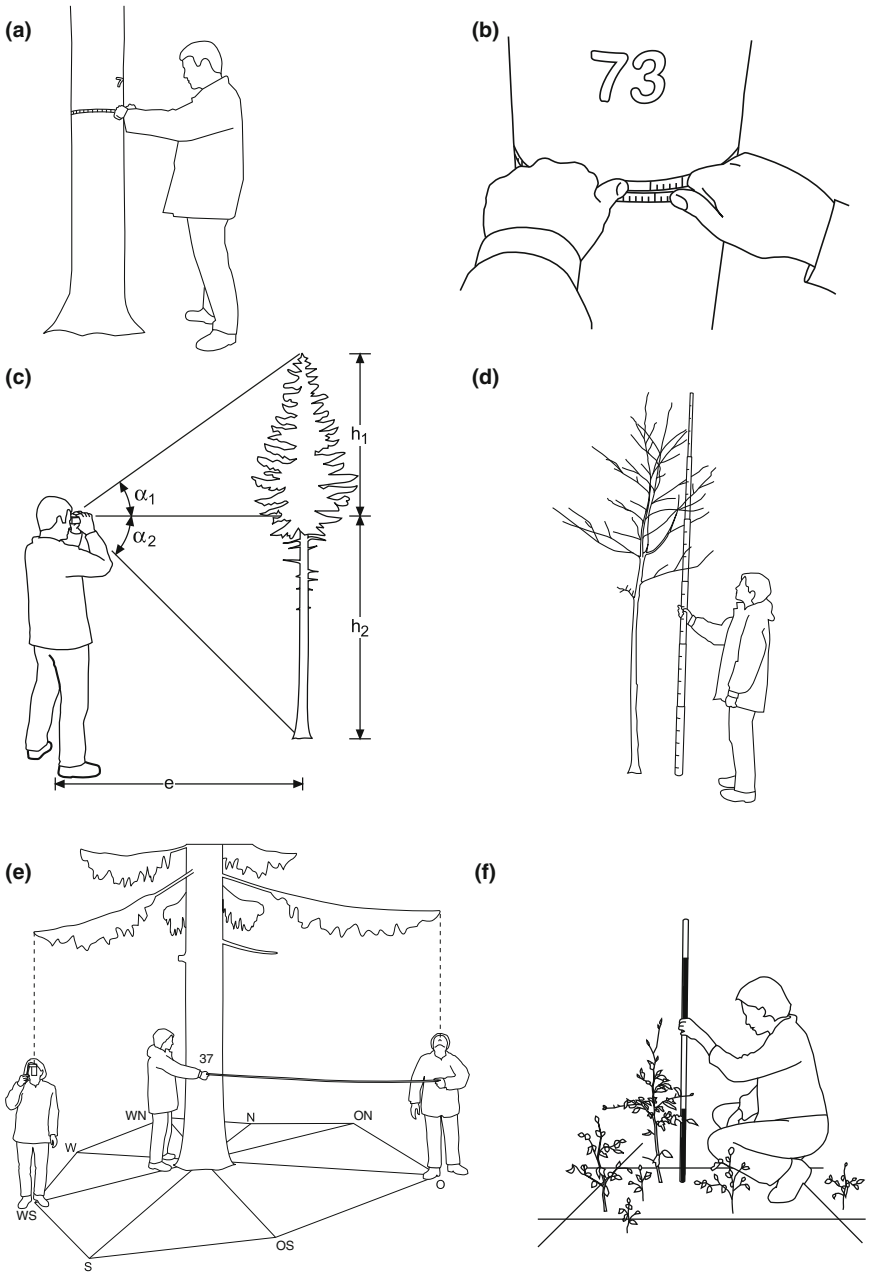

Fig. 3.6 Essential steps for measuring standing trees. (**a**) Measuring the diameter at breast height at 1.30 m with a girth tape; (**b**) the position of the measuring tape should be horizontal. (**c**) Measuring tree height based on trigonometric principles. (**d**) Measuring tree height or retracing shoot length with a telescopic height yardstick. (**e**) Projection of tree crowns by vertical sighting (*right*) and optical plummet (*left*). (**f**) Survey of regeneration on sample quadrates

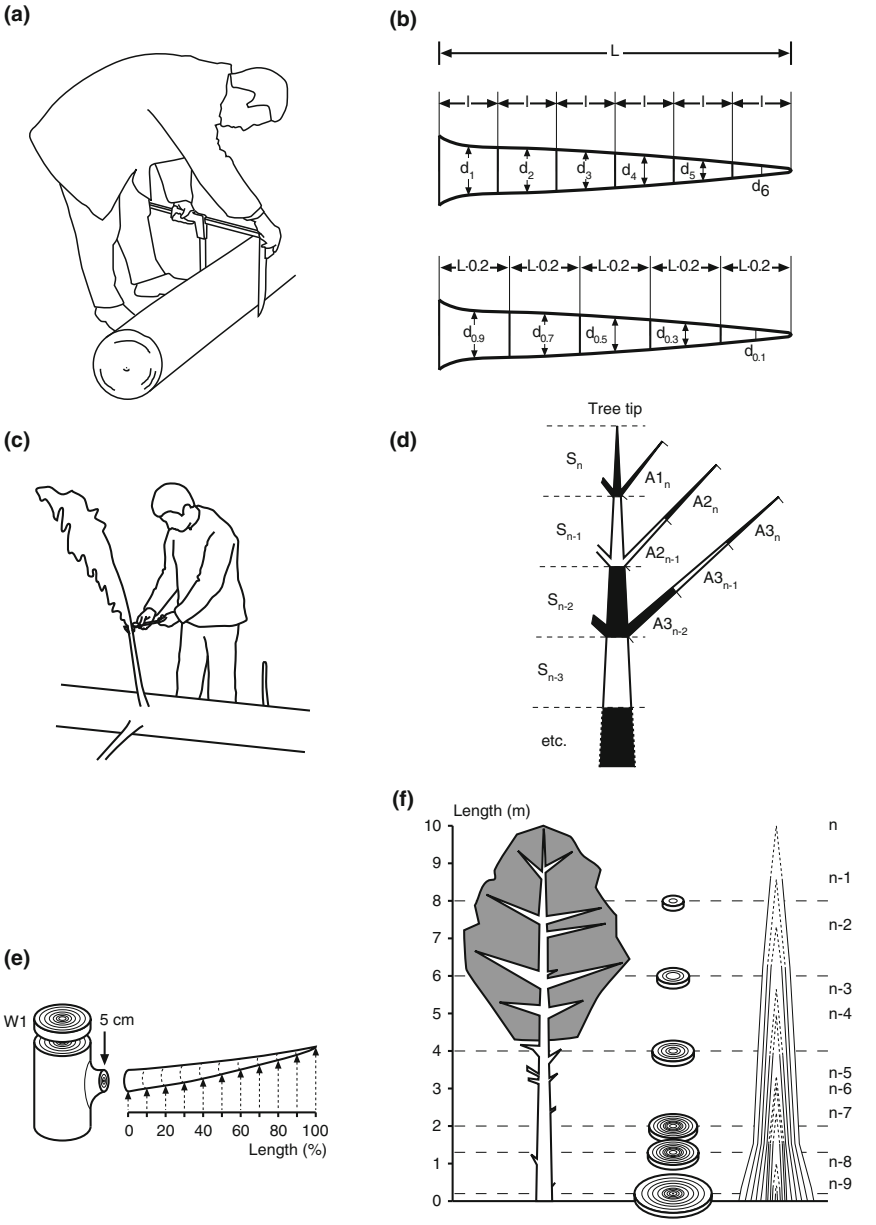

Fig. 3.7 Selected steps of measuring lying trees. (**a**) Stem diameter measurements are made in two directions perpendicular to one another using a calliper. (**b**) To calculate the stem volume, the diameter is measured on sections of equal absolute length (*above*) or relative length (*below*). (**c**) Measure the branch length and branch diameter. (**d**) Measure the annual increment of the leading shoot length retrospectively on the stem and branches. (**e**) Analyse the stem and branch disks near whorls to reconstruct branch development. (**f**) Analyse the stem development by retracing the leading shoot length and tree ring width on stem disks

removed trees are differentiated. To reconstruct stand development, stump inventories and deadwood surveys are usually conducted. For determining crown radii and crown projection area, there are two frequently applied methods: The vertical sighting method (Preuhsler 1979) is quick though rather inaccurate (Fig. 3.6e, right) compared to the projection method, which uses a plummet and is very accurate but time consuming (Röhle and Huber 1985; Röhle (1986) (Fig. 3.6e, left). To inventory the regeneration, the stand is divided into sample squares. At each sample quadrate, the number of seedlings is counted, and the tree species and height class is recorded. The height and shoot length of selected trees is measured (Fig. 3.6f).

3.7.2.2 Selected Measurements on Lying Trees

On experimental plots, volume measurements, stem analyses, and measurements retracing shoot length may be carried out in sections on lying sample trees. The measurement of volume in sections is mainly useful for determinations of stem form, stem volume, form factor, form-factor series, and stem form functions. To determine the volume, the lying stem is divided into sections of equal absolute length (e.g. 2 or 4 m), or in sections of equal relative length (e.g. section lengths = total length/5) (Fig. 3.7a and b). Measurements on lying sample trees can include measurements of (green) branch length, branch diameter, branch dry weight, and foliage weight (Fig. 3.7c). For the reconstruction of the crown morphology, annual increment of the leading shoot length can be measured retrospectively on the stem and branches (Fig. 3.7d). For branch analysis and further crown growth reconstruction, branches from different heights within the crown are selected for measurement. Branch disks are taken from these branches as illustrated in Fig. 3.7e. The stem disks should be extracted directly above the branch whorl to determine relationships between stem and branch ring width development, areas of sapwood that conduct water on the stem and branches, etc. An analysis of stem development and the three-dimensional stem structure is possible by retracing the leading shoot length back along the stem axis and analysing the year rings on stem disks. In Fig. 3.7f, the dotted lines represent the measurements retracing the leading shoot length facilitate the reconstruction of the height development of the tree from the tree top to the stem base; the dashed lines represent the analysis of year rings on stem disks, which delivers measurements for the reconstruction of diameter and stem form development.

Summary

Forests are difficult to investigate due to their longevity, their spatial dimension, and their heterogeneity. Forest science successfully established appropriate research institutions for continuous large-scale investigations on forest growth and yield science. Since the mid-nineteenth century an international scientific community has grown, which has set up a network of long-term experiments, standardised

measurement and data evaluation methods, and developed tree and stand growth models for scientific and practical application.

(1) Commencing in the 1860s, a network of long-term growth and yield experiments was established. In Germany alone this network comprised several thousand individual plots, the oldest of which have been observed for more than 130 years and remeasured more than 20 times. Thanks to the far-sightedness of the founding fathers of the long-term experiments we can utilise the data today, e.g. to record growth trends on a large scale, to analyse the consequences of climate change or to parameterise growth models. The motto "From supposed qualitative silvicultural experience to sound quantitative knowledge" has and continues to bear its fruits.
(2) The first forest research stations were established from 1870 onwards by the founding fathers Franz v. Baur, Bernhard Danckelmann, Ernst Ebermayer, August v. Ganghofer, Karl Gayer, Carl Heyer, Gustav Heyer, Friederich Judeich, and Arthur v. Seckendorff-Gudent in Baden, Bavaria, Prussia, Saxony, and Württemberg in order to support the establishment of long-term growth and yield experiments and practical application of results.
(3) These and other Forest Research Stations established later developed the Association of German Forest Research Stations (Verein Deutscher Forstlicher Versuchsanstalten) with the aim of promoting systematic experimental forest research by the standardisation of working plans, the development of uniform measurement methods, the standardisation of silvicultural treatments, the division of tasks, and the joint analysis and publication of results.
(4) The Association of German Forest Research Stations led to the formation of the International Forest Research Stations (Internationaler Verband Forstlicher Versuchsanstalten) in 1892. Therefore, the above mentioned founding fathers of experimental forestry prepared the way for the establishment of the International Union of Forest Research Organisations (IUFRO) in the year 1929.
(5) The network of experimental plots consists of scientific experiments where the treatments are controlled by the leading investigator. Most common are planting experiments, provenance experiments, planting and plant spacing experiments, thinning experiments, fertiliser experiments, stand regeneration experiments, mixed stand experiments, and experiments for the determination of disturbance factors.
(6) Practical experiments are investigations in the broadest sense in which local foresters are in charge of the treatments. The roll of the leading investigator is confined to the documentation of operations and survey of the investigations. Examples are investigations of new regeneration methods, conversion trials and practical investigations for close-to-nature forest management.
(7) The possibility of relocating experimental plots for decade-spanning observations, of identifying the trees and measuring positions for repeated surveys, and of buffering of experimental plots from the regular forest management in neighbouring stands is ensured by permanently marking the whole experimental area, the plots, and the surroundings. Tree numbers and the measuring position at 1.3 m height are marked on the individual trees. Typically, also the

x, y, and z coordinates of the stem base are recorded for an exact reconstruction of the stand structure.

(8) The mature stand is recorded to determine the wood volume from individual trees. Diameter measurements are carried out with a girth tape. Height measurements are taken from a few sample trees using measuring instruments based on trigonometric principles. The form factor is not explicitly determined but is obtained from standard volume tables or form-factor functions. In the survey of mature stands, remaining and removed trees are differentiated. To reconstruct stand development, stump inventories and deadwood surveys are usually conducted.

(9) The reconstruction of the development of single trees and stands is possible using increment boring and subsequent core analysis. As these techniques cause damage, core extractions should be avoided inside the plots in long-term experimental areas. The use of thinned stems or of stems outside the plots is recommended.

(10) The trees removed from long-term experimental plots are available for measurement as lying trees. The volume determinations in sections along the stem assist determinations of stem form, stem volume, and form factor. Crown structural analysis reconstructs the crown development by retracing the shoot along the stem axis and branches. In stem analyses, the stem is dissected along its entire length; the extracted stem discs facilitate an accurate reconstruction of stem development.

(11) Measurements on long-term experiments deliver time series, sometimes without immediate benefit. However, the resulting datasets are of singular importance in long-time analyses of forest growth; just as today we base our computer models on the data that our great-grandfathers measured. The forest science approach is long term and large scale and therefore in some ways against the "zeitgeist". Nevertheless, the maintenance and expansion of a network of long-term experimental areas require that scientific and administrative institutions are far-sighted enough to perceive the tremendous importance of long-term research projects for the purpose of gaining knowledge about long-term processes.

Chapter 4
Planning Forest Growth and Yield Experiments

4.1 Key Terminology in the Design of Long-Term Experiments

The combined plant spacing–thinning experiment Weiden 611 (WEI 611) for Scots pine includes 24 plots near Weiden in 1974 in the central Upper Palatinate Region in Bavaria (Oberpfälzer Becken und Hügelland, growth region 9) on moderately dry sandy soil with poor nutrient status (Fig. 4.1). This long-term experimental plot will assist the following introduction of terms used in research planning.

Experimental Question. The most common question underlying forest growth and yield science investigations is, what effect does a specific treatment have on the growth of the given research object? In our example (WEI 611), the question is, what effect does plant spacing and thinning have on the qualitative and quantitative aspects of yield (e.g. stem shape, branching, annual volume growth, gross volume yield) of Scots pine? This question is tested for a given range of plant spacing variants (1.25 m × 0.4 m to 2.5 m × 1.6 m) and thinning regimes (maximum density to a density reduced to 50%).

Object of the Investigation. In our example, the object of the investigation is a Scots pine stand. Diameter and height are measured for all individual trees, or a representative sample. The investigation was established on a representative site in growth region 9 in Bavaria to ensure the transferability of the experimental results to forestry practice.

Experimental Treatment. A treatment describes the factor, or factors, imposed on the object to test its effects. The treatment may encompass one or more factors (e.g. pruning and fertilisation) implemented at different levels (e.g. different pruning heights, fertiliser amounts). In our example, plant spacing and thinning form the treatment, although plant spacing does not represent a "treatment" as such. The thinning involves repeated thinning operations during the entire stand rotation. Continuity in the treatments and the elimination of subjective influences can be achieved by defining thinning operations quantitatively (Chap. 5). In our example, a tree number on unthinned control plots provides a reference for the 30–50% reduction in tree number in thinning from above operations on the plots designated for silvicultural treatment.

H. Pretzsch, *Forest Dynamics, Growth and Yield: From Measurement to Model*,
DOI: 10.1007/978-3-540-88307-4_4,

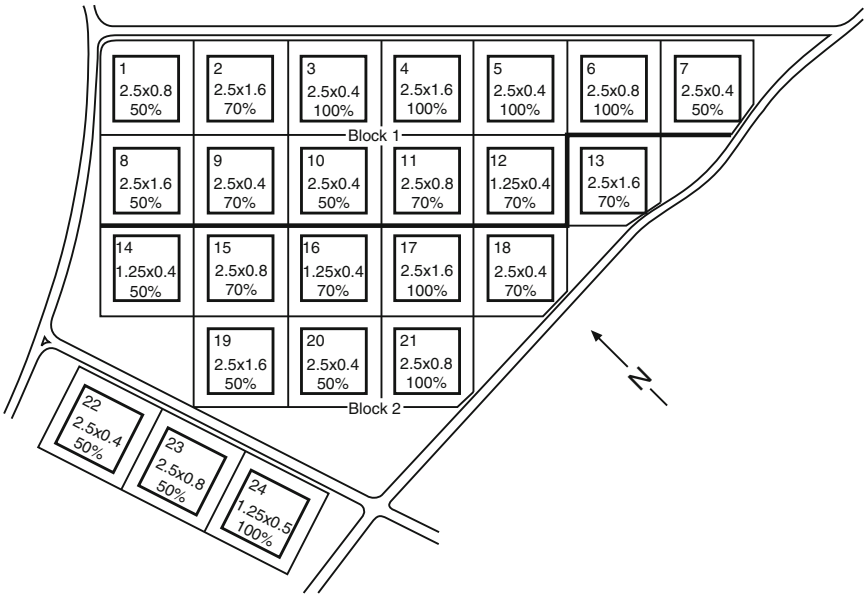

Fig. 4.1 Design of the Scots pine plant spacing–thinning experiment Weiden 611. The two-factor experiment tests the effect of four plant spacing variants and three thinning regimes with two replications each (in two blocks) on the growth of Scots pine. The resulting experimental design comprises $4 \times 3 \times 2 = 24$ trial plots

Experimental Factor. An experimental factor describes the type or types of treatments. Our experimental design comprises two experimental factors: the factor plant spacing, and the factor thinning severity. The plant spacing (factor 1) is divided into four treatment levels: $1.25\,\mathrm{m} \times 0.4 \mathrel{\hat{=}} 20{,}000$ plants ha^{-1}, $2.50\,\mathrm{m} \times 0.4\,\mathrm{m} \mathrel{\hat{=}} 10{,}000$ plants ha^{-1}, $2.50\,\mathrm{m} \times 0.8\,\mathrm{m} \mathrel{\hat{=}} 5{,}000$ plants ha^{-1}, and $2.50\,\mathrm{m} \times 1.4\,\mathrm{m} \mathrel{\hat{=}} 2{,}500$ plants ha^{-1}. The thinning (factor 2) is divided into three treatment levels: no thinning; reduction in tree number to 70% of the untreated control plot; and reduction in tree number to 50% of the untreated control plot. A thinning from above is implemented to reduce tree number.

Treatment Variants. Consequently, there are 4×3 treatment variants, which can also be described as experimental units or plots. The experimental unit is that part of the object of investigation upon which the treatment is conducted. In our experimental design there are 24 experimental units, or plots. They consist of an area of $32.0\,\mathrm{m} \times 32.5\,\mathrm{m}$ in size and a buffer strip of 10 m to protect the plots from edge effects.

Buffer Strips. These strips border on a plot, protecting it from the different treatments in adjacent plots or from the edge effects at the boundary of the experimental plot. It receives the same treatment as the plot and is delineated from the neighbouring plot and outlying investigation area by thin lines, as in Fig. 4.1.

Target Response Variables or Test Variables. If a forest stand is the object of the investigation, the variables needed to represent the stand might be mean or top

height, basal area, and standing volume. If the objects of the investigation are the individual trees, the target variables might be diameter, basal area, volume increment, crown volume, or the biomass. The explanatory variables and the response variables are not necessarily identical. For example, the response variable crown volume is derived from the explanatory variables tree height, crown base height, and crown radii.

Replication. This indicates how many times a treatment variant occurs in the experimental design. In our example the treatment variants are replicated twice, so that the total result is 24 plots ($\hat{=}$ 4 plant spacing $\times$ 3 thinning severities $\times$ 2 replications). Any variation in stand history of the experimental plots, in their site conditions, and in the biotic or abiotic disturbance factors make it difficult to keep all conditions, except the planned treatment, equal in field experiments. Adequate, frequent replications help differentiate between biological variability in the data and differences due to the applied treatment.

Randomisation. If the site conditions of all 24 plots were similar, the results from a completely random assignment of the 12 treatment variants to the plots (complete randomised design) would contain no systematic error. However, based on prior information gained from site mapping, we need to distinguish two blocks with different site conditions in our example (cf. Fig. 4.1, block 1 above, block 2 below). Within these two blocks, the treatment variants are assigned randomly to the plots (block design with randomisation within the blocks).

Block Design. The formation of blocks can eliminate sources of systematic error, e.g. a site gradient on the experimental plot. In our example, block 1, with plots 1–12, comprises impoverished sandy soils; and block 2, with plots 13–24, comprises impoverished coarse loamy sand. In each block, all 12 treatment variants are represented (complete block design) so that the site differences between the blocks can be eliminated in the analysis.

4.2 The Experimental Question and its Four Component Questions

The structure of an investigation is decided upon once the experimental question has been formulated clearly and precisely with its four component questions. This rather trivial principle is often violated, in which case a more resource-intensive approach may not provide results that are more meaningful.

4.2.1 Which Question Should Be Answered?

Here, a decision about what type of treatment needs to be tested for its effects on growth and whether, when testing multiple treatments, interactions between them shall be dealt with in the investigation. If the effects of different fertilisations and

soil treatment methods on stand growth are to be investigated in a Scots pine stand at the same time, then the interaction between these two treatments may also be part of the experimental question. Furthermore, one needs to determine whether the investigation should produce qualitative or quantitative results. For example, the question of whether Douglas fir responds to pruning live branches with a reduction in growth aims for a purely qualitative result. In this case a simple yes–no answer is required. A quantitative result, for instance, is the outcome of an investigation of the effect of increasing nitrogen fertiliser amounts on the growth of Scots pine. In this case the question is not confined to testing whether the Scots pine responds to fertilisation. Rather the question asks to what extent its growth changes by increasing fertiliser applications.

4.2.2 With What Level of Accuracy Should the Question be Answered?

The desired level of accuracy determines the number of replications required in an investigation. One, two or three replications or more means that a certain treatment variant is repeated once, twice or three times and so on in an experimental design. Guidance for determining the necessary number of replications to achieve a particular level of accuracy may be found in Cochran and Cox (1957), Munzert (1992), Pretzsch (2002), and Rasch et al. (1992).

4.2.3 What Level of Spatial–Temporal Resolution is Wanted in the Explanation?

Process and structures in forest ecosystems can be observed at very different spatial and temporal scales. The resolution is dependent on the aim and purpose of the experiment. These indicate whether, e.g. in a fertiliser trial, tree diameter only is measured or the crown, branch, and root growth as well and also whether the measurements need to be taken in time intervals of seconds, minutes, days, years, or every 5 years.

4.2.4 Why and for What Purpose Should the Question be Answered?

This question aims at defining the level of validity desired for the result, most importantly in terms of the spatial and temporal range. For example, conclusions about the success of fertilisation applied in different amounts are only valid for a larger

region and a broad range of sites if the experiment is widespread across the region. If only local validity is desired, a restriction to a single site is sufficient.

4.3 Biological Variability and Replicates

4.3.1 Total Population and Sample

The measurements on experimental plots always represent a sample of the population from which conclusions about the characteristics and relationships of the population (in statistical terms) can be drawn. As a rule, the population remains essentially unknown. Multiple samples of a population usually contain different population elements and therefore differ from each. Hence, the sample estimates are associated with a certain error: the larger the sample, the smaller the error. Ultimately, in accordance with the law of large numbers, the deviation between the sample and population approaches zero.

4.3.1.1 Overview of the Determination of the Number of Replicates, Plot Size, and Number of Trial Plots

The following steps outline the procedure for deriving the number of replicates needed, the area size and the number of plots for investigations of individual trees or stands:

(1) Measurement or estimation of the variability in the target variables (e.g. mean height, mean diameter, standing volume, volume growth).
(2) Defining the accuracy required and level of confidence for the response variables, or for the analysis of differences between treatment variants.
(3) Preliminary calculation of the number of replicates needed in relation to the variability, level of confidence, and accuracy required.
(4) Determination of the size of the experimental plot in total as a result of the number of replicates and the age-related growing space of a given tree species.
(5) Division and layout of the total area required into a few large, or many small plots depending on site conditions (e.g. homogeneity) and technical conditions (e.g. ploughing in strips, planting in rows, ozone-fumigating individuals or cohorts).

Although in practice deviations from this strict procedure often occur, these steps identify critical tasks for goal-oriented and transparent research planning (Köhl 1991).

The more measurements taken and the greater the skills in arranging them, the better estimated sample approximates the actual population value. The number of replicates required increases with the variability of the target response variable and with the desired level of confidence and accuracy of the result. In research planning,

the number of replicates needed can be calculated prior to the investigation so that the number of trees that must be measured for a given question can be estimated. The experimental design needs to encompass an area sufficiently large to support the number of trees required. In the case of long-term trials, plot size must be sufficiently large at the outset to still maintain a sufficient number of trees at the end of an observation period to produce the desired accuracy.

If the tree number required is known, the corresponding area can be derived from species-specific relationships between required growing area (or growing space) and age. The homogeneity of the site and, possibly, the need to eliminate systematic error by forming blocks determines whether a design gives preference to one large plot or many smaller plots. The larger the plots selected are, the smaller are the degrees of freedom, and the coefficient of variation. A reduction in plot size results in an increase in the degrees of freedom, as well as in the variation among sample units. The effort expended in experimental layout and survey is minimised by selecting medium-sized sample areas.

The optimal plot size for given conditions can only be determined accurately using computerised sample simulation. In practice, however, technical aspects and site factors largely determine plot size. The variation between the experimental units declines with increasing plot size. In individual plots, angle count samples, or six tree-sample units [according to Prodan (1968, 1973)], the coefficient of variation for the target variables height, diameter, stem volume, or volume growth rate can be 50% or more. With increasing plot size, the coefficient of variation is reduced to the extent that in fertilisation or thinning trials with plot sizes ranging from 0.1 to 0.01 ha, often two to three replicates per treatment variant produce sufficient accuracy in the target variables and facilitate an analysis of significant differences between treatment variants.

4.4 Size of Experimental Plot and Trial Plot Number

A plot comprises the measurement area and the surrounding buffer strip. To avoid edge effects, the surrounding strip should receive the same treatment as the plot and be at least 7.5 m wide. This ensures that trees in a mature stand situated close to the perimeter of the plot have at least one neighbouring tree outside the area treated similarly. In soil treatment and fertiliser experiments, wider buffer strips are recommended in order to minimise the effects of lateral nutrient transfer and root competition between plots.

The size of the experimental plot needed is derived from the defined minimum tree number required to answer the experimental question. Given the minimum tree number and known tree number–age relationships (typical stocking requirements for tree species), the area required can be estimated. The resulting measurement area may constitute one or many plots. The decision is usually dependent on technical constraints, on silvicultural, or on site conditions. On heterogeneous experimental plots, a division of the area into two or more blocks may be required to eliminate

systematic errors. The increase in the technical effort involved and the area required for buffer strips are reasons to restrict this division. If the treatment variants can be set up for individual trees (e.g. pruning or release growth) with little effort, then a fragmentation down to an individual tree plot is possible.

In growth and yield research at the stand level, the minimum tree number per plot ranges from 40 to 80 trees depending on the experimental question, the experimental conditions, and the yield elements under consideration. These values are more or less standard for pure evenaged stands. From this minimum tree number and the mean area available for growth for each tree, one obtains the size of the measurement area, which together with the buffer strip comprises the required area per treatment unit. The site conditions at the experimental plot, the tree species under investigation, the stand age or the age range in long-term observations, and the stand management, all have a major influence on the area or growing space trees require for growth.

Figure 4.2 shows the relationship between age and tree number for Norway spruce and Sessile oak on plots 0.01, 0.02, . . . , 0.2 ha in size. If a Norway spruce investigation established at the age of 30 years still should have a minimum of 50 trees per plot at the age of 100 years, then the research plot should be at least 0.1 ha in size at the outset. With an area of 0.05 ha, the desired tree number would already be too low at age 50. Due to the more rapid reduction in tree number and the lower final tree number in Sessile oak stands, large areas are needed to have a sufficient number of trees still present in the final stand (Fig. 4.2b).

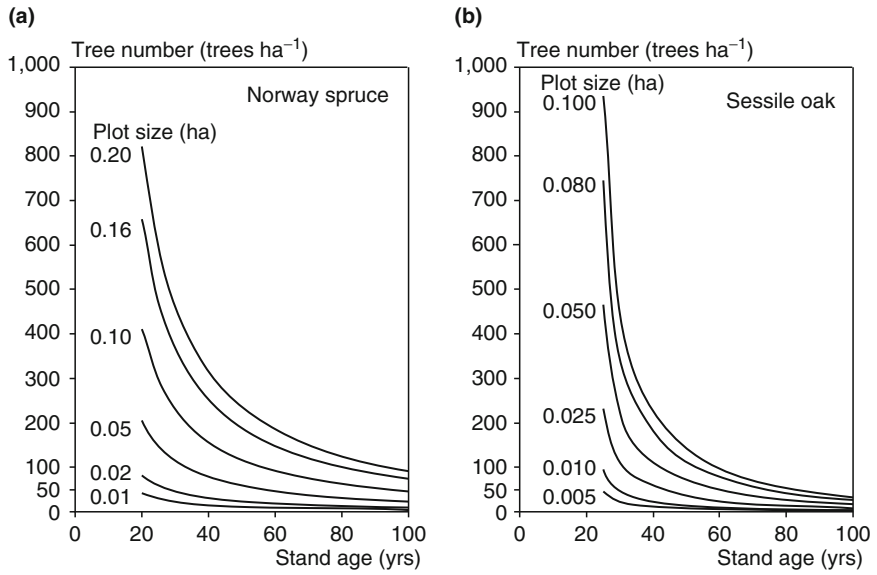

Fig. 4.2 The expected tree number in relation to size of the measurement area $(0.01, 0.02, \ldots, 0.2$ ha) and age of (**a**) Norway spruce and (**b**) Sessile oak based on the tree number–age relationships in the Norway spruce yield tables from Assmann and Franz (1963), upper height site index 40, moderate yield level; and the Sessile oak yield tables from Jüttner (1955), moderate thinning, yield class II, respectively

4.5 Block Formation and Randomisation: Elimination of Systematic Error

When, for an experimental plot, no systematic error is expected because of site gradient or edge effects, a random assignment of the treatment variants to the plots may be appropriate (Linder 1951). This creates a completely randomised experimental design in which both the technical layout of experimental plots and the analysis of variance are simple to manage. Unfortunately, this type of design is usually unsuitable for field experiments because of the inhomogeneous nature of site conditions.

In the following examples, the experimental plot is overlaid by a dot grid where the density of the dot pattern reflects the (in-) homogeneity of the site conditions. A regular point density over an entire area (e.g. Fig. 4.3) indicates more or less homogeneous conditions. An increase in point density in one or more directions (e.g. Fig. 4.4) symbolises a site gradient, which needs to be taken into account in the experimental design.

If a homogeneous experimental plot is available for a thinning trial of 15 plots with five treatment variants (basal area density of the treatment variants $1 \triangleq 100\%$, $2 \triangleq 85\%$, $3 \triangleq 70\%$, $4 \triangleq 55\%$, and $5 \triangleq 40\%$) and three replicates ($5 \times 3 = 15$ plots), shown in Fig. 4.3 by a largely homogeneous point density, then a random allocation of treatment variants on the 15 plots is justified. To allocate the five treatment variants onto 15 plots randomly, the plots were numbered first (Fig. 4.3a), and then the random numbers specifying the allocation were taken from random number tables or random number generators. Assuming site homogeneity, which is rarely the case in field experiments, the concentration of treatment variant 1 (basal area density $\triangleq 100\%$) in the northwest section of the experimental plot is no cause for concern (Fig. 4.3b).

If one expects site conditions to introduce systematic error within the experimental plot, these can be eliminated by establishing blocks. If a site gradient is evident

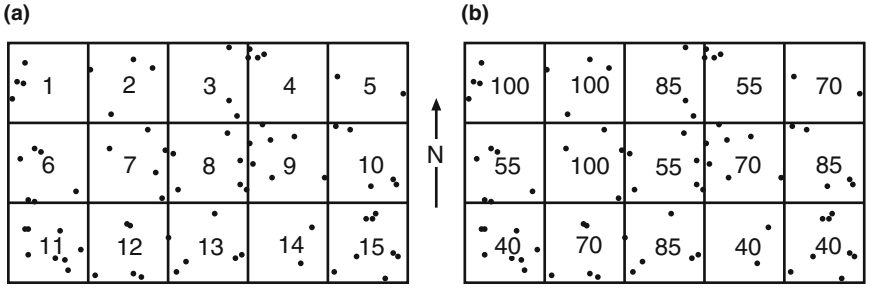

Fig. 4.3 Experimental design for a Norway spruce thinning trial comprising 15 plots on a homogeneous experimental plot. The thinning trial encompasses five treatment variants (basal area density $1 \triangleq 100\%$, $2 \triangleq 85\%$, $3 \triangleq 70\%$, $4 \triangleq 55\%$, and $5 \triangleq 40\%$) with three replicates ($5 \times 3 = 15$ plots): (**a**) For the allocation of treatment variants the plots were numbered from 1 to 15. (**b**) By drawing random numbers the five treatment variants were randomly allocated to the 15 trial plots. The numbers entered in the trial plots describe the basal area density in relation to the untreated control plots

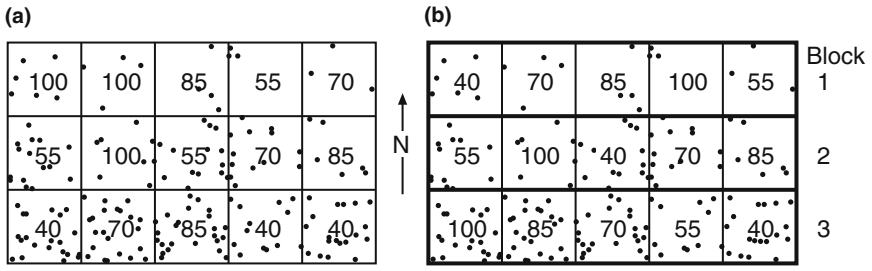

Fig. 4.4 Experimental design for a Norway spruce thinning trial comprising 15 plots on an inhomogeneous experimental plot (**a**) with random allocation of treatment variants and (**b**) with block subdivisions. The increasing density of points from north to south indicates site improvement. (**a**) Under inhomogeneous site conditions with an improvement in site conditions from north to south, a completely random allocation may produce distortion in results. Here treatment variant 1 (basal area density 100%) dominates in the poorer sites in northern part of the experimental plot, treatment variant 5 (basal area density 40%) lies in the favourable, southern part. (**b**) By subdividing the experimental plot into three blocks 1, 2, and 3, for which homogeneous conditions exist, prior information about the experimental plot can be used effectively, systematic sources of error removed, and the residual standard deviation minimised in the analysis of variance

at a site, with improved growth conditions from the north to the south, indicated in Fig. 4.4 by an increase in point density, a completely randomised layout would not take this prior knowledge of site differences into account, leading to a potential bias in the results. In a random allocation, as shown in Fig. 4.4a, the treatment variant 1 (basal are density $\hat{=}$ 100%) would be disadvantaged systematically by its location, and treatment variant 5 (basal area density $\hat{=}$ 40%) would be allocated systematically to favourable sites. The formation of blocks in Fig. 4.4b eliminates systematic error effectively as the site conditions in blocks 1, 2, and 3 are homogeneous, and each block contains all treatment variants. This type of block design eliminates variation in one direction. Latin squares and Latin rectangles are suitable for the elimination of systematic error in two directions.

4.6 Classical Experimental Designs

The experimental question and its four components influence the experimental design. Table 4.1 outlines the most important experimental designs for long-term experiments. The investigation designed may be one factor or multifactor depending on whether the aim is to test the effect of one or more factors on forest growth. The accuracy desired of the answer to the experimental question determines the number of replications. As discussed in the previous sections, site homogeneity may be problematic when the number of plots increases. Whereas a randomised design is recommended for homogeneous site conditions, potential sources of systematic error in one or more directions can be eliminated on inhomogeneous sites by adopting

Table 4.1 Traditional designs for field experiments. The number of treatment factors (e.g. thinning, fertilisation, pruning) and the degree of homogeneity of the site conditions determine the choice of the experimental design

Site conditions	Treatment	
	Mono-factorial	Multi-factorial
homogeneous	randomized design	randomized design
heterogeneous	mono-factorial block design	multi-factorial block design
	Latin square	multi-factorial Latin square and rectangle split-plot design split-block design trial series disjunct experimental plots

a block design. The validity of results increases in order from single investigations to disjunct experimental plots to trial series. Recommendations for forestry practice can be derived best from experiments when the investigations are repeated on different sites inventoried over long periods of time. Therefore, disjunct experimental plots and trial series are of particular practical relevance. Deviations from a randomised assignment of treatment variants to plots are characteristic of forestry field experiments. To exclude systematic error sources, block designs or Latin squares can be used. Furthermore, split-plot or split-block designs can be used to ease the implementation of investigations (Table 4.1).

4.6.1 One-Factor Designs

Older examples of one-factor experimental designs are the thinning trials with three thinning grades, established in the nineteenth century in the initial stages of forest yield science research and, in many cases, still observed today. They test the effect of light, moderate and heavy thinning (A, B, and C grade) on stand growth (cf. Chaps. 5 and 6). More recent examples of one-factor design include nitrogen enhancement and other fertilisation, plant spacing, and provenance trials where the effect of only one factor on growth is investigated.

4.6.1.1 Completely Randomised Designs

The distribution of treatment variants on the plots should be objective and avoid systematic errors. However, the random distribution of experimental error across the treatment variants is difficult to achieve in field experiments because the probability of site heterogeneity in the experimental plot increases with increasing area used.

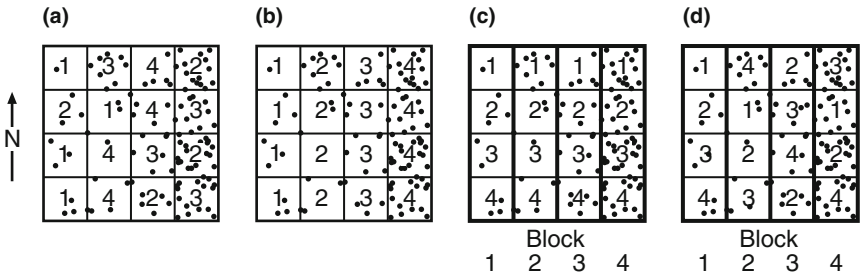

Fig. 4.5 Different options for allocating treatment variants (variants 1, 2, 3, and 4) with four replicates on inhomogeneous sites. The improvement in site conditions from west to east is depicted by the increase in point density: (**a**) completely random allocation, (**b**) systematic allocation of treatment variants, (**c**) blocking with systematic allocation within blocks 1–4, and (**d**) blocking with random allocation of treatment variants to trail plots within blocks 1–4

The influence of site as an exogenous factor can blot out or bias the effects of the treatment being tested in some circumstances. If, e.g. a thinning trial comprising 16 plots with four treatment variants and four replicates ($4 \times 4 = 16$) are established on a heterogeneous experimental plot, different methods may be used to allocate the treatment variants to the plots. The increasing point density from west to east in Fig. 4.5a represents a gradual improvement in site quality within the experimental plot. The random allocation of the treatment variants to the plots by drawing numbers or by random number generation represents the first method (Fig. 4.5a).

The method of drawing numbers involves the preparation of as many cards as there are experimental units, on which the treatment variants are inscribed. The number of cards prepared for a treatment variant corresponds to the number of replicates (inscription on the lots: 1, 1, 1, 1, 2, 2, 2, 2, 3, 3, 3, 3, 4, 4, 4, 4). For each plot, commencing in the northwest and finishing in the southeast of the experimental plot, for example, one card is drawn and cannot be returned. The treatment variant written on the card is then assigned to the respective plot.

When random numbers are used, the plots are numbered sequentially, in our example from the northwest beginning with 1 and finishing in the southeast with the number 16. Random number tables, or a random number generator, are then used to extract a series of random numbers. One of many possibilities for assigning treatment variants to the plots is to assign treatment variant 1 to the first four random numbers drawn lying between 1 and 16 (e.g. plots 1, 6, 9, and 13 are drawn). The next four random numbers generated between 1 and 16 are allocated to treatment variant 2 (e.g. plots 4, 5, 12 and 15) and so on. Random numbers already assigned are ignored, as are the random numbers that do no lie between 1 and 16. In our example, treatment variant 1 is concentrated in the western side of the experimental plot on the poorer sites, so that a negative systematic error would be expected from the outset (Fig. 4.5a). A systematic allocation of treatment variants to plots, resulting in the plan shown in Fig. 4.5b, would enhance this error.

4.6.1.2 Block Designs

Block formation aims to eliminate systematic exogenous disturbance factors, which are not the object of the trial. The aim of the block layout is to minimise the site variation within blocks. The residual variation in the subsequent analysis of variance, which compares the variation arising from the treatments to the random variation, can be reduced effectively by block formation, enhancing the sensitivity of the investigation.

In our example (Fig. 4.5c), blocks are best aligned from west to east, and the treatment variants are distributed so that all variants are present in each of the four blocks. If the four factor levels are ordered systematically within the blocks 1–4, however, the danger of a one-sided error still exists because treatment level 1 is only represented in the northern and level 4 only in the southern part of the block (Fig. 4.5b). Therefore, a combination of block building and random assignment of treatment variants within the blocks (Fig. 4.5d) avoids systematic errors most effectively. The Scots pine plant spacing and thinning experiment Weiden 611 provides a practical example of a block design (cf. Fig. 4.1).

4.6.1.3 Latin Squares

Whereas block designs are suitable for eliminating site gradients in one direction, Latin squares eliminate systematic site differences in two directions by duplicate block formation.

For example, we assume that a thinning trial with six thinning variants (1, 2, 3, 4, 5, and 6) and six replicates needs to be established on a slope with a gradual improvement in nutrient supply from the west to the east and aspect differences from the north to the south because there is no other suitable area for the experimental plot available. In such a case, the site differences at the experimental plot can be excluded to a certain extent by selecting a 6×6 Latin square (Fig. 4.6). Here, the

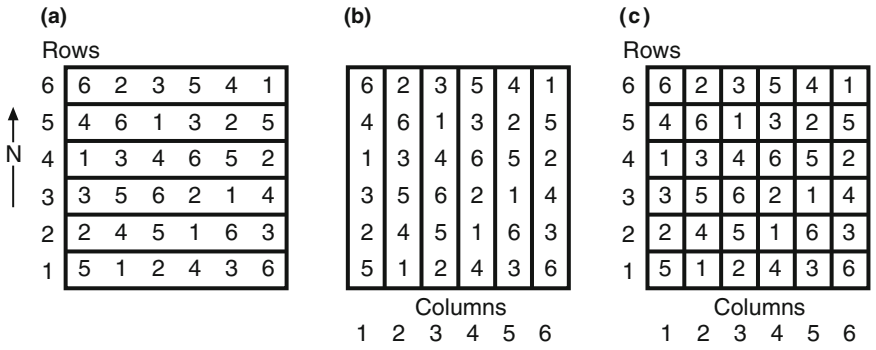

Fig. 4.6 Latin squares eliminate systematic error in two directions. Horizontal blocks (*rows*) and vertical blocks (*columns*) are overlaid so that each of the six treatment variants in each block occurs exactly once. A 6×6 Latin square is presented

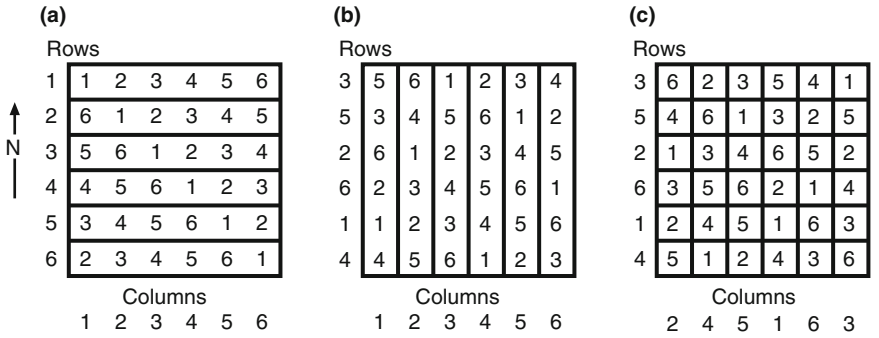

Fig. 4.7 Generation of a 6×6 Latin square in three stages (from Mudra 1958): (**a**) systematic distribution of treatment variants on the plots, (**b**) random redistribution of columns (1)–(6) using random numbers, and (**c**) random redistribution of rows using random numbers

six treatment variants with the six replicates are distributed representatively across the area. A Latin square ensures that all treatment variants occur in the north, south, east, and west with the same frequency to eliminate systematic error. It consists of horizontal blocks (rows), which remove the first gradient, and vertical blocks (columns), which eliminate the second gradient. In our case the Latin square consists of horizontal blocks that exclude the aspect gradient and vertical blocks, which exclude the nutrient gradient.

To develop a Latin square the treatments 1–6 are spread out systematically on the blocks (Fig. 4.7a) so that the first row represents the treatments in the order 1, 2, 3, 4, 5, and 6; the second block in the order 6, 1, 2, 3, 4, and 5; and so on. In the second step, the rows are redistributed using random numbers generated or drawn (Fig. 4.7b). Once this step has been completed, the treatments are randomly distributed in the columns. In the third step, the procedure is repeated for the columns also to remove the systematic distribution in rows (Fig. 4.7c). This way, the treatment variants are distributed randomly both within the rows as well as in the columns, and each number occurs only once in each row and each column.

4.6.2 Two-Factor or Multifactor Analysis

This experimental design is particularly important as it tests the effect of two or more treatment factors on the growth of individual trees or stands. Examples of two-factor analyses include plant spacing–thinning trials, fertilisation–thinning trials, or species mix–thinning trials. In plant spacing–thinning experiments, the effect of both plant spacing (factor 1) and thinning (factor 2) on stand growth is tested in the same investigation. Factor 1 and factor 2 are further divided into levels (variable plant spacing and thinning grades) and replicated. The advantage of testing multiple factors in one investigation over testing factors in separate experiments in isolation is that multifactor investigations provide results about main effects as well as

interactions between factors. In a combined plant spacing–thinning experiment, the objective is to determine, firstly, the effect of plant spacing on stand development, secondly, the effect of different thinning grades on stand development, and finally, information about the interactions between plant spacing and thinning.

Thus, in an analysis of variance both the effects of the main factors (factors 1 and 2) as well as their interactive effects (combined effects of factors 1 and 2) on the variables selected are investigated. Modern silvicultural prescriptions mostly combine different treatments (thinning, pruning, fertilisation, soil treatments), and these are supported best by multifactor analyses. One limitation of a multifactor analysis is the rapid increase in the number of plots and experimental space required with an increasing number of factors, factor levels, and replications. In a two-factor investigation in which five different initial spacing variants and four thinning grades with five replicates of each are to be tested, $5 \times 4 \times 5 = 100$ plots are needed. In such multifactor investigations, usually block designs are needed to overcome site inhomogeneity.

4.6.2.1 Multifactor Block Designs

Figure 4.8 illustrates two different examples of a two-factor block design in which two levels of the first factor are investigated and four levels of the second factor. In the convention for describing treatment variants the first number represents the level

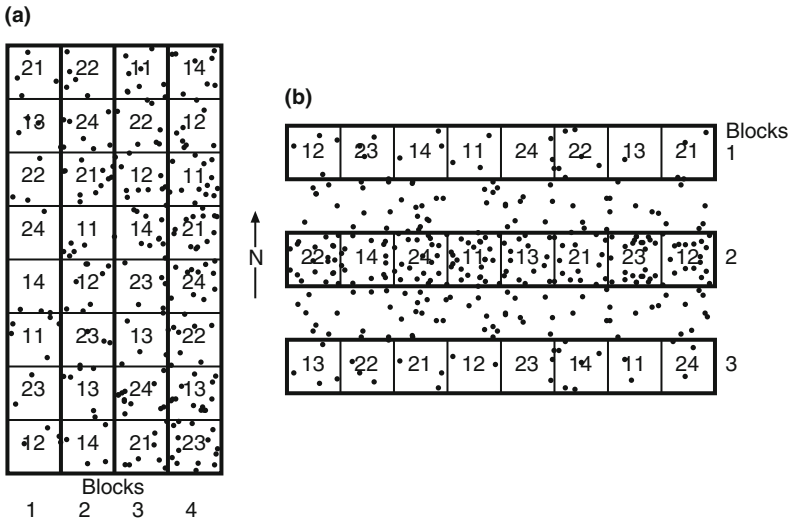

Fig. 4.8 A two-factor experimental design in block layout for systematic site gradients. (**a**) The growing conditions improve from block 1 to block 4. In blocks 1–4 eight factor combinations $(11, 12, 13, \ldots, 23, 24)$ are represented. (**b**) Horizontal blocks 1, 2, and 3 are established in response to the site improvement from the perimeter towards the central axis of the experimental plot. Within the blocks, the eight factor combinations are allocated randomly to the plots

of the first factor and the second number the level of the second factor, and so on. In a two-factor investigation the plot code 24 indicates that a test of the second level of factor 1 and fourth level of factor 2 are being conducted on the plot.

In the first example (Fig. 4.8a), the improvement in site quality from west to east is eliminated by the formation of the blocks 1–4. In the second example (Fig. 4.8b), the establishment of three blocks eliminates the effect of site quality, which improves from north to south along the central axis of the experimental plot. The $2 \times 4 = 8$ plots within a block represent all the treatment variants under investigation. They are randomly arranged within the block. The blocks represented by 1–4 and 1–3 are arranged so that homogeneous conditions dominate within the blocks, whereas the conditions among the blocks aligned at right angles to the site gradient differ considerably.

4.6.2.2 Multifactor Latin Square and Rectangles

Quadratic experimental designs occur only when the number of treatment variants, i.e. the number of possible combinations of the treatment levels, corresponds to the number of replications. Figure 4.9a shows a two-factor Latin square with four factor level combinations (11, 12, 21, 22) and four replicates. It eliminates sources of systematic errors potentially arising from north–south and east–west site gradients to the extent possible.

Multifactor rectangles are comparatively more flexible as the number of treatment levels and the replications can be nominated as desired. In each row and each column, all possible treatment levels are randomly allocated and represented just once. Figure 4.9b shows a 2×4 Latin rectangle with four replicates. The product of the level number of the first and second factors and the number of replications

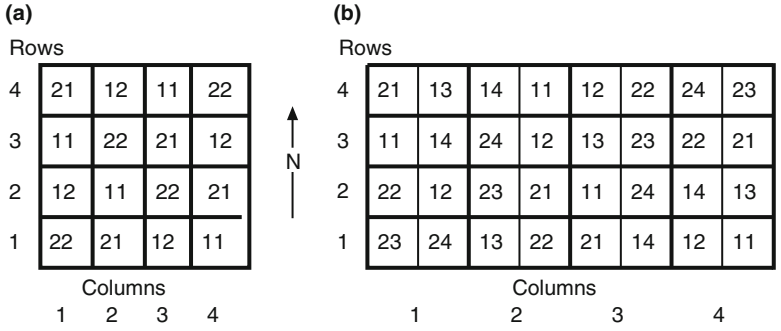

Fig. 4.9 Design of a 4×4 two-factor Latin square and a 2×4 Latin rectangle with four replicates. (**a**) Multifactor Latin squares are only possible if the number of factor combinations is equal to the number of replications. In the example, according to the four factor combinations (11, 12, 21, 22) and four replications, four rows and columns are established. (**b**) Latin rectangle for the elimination of systematic error in two directions. The factor combinations 11, 12, 13, 14, 21, 22, 23, 24 occur in each row and column once

$2 \times 4 \times 4 = 32$ produces the number of plots needed. The effect of one-sided error caused by site heterogeneity in the experimental plot is counteracted once again by the establishment of vertical and horizontal blocks.

4.6.2.3 Effect of Interactions

Often, the interactions between two factors are of primary interest, whereas the main effects, e.g. the isolated effect of fertiliser application and thinning grades on growth, is known. The existence and intensity of interactions between two or more factors can be recognised by the influence of the levels of one factor on the mean level of the factor combinations.

Figure 4.10a shows graphically the effect of fertiliser (factor 1: factor levels 0, N, NPK) and thinning severity (factor 2: basal area density 100%, 85%, 70%, and 55%) on gross volume yield. The factor levels 0, N, and NPK represent the unfertilised variant (0 or control plot), nitrogen fertilisation, and nitrogen–phosphorus–potassium fertilisation, respectively. An optimum curve is obtained from both the cumulative effect of all three fertilisation variants (broken line) as well as the isolated effect of the fertilisation variants 0, N, and NPK (solid line) in relation to basal area density. In general, total production increases for a moderate reduction in basal area density from 100% to 85%, and then declines with increasing thinning severity (Chap. 10). We observe this response pattern to thinning operations for all fertilisation variants. Thus, the lines run parallel to one another and do not reveal any interaction between fertilisation and thinning.

In the second example, a positive interaction between thinning and fertilisation is apparent (Fig. 4.10b). Whereas the growth on the unfertilised plot declines with

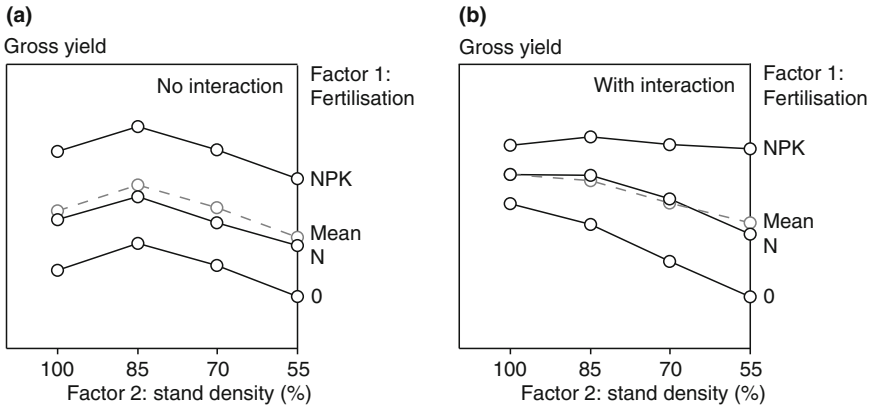

Fig. 4.10 Analysis of total volume yield in a two-factor investigation: factor 1, fertilisation with the factor levels 0, N, NPK; factor 2, thinning with the factor levels basal area density 100%, 85%, 70%, and 55%, (**a**) without and (**b**) with interaction. The deviation from a parallel orientation of the lines, obtained from joining the factor level mean, reveals the interaction effects (from Pruscha 1989, p. 131)

thinning severity, the NPK fertiliser largely compensates for the reduction in growth caused by thinning. We describe the interaction between two or more factors as positive, negative, or zero, if the factors in one or more level combinations have a higher, a lower, or the same influence on the mean level in relation to the sum of the individual influences of both factor 1 and 2. The occurrence and intensity of the interactions are recognisable by the degree of nonparallelism of the lines obtained by plotting the level mean for factor 1 in relation to factor 2.

4.6.3 Split-Plot and Split-Block Designs

These designs are selected when one or more of the factors investigated either cannot be established as plots or can be established only with insupportably high technical or silvicultural effort. This is the case, for instance, in the European beech underplanting trial under a mature Scots pine stand presented in Fig. 4.11. The investigation should test the effect of different canopy densities (factor 1: degree of crown cover 0.4, 0.6, 0.8, and 1.0) in the mature Scots pine stand and different plant spacing for the underplanted European beech (factor 2: 1.0×1.5 m, 1.0×2.0 m and 1.0×3.0 m) on growth of both species. A random allocation of crown density on plots, as shown in Fig. 4.11a, would be impractical due to the large area required, the edge effects, and the complexity involved in future secondary thinning operations. Therefore, the factor levels for crown cover are not randomly arranged but are in columns or lines (Fig. 4.11b). As with the example of canopy opening up, similar designs may also be necessary for large-area investigations of irrigation, soil treatments, fertilisation, or drainage. In addition to the technical arguments, split-plot and split-block designs also allow one factor to be tested at a higher level of accuracy than a second or a third.

4.6.3.1 Split-Plot Design

In the two-factor split-plot design, one factor is assigned to large plots (main unit). To test the second factor, each large plot is divided into small plots (subunits) so that the levels of the second factor are randomly located in a large plot. In our 4×3 split-plot design with two replicates (Fig. 4.11b), the factor levels for crown density (0.4, 0.6, 0.8, and 1.0) are established on large plots as the main units (units of three levels enclosed by bold frame). This design requires a smaller area than otherwise would be needed to reduce the edge effects. In addition, it is assumed that crown density will have a significant effect on the growth of European beech underplanting (strong effect), so that two replicates appear sufficient to document the canopy effects. As different plant spacings (factor 2: 1.0×1.5 m, 1.0×2.0 m, 1.0×3.0 m) can be tested on small areas and since little is known about its effect on European beech growth, this factor is tested on subunits with eight replicates and gives a higher level of accuracy. The major advantages of such split-plot designs (Fig. 4.11b) over

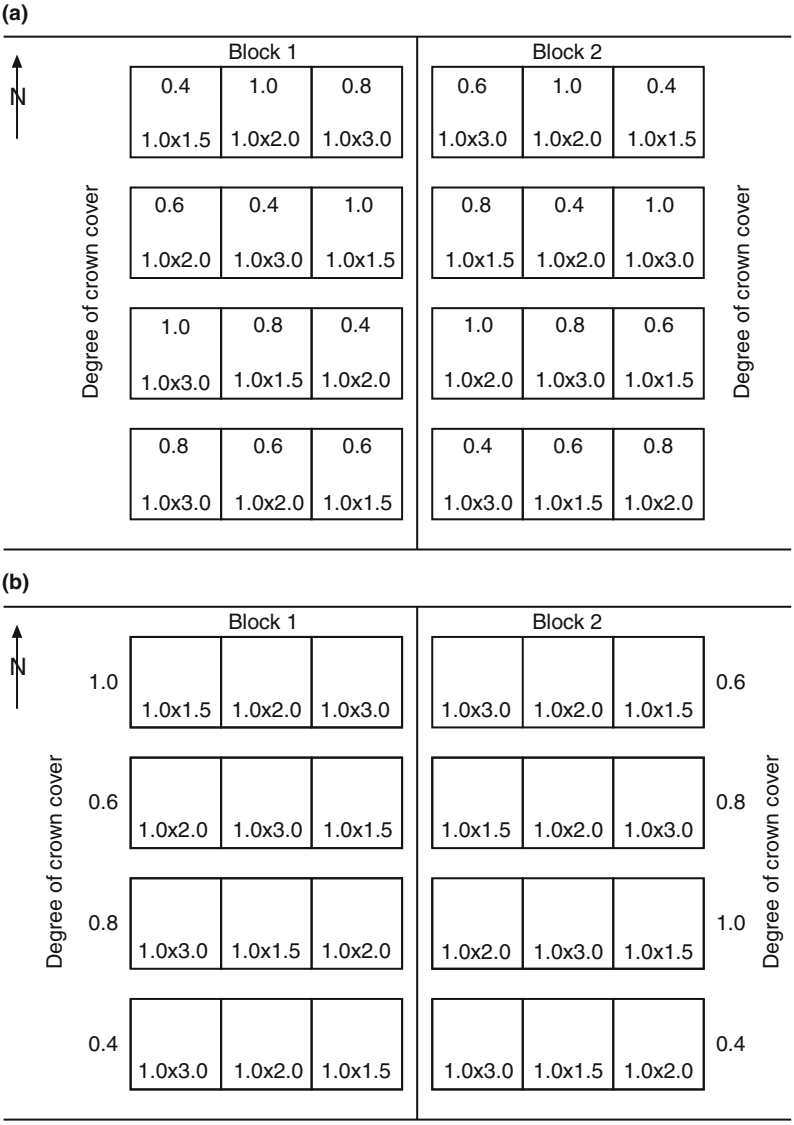

Fig. 4.11 A two-factor investigation to test the combined effects of crown density (factor levels: 0.4, 0.6, 0.8, and 1.0) and plant spacing (factor levels: 1.0 m × 1.5 m, 1.0 m × 2.0 m, and 1.0 m × 3.0 m) on the growth of a European beech underplanting below a mature Scots pine canopy. To exclude systematic error, the treatments were replicated twice in the blocks 1 and 2: (**a**) completely randomised allocation of treatments on plots and (**b**) split-plot layout, in which the main unit comprises large plots with the same crown cover, and the subunits comprise smaller trial plots with defined crown cover and plant spacing

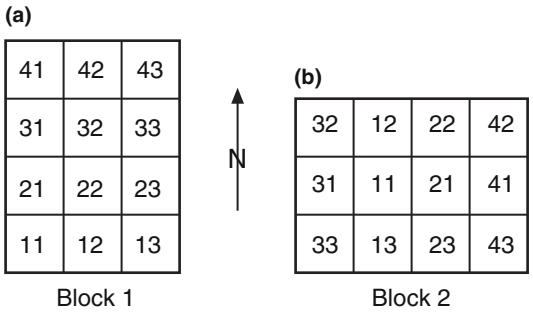

Fig. 4.12 A two-factor split-block design with two replications in blocks. To ease the establishment of the layout, plots with the same factor levels are arranged in strips across the blocks from west to east and north to south

completely randomised designs (Fig. 4.11a) are the ease with which they can be established, the smaller area required, and the better correspondence between the number of replicates selected for levels of factor 1 and factor 2 and the experimental question.

4.6.3.2 Split-Block Design

In a two-factor or multifactor investigation, if the factors under investigation can only be studied on large plots, then split-block designs are necessary. Figure 4.12 shows an example of a 4×3 split-block design with two replicates between the blocks. The levels of factors 1 and 2 are assigned to the plots such that they are arranged in horizontal and vertical strips. The randomisation is limited even more here than for the split-plot design, where at least the subunits are randomly distributed within the main unit. If factor 1 was plant spacing and factor 2 was soil preparation, then the planting could be carried out in block 1 and block 2 in the rows and columns, respectively. The soil treatment also could be conducted in large-scale rows or columns running perpendicular to these. In this way the use of machinery is made easier, damage and error sources are avoided, and the factors 1 and 2 can be tested with equal accuracy. Such split-block designs may be analysed by a two-factor analysis of variance with two main factors testing for interactions (Bätz et al. 1972; Mudra 1958; Rasch et al. 1973).

4.6.4 Trial Series and Disjunct Experimental Plots

Single experiments based on the experimental designs discussed so far have a limited practical relevance given the local validity of the results obtained. However, field experiments mostly aim to provide recommendations that are more general. If, e.g. in a provenance experiment on a selected site, the quantitative growth

performance, the yield, and resistance characteristics of different provenances of a commercial tree species were to be investigated in a single experiment with considerable accuracy, the recommendations for provenance selection still could be made only for the immediate locality. Generalisations about the characteristics of provenances in relation to environmental conditions and recommendations for the selection of the most suitable provenances require replications on different sites and repeated survey over many decades (Schober 1961). Therefore experimental questions, e.g. about the relationship between provenance selection and growth, thinning and growth, or stand establishment techniques and juvenile growth, have been investigated by establishing trial series or disjunct experiments since the very beginning of experimental forestry. Such experimental designs replicate the treatment variants to be tested on different experimental plots in different growth regions.

We call experimental designs with more than one replicate per experimental plot a trial series. If only one replicate is carried out per experimental plot, we speak of disjunct experiments (Fig. 4.13). Whereas, in the past, trial series and disjunct experiments mostly developed by gradually expansion of the regional and

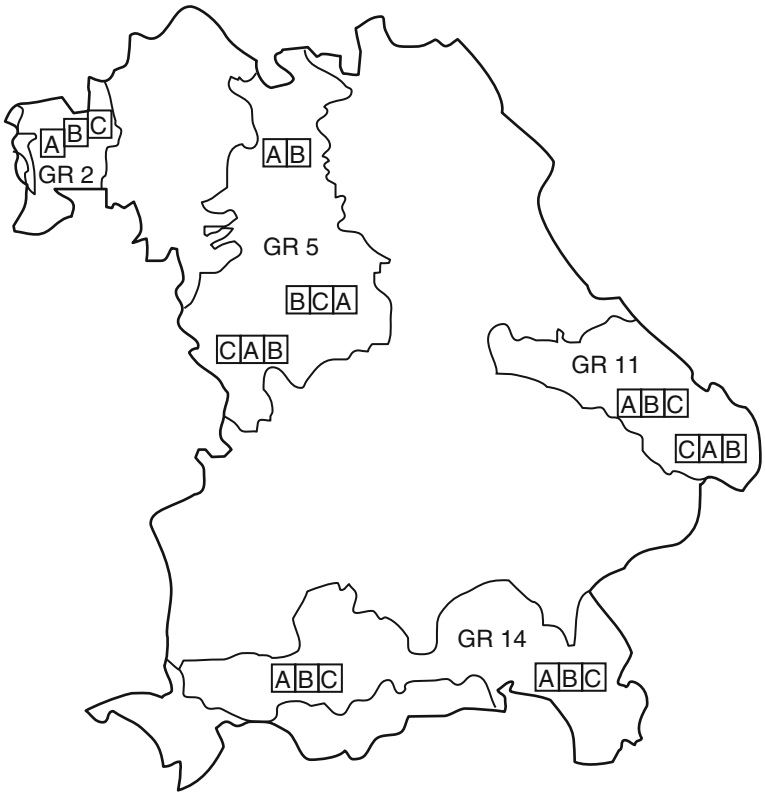

Fig. 4.13 Disjunct investigations arise when, e.g. thinning trials with equal factor levels (typically A, B, and C grade) are established in different growth regions (GR). They can be regarded as two-factor investigations with the factors treatment and site. Examples include the conventional thinning trials with three thinning grades from the yield science experiments

large-scale networks of experimental plots, in the last two to three decades many trial series have been conceived nationally or internationally with replications over a wide range of site conditions. Examples of this include the provenance, growing space, and thinning trials for Norway spruce, European larch, or Douglas fir coordinated by IUFRO.

When planning regional or large-scale experiments of this kind, one needs to decide which concept is best suited to answering the experimental question: the selection of a few experimental plots where the experimental question can be investigated accurately with many replicates or the selection of many experimental plots where only one or a few replicates may be observed.

The approach depends upon the response variables of interest. For example, in the investigation of the growth behaviour of different provenances on different sites, if one is especially interested in a broad distribution across different sites, then the establishment of many experimental plots with little replications on each experimental plot is recommended. In contrast, if one can assume that the kind, severity, and intensity of thinning affects tree and stand growth most, then the variation between the sites is less important. Hence, in this case, the establishment of fewer but more comprehensive investigations with multiple replicates may be recommended.

4.7 Special Experimental Designs and Forest Growth Surveys

4.7.1 From Stand to Individual Tree Experiments

Standard long-term experiments are established on a number of plots, 0.1–1.0 ha in size, which form the mensuration and treatment unit. This conventional approach was often found to be limiting in view of the large areas required, especially in multifactor investigations. An effective reduction in the area needed demanded a reduction in the plot size, limiting the number of factors and factor levels, or a minimising the replications. Nelder (1962) reduced the area requirement in a clever approach for arranging trees (Fig. 4.14). Plots still form the experimental and sample units in his experiments, but they are designed concentrically with a gradual change in stand density (Pretzsch 2002, pp. 69–73). The experimental designs from Weihe (1968 and 1970), Ehrenspiel (1970), Le Tacon et al. (1970), and Franz (1981) go one step further by selecting individual trees as the investigation and survey unit.

A section of the experimental layout of the combined clone-growing space investigation VOH 622 for Norway spruce near Vohenstrauß/Bavaria (Fig. 4.15) illustrates the fundamental difference between plot and individual tree designs. VOH 622 is part of an international trial series that tests the effect of clones (treatment factor levels: different Norway spruce clones from Germany and neighbouring countries) and plant spacing (treatment factor levels: 1.25 m × 2.5 m, 2.5 m × 2.5 m, 2.5 m × 5.0 m, and 5.0 m × 5.0 m) on the growth of Norway spruce. Individual trees form the investigation and survey units. They are arranged in plots for practical reasons (Fig. 4.15a). The four plant spacing levels are replicated twice, and

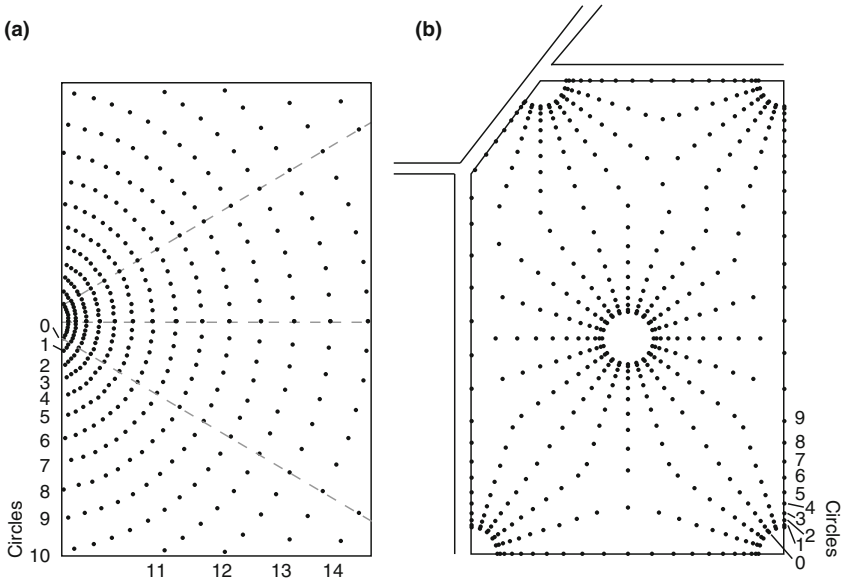

Fig. 4.14 Two setups of individual tree-based spacing experiments according to Nelder (1962). Starting from a centre, the trees are located on concentric circles and radii in such a way that the area available for tree growth increases systematically with increasing distance from the origin: (**a**) semicircle planting scheme and (**b**) full circle in combination with another four quarter circles after Pretzsch (2002, p. 70)

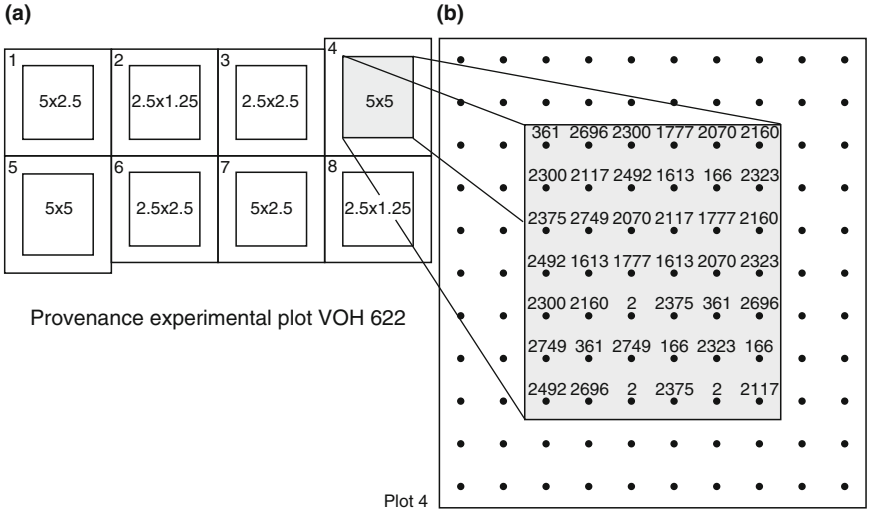

Fig. 4.15 Part of the design of the individual-tree-oriented Norway spruce clone trial at Vohenstrauß 622. (**a**) On eight plots in total the effect of 14 main clones and five plant spacing variants on the growth of Norway spruce is tested. (**b**) Each of the individual plots contains 14 Norway spruce clones with three replicates, supplemented by additional clones for the closer spacing. For plot 4 (5 m × 5 m) the basic design is presented with the numbers of the clones

three of each of the 14 clones are planted on each plot, producing a total of $4 \times 2 \times 14 \times 3 = 336$ samples for statistical analysis. A buffer strip (outer rectangle in Fig. 4.15b) surrounds each plot (inner rectangle in Fig. 4.15b) to avoid edge effects. The plant arrangement in the plot (black dots) is continued into the buffer strip.

To test factor 1 (clone), the various clones to be tested are distributed randomly across the plot under the condition that similar clones do not occur as neighbours. In addition to the 14 clones represented equally on the plots, additional clones are included to fill in the area according to the spacing defined by test factor 2 (plant spacing). Whereas factor 1 can be varied by selecting clones on an individual-tree basis, planting and future silvicultural operations make is easier to vary factor 2 on an area basis. The result is a two-factor split-plot design in which the plots with different plant spacing form the main units and the clones, i.e. the individual trees in plots, form the subunits. If identical experimental designs, e.g. in Baden-Württemberg, Lower Saxony, Rhineland-Palatinate, and Schleswig-Holstein, were also included in the analysis, then a three-factor trial would result with the factors site, clone number, and growing space with a sample size of $4 \times 336 = 1{,}344$ trees.

Existing long-term experimental plots can be incorporated into individual-tree approaches by recording the coordinates of all individual trees and stumps and, subsequently, the crown dimensions (Fig. 4.16). In a discussion of the transition towards new experimental designs, Prodan (1968, p. 239) stated, "… that data from long-term experimental plots do not lose importance in any way. Rather, the more radical the method of analysis becomes, the more important the basic data that facilitate testing in all directions will be in the future …" (translation by the author). Until now, the long-term experimental plots were mainly analysed at the plot level in

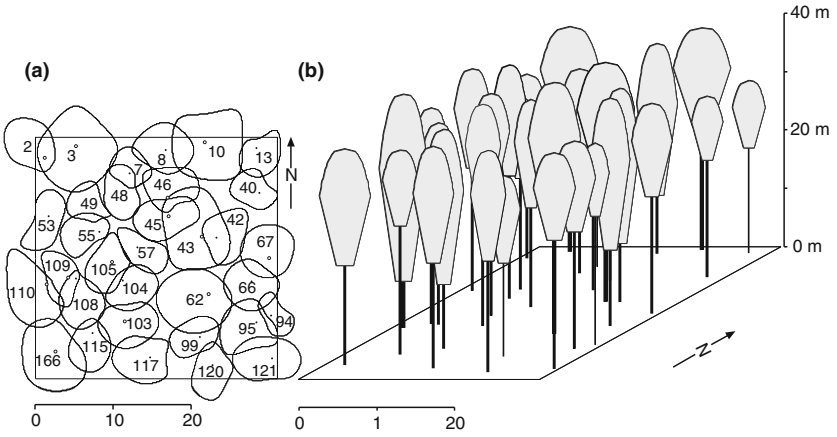

Fig. 4.16 Retrospective measurement of tree coordinates and crown expansion on the thinning trial Fabrikschleichach 15 in Forest District Eltmann, monitored for 130 years. (**a**) Part of the crown projection map following the survey in autumn 1981. (**b**) Three-dimensional stand structure providing a basis for individual-tree research

terms of the target response variables diameter, volume, etc.; however, they comprise a considerable potential knowledge of individual-tree growth. In Chapters 7–9 there will be introduced analytical methods that encompass the information potential from stand investigations of individual-tree dynamics. This transition to the individual-tree level in experimental designs and analysis represents a change in scale that also has been adopted in the analysis, modelling, and simulation of fauna and flora populations since the 1960s. It recognizes that stand development can be understood and represented better when the stand is divided into a mosaic of individuals acting together in a spatial–temporal system. The transition to individual-based approaches stretches from the planning and design of experiments through to the analysis and modelling of forest growth (Chap. 11).

4.7.2 Experiments and Surveys of Growth Disturbances

Field experiments and inventories for the identification of disturbances (e.g. drop in the ground water table, emissions, thawing salt damage) aim to prove and quantify the effect of disturbances on forest structure, growth, and yield. Whereas on conventional experimental plots, treatments (e.g. amount of fertiliser, thinning grade) are designated to the experimental units (plots, trees) randomly, systematically, or in stratified blocks, designs for the revelation of disturbance factors on growth are usually spatially determined by the given pattern of disturbances. Therefore, the experimental units are arranged so that they represent the different levels of intensity of the disturbance. Field experiments in which the disturbance factors are experimentally controlled, e.g. through acid sprinkling, drying up, or fumigation with ozone, are extremely resource intensive and are confined to a few research stations [e.g. ozone fumigation experiment Kranzberg Forest, cf. Matyssek et al. (2005); Pretzsch and Schütze (2005, 2008)].

When the disturbances cannot be initiated actively, plots are distributed spatially in a study region to cover different factor levels (e.g. different distances from the point source, damage from sulphur emissions, or rates of salt uptake). To quantify growth responses to salt or pollution within the vicinity of a motorway, one selects sample trees or plots at different distances from the road. The growth response to changes in the ground water table due to the construction of boat canals or the removal of drinking water at specific points can be tested best by growth surveys on sample plots arranged in zones parallel or concentric to the source of disturbance. The same applies for proving growth losses arising from point emission sources such as power stations, ironworks, or ceramic factories (cf. Chap. 14). Here also, plots are arranged to account for the spatial distribution of the harmful substances. Although the plot selection and allocation of treatments differs from that of conventional experiments, making it more difficult to meet ceteris paribus conditions, we include such layouts in investigations or experiments.

The following example elaborates the difference between such experimental designs and conventional ones (discussed previously). To investigate the effects of

distance and direction (=location) from a brown coal power plant (factor 1) and the temporal nature of sulphur emissions (factor 2) on the growth behaviour of Scots pine stands in the vicinity of a brown coal power station, 103 sample plots were established (Franz and Pretzsch 1988; Pretzsch 1989b). This example relates to the brown coal power station at Schwandorf, one of the major sources of pollution in Bavaria from 1960 to 1980 producing an emissions volume of 20–40 t SO_2 per hour. By arranging the study plots in concentric circles at 5, 15, and 30 km distance around the power station, the effect of distance and direction (= location, factor 1) on growth in the surrounding Scots pine stands could be tested. Twenty-three sample plots were located on the inner circle (5-km radius). On the middle (15 km) and outer (30 km) circles, there were 33 and 47 plots, respectively (Fig. 14.9).

For an analysis of variance, the stands can be grouped according to different aspects. The first option is to form three groups of sample plots at the same distance from the power station (factor 1: position with three levels). As the damage is also presumed to be dependent upon direction, the plots may also be grouped by distance and direction. This second option leads to 12 groups (Fig. 14.10): group 1, distance 5 km, 1st quadrant; group 2, distance 5 km, 2nd quadrant; ...; group 12, distance 30 km, 4th quadrant (12 levels).

To test the influence of the emissions over time (factor 2) on the increment behaviour, core samples were obtained from 20 predominant or dominant Scots pine trees on each sample plot. These samples were used to retrospectively calculate the annual and periodic annual increment of stand basal area and volume over the previous 40 years. All sample plots were set up in normally stocked early mature Scots pine stands with an average site class. This resulted is a split-plot design with location as the main unit and the 40 annual increment values as the (temporal) subunits.

The experimental design allows one to test whether location and time influence Scots pine growth in the area surrounding the brown coal power station. Furthermore, the interaction between location and time can also be analysed. By stratifying the sample plots into 12 groups in the same location, as represented in Fig. 14.10, the spatial distribution pattern of growth losses from 1971 to 1973 and 1980 to 1982 could be identified and quantified. With the conversion from low to high chimneys in the 1970s because of political pressure, the emissions were transferred from closer regions to regions that are more distant. This spatial change in pollution arising from the power station is reflected in the spatial–temporal characteristics of the growth losses, which can be found in the surrounding Scots pine stands.

4.7.3 Artificial Time Series or Growth Series

4.7.3.1 Recording Stand Level Data

Artificial time series or growth series are conventional designs for recording growth of pure stands. In the absence of long-term experimental plots, where age development is documented in long-term observation (real time series), artificial time series

are constructed from adjacent stands spanning the desired age spectrum (Fig. 1.3, vertical chronosequence). For this purpose, a series of growth and yield observation plots are set up on a predetermined site unit. A complete inventory of these sites is carried out, which also may include the extraction of core samples to reconstruct the growth process. The sample plots cover the entire age spectrum (e.g. age of plot $1 \hat{=} 40$ years, age of plot $2 \hat{=} 90$ years, ..., age of plot $6 \hat{=} 150$ years) so that these site units represent the temporal stand development one over time. As the past development of the growth series plots also is recorded by measurements retracing shoot development, stem analyses, or increment cores, one can test whether a section of the real time series follows the pattern of an artificial time series. The comparison of the height growth development is particularly valuable for this test on compatibility as it is independent of management. In the past, the growth series concept was used primarily to record the cumulative and mean values in pure evenaged stands to construct yield tables (Chap. 11).

4.7.3.2 Recording Individual-Tree Dynamics

When the design of these conventional artificial time series is expanded to include measurements of crown, growing space, tree position, and growth characteristics of individual trees (Fig. 4.17), one can develop a very valuable database for the analysis

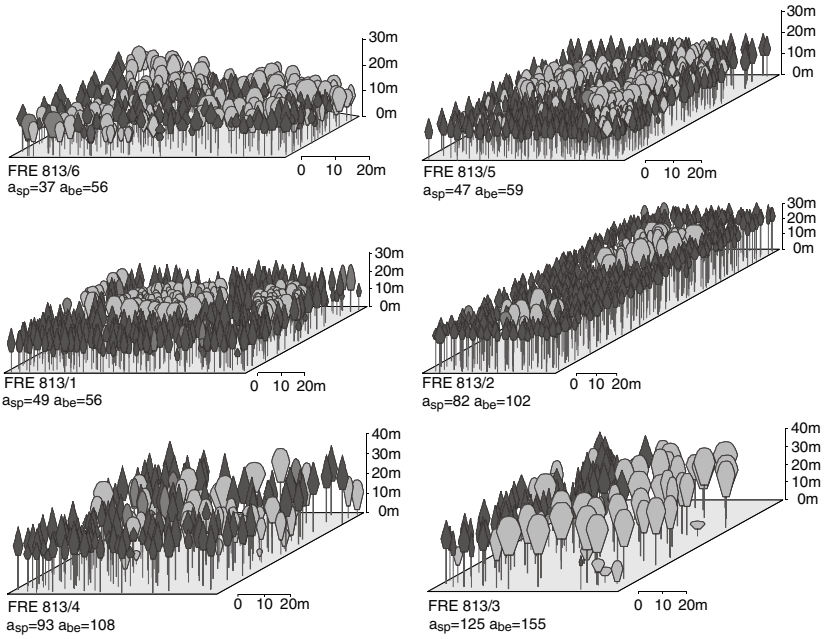

Fig. 4.17 Parts of the time series FRE 813 in the year 1994; artificial time series from young (*top left*) to mature mixed stands (*bottom right*). Stand ages (a_{sp} and a_{be} of Norway spruce and European beech, respectively) refer to the year 1994. All plots were inventoried 1994 and 1999 by measurement of tree positions, crown dimensions, tree diameter, and tree height

and modelling of mixed stands (Pretzsch and Schütze 2008). Since the 1990s, artificial age series of this kind have been established to obtain the individual tree data needed to parameterise mixed stand models; earlier, such precise data were rarely available from long-term plots. With this aim in mind, species-specific growth responses of diameter, height, and crown dimensions and mortality of individual trees should be recorded on artificial age series for the widest age spectrum possible and for different levels of competition. The primary aim of the establishment and survey of individual-tree-based age series is not to record stand mean values, but the structural and the growth and yield characteristics of individual trees. The methods introduced in Chapters 7–9 can be used to derive relationships between the spatial growth arrangement and growth behaviour of individual trees from the time series data. These relationships are required for the description and individual-tree-based modelling of growth in pure and mixed stands. Although the experimental design aims to obtain individual-tree data, typically plots 0.1–1.0 ha in size are set up. In this way, the inventory data relate to a unit area, and the trees in the area may be recorded and managed more easily and efficiently than would be the case in individual-tree designs.

To analyse growth and yield in mixed stands, parameterise individual-tree models and support management decisions in mixed stands, about 20 artificial time series with about 100 plots in total were established recently in the main mixed stands in Bavaria in the last decade specifically for spatial inventory. As an example, Fig. 4.17 shows parts of the age series FRE 813 in the year 1994. All plots were inventoried 1994 and 1999 by measurement of stem position, crown dimension, tree diameter, and tree height. In addition to the individual tree data, time series also deliver information about structural dynamics, growth, and yield at the stand level (Fig. 4.18).

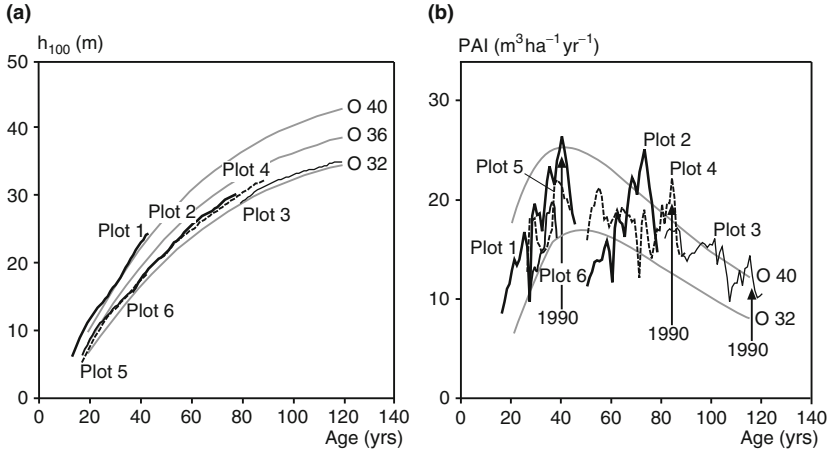

Fig. 4.18 Development of (**a**) top height h_{100} of Norway spruce and (**b**) periodic annual volume increment ($m^3\,ha^{-1}$ per year) on the plots 1–6 of artificial time series FRE 813 in relation to the yield table by Assmann and Franz (1963), top height O32, O36, and O40. The development is plotted by stand age of Norway spruce; the growth in the calendar year 1990 is covered by young, medium-aged, and old stands

Summary

The longevity of forests extends well beyond the working life of a researcher. The variation in site conditions and the diversity in growth processes prohibit the generalisation of results from isolated, local investigations. These forest characteristics make experimentation difficult and require specific research methods that, in terms of spatial and temporal scale, go well beyond the standard methods for physics, medicine, or agriculture. The basic terminology for the design of long-term experimental areas includes the experimental question, the experimental treatment, treatment factors, factor levels, plots, buffer strips, measured and target variables, replications, randomisation, and block formation.

(1) In an experiment, all other factors should be constant except the factor under investigation, which is modified according to the specifications of the study design to analyse its effect on tree or stand development. In this way, experiments can provide clear relationships between cause and effect, e.g. between ozone fumigation and tree growth. In contrast to experiments, inventories just provide data for correlations between cause and effect parameters. Known examples of latter survey type are forest inventories at the enterprise, state, or national level and the monitoring of natural forest reserves.
(2) An experimental question comprises four separate component questions: What do we want to know? What is the desired level of explanation (spatial–temporal scale, e.g. individual tree or stand, daily or annual increment)? What level of accuracy is required? What is the purpose of answering the question? Once the experimental question is clearly formulated, the design, treatments, and analysis of the investigation are planned accordingly to attain the best possible answer to the question.
(3) Of high relevance for growth and yield science as well as for practical ecosystem management are experiments on provenance trials, planting techniques, and plant spacing, thinning, fertilisation, regeneration, species composition, and experiments for the determination of disturbance factors (e.g. lowering of ground water level, increase of ozone concentration, load of thawing salt in forests close to roads).
(4) The site conditions and the number of treatment factors to be investigated influence the selection of the most suitable experimental design. Whereas under homogeneous site conditions, a randomised design is recommended, on inhomogeneous sites, systematic sources of error in one or more directions can be eliminated by block designs and Latin squares. Depending on whether the effect of one, two, or more treatment factors on growth shall be tested, a one-factor, two-factor, or multifactor experimental design results (multifactor block designs, Latin squares, Latin rectangles, split-plot, and split-block designs).
(5) The thinning experiments with the three grades A, B, and C established in the initial stages of forest research in the nineteenth century, and still monitored today, are typical one-factor experimental designs. Recent examples

of one-factor experiments investigate the effect of fertilisation, plant spacing, and provenance as treatment factors. Design options include completely randomised designs for homogeneous sites, simple block designs to eliminate site gradients, and multiple block designs or Latin squares to exclude site gradients in several directions.

(6) Two-factor and multifactor designs analyse the effects of two or more treatment factors and their interactive effects on stand or individual-tree growth. As modern treatment methods generally combine different management techniques (thinning, pruning, fertilisation, soil treatment), the complex decision support can be obtained only from multifactor investigations. Suitable designs include multifactor blocks, multifactor Latin squares and rectangles as well as split-plot and split-block designs.

(7) Two-factor or multifactor investigations analyse the effect of interactions between the treatment factors. From a combined plant spacing and thinning trial, not only can the effect of plant spacing on stand development and the effect of different thinning regimes on stand development be studied, but also the interaction between plant spacing and thinning. Whereas the main effect of the factors is usually known, the interaction or combined effects are rarely understood.

(8) Scattered experimental areas and trial series replicate the treatment factors on different sites. In contrast to recommendations from single experiments, which are only locally valid, scattered experimental experiments and trial series, which cover a range of sites surveyed over long periods, provide results that allow making recommendations that are more general.

(9) Investigations and surveys for the diagnosis of growth disturbances (e.g. sinking ground water table, thawing salt damage) aim to show and quantify the effects of disturbance on growth. Whereas in conventional studies, planned treatments (e.g. fertiliser dose, thinning grades) are allocated to the plots randomly, systematically, or in blocks, designs for the determination of disturbance factors are spatially oriented at the source. The plots are arranged so that their location represents different levels of treatment.

(10) Due to the lack of long-term experimental areas that would show real time series, artificial age series (=growth series) can be established that produce an artificial time series from adjacent stands of different age classes. Repeated spatially explicit inventories can supply data for analysis and modelling of a broad range of pure and mixed species stands.

Chapter 5
Description and Quantification of Silvicultural Prescriptions

Since the initial simple thinning instructions for individual stands of the nineteenth century, silvicultural prescriptions have continued to become more specific in Central Europe. Today, they focus on individual trees and their spatial growth arrangement. The quantitative prescriptions below assist the silvicultural regulation of trial stands. In parameterised form, they are also an element of simulation models for forest stands (cf. Chaps. 11 and 13); in simplified form, they can be used as silvicultural prescriptions in forest management practice.

The research question establishes what experimental factors are to be investigated to identify how they affect forest growth. For example, when the effects of thinning are to be tested in an experiment, one might investigate the different levels – light, moderate and heavy thinning. The results of experiments are both scientifically beneficial and of practical use only when the different factor levels are defined clearly. Factor levels are only fixed once they have been defined quantitatively. This ensures that they are objective, reproducible and therefore largely independent of the leading scientist at the time, which is very important for trans-generational management of experimental plots (Wiedemann 1928).

Experimental results and findings are readily applied in forest practice when the experimental factors and factor levels have been defined as clearly and objectively as possible. Quantitative definitions make investigation results particularly relevant to forest management, and hence readily transferable to forest practice. Assmann (1961a, 1970), and subsequently Abetz and Mitscherlich (1969) recommended addressing the following three factors for clear definitions of thinning and tending operations (Fig. 5.1)

- Kind of thinning
- Severity of thinning
- Intensity of thinning

These three experimental factors help quantify systematically the desired thinning treatments. A quantitative definition of the kind, severity and intensity of thinning can be transferred readily from thinning trials to other experimental factors such as fertilisation, species mixtures and regeneration and soil treatments. In mixed stands, the kind, severity and intensity of thinning are defined separately for each

H. Pretzsch, *Forest Dynamics, Growth and Yield: From Measurement to Model*,
DOI: 10.1007/978-3-540-88307-4_5,

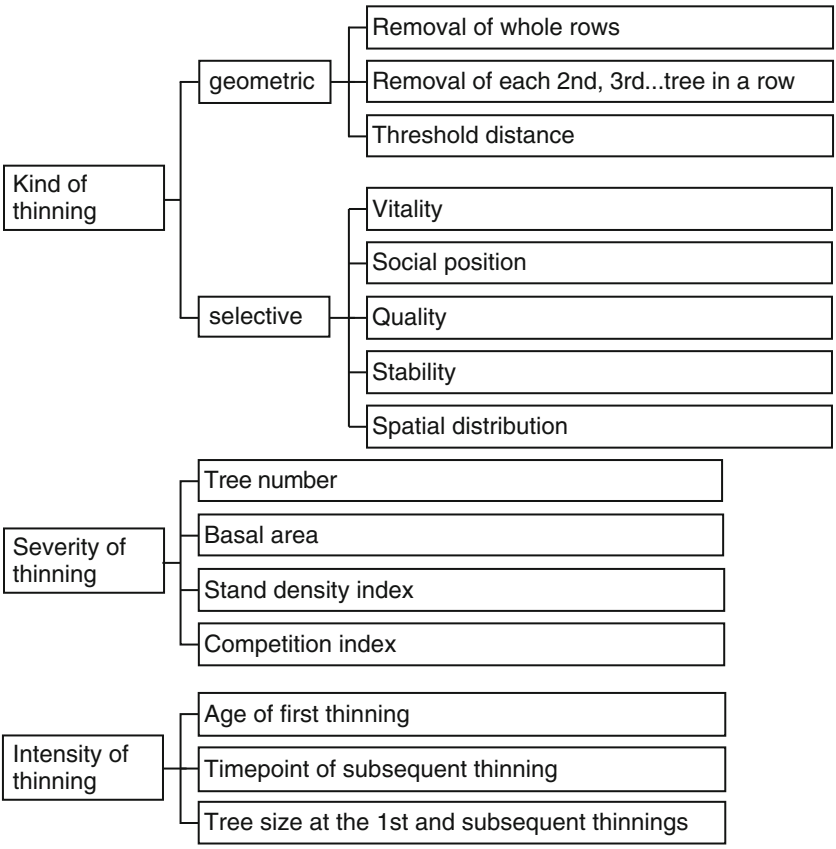

Fig. 5.1 Kind, severity and intensity of thinning as key criteria for silvicultural prescriptions and approaches for quantifying them

tree species present. Specifications of the kind of thinning operations include details about the desired species mixture in the mature stand, and also the structure of the species mixture:

- Single tree mixture (cluster diameter < 5 m)
- Mix in small clusters (cluster diameter 5–10 m)
- Mix in groups (cluster diameter 10–20 m)
- Mix in patches (cluster diameter 20–40 m)

The three experimental factors of thinning are presented in Fig. 5.2 for a European beech thinning trial with three factor levels. The basal area development for the first factor level, a light thinning from below, is represented by the dashed line. It provides a reference basal area for near-natural stand density (A grade). The two curves below it represent moderate and heavy selective thinning. In both, the basal area is considerably different from the reference curve. We use these two thinning variants to explain the kind, severity and intensity of thinning.

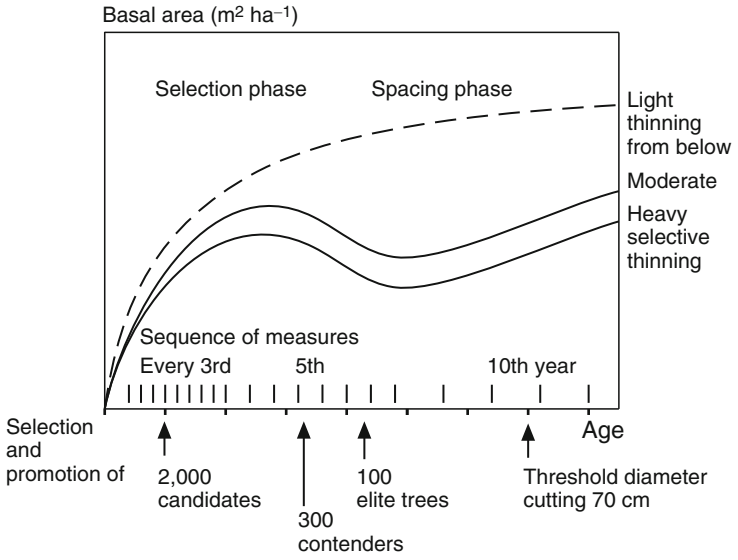

Fig. 5.2 Kind, severity and intensity of thinning plotted for a light thinning from below, and a moderate and heavy selective thinning in European beech stands. From a large number of candidates to a smaller number of contenders, an ongoing selection process gradually reduces the number of selected trees until finally a small number of superior trees is left (Schädelin 1942). Basal area curves determine the density at the stand level

The kind of thinning is characterised by the selection and promotion of the most vigorous individual trees. In the first quarter of the rotation period (R/4), 2,000 candidates are selected and, of these, 300 are identified as contenders by the end of the first half of the rotation period (R/2). After R/2, an increment thinning regime is adopted in the area surrounding 100 superior trees (elite trees). The suitability of this collective of the best growing stock for the final stand is checked repeatedly. Their growth is promoted by the removal of competitors with a thinning from above. (R = rotation turns; e.g. 100 years).

The severity of thinning is defined by a specified target basal area, which is maintained mainly by eliminating competition adjacent to the candidates, contenders or elite trees. The set target basal area aims at leaving a relatively dense crown cover during the first half of the rotation period to promote height growth and self-pruning. Thereafter, increment thinning is adopted to promote diameter growth of the superior trees as much as possible. Moderate and heavy selective thinning differs in the number of trees removed and the density of the remaining stand. They are carried out to promote the candidates, the contenders and ultimately the superior trees (Schädelin 1942).

The intensity of thinning varies from a 3-year thinning cycle in the juvenile phase to a 5-year cycle in the early-mature growth phase, and a 10-year cycle in the mature stand. The superior trees are harvested once the final diameter of 70 cm has been reached.

We began with this example to demonstrate the specific concepts of silvicultural prescriptions in Europe, which define measures for the stand and for individual trees. The manner of quantifying the kind, severity and intensity of thinning may differ completely from this example (Fig. 5.1). Initially, thinning was defined at the stand or tree collective level (Schwappach 1908, 1911; Wiedemann 1932, 1951). Reventlow (1879) initiated the definition and implementation of thinning regimes in relation to individual trees and their growth. The terms candidate, contender, superior trees and reserve trees (Kandidaten, Anwärter, Elitebäume, Reserve) date back to the Swiss silviculturist Schädelin (1942, p. 60 ff) who recognised the individual role of trees in the stand. In current central European forestry practice, a restricted number of high quality trees are frequently selected in the early phase of stand development. These trees are recorded subsequently in inventories, and painted with white dots or rings for recognition and promotion in successive silvicultural operations.

5.1 Kind of Thinning

5.1.1 Thinning According to Social Tree Classes by Kraft (1884)

Historically, the approach for defining silvicultural operations was outlined by Kraft (1884). Given the crown expansion, which is closely related to growth performance, and relative tree height, which reflects tree dominance, the trees within a stand are assigned to one of five social classes (Fig. 5.3). The classification is based entirely on biological criteria: economic or ecological aspects are not considered. The following tree classification, cited from Kraft (1884, pp. 22–23), is still part of the standard forest science and forestry knowledge, and assists in the understanding of questions related to thinning. The five social classes adopted by Kraft are:

1. “Predominant trees with exceptionally well-developed crowns.
2. Dominant trees, forming the main stand as a rule, with relatively well-developed crowns.
3. Low co-dominant trees. Crown shape is still normal, and hence the trees are similar to those in the second tree class in this respect, yet they are relatively weakly developed and restricted, often already with the onset of degeneration (e.g. with somewhat dry shoots at the crown perimeter; oak crowns often reveal the onset of gnarled crown twig growth as well). This third social class forms the lower limit of the dominant trees.
4. Dominated trees, with crowns more or less dying back, restricted on all sides or on two sides, or with one-sided (flag-shaped) development; gnarled twig growth in oak.

    a. Intermediate trees, essentially free of canopy cover with restricted lateral crown growth.

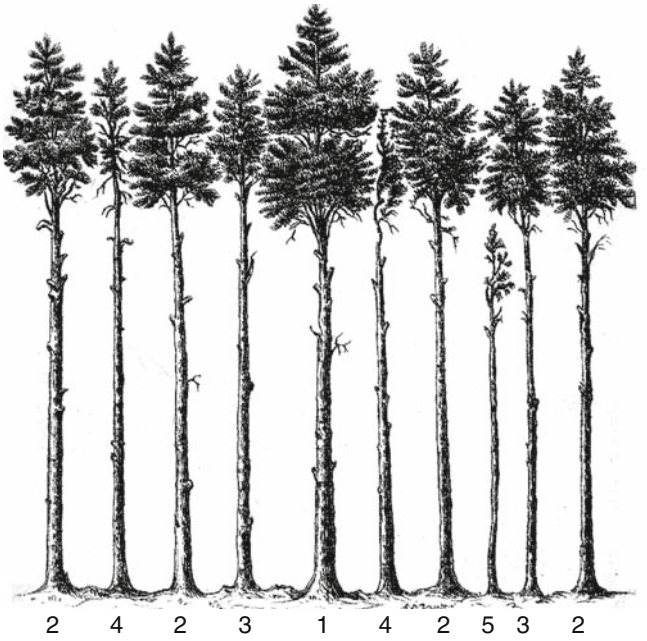

Fig. 5.3 Tree classes 1–5 (predominant to very suppressed stems with dying or dead crowns) for evenaged forest stands from Kraft (1884) provide an example of a qualitative estimate of the competitive status of individual trees within the stand. Criteria for classification are crown size and tree height

b. Partially overtopped crowns; the upper crown free, the lower crown under canopy cover, or dead as a result of canopy cover.

5. Entirely overtopped trees.

a. With crowns capable of growth (only in shade tolerant tree species).
b. With dead or dying crowns' (translation by author)."

Kraft (1884, pp. 38–39) used these tree social classes to define thinning grades (thinning grade defines the kind and severity of thinning):

"The thinning can be related to the tree classes as follows:
Grade 1. Light thinning: utilisation of the fifth tree class.
Grade 2. Moderate thinning (usually the uppermost, though rarely reached, limit of standard thinning practices): utilisation of tree classes 5 and 4^{b}.
Grade 3. Heavy thinning: utilisation of tree classes 5, 4^{b} and 4^{a}.

The last grade forms the extreme [upper] limit of thinning practices. Silvicultural practices beyond this limit are regarded as an opening up of the canopy (temporary to permanent opening up).

Between thinning grades 2 and 3, a middle grade 2^a, describing a moderate to heavy thinning, can be included. It is confined to smaller trees with weakly developed crowns, or to severely crowded trees in class 4^a in addition to the classes 4^b and 5. In common practice, which often lags behind the natural process of tree mortality instead of supporting and accelerating it, this intermediate grade is rarely achieved; the characteristics of this thinning grade are, unfortunately, rather vague as it does not fit into the clearly defined tree classes.

The use of tree classes facilitates the implementation of thinning operations. Furthermore, it ensures the thinning operations are implemented similarly. In addition, and equally important, once the overseer of the operations has grasped the nature of the tree classes through practical training in the forest (which happens quickly in my experience), he can direct thinning operations more easily (translation by author)."

Kraft's silvicultural prescriptions define the kind of thinning by the tree classes to be removed. The number of trees removed in the different social classes determines whether a light, moderate or heavy thinning has been applied, and thus quantifies the severity of thinning. Compared to all subsequent thinning definitions, the three thinning grades defined above (includes kind and severity of thinning) represent a very cautious method for raising high volume single-layered stands from the nineteenth century. The kind and severity of thinning are defined qualitatively, omitting details about the timing of the first thinning and the thinning cycle. Yet, Kraft's definitions, with the classification of trees within the stand, represent the beginning of silvicultural tending regimes, which have since become increasingly intensified, specialised and precise. Although Kraft's definitions of thinning operations are merely of historical significance today, his tree classes still provide a standard for tree dominance classes used today.

5.1.2 Thinning According to Combined Tree and Stem Quality Classes from the Association of German Forest Research Stations (1902)

In the working plans of the Association of German Forest Research Stations from 1902 (Verein Deutscher Forstlicher Versuchsanstalten 1873, 1902), the kind of thinning (e.g. thinning from below, thinning from above, open-stand thinning) and the severity of thinning, i.e. the extent of density reduction (e.g. light, moderate, heavy thinning) were defined on the basis of combined tree and stem quality classes. The following text is cited from the 1902 working plan from the Association of German Forest Research Stations:

"I Principles
§2

The trees within a stand can be differentiated as follows:

I. Dominant trees. These comprise all trees that are present in the upper crown canopy as:

1. Trees with normal crown development and good stem form.
2. Trees with abnormal crown development or poor stem form.

This includes:

a) Crowded trees
b) Poorly formed wolf trees
c) Other trees with defective stem formation, particularly forked trees
d) So-called whips
e) Unhealthy trees of all types

II. Dominated trees. These comprise all trees that are not present in the upper crown canopy.

In this group one finds:

3. Slow growing trees, yet free of canopy cover, that are considered in soil and stand tending treatments.
4. Suppressed (lower storey, overtopped) trees, yet still with the capacity for growth, that are considered in soil and stand tending treatments.
5. Dying and dead trees no longer considered in soil and stand tending treatments, including bowed saplings as well.

§3

Thinning essentially applies to the removal of dead and dying, slow growing, unhealthy trees, trees with an irregularly formed crown or bole, or those trees that, despite a good crown and bole form, are detrimental to the remaining, more valuable trees with greater growth potential. Thus, in thinning operations, the trees in the classes 5–2 are removed partially or totally and, in exceptional cases, stems in class 1 are removed if it is deemed necessary to break up a group.

In contrast, in operations to open up the canopy, essentially trees with strong, healthy growth that do not impact on remaining neighbouring trees as yet are removed, some larger and some smaller trees in tree class 1 with the aim of creating permanent gaps in the canopy. This strategy should be continued for the duration of stand rotation, or at least for a long period as, for example, in Seebach's approach to stand opening up.

§4

The following thinning grades are differentiated in thinning operations:

I. Thinning from below

1. Light thinning (A grade). This is limited to the removal of dying and dead trees, as well as any bowed pole wood (5) for the purpose of delivering material for comparative growth investigations only.

2. Moderate thinning (B grade). This encompasses the dying and dead, bowed, suppressed trees, any whips, the most dangerous and poorly formed wolf trees that cannot be rendered harmless by pruning, and unhealthy trees (classes 5, 4 and part of 2).
3. Heavy thinning (C grade). This removes all trees except those in class 1 so that only trees with normal crown development and good stem form remain, which, with the breaking up of any groups on all sides, have space to develop their crowns freely while maintaining continuous crown cover.

II. Thinning from above

This operation is undertaken in the upper canopy space to achieve a special tending regime for that component of dominant trees destined to become the future final crop. Here two thinning grades are differentiated:

1. Light thinning from above (D grade). This is limited to the extraction of dying or dead, bowed trees, followed by the poorly formed and unhealthy trees, the forked trees, wolf trees, whips, as well as those trees that must be removed to break up groups of equally valuable trees. Thus thinnings include tree class 5, a large part of tree class 2 and individual stems from tree class 1. The removal of the poorly formed wolf trees, and other trees with defective bole form, in particular the forked trees, can be carried out in more than one thinning operation if such trees are present in large numbers to avoid opening up the canopy too severely. During the first thinning, pruning or the removal of forked trees is recommended to eliminate potential detrimental effects to the remaining stand. This thinning grade is adopted primarily in young stands.
2. Heavy thinning from above (E grade). The aim of this thinning grade is to tend specifically a known number of the future crop trees identified. For this purpose, in addition to removing the dying, dead, bowed and unhealthy trees, all those trees are removed that inhibit the good crown development of the future crop trees; that is class 5 and stems in class 1 and 2. This thinning grade appears to be suitable mainly for more mature stands.

§5

Investigations of the influence of increment felling are conducted using volume increment to determine whether, and to what extent, perpetual interruptions to the crown canopy by means of the heaviest thinning grade are capable of increasing the growth of the whole stand or individual trees above a desired amount. Additionally, the aim also is to identify when growth begins to fall again as a consequence of too large a reduction in tree number, and the limit to the increase in individual tree growth.

For this purpose, subject to other special investigations, e.g. for Seebach's opening up operations, two intensities of stand opening up need to be differentiated:

1. Light opening up (L-I grade); and
2. Heavy opening up (L-II grade).

The former thinning strategy removes 20–30%, and the latter 30–50% of the stem basal area of the adjacent reference plots in a C grade thinning. The heavy opening up can be increased above the stated level to maximise the increment. The conversion from a closed stand to clearances should occur gradually."

Figure 5.4 indicates the tree classes that are removed completely or partially in a thinning from below, an opening up and a thinning from above based on the 1902 instructions. It shows clearly that an increase in thinning, commencing with the inferior trees, takes place from the A grade to the opening up, L II grade. The light and heavy opening up, L I and L II respectively, are defined in terms of the basal area removed, thereby providing a quantitative definition of the thinning intensity. The light and heavy thinnings from above leave the slow-growing and suppressed trees (tree classes 3 and 4). The aim of a heavy thinning from above is to promote the future crop trees already selected.

For all shortcomings and inadequacies perceived today, the combined tree and stem quality classification, and the definition of management strategies developed from them, are still a very important reference as most of the long-term thinning experiments, which are surveyed still, are guided by this standard. The thinning trials following these thinning grades form the database for our pure stand yield tables, and the thinning variants in these yield tables are based on the thinning definitions from 1902. Separate yield tables have been set up for light, moderate and heavy thinnings from below, or light and heavy thinnings from above. Thus the A, B, C, D and E grades defined in the working plan from the Association of German Forest Research Stations form a reference in this respect. The definition of the grade of thinning is based on the tree classes developed in 2 from tree dominance and stem

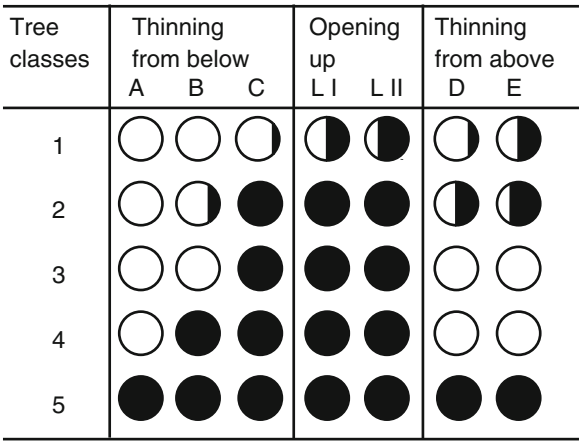

Fig. 5.4 Diagram of thinning from below (A = light, B = moderate, C = heavy), opening up of the canopy (L I = light, L II = heavy) and thinning from above (D = light, E = heavy) based on the definitions from the Association of German Forest Research Stations (Verein Deutscher Forstlicher Versuchsanstalten, 1873, 1902): the *partially, or entirely black circles* represent partially, or completely removed tree classes respectively

quality. The combined tree and stem quality classes defined in 2 differ from the tree classes defined by Kraft (1884) in that they also incorporate qualitative criteria in addition to tree dominance. From today's perspective, these definitions of thinning lack details about the timing of the first thinning and the thinning cycle for all treatment variants, the criteria for the selection of future crop trees for a heavy thinning from above, and sufficient detail about the kind and manner of releasing these future crop trees.

5.1.3 Thinning After the Selection of Superior or Final Crop Trees

The first step in this silvicultural practice is to identify a number of so-called superior trees or future crop trees, which then become the focus of further management interventions. In a second step, these superior trees are promoted in the long-term by removing a defined number of competitors. Additional tending measures are undertaken in the space between these trees, the area of which varies according to the number of superior trees or future crop trees and the number of competitors to be removed. By future crop trees we mean the trees with good, vigorous growth, which are selected and permanently marked at the pole or young timber stage, and thereafter maintained and systematically promoted until they reach a desired target diameter. Once selected, future crop trees are kept strictly until the final cut. According to Assmann (1961a, p. 268) these "[...] child prodigies selected at a young age [...]" are associated with considerable uncertainty because of this early, and rigid selection process. In contrast, the concept of selective thinning appears more flexible. Superior trees are also selected at a top height of 8–12 m, but their suitability for the final stand is reevaluated in each subsequent silvicultural operation. The original selective thinning (Auslesedurchforstung) defined by Schädelin (1942) clearly shows the gradual progression to the final number of crop trees, which is associated with greater flexibility in, yet more resource intensive, silvicultural measures compared with the earlier, rigid specification of future crop trees. Beginning with a large number of candidates, then progressing to a smaller number of contenders, the number of trees selected becomes gradually smaller in an ongoing selection process until, finally, a small number of superior trees remains (Schädelin 1942). Each method differs essentially in the level of risk, the intensity of decision-making and the spatial concentration of tending measures.

Selective thinning and crop tree thinning should not be confused with selection thinning (Plenterdurchforstung) or the selection forest system (Plenterwald). In selection thinning, developed by Borggreve (1891), dominant trees are removed in the late pole stage to increase intermediate yield, promote subdominant trees and prolong the rotation length. In contrast, the selection forest system describes an unevenaged, typically mixed-species forest with an inverse J-shaped size distribution in which mainly the medium and high diameter classes are harvested (Knoke 1998; Pretzsch 1985a; Schütz 1997).

Table 5.1 Criteria from different authors for the selection of superior trees and future crop trees (from Schober 1988a, b)

Heck (1898)	Leibundgut (1966)	Rank	Abetz (1974)
Healthy tree, tall crown size, high increment	Crown size	1	Vitality regarding social position and crown size
Stem quality	Stem shape	2	Quality (stem shape)
Spatial distribution	Spatial distribution	3	Spatial distribution
Stability considering wind and storm			Stem stability (h/d-ratio)

Vitality is the first criterion for the selection of superior trees or future crop trees. It is revealed in crown size, tree dominance status, or tree growth. The second selection criterion is stem quality, often defined by stem form, or the degree of branching or damage. Third, a regular distribution of superior trees or future crop trees should result, attained by establishing a minimum distance between trees. Another criterion might include individual-tree stability, characterised by slenderness or crown length. These criteria should be ranked: the ranking adopted by Abetz (1975) of vitality, quality followed by distribution is one option (Table 5.1). Kató and Müldner (1978) and Kató (1979, 1987) recommend another system of ranking, introduced in their "qualitative group selection thinning" method, in which the trees selected for promotion may also be selected in clumps. This method is particularly appropriate when the vigorous superior trees or future crop trees that meet the qualitative criteria are distributed irregularly across the stand, such that a sufficient number of vigorous growing stocks can only be obtained by including trees in clusters.

5.1.3.1 Tree Number and Distance Regulation

Given the number of superior trees or future crop trees n in a mature evenaged forest stand, the mean area available for tree growth a is determined as

$$a = \frac{10{,}000}{n}, \tag{5.1}$$

where a represents mean area available for tree growth and n is the target number of future crop trees or superior trees in the mature stand. Conversely, the target area available for tree growth a in the mature stand determines the final number of future crop trees or superior trees per hectare is

$$n = \frac{10{,}000}{a}. \tag{5.2}$$

If the estimated target area available for tree growth a in a mature European beech stand is $a = 100\,m^2$ per tree, then no more than $n = 100$ future crop trees should be specified. The number of future crop trees, or the final number of superior

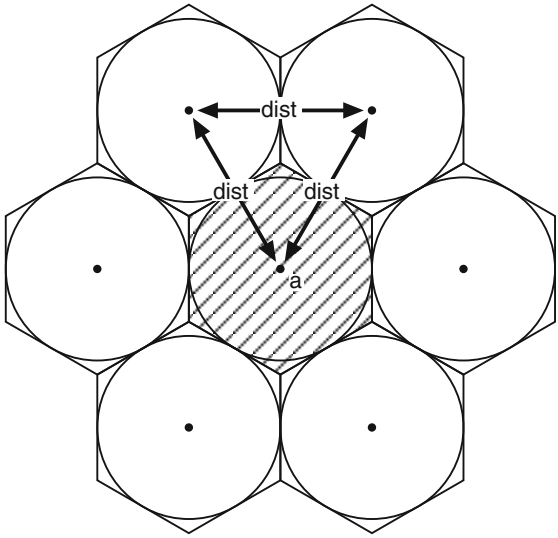

Fig. 5.5 Triangular arrangement of trees produces hexagonal growing areas: dist = distance to the next neighbours; a = mean growing area of individual trees (*hatched*)

trees, determines the upper limit for the degree of release. From the number of future crop trees n, the mean distance dist between the future crop trees is derived from

$$\text{dist} = \frac{1}{\sqrt{\text{n}}} \times 107.46, \tag{5.3}$$

where a triangular arrangement of trees is assumed (cf. Fig. 5.5). In this case, the area available for tree growth approximates a regular hexagon. The relationship between the mean tree distance dist, the mean area available for tree growth a and the number of future crop trees per hectare n is given by

$$\text{dist} = \sqrt{\text{a}} \times 1.0746 = \sqrt{\frac{10{,}000}{\text{n}}} \times 1.0746 = \frac{1}{\sqrt{\text{n}}} \times 107.46. \tag{5.4}$$

This relationship can be applied in the experimental planning phase to calculate the potential number of future crop trees for the area available for tree growth desired in the mature phase (Fig. 5.6a), followed by the mean distance between the selected final crop trees, dist (Fig. 5.6b). The mean distance measure then guides the selection of regularly distributed future crop trees on plots. Distances below, or above this mean distance reduce, or increase the degree of release possible during the experiment respectively.

The number of superior trees or future crop trees to be selected depends, firstly, on the tending regime to be investigated and the timing of selection. Schober (1988a, b) investigated the following ranges in the number of future crop trees for the tree species listed below (trees per hectare): Norway spruce 150–400,

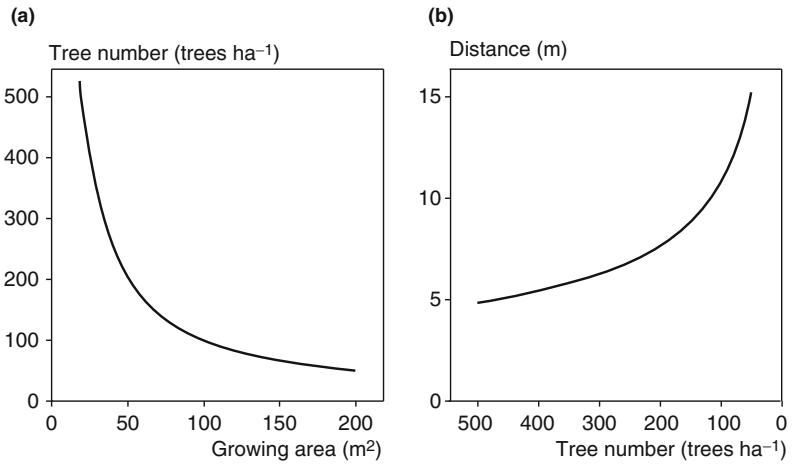

Fig. 5.6 Relationship between (**a**) area available for growth and tree number per hectare, and (**b**) tree number and mean distance to nearest neighbour for triangular spacing. These relationships (**a**) can be applied for determining the number of future crop trees in relation to the area available for growth in the final stand, and (**b**) shows the mean distance between them

Table 5.2 Future crop tree numbers, mean and minimum future crop tree distances (in brackets) derived from crown measurements in pure and mixed stands by Abetz (1974)

Tree species	Norway spruce	Silver fir	Douglas fir	Scots pine	European larch	European beech	Sessile/ Common oak
Number of future trees (trees ha^{-1})	400	300	100	200	100	110	60
Norway spruce	5.7 (4.0)						
Silver fir	6.2 (5.0)	6.6 (4.0)					
Douglas fir			11.5 (8.0)				
Scots pine	7.0 (6.0)	7.3 (6.0)		8.1 (5.0)			
European larch		9.0 (7.0)		9.8 (8.0)	11.5 (5.0)		
European beech	8.5 (7.0)	8.7 (7.0)		9.5 (7.0)	11.2 (8.0)	11.0 (5.0)	
Sessile/Common oak				11.4 (8.0)	13.1 (9.0)	12.9 (9.0)	14.8 (6.0)

Silver fir 300, Scots pine 200–300, Douglas fir 100–200, European beech 90–120, European larch 100, Sessile oak 50–100.

Table 5.2 indicates the target mean and minimum distances targeted between future crop trees in pure and mixed stands for the given number of future crop trees.

Abetz (1974) derives these distances empirically using tree distance and crown radial measurements at experimental plots comprising pure and mixed stands of the dominant tree species in Europe. The number of future crop trees often is fixed according to the number of trees possible and the area required for growth in the mature stand. By comparison, in stands treated by selective thinning, the number of trees selected is usually greater since the selection process is continual, carried out from the first selection through to the final stand.

5.1.4 Thinning Based on Diameter Class or Target Diameter

By sorting the trees in a stand into diameter classes with a width of 1 or 5 cm, for example, a stem number–diameter distribution is obtained in which the mean diameter, variation, skewness and excess of the frequency distribution reflect the underlying stand structure. The stem number–diameter distribution of an evenaged pure stand can be approximated by a normal distribution, whereas that of mixed-species mountain forests and selection forests is approximated best by an exponential inverse J-shaped distribution (Pretzsch 1985a). Assmann (1961a) described the diameter classes as numerical tree classes because the trees within a class, like the tree classes defined by Kraft, are comparable in size and social status.

Therefore, the kind of thinning can also be defined by specifying the stem number–diameter distribution to be maintained. By comparing the actual stem number–diameter distribution with the desired, programmed distribution, the treatment is regulated. When the desired tree number is surpassed, a thinning is carried out to reduce it.

Figure 5.7 provides an example of this method for the silvicultural treatment of the selection forest experiment, Freyung 129. An equilibrium curve is obtained from

$$n = k \times e^{-a \times d}, \tag{5.5}$$

which describes a declining exponential distribution that can be represented as a line in the semi-logarithmic coordinate system

$$\ln(n) = \ln(k) - a \times d, \tag{5.6}$$

where n represents tree number per diameter class, d diameter class, k intercept, a the slope of the line and ln the natural logarithm. The presentation of the stem–diameter distributions in semi-logarithmic coordinate system (Fig. 5.7) shows clearly whether the stem number lies above or below the reference curve. The curve parameters k and a can be determined from the target diameter d_t and the corresponding stem number n_t in this diameter class, and the mean diameter of the first diameter class d_i

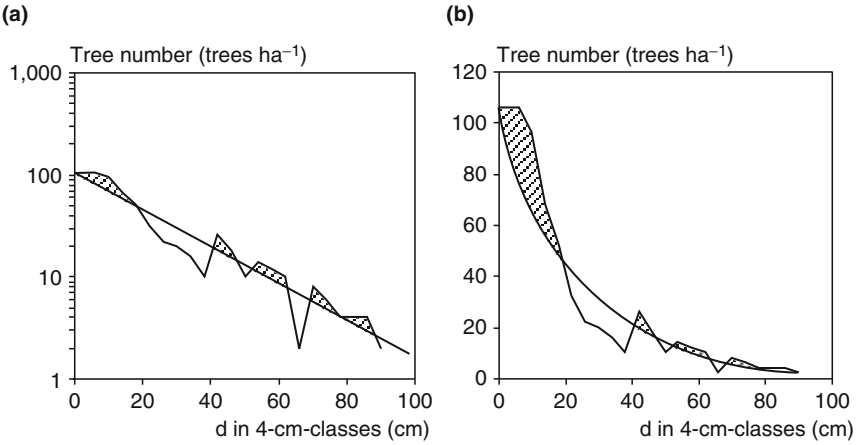

Fig. 5.7 Silvicultural prescriptions using target stem number–diameter distributions. Observed stem number–diameter distribution (*black solid jagged line*) for the selection forest experiment Freyung 129, plot 1, and corresponding equilibrium curves are displayed (**a**) on a semi-logarithmic scale, and (**b**) linearly: *hatched areas* between observed tree numbers and the model curve indicate required thinning; *white areas* indicate diameter classes with an undersupply of trees

and the corresponding stem number n_i, respectively. The curve parameter a reflects the process of recruitment:

$$a = \frac{\ln(n_t) - \ln(n_i)}{d_t - d_i}, \tag{5.7}$$

where k is determined by

$$k = n_i \times e^{ad_i}. \tag{5.8}$$

Schütz (1997) suggests a simple algorithm for determining equilibrium curves for selection forests to obtain the desired distributions. These approximate exponential distributions as a rule. Diameter distribution models and individual-tree models offer an even more convincing approach for the derivation of reference curves (cf. Chap. 11). No matter how the reference curve is developed, its application is rather simple. The desired stem number–diameter distribution is compared to the actual distribution. Any deviation from the equilibrium curve can be addressed by removing the excess tree numbers in the diameter classes. In our example (Fig. 5.7), intensified thinning in the middle and large tree classes improved the regeneration conditions and recruitment.

The final cutting can also be quantified by a threshold diameter, derived in relation to ecological and economical considerations. In this case, all trees, or a defined proportion of those trees exceeding the final diameter stipulated, are removed in each thinning operation. The severity of the thinning is governed by prescribing the portion of the trees outside the threshold that need to be removed (cf. Sect. 2). Figure 5.8 provides an example of the development of the stem number–diameter

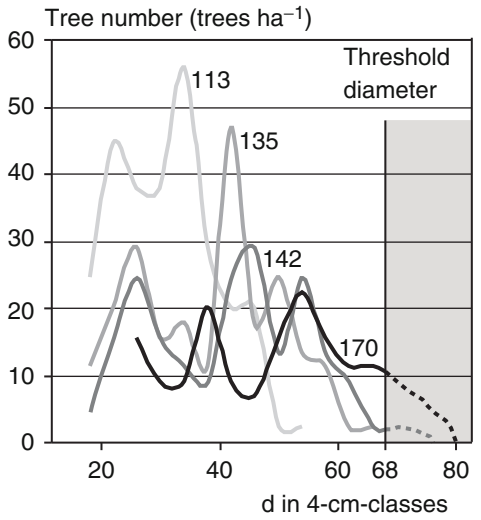

Fig. 5.8 Quantifying kind of thinning by setting a target diameter of 68 cm, above which all trees or a defined portion of trees are removed. The stem number–diameter distributions are presented for the European beech thinning experiment, Wieda 99, plot 1, at the age of 113, 135, 142 and 170 years. The right tail of the distribution is capped in target diameter free utilisation

distribution for the European beech thinning trial, Wieda 99, plot 1, at the age of 113–170 years. It shows how the distribution gradually approaches the target diameter. In each thinning, the trees over 68 cm diameter at breast height (cf. Fig. 5.8, hatched area) are removed. The first thinning occurred at 135 years of age. By the time the trees are 170 years old, the majority of the right tail of the stem number–diameter distribution has been removed.

5.2 Severity of Thinning

The target stand density may be defined at the stand or tree level. A definition incorporating both levels is also possible, and is being used increasingly. In this case, the degree of release can be quantified for the individual superior trees or the future crop trees on a trial plot (e.g. 1, 2, 3… competitors removed to keep distance to nearest neighbour above a given threshold). Furthermore, any additional thinning required in the areas between the vigorous growing stock being promoted can be quantified by stipulating a stand density measure (e.g. stem number, stand basal area, stand density index SDI). The combined individual tree and stand level definitions of thinning makes the kind and intensity of thinning operations more precise, and improves the comparability of results from different experiments. As the structural distribution of removals is specified in addition to the absolute level of stand density, the potential for subjective interpretation and implementation of silvicultural

prescriptions is restricted. In long-term experiments, both stand density and severity of thinning should be specified for the entire survey period, i.e. potentially 50 or 100 years.

5.2.1 Thinning Based on a Target Stand Density Curve

The instructions from the Association of German Forest Research Stations regulate the desired stand density qualitatively by specifying the complete or partial removal of trees in the classes 5, 4, 3, 2 and 1. With this definition, however, the thinning severity and the corresponding stand density are not specified clearly because differences in tree dominance and the distribution of tree number in tree classes is site-dependent, and may be managed somewhat subjectively.

The number of trees to be removed per hectare would appear to be a more appropriate measure of the severity of thinning. The target stem number per hectare, a measure of the remaining stand density, can be applied successfully in the implementation of a trial, in the juvenile stand phase and in the pre-commercial thinning phase. However, as the stand develops and the diameter range expands, the usefulness of stem number per hectare for controlling stand density declines. In contrast to the early growth phase, when trees are similar in size with correspondingly similar values for stem number, percentage basal area and percentage volume removed, tree size varies considerably in early-mature and mature stands, which means that the removal of the same percentage stem number may lead to very different reductions in basal area. Consequently, stand basal area is more appropriate for managing density because it combines the yield elements, stem number per hectare and stand mean diameter. However, due to the errors associated with height measurements and form factor determinations, stand volume per hectare provides inaccurate stand density values, and, therefore, is an unsuitable control parameter for stand density.

Although Curtis (1982), Hart (1928) and Becking (1953), among others, recommend the use of stand density indices and stand management diagrams to manage stand density or the severity of thinning, they have not been applied in practice in Europe. Stand density management diagrams (SDMD), a common tool for regulating the stand density of many species in US and Canada, adopt the self-thinning line as the upper boundary and reference for definition of density levels (Chap. 10, Sect. 10.4). This is the most prominent silvicultural application of the self-thinning rule (Oliver and Larson 1990, pp. 352–353).

5.2.2 Approaches for Regulating Thinning Severity and Stand Density

To test a hypothesis, or reveal a relationship between thinning and stand or tree growth, a defined thinning regime needs to be maintained in the experimental plots

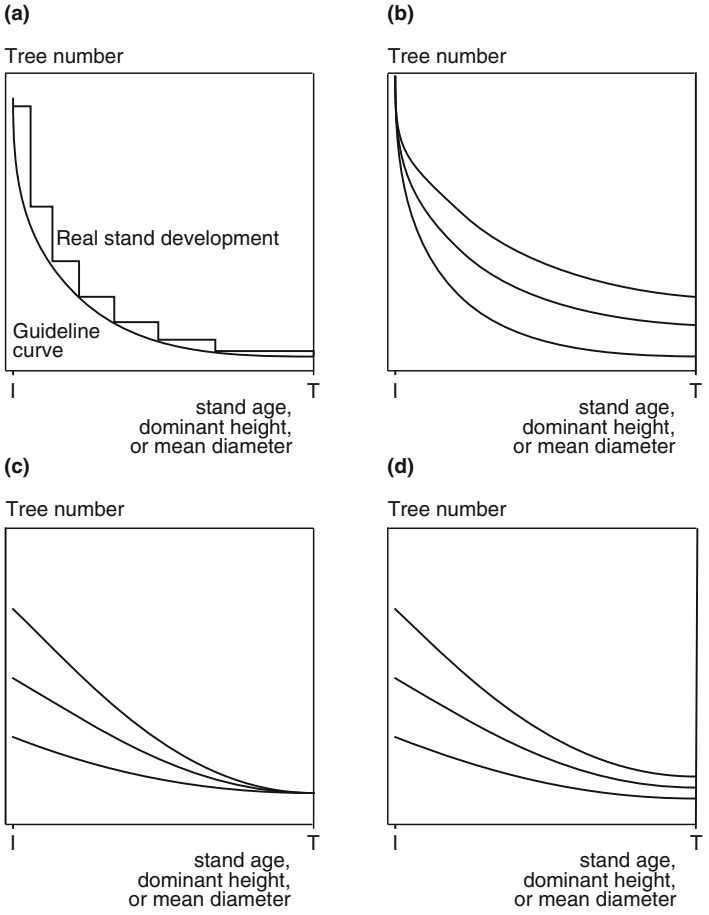

Fig. 5.9 Curves for setting stand density and specifying the thinning from the initial state (I) to the target state (T) of the long-term experiment. (**a**) Stand density (*stepped line*) is guided along the optimum density curve. This gives the corresponding severity of thinning (*step heights in the curve*). (**b**) With an equal stand density at the beginning of the experiment, different density levels (factor levels) are established and maintained until the end of the long-term inventory. (**c**) With different stand densities and a corresponding range of areas available for growth at the beginning of the experiment, the treatments aim for the same stand density in the final stand phase. (**d**) The density levels at the beginning of the experiment are maintained for the duration of the survey

in the long-term. The establishment of curves for the desired development of stand basal area or stem number by stand age, top height or mean diameter, as shown in Fig. 5.9, provides clear quantitative guidelines for the severity of thinning. Stand density (ordinate) can be described by stem number, basal area, volume or stocking density. The age, top height or diameter indicates the development phase of the stand (abscissa). The reference curve, outlining the pathway stand density should follow, should be defined precisely for each plot (Fig. 5.9a). The derivation of a reference curve, or a series of reference curves, may be theoretically based, for example when

the site-specific maximum density is used (derived from A grade plots of the same trial), or obtained from a theoretical site-specific or species-specific maximum density (Franz 1965, 1967b; Sterba 1975, 1981).

Given the underlying question and hypothesis, most spacing and thinning experiments can be assigned to one of the silvicultural regimes for managing stand density as presented schematically in Fig. 5.9. An investigation of the question as to what growth and yield results when different densities are established and developed further in stands with identical structures at the outset leads to the system of curves in Fig. 5.9b. Examples of this concept of density management may be found in traditional thinning trials, increment thinning trials and natural regeneration trials. Ultimately, these trial plots all have different density levels (e.g. A, B and C grade). The system of target curves in Fig. 5.9c applies to research in many spacing trials because it answers the question, what density regime achieves best the predefined target density. Spacing trials, comprising plots with different densities, yet the same number of superior trees or future crop trees selected for promotion, provide examples of this approach. If the research question is concerned with the effect of different initial stand states, different density regimes in the investigation period and different final densities, then we obtain the system of target curves presented in Fig. 5.9d. Growing space trials with different numbers of superior or future crop trees present examples of this approach in silvicultural management. A change in treatment concept during the investigation is only justifiable under exceptional circumstances (e.g. disturbance of plots by disasters, change in research aims in the mature phase from thinning to underplanting or regeneration).

Assuming the size, quality and spatial distribution of trees within a stand are relatively homogenous, the subject tree number, alone, is an efficient means of setting and regulating stand density. This applies especially in evenaged forests that have developed after a large-scale fire. Figure 5.10 shows a stand density management diagram (SDMD) for boreal conifers (adapted from Weetman 2005, p. 7) with four different thinning regimes quantified by the stem number–mean volume trajectories (shown in the ln–ln-scale). The upper boundary line (solid black line) represents the maximum stand density under self-thinning and is derived empirically from unthinned stands. The area below the line gives the possible tree number–mean volume relationships.

Trajectories 1–4 all commence with dense natural regeneration. Trajectory 1 describes unthinned stand development yielding high total volume at low cost, but with a low mean tree volume. Trajectory 2 describes moderately dense stands established by frequent light commercial thinning to maximise volume production. In trajectory 3, a moderate pre-commercial thinning reduces the high initial density to one that allows for a single commercial thinning, and trajectory 4 applies a heavy pre-commercial thinning, reducing the tree number reduction to the final level. The latter thinning scenario represents the minimax-approach, in which a minimum number of trees at the beginning go unthinned for a long period of time to accumulate maximum standing volume. Bégin et al. (2001) list the available SDMDs for a large number of tree species as guidelines for stand management.

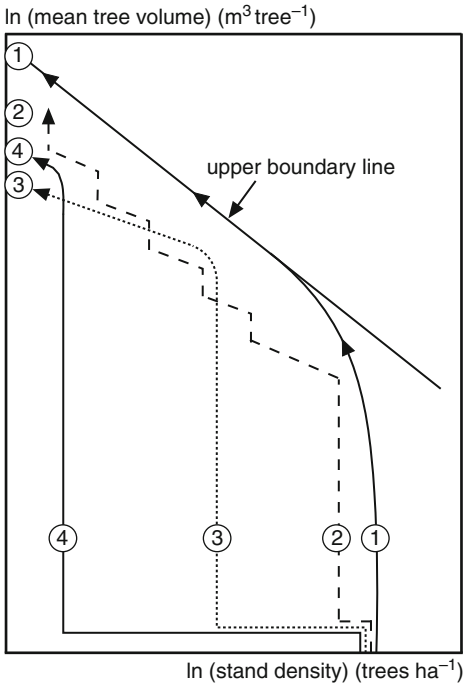

Fig. 5.10 Stand density management diagram (SDMD) for boreal conifer stands with four trajectories representing various thinning concepts (adopted by Weetman 2005, p. 7). The upper boundary line (*black solid line*) represents the maximum stand density and is derived empirically from unthinned stands. The area below this threshold stand density outlines the possible tree number–mean tree volume relationships. Trajectories 1–4 all begin with dense natural regeneration, and subsequently quantify different silvicultural prescriptions explained in the text. Note the ln–ln-scaling of the axes

5.2.3 Selection of Density Classes

The experimental factor levels should not be confined to densities commonly used in practice, but also include extreme values such as maximum density and solitary behaviour. The availability of such information about the extremes enables general relationships between density and growth responses to be derived. The density regimes, presented in Fig. 5.9 as target curves for the remaining stem number, can also be defined by the final basal area, or standing volume. They are derived using one of the following methods.

In the first method, a normative target density curve is derived from the initial and final densities used in practice. Occasionally the desired initial and final densities are plotted as a semi-logarithmic curve (abscissa: age, mean height, or top height; ordinate: stem number) producing a straight line. In this way, curves that decline exponentially are represented in the linear coordinate system.

The second method bases thinning intensity on the local expected maximum density. To this end, an experimental design incorporates one untreated experimental factor level, which serves as a control for the other plots. The untreated plot provides the upper limits for the system of target curves (uppermost line in Fig. 5.9b–d), and serves as a control for other factor levels (e.g. tree number 100%, 80%, 60% and 40%).

In the third method, untreated control plots are missing on the experimental plot at the outset, or they drop out during the course of the experiment. In these cases the maximum density can be derived with the analytical methods developed by Franz (1965, 1967b) or Sterba (1975, 1981) for use as a control.

The advantage of methods 2 and 3 is that the target curves are based on the upper biological limit of the site throughout the entire observation period.

To define density classes as percentages of the A grade conditions (e.g. experimental factor levels 1, 2 and 3 correspond to a maximum tree number, 80%, and 60% of the maximum basal area respectively), one needs to account for the characteristic changes in growth responses to these density reductions with age. Whereas it may be useful to investigate a density reduction to 60% of the A grade level in the juvenile phase when the capacity to respond is high, a similar reduction in a mature stand might result in the stand being opened up too much unnecessarily. Mature stands are more sensitive to the same relative reductions in density because their capacity to respond declines. The percentage reductions should therefore become smaller with increasing age so that the target density curves converge.

In addition to the practice of maintaining stand density on a constant, continuous course, target density curves comprising alternating phases of extreme rises and falls in density are conceivable. For example, the minimax-method of maintaining density pursues the lowest possible density (min) together with the greatest possible stimulation of diameter growth of the remaining trees in the juvenile phase. This is followed by a phase in which the aim is to achieve maximum density (max) to keep the productivity of the stand as high as possible (Zeide 2005).

5.2.4 Management of Stand Density in Fertilisation and Provenance Trials

Clear, quantitative descriptions of thinning strategies on long-term experimental plots are also necessary to test the effects of fertilisation, provenance selection or soil treatments on tree and stand growth. When establishing fertilisation experiments, the stand density on all plots should be comparable and, during the survey periods, thinning on the experimental plot should be limited to dying or unhealthy trees. In this way, growth responses to fertilisation can be differentiated from responses to thinning operations. If, after 5–10 years, the effect of fertilisation on tree or stand growth has been tested, and thinning is necessary due to the increase in stand density, the unfertilised plots should be thinned at the same relative intensity as the plots with different fertilisation treatments. If 10%, 20% or 30% of the stem

number or basal area is removed from the plots most affected by fertilisation, the adjacent plots should also be adjusted to this same relative stem number or basal area density (Abetz et al. 1964; Franz 1967a).

The use of the same relative density is also recommended in provenance trials, as this is the only method that takes into account the different growing space requirements of different provenances. Equivalent stem numbers or basal areas in all provenances in an experiment eliminate any provenance differences in spatial occupancy patterns and growth rates (Schober 1961).

In all investigations set up to test disturbance factors (salt, insect infestations, atmospheric pollution) on forest growth, thinning treatments of the same intensity are recommended for all plots because then the responses to the disturbance factors largely can be isolated from silvicultural management activities. As with thinning trials, all experiments that aim to identify cause–effect relationships should include so-called 0-plots, i.e. plots representing untreated tree and stand dynamics.

5.2.5 Individual Tree Based Thinning Prescriptions

Even when a target density curve is defined clearly at the stand level, there are still opportunities for promoting individual trees or particular collectives. A defined stand density can be established by the moderate release and promotion of many of the remaining trees, or the strong release and promotion of fewer trees. There are essentially three methods available for managing the degree of release of superior trees or future crop trees objectively, and the severity of thinning in their vicinity, as follows.

First, the liberation of central trees by removing all stand neighbours within a defined radius of, for example 2, 3, . . . , 6 m.

Second, the use of a given competition index for the central trees where competitors are removed, beginning with the first, second, . . . , nth neighbour, until the defined competition index is reached. Position-dependent competition indices are applied here; they are calculated for all central trees prior to thinning operations and used for planned tree removals (cf. Chap. 8).

Third, pair-wise comparisons between superior trees or future crop trees and their competitors are used for identifying whether a neighbouring tree is a competitor for a superior or future crop tree, and thus for regulating the release of these trees individually, e.g. by adopting the A-value from Johann (1982).

Thinning Using the A-Value from Johann (1982)

In this approach a neighbouring tree i of a future crop tree j is removed if its distance to the future crop tree $Dist_{ij}$ is below a threshold distance T_{Dist}. T_{Dist} calculated from

$$T_{Dist} = \frac{h_j}{A} \times \frac{d_i}{d_j}, \tag{5.9}$$

where h_j is the height of the future crop tree, d_i is the diameter of the neighbour, d_j is the diameter of the future crop tree, and A is a proportionality quotient defined in the investigation, determining the degree of release.

The neighbouring trees are removed when their actual distance to the selected superior tree, or future crop tree, is below that calculated in (5.9), that is when the neighbour is too close to the superior or future crop tree. The taller the subject tree j (h_j), and the greater the size ratio of competitor i to the subject tree j (d_i/d_j), the broader the zone of elimination of competitors. In contrast, the higher the *A*-value is set, the lower the release of the individual central trees:

$$\mathrm{Dist}_{ij} < \mathrm{T}_{\mathrm{Dist}} \tag{5.10}$$

or

$$\mathrm{Dist}_{ji} < \frac{h_j}{A} \times \frac{d_i}{d_j}. \tag{5.11}$$

T_{Dist} marks the threshold distance for a given A-value below which a neighbouring tree is removed, and above which a tree is kept in the stand. Johann (1982) recommends A-values of 4, 5 and 6 for evenaged pure Norway spruce stands, which equate with heavy, moderate and light releases respectively. If a superior or final crop tree has a height of $h_j = 20\,\mathrm{m}$ and diameter at breast height of $d_j = 20\,\mathrm{cm}$ and its neighbour a diameter at breast height of $d_i = 10\,\mathrm{cm}$, the limiting distances $T_{Dist_{ij}}$ for A-values of 4, 5 and 6 are

$$\mathrm{T}_{\mathrm{Dist\,A=4}} = \frac{20\,\mathrm{m}}{4} \times \frac{10\,\mathrm{cm}}{20\,\mathrm{cm}} = 2.5\,\mathrm{m},$$

$$\mathrm{T}_{\mathrm{Dist\,A=5}} = \frac{20\,\mathrm{m}}{5} \times \frac{10\,\mathrm{cm}}{20\,\mathrm{cm}} = 2.0\,\mathrm{m}, \text{ and}$$

$$\mathrm{T}_{\mathrm{Dist\,A=6}} = \frac{20\,\mathrm{m}}{6} \times \frac{10\,\mathrm{cm}}{20\,\mathrm{cm}} = 1.67\,\mathrm{m}.$$

Competitors of selected superior trees or future crop trees inside these threshold distances are removed. Figure 5.11 shows the outcomes of a thinning using Johann's (1982) A-value method. The calculation of tree removals is carried out for plot 21 on the 29-year-old Scots pine experimental plot, Weiden 611. As the A-values decrease, the tolerance level of competition on the subject tree j declines, and the number of trees i to be removed increases.

When thinning trials are established based on the German Union of Forest Research Organisations' recommendations (Deutscher Verband Forstlicher Forschungsanstalten 1986a, b), A-values of 4 and 5 are mandatory in experiments. With a linear increase in tree dimensions (height, diameter), a quadratic and cubic increase in area and space required for tree growth, and not a linear one as assumed in (5.9), is required. In (5.9), the application of a proportionality factor A between tree height and the threshold distance T_{Dist} to a neighbour in young or mature stands results in release operations that are too light or too heavy respectively. To avoid release operations that are too light in juvenile stands, and extremely heavy

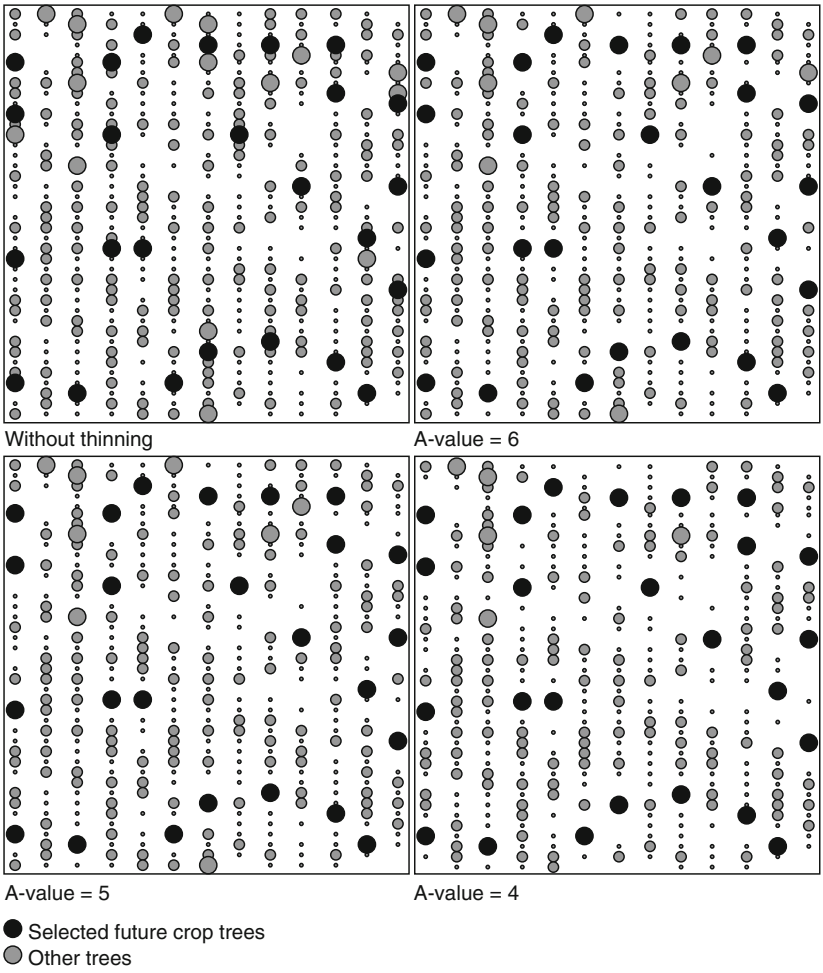

Fig. 5.11 Density reduction on the experimental plots Weiden 611, plot 21 by specifying the A-values by Johann (1982) from A = 6,5 and 4. The selected future crop trees are highlighted in *black*, other trees in *grey*. *Size of the circles* is proportional to tree diameter. As the A-value declines, the competition tolerated in the stand also declines, and the number of trees removed increases

in mature stands, the quotient h_j/A is replaced by the value 2 for juvenile stands, and 6 for mature stands. Figure 5.11 shows the rule recommended for the release of future crop trees in a Norway spruce thinning trial using A-values of A = 4 to A = 6 (Deutscher Verband Forstlicher Forschungsanstalten 1986a, b). Trees neighbouring superior trees or future crop trees are removed when $Dist_{ij} < T_{Dist}$. As the height of the subject tree increases, Fig. 5.12 indicates the threshold distance up to which trees of similar size ($d_i = d_j$) are removed for A-values of 4 and 6. If $h_j/A \leq 2\,m$, then $T_{Dist} = 2d_i/d_j$. If $2\,m < h_i/A < 6\,m$, then the threshold distance is $T_{Dist} = \frac{h_i}{A}\frac{d_i}{d_j}$.

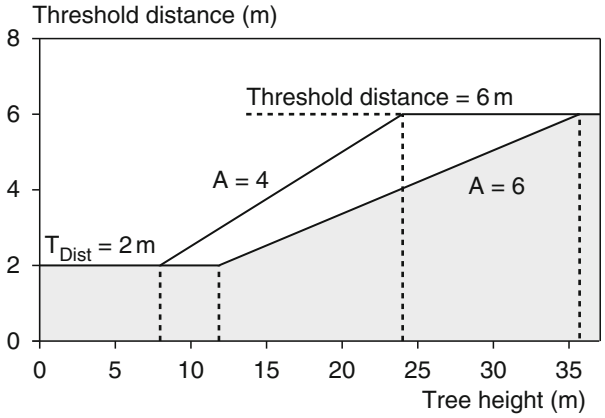

Fig. 5.12 Rules for releasing the selected and future crop trees using the A-values A = 4 and 6. Neighbours of the central tree are removed when their distance $Dist_{ij} < T_{dist}$ (Deutscher Verband Forstlicher Forschungsanstalten 1986a, b)

If the ratio $h_j/A \geq 6\,m$, then $T_{Dist} = 6d_i/d_j$ applies. When the selected trees or future crop trees follow the line $A = 4,5$ or 6, then a very heavy, heavy or moderate release of future crop trees results respectively.

5.3 Intensity of Thinning

The timing of the pre-commercial thinning and the subsequent repeated commercial thinnings is specified either for an absolute stand age (e.g. first thinning at 20 years of age, second thinning at 25 years of age) or for a predefined minimum mean tree size parameter (e.g. mean height, top height, mean diameter). Assmann (1961a) characterises the beginning and intensity of repeated thinning as the intensity of the thinning. He differentiates:

Level 1 (extensive). First thinning when mean height is greater than 12 m, and the average thinning interval greater than 5 years.
Level 2 (intensive). First thinning at a mean height of 8–12 m, average thinning interval 3–5 years.
Level 3 (very intensive). First thinning before mean height reaches 8 m, average return time 3 years or less.

Linking the time of thinning to diameter or height development infers that the increase in stand space needed is dependent primarily on tree size, and less on the time frame. For the treatment of Norway spruce stands, Abetz (1975) recommended thinning operations after 2-, 3- or 4-m height increments (Fig. 5.13). If a silvicultural prescription specifies the reduction in stem number to the target stem number

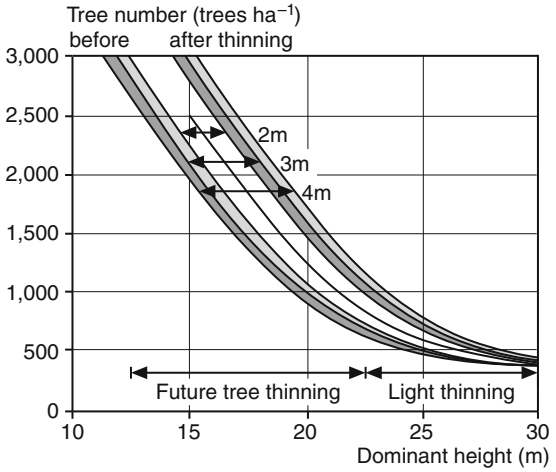

Fig. 5.13 Tree number–mean height curves as decision support for thinning Norway spruce stands (Abetz 1975). The target stem number before and after thinning is given for different thinning intervals. As thinning occurs after top height increments of 2, 3 and 4 m the curves are based on site-specific size growth

on the curve after each 3-m increment in top height, then the thinning intensity on sites with more vigorous growth will be higher than on sites with less vigorous growth, since, on the former sites, a 3-m increase in height in the juvenile phase might be achieved in 3 years, but require 6 years on the latter. A thinning schedule based on mean height, top height or diameter is appropriate for the definition and implementation of tending guidelines. Problems occur on experimental plots when the height development on plots varies significantly as then, strictly speaking, the thinning operations should occur at different times. In other words, the plots should be inventoried at different times and the experiments revisited in different years, substantially increasing the amount of work involved. Apart from the insupportably high work effort required, data from the plots with inventory and growth periods of different lengths would be associated with different climatic conditions. The effect of climate and treatment on growth behaviour could not be distinguished from each other. One solution might be to base the thinning intensity on the development of a control plot, e.g. an A grade plot, to prescribe the timing of operations for the whole experiment.

In Chap. 11, site-specific differences in total volume production for a given top height or mean height are outlined. These differences in the general, special and subdivided special yield levels must be considered when establishing the stem optimum stocking curves. By following set optimum stocking curves over extreme sites, local differences in stand production potential are evened out.

5.4 Algorithmic Formulation of Silvicultural Prescriptions for Forest Practice and Growth and Yield Models

Since the stand-based, quantitative forest management instructions of the eighteenth century (e.g. von Carlowitz 1713; Paulsen 1795), forestry and forest science have progressed to quantitative individual-tree and stand based silvicultural prescriptions. With this transition, the regulation of thinning trials has gradually become increasingly objective. In addition, the measured effects of thinning can be related directly to interventions in stand dynamics, so that general relationships between the treatment and tree and stand growth can be identified (Assmann 1961; Pretzsch 2005b; Zeide 2001, 2002). As long as silvicultural prescriptions for experimental plots are fixed in a detailed and quantitative way, experimental results can be used to produce management guidelines, and in simulation models. In addition, by refining experiments and their silvicultural treatments, management guidelines and forest growth models now can define thinning at the stand and tree level spatially as well as temporally.

An example of silvicultural prescriptions for Norway spruce stands in Bavaria is given in Fig. 5.14. It represents one of a set of treatment concepts integrated in the individual-tree simulator SILVA 2.2 (Chap. 13). These treatments are used for scenario analyse at the stand, strata, enterprise or state level (Pretzsch et al. 2005a, b; Moshammer 2006).

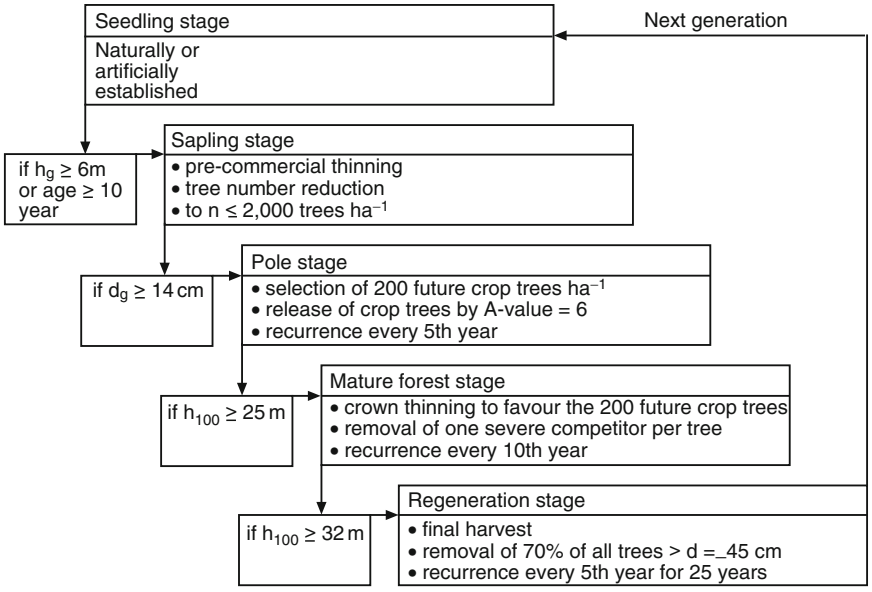

Fig. 5.14 Silvicultural prescription applied by the individual-tree simulator SILVA 2.2 for the management of Norway spruce stands in Bavaria. The example represents one of several treatment options applied for long-term timber volume prognosis at the state level and management plans at the enterprise level (cf. Chap. 13)

At every growth stage, from the seedling stage to the regeneration stage, the kind, severity and intensity of thinning treatments is fixed separately. Thresholds for stand height or mean diameter regulate the transition from one stage to the next. In the pre-commercial thinning stage, the treatment is quantified at the stand level, prescribing the reduction in tree number to below 2,000 trees per hectare. Subsequently, thinning concentrates on the promotion of a limited number of future crop trees. With a position-dependent individual-tree model, these trees can be promoted in a simulation run by applying the A-value = 6. Thinning intensity changes from one development stage to the next, and is prescribed by the thinning interval in years. By integrating different silvicultural prescriptions, forest simulation programs can be applied in scenario analysis. The expected long-term results of different treatment options produced in the scenarios assist managers in decision making.

Summary

The removal of trees is the most important measure for steering stand development. It changes the stand structure and triggers specific growth responses in the remaining stand. By removing trees the investigator or practitioner aims to modify resource allocation in a certain way, e.g., direct it to a specific tree collective or promote stability. Tree removals present a very effective lever for controlling the resource partitioning and biomass allocation between the trees in the remaining stand. It is necessary to quantify where, and how, this lever can be used to change the spatial occupancy pattern in stands through removals. By numerically fixing the spatial-temporal course of silvicultural intervention on experimental plots, the formulation of thinning guidelines and the integration of silvicultural prescriptions in simulation models become objective and reproducible. Furthermore, a clear quantification of the treatment or tending strategies also assists the transfer and the ability to manage recommended treatments in forestry practice.

(1) The best definition of thinning operations in the stand structure is given using three criteria: kind of removals, severity of removals, and timing and intensity of removals.
(2) The kind of removals characterises the structural changes in the spatial occupancy pattern. The severity of removals quantifies to what extent thinning operations lower the stand density in order to promote the remaining trees. The timing and intensity of removals defines the intervals between the removals (for which structure and quantity has to be specified).
(3) The relationships of the social or biological-technical tree classes from Kraft (1884) or the Association of German Forest Research Stations (Verein Deutscher Forstlicher Versuchsanstalten, 1873, 1902) provide a practical yet imprecise quantification of the kind and severity of thinning. Depending on whether the emphasis of the removals lies in the lower or the upper strata, a thinning from below, an opening-up of the tree crowns or a thinning from above is carried out.

(4) Removals according to numeric tree classes are determined by specified diameter classes or diameter limits. In this way, equilibrium curves in selection forests or target diameters in age class forests can be defined.
(5) The types of operations that, in a first step, select a number of well-developed crop trees according to the criteria vitality, quality and distance, and then, in a second step, favour these trees through removal of competitors, are described as selection and future crop tree thinning.
(6) The quantity of removals at the stand level can be given by prescribing a defined target stem number, a basal area development or a prescribed ln (mean tree volume)–ln (tree number)–trajectory (SDMD). For the promotion of trees, tree removals in the surrounding area may be carried out by specifying the number of competitors to be removed, by prescribing a radius of release, or by prescribing a target competition index. The definition of the quantity of removals becomes very precise when it is specified for both individual tree level as well as stand level. That is when the degree of release of the individual trees selected is stipulated as well as the degree of opening up in the areas in between.
(7) The thinning schedule of removals can be defined by prescribing the stand age at which operations must occur. If the timing of the operations is linked to a dendrometric parameter, such as tree diameter or tree height, the rate of growth determines the interval between operations (e.g., thinning after a height increment of 3 m, or diameter increment of 5 cm). As there is an allometric relationship between tree size and growing space requirements, size growth indicates the need of operations better than tree age.
(8) To clarify management activities, the kind of thinning, severity of thinning and intensity of removals must be given for the entire rotation time. If the target values of the quantity of removals are related to neighbouring control stands or A-grade stands, the site-specific natural development with age may serve as a reference.

Chapter 6
Standard Analysis of Long-Term Experimental Plots

Overview of Standard Analysis

The standard analysis of forest growth experimental plots essentially aims to record the variables summarised in Table 6.1, which characterise a given stand at the time of inventory, and any changes in the periods between inventories. These variables are the response variables, which are determined in an experiment and are needed to answer the research question. For example, the diameter and height of individual trees are measured to analyse the relationship between severity of thinning and stand growth in a thinning trial. These measures are used then to calculate the actual response variables needed, such as stand volume and stand growth. The response variables determined from long-term experimental plots are, as a rule, the cumulative and mean values of stand data per hectare.

In this chapter, the various stand analysis methods, and the analytical steps involved, are introduced by adopting data from the European beech thinning plot Fabrikschleichach 15 (FAB 15/1-3) in Bavaria. Here, the trial plots have been monitored since spring 1871, and conform to the conventional classification into A, B and C grade plots. The steps undertaken in standard analysis include: plausibility controls; treatment of absent or incorrect measurements; derivation of diameter–height (age) relationships; calculation of individual-tree volume from diameter, height and form factor; calculation of mean and cumulative values at the time of inventory from stand level inventory data; calculation of growth and yield values; and presentation of results in tables and graphs.

The Aim of Standard Analysis

The response variables determined in the standard analysis (the variables tested in an experiment) are used to test hypotheses, and thereby answer the research question. To this end, the response variables are analysed further with inference statistics

H. Pretzsch, *Forest Dynamics, Growth and Yield: From Measurement to Model*,
DOI: 10.1007/978-3-540-88307-4_6,

Table 6.1 Overview of the most important stand data, commonly used abbreviations and units (Johann 1993). A description of the variables is given as the headings of the standardised results tables (Table 6.2a–6.2c)

Variable	Short cut	Unit
Year of survey	year	–
Age	age	year
Tree species	sp	–
Tree number	N	
Dominant height	h_{100}	m
Dominant diameter	d_{100}	cm
Slenderness of dominant trees	h_{100}/d_{100}	m/cm
Mean height	h_q	m
Mean diameter	d_q	cm
Slenderness of mean tree	h_q/d_q	m/cm
Stand basal area	BA	$m^2\,ha^{-1}$
Standing volume	V	$m^3\,ha^{-1}$
Gross volume yield	GY_V	$m^3\,ha^{-1}$
Mean basal area density	mBA	$m^2\,ha^{-1}$
Periodic annual increment basal area	PAI_{BA}	$m^2\,ha^{-1}yr^{-1}$
Periodic annual increment volume	PAI_V	$m^3\,ha^{-1}yr^{-1}$
Mean annual volume increment	MAI_V	$m^3\,ha^{-1}yr^{-1}$
Length of survey period	per	yr

methods, for example with the t-test, analysis of variance and covariance, regression analysis, discriminance analysis or factor analysis. These statistical methods enable one to test the underlying hypotheses of the investigation (cf. Chap. 12). The textbooks from Bätz et al. (1972), Bortz (1993), Linder (1951, 1953), Mudra (1958), Pruscha (1989), Rasch (1987), Rasch et al. (1973), Überla (1968) and Weber (1980) are regarded as standard texts for inference statistics methods.

The response variables resulting from the standard analysis, shown in Table 6.1, are then adjusted to render the research outcomes relevant to forestry practice, which relies on mean and cumulative values of stand level data per hectare for the planning, implementation and control of activities at the stand and forest estate level. The construction of forest growth models (cf. Chap. 11) is based on the extensive spatial-temporal database from these experimental plots; the standardised analysis of data derived from these plots is designed specifically for constructing yield tables. Investigations of long-term growth trends provide an example of longitudinal studies (analysis of time series) (Kenk et al. 1991; Pretzsch 1999; Spiecker et al. 1996). Large-scale scattered analyses of site-productivity relationships for tree species (Kahn 1994; Moosmayer and Schöpfer 1972) or vitality (Mayer 1999; Schöpfer and Hradetzky 1983, 1988) are examples of cross-sectional analyses (analysis of data inventoried at a given point in time at different locations).

Furthermore, the organisation of data, test of plausibility, and the standardised analysis of inventory data are paramount for the management of the investigation

and any control measurements in subsequent periods. For example, stand inventory data are essential for controlling the target tree number or target basal area in an investigation to quantify the amount of thinning necessary (cf. Chap. 3).

6.1 From Measurement to Response Variables

The derivation of response variables is more complicated for study sites in forest stands than in agricultural crops. Whereas biomass production in a rye or corn field can be determined by harvesting and weighing the whole crop after one growing season, entirely different methods are required for trees, which are considerably larger and longer living than humans. To obtain the response variables, a standard analysis procedure is followed. This procedure ranges from testing the plausibility of the original data through to the compilation of tree parameters into stand cumulative and mean values. With these variables, the remaining, removed and total stand can be described at the time of each inventory. The growth in the interval between inventories can be calculated from the change in standing volume from one inventory to the next.

The main response variable, standing volume, can be calculated, for example, from the measured variables tree diameter at 1.3 m height ($d_{1.3}$), tree height (h) and form factor ($f_{1.3}$). The diameters of all trees on the plot must be measured; the height is determined usually by sampling. To calculate the standing volume, firstly the diameter–height curves for the tree species present on the plot are calculated by regression analysis, and then estimating the height of all trees from the diameter–height curves. Next, form factors $f_{1.3}$ are obtained for all trees in relation to diameter and estimated height from form factor functions or form factor tables; thus $f_{1.3}$ is a function of $d_{1.3}$ and h. Then, based on basal area ($ba_{1.3} = {d_{1.3}}^2 \times \pi/4$), height and form factor, the stem volume $v_i = ba_{1.3,i} \times h_i \times f_{1.3,i}$ of all $i = 1 \ldots n$ trees on the plot can then be calculated. Once the volumes of all the trees are added together we obtain standing volume, the desired response variable,

$$V = \sum_{i=1}^{n} v_i = \sum_{i=1}^{n} ba_{1.3,i} \times h_i \times f_{1.3,i}, \tag{6.1}$$

which is projected to 1 ha as a rule. The extremely time consuming nature of a complete inventory of tree height, or individual-tree volume calculations in sections, make it more feasible to obtain tree height from regression equations, and form factors from tables. Moreover, the statistical relationships between form factor, diameter and height are so close-fitting, due to the allometric relationships existing between them, that the accuracy of regression estimates of tree height as a function of diameter, or form factors from general functions in relation to diameter and height is often more that sufficient. For each inventory, the volume of the remaining and removed stands needs to be calculated separately to quantify the development of the total volume production over time, standing volume, the volume of utilisable intermediate thinnings and the volume growth, which represent the response variables in many investigations (cf. Table 6.1).

6.2 Importance of Regression Sampling for Standard Analysis

6.2.1 Principle of Regression Sampling

Regression analysis produces a functional relationship between a dependent variable y and one or more independent variables. As such it is essential for the derivation of stand parameters. Through regression analysis, the dendrometric variables that are difficult and time consuming to measure, such as tree height, crown base height and diameter growth, can be estimated by regression sampling in the following steps.

First, a collective of trees is selected for which both the variables readily obtained, such as tree diameter $d_{1.3}$, and those that require more effort, such as tree height h, are measured.

Thus, for deriving functional relationships by regression analysis between the more, and less easily measured variables, measured pair values, e.g. diameter–height values, are available.

Then, a regression analysis is carried out to estimate the function parameters for the desired statistical relationship, e.g. $h = f(d_{1.3})$. If the relationship is linear, for example $\hat{y} = a + b \times x$, then the regression coefficients a and b, and the parameters for the goodness of fit of the statistical relationship (covariance, correlation coefficient and coefficient of determination) are calculated.

With the derived function, the variables requiring more effort to measure can be estimated from the variables that are easily measured, which have been recorded for all trees in the stand. In the example given, by inserting the $d_{1.3}$ values on the right side of the linear equation $\hat{y} = a + b \times x$ together with the estimated model parameters a and b, the estimated values for all tree heights are produced on the left side.

6.2.2 Linear Transformation

In forest stands, and in nature in general, linear relationships between parameters are rare; as a rule non-linear relationships are found. These non-linear relationships between variables can be transformed into a linear form in many cases so that they can be subject to linear regression analysis.

Logarithmic transformation is particularly useful. The effect of this transformation is shown in Fig. 6.1 for European beech study site Ebrach 133, plot 5 after the 1984 inventory. The non-linear relationship between tree diameter and tree height, where the increase in height tapers off with increasing tree diameter (Fig. 6.1a), can be linearised by a logarithmic transformation of the diameter values (x-axis) (Fig. 6.1b). In this example, a logarithmic relationship $\hat{y}_i = a + b \times \ln x$ is assumed between the diameter x and height y variables. By substituting $x' = \ln x$ in the equation, the linear function $\hat{y}_i = a + b \times x'$ is obtained. With this logarithmic transformation of x values, some non-linear relationships can be changed to linear ones so that a linear regression analysis can be performed.

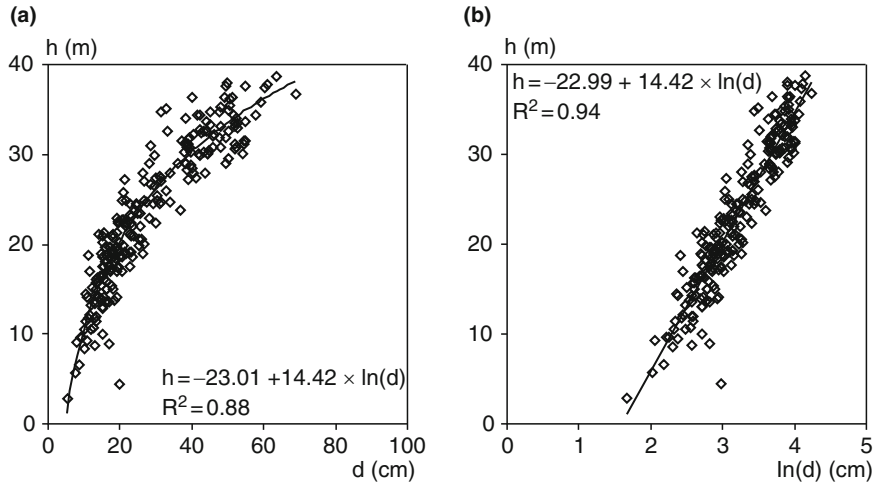

Fig. 6.1 (**a**) Non-linear relationship between tree diameter $d_{1.3}$ and tree height h for European beech on the trial plot Ebrach 133/5, in the 1984 inventory. (**b**) Result of a linear logarithmic transformation of tree diameter $d_{1.3}$ on the x axis. The regression coefficients and coefficients of determination obtained from smoothing with a non-linear regression are not significantly different from those obtained from a linear regression applied after the transformation of variables

However, such transformations change the measured variables adopted, resulting in a certain distortion when the regression predictions are retransformed. In Fig. 6.1a, the regression equation is fitted without transformation by a non-linear regression analysis, leading to somewhat different parameters and coefficients of determination compared to linear transformation (Fig. 6.1b). In general, the size of the distortions from the linear transformation in this example is tolerable. If this were not the case, non-linear regression or correction methods could be adopted instead (Vanclay 1994).

Figure 6.2 shows (a) the most common curvilinear relationships, and (b) their linear transformations.

Curve 1 represents a stand height curve (Assmann 1943; Prodan 1951; Schmidt 1967) ($y = a + b \times \ln x$). It can be linearised by a logarithmic transformation of the x-axis while the y-axis remains unchanged ($x' = \ln x,\ y' = y$).

Curve 2 describes an exponential relationship. A gradually increasing exponential function can be used to model the relationship between the tree diameter and stem volume of individual trees (Prodan 1961), whereas a declining exponential function can be used for the relationship between tree number and diameter in selection stands ($y = a \times b^x$, with $b > 0$) (Assmann 1961a; Knoke 1998; Meyer 1953; Pretzsch 1985a). A linear relationship results when the logarithm of the y-axis is obtained, while the x-axis remains the same ($x' = x,\ y' = \ln y$).

Curve 3 represents an allometric relationship ($y = a \times x^b$) found, for example, between tree number per hectare and mean diameter, or between mean plant weight and plant density in woody and herbaceous stands (Pretzsch 2000; Reineke 1933;

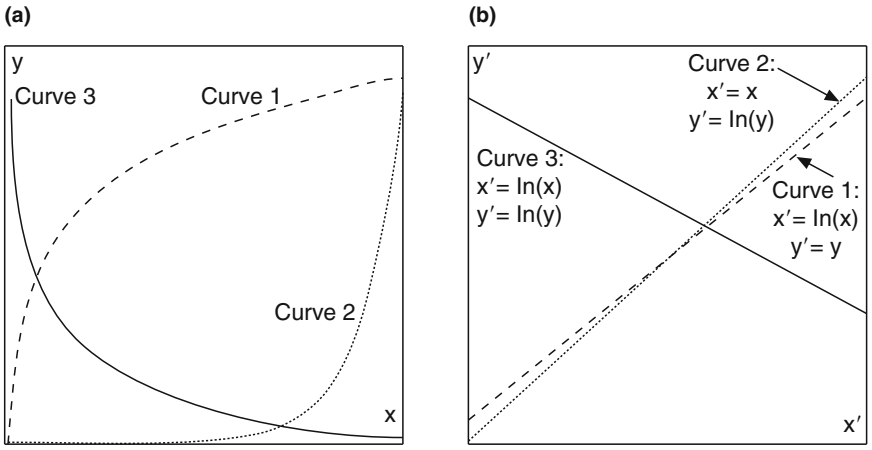

Fig. 6.2 Curvilinear relationships commonly occurring, and instructions for their transformation. (**a**) The following functional relationships underlie the curvilinear relationships: curve 1: $y = a + b \times \ln x$, curve 2: $y = a \times b^x$, and curve 3: $y = a \times x^b$. (**b**) The linearization is carried out separately by the following axes transformations: curve 1: $x' = \ln x$, $y' = y$, curve 2: $x' = x$, $y' = \ln y$ and curve 3: $x' = \ln x$, $y' = \ln y$

Yoda et al. 1963). In this case the relationship is linearised by obtaining the logarithm of both the x and y axes ($x' = \ln x, y' = \ln y$).

This introduction of the application of regression analysis and linear transformation should provide some background for the stand height curves presented below. For a deeper understanding of linear and non-linear regression analysis, the transformation of independent and dependent variables, testing regression coefficients or the calculation of standard error, one can refer to statistical textbooks (Bortz 1993; Linder 1951, 1953; Weber 1980).

6.3 Determination of Stand-Height Curves

Physical and physiological factors create non-linear statistical relationships between tree diameter and height in forest stands. By plotting diameter and height values following the inventory of a pure evenaged stand on a Cartesian coordinate system, one obtains a point cloud, which can be evened out graphically or by regression analysis to display a characteristic increase in height as tree diameter increases (cf. Fig. 6.1). The stand height curve resulting represents the relationship between tree diameter and height at time of inventory. Given this general relationship, tree height measurements taken during the inventory of study sites can be confined to a tree collective (regression sampling). The heights of those trees whose tree height is not recorded are then read off the regression curve on the basis of their known diameter measurements.

6.3.1 Function Equations for Diameter–Height Relationships

Some of the more important functions, which have proven useful for smoothing data by regression analysis (Schmidt 1969), are presented below.

The following function was used by Assmann (1943):

$$h = a_0 + a_1 \times d + a_2 \times d^2. \tag{6.2}$$

This second degree parabola produces a linear equation of the form $z = b_0 + b_1 \times x + b_2 \times y$ by substituting $z = h$, $x = d$ and $y = d^2$ according to Prodan (1951):

$$h - 1.3 = \frac{d^2}{a_0 + a_1 \times d + a_2 \times d^2}. \tag{6.3}$$

A transformation produces the equation $\frac{d^2}{h-1.3} = a_0 + a_1 \times d + a_2 \times d^2$ so that, with $z = d^2/(h - 1.3)$, $x = d$ and $y = d^2$, a linear equation of the form $z = b_0 + b_1 \times x + b_2 \times y$ is obtained and can be fitted to the data by linear regression analysis.

A second degree parabola, and Prodan's (1951) function, according to Assmann (1943) and Prodan (1951) respectively, can be used for stand height curves in selection forests, mixed-species mountain forests, virgin forests as well as for the derivation of crown base height curves. They are able to model height or crown base height increase up to a certain diameter, and the subsequent decline, which can occur in forest stands of this nature (Prodan 1965; Pretzsch 1985a; Preuhsler 1979).

The following functions (6.4)–(6.8) have proven useful for evenaged and single-layered stands.

The function from Petterson (1955) is

$$h = 1.3 + \left(\frac{d}{a_0 + a_1 \times d}\right)^3. \tag{6.4}$$

A linear transformation of this function (6.4) is carried out in the following three steps:

$$\frac{1}{h - 1.3} = \left(\frac{a_0 + a_1 \times d}{d}\right)^3,$$

$$\left(\frac{1}{h - 1.3}\right)^{1/3} = \frac{a_0 + a_1 \times d}{d},$$

$$\left(\frac{1}{h - 1.3}\right)^{1/3} = a_0 \times \frac{1}{d} + a_1.$$

If we set $y = \left(\frac{1}{h-1.3}\right)^{1/3}$ and $x = \frac{1}{d}$ we obtain the linear equation $y = b_0 + b_1 \times x$.

The function from Korsun (1935) is

$$h = e^{\left[a_0 + a_1 \times \ln d + a_2 \times \ln^2 d\right]}. \tag{6.5}$$

The logarithm of this equation is $\ln h = a_0 + a_1 \times \ln d + a \times \ln^2 d$ and, after substituting $z = \ln h$, $x = \ln d$ and $y = \ln^2 d$, a linear equation of the form $z = b_0 + b_1 \times x + b_2 \times y$ results.

The semi-logarithmic function (cf. Fig. 6.1) is

$$h = a_0 + a_1 \times \ln d. \tag{6.6}$$

By substituting $y = h$ and $x = \ln d$, the linear equation $y = b_0 + b_1 \times x$ is obtained.

The function from Freese (1964) is

$$h = e^{[a_0 + a_1 \times \ln d + a_2 \times d]}. \tag{6.7}$$

The logarithm of this equation is $\ln h = a_0 + a_1 \ln d + a_2 d$ and, after substituting $z = \ln h$, $x = \ln d$ and $y = d$, the linear equation $z = b_0 + b_1 \times x + b_2 \times y$ is obtained.

The function from Michailoff (1943) is

$$h = 1.3 + a_0 \times e^{-\frac{a_1}{d}}. \tag{6.8}$$

The transformations $\ln(h - 1.3) = \ln a_0 - a_1/d$ and $\ln(h - 1.3) = \ln a_0 - a_1 \times \frac{1}{d}$ enable the substitution $y = \ln(h - 1.3)$ and $x = 1/d$, resulting in the linear equation $y = b_0 + b_1 \times x$.

The important statistical parameters for selecting the most suitable regression curve are the residual standard deviation $s_{h\hat{h}}$ (6.9) and the coefficient of determination R^2 (6.10).

6.3.2 Selection of the Most Suitable Model Function

The residual standard deviation quantifies the standard deviation between the observed height values h_i and the corresponding estimated values $\hat{h}_i$ on the regression curve. The residual standard deviation of a regression with two parameters (e.g. $y = a + b \times x$) is

$$s_{h\hat{h}} = \sqrt{\frac{\sum_{i=1}^{n} \left(h_i - \hat{h}_i\right)^2}{n - 2}}, \tag{6.9}$$

where the denominator for a regression equation with k parameters is (n–k). The ratio of this standard deviation to the mean height $\overline{h}$ gives the coefficient of variation, which can also be used to identify the outliers of the observed height values (Schmidt 1967). In contrast, the coefficient of determination quantifies the relative proportion ($R^2 = 0$–100%) of the variance in the observed height values s_h^2 explained by the regression line (total variance minus residual standard deviation). For example, if all the height values recorded lie on the regression curve, then $s_{h\hat{h}}^2$ in the numerator of

$$R^2 = \frac{s_h^2 - s_{h\hat{h}}^2}{s_h^2} \times 100, \tag{6.10}$$

is equal to 0, and the maximum value of R^2 is obtained ($R^2 = 100\%$). The greater the differences between the observed and estimated values, the smaller the numerator in (6.10) and therefore also R^2.

As the shape of the curve is determined by the regression function selected, and the underlying diameter–height values ultimately only represent a tree collective in the stand, the selection of the best regression function should not be based only on the residual standard deviation, the correlation coefficient or the coefficient of determination. A test of their biological plausibility is equally important.

6.4 Diameter–Height–Age Relationships

In forest stands with more or less constant tree number–diameter distributions, trees with a given diameter always have a similar social position in the stand. Figure 6.3a shows the diameter–height data for Norway spruce in the selection forest Freyung 129, plot 31 from the first inventory in June 1980, and repeated inventories in 1987, 1993 and 1999. In this stand, trees with a diameter of 10 cm always occur in the lower stand. Trees with a diameter of 80 cm always belong to the dominant stratum. Therefore, height growth in the individual diameter classes remains almost constant, and the position of the stand height curve stationary over time. This applies so long as the vertical structure of the stand, and, consequently, the specific competition

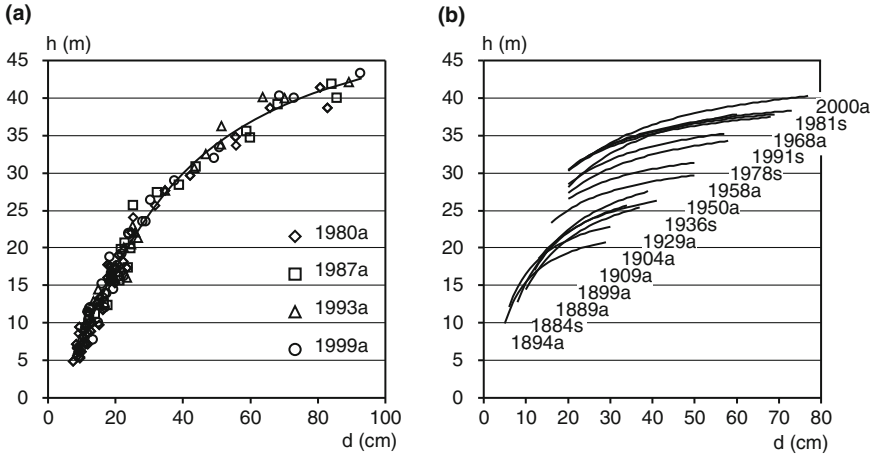

Fig. 6.3 Comparison of the development of stand height curves in (**a**) a Norway spruce–Silver fir–European beech selection forest and (**b**) an evenaged European beech forest. (**a**) On the selection forest site FRY 129/31, the shift in the stand height curve for Norway spruce in the inventories 1980a, 1987a, 1993a and 1999a is minimal due to the static nature of the tree number–diameter distribution. (**b**) The shift in the stand height curves at the European beech thinning trial FAB 15/2 from the height inventory 1884a to the most recent inventory 2000a (s and a = inventory in spring and autumn respectively)

between trees in the different diameter classes do not change. Under these conditions, found for example in selection forests in a balanced state, and occasionally in virgin forest stands and mixed-species mountain forests, the stand height curve coincides with the height growth curve, imitating its S-shaped form (6.2) or (6.3).

In contrast, stand height curves in pure evenaged stands shift from inventory to inventory. Figure 6.3b shows the layers of stand height curves for the pure European beech stand FAB 15/2 from the first height inventory in autumn 1884 (aged 61 years) through to the most recent inventory in autumn 2000 (aged 178 years). In such stands, the trees with the same diameters of, e.g. 30 cm, belong to completely different dominance classes as stand age advances. Trees of this size that belonged to the dominant class in the initial inventory, represented the average height stratum in the 1950s and, in the last inventory, the lower stratum. With increasing age, the stand height curve shifts upwards to the right, and, at the same time, the slope declines as the self-thinning process drops off. In mature stands, the stand height curve may run almost parallel to the x axis, for example in stands after a heavy thinning from below or opening up.

However, stand height curves from repeated inventories often deviate from these relationships; they shift in an apparently implausible manner in stands with a stable character, or cut across one another in pure evenaged stands (cf. Fig. 6.3b). The causes of this behaviour may be, e.g. the presence of systematic measuring errors, varying the trees measured for height, or selecting a measurement tree collective that is too small. Some inventory data provide neither height measurements nor stand height curves. This applies, e.g. to the inventories in 1871s, and 1882s at the FAB 15 sampling plot where height measurements were particularly prone to error or limited due to the effort required to record them. The methods introduced below may be used to identify and correct isolated implausible measurements, to identify, eliminate and replace implausible height curves with ones representing the expected relationship, and to interpolate or extrapolate the missing stand height curves from the existing curves.

To introduce the plausibility test and adjust stand height curves, we adhere to the example of the European beech thinning experiment FAB 15. Some stand height curves on plot 2 are clearly biased, and do not correspond to the otherwise regular shift (Fig. 6.3b). The calendar years recorded show the layers of curves in relation to their height position at the end of the curves. It shows a deviation in the height curves from the 1894a, 1904a, 1909a, 1968a and 1991s inventory data to a greater or lesser extent from systematic layering. The curves for the first two inventories in 1871s and 1882s are missing, and need to be supplemented for volume calculations. The variation in the stand height curve layers on this plot may be the due to numerous changes in measuring techniques, changes in the tree collective selected for height measurements, upgrowth from the lower storey and consequent expansion of the tree measurement collective, or to measurement being impeded by dense stand conditions.

In the following discussion, the most common methods for adjusting stand height curves are introduced. The methods outlined differ in the extent to which they have moved away from original data in favour of a biologically tenable model hypothesis

for stand height curve development. The application of these methods is an essential step in standard analysis procedures. They have considerable influence on all height-dependent response variables (including mean height, standing volume, volume growth, total volume production) and should therefore be listed in the analysis results.

6.4.1 Method of Smoothing Coefficients

Johann (1990) uses the specific change in the height curve parameters with age to adjust implausible height curves, and to interpolate in, or extrapolate beyond a series of height curves respectively. His method of smoothing stand height curves (cf. Pollanschütz 1974; Schadauer 1999) involves firstly estimating the regression coefficients for stand height curves separately at the time of inventories $1, \ldots, n$ by regression analysis after stipulating an appropriate smoothing function (6.2)–(6.8). When a two-parameter function is applied, the regression coefficients $a_1, \ldots, a_n$ and $b_1, \ldots, b_n$ result. In the second step, the regression coefficients a and b are smoothed over stand age, where $\hat{a} = f(\text{age})$ and $\hat{b} = f(\text{age})$. According to Johann (1990) the functions

$$\hat{a} = a_{10} + a_{11} \times \text{age} + a_{12} \times \text{age}^2, \tag{6.11}$$

$$\hat{b} = b_{10} + b_{11}/\text{age}, \tag{6.12}$$

or

$$\hat{a} = a_{10} + a_{11}/\text{age}, \tag{6.13}$$

$$\hat{b} = b_{10} + b_{11} \times \ln\text{age} + b_{12} \times \text{age}^2 \tag{6.14}$$

have proven useful for smoothing parameters, provided Michailoff's (1943) function applies for the coefficients [cf. (6.8)]. Thus, for a given age, the following procedure is possible: age → regression coefficients of the height curves → stand height curves → reading off the heights for given $d_{1.3}$ values.

In the following example, we use Michailoff's (1943) equation to smooth the stand height curves from the experimental plot FAB 15/2 (cf. Fig. 6.3b). Some stand height curves do not fit in with the shift in the other stand height curves. Figure 6.4 shows the development in coefficients a and b for the curve series by age. Stand height curves demonstrating considerable distortion may be identified here by their outlying, implausible coefficients. By removing the outliers the coefficients are evened out over stand age. The solid line shows the resulting smoothed curve $\hat{a} = f(\text{age})$ and $\hat{b} = f(\text{age})$, producing the two-tiered system of functions required to determine the age-specific stand height curve coefficients a and b for the development of age-specific stand height curves. Stand height curves smoothed using this method are depicted in Fig. 6.5. The measured (solid lines), and adjusted (dashed lines) stand height curves are compared with data from the 1884s, 1894a, 1950a,

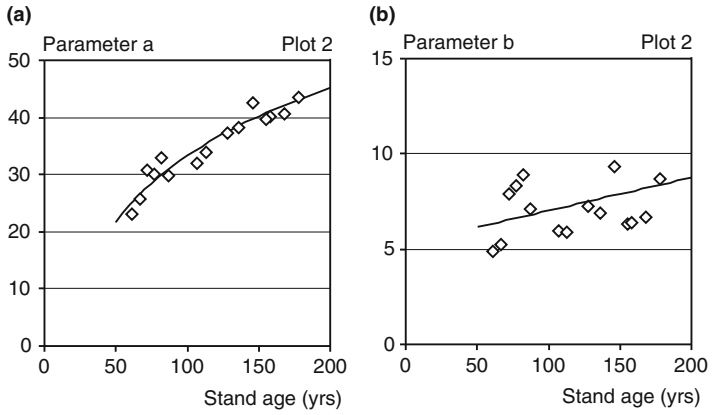

Fig. 6.4 Methods of smoothing coefficients from Johann (1990), presented for the trial plot FAB 15/2. The sequential smoothing of the stand height curves using the Michailoff (1943) function produces the parameters a and b (*left and right*). These coefficients are smoothed with age by regression analysis

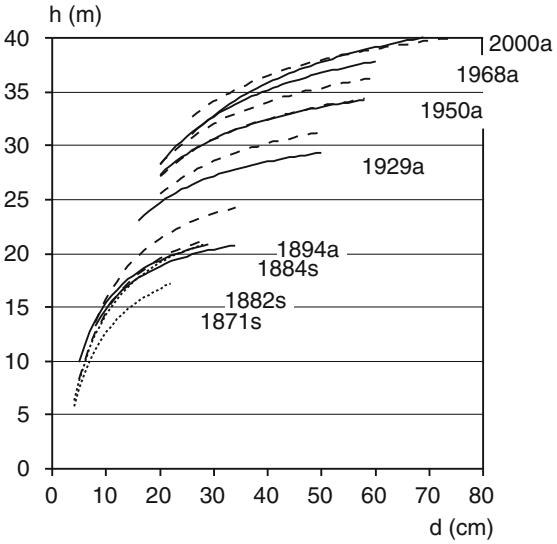

Fig. 6.5 The adjusted stand height curves (*dashed line*) and extrapolated stand height curves (*dotted line*) using Johann's (1990) method of smoothing coefficients compared to the original diameter–height curves (*solid line*). As the method of smoothing permits the calculation of stand height curves for any age, absent or untenable stand height curves may be extrapolated or replaced accurately

1968a and 2000a inventories. In addition, the extrapolated stand height curves for 1871 and 1882 (dotted lines), in which diameter but not height measurements are available, also are plotted.

In the multiple regression approach, $h = f(d, age)$, all available measurements from successive inventories are used, yet the influence of the diameter–height inventory data on the system of curves as a whole depends on the sample size. In the method of smoothing coefficients, however, the diameter–height data from all inventories included have an equal weighting, even when the measured tree collectives differ in size. In this method, any implausible stand height curves, which are associated with systematic error, are identified by their stand height curve parameters a and b.

6.4.2 Growth Function Methods for Strata Mean Trees

Röhle (1999) suggests an alternative method in which the trees measured for height in each inventory are allocated firstly to three strata according to their diameter. These strata comprise the lower, middle and upper strata, where stratum L comprises the smallest 40%, stratum M the middle 30% and the stratum U the largest 30% trees (L $\hat{=}$ 0–40%, M $\hat{=}$ 40–70% U $\hat{=}$ 70–100%). For each stratum, the mean height and mean diameter are calculated. Figure 6.6a, b shows this approach for the experimental plot FAB 15/2 for the year 2000 inventory. If the data are stratified, and the mean values determined at each inventory time point, we obtain the paired values $\left(\bar{d}_L, t\right)$, $\left(\bar{d}_M, t\right)$, $\left(\bar{d}_U, t\right)$ and $\left(\bar{h}_L, t\right)$, $\left(\bar{h}_M, t\right)$, $\left(\bar{h}_U, t\right)$ at any time $t_1 \ldots t_n$. From

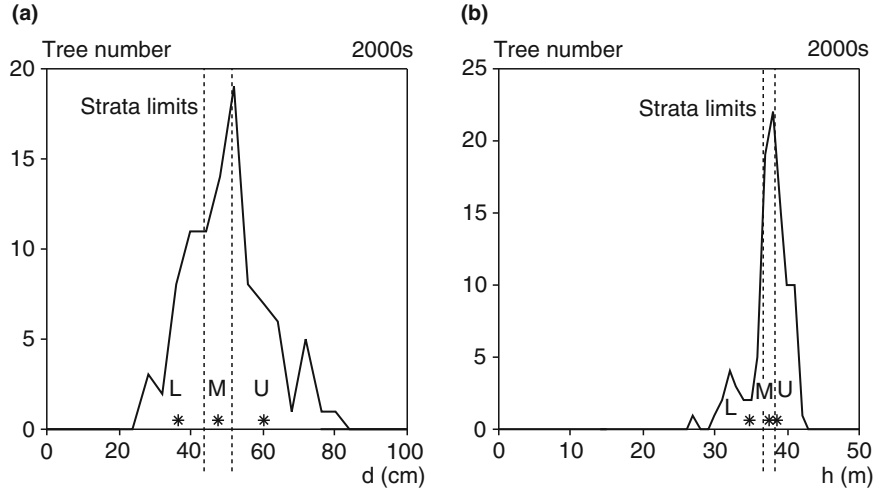

Fig. 6.6 In the methods of growth functions for strata mean trees from Röhle (1999), the mean diameter and mean height are determined firstly for the lower, middle and upper spectrum (L, M, U) of the (**a**) the tree number–diameter frequency and (**b**) the tree number–height frequency respectively. The division into the strata L (the 40% smallest), M (the next 30% taller) and U (the 30% largest) is presented for the example of the diameter–height paired values from the inventory 2000a

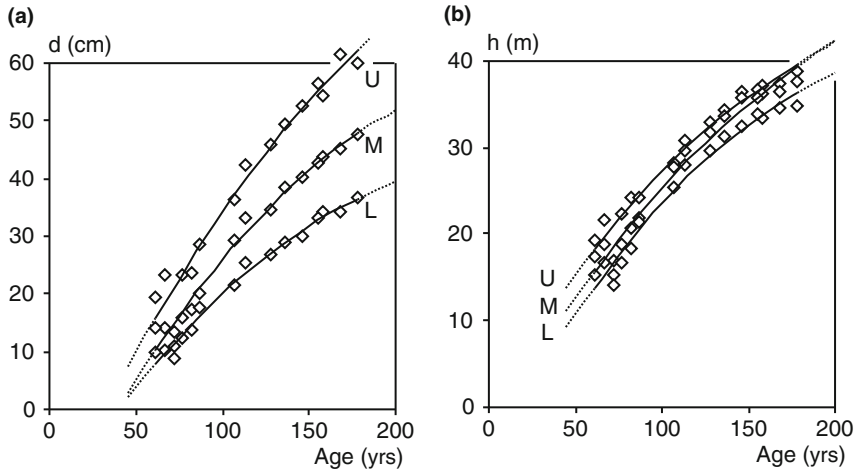

Fig. 6.7 Method of growth functions for strata mean trees from Röhle (1999). The strata specific (**a**) mean diameters and (**b**) mean heights are plotted by age and smoothed using appropriate growth functions (cf. Chap. 10, Sect. 10.3.2) by regression analysis (*solid lines*)

these paired values, three age–mean diameter curves and three age–mean height curves,

$$\overline{d}_L = f(age), \overline{d}_M = f(age), \overline{d}_U = f(age) \text{ and}$$
$$\overline{h}_L = f(age), \overline{h}_M = f(age), \overline{h}_U = f(age) \qquad (6.15)$$

can be fitted by regression analysis for each strata (Fig. 6.7a, b). For a given stand age, these growth functions calculate the age-typical mean height and mean diameter for the three strata, which clearly determine the three-parameter stand height curve for that age. A stand height curve is fitted to these three point series by regression analysis for each inventory time point (Fig. 6.8). The height corresponding to the diameter of trees in the stand is read off the stand height curves typical for a given age.

The series of curves presented in Fig. 6.8 for FAB 15/2 was obtained from the strata mean values from 15 inventories; the stand height curves from the 1871 and 1882 inventories were unavailable, and those from the 1924 inventory data appeared distorted due to the poor stratification and needed to be amended. The mean diameter values, and mean height values were smoothed with the functions $d_{1.3} = a_0 + a_1 \times age + a_2 \times age^2$, and $\ln h = b_0 + b_1 \times \ln age + b_2 \times \ln^2 age$ respectively. As Fig. 6.8 shows, the method facilitates the inclusion of missing, or the adjustment of implausible stand height curves. The stand height curve from 1924, omitted because of its implausibility, was supplemented by interpolation (Fig. 6.8, dashed line). The extrapolation of curves outside the existing series of curves, for example to reconstruct the absent stand height curves for 1871 and 1882 (Fig. 6.8, dotted lines), may produce implausible results.

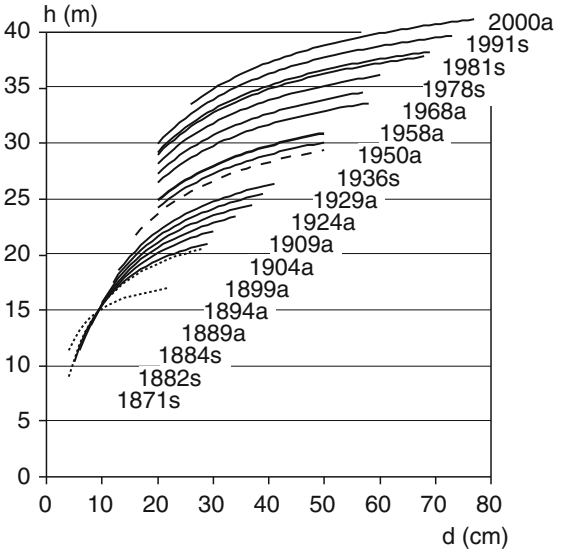

Fig. 6.8 Adjustment of stand height curves using methods of growth functions for strata mean trees. For each age, the diameter–height paired values for the lower middle and upper stratum are available. These may be used as location points for developing the system of stand height curves presented: interpolated (*dashed line*) and extrapolated (*dotted line*) stand height curves

6.4.3 Age–Diameter–Height Regression Methods

This method is useful when at least three repeated height measurements have been carried out in inventories. From the three values of diameter, height and age of trees measured at different points in time, an age–diameter–height curve is derived by regression analysis (Pollanschütz 1974):

$$\hat{h} = f(d, age)\,. \tag{6.16}$$

If the functional relationship is known, then interpolation between the existing inventories is possible to supplement any missing inventory data or replace an implausible stand height curve. Hence, for any diameter and age, the corresponding tree height can be read off the age–diameter–height curve developed. An extrapolation is also possible provided one is cautious, when the lower or upper curves of a series need to be added or adjusted.

Figure 6.9 shows the results of smoothing for the experimental plot FAB 15/2, with the function $\hat{h} = a_0 + a_1 \times \ln d_{1.3} + a_2 \times age + a_3 \times \ln(d_{1.3} \times age)$. Compared to the stand height curves derived from measured values (Fig. 6.3b), and those adjusted by smoothing coefficients (cf. Fig. 6.5), the age–diameter–height curves are considerably steeper in the first and second thirds of the observed growth period. In addition to the function above, this method allows one to fit the functions obtained in the two separate steps with the coefficient estimation methods. Due to insufficient or unequal weighting of data (changing sample size, weighting earlier inventories

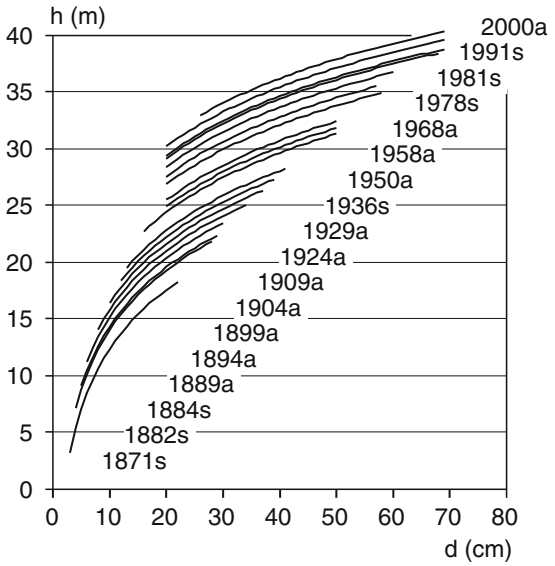

Fig. 6.9 Age–diameter–height regression for the European beech trial plot FAB 15/2 from inventories 1871s to 2000a, smoothing the relationship $\hat{h} = f(d_{1.3}, age)$ by multiple linear regression calculations. The relationship $\hat{h} = a_0 + a_1 \times \ln d_{1.3} + a_2 \times age + a_3 \times \ln(d_{1.3} \times age)$ is used to smooth the curves by regression analysis

with large sample size or initial, complete inventories too highly), the calculation of age–diameter–height curves in the inventory years included, often produces less favourable results than the methods for estimating coefficients.

6.5 Form Factors and Volume Calculations for Individual Trees

If we assume that a tree is shaped like a cylinder with height h and basal area $ba_{1.3}$ at 1.3 m height (cf. Fig. 6.10), then the form factor $f_{1.3}$ gives the reduction factor that the cylinder volume needs to be multiplied by to obtain tree volume. Therefore, the form factor can also be called the reduction factor, which reduces the volume of a cylinder ($c = ba_{1.3} \times h$) to tree volume ($v = f_{1.3} \times c$). Conversely, the form factor expresses the proportion of a cylinder filled by the tree (Fig. 6.10). The form factors are applied to merchantable wood or stemwood, which indicate whether volume determinations include all aboveground wood with a diameter greater than 7 cm or the tree shaft respectively.

Bülow (1962) traced the definition of the smallest diameter of 7 cm for merchantable wood back to the forest and wood regulations of salt industry forests in Reichenhall, Bavaria, from 1529. These stipulated that trees with diameters smaller than the cutting width of a manual brush hook were to be left undamaged. It was

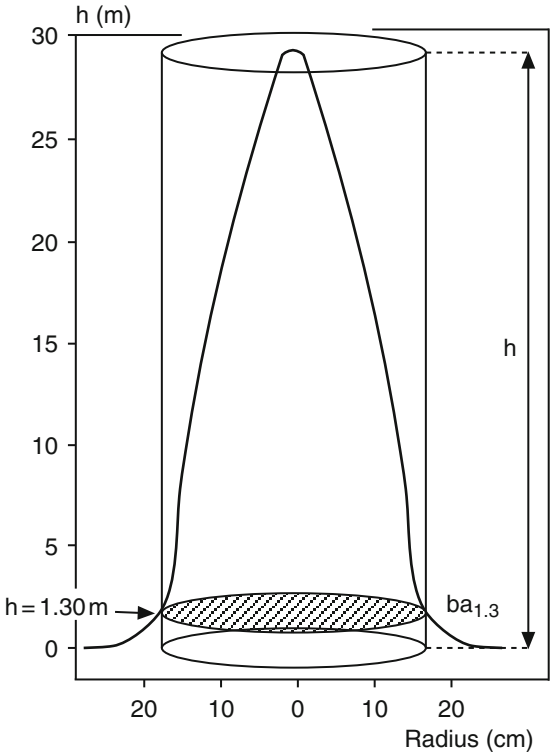

Fig. 6.10 The form factor $f_{1.3}$ is the factor that reduces the volume of a cylinder ($c = ba_{1.3} \times h$) to tree volume $v = c \times f_{1.3}$. A form factor of $f_{1.3} = 0.5$ would mean that the tree fills half of the reference cylinder ($v = ba_{1.3} \times h \times 0.5$)

permitted to use and fell trees with diameters greater than this width, which was 7.2 cm. "It is not coincidental, and admirable, that our merchantable wood limit today coincides with the manual brush hook cutting width from 1529" (Bülow 1962, p. 189).

6.5.1 Form Factors

The form factor $f_{1.3}$ is not determined explicitly for each experimental plot inventory. Rather, the form information is derived deductively from form factor tables, form factor or form height functions, or volumes function in relation to diameter and height. The form factor functions [cf. (6.17)] present one way of deriving volume deductively in relation to diameter and height:

$$f_{1.3} = f(d, h)\,. \tag{6.17}$$

A second option is to obtain the product of height and form factor from form height functions [cf. (6.18)]:

$$hf_{1.3} = f(d,h)\,, \tag{6.18}$$

where the form height only needs to be multiplied by tree basal area to determine tree volume. A third option is to use the volume functions or volume tables,

$$v = f(d,h)\,, \tag{6.19}$$

which give stem volume directly in relation to diameter and height. These functions, or the corresponding tables, provide the same stereometric information as already shown. However, they process it differently for the computation of the standard analysis. We use the functions for merchantable wood from Franz et al. (1973), or for stemwood from Kennel (1969) to illustrate the development of the form factor ($f_{1.3}$) for Norway spruce trees with h/d ratios of 1.0, 0.8 and 0.6 (Fig. 6.11).

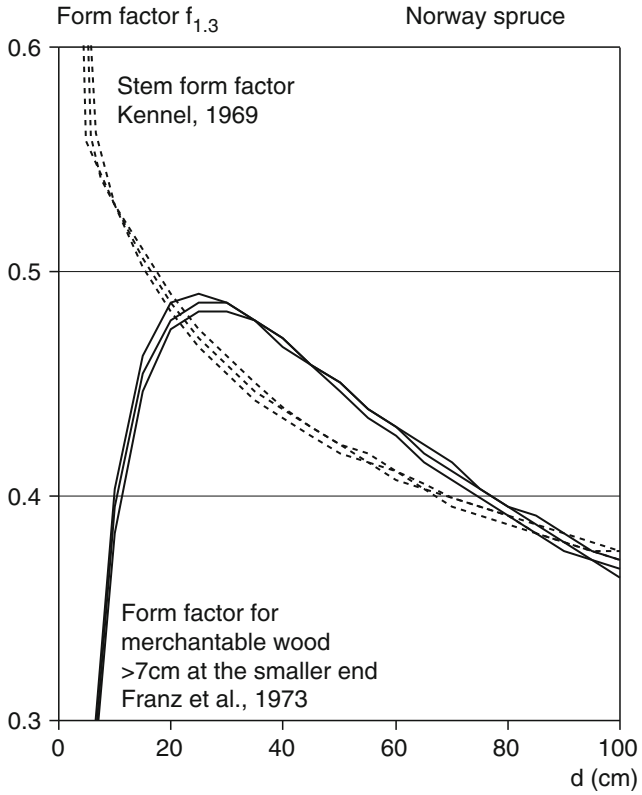

Fig. 6.11 Development of form factors $f_{1.3}$ for merchantable timber according to Franz et al. (1973) (*solid line*) and the stem wood according to Kennel (1965b, 1969) (*dashed line*) by diameter $d_{1.3}$. The merchantable timber form factors for Norway spruce are presented with h/d values of 1.0, 0.8 and 0.6

6.5.2 Volume Calculations for Individual Trees

The volume calculation assumes that tree height is measured in meters, and tree diameter in centimeters. Thus to obtain the volume in m^3, the values must be divided by 10,000:

$$v = d^2 \times \frac{\pi}{40{,}000} \times h \times f_{1.3}. \tag{6.20}$$

6.6 Stand Mean and Cumulative Values at the Time of Inventory and for the Periods Between Inventories

The stand mean and cumulative values discussed below characterise the long-term experimental plots at the time of inventory, and their development in the intervals between successive inventories. They are the variables that are the target of long-term investigations. A more detailed introduction is available in the forest mensuration textbooks from Avery and Burkhardt (1975), Bruce and Schumacher (1950), Kramer and Akça (1995), Loetsch and Haller (1964), Loetsch et al. (1973), Meyer (1953) and Prodan (1951, 1961, 1965).

6.6.1 Reference Area

To extrapolate response variables from a plot to the standard area of 1 ha, the extrapolation factor E is used:

$$E = \frac{1}{A}, \tag{6.21}$$

where A is the size of the plot in hectares. For a 2 ha plot, the extrapolation factor $E = 0.5$, and for a 0.25 ha plot, $E = 4$.

6.6.2 Tree Number

If the tree number n per plot is known, then the tree number per hectare N is obtained from

$$N = \frac{n}{A} = n \times E. \tag{6.22}$$

The procedure for extrapolating stand basal area, standing volume and growth and yield data to 1 ha is analogous. In a standard analysis, tree number, mean diameter, mean height, slenderness, basal area and volume are calculated for the strata remaining stand, removed stand and total stand.

6.6.3 Mean Diameter and Mean Diameter of the Top Height Tree Collective

To quantify the diameter structure of a stand, the following parameters are used: arithmetic mean diameter $\overline{d}$, quadratic mean diameter d_q, Weise's mean tree diameter d_W, median basal area tree diameter d_Z, Hohenadl's mean tree diameters d_- and d_+, and the quadratic mean diameter of the tree collective comprising the 100 trees with the largest diameters nominated for top height measurement d_{100}. Both historical and practical factors have led to the development of a range of measures of mean diameter. In the following section, we introduce the arithmetic mean diameter $\overline{d}$, quadratic mean diameter d_q and the mean diameter of the top height tree collective d_{100}, which are applied frequently.

The arithmetic mean diameter, important for the mathematical description of tree number–diameter distributions, is calculated either from the individual diameter values from the trial plot:

$$\overline{d} = \frac{d_1 + d_2 + \cdots + d_N}{N} = \frac{1}{N} \times \sum_{i=1}^{N} d_i, \tag{6.23}$$

or from the tree number n_i per diameter class d_i:

$$\overline{d} = \frac{n_1 \times d_1 + n_2 \times d_2 + \cdots + n_k \times d_k}{n_1 + n_2 + \cdots + n_k} = \frac{\sum_{i=1}^{k} (n_i \times d_i)}{\sum_{i=1}^{k} n_i}, \tag{6.24}$$

where n_i = tree number in diameter class i, d_i = mean diameter of each diameter class, k = number of diameter classes, and N = tree number in the stand $N = \sum_{i=1}^{k} n_i$.

The diameter of the mean basal area tree, or the quadratic mean diameter d_q, is of particular practical importance because, in evenaged stands, this tree corresponds approximately to the tree of mean volume. If one multiplies the volume of this tree by the tree number per hectare, standing volume is obtained. Therefore many yield tables, tariff or tending prescriptions are based on the mean basal area tree. It is calculated from the arithmetic mean of the basal area of all trees at breast height $ba_{1.3}$ in a stand:

$$\overline{ba} = \frac{\sum_{i=1}^{N} ba_i}{N} = \frac{\sum_{i=1}^{k} n_i \times ba_i}{N}. \tag{6.25}$$

This mean basal area of all trees is used then to obtain d_q:

$$d_q = 2 \times \sqrt{\frac{\overline{ba}}{\pi}}. \tag{6.26}$$

The quadratic mean diameter can also be determined directly from the individual diameter measurements $d_{i,i=1...N}$ from

$$d_q = \sqrt{\frac{\sum_{i=1}^{N} n_i \times d_i^2}{N}}. \tag{6.27}$$

The diameter d_{100} of the 100 largest trees is calculated from the largest end of the diameter lists. The sum basal areas of the 100 largest trees per hectare, $sba_{100} = \sum_{i=1}^{100} ba_i$, is determined. By dividing this value by the tree number 100, the mean basal area of the 100 largest trees per hectare $\overline{ba}_{100} = sba_{100}/100$ is obtained from which the mean diameter of the top height tree collective can be determined:

$$d_{100} = \sqrt{\frac{\overline{ba}_{100}}{\pi} \times 4}. \tag{6.28}$$

6.6.4 Mean and Top Height

In a standard analysis, the mean and top heights are always read off the stand height curve. Thus, the mean diameter and the mean diameter of the top height tree collective, introduced above, serve as input parameters for the diameter–height function. The mean and top heights, with relative dimensions in the order given below, are then either taken from the curve or calculated using the appropriate stand height function (Fig. 6.12).

Lorey's mean height h_L corresponds to the height of the mean basal area tree (Lorey 1878). It is significant today because most of the older yield tables use this height as a variable for site quality assessment. The use of the height of the mean basal area tree and top height as parameters for yield tables began in the 1960s and 1970s. Lorey's mean height is calculated from

$$h_L = \frac{n_1 \times ba_1 \times h_1 + n_2 \times ba_2 \times h_2 + \cdots + n_k \times ba_k \times h_k}{n_1 \times ba_1 + n_2 \times ba_2 + \cdots + n_k \times ba_k} = \frac{\sum_{i=1}^{k} n_i \times ba_i \times h_i}{\sum_{i=1}^{k} n_i \times ba_i}, \tag{6.29}$$

where n_i represents number of trees in diameter class i, ba_i basal area of a tree in the given diameter class, h_i mean height in the diameter class and k number of diameter classes.

Conversely, the mean height in the diameter class h_i is taken from the stand–height curve in relation to the corresponding diameter d_i. The somewhat

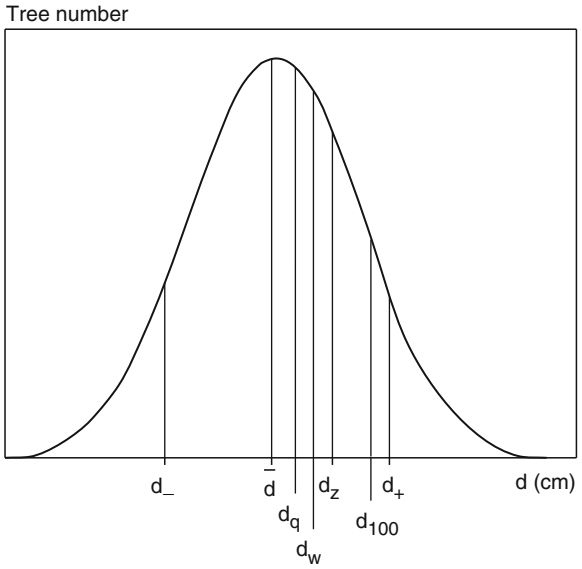

Fig. 6.12 Graph presenting the tree number–diameter distribution with the relative position of the mean diameter and mean diameter of the top height tree collective (from Kramer and Akça 1995). In the case of even aged stands applies mostly $d_- < \overline{d} < d_q \approx d_W < d_Z < d_+ \gtrless d_{100}$

complicated calculation of this height can be simplified by stratifying the stand into five classes with the same tree number or the same basal area:

$$h_L = \frac{h_1 + h_2 + h_3 + h_4 + h_5}{5}, \tag{6.30}$$

where $h_1, \ldots, h_5$ represents mean heights in classes with the same tree number or the same basal area.

The aim of the somewhat complicated calculation of Lorey's mean height, impressive at the time of its introduction in the nineteenth century given that it was calculated largely manually, was to find a robust description of stand height that, in the form of an age–mean height relationship, would become the basis of yield tables at the time.

We describe the tree collective at the right tail (large end) of the tree number–diameter distribution as top height trees. Definitions of the limit of this collective differ. Either the largest 20% of trees, or a fixed number of 100 or 200 of the largest trees form the collective for top height. The relative and absolute values of dominant diameter and top height are not abbreviated uniformly. Whereas $d_{100}, d_{200}, h_{100}, h_{200}$ always relate to the 100 or 200 largest trees respectively, the descriptions d_o and h_o commonly refer to relative and absolute and tree collectives. In such cases one must note, or query the nature of determinations of dominant diameter or top height in question.

6.6.5 Slenderness h_q/d_q and h_{100}/d_{100}

Standard analysis incorporates the calculation of slenderness to characterise the stability of the remaining trees and the structural features of the removed trees. The height and diameter of either the mean basal area tree (h_q/d_q) or the top height tree (h_{100}/d_{100}) are used. The height is entered into the equation in meters, and the diameter in centimeters. Slenderness values usually fall within the range 50–150; slenderness values below 80 are generally an indicator of adequate individual tree stability. The slenderness of the trees removed from a stand in an intermediate thinning from below is usually much higher than the remaining stand. In a thinning from above, the slenderness of the remaining and the removed stand are similar because the dominant, stable trees are generally removed.

6.6.6 Stand Basal Area and Volume

Basal area BA, and volume V are calculated for the remaining, removed and total stand per hectare by adding the basal area, and volume of all individual trees in the measurement tree collective and the total stand respectively:

$$\mathrm{BA} = \frac{\sum_{i=1}^{N} \mathrm{ba_i}}{\mathrm{A}} = \frac{\sum_{i=1}^{N} \frac{\mathrm{d_i^2}\times\pi}{4}}{\mathrm{A}} = \frac{\pi/4 \times \sum_{i=1}^{N} \mathrm{d_i^2}}{\mathrm{A}}, \tag{6.31}$$

$$\mathrm{V} = \frac{\sum_{i=1}^{N} \mathrm{ba_i}\times \mathrm{h_i} \times \mathrm{f_{1.3i}}}{\mathrm{A}} = \frac{\sum_{i=1}^{N} \frac{\mathrm{d_i^2}\times\pi\times \mathrm{h_i}\times \mathrm{f_{1.3_i}}}{4}}{\mathrm{A}} = \frac{\pi/4 \times \sum_{i=1}^{N} \mathrm{d_i^2}\times \mathrm{h_i} \times \mathrm{f_{1.3_i}}}{\mathrm{A}}, \tag{6.32}$$

where BA is stand basal area, V the volume and A the plot size in ha.

The mean basal area density, the density measure determined in the standard analysis, is based on the basal areas at the time of inventory. The mean basal area density in the periods between inventories $1, \ldots,$ n is

$$\mathrm{mBA} = \frac{\left(\frac{\mathrm{bBA_1}+\mathrm{eBA_1}}{2}\right)\times \mathrm{per_1} + \left(\frac{\mathrm{bBA_2}+\mathrm{eBA_2}}{2}\right)\times \mathrm{per_2} + \cdots + \left(\frac{\mathrm{bBA_n}+\mathrm{eBA_n}}{2}\right)\times \mathrm{per_n}}{\mathrm{per_1}+\mathrm{per_2}+\cdots+\mathrm{per_n}}. \tag{6.33}$$

Here, mBA is mean basal area density, bBA the stand basal area at the beginning of an inventory period, eBA is the stand basal area at the end of an inventory period and per is the number of years in the period between inventories. Therefore, the mean basal area density represents the average of the stand basal areas at the beginning and end of each growth period weighted according to the length of the growth period. It characterises stand density in one or more periods between inventories, and is an appropriate measure for quantifying stand density.

6.6.7 Growth and Yield Characteristics

The gross volume growth G, equivalent to gross volume increment I, is obtained from the standard analysis of long-term trial plots or with the control methods used in forestry practice (cf. Fig. 2.5):

$$I = V_{2\,\text{remain}} - V_{1\,\text{remain}} + V_{\text{removed}}, \tag{6.34}$$

where I = volume increment, $V_{1\text{remain}}$ = standing volume at the beginning of the inventory period, $V_{2\,\text{remain}}$ = standing volume at the end of the inventory period, and V_{removed} = volume removed in the period between inventories (utilisable thinnings plus mortality). The growth and increment of stand basal area is calculated analogously.

This approach gives the volume increment during the period between successive inventories, which, when divided by the length of the period (per in years) produces the periodic annual increment (PAI) in volume for that period:

$$\text{PAI} = (V_{2\,\text{remain}} - V_{1\,\text{remain}} + V_{\text{removed}})/\text{per}. \tag{6.35}$$

If the length of the period between inventories is just 1 year (per = 1), then we get the current annual increment (CAI) in volume. PAI and CAI are important for estimating the stand growth phase in the period between inventories, planning future stand treatment, analysing thinning responses and calculating the quantity of removals.

The volume yield equals the total volume production and is the sum of the volume growth in the periods up to the current inventory period. Yield is calculated by adding the current standing volume and the sum of the volume removed in all previous periods:

$$\text{Volume yield} = \text{standing volume} + \text{volume of removed stand}. \tag{6.36}$$

The volume of the remaining stand is the "visible", or net, component of the total volume production (=volume yield). The sum of the thinned volume (utilisable and non-utilisable thinnings) must be added to the current standing volume to obtain total volume production. This removed volume may amount to 20–60% of the total volume production depending on the self-thinning and the intensity of thinning operations. Trial plots that have been observed and measured since stand establishment enable the total volume production to be calculated from the current standing volume and the sum of the volume removed in each intermediate thinning carried out.

The division of the total volume production at time t by age:

$$\text{MAI}_t = \frac{\text{Gross volume yield}_t}{\text{age}} \tag{6.37}$$

produces the mean annual increment (MAI). It expresses volume growth produced in a stand from the time of establishment to the present in each year. The MAI in volume and in timber value play a key role in determining the time of stand harvest.

6.7 Results of Standard Analysis

6.7.1 Presentation in Tables

6.7.1.1 Analogy Between Results Tables and Yield Tables

The information contained in the results tables from long-term trial plots is explained with the example of the European beech thinning trial plots FAB 15/1-3. The structure of the tables largely corresponds to that of the yield tables (cf. Chap. 11). This is because the yield tables are essentially based on the results of long-term trial plots, and they describe stand development with stand level mean and cumulative values. The analysis results provided for the A, B and C grade plots clearly present the investigation results in tables and graphs. Yet, as this is one of the oldest existing thinning trials, we also become acquainted with stand growth relationships. The headings of the results table (cf. Table 6.2a–c) comprise the institution undertaking the investigation, the description, number and silvicultural treatment on the trial plots, the date of analysis and size of the plot and reference area (usually 1 ha). The results table headings differentiate three strata: remaining stand, removal stand and total stand.

For each inventory time point, the important stand mean and cumulative values are entered by stand age for the three strata mentioned above. In our example, the growth period considered ranges from 1871 to 2000. All 18 inventories were sometimes conducted in spring (s) and sometimes in autumn (a); the season is denoted after the year of inventory. The inventories cover the ages of 48–178 years. For each of the inventories, the characteristics of each tree species present are given separately in the stand descriptions, and in total for the remaining stand, the removed stand and the total stand. In the European beech stand mentioned above, we include the few admixed specimens of Sessile oak and Common maple with the European beech so that the stratum (European beech) characterises the total stand.

6.7.1.2 Structure and List of Variables in Results Tables

The following data are recorded for the remaining stand: tree number (N), top height (h_{100}), mean diameter of the top height tree collective (d_{100}), slenderness of the top height trees (h_{100}/d_{100}), height of the mean basal area tree (h_q), quadratic mean diameter (d_q), slenderness of the mean basal area tree (h_q/d_q), basal area of the remaining stand (BA) and standing volume (V). In the following example, top height and mean diameter of the top height tree collective are determined from the height

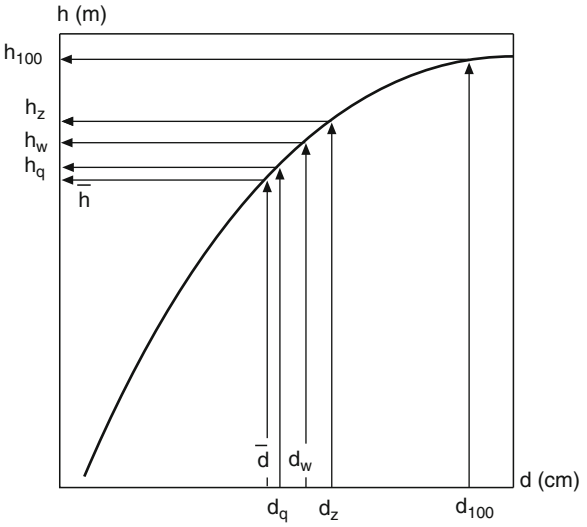

Fig. 6.13 Diameter–height curve (*stand height curve*) and the relative position of important stand mean heights and stand upper heights presented graphically (from Kramer and Akça 1995)

and diameter of the mean basal area tree of the 100 trees with the largest diameter per hectare respectively (Fig. 6.13).

The following data are recorded for the remaining stand: tree number (N), top height (h_{100}), mean diameter of the top height tree collective (d_{100}), slenderness of the top height trees (h_{100}/d_{100}), height of the mean basal area tree (h_q), quadratic mean diameter (d_q), slenderness of the mean basal area tree (h_q/d_q), basal area of the remaining stand (BA) and standing volume (V). In the following example, top height and mean diameter of the top height tree collective are determined from the height and diameter of the mean basal area tree of the 100 trees with the largest diameter per hectare respectively (Fig. 6.13).

The standardised list of variables for the removed stand includes: tree number (N), height of the mean basal area tree of the removed trees (h_q), quadratic mean diameter of the removed trees (d_q), slenderness of the removed stand components (h_q/d_q), basal area of the removed stand (BA) and volume of the removed stand (V).

The following standard variables are provided for the entire stand: gross volume yield (GY_V), mean basal area density (mBA), periodic annual basal area increment (PAI_{BA}), periodic annual volume increment (PAI_V), mean annual volume increment (MAI_V), period between successive inventories (per), total stand basal area before thinning (BA) and total standing volume before thinning (V).

The values given in the rows for the mean basal area density (mBA), the periodic annual basal area increment (PAI_{BA}), the periodic annual volume increment (PAI_V) and the period between successive inventories (per) relate to the preceding inventory period. Thus, in the second row of Table 6.2b, the values given for the mean basal area density ($mBA = 30.3\,m^2\,ha^{-1}$), basal area increment

($PAI_{BA} = 0.7\,m^2\,ha^{-1}\,yr^{-1}$) and volume increment ($PAI_V = 8.7\,m^3\,ha^{-1}\,yr^{-1}$) for the moderately thinned plot FAB 15/2 at the inventory time point 1882s relate to the 11 year inventory period from 1871s to 1882s.

6.7.1.3 Contents of Results Tables

Remaining Stand

In the result tables for A, B and C grade trial plots (Table 6.2a–c), a clear exponential reduction in tree number is evident from the beginning of the trial to the last inventory, where a light thinning from below, moderate thinning and a heavy thinning leave 393, 234 and 159 trees per hectare respectively. With this variation in thinning grade, mean diameter of the top height tree collective can be increased from 54.4 cm for A grade to 60.1 cm for B grade and 63.0 cm for C grade by the year 2000.

In the 130 year observation period, the standing volume, expressed in cubic metres of merchantable timber per hectare, increases from 117 to $136\,m^3\,ha^{-1}$ at the age of 48 years to 848–$1,015\,m^3\,ha^{-1}$ at the age of 178 years. On the moderately and heavily thinned plots, FAB 15/2 and 3, the volume growth is slowed by the periodic thinning treatments. Slenderness decreases noticeably with increasing thinning grade. Under high stand densities, the trees striving for light emphasise height growth at the expense of diameter growth. In the survey year 2000, a gradual reduction in h_q/d_q values of 81, 73 and 68 was found for the A, B and C grade trials respectively.

Removed Stand

Trees that drop out of a stand in the intervals between inventories either as a result of natural thinning processes or thinning operations are recorded at the time of inventory. The removed stand recorded in Table 6.2a for the inventory time point 1882s (1,044 trees per hectare, mean height 3.4 m, mean diameter 3.2 m, slenderness 106, basal area $0.84\,m^2\,ha^{-1}$) comprises trees that died in the 11 year growing period 1871s–1882s. On plots where a moderate or heavily thinning from below was carried out, the cumulative values of those trees harvested as part of trial management before 1882s are recorded.

The increase in thinning grade from A grade to C grade is evident from the increase in tree numbers, basal area and volume removed from the stand. As more and more small and moderate-sized trees are removed, the height and diameter of the removed trees increases. The relatively low slenderness of the removed trees in the C grade trial in the second half of the 130-year trial period shows that this stand only contains a few small and moderate-sized trees. Thus the height and diameter measurements of the trees extracted in thinning operations approximate those of the remaining dominant stand. The ratio of the diameter of the removed stand to that

Table 6.2a Table of results of a standard analysis for the A grade European beech thinning trial FAB 15 (first inventory 1871s, current repeated inventory 2000a) are used to demonstrate the standardised form for presenting stand level data. Table headings are explained in the text and in Table 6.1. European beech thinning trial plot FAB 15/1, A grade, light thinning from below

Lehrstuhl für Waldwachstumskunde der TU München — Plot size: 0.3690 ha
Experimental plot FAB 15/1 A grade — All data refer to 1 ha

		Remaining stand										Removal stand						Total stand							
Year	Age year	sp	N	h_{100} m	d_{100} cm	h_{100}/d_{100}	h_q m	d_q cm	h_q/d_q	BA m^2	V m^3	N	h_q m	d_q cm	h_q/d_q	BA m^2	V m^3	GY_V m^3	mBA m^2	PAI_{BA} m^2yr^{-1}	PAI_V m^3yr^{-1}	MAI_V m^3yr^{-1}	per yr	BA m^2	V m^3
1871s	48	E. beech	6,220	16.6	18.6	89	9.3	7.5	124	28.22	120	0	0	0	0	0	0	120				2.5		28.2	120
1882s	59	E. beech	5,176	19.2	21.2	90	11.6	8.7	133	31.42	179	1,044	3.4	3.2	106	0.84	0	179	30.2	0.4	5.4	3.0	11	32.3	179
1884s	61	E. beech	2,639	19.9	22.3	89	14.3	11.4	125	27.19	188	2,537	6.6	5.1	129	5.28	8	196	31.9	0.5	8.3	3.2	2	32.5	196
1889a	67	E. beech	2,368	21.7	25.3	85	16.3	13.2	123	32.76	265	271	7.2	5.3	135	0.61	1	274	30.3	1.0	13.0	4.1	6	33.4	266
1894a	72	E. beech	2,135	22.9	27.4	83	17.8	14.7	121	36.34	324	233	9.3	6.5	143	0.77	2	335	34.9	0.9	12.2	4.7	5	37.1	326
1899a	77	E. beech	1,853	23.9	28.8	82	19.0	15.9	119	37.02	354	282	11.5	7.8	147	1.34	5	370	37.4	0.4	7.1	4.8	5	38.4	359
1904a	82	E. beech	1,583	24.8	30.4	81	20.4	17.4	117	37.96	389	270	12.8	8.5	150	1.56	8	413	38.3	0.5	8.6	5.0	5	39.5	397
19093	87	E. beech	1,177	25.7	31.8	80	22.1	19.9	111	36.99	410	406	15.0	10.1	148	3.26	21	454	39.1	0.5	8.3	5.2	5	40.3	431
19243	102	E. beech	830	28.1	35.8	78	25.3	24.6	102	39.51	502	347	18.4	12.5	147	4.23	36	583	40.4	0.4	8.5	5.7	15	43.7	538
1929a	107	E. beech	700	29.0	37.4	77	26.7	26.8	89	39.37	529	130	22.3	16.1	138	2.70	29	638	40.8	0.5	11.2	6.0	5	42.1	558
1936s	113	E. beech	613	29.7	39.0	76	27.5	28.8	85	40.09	555	87	22.2	16.4	135	1.90	20	685	40.7	0.4	7.8	6.1	6	42.0	576
1950a	128	E. beech	499	31.5	42.6	73	29.7	32.7	90	41.98	630	114	25.4	20.2	125	3.79	48	808	42.9	0.4	8.2	6.3	15	45.8	678
19583	136	E. beech	477	32.4	44.4	72	30.6	34.1	89	43.54	676	22	30.2	32.6	92	1.81	28	882	43.7	0.4	9.2	6.5	8	45.3	704
19683	146	E. beech	461	33.5	47.2	70	31.7	36.2	87	47.50	769	16	27.8	23.1	120	0.68	9	984	45.9	0.5	10.2	6.7	10	48.2	778
1978s	155	E. beech	444	34.5	49.7	69	32.8	38.3	85	51.15	857	17	28.1	22.7	123	0.66	9	1,082	49.7	0.5	10.9	7.0	9	51.8	867
1981s	158	E. beech	436	34.8	50.7	68	33.1	39.2	84	52.50	891	8	28.7	23.7	121	0.36	5	1,120	52.0	0.6	12.8	7.1	3	52.9	896
1991s	168	E. beech	406	35.6	52.3	68	34.1	41.1	82	53.90	944	30	32.4	33.0	98	2.51	42	1,216	54.5	0.4	9.6	7.2	10	56.4	986
2000a	178	E. beech	393	36.5	54.4	67	34.9	42.6	81	56.30	1,015	13	32.8	32.8	100	1.15	19	1,306	55.7	0.4	9.0	7.3	10	57.4	1,034

Table 6.2b Table of results of a standard analysis for the B grade European beech thinning trial FAB 15 (first inventory 1871s, current repeated inventory 2000a) are used to demonstrate the standardised form for presenting stand level data. Table headings are explained in the text and in Table 6.1. European beech thinning trial plot FAB 15/2, B grade, moderate thinning from below

Lehrstuhl für Waldwachstumskunde der TU München — Plot size: 0.3670 ha
Experimental plot FAB 15/2 B grade — All data refer to 1 ha

		Remaining stand										Removal stand						Total stand							
Year	Age year	sp	N	h_{100} m	d_{100} cm	h_{100}/d_{100}	h_q m	d_q cm	h_q/d_q	BA m^2	V m^3	N	h_q m	d_q cm	h_q/d_q	BA m^2	V m^3	GY_V m^3	mBA m^2	PAI_{BA} m^2yr^{-1}	PAI_V m^3yr^{-1}	MAI_V m^3yr^{-1}	per yr	BA m^2	V m^3
1871s	48	E. beech	3,831	16.2	18.1	89	11.9	9.1	130	26.54	136	2,371	6.2	4.2	147	3.32	0	136				2.8		29.9	136
1882s	59	E. beech	2,450	19.8	22.6	87	15.7	12.1	129	29.45	219	1,381	10.5	6.5	161	4.57	12	231	30.3	0.7	8.7	3.9	11	34.0	231
1884s	61	E. beech	1,638	20.4	23.7	86	17.6	14.9	118	28.79	242	812	12.1	7.6	159	3.64	13	268	30.9	1.5	18.0	4.4	2	32.4	255
1889a	67	E. beech	1,509	21.9	25.4	86	19.0	15.9	119	30.13	276	129	13.5	8.3	162	0.96	6	308	29.9	0.4	6.7	4.6	6	31.1	282
1894a	72	E. beech	1,090	23.3	28.3	82	21.2	19.5	108	31.93	329	419	16.9	11.3	149	4.21	31	392	33.1	1.2	16.8	5.4	5	36.1	360
1899a	77	E. beech	965	24.3	29.1	83	22.3	20.9	106	32.50	356	125	18.8	13.1	143	1.73	15	433	33.1	0.5	8.3	5.6	5	34.2	371
1904a	82	E. beech	760	25.4	30.6	83	23.7	23.0	103	31.06	362	205	21.0	16.0	131	4.05	41	480	33.8	0.5	9.4	5.9	5	35.1	403
1909a	87	E. beech	575	26.4	32.2	81	24.9	25.1	99	27.96	345	185	23.5	20.5	114	5.86	67	530	32.4	0.6	10.0	6.1	5	33.8	412
1924a	102	E. beech	528	29.2	37.2	78	27.8	29.5	94	35.26	489	47	24.1	18.0	133	1.17	14	688	32.2	0.6	10.5	6.7	15	36.4	503
1929a	107	E. beech	452	30.0	38.9	77	28.8	31.4	91	34.68	500	76	27.1	24.5	110	3.29	44	743	36.6	0.5	10.9	6.9	5	38.0	543
1936s	113	E. beech	447	30.9	40.5	76	29.7	32.8	90	37.31	557	5	26.3	20.6	127	0.22	3	802	36.1	0.5	10.0	7.1	6	37.5	560
1950a	128	E. beech	370	33.0	44.5	74	31.9	36.8	86	39.04	631	77	30.5	29.7	102	4.98	76	953	40.7	0.4	10.0	7.4	15	44.0	707
1958a	136	E. beech	340	34.1	47.3	72	33.0	39.1	84	40.44	680	30	32.3	34.9	92	2.83	46	1,048	41.2	0.5	11.9	7.7	8	43.3	726
1968a	146	E. beech	330	35.3	50.1	70	34.2	41.5	82	43.89	768	10	35.1	47.7	73	1.71	30	1,167	43.0	0.5	11.9	8.0	10	45.6	799
1978s	155	E. beech	325	36.5	53.6	68	35.3	43.9	80	48.20	875	5	35.5	45.2	78	0.87	16	1,289	46.5	0.6	13.6	8.3	9	49.1	891
1981s	158	E. beech	316	36.8	54.8	67	35.7	45.1	79	49.28	906	9	33.3	32.1	103	0.66	11	1,331	49.1	0.6	13.9	8.4	3	49.9	917
1991s	168	E. beech	297	37.8	57.2	66	36.7	47.2	77	50.94	969	19	36.5	45.7	79	2.76	52	1,446	51.5	0.4	11.5	8.6	10	53.7	1,021
2000a	178	E. beech	234	38.8	60.1	64	38.0	51.5	73	48.01	950	63	35.7	37.2	95	6.91	127	1,554	52.9	0.4	10.8	8.7	10	54.9	1,077

Table 6.2c Table of results of a standard analysis for the C grade European beech thinning trial FAB 15 (first inventory 1871s, current repeated inventory 2000a) are used to demonstrate the standardised form for presenting stand level data. Table headings are explained in the text and in Table 6.1. European beech thinning trial plot FAB 15/3, C grade, heavy thinning from below

Lehrstuhl für Waldwachstumskunde der TU München — Plot size: 0.3650 ha
Experimental plot FAB 15/3 C grade — All data refer to 1 ha

		Remaining stand										Removal stand						Total stand							
Year	Age	sp	N	h_{100}	d_{100}	h_{100}/d_{100}	h_q	d_q	h_q/d_q	BA	V	N	h_q	d_q	h_q/d_q	BA	V	GY_V	mBA	PAI_{BA}	PAI_V	MAI_V	per	BA	V
	year			m	cm		m	cm		m^2	m^3		m	cm		m^2	m^3	m^3	m^2	m^2yr^{-1}	m^3yr^{-1}	m^3yr^{-1}	yr	m^2	m^3
1871s	48	E. beech	2,442	15.2	18.0	84	12.3	10.4	118	21.86	117	3,626	7.1	4.8	147	6.48	3	120				2.5		28.3	120
1882s	59	E. beech	1,513	19.0	22.7	83	16.5	14.5	113	25.41	199	929	14.4	10.6	135	8.25	50	252	27.8	1.1	12	4.3	11	33.7	249
1884s	61	E. beech	1,252	19.6	23.7	82	17.4	15.8	110	24.98	209	261	14.1	9.8	143	1.97	11	273	26.2	0.8	10.4	4.5	2	27.0	220
1889a	67	E. beech	1,110	21.2	25.4	83	19.1	17.3	110	26.40	244	142	15.5	10.6	146	1.32	9	317	26.4	0.5	7.4	4.7	6	27.7	253
18943	72	E. beech	830	22.6	27.6	81	20.9	20.1	103	26.65	272	280	18.1	13.4	135	4.01	34	379	28.5	0.9	12.4	5.3	5	30.7	306
18993	77	E. beech	654	23.8	29.3	81	22.3	22.2	100	25.31	278	176	20.4	16.7	122	3.8*j*	38	422	27.9	0.5	8.6	5.5	5	29.2	315
1904a	82	E. beech	481	25.0	31.0	80	23.7	24.5	96	22.54	264	173	22.6	20.6	109	5.72	63	472	26.8	0.6	9.9	5.8	5	28.3	327
1909a	87	E. beech	343	26.1	32.7	79	25.0	26.9	92	19.45	242	138	24.4	24.3	100	6.18	74	524	24.1	0.6	10.4	6.0	5	25.6	316
19243	102	E. beech	274	29.2	38.8	75	28.4	33.5	84	24.06	343	69	26.6	25.2	105	3.25	43	668	23.4	0.5	9.6	6.5	15	27.3	386
19293	107	E. beech	250	30.1	40.5	74	29.4	35.6	82	25.04	371	24	28.0	28.4	98	1.35	19	714	25.2	0.5	9.3	6.7	5	26.4	389
s1936s	113	E. beech	247	31.1	42.3	73	30.4	37.2	81	27.16	417	3	0	0	0	0.12	2	762	26.2	0.4	8.0	6.7	6	27.3	419
1950a	128	E. beech	239	33.4	46.9	71	32.7	41.2	79	32.28	538	8	31.0	31.7	97	0.64	10	893	30.0	0.4	8.7	7.0	15	32.9	548
19583	136	E. beech	212	34.5	49.0	70	33.8	43.6	77	31.52	545	27	33.5	41.5	80	4.08	71	971	33.9	0.4	9.7	7.1	8	35.6	616
1968a	146	E. beech	212	35.9	52.9	67	35.2	46.6	75	36.14	654	0	0	0	0	0	0	1,080	33.8	0.5	10.9	7.1	10	36.1	654
1978s	155	E. beech	212	37.1	56.5	65	36.3	49.5	73	40.72	767	0	0	0	0	0	0	1,192	38.4	0.5	12.5	7.4	9	40.7	767
1981s	158	E. beech	212	37.4	57.6	64	36.7	50.3	72	42.11	802	0	0	0	0	0	0	1,228	41.4	0.5	11.9	7.5	3	42.1	802
1991s	168	E. beech	206	38.6	60.7	63	37.8	52.9	71	45.33	896	6	36.8	45.1	81	0.88	17	1,338	44.2	0.4	11.0	7.7	10	46.2	912
20003	178	E. beech	159	39.6	63.0	62	39.1	57.4	68	41.22	848	47	37.6	45.6	82	7.62	148	1,438	47.1	0.4	10.0	7.8	10	48.8	996

of the remaining stand characterises the type of thinning. For operations described as thinning from below, the mean diameter of the removed stand is much lower than the mean diameter of the remaining stand. In contrast, if the aim is to conduct thinning operations in the dominant stand layer, then the mean diameters of the removed and remaining stands are similar (cf. Table 6.2c).

Total Stand

The category total stand comprises the total volume production (gross volume yield GY_V) of the stand at the time of each inventory. The mean annual volume increment (MAI_V) was calculated by dividing total volume production by age. The period length (per) expresses the length of the interval between successive inventories in years. The last two columns in Table 6.2a show the basal area and the standing volume of the total stand before thinning (BA and V, respectively). These values are based on the remaining, and the removed stand recorded in each inventory. On plot 2 (Table 6.2b), for example, a total volume of 1,077 $m^3 ha^{-1}$ was recorded in the 2000a inventory, at which time 127 $m^3 ha^{-1}$ was thinned, leaving 950 $m^3 ha^{-1}$ in the stand.

In the last inventory, the total volume production amounted to 1,306–1,554 $m^3 ha^{-1}$, of which 1,015, 950 and 848 $m^3 ha^{-1}$ still remain in the A grade, B grade and C grade stands respectively. The development of the periodic annual volume increment (PAI_V) enables the first growth maximum to be identified in the first half of the growth period (60–80 years old); in the last third of the growth period (136–178 years old), the increment values once again reach the highest values of the juvenile phase. Thus, up to the present, the values of the mean annual increment (MAI_V) show no evidence of culmination; rather, in past decades, they have continued to increase.

6.7.2 Stand Development Diagrams

As a reference for the expected change in stand yield with age, we apply the European beech yield table from Schober (1967), moderate thinning, for the site classes I, II and III (Figs. 6.14–6.23, gray lines). This site class range is selected because the A grade, a somewhat inferior site, falls within the range of site classes II–III. The age–height development of B and C grades largely follows site class II (cf. Fig. 6.18). The site class has improved on all plots since trial establishment by more than half a class.

6.7.2.1 Tree Number

On the A, B and C grade plots, the tree number declines exponentially from the initial 6,220, 6,202 and 6,068 trees per hectare to 393, 234 and 159 trees per

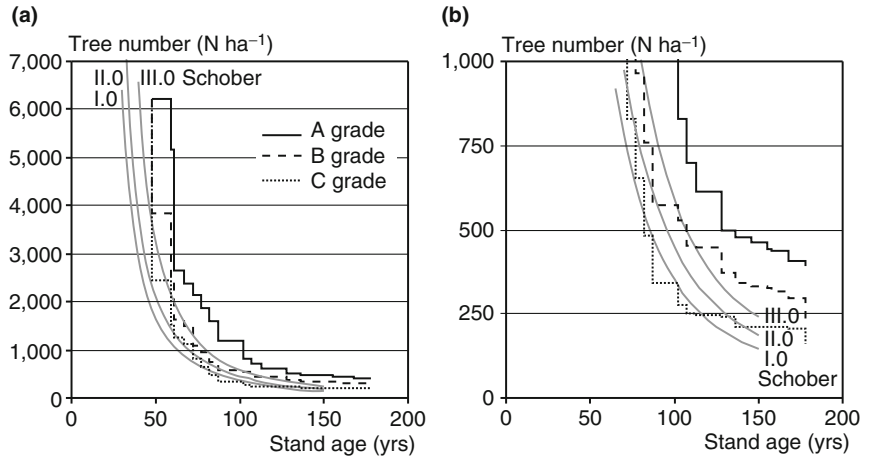

Fig. 6.14 Tree number development on the European beech trial plot FAB 15 for (**a**) the total observation period and (**b**) magnified for the age range 102–178 years. The tree number per hectare is presented for the A grade (*solid line*), B grade (*dashed line*) and C grade (*dotted line*). The curves from Schober's (1967) European beech yield tables, moderate thinning, for the I., II., and III. site classes are plotted for reference (*gray lines*)

hectare respectively (Fig. 6.14). As the reduction in tree number arising from mortality or thinning is always recorded at the end of the survey period, the graph characteristically is stepped. While the development in tree number in the A grade plot represents the maximum number of trees possible at a given age (*solid line*), the density decreases considerably on plots 2, and 3 due to the moderate (*dashed line*), and heavy (*dotted line*) thinnings from below respectively. The tree numbers on the treated plots in the first third of the observation period are clearly higher than in the yield tables (Fig. 6.14a). In the second third, they decline to the level of the tables, and, from the age of 100 years, remain much higher than the table values (Fig. 6.14b).

6.7.2.2 Age–Diameter Development

The thinnings from below carried out in accordance with the instructions from the Association of German Forest Research Stations (1902) (cf. Chap. 5) cause a continuous increase in mean diameter on the moderately and heavily thinned plots (Fig. 6.15a). At the end of the observation period, the diameter on these plots exceeds that of the A grade plot by 14.8 cm on the C grade and 8.9 cm on the B grade plots. This increase in diameter results, in part, from an arithmetic shift in the mean diameter as a result of the thinning from below. However, the increased availability in growing space, which promotes the growth of the remaining trees, also contributes.

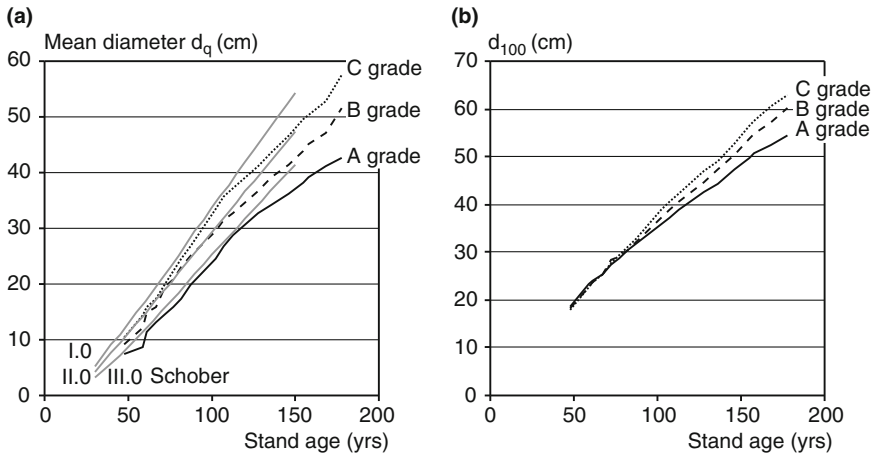

Fig. 6.15 Development of (**a**) the quadratic mean diameter d_q and (**b**) the quadratic mean diameter of the top height tree collective d_{100} on the European beech thinning trial plot FAB 15. The increase in diameter resulting from the treatment is recognisable from the A grade (*solid line*) through the B grade (*dashed line*) to C grade (*dotted line*). The curves from Schober's (1967) European beech yield tables, moderate thinning, for the I., II., and III. site classes are plotted for reference (*gray lines*)

The diameter of the 100 largest trees per hectare (d_{100}) is increased by moderate and heavy thinning from below by 5.7 and 8.6 cm compared to the A grade plot respectively. As d_{100} largely is unaffected by an arithmetic shift after a thinning from below, the diameter increase essentially represents the response to thinning. The operations carried out are expressed in the tree numbers; compared to the A grade plot (100%), 60% and 40% of trees on the B grade and C grade stands are present at the age of 178 years respectively.

6.7.2.3 Tree Number–Diameter Frequencies

Tree number–diameter distributions show the way in which the growing space is divided up between trees; that is whether it is occupied by a few large trees, or many small trees. Figure 6.16 shows the development of tree number–diameter frequencies for the three plots in the European beech thinning trial FAB 15/1-3 (light thinning, moderate thinning and heavy thinning) from 1871s to 2000a. The logarithmic transformation of the tree numbers for each 4 cm diameter class, undertaken to display the data, curbs the high occupancy numbers and increases the relatively low occupation frequencies.

The tree number–diameter distributions continue along the $d_{1.3}$ axes from the beginning of the experiment to the present, changing in form. In view of the variable frequency of inventory, especially during the war years, different time intervals occur between the distributions. The diameter increase is accompanied by an expansion of growing space such that fewer and fewer trees have sufficient growing

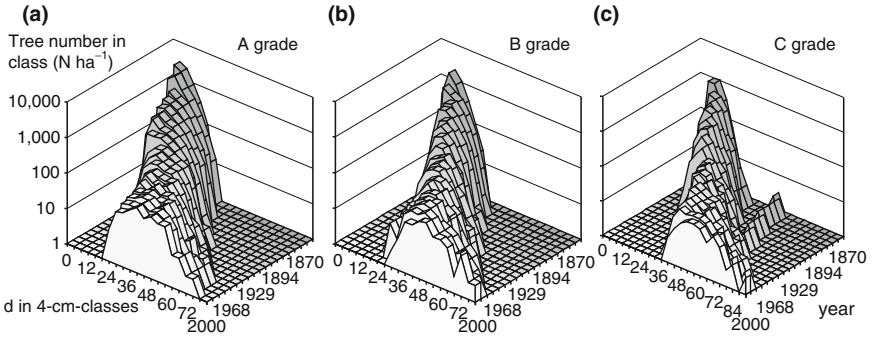

Fig. 6.16 (**a–c**) Tree number–diameter distributions for A, B and C grades at the European beech thinning trial plot FAB 15, from the first inventory in 1871 to the most recent repeated inventory in autumn 2000. The tree–diameter distributions of the total stand are presented in 4 cm diameter classes

space on the trial plot. The A grade plot, left entirely to self-thinning processes (Fig. 6.16a), reveals the characteristic right shift, levelling out and increasing variation in the tree number–diameter distribution. In the 2000a inventory, at the age of 178 years, the diameter ranged from 16 to 70 cm. On the B and C grade plots, the moderate and heavy thinning from below, respectively, produce a more rapid shift to the right and levelling out in the tree number–diameter distributions. The diameter range is cut off in the small diameter range after a thinning from below. The largest trees achieve diameters over 80 cm, and the diameter classes at the large end of the tree number–diameter frequencies reveal much higher occupancies than for a light thinning from below.

6.7.2.4 Stand Height Curves and Mean Height Values

The graphic depiction of results always comprises the adjusted stand height curves as well, which underlie the mean height and volume calculations (Fig. 6.17a–c). On all three plots, we recognise the characteristic shift of the initially rather steep diameter height curves upwards to the right as the curves level off. The series of stand height curves provides deeper insight into stand structure and stand dynamics.

On the A grade plot, we see a relatively wide range in height and diameter. For example, in the 2000a inventory, the range in variation of the smoothed tree height and diameter is 8 m and 45 cm respectively. The moderate, and heavy thinning from below result in an increase in the maximum diameter by 10–20 cm, yet reduces the range in variation of height and diameter to 4 m and 35 cm, respectively. The development of the stand height curves characterises the relatively high structural diversity of the A grade plots. The B and C grade plots develop more and more towards tall European beech forests, where variation in tree diameter still is found, but where tree height is very similar.

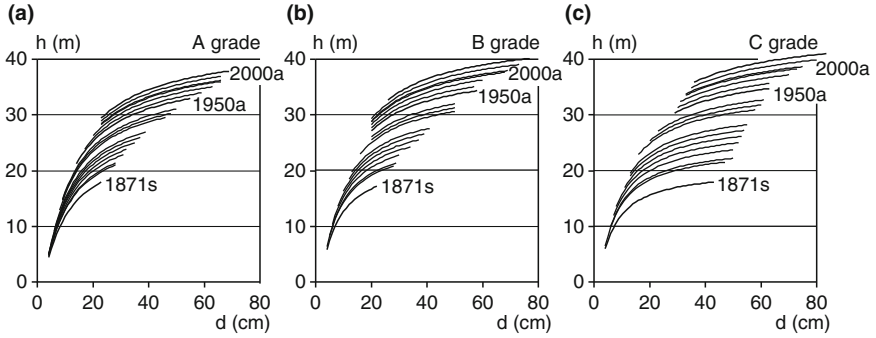

Fig. 6.17 Shift in stand height curves from the first inventory in 1871 to the most recent repeated inventory in autumn 2000 calculated using the method of smoothing coefficients. The layering of stand height curves for (**a**) A grade, (**b**) B grade and (**c**) C grade is presented. The height curves from the inventories 1871s, 1950a and 2000a are highlighted to assist comparisons

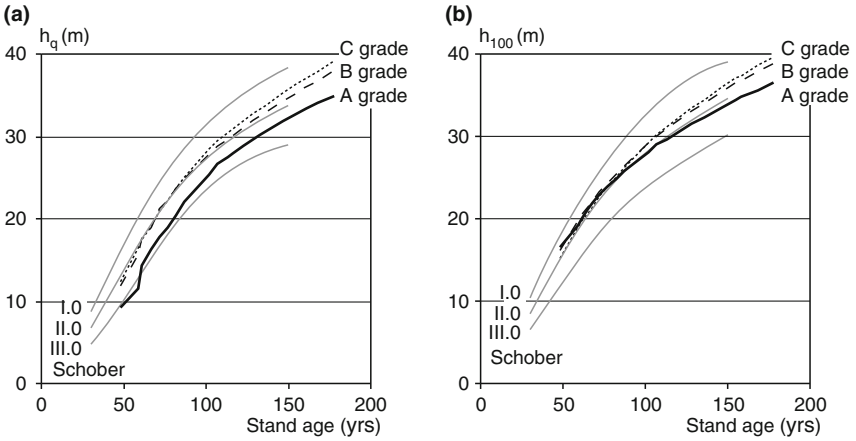

Fig. 6.18 Development of the (**a**) mean height h_q and (**b**) top height h_{100} on the European beech thinning experimental plots FAB 15. The increase in the mean and top height levels from A grade (*solid line*) to the B and C grades (*dashed and dotted lines* respectively) is essentially due to the effects of the treatments, but also to a certain inferiority of the A grade site. The curves from Schober's (1967) European beech yield tables, moderate thinning, for the I., II., and III. site classes is provided for reference (*gray lines*)

Depending on the aim of analysis, the mean and top height values (h_q, h_{100}) can be read from the stand height curves. Figure 6.18 shows (a) the height development of the quadratic mean diameter, and (b) the mean basal area tree of the 100 largest trees per hectare for A, B and C grade plots (solid line, dashed line and dotted line). For the purpose of site quality assessment from the mean height or top height, these age–height curves are usually compared to the height series in the conventional yield tables. In Fig. 6.18 the European beech yield tables for moderate thinning from Schober (1967) are used as a reference.

6.7.2.5 Slenderness h_q/d_q and h_{100}/d_{100}

The ratio of height to diameter, giving the slenderness or h/d values, is an indicator of the thinning effects, stem form and stability of individual trees. Greater slenderness indicates an intensification of height growth over diameter growth (survival strategy), whereas lower slenderness indicates superior diameter growth relative to height growth (stabilising strategy). Figure 6.19 shows the development of slenderness of (a) the quadratic mean diameter tree, and (b) the mean top height tree for all three treatments.

On all plots, slenderness has continued to decline since the beginning of the trial. The decline becomes increasingly evident with heavier thinning operations. As the tree number, and hence the competition for light, is higher on the A grade plot, the trees strive foremost for light at the expense of diameter growth. The lower tree numbers on the B and C grade plots provide the trees with adequate light, enabling greater nutrient allocation to the lower stem. Therefore, the different h/d values reflect the effect of silvicultural practices on the allocation behaviour of individual trees. Whereas this response is especially clear for the quadratic mean diameter trees (Fig. 6.19a), the effects on the largest 100 trees per hectare, which benefit less from a thinning from below operation, are much less evident (Fig. 6.19b).

6.7.2.6 Development of Stand Basal Area and Stand Volume

The sawtooth lines in Fig. 6.20a, b show the development of basal area and standing volume over time on the three plots considered. The A grade plot represents the

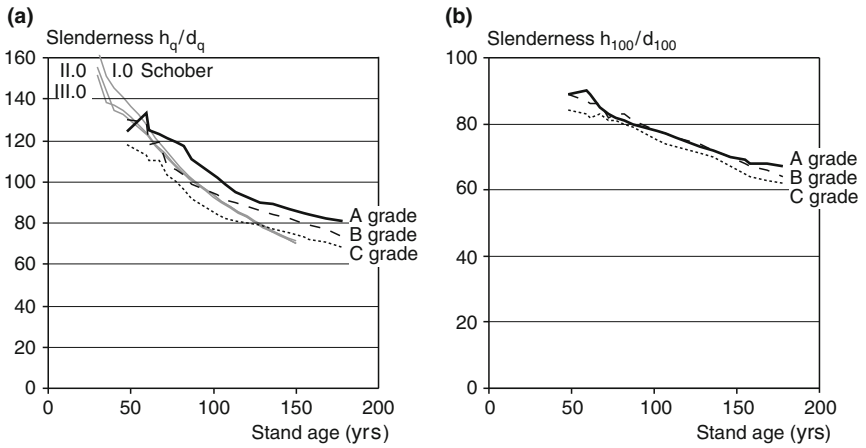

Fig. 6.19 Development of slenderness for the (**a**) mean tree (h_q/d_q) and (**b**) top height tree (h_{100}/d_{100}) on the European beech thinning trial plots FAB 15. The increase in thinning grade is revealed by a reduction in slenderness from A grade (*solid line*), to C grade (*dotted line*). The curves from Schober's (1967) European beech yield tables, moderate thinning, for the I., II., and III. site classes is provided for reference (*gray lines*)

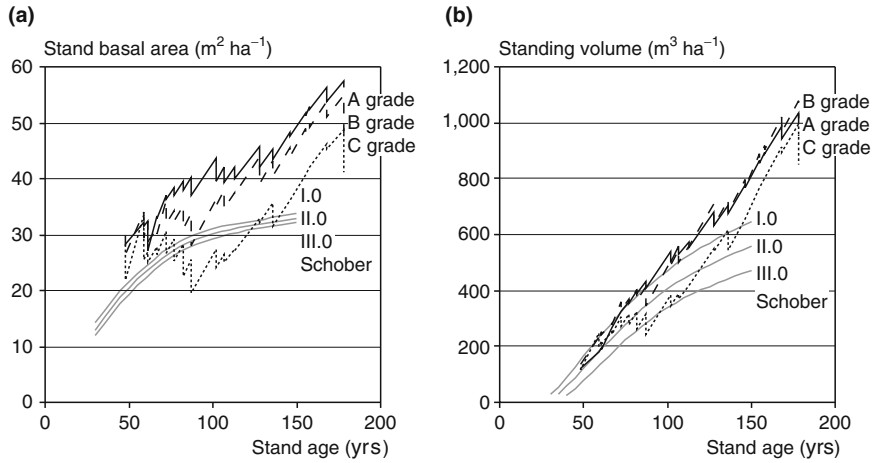

Fig. 6.20 Development of the (**a**) stand basal area and (**b**) standing volume on the European beech thinning trial FAB 15. The basal area, and volume of the remaining stand for the A grade (*solid line*), B grade (*dashed line*) and C grade (*dotted line*) are presented respectively. The curves from Schober's (1967) European beech yield tables, moderate thinning, for the I., II., and III. site classes is provided for reference (*gray lines*)

maximum density on the given site. A comparison with the yield tables indicates that the stand basal area and volume on the untreated plot FAB 15/1 rises well above the expected yield table values. This shows, once again, the value of only lightly thinned or untreated trial plots. They reflect the maximum possible density on a given site. Without knowledge of the maximum possible density, forestry practice would be in danger of under-exploiting the productivity potential of stands.

The corresponding sawtooth lines for moderate and heavy thinnings reflect the silvicultural practices in the trial; the perpendicular drops in basal area and standing volume are due to the thinning operations at the time of each inventory. The gap in trial activity during World War I and II in the stand age ranges 87–102 and 113–128 years can be seen by the marked climb in stand density on the B and C grade plots (tending operations omitted). We attribute the climb in density in the past two to three decades, which is well above the expected yield tables values, to large-scale influences, such as climate change and nitrogen inputs (Chap. 14).

6.7.2.7 Periodic Annual Increment of Basal Area and Volume

The response of a stand to different thinning grades can be determined from the periodic annual increment of basal area and volume (Fig. 6.21a,b). The periodic annual increments for the period between inventories, derived from the repeated inventory of the trial plots, are usually plotted above the midpoint of the period. The periodic annual increment is calculated for different intervals, depending on the inventory cycle. The longer the period between inventories, the flatter the PAI curves.

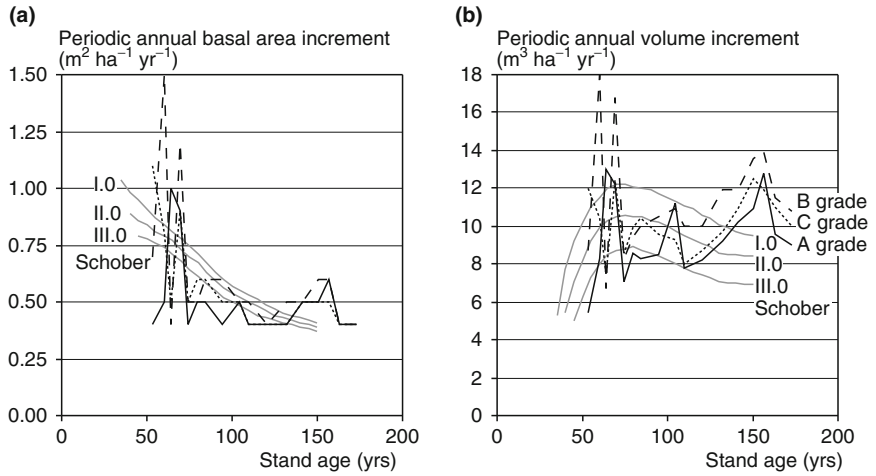

Fig. 6.21 Development of the (**a**) periodic annual basal area increment and (**b**) periodic annual volume increment in the 17 increment periods from the first inventory in spring 1987 to the most recent repeated inventory in autumn 2000. The development for the A grade (*solid line*), B grade (*dashed line*) and C grade (*dotted line*) are presented. The curves from Schober's (1967) European beech yield tables, moderate thinning, for the I., II., and III. site classes is provided for reference (*gray lines*)

In short periods, weather patterns influence PAI, producing greater oscillations in the increment curve.

In the first third of the growing period, the periodic annual basal area and volume increment achieve the highest values as expected. The moderate and heavy thinnings result in increased growth on the B and C grade plots (Fig. 6.21, dashed and dotted lines respectively) compared to the A grade plot (solid line). After the typical age dependent decline in growth in the second third of the life period, growth rises once again from the age of 120 years, which is atypical of this stand phase. The presence of an A grade plot in the experimental design assists the interpretation of this finding. As an increase in increment atypical of age can be discerned on all plots, it is caused not only by the silvicultural treatment but also influenced by external factors. From the 1960s onwards, the actual growth increment over time clearly deviates from the expected increment from Schober's (1967) yield table for moderate thinning (cf. Chap. 14).

6.7.2.8 Total Volume Production (=Gross Volume Yield) and Mean Annual Increment

The total volume production is the sum of volume growth since stand establishment (Fig. 6.22a). The total volume production of the A grade plot represents the site productivity potential, and the B and C grade curves indicate the extent of change in total volume production brought about by moderate and heavy thinning.

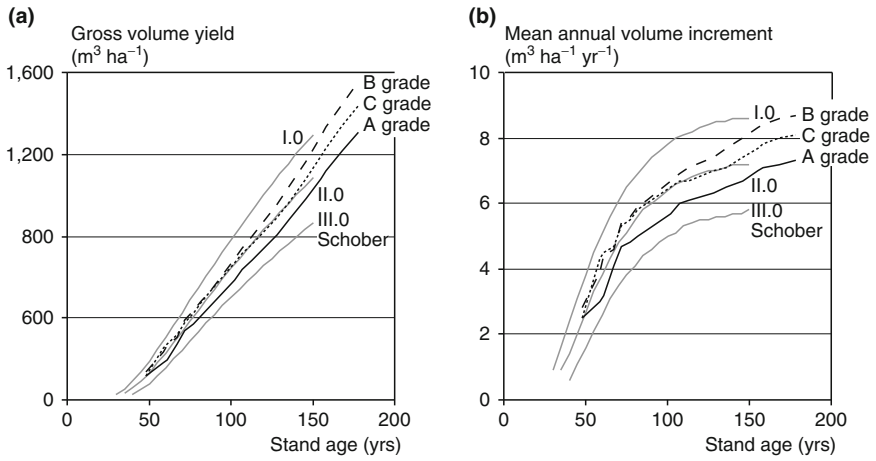

Fig. 6.22 Development of (**a**) gross volume yield and (**b**) mean annual increment in volume MAI_V on the European beech thinning trial FAB 15. The growth and increment process for the A grade (*solid line*), B grade (*dashed line*) and C grade (*dotted line*) are presented respectively. The curves from Schober's (1967) European beech yield tables, moderate thinning, for the I., II., and III. site classes is provided for reference (*gray lines*)

In comparison with the A grade plot, the total volume production of the B and C grade plots increases by 18% and 10% respectively. When the A grade plot's inferior site index (Fig. 6.18) is considered in the interpretation of development over time, the total volume production and mean annual increment curves of the plots appear quite similar. This suggests the well known fact that although the different thinning grades lead to a different resource distribution between trees, and different tree number–diameter frequencies and percentage intermediate yields, the total production resulting remains largely the same (Pretzsch 2005b). Clearly the relatively heavy thinning operations on the C Grade plot do not cause any noticeable losses in productivity by area (cf. Chap. 10). A comparison of the mean annual volume increment (MAI_V) curve (Fig. 6.22b) with the yield table highlights the atypical increase in growth by age on all three plots. In contrast to the values expected from the yield tables, even at the age of 178 years, no culmination in the MAI_V is evident.

6.7.2.9 Percentage Volume Increment and Percentage Intermediate Yield

Figure 6.23a shows the exponential decline in percentage volume increment $PAI_{\%} = PAI/V \times 100$ by age characteristic of age class forests. The calculation is based on the PAI in the interval between inventories, and the standing volume at the beginning of the respective inventory period $V_{n\ remain}$ (cf. Fig. 2.5). In the early growth phase, when standing volume is still low, yet volume growth is high, percentage volume increments of 10–15% are achieved. Over time, the percentage volume increment declines for A, B and C grade treatments to values between 1% and 2%. On all

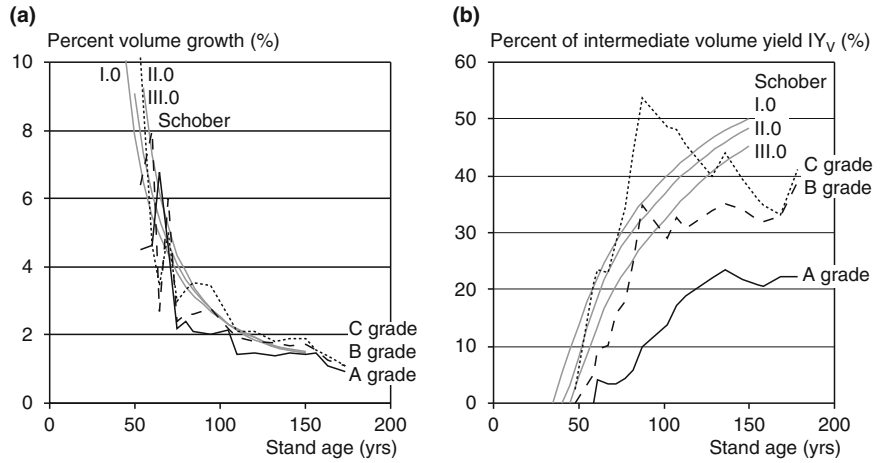

Fig. 6.23 Percentage volume increment and percentage intermediate yield for the European beech thinning trial FAB 15. With increasing thinning grade, both the (**a**) percentage volume increment and the (**b**) percentage intermediate yield in volume increase. The percentage development for the A grade (*solid line*), B grade (*dashed line*) and C grade (*dotted line*) are presented. The curves from Schober's (1967) European beech yield tables, moderate thinning, for the I., II., and III. site classes is provided for reference (*gray lines*)

three plots, about 1% of the standing volume is still produced annually at the age of 178 years due to the undiminished volume growth.

The percentage intermediate yield (IY_V (%) = whole tree turnover/gross volume yield $\times$ 100) relates the sum of all removals recorded in all inventories to total volume production (Fig. 6.23b). On the A grade plot, the percentage intermediate yield increases continuously from the beginning of observation period and amounts to about 20% at the stand age of 178 years. The moderate and heavy thinning operations in the first and second third of the growing period considered cause the percentage intermediate yield on the B and C grade plots to increase by 35% and 55% respectively. Given the very different treatment, the differences in the total volume production are remarkably small. This is due to the capacity of European beech to compensate, or even overcompensate, for thinning operations of any intensity by increasing its rate of growth (Chap. 10, Sect. 10.5).

Summary

Due to the long time periods of observation, dating back to the 1860s and 1870s for many sample plots, and the ongoing management of the plots in accordance with the prescribed research plans, standards for the data collection, organisation and analyses are of particular importance. Only when standard collection and analysis protocols are applied to past survey data, can the time series, so valuable in

forest growth research, be obtained for the entire lifespan of trees or stands. In this chapter we adopt the European beech sample plot FAB 15, one of the oldest existing thinning trials, to illustrate the results of the standardised analysis at the stand level, presenting a description of the fundamental characteristics of stands and their long-term responses to thinning.

(1) The aim of standard analyses of study sites is to obtain stand level mean and cumulative values such as mean diameter and mean diameter of the top height tree collective, mean and top height, stand basal area and standing volume per hectare. In repeated inventories, the periodic annual increment, mean annual increment, and total yield for basal area and volume are calculated. All stand characteristics are calculated for the remaining, removed and total stand.
(2) Standard analysis begins with a plausibility control, which checks for any missing or recruited trees, and tests the plausibility of the diameter and height measurements.
(3) The treatment of missing or incorrect measurements must be consistent, transparent and documented. Where possible, corrections should be based on supplementary surveys (e.g., stem analysis, shoot length measurements), statistical relationships (e.g., diameter increment curves, stand height curves) or model predictions (yield tables, dynamic growth models).
(4) In a regression analysis, size parameters that are difficult to measure, or can only be measured with considerable effort (e.g., tree height, crown base height, diameter increment), can be estimated from parameters that are easier to measure. First, a tree collective is selected where both the easy and difficult aquirable parameters are measured. Then, a functional relationship between the easy and difficult measurable parameters is derived by a regression analysis: difficult parameter = f [easy parameter(s)]. Finally, the easy measurable parameters for all trees (e.g., diameter) are used to estimate the difficult parameters for all trees with the derived function (e.g. height = f [diameter]).
(5) Due to the close allometric relationship between tree diameter and tree height, a number of functions are available that can be used to describe statistically the relationship $h_i = f(d_i)$ by regression analysis. The plausibility of the function curve and statistical measures (coefficient of determination, standard error, significance of the parameter) indicate the most appropriate function to select.
(6) To determine the volume of a tree i with the formula $v_i = ba_{1.3,i} \times h_i \times f_{1.3,i}$, the form information is not determined explicitly by measurement on the plot, but deduced from tree diameter and height using appropriate form factor tables, form factor or form height functions, or volume tables.
(7) When the diameter measurements of all trees in a stand $d_{1.3,i}$ or $ba_{1.3,i}$, the height values h_i (typically from diameter-height regressions) and the form factor $f_{1.3,i}$ (typically derived deductively $f[d_{1.3,i}, h_i]$) are known, the stem volume $v_i = ba_{1.3,i} \times h_i \times f_{1.3,i}$ is calculated for all $i = 1 \ldots n$ trees. The sum of these values is the stand volume $V = \sum_{i=1}^{n} v_i$.
(8) The cumulative values (per hectare) and mean values of the stand are calculated from individual tree parameters (height, diameter, basal area, form factor, volume). In mixed stands, this calculation is conducted for each tree species

separately and for the stand. In addition, the analysis differentiates between the remaining stand, the removed stand (mortality and removals) and the total stand.

(9) When a stand has been inventoried repeatedly, the periodic annual volume increment (PAI), the yield (standing volume + sum of removed volume), mean annual volume increment (MAI), and the intermediate volume yield (IY_V = whole tree turnover) can be calculated.

(10) The tabular and graphic presentation of results from forest growth sample plots generally encompasses the age development of tree number, mean diameter and mean diameter of the top height tree collective, mean and top height, tree number-diameter frequencies, stand height curves, slenderness, stand basal area and stand volume, periodic basal area and volume increment, total yield and mean annual increment, percentage volume increment, and percentage intermediate volume yield (IY (%) = whole tree turnover/total yield × 100).

Chapter 7
Description and Analysis of Stand Structures

The spatial structure, that is the horizontal and vertical spatial arrangement of individual trees and other plants at a given point in time, determines the integrity and stability of a forest to a large extent. While this applies to all forest types, it is particularly relevant in shaping the forests of the future, and the transition from homogeneous evenaged stands to structurally-rich mixed stands with complex intraspecific and interspecific interactions. Not only does stand structure affect stand dynamics, growth and yield, it also affects a broad spectrum of forest functions including protection and recreation. Thus, in this chapter, considerable importance is placed on recording, quantifying, modelling and predicting tree growth and forest stand structure (Table 7.1).

Landscape structures, forest stands and trees themselves are all features on which, in which or through which physical, biochemical ecological and socio-economic processes take place. Before we emphasise the effect of stand structure on stand dynamics and the importance of spatial models for predicting growth, yield, and aesthetic value for humans, we show that spatial structure also influences habitat, and plant and animal species diversity (Fig. 7.1). For example, landscape and stand structures determine the occurrence and population dynamics of brown bears, owls and woodpeckers to such an extent that habitat suitability and the development of a population can be inferred directly from given structures (Letcher et al. 1998; McKelvey et al. 1993; Wiegand 1998). Altenkirch (1982), Ammer et al. (1995), Ammer and Schubert (1999), and Ellenberg et al. (1985), among others, point to the close relationship between tree and stand structure, and the presence of birds, beetles, spiders, lacewings and soldier beetles. Although, despite this research, there are still gaps in knowledge about the relationships between stand structure and the diversity of plant and animal species, and ecological stability, current knowledge indicates that the diversity of the plant and animal species present increases with increasing structural differentiation. Consequently, structural parameters at the macro, meso, and micro level are very good indicators of the ecological diversity and stability of forest ecosystems, and the type of management (Haber 1982). In Fig. 7.1 stand structure is represented only schematically on the abscissa. However, the parameters presented in Table 7.1, introduced in this chapter, provide a quantitative description of stand structure.

H. Pretzsch, *Forest Dynamics, Growth and Yield: From Measurement to Model*,
DOI: 10.1007/978-3-540-88307-4_7,

Table 7.1 A qualitative and quantitative description of stand structure

Structural feature	Qualitative description	Numerical quantification	Section
Horizontal tree distribution pattern	Random, regular, clustered	Aggregation index by Clark and Evans (1954)	7.3.2.1
		Pielou's distribution index (1959)	7.3.2.2
		Clapham's (1936) variance-mean value index	7.3.3.1
		Dispersion index by Morisita (1959)	7.3.3.2
		Ripley's K-function (1977)	7.3.4
		Besag's L-function (1977)	7.3.5
		Pair correlation function by Stoyan and Stoyan (1992)	7.3.6
Stand density	Sparse, spacious, gappy, dense, crowded, packed	Stocking density with reference to yield tables	7.4.1.1
		Natural stocking density	7.4.1.2
		Percentage canopy cover	7.4.2
		Mean basal area over a period by Assmann (1970)	7.4.3
		Stand density index by Reineke (1933)	7.4.4
		Crown competition factor	7.4.5
Tree size differentiation	Mono-layered, two-layered multilayered	Coefficient of variation of tree sizes	7.5.1
		Diameter differentiation by Füldner (1995)	7.5.2
Structural and species diversity	Pure stand, two-species mixture, multiple-species mixture	Species richness	7.5.3.1
		Species diversity by Hattemer (1994)	7.5.3.1
		Diversity index by Shannon (1948)	7.5.3.1
		Standardized diversity und standardized evenness	7.5.3.2
		Species profile index by Pretzsch (1995)	7.5.3.3
		Standardized species profile index	7.5.3.4
Tree species intermingling	Single tree mixture, groups, clusters, rows, patches	Species intermingling index by Füldner (1996)	7.6.1
		Index of segregation by Pielou (1977)	7.6.2

Stand structure parameters are useful for analysing and modelling forest stand dynamics. They are also useful indicators of the state and development of forest ecosystems, and for applied management practice (MCPFE 1993). In comparison with direct quantitative measurements of biodiversity, stability or sustainability (counting plant and animal species, assessment of matter balance etc.), the use of structural parameters is advantageous as the data can be collected readily, or already exists in forest inventory data (Chap. 1, Sect. 1.3).

Conventional approaches for measuring, analysing, and modelling forest stands are based on stand level data, such as mean diameter, dominant height, or volume per hectare. As such, they ignore the three-dimensional nature of stand structure, its most important characteristic. The recognition of a stand as a spatial, structural–functional collective of individual trees paves the way for recognising the individual trees within the stand, and hence the level at which fitness is maximised. It is the individual tree, not the stand as a collective, which represents the critical unit in the

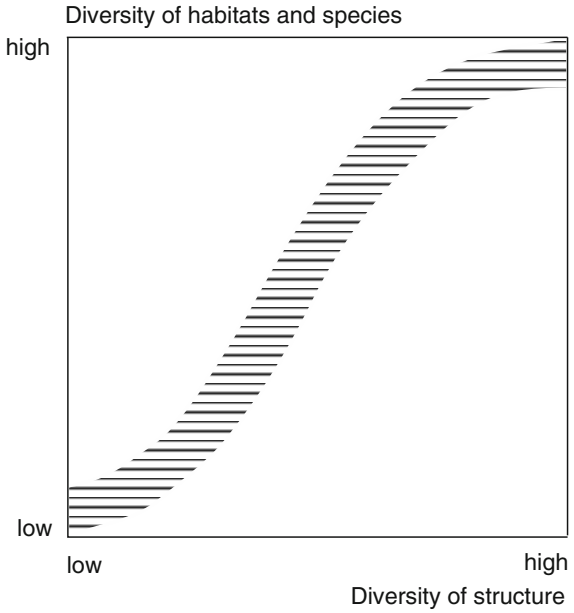

Fig. 7.1 Relationship between structure, and habitat diversity and species diversity (adapted from Begon et al. 1998)

maximisation of fitness (survival, reproduction, number of progeny in relation to the neighbour). Approaches that abstract the stand from mean or cumulative stand values overlook the key role of the individual tree and structure in stand dynamics. The anthropocentric notion that the trees within a stand work together in a division of labour for the common good of the population with the aim of maximising resource production, is misleading.

7.1 Structures and Processes in Forest Stands

7.1.1 Interaction Between Structures and Processes

The interaction between structures and processes in dynamic systems can be illustrated by a river system. The riverbed, itself, influences water flow, the current, and the formation of whirlpools, and swirling. Consequently, the structure of the riverbed has a direct effect on water flow. Conversely, through the processes of removal, deposition, and hollowing out, the water flow changes the riverbed. The flow of water affects the riverbed with time, leading to the formation of meanders, for example. The feedback mechanism, characteristic of many dynamic systems, becomes apparent in this example. The structure determines the processes directly and immediately whereas, in turn, the processes modify structures over a longer period of time in a slower feedback system. The existence of this feedback system means

an understanding of the processes is only possible if one recognises the structural patterns these processes follow. Given that processes modify structures, the resulting structures, which can be readily measured, assist the interpretation of processes that are often more difficult to measure or observe. Interactions similar to those between the riverbed and water flow in a stretch of water also occur between an organisational structure and the production process in a business enterprise. Senge (1994) defines archetypal system structures associated with typical system behaviour. He considers the recognition of structures to be essential for a deeper understanding of developments that can be influenced effectively, or diverted if undesirable, through structural change.

Stand structure, of primary importance in ongoing processes, has particular relevance in forest ecosystems. Since trees are rooted in the ground, and develop and acquire their structure over prolonged periods, their existing structures enable them to influence those factors, which, in turn, influence growth, such as light, temperature and precipitation. Consequently, the tree and stand structures, which have developed in a forest ecosystem, have a major influence on the life cycle of all organisms within the stand. Crown size, branching, and needle and root development affect processes such as light absorption, water interception evapotranspiration, photosynthesis and respiration to a large extent. Conversely, the latter processes influence the growth of trees and the life cycle of the surrounding organisms. Stand structure determines the competition among trees in a stand for resources, biomass production in the stand, and the growing conditions for ground vegetation and forest fauna. Similarly, stand structure plays a central role in system renewal. In this case, structure influences pollination, seed dispersal, germination and development of regeneration.

Aboveground, the trees in a forest interact through two feedback loops proceeding at different time scales (Fig. 7.2). In the first feedback loop, tree growth → growth conditions → tree growth, which proceeds quickly, neighbouring trees influence one another through their physiological activity. For example, if the moisture and carbon dioxide content of the atmosphere in any part of the crown space changes due to evapotranspiration and assimilation, then the growth conditions of the neighbouring trees change almost simultaneously. The second feedback loop, tree growth → stand structure → growth conditions → tree growth, proceeds more

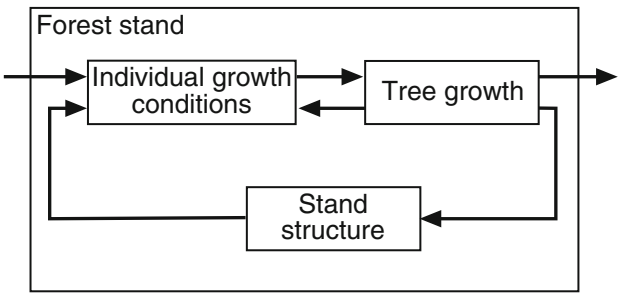

Fig. 7.2 Important feedback loop determining forest stand dynamics: tree growth → stand structure → individual growth conditions → tree growth

slowly and the trees influence one another via structural changes. Growth brings about change in tree and stand structure. These structural changes affect the spatial arrangement of a tree and that of its neighbours, thereby influencing growth behaviour. For example, the development opportunities for a tree growing under favourable light conditions are better than a heavily shaded neighbour by virtue of its higher photoproduction. It can compete more easily, and change stand structure and its own spatial arrangement in its favour. The development of any tree within a stand collective is affected by its neighbours and, in turn, influences its neighbour's development (Hari 1985).

In forestry, the influence of structure on growth processes in forest ecosystems is used to influence the direction of forest development (Pretzsch 1996b). Forestry practices such as the establishment of structural mixes, planting in rows or square systems, thinning trees, pruning or coppicing trees alter the stand structure, and thereby affect growing conditions like radiation supply, water consumption, and nutrient turnover in forest soils. Most silvicultural measures make use of the feedback loop in Fig. 7.2: they interfere with the stand structure to regulate *indirectly* the growth processes in the remaining stand. However measures such as fertilisation and the dispersal of fungicides or insecticides have a *direct* affect on growth.

7.1.2 Effect of Initial Structure on Stand Development

The compound interest effect of the initial stand structure on stand development is illustrated in Fig. 7.3 by the long-term development of Norway spruce–European beech mixed stands. In stands A and B, aged 30 years, the stand cumulative and mean values, and frequencies of individual-tree size are similar. Only the structural mix differs. In stand A, individual Norway spruce and European beech trees typically occur in isolation. In stand B, groups and patches of Norway spruce and European beech are evident. All else being equal, this initial structural difference affects stand development considerably up to 150 years of age. Whereas, in stand A, the percentage of European beech in the 150-year-old stand has dropped to 25%, in stand B it has increased to 48% (basal area percentage). In stand A, growth surpasses the periodic annual increment, producing $3.0\,m^3\,ha^{-1}\,yr^{-1}$ (merchantable timber) in 50–80-year-old stands, thereafter falling to $0.51\,m^3\,ha^{-1}\,yr^{-1}$ in 150-year-old stands. The effect of the initial stand structure on stand development is reflected both in the tree species composition and in the absolute growth.

In this example, computer simulations were carried out with the stand growth simulator SILVA 2.2 (cf. Chap. 13). At the beginning of the simulation, stands A and B are 30 years old. In each stand, the mean height of Norway spruce and European beech is 14.4 and 10.3 m respectively, and the basal area about $22\,m^3\,ha^{-1}$. Both stands comprise 64% Norway spruce and 36% European beech. In stands with an average water and nutrient supply in growth region 12.7 Central Swabian "Schotterriedelland and Hügelland", the expected stand development is modelled assuming Norway spruce growth to be superior to European beech. Stand

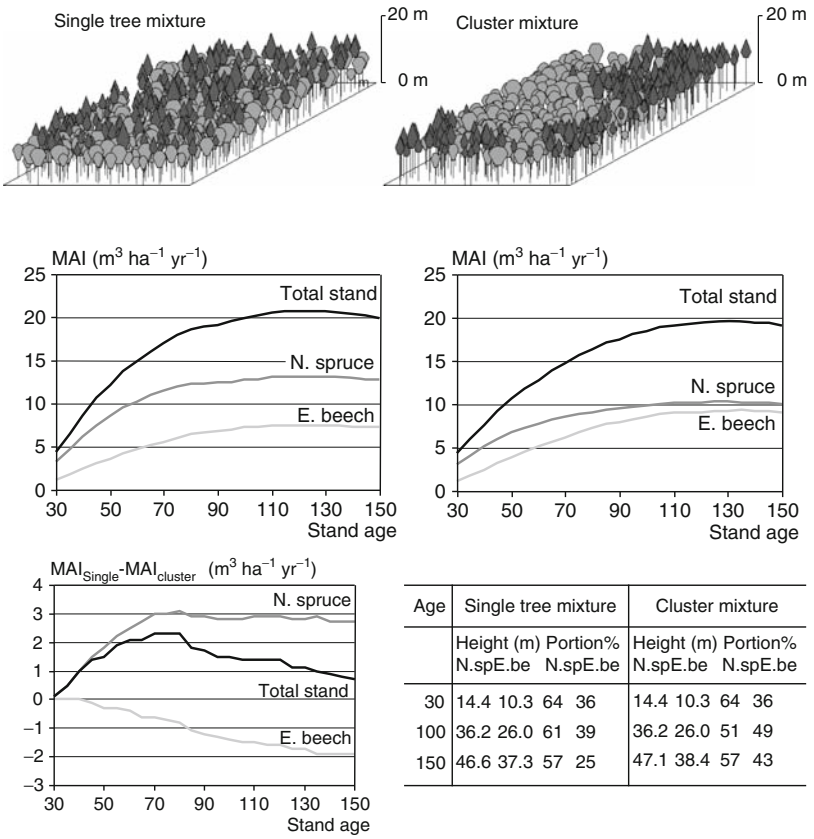

Age	Single tree mixture				Cluster mixture			
	Height (m)		Portion%		Height (m)		Portion%	
	N.spE.	be	N.spE.	be	N.spE.	be	N.spE.	be
30	14.4	10.3	64	36	14.4	10.3	64	36
100	36.2	26.0	61	39	36.2	26.0	51	49
150	46.6	37.3	57	25	47.1	38.4	57	43

Fig. 7.3 The development of two Norway spruce–European beech mixed stands with identical initial cumulative and mean stand values at age 30 but different initial structures. The single-tree mixture (*left*) results in more rapid and early growth, a higher culmination in mean annual volume increment and a greater contribution from Norway spruce to stand growth. In the cluster mixtures, European beech is less suppressed and comprises nearly 50% of total stand growth

development predictions up to the age of 150 years assume A grade conditions (light thinning) for the two stands, differing only in their initial stand structures.

Norway spruce's initial lead in single-tree mixtures, with a height superiority of 4.1 m, is enhanced in subsequent years when the percentage of European beech in the stand decreases from an initial 36–25% by the age of 150 years. The suppression of European beech trees in single-tree mixtures allows Norway spruce to dominate across the entire area to varying degrees, and enhance its growth at the expense of European beech. In contrast, the slower growing European beech faces less competition when Norway spruce occurs in patches, gaining advantage over Norway spruce to attain 43% of the percentage mix in a 150-year-old stand and contribute 50% of mean annual volume increment (MAI) of the stand. The MAI, and ΔMAI over time, shown in Fig. 7.3, indicate that the selection of single-tree mixtures over groups or clumped mixtures results in a more rapid increase in MAI, a higher absolute MAI,

and a reduction in the contribution of beech to MAI. At 150 years of age, the stand basal area is 44.4–48.4 $m^2\,ha^{-1}$, standing merchantable volume 857–956 $m^3\,ha^{-1}$, and there are 147–159 trees ha^{-1}.

7.2 Descriptions of Stand Structure

The wealth of information available from crown maps and stand profile diagrams induced Bonnemann (1939), Köstler (1953) and Mayer (1984) to illustrate special silvicultural systems, forest tending measures and regeneration methods with artistic, hand drawn sketches. A few crown maps and stand profile diagrams provide a far more accurate impression of the Scots pine–European beech mixed stands Bonnemann investigated than descriptions of stands with stand level data by hectare (Fig. 7.4). However, the above-mentioned authors provided graphical illustrations of the structural archetypes selected only, omitting to disclose any quantitative information contained within them. Consequently, the two approaches, the visualisation of individual trees to describe the spatial stand structure, and the description and modelling of stands with stand level data, were undertaken independently of one another.

In contrast, the methods introduced in this section for the spatial modelling and visualisation of stand structure facilitate the description, analysis and modelling of stands at the same level. Whereas it is more difficult to associate stand level data descriptions with a particular stand structure, by representing stand structure in relation to the individual trees within it, we reach a scale that is consistent with our capacity

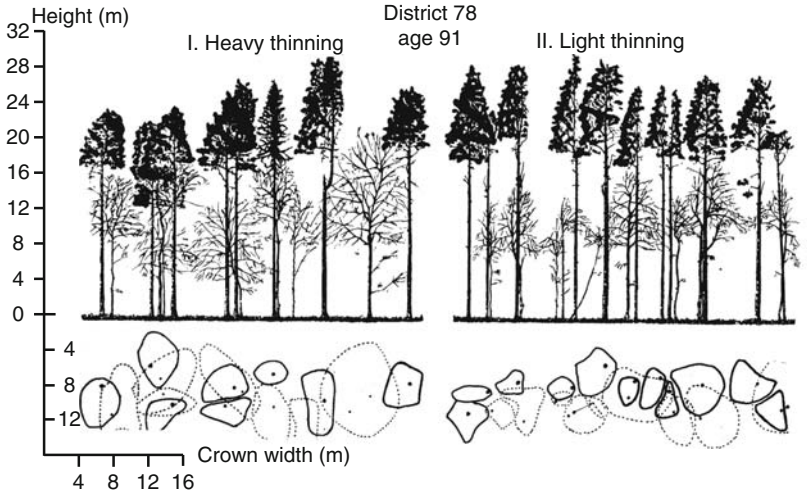

Fig. 7.4 The sketch of the sectional view (*above*) and crown projections (*below*) reveals better development of Scots pine crowns and more favourable development of European beech crowns on the heavily thinned Scots pine–European beech experimental plot, Waldau 78, compared to the lightly thinned plot (after Bonnemann 1939, p. 38)

to visualise, and to measure, analysis and reproduce it. Where, previously, structural information was only available for archetypal forests by way of example, information is now more widely available from experimental plots, and indicator, inventory and sample plots. Thus, the difficulty of envisaging development from rather abstract stand level data in the past no longer applies today because the description, analysis and modelling of forests is undertaken at the same resolution at which humans perceive the forest.

Methods of scientific visualisation are being developed with stand profile diagrams, crown maps, stand inspections, and walk-through, fly-through and landscape simulations (cf. Chap. 11). These methods serve to illustrate the natural development of, and human operations in the forest. They are also useful tools in forest science teaching and research, and in forestry practice. Yet their relevance also extends to other disciplines, such as landscape planning and nature conservation. We understand scientific visualisation as the application of graphic programs for processing and optimising the knowledge contained within measurements and simulation results (Brodlie et al. 1992).

7.2.1 Tree Distribution Maps and Crown Maps

7.2.1.1 Representing Crown Projection Area by Polygons and Circles

Applying stem coordinates and data from crown projections (four or eight crown radii projections) the program KROANLY (Pretzsch 1992a, c) produces and numerically analyses crown maps. The program KROANLY contains a graphic routine that produces crown maps following the selection of any one of the three methods of calculation outlined below. In the first method of calculation, the radii are evened out linearly, representing the crown perimeter as a polygon. In the second method, the graphic program depicts the crown as a circle with a radius $\bar{r}_q$, which corresponds to the quadratic mean of four or eight radial measurements $r_1, \ldots, r_n$:

$$\bar{r}_q = \sqrt{(r_1^2 + r_2^2 + \cdots + r_n^2)/n}. \tag{7.1}$$

This option, for example, uses the individual tree growth model SILVA 2.2 (Pretzsch, 2001) to depict graphically the simulated growth processes (cf. Chap. 13). In the third calculation method, the crown radii measured are evened out by a cubic polynomial, and the crown perimeter is reproduced by a smooth spline function.

7.2.1.2 Cubic Spline Functions

Spline functions smooth the connection between n points defined by their coordinates x_k and y_k ($k = 1, \ldots, n$) in a Cartesian coordinate system. Growth and yield

research applies spline functions to smooth out time series data, to approximate stem cross sections, and in graphic reproductions and determinations of crown projection area from sampled crown projections. The connection of n points (x_1, y_1) to (x_n, y_n) by a line would produce a polygon. However, if $n-1$ polynomials of the third degree are used to interpolate between the points instead, then the resulting spline connects the n sample points smoothly so that it can be continuously differentiated twice at the points connecting the polynomials. The $k = 1, \ldots, n$ points produce $n-1$ intervals. For each of these intervals a cubic polynomial

$$f_k(x) = a_k(x - x_k)^3 + b_k(x - x_k)^2 + c_k(x - x_k) + d_k \tag{7.2}$$

is derived, where the parameters a_k, b_k, c_k and d_k are selected so that the polynomial passes through the given points, connecting with neighbouring polynomials at these points in such a way that it can be continuously differentiated twice at these points (x_1, y_1) to (x_n, y_n). The coefficients a, b, c, and d of the $n-1$ polynomials can be determined by Gaussian elimination based on the given point series (Späth 1983). By solving a system of linear–quadratic equations, we obtain the second derivation of the cubic polynomial y_k'' at the points $k = 1, \ldots, n$. This approach is suitable in cases where the increase in x values in the interval $[a, b]\, a = x_1 < x_2 \ll x_n = b$ is strictly monotone. This occurs when, for example, cubic spline functions are used to smooth data in time series analyses (cf. Chap. 12).

A linear interpolation between the points presented in Fig. 7.5, which may originate from crown projections, for example, would produce a polygon that does not

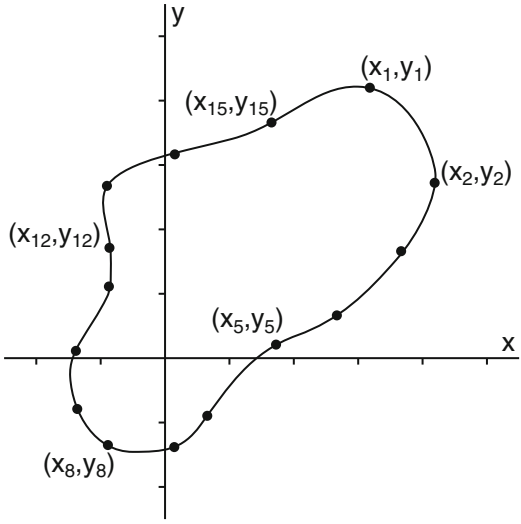

Fig. 7.5 Interpolation between $k = 1, \ldots, n$ points $(x_1, y_1, \ldots, x_n, y_n)$ in a plane with a closed, smooth spline function. The series of n points for a closed line produces n cubic polynomials (after Späth 1983)

approximate a typically round crown perimeter satisfactorily. If a closed smooth curve is drawn through these point then $x_1 = x_n$ and $y_1 = y_n$. By solving a system of linear equations, the $n-1$ derivations determine y'_k, which is then used to calculate the parameters of n cubic polynomials. If the x values are not assumed to be monotone, the curve through the points (x_k, y_k) where $k = 1, \ldots, n$ is described parametrically by the two functions of a curve parameter t:

$$x = x(t), \tag{7.3}$$

$$y = y(t). \tag{7.4}$$

The t_n values can be selected from the angle between the null point of the coordinate system and a point on the spline function measured in radians. By adopting monotone values $t_1 < t_2 \ll t_n$, and interpolating between the points (t_k, x_k) and (t_k, y_k), where $k = 1, \ldots, n$, one obtains a cubic spline every time. For any values t_1–t_n, one obtains the x and y values of a closed spline function.

In Fig. 7.6, crown maps produced by closed cubic spline functions show the development of the Norway spruce–European beech long-term experiment Zwiesel 111/3 established in 1954 in the Bavarian Forest. European beech crowns are shaded light grey, Norway spruce crowns dark grey, and multiple crown cover is shown in black. In Fig. 7.6a the stem positions and crown maps for 1954, the year of establishment, are recorded. Figure 7.6b shows the distribution of stems removed during the 1982 thinning operation, and Fig. 7.6c shows the area in 1982 after thinning.

7.2.1.3 Crown Projection Area

With KROANLY, the crown projection area, calculated by any of the three smoothing methods outlined above, can be determined for the entire stand, for particular stand components, for example tree species groups, or for individual trees. The crown projection area (cpa) is determined by linear approximation (method 1) using the Cartesian coordinates of the polygon points measured according to Gauss' area formula:

$$\text{cpa} = \frac{1}{2} \sum_{i=1}^{n} x_i \times (y_{i-1} - y_{i+1}). \tag{7.5}$$

The variables x_i, y_i describe the Cartesian coordinates of $i = 1, \ldots, n$ polygon points, where points $y_{i-1} = y_n$ when $i = 1$ and points $y_{i+1} = y_1$ when $i = n$. To approximate the crown by a circle (method 2), the area is calculated using the area formula for a circle:

$$\text{cpa} = \bar{r}_q^2 \times \pi. \tag{7.6}$$

By evening out the crown radii with a cubic spline (method 3), n third degree polynomials result. With these, the x and y values are obtained by iteration after entering t, providing the input data for area calculations with the Gauss formula (7.5).

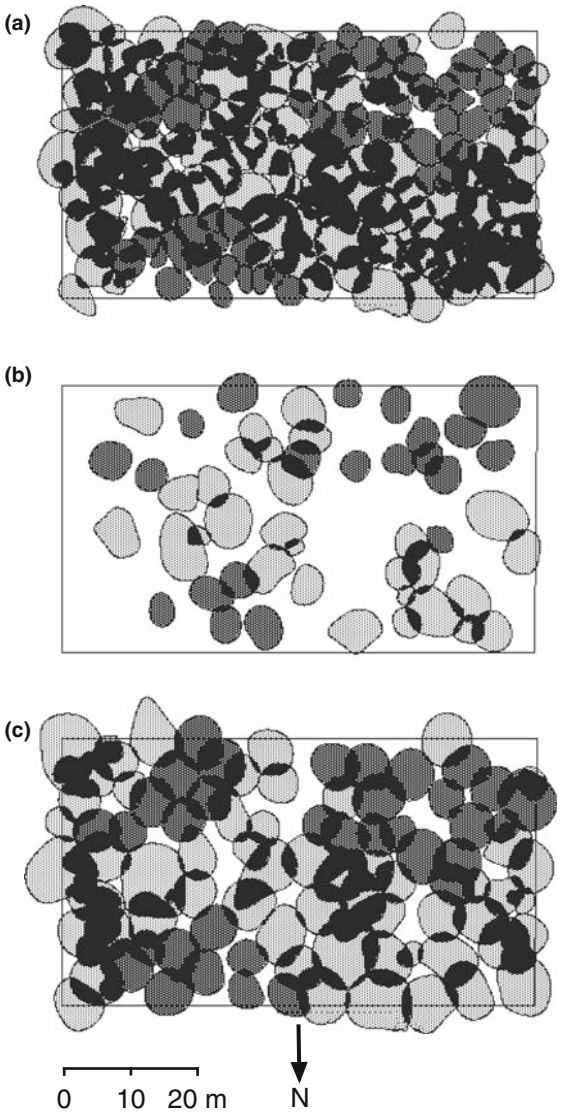

Fig. 7.6 Crown maps for the Norway spruce–European beech mixed stand experimental plot, Zwiesel 111/3. Norway spruce and European beech are indicated by *dark grey and light grey hatching* respectively. Crown projection areas with multiple canopy cover are marked black: (**a**) the initial stand in 1954, (**b**) thinning removals in 1982 and (**c**) stand in1982 after thinning are shown

By selecting a small interval for t, the crown surface area values resulting are realistic and biologically more tenable than the values obtained by linear interpolation frequently used.

7.2.2 Three-Dimensional Visualisation of Forest Growth

7.2.2.1 Crown Shape Models

The crown shape models outlined below are based on renowned crown investigations from Assmann (1961a), Badoux (1946), Burger (1939), Hampel (1955) and Mang (1955). The model adopts average, species-specific crown shapes determined in crown investigations. They are acknowledged to be smoothed approximations of crown shapes that, in reality, are more irregular with fractal dimensions (Kurth 1999; Zeide 1998). The biometric reproduction of crown perimeter can be carried out for different species in a standard calculation procedure describing the change in crown radius (r) with increasing distance (dist) from the tip (Fig. 7.7). In the sunlit crown with length l_o, which is exposed to direct sunlight, the crown radii (r_o) are calculated as a function of the distance from the tip in the function:

$$r_o = a \times dist^b \tag{7.7}$$

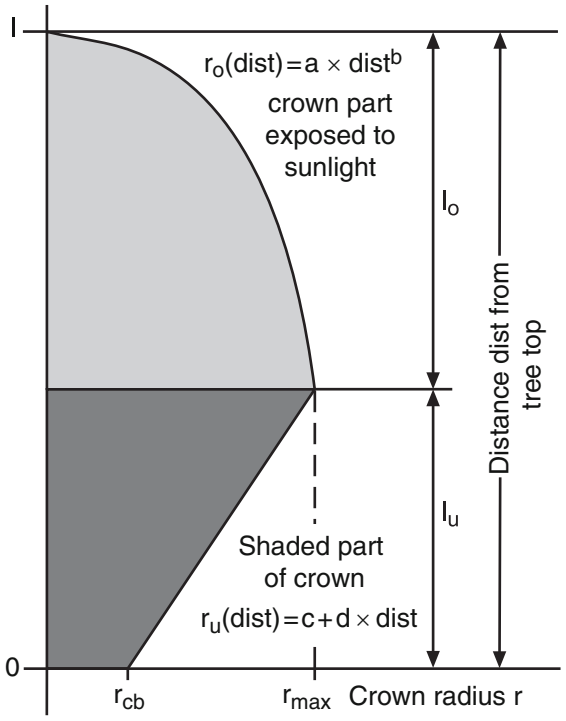

Fig. 7.7 The radius of the sunlit crown l_o is described by the function $r_o = a \times dist^b$ with species-specific parameters a and b. The shaded crown l_u is modelled by the linear equation $r_u = c + dist \times d$. The parameters and variables are: r = crown radius, l = crown length, r_o = sunlit crown radius, l_o = length of sunlit crown, r_u = shaded crown radius, l_u = length of the shaded crown, r_{max} = largest crown radius, r_{cb} = crown radius at crown base, dist = distance from the tip of the tree, and a, b, c, d = species-specific crown shape parameters (cf. Table 7.2)

Table 7.2 Crown shape models for the sunlit and shaded crown for main tree species in Europe. The shape of the sunlit crown is calculated by the parabolic equation $r_o = a\,\mathrm{dist}^b$, the shape of the shaded crown by the linear equation $r_u = c + \mathrm{dist} \times d$. The derivation of parameters a, b, c, and d are given in the table: a description of variables is given in Fig. 7.7

Tree species	Upper crown			Lower crown		
	a	l_o	b	c	d	r_{cb}
Picea abies	r_{max}/l_o	$l \times 0.66$	1.00			$r_{max} \times 0.50$
Abies alba	$r_{max}/(l_o)^{0.5}$	$l \times 0.50$	0.50			$r_{max} \times 0.50$
Pinus silvestris	$r_{max}/(l_o)$	$l \times 0.68$	0.50	for all species $c = r_{max} - d \times l_o$		$r_{max} \times 0.63$
Larix decidua	$r_{max}/(l_o)$	$l \times 0.66$	0.50			$r_{max} \times 0.50$
Fagus silvatica	$r_{max}/(l_o)^{0.33}$	$l \times 0.40$	0.33		for all species $d = \frac{r_{cb} - r_{max}}{1 - l_o}$	$r_{max} \times 0.33$
Quercus petaea	$r_{max}/(l_o)^{0.33}$	$l \times 0.39$	0.33			$r_{max} \times 0.36$
Pseudotsuga menziesii	$r_{max}/(l_o)$	$l \times 0.66$	0.50			$r_{max} \times 0.50$
Acer pseudoplatanus	$r_{max}/(l_o)^{0.33}$	$l \times 0.35$	0.52			r_{max}
Alnus glutinosa	$r_{max}/(l_o)^{0.5}$	$l \times 0.56$	0.50			r_{max}

using the individual tree parameter a and the species-specific exponent b. The radii (r_u) in the shaded crown with length l_u are calculated using the linear equation with the individual tree parameters c and d:

$$r_u = c + \mathrm{dist} \times d. \tag{7.8}$$

In Table 7.2, the input variables, total crown length ($l = l_o + l_u$) and mean crown radius (r_{max}), are needed to determine the parameters a, b, c and d in the crown shape model for different tree species. The meaning of the variables is apparent in Fig. 7.7. With the input data tree height, crown base height, mean crown radius, and with the species-specific crown shape parameter, one can calculate the spatial expansion of the crown, crown volume and crown surface area (Table 7.2).

For Norway spruce, the crown shape model assumes that crown width is greatest at 66% of the crown length from the tip ($l_o = l \times 0.66$). This height is used to define the boundary between the sunlit crown, represented as a conical tip for Norway spruce, and the shaded crown, which is approximated by a frustum. The greatest crown width is obtained by doubling the mean crown radius. A circle represents crown surface area. At crown base height, the crown radius r_{cb} is estimated to be half the greatest crown radius ($r_{cb} = r_{max} \times 0.50$). For European beech, the model assumes that the greatest crown width occurs at 40% of crown length from the tip of the tree ($l_o = l \times 0.40$). The shape of the sunlit and shaded crown is represented by a cubic parabola, and frustum respectively. The crown diameter at crown base height is estimated as 33% of the greatest crown width ($r_{cb} = r_{max} \times 0.33$). In the model for Silver fir, the greatest crown diameter is set at 50% of the crown length ($l_o = l \times 0.50$). The shape of the sunlit and shaded crown is defined by a quadratic parabola, and frustum respectively. At the crown base, crown width is defined as half the greatest crown width, as with Norway spruce ($r_{cb} = r_{max} \times 0.50$).

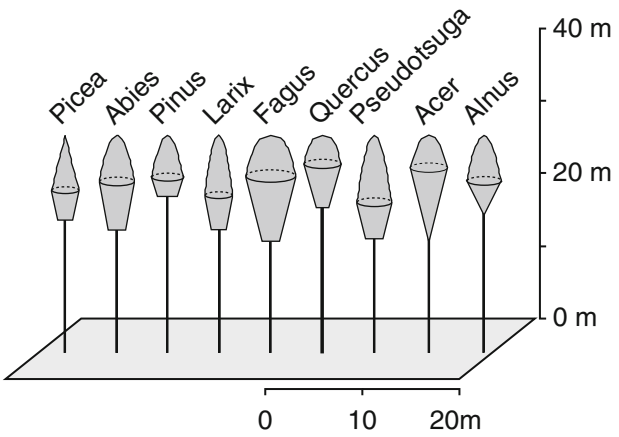

Fig. 7.8 Comparison of the crown shapes of different tree genera for trees with a tree height of 24 m and a diameter at breast height of 30 cm. The crowns reflect a lateral extension expected under medium stand density

The species-specific nature of crown shape parameters warrants the development of specific crown models. These are presented in Fig. 7.8 for trees with similar-sized stems.

7.2.2.2 Profile Diagrams and Front Views

Based on species-specific crown shape models, the program AUFRISS (Pretzsch 1992c) produces profile diagrams of any section of a stand. Stand profile diagrams facilitate the presentation and analysis of research results. Yet, as a component of the individual-tree growth simulator SILVA 2.2 (Pretzsch 2001), AUFRISS also allows one to follow simulated stand development visually, and influence thinning operations interactively.

Figure 7.9a and c show profile diagrams for 5 m wide strips in the pure Norway spruce stand, ZWI 111/5, and the pure European beech stand, ZWI 111/4. In the 1982 survey year, both stands received a light thinning from above to open up the crown. Vigorous trees with wide crowns, able to compete favourably, dominate the stands. The Norway spruce–European beech mixed stand, Zwiesel 111/3, in Fig. 7.9b, comprises a grouped mixture of Norway spruce and European beech. In the Norway spruce–Silver fir–European beech selection forest, Freyung 129/2, both individual-tree mixtures and group mixtures of Norway spruce, Silver fir and European beech of different ages and sizes are found in close proximity (Fig. 7.9d). The Silver fir adapts to the amount of growing space available by developing a relatively wide crown.

The profile diagrams provide a pseudo three-dimensional representation of the stand observed at an oblique angle from above. By offsetting the image of trees, and building up the picture from back to front, a three-dimensional impression is

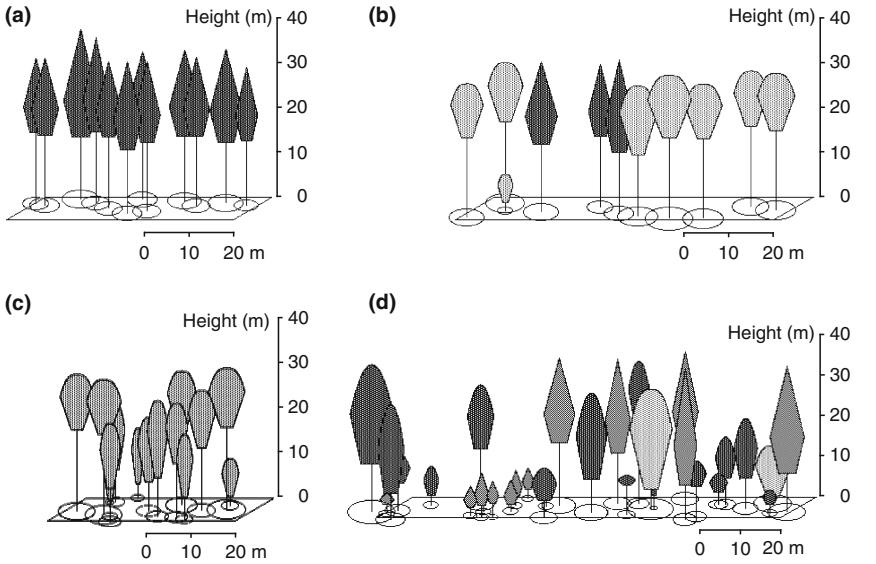

Fig. 7.9 Profile diagrams for 5 m wide zones in pure and mixed stands of Norway spruce (*dark grey*), Silver fir (*grey*), and European beech (*light grey*): (**a**) pure Norway spruce stand, Zwiesel 111/5, in 1982 after thinning, (**b**) Norway spruce–European beech mixed stand, Zwiesel 111/3, in 1982 after thinning, (**c**) pure European beech stand, Zwiesel 111/4, in 1982 before thinning, and (**d**) Norway spruce–Silver fir–European beech selection forest experiment plot, Freyung 129/2, in 1980

produced. Although the perspective is not accurate, it provides a view over the entire stand. Trees are depicted according to their size without taking their distance from a given viewpoint into account. Consequently, the trees in the background appear higher than those in the foreground. Topography, an essential structural characteristic of stands, has been omitted. This approach requires less calculation time, and yet provides an adequate impression of the stand.

Whereas these visualisation methods permit trees and stands to be presented from only one defined angle of vision, the program TREEVIEW facilitates stand views from any desirable position (Pretzsch and Seifert 1999; Seifert 1998). Figure 7.10a shows two European beech groups surrounded by areas of pure Norway spruce with mixed zones at the centre of the Norway spruce–European beech mixed stand experimental plot, Freising 813/1 (Chap. 9, Sect. 9.3). In addition to producing static representations of this kind, the program allows the user to move through the stand in real time. The user may elect to pass through the stand at ground level and, during this virtual "walk-through", gain a realistic terrestrial perspective of the stand. One controls the direction of the walk-through with the keyboard and mouse. Furthermore, movement through the stand above the forest floor is also possible. This option affords free movement through the stand in all directions, a virtual "fly-through", so that the user gains an impression of stand structure that is not possible when confined to the forest floor. These different perspectives are possible when all trees are modelled individually as three-dimensional shapes. Individual-tree data

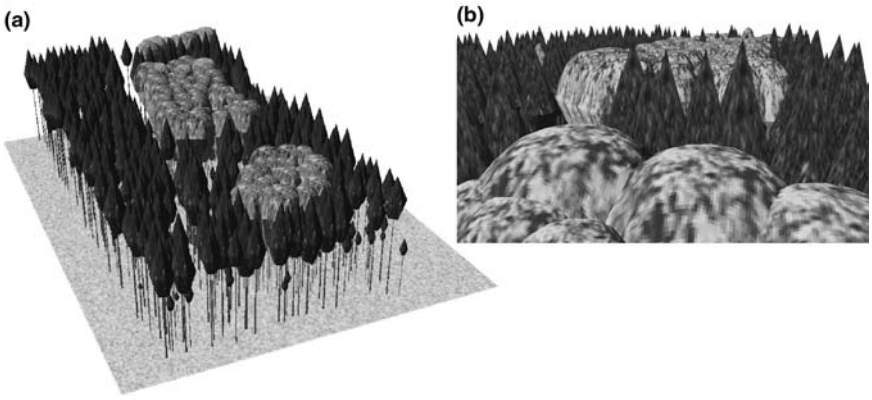

Fig. 7.10 View of the Norway spruce–European beech experimental plot Freising 813/1 near Freising, from different perspectives

Fig. 7.11 The program TREEVIEW is based on crown shape models and develops every tree form individually. The crown surface area is constructed from a system of triangles

from experimental plot surveys or from the results of position-dependent individual-tree models provide the database needed. From crown shape models and stem form models, crowns and stems are reproduced by rotational symmetry. First, the crown is approximated by a cone and frustum. Then, these are transformed into pyramids and truncated pyramids for graphical reproduction because, in the end, the crown perimeter is constructed from a number of triangles forming the surfaces of the pyramids (Fig. 7.11). The realism is enhanced by projecting species-specific patterns adopted from photographs onto tree crowns and stem surfaces.

Three-dimensional visualisation supports comprehensive stand planning and control measures, not only for individual stands but also for entire regions. Three-dimensional landscape images can be produced from data available for topography,

surface structure, stand boundaries and stocking level data. The user may choose his viewing position. Linked to an individual-tree growth model, landscape imaging enables one to create images of forest condition as well as realistic forest development, such as long-term changes in the landscape due to afforestation, forest conversion or reforestation. The landscape visualisation program L-VIS (Seifert 1998) produces stand images analogous to the program TREEVIEW (Chap. 11).

7.2.3 Spatial Occupancy Patterns

7.2.3.1 Rasterising Forest Stand Structure

Contrary to using spatial stand structure data to the fullest extent, the mere conversion of stem positions and crown expansion data into tree distribution maps, crown maps, and profile diagrams results in an information loss. This is particularly significant in multi-layered stands, where the spatial structure of the stand is projected only in one plane. Thus, crown maps of structurally diverse, multi-layered stands reveal crown overlap that is the lateral competition between neighbouring trees, which does not occur in reality. Yet if we produce horizontal cuts at different heights within a stand, we obtain a series of spatial occupancy maps that reflect the presence of tree crowns at different heights in the canopy, revealing the spatial stand structure.

To help characterise the crown space and tree neighbourhood of each tree within the stand, the program RAUM (Pretzsch 1992a,c) was developed. The program contains a three-dimensional matrix able to store data for each cubic meter of stand space in a trial plot (Fig. 7.12). For example, a (20, 20, 25) matrix would be required to record spatial data in a stand measuring $20\,\mathrm{m} \times 20\,\mathrm{m}$ with a maximum height of 25 m. The stand space would then consist of $10,000$ cells $1\,\mathrm{m}^3$ in size, and the data allocated to the cell centre point. For example, the points with the coordinates (0.5, 0.5, 0.5) and (1.5, 1.5, 4.5) form the centre of the cells (1, 1, 1) and (2, 2, 5) respectively. Cell size can be made larger or smaller depending on the level of accuracy desired. In the following example the cells are $1\,\mathrm{m}^3$ in size.

In a trial plot, the data for all trees are entered into the matrix one by one. Given the stem coordinates, crown radii, tree height and crown base height, the species-specific crown model transforms the spatial expansion of trees to Cartesian coordinates and places them in the matrix. The trees and tree species at all cell centre points in the matrix and the frequency of occurrence are determined by a dot count. These results are stored in the spatial matrix, producing a grid image of the actual stand structure, which generalises the exploitation of the crown space by tree crowns and the presence of different tree species at different heights within the crown. Based on this information, the program RAUM produces horizontal sections through the stand space creating vertical profiles of the canopy. The spatial matrix data can also be analysed as a numerical dot count statistic. This database is ideal for investigations

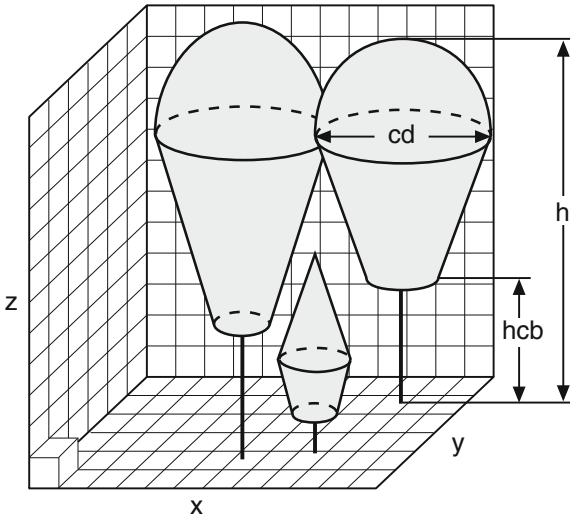

Fig. 7.12 Spatial analysis of tree and stand structure by digitising tree expansion and constructing stand structure from voxels. For every voxel, information about the presence and frequency of different tree species is stored in a three dimensional matrix for further analysis (cf. Figs. 7.13–7.15): variables h = tree height, hcb = height to crown base, cd = crown diameter, x, y, z = stem coordinates

into intraspecific and interspecific competition, and neighbourhood relationships in forest stands.

7.2.3.2 Horizontal Cross-Sections

Figures 7.13–7.15 show the results of a structural analysis with the program RAUM exemplified by the experimental plots near Zwiesel and Freyung in the Bavarian Forest, described previously (cf. Fig. 7.9). Figure 7.13a and c show the results of a dot count along horizontal planes through the crown space of the pure European beech stand ZWI 114/1 (surveyed 1982, after thinning) at a height of 25 m (Fig. 7.13a) and 30 m (Fig. 7.13c). In the horizontal plane at height 25 m, European beech crown occupancy is high and many cells, shown in black, indicate multiple occupancy. The canopy is much more open above and below this main competition zone at 25 m height. At a height of 30 m, for example, the crowns barely overlap.

The canopy structure in the pure Norway spruce stand ZWI 111/5 (surveyed 1982, after thinning) is very similar. Here, we also see a relatively dense crown closure and multiple crown overlap at 25 m height (Fig. 7.13b) whereas, in the upper crown space, Norway spruce crowns rarely touch (Fig. 7.13d).

In the Norway spruce–European beech mixed stand ZWI 111/3 (surveyed 1982, after thinning), the Norway spruce and European beech crowns overlap in a distinctly broader height zone (Fig. 7.14). In contrast to the pure stands, a clear competition zone within a narrow height range could not be found. Instead,

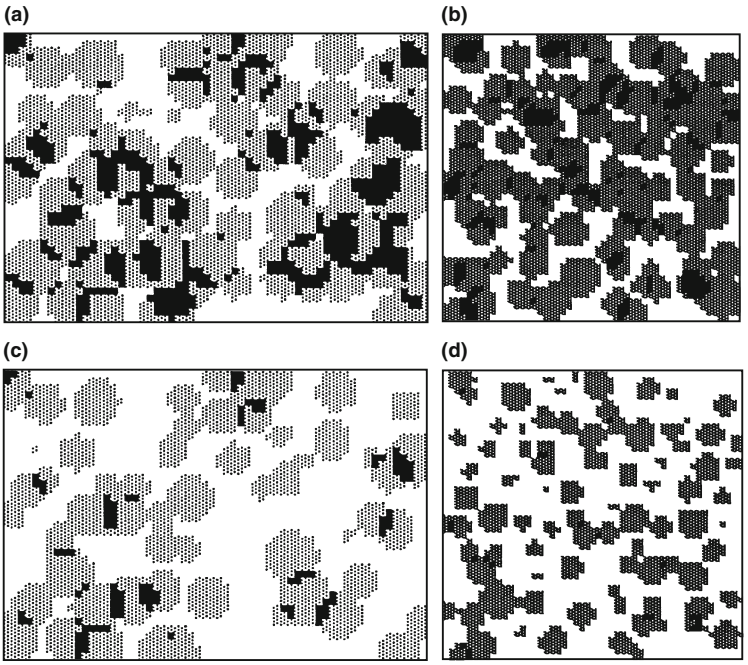

Fig. 7.13 Horizontal cross-sections through the crown space of the pure European beech stand, Zwiesel 111/4, surveyed in autumn 1982 after thinning (**a, c**) and the pure Norway spruce stand, Zwiesel 111/5, inventoried in autumn 1982 after thinning (**b, d**). Cross-sections are shown at a height 25 m (**a, b**), and at a height 30 m (**c, d**). Spatial occupancy of European beech is shown in *light grey*, of Norway spruce in *dark grey*, and multiple-occupancy is shown in *black*

horizontal planes at 20, 25 and 30 m height indicated that European beech (light grey) dominated the lower canopy (20 m). In the mid height range (25 m), Norway spruce (dark grey) and European beech frequencies were similar. The crowns used a large portion of the available growing space. In the upper crown space (30 m), neighbouring crowns rarely overlapped.

In the Norway spruce–Silver fir–European beech selection forest near Freyung 129/2 (surveyed 1980) in the Bavarian Forest, Norway spruce (dark grey), Silver fir (grey) and European beech (light grey) are distributed more widely throughout all height strata (Fig. 7.15) than in the stands described earlier. Multiple cell occupancy (black) is rare. The horizontal plane at 5 m height (Fig. 7.15a) shows a relatively sparse presence of ingrowth in the selection forest, which is growing with almost no lateral mechanical restriction. The structure of the middle and upper canopy layers which can be recognised in the horizontal planes at 15 and 25 m height respectively (Fig. 7.15b and c), influences the growth processes in the crown space below.

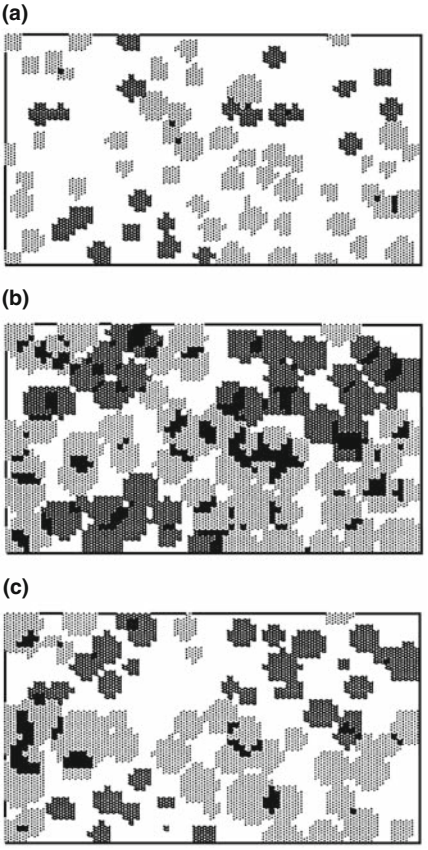

Fig. 7.14 Horizontal cross-sections through the crown space of the Norway spruce–European beech experimental plot Zwiesel 111/3 after the results of the inventory in autumn 1982, after thinning. Horizontal cross-sections at heights (**a**) 20 m, (**b**) 25 m, and (**c**) 30 m. Spatial occupancy of European beech is shown in *light grey*, of Norway spruce in *dark grey*, and multiple-occupancy is shown in *black*

7.3 Horizontal Tree Distribution Patterns

Two approaches may be useful for quantifying horizontal tree distribution patterns: indices calculated from the distances between trees, or from occupation frequencies in sample squares, and which express the mean distribution pattern as a single value; and correlation functions describing changes in the distribution pattern with increasing distance from given tree positions or random points. In contrast to indices, the K-, L- and pair correlation functions provide much more information. Yet, the calculations involved are more complicated and more difficult to interpret. Both approaches use the two-dimensional Poisson distribution, introduced in the following section, as a reference for the identification of distribution patterns.

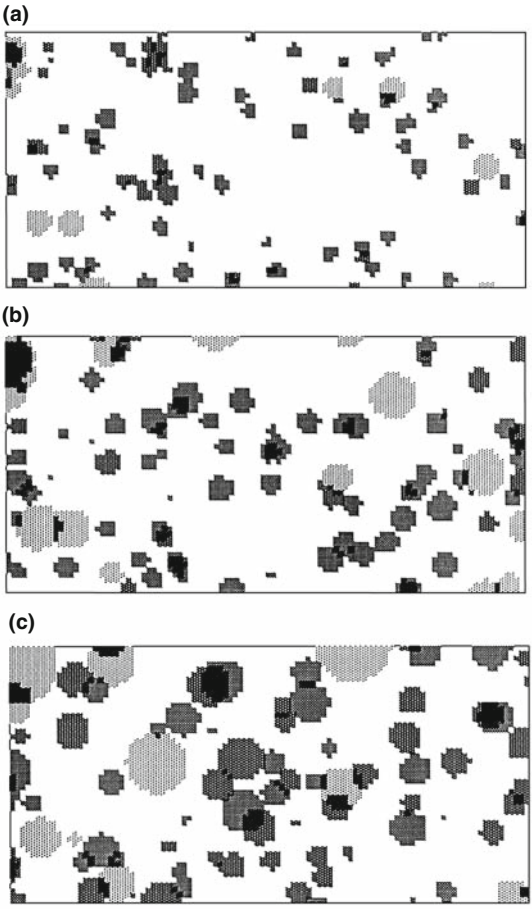

Fig. 7.15 Horizontal cross-sections through the crown space of a Norway spruce, Silver fir and European beech selection stand in Forest District Freyung (experimental plot FRY 129/2, inventory autumn 1980) at heights (**a**) 5 m, (**b**) 15 m, and (**c**) 25 m. Spatial occupancy of European beech, Norway spruce, and Silver fir is shown in *light grey*, *dark grey*, and *grey* respectively. Multiple occupancy of voxels is shown in *black*

7.3.1 Poisson Distribution as a Reference for Analysing Stand Structures

The Poisson forest is a reference for the analysis and interpretation of distribution indices and correlation functions; it is a horizontal tree distribution pattern arising from an entirely randomly distribution of trees across a given area. Siméon Denis Poisson (1781–1840) was a French mathematician and physicist who introduced the Poisson distribution to probability theory as a limiting case of the binomial distribution. If we produce randomly distributed x and y coordinates on a 10 m $\times$ 10 m area,

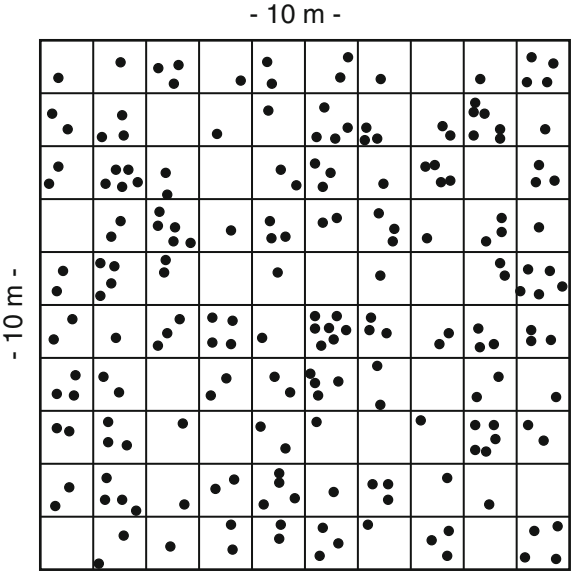

Fig. 7.16 Two-dimensional Poisson distribution from stem charts on a $10\,m \times 10\,m$ square sample plot. A count of the sample squares produces $N = 200$ trees on an area $A = 100\,m^2$, thus $\lambda = 2$, and the underlying Poisson distribution is $p_n = \frac{2^n}{n!} \times e^{-2}$

as shown in Fig. 7.16, we obtain a random distribution, which is called a Poisson distribution. In random distributions, there are areas of higher and lower density. In Fig. 7.16, the sample squares rarely have 5, 6, 7, or more trees. Many of the squares are unoccupied or have only a few points. Thus a random or Poisson distribution does not result in a regular square or hexagonal spacing of trees. The number of telephone calls received at a reception desk provides an example of a one-dimensional random distribution over time. There are long periods where no telephone calls, or very few occur. At other times there are numerous telephone calls. The Poisson distribution is applicable to historical statistics for the number of Prussian Calvary men killed by kicking horses, or for the number of child suicides in Prussia. The first raindrops falling on a dry road or the location of fallen beechnuts on the forest floor in a European beech forest provide examples of two-dimensional random, or Poisson distributions.

To analyse the distribution of trees on the area represented in Fig. 7.16 quantitatively, one can cover the plot with a square grid and record the frequency of trees present in each square. This results in many squares in which no or just a few trees are present. A few squares are occupied by a large number of trees. This pattern is analogous to the number of telephone calls in set time intervals described in the example above. The number of squares with a particular occupancy follows the Poisson distribution. This distribution comprises the parameter λ only, which represents the mean number of stems in the square, and equals the mean μ and the variance of the distribution σ^2 ($\lambda = \sigma^2 = \mu$). The Poisson distribution,

$$p_n = \frac{\lambda^n}{n!} \times e^{-\lambda} \tag{7.9}$$

describes the probability of $0, 1, 2, \ldots, n$ trees occurring in a randomly selected sample plot. The constant e is Euler's number ($e = 2.718282$). In our example there are 200 trees on an area of $100\,m^2$, resulting in $\lambda = 2$ trees m^{-2}. By entering $\lambda = 2$ into (7.9), the probability and frequency of occurrence of $n = 0, 1, 2, \ldots, \infty$ counts per square expected for a Poisson distribution can be calculated by

$$\begin{aligned}
P_0 &= \frac{2^0}{0!} \times e^{-2} = 0.1353 \times 100 = 14, \\
P_1 &= \frac{2^1}{1!} \times e^{-2} = 0.2706 \times 100 = 27, \\
P_2 &= \frac{2^2}{2!} \times e^{-2} = 0.2706 \times 100 = 27, \\
P_3 &= \frac{2^3}{3!} \times e^{-2} = 0.1804 \times 100 = 18, \\
P_n &= \frac{2^n}{n!} \times e^{-2} = \cdots .
\end{aligned} \tag{7.10}$$

and then compared to the real frequencies (Fig. 7.17). In this example we obtain quite a good approximation between the expected and the observed frequency. In selection forests, virgin forest stands, forests with continuous forest cover, and near-natural mixed forests in the regeneration phase, we see that stems positions often follow a Poisson distribution. As the Poisson forest can be described readily with biometric parameters, and is also clearly the result of an entirely independent placement of trees, it provides an appropriate reference for other distributions that deviate from it. Figure 7.18 shows more regular (Fig. 7.18a and b), Poisson (Fig. 7.18c) and clumped (Fig. 7.18d) tree distribution patterns. The growing space occupied by trees differs in stands with regular, random or clumped tree distributions. The development opportunities differ accordingly, and the more stands deviate from a regular distribution, the more effort required to inventory them.

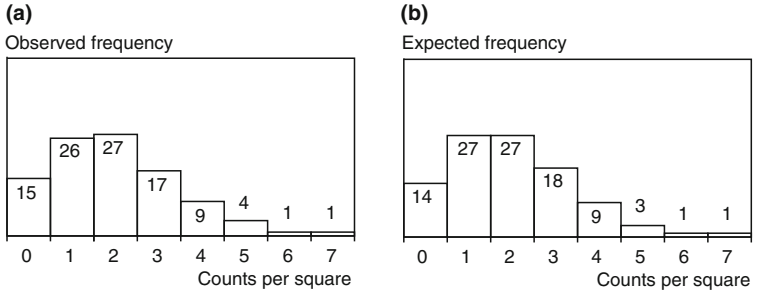

Fig. 7.17 Comparison of (**a**) observed frequencies of sample squares with an occupancy of $0, 1, \ldots, 7$ trees per square and (**b**) expected frequency according to a Poisson distribution. The agreement between the observed and expected values suggests a Poisson distribution

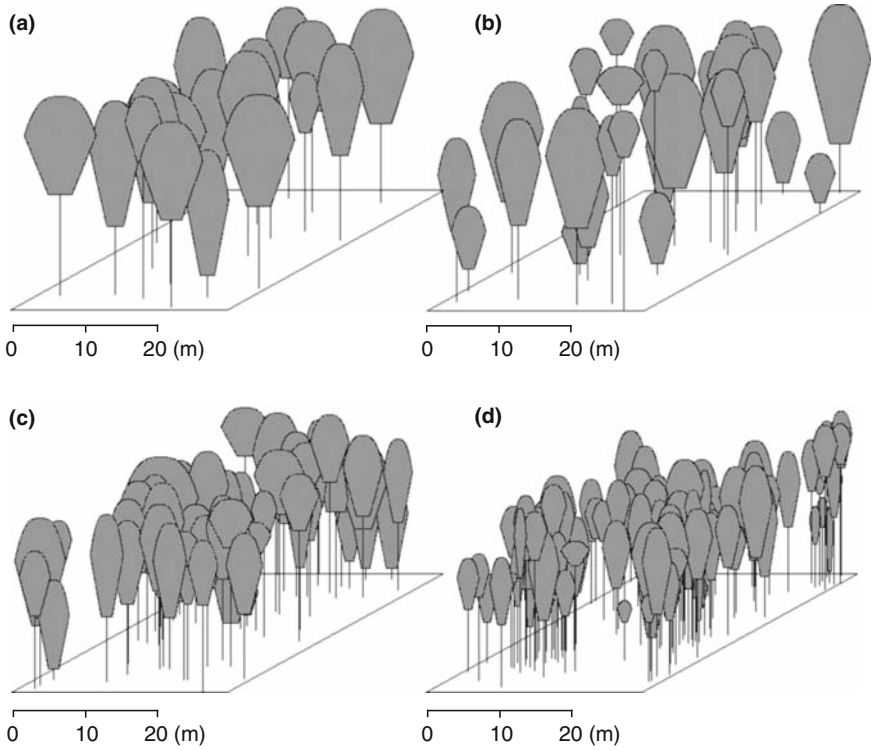

Fig. 7.18 Regular, random, and clumped tree distribution patterns in European beech stands. Stands (**a, b**) represent a more or less regular distribution, (**c**) a random, or Poisson distribution, and (**d**) a clumped horizontal distribution

7.3.2 Position-Dependent Distribution Indices

Indices of this kind are based on the distance to the nearest neighbour, or the position of all trees. They test whether a given tree distribution pattern is purely random, or whether it tends to be regular or clumped. The first group of methods is based on the distances from individual trees to their nearest neighbour. The aggregation index R from Clark and Evans (1954) provides an example. Eberhardt (1967), Prodan (1973) and Smaltschinski (1981) discuss other indices of this type. The second group of methods, for which we present Pielou's index (1959), is based on the distances between random points and actual tree positions. Among others, Hopkins (1954) and Thompson (1956) have developed indices of this type. Pielou (1975, 1977), Ripley (1977, 1981), and Upton and Fingleton (1985, 1989) provide a broad overview of both groups of methods. In this section we have been able to single out only those methods used frequently in forestry research.

7.3.2.1 Clark and Evans' (1954) Aggregation Index

Clark and Evans' index R describes the relationship between the observed mean distance to the nearest neighbour $\bar{r}_{observed}$ in an area and the expected mean distance $\bar{r}_{expected}$ in a purely random tree distribution:

$$R = \frac{\bar{r}_{observed}}{\bar{r}_{expected}}. \tag{7.11}$$

Theoretically, R lies between 0 (greatest clumping, all objects occur at the same point) and 2.1491 (strictly regular hexagonal pattern), and indicates whether the trees are distributed regularly, randomly or in clumps across an area. Aggregation values below 1.0, approximately 1.0 and higher that 1.0 indicate a tendency towards clumping, a random distribution and a more regular distribution respectively. R is determined by methods of the nearest neighbour. The distances $r_{i,i...n}$ to the nearest neighbour is measured for all n trees on a trial plot of the area A (Fig. 7.19). The mean distance to the nearest neighbour is calculated by

$$\bar{r}_{observed} = \frac{\sum_{i=1}^{n} r_i}{n}. \tag{7.12}$$

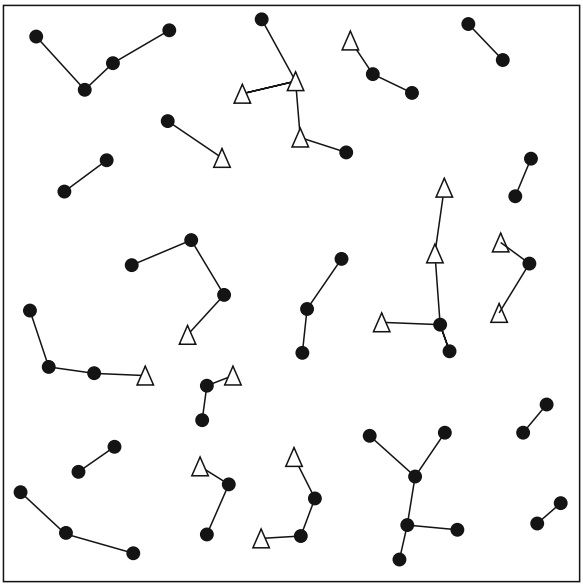

Fig. 7.19 To calculate the distribution index R by Clark and Evans (1954) the distance from every tree to its nearest neighbour is recorded. In mixed stands it is also useful to record the species of the basic tree and its nearest neighbour. Species symbols indicating the stem base points are given as well as examples of distances of some trees to their nearest neighbours

The actual observed distance to the nearest neighbour is related to the expected mean distance $\bar{r}_{expected}$ for a random tree distribution in

$$\bar{r}_{expected} = \frac{1}{2 \times \sqrt{\rho}}, \tag{7.13}$$

where ρ is the number of trees per unit area ($\rho = n/A$). Therefore, the aggregation index R indicates the difference between the observed distribution pattern and a purely random, or Poisson distribution. Based on $\bar{r}_{observed}$, the mean distance $\bar{r}_{expected}$ and the standard error of the mean distance in a random distribution,

$$\sigma_{\bar{r}_{expected}} = \frac{0.26136}{\sqrt[2]{n^2/A}} \tag{7.14}$$

produces

$$T_R = \frac{\bar{r}_{observed} - \bar{r}_{expected}}{\sigma_{\bar{r}_{expected}}}, \tag{7.15}$$

a standard, normally distributed text statistic, which can be used to test the significance of a deviation from a random distribution towards an even distribution or clumping. The edge effect arising from the spatial limitations of experimental plots can be eliminated by replacing the expected mean distance to the nearest neighbour, $\bar{r}_{expected}$, and the standard error of the mean distance in a random distribution in (7.13) and (7.14) with the boundary correction factor from Donnelly (1978) for areas with compact shapes:

$$\bar{r}_{corr} = 0.5\sqrt{\frac{A}{n}} + 0.051368 \times \frac{P}{n} + 0.041 \times \frac{P}{n^{\frac{3}{2}}} \tag{7.16}$$

and

$$\sigma_{\bar{r}_{corr}} = \sqrt{0.0703 \times \frac{A}{n^2} + 0.037 \times P \times \sqrt{\frac{A}{n^5}}}, \tag{7.17}$$

where A is the area (in m^2), n the number of observations, and P the circumference of the area (in m).

In the following examples we applied the aggregation index R according to the resulting correction formulas

$$R_{corr} = \frac{\bar{r}_{observed}}{\bar{r}_{corr}} \tag{7.18}$$

for the distribution index, and

$$T_{R_{corr}} = \frac{\bar{r}_{observed} - \bar{r}_{corr}}{\sigma_{\bar{r}_{corr}}} \tag{7.19}$$

for the standard normally distributed test statistic. If the latter result is greater than 1.96, 2.58, or 3.30, a significant deviation from the random distribution occurs, with the probability of error of 5, 1, and 0.1% respectively.

The aggregation indices for the tree distribution patterns presented in Fig. 7.20a and b are $R = 1.4^{**}$ and 1.2^{*} respectively. These indices are typical of the more regular tree distributions found in age class forests that have undergone thinning from below. A value of $R = 1.0$ (Fig. 7.20c) indicates a random, or Poisson distribution pattern common in selection forests and virgin forests. An aggregation index of $R = 0.9$ (Fig. 7.20d) suggests a tendency towards clumping, which occurs, for

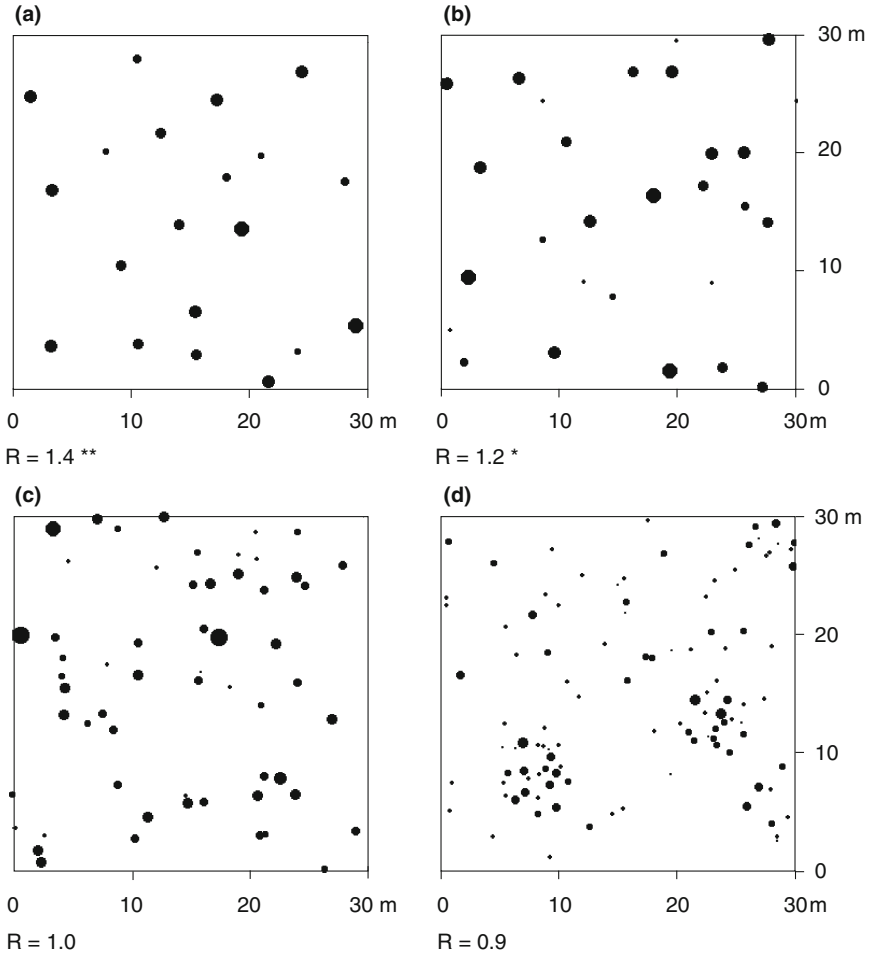

Fig. 7.20 Identification of four horizontal tree distribution patterns with the aggregation index R from Clark and Evans (1954). The *symbol* size is proportional to the stem diameters at 1.30 m height. Values of R above 1.0 indicate a tendency towards a regular distribution, and values below 1.0 a tendency towards clumping. For random distributions, index $R \approx 1.0$

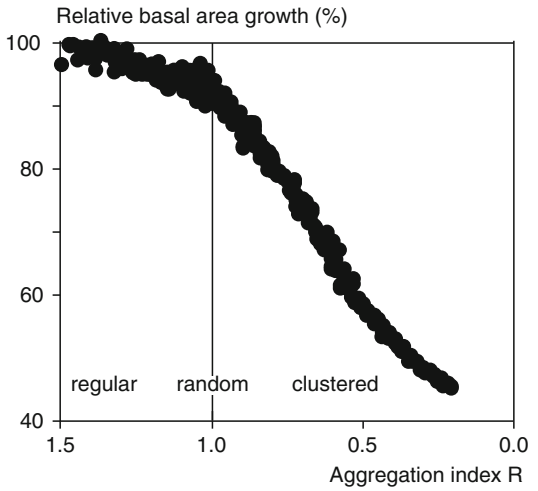

Fig. 7.21 Relationship between the aggregation index R and the relative stand basal area growth (%) derived from the results of 10,000 simulation runs with different tree distribution patterns, ranging from regular to very clustered tree distributions. The basal area growth of each simulation run is set into relation to the maximum basal area growth (100%), which is produced in regularly structured stands with closed canopies (after Pretzsch 1995)

example, in cohort structures in Norway spruce forests in mountainous regions. The symbols *, ** and *** indicate that tree patterns deviate from a random distribution with a probability error of 5, 1 and 0.1% respectively.

Distribution indices of the total population, ranging from R = 1.0 to 1.4, were derived for 53 European beech–European larch mixed stands in Lower Saxony. This indicates that the tree distributions range from random to regular. As stands develop, regularity increases (Pretzsch 1993, 1997). Biber (1997) obtains similar results from investigations of structure in 113 long-term plots in pure and mixed stands in Bavaria comprising Norway spruce, Silver fir, and European beech ranging in age from 19 to 250 years. The aggregation values R of these stands ranged from 0.9 to 1.9, tending towards a regular distribution pattern on average with R = 1.25. The same dataset was applied to quantify the effect of tree distribution patterns on stand growth (Pretzsch 1995). The results showed that maximum stand basal area increment ($m^2\,ha^{-1}\,yr^{-1}$) occurs in stands with a regular tree distribution (Fig. 7.21). About 95% of the maximum increment is attained in random distributions (R = 1.0). For aggregation indices below R = 0.9, the basal area increment declines almost linearly (Fig. 7.21).

7.3.2.2 Pielou's (1959) Distribution Index

Alternatively, instead of using distances between trees, the distance to the nearest neighbour can be determined from random points selected on an area. Assuming a Poisson distribution, the distribution of random points generated is equally as

random as the trees. Thus, on average, methods based on distances from tree to tree produce the same results as methods based on distances from random points to trees. Pielou's (1959) Index I_P,

$$I_P = \pi \times \lambda \times \bar{r}^2 \tag{7.20}$$

is based on the distances from n random points to tree positions. If we imagine a circle around each random point with a radius given by the distance to the nearest neighbour, we get n circles with the radii $r_{i,i=1\ldots n}$. Then we can calculate the mean of the square distances $\bar{r}^2$, and the mean area occupied by a tree, $\bar{r}^2 \times \pi$. Assuming a Poisson distribution, the product of the point density $\lambda = n/A$, and the average area a tree occupies $\bar{r}^2 \times \pi$ produces the value $(n-1)/n$ (Moore 1954):

$$I_P = \pi \times \lambda \times \bar{r}^2 = (n-1)/n. \tag{7.21}$$

The number of distance measurements in the calculation of the distribution index is given by n, where $\lambda = n/A$ represents the number of plants per unit area and

$$\bar{r}^2 = \frac{\sum_{i=1}^{n} r_i^2}{n} \tag{7.22}$$

represents the mean distance squared between the random points and the position of the nearest tree. To calculate $\bar{r}^2$, we cast n random points across an area, and then determine the distances $r_{i,i=1\ldots n}$ from these points to the position of the nearest tree. In large samples, the quotient $I_P = (n-1)/n$ approaches the value 1.0 when the point distribution is entirely random.

If the index $I_P = \pi \times \lambda \times \bar{r}^2$, calculated for a given tree distribution pattern, does not deviate significantly from $(n-1)/n$, the tree distribution pattern is random. For a clumped distribution pattern, one would expect a predominance of large point-to-tree distances $r_{i,i=1\ldots n}$, with correspondingly high $\bar{r}^2$ values, and hence a higher I_P value. Conversely, for a regular tree distribution pattern, only a few large, above-average squared distance values would be found, and hence $I_P = \pi \times \lambda \times \bar{r}^2$ would be smaller than $(n-1)/n$. The significance of any deviation in the index I_P from the expected value $(n-1)/n$ can be tested since, for a Poisson distribution, the product $(2n\,I_P)$ describes an χ^2-distribution with 2n degrees of freedom (Pielou 1959).

For sample sizes of $2n > 100$, common in studies of this nature, 95 and 99% confidence intervals can be calculated by

$$I_{P\,crit} = \frac{1}{4 \times n} \times \left(\sqrt{4n-1} \pm 1.9600\right)^2 \tag{7.23}$$

and

$$I_{P\,crit} = \frac{1}{4 \times n} \times \left(\sqrt{4n-1} \pm 2.3263\right)^2 \tag{7.24}$$

respectively. If the observed values lie below or above these confidence intervals it indicates a significant trend towards regularity, or clumping respectively.

Pielou (1959) also developed a useful test to analyse the difference in distribution patterns between two populations, which I_P identifies as non-random.

In his investigations of 13 stand types in Northern Ontario, Payandeh (1974) found I_P index values between 0.593 and 2.116. In near-natural coniferous stands patterns reached from aggregated to clumped distributions, with index values up to $I_P = 2.116$. The distribution of trees in natural broadleaved mixed forests were overwhelmingly random with $I_P = 1.0$. The artificially established stands differed considerably, with I_P values below 0.6. Differences in structure and structural diversity have far-reaching consequences for data sampling in, and modelling such stands (Vries 1986).

7.3.3 Distribution Indices Based on Sample Quadrats

From the large palette of plot-count methods available, we focus on the indices from Clapham (1936) and Morisita (1959). These indices have proven particularly useful in forestry research. After repeated use of such indices in forestry research, we gain some knowledge of the range in values derived for different stand structures. These values provide a framework for the accurate interpretation of individual results. Cox (1971), David and Moore (1954), Loetsch (1973) and Douglas (1975), among others, describe other indices of this nature.

7.3.3.1 Clapham's (1936) Variance–Mean Ratio

The relative variance I_c, also called the variance–mean ratio, is based on the number of plants in sample squares. If m sample squares are being assessed, and $n_{j,j=1\ldots m}$ gives the number of plants in square j, then the mean plant number per square is

$$\bar{n} = \frac{\sum_{j=1}^{m} n_j}{m}, \tag{7.25}$$

the total number of plants is

$$n = \sum_{j=1}^{m} n_j = \bar{n} \times m, \tag{7.26}$$

and the variance in plant number per quadrat s_n^2 is

$$s_n^2 = \frac{\sum_{j=1}^{m} \left(n_j - \bar{n}\right)^2}{m-1}. \tag{7.27}$$

Thus, we can calculate the relative variance, or the variance–mean ratio,

$$I_c = \frac{s_n^2}{\bar{n}} \tag{7.28}$$

from the variance in plant number per square and the mean plant number per square. The variance calculated is related to the mean occupancy $\bar{n}$. So, as for a Poisson distribution where

$$s_n^2 = \bar{n} = \lambda \tag{7.29}$$

applies, one obtains an index value $I_c = 1.0$ and the distribution corresponds to a Poisson-distribution (cf. Sect. 3.1). The following three cases can be distinguished: when, in a Poisson distribution, the variance in the numerator and the mean in the denominator of (7.28) are equal, then, $s_n^2 = \bar{n}$, and $I_c = 1.0$, indicating a purely random distribution; when the variance s_n^2 is greater than the mean $\bar{n}$, many squares have a very high or very low occupancy, then $s_n^2 > \bar{n}$ and $I_c > 1.0$, indicating clumping; and, finally, when the variance is less than the mean plant number per square, then $s_n^2 < \bar{n}$, and $I_c < 1.0$, and a regular distributions occurs.

According to Hoel (1943) the product of $(m-1)$ and I_c

$$T = (m-1) \times \frac{s_n^2}{\bar{n}} \tag{7.30}$$

represents the dispersion index T for a random distribution χ^2_{m-1}, when $m > 6$ and $\bar{n} > 1$ (Kathirgamatamby 1953). Pielou (1977) maintains the index changes more quickly when clumping occurs than for a more regular distribution.

In the example presented in Fig. 7.22, taken from the tree distribution pattern in Fig. 7.16, the $m = 100$ squares produces a mean tree number per square of $\bar{n} = 2.0$

- 10 m -

- 10 m -										
	1	1	3	1	2	2	1	0	1	4
	2	3	0	1	1	4	3	2	6	1
	2	5	2	0	2	3	1	4	0	3
	0	2	5	1	3	2	3	1	3	1
	2	4	2	0	1	0	1	0	2	5
	2	1	3	4	1	7	3	2	3	3
	3	2	0	2	2	4	2	0	2	1
	2	3	1	0	2	1	0	1	5	2
	2	4	1	2	4	1	3	1	1	0
	0	2	1	2	2	3	1	3	0	4

Fig. 7.22 Calculation of the variance–mean ratio by Clapham (1936) from the frequency of occupation in sample squares. The analysis of $m = 100$ squares produces a mean tree number per square of $\bar{n} = 2.0$, a variance of occupancy of $s_n^2 = 2.18$ and thus a relative variance of $I_c = 1.09$, indicating a random or Poisson distribution

with a variance of $s_n^2 = 2.18$. Thus, the variance mean index is $I_c = 1.09$, indicating a random distribution. The test value $T = 99 \times 1.09 = 107.91$ lies below the 5, 1 and 0.1% upper confidence limits for the χ^2-distribution with 99 degrees of freedom, which are 123, 135 and 148 respectively. Therefore, it can be assumed that this distribution is not significantly different from a random distribution.

7.3.3.2 Morisita's (1959) Index of Dispersion

The index developed by Morisita (1959) is also based on frequencies in sample squares, and tests whether the distribution pattern is significantly different from a random distribution. This is determined by recording the distribution pattern across q squares, which is obtained by counting occupancy in the squares $n_1, \ldots, n_q$. The total number of objects n is calculated by

$$n = \sum_{i=1}^{q} n_i. \tag{7.31}$$

The index of dispersion from Morisita is calculated from the number of squares q, the occupancy of the squares $n_1, \ldots, n_q$, and the total number of objects n in

$$I_\sigma = \frac{q \sum_{i=1}^{q} n_i \times (n_i - 1)}{n \times (n-1)}. \tag{7.32}$$

The probability that two trees randomly selected from the distribution are found in the same square is

$$\sigma = \frac{\sum_{i=1}^{q} n_i \times (n_i - 1)}{n \times (n-1)}. \tag{7.33}$$

If the distribution is entirely random, such as in a Poisson forest, the expected probability that two randomly selected trees are located in the same square is

$$E(\sigma) = \frac{1}{q}. \tag{7.34}$$

The index I_σ is the quotient of the observed probability σ for the given distribution and the expected probability $E(\sigma) = 1/q$ when the distribution is random:

$$I_\sigma = \frac{\sigma}{E(\sigma)} = \frac{\sum_{i=1}^{q} n_i \times (n_i - 1)}{n \times (n-1)} \Big/ \frac{1}{q}. \tag{7.35}$$

If the observed probability and the expected probability for a Poisson distribution are equal, then $I_\sigma = 1$ and the distribution is random. If the probability that two selected trees occur in the same square is greater than the expected probability for a Poisson distribution, then $I_\sigma > 1$, which indicates clumping or aggregation. A regular distribution occurs when $I_\sigma < 1$. Based on the F-test, Morisita (1959) developed the test statistic

$$F_0 = \frac{I_\sigma \times (n-1) + q - n}{q-1} \tag{7.36}$$

for testing the deviation from an entirely random distribution. By comparing F_0 with the table value for $F_{q-1,\alpha}$, one can test whether a deviation from the random distribution is significant. If F_0 is greater than the table value, a significant deviation at the level α exists. As with other indices based on sample squares, Morisita's index of dispersion is also dependent on the size of the sample squares.

7.3.3.3 Selecting Sample Square Size

There is no prescription for deciding what square size to use. If the entire observation area were divided into two or three squares only, with half or one third of the recorded points respectively, we would find out as little about the distribution pattern as if the area were divided into squares so small they contained one sample point at the most. Many authors (Upton and Fingleton 1985) suggest that the size of squares should be selected so that 1.0–4.0 objects are present, on average, in each square. If a Poisson distribution occurs, then the λ values 1.0 and 4.0 would result in 37 and 2% unoccupied squares, respectively. When the percentage of unoccupied squares in the survey grid is higher or lower, then the increase in data collected would not indicate a corresponding gain in information, or the decrease in data collected would compromise the level of detail obtained respectively.

In practice, sample square size, particularly for the sampling of seedlings, regeneration or the lower stand, is usually dependent on technical considerations (ease of keeping track of squares, resources for measuring the squares, desired accuracy of pattern recognition), and usually ranges from $1\,m \times 1\,m$ to $5\,m \times 5\,m$ at experimental plots. With small sample squares, detailed analyses of regeneration structure can be carried out, for example, to understand seed dispersal patterns on a mature forest floor. Larger sample squares are appropriate when an investigation aims to gain a comprehensive overview of the state of regeneration throughout the stand.

When in doubt, smaller sample squares should be used, or tree positions explicitly measured. If necessary, the sample squares can then be aggregated into larger units afterwards. Furthermore, the analysis can be undertaken independent of scale. If an analysis of distribution commences with a certain number of sample squares, and then every four sample squares are aggregated, followed by every 16 sample squares, and so on in sequence, clumping may be identified at different resolutions.

7.3.4 K-Function

The K-function defined by Ripley (1977), its transformation into the L-function by Besag (1977), and the pair correlation function from Stoyan and Stoyan (1992) enable tree distribution patterns to be quantified more precisely and clearly than the structural indices mentioned above. Whereas the structural indices simply provide details about the position of the nearest neighbour, or the variation in density across the area, the K-, L-, and pair correlation functions produce statements about change trends in stand structure around individual trees as the distance from a standpoint increases (cf. Fig. 7.23a–c). In all three functions, the results of the underlying algorithms are related to theoretical frequencies of randomly distributed trees. The functions identify the extent to which the tree distribution pattern is more or less dense than the Poisson distribution as the distance r from the tree base increases. The two-dimensional Poisson distribution, introduced in Sect. 3.1 is used again as a reference. By virtue of the more time consuming computations, and more sophisticated interpretations undertaken, these functions provide more meaningful statements about the distribution patterns than structural indices. Consequently, primarily the correlation functions are used in research. Nevertheless the indices presented are useful for quantifying structure and structural changes in practice as they are calculated readily and, the fixed range in values interpreted readily.

In the application of the above-mentioned functions, we assume that the tree distribution patterns are homogeneous and isotropic. Homogeneity occurs when point configurations in different areas of the point distribution are similar, and any differences merely random. Inhomogeneity in the point distribution occurs when the area investigated touches the stand boundary or spans sites with clear variation

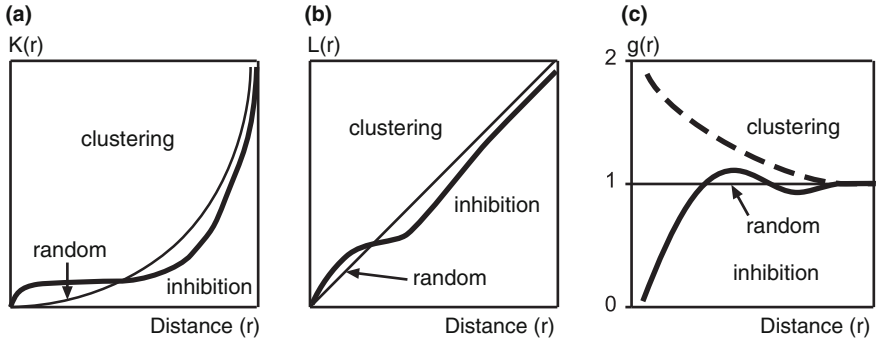

Fig. 7.23 K-function, L-function and the pair correlation function g(r) diagnose stem distribution patterns in relation to distance r from the stem base point (*from left to right*). Clustering or inhibition of trees is evident relative to a random tree distribution, shown as (**a**) a parabola $K(r) = \pi \times r^2$, (**b**) angle bisector line $L(r) = r$, or (**c**) as a line parallel to the abscissa $g(r) = 1.0$

in environmental conditions and resource supply. In this case, tree density and distribution patterns may change gradually due to changes in site conditions. Proof of homogeneity is based largely on scientific evidence, for example, that stand conditions, fertilisation measures, or treatments are uniform. Whereas homogeneity indicates that distribution patterns do not vary when a shift or translation is applied, isotropy describes distribution patterns that are independent of the rotations about an origin. If a point distribution is both homogeneous and isotropic it is termed motion invariant since neither a shift nor rotation about any point will change the distribution pattern systematically (Stoyan and Stoyan 1992).

To illustrate the information gained from them, the K-, L- and pair correlation functions are calculated for the tree distributions shown in Fig. 7.24, which have regular (a, d), random (b, e) and clumped (c, f) distributions in Norway spruce stands. Figure 7.24a–c shows the stand structure in the early growth phase. The stand structures were extrapolated over 100 years without treatments using the stand simulator SILVA 2.2 (Chap. 13), producing the mature stand structures illustrated in Fig. 7.24d–f. These structures represent the spectrum of tree distribution patterns frequently observed in European forests.

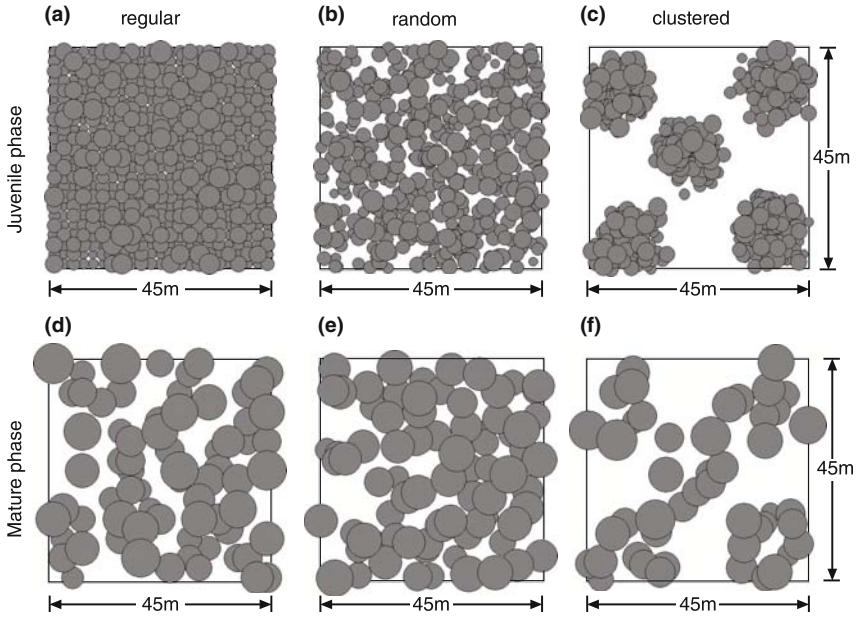

Fig. 7.24 Distribution patterns as examples of the application of K-, L- and pair correlation functions in Norway spruce stands. The tree distribution patterns are presented for a regular, random and clumped tree distribution (*from left to right*). The upper maps (**a–c**) show stands in the juvenile growth phase, and the maps below (**d–f**) show the same stands in the mature growth phase

7.3.4.1 Methodological Principles

To quantify the change in a distribution pattern with increasing distance from the tree base point using the K-function, a circle with the radius r is drawn around every tree in the tree distribution map. The number of trees located within this circle, excluding the centre tree, is counted. The radius is increased gradually, and the trees located within the circle recounted after each increment. A transformation of the results of these counts, explained below, gives the K-function (Fig. 7.23a). It gives the mean number of trees for a given radius r, and is defined as

$$\lambda \times K(r) = n_r, \text{ for } r \geq 0. \tag{7.37}$$

where $\lambda \times K(r)$ indicates the mean number of trees at a distance less than r from any point in the distribution. The number of trees is determined by drawing a circle around the base of every tree in the point distribution, then increasing the radius as described above counting the number of points n_r inside. The results are standardised by dividing this number of points, which is dependent on the radius, by the mean density λ, giving the K-function,

$$K(r) = \frac{n_r}{\lambda}. \tag{7.38}$$

In this equation, n_r represents the mean number of tree base points in a circle with radius r drawn around the tree base points. The intensity of the points is represented by λ, which indicates the mean number of points per unit area. According to Ripley (1977), the K-function for a random distribution in a Poisson forest would be the parabola

$$K(r) = \pi \times r^2, \text{ for } r \geq 0. \tag{7.39}$$

Thus, with increasing radius r, we obtain a quadratic increase in the expected number of trees in the concentric circles drawn around the tree base points. The positive deviations from this parabola, found for small tree distances as shown in Fig. 7.23a, indicate aggregation and clustering in the distribution pattern. Negative deviations from the parabola indicate inhibition, or a tendency towards regularity. The K-function depicted in Fig. 7.23a shows a tree distribution pattern in which nearby trees occur in clusters, for example in clumps or groups, becoming less dense further away.

For n trees on an experimental plot with size A, Ripley's K-function is estimated for a specified radius r by

$$\hat{K}(r) = \frac{1}{\lambda} \times \sum_{i=1}^{n} \sum_{j=1}^{n} \frac{P_{ij}(r)}{n-1} \tag{7.40}$$

with

$$P_{ij}(r) = \begin{cases} 1 & \text{if} \quad r_{ij} \leq r \\ 0 & \text{if} \quad r_{ij} > r \end{cases}, \tag{7.41}$$

where r_{ij} is the distance between tree i and tree j, and $\lambda = n/A$ represents the mean point density. At this stage it is important to note that methods for boundary correction may need to be used when the radius r extends beyond the boundary of the experimental plot.

7.3.4.2 Practical Example

What do the K-functions look like for regular, clumped and random structures in the Norway spruce stands we presented earlier by way of example (cf. Fig. 7.24)?

The stepped K-function in the regularly stocked Norway spruce stand (Fig. 7.25a) indicates a high degree of regularity in the initial and mature stand (grey and black lines respectively). A periodicity is evident in zones that deviate from the Poisson-forest (parabola shown by a thin line) positively or negatively (aggregation and inhibition respectively). If the sample circle with the radius r meets a row of trees, a zone of clustering results; in between an area of lower density, or inhibition, occurs. This explains the stepped K-functions resulting.

The Norway spruce stand with a random structure initially (Fig. 7.24b) largely maintains this structure until the end of the prediction period (Fig. 7.25b). A tendency towards regularity, strived for in managed forests, is barely distinguishable in the K-function. However, for small radii, a slight thinning out of the structure as a result of competition is discernible.

The initially clumped Norway spruce stand (Fig. 7.24c) reveals zones of clustering in the initial stand within 10 m of the centre tree, and zones of inhibition at greater distances in the zone between clusters (Fig. 7.25c). In the final stand, these clusters have largely dissipated through the self-thinning process so that the

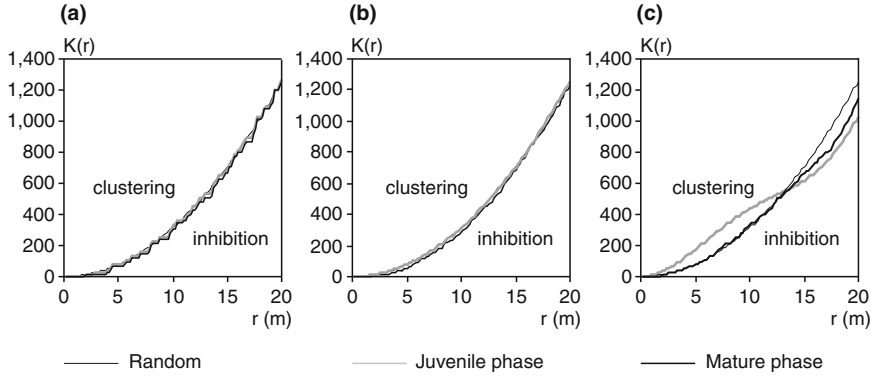

Fig. 7.25 K-functions for (**a**) regular, (**b**) random, and (**c**) clumped Norway spruce stands in the juvenile growth phase (*grey line*) and mature phase after self-thinning over 100 years (*black line*). As a reference, the parabola $K(r) = \pi \times r^2$ produced in the event of a Poisson distribution is shown. The analysis is based on the stands presented in Fig. 7.24

distribution pattern in zones at distances of 12–13 m tends to be random. Although less distinctive, the lower density evident in the zones between the clusters initially is maintained over time.

7.3.5 L-Function

7.3.5.1 Methodological Principles

The transformation of K(r) developed by Besag (1977) has proven useful for identifying, and statistically testing deviations in the observed point distribution from the random distribution. This transformation,

$$L(r) = \sqrt{\frac{K(r)}{\pi}}, \quad \text{for } r \geq 0 \tag{7.42}$$

linearises K(r) when the distribution is entirely irregular and stabilises the variance. The L-function for a Poisson forest is,

$$L(r) = r, \quad \text{for } r \geq 0, \tag{7.43}$$

which forms the angle bisector in the graph presented (Fig. 7.26). Besag's (1977) L-function is interpreted similarly to the K-function. The function values K(r) are merely transformed to represent the Poisson forest by the angle bisector. Positive deviations from this angle bisector indicate clustering, and negative deviations indicate inhibition in a particular stand up to a given radius r. The L-function simply

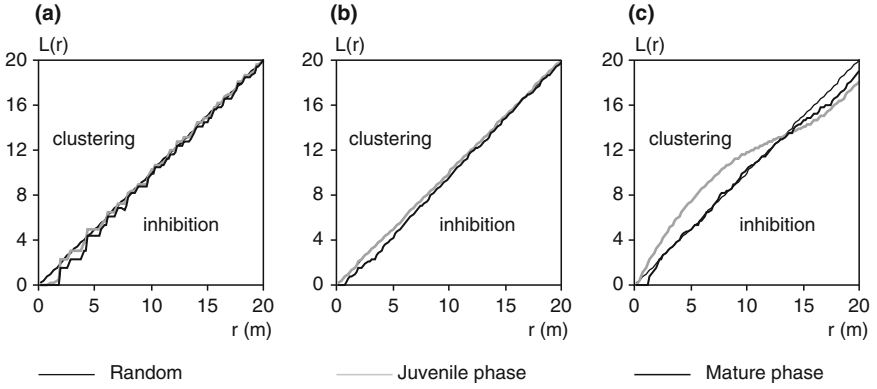

Fig. 7.26 L-functions for (**a**) regular, (**b**) random, and (**c**) clumped Norway spruce stands in the juvenile growth phase (*grey line*) and mature phase after self-thinning over 100 years (*black line*). As a reference, the angle bisector line L(r) = r produced in the event of a Poisson distribution is shown. The analysis is based on the stands presented in Fig. 7.24

reflects the information from the K-function in linear form, with the advantage that deviations from the straight line and angle bisector are more easily recognised than deviations from a parabola.

7.3.5.2 Practical Example

In the regularly structured Norway spruce stand, the distribution pattern is described by a stepped L-function (Fig. 7.26a). In this graph, the angle bisector represents the L-function of a random distribution so that a deviation from this reference is more evident. In the initial (grey line), and the mature stand (black line), the effect of the regular square spacing is evident in the strong inhibition up to distances of 2 m and the continuous, moderate inhibition up to 4 m. In zones at greater distances, the alternating clustering, when plant rows occur, and inhibition, in the zones between, is no longer as clear because it becomes more difficult to separate plant rows from the in-between zones as the radius increases. Whereas the L-function in the initially randomly structured Norway spruce stand follows the reference curve for a random distribution, the change brought about by self-thinning over 100 years causes inhibition within 10 m of the trees (Fig. 7.26). The L-function for the final stand (black line) points to inhibition caused by competition in the vicinity of trees in the final stand. Furthermore, the clumping in the initial stand and the change to a more random structure over time (Fig. 7.26c) is more evident when represented by the L-function.

7.3.6 Pair Correlation Functions for Detailed Analysis of Tree Distribution Patterns

7.3.6.1 Methodological Principles

Before the estimation function for the pair correlation function g(r) is introduced in detail (7.47), the principle and meaningfulness of the function is explained by outlining the procedure followed to derive it. A tree distribution on a plot W with an area A, n observed points and point density $\lambda = n/A$ is analysed. A ring with a mean radius r is drawn around every tree base point in the tree distribution (Fig. 7.27). By counting the trees on the ring, the mean number of tree pairs at a given distance r can be determined. By increasing the radius r of the ring gradually, and repeating the count, the number of tree pairs is determined in relation to distance. The occupation densities found are then related to the expected frequency for the Poisson distribution. The function g(r) expresses the extent to which the tree distribution pattern changes with increasing distance, whether the distribution remains random within the entire observation area, and whether accumulation can be identified at certain distances, as might be expected for square spacing, for example. The function identifies the distance at which deviations from the random distribution occur, and whether these deviations indicate clumping or regularity.

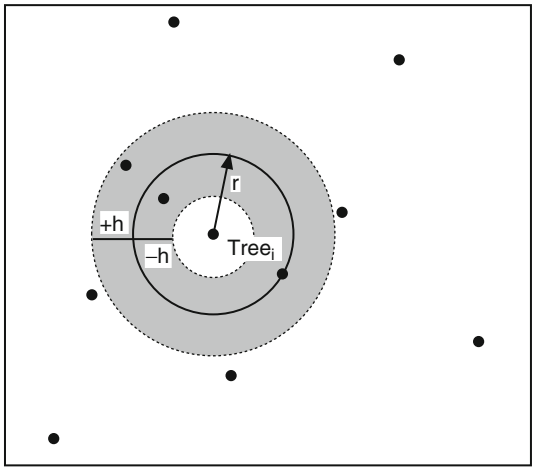

Fig. 7.27 To estimate the pair correlation function g(r), the positions of all trees that occur within r ± h (r = actual radius, h = bandwidth around r) are recorded in relation to each stem base point (*range between dotted circles*). The closer the neighbouring trees (*black points*) are to the circle with radius r (*black line*) the more they influence the value of the pair correlation function. After an analysis of the area surrounding each tree, r is increased by a given value and the algorithm is repeated

If the pair correlation function $g(r) = 1.0$, it indicates that the number of tree pairs at a distance r accords with the expected number in a Poisson distribution (Fig. 7.23c). If g(r) is 1.0 for all r, then an entirely random distribution is apparent. If $g(r) > 1.0$, then the point pairs at distance r are more frequent than for a Poisson distribution of the same intensity, indicating clumping. If $g(r) < 1.0$, then the number of point pairs at a distance r is lower than for a Poisson distribution. Hence segregation is observed. For small r, below the minimum distance observed between trees in the stand r_0, the pair correlation function $g(r) = 0$. As r increases, g(r) approaches the value 1.0. For the g-function, and similarly for the K- and L-functions, the radius r and the circle it describes will eventually reach a size at which λ, the intensity recorded, does not deviate from the total intensity of the area. Above this radius, a deviation from the random distribution can no longer be detected, and the correlation functions lose their meaningfulness from this point on.

A hard core that is a minimum distance within which no neighbours occur or neighbours rarely occur is typical for tree distribution patterns in pure evenaged stands (lower continuous line in Fig. 7.23c). Due to the competition for resources, the point density in close proximity to the trees is sparser than for a random distribution. When the distance r increases, the density also increases and oscillates as it approaches the 1.0 line. The more apparent regularity of the distribution pattern, the more distinct and consistent the oscillations. However, a completely different pair correlation function is found in a Sessile oak–European beech mixed stand for example (upper broken line in Fig. 7.23c). Here, to protect the Sessile oak trees, they are interspersed with European beech. The minimum distance between trees defines

the hard core. Outside, clustering occurs, which only converts to a random distribution at greater distances. The two pair correlation functions in Fig. 7.23c (below and above) demonstrate the stand structure limits.

7.3.6.2 Algorithms for Estimating the Pair Correlation Function

Before calculating the pair correlation function g(r), the following decisions need to be made. First, one needs to establish the smallest radius r_{min} and the largest radius r_{max}, defining the beginning and endpoint of the tree distribution pattern analysis. The size of the area needs to be considered when setting the value rmax to ensure the edge effect is tolerable. Second, the gradation Δr, needed to estimate g(r), must be determined. Third, the width h of the ring in which the point distribution is analysed needs to be defined (Fig. 7.27). The gradations and the width h determine the sensitivity of the analysis. Large gradations and widths produce smoothed functions, whereas smaller gradations and widths result in greater oscillations in the pair correlation function. The procedure for calculating the pair correlation function is outlined in the following nine steps:

1. The assumed initial radius r for g(r) is r_{min}.
2. A circle with the radius r is drawn around any tree i with tree base point at point q_i.
3. All trees within the stand j are checked to determine whether they lie on the ring $r \pm h$. The trees on the ring are counted and weighted more heavily the closer they are to the mean radius r in the band $r \pm h$. If q_i is the stem base point of the tree at the centre of the ring, and q_j the stem base point of another tree, then the auxiliary variable Z_j is calculated according to

$$Z_j = k_h \times \left(r - \left\|q_j - q_i\right\|\right), \tag{7.44}$$

   where $\left\|q_j - q_i\right\|$ represents the Euclidean distance between the points q_j and q_i. By applying an appropriate core function $k_h(t)$ with $t = r - \left\|q_j - q_i\right\|$ (Stoyan and Stoyan 1992, p. 389), Z_j is greater than zero only if the distance between q_j and q_i lies within the width $r \pm h$. Outside this bandwidth, the core function adopts the value 0. Furthermore, Z_j increases as the distance between the two points approaches r.
4. The expression Z_i is calculated from the sum of all Z_j:

$$Z_i = \sum_{\substack{j=1 \\ (j \neq i)}}^{n} Z_j. \tag{7.45}$$

5. The steps 2–4 are carried out for all trees in the area W so that a value Z_i is known for all trees.
6. All Z_i are summed to obtain the expression Z:

$$Z = \sum_{i=1}^{n} Z_i. \tag{7.46}$$

7. Z is placed in (7.47) to obtain an estimate of g at the point r:

$$\hat{g}(r) = \frac{Z}{2 \times \pi \times r \times \hat{\lambda}^2 \times \gamma(r)}. \tag{7.47}$$

   The numerator in (7.47) describes the point density determined by counting the points in each ring with radius r. The denominator describes the theoretical, expected frequency of occupation for the Poisson distribution, where $\lambda = n/A$ represents the mean point density and $\gamma(r)$ evens out of the edge effect.
8. In the next analytical cycle (Steps 2–8) r is increased by Δr.
9. As long as $r \leq r_{max}$, the steps 2–8 are repeated. For each radius r a value $\hat{g}(r)$ is derived and produces the pair correlation function.

In summary, given the coordinates of the points $q_{i,i=1\ldots n}$, the pair correlation function $\hat{g}(r)$, is estimated by the equation

$$\hat{g}(r) = \frac{1}{2 \times \pi \times r \times \hat{\lambda}^2 \times \gamma(r)} \sum_{i=1}^{n} \sum_{\substack{j=1 \\ (j \neq i)}}^{n} k_h \times \left(r - \left\|q_j - q_i\right\|\right), \quad \text{for } r > 0, \tag{7.48}$$

where $\hat{g}(r)$ is the estimate of the pair correlation function at the point r, q_i, q_j are points i and j with the coordinates x_i, y_i and x_j, y_j, $\left\|q_j - q_i\right\|$ represents the Euclidean distance between q_j and q_i calculated from $\left\|q_j - q_i\right\| = \sqrt{\left(x_j - x_i\right)^2 + \left(y_j - y_i\right)^2}$, n is the number of points in the study area W, and $k_h(t)$ is the kernel function, which constructs a bandwidth around r, and includes the weighted points in the numerator. Stoyan and Stoyan (1992, p. 389) recommend the Epanecnikov-kernel function (7.49). The term $\gamma(r)$ in (7.48) represents a function for edge correction in the pair correlation function (cf. Stoyan and Stoyan 1992, p. 141).

The reasons for applying the core function $k_h(t)$ is that all point pairs, whose distances approximate r, should be included. The Epanecnikov kernel (Stoyan and Stoyan 1992) may be used:

$$k_h(t) = \begin{cases} \frac{3}{4h} \times \left(1 - \frac{t^2}{h^2}\right), & \text{if} \quad -h \leq t \leq h \\ 0, & \text{if} \quad t > h \text{ or } t < -h \end{cases}, \tag{7.49}$$

where h is the bandwidth of the kernel function. The selection of h is generally more important than the selection of the kernel function. A small h produces detailed pair correlation functions, whereas a large h results in smoother pair correlation functions. Stoyan and Stoyan (1992) recommend that size of h be determined from the equation $h = c \times \lambda^{-1/2}$, where $c = 0.1, \ldots, 0.2$.

The relationship between the pair correlation function g(r) and Ripley's K-function is

$$g(r) = \frac{\frac{dK(r)}{dr}}{2 \times \pi \times r}. \tag{7.50}$$

This equation highlights the fact, graphically presented at the outset, that K(r) records the cumulative point density on the circular band with the radius r and g(r) determines the point density on each of the circular bands with radius r. By deriving K(r) from r, one obtains a pair correlation function for analysing the changes in spatial occupation with increasing distance in more detail than the K- and L-functions, which show the cumulative occupation density instead.

7.3.6.3 Examples of Pattern Analysis using the Pair Correlation Function

As the pair correlation function does not register an aggregated tree frequency with increasing distance but rather registers the changes in the frequency with increasing distance, it is more sensitive than the K- and L-functions, and also reveals small changes in the distribution pattern. Using the pair correlation function, we characterise the horizontal tree distribution patterns for Norway spruce stands with regular, clumped and random structures presented earlier (Fig. 7.24).

In a stand with a regular distribution pattern, the pair correlation function produces a periodic sequence of maxima and minima for the initial and final stand (Fig. 7.28a, grey and black lines respectively), highlighting the very high degree of order in the tree distribution pattern. Positive deflections mark clustering coinciding with the occurrence of plant rows, and negative deflections mark the in between zones. The decline in amplitude with stand age results from the self-thinning processes over the 100 year prediction period as competition eliminates the immediate neighbours of the dominant and predominant trees. Initially, the pair correlation functions of the randomly structured Norway spruce stand (Fig. 7.28b) oscillate about the reference line representing a random distribution. After 100 years, the stand clearly has become less dense in close proximity to the remaining trees.

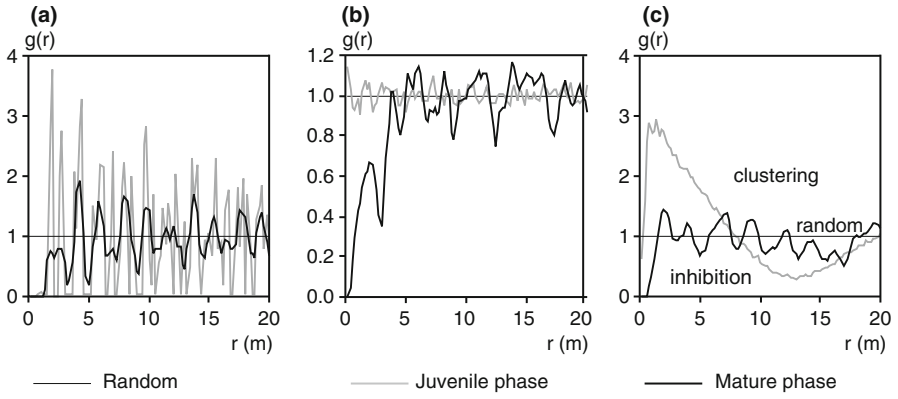

Fig. 7.28 Pair correlation functions for a (**a**) regular, (**b**) random, and (**c**) clumped Norway spruce stand in the juvenile growth phase (*grey line*) and mature phase after self-thinning over 100 years (*black line*). As a reference, the line $g(r) = 1.0$ parallel to the abscissa produced in the event of a Poisson distribution is shown. The analysis is based on the stands presented in Fig. 7.24

The first maximum is observed at distances of 5–7 m. Thereafter, at multiples of this distance, clustering and inhibition are found periodically within the stand. This corresponds to the fact that vigorous dominant and predominant trees in mature Norway spruce stands are about 7–8 m apart. The distinctive clumping in the initial stand (Fig. 7.28c) is more evident in the pair correlation function than in either the K- or L-function. Through self-thinning processes, clumping in the initial stand (grey line) gradually becomes random to regular over time. Similarly, in the mature stand (black line), segregation in the regular, random and clumped stands occurs as a result of self-thinning close to the trees. At greater distances, inhibition and clustering occur periodically, resulting in a more regular distribution of trees in the final stand, which probably facilitates the best possible exploitation of the stand resources.

7.4 Stand Density

7.4.1 Stocking Density

7.4.1.1 Stocking Density with Reference to Yield Tables

These approaches use the appropriate yield table values, e.g. stand basal area or standing volume, as a reference for quantifying stocking density. The observed basal area of a given stand ($m^2\ ha^{-1}$), or the observed standing volume (m^3 merchantable timber ha^{-1}) is related to the expected values from the yield tables. For a given species, the yield table for moderate thinning is usually relevant. Stocking density is used in descriptions of stand density, estimations of volume increment in stands in which the density does not conform to the yield tables, definitions of thinning, and for quantifying the stand opening up needed to promote regeneration.

The stocking density SD, based on stand basal area, for pure and mixed stands with n tree species is calculated as follows:

$$SD^{yt} = \sum_{i=1}^{n} \frac{BA^{obs}_{\text{tree species}_i}}{BA^{yt}_{\text{tree species}_i}}, \tag{7.51}$$

where BA^{obs} reflects the actual stand basal area, and BA^{yt} the basal area values per hectare from the relevant yield tables. The stocking density is calculated analogously in relation to standing volume. In practice, the derivation of the mixture proportion of tree species in mixed stands is based on the stocking density. To obtain the growing space requirements of each species, forest practice adjusts the observed basal area proportions in mixed stands (BA^{obs}) by the basal area predicted in the yield tables for pure stands (BA^{yt}) on the given site. The mixture proportion of species i in a mixed stand with n species is

$$\text{Mixing proportion}_{\text{species}_i}(\%) = \frac{\frac{\text{BA}^{\text{obs}}_{\text{species}_i}}{\text{BA}^{\text{yt}}_{\text{species}_i}}}{\sum_{j=1}^{n} \frac{\text{BA}^{\text{obs}}_{\text{species}_j}}{\text{BA}^{\text{yt}}_{\text{species}_j}}} \times 100. \tag{7.52}$$

Thus, the calculation of stocking density and the mixture proportion incorporates the species-specific growing area. In this formula, the relationship between species basal area in the pure stand, which expresses the species-specific packing density, is used to adjust the observed basal areas to determine a species' share of the stand area. Although this approach is frequently used in forest practice, more convincing approaches for calculating mixture proportions are common in forest science (Chap. 9, Sect. 9.3.3).

7.4.1.2 Natural Stocking Density

The natural stocking density SD^{nat} is given by the quotient

$$\text{SD}^{\text{nat}} = \frac{\text{BA}^{\text{obs}}_{\text{stand}_i}}{\text{BA}^{\text{obs}}_{\text{max}}} \tag{7.53}$$

with the observed stand basal area of a given stand in the nominator, and the maximum basal area possible per hectare on neighbouring untreated control plots in the denominator.

7.4.2 Percentage Canopy Cover (PCC)

The percentage canopy cover, another measure of stand density, indicates the percentage of stand area covered by crowns:

$$\text{Percentage canopy cover}\,(\%) = \frac{\text{area of crown projection}}{\text{total area}} \times 100. \tag{7.54}$$

The stocking density and the percentage canopy cover are not necessarily synchronous. For example, if the stocking density and percentage canopy cover in a European beech stand were reduced significantly by a thinning from above, the percentage canopy cover would recover rapidly as the crowns expand quickly to occupy the increased space available. In contrast, stocking density, based on basal area or standing volume would only increase gradually; crown expansion occurs more quickly and substantially than diameter increment, which determines stocking density. Thus, stocking density and canopy cover are indicators of different aspects of density. The former relates to the density of the standing volume, and the latter relates to the density of the canopy space.

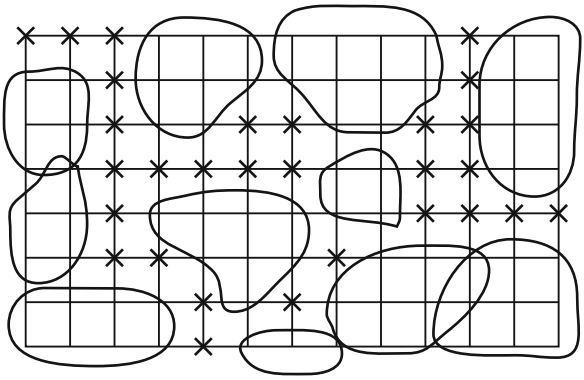

Fig. 7.29 The percentage canopy cover PCC is obtained from a dot count on crown projection maps. For a total of 104 grid points, tree crowns were counted at 75 points, so that the percentage canopy cover is $(75/104) \times 100 = 72.1\%$

Canopy cover is generally analysed by dot counts of crown maps. A grid is laid over the map (Fig. 7.29), and a dot count conducted to determine the percentage canopy cover. The percentage canopy cover is obtained from the number of dot points covered by the crown divided by the total number of grid dot points. The distance between grid lines can be nominated according to the recording density desired. A computer search program carries out a dot count, checking each intersection point on the grid to determine whether a dot point has no canopy cover, or whether it is covered by one, two, three or more crown layers, and the tree species. Conclusions about the nature of canopy cover in the stand can be drawn from the frequency of occurrence of each stand characteristic.

The three calculation methods introduced in Sect. 7.2.1 for drawing crown periphery and analysing canopy cover are presented for the Silver fir–Norway spruce long-term experimental plot, WOL 097/3 Starnberg, by way of example. Figure 7.30 shows the crown map for this site in 1988 after the crown contours are evened out with spline functions, and the canopy cover resulting from one or more crowns (grey and black respectively). The percentage canopy cover for the total stand, recorded in Table 7.3, was determined by a dot count for each stand characteristic (no canopy, one canopy layer, two canopy layers, etc.) at 60,000 points on a grid with lines 20 cm apart. To analyse the crown map, the circumference of the crown projections were reproduced using three different methods: in method 1 the crown corner points are joined with a line to form a polygon; method 2 produces a simplified crown projection by drawing a circle with a radius defined by the quadratic mean of the crown radii around each tree; and in method 3, spline functions are used to connect eight radii for each tree (cf. Fig. 7.30).

The dot count statistic for the spline, and circular crown projection produced total canopy cover values that were 2–3% higher and 2–3% lower than the linear approximation respectively. Multiple canopy cover is identified more frequently in the non-linear approximations (methods 2 and 3) than in linear approximations because they

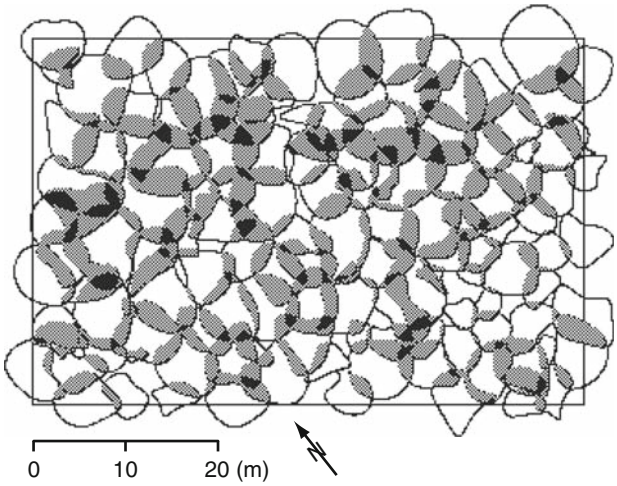

Fig. 7.30 Crown projection maps of the Silver fir–Norway spruce experimental plot WOL 097/3, near Starnberg from the inventory in spring 1988, presented using spline functions. Areas covered by one crown are marked *white*, by two crowns *grey*, and areas covered by more than two crowns are marked in *black*

Table 7.3 Percentage canopy cover PCC in the Silver fir–Norway spruce mixed stand, Wolfratshausen 097/3 near Starnberg. Results of canopy cover analyses from three different methods for evening out crown radii are listed: linear approximation of the eight crown radii, approximation of the crown surface area using circles, and use of spine functions to connect the radii

Method for evening out	Uncovered (%)	Covered (%)	Onefold (%)	Twofold (%)	Threefold (%)	Fourfold (%)
Linear	10.3	89.7	61.6	26.1	2.0	0.0
Circle	12.7	87.3	48.4	33.7	5.2	0.0
Spline	7.4	92.6	54.3	33.2	4.6	0.5

produce a more rounded crown shape. A series of test calculations for additional study plots confirmed that the total canopy cover values from the spline approach were up to 10% higher than those from the linear approximation. These systematic differences, inherent in the method applied, should be taken into account in the interpretation of the canopy cover values from different methods.

7.4.3 Mean Basal Area, mBA, by Assmann (1970)

The density measures, periodic mean basal area (mBA) and relative periodic mean basal area (mBA_{rel}), are frequently used in the analysis and modelling of stand growth, management of thinning trials, and for the regulation of stand density in silvicultural prescriptions. If bBA is the basal area at the beginning of a growth

period, eBA the basal area at the end of that growth period, and m indicates the number years in the growth period, then, for the growth periods $1, \ldots, n$,

$$mBA = \frac{\left(\frac{bBA_1+eBA_1}{2}\right) \times m_1 + \left(\frac{bBA_2+eBA_2}{2}\right) \times m_2 + \cdots + \left(\frac{bBA_n+eBA_n}{2}\right) \times m_n}{m_1 + m_2 + \cdots + m_n}. \tag{7.55}$$

Thus, the periodic mean basal area in period $1 \ldots n$ (mBA) is determined from the means of the basal area at the beginning and end of the each growth period $1, \ldots, n$, weighted by the length of the growth periods.

When the observed mBA of a stand is determined according to (7.55) and divided by the periodic mean basal area in period $1 \ldots n$ of an untreated stand on a similar site with maximum stocking (self-thinning conditions), then the relative periodic mean basal area (mBA_{rel}) is

$$mBA_{rel} = \frac{mBA_{obs}}{mBA_{max}}. \tag{7.56}$$

As the relative periodic mean basal area (mBA_{rel}) uses the maximum stand basal area as a reference, it is a biologically meaningful measure for quantifying stand density. In managed stands mBA_{rel} ranges from 0–1.0; $mBA_{rel} = 0.7$ when 30% of the basal of the unthinned stand is removed. Assmann (1971, pp. 216–235) applied mBA_{rel} to define the dependence of growth on stand density (maximum, optimum and critical mBA_{rel}), and for quantifying density and estimating volume growth in relation to thinning severity (Chap. 5, Sect. 5.2.2). He named mBA_{rel} the natural stocking rate, and used mBA_{rel} to derive the "growth reduction tables" appended to the Norway spruce yield table (Assmann and Franz 1963).

7.4.4 Quantifying Stand Density from the Allometry Between Mean Size and Plants per Unit Area

At the stand level, allometry is investigated mainly with respect to the self-thinning rules, which describe the relationship between plant size or weight and number of viable plants per unit area (Long 1984; Weller 1987, 1990; White 1981). The rules proposed by Reineke (1933) for woody plants, and by Yoda et al. (1963) for herbaceous plants are well-known outcomes of allometric investigations. Figure 10.13 in Chap. 10, Sect. 10.4 shows the common principle of Reineke's rule (1933), and the $-3/2$ power rule by Yoda et al. (1963). Both authors define the relationship between average plant size, or average plant weight and plant number as a straight line in a double-logarithmic scale. The stand density index SDI, introduced later, is based on the self-thinning rule Reineke (1933) introduced for densely stocked pure evenaged stands.

7.4.4.1 Stand Density Rule from Reineke (1933)

The stand density rule from Reineke (1933) describes the relationship between mean diameter d_q and stem number N per hectare in a fully stocked, unmanaged, pure evenaged stand:

$$N = a \times d_q^b. \tag{7.57}$$

This relationship can be represented by a straight line in the double logarithmic coordinate system:

$$\ln N = \ln a + b \times \ln d_q \tag{7.58}$$

with the intercept ln a and slope b. Reineke (1933) postulated $N \propto d_q^b$, with $b = -1.605$; i.e. an increase in the mean diameter d_q by 1% results in a decrease in tree number N of $b = 1.605\%$ for all species. Reineke's exponent was analysed and differentiated for different tree species (Pretzsch 2005; Pretzsch and Biber 2005), site conditions (von Gadow 1986), and stand histories (Rio et al. 2001) (cf. Chap. 10, Sect. 10.4).

7.4.4.2 Stand Density Index from Reineke (1933)

Reineke (1933) based his stand density index SDI on this allometric relationship between stem number N and quadratic mean diameter d_q:

$$SDI = N \times \left(\frac{25}{d_q}\right)^{-1.605}. \tag{7.59}$$

For a stand with an observed quadratic mean diameter d_q and an observed tree number N per hectare, the index SDI indicates the expected number of trees in a stand with an index diameter of $d_q = 25\,\text{cm}$. In other words, SDI reflects the number of trees a stand has when $d_q = 25\,\text{cm}$. It is assumed that the number of trees decreases according to the stand density rule with gradient $b = -1.605$, i.e. the expected tree number is extrapolated from the observed tree number with the slope b in the stand with $d_q = 25\,\text{cm}$ (Fig. 7.31).

The extrapolation from an observed quadratic mean diameter d_q and tree number N to an index diameter of $d_q = 25$ is illustrated in Fig. 7.31. The tree numbers $N_1, \ldots, N_6$ are plotted against the mean diameter $d_{q_1}, \ldots, d_{q_6}$ in a double logarithmic grid for a forest stand at the survey time points $t_1, t_2, t_3, \ldots, t_6$. To quantify the stand density at the survey time point t_1 or t_6 with the stand density index, a line with a slope $b = -1.605$ is drawn through the points t_1 or t_6 so that the expected stem number for a stand with a quadratic mean diameter $d_q = 25$ can be read off the graph. Stand density indices result, which, in our example, have the values $SDI(t_1) = 200$ and $SDI(t_6) = 2{,}000$ respectively, and indicate the tree number per hectare this stand would have if the stand density remained constant in the time taken for the stand to attain a quadratic mean diameter $d_q = 25$.

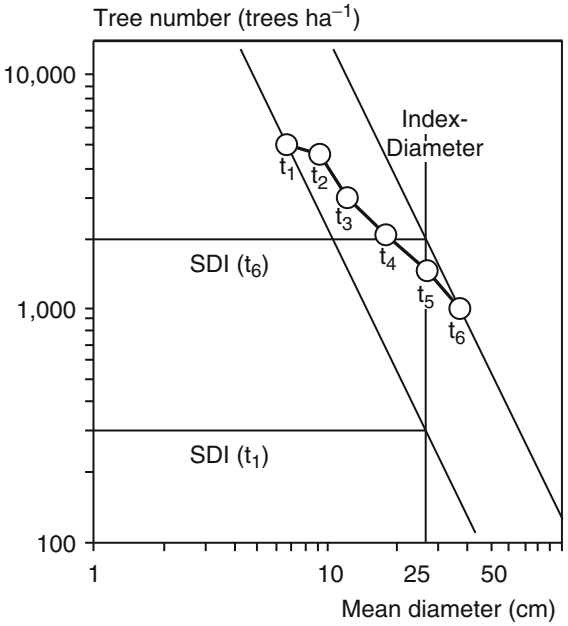

Fig. 7.31 To quantify the stand density with the stand density index SDI, stem number development can be plotted against mean diameter giving the trajectory $t_1 \rightarrow t_2 \rightarrow t_3, \ldots, t_6$ in the double logarithmic net. To quantify the density in the development stage, t_1, or t_6, e.g., a line is drawn through these points with the gradient $b = -1.605$. One can then determine the stem number that a stand with an index diameter of $d_q = 25\,\text{cm}$ would have for the $\text{SDI}(t_1) = 200$ and $\text{SDI}(t_6) = 2,000$ respectively

Table 7.4 Range in values of stand density index SDI by Reineke (1933) for the main tree species (adapted from Sterba 1991). For example, the maximum stocking density expected in Norway spruce and Silver fir stands with a mean diameter of $d_q = 25\,\text{cm}$ ranges from 900 to 1,100 and 800 to 1,000 trees per hectare respectively

Species		Norway spruce	Silver fir	Douglas fir	European larch	Scots pine	European beech	Common/ Sessile oak
SDI (trees per ha)	from	900	800	700	500	600	650	500
	to	1,100	1,000	900	600	750	750	600

Sterba (1991) provides stand density indices for the main tree species at maximum stocking densities. These vary according to the spatial requirements of tree species and site characteristics (Table 7.4). Whereas one can expect 900–1,100 trees per hectare with a quadratic mean diameter of $d_q = 25\,\text{cm}$ in a Norway spruce stand with maximum stocking density and optimal growing conditions, and similarly high values for Silver fir and Douglas fir, the stand density indices for Sessile oak and European larch are only about half that, with 500–600 trees per hectare. Moderate values of 600–750 trees per hectare with a quadratic mean diameter of $d_q = 25\,\text{cm}$

are found for Scots pine and European beech. Reineke's SDI is frequently used in density estimation (Zeide 2004) and density control (Bégin et al. 2001).

7.4.5 Crown Competition Factor CCF

The crown competition factor CCF indicates the relationship between the total crown projection area, of all trees in a stand and stand area, A. It is a relative measure of the packing density in the crown space. The greater the crown projection area is in a stand with a given stand area A, the stronger the packing density in the crown space, and the higher the crown competition factor CCF. There is a significant difference between percentage canopy cover PCC and CCF (Sect. 7.4.2). Whereas PCC is calculated from the observed crown areas of individual trees, CCF is based on the potential crown area expected for each tree under optimal growing conditions. The potential crown area is calculated from tree diameter at breast height in a given relationship. To derive a relationship for the estimation of potential crown area, the linear relationship

$$cd = a_0 + a_1 \times d, \tag{7.60}$$

is fitted to pairs of crown diameter values, cd, and the diameters at breast height, d, of trees with maximum crown extension, for example solitary trees. The crown diameter, $cd = 2 \times \bar{r}_q$, is usually obtained from the quadratic mean of multiple crown radii measurements per tree $\bar{r}_q = \sqrt{(r_1^2 + r_2^2 + \cdots + r_n^2)/n}$. Potential crown projection area cpa is estimated by

$$cpa = (a_0 + a_1 \times d)^2 \times \pi/4 \tag{7.61}$$

from the diameter at breast height, d. Circular crown projections are assumed in this calculation. The crown competition factor CCF for a forest stand with an area A and tree number n is given by a quotient of the sum of the potential crown projection areas $cpa_1 \ldots cpa_n$ expected for solitary trees and the stand area A multiplied by 100:

$$CCF = \frac{1}{A} \times \sum_{i=1}^{n} cpa_i \times 100. \tag{7.62}$$

For a better understanding, crown competition factors of different stands are presented in Fig. 7.32. In the absence of high crown competition, that is when solitary trees occur, the crown competition factor is below 100% (Fig. 7.32a). If the stand density increases to the extent that the trees just achieve their maximum crown projection area, such that crown development is not limited by neighbouring competition and yet the entire stand is under canopy cover, then the crown competition factor is about 100% (Fig. 7.32b). Once the trees in the stand can no longer achieve maximum crown projection area cpa without touching their neighbours, it indicates

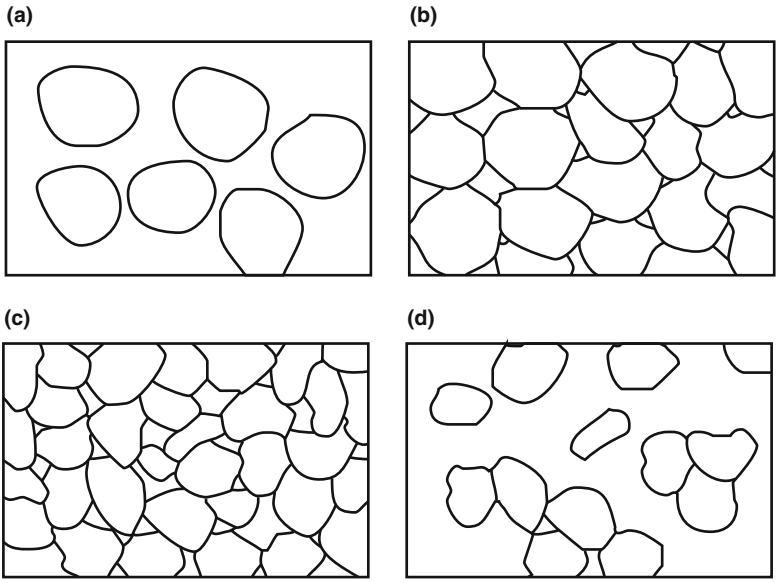

Fig. 7.32 Description of stand density by the crown competition factor CCF (adapted from Oliveira 1980, p. 56) for (**a**) stand in growth phase before crown closure (CCF = 50%), (**b**) when complete crown closure is reached (CCF = 100%), (**c**) when crown extension is restricted due to competition (CCF = 200%), and (**d**) crown competition factor of stand (**c**) after thinning (CCF = 100%)

increased competition in both the crown and root spaces, and the CCF value exceeds 100% (Fig. 7.32c). Figure 7.32d shows the stand illustrated in Fig. 7.32c after thinning. The remaining trees still have a CCF value of 100% because they would cover the entire stand if the trees were able to achieve their maximum crown size. Thus the crown competition factor CCF can be interpreted readily in relation to the crown projection area expected in respective stands with maximum crown extension.

7.4.6 Density of Spatial Occupancy and Vertical Profiles

The results from the digitised occupancy of the crown space, shown in Sect. 7.2.3, can be used as statistics for the vertical distribution of crowns in a stand. An example is provided in Fig. 7.33a–c for the experimental plots Zwiesel and Freyung in the Bavarian Forest. These graphs clearly show the percentage of stand space occupied by different tree species at these sites. The percentage spatial occupancy by the crown is shown at 1 m height intervals on the left hand side, and for Norway spruce, Silver fir, and European beech in the centre as well as for all tree species together (SUM). The percentage spatial occupancy was calculated with the program RAUM (Pretzsch 1992a,c), which cuts horizontal planes through the canopy at 1 m height intervals beginning from the forest floor and extending to the treetops. In a search run, each horizontal plane is analysed to determine the number of voxels it

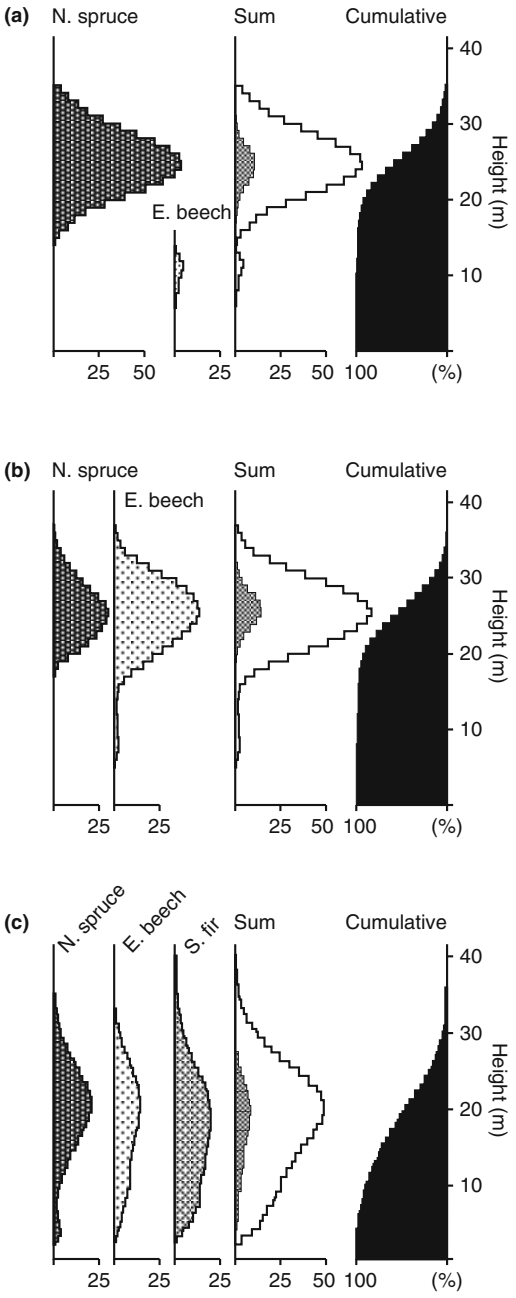

Fig. 7.33 Vertical profile of spatial occupancy for the experimental plots presented in Fig. 7.9 for (**a**) pure Norway spruce stand Zwiesel 111/5, autumn 1982, after thinning, (**b**) Norway spruce–European beech mixed stand Zwiesel 111/3, autumn 1982, after thinning, and (**c**) Norway spruce–Silver fir–European beech selection forest Freyung 129/2, autumn 1980

occupies (cf. Fig. 7.12) and the portion of these cells occupied by different species. Once the search has been completed at all 1 m height intervals, we obtain the percentages for the vertical profile of the canopy, shown in Fig. 7.33. On the right hand side of Fig. 7.33 (cumulative), the cumulative frequency of the presence of tree crowns within the crown space is also provided. The cumulative frequency distribution shows an increase in the spatial occupancy from the treetops to the forest floor. This gradient is an indicator for light extinction within the crown space.

Figure 7.33a shows the vertical profile of the canopy cover in the pure Norway spruce stand Zwiesel 111/5 (survey in autumn 1982), where the crowns meet in a narrow height zone at about 25 m. At this height range, as the cumulative graph shows, crowns occupy about 75% of the cells in the spatial matrix, and multiple occupancies at cell midpoints of the spatial matrix (grey density curve in the SUM category) are most frequent. In the Norway spruce–European beech mixed stand Zwiesel 111/3 (survey in autumn 1982), the frequency distribution by height is broader (Fig. 7.33b). The cumulative frequency distribution is trapeze-shaped. In the Norway spruce–Silver fir–European beech selection forest Freyung 129/2 (survey autumn 1980), all species present are found distributed along the entire height range. The cumulative frequency distribution is triangular, indicating a more intense light penetration into the lower storeys (Fig. 7.33c).

7.5 Differentiation

7.5.1 Coefficient of Variation of Tree Diameters and Heights

The coefficient of variation of both diameter and height, frequently are used to quantify the size heterogeneity within a stand. The coefficients VAR_d

$$VAR_d = \frac{\sqrt{\sum_{i=1}^{n} \frac{(d_i - \bar{d})^2}{n-1}}}{\bar{d}} \times 100, \tag{7.63}$$

where $\bar{d}$ = arithmetic mean diameter and d_i = diameter at breast height of the $i = 1, \ldots, n$ trees in a stand and, analogously, VAR_d is used to analyse tree size variation, sample size, stand stability or conversion capacity.

7.5.2 Diameter Differentiation by Füldner (1995)

The diameter differentiation T_i quantifies diameter heterogeneity in the immediate neighbourhood of a tree i (Füldner 1995, 1996; Gadow 1993). For a central tree $i, i = 1, \ldots, n$ and its nearest neighbours $j, j = 1, \ldots, m$, the diameter differentiation

T_i is defined as

$$T_i = \frac{1}{m} \times \sum_{j=1}^{m} r_{ij} \tag{7.64}$$

with

$$r_{ij} = 1 - \frac{\min(d_i, d_j)}{\max(d_i, d_j)}, \tag{7.65}$$

where n is the number of central trees, and d_i, d_j are the diameters of the central tree and its neighbours respectively.

The principle of the structural quartet is presented in Fig. 7.34; it comprises a central tree i and its $n = 3$ nearest neighbours. Füldner (1995) found that the structural quartet, comprising a central tree and its three nearest neighbours, is particularly suitable for calculating structural parameters. Based on diameters of the central tree and its three nearest neighbours, the diameter differentiation in this example is

$$T_i = \frac{\left(1 - \frac{40}{40}\right) + \left(1 - \frac{40}{60}\right) + \left(1 - \frac{20}{40}\right)}{3} = \frac{0.00 + 0.33 + 0.50}{3} = 0.28. \tag{7.66}$$

The values of T_i may range from 0 to 1.0. If diameter differentiation is low, as in plantations or mature stands managed for future crop trees, then the T_i values approach 0. The maximum diameter differentiation in selection forests or in mixed-species mountain forests produces T_i-values close to 1.0. If required, the

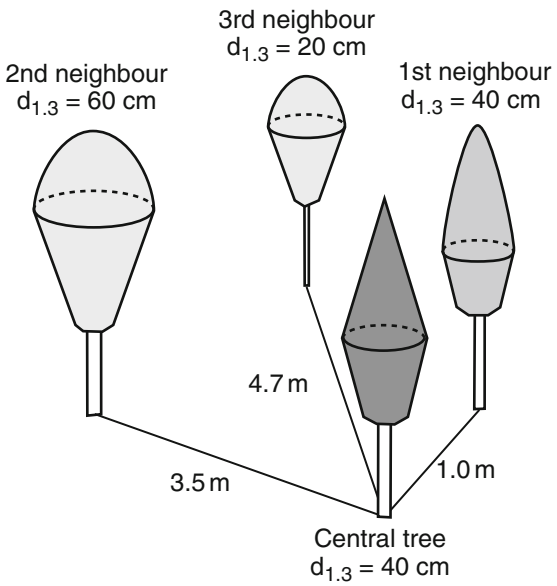

Fig. 7.34 The structural quartet consists of a central tree i and its three nearest neighbours $j = 1, \ldots, n$. According to (7.66), the diameter differentiation for the group presented is $T_i = 0.28$

mean diameter differentiation within a stand can be calculated by obtaining the mean of all T_i values:

$$\overline{T} = \frac{1}{n} \times \sum_{i=1}^{n} T_i. \tag{7.67}$$

Ideally, the stem coordinates and the diameter at breast height of all trees in a stand are known after complete sampling. This affords another way of determining the mean diameter differentiation for a stand. In the calculation of the structural parameters from data recorded in a complete sampling, each tree $i, i = 1, \ldots, n$ is a central tree just once. For each individual tree i, the three nearest neighbours are determined independently. However, in this approach, information about the stand-specific growth arrangement between the centre tree and its first, second and third nearest neighbours is lost. Hence Füldner (1995) suggests that $\overline{T1}$ be calculated:

$$\overline{T1} = \frac{1}{n} \times \sum_{i=1}^{n} T1_i, \tag{7.68}$$

where $T1_i$, is the diameter differentiation between tree i and its first neighbour calculated in (7.64). $\overline{T1}$ quantifies the mean diameter differentiation between the central tree and its first neighbour. Similarly $\overline{T2}$ and $\overline{T3}$ can be calculated, so that the average neighbourhood can be characterised for all trees within the stand in relation to their first, second, and third neighbours.

In the following, the pure and mixed stands comprising Norway spruce, Silver fir and European beech, illustrated in Fig. 7.35, serve as an example for the calculation of the mean T values, $\overline{T}$ and $\overline{T1}$, $\overline{T2}$, and $\overline{T3}$. To underline the diameter differentiation, we depicted the diameters after magnification by a factor of 10. The $\overline{T}$-values range from 0.22 in the pure Norway spruce stand to 0.46 in the Norway spruce–

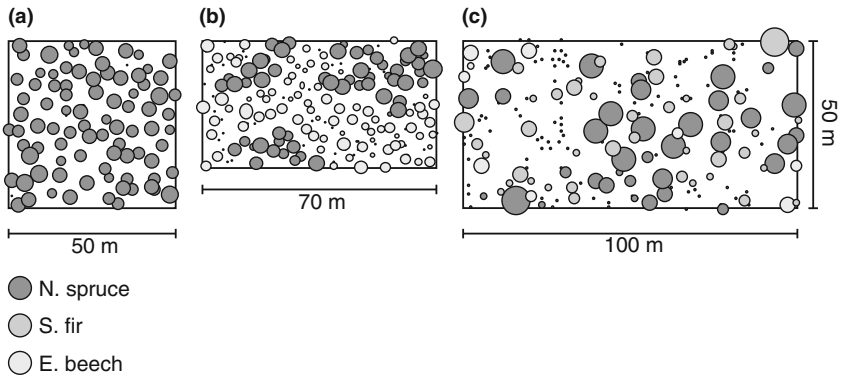

Fig. 7.35 An example showing the calculation of the mean diameter differentiation $\overline{T}$ and the diameter differentiation between the central tree and the first, second and third neighbour $\overline{T1}$, $\overline{T2}$, and $\overline{T3}$ respectively. The values for diameter differentiation in (**a**) the pure Norway spruce stand are $\overline{T} = 0.22$, $\overline{T1} = 0.23$, $\overline{T2} = 0.23$ and $\overline{T3} = 0.21$, (**b**) the Norway spruce–European beech mixed stand, $\overline{T} = 0.32$, $\overline{T1} = 0.32$, $\overline{T2} = 0.31$ and $\overline{T3} = 0.32$, and (**c**) the Norway spruce–Silver fir–European beech selection forest $\overline{T} = 0.46$, $\overline{T1} = 0.48$, $\overline{T2} = 0.46$ and $\overline{T3} = 0.45$

Silver fir–European beech selection stand. In the pure Norway spruce stand, a detailed analysis of the neighbourhood relationships produced $\overline{T1}$, $\overline{T2}$, and $\overline{T3}$ values of 0.23, 0.23, and 0.21 respectively. In the two-layered mixed stand comprising Norway spruce and European beech, the values of $\overline{T1}$, $\overline{T2}$, and $\overline{T3}$ were 0.32, 0.31, and 0.32 respectively. The largest diameter differentiation in the immediate neighbourhood is found in the selection forest, where the values of $\overline{T1}$, $\overline{T2}$, and $\overline{T3}$ were only calculated for trees with $d_{1.3} \geq 7\,\text{cm}$ and amounted to 0.48, 0.46, and 0.45 respectively.

7.5.3 Species Richness, Species Diversity, and Structural Diversity

7.5.3.1 Species Richness and Species Diversity

We adopt the terms species richness and species diversity from genetics (Hattemer 1994; Konnert 1992). Species richness R is defined as the observed number of genotypes, alleles or species. In a mixed stand comprising four species, the species richness R is independent of the frequency distribution of these four species, and simply, $R = 4$.

In contrast, species diversity considers the number and frequency of the species present. If all the occurring genotypes, alleles or species have the same frequency of occurrence, then diversity is at a maximum. The diversity declines as the frequencies become less even. One parameter borrowed from genetics serves to quantify genetic diversity:

$$D = \left[\sum_{i=1}^{n} (p_i)^2\right]^{-1} \tag{7.69}$$

with $i, i = 1, \ldots n$ indicating the number of species present and p_i the relative frequency of the species i.

The Shannon diversity index H is another measure for quantifying diversity, and is also based on the number and frequency of species present. This index, developed by Shannon and Weaver for use in information theory, was successfully transferred to the description of species diversity in biological systems (Shannon 1948):

$$H = -\sum_{i=1}^{S} p_i \times \ln p_i. \tag{7.70}$$

Here, S represents the number of species present, p_i the proportion of a species in the population $(p_i = n_i/N), n_i$ the number of individuals of a species i, and N the total number of individuals.

The sum of the products of the proportion of species in the stand p_i and the logarithmic proportion of the species $\ln p_i$, for all S species occurring, multiplied by -1 produces the index H for species diversity. As the logarithmic transformation of the species proportion is a multiplier in the equation, the index increases dis-

proportionately with the presence of rare and dominant species. This increase is disproportionately high for rare species, and disproportionately low for dominant species, in agreement with the concept that a number of rare species contributes more to species diversity than a few dominant species (cf. Table 7.5).

7.5.3.2 Standardised Diversity, or Evenness E

For a stand with a given number of species S the maximum diversity is

$$H^{max} = \ln S \tag{7.71}$$

and a standardised diversity is obtained from the quotient of the species diversity H (7.70) and the maximum diversity (7.71):

$$E = \frac{H}{H^{max}} \times 100, \tag{7.72}$$

where H represents species diversity, H^{max} maximum species diversity, E standardised diversity or evenness, and S the number of species present in the stand.

When species intermingling is greatest, that is when the proportion of each species present is the same, $E = 100$. E approaches 0 as species diversity decreases. To provide an example, Table 7.5 shows the calculation of the Shannon diversity index H, the maximum diversity H^{max} and the standardised diversity E for three mixed species mountain forest stands, each with a different species intermingling. In stand A, Norway spruce, Silver fir, European beech, and Sycamore maple are all present in equal proportions, at 25% ($p_i = 0.25$). Thus the Shannon diversity index H is equal to the maximum diversity H^{max}, and the evenness is $E = 100\%$. The more unbalanced the proportional intermingling of the four species in stand B and stand C becomes, the lower the species diversity H. In stand B and stand C only 77, and 31%

Table 7.5 Calculation of Shannon's (1948) diversity index H, maximum diversity H^{max} and evenness E (cf. (7.70)–(7.72) respectively) for three mixed-species mountain forest stands (A, B and C) comprising different species mixes of Norway spruce, Silver fir, European beech and Sycamore maple

Tree species	Forest stand A			Forest stand B			Forest stand C		
	p_i	$\ln p_i$	$p_i \times \ln p_i$	p_i	$\ln p_i$	$p_i \times \ln p_i$	p_i	$\ln p_i$	$p_i \times \ln p_i$
Picea abies	0.25	−1.3863	−0.3465	0.60	−0.5108	−0.3065	0.90	−1.1054	−0.0948
Abies alba	0.25	−1.3863	−0.3465	0.20	−1.6094	−0.3219	0.05	−2.9957	−0.1498
Fagus silvatica	0.25	−1.3863	−0.3465	0.15	−1.8971	−0.2846	0.03	−3.5066	−0.1052
Acer pseudoplatanus	0.25	−1.3863	−0.3465	0.05	−2.9957	−0.1498	0.02	−3.9120	−0.0782
H			1.3863			1.0628			0.4280
H^{max}			1.3863			1.3863			1.3863
E (%)			100			77			31

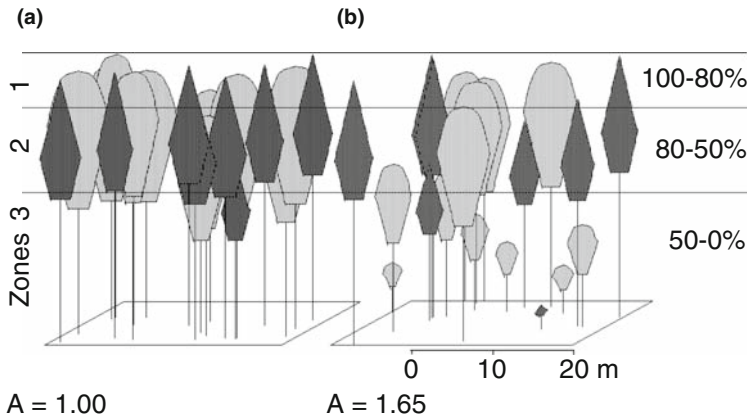

Fig. 7.36 To determine the species profile index A, a stand is divided into three height zones. Zones 1, 2 and 3 range between 100–80%, 80–50% and 50–0% of the maximum height of the stand respectively. To calculate index A, species proportions are recorded by tree species and height zones

of the maximum diversity is reached respectively (E = 77 and 31%, respectively). The Shannon index, and the standardised diversity for a completely even species intermingling are at a maximum, and they decrease as the balance between species decreases. In pure stands, $p_i = n_i/N = 1$ and $H = 0$ because $\ln 1 = 0$. Consequently, $H^{max} = 0$ and $E = 0$, which indicates minimal species diversity.

As the evenness E gives the ratio of observed stand diversity to maximum diversity for a given number of species S, we obtain a standardised or relative diversity, which expresses as a percentage the extent to which a stand with a given number of species S approximates the maximum possible diversity when the proportion of species is entirely even. Therefore, the evenness E may also be used to characterise stands with different numbers of species S in terms of the degree of approximation to, or deviation from maximum diversity and disorder. Since the index H considers the species proportion only, not the spatial occupancy pattern, forest stands with vastly different structures, such as those presented in Fig. 7.36 for example, have the same diversity indices H = 0.67.

7.5.3.3 Species Profile Index by Pretzsch (1995)

Index A for species profiles (Pretzsch 1995), outlined below, is based on the diversity index H by Shannon (1948). In addition to the proportion of the species within a stand, index A takes into account the presence of these species in different height zones. Although, in the determination of index A in the example below, the trees in a stand are assigned to three height zones, any other number of height or diameter zones may be adopted.

To calculate index A, the stand is divided into three height zones $j = 1$, $j = 2$ and $j = 3$, which constitute 0–50%, 50–80% and 80–100% of the maximum stand height

Table 7.6 Mixture proportions of the two Norway spruce–European beech mixed stands, shown in Fig. 7.36 from which the species profile index A is calculated. The species proportions p_{ij} for the three zones and two species are listed

	Species proportion in stand 1		Species proportion in stand 2	
	N. spruce	E. beech	N. spruce	E. beech
Layer 1	0.35	0.55	0.25	0.25
Layer 2	0.05	0.05	0.10	0.10
Layer 3	0.00	0.00	0.05	0.25

respectively (Fig. 7.36). Index A equals

$$A = -\sum_{i=1}^{S}\sum_{j=1}^{Z} p_{ij} \times \ln p_{ij} \tag{7.73}$$

where S represents the number of species present, Z the number of height zones (3 in this example), N the total number of individuals, n_{ij} the number of individuals of the species i in zone j, and p_{ij} the proportion of a species in the height zone $p_{ij} = n_{ij}/N$. The number of individuals of species i in zone j are counted. By calculating the sum of the products of the proportion of a species and the logarithmic proportion of that species for $i = 1{-}S$, and for the height zones $j = 1{-}Z$, one obtains an index that quantifies the overall species diversity and the vertical spatial occupancy of the species present in the forest stand.

Table 7.6 summarises the division of Norway spruce and European beech in the stand depicted in Fig. 7.36 into the height zones 1–3. For the largely single-layered stand 1 (Fig. 7.36a), $A = 0.35 \times \ln(0.35) + 0.05 \times \ln(0.05) + \cdots + 0.05 \times \ln(0.05) = 1.00$. For stand 2, which has greater structural variability (Fig. 7.36b), $A = 0.25 \times \ln(0.25) + 0.10 \times \ln(0.10) + \cdots + 0.25 \times \ln(0.25) = 1.65$. As for the Shannon index H, rare species and trees present in the less occupied height zones produce a disproportional increase in index A. Any deviation from the single-layered pure stand is recognised by a distinct increase in the species profile index A. Instead of classifying individual trees into height zones, and given that tree diameter data are more frequently available than tree height data, diameter classes $j = 1, \ldots, Z$ can also be developed. However, depending on tree species and treatment, trees of a given diameter may differ significantly in height, and thus height still appears a more appropriate measure for an index explicitly used to characterise vertical structural differentiation.

7.5.3.4 Standardised Species Profile Index

The maximum value of the A index for a given number of species S and zones Z is

$$A_{max} = \ln(S \times Z). \tag{7.74}$$

Therefore index A can be standardised according to

$$A_{rel} = \frac{A}{\ln(S \times Z)} \times 100, \tag{7.75}$$

so that comparisons can be made between stands in which the naturally occurring species differ, for example tropical mountain rainforests with a higher number of species and Central European mixed-species mountain forests. In such comparisons, the standardised index indicates the extent to which the structure of the stand in question approximates the maximum possible structural differentiation under the given the natural conditions.

For the stands presented in Fig. 7.36, the relative species profile index would be $A_{rel} = (1.0/1.79) \times 100 = 56\%$, and $A_{rel} = (1.65/1.79) \times 100 = 92\%$ respectively. This suggests that the stand presented in Fig. 7.36b approximates the maximum structural differentiation possible when the total number of individuals N is distributed evenly across species and zones. Index A quantifies the stand feature termed structural diversity in forestry (Fig. 7.37). This is lowest in single-layered pure stands (a). It increases in pure stands with two or more layers (b), still further in mixed stands (c), and achieves its greatest value in highly structured mixed stands (d). This is reflected by a rise in A from 0.29 to 2.02. The A_{rel}-index, which quantifies the relative degree of structural diversity, i.e., the observed diversity in relation to the maximum structural diversity for the given number of species and number of zones distinguished, ranges from $A_{rel} = 26.5$ to 93.5%.

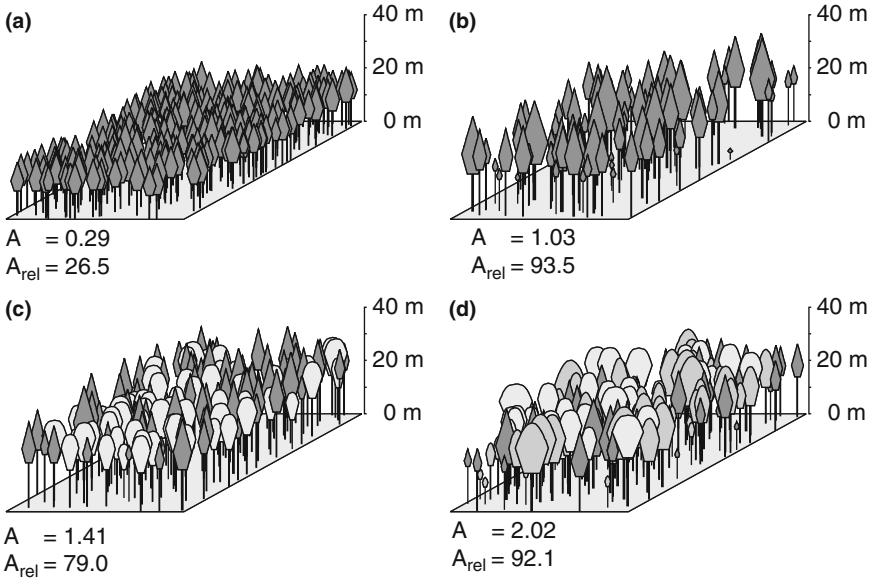

Fig. 7.37 Species profile index A and the standardised species profile index A_{rel} for (**a**) a monolayered stand of Norway spruce, (**b**) a two-layered stand of Norway spruce, (**c**) a two-layered stand of Norway spruce and European beech, and (**d**) a multi-layered stand of Norway spruce, European beech, and Silver fir

7.6 Species Intermingling

7.6.1 Species Intermingling Index by Füldner (1996)

7.6.1.1 Methodological Principles

The species intermingling index M_i by Füldner (1996) describes the spatial structure of the species mixture in a stand. Index M_i is defined as the proportion of neighbours of another species:

$$M_i = \frac{1}{n} \times \sum_{j=1}^{n} v_{ij}, \tag{7.76}$$

where i is the centre tree, j refers to the neighbouring trees j, $j = 1, \ldots, n$, and n represents the number of neighbours included in the analysis. The parameter v_{ij}:

$$v_{ij} = \begin{cases} 0, & \text{if neigbour j belongs to the same species as central tree i} \\ 1, & \text{if neigbour j belongs to a species different from central tree i} \end{cases} \tag{7.77}$$

is a dual discrete variable that takes the value 0 when the neighbour considered j belongs to the same species as the centre tree i. If the neighbour j belongs to another species then $v_{ij} = 1.0$. For a structural quartet $(n = 3)$, M_i can take on four discrete values as shown in Fig. 7.38 (Füldner 1996): $M_i = 0.00$ when all trees in the quartet belong to the same species; $M_i = 0.33$ when one centre tree neighbour belongs to another species; $M_i = 0.67$ when two of the three centre tree neighbours belong to a different species; and $M_i = 1.0$ when all neighbours of the centre tree belong to another species. In the latter case, e.g., M_i is calculated as follows:

$$M_i = \frac{v_{i1} + v_{i2} + v_{i3}}{n} = \frac{1+1+1}{3} = 1.0. \tag{7.78}$$

To calculate the mean species intermingling index of a stand, the individual M_i values are added together and divided by the number of individual trees in the stand N:

$$\overline{M} = \frac{1}{N} \times \sum_{i=1}^{N} M_i, \tag{7.79}$$

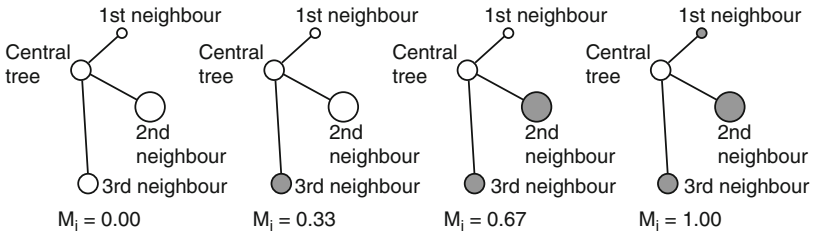

Fig. 7.38 Possible values for the discrete variable species intermingling index M_i in the structural quartet are $M_i = 0.00, 0.33, 0.67$ or 1.00 (*from left to right*)

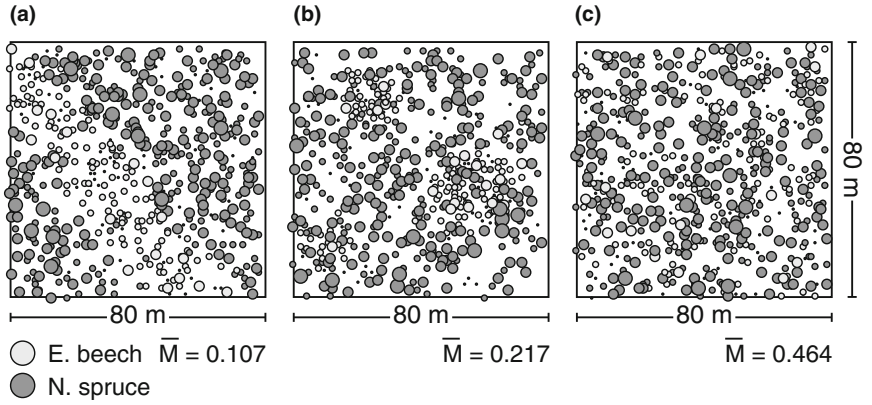

Fig. 7.39 Examples of tree species intermingling patterns, and the behaviour of index $\overline{M}$. European beech is added to the Norway spruce stand in (**a**) a large cluster, (**b**) in groups, and (**c**) single-tree mixture

where N is the number of the central trees considered in the stand. For $\overline{M}$, $0 \leq \bar{M} \leq 1$ applies. The mean value $\overline{M}$ can be determined for the total stand, or for any species present. The larger the species-specific value $\overline{M}$, for example, the more intensive individual trees of that species intermingle with the other species present. Lower values indicate the occurrence of species in groups or patches.

7.6.1.2 Practical Example

Figure 7.39 shows a Norway spruce–European beech mixed stand with tree diameters magnified eightfold. European beech is added to the Norway spruce stand (a) as a large cluster, (b) in groups and (c) in a individual-tree mixture. The $\overline{M}$ values calculated for European beech in these stands are 0.107, 0.217, and 0.464 respectively. From the cluster to the individual-tree mixture (Fig. 7.39a–c), the species intermingling and interspecific competition increases, as the species intermingling index $\overline{M}$.

7.6.2 Index of Segregation from Pielou (1977)

7.6.2.1 Methodological Principles

In contrast, the index of segregation S, developed by Pielou (1977), describes the intermingling of two tree species or species groups using the nearest neighbour methods (cf. Sect. 3.2). To calculate this index, we record whether trees belong to species 1 or 2 for all trees N on the plot. We can calculate the total number of trees

Table 7.7 Table presenting the variables used in the calculation of the segregation index S by Pielou (1977), and the test statistic T_S. For a description of variables, see (7.81) and (7.82)

		Nearest neighbour		
Starting point tree		Species 1	Species 2	Total
	Species 1	a	b	m
	Species 2	c	d	n
	Total	v	w	N

from the sum of m and n, the number of species 1 and 2 respectively ($N = m + n$). In addition, the tree species of the nearest neighbour is recorded, so that the number of trees with neighbours of the same species (a, d) or of different species (c, b) is known (Table 7.7). The index of segregation S is obtained as

$$S = 1 - \frac{\text{observed number of mixed pairs}}{\text{expected number of mixed pairs}} \tag{7.80}$$

and lies between -1.0 and $+1.0$. The expected number of mixed pairs describes a random, and hence entirely independent distribution of tree species. The index of segregation S is calculated from the basic parameters provided in Table 7.7 as follows:

$$S = 1 - \frac{N \times (b + c)}{(v \times n + w \times m)}. \tag{7.81}$$

To test the segregation indices for possible significant deviations from an independent distribution of two mixed species, Upton and Fingleton (1985) developed the following χ^2 distributed test statistic:

$$T_S = \frac{(N-1) \times (|a \times d - b \times c| - N/2)^2}{m \times n \times v \times w}. \tag{7.82}$$

If the observed number of mixed pairs is higher than expected, then $S < 0$, indicating a close connection or association between the two species. However, if the observed number of mixed pairs is lower than expected, then $S > 0$ and shows segregation, that is a spatial separation of these species. If $S \cong 0$, it means the observed number of mixed pairs corresponds to the expected number, which, in turn, means the distribution of the two species is independent of one another. To eliminate any edge effects, only plants whose distances from the border of the sample plot are greater than the distances to the nearest neighbour are included in the calculation of S.

7.6.2.2 Practical Example

The European beech–European larch mixed stands in the Solling, Lower Saxony, presented in Fig. 7.40, reveal a broad range of intermingling intensity. Whereas

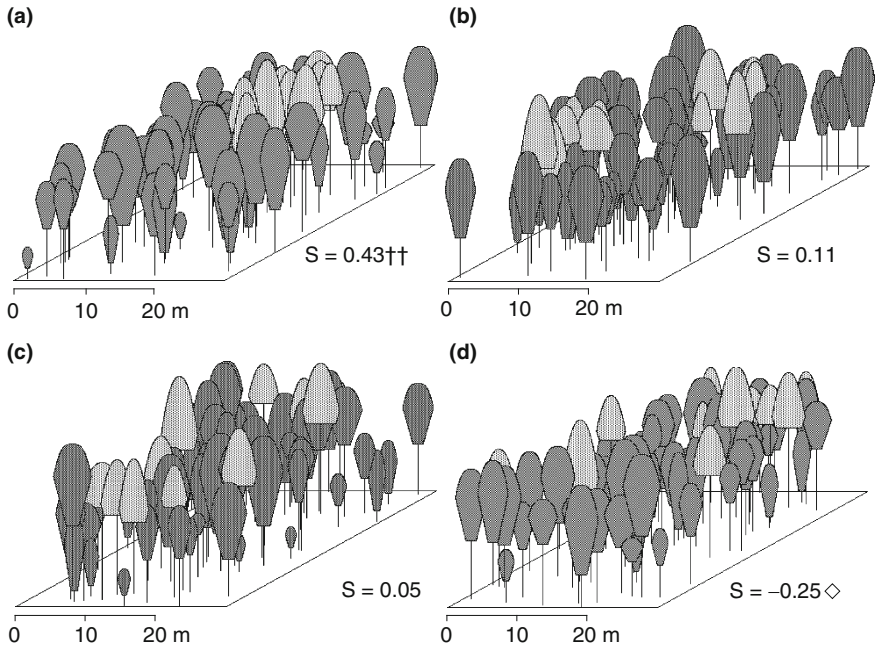

Fig. 7.40 Identification of species intermingling of European beech (*dark grey*) and European larch (*light grey*) with the index of segregation by Pielou (1977). S values above 0 show a tendency towards segregation (**a, b**), values below 0 a tendency towards association (**d**), and independent occurrence of species is indicated by S values around 0 (**c**). The symbols two daggers and open diamond show statistically significant segregation or aggregation tendencies; the number of 1, 2 or 3 symbols refers to the error probability of 5, 1, and 0.1%

patches and group mixtures (Fig. 7.40a and b) produce segregation values of 0.43 (two daggers) and 0.11 respectively, the segregation values of clumps and individual-tree mixtures (Fig. 7.40c and d) decline to −0.25 (open diamond). High segregation values suggest low interspecific but marked intraspecific competition. In comparison, low S values suggest species association, and the dominance of interspecific competition. The symbol two dagger indicates that segregation is significant with a 1% probability of error, and open diamond indicates significant association with a 5% probability of error. The statistical level of confidence results from using the χ^2 distribution test statistic presented in (7.82).

Summary

As trees are firmly anchored in the ground and develop their structures gradually over long periods of time, the emerging structures can influence environmental conditions and resource supply within the stand (light, temperature, precipitation, deposition etc.). In this way, the tree and stand structures that have developed in

forest ecosystems have a major influence on all life processes within the stand. The methods of description, quantification, three-dimensional reproduction, and the visualisation of tree, stand and landscape structures outlined in this chapter support the understanding, modelling and prediction of forest development. Forest management makes use of the central importance of structure in forest ecosystem processes by analysing and modifying them (extraction of trees, enhancing structural heterogeneity, variable plant spacing, etc.) to regulate growth processes, habitats, species diversity and stability of forest ecosystems. The horizontal distribution pattern, stand density, differentiation and species intermingling constitute the most important aspects of stand structure, and the most important conditions of growth for individual trees within a stand.

(1) The feedback loop, tree growth → stand structure → growth conditions → tree growth, is essential for understanding and managing forest development. The initial stand structure at the stand establishment or the beginning of a growing season largely sets the framework for future stand development. Predictions should therefore include initial structure data. This applies particularly to development predictions in highly diverse stands.
(2) Charts with tree coordinates and crown maps form the basis for analyses of spatial occupancy in a stand and the growing space available for individual trees. By reproducing the crown periphery with polygons, circles and cubic splines, the modelled outcomes approximate the reality more closely.
(3) The spatial reproduction of tree crowns from generalised crown shape models pave the way for the spatial reproduction of stand structure.
(4) Data from stand surveys, and predictions from simulation runs can be visualised by modelling the spatial stand structure. The models produce stand profile diagrams, front views, walk-throughs in real time and landscape images. Models of spatial structures at the tree, stand and landscape levels correspond to the biological level of observation, and thereby assist information transfer in consultations, participatory planning, training and teaching.
(5) Given the stem coordinates, the crown radii, tree height, crown base height and species-specific crown models, the spatial expansion of trees can be digitised and transferred into a three-dimensional matrix of voxels. A dot count can be carried out to determine the presence of trees and species in all voxels, and to develop cross-sections through the matrix to assist visualisation. The data entry in voxels (which species, how many dots, species intermingling, etc.) is useful for further statistical analysis of space sequestration.
(6) The single-tree-based three-dimensional analysis and visualisation adopts the individual tree as the basic unit of the stand, and expresses the results on the scale of biological observation and silvicultural operations. The individual tree also forms the unit for the maximisation of fitness (survival, reproduction, number of progeny relative to its neighbours). The three-dimensional and individual-tree based analysis of structure and function achieves a consistency in the levels of biological knowledge, perception, measurement, analysis and modelling.

(7) The distribution indices by Clark and Evans (1954), Pielou (1959), Clapham (1936) and Morisita (1959) compare the measured tree distances or occupation densities in sample squares with values expected for a Poisson distribution (random distribution), $p(n) = \lambda^n / n! \times e^{-\lambda}$. The Poisson distribution forms the reference for measures of regularity, randomness and clumping of tree positions.

(8) The results from the K-, L- and pair correlation functions indicate the change in structure of single-tree neighbourhoods with increasing distance from the standpoint. The functions identify the extent to which a measured tree distribution pattern becomes more or less dense than the Poisson distribution with increasing distance r from the stem base points.

(9) The stocking density from the yield tables, natural stocking density, percentage canopy cover, mean basal area by Assmann (1970), stand density index SDI from Reineke (1933) and the crown competition factor CCF all quantify the density of spatial occupancy and the mean competition within a stand. They are used to analyse and model the relationship between density and growth, and to quantify silvicultural prescriptions for stand management guidelines.

(10) The coefficient of variation of tree sizes (e.g. height or diameter), used to quantify the structural heterogeneity of plant communities, supports considerations of sample size, assessments of frequencies of individual-tree size and stand stability or conversion capacity. Diameter differentiation by Füldner (1995) quantifies heterogeneity in a tree's immediate neighbourhood in relation to the size variation of its three nearest neighbours.

(11) Species richness and species diversity can be described using the following indices: species richness, species diversity by Hattemer (1994), diversity index by Shannon (1948), standardised diversity, standardised evenness, species profile index from Pretzsch (1995) and standardised species profile index. These measures can be used to quantify the heterogeneity of diameter, height and species in an entire stand, in the vicinity of individual trees or for different height zones in the stand.

(12) To measure species intermingling, e.g., whether two species occur single tree wise, in clusters, groups or in patches, species intermingling and segregation indices are useful. Füldner (1996) derived a species intermingling index from the proportion of neighbours belonging to a different species. Pielou (1977) developed a segregation index based on nearest neighbour methods, where the observed number of mixed tree pairs is compared to the expected number of mixed tree pairs in a random distribution.

Chapter 8
Growing Space and Competitive Situation of Individual Trees

When resource availability in a stand is lower than required for optimal tree growth, the individual trees are in direct competition with one another. In this sense, competition indices and related measures introduced in this chapter can be regarded as aggregated measures for the resource availability of the individual trees in a stand. Competition indices make use of tree species, diameter, height, crown size and distance to stand neighbours to quantify the competitive situation of individual trees and the impact on growth. Competition indices are termed position-dependent when the distances to neighbouring trees are involved in the calculation, and position-independent if not.

In view of the different competition strategies in the crown and root space and the influence of tree species, site and stand structure on competition, the characterisation of resource availability by simple aggregated competition indices is essentially limited. However, competition indices have attained considerable importance in growth and yield research and modelling because they are easy to calculate, and the tree and the stand variables used are readily available. They quantify a tree's competitive situation in a highly aggregated form, and permit a simplified expression of spatial competitive processes about which we have only a limited understanding. The applicability of competition indices and other measures for determining the spatial growth arrangement of individual trees extends from pure description, to modelling and managing of tree and stand growth. The social tree classes already introduced for even-aged stands from Kraft (1884) provide an example of the qualitative estimation of the growth arrangement of individual trees based on tree height and crown size (cf. Chap. 5). Johann (1983) uses the A-value, a position-dependent competition index, to quantify thinning on experimental plots and in practice. As competition indices are a measure of an individual tree's resource supply, they play a key role in individual-tree simulators (cf. Chap. 11).

H. Pretzsch, *Forest Dynamics, Growth and Yield: From Measurement to Model*,
DOI: 10.1007/978-3-540-88307-4_8,

8.1 The Stand as a Mosaic of Individual Trees

Recent investigations on the development dynamics in animal and plant populations point out that the understanding of population development is enhanced significantly when the stand is broken down into a mosaic of individuals and interactions in a dynamic spatial–temporal system. Consequently, the following methods will be based on individual-tree growth data from stand surveys to provide a differentiated picture of the stand development. The knowledge from the traditional representation of stand development by the cumulative and mean values and frequency distributions of individual tree characteristics appears to be exploited fairly well. In contrast, the transition to an approach that explains stand development with respect to individual trees creates new opportunities for understanding and predicting stand growth. As traditional approaches for the investigation and representation of stand development pay little attention to the spatial configuration of stands, and assume a largely uniform appearance and behaviour of trees in the stand, they ignore the heterogeneity present in stand structure, and thereby the most important stand characteristic. In contrast, investigations that focus on the individual, perceiving the stand to be a heterogeneous mosaic of individual trees, place particular importance on spatial configuration and individual differences between trees, and use these characteristics to explain and predict future development. Total stand development is derived from the interactions taking place between individual trees.

The transition from stand-based approaches to individual tree approaches reflects a fundamental paradigm shift in all research disciplines concerned with stand or population development. Huston, DeAngelis and Post (1988) reviewed a number of studies on the dynamics of populations, biological communities and ecosystems, including forestry research, and came to the conclusion that the transition from stand to individual-based concepts and models is a crucial step towards a more profound understanding of population development processes.

8.2 Position-Dependent Competition Indices

Detailed surveys of long-term experimental plots, inventory and monitoring plots, and remote sensing images contribute to a continuously expanding tree database. This database comprises tree species, stem base position, diameter, height, crown length, crown radius and crown transparency, and provides the data required for the calculation of position-dependent competition indices. The indices are calculated in two steps: in the first step, for each tree, the neighbouring trees that compete with the tree in question for resources are determined. In the second step, the strength of competition from each of the neighbours identified on that tree is calculated. Numerous methods are available for the identification of competitors, and for quantifying their competitive strength. The result is always a dimensionless competition index that characterises resource availability, and hence the growing conditions of each individual tree.

8.2.1 Example of Competitor Identification and Competition Calculation

In the first example of the general approach, the position-dependent competition index KKL, used frequently, is presented (Pretzsch 1995; Bachmann 1998). To calculate the KKL, an upside-down search-cone with a 60° opening angle is placed on the tree under investigation j, which we call the central tree (Fig. 8.1), with an insertion height of the cone apex at p = 60% of the tree height. All trees whose crowns fall within this search cone are regarded as competitors. The angle $BETA_{ij}$, the angle between the surface line of the search cone and the line connecting the tip of the competitor tree i with the cone apex on the central tree j, is calculated for all competitors. The closer and taller the competitor compared to the central tree, the greater the angle BETA and the competitive strength of this neighbour. The angle $BETA_{ij}$ in radians, $BETA_{ij}(\text{radian}) = \frac{\pi}{180} \times \beta_{ij}$, is determined for all competitors, and then added together to obtain the competition index:

$$KKL_j = \sum_{\substack{i=1 \\ i \neq j}}^{n} BETA_{ij} \times \frac{KQF_i}{KQF_j}, \tag{8.1}$$

as a relative measure of the competition on the central tree j from its neighbours. Since not only distance and relative height of neighbours affect competition, but also the size of the central tree in relation to its neighbour, the angle calculated is

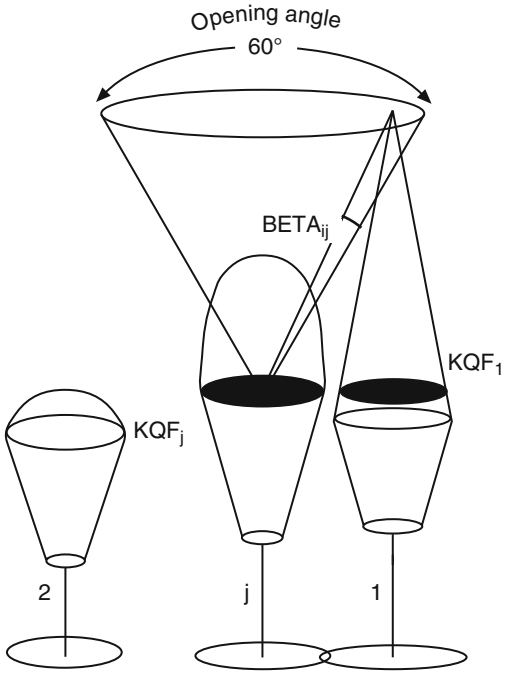

Fig. 8.1 Crown competition KKL_j is determined by the search cone method in relation to tree height and crown size ratios between the central tree j and its neighbours i = 1,...,n; variables are explained in the text

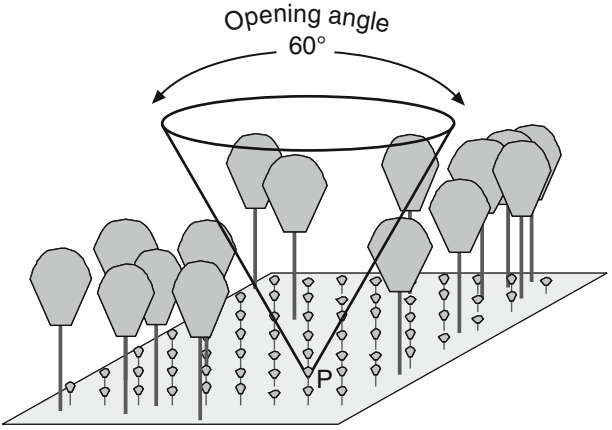

Fig. 8.2 To quantify growth conditions at the forest floor, the stand area is divided into a grid of sample points $p = 1, \ldots, m$. By calculating KKL_p at each point p competition indices are obtained that are useful in the analysis and modelling of regeneration

weighted by the ratio of the crown cross-sectional area of neighbour i at the height of the cone apex KQF_i to the crown cross-sectional area of the central tree at the height of the cone apex KQF_j.

As the competition index KKL is based on size and distance relations between the central tree and its neighbour, mature and young stands with different absolute, yet similar relative dimensions, produce the same indices. A more detailed competition and growth estimation additionally may include light transmission of neighbouring trees, and the tree species or tree species groups to which neighbouring trees belong (Pretzsch 2001).

This principle for quantifying competition in the crown space can also be transferred to the understorey and tree regeneration layer (Fig. 8.2). If the diameter, height, crown size and the position of regeneration are known, their competitive situation can be calculated according to (8.1). When information on the regeneration layer is incomplete or missing, another simple method can be used to characterise the growing conditions at the forest floor. In this method, a grid, with a grid density adapted to the information required, is laid over the forest floor. At every grid point P we place an imaginary tree with height 1.67 m, and crown diameter 1.12 m, which corresponds to a crown cross-sectional area of $1\,m^2$. At 60% of the height of this standard tree, i.e. at 1.0 m, we insert the upside-down search cone with an opening angle of 60°. Then, the competition at the grid point P can be quantified by

$$KKL_P = \sum_{i=1}^{n} BETA_{iP} \times KQF_i \tag{8.2}$$

This formula is analogous to (8.1), only the denominator KQF_j is equal to 1, since the crown cross-sectional area of the standard tree is $KQF_j = 1.0\,m^2$. KKL_p gives

a dimensionless measure of the growing conditions at point P relative to an imaginary standardised regenerating tree. Once this analysis is carried out at all grid points, indices characterising the development conditions of the regeneration are available for the whole area. These index values are useful in the analysis of spatial distribution patterns of the regeneration in the initial phase, as well as for explaining and managing height growth, density and mortality in the understorey and regeneration.

The grid-like segmentation of the stand area and the subsequent calculation of KKL_P may be used to analyse the inventories of regeneration. When inventories of regeneration are carried out in sampling squares of $2.5\,m \times 2.5\,m$ or $5.0\,m \times 5.0\,m$, the grid points P should be placed at the centre of the sampling squares so that the actual standardised competition index can be calculated for each survey square. A statistical analysis may reveal possible relationships between spatial distribution and growth, density and mortality of the regeneration and the overstorey stand structure. Therefore the modified competition index in (8.2) can be applied by individual-tree simulation models.

Figure 8.3 shows the frequency distribution of diameter at breast height, crown density, mean annual basal area increment and competition index KKL for the 1.5 ha selection forest experimental plot FRY 129/1–3 in Forest District Freyung, in the Bavarian Forest. The three adjacent plots 1–3 represent fertile soils, and show high growth rates and high net yields of $499–588\,m^3\,ha^{-1}$ merchantable timber volume. Silver fir dominates the lower and middle stand layers, Norway spruce forms the upper layer, and European beech is present only as a subordinate tree species. The frequency distributions of diameter, crown density and annual basal area increment highlight the heterogeneous stand structure, which is also reflected in the broad frequency distribution of the index KKL (cf. Fig. 8.3d), ranging from 0 (dominant, open grown trees) to over 30 (suppressed trees).

8.2.2 Methods of Competitor Identification

There are four common approaches for the identification of neighbouring trees that compete with the central tree for inclusion in subsequent calculations of the competition index.

8.2.2.1 Fixed Radius Method

The first option is to draw a circle around the central tree j with a fixed radius r and count those neighbours $i = 1, \ldots, n$ as competitors whose distance $dist_{ij}$ from the central tree is smaller than the search-radius r. In his position-dependent individual-tree model for Canadian pine forests, Hegyi (1974) uses a radius of $r = 10\,ft = 3.048\,m$. His competition index DCI,

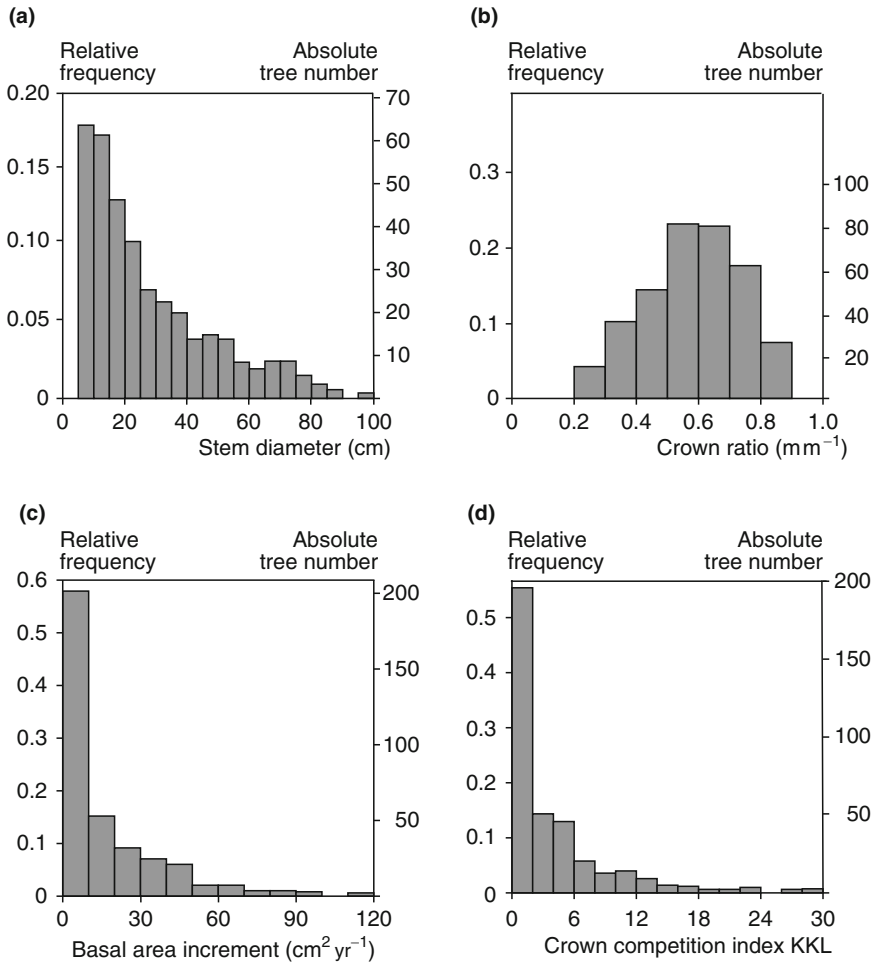

Fig. 8.3 Frequency distributions of (**a**) diameter at breast height, (**b**) crown ratio, (**c**) mean annual basal area increment, and (**d**) competition index KKL for a total of 1,016 trees in the Norway spruce-Silver fir-European beech selection forest experiment Freyung 129

$$DCI_j = \sum_{\substack{i=1 \\ i \neq j}}^{n} \left(\frac{d_i}{d_j} \times \frac{1}{dist_{ij}} \right) \tag{8.3}$$

considers all $i = 1, \ldots, n$ neighbours falling within the search circle drawn around the central tree j (Fig. 8.4). However, any fixed search radius is only adequate for a certain tree size or stand stadium, and proves a severe disadvantage when implemented in growth model, particularly in long-term growth prognoses.

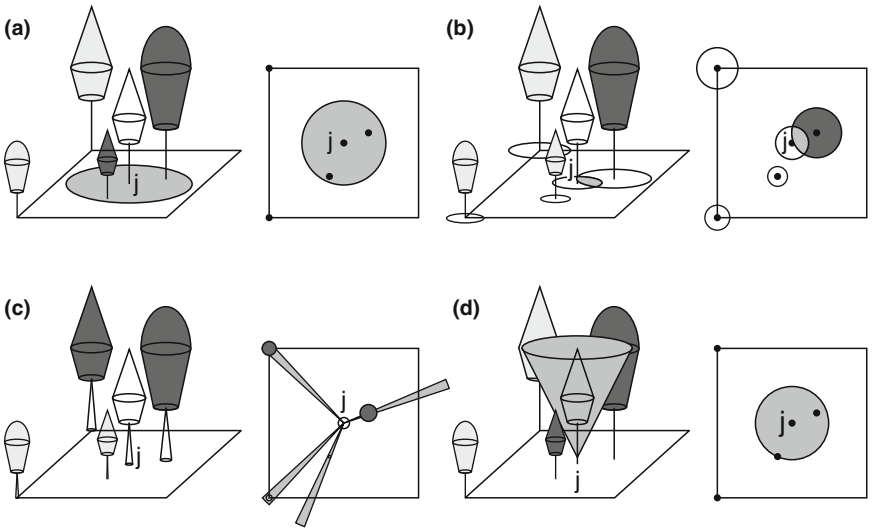

Fig. 8.4 Methods for identifying competitors of the central tree j, illustrated by stand profiles and crown projection maps. Competitors are identified from (**a**) a fixed search radius around tree j, (**b**) crown overlap, (**c**) horizontal, and (**d**) vertical angle count samples. The colours were specified as follows: the central tree j (*white*), the competitors identified by each method (*dark grey*) and unconsidered trees (*light grey*)

8.2.2.2 Crown Overlap Methods

The second group of methods used by Bella (1971), Alemdag (1978), and Pretzsch (1992a), among others, regards those trees as competitors whose actual crown, potential crown, or growing area overlap with that of the central tree (Fig. 8.4b). If the actual crown radius of the central tree and its competitors (cr_j and cr_i respectively) is used in the identification of competitors, a tree is a competitor if

$$dist_{ij} < \left(cr_i + cr_j\right). \tag{8.4}$$

If the potential crown radius is used in this test instead, then a known relationship for individual trees or predominant trees is needed, which expresses the potential crown radius cr_{pot} as a function of tree diameter or tree height. An allometric equation [e.g. $\ln(cr_{pot}) = a + b \times \ln(d)$] is usually developed for this purpose (Pretzsch 1992a). Once the potential crown radii of the central tree j and its neighbours i ($cr_{pot\,j}$ and $cr_{pot\,i}$, respectively) are known, the same procedure as in (8.4) is followed. If the actual or potential crown parameters are unknown, the identification of competitors may be carried out according to the following rule: tree i is a competitor of the central tree j when $dist_{ij} < (d_i^2 + d_j^2) \times mult$. Variables d_i^2 and d_j^2 represent the squares of the diameters and mult is a multiplier, for which Alemdag (1978) proposes the values 0.0085, 0.0090, or 0.0095. The larger the multiplier is, the larger the search circle, and, therefore, the more competitors included in the competition calculation.

8.2.2.3 Angle Count Sampling

If angle count sampling from Bitterlich (1952) is employed as the search method (Fig. 8.4c), the identification of competitors is dependent on their distance and diameter. A tree is included as a competitor in the competition index if its distance $dist_{ij}$ to the central tree is

$$dist_{ij} < d_i \times \frac{50}{\sqrt{ACF}}. \tag{8.5}$$

In angle count sampling the diameter d_i of the neighbour is multiplied by factor $50/\sqrt{ACF}$ as for the control of boundary trees. The boundary distances, up to which a tree is regarded as a competitor, for the most frequently used angle count factors ACF = 1, 2, and 4 are $d_i \times 50.00$, $d_i \times 35.36$, and $d_i \times 25.00$, respectively. The basal area factors 1, 2, and 4 correspond to the opening angles of $\alpha = 1.15°, 1.62°$, and 2.30°, respectively. Thus, for small angle count factors and boundary angles, many neighbours are included as competitors, whereas, for large ACF values and boundary angles, only a few trees meet the criteria for inclusion in the group of competitors (Lorimer 1983; Tomé and Burkhart 1989).

8.2.2.4 Search Cone Methods

Pukkala and Kolström (1987), Pukkala (1989), Biging and Dobbertin (1992) and Pretzsch (1995) transfer the horizontal identification principle in the angle count sampling method to a vertical identification method depending on tree height of competitors. For this purpose a search cone is set up at the stem base of the central tree j (Fig. 8.4d). For an opening angle of the search cone β, the angle α between the (horizontal) forest floor and the search cone margin is $\alpha = 90 - \beta/2$. Only the neighbouring trees whose crowns reach into the search cone are regarded as competitors, where

$$dist_{ij} < h_i \times \tan\alpha^{-1}. \tag{8.6}$$

If the apex of the search cone is not positioned at stem base but at the crown base height of the central tree hcb_j instead, then a neighbouring tree with height h_j is a competitor when

$$dist_{ij} < (h_i - hcb_j) \times \tan\alpha^{-1}. \tag{8.7}$$

The correlation between the competition index and the annual basal area increment for the trees in the stand represents one criterion for selecting suitable height positions and opening angles β for the search cone. In a mixed species mountain forests in Bavaria, Bachmann (1998) found the strongest correlation between competition index and basal area growth when the search cone is placed at 50, 10, and 70% of the tree height for Norway spruce, Silver fir, and European beech respectively. The optimal opening angle is dependent on species, and lies between 20 and 60° in the regeneration phase and otherwise between 60 and 100°.

8.2.3 Quantifying the Level of Competition

Once the competitors have been identified, the strength of competition they exert on the central tree j is calculated. Three methods are appropriate for this task: crown overlap or competitive influence zones, ratio of tree size dimensions, and ratio of crown size of the central tree to its neighbours. These methods are presented using well-known indices as examples. A comprehensive overview of these methods is available in Dale, Doyle and Shugart (1985), Biging and Dobbertin (1992) and Bachmann (1998).

8.2.3.1 Crown Overlap or Competitive Influence Zones

The crown overlap index from Bella (1971) belongs to the methods based on crown overlap and competitive influence zones (Fig. 8.5). For each of the $i = 1, \ldots, n$ competitors, the overlapping area o_{ij} with the central tree crown is determined. To calculate the competition index B, the overlap areas are not simply related to the crown projection area of the central tree $cpac_j$, but weighted by the diameter ratio d_i/d_j:

$$B = \sum_{\substack{i=1 \\ i \neq j}}^{n} \frac{o_{ij}}{cpac_j} \times \frac{d_i}{d_j} \tag{8.8}$$

The overlapping area expresses competition in respect to space occupation. The diameter ratio expresses the proportion of size between central tree and its neighbours. Thus, even when trees in the understorey in the immediate vicinity of the central tree produce high o_{ij} values, their contribution to index B is weakened due to the low quotient d_i/d_j. The overlapping area o_{ij} can be calculated from the actual crown projection area, potential crown extension or theoretical competitive influence zones.

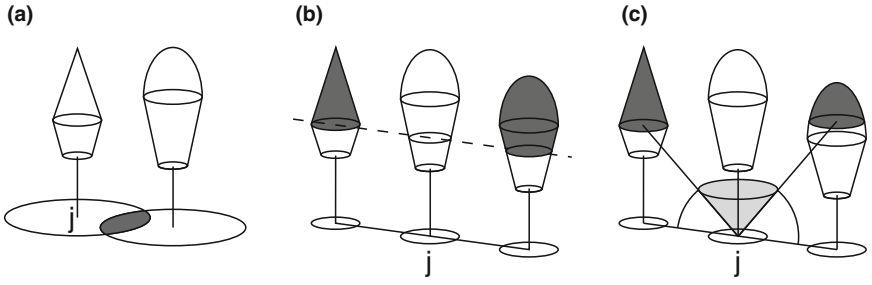

Fig. 8.5 Methods for quantifying the strength of competition: determination of (**a**) crown overlap, (**b**) crown size ratios of the central tree to its neighbours at a fixed reference height, and (**c**) at variable reference heights. The central tree j and the relevant characteristics of competitors or their overlap area (*dark grey*) are shown for each of the illustrated methods

8.2.3.2 Ratio of Tree Size Dimensions

The index from Martin and Ek (1984) provides a good example for this group of methods. It relates the diameters d_i of all competitors identified to the diameter of the central tree d_j, and then determines the sum of the quotients to obtain the competition index ME:

$$ME = \sum_{\substack{i=1 \\ i \neq j}}^{n} \frac{d_i}{d_j} \times e^{-\left[\frac{16 \times dist_{ij}}{d_i + d_j}\right]}. \tag{8.9}$$

The quotients are weighted by the exponential function where the contribution of a competitor to the competition index decreases with increasing distance and decreasing diameter.

The A-value from Johann (1982) has a special place in this group of methods as it is used for quantifying as well as for controlling individual tree development on experimental plots (cf. Chap. 5). Johann quantifies the competition between a central tree j and its neighbour i by the A-value:

$$A_{ij} = \frac{h_j}{E_{ij}} \times \frac{d_i}{d_j}, \tag{8.10}$$

where A_{ij} represents the competition index, h_j the height of the central tree j, d_j the diameter at breast height of the central tree j, d_i the diameter of the neighbouring tree, and E_{ij} represents the distance between the central tree j and neighbour i.

The competition value A_{ij} increases with increasing tree height of the central tree, decreasing distance to the neighbour i, and increasing diameter ratio of the neighbour to the central tree d_i/d_j. The transformation of (8.10) produces

$$E_A = \frac{h_j}{A} \times \frac{d_i}{d_j} \tag{8.11}$$

which enables one to determine the distance between the central tree j and neighbour i for a given competition value A. If, for example, a central tree has a height of 20 m and a diameter at breast height of 20 cm, and its neighbour has a diameter at breast height of 10 cm, then, according to (8.11), A-values of 4, 5 and 6 result in E_A values of $E_A = 2.50$ m, 2.00 and 1.67 m, respectively. Johann (1982, 1983) calculates expected distances E_A to a neighbour for different tree sizes and competition values A, and uses it to quantify and control thinning (Chap. 5). A neighbour of the central tree j is removed when its distance to the central tree E_{ij} is smaller than the distance limit E_A calculated in (8.11) for a given A-value. The competition index from Hegyi (1974), introduced previously in (8.3), also belongs to the methods based on the ratio between stem sizes.

8.2.3.3 Ratio of Crown Size of the Central Tree to Its Neighbours

Methods in the third group relate crown cross-sectional area, crown surface area, or crown volumes of competitors and the central tree to one another. According to Biging and Dobbertin (1992) and Bachmann (1998), they produce competition indices with a particularly strong correlation to individual tree growth. Crown shape models provide the crown extension data for each tree, which are required at different tree heights (cf. Chap. 7, Sect. 7.2.2.1). They also facilitate the calculation of the crown cross-sectional area at any tree height, and the crown surface area or the crown volume above this height. To calculate the competition on the central tree j, Biging and Dobbertin (1992) suggested cutting the crown of all competitors and the central tree at a defined reference height p of the central tree (Fig. 8.5b). Next, at this reference height, the crown cross-sectional area CC, the crown surface area CM, and crown volumes CV of the crown section above this height are obtained from crown shape models. The crown size of competitors and central tree are compared, as shown for crown volume in (8.12) and for crown surface area in (8.13). However, a comparison of the crown cross-sectional area CC is equally possible. The ratios are then summed up to obtain the competition indices BDV_f and BDM_f:

$$BDV_f = \sum_{\substack{i=1 \\ i \neq j}}^{n} \frac{CV_i}{CV_j \times \left(dist_{ij} + 1\right)} \tag{8.12}$$

$$BDM_f = \sum_{\substack{i=1 \\ i \neq j}}^{n} \frac{CM_i}{CM_j \times \left(dist_{ij} + 1\right)}. \tag{8.13}$$

The inclusion of the distance $dist_{ij}$ to the neighbour strengthens the contribution of closer trees to competition, and weakens the contribution of those further away. The subscript f indicates that the reference height is fixed in the calculation of the crown parameters.

Biging and Dobbertin (1992) developed an alternative method of determining the reference height. Instead of choosing a predefined fixed reference height for the central tree, they calculated the crown cross-sectional area, crown surface area or crown volume of the competitors at the height at which their stem axes are intersected by the surface line of the search cone (Fig. 8.5c). Consequently, the reference height is variable, and dependent on the opening angle and the height at which the search cone is positioned, which is expressed by the subscript v in (8.14) and (8.15). Again, to calculate the competition index, the ratio between the crown dimensions of neighbour and central tree is obtained:

$$BDV_v = \sum_{\substack{i=1 \\ i \neq j}}^{n} \frac{CV_i}{CV_j} \tag{8.14}$$

$$BDM_v = \sum_{\substack{i=1 \\ i \neq j}}^{n} \frac{CM_i}{CM_j}. \quad (8.15)$$

For the central tree, the entire crown, or the crown at 66% of the tree height is adopted. Equations (8.14) and (8.15) can also be carried out for crown cross-sectional areas. The distance to competitors is taken into account indirectly, as the cone surface line cuts more distant competitors at higher heights. Thus, the contribution of crown cross-sectional area, crown surface area and crown volume of competitors to the indices decreases with increasing distance.

8.2.4 Evaluation of Methods

Bachmann (1998) tested the suitability of 229 position-dependent competition indices for estimating a tree's increment. A brief presentation of his data and methods will help interpreting the method combinations he investigated. Tables 8.1 and 8.2 summarise the most successful methods for determining competition indices. To ensure that his analysis was valid for a wide range of forest types, Bachmann (1998) based his study on 742 trees in extremely structurally diverse plots on the mixed species mountain forest long-term experimental plots at Garmisch-Partenkirchen 115. These research plots are located in the growth region 15.8 in the Karwendel and Wetterstein Mountain Ranges situated 1,200–1,472 m above sea level where medium soil fertility prevail. At this mixed forest site, comprising Norway spruce, Silver fir, and European beech, some individuals were 385-years-old. Total yields in these uneven-aged forests range from 404 to 736 $m^3\,ha^{-1}$ merchantable timber over bark. Since the establishment of the experiment in 1954, structural changes at these sites have been recorded thoroughly in six surveys. Tree height ranges from 2.3 to 39.1 m with a mean height of 23.5 m. Diameter ranges from 4.0 to 74.0 cm with a mean value of 35.0 cm. The trees included in competition investigations range from suppressed through co-dominant to predominant trees. However, abrupt changes in the competitive situation, through concentrated thinning operations or hazards occurred only very rarely.

As part of his investigation, Bachmann (1998) combined four different methods for identifying competitors with three methods for quantifying competition. Competitors were identified by one of the following methods: fixed search radius, crown overlap, horizontal angle count sampling, and vertical search cones.

The four methods for identifying competitors were modified in discrete steps by changing the basal area factor in the horizontal angle count sampling, for example, or by changing the opening angle and the height at which the vertical search cone was positioned. In addition, he combined the four methods of identification mentioned above with the following methods of calculating competition: crown overlap and competitive influence zones, ratio of stem sizes, and ratio of crown sizes.

The algorithms used to quantify competition were also modified, for example by gradually adjusting the reference height ($p = 10 \ldots 90\%$) when determining the

ratio of crown dimensions of the central tree to its competitors. This results in very different method combinations and corresponding competition indices. All method combinations were systematically applied to the 742 sample trees and each survey period. By correlating the competition indices with the mean periodic basal area increment of trees in the same 5 year survey period, their suitability was validated. For a more detailed understanding, the 742 trees were stratified according to tree species (Norway spruce, Silver fir, and European beech) and height classes (0–50%, 51–80% and >80% of stand height). Thus, the correlation between competition indices and basal area increment could be determined for each stratum. Within these strata, the method combinations were listed in order of the level of correlation. Therefore, one can identify the indices that correlate more, or less closely with tree growth for each tree species and height class.

Table 8.1 summarises 10 of the 229 method combinations, which provided, on average, the highest correlation between competition index and basal area increment. The correlation coefficient from Spearman provides an average of the nine strata, i.e. the three tree species and height classes. Table 8.2 shows the 10 best method combinations for Silver fir in the understorey (stratum: *Abies alba* Mill., 0–50% stand height). The stratum-specific correlation coefficient is considerably higher than the mean correlation coefficient obtained in Table 8.1.

The different orders in the tables illustrate a fact that is of fundamental importance for the selection of competition indices. The search for indices most suitable for a particular stratum (Table 8.2) leads to a different approach than the search

Table 8.1 Overview of the ten best of 229 combined methods for determining competition for contested resources by competition indices (after Bachmann 1998). Order of methods according to the highest average correlation between the competition index and the mean periodic basal area increment for the nine strata comprising Norway spruce, Silver fir, and European beech in the lower, middle and upper storey. The relative height of the search cone position (A) and the opening angle in degrees (O) are given for the search cone method. To quantify competition, methods of the angle sums (KKL) and crown size relationships (BDV, BDM) are particularly useful. P reflects the reference height ($p = 10 \ldots 90\%$) when determining the ratio of crown dimensions of the central tree to its competitors. The Spearman correlation coefficient between competition index and annual basal area growth of the trees amounts to 0.57–0.58. Explanation of the relevant algorithm is given in the text

Ranking	Competitor selection			Quantification of competition			Correlation coefficient	Formula
1	Search cone	A = 50%	O = 60°	Angle sum	KKL	p = 50%	0.58	8.1
2	Search cone	A = Kra	O = 80°	Crown proportion	BDV	p = 50%	0.58	8.12
3	Search cone	A = 70%	O = 50°	Crown proportion	BDM	p = 66%	0.58	8.13
4	Search cone	A = 50%	O = 50°	Angle sum	KKL	p = 50%	0.58	8.1
5	Search cone	A = 60%	O = 60°	Crown proportion	BDM	p = 66%	0.58	8.13
6	Search cone	A = 60%	O = 60°	Angle sum	KKL	p = 60%	0.58	8.1
7	Search cone	A = 60%	O = 70°	Angle sum	KKL	p = 60%	0.58	8.1
8	Search cone	A = 40%	O = 50°	Angle sum	KKL	p = 40%	0.58	8.1
9	Search cone	A = 50%	O = 70°	Angle sum	KKL	p = 50%	0.57	8.1
10	Search cone	A = Kra	O = 60°	Crown proportion	BDV	p = 50%	0.57	8.12

Table 8.2 Overview of the ten best of 229 methods for determining competition indices for Silver fir in the understorey according to Bachmann (1998). Order of methods according to the highest average correlation between competition index and annual basal area growth in a given survey period. For the search cone method the relative height of the search cone position (A) and the opening angle in degrees (O) are given. If A = SF, or A = Kra, the search cone is set at the stem base and the crown base respectively. For the horizontal angle count sampling method angle count factor ACF and the opening angle O are given. To quantify competition, methods of the crown size relationships (BDV, BDM) and angle sums (KKL) are particularly useful. P reflects the reference height (p = 10…90%) when determining the ratio of crown dimensions of the central tree to its competitors. The Spearman correlation coefficient between competition index and annual basal area growth of the trees amounts to 0.91–0.97. Explanation of the relevant algorithm is given in the text

Ranking	Competitor selection			Quantification of competition			Correlation coefficient	Formula
1	Search cone	A = SF	O = 40°	Crown proportion	BDV	p = 66%	0.97	8.12
2	Search cone	A = SF	O = 60°	Crown proportion	BDM	p = 50%	0.95	8.13
3	Search cone	A = SF	O = 20°	Crown proportion	BDM	p = 66%	0.95	8.13
4	Angle count	ACF = 2.295	O = 1.74°	Crown proportion	BDV	p = 50%	0.93	8.12
5	Search cone	A = SF	O = 70°	Crown proportion	BDV	p = 50%	0.93	8.12
6	Search cone	A = Kra	O = 80°	Crown proportion	BDV	p = 50%	0.93	8.12
7	Search cone	A = 70	O = 30°	Angle sum	KKL	p = 70%	0.93	8.1
8	Angle count	ACF = 2.295	O = 1.74°	Crown proportion	BDM	p = 50%	0.91	8.13
9	Search cone	A = SF	O = 80°	Crown proportion	BDM	p = 50%	0.91	8.13
10	Search cone	A = SF	O = 100°	Crown proportion	BDM	p = 50%	0.91	8.13

for an index that provides the most robust results for different strata (Table 8.1). For individual analyses, algorithms most appropriate to the particular case should be used. However, robust, nonspecific competition indices should be employed in individual-tree oriented stand simulators designed for a broad spectrum of tree species, stand structures, site conditions (e.g., different limiting factors) and silvicultural management options.

In a comprehensive view, the list of methods in Tables 8.1 and 8.2 indicates good performances of search cone methods for competitor identification. Opening angles between 20° and 100°, especially between 50° and 70°, and placement heights at 0–70% of the tree height or at the crown base, are recommended. The horizontal angle-count sample with a basal area factor between 2 and 3 is also listed twice among the 10 most suitable methods for competitor identification. Methods that employ a fixed search radius, or crown overlap were inferior.

Of the methods available for quantifying competition, the weighted angle sum according to (8.1) and the ratio of crown sizes according to (8.12) and (8.13) with a fixed reference height of p = 40% to p = 70% of tree height proved particularly suitable. Both cases involved methods that related crown size of the central tree to that of its neighbours. Methods for calculating competition from crown overlap or competitive influence zones, ratios of stem size, and methods that incorporated ratios of crown sizes at different heights [(8.14) and (8.15)] proved less accurate.

8.3 Position-Independent Competition Measures

Position-independent descriptions of competition at the stand level can be obtained from measures of density such as stocking density, stand density index, or crown density (Chap. 7, Sect. 7.4). Here, we will introduce methods that estimate the competition on each tree due to the presence of larger or higher trees.

8.3.1 Crown Competition Factor

The first group of methods builds on the crown competition factor, which assumes that all trees achieve their potential crown extension and relates the sum of their potential crown projection areas $\sum_{i=1}^{n} cpa_{poti}$ to the stand area A. The calculation of cpa has been elaborated in the Chap. 7, Sect. 7.2.1.3. CCF provides a relative measure of the mean competition within a stand:

$$CCF = \frac{1}{A} \times \sum_{i=1}^{n} cpa_{poti}. \tag{8.16}$$

If the crown competition factor CCF approaches 1, the entire stand area is covered by the canopy, and this represents the extent crowns can develop without creating over lapping. As long as excess light resources are available CCF < 1. Typically, however, competition for light eventually leads to CCF > 1. If only those trees in the stand with diameters larger than the central tree j ($d_i > d_j$) are included in this calculation, then

$$CCFL = \frac{1}{A} \times \sum_{\substack{i=1 \\ d_i > d_j}}^{n} cpa_{poti}. \tag{8.17}$$

This crown competition factor, based only on trees larger than the central tree, provides an individual measure of the social position of a tree within the stand. In Fig. 8.6 the relationships of central trees (black rectangles) in the (a) understorey, (b) sub-canopy and (c) upper canopy are illustrated. The grey crowns indicate the (larger) neighbours that were included in the CCFL calculation of the respective central tree. In the calculations of CCFL for these central trees, the number of neighbouring trees included ranges from many to none (crowns shown grey). For the understorey central tree (Fig. 8.6a), eight trees are included in the CCFL, resulting in a CCFL $= 0.5$. The sub-canopy central tree (Fig. 8.6b), and the upper canopy (Fig. 8.6c) has two neighbours, and no neighbours respectively, with CCFL $= 0.1$ and CCFL $= 0.0$.

When the competition measures CCF and CCFL are based on potential crown dimensions, they quantify the maximum extension limits of individual trees. If, in (8.16), the actual crown size is used instead of the potential crown size, the index indicates the extent to which a stand actually occupies the available space. Biging and Dobbertin (1995) test the actual crown volume and crown surface area in addition

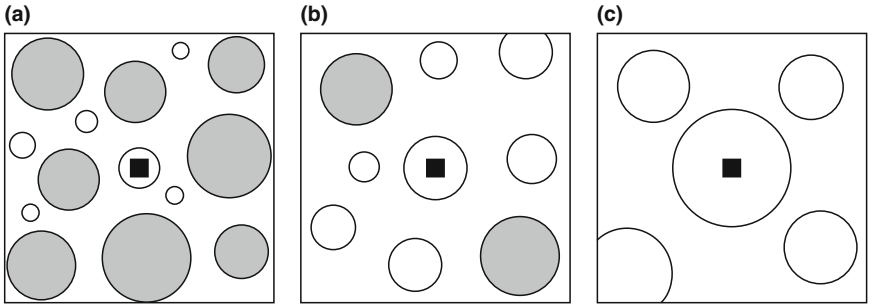

Fig. 8.6 CCFL values calculated for a (**a**) understorey, (**b**) co-dominant, and (**c**) predominant trees were CCFL = 0.5, 0.1 and 0.0 respectively. The central tree (*black*) and the competitor trees included in the calculation (*grey*) are shown

to the crown cross-sectional area in the calculation of CCFL values. However, an increase in the correlation between the resulting indices and tree growth compared to the CCFL based on crown area was not found.

8.3.2 Horizontal Cross-Section Methods

A second group of methods derive the individual competition index for (a central) tree j by constructing an imaginary horizontal plane through the entire stand at a specific, defined height of tree j (Fig. 8.7). When the crown cross-sectional areas KQF (or analogously their crown surface areas KMF or crown volumes KV) of all neighbours at this height p, shown in black, above this plane are added up and divided by the plot area A:

$$\mathrm{KKQ} = \frac{1}{\mathrm{A}} \times \sum_{\substack{\mathrm{i}=1 \\ \mathrm{i}\neq\mathrm{j}}}^{\mathrm{n}} \mathrm{KQF_i}, \tag{8.18}$$

$$\mathrm{KKM} = \frac{1}{\mathrm{A}} \times \sum_{\substack{\mathrm{i}=1 \\ \mathrm{i}\neq\mathrm{j}}}^{\mathrm{n}} \mathrm{KMF_i}, \tag{8.19}$$

$$\mathrm{KKV} = \frac{1}{\mathrm{A}} \times \sum_{\substack{\mathrm{i}=1 \\ \mathrm{i}\neq\mathrm{j}}}^{\mathrm{n}} \mathrm{KV_i}, \tag{8.20}$$

then we obtain the dimensionless competition indices KKQ, KKM, and KKV, which show the relative positions of the trees in the vertical structure of the stand [(8.18)–(8.20)]. In contrast to position-dependent approaches, where only neighbouring trees are identified, all trees in the stand cut by the horizontal plane are identified as competitors in this approach.

For example, the dominant Norway spruce j in Fig. 8.7a has a small KKQ value since the plane (horizontal line) intersects only a few trees at 60% of its height

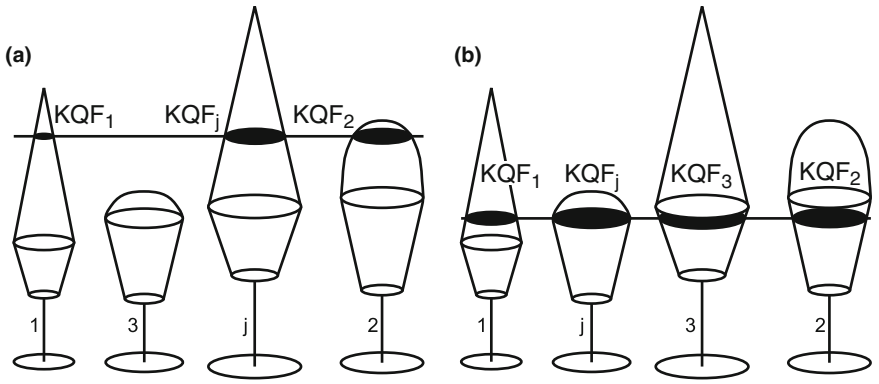

Fig. 8.7 Determination of the position-independent competition index KKQ for (**a**) a co-dominant Norway spruce and (**b**) subdominant European beech. The crown cross-sectional area KQF of all trees at the experimental trial plot is determined at 60% of the height of the central tree j according to known crown form models (*black circular plane*)

and the sum of the potential competitors' crown cross-sectional areas is relatively small. On the other hand, the European beech j in Fig. 8.7b belongs rather to the sub-canopy. It receives a high KKQ value, since the horizontal plane at 60% of its height intersects many potential competitors' crowns. Crown shape models (Chap. 7, Sect. 7.2.2.1) are employed in the calculation of the competition indices KKQ, KKM, and KKV.

Investigations by Pretzsch (1995) and Biging and Dobbertin (1995) emphasise the suitability of the index KKQ for reference heights p between 60% and 75% of tree height. Biging and Dobbertin (1995) tested the suitability of the indices KKQ, KKM and KKV by estimating individual-tree volume growth for selected stands of *Abies concolor* and *Pinus ponderosa*. First, they estimated volume growth only from stem diameter, height and crown length, and then checked whether the inclusion of the above-mentioned competition indices improved the growth estimation. Using the percentage reduction in the mean quadratic error as a measure of the suitability of the competition indices, they employed various reference heights ranging from p = 25–100%. Plotting the reduction in mean quadratic error for each, they could identify the optimal reference height (Fig. 8.8). This optimal height lies between p = 60–80% of the central tree's height regardless of the tree species and crown measure used in the calculation of the competition index.

8.3.3 Percentile of the Basal Area Frequency Distribution

The competitive situation of individual trees in the stand can also be derived from the relative position of the tree in the stand basal area frequency distribution as illustrated in Fig. 8.9a–d. In this method, the stand basal area frequency distribution (a) is converted to an absolute cumulative distribution in which each basal area class

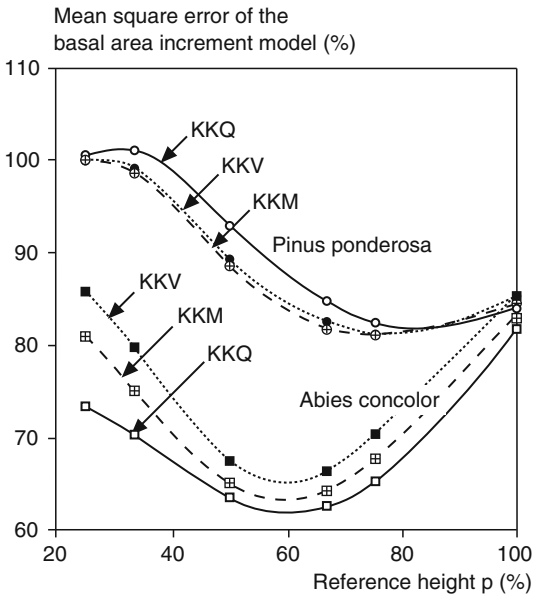

Fig. 8.8 Influence of selected reference height p on the quality of the growth prediction by the competition indices KKQ, KKV, and KKM. For the tree species *Pinus ponderosa* and *Abies concolor*, the influence of the chosen reference height p on the mean quadratic error of the basal area increment model is given. The 100% reference corresponds to the modelling results without competition index (after Biging and Dobbertin 1995)

contains the sum basal area of all trees within and below a given class (b). The cumulative basal area distribution is converted to percentages by dividing each class value by the total basal area (c). Then, the social rank of each tree is expressed by its relative position in this distribution as its percentile (PCT) (d). In their STAND PROGNOSIS MODEL, Wykoff, Crookston and Stage (1982) use the percentiles to model the growth response of individual trees to competition (Chap. 11).

8.3.4 Comparing Position-Independent with Position-Dependent Competition Indices

Essentially, the available database and the information requirements determine whether position-independent or position-dependent competition indices should be used in the description, modelling or management of individual-tree growth. If stem coordinates and stem and crown size are known, then position-dependent indices may be used for a more detailed characterisation of resource availability. That Lorimer (1983) and Martin and Ek (1984), following their modelling investigations, came to the conclusion that the inclusion of tree position did not significantly improve growth estimations may be for the following reasons. In untreated natural forest stands, tree size may represent the competition so well that competition indices do not produce better estimate of growth increment; alternatively, these investigations were largely carried out in pure even-aged stands, and hence the inclusion of position did not improve growth estimations because the competitive conditions varied only minimal anyway; finally, the comparisons were sometimes based

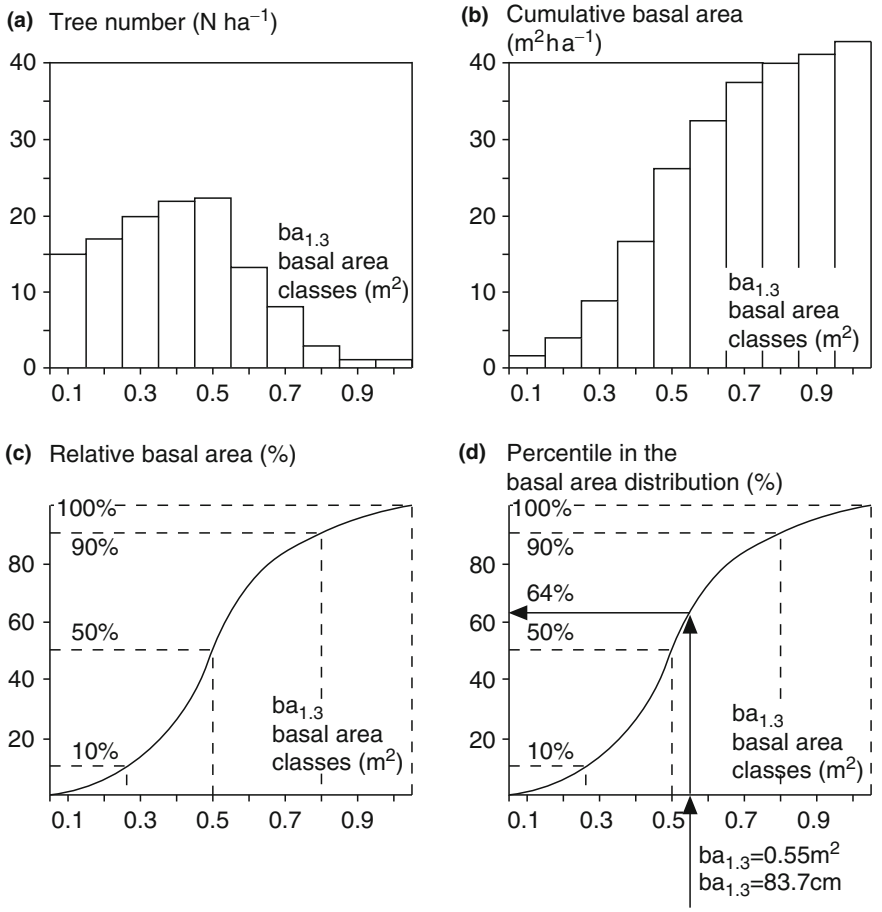

Fig. 8.9 Description of the competitive situation of an individual tree by its percentile in the basal area frequency distribution (presented graphically): (**a**) tree number distribution in classes of similar basal area; (**b**) absolute cumulative basal area by basal area class; (**c**) percentage of cumulative basal area by basal area class; (**d**) determining the percentile of a tree from the percentage basal area distribution

on such small sample plots that position-dependent identification methods identified a large proportion of trees as competitors, and any differences between position-dependent and position-independent models were not discernable due to the small sampling areas (Biging and Dobbertin 1995).

So what is the advantage of position-dependent competition indices? Figure. 8.10 depicts the behaviour of a position-dependent and position-independent growth model compared to the actual basal area increment of a stand (=100%). The position-dependent model 1 uses the competition index KKL (8.1). The position-independent model 2 uses the competition index KKQ (8.18) with a horizontal plane height at p = 60% of the height of the central tree. We characterise the horizontal

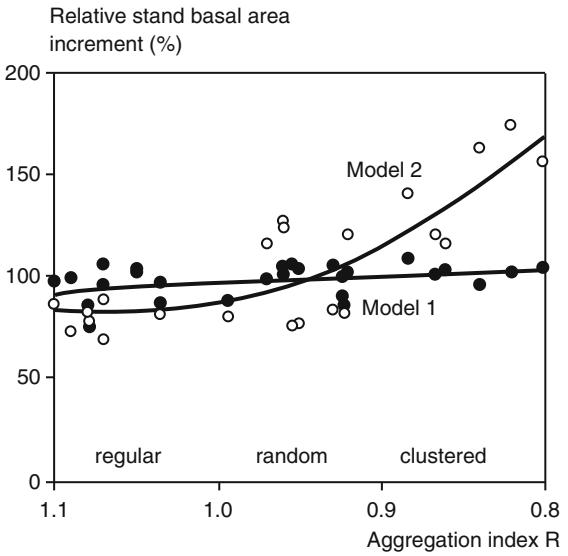

Fig. 8.10 Results of the increment estimate from a position-dependent model 1 (*black dots* and *thick black line*) and a position-independent model 2 (*open circles* and *thin black line*) in stands with different degrees of spatial heterogeneity. Whereas model 1 presents the actual basal area growth (100%) for the total range of aggregation values R (by Clark and Evans 1954), model 2 deviates from reality with increasing structural variation

tree distribution pattern in the stand investigated with the aggregation index R from Clark and Evans (1954) outlined in the Chap. 7, Sect. 7.3.2.1. For the regularly to randomly distributed stem positions characteristic of pure even-aged stands, the inclusion of tree position produces only slightly better estimations of stand basal area increment. If we use both models in forest stands that are structurally more diverse, such as mixed species mountain forest stands or selection forest stands with a clustered horizontal tree distribution pattern, then the position-dependent model is more reliable. When compared to actual stand basal area increment (=100%), model 1 provides relatively accurate predictions of increment across the entire range of values for the aggregation indices, that is from R = 1.1 (tendency towards regularity) to R = 0.8 (tendency towards clumping), deviating from the actual values by 10% at most. The position-independent model 2 produces values close to the actual values only for regular distribution patterns. For irregular or clustered distributions, model 2 produces increment values up to 80% above the actual values.

This model comparison elaborates an important aspect in the calculation of competition. In stands with homogeneous structures, both position-independent and position-dependent models provide similarly accurate estimations of stand increment. As stand structure becomes more heterogeneous, where clustered tree distribution patterns occur, position-independent individual-tree models quickly lose validity. Hence, when growth models need to be applied across a broad range of stand structures, species mixtures, growth limiting factors, regeneration methods and thinning regimes, position-dependent models clearly are preferred.

8.4 Methods Based on Growing Area

8.4.1 Circle Segment Method

Alemdag (1978) breaks up the stand surrounding a central tree j into as many imaginary circle segments as there are competitors (Fig. 8.11). The sum of the area of these n segments produces the area available for tree growth A. By dividing the number of competitors n by this area A, a measure of competition A_n is obtained, which increases with an increasing number of competitors and decreases with increasing area available for growth:

$$A_n = \frac{n}{A}. \tag{8.21}$$

To calculate the area available for growth, expressed by the circle segments, the diameter of the central tree, the diameter of the competitors and the distance to the competitors are used:

$$A = \sum_{i=1}^{n} \pi \times \left[\frac{dist_{ij} \times d_j}{d_i + d_j}\right]^2 \times \left[\frac{d_i}{dist_{ij}} \Big/ \frac{\sum d_i}{\sum dist_{ij}}\right]. \tag{8.22}$$

The first term in (8.22) defines the radius of the circle segments. The second term defines the opening width of the segments. Thus, the radius of the segments increases with increasing distance to the neighbour and the diameter of the central tree. Further, the segment width is dependent on the diameter–distance ratio of the neighbour considered in relation to all competitors.

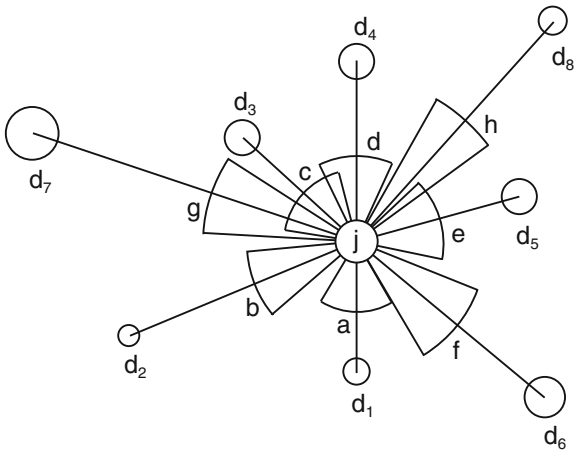

Fig. 8.11 Calculation of available growing area for the central tree j in relation to the diameters ($d_1, \ldots, d_8$) and the distances dist to its eight competitors (after Alemdag 1978). The area available for growth A is obtained from the sum of the areas of the eight circle sectors (a, . . . , h)

8.4.2 Rastering the Stand Area

Whereas Alemdag's index is based on an imaginary growing area and calculated merely from diameter and distance measures, Faber (1981, 1983) and Nagel (1985) adopted methods that partition the entire stand area between its trees. They divided the entire stand area into small cells of, for example, about 10 cm × 10 cm. Each cell is then assigned to the tree that exerts the greatest competition FK (Fig. 8.12). Faber (1981) calculated the strength of competitive FK of a tree on a given cell as a function of the stem volume v and distance dist of the trees next to it:

$$FK = \frac{v^x}{dist^2}. \tag{8.23}$$

The exponent x in (8.23) is either set to 1.0, or it is optimised empirically to obtain the maximum correlation between the area available for growth and actual tree growth in a given period. Nagel (1999) simplified Faber's approach by calculating the strength of competition NK from the basal area $ba_{1.3}$ of all relevant trees and their distance to the cell under consideration:

$$NK = ba_{1.3} \times e^{-dist}. \tag{8.24}$$

Figure 8.13 shows the strength of competition NK for two example trees 1 and 2 decreasing with distance. The shown point (x, y) is assigned to the tree 1 which exerts the greater competition. The area available for the growth of a tree is obtained from the sum of the area of all cells k allocated to that tree. For a cell area of 0.01 m^2, assumed in the example, the k counted cells would result in an area available for

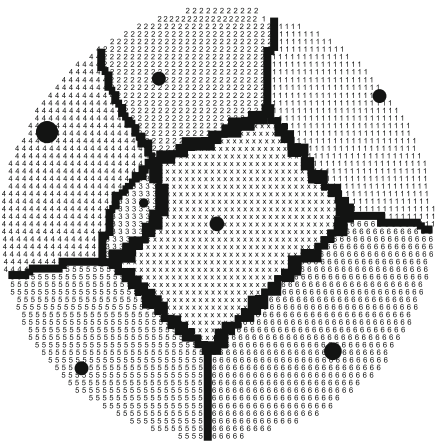

Fig. 8.12 Results of a calculation of the area available for growth using the method from Faber (1981, 1983). The *black dots* represent the stem base of individual trees in the stand. The *filling symbols* show to which tree each grid point has been assigned. The grid points assigned to the central tree are characterised by x. The *black lines* define the boundaries of the area available for growth for the respective trees (after Nagel 1985)

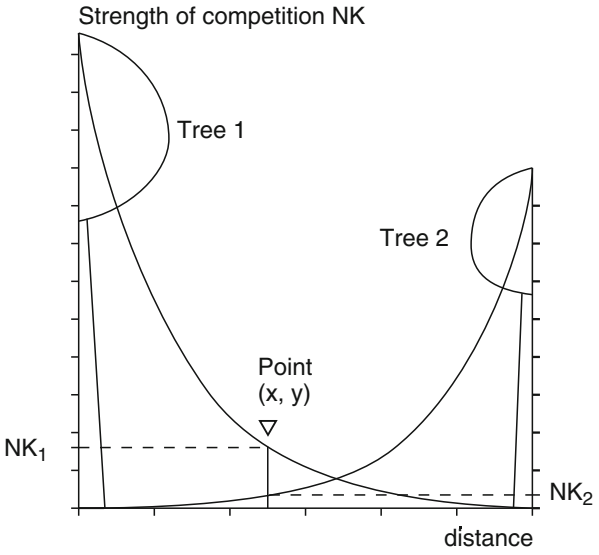

Fig. 8.13 Determination of the strength of competition NK around two neighbouring trees in relation to their size and distance. The point (x, y) is assigned to tree 1 as its strength of competition is greatest at this point (after Nagel 1985, p. 39)

growth $S_j = k \times 0.01 m^2$. For a known growing area S_j, which can be derived from (8.23) or (8.24) as desired, the corresponding potential tree number per hectare is

$$N = \frac{10{,}000}{S_j}. \tag{8.25}$$

The stem number N provides a measure of stand density and the strength of competition on tree j. As the methods from Faber (1981, 1983) and Nagel (1985) allocate the total stand area to the standing trees, they may be used to investigate the efficiency of occupation of the area available for growth in more or less mono-layered pure stands. Both methods divide the stand area among the trees in the stand in proportion to distance and size. This simplified distribution of the area available for growth is limited to mono-layered stands and can hardly be applied in multi-layered stands where the space occupation strategies vary with species and height strata.

8.4.3 Growing Area Polygons

Brown (1965) transferred the Thiessen and Voronoi polygons from geodesy and astronomy to the description of the area available for the growth of a tree. In this method, the available stand area is completely divided between the standing trees. On a tree distribution map (Fig. 8.14a) distance lines are drawn from the central

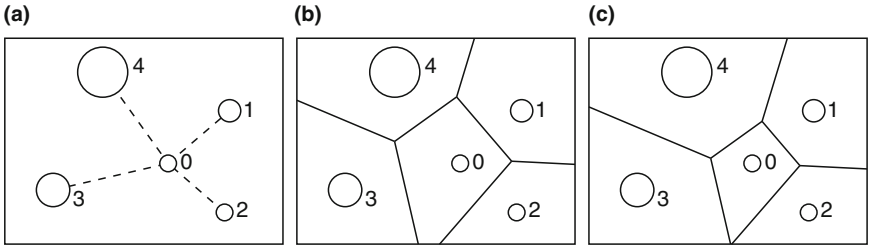

Fig. 8.14 Determination of area available for growth through polygons that were (**b**) not weighted, and (**c**) weighted by diameter ratios. On the tree distribution map (**a**) the connecting lines from each tree and its perpendicular bisecting lines are determined. The point at which they intersect becomes a polygon corner (**b**). By weighting distance ratios by tree size the allocation of the growing area becomes size dependent (**c**)

tree 0 to its neighbours $n = 1,\ldots,4$. The perpendicular lines bisecting the distance lines between two neighbours are determined (Fig. 8.14b). The points at which these bisectors intersect form the corners of the polygons representing the growing area. Trees whose bisectors lie outside the polygons created are not regarded as neighbours. This way, the stand area is divided among the trees without leaving gaps. The area available to tree 0 for growth derived by this method is shown in Fig. 8.14b. It is based on the distribution pattern of stems and not on the size of the trees concerned.

Jack (1968), Fraser (1977) and Pelz (1978) do not place the perpendicular lines at the centre of the distance lines. Rather they divide the distance proportional to the size ratio of the central tree to its neighbour. In our example (Fig. 8.14c), the division is carried out in proportion to diameter so that the area allocated to tree 0 is distinctly smaller because its diameter is considerably smaller than that of its neighbours. Pelz (1978) analysed different weighting options on a trial plot with the species *Liriodendron tulipifera*. In this analysis, he considered tree diameter ($d_{1.3}$), height (h), basal area ($ba_{1.3}$) and the product of basal area and height ($ba_{1.3} \times h$), and concluded that the allocation of available area improved in the order ($d_{1.3} < h < ba_{1.3} < ba_{1.3} \times h$). He adopted the correlation between the area available for growth and basal area growth of the trees in the stand as his assessment criterion.

By weighting the distance relationships by basal area, or the product of basal area and height, correlation values up to 0.8 were obtained (Pelz 1978), making the estimations of tree growth from this method as accurate as those from the competition indices introduced. Whereas, in the competition indices discussed, information about resource availability is aggregated into a dimensionless number, which indicates the restriction in resource supply, methods based on the area available for growth indicate the resource supply by the available square metre per tree. By transferring these methods from the two-dimensional area available for growth to the three-dimensional growing space, which is more useful in highly structured stands, a measure of growing space in cubic metres is obtained (Pelz 1978).

8.5 Detailed Analysis of a Tree's Spatial Growth Constellation

8.5.1 Spatial Rastering and Dot Counting

The dot count principle introduced in the Chap. 7, Sect. 7.4.2 for analysing the crown space of an entire stand can also be used to carry out a detailed analysis of the spatial structure surrounding individual trees. It adopts the three dimensional matrix produced in the Chap. 7, Sect. 7.4.6 which contains digitised data for crown space occupation. The lateral restriction of a tree crown and the shading by neighbouring trees have proven particularly relevant for determining the spatial arrangement of individual trees in highly structured forests, and for predicting their growth (Assmann 1953/1954). The lateral crown restriction of individual trees, which we represent as ε, and their shading, represented by ω, can be derived by a dot count, as done, e.g. by the program ANALYSE (Pretzsch 1992a). This program may also be used to determine other parameters for measuring the surrounding forest structure of individual trees.

The lateral crown restriction ε of the individual trees in a stand, and the change Δε as a result of thinning treatments can be calculated in the following procedure.

The potential crown diameter cd_{pot} is determined for the subject tree A from a previously derived relationship between tree height h and potential crown diameter cd_{pot}. The circular plane with diameter cd_{pot} marks the area occupied by tree A under optimal growing conditions. However, this area is usually reduced by competition from its neighbours (Fig. 8.15).

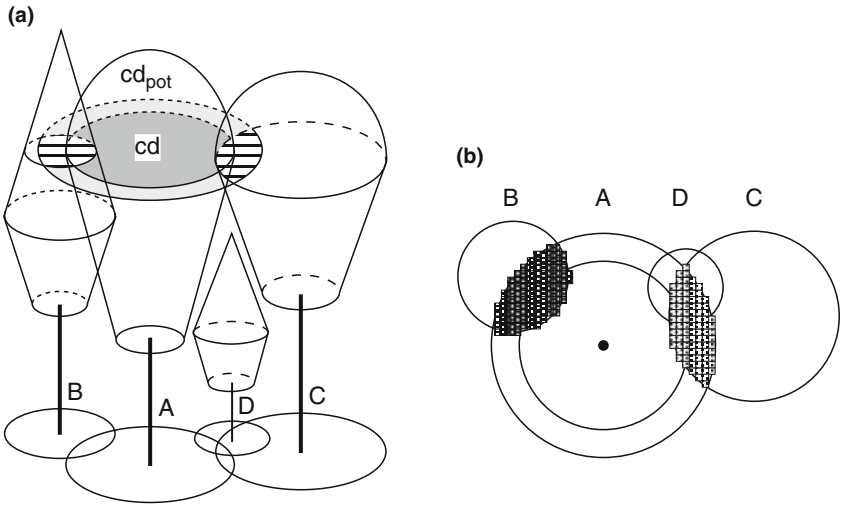

Fig. 8.15 Determination of the lateral crown restriction ε of tree A by its stand neighbours. (**a**) The circular plane with potential diameter cd_{pot} of tree A forms the reference area for the determination of crown overlap (*hatched area*). (**b**) The overlap areas are obtained from a dot count; the overlap of neighbouring Norway spruce (*left*) and European beech (*right*) is highlighted in *dark grey* respectively *light grey*

To determine the lateral crown restriction ε of tree A, the area of overlap of all neighbouring crowns (Fig. 8.15a, trees B and C) with the potential crown width of the central tree A, represented by the hatched area in Fig. 8.15a, is determined. Figure 8.15b visualises the spatial arrangement of trees A–D in the horizontal plane, and shows that the overlap area is determined by means of dot count in the three dimensional matrix, which contains stand structure in grid form. In the height layer, where the lateral restriction of tree A from its neighbours occurs, a dot count is carried out for each grid point. This reveals whether a certain point is overlapped not at all, or once, twice, thrice or more by crowns from neighbouring trees. By relating the overlap area recorded in the dot count to the total potential crown area for each tree, one obtains a relative measure ε for lateral crown restriction of the individual trees by its neighbours.

The entire procedure is repeated for the stand structure after thinning so that ε_{before} and ε_{after} for each tree, and the lateral release $\Delta\varepsilon = \varepsilon_{before} - \varepsilon_{after}$ can be quantified.

The dot count statistic delivers not only a total value of ε for each tree, referred to as ε_{tot} in future, but can also distinguish between the tree species responsible for the lateral crown restriction of the central tree by classifying ε_{tot} by tree species. In a hypothetical example of a mixed Norway spruce–European beech stand, an overlap analysis for a tree produces the following results: $\varepsilon_{tot} = 0.75$, with $\varepsilon_{sp} = 0.25$, and $\varepsilon_{be} = 0.50$. This means that adjacent tree crowns overlap the central tree by 75%, and the lateral crown restriction from European beech is twice that of Norway spruce. The numerical recording of lateral restriction and its classification by tree species provides the information necessary to analyse the species-specific effect on, and response to competition from experimental plot data (Pretzsch 1992c).

To determine the shading ω of a tree, we construct a search cone at $p = 70\%$ of the central tree height with an opening angle of $\alpha = 60^\circ$ (Fig. 8.16) where p and α can be varied to meet the investigation aims. Then, a dot count searches all cells filled by adjacent tree crowns within the three-dimensional search cone. Each of these grid points is weighted by the reciprocal of the quadratic distance between the cell centre and the cone apex so that the shade index ω becomes

$$\omega = \sum_{i=1}^{n} \sum_{j=1}^{m} \sum_{k=1}^{u} \frac{R_{ijk}}{E_{ijk}^2}. \tag{8.26}$$

In this formula, R_{ijk} is set to 0 if no crown meets the grid point R_{ijk}, and to 1, 2, 3 ... if 1, 2, 3, ... crowns meet the grid point R_{ijk}. E_{ijk} represents the distance from R_{ijk} to the apex of the search cone. The variables n, m, u indicate the number of cells in the x, y, and z direction of growing space, and i, j, and k the coordinates of cells.

The canopy cover from neighbouring crowns is weighted stronger than canopy cover from more distant trees. The shade index ω is a dimensionless indicator of the shading of a tree by its neighbours. As for the lateral crown restriction ε, in addition to the total shading $(\omega = \omega_{tot})$, the species-specific contributions can be calculated. Thus, the results of a shading analysis for a tree in a hypothetical, mixed Norway spruce-Silver fir-European beech stand might be: $\omega_{tot} = 8.0$ with

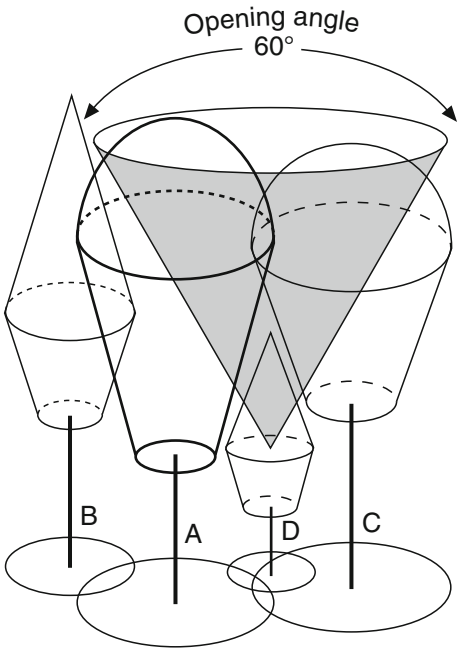

Fig. 8.16 Determination of the shading ω of tree D by a dot count in the search cone area

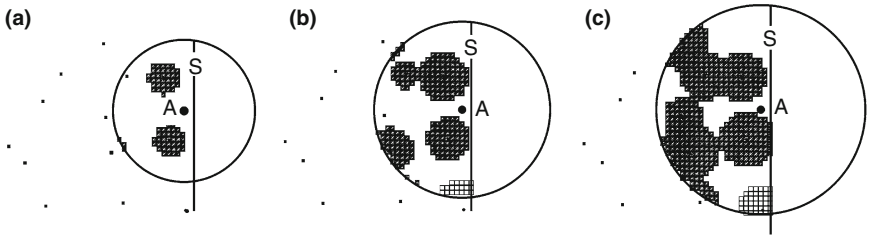

Fig. 8.17 Shading analysis by dot count within the search cone for tree A (stem base shown by *black dot*) at heights (**a**) h = 13.3 m, (**b**) h = 15.3 m, and (**c**) h = 17.3 m. The crowns of the neighbouring Norway spruce (*grey grid squares*) and European beech (*white grid squares*) reach into tree A's search cone. The secant S indicates the experimental trial plot border, on the right side of which there is no information about neighbouring trees

$\omega_{sp} = 4.0$, $\omega_{fir} = 3.0$, and $\omega_{be} = 1.0$. In this case, the shade cast on this tree comes primarily from Norway spruce and Silver fir and only minimally from neighbouring European beech trees. If a shading analysis is carried out before and after thinning, $\Delta\omega$ provides a meaningful measure of the opening up of the tree crowns through thinning.

Figure 8.17 provides an example of shading relationships within a search cone for a tree at the plot edge in the Norway spruce–European beech mixed stand, Zwiesel 111/3. The results of the dot count from three search cone cross-sections at the

heights (a) 13.3 m, (b) 15.3 m and (c) 17.3 m (Fig. 8.17) are displayed. The stem base of the central tree A is shown as a black dot at the centre of the search cone. The crowns of the neighbouring Norway spruce (dark grey grid squares) and European beech (lighter grid squares) reach into the search cone around tree A. Due to the increasing opening width of the search cone with height, the search circle area A increases from image (a) to (c). The points outside the search cone represent stem positions of trees disregarded in the structural analysis. The secants (S) indicate the edge of the experimental trial plot. As the search cone extends beyond the edge, different methods for dealing with the edge effect may be used (cf. Sect. 8.7 of this chapter).

8.5.2 Calculation of Spatial Distances

An increasing number of tree distribution maps and repeated crown surveys are available from extensive surveys of experimental plots. They contain information about growth behaviour of individual trees that has by far not yet been exhausted. In this section, a method is presented that allows spatial structural measures to be extracted from crown maps. These structural measures, together with growth rates of the respective trees, can reveal crown dynamics.

We will now investigate the relation between lateral crown restriction and radial crown growth more closely. The influence of crown distance and tree species of the neighbours on the crown development of the central tree can be quantified by calculating the distance to neighbouring crowns along eight tree crown radii (1 = north, 2 = northeast, 3 = east, ..., 8 = northwest). This procedure is implemented, for example, in the program ABSTAND from Pretzsch (1992b) with a spatial stand model.

A 3D-crown shape model produces a spatial image of the stand structure from stem coordinates, the eight crown radii, tree height and height to the crown base (Fig. 8.18). In this model, the horizontal crown plane is described by an octagon given by the eight crown radii in the directions N, NE, etc. to NW. The vertical crown shape is modelled from the crown shape function in the Chap. 7, Sect. 7.2.2.1 for each crown octant separately. Then the crown shape model calculates the height of the maximum crown width, which is also the boundary between light and shade crown, and the crown shape function determines the horizontal crown extension at that height. The program ABSTAND then draws a horizontal cross-section through the stand crown space at a height corresponding to the greatest crown width of central tree. Next, as shown in Fig. 8.19 for a Norway spruce tree in a mixed Norway spruce–European beech forest on the long-term experimental trial plot Zwiesel 111/3, lines are drawn in all eight directions on this plane until they meet a neighbouring crown. The program registers both the distance and species of the neighbouring crowns. In direction 2 and 3, for example, the lines meet a European beech (light grey), and, in direction 7 the line meets a Norway spruce (dark grey).

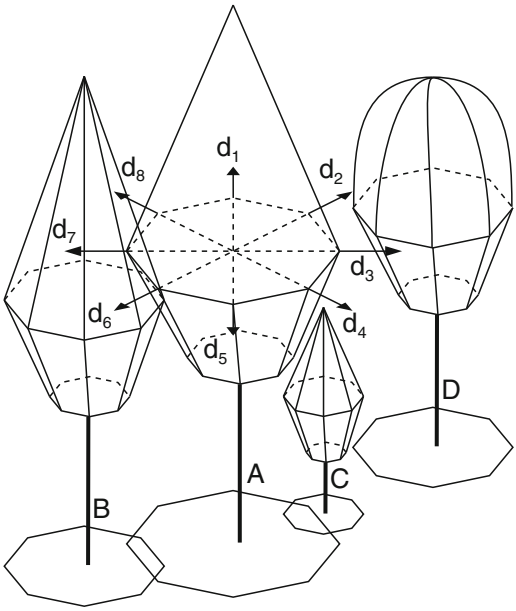

Fig. 8.18 Determination of the lateral crown restriction of individual trees: distances from the crown perimeter of tree A to the neighbouring crowns are determined in eight directions

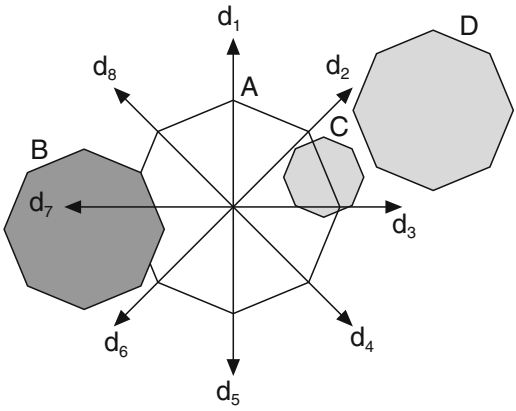

Fig. 8.19 For a refined analyses of the competitive situation of a tree the distances from the central tree's crown to its neighbours in all eight directions can be extracted from stem charts and crown maps. A–D: central tree and neighbours, $d_1, \ldots, d_8$: direction specific distance between the central tree crown and neighbouring crown at the height of the circular plane

Where crowns almost touch each other, the distance is about zero, where there is a gap, the distance assumes positive values (trees A and D); overlapping crowns are recorded as negative distances (trees A and B). If the tree is released by thinning on one side, then distances of many metres may be recorded in this direction (Fig. 8.19, d_1, d_4, d_5, d_6, d_8). The 3D-approach to distance calculations is especially useful in stands with strong vertical structures. Distance calculations from crown maps in such stands would frequently identify crowns touching where, in reality, they do not (cf. Fig. 8.19, trees A and C).

8.5.3 Crown Growth Responses to Lateral Restriction

The eight direction-specific distances to neighbouring crowns, and the species of each neighbour were registered in the program ABSTAND for all trees in the mixed Norway spruce–European beech stand, at the long-term experimental trial plots Zwiesel 111/1, 4, and 5. In addition, from repeated surveys, the initial and final crown radii, and hence changes in radii, are available for several survey periods.

From these data, and the spatial distance calculated, species-specific functions defining relationships between crown distance and radial crown development can be derived (Fig. 8.20). The functions describe the relative changes in crown radii of Norway spruce and European beech in relation to the crown distance to neighbours. A change in radius of +100% means that a tree expands its crown radius without lateral restriction, and achieves the potential crown radial increment. The curves in Fig. 8.20 show not only the decline in crown radial increment as the central tree crown becomes increasingly interlocked with neighbouring crowns, but also the crown distance at which a crown dieback commences (below the dotted 0-line). As the program ABSTAND records tree species as well as distance to the neighbour, separate functions can be derived for the following neighbourhood situations: N. sp. → N. sp. and N. sp. → E. be. (Fig. 8.20a), and E. be. → E. be. and E. be. → N. sp. (Fig. 8.20b).

The functions reveal an interesting species-specific competition behaviour: when a Norway spruce grows towards another Norway spruce, the decrease in radial increment after an overlap of 1.0 m is almost linear. Yet, if it grows towards a European beech, a decrease in radial increment is observed much later. Effectively, this leads to

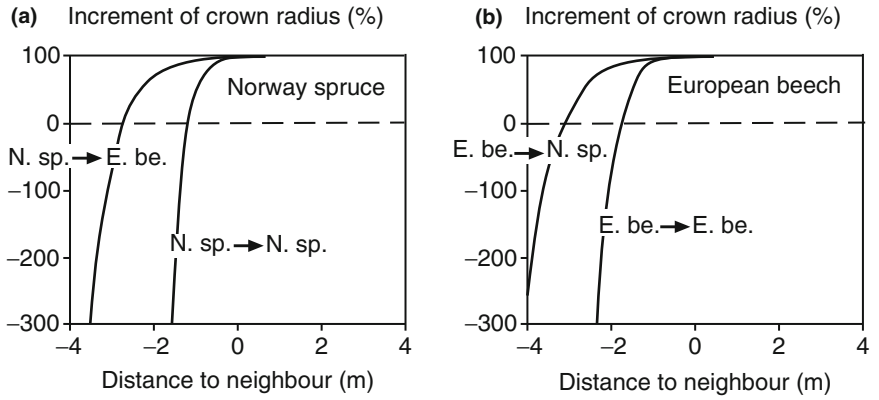

Fig. 8.20 Influence of the distance to the neighbouring crown (dist) on the relative radial crown increment (icr in %). (**a**) Radial crown increment of Norway spruce in a Norway spruce (N. sp → N. sp.), and a European beech (N. sp. → E. be.) neighbourhood. Estimation functions: $icr_{sp \to sp} = 1.0 - e^{-3.84 \times (dist+1.2)}$ and $icr_{sp \to be} = 1.0 - e^{-1.71 \times (dist+2.7)}$. (**b**) Radial crown growth of European beech in a European beech (E. be. → E. be.), and a Norway spruce (E. be. → N. sp.) neighbourhood: $icr_{be \to be} = 1.0 - e^{-2.56 \times (dist+1.8)}$ and $icr_{be \to sp} = 1.0 - e^{-1.49 \times (dist+3.1)}$

a tighter interlocking of a Norway spruce crown with neighbouring European beech than with neighbouring Norway spruce. Similarly, the crown interlocking for a European beech growing towards a Norway spruce is also tighter than for European beech in pure stands. This finding confirms the results from Kennel (1965a) that mixed Norway spruce and European beech stands are more productive than pure stands at this site because they can use the available growing space with more flexibility and efficiency. For Norway spruce and European beech, a reduction in lateral crown expansion of more than 5% only occurs when crowns interlock by 1.0–2.0 m, and the crowns recede only after the crowns overlap by 2.0–3.0 m. Thus the crown growth dynamics of Norway spruce and European beech differ considerably from the light-demanding species European larch, which shows a clear reduction in the growth of side branches once the distances from branches to the neighbouring crown fall below 40 cm (Schütz 1989).

Based on the position-dependent crown growth functions, the crown cross-sectional development at a trial plot can be simulated for each individual tree in relation to its neighbourhood. Figure 8.21 shows the crown map for a 20 m × 20 m section of the experimental trial plot ZWI 111/3 in 1954, the year the simulation run begins. The crown development of Norway spruce and European beech, 60 and 80 years old at this time respectively, was simulated for a 50-year period at 5-year intervals. The interim results at times t = 10 years, t = 30 years, and t = 50 years (Fig. 8.21b–d) show how the crowns expand and respond to increasing restriction by developing oval and eccentric crown shapes. To develop the crown perimeter, the eight crown radii are connected by a cubic spline using the algorithms from Späth (1983) (cf. Chap. 7, Sect. 7.2.1.2).

8.6 Hemispherical Images for Quantifying the Competitive Situation of Individual Trees

8.6.1 Fish-Eye Images as a Basis for Spatial Analyses

Biber (1996) introduced a method for quantifying the competitive situation of individual trees at the forest floor, or in the crown space through the computational construction and analysis of hemispherical images. The aim of his method is to calculate the diffuse site factor and sky factor, which Anderson (1964) developed and Olsson et al. (1982) applied to quantify growing conditions in forest stands. The diffuse site factor represents the relative light intensity at a defined point within the stand. The light intensity of a completely overcast sky provides the reference measure (100%). The sky factor indicates the proportion of free sky in a circle described by an angle of 10° around the zenith. Whereas the diffuse site factor correlates closely with diffuse radiation at the point, the sky factor correlates closely to precipitation measured at this point. Both factors can be determined directly from radiation, light intensity or crown projection measurements. Alternatively, these variables may be extracted

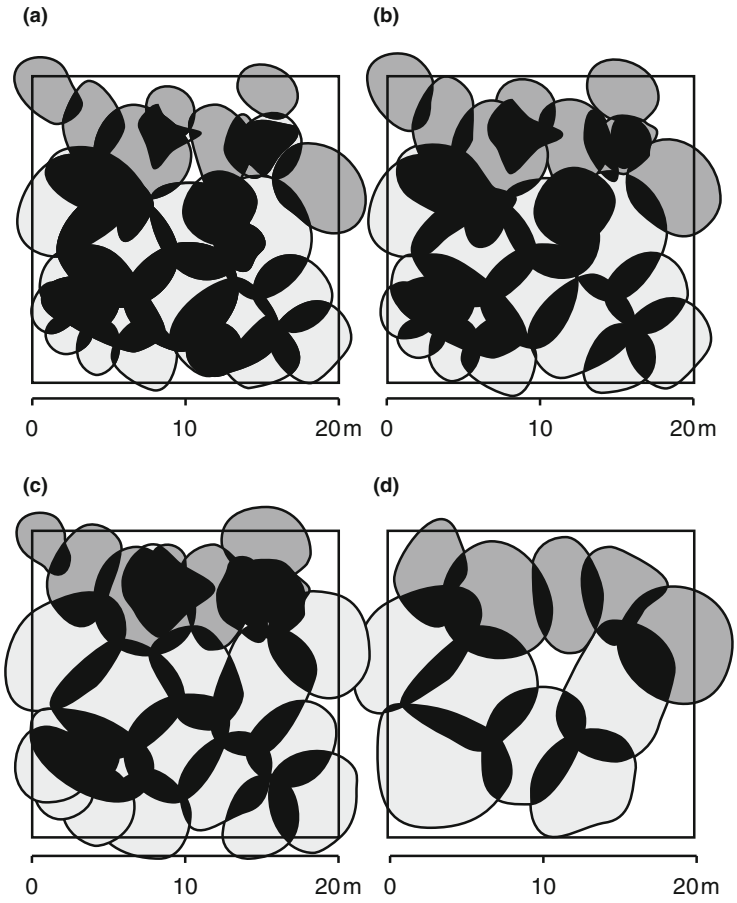

Fig. 8.21 Crown cross-sectional area development resulting from a simulation run with SILVA 2.0 over 50 years. The crown map for a 20×20 m section of the experimental trial plot Zwiesel 111/3 is presented in a 50 year simulation run at the time (**a**) t = 0 year, (**b**) t = 10 years, (**c**) t = 30 years, and (**d**) t = 50 years

from hemispherical photographs (fish-eye photos) using a method developed and used by Wagner (1994) in stand regeneration investigations. Figure 8.22 shows fish-eye photographs from (a) an open and (b) a sparsely stocked area of a 114-year-old Scots pine stand in Forest District Fuhrberg.

Whereas direct measurements require considerable technical equipment, fish-eye photos, which are produced relatively easily, facilitate a comparatively simple analysis of the above-mentioned factors. Further, they store the spatial stand structure data at the respective points permanently. Biber's (1996) method does not make use of actual photographs, but computes a hemispherical image at a point AP from the available stand data. By analysing the shades of grey, Nagel et al. (1996) showed that close approximations of the diffuse site factor (DIFFSF) and sky factor (SF)

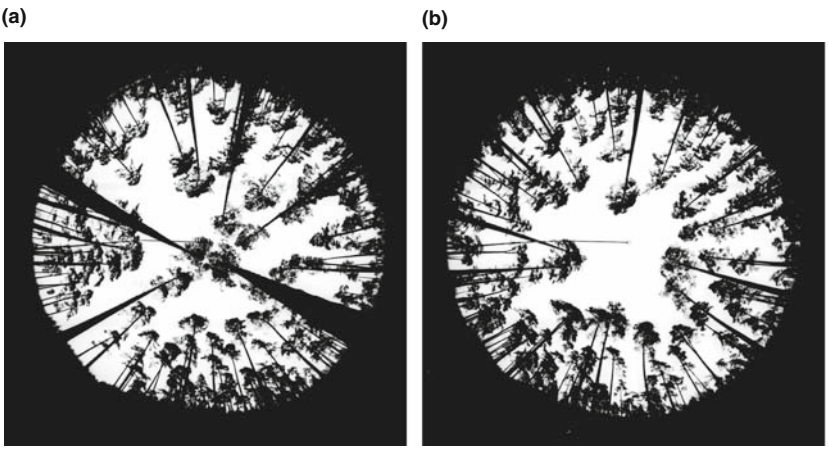

Fig. 8.22 Fish-eye photography from a 114-year-old Scots pine stand in Forest District Fuhrberg in Lower Saxony. The pictures show (**a**) an open, and (**b**) sparsely stocked part of the Scots pine stand. Yield class I.–II. by Wiedemann (1943a) with moderate thinning, and a stocking density with reference to this yield table of stocking density SD = 0.5 (Photo by courtesy of Sven Wagner)

can be obtained. The data required for this approach are the same as those required to calculate position-dependent competition indices, primarily comprising tree species, diameter, height, crown base height, crown radius and the position of all trees. DIFFSF and SF, two ecologically important variables, can be calculated at any point within the stand from the method outlined below. Biber (1996) successfully employs the data from the computed hemispherical images to parameterise and control individual-tree growth in a simulator for mixed Norway spruce–European beech stands.

8.6.2 Methodological Principles of Fish-Eye Projection in Forest Stands

In the fish-eye approach for developing hemispherical images, points are projected from hemispheric angles on concentric circles around the point AP, which is located at the centre, i.e. the zenith, of the image (Fig. 8.23). The position of the treetop P (Fig. 8.23a) under the hemispherical angle α above the projection plane, is converted to point P' on the projection plane (Fig. 8.23b) by the following formulae:

$$X_{P'} = r \times \left(1 - \frac{\alpha}{90^\circ}\right) \times \cos\left(\beta - 90^\circ\right) \text{ and} \tag{8.27}$$

$$Y_{P'} = r \times \left(1 - \frac{\alpha}{90^\circ}\right) \times \sin\left(\beta - 90^\circ\right), \tag{8.28}$$

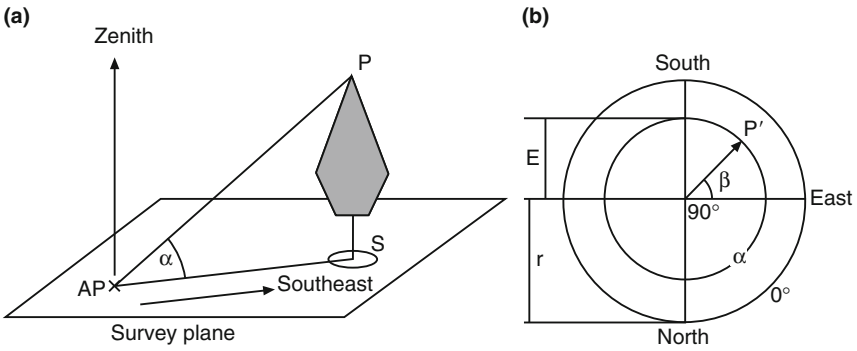

Fig. 8.23 Principle of a fish-eye projection of the tree top P (**a**) from the 3D-space onto the 2D-projection plane and (**b**) the results of projection. At the centre point AP the fish-eye lens is directed to the zenith and projects all points above this level on the given survey plane through AP. P can be converted to P′ using (8.27) and (8.28). r represents the radius of the periphery of the fish-eye image at $\alpha = 0°$, E the distance between AP and P projected onto the survey plane

where $X_{P'}, Y_{P'}$ are Cartesian coordinates of the point P′, α represents the hemispherical angle at the point P, β the horizontal direction of point P in relation to the point AP, and r the radius of the fish-eye image, also the scale parameter.

The angle α is obtained from

$$\alpha = \arctan\left(\frac{\overline{PS}}{\overline{APS}}\right). \tag{8.29}$$

In this way each point above the projection plane can be projected onto it. The actual distance E between the point AP and the projection point P in a fish-eye image with the radius r is

$$E = r \times \left(1 - \frac{\alpha}{90°}\right) \quad \text{for } [0° \leq \alpha \leq 90°]. \tag{8.30}$$

Thus, an object under a given hemispherical angle is projected linearly on the radius of the fish-eye image. To project whole trees onto the projection plane, the trees are divided into sections of equal length from the crown top P to the stem base S (Fig. 8.23a). The cross-sections of the crown and stem for each section are reproduced by eight-sided regular polygons whose corner points are projected onto the projection plane using the methods described. Depending on the projection angle, the regular polygons become symmetrical or asymmetrical areas in the fish-eye image. After projecting the crowns and stems of all trees in the stand that are visible from a given point AP onto the projection plane, the surface is covered to a certain degree. Biber (1996) classifies the projected points P′ with different shades of grey according to onefold and multiple cover, cover from different tree species, and cover from stem or crown.

He recommends the number of trees to include in a survey, and develops methods for edge correction. From a dot count of grey shades in the fish-eye image, the cover is represented by an intensity histogram from the two ecological variables, diffuse site factor and sky factor, can be derived.

8.6.3 *Quantifying the Competitive Situation of Individual Trees in a Norway Spruce–European Beech Mixed Stand*

If the three-dimensional stand structure is known, as in our example of a mixed stand of Norway spruce and European beech in Fig. 8.24, then fish-eye images can be simulated at any points AP 1 to AP 5 in the stand space. In doing so, tree sections found above the projection plane through AP 1 to AP 5 are projected onto the projection plane creating the hemispherical images as described previously. From these images, we can see how the coverage by stems and crowns decreases with increasing height from AP 1 to AP 5. When the grey values and coverage of simulated images are analysed, a height profile of the diffuse site factor can be derived (Fig. 8.25). It is not only based on the five points AP 1 to AP 5 presented in the example, but on an entire survey at 1 m height intervals, amounting to 41 analyses in total. The height profile in Fig. 8.25 reproduces well the reduction in the diffuse radiation from the upper canopy to the forest floor.

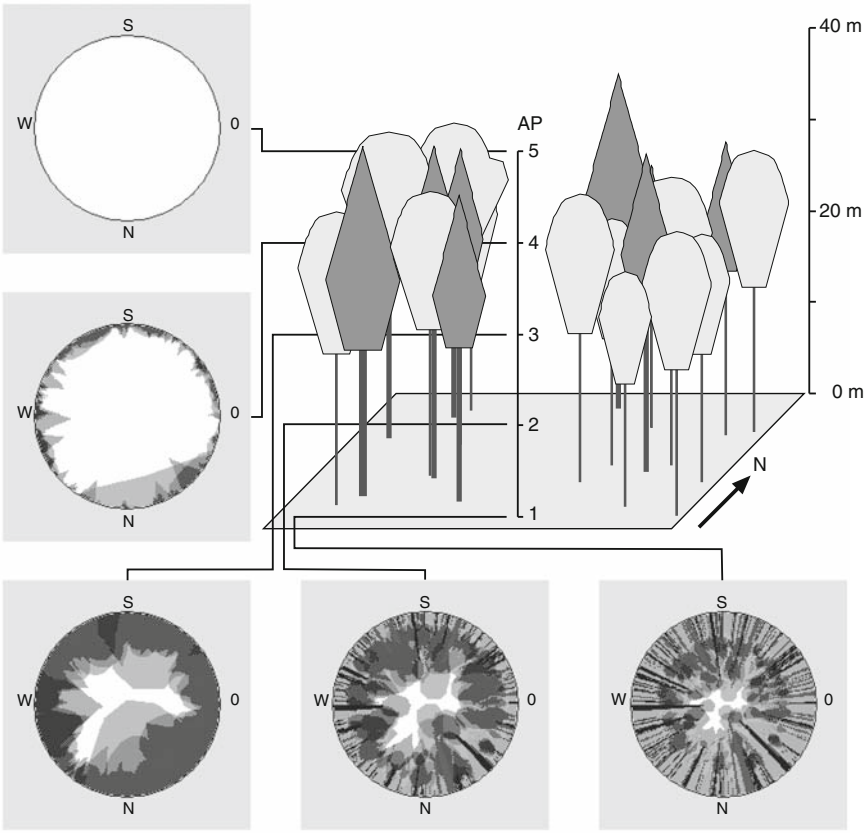

Fig. 8.24 Example of the calculation and analysis of hemispherical images at the points $AP_1, \ldots,$ AP_5 in a mixed Norway spruce–European beech stand

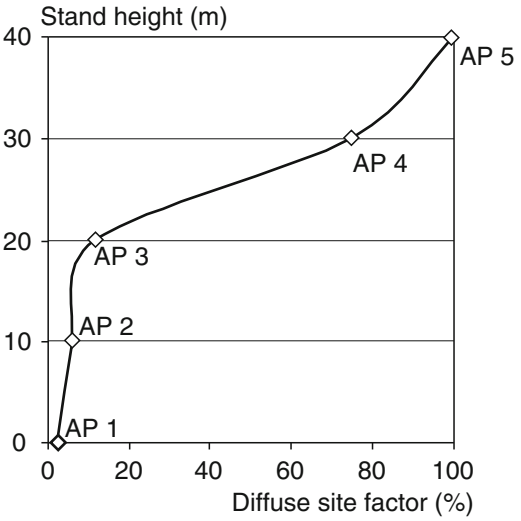

Fig. 8.25 Computational hemispherical images can deliver reliable results about the radiation conditions in the form of a diffuse site factor at locations within the stand that are difficult to reach with instruments. Towards the upper crown space the cover from stem and crown decreases

The values of DIFFSF and SF derived by this method correlate closely with the measured values of these variables at the same points (Nagel et al. 1996). A large number of survey points, for which the grey values of both fish eye photographs and simulated hemispherical images were analysed, facilitate the derivation of the following relationships between the estimated and measured factors:

$$\mathrm{DIFFSF}_{\mathrm{measured}} = \mathrm{DIFFSF}_{\mathrm{estimated}}, \tag{8.31}$$

$$\mathrm{SF}_{\mathrm{measured}} = -18 + 1.25 \times \mathrm{SF}_{\mathrm{estimated}}. \tag{8.32}$$

8.7 Edge Correction Methods

8.7.1 Edge Effects and Edge Correction Methods

For trees located near the boundary of monitoring plots, the indices introduced in this chapter can only supply incomplete or imprecise information. The closer the tree is to the boundary, the greater the unknown portion of the tree's surroundings outside the experimental trial plot. One possibility for avoiding the edge effects in structural analysis is to include only those trees whose entire surroundings is known, i.e. the centre of the experimental trial plot. Yet, the number of trees with no edge effects is often comparably small, particularly for small plots, and plots with a high circumference to area ratio. The edge effect is especially problematic in position-dependent modelling and forest growth predictions when the long-term development of a stand is based on a small sample area without information about

the external stand structure. The edge effect may be evened out by one of three groups of methods: methods, which extrapolate the stand structure on the trial plot beyond the plot boundary by mirroring, shifting, linear expansion; methods where the expected competition situation outside the plot is estimated from the individual tree surroundings inside the plot; and structure generation methods based on generalised stem-distance functions, which are calibrated for the experimental plot and then used to generate a hypothetical stand around the plot with similar structural characteristics.

8.7.2 Reflection and Shift

In the reflection method, stand structure on a plot is mirrored along the axes formed by the plot boundary line, with point reflections at the plot corner points so that, ultimately, the plot is surrounded by reflected images of itself along its perimeter (Fig. 8.26). If the competitive zones of trees in the core area extend beyond the edges produced by the reflection, the reflection is repeated so that the core area, comprising eight images from the first reflection, is surrounded by 16 more images after the second reflection. The resulting 25 areas provide the basis for quantifying competition for all trees in the core area.

In the shifting method, an exact copy of the monitoring area is shifted along its sides and corners (Fig. 8.27). Again, if the zones of competitive influence of the

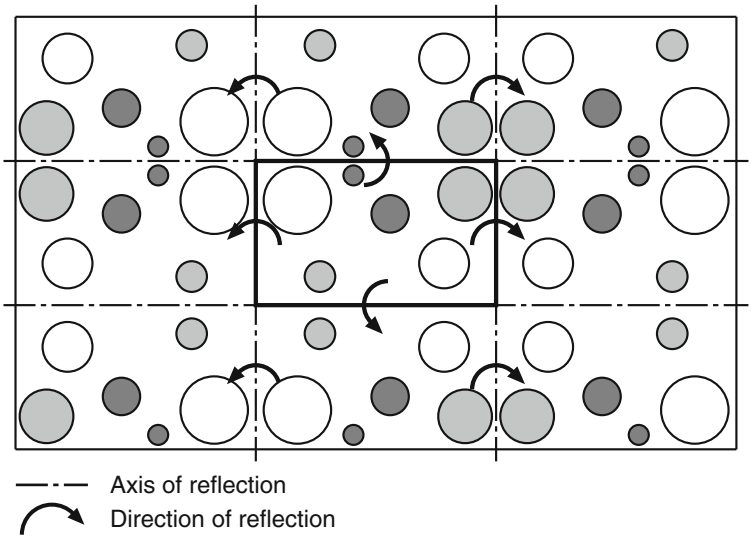

Fig. 8.26 Correction of the edge effects by mirroring the stand structure of the experimental trial plot at the plot boundaries and corners. The true experimental trial plot is depicted by the *bold inner rectangle*

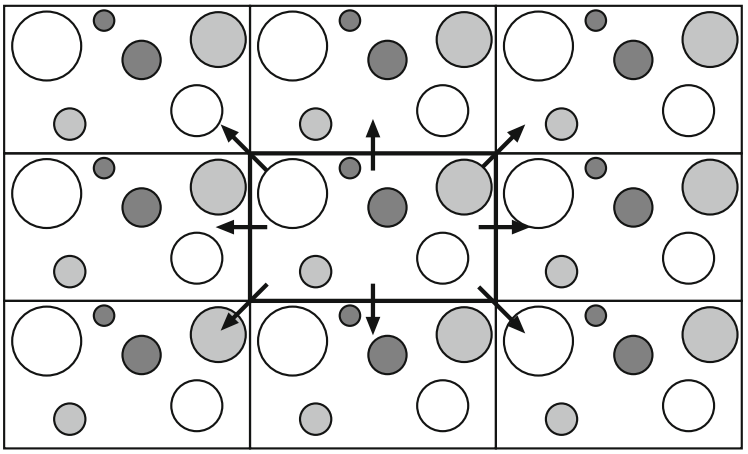

Fig. 8.27 Correction of the edge effects by shifting of the stand structure at the experimental trial plot, which is then surrounded by eight identical stand sections. The true plot is depicted by the *bold inner rectangle*

trees in the monitoring plot extend beyond the edge created by these eight images then the edge can be extended by another shifting, creating 16 image repetitions.

Although both methods produce a somewhat artificial periodicity in the spatial stand structure, they deliver equally effective corrections of competition estimations for edge trees (Monserud and Ek 1974; Windhager 1997; Radtke and Burkhart 1998; Biber 1999). In axis and point reflections, periodicity is dependent on the position of individual trees in relation to the boundary. Here, unnatural spatial structures, such as extremely dense or extremely sparse neighbourhoods, can be produced, which occasionally result in outliers in the competition indices (Biber 1999). In their investigations in regularly structured even-aged forests Radtke and Burkhart (1998) found that an axis mirroring passing through the outermost tree row of the plot proved effective, and avoided atypical neighbourhood relationships. The shifting method generates a very regular periodicity. However, this method also may lead to implausible neighbourhood relationships, for example such as concentration of large mature trees.

8.7.3 Linear Expansion

The disadvantages of reflection and shifting methods are that they produce periodicity at the tree or stand level, and their application is limited to rectangular monitoring plots. When employing reflection or shifting methods on, for example, circular, sample areas, empty areas are created. To overcome this disadvantage, Martin et al. (1977) developed the linear expansion method. This method

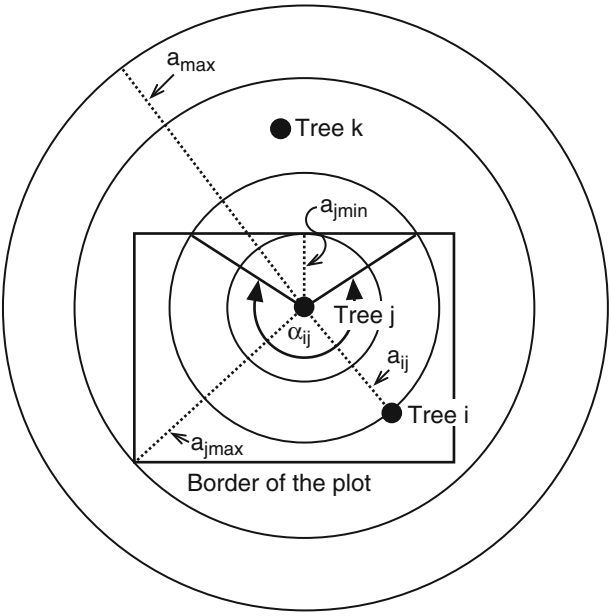

Fig. 8.28 To calculate the competition for central tree j located close to the plot boundary (*bold rectangle*) three distance zones are defined, for which different information is available. Zone 1 covers all trees within the inner circle. Information on the competition of trees within this zone where $a_{ij} < a_{jmin}$ is complete. For the trees in zone 2 which reaches from a_{jmin} to a_{jmax} and covers, e.g., tree i the study plot provide just incomplete information about neighbourhood and competition of tree j. In the distance beyond a_{jmax} no values are available for quantifying individual competition of tree j

recognises that, even for edge trees, a part of the zone of influence always lies within the observation zone. The linear expansion method regards that part of the influence zone inside the monitoring plot as representative for the overall competition. The competitive situation within the plot is extrapolated linearly over the total area.

In the next example, we calculate the competition index CI_j for tree j close to the boundary in Fig. 8.28 (black circle at the centre of the search radii):

$$CI_j = \sum_{i=1}^{n} c_{ij}. \tag{8.33}$$

Typically only its $i = 1, \ldots, n$ competitors located within the plot (black rectangle) are known. The circle with radius a_{max} indicates the search space around the tree j (centre) located near the boundary. This radius delineates the zone of influence of possible competitors, which extends well beyond the plot boundary. Clearly, the plot provides only an incomplete picture of the spatial surrounding and competitive situation of tree j. The competition indices of edge trees would be underestimated systematically if the stand structure and competitors outside the monitoring plot were ignored. In Fig. 8.28, three distances zones can be differentiated around tree j,

indicated by the dotted radii a_{jmin}, a_{jmax} and a_{max}. In the first zone, trees are found whose distances from the central tree a_{ij} are smaller than a_{jmin}. In the second zone, the distances range from a_{jmin} to a_{jmax}, and, in the third zone, from a_{jmax} to a_{max}. The first radius a_{jmin} generates the largest possible circle around tree j that still lies entirely within the plot area. The radius a_{jmax} defines the largest circle around tree j that still touches the experimental trial plot. The radius a_{max} represents the search radius for the identification of competitors from tree j. These three zones provide very different information about the competitive situation for central tree j and they make specific contributions to the competition index CI_j.

Information about the contribution of trees at distances $a_{ij} < a_{jmin}$ to competition is complete as the entire search space falls within the research plot (Fig. 8.28). The contribution to competition from trees in this zone is determined using standard calculation methods without the need for correction.

The research plot only partially documents the competition from trees at distances $a_{jmin} < a_{ij} < a_{jmax}$. For example, the characteristics of a tree k, which falls within this zone, could not be included in the competition calculation as it was not measured. In this zone, the linear expansion method assumes that competition in the research plot is representative of competition in the entire search radius a_{ij}, and the contribution to competition in the search-circle outside the research plot is the same as inside. The portion of the search space outside the research plot depends on the distance a_{ij} between the central tree j and the competitors i. For example, for tree i in Fig. 8.28, the competition relationships in the circle sector with angle α_{ij} are known. However, the relationships in the section $360^\circ - \alpha_{ij}$ are unknown. Hence, we extrapolate the competitive behaviour in the total 360°-search space from the circle sectors that lie completely within the research plot. As shown in Fig. 8.29, the angle α corresponding to the circle sectors carrying information often consists of various circle segments α_1 to α_n. The portion of the circle for which the information about competition is complete is given by $P_{ij} = \alpha/360^\circ$. The reciprocal factor $E_{ij} = 360^\circ/\alpha$ can be used to estimate the total competition from the competition c_{ij} of $i = 1, \ldots, n$ trees on a plot:

$$CI_j = \sum_{i=1}^{m} E_{ij} \times c_{ij} = \sum_{i=1}^{m} 360^\circ/\alpha_{ij} \times c_{ij}. \tag{8.34}$$

For trees whose distances are $a_{ij} < a_{jmin}$, the angle α and projection factor E are $\alpha = 360^\circ$ and $E_{ij} = 1.0$ respectively.

For those trees whose distance a_{ij} falls within the radius $a_{jmax} < a_{ij} \leq a_{max}$, information about the competition they exert on tree j is unavailable. For small plots, large central trees and large competitors, the contribution to competition from this third zone may be considerable, and should not be ignored. Therefore, according to Martin et al. (1977), the size of the plot for individual-tree analyses should be chosen such that $a_{max} < a_{jmax}$ for all $j = 1, \ldots, n$. If this is not possible, then, according to Martin et al. (1977), the contribution to competition from such trees in the zone $a_{jmax} < a_{ij} \leq a_{max}$ can be estimated by determining the mean competition ratios for discrete size classes of central trees j and neighbours i and defined distance classes between a_{jmax} and a_{max}, and then adding them to the competition index CI_j.

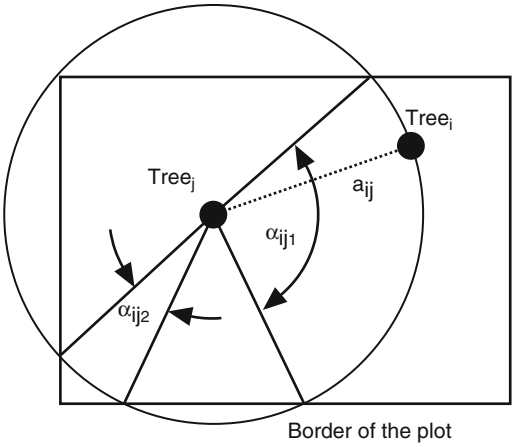

Fig. 8.29 The estimation of competitive influences from neighbours in the distance interval $a_{jmin} < a_{ij} \leq a_{jmax}$ (cf. Fig. 8.28, zone 2) is obtained sometimes from more than one circle sector depending on the plot shape and the location of the tree j. In this example, the radius is a_{ij}, and two circle sectors with angles α_{ij1} and α_{ij2} are used to calculate the competition index. The expected competition in the remaining areas for which data are unavailable are extrapolated from the spatial arrangement of the trees within the two circle sectors, lying entirely within the experimental trial plot

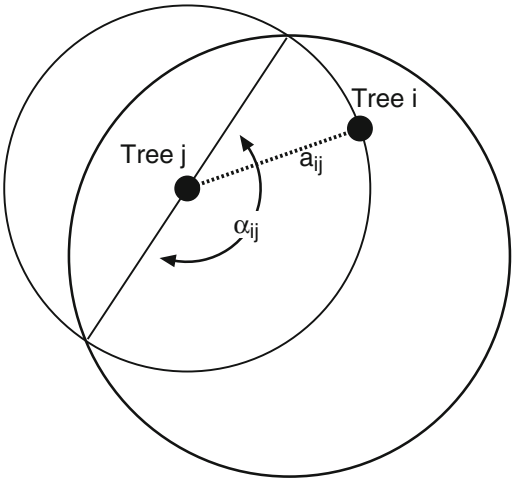

Fig. 8.30 The linear expansion method can also be used for circular experimental trial plots, for which the mirroring and shifting techniques are unsuitable. The spatial competitive situation in the circle sectors that extend beyond the plot boundary is estimated from the competition relationships in the circle sector with radius a_{ij} and angle α_{ij}

8.7.4 Structure Generation

This method relies on the structure generator STRUGEN, which produces stand structures close to reality in a given area around the observation plot (Pretzsch 1997, 2001). The tree distribution within the plot is used to generate a random tree distribution on a larger area using an inhomogeneous Poisson process (Fig. 8.31). The regulation of distance in relation to size and species is controlled by a parametric system of equations calibrated from an extensive database (Pretzsch 1993).

In the procedure used by the structure generator STRUGEN to compensate for edge effects (Pretzsch 1998; Pretzsch 2001), trees from inside the plot are copied to random coordinates in the area surrounding the monitoring plot. Then, the equation (8.35) is used to calculate the expected distance $DIST01_{exp}$ between the tree positions produced and its nearest neighbours in relation to observed distance $DIST02_{obs}$, and CDTm0, CDTm1, and CDTm2:

$$DIST01_{exp} = a_0 + a_1 \times DIST02_{obs} + a_2 \times CDTm0 + a_3 \times CDTm1 + a_4 \times CDTm2 \tag{8.35}$$

where $DIST01_{exp}$ represents the expected distance from reference tree to the nearest neighbour (in m), $DIST02_{obs}$ is the observed distance from reference tree to second closest neighbour (in m), and CDTm0, CDTm1, CDTm2 are the ratios of the crown diameter (in m) to the species-specific transmission coefficient calculated for the reference tree, its first and second neighbour, respectively. The transmission coefficients are: 1.0 for European beech, 1.0 for Silver fir, 0.8 for Norway spruce, 0.6 for Sessile oak, and 0.2 for Scots pine. The regression coefficients $a_0 = 0.0835$, $a_1 = 0.6761$, $a_2 = 0.0065$, $a_3 = 0.0031$, and $a_4 = -0.0039$ are species-unspecific; the species effect is included in the transmission coefficients.

If the observed distance to the nearest neighbour $DIST01_{obs}$ is considerably smaller than the expected distance $DIST01_{exp}$ of the reference tree to its nearest neighbour, then the stem position produced is not accepted as a tree coordinate. The scattering process continues until a tree coordinate is produced where the expected

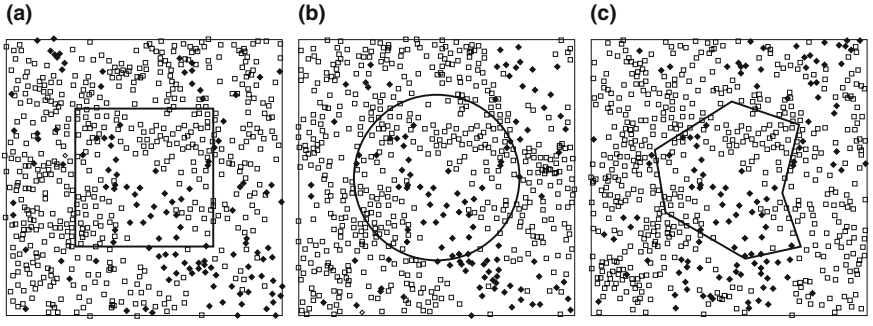

Fig. 8.31 Generation of a border area by structure generation. A (**a**) rectangular, (**b**) circular and (**c**) irregular monitoring plot (*thick lines*) with recorded stem locations is presented. Structure generation produces a gapless border area regardless of the original area's shape (cf. Biber 1999)

and observed distance to the nearest neighbour are close. The regression model for the size- and species-dependent distance function (8.35) is parameterised using data from long-term experimental plots (Pretzsch 1993; Pretzsch and Kahn 1998). Of course, natural variation does arise in this function. According to Pretzsch and Kahn (1998), the standard deviation of tree distances is normally distributed about the mean distance and increases with the $DIST01_{exp}$ as in (8.36):

$$S_{DIST01} = b_1 \times \left(1 - e^{-b_2 \times DIST01}\right) \tag{8.36}$$

where S_{DIST01} is the standard deviation of distances from the reference tree to the nearest neighbour (in m). The regression coefficients b_1, b_2 are species-unspecific and amount to 5.7007 and 0.0585. If the expected distance DIST01 to the next neighbour and the standard deviation S_{DIST01} are known, a randomly generated coordinate can be accepted or rejected using the following procedure: from (8.36) and (8.37) the mean value and standard deviation of the expected distance to the next neighbour $DIST01_{exp}$ are estimated for the generated tree. Then the probability of the observed distance $DIST01_{obs}$ can be determined from the normal distribution function of the mean value of $DIST01_{exp}$ and the standard deviation S_{DIST01}. If this probability is smaller than an uniformly distributed random number, then the distance between the reference tree and its next neighbour is rejected as unacceptable, and a new point is drawn. Otherwise the tree with this distance and size is accepted and established. The scattering process continues until the tree density in the surrounding area is identical to that of the experimental plot.

Thus far, the process is a deductive one that employs as generally valid assumed equations for the generation of a structure in the area surrounding the true plot. As Biber (1999) also uses the structural information from the monitoring plots, i.e. the height distribution, basal area, species mixture and site-specific distance relations, he expands this method with inductive elements. Compared to methods by Radtke and Burkhart (1998), that develop the surrounding area from a homogeneous Poisson forest, the structure generation using STRUGEN is a notable improvement due to the regulation of distance by size.

8.7.5 Evaluation of Edge Correction Methods

Three methods for treating edge effects were introduced: methods of mirroring and shifting, linear expansion, and generation of stand structure. Whereas reflection and toridorial shift cannot be transferred directly to circular plots or amorphous areas, the linear expansion method can be applied universally. It is also suitable for the correction of edge effects for circular or amorphous plots (Fig. 8.30). Similar to the reflection method, the linear expansion method also produces a systematic increase, or decrease in competition for trees close to the boundary facing strong, or little competition respectively as the competitive situation outside the plot is extrapolated from that inside the plot. In contrast, in a shift any unnaturally small or large

distances are produced rather randomly, not systematically. Structure generation relies on both distance functions deduced from long-term experimental plots as well as structural information obtained inductively from the monitoring plot itself to generate the stand structure outside the plot boundary. The advantages of this method are that it can be used for areas of any shape, does not result in periodicity, produces biologically plausible tree distances, and extrapolates macro-structures of the plot, such as mixtures of different tree species, beyond the area boundary (Fig. 8.31).

Comparisons of the effectiveness of reflection, shifting, linear expansion and structural generation for edge correction seldom have been carried out. Investigations are generally confined to the comparison of two methods at one or only a few experimental plots with little variation in shape and forest structure. Investigations by Martin et al. (1977) showed linear expansion was somewhat superior to the shifting method for long and small rectangular areas in pure and mixed stands in Ontario. Windhager (1997) employed linear expansion and reflection methods in a large number of mixed Norway spruce–Scots pine stands in Austria, and concluded that the methods were equally effective in eliminating edge effects in competition estimates. In investigations by Radtke and Burkhart (1998), the results of the shifting, reflection and a simple structural generation for edge correction were equally good in pure even-aged pine stands. In contrast, structural generation proved better in mixed stands of Norway spruce, Silver fir, and European beech than the reflection and shifting methods. Combined methods that repeat the reflected or translated plot area for a given distance, and generate the structure in between can be assumed to produce equally good results.

Summary

The transition from the focus on stands to approaches based on individual trees indicates a fundamental paradigm shift for all disciplines concerned with stands, populations, biological communities and ecosystems. The resolution of the stand into a mosaic of individuals that interact as a dynamic spatial-temporal system allows new advances in the analysis, modelling and prediction of forest stand development.

(1) By competition we refer to the interaction between trees through spatial occupancy and resource exploitation. The essential resources are carbon dioxide, water, nutrients and light as an energy source.
(2) Competition indices quantify the space occupation and spatial constellation of individual trees within a stand and indicate the associated access to resources in one or a few surrogate variables.
(3) Competition indices combine information on tree species, diameter, height, and crown size, to quantify the spatial growth constellation of a tree in relation to its neighbours. Competition indices may be position-dependent or position-independent depending on whether the distance to stand neighbours is used in the calculation or not.

(4) As competition indices reflect the spatial growth constellation of individual trees within a stand they may also be used for the silvicultural prescriptions on experimental plots and to estimate the growth reactions in individual based simulation models.
(5) For homogeneous stands, position-dependent or position-independent models may be used to estimate stand growth with equal accuracy. However, for heterogeneous stands, e.g. unevenaged pure and mixed stands, position-independent competition indices are inappropriate.
(6) The first step for position-dependent competition indices is to select the neighbouring trees that compete with the centre tree for resources (fixed search radius, crown overlap, angle count sample, search cone methods). In a second step, for each of the selected neighbours the strength of competition it imposes on the centre tree is quantified (crown overlap or overlap of competitive influence zones, stem size ratio, crown size ratio between the centre tree and neighbour). Methods that use a search cone to select competitors and quantify competition in relation to crown size produce competition indices with the highest correlation to growth.
(7) Stand level density characteristics such as stocking density, stand density index and canopy density are appropriate for describing mean competitive stress in a stand with position-independent methods. Methods like the crown competition factor, horizontal plane methods, percentile of the basal area frequency distribution quantify the relative position of individual trees in the social rank order within the stand and reflect their access to contested resources.
(8) Methods based on the growing area (circle segment methods, rasterising the stand area, representing the growing area as polygons) quantify the spatial growth constellation of individual trees by assigning the entire stand area to individual trees according to biological growth laws. They allow an efficient calculation of space occupation and space exploitation.
(9) A three-dimensional analysis of stand space (determination of the lateral restriction, shading) is possible by rasterising the three-dimensional stand model into voxels. This type of analysis yields the highest potential for understanding space occupation strategies in heterogeneous forest stands.
(10) Hemispherical images are useful in the quantification of spatial growth constellation as they provide a circular picture of the entire hemisphere above a given stand point of a tree. Hemispherical images can be produced photographically or arithmetically from stand structure data. The grey value analysis allows calculating the diffuse site factor and sky factor, which are closely related to the relative light intensity, and the precipitation recorded at the measuring point, respectively.
(11) To analyse the spatial growth constellation of individual trees at the edge of a site, edge correction methods are necessary. If only those trees further away from the plot boundary were included in the individual-tree analysis of the study site, then a representative number of trees would only on very large plots be available for evaluation. Reflection, shifting, linear expansion and structure

generation can correct edge effects so that the database for trees in the vicinity of the boundary is completed.

(12) The applicability of competition indices and other measures for determining the spatial growth constellation of individual trees extends from pure description, to modelling and managing of tree and stand growth. As competition indices are a measure for the individual tree's resource supply they play a key role in individual-tree simulators.

Chapter 9
Effects of Species Mixture on Tree and Stand Growth

In this chapter we shall focus on analysing how tree species diversity and forest productivity are interrelated; a question of particular relevance to forestry practice. The methods presented are applied to mixed stands consisting of two species. Two-species mixtures, especially those where each species is present singly or in groups, prevail in mixed forests in Europe (Bartelink and Olsthoorn 1999), and have been studied scientifically more intensively than any other (Kelty 1992; Piotto 2007; Pretzsch 2005a; Scherer-Lorenzen 2005). However, all methods presented here apply equally to other mixtures.

9.1 Introduction: Increasing Productivity with Species Mixtures?

The increase in resource uptake of mixed species stands, e.g. due to spatial or temporal niche differences, or to the denser occupation of the crown and root space, does not explain fully the increase in productivity found in species mixtures. One can expect an increase in productivity only when the additional resources are allocated to growth rather than to looking after, impeding or poisoning neighbours or other like strategies. To understand the effect of species mixtures on stand productivity, we need to look at the niches of each species and the differences between them. Furthermore, we need to investigate the competition strategies of each species, and their allocation behaviour under selection pressure for intraspecific and interspecific competition. For practical reasons, the following discussion focuses on the increase in aboveground productivity of stands (tons per hectare per year) or single trees (kilogrammes per square metre per year) in species mixtures; growth reductions can be traced with the same principle.

H. Pretzsch, *Forest Dynamics, Growth and Yield: From Measurement to Model*,
DOI: 10.1007/978-3-540-88307-4_9,

9.1.1 Fundamental Niche and Niche Differentiation

The overlap in fundamental niches of species is a necessary, though insufficient prerequisite for determining whether species can co-occur in mixtures (Fig. 9.1a). A species mixture may occur only on sites that, in terms of resource availability and environmental conditions, fall within this area of overlap (Fig. 9.1b, hatched area). If a site lies at the centre of the fundamental niche of species 1 (Fig. 9.1b, site p), then higher competition is expected from its own species than from species 2 because species 2 occurs at the fringe of its niche at site p. Under steady state conditions, the competitive strength of species 1 decreases towards the periphery of the niche. However, under changing growth conditions (environmental conditions, resource availability; Fig. 9.1c), the site p represents the area of worst possible conditions (pessimum) or mortality for species 2.

Through the influence of the two species on each other (e.g. overshadowing, poisoning, suppression in the root space), the width of the fundamental niche of each species may be restricted to a narrower, realised niche. The area of possible

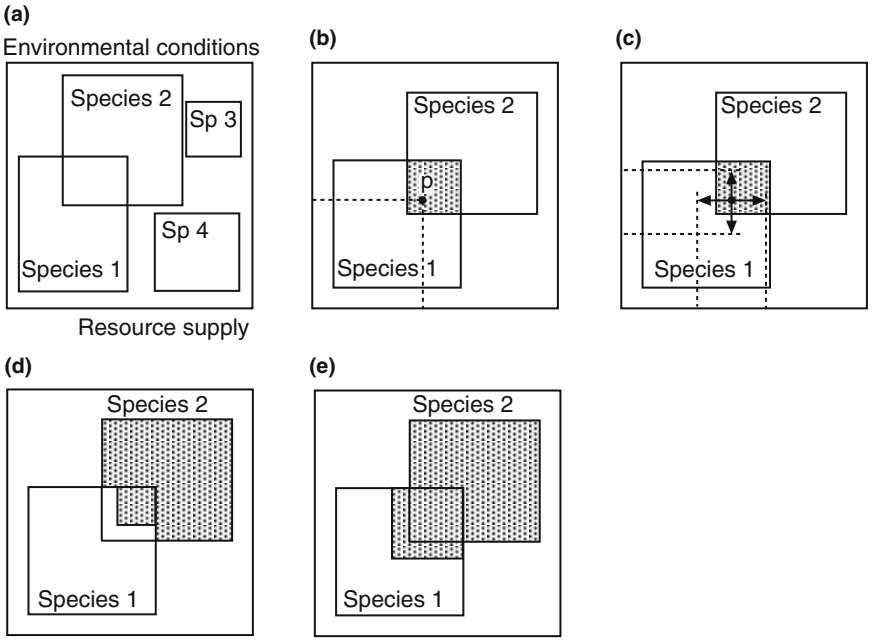

Fig. 9.1 Overlap of fundamental and realised niches as a prerequisite for a stable, productive species mixture. (**a**) Fundamental niches of species defined by their potential occurrence in a matrix of resource supply and environmental conditions. (**b**) Species 1 and 2 have a common niche (*dotted area*) which includes site p. (**c**) Resource supply or environmental conditions at site p can fluctuate (*arrows*) so that they extend beyond the fundamental niches of species 1 and 2. (**d**) The realised niche of species 2 can be restricted (*dotted area*) due to competition by species 1. (**e**) The niche of species 2 can be extended (*dotted area*) with the admixture of species 1

coexistence of two species, therefore, may be smaller than the intersection of their fundamental niches. For example, species 1 causes a reduction in the fundamental niche of species 2, so that species 1 and 2 can coexist only in the dotted area (Fig. 9.1d). This reduction in the realised niche, or even competitive exclusion of a species, occurs frequently when the initial height (initial state) or the height growth development (species-specific ontogenesis) of one species is very inferior to the other. The relatively limited access of this species to light can lead to a permanent decline, and ultimately to the elimination of a species in the stand. The more asymmetrical the competitiveness of two species is, the more unstable the species mixture (Wiedemann 1951, pp. 131–133). In practice, asymmetrical competition can be regulated by promoting one species or inhibiting the other depending on the species composition the treatment aims to achieve (Mitscherlich 1970).

The realised niche of a species can also be extended by coexistence with another species. For example, N_2-fixation by *Alnus* species enables Norway spruce to advance into otherwise relatively inaccessible moor sites. Figure 9.1e depicts this arrangement. Here, the area of possible coexistence of species 1 and 2 extends beyond the fundamental niche of species 2.

That two species are able to exist and coexist in the same niche does not mean that they use the same strategies to access the available resources. For example, they may be variously dependent on the environmental conditions, or have asynchronous temporal growth patterns. Their niches may be differentiated effectively, e.g. by adjusting their competitive abilities to the site conditions (temporally and spatially). Niche differentiation may relax resource competition, as occurs, for example, with the combination of shade tolerant and intolerant trees, flat and deep rooted systems, and early and late successional species. For given site conditions (site p), species 1 and 2 may access resources in different spaces or at different times (Fig. 9.2a,b).

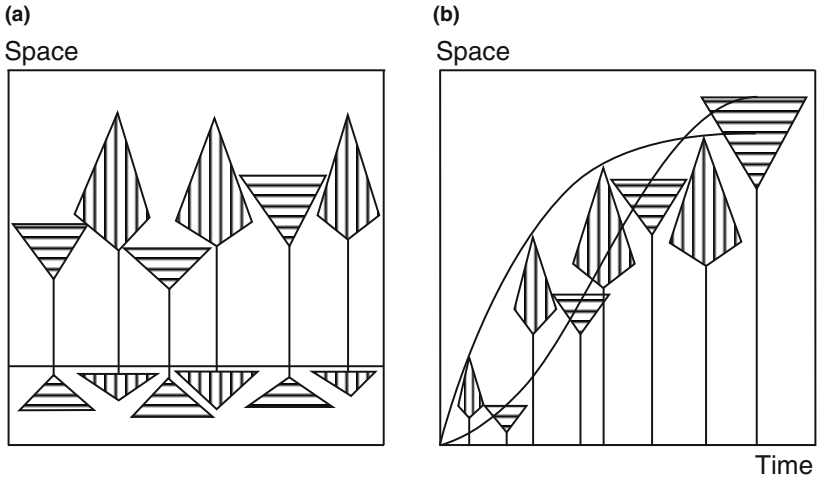

Fig. 9.2 Coexistence of species 1 and 2 at site p can be stabilised, and productivity increased through spatial or temporal niche differentiation by (**a**) layering in the crown or root space, or (**b**) asynchronous growth patterns of the species

The capacity of a species to fix nitrogen is, in its effect, comparable to niche differentiation. It reveals an important effect of niche differentiation and more thorough resource acquisition: that is, although differences in resource acquisition (e.g. N_2-fixation of *Alnus* species, base pump effect of the deep-rooted *Fagus* or *Abies* species) benefit individual trees initially, the nitrogen fixing species increases the turnover of plant material (nutrients in transported leaves and fine roots), and thereby the amount of resources introduced into the nutrient cycle, which become available to other individual trees of one or the other species (Rothe and Binkley 2001; Piotto 2007).

In contrast, in pure stands, genetically similar individuals with similar strategies compete for the same pool of resources. The greater the niche differentiation achieved by mixing species, the more relaxed interspecific resource competition becomes, and therefore, the likelihood of access to additional resources increases. Additional, available resources, however, are not necessarily used to the fullest extent, nor used inevitably to increase biomass productivity.

9.1.2 Maximizing Fitness isn't Equivalent to Maximizing Productivity

If, in the nature of things, the highest productivity is expected in a mixed forest, this comes from a largely anthropological notion that trees in a stand tap resources in a division of labour for the common good with the aim of maximising productivity (Cotta 1828, p. 115). Furthermore, it is assumed that mixed stands tap the available resources more thoroughly (temporal, spatial, temporal–spatial differentiation) so that, inevitably, trees will grow more in mixed stands than in pure stands (Gayer 1886; Möller 1922). This is a very dubious biological supposition because the dynamics of pure and mixed stands are not driven by the target of a species, population or cohort to achieve maximum productivity, but by individual trees striving for maximum fitness. According to the theory of natural selection, the fitness of the individual is maximised by survival and seed production so that the number of its progeny is higher than that of competing neighbours. The abundance of a genotype, not the productivity of the stand, or of a species, is maximised.

Anything that ensures the success of a tree's reproduction, e.g. sit-and-wait, inhibition or poisoning of a neighbour, or mechanical abrasion of neighbouring crowns by wind-induced swaying, will help it. A tree does not necessarily need to grow and produce rapidly. Even if a tree does not increase the number of its progeny, it improves its fitness by reducing the number of progeny of its neighbours. A reduction in the fitness of its neighbours also makes it "fitter", since fitness is determined by the number of progeny of an individual *relative* to the progeny of a neighbour.

Thus, when individual trees of two species that have coevolved and adapted interspecific as well as intraspecific strategies to increase their fitness are mixed, most likely, they have developed numerous, ingenious adaptation strategies for allocating resources to outlasting, inhibiting or poisoning neighbours in addition the

more straightforward "faster growth" and "higher production". Investments of this kind may prove more effective for increasing fitness and abundance than increasing aboveground biomass production. Growth loss under increasing competition may be attributable in part to increased energy consumption in the attempt to produce allelopathic or toxic effects on neighbours (Tubbs 1973). If a tree allelopathically restricts, or inhibits its neighbour, it will consume energy (poison is costly for the tree). Yet, as long as the costs of producing toxic compounds and substances, and of interventions are lower than those involved in reducing competition, this strategy gives the aggressor a *relative* advantage.

A tree, for example European beech, which stores many nutrients in the stem and bark, does not increase its productivity, but withdraws permanently these nutrients from its competitors, thereby reducing their productivity. This is effective primarily when the neighbour belongs to another species that does not share this characteristic because, then, the withdrawal is a real hindrance for that neighbour. Creating empty crown space, mechanical abrasion and crown shyness, which are particularly widespread in mature pure evenaged stands, also can reduce the productivity of an area. However, as long as the loss of crown biomass, and the efficient leaf mass of larger trees, with their superior height and wider crown sway, is less than that of smaller trees, they still have a relative advantage even if total productivity decreases.

9.1.3 The Balance Between Production Promoting and Inhibiting Effects is Important

Whether a mixed stand is better or worse off than a neighbouring pure stand on a comparable site is dependent on the balance of factors enhancing or restricting growth. On the one hand, through niche differentiation, potentially more total, and species-specific resources may be available for growth and the development of tree form, and hence competitor displacement. On the other hand, mixtures may also trigger adaptation strategies for the maximisation of fitness, in which the resources are invested in displacing, inhibiting or poisoning competitors at the expense of production.

One would expect higher productivity in mixed stands than in pure stands when the differences between niches of the mixed species is particularly marked, and the investment in competition strategies for increasing growth high, i.e. when losses from investing in other strategies are low. In this case, the enhanced resources available are allocated to growth rather than to inhibition, or to inducing the mortality of neighbours. In contrast, a reduction in the production of mixtures might be expected when species with similar niches are combined, and interspecific competition in the form of production minimisation strategies eventuates (e.g. allelopathy, mechanical crown abrasion).

In fact, empirical findings to date show that overyielding often is found when an increase in resource uptake arises from niche differentiation and promotion (shade tolerant and intolerant tree species, early and late successional species, shallow and deep rooting species), and the mixed species exhibit an almost symmetrical competition (Bauhus et al. 2000; Garber and Maguire 2004; Pretzsch 2005a). Here, the species allocate the additional resources obtained to overtopping one another rather than to other strategies for inhibiting the competing species. Examples of such investigations include the evenaged mixtures of Norway spruce and European beech (Kennel 1965; Pretzsch and Schütze 2008; Wiedemann 1942), Scots pine and European beech (Bonnemann 1939), European larch and Norway spruce (Zöhrer 1969), and Scots pine and Silver fir (Garber and Maguire 2004). Investigations identifying neutral mixture effects or reduced productivity largely include species mixtures comprising light demanding species such as Scots pine and white birch (Frivold and Frank 2002), and Scots pine and Sessile oak (Kramer 1988, pp. 279–280), or mixtures with permanent asymmetrical competition (Spellmann 1996; Wenk et al. 1990, pp. 378–383).

Investigations, which are useful for the comparison of many species mixtures with pure stands on similar plots, are entirely nonexistent. Investigations of other mixtures address only a limited range of study sites. Consequently the following discussion about the site dependency of the effects of species mixtures is to some extend theoretical.

With adequate water and nutrient supply, and with light as the primary limiting factor, complementary niche differentiation, such as shade intolerant and shade tolerant tree species, would prove particularly advantageous. In this event, increased productivity from aboveground niche differentiation is expected, especially on fertile sites (good site quality) because better light conditions are the most important factor affecting growth. On sites where soil resources are limiting for growth, niche differentiation in the soil space, such as a combination of deep and shallow rooting trees, is advantageous. The less favourable and less fertile the soil is (the more eccentric the location of the given site in the niche), the more likely a species mixture will result in a production increase. However, the absolute effect might be much smaller than under light limiting conditions, since, on sites with limiting soil resources, primarily a greater investment in root mass is needed to tap additional resources. Moreover, the increased investment in defence occurs at the expense of growth (Herms and Mattson 1992).

Forest managers who focus on stand yield would prefer mixed stands in which the maximisation of fitness primarily takes place in the production of aboveground biomass, that is in overtopping. They prefer silvicultural practices that permanently regulate stand growth largely by promoting growth and less through inhibition, elimination and competition. Yet higher productivity in mixed stands of this kind does not permit one to draw conclusions about the naturalness or stability of the remaining population, or the adaptability of these stands (Harper 1977, pp. 776–778).

9.2 Framework for Analysing Mixing Effects

9.2.1 Ecological Niche

The analysis of the productivity $p_{1,2}$ of a mixed stand consisting of two species usually is carried out in relation to the productivity p_1 or p_2 of the corresponding pure stand at the same site. For species interaction without synergistic effects, productivity $p_{1,2}$ of a mixed stand is represented as the productivity of the pure stands weighted by the proportion of each species in the mixture m_1 and m_2; i.e. $p_{1,2} = m_1 \times p_1 + m_2 \times p_2$. Species ecological niches and their compatibility are a crucial factor in the analysis of species as they affect biomass productivity at any given site. Yet, first, we need to distinguish between the "fundamental niche", which reflects the totality of environmental variables and functional roles to which a species is adapted, and the "realised niche" which is the niche a species occupies in natural communities (Helms 1998, p. 123). The opportunity to enhance biomass productivity by mixing species depends both on the differences in the species' fundamental niches and their ability to realise different niches.

Here, two examples are presented to explain the relationship. In one, the species occupy similar, and in the other different fundamental niches (Fig. 9.3a,b). The unimodal dose–response curves represent the different niches inasmuch as they reflect the dependence of productivity on growth conditions typical of the species. For simplicity, growth conditions are plotted in one dimension only on this graph, and consist of the n-dimensional vectors of environmental factors (e.g. temperature, soil pH-value, storm–snow load) and availability of resources (e.g. irradiation, water, nutrient supply, atmospheric carbon dioxide, etc.).

In the first case (Fig. 9.3a), the tree species 1 and 2 occupy similar niches, yet their growth clearly differs on the given site. In this case, productivities p_1 and p_2

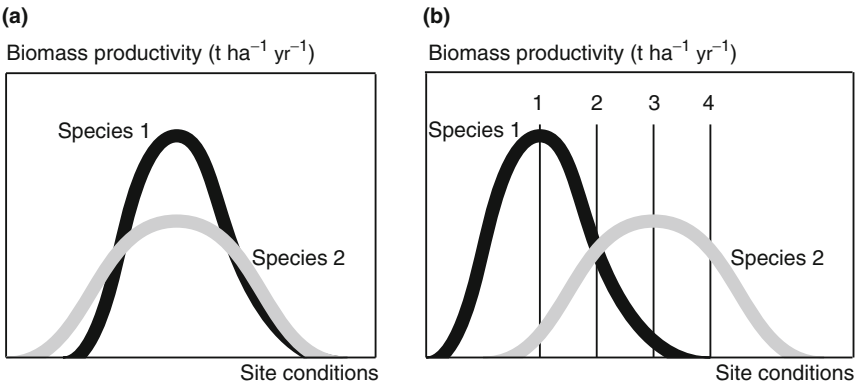

Fig. 9.3 Dry biomass productivity of various tree species in relation to site conditions. (**a**) Growth of two tree species with similar fundamental niches but different levels of productivity. (**b**) Growth of two tree species with different niches. Numbers 1–4 below the abscissa represent different site conditions producing different growth responses by species 1 and 2 (cf. Fig. 9.4)

of the superior and inferior tree species respectively, vary to the extent that, usually, the addition of the inferior tree species will cause a reduction in stand productivity as, for example, found for the superiority of Douglas fir over Scots pine, or of Red oak over Sessile oak across a wide range in ecological amplitude for these species. Both these examples compare an indigenous species with an exotic species; corresponding examples for two indigenous species are lacking.

Relationships become more complicated if the species in the mixture occupy distinctly different niches (Fig. 9.3b). Let us assume species 1 and 2 are mixed in stands on four different sites (site conditions 1–4). The growth relationships will vary considerably with site conditions. On site 1, optimal for species 1, the addition of species 2, inferior on this site, will become a burden and reduce productivity on the site. On site 2, well suited to both species, productivity is in balance. On site 3, optimal for species 2, the inferior species 1 will slow down growth. Examples of this effect of inferiority may be found in mixed European beech and Sessile oak stands on moist calcareous sites, and mixed Norway spruce and European beech stands on acidic, cool and moist sites. The Sessile oak in the former and European beech in the latter stand can be sustained only by silvicultural treatment. On site 4, species 1 will disappear eventually, whereas species 2 will achieve high productivity.

9.2.2 Site–Growth Relationships

Figure 9.4a–d depicts the productivities p_1 and p_2 of species 1 and 2, respectively, on sites 1–4 (cf. Fig. 9.3b). The right-hand and left-hand ordinates plot productivities for species 1 and 2 in pure stands, the abscissa the mixture proportion. For sites 1–4 the resulting relationships are $p_1 > p_2$, $p_1 = p_2$, $p_1 < p_2$, and $p_1 < p_2$ with $p_1 = 0$, respectively. This example explains why the site-related productivity relationships diverge, and warns against generalising results obtained from a limited spectrum of site conditions.

If the mixed species do not interact at all, or if effects of the mixture on growth cancel each other, productivity $p_{1,2}$ in the mixed stand will lie on the straight reference line between p_1 and p_2 (dashed lines). In this case, an increase in the mixture proportion would be reflected in a proportional increase in $p_{1,2}$.

If growth deviates positively or negatively from this straight reference line (convex and concave curves in Fig. 9.4, respectively), this is indicative of a species interaction that will increase, or reduce productivity respectively. Positive deviations and their causes are of special interest.

9.2.3 Risk Distribution

If one species in a mixture is more sensitive to disturbances, the more robust species may then, on account of its better adaptation, profit from the weakening or mortality of the inferior species. Assuming, e.g. a shift in environmental factors and

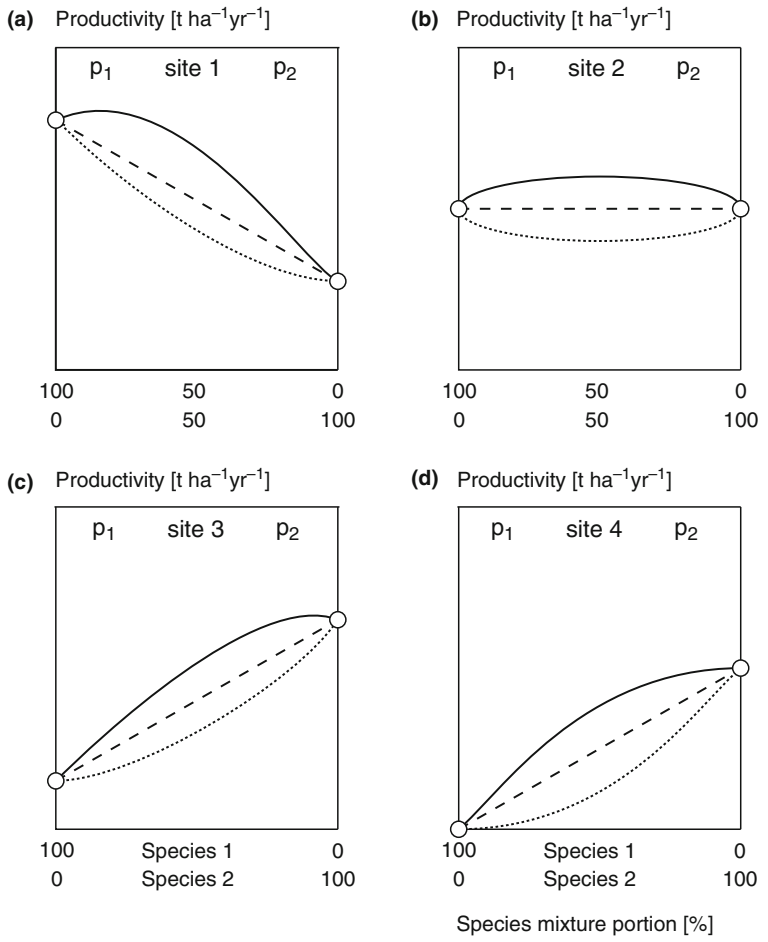

Fig. 9.4 Dry biomass productivity for two species in pure and mixed stands under different site conditions 1–4 (cf. Fig. 9.3b). Dry biomass productivities p_1 and p_2 of species 1 and 2 are shown for pure stands (*left and right ordinate respectively*). The connecting lines show expected productivity values $p_{1,2}$ in the mixture with different mixture proportions. The linear connecting lines (*dashed*) represent neutral effects between species 1 and 2, and the continuous and dotted lines reflect positive and negative effects of the species mixture respectively

resource availability affects species 1 unfavourably (Fig. 9.5, arrow 1 → 3), a significant decrease in productivity in pure stands would result. However, if a second species were added to the stand that is better adapted to the new growth conditions this species would have a stabilising effect on growth. Species 2 would make better use of available resources and, consequently, species 2 can improve its productivity and space sequestration. The same would happen if one species disappeared completely after a biotic calamity, or through natural mortality. In this case, the species remaining would contribute to the recovery of the loss in productivity through accel-

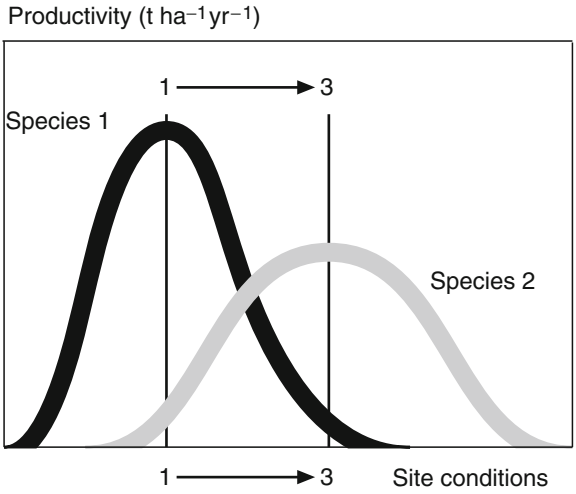

Fig. 9.5 Dry biomass productivity for species 1 and 2 (*black and grey lines*, respectively) in relation to site conditions. The shift in site conditions from 1–3 (*arrows*) results in considerable growth loss for species 1. If species 1 and 2 are mixed, species 2 is able to compensate for a loss in biomass productivity

erated growth, as the insurance hypothesis proposes. This buffering by the remaining species would improve with the regularity of its spatial distribution within the stand. In both cases, the advantage of species mixtures lies in risk distribution arising from silvicultural diversification.

The greater the niche variation between the constituent species of a mixed stand, the more elastic its response will be to disturbances. The annual radial increments from the Norway spruce–European beech experimental plot Schongau 814 in the period 1960–1995 (Fig. 9.6) provides an example. In contrast to European beech, Norway spruce reacted to the 1976 drought with a large decline in growth (Fig. 9.6a). In pure Norway spruce stands, this would cause serious productivity losses. In Norway spruce–European beech mixtures, disturbances of this kind can be mitigated by the compensatory growth of European beech (Fig. 9.6b) postulated in the insurance hypothesis (Yachi and Loreau 1999; Pretzsch 2005a).

Unfortunately, yield comparisons between pure and mixed stands usually refer to more or less undisturbed stands. Plots affected by calamities or unplanned use are abandoned, and only undisturbed plots are kept under continual observation. Therefore statements about inferiority or superiority of species from such experiments apply merely to "normal" circumstances. If response patterns after disturbances were considered also, yield comparisons would become more realistic. In the following, the example of Norway spruce and European beech serves to illustrate that pure stands comprising these species respond in rather different ways to disturbances through thinning or natural density reduction, e.g. by wind-throw or ice-breakage, than mixed stands.

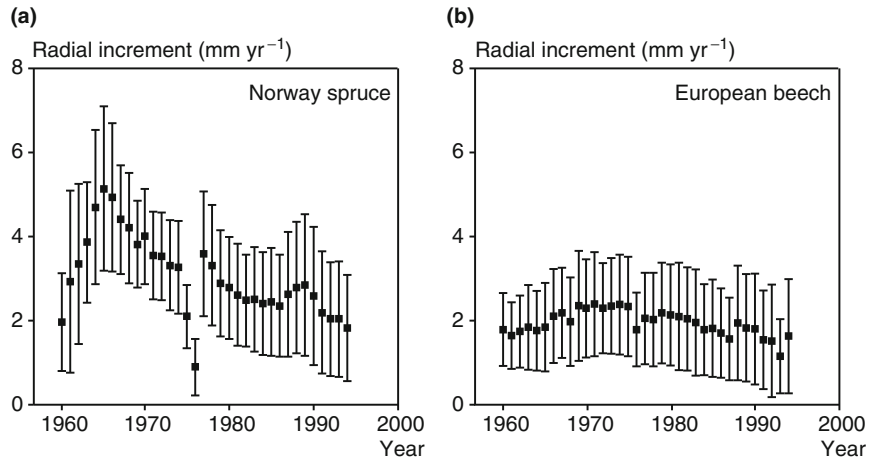

Fig. 9.6 Mean ± standard deviation of annual ring width (**a**) for Norway spruce and (**b**) European beech on the mixed stand experimental plot Schongau 814 (n = 193 and n = 87 for Norway spruce and European beech respectively). Here, Norway spruce responds more sensitively to the 1976 drought than European beech

Moreover, mixed stands compensate more easily for variations in stand density. This characteristic enables mixed stands to maintain stable growth rates despite a lack of treatment, maximum density, or a reduction in density after silvicultural treatments or calamities. In pure stands, an optimum relationship exists between density and growth. The overlap in different response patterns of Norway spruce and European beech leads to a much wider plateau in the density–growth relationship of mixed stands than for the corresponding pure stands. The broad saddle in the resulting curve looks similar to the much discussed curve by Langsaeter (1941, p. 173, Fig. 9.3). In contrast to the pure stands under investigation, only a slight, statistically insignificant decrease in growth occurs as the stand approaches maximum density.

This important relationship is represented schematically in Fig. 9.7. The mixture (black line) is compared to two pure stands (grey lines). In the case of the first pure stand (upper grey line), we assume the productivity of pure stands is superior to mixtures at medium density. Whenever density is reduced following some kind of disturbance, pure stands will suffer considerable growth loss and become inferior. By contrast, growth in the mixed stand remains stable over a wide range of densities. Even though mixed stands may be inferior under "stable" conditions they may become superior on account of their greater resilience to perturbation or nontreatment.

The second pure stand (lower grey line) is less productive than the mixture even under "normal" conditions. In this case, positive or negative deviations from average density, e.g. on account of lack of treatment or unplanned disruption of the pure stand's canopy, lead to inferior productivity.

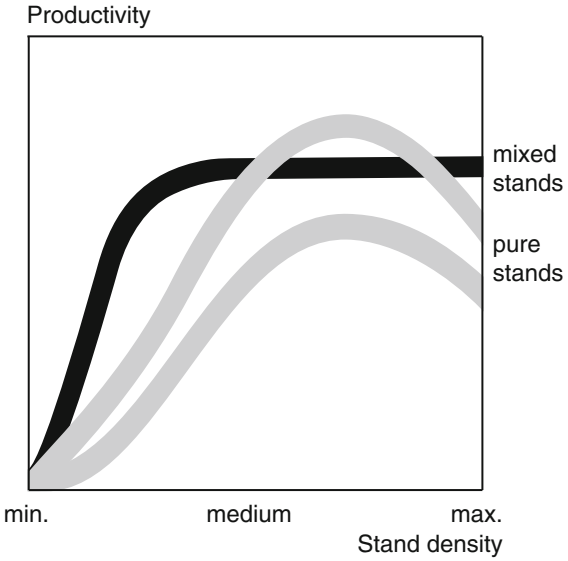

Fig. 9.7 Schematic representation of relationships between stand density and biomass productivity in pure and mixed stands. The overlap in different Norway spruce and European beech response patterns can lead to a much wider plateau in the density–growth relationship for mixed stands than for the pure stands. This reflects the greater growth resilience in mixed stands (*black line*) compared to pure stands (*grey lines*)

9.2.4 Comparison of Mixed Stands with Neighbouring Pure Stands: Methodological Considerations

In the unlikely case that the growth of species 1 and 2 is identical, then the productivity $p_{1,2}$ of a mixed stand of both might be the same as the productivity of species 1 or 2 in a monoculture, i.e. $p_{1,2} = p_1 = p_2$. Thus the productivity of pure and mixed stands would be identical, and, as neither species changes absolute level of growth or growth patterns, the initial productivity ratio and proportional mix ratio of the species also remain unchanged during stand development. In this, and all subsequent examples p refers to aboveground biomass growth of a stand in a given time period (tons per hectare per year).

In the case, that the mixed species 1 and 2 differ in productivity ($p_1 \neq p_2$), yet strictly adhere to their development trends in the pure stand, the productivity $p_{1,2}$ of the mixed stand equals the productivity achieved by both species in pure stands (p_1, p_2), weighted by their mixture proportions (m_1, m_2): $p_{1,2} \cong p_1 \times m_1 + p_2 \times m_2$.

Let us assume the dry biomass productivity of Norway spruce in a pure stand is $p_1 = 8.0$ tons per hectare per year, and that of European beech is $p_2 = 4.8$ tons per hectare per year on a specific site. Let us further assume that the European beech added to the Norway spruce stand comprises 50% of the stand (mixture proportions of species 1 and 2 are $m_1 = 0.5$ and $m_2 = 0.5$, respectively), and that neutral

interactions between the species prevail. This would reduce the productivity in the mixed stand to $p_{1,2} = 0.5 \times 8.0\,t\,ha^{-1}\,yr^{-1} + 0.5 \times 4.8\,t\,ha^{-1}\,yr^{-1} = 6.4\,t\,ha^{-1}\,yr^{-1}$, i.e. down to 80% of the pure Norway spruce stand, which is equivalent to a loss in productivity of 20%. Thus, the productivity in the mixed stand may exceed considerably, or fall below one of the neighbouring pure stands. Yet, as long as $p_{1,2}$ equals the proportional weighted sum of the productivity in comparable neighbouring pure stands, we observe a simple replacement with a neutral effect on the stand's overall productivity. A replacement of this kind involves the *redistribution of available resources* from one species to another, not an exploitation of more or less resources.

A direct positive mixing effect is assumed when the mixed stand productivity $p_{1,2}$ is greater than the productivity of the two pure stands of similar size ($p_{1,2} > p_1 \times m_1 + p_2 \times m_2$), or when the mixed stand productivity even exceeds the sum productivity of pure stands of species 1 and 2 ($p_{1,2} > p_1$ and $p_{1,2} > p_2$). These cases are referred to as ordinary overyielding and transgressive overyielding respectively. Analogously, underyielding means $p_{1,2} < p_1 \times m_1 + p_2 \times m_2$ or $p_{1,2} < p_1$ and $p_{1,2} < p_2$. Overyielding can be caused either by an *occupation of more space*, e.g. arising from denser tree spacing, a multi-layered exploitation of light, or a reduction in empty spaces arising from crown shyness. Alternatively, overyielding may result from *a more efficient exploitation of a given space* in the mixed stand than for the same space in the monoculture, e.g. by an increase in leaf area density and crown efficiency.

Usually the growth of the neighbouring pure stands (p_1, p_2) serves as reference for the detection of any (positive or negative) mixing effects. However, this comparison can be rather misleading, especially if it is based on the periodic annual volume increment or biomass growth in only one survey period. With the exception of a direct replacement, which has a neutral effect on productivity, even minor initial mixing effects can result in considerable compound interest effects for stand dynamics considerably in the long term. When one species grows quicker and overtops its interspecific competitors, especially in the stand development phases, it can increase its mixture proportion by edging out and replacing the other species. A quicker or slower growth of one of the species complicates the analysis of mixing effects because the growth on the mixed plot becomes increasingly less comparable with that on the pure stand plot.

If the growth of a species is superior in a given mixed stand to that in the neighbouring pure stand, the superior growth can result in an earlier and higher culmination in growth (Fig. 9.8, left). However, this advanced tree growth is associated with increased maintenance costs, and accelerated aging. Consequently, species growth may culminate earlier, but decline quicker thereafter, entering into a phase of lower growth earlier than in the neighbouring pure stand. A comparison of growth at age t_1 would indicate superiority, yet, at age t_2, an inferiority of the species in the mixed stand. For a more comprehensive understanding of species growth in a pure vs mixed stand, the comparison should cover several stand ages. This way, the comparison reveals whether the species considered benefits from the mixture only temporally (Fig. 9.8, left), or continuously (Fig. 9.8, right).

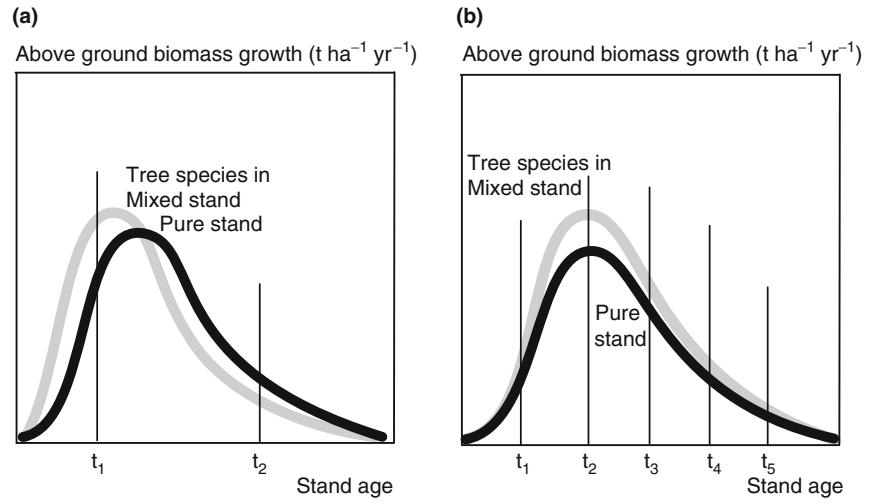

Fig. 9.8 Unimodal biomass growth curves of a species in a pure stand (*black*) and in a neighbouring mixed stand (*grey*) presented schematically. (**a**) If mixing alters a species' growth curve, comparison of increment at time t_1 and t_2 yield inconsistent results. In this case, the comparison reflects accumulated difference due to altered aging, rather than differences in productivity between mixed and pure stand under ceteris paribus conditions. (**b**) If mixing only increases the level of biomass productivity without altering the rhythm of the increment curve, comparison at time $t_1 \ldots t_5$ deliver consistent results

Although investigations based on periodic comparisons, e.g. by Kennel (1965), Mettin (1985) or Rothe (1997), may provide practical relevant information about mixed species stands, when they neglect size or age effects, their conclusions about superior or inferior productivity of mixed vs pure stands remain questionable. Mitscherlich (1970, p. 122) and Wiedemann (1942) show distinctly how mixing can alter the ontogenetic aging of the trees, the progress of stand development and the shape of the growth curves. The further ahead or behind one stand is in relation to the other, the more questionable a comparison of their mean annual growth in a given period becomes because this may simply represent different development stages. One method for avoiding such confusion is to survey pure and neighbouring mixed stands over long periods: over decades or even centuries. Then, the accumulated total biomass production from each successive survey is balanced, and the overall performance of mixed stands can be compared to pure stands. However, complete long-term trials in mixed stands are rare, and hardly representative of all site conditions (Pretzsch 2005a; Spellmann 1996). Chronosequences of stands offer another approach for examining the persistence of mixing effects (Fig. 9.8b). By analysing the productivity of mixed vs pure stands at several stand ages $t_1 \ldots t_5$ instead of only for a selected period, the duration of a mixture's superiority can be substantiated (Sects. 9.3 and 9.4 of this chapter).

9.3 Quantifying Effects of Species Mixture at Stand Level

9.3.1 Cross-Species Diagrams for Visualising Mixture Effects

Early mixed stand experimental plots consisted mostly of one plot with the species in mixture, and two neighbouring plots representing their growth in monocultures (Kennel 1965; von Lüpke and Spellmann 1999; Wiedemann 1943b). Recent designs comprise several mixed plots with different mixture proportions and patterns and, like their predecessors, nearby plots, which represent species performance in monoculture (Kelty and Cameron 1995; Pretzsch 1992a; Scherer-Lorenzen et al. 2005). Cross-species diagrams offer a powerful tool for revealing species interactions, especially for the extended design, as they represent the results of quantitative comparisons, shown in the following section, at the stand level.

In such diagrams, biomass productivity (t ha^{-1} yr^{-1}) at, or total biomass production (t ha^{-1}) till a given age for the pure stand of species 1 (p_1) is plotted on the left-hand ordinate, while that for species 2 (p_2) is plotted on the right-hand ordinate (Fig. 9.9). The upper, connecting lines (accentuated by rhombuses) represent

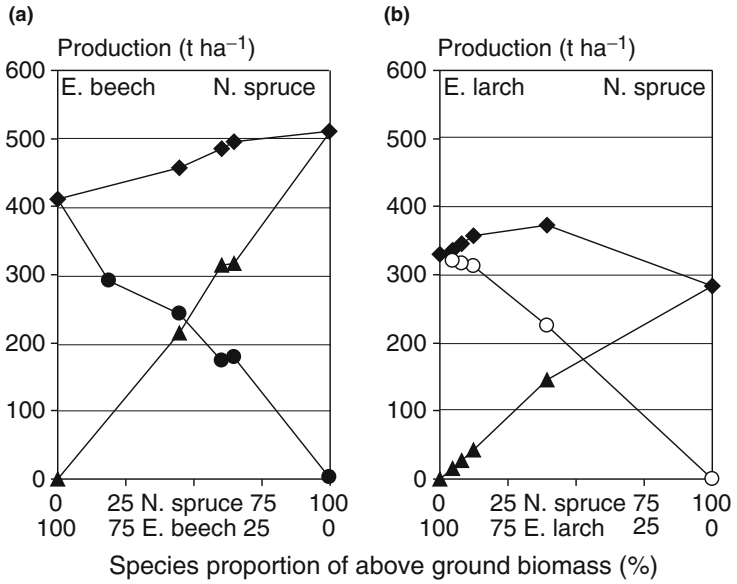

Fig. 9.9 Cross-species diagrams for visualising mixing effects: a typical response pattern of dry biomass production in two-species mixtures. (**a**) Norway spruce and European beech in submontane areas with neutral effects. (**b**) European larch and Norway spruce in sub-alpine areas showing beneficial responses to species mixing. The dry biomass production from pure stands of species 1 is plotted on the *left-hand ordinates*, and that for species 2 on the right-hand ordinates. The *upper connecting lines* (*accentuated by rhombuses*) represent total production $p_{1,2}$ of the mixed stand. The production for each species $p_{1,(2)}$ and $p_{(1),2}$ is shown (*triangles and circles*, respectively). Data are from (**a**) Pretzsch (1992a) and (**b**) Zöhrer (1969)

total production $p_{1,2}$ of the mixed stands for different mixture proportions. The mixing effect for the mixed European beech–Norway spruce stands (Fig. 9.9a) can be analysed on three mixed-species plots, and for the European larch–Norway spruce experiment, on four mixed stands. In addition, the production of each species $p_{1,(2)}$ and $p_{(1),2}$ is shown for each mixture (triangles and circles respectively). Data for Fig. 9.9 a and b originate from Pretzsch (1992a) and Zöhrer (1969) respectively.

With growth-neutral mixture effects, the production of the mixed plots will lie on the straight lines connecting the two pure stands. Deviations in the observed values from the straight reference lines reveal whether the stand gains or loses in the mixture overall. Concave (seen from below) upper lines indicate positive mixing effects, convex lines growth losses due to species mixing. In the same way the individual species lines of $p_{1,(2)}$ and $p_{(1),2}$ (forming a cross) indicate whether a species gains or loses by mixing. Again concavity indicates benefit, and convexity loss due to the mixing.

The European beech–Norway spruce experimental plot Zwiesel 111 (Fig. 9.9a) shows neutral effects from species interaction. On all trial plots within this experimental plot, total dry biomass production increases in proportion to the share of the constituent species in the mixture. Thus, the total production from mixtures lies between the pure stand plots. Accordingly, production gains are solely attributable to European beech being replaced by Norway spruce, which grows faster on this site, and not to beneficial interactions between the two species. Norway spruce's production (triangles) increases in proportion to its share in the mixture; the same applies for European beech.

Zöhrer (1969) provides evidence that the biomass production of European larch–Norway spruce mixtures in the Salzburger Land is superior to that of pure stands on identical sites (Fig. 9.9b). With the increase in the Norway spruce proportion, total yield is disproportionately high, until it reaches a peak at 40%, and then declines to the value of the pure Norway spruce stand. The position of the resulting data above the line connecting the dry biomass production of both pure stands is indicative of the beneficial effects of species interactions in the mixture. The European larch–Norway spruce mixture surpasses the pure Norway spruce stand by 22–28%, and the pure European larch stand by 2–13%; in other words it provides an example of transgressive overyielding (9.3). In these examples the comparison between pure and mixed stands is based on long-term experimental plots for which the total production data is available from stand establishment to an advanced stand age. Subsequent examples are based mainly on biomass productivity ($t\,ha^{-1}\,yr^{-1}$) over shorter survey periods.

9.3.2 Nomenclature, Relations and Variables for Analysing Mixture Effects

We developed a framework for analysing the effects of species mixtures in relation to stand and tree parameters. In the following introduction, the key variable,

aboveground biomass productivity p ($t\,ha^{-1}\,yr^{-1}$), provides an example. We consider an experimental arrangement where one plot contains pure Norway spruce, one plot pure European beech, and a third plot, both species in mixture.

For consistency with subsequent examples, we denote the biomass productivity p of the pure Norway spruce stand as p_{sp}, the European beech stand as p_{be} and the mixed stand as $p_{sp,be}$. In the mixed stand, we refer to the biomass productivity per ha of Norway spruce as $p_{sp,(be)}$, and of European beech as $p_{(sp),be}$. To obtain these variables, we need the share of productivity of both species, $pp_{sp,(be)}$ and $pp_{(sp),be}$, and their mixing proportions m_{sp} and m_{be}. This enables us to calculate $p_{sp,(be)} = pp_{sp,(be)}/m_{sp}$ and $p_{(sp),be} = pp_{(sp),be}/m_{be}$. The share $pp_{sp,(be)}$ represents Norway spruce's contribution to biomass productivity in the mixed stand, and $p_{sp,be} = pp_{sp,(be)} + pp_{(sp),be}$. In contrast $p_{sp,(be)}$ reflects the contribution $pp_{sp,(be)}$ scaled up to 1 ha by the mixture proportion of this species, i.e. $p_{sp,(be)} = pp_{sp,(be)}/m_{sp}$.

Now we can calculate

$$\widehat{p}_{sp,be} = p_{sp} \times m_{sp} + p_{be} \times m_{be}, \tag{9.1}$$

which represents the expected biomass produced by a mixed stand if the productivity of both species is the same as in neighbouring pure stands with the same area. If the observed productivity in the mixed stand is higher than the expected productivity $\widehat{p}_{sp,be}$, i.e.

$$p_{sp,be} > p_{sp} \times m_{sp} + p_{be} \times m_{be} \tag{9.2}$$

we find overyielding. When even

$$p_{sp,be} > p_{sp} \text{ and } p_{sp,be} > p_{be} \tag{9.3}$$

we notice transgressive overyielding of the mixed stand compared with both species in pure stands.

The following quotients apply the above-mentioned variables to compare pure and mixed stands: the ratio $p_{sp} : p_{be}$ compares the productivity of the species considered in monoculture. The ratio $p_{sp,(be)} : p_{(sp),be}$ addresses the same relation in the mixed stand. It reveals how mixing changes the relative strength of both species. Over-, or underyielding can be quantified by the ratio $p_{sp,be} : \hat{p}_{sp,be}$, which amounts to 1.0 when mixed stand growth is similar to the neighbouring pure stands with the same area. However, values above or below 1 indicate, and quantify overyielding and underyielding respectively. For example, $p_{sp,be} : \hat{p}_{sp,be} = 1.5$ indicates overyielding by 50%. Transgressive overyielding is indicated by $p_{sp,be} > p_{sp}$ and $p_{sp,be} > p_{be}$. The ratios $p_{sp,(be)} : p_{sp}$ and $p_{(sp),be} : p_{be}$ show which species causes overyielding or underyielding. They relate the productivity of each species in mixed stands to its productivity in the neighbouring monoculture. Other variables, e.g. diameter d, crown length cl, and crown projection area cpa are named and applied analogously.

During inventories, standing volume is measured in $m^3\,ha^{-1}$ and stand productivity in $m^3\,ha^{-1}\,yr^{-1}$. Volume is mostly given as merchantable wood >7 cm minimum diameter at the smaller end. The standing volume is multiplied by the species-specific wood density so that the productivities of species with different

specific wood densities are comparable, and the mixture proportions plausible (Trendelenburg and Mayer-Wegelin 1955). Kennel (1965), for example, assumed a wood density of 390 $kg\,m^{-3}$ for Norway spruce and 560 $kg\,m^{-3}$ for European beech. He showed that the mixture did not change the wood density significantly, and compared the stock and growth of standing aboveground stem biomass in pure and mixed stands. Wood densities for other relevant species are listed in Chap. 2, Table 2.8.

Alternatively, one can apply species-specific biomass functions at the tree level, which can be extrapolated to derive the total standing aboveground biomass ($t\,ha^{-1}$) and total biomass productivity ($t\,ha^{-1}\,yr^{-1}$) of stands, including branch and leaf biomass (Pretzsch and Mette 2008).

9.3.3 Mixture Proportion

To identify any productivity benefit or loss due to species interaction, mixture proportions of species 1 and 2 (e.g. m_{sp} and m_{be}) in the mixed stands need to be calculated and applied in (9.1) and (9.2), or in the cross-species diagram in Fig. 9.9. However, the different conventions for calculating mixture proportions can produce contrasting results.

Simple approaches for deriving the mixture proportions use tree number N (trees per hectare), stand basal area BA (square metres per hectare) or standing stem volume V ($m^3\,ha^{-1}$) for the total stand and for each species. Suppose we analyse a mixed stand of Norway spruce and European beech. Then, the mixture proportion of Norway spruce based on tree number is determined from $m_{sp}(N) = N_{sp}/(N_{sp} + N_{be})$. The portions $m_{sp}(BA)$ and $m_{sp}(V)$ are calculated analogously. These methods do not take into account species-specific mean tree size, growing space requirements, and tree packing densities adequately. Norway spruce may comprise numerous small trees N_{sp} and European beech only a few, yet tall trees N_{be}. In this case, the mixture proportion $m_{sp}(N)$ would overestimate Norway spruce's share of the stand area and resources. Mixture proportions based on BA or V take into account species-specific sizes. However, depending on the species-specific crown allometry and specific wood density R (cf. Chap. 2, Table 2.8), very different leaf area, living tree biomass and growing space requirements may underly a given basal area BA or standing volume V. Thus, it is important to consider species-specific density and growing space requirements when calculating the mixture proportions $m_1 \ldots m_n$.

To consider the species-specific growing space requirements, forest practice adjusts observed basal area proportions in mixed stands ($BA_{obs\,sp}$, $BA_{obs\,be}$) by the basal area predicted in the yield tables for pure stands ($BA_{Y\,sp}$, $BA_{Y\,be}$) on the given site. The mixture proportion of Norway spruce $m_{sp}(BA_Y)$, e.g. is

$$m_{sp}(BA_Y) = \frac{BA_{obs\,sp}/BA_{Y\,sp}}{BA_{obs\,sp}/BA_{Y\,sp} + BA_{obs\,be}/BA_{Y\,be}}. \tag{9.4}$$

In other words, the relationship between the basal areas of both species in the pure stand, which expresses the species-specific packing density, is applied to adjust observed basal areas of Norway spruce and European beech to their share of stand space and resources.

As, in our case, neighbouring plots represent the species basal area in pure stands, we can use the measured basal areas on the nearby reference plots to adjust the observed basal area proportions in mixed stands giving

$$m_{sp}(BA_{ref}) = \frac{BA_{obs\,sp}/BA_{ref\,sp}}{BA_{obs\,sp}/BA_{ref\,sp} + BA_{obs\,be}/BA_{ref\,be}}. \tag{9.5}$$

If total crown projection area CPA_T ($m^2\,ha^{-1}$) is available for both of the species occurring ($CPA_{T\,sp}$ and $CPA_{T\,be}$ respectively), Assmann (1961) and Kennel (1965) favour its application for calculating the mixture proportions: e.g. $m_{sp}(CPA_T) = CPA_{T\,sp}/(CPA_{T\,sp} + CPA_{T\,be})$. The same method can be based only on the projection area of the dominant crowns and yields, $m_{sp}(CPA_D)$, and $m_{be}(CPA_D)$ respectively. However, again, a given crown projection area may reflect very different leaf areas, and living stem biomass, and hence very different resource consumption.

The following three methods aim to provide an even better quantification of the mixing proportions by considering the species-specific biomass. Assmann (1961), and others apply specific wood density for the species present (e.g. $R_{sp} = 0.39\,g\,cm^{-3}$ and $R_{be} = 0.56\,g\,cm^{-3}$ for Norway spruce and European beech respectively) to calculate the mixture proportions on the basis of basal area proportions:

$$m_{sp}(BA_R) = \frac{BA_{obs\,sp} \times R_{sp}}{BA_{obs\,sp} \times R_{sp} + BA_{obs\,be} \times R_{be}}. \tag{9.6}$$

Keller (1995) criticised the adjustment with the untransformed specific wood density R. He argued that R represents a density in relation to space, but that the basal area should be corrected by relating density to area, i.e. $\sqrt[3]{R^2}$. Supposing a stem is a stereometric body with the volume v, basal area ba, and diameter d, then simple geometrical scaling yields allometry $v \propto d^3$ and $ba \propto d^2$, and thus $ba \propto v^{2/3}$. As volume is proportional to weight ($v \propto w$), $ba \propto w^{2/3}$. This means the relationship between two volumes corresponds to a relationship between the respective basal areas raised to the power of 2/3. Applying the ratio of the specific wood densities of Norway spruce to European beech, 0.39 : 0.56, the ratio of the basal areas becomes $0.39^{2/3} : 0.56^{2/3} = 0.534 : 0.679 = 1 : 1.272$. Given this relationship, the basal area of Norway spruce should be weighted by $\sqrt[3]{R_{sp}^2}$ and that of European beech by $\sqrt[3]{R_{be}^2}$ in to the following equation:

$$m_{sp}(BA_{R^{2/3}}) = \frac{BA_{obs\,sp} \times \sqrt[3]{R_{sp}^2}}{BA_{obs\,sp} \times \sqrt[3]{R_{sp}^2} + BA_{obs\,be} \times \sqrt[3]{R_{be}^2}}. \tag{9.7}$$

A similar approach applies to the aboveground biomass of the species present, calculated with biomass functions of the type w = f (tree diameter and/or tree height), to obtain $m_{sp}(W) = W_{sp}/(W_{sp} + W_{be})$. This approach assumes that the share of aboveground biomass of each species expresses best their competitive access to above and belowground resources, and thus their proportion in the mixture.

As the productivity and mixture proportions always relate to 1 ha, a mixture proportion of $m_{sp} = 0.8$ would mean that 0.8 ha or 80% of the growing space and resource are sequestrated by Norway spruce. In the following section we apply a whole series of methods to show the broad differences in the results.

9.3.4 Examining Effects of Species Mixture on Biomass Productivity in Norway Spruce–European Beech Stands: An Example

We applied the methods introduced above on 37 experimental plots in pure evenaged, and mixed stands of Norway spruce and European beech spanning 37–155 years of age (Pretzsch and Schütze 2008). The site conditions at the plots ranges from warm, dry and base-rich to cool, wet and acidic sites. They are located in prealpine areas of Southern Bavaria, near Schongau (SON) and Freising (FRE), where both European beech and Norway spruce are highly productive and approximately equally competitive. One pure Norway spruce plot, one pure European beech plot and a mixed Norway spruce–European beech plot are present on most of the 14 sites considered.

Table 9.1 displays the key information for the subsequent detailed analysis of mixing effects on the stand. The periodic annual increment in aboveground biomass production in the pure stands (left) ranges from $p_{sp} = 5.0{-}13.4$ (t ha^{-1} yr^{-1}) for Norway spruce and $p_{be} = 3.8$–18.1 (t ha^{-1} yr^{-1}) for European beech stands. Standing biomass in the pure Norway spruce stand, $W_{sp} = 137$–683 (t ha^{-1}), is similar to that of pure European beech, $W_{be} = 73$–807 (t ha^{-1}). Yet of the pure stands, European beech tends to be superior in FRE 813, whereas, Norway spruce is superior in SON 814. Total biomass productivity of the mixed stands $p_{sp,be}$ (right) ranges from $p_{sp,be} = 7.4$–13.6 (t ha^{-1} yr^{-1}), and remains more stable with stand development than in the pure stands. In the mixture, standing biomass ranges from $W_{sp,(be)} = 92$–399 (t ha^{-1}) for Norway spruce, and $W_{(sp),be} = 84$–340 (t ha^{-1}) for European beech. Ranging from $W_{sp,be} = 177$–649 (t ha^{-1}), total biomass is more stable over time in mixed stands, yet not considerably different from the standing biomass in pure stands.

Standing biomass of the mixed stand is used to evaluate the mixture proportions with $m_{sp} = W_{sp,(be)}/W_{sp,be}$ for Norway spruce, and similarly with m_{be} for European beech. Mixture proportion (ratio of aboveground biomass Norway spruce: European beech) is 0.53:0.47 on average, and ranges from 0.35:0.65 to 0.64:0.36. The biomass productivity p_{sp} and p_{be} of the pure stands, and the species proportions m_{sp} and m_{be} of standing biomass in the mixed stand (left part of the table)

Table 9.1 Aboveground standing biomass and periodic annual biomass growth on the plots FRE 813/1–6 and SON 814/1–9. Missing values for the mixed stand in the table stem from missing mixed plots or unrepresentative small plots (<0.05 ha): [a]stand age refers to Norway spruce; [b]biomass production of the pure stands p_1 and p_2 (*left part of the table*) and species mixing proportions m_1 and m_2 of standing biomass in the mixed stand (*left part of the table*) are used to calculate the expected annual biomass production $\hat{p}_{sp,be} = p_1 \times m_1 + p_2 \times m_2$, which serves as reference for assessing total mixed stand productivity

Age series	Plot	Age[a]	Pure stands observed				Mixed stands expected	Mixed stands observed					
			N. spruce		E. beech		Total $\hat{p}_{sp,be}$	N. spruce		E. beech		Total $p_{sp,be}$	
			Standing biomass ($t\,ha^{-1}$)	Biomass productivity ($t\,ha^{-1}\,yr^{-1}$)	Standing biomass ($t\,ha^{-1}$)	Biomass productivity ($t\,ha^{-1}\,yr^{-1}$)	Biomass productivity[b] ($t\,ha^{-1}\,yr^{-1}$)	Standing biomass ($t\,ha^{-1}$)	Biomass productivity ($t\,ha^{-1}\,yr^{-1}$)	Standing biomass ($t\,ha^{-1}$)	Biomass productivity ($t\,ha^{-1}\,yr^{-1}$)	Standing biomass ($t\,ha^{-1}$)	Biomass productivity ($t\,ha^{-1}\,yr^{-1}$)
FRE 813	6	42	137	11.6	73	6.8	9.3	92	6.5	84	5.7	177	12.2
	5	47	166	12.8	362	18.1	–	–	–	–	–	–	–
	1	49	255	11.3	424	11.6	11.5	142	5.8	263	5.5	406	11.3
	2	82	358	8.2	807	9.9	–	–	–	–	–	–	–
	4	93	209	5.0	409	8.5	6.3	285	6.2	161	3.8	446	10.0
	3	120	337	5.1	358	7.2	5.9	303	4.3	193	3.3	496	7.6
SON 814	7	55	308	12.3	343	11.5	–	–	–	–	–	–	–
	4	60	480	13.4	371	11.4	–	–	–	–	–	–	–
	9	65	517	9.8	330	8.9	9.3	145	3.7	185	5.1	330	8.8
	8	70	321	9.6	253	8.9	9.3	213	7.1	142	5.0	355	12.1
	5	90	363	8.7	422	9.6	9.2	242	4.9	340	8.7	582	13.6
	1	110	683	10.4	392	3.8	7.9	255	4.5	154	2.9	409	7.4
	2	115	684	6.8	406	7.3	–	–	–	–	–	–	–
	3	120	683	10.4	493	6.9	9.1	399	5.9	250	3.7	649	9.6

are used to calculate the expected annual biomass productivity $\widehat{p}_{sp,be}$ in (9.1). In six out of nine cases, i.e. in 67% of the observations, we find that total productivity in the mixed stand exceeds expected productivity ($p_{sp,be} > \widehat{p}_{sp,be}$). Thus, productivity in the mixed stand is superior to that expected in pure stands of the same size. In five out of nine cases (plots FRE 813/6, 4, 3 and SON 814/8, 5), the productivity of the mixed stand even exceeds the productivity of the pure Norway spruce, and pure European beech stands ($p_{sp,be} > p_{sp}$ and $p_{sp,be} > p_{be}$), and substantiates evidence for transgressive overyielding.

To assess the relative productivity of Norway spruce compared to European beech, we apply the quotient $p_{sp} : p_{be}$, which relates the periodic annual increment in biomass of the pure Norway spruce stand p_{sp} to the pure European beech stand p_{be}. Table 9.2 displays the results by plots, age series, and in total. On the FRE 813 plots, the productivity of Norway spruce is slightly lower than European beech (0.92:1), whereas SON 814 shows a distinct (but not statistically significant) superiority of Norway spruce (1.31:1). For this, and all subsequent quotients, we use the t-test to analyse whether the quotient deviates from 1.0 for the plots and the chronosequence. Quotients significantly ($p < 0.05$) above, and below 1.0 are set in bold numbers.

Table 9.2 Ratios for comparing stand level productivity of pure stands to a Norway spruce–European beech mixed stand: $p_{sp} : p_{be}$, stand productivity ratio of pure Norway spruce–pure European beech; $p_{sp,(be)} : p_{(sp),be}$ productivity ratio of Norway spruce–European beech in mixture; $p_{sp,be} : \hat{p}_{sp,be}$ observed productivity ratio of the mixed stand to productivity expected from pure stands of the same size; $p_{sp,(be)} : p_{sp}$ productivity ratio of Norway spruce in mixture to Norway spruce in a pure stand; $p_{(sp),be} : p_{be}$ productivity ratio of European beech in mixture to European beech in a pure stand. All quotients are based on periodic annual biomass growth ($t\,ha^{-1}\,yr^{-1}$)

Age series	Plot	$p_{sp} : p_{be}$	$p_{sp,(be)} : p_{(sp),be}$	$p_{sp,be} : \hat{p}_{sp,be}$	$p_{sp,(be)} : p_{sp}$	$p_{(sp),be} : p_{be}$
FRE 813	6	1.71	1.04	1.31	1.07	1.76
	5	0.71	–	–	–	–
	1	0.97	1.96	0.98	1.46	0.72
	2	0.82				
	4	0.59	0.93	1.59	1.94	1.22
	3	0.71	0.83	1.29	1.40	1.20
FRE 813/1–6		0.92	1.19	**1.29**	**1.47**	1.23
SON 814	7	1.06	–	–	–	–
	4	1.18	–	–	–	–
	9	1.11	0.93	0.94	0.86	1.02
	8	1.07	0.95	1.30	1.23	1.39
	5	0.90	0.78	1.47	1.34	1.55
	1	2.76	0.93	0.93	0.69	2.07
	2	0.93	–	–	–	–
	3	1.51	0.99	1.06	0.92	1.40
SON 814/1–9		1.31	**0.91**	1.14	1.01	**1.49**
Total		1.14	1.04	**1.21**	1.21	**1.37**

The ratio $p_{sp,(be)} : p_{(sp),be}$ compares the productivity of Norway spruce to European beech in the mixed stand, where $p_{sp,(be)} = pp_{sp,(be)}/m_{sp}$ and $p_{(sp),be} = pp_{(sp),be}/m_{be}$ are the species-specific and area-related productivities in the mixture. Mixing extends the ratio of Norway spruce to European beech to 1.19:1 for FRE 813, and reduces it to 0.91:1 for SON 814. In other words, the mixture fosters Norway spruce in FRE 813, but European beech in SON 814. In total, the productivity ratio of Norway spruce to European beech is 1.14:1 in monocultures, and 1.04:1 in mixture; i.e. it is closer, though not significant at the level $p < 0.05$.

The quotient $p_{sp,be} : \hat{p}_{sp,be}$ reveals overyielding by mixing. It relates the observed total biomass productivity of the mixed plots $p_{sp,be}$ to the productivity of a combination of pure stands of the same size $\hat{p}_{sp,be}$ (cf. (9.1)). We notice an average overyielding in a mixture of 1.29 on the FRE 813 plots, and 1.14 on the SON 814 plots. Therefore, the mean productivity increases in these mixtures by 29 and 14% respectively. In total, $p_{sp,be} : \hat{p}_{sp,be}$ is 1.21 (Table 9.2, bottom).

By relating the productivity of each species by area in mixed stands $p_{sp,(be)}$ and $p_{(sp),be}$ to the productivity in the neighbouring pure stands, p_{sp} and p_{be} respectively, we identify which species is responsible for overyielding in the mixture. The quotient $p_{sp,(be)} : p_{sp}$ on FRE 813 and on SON 814 age series ranges from 1.07 to 1.94 and 0.69 to 1.34 respectively. On FRE 813, Norway spruce increases growth in the mixture significantly by a factor of 1.47. In contrast, the ratio $p_{(sp),be} : p_{be}$ at these sites ranges from 0.72 to 1.76 and 1.02 to 2.07 respectively. Thus, in the age series SON 814, European beech increases the growth in the mixture significantly by a factor of 1.49 on average.

In this example, we calculate the mixture proportion on the basis of the standing aboveground biomass of Norway spruce and European beech in the mixed stand ($W_{sp,(be)}$ and $W_{(be),sp}$), and the total biomass of the mixed stand ($W_{sp,be}$). However, we use the 14 mixed stand plots to show the differences between the introduced methods for calculating mixture proportions: the results differ markedly (Fig. 9.10). When basal area, corrected by the yield table values, is used, we obtain the lowest mixture proportion of $m_{sp}(BA_Y) = 0.57$ on average, whereas when crown projection area of dominant trees is used, we obtain the highest mixture proportion of $m_{sp}(CPA_D) = 0.75$. In other words, the mixture proportion varies by 18 points, between 0.57 and 0.75, depending on the method applied. Consequently, the choice of the applied method will considerably affect $\widehat{p}_{sp,be}$ (cf. (9.1)), and all subsequent calculations and comparisons between pure and mixed stand productivity.

The mixture proportion $m_{sp}(W)$ we applied is in line with $m_{sp}(BA_Y)$, $m_{sp}(BA_{ref})$, $m_{sp}(BA_R)$, and $m_{sp}(BA_{R^{2/3}})$, which all take into account the species-specific growing space requirements. The proportions $m_{sp}(BA), m_{sp}(CPA_T)$, and $m_{sp}(CPA_D)$ do not consider the species-specific packing density, and therefore overestimate the proportion of Norway spruce.

In our example, we found prevailing transgressive overyielding, i.e. $p_{sp,be} > p_{sp}$ *and* $p_{sp,be} > p_{be}$. In this case $p_{sp,be} > p_{sp} \times m_{sp} + p_{be} \times m_{be}$ applies for all proportions of species mixtures (e.g. $m_{sp} : m_{be} = 0.9 : 0.1,\ 0.8 : 0.2 \ldots 0.1 : 0.9$ etc.). Therefore, the identification of transgressive overyielding is not affected by the method used to calculate the mixture proportion because the linear combination $p_{sp} \times m_{sp} + p_{be} \times m_{be}$ never can exceed p_{sp} or p_{be}.

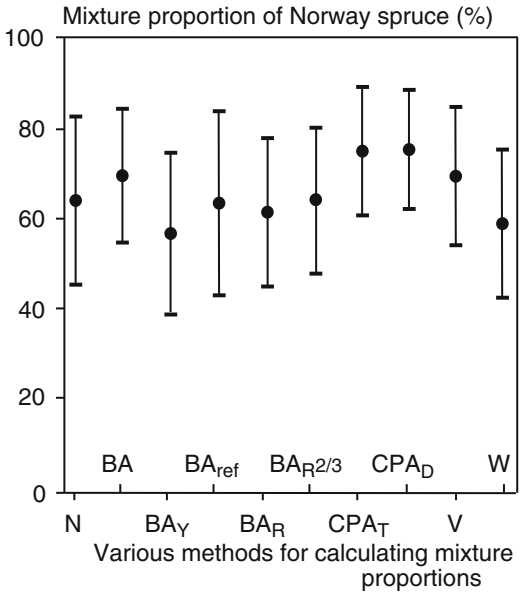

Fig. 9.10 Results from 10 different methods for calculating the mixture proportion of Norway spruce for 14 mixed stand plots (cf. Table 9.1). *From left to right*, the results are shown of calculations based on (average mixture proportion and standard deviation) stem number $m_{sp}(N)$, basal area $m_{sp}(BA)$, basal area corrected by yield table $m_{sp}(BA_Y)$, basal area corrected by measured basal area of neighbouring pure stands as reference $m_{sp}(BA_{ref})$, basal area corrected by specific wood density R $m_{sp}(BA_R)$, basal area corrected by $\sqrt[3]{R^2}$ resulting in $m_{sp}(BA_{R^{2/3}})$, total crown projection area $m_{sp}(CPA_T)$, crown projection area of dominant trees $m_{sp}(CPA_D)$, standing stem volume $m_{sp}(V)$, and standing above ground tree biomass $m_{sp}(W)$

9.3.5 Examining Mean Tree Size in Norway Spruce–European Beech Stands: An Example

Here, we apply the arithmetic mean diameter d, crown length cl, crown projection area cpa, and the aboveground tree biomass w to analyse whether the trees in pure, and neighbouring mixed stands are equal in size. Any difference in mean size indicates that trees in pure and mixed stands are in different ontogenetic phases. This would mean that our stand-level scale of comparison in the last section is flawed, since, although the neighbouring stands are at a similar physical age, they are at divergent development stages due to the mixing.

The absolute size and size difference between trees in pure and mixed stands is of as much interest in forest practice as the size relationships between trees on thinned and unthinned plots of thinning trials. To reveal any differences between tree size in mixed and pure stands, we apply ratios that relate tree sizes in mixed stands to those in the corresponding pure stands. These ratios are similar to the quotients applied in the previous section for comparisons of productivity.

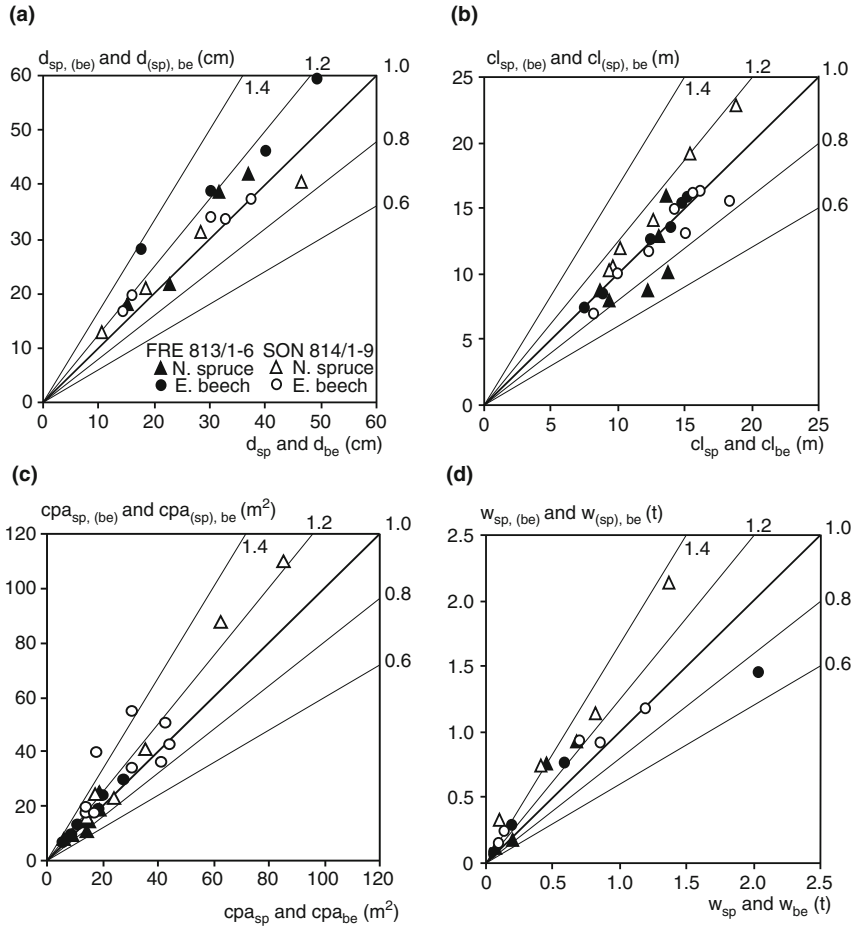

Fig. 9.11 Comparison between mean tree size in pure stands (abscissa) and mixed stands (ordinate) of Norway spruce (*triangles*) and European beech (*circles*) with respect to (**a**) arithmetic mean diameter d, (**b**) crown length cl, (**c**) crown projection area cpa, and (**d**) aboveground tree biomass w. The *filled and unfilled symbols* represent plots in FRE 813 and SON 814 respectively. *Symbols on or near the bisection line* reflect equivalent pure and mixed stand mean size; the *values exceeding the line* (>1.0) indicate that mixed stand trees are superior in size, and vice versa

Figure 9.11 reveals whether the trees in mixed stands are larger than members of the same species in neighbouring pure stands. The quadrants in the graphs are divided into sectors where tree size in the mixed (ordinate) and pure stand (abscissa) is equivalent. The bisector line represents equal sizes in the mixed and pure stand (quotient = 1.0). Above this line, in the sector 1.0–1.1, 1.1–1.2 etc., trees in the mixture are superior by 0–10%, 10–20% etc. Below the bisector, e.g. in the sector 0.9–1.0, 0.8–0.9 etc., trees in mixed stands are inferior. In Fig. 9.11, Norway spruce is represented by triangles and European beech by circles; solid symbols represent the FRE 813/1–6 age series, and unfilled symbols the SON 814/1–9 age series.

Overall, more observations lie above the bisector line than below. In the case of Norway spruce, the quotients for d, cl, cpa, and w lie between 0.96–1.56, 0.72–1.18, 0.77–1.29, and 0.90–2.97 respectively. Diameter and tree biomass is considerably higher in the mixed stands (Fig. 9.11a, d), whereas crown length and crown projection area of Norway spruce are less affected by mixing (Fig. 9.11b, c). In the case of European beech, the quotients for d, cl, cpa, and w lie between 0.87–1.23, 0.84–1.25, 0.94–2.23, and 0.71–1.66 respectively. In addition, the figure shows that the superiority of mixed vs pure stands increases with size, i.e. trees in the mixed stand can increase their lead as the stand develops. Table 9.3 shows that the superiority in the size of Norway spruce in mixed stands is statistically significant ($p < 0.05$) in most of the tree attributes analysed. Although the tree diameter and tree biomass of Norway spruce are particularly superior in mixed stands (+21 and +64%), European beech (not show in the table) is not only superior in diameter and biomass (+9 and +27%, respectively), but also in length and projection area of tree crowns (+4 and +29%).

Table 9.3 Trees size of Norway spruce in mixed stands (FRE 813/1–6 and SON 814/1–9) in relation to tree size in the corresponding pure stand. The ratio $d_{sp,(be)} : d_{sp}$, for example, relates mean diameter of Norway spruce in the mixed stand to mean diameter of Norway spruce in the neighbouring pure stand. Such ratios are listed for mean tree diameter d, crown length cl, crown projection area cpa, and aboveground tree biomass w. Ratios deviating significantly from 1.0 are given in bold numbers (significance on level $p < 0.05$). Ratios CI and EEX are discussed in Sect. 9.4

Age series	Plot	Norway spruce					
		$d_{sp,(be)} : d_{sp}$	$cl_{sp,(be)} : cl_{sp}$	$cpa_{sp,(be)} : cpa_{sp}$	$w_{sp,(be)} : w_{sp}$	$CI_{sp,(be)} : CI_{sp}$	$EEX_{sp,(be)} : EEX_{sp}$
FRE 813	1	0.96	0.73	0.77	0.9	1.18	1.22
	2	–	0.72	0.95	–	2.07	1.14
	3	1.14	1.18	1.29	1.37	1.51	0.80
	4	1.22	0.98	0.97	1.63	1.39	1.22
	5	–	0.86	1.24	–	0.76	1.29
	6	1.19	1.00	0.99	1.52	1.24	1.86
FRE 813/1–6		**1.13**	0.91	1.03	**1.36**	**1.36**	1.25
SON 814	1	1.14	1.00	1.15	1.39	0.72	2.11
	2	–	0.96	1.07	–	0.79	1.51
	3	1.20	1.04	–	1.56	–	–
	4	–	0.94	1.14	–	0.81	1.36
	5	1.27	1.04	0.99	1.80	0.90	1.18
	7	–	0.98	1.06	–	1.37	0.82
	8	1.56	–	1.06	2.97	1.25	1.39
	9	–	–	–	–	–	–
SON 814/1–9		**1.29**	0.99	**1.08**	**1.93**	0.97	**1.40**
Total		**1.21**	0.9	1.06	**1.64**	1.17	**1.32**

9.4 Quantifying Mixture Effects at the Individual Tree Level

If mixing alters a species' biomass productivity ($t\,ha^{-1}\,yr^{-1}$) compared to the pure stand, the mixing effect should also be reflected at the individual tree level. For the detection of mixing effects at the tree level, we apply efficiency parameters that relate the biomass or biomass growth of a plant to the resources used (Kozovits et al. 2005; Matyssek et al. 2005; Reiter et al. 2005). However, we replace resource supply by the area available for tree growth or growing space (Pretzsch and Schütze 2005, 2008). The resulting efficiency parameters quantify the growth or yield of an individual tree per unit area available for growth, and offer a strong tool for tracing mixing effects from the stand to the plant level.

To reveal any mixing effects on the efficiency of individual trees, we need to eliminate the effect of tree size and competition status first so that the comparison is not flawed. Differences between the efficiency of a crown in a mixed stand and a pure stand for trees of equal size and competition status provides evidence for mixing effects, and helps quantify them. Consequently, in the following sections, we present efficiency parameters, methods for eliminating size and competition effects, and examples that show the effects of species mixing at the individual tree level. The methodology presented also enables the mixing effects in undesignated mixed-species plantations or naturally established stands to be revealed (Bristow et al. 2006; Pretzsch and Schütze 2005).

9.4.1 Efficiency Parameters for Individual Tree Growth

Efficiency parameters relate a plant's biomass or biomass growth to the resources used. Whereas biomass or growth can be evaluated easily from successive inventories, resources available to, and utilised by a tree are difficult to measure directly in a mature forest stand. Consequently, the growing space, or area available for tree growth often is used as a surrogate variable for resources. The approaches commonly used quantify area available for tree growth in relation to crown projection area (Assmann 1961; Sterba and Amateis 1998; Webster and Lorimer 2003).

We examine species space sequestration in a given period using the following parameters: cpa = crown projection area at the beginning of the growing season (m^2); w = aboveground tree biomass at the beginning of the growing season (kg); and $\Delta w = (w_2 - w_1)/n$ = mean annual biomass/increment in the growing season of length n ($kg\,yr^{-1}$). These parameters are used to calculate the efficiency of space occupation (EOC):

$$EOC = cpa/w, \tag{9.8}$$

efficiency in space exploitation (EEX):

$$EEX = \Delta w/cpa, \tag{9.9}$$

Table 9.4 Space occupation efficiency EOC ($m^2\,kg^{-1}$), space exploitation efficiency EEX ($kg\,m^2\,yr^{-1}$), and biomass investment efficiency EBI ($kg\,kg^{-1}$) for Norway spruce and European beech by crown projection area classes (cpa $< 10\,m^2$, 10–$16\,m^2$, $>16\,m^2$), and competition index classes (CI < 1, CI $= 1-2$, CI > 2). For an explanation of efficiency parameters, see (9.8)–(9.10)

		EOC ($m^2\,kg^{-1}$) cpa-class (m^2)				EEX($kg\,m^{-2}\,yr^{-1}$) cpa-class (m^2)				EBI ($kg\,kg^{-1}$) cpa-class (m^2)			
	n	<10	10–16	>16	mean	<10	10–16	>16	mean	<10	10–16	>16	mean
Norway spruce													
CI < 1	63	0.027	0.044	0.040	0.040	2.348	1.584	1.788	1.781	0.059	0.061	0.065	0.062
CI = 1–2	24	0.044	0.067	–	0.055	1.123	0.773	–	0.963	0.046	0.040	–	0.043
CI > 2	17	0.188	0.236	–	0.199	0.149	0.038	–	0.123	0.018	0.007	–	0.015
Mean	104	0.093	0.068	0.040	**0.069**	1.076	1.224	1.788	**1.321**	0.039	0.051	0.065	**0.050**
SDev (±)		0.114	0.069	0.014	0.082	1.024	0.778	0.884	0.931	0.023	0.024	0.024	0.026
European beech													
CI < 1	22	–	–	0.073	0.073	–	–	0.554	0.554	–	–	0.035	0.035
CI = 1–2	22	0.040	0.051	0.087	0.068	1.097	0.690	0.504	0.606	0.042	0.033	0.037	0.035
CI > 2	35	0.134	0.207	0.153	0.155	0.105	0.301	0.513	0.231	0.012	0.024	0.038	0.020
Mean	79	0.125	0.122	0.091	**0.108**	0.195	0.472	0.534	**0.425**	0.015	0.028	0.036	**0.028**
SDev (±)		0.075	0.144	0.071	0.094	0.343	0.430	0.420	0.423	0.017	0.022	0.023	0.023

and efficiency in biomass investment (EBI):

$$\mathrm{EBI} = \Delta w/w = \mathrm{EOC} \times \mathrm{EEX}. \tag{9.10}$$

For instance, for the mixed stand of Norway spruce and European beech (FRE 813/1), Table 9.4 shows that efficiency parameters are highly dependent on tree size and competitive status. We demonstrated the effect of tree size and competitive status on the efficiency parameters by allocating the 104 Norway spruce trees and 79 European beech trees to a 3×3 matrix by crown size (cpa) and competition index (CI). The size classes are cpa $< 10\,m^2$, 10–$16\,m^2$, and $> 16\,m^2$; classes of increasing competitive stress are CI < 1, 1–2, CI > 2 (cf. (9.11)). The competition index CI quantifies whether tree crown growth is free, restricted or overtopped (Pretzsch 2001, p. 220).

A comparison of overall mean EOC values (Table 9.4, bold numbers) between Norway spruce ($0.069\,m^2\,kg^{-1}$) and European beech ($0.108\,m^2\,kg^{-1}$) shows that the crown projection area of the latter is 57% greater on average for the same biomass. EEX for Norway spruce ($1.321\,kg\,m^{-2}\,yr^{-1}$) is about three times that of European beech ($0.425\,kg\,m^{-2}\,yr^{-1}$). Maximum EEX is reached when trees have a small crown and CI is low. As cpa increases, the efficiency with which Norway spruce and European beech exploit space decreases rapidly. Despite differences in crown size, EEX declines even more rapidly under competition. The percentage biomass growth, obtained by multiplying EBI by 100, is 5% and 2.8%, on average, for Norway spruce and European beech. Thus the efficiency of biomass investment of Norway spruce is approximately twice that of European beech. This relationship

between the two species persists throughout all strata (cf. Table 9.4). EBI clearly decreases from small to large crowns, and from trees with good to trees with poor access to light.

9.4.2 Application of Efficiency Parameters for Detecting Mixture Effects

An unadjusted comparison of crown efficiencies in pure and mixed stands would be misleading. Crown efficiency depends on size and competitive status, and unadjusted comparisons would compare the role of a species in mixed and pure stands rather than its crown efficiency. Therefore, before we make a comparison, we need to eliminate size and competition effects. Thus cpa and CI are used as independent variables in models that analyse crown efficiency in relation to lateral expansion and the vertical position of the crown. Space occupation efficiency EOC is analysed with the model using crown size cpa and competition index CI for each species:

$$\ln(\mathrm{EOC}) = a_0 + a_1 \times \ln(\mathrm{CI}+1) + a_2 \times \ln(\mathrm{cpa}). \tag{9.11}$$

By adding the value 1.0 to CI-values, we prevent an undefined result from the $\ln(\mathrm{CI}+1)$ when $\mathrm{CI}=0$. The antilogarithm of (9.12) ($\mathrm{EOC} = e^{a_0} \times (\mathrm{CI}+1)^{a_1} \times \mathrm{cpa}^{a_2}$) gives an allometric relationship between efficiency parameters and tree attributes. Space exploitation efficiency EEX and biomass investment efficiency EBI are examined in the same way.

Figure 9.12 displays the relationships between the crown efficiency parameters considered and the tree attributes CI and cpa for the tree collective from plot FRE 813/1 presented in Table 9.4.

EOC increases when crown projection area and competition increase. Norway spruce trees and European beech trees in the understorey ($\mathrm{CI}=2.5$) occupy much more growing space for a given biomass than do dominant trees ($\mathrm{CI}=0.5$) of the same size. While this tendency is similar for both species, the level of EOC and range in crown size of each differs considerably. Norway spruce trees with small crowns are more efficient than European beech trees of the same size. However, this apparent superiority of Norway spruce is not relevant at the stand level. The solid parts of the curves in Fig. 9.12 (top) represent the ranges in the observations, and show that Norway spruce dominates in small size classes with low EOC-values, whereas European beech reaches twice the size of Norway spruce and achieves high EOC-values.

EEX is at a maximum when small crowns have access to the upper canopy layer, but decreases exponentially with increasing crown size and CI (cf. Fig. 9.12, centre). The absolute EEX of predominant Norway spruce is considerably higher than European beech. The exponents $a_1 = -3.05$ (N. spruce) vs -1.64 (E. beech) for CI and $a_2 = -0.84$ (N. spruce) vs -0.69 (E. beech) for crown size cpa indicate that the decrease in EEX arising from an increase in size and in CI is steeper for Norway spruce than for European beech.

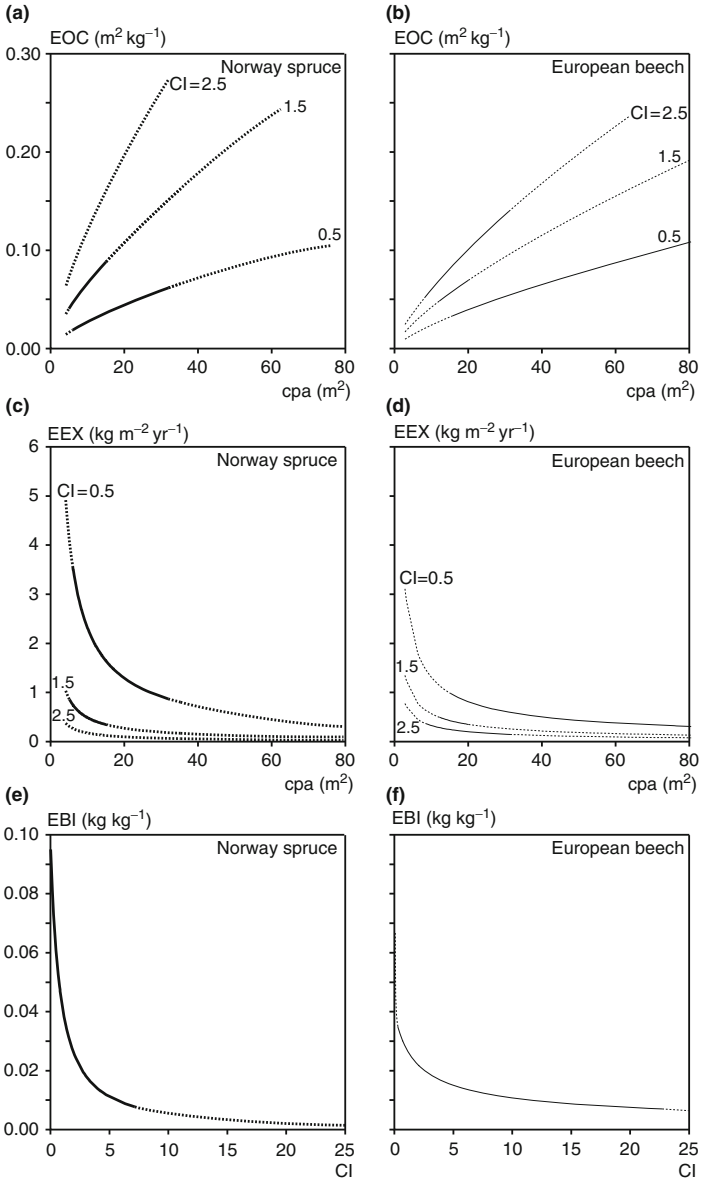

Fig. 9.12 Space occupation efficiency EOC ($m^2\,kg^{-1}$) (*top*), space exploitation efficiency EEX ($kg\,m^{-2}\,yr^{-1}$) (*middle*), and biomass investment efficiency EBI ($kg\,kg^{-1}$) for Norway spruce (*left*) and European beech (*right*) in relation to competition index CI, and crown projection area cpa (m^2): solid parts of the curves represent the ranges covered by observations. Regression equations for Norway spruce (n = 104): $\ln(EOC) = -5.97 + 1.76 \times \ln(CI+1) + 0.71 \times \ln(cpa)$, $R^2 = 0.78$, $p < 0.001$; $\ln(EEX) = 4.02 - 3.05 \times \ln(CI+1) - 0.84 \times \ln(cpa)$, $R^2 = 0.85$, $p < 0.001$; $\ln(EBI) = -2.33 - 1.21 \times \ln(CI+1)$, $R^2 = 0.58$, $p < 0.001$; For European beech (n = 79): $\ln(EOC) = -5.88 + 1.12 \times \ln(CI+1) + 0.73 \times \ln(cpa)$, $R^2 = 0.85$, $p < 0.001$; $\ln(EEX) = 2.53 - 1.64 \times \ln(CI+1) - 0.69 \times \ln(cpa)$, $R^2 = 0.85$, $p < 0.001$; $\ln(EBI) = -3.21 - 0.55 \times \ln(CI+1)$, $R^2 = 0.21$, $p < 0.001$

Therefore, European beech is more efficient in occupying space, but with only one third of the efficiency of Norway spruce in exploiting space occupied. Size seems to be an ambiguous tree characteristic. On the one hand, it ensures privileged access to light, and limits competitor access to contested resources. On the other hand, size boosts energy consumption for maintenance so that size growth is coupled with a decline in EEX.

EBI was found to be independent of crown projection but dependent on CI (cf. Fig. 9.12, bottom). The different growth percentages of Norway spruce and European beech are revealed by the respective equations in Fig. 9.12 (bottom). When converted to the antilogarithm form, $EBI = e^{a_0} \times (CI+1)^{a_1}$, $e^{-2.33} = 0.097\,kg\,kg^{-1}$ and $e^{-3.21} = 0.040\,kg\,kg^{-1}$ give EBI when $CI = 0$, which shows that Norway spruce is 243% more efficient than European beech. However, if competition CI increases, Norway spruce's EBI decreases by exponent $a_1 = -1.21$, and European beech's merely by exponent $a_1 = -0.55$. European beech occupies space with lower biomass investment, especially in the understorey, yet exploits it more efficiently than Norway spruce because of its tolerance to shade.

We extend the model, dependent only on size and competition so far, to compare tree growth in pure and mixed stands, and quantify mixing effects at the tree level (9.11):

$$\ln(EEX) = b_0 + b_1 \times \ln(cpa) + b_2 \times \ln(CI+1) + b_3 \times pm. \tag{9.12}$$

The binary dummy variable pm indicates whether the tree belongs to a pure stand $pm = 0$ or mixed stand $pm = 1$.

The regression was calculated for each plot of the series FRE 813/1–6 and SON 814/1–9, and for both species (15 plots $\times$ 2 species $= 30$ strata). The regression aims to quantify the influence of mixing (pm) on crown efficiency (EEX) once size and competition effects are eliminated. By adding 1.0, the term $\ln(CI+1)$ is defined when $CI = 0$. The term $b_3 \times pm$ represents the mixing effect. This becomes apparent when we rearrange (9.12) to

$$EEX = e^{b_0} \times cpa^{b_1} \times (CI+1)^{b_2} \times e^{b_3 \times pm} \tag{9.13}$$

The crown efficiency EEX in (9.13) remains unchanged for the pure stand, where $pm = 0$ and $e^{b_3 \times pm} = 1$. If $pm = 1$, crown efficiency is multiplied by $mult = e^{b_3}$, which represents directly the synergic effect of mixing on crown efficiency.

As cpa is one of the determinants of EEX (cf. (9.9)), it is included on both sides of (9.11) and (9.12). This increases the reported significance level, and the R^2 of the overall model. However, for our purposes, cpa should not be replaced by another dependent variable to obtain optimal parameter estimates for explaining EEX. Omitting cpa as an explanatory variable would mean that Δw is directly proportional to cpa, which makes no sense biologically. The biological plausibility of (9.12) ensures meaningful parameter estimates.

Altogether 2,630 trees (889 and 797 Norway spruce, and 455 and 489 European beech in the pure and mixed stands respectively) were available for the analysis. Parameter b_3 is of particular interest to us as it quantifies the effect of mixing on

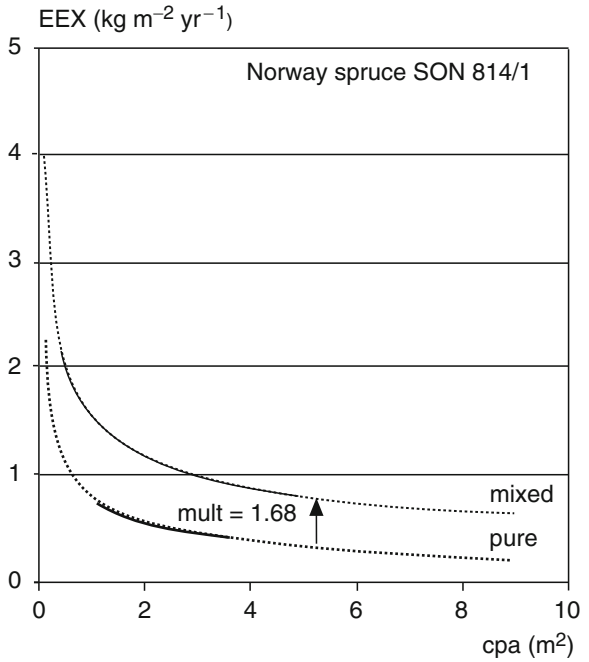

Fig. 9.13 Principle for the detection of mixing effects at the individual tree level by the multiplier mult $= e^{b_3 \times pm}$ (cf. (9.13)). EEX of crown projection area for spruce on plot SON 814/1 in relation to crown projection area cpa according to equation EEX $= e^{1.39} \times cpa^{-0.41} \times (CI+1)^{-1.30} \times e^{0.52 \times pm}$. EEX in the pure stand (pm $= 0$, lower curve) is shifted upwards by mult $= e^{0.52} = 1.68$ in the neighbouring mixed stand where pm $= 1$ (upper curve). To demonstrate, CI is set constant to 0.5

crown efficiency. In our example, we use Norway spruce on plot SON 814/1 to interpret b_3 (Fig. 9.13). Linear regression gives $\ln(EEX) = 1.39–0.41 \times \ln(cpa) - 1.30 \times \ln(CI+1) + 0.52 \times pm$ with $b_3 = 0.52$, and thus mult $= e^{0.52} = 1.68$. The lower curve in Fig. 9.13 represents the dependence of EEX on cpa in the pure stand. Here CI is set constant to CI $= 0.5$, which represents a dominant tree. The upper curve shows the same relationship as in the neighbouring mixed stand. Multiplier mult $= e^{0.52}$ raises the curve by a factor of 1.68, indicating Norway spruce crown efficiency increases by 68% with the admixture of European beech under ceteris paribus conditions.

Figure 9.14 summarises the mixing effect on crown efficiency (mult $= e^{b_3}$) for all plots in the age series FRE 813 and SON 814. The specific plot values of mult are depicted in relation to mean stand height for Norway spruce (left) and European beech (right) separately. When mult $= 1.0$, crown efficiency in the mixed stand equals that in pure stand. In contrast, mult > 1.0 or mult < 1.0 indicates that mixing stimulates or reduces crown efficiency respectively. $Mult_{sp}$ ranges from 1.0 to 3.0 in Norway spruce (left), and indicates that positive mixing effects prevail. This applies to all stand development phases from mean height 15–40 m, i.e. the positive effect

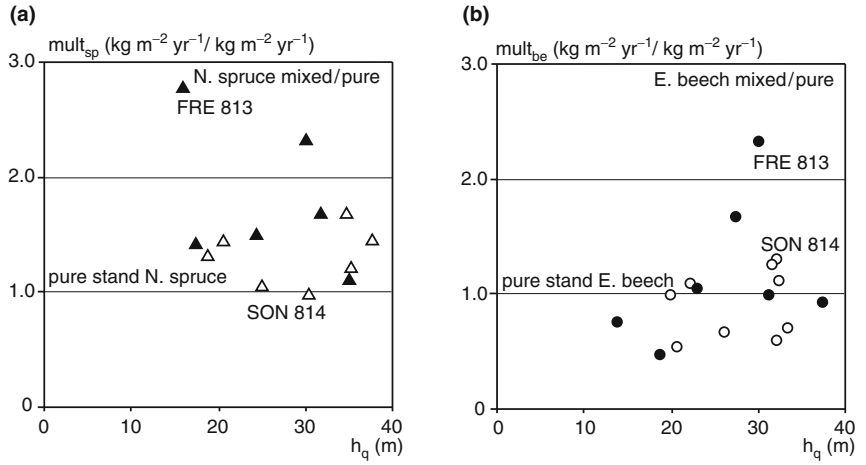

Fig. 9.14 Multipliers (**a**) mult_{sp} for Norway spruce and (**b**) mult_{be} for European beech respectively (cf. (9.13)) over stand mean height of the corresponding plots: symbols above the 1.0-line indicate a positive effect of thinning on crown efficiency; symbols below the 1.0-line reflect a reduction in crown efficiency in the mixed stand compared to the corresponding pure stand. The *filled and unfilled symbols* represent plots in FRE 813 and SON 814 respectively

is continuous and independent of stand development stage. For European beech, $\text{mult}_{be} = 0.5$–1.5 (right). The slightly positive and negative mixing effects are balanced out, and positive effects seem to dominate as stand development progresses.

An integrated evaluation produces $\text{mult}_{sp} = 1.53 \pm 0.14$ (mean and standard error) for Norway spruce, and $\text{mult}_{be} = 0.95 \pm 0.09$ for European beech. A t-test for significant deviation from mult = 1.0 (pure stand conditions) reveals significant positive mixing effects for Norway spruce ($p < 0.001$, $n = 13$). The same test reveals no significant mixing effects for European beech ($p < 0.05$, $n = 15$). Results at the stand level indicate that Norway spruce also benefits from mixtures at the individual-tree level, where, unlike the stand level, European beech crown efficiency responds neutrally rather than positively to mixing.

The mixing effect on crown efficiency quantified by mult (Fig. 9.14) should not be confused with the mixing effect on mean crown efficiency EEX (Table 9.4); whereas the former expresses the effect of mixing on crown productivity under ceteris paribus conditions, the latter expresses the average crown productivity in the real stand and also depends on the frequency distribution of crown sizes and competitive status.

9.4.2.1 Evidence of Mixing Effects at the Stand Level with Explanation at the Individual-Tree Level

Here, explanation means tracing a phenomenon observed at one level to the next higher level. In our case, findings at the stand level can be substantiated by analysis at the tree level (Table 9.5).

Table 9.5 Summary of the effects of mixing Norway spruce and European beech. For key variables at the stand, mean tree and individual tree level, the performance of the mixture is given in relation to the corresponding pure stand. Values greater than 1.0 reflect superiority of the mixed stand, values close to 1.0 reflect equality of mixed and pure stands, and values less than 1.0 indicate inferiority of the mixed stand: p_{sp}, p_{be} = productivity in Norway spruce, and European beech pure stands; $p_{sp,(be)}, p_{(sp),be}$ = productivity of Norway spruce, and of European beech in the mixed stand; $p_{sp,be}, \hat{p}_{sp,be}$ = observed, and expected productivity in the mixed stand; d stem diameter at 1.30 m; cl crown length; cpa crown projection area; w above-ground biomass; CI competition index; EEX crown efficiency; mult mixing effect on crown efficiency

	FRE 813	SON 814	Total
Stand			
$p_{sp} : p_{be}$	0.92	1.31	1.14
$p_{sp,(be)} : p_{(sp),be}$	1.19	0.91	1.04
$p_{sp,be} : \hat{p}_{sp,be}$	1.29	1.14	1.21
$p_{sp,(be)} : p_{sp}$	1.47	1.01	1.21
$p_{(sp),be} : p_{be}$	1.23	1.49	1.37
Mean tree scale			
$d_{sp,(be)} : d_{sp}$	1.13	1.29	1.21
$d_{(sp),be} : d_{be}$	1.09	1.10	1.09
$cl_{sp,(be)} : cl_{sp}$	0.91	0.99	0.95
$cl_{(sp),be} : cl_{be}$	1.16	0.95	1.04
$cpa_{sp,(be)} : cpa_{sp}$	1.03	1.08	1.06
$cpa_{(sp),be} : cpa_{be}$	1.22	1.34	1.29
$w_{sp,(be)} : w_{sp}$	1.36	1.93	1.64
$w_{(sp),be} : w_{be}$	1.26	1.27	1.27
Individual tree scale			
$CI_{sp,(be)} : CI_{sp}$	1.36	0.97	1.17
$CI_{(sp),be} : CI_{be}$	0.51	0.75	0.64
$EEX_{sp,(be)} : EEX_{sp}$	1.25	1.40	1.32
$EEX_{(sp),be} : EEX_{be}$	1.16	1.25	1.21
$mult_{sp}$	1.81	1.30	1.53
$mult_{be}$	0.99	0.92	0.95

Norway spruce's productivity at the stand level is much higher in mixture than in pure stands (cf. $p_{sp,(be)}$: p_{sp} in Table 9.5) even though its crown efficiency is strongly affected by the mixture (cf. $mult_{sp}$ in Table 9.5). An analysis of individual trees revealed that Norway spruce crown efficiency rises by 81 and 30% in FRE 813 and SON 814 respectively (cf. $mult_{sp}$, Table 9.5). Under ceteris paribus conditions (i.e., equal size, equal competition index CI), Norway spruce produces more biomass for a given radiation level in mixture. As suggested by Rothe (1997), Wiedemann (1942, 1943b), and Mettin (1985), European beech may foster crown efficiency in Norway spruce. Unlike the shallow-rooted Norway spruce seeking resources just below the surface, the European beech root system extends further down to soil layers richer in nutrients (Bolte and Villanueva 2006; Schmid 2002; Schmid and Kazda 2002). Some of the scarce nutrients (nitrogen, phosphate, calcium, potassium) are transferred to the stand parts stocked with Norway spruce by means of leaf shedding in autumn.

The higher positive effect on Norway spruce growth found on the site in FRE 813 (suboptimal for Norway spruce) than on SON 814 (optimal for Norway spruce) appears plausible. The more photo-production is limited by a shortage of nutrients on a given site, the more distinct the increase in efficiency with an improved supply of those nutrients (Körner 2002, p. 928; Schulze et al. 2002; p. 359). Moreover, the nutrient supply may improve in the mixed stand as, compared to the pure stands, the soil temperature and mineralisation are superior (Rothe 1997; Wiedemann 1942). Radiation reaches deep into the stand and stimulates decomposition processes, especially in fall and spring, when European beech leaves are absent. On the one hand, the crowns assimilate more carbon due to the increased crown efficiency. On the other hand, the photo-production compensation point probably shifts to the left as mineral nutrients either are incorporated in enzymes and pigments, or activate directly the process of photosynthesis (Larcher 2003; pp. 134–136). Thus, a lower radiation level already can yield a positive net production. As result, Norway spruce grows quicker here, with a total mean diameter and mean tree biomass 21 and 64% greater than Norway spruce of the same age in the neighbouring pure stand (cf. $d_{sp,(be)} : d_{sp}$ and $w_{sp,(be)} : w_{sp}$, in Table 9.5). Crown length cl and crown projection area cpa hardly differ between pure and mixed stands. Thus, the increased Norway spruce productivity at the stand level accompanies the accelerated size growth at the tree level.

European beech behaves different. Its productivity at the stand level is also higher in mixture than in pure stands (cf. $p_{(sp),be}$: p_{be} in Table 9.5). Yet European beech crown efficiency largely is unaffected by the mixture (cf. $mult_{be}$ in Table 9.5). It even decreases slightly to 0.99, 0.92, and 0.95 in FRE 813, SON 814, and in total respectively. A thorough analysis of crown length, crown projection area and competition index reveals that European beech occupies the available space in an omnipresent way (Table 9.5). Crowns are not more efficient, but they are larger, more scattered and in better positions than in the pure European beech stand. Under interspecific competition, they are able to penetrate and occupy crown space with a relative low biomass investment (Pretzsch 1992b; Pretzsch and Schütze 2005, 2008), and, with their sit-and-wait strategy, they are able to fill niches, which are heavily contested under intraspecific competition in the pure European beech stand (Pretzsch 2005a). In summary, the overyielding of European beech is an effect of multi-layering, adaptation, gap dynamics and high efficiency of space occupation.

9.5 Productivity in Mixed Forest Stands

9.5.1 The Mixed Stands Issue: A Central European Review and Perspective

Hartig (1791, p. 134), regarded by many as the forefather of forest science, commented on the mixed stands issue as follows: "... the mixing of deciduous and coniferous species is not advantageous as coniferous trees generally tend to supplant

deciduous ones, and because one type of tree impedes the growth of the other: thus no mixed deciduous and coniferous forests should be established with intent" (this, and all subsequent quotations are translated by the author). Concerned about serious production losses in mixed stands, Hartig (1804, p. 40) recommended: "All mixed stands with coniferous and deciduous species should be converted into pure stands of the constituent species, as soon as circumstances permit". Von Cotta (1828, p. 115) contradicted this: "Endeavours to establish pure stands everywhere is based on an old and highly detrimental prejudice [...]. Since not all tree species utilise resources in the same manner, growth is livelier in mixed stands, and neither insects nor storms can damage them as much as in pure stands. In addition, a wider range of timber will be available everywhere to satisfy different demands [...]". This opinion was supported by Gayer (1886, p. 31): "The mixed forest does not only produce more, but also more valuable commercial timber than that grown in pure stands". Statements by Möller (1922, pp. 41–42) are even more optimistic: "[...] if we design stands of shade-intolerant and shade-tolerant tree species, [...] the potential for timber production is raised even more, the reason being that it is now possible to go much further in the stratification of age classes than in the design of pure stands with only a single layer". Wiedemann, a professional yield scientist, dampens the optimism voiced by the above silviculturalists (1951, p. 341) saying "[...] even in silviculture, room must be given to hard facts not just emotions". It was not until data were evaluated from long-term experiments, under observation in many European countries since the founding of the Forest Experimental Stations between 1870 and 1880 (cf. Chap. 3) that a clearer picture was conveyed of the growth and yield in pure and mixed stands for different species and sites.

Early evaluations of long-term experimental plots reveal far greater productivity in Norway spruce and Douglas fir monocultures than in any mixture on many sites in temperate and boreal zones (Assmann 1970; Schober 1975; Schwappach 1912; Wiedemann 1949). Whenever the primary objective was to maximise aboveground biomass productivity, then, on many sites, there seemed to be no alternative to pure stands of these species. Similar advantages of monospecific stands were noted for *Pinus* species in the Mediterranean, and for *Eucalyptus* and *Albizia* species in subtropical and tropical climatic zones (Kelty 1992; Weck 1955).

9.5.2 Benchmarks for Productivity of Mixed Stands Compared to Pure Stands

As the start of regular forest management and systematic forestry sciences, the primary objective was sustainable timber production (Carlowitz 1713; Hartig 1791, 1804; Cotta 1828). There was widespread belief that, in the wake of sustainable timber production, other forest functions, such as protective and recreational functions, would also be fulfilled automatically. That proved to be incorrect: on the contrary, all forest functions need to be regarded explicitly. Today, there is international consensus that the multiple functions of forests include the protection of

forest resources, health and vitality of forest ecosystems, the production of wood and other forest products, biological diversity, and protective and socioeconomic functions (MCPFE 2000). In particular, the sustainability of biodiversity is becoming an imperative, similar to the sustainability of timber production in the past, reshaping the old question about the relationship between biodiversity and productivity.

Systematic yield gains by up to 30% and 50% for natural grasslands and forest ecosystems, respectively, in the transition from monocultures to two-species mixtures (Caspersen and Pacala 2001; Hector et al. 1999; Loreau et al. 2001; Pfisterer and Schmid 2002) can be expected in managed pure and mixed stands only to a very limited extent. Presumably, in European boreal and temperate forests, niche differentiation is comparatively low given the species reduction in the course of the ice ages, and also the much slower evolutionary and co-evolutionary processes of long-lived trees. This may explain why the advantages of resource use efficiency and productivity of mixed stands over pure stands is much lower in long-lived woody ecosystems than in short-lived herbaceous stands.

9.5.2.1 Range of Productivity Increase and Decrease by Mixing

Mixed stand growth and yield research was always driven by the notion that mixing two or more species may result in a surplus of biomass productivity compared with the corresponding pure stands (Dietrich 1927, 1928; Gayer 1886; Hartig 1791; Möller 1922). While monocultures are mostly man-made, frequently mixed stands occurred in the natural state in the absence of forest management. Perhaps, by separating species into monocultures, special characteristics, potential mutualism, and their general capacity to exploit resources successfully, and, hence, also their environmental potential remain unused.

However, even for mixtures of Norway spruce and European beech, the mixture most investigated in central Europe, this question has not been answered satisfactorily as yet. Early investigations by Schwappach (1909), Wimmenauer (1914), Dietrich (1927, 1928), Hofmann (1923), Flury (1926, 1931), and Zimmerle (1949) provided basic growth and yield data, highlighting the alteration of growth curves at the tree and stand level by mixing, and showed a stabilising effect on productivity and stand structure in the event of disturbances. However, their comparisons with pure stands were questionable, as they were based on yield tables and not neighbouring pure stands with equivalent site conditions. More sophisticated comparisons were based on one or more mixed stands, differing in proportion or spatial pattern of species mixing, with the two adjacent pure stands of Norway spruce and European beech. Such studies compare volume production in pure and neighbouring mixed stands (Wiedemann 1942; Spellmann 1996), basal area growth (Rothe 1997), or dry mass production of stem-wood exclusively (Burger 1941; Kennel 1965). By covering site conditions from warm, dry and base-rich to cool, wet and acid sites, these investigations showed that the relationship between the aboveground biomass productivity of both species strongly depends on the particular site conditions. The relationship of aboveground biomass production between pure Norway spruce and

pure European beech stands can be 1:1, i.e. balanced, on temperate, humid and calcareous sites. However, it moves towards 2:1 on cool, wet and acid sites, as they are more favourable for Norway spruce (Assmann 1961, pp. 351–355).

The evaluation of the few available long-term experiments showed that, when European beech is added to typical Norway spruce sites, the mixture causes a 20% reduction in productivity compared to pure stands under the same conditions. Yet when Norway spruce is added to typical European beech sites it can result in +10% in productivity compared to pure stands under the same conditions (Pretzsch 2005a). Kennel (1965) studied mixtures of Norway spruce and European beech in the Bavarian alpine foothills, the Bavarian Forest and the Harz mountains in Lower Saxony, as did Burger (1941) in Switzerland. These studies revealed a 6% increase in volume productivity in most of the mixed stands. However, biomass productivity showed no significant increase in all cases. Only in temperate, humid climate in the prealpine areas of Southern Bavaria on nutrient-rich soils, where both European Beech and Norway spruce are highly productive and about equally competitive, do mixed stands of these species produce 1.14–1.29 times more biomass than the corresponding pure stands with the same area (Pretzsch and Schütze 2008). In most available studies, however, the productivity of the Norway spruce and European beech mixed stand occupies a position between the pure stands of each species.

In a study of Norway spruce and Silver fir by Jensen (1983), pure stands also form the boundaries of productivity of the mixed species stands. Along a West–East transect through Jutland, in Denmark, he models the effects of site condition on the growth relationship between Norway spruce and Silver fir: in the coastal dune belt, Silver fir is superior to Norway spruce; the adjacent Riss-glacial landscape produces equivalent growth of Silver fir and Norway spruce; on the old inland moraines of the Würm glacial period, however, dry biomass productivity of Silver fir is inferior to Norway spruce. The decisive factor for the inland superiority of Norway spruce is its adaptability to low water supplies on acidic sites. In contrast, Silver fir profits from better water availability and the more favourable nutrient supply in the coastal region. Even here, the effects of species interaction in mixture amount to productivity increases of about only 5% of the corresponding pure stands (Jensen 1983, pp. 200–210). The overyielding caused by Norway spruce is not sufficiently strong to cause transgressive overyielding.

Yield limitations in species mixtures comprising shade-tolerant trees, such as Norway spruce–European beech and Norway spruce–Silver fir, are not transferable to mixtures consisting of shade-intolerant and shade-tolerant trees. Frivold and Kolström (1999) studied Silver birch, Scots pine and Norway spruce growth in Finland, Sweden and Norway. They emphasised that the potential superiority or inferiority of these species in mixtures is related to site conditions. Depending on site conditions, the effects of species interaction may be unfavourable, neutral or beneficial, and, in the latter case, even lead to overyielding of mixed stands over the more productive pure stands. In Southern and Central Finland, the productivity of Scots pine–Silver birch mixtures surpass pure Scots pine and pure Silver birch stands by 10 and 14%, respectively (Mielikäinen 1980). For Norway spruce–Silver birch mixtures, a 10–15% increase in productivity may

occur compared to the corresponding pure stands of these species depending on the site (Mielikäinen 1985). In the oceanic regions of Norway and Sweden, Silver birch loses some growth capacity compared to coniferous species. There, the yields of Scots pine–Silver birch mixtures are not greater than the pure stands, whereas Norway spruce–Silver birch mixtures show a beneficial effect from mixtures only during the juvenile growth period (Frivold and Frank 2002).

Zöhrer (1969) provides evidence that the biomass productivity of European larch–Norway spruce mixtures in the Salzburger Land is superior to that of pure stands on identical sites (Fig. 9.9). The European larch–Norway spruce mixture, therefore, surpasses the pure Norway spruce stand by 22–28%, and the pure European larch stand by 2–13%. For mixed stands, comprising shade-intolerant and shade-tolerant species such as Sessile oak–European beech, Scots pine–Norway spruce and Scots pine–European beech, Bonnemann (1939) and Wiedemann (1943b, 1951) found similar beneficial effects from species interactions after 50 years of observation. In long-term Scots pine–European beech experimental plots in the Dübener Heide, Dittmar et al. (1986) noted beneficial interaction effects of 7–25% compared to the pure stands depending on the age and structure of the mixture. Burger (1941) and Wimmenauer (1941) note the same strong superiority in European larch–European beech mixtures.

DeBell et al. (1989) claim a 50% higher superiority in mixtures of *Eucalyptus saligna* and the leguminous and nitrogen fixing tree species *Albizia falcataria* in Hawaii. Other examples showing similar benefits of mixing are summarised by Kelty (1992) or Piotto (2007). Compared to these yield relationships in the subtropics, the maximum mixture effects of -20 to $+$ 30% for commercial tree species in temperate and boreal zones appear rather moderate.

Mixture effects may vary considerably depending on species mixture, site, silvicultural treatment and risks. In comparison with pure stands, resource utilisation, and thus growth can be improved by almost 30% by combining early and late successional species, ontogenetically early and late culminating species, and shade-intolerant and shade-tolerant tree species. However, where ecological niches and functional characteristics are similar, species may compete for the same resources in crown and root systems. Here, the consequence of species interactions may be negative with a reduction in productivity by 20%.

9.5.3 Spatial and Temporal Niche Differentiation as a Recipe for Coexistence and Cause of Surplus Productivity

There is especial potential for increased productivity on a site in mixtures of similarly productive species that complement each other in the spatial–temporal utilisation of space due to the resulting reduction in competition (Kelty 1992). This can be achieved by joint growing space occupation through shade-intolerant species (e.g. European larch, Scots pine), semi-shade-tolerant species (e.g. Norway spruce, Douglas fir) and shade-tolerant trees (e.g. European beech, Silver fir). This kind of

stratification, using species of different shade tolerance, will allow light transmitted through the upper canopy to be used by the layers underneath (Fig. 9.2a).

Gains in productivity are also achieved in tree mixtures where the temporal development in the growing season, and in the ageing process complement one another. Let us assume the growth of species 1 in a two-species mixture culminates early and then declines rapidly. The decrease in total growth can then be compensated for by the addition of species 2, the development of which is anti-cyclic to that of the other. Assmann (1970) shows that species-specific periodicity is reflected in different time scales. Species, which culminate early in the season, also exhibit the same characteristic in their lifespan. Mixtures of species that have anti-cyclic seasonal growth characteristics also often complement one another in the ageing process (Fig. 9.2b).

Complementary temporal and spatial use of resources, e.g. in Norway spruce–European beech mixtures, may also occur in combined form. In spring, before European beech leafing, more intensive light can penetrate the stand and curtail the winter dormancy of Norway spruce. This prolongs its growing season, which is generally longer than that of European beech (Schober 1950/51). With this kind of "job-sharing", for example, Norway spruce and European beech in mixtures may draw advantages in resource utilisation (Mitscherlich 1952). The closer, and more intensive the mixing of Norway spruce and European beech is, the stronger the beneficial interaction effects (Ellenberg et al. 1986).

Many of the European forest stands are "artefacts", designed with very productive species such as Norway spruce and Douglas fir cultivated outside their natural habitats. Often, genetic variation in these species no longer reflects natural selection but human choice based on commercial criteria. Therefore these forests are not designed for optimum niche utilisation by species in the mixture. Niche overlapping and risks may occur, revealed by unfavourable effects from species interactions in the mixture.

9.5.4 Crown Shyness

Crown shyness provides a good example of the fact that the effective increase in fitness at the individual level is linked in no way to an increase in productivity at the stand level or the population level. High trees sway in a wider radius and can keep their neighbours at a distance in the upper crown without considerable loss in the highly productive leaf mass. Such responses to disturbance by wind are useful for superior trees, but temporarily create empty, unused spaces in the crown canopy and losses in stand productivity.

Especially in one-layer pure stands, tree sway caused by wind can lead to crown shyness gaps (Fish et al. 2006; Putz et al. 1984; Rudnicki et al. 2003). These gaps create empty spaces between tree crowns, which also occur in fully stocked stands but which do not result from tree fall. Mechanical abrasion of buds, leaves, and branches caused by trees knocking into one another can create a halo of empty space around tree crowns. Thus, canopy cover, even on completely unmanaged pure stands

on very fertile sites, might only amount to 90–95% of the stand area. Apart from the fact that mechanical abrasion results in a higher turnover, that is a net growth loss, gaps are created as well. The abrasion of crown edges by wind-induced tree sway can lead to a decline in crown closure, leaf area and stand productivity, particularly in one-layer stands (Meng et al. 2006).

Species and structural diversity can restrict such gaps in the crown canopy by reducing the stem slenderness, restricting collision among trees of the same height, and therefore the loss in biomass. Furthermore, structural diversification (two layers or more; combination of somewhat more vertical and lateral crowns) can also restrict crown shyness, or by better closure of gaps caused by crown shyness.

9.5.5 Growth Resilience with Structural and Species Diversity

The combination of several species is synonymous with the distribution of risk. As a rule, mixed stands are more elastic in their response to changing site conditions, and show greater resilience in the face of natural losses or calamities.

Let us assume a pure Norway spruce stand on a site in the Bavarian alpine foothills with acidic soil and a good water supply, where Norway spruce growth far surpasses that of European beech, but to which European beech is added to raise stand biodiversity and aesthetic value. The replacement of Norway spruce by the slower-growing European beech, in the absence of development disturbance, causes considerable yield loss under steady state conditions (Chaps. 13 and 14). However, the relationship changes when site conditions are unstable. This has been shown in simulation studies on the effect of climate change on the growth of pure and mixed Norway spruce and European beech stands in Germany (Pretzsch and Ďurský 2002). Let us assume that temperatures within the growing season rise by 2°C for the above site, precipitation in the growing season drops by 10%, and the growing season is prolonged by 10 days. This would cause a decrease in Norway spruce productivity by over 10% on that particular site. The substitution of 30% of the Norway spruce trees by European beech, which is better adapted to the assumed change in climatic conditions, could overcompensate for the climate-related growth losses in Norway spruce. In view of the increasing disturbances to which our forest ecosystems are being subjected through air pollution and climate change, opportunities to benefit from the distribution of risk through species mixtures most likely will rise in the future (Lindner and Cramer 2002).

While Norway spruce is overwhelmingly superior to European beech on many sites under normal conditions, storm damage in Norway spruce stands is four times as high as in European beech stands (von Lüpke and Spellmann 1999). To a large extent, mixtures can overcome this kind of perturbation, equivalent to an abrupt reduction in stand density from a medium to lower level, without further growth reductions (Fig. 9.7). The decisive factor here, in essence, is the probability of disturbance and damage occurrence. The striking superior productivity of artificial pure

stands often is short-lived, and, in the event of potential major disturbances, may become inferior (Knoke et al. 2005).

The analysis of productivity at the stand, mean tree and individual tree level reveals possible increases or decreases in growth. Net growth is a nonspecific indicator, which indicates the existence of a mixture effect, yet does not reveal details of the causes. Intraspecific and interspecific interactions, which partially inhibit, and partially promote growth, may be the cause of a positive or negative species mixture effect. A possible increase in growth through species mixture is extremely relevant for forest management. We have seen that superior productivity is a desirable, though not necessarily sufficient prerequisite for superior fitness of a tree or for the success of a species in a mixed stand. Productivity contributes to the understanding of intraspecific and interspecific interactions. Superior or inferior growth is not synonymous with higher or lower fitness, closeness to nature or stability, just as maximum fitness of a species is not expressed by the maximisation of its production at the stand level.

Summary

In this chapter we analyse how tree species diversity and forest productivity are interrelated, a question of particular relevance to forestry practice. The methods presented concentrate on mixed stands consisting of two species. The analysis of the production of a mixed stand is usually carried out in relation to the production of corresponding pure stands at the same site. The benefits of species interactions that enhance mixed-stand growth are of particular interest in this context. A series of mixed and adjacent pure stands of Norway spruce and European beech is analysed to demonstrate the options for detecting species interactions.

(1) Whether productivity of a mixed stand is better or worse than an adjacent pure stand on a similar site is dependent on the balance of factors that enhances and inhibits productivity. On the one hand, niche differentiation may provide more overall and species-specifically available resources that can be invested into growth (productivity increase). On the other hand, mixtures can also trigger adaptation strategies for the maximisation of fitness that invest resources in displacing and inhibiting the growth of the competitor at the cost of productivity.
(2) The potential productivity of a species increases the more it approximates the centre of its "fundamental niche." The performance potential of a species in a mixed stand will improve as the resource supply and environmental conditions in its fundamental niche approach the optimum conditions for that species. Consequently, the admixture of a poorly adapted species may burden the superior one, resulting in a decrease in total stand productivity (under steady state conditions). However, species differentiation in the "realised niche" (e.g., shade-tolerance and shade-intolerance) also can lead to a better exploitation of resources and increase total stand productivity.

(3) When environmental conditions oscillate or change gradually, species mixtures can contribute to risk distribution and stabilise total stand productivity in the long-term. The striking superior productivity of artificial pure stands often is short-lived, and, in the event of potential major disturbances may become inferior. The probability of the occurrence of disturbances and damage is a decisive factor in the relative long-term performance of pure and mixed stands.

(4) The expected productivity, $\widehat{p}_{1,2} = p_1 \times m_1 + p_2 \times m_2$, where p_1 and p_2 denote the productivity of neighbouring pure stands of species 1 and 2, and m_1 and m_2 the mixture proportions of the species in the mixed stand, plays a key role in detecting mixture effects at the stand level. The productivity $\widehat{p}_{1,2}$ quantifies the expected productivity of a mixed stand when the joint productivity of species 1 and 2 is the same as in neighbouring pure stands with the same area.

(5) If the observed productivity in the mixed stand $p_{1,2}$ is higher than the expected, i.e., $p_{1,2} > p_1 \times m_1 + p_2 \times m_2$, we have overyielding, and when $p_{1,2} > p_1$ and $p_{1,2} > p_2$ we have transgressive overyielding of the mixed stand compared to the pure stands. Analogously, we refer to underyielding and transgressive underyielding when the mixed stand is inferior.

(6) Productivity comparisons should be based on net or gross biomass growth to reflect the species performance as accurately as possible. The applied mixture proportions m_1, m_2 should reflect the species growing space, growing space sequestration and access to resources. Therefore mixture proportions based on standing biomass W or stand basal area adjusted by the transformed wood density, $\sqrt[3]{R^2}$ (e.g., m(W), m($BA_{R^{2/3}}$)) seem appropriate, whereas the application of stem number, basal area, or standing volume may give flawed mixture proportions.

(7) The ratios $p_{1,(2)} : p_1$ and $p_{(1),2} : p_2$ indicate the species causing over- or underyielding. They relate each species' productivity in mixed stands to its productivity in the neighbouring monoculture. Other variables, e.g., diameter d, crown length cl, and crown projection area cpa may be applied analogously.

(8) A comparison of mean tree size, e.g., tree diameter d ($d_{1,(2)} : d_1$ and $d_{(1),2} : d_2$), shows whether trees in the mixed stand are larger or smaller than those of the same species in the neighbouring pure stands. The greater the difference, the more questionable a comparison of their mean annual growth in a given limited period is because the stands simply may be in different development stages (age and size effect).

(9) Analyses at the individual tree level help separate age and size effects from mixing effects. When crown efficiency of individual trees in pure stands exceeds crown efficiency in mixed stands, even after size and competition effects are eliminated, this indicates the presence of mixing effects, which can then be quantified.

(10) As long as a comparison is merely based on one, more or less narrow phase of stand development, it remains hard to judge whether an observed (positive or negative) mixing effect is overall or merely a temporary phenomenon caused by diverging growth rhythms of the pure and mixed stands. However, with the

analysis of crown efficiency any effects can be traced down to the individual tree level, and the cause and amount of mixing effect determined.

(11) Compared to pure stands, growth in mixed stands can be increased by almost 30% by combining early and late successional species, ontogenetically early and late culminating species, or shade-intolerant and shade-tolerant tree species.

(12) In such European forests, where species niches are similar, negative effects from species interactions may lead to a reduction in productivity by 20%. In contrast to these moderate findings in temperate and boreal forests, superiority of mixed stand in comparison to pure stands can amount to 50% in tropical and subtropical forests.

(13) An analysis of the productivity at the stand, mean tree and individual tree level indicates an increase or decrease in growth. As such, it provides an important starting point for revealing and understanding intraspecific and interspecific interactions in pure and mixed stands. Over- or underyielding is not synonymous with higher or lower fitness, closeness to nature or stability, just as the maximum fitness of a species is not expressed by the maximisation of its production at the stand level.

Chapter 10
Growth Relationships and their Biometric Formulation

In forest ecosystems, biological variability makes it difficult to reveal strict functional laws as in physics or mathematics. We must be content with stochastic relationships, which we call biological relationships or rules. The growth relationships at the individual-tree and stand level, the biological variability of these relationships are of particular interest in forest growth and yield science. This chapter introduces a number of established growth relationships, and shows how to separate deterministic components from stochastic components of growth, which is important when simulating the growth behaviour of biological systems in models.

10.1 Dependence of Growth on Environmental Conditions and Resource Availability

Environmental conditions (e.g. temperature, humidity, acidity, storms and other risks) affect plant growth, and plants, in turn, affect environmental conditions. While environmental conditions cannot be consumed by plants, resources (e.g. radiation, water, nutrient minerals, CO_2, O_2) are consumed by the plant. The relationships introduced below relate growth directly to primary environmental and resource variables. However, the substitution of the variables the area available for tree growth (m^2 per tree), the growing space (m^3 per tree), and geometrically derived competition indices for resource supply is common in growth and yield science. They are used analogously to the primary variables, but are easier to measure. In the following discussion, we refer to these primary or surrogate environmental and resource variables as growth factors.

10.1.1 Unimodal Dose–Effect-Curve

The growth response of an organism follows a unimodal dose–effect-curve when the dose of a particular growth factor is increased under *ceteris paribus* conditions

H. Pretzsch, *Forest Dynamics, Growth and Yield: From Measurement to Model*,
DOI: 10.1007/978-3-540-88307-4_10,

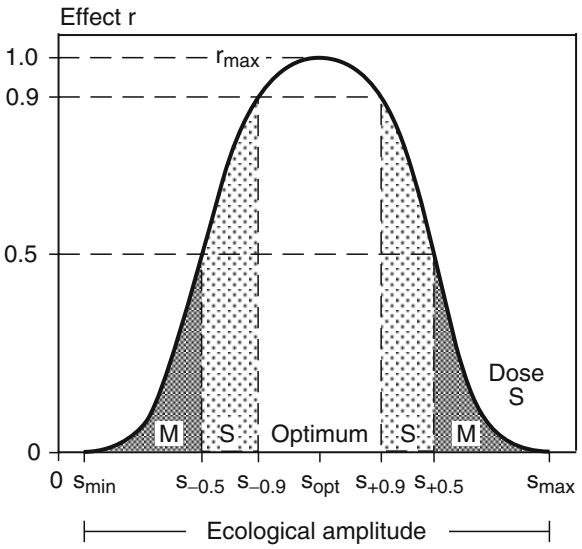

Fig. 10.1 Dose–effect-function with ecological amplitude ($s_{min} - s_{max}$), minimum (s_{min}), maximum (s_{max}), optimum (s_{opt}) as well as ranges of minimum, maximum, suboptimum and optimum supply (M, S and O)

(Fig. 10.1). In this curve, growth commences above a certain threshold value (minimum), increases up to an optimum, and at some point decreases until it becomes zero again at a certain maximum value. The minimum and maximum values (s_{min}, s_{max}) are called the cardinal points of the dose–effect-function, and enclose the tolerance space (ecological amplitude) of an organism in response to the growth factor s. The ecological optimum (O) includes not only the point s_{opt}, but also the entire range from $s_{-0.9}$ to $s_{+0.9}$, where growth response is $r \geq r_{max} \times 0.9$. The intervals $s_{-0.5}$ to $s_{-0.9}$ and $s_{+0.9}$ to $s_{+0.5}$ restrict the sub-optimal range (S), whereas r-values of $r < r_{max} \times 0.5$ limit the range of minimum or maximum values (M) (Fig. 10.1).

The position and range of the ecological amplitude, the position of the optimum within this amplitude, and curve division into progressive and regressive branches depend, e.g. on the growth factor and species. The combined ecological amplitude of several growth factors and their combined effect on growth determines the ecological niche of an observed organism. The path of the dose–effect-curve in the progressive or regressive branches can be assumed as linear for simplicity (Kahn 1994), as monotone ascending or monotone descending with and inflection point (Mitscherlich 1948; Müller 1991), or without (Thomasius 1990).

The dose–effect-functions in Fig. 10.2 show how height growth of various tree species responds to different levels of precipitation during the growing season. The curves show the different ecological amplitudes observed for different tree species. For example, Sessile oak (dashed and dotted line) achieves higher height growth at lower precipitation levels than Silver fir (broken line). For optimal height

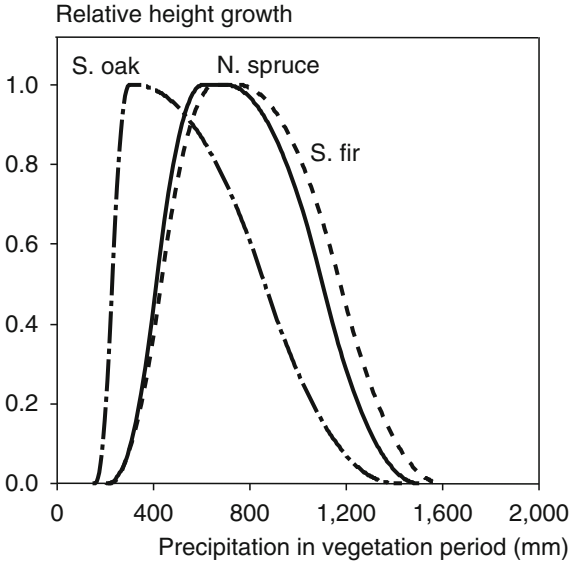

Fig. 10.2 Response of relative height increment of Norway spruce, Silver fir and Sessile oak to different precipitation conditions during the growing season (after Kahn 1994)

growth of Silver fir, precipitation levels need to be about 300 mm higher. The Norway spruce response curve (continuous line) lies between these two tree species.

10.1.2 Dose–Effect-Rule by Mitscherlich (1948)

The dose–effect-rule by Mitscherlich (1948) describes the left, progressive branch of the dose–effect-curve. This rule describes an increase in growth dw_p, triggered by a change in resource supply ds, in relation to the difference between maximum growth w_{max} (under optimal supply) and actual growth w_p:

$$\frac{dw_p}{ds} = c_p \times \left(w_{max} - w_p\right). \tag{10.1}$$

According to this equation, the expected change in growth resulting from a change in a growth factor s is proportional to the difference between maximum and actual growth $w_{max} - w_p$. The proportionality factor c_p stipulates the strength of the effect of a given growth factor. As the benefit from an additional increase in the growth factor s decreases when the optimal supply is reached, this rule is also called the rule of declining marginal benefit. For example, it is used often for the description of the relationship between consumption and benefit in the field of economics (Samuelson and Nordhaus 1998).

The integration of the differential equation (10.1) produces the Mitscherlich function

$$w_p = w_{max} \times \left(1 - e^{-c_p \times s}\right), \tag{10.2}$$

which describes the asymptotic approach of an increase in growth factor w_p maximum growth w_{max}. The factor c_p specifies the slope of the function. The logarithmic function

$$\ln\left(w_{max} - w_p\right) = -c_p \times s + \ln w_{max} \tag{10.3}$$

shows the relationship between the growth factors and the logarithm of the difference $w_{max} - w_p$. This means that the difference between maximum growth and actual growth does not decrease linearly, but exponentially with a gradual increase in growth factors (Fig. 10.3). To shift the Mitscherlich curve to the threshold s_{min}, as illustrated in Fig. 10.4, we extend the Mitscherlich's function as follows:

$$w_p = \begin{cases} w_{max} \times \left(1 - e^{c_p \times (s - s_{min})}\right), & \text{if} \quad s \geq s_{min} \\ 0 \qquad\qquad\qquad\qquad\quad , & \text{if} \quad s < s_{min} \end{cases}. \tag{10.4}$$

Mitscherlich (1948) extended this function to represent the right, declining branch of the dose–effect-curve, which reflects an overdose. By multiplying the positive

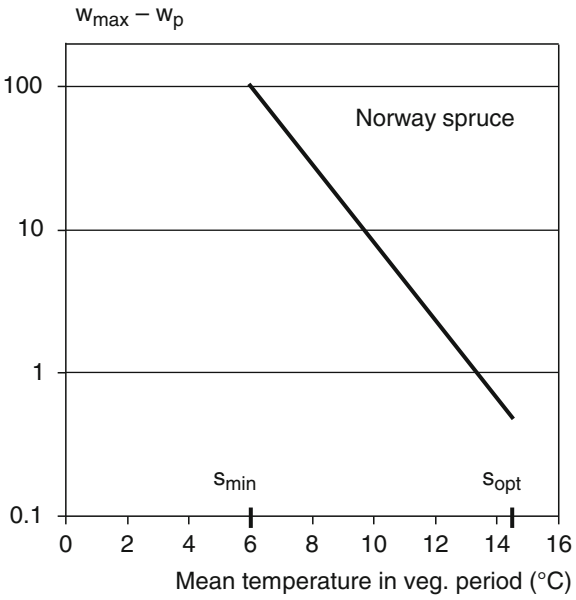

Fig. 10.3 For Norway spruce, the difference between maximal height increase and the observed increase decreases exponentially with increasing dose of s_{min} to s_{opt}; this corresponds to a linear decrease in half-logarithmic coordinate system

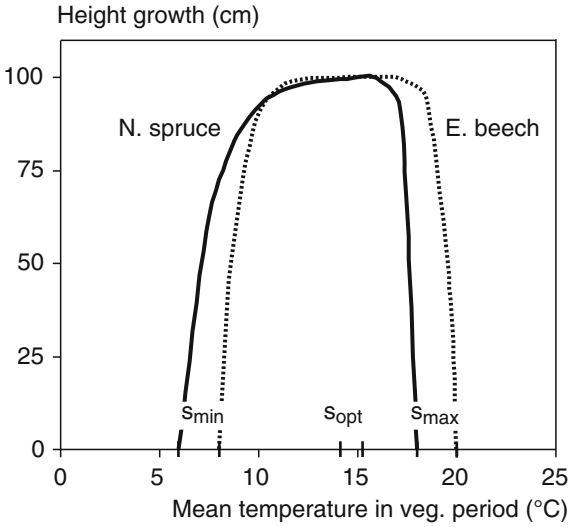

Fig. 10.4 Response of annual height increment of Norway spruce and European beech to different mean temperatures during the growing season. Progressive and regressive branches can be reproduced by the equation $w = w_{max} \times \left(1 - e^{-c_p \times (s - s_{min})} - e^{-c_d \times (s_{max} - s)}\right)$. For Norway spruce: $c_p = 0.63$, $c_d = 3.03$, $s_{min} = 6°C$, $s_{opt} = 14.5°C$, $s_{max} = 18°C$; for European beech: $c_p = 1.14$, $c_d = 1.83$, $s_{min} = 8°C$, $s_{opt} = 15.2°C$, $s_{max} = 20°C$

branch of the function by a declining exponential function with the proportionality factor c_d, a unimodal dose–effect-curve can be generated:

$$w = w_{max} \times \left(1 - e^{-c_p \times s}\right) \times e^{-c_d \times s}. \tag{10.5}$$

In this function, $\left(1 - e^{-c_p \times s}\right)$ describes the rise of the curve in the progressive range, and $e^{-c_d \times s}$ the fall of the curve in the declining range. According to Thomasius (1990), a smoother, unimodal dose–effect-curve is obtained by modelling growth w as

$$w = w_p - w_d, \tag{10.6}$$

i.e. by obtaining the difference between the progressive component $w_p = w_{max} \times \left(1 - e^{-c_p \times (s - s_{min})}\right)$ and the declining component $w_d = w_{max} \times e^{-c_d \times (s_{max} - s)}$, rather than the product of these components as in Mitscherlich's equation (10.5).

The resulting dose–effect-function is

$$w = w_{max} \times \left(1 - e^{-c_p \times (s - s_{min})} - e^{-c_d \times (s_{max} - s)}\right), \tag{10.7}$$

where s expresses the growth factor, and s_{min} and s_{max} the upper, and the lower limits of the ecological amplitude respectively. The relationship between mean temperature during the growing season and annual height growth for Norway spruce and European beech (Fig. 10.4) are described by (10.7).

10.1.3 Combining the Effects of Several Growth Factors

To model the effects of several factors $(s_1, s_2, \ldots, s_n)$ on tree, or stand growth, the responses r_1 to r_n $(r_1 = (1 - e^{-c_{p1} \times s_1}) \cdots r_n = (1 - e^{-c_{pn} \times s_n}))$ can be multiplied $(w_p = w_{max} \times r_1 \times r_2 \cdots r_n)$. For the left, progressive branch of the dose–effect-curve, this results in

$$\begin{aligned} w_p &= w_{max} \times \left(1 - e^{-c_{p1} \times s_1}\right) \times \left(1 - e^{-c_{p2} \times s_2}\right) \cdots \left(1 - e^{-c_{pn} \times s_n}\right), \\ &= w_{max} \times \prod_{i=1}^{n} \left(1 - e^{-c_{pi} \times s_i}\right). \end{aligned} \tag{10.8}$$

In addition, as in the entire dose–effect-curve in (10.5) or (10.7), several growth factors can be combined by multiplication. This way, the combined effect of mean temperature (s_1) and precipitation (s_2) on Norway spruce height growth in (10.8) produces the two-dimensional, unimodal function $w = 100 \times \left(1 - e^{-0.63 \times (s_1 - s_{1\,min})} - e^{-3.03 \times (s_{1\,max} - s_1)}\right) \times \left(1 - e^{-0.00918 \times (s_2 - s_{2\,min})} - e^{-0.0325 \times (s_{2max} - s_2)}\right)$ with $s_{1\,min} = 6°C$, $s_{1\,max} = 18°C$, $s_{2\,min} = 220\,mm$, and $s_{2\,max} = 1{,}500\,mm$. Figure 10.5 shows the progressive branch. By multiplying the responses $r_1, r_2, \ldots, r_n$, the lowest response is always the restricting factor. Compensation, substitution, or enhancement among the growth factors remains unaccounted for.

A much more flexible combination of responses is possible if the operators are not linked purely by multiplication. For this, Zimmermann and Zysno (1980)

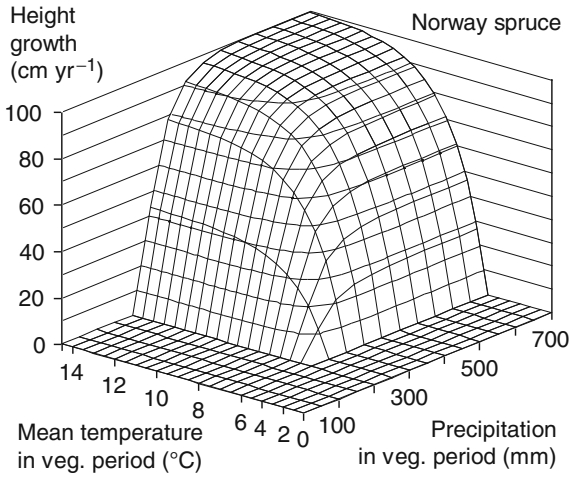

Fig. 10.5 Response of annual height increase of Norway spruce to different mean temperatures s_1 and precipitation levels s_2 during the growing season. The progressive branch of the dose–effect-function is reconstructed according to the equation $w = 100 \times \left(1 - e^{-0.63 \times (s_1 - s_{1\,min})} - e^{-3.03 \times (s_{1\,max} - s_1)}\right) \times \left(1 - e^{-0.00918 \times (s_2 - s_{2\,min})} - e^{-0.0325 \times (s_{2\,max} - s_2)}\right)$ with $s_{1\,min} = 6°C$, $s_{1\,max} = 18°C$, $s_{2\,min} = 220\,mm$, and $s_{2\,max} = 1{,}500\,mm$

developed the γ-aggregation, which combines a minimum-operator r_{mult}, equivalent with a multiplicative, non-compensatory "and" (cf. (10.9)):

$$r_{mult} = \prod_{i=1}^{n} r_i = r_1 \times r_2 \times \cdots \times r_n \tag{10.9}$$

and a maximum operator r_{1-mult}, which is equivalent with an entirely compensatory "or":

$$r_{1-mult} = 1 - \prod_{i=1}^{n} (1 - r_i) = 1 - (1 - r_1) \times (1 - r_2) \times \cdots \times (1 - r_n) \tag{10.10}$$

into the combined effect r_{comb}:

$$r_{comb} = \left(\prod_{i=1}^{n} r_i \right)^{1-\gamma} \times \left(1 - \prod_{i=1}^{n} (1 - r_i) \right)^{\gamma}. \tag{10.11}$$

The aggregation exponent γ assumes values between 0 and 1. The former enforces non-compensatory factor multiplication and the latter enforces compensation effects between the growth factors. In Chap. 13, the aggregation operator γ in (10.11) is fitted to growth and site variables in order to develop individual tree hybrid models (cf. Chaps. 1 and 11).

10.2 Allometry at the Individual Plant Level

The growth process of humans, animals and plants leads to characteristic changes in the proportions of their organs. This is because certain organs grow quicker than others. Examples of age-dependent changes in proportions include the decrease in the size of the human head relative to the total body size during their ontogeny, between pincer size and body size of crabs, or between height and crown size of trees (Fig. 10.6). For humans and mammals, for example, the infant-like characteristics of a big head, big eyes and mouth in relation to the total body trigger nurturing responses in adults. With increasing age, this disarming appearance vanishes. In many cases, the disproportional dynamic morphology with which, the shape of humans, animals or plants changes can be described by a so-called allometric relationship.

10.2.1 Allometry and Its Biometric Formulation

Allometry is concerned with the description and causality of deterministic size relations in and between organisms. As size and shape relations reflect the result of the phylo- and ontogenetic evolution towards a functional optimisation (Niklas 1994, p. 1), the study of allometry seeks to understand the adaptations of living organisms

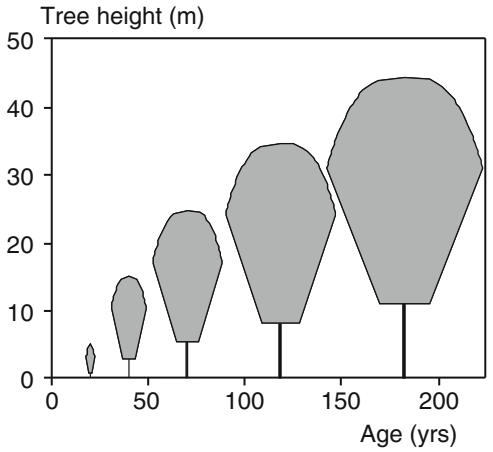

Fig. 10.6 Un-proportional shape development of a European beech under solitary conditions. In many cases, the changing relationships between tree dimensions such as height (h), crown diameter (cd) and crown length can be described by the allometric equation (e.g. $cd \propto h^{\alpha}$, here applies $\alpha_{cd,h} = 1.2$)

to their environment. The principle of the similarity of forms, postulated by Galileo Galilei, was transferred to allometric relationships between the length, surface, content and biomass of organisms or their organs by Spencer (1864) and Thompson (1917). In the early 1930s, Huxley (1932) and Teissier (1934) formulated a "relative growth equation", which, today is accepted widely as the allometric equation:

$$\frac{\frac{dy}{dt} \times \frac{1}{y}}{\frac{dx}{dt} \times \frac{1}{x}} = \alpha, \tag{10.12}$$

where y represents the dimension of the first, and x the dimension of the second organ, or of the entire body. Thus, (10.12) relates the relative growth rate of the first organ in the numerator, to the relative growth rate of the second organ, or entire body, in the denominator. α determines the ratio of relative growth rates of y and x, and is called the allometric exponent. The integrated and logarithmic representations of (10.12), which make it clear why α is referred to as an exponent (for clarity, we use α for allometry of individuals and β for allometry at the stand level in Sect. 10.4) are better known:

$$y = a \times x^{\alpha}, \tag{10.13}$$

$$\ln y = \ln a + \alpha \times \ln x. \tag{10.14}$$

Bertalanffy (1951, pp. 311–315) uses the allometric principle to model changes in the shapes of plants and animals. The allometric exponent α can be understood as the key to the distribution of the growth resources: when x increases by 1%, y increases by α%. Plotted in a double logarithmic coordinate system (Fig. 10.7), the allometric equation describes a straight line where the allometric exponent α

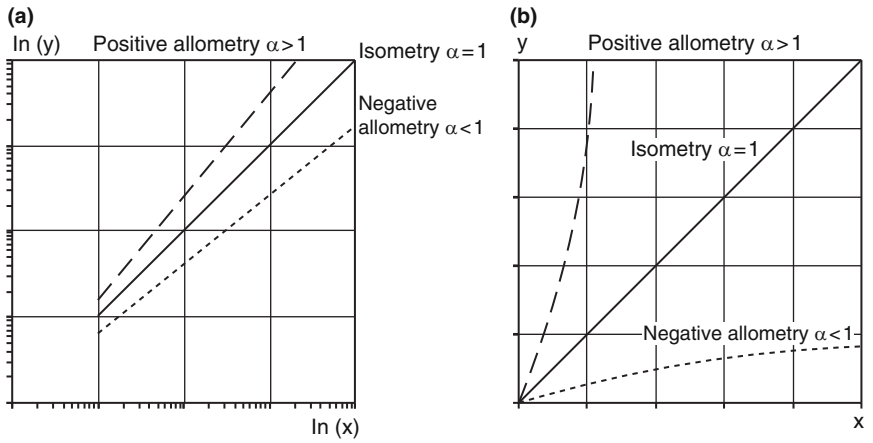

Fig. 10.7 Positive and negative allometry ($\alpha > 1$, $\alpha < 1$) and isometry ($\alpha = 1$) between dimension measures y and x in (**a**) double-logarithmic and (**b**) Cartesian coordinate system

determines the slope, and the allometric factor a gives the value of y at $x = 1$. If y increases faster than x, the allometric exponent α is greater than 1. This is called "positive allometry". If $\alpha = 1$, growth is isometric, i.e. original proportions remain unchanged during growth. If the allometric exponent α is lower than 1, we call this "negative allometry". In this case, the growth of y drops behind x. This applies to the example given above, for the development of human head size in relation to total body size as a child ages.

The physiological interpretation of the allometric equation becomes even more obvious after rearranging (10.12) to

$$\frac{dy}{dx} = \alpha \times \frac{y}{x}. \tag{10.15}$$

Here, allometry is regarded as the result of a distribution process, in which the growth resources of the entire organism are distributed between the organs according to a certain distribution key. The allometric exponent α in (10.15) describes the manner in which the resources are distributed relative to the proportions of y and x, and functions as a distribution constant. Hence, the allometric exponent α is a measure of an organism's internal distribution strategy and balance.

10.2.2 Examples of Allometry at the Individual Plant Level

10.2.2.1 Height and Diameter Allometry

Figure 10.8 shows, in a schematic array, the diameter–height–allometry of three trees which, commencing with equal height–diameter ratios in the early growth phase, develop different relative diameter and height growth rates due to the

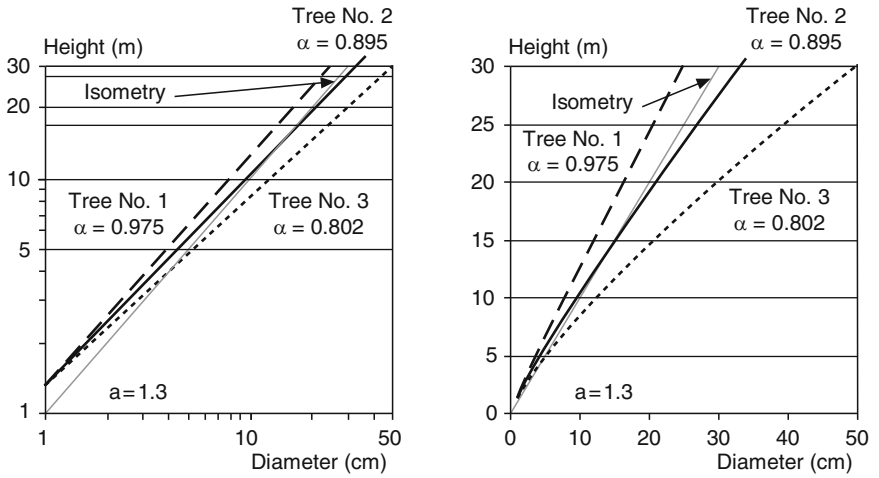

Fig. 10.8 Starting from equal height–diameter relations during youth, competition within the stand triggers different relative diameter and height growth rates of Trees 1 (high competition), 2 (medium density) and 3 (open-grown) (cf. Thomasius 1990). Allometric exponent of $\alpha_{h,d} = 0.975, 0.895$, respectively. $\alpha_{h,d} = 0.802$ reflect the individual allocation keys and result in h/d-relations of $h/d = 1.2, 0.9$, and 0.6 at a tree height of 30 m

competitive situation in the stand (adapted from Thomasius 1990). Because of strong competition, Tree 1 increases its height growth relative to its diameter growth, in the attempt to reach the upper crown space with good light conditions. Its allometry amounts to $\alpha_{h,d} = 0.975$ and its slenderness ratio increases to 1.2 at the expense of stability (survival strategy). In contrast, the larger growing space availability (less competition, better resource supply) of Tree 2 and Tree 3 leads to a decreasing h–d–allometry from $\alpha_{h,d} = 0.895$ to 0.802. This signifies that height growth rate slows down compared to diameter growth rate (stabilisation strategy).

At this point, we should mention that the description of the h–d relation by the allometric equation is essentially an approximation. At maturity, height growth slows down and almost ceases while diameter continues to increase almost constantly. Therefore, in forestry, h–d relations commonly are described by the Petterson equation (Petterson 1955), which, literally speaking, is only another type of allometric relationship (Chap. 6).

10.2.2.2 Crown Width and Tree Height Allometry

The relationship between tree height and crown width is a good example of positive allometry relevant to the silvicultural management of pure and mixed stands of Norway spruce and European beech. Figure 10.9 displays the different space sequestration strategies of both species (allometry growing space $\propto$ size$^{\alpha}$). Crown width, and hence also the growing space requirement, increases with increasing tree height.

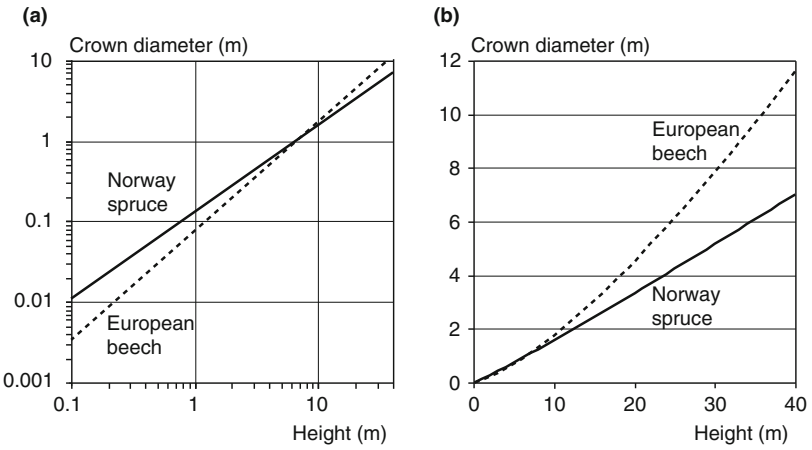

Fig. 10.9 Allometric relation between height (h) and crown diameter (cd) of Norway spruce (*continuous line*) and European beech (*broken line*) at long-term experimental plots Zwiesel 111. The $\alpha_{cd,h}$-allometry shows the stronger crown expansion of European beech ($\alpha_{cd,h} = 1.36$) compared with Norway spruce ($\alpha_{cd,h} = 1.07$) in (**a**) double-logarithmic and (**b**) Cartesian coordinate system

Norway spruce exhibits an allometric exponent of $\alpha = 1.07$, European beech a significantly higher positive allometry of $\alpha = 1.36$. Consequently, for an equal increase in size, European beech demand for increased growing space is higher than that of Norway spruce. Although the Norway spruce tables from Assmann and Franz (1963, dominant height 40 m at age 100) and Schober's (1967) European beech tables (yield class 1.0, moderate thinning) show that, at a dominant height of 18 m, both species have a stocking of approximately 2,000 trees ha^{-1}, at a height of 30 m, spruce still has more than 900 trees ha^{-1} whereas there are less than 400 trees ha^{-1} in the beech stands.

Environmental changes can lead to deviations in allometric development, i.e. abrupt changes in the allometric exponent α. For example, for Norway spruce and Silver fir in the low mountain ranges, high pollution exposure often was found to lead to a major reduction in diameter growth in relation to height growth, ultimately resulting in the absence of entire annual tree rings (Elling 1993; Franz and Pretzsch 1988; Röhle 1987). This resulted in a slenderness of the trees in early mature Norway spruce and Silver fir stands that is normally typical for stands in the pole stage. After the reduction in the pollution exposure, form rejuvenated producing a shift back towards the favouring of diameter growth, so that the temporary increase in h/d-values approached age-specific values once again.

10.2.3 Detection of Periodic Changes in Allometry

In plots with double-logarithmic scales, deviations from allometric behaviour are apparent by the deviations from the linear slope. For a detailed analysis of x–y-allometry, the slope

$$\alpha_i = \frac{\ln(y_{i+1}) - \ln(y_i)}{\ln(x_{i+1}) - \ln(x_i)} = \frac{\ln(y_{i+1}/y_i)}{\ln(x_{i+1}/x_i)} \tag{10.16}$$

can be calculated from the pairs of variables $y_{i=1,\ldots,n}$ and $x_{i=1,\ldots,n}$ from consecutive surveys, which are commonly available from long-term observations. Thus, the allometric exponent α_i can be quantified for the period between two surveys. For infinitely small time steps

$$\alpha_i = \Delta y/y/\Delta x/x, \tag{10.17}$$

applies which is equal to the allometric relation in (10.13). As long as the relationship between $\ln(y)$ and $\ln(x)$ is linear for a certain period, (10.16) and (10.17) are equivalent.

In Fig. 10.10, we illustrate the usefulness of slope α_i for quantifying the effect of (a) competition, and (b) long-term ozone fumigation on the h–d–allometry ($\alpha_{h,d}$) of European beech and Norway spruce, respectively. Figure 10.10a shows the h–d–allometry of beech in the Norway spruce–European beech mixed stand near Freising FRE 813/1 in the period 1994–2005. The calculation of $\alpha_{h,d} = \ln(h_{2005}/h_{1994})/\ln(d_{2005}/d_{1994})$ produces $\alpha_{h,d} = 0.85$, on average, with a range of $\alpha_{h,d} = 0.1$–3.5. This means, when diameter increases by 1%, height increases on average by 0.85. However, thorough analysis reveals that, in case of small understorey trees, a diameter increase of 1% corresponds with a height growth of up to 3.5% (steep slopes on the left of Fig. 10.10a), whereas, in case of dominant trees,

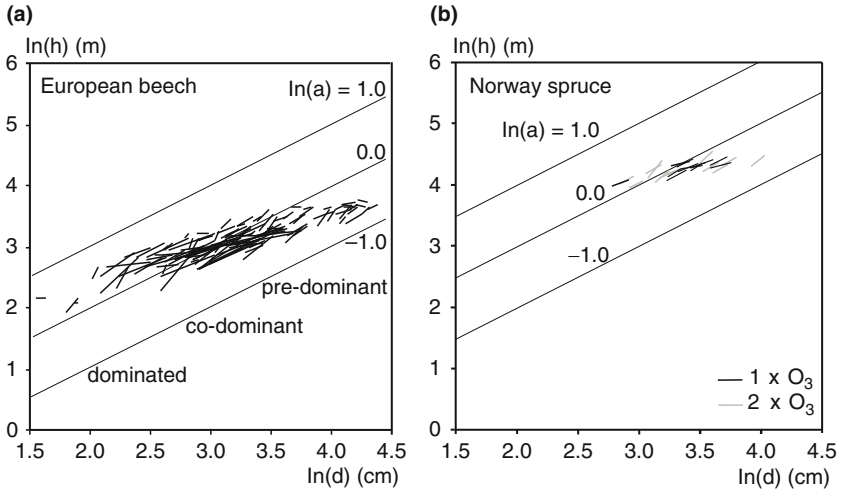

Fig. 10.10 Change of h–d-allometry ($\alpha_{h,d}$) of (**a**) European beech under competitive stress and of (**b**) Norway spruce under ozone stress, shown in a double-logarithmic coordinate system. (**a**) For European beech ($n = 107$), the h–d-allometry is shown for the period 1994–2005. (**b**) For Norway spruce ($n = 19$) trees under ambient ozone (*thin lines*; $1 \times O_3$) show smaller slopes than trees under double ozone fumigation (*bold lines*; $2 \times O_3$). The straight lines serve as a reference, and display the expected allometry under geometric similitude ($\alpha_{h,d} = 1$). Lines $\ln(h) = \ln(a) + \alpha_{h,d} \times \ln(d)$ with $\ln(a) = -1.0, 0, -1.0$ reflect different absolute levels for the expected development under geometric similitude

a corresponding height growth of 0.1–0.5% was found (shallow slopes in the right part of Fig. 10.10a).

In Fig. 10.10b, the application of $\alpha_{h,d}$ shows how long-term ozone fumigation in the same stand changes the h–d–allometry of Norway spruce. Under ambient ozone concentrations ($1 \times O_3$), the slope $\alpha_{h,d} = \ln(h_{2007}/h_{2000})/\ln(d_{2007}/d_{2000})$ for Norway spruce produces $\alpha_{h,d}(\pm SE) = 0.81(\pm 0.08)$, whereas a raised ozone concentration of $2 \times O_3$ results in significantly higher values of $\alpha_{h,d}(\pm SE) = 1.32(\pm 0.14)$. In other words, under ozone stress, diameter growth declines compared to height growth so that stems become more slender and less stable (Pretzsch 2008).

10.3 Growth and Yield Functions of Individual Plants

In general, growth is defined as an increase in yield, i.e. volume or biomass, with age (time). The "growth" of size measures such as height, diameter or basal area is also referred to as increment (cf. Chap. 2). Despite the complexity of the processes involved, growth and yield at the scale of the individual organism often exhibit astonishing regularity, which can be described with relatively simple functions.

10.3.1 Physiological Reasoning and Biometrical Formulation of Growth Functions

We introduce Bertalanffy's (1951) function as an example for a growth function, which is deduced theoretically by combining ecophysiological reasoning and the allometric relationships introduced in the previous section. In his attempt to explain one of the most fundamental processes, Bertalanffy describes the body mass growth rate dw/dt as the result of the assimilation and respiration processes in an organism. Both assimilation and respiration are modelled as functions of body mass w, and the growth rate is derived from the difference between positive assimilation and negative respiration:

$$\frac{dw}{dt} = a \times w^{\alpha_1} - b \times w^{\alpha_2}. \tag{10.18}$$

Assimilation and respiration are proportional to the body mass raised to the power of α_1 and α_2, respectively. The allometric factors a and b are species-specific constants. Exponents α_1 and α_2 are set according to Rubner (1931), who claimed that the increase in assimilation is proportional to the surface (leaf area, surface area of an animals lungs and intestine), and the increase in respiration proportional to an organism's weight or volume. On basis of Rubner's surface–volume relationship, Bertalanffy (1951) describes the assimilation process in relation to surface, which can be expressed as weight to the power of $2/3$ (anabolism $\propto a \times w^{2/3}$). Simultaneously, the respiration process is proportional to weight (catabolism $\propto$

$b \times w$). Consequently, (10.18) becomes

$$\frac{dw}{dt} = a \times w^{2/3} - b \times w. \tag{10.19}$$

By solving this differential equation with the initial value w_0 for the initial point of time t_0, and setting $A = (a/b)^3$ and $k = b/3$, one obtains the yield w as a function of time,

$$w = A \times \left(1 - e^{-k \times t}\right)^3. \tag{10.20}$$

When growth follows this function, at the time of increment culmination t_{culm}, which occurs at the function's inflection point, 29.63% of ultimate size dimension has been reached ($w_{tinf} = A \times 0.2963$). The inflection point is given by $t_{inf} = -\ln(1/3)/k$. Bertalanffy (1951) maintains that (10.20) is appropriate for descriptions of weight or volume development (volume $\propto$ weight) for animals and microorganisms when assimilation is proportional to the surface, i.e. to the power of 2/3 of weight, and if respiration is proportional to weight or volume.

10.3.2 Overview Over Approved Growth and Yield Functions

Even though, assimilation and respiration processes upon which tree growth is based are not yet completely understood in detail, growth and yield functions such as that from Bertalanffy perform surprisingly well. These functions describe changes in tree diameter, height or volume over time, and define growth as balance of increase and loss effects.

The following growth and yield functions (yield function results from the integration of the growth function, growth function from the first derivative of the yield function) try to quantify the principles of tree growth at the macro level (Wenk et al. 1990). Growth and yield functions are applied, e.g. in growth models for the prognosis of yield (Chap. 11), or as reference functions for the quantification of growth losses following disturbances (Chap. 14). Therefore, the biological plausibility of growth functions and the ability to extrapolate them is at least as important as their flexibility. An optimised statistical fitting with polynomials would abandon the possibility of interpreting curve parameters within a biological context. The extrapolation of growth functions beyond the observed data range, important in modelling or diagnosis of disturbances, using polynomials would be questionable.

Besides the frequently-used growth functions, Table 10.1 also lists some less well-known functions such as those from Korf (1939), Levakovic III (1935) and Hossfeld IV (in Peschel 1938), or from Zeide (1993) and Kiviste (1988), which proved to be appropriate for modelling tree growth. The column containing yield functions describes the age-dependence (t) of y (e.g. weight, diameter, height), the growth function describes the derivation $y'(=dy/dt)$ of the yield function over time. Since the underlying expansion and reduction processes are concealed in these functions, Table 10.1 also splits the growth y' into its expansion and reduction

Table 10.1 Overview of important growth functions, including name, integrated form, differential form as well as their composition into expansion and reduction components. y = dimension of tree or stand (height, diameter, volume), t = age, y' = increment, a, b, c, and d = function parameters, ln = natural logarithm. For clarity reasons, parameter and variables are combined without multiplication operators: $(b/a)\,y^2 = b/a \times y^2$ (according to Zeide 1993)

Function	Yield	Growth	Expansion component	Reduction component
Hossfeld IV	$y = t^c/(b+t^c/a)$	$y' = bct^{c-1}/(b+t^c/a)^2$	cy/t	cy^2/at
Gompertz	$y = a\,e^{-b\,e^{-ct}}$	$y' = abc\,e^{-ct}e^{-b\,e^{-ct}}$	$c\ln(a)y$	$cy\ln(y)$
Logistisch	$y = a/(1+c\,e^{-bt})$	$y' = abc\,e^{-bt}/(1+c\,e^{-bt})^2$	by	$(b/a)y^2$
Monomolecular	$y = a(1-c\,e^{-bt})$	$y' = abc\,e^{-bt}$	ab	by
Bertalanffy	$y = a(1-e^{-bt})^3$	$y' = 3ab\,e^{-bt}(1-e^{-bt})^2$	$3a^{1/3}by^{2/3}$	$3by$
Chapman-Richards	$y = a\,(1-e^{-bt})^c$	$y' = abc\,e^{-bt}(1-e^{-bt})^{c-1}$	$a^{1/c}bcy^{(c-1)/c}$	bcy
Levakovic III	$y = a(t^2/(b+t^2))^c$	$y' = 2bcy/t(b+t^2)$	$2cy/t$	$2a^{-1/c}cy^{(c+1)/c}/t$
Korf	$y = a\,e^{-bt^{-c}}$	$y' = abct^{-c-1}\,e^{-bt^{-c}}$	$c\ln(a)y/t$	$cy\ln(y)/t$

components (differential formulation), as demonstrated earlier for Bertalanffy's function. In an example, the expansion and reduction components (see columns 4 and 5, Table 10.1) are deduced in the mono-molecular equations

$$y = a \times \left(1 - c \times e^{-b\times t}\right), \tag{10.21}$$

$$y' = a \times b \times c \times e^{-b\times t}. \tag{10.22}$$

Rewriting (10.21) as $y = a - a \times c \times e^{-b\times t} \Leftrightarrow a - y = a \times c \times e^{-b\times t}$, we can substitute $a \times c \times e^{-b\times t}$ in (10.22) by $a - y$. Then growth (10.22) can be described by $y' = b \times (a - y)$ or

$$y' = a \times b - b \times y. \tag{10.23}$$

Here, the production component ($a \times b$) and reduction component ($b \times y$) become visible, and separate from each other. The production and reduction components of all growth functions listed in Table 10.1 can be expressed in a similar way. We recognise Bertalanffy's (1951) growth function, where the expansion component is dependent on $\alpha_1 = 2/3$ power of y, whereas the reduction is proportional to y ($\alpha_1 = 1$) (cf. (10.18) and (10.19)). Production and reduction components of the growth functions mentioned clearly assume very different forms. The reduction component can be expressed in many ways, which reflect the variety of factors restricting growth; the limitation of resources, competition, energy input for reproduction, biotic and abiotic disturbance factors.

Richards' (1959) function

$$y = a \times \left(1 - e^{-b\times t}\right)^c \tag{10.24}$$

is thought to be the most frequently used function that has three parameters. It is similar to Bertalanffy's (1951) function, except that the fixed exponent, 3 (in Bertalanffy) is replaced by c (in Richards), which means the inflection point is flexible. Kahn (1994) and Pretzsch and Kahn (1996) successfully applied Richards' (1959) growth function in a site-dependent height growth model for long-term experimental plots, and in the growth simulator SILVA (cf. Chap. 13).

Figure 10.11 shows the flexibility of Richards' (1959) function $y = a \times \left(1 - e^{-b \times t}\right)^c$ for modelling height. By varying the parameters a, b and c, which control the asymptote, slope, and the location of the function's inflection point, respectively, a broad range of height growth curves can be fitted. Nevertheless, the increased flexibility, which was obtained by generalising Bertalanffy's (1951)

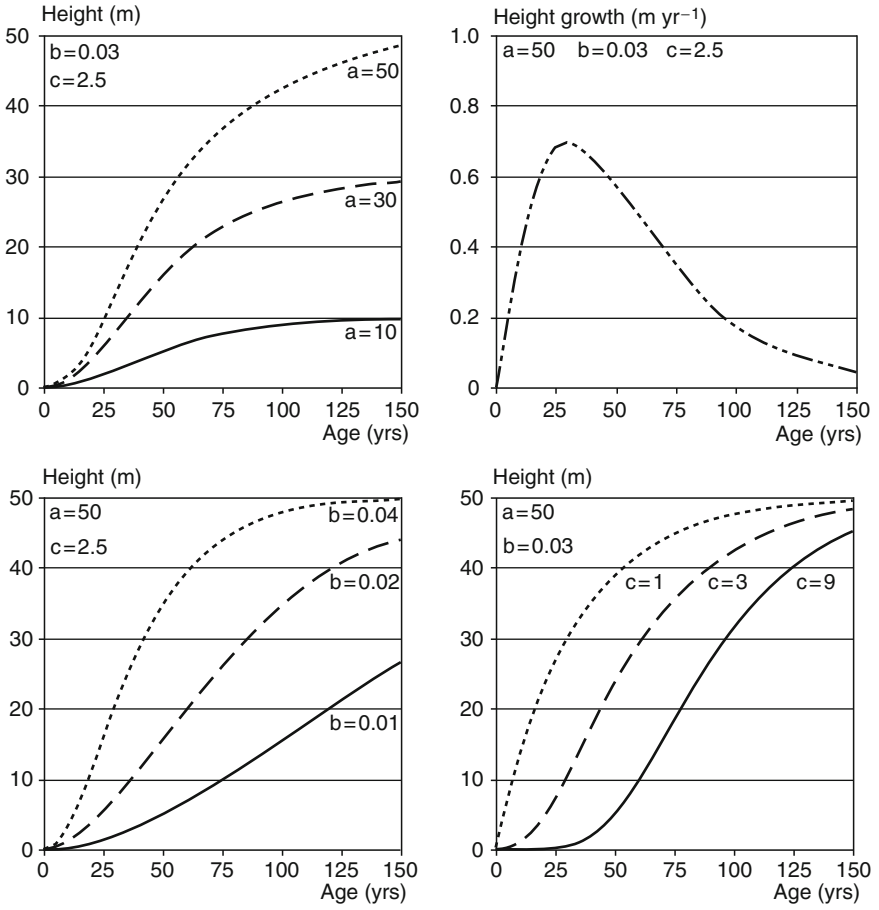

Fig. 10.11 Applying the function of Richards' (1959) $y = a \times \left(1 - e^{-b \times t}\right)^c$ for modelling height growth and height increment. By varying parameters a, b and c (asymptote, slope and position of inflection point), a broad range of height growth curves can be fitted

approach, is accompanies by a loss in biological plausibility of the surface–volume dependence of the metabolic balance, and produces unstable parameter estimations.

The functions from Korf (1939) or Levakovic III (1935) also are growth functions with three parameters, yet they avoid this drawback. According to Kiviste (1988) and Zeide (1972, 1989, 1993), they often achieve better results in biological plausibility and statistical fitting (standard error). The Formula IV from Hossfeld performs particularly well for modelling tree and stand volume growth. For height and diameter growth, it also achieves the accuracy of Richards' equation. The function by Gompertz (1825), which was originally created to describe age distributions of human populations, has an inflection point at $0.3679 \times A$, and also performs quite well in comparison with other functions. The monomolecular function (cf. (10.1) and (10.2)) is well suited to modelling dose–response effects (Sect. 10.1), but largely unsuitable for modelling growth due to the lack of an inflection point, and limited biological plausibility. Even though the logistic growth function is very common in the field of ecology, it often falls behind other functions because of its inflexibility. This is due to the fixed inflection point, at $0.5 \times A$, and the arbitrary definition of reduction processes which raise the size parameter to the power of 2 $((b/a) \times y^2)$. The comparisons undertaken by Kiviste and Zeide emphasise the special flexibility and biological interpretability of the functions from Gompertz, Levakovic III, Korf and Hossfeld IV. They recommend the user to choose biologically plausible functions, which provides the best possible statistical fitting, as indicated by the standard error.

10.3.3 Relationship Between Growth and Yield

Using the yield tables for Norway spruce from Assmann and Franz (1963, site index O 40), Fig. 10.12 shows the relationship between growth (equivalent with increment) and yield curves for the parameter height. When plotting the height h against age (t), the height yield curve results (cf. Fig. 10.12a):

$$h = F(t). \tag{10.25}$$

Assuming unhindered growth or constantly limited growth, the yield function exhibits the typical sigmoid shape (S-shape). The curve of the current annual height increment (CAI_h), i.e. height growth, is shown in Fig. 10.12b:

$$CAI_h = f(t) = F'(t) = \frac{dh}{dt}. \tag{10.26}$$

CAI_h is the first derivation of the yield function; the yield function $F(t)$ is the integral of growth function

$$h = F(t) = \int_0^t CAI_h \, dt = \int_0^t f(t) \, dt. \tag{10.27}$$

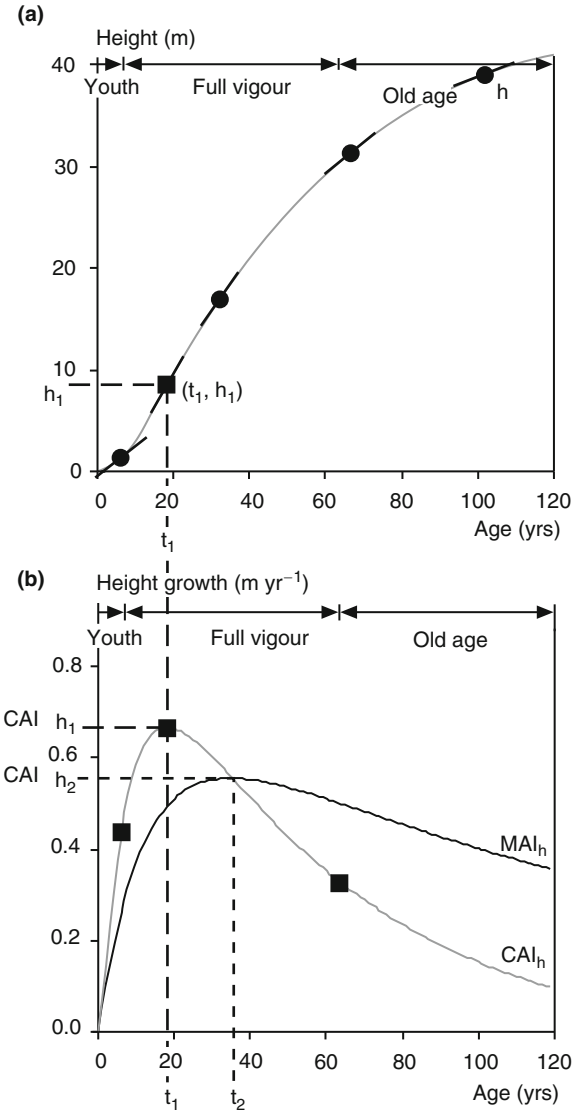

Fig. 10.12 Relationship between tree height development over time (*black continuous line*) and current annual increment CAI_h (*grey continuous line*). The dominant height development for site class 40 of Norway spruce yield table from Assmann and Franz (1963) is shown. As (**a**) the yield function is the integral of (**b**) the growth function, yield function's inflexion point (t_1, h_1) coincides with the growth function's (t_1, CAI_{h1}) culmination point

Therefore, culmination point of the growth curve (t_1, CAI_{ht1}) and the inflection point of the yield curve (t_1, h_1) meet at the same age t_1. The mean annual height increment MAI_h can be calculated by dividing the height h_t, which has been reached

at a given point in time, by the corresponding age t:

$$MAI_{ht} = \frac{h_t}{t} = \frac{\int_0^t f(t)\,dt}{t} = \frac{F(t)}{t}. \tag{10.28}$$

Mean annual volume increment MAI_V results, analogous to the volume yield Y_t that has accumulated at a given age t, divided by the age t ($MAI_{Vt} = Y_V/t$). The function of mean annual growth (MAI_h or MAI_V, respectively) culminates later than the current annual growth. It can be shown that the MAI culminates (MAI_{max}) at the point where the MAI curve intersects with the current annual increment (t_2, h_2) (cf. Fig. 10.12b). The mean annual increment culmination point is derived by setting the first derivative of mean increment equal to zero:

$$MAI'_h = \frac{d\frac{F(t)}{t}}{dt} = \frac{F'(t) \times t - F(t)}{t^2} = 0. \tag{10.29}$$

The differential MAI'_h is zero, when $F'(t) \times t - F(t) = 0$. That is the case, when

$$F'(t) = \frac{F(t)}{t}. \tag{10.30}$$

Consequently, MAI ($= F(t)/t$) culminates when it equals CAI ($= F'(t)$). As shown in Fig. 10.12a, the inflexion point of the yield function (t_1, h_1) coincides with the CAI culmination point (t_1, CAI_{h1}). MAI culminates at the intersection point with CAI right downward branch (t_2, CAI_{h2}).

10.4 Allometry at the Stand Level: The Self-Thinning Rules from Reineke (1933) and Yoda et al. (1963)

As plants grow in size, their demands on resources and growing space increase. If resources are no longer sufficient for all individuals, self-thinning commences, and the number of plants N per unit area decreases. Although the principle of allometry was derived for individual trees, its application to plant communities in which self-thinning occurs produces some important conclusions (Reineke 1933; Yoda et al. 1963). Figure 10.13 is a schematic representation of the relationship between average plant size and density on the double logarithmic scale. The upper self-thinning, or limiting boundary line, marks the maximum possible density for a species at a given average plant size, or weight in evenaged pure stands under optimum site conditions. The lower self-thinning lines mark the characteristic boundary relationship for any stand under sub-optimum growing conditions. Given three stands A, B, and C growing under optimum and sub-optimum conditions respectively, the size–density relationships of each stand initially approximate their stand-specific self-thinning lines, and, subsequently, deviate from this line, at different absolute levels, but with similar gradients.

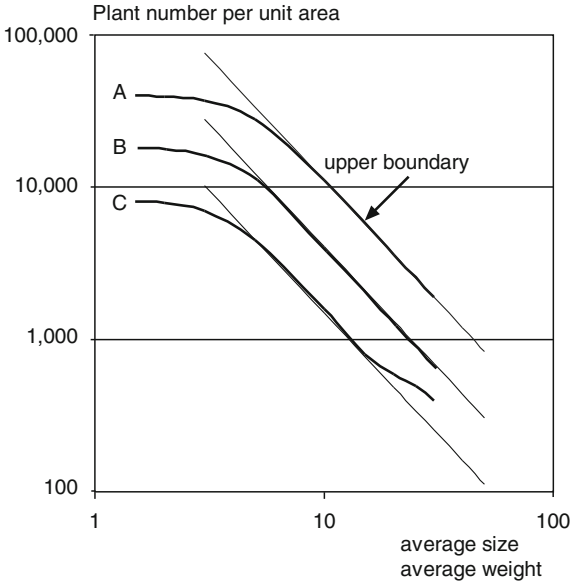

Fig. 10.13 The common principle of Reineke's rule (1933) and the $-3/2$ power law by Yoda et al. (1963) for evenaged plant populations. The relationship between average plant size or average weight and plant number forms a straight line in a double-logarithmic scale. The *upper, middle and lower straight lines* represents the self-thinning line of the plant populations A, B and C, and delineate the decrease of plant number under optimal, medium and poor site conditions, respectively. Initially the population density remains rather constant until the limited resources enhance competition and lead to self-thinning. A deviation from the self-thinning line, such as the last section of the trajectory C, occurs when environmental conditions and resource supply change

The size–density allometry of plants under self-thinning provides information relevant to ecophysiology and production economics; because, under self-thinning conditions, size–density allometry reveals the species-specific critical demand for resources and growing space of average trees at a given mean size.

10.4.1 Reineke's (1933) Self-thinning Line and Stand Density Index

For the relationship between tree number N and quadratic mean diameter d_q in fully stocked, evenaged forest stands Reineke (1933) defined the "stand density rule"

$$N = b \times d_q^{-1.605}. \tag{10.31}$$

Reineke's rule can be represented on the log–log scale as a straight line:

$$\ln N = b' - 1.605 \times \ln d_q \tag{10.32}$$

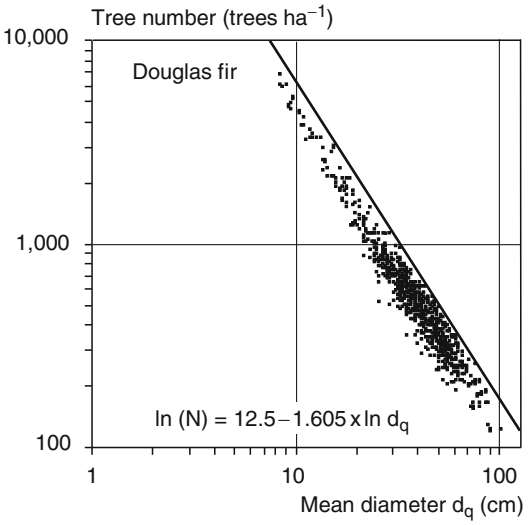

Fig. 10.14 Relationship between stem number per hectare and mean diameter for evenaged Douglas fir stands (*Pseudotsuga menziesii* Mirb.) from inventories in Washington and Oregon. The upper envelope of the point cloud $\ln N = \ln(b) - \beta \times \ln d_q$ with the absolute level $\ln(b) = 12.5$ and the slope $\beta = -1.605$ (according to Reineke 1933) also are shown

with the intercept $b' = \ln b$ and the slope $\beta_R = -1.605$ (note that we substitute α as the allometric exponent on individual plant level by β for the stand level; the subscript R stands for Reineke). Reineke obtained this scaling rule by plotting d_q and N for untreated forest inventory plots in the USA on a log–log grid (Fig. 10.14). He found very similar allometric exponents for various tree species, stand structures, and sites, and hence concluded that the rule had a general validity of $\beta_R \cong -1.605$ for forest stands. Reineke's rule has gained considerable importance for the quantification and control of stand density, and for modelling stand development in pure (Bergel 1985; Ducey and Larson 1999; Long 1985; Newton 1997; Pretzsch 2001; Puettmann et al. 1993; Sterba 1975, 1981, 1987), and mixed stands (Puettmann et al. 1992; Sterba and Monserud 1993). Reineke (1933) used the allometric exponent $\beta_R = -1.605$ to develop his stand density index $SDI = N \times (25.4/d_q)^{-1.605}$. The SDI describes stand density in relation to the quadratic mean diameter d_q and the number of trees per hectare N by calculating the expected number of stems per hectare for a 10 inch mean diameter (=25.4 cm; 1 inch = 2.54 cm). In Europe, an index diameter of 25 cm is used, so that

$$SDI = N \times (25/d_q)^{-1.605}. \tag{10.33}$$

According to Zeide (2004, p. 7), Reineke's density assessment with the SDI "may be the most significant American contribution to forest science". But, like Gadow (1986), and Pretzsch and Biber (2005) he questions the general validity of exponent $\beta_R \cong -1.605$.

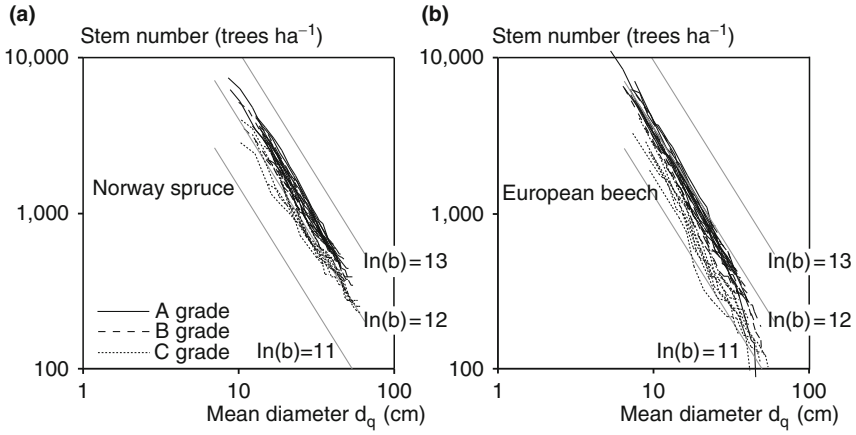

Fig. 10.15 ln(N)–ln(d)-relationship for untreated, fully stocked stands of pure (**a**) Norway spruce (n = 9) and (**b**) European beech (n = 9) (Pretzsch and Biber (2005): *reference lines* $\ln(N) = \ln(b) - 1.605 \times \ln(d_q)$ follow Reineke (1933) with $\ln(b) = 11, 12, 13$

Pretzsch and Biber (2005) reevaluate Reineke's rule based on 28 fully stocked pure stands of European beech, Norway spruce, Scots pine, and Sessile oak in Germany, which have been inventoried since 1870. Figure 10.15 shows the $\ln(N)$–$\ln(d_q)$-relationships for Norway spruce and European beech. OLS regression of the model $\ln(N) = b' + \beta_R \times \ln(d_q)$ results in β_R values of -1.789 for European beech, -1.664 for Norway spruce, -1.593 for Scots pine and -1.424 for Sessile oak. The allometric exponent for European beech differs significantly from the other species. There is also a significant difference between the β_R-values for Norway spruce and Sessile oak. With the exception of Scots pine, the allometric exponents deviate significantly (European beech) and almost significantly (Norway spruce, Sessile oak) from the exponent $\beta_R = -1.605$ postulated by Reineke (1933). This shows that, if species-specific allometry is ignored, serious errors in the estimate and control of density may be the consequence when using the Stand Density Index $SDI = N \times (25/d)^{-1.605}$. Physiologically, the Reineke exponent demonstrates how strong a species enforces self-thinning for a given increase in diameter, or, in the words of Zeide (1985), the species' self-tolerance. According to the results from above, European beech exhibits the highest self-thinning, or lowest self-tolerance, and Sessile oak the lowest self-thinning, or highest self-tolerance (cf. Pretzsch and Biber 2005; Pretzsch 2006a).

10.4.2 −3/2-Power Rule by Yoda et al. (1963)

With no knowledge of the stand density rule by Reineke (1933), Kira et al. (1953) and Yoda et al. (1963) discovered the $-3/2$ power rule of self-thinning, initiating probably the most prominent controversial discussion of a scaling rule. It describes

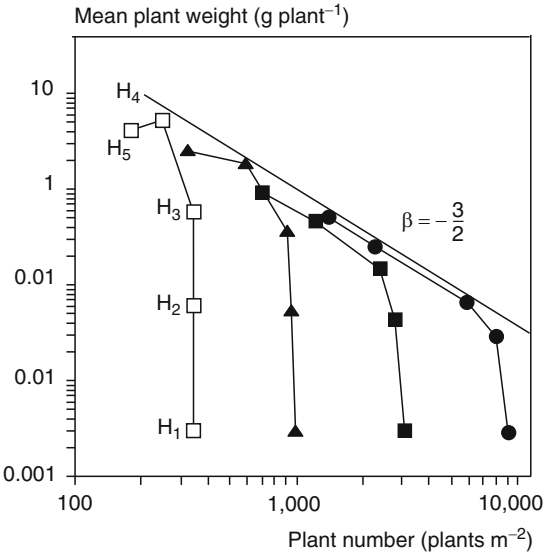

Fig. 10.16 Development of the relationship between density (plants m^{-2}) and average plant weight (g $plant^{-1}$) in populations of English Ryegrass (*Lolium perenne* L.) with different initial densities under optimal light ambience. The data points H_1, H_2 etc. represent numbers at different developmental phases (according to Harper 1977)

the relationship between the average shoot weight $\bar{w}$ and the plant number N per unit area in evenaged and fully stocked monospecific plant populations as

$$\bar{w} \propto N^{-3/2} \tag{10.34}$$

with the species invariant scaling exponent $\beta_Y = -3/2$ (Fig. 10.16). Yoda et al. (1963) assume that plants are simple Euclidian objects, and all plant parts are related to each other isometrically. Yoda's allometric exponent $\beta_Y = -3/2$ can be reformulated in several ways based on the cubic relationship between plant diameter $\bar{d}$ and biomass $\bar{w}$:

$$\bar{w} \propto \bar{d}^3 \tag{10.35}$$

and the quadratic relationship between $\bar{d}$ and occupied growing area $\bar{s}$ as the inverse of the number of plants per hectare $N\,(\bar{s} = 1/N)$:

$$\bar{s} \propto \bar{d}^2. \tag{10.36}$$

Inserting (10.35), (10.34) can be written as $\bar{d} \propto N^{-1/2}$ or $N \propto \bar{d}^{-2}$, which is similar to Reineke's (1933) formulation of the stand density rule, but which predicts a Reineke exponent of $\beta_R = -2$ instead of -1.605. The relationship between shoot biomass per unit area W and plant number N is similar as $W \propto N^{-1/2}$, since $W = \bar{w} \times N$, $W \propto N \times N^{-3/2} \propto N^{-1/2}$.

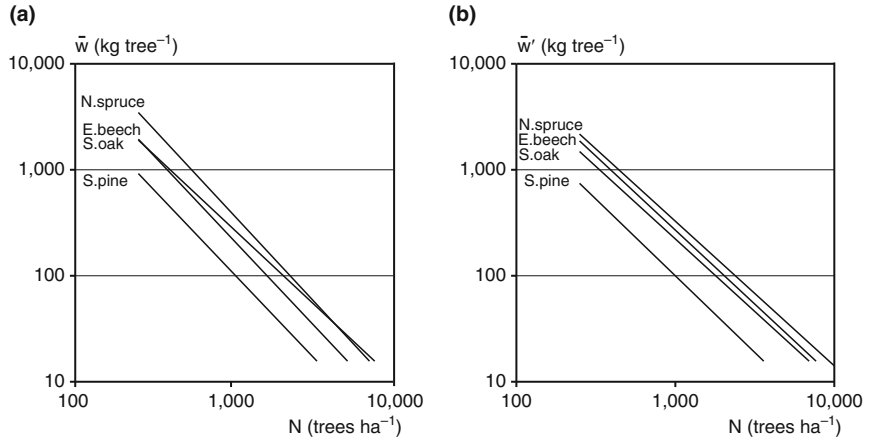

Fig. 10.17 Relationship between logarithmic mean plant biomass $\ln \bar{w}$ and tree number per unit area ln N for untreated, fully stocked, pure European beech, Norway spruce, Scots pine, and Sessile oak stands: self-thinning slopes (**a**) for $\bar{w}$ = total mean above ground biomass per tree and (**b**) $\bar{w}'$ = living mean above ground biomass per tree

Figure 10.17a depicts the $\ln \bar{w} - \ln N$ lines for the four tree species European beech, Norway spruce, Scots pine, and Sessile oak already considered in the previous section. As can be seen, a wide range of stem numbers and biomass is covered by the dataset. Mean shoot biomass per plant $\bar{w}$ of European beech, Norway spruce, Scots pine, and Sessile oak, ranges from 9.7 to 1,809.9 kg, 13.5 to 1,514.4 kg, 12.9 to 331.7 kg and 93.4 to 982.1 kg respectively. For $\bar{w} \propto N^{\beta_Y}$, OLS regression yielded $\beta_Y = -1.403, -1.614, -1.575$, and -1.592 for European beech, Norway spruce, Scots pine, and Sessile oak. Again, we find species-specific differences, which can be interpreted analogously to Reineke as self-thinning, or self-tolerance, with respect to plant weight. The formulation of the Yoda rule with exponent β_Y on the side of the stem number results in an increase in the self-thinning (decrease in self-tolerance) in the order: European beech, Scots Pine, Sessile oak, Norway spruce (cf. also Pretzsch 2006a). The difference in the exponents from Reineke and Yoda arises from the different allometry between mean quadratic diameter and mean plant weight. By rearranging the Yoda rule to $N \propto \bar{w}^{1/\beta_Y}$, and substituting it in Reineke's rule, $N \propto \overline{d_q}^{\beta_R}$, one obtains $\bar{w}^{1/\beta_Y} \propto \overline{d_q}^{\beta_R} \Leftrightarrow \bar{w} \propto \overline{d_q}^{\beta_Y \times \beta_R}$. For the four species considered, the relation produces exponents of 2.508, 2.686, 2.509 and 2.267 for beech, spruce, pine and oak, respectively. The original exponents from Yoda and Reineke result in an exponent of $\bar{w} \propto \overline{d_q}^{2.4075}$ (Pretzsch 2002, pp. 37–38).

Unlike herbaceous plants, many tree species develop a stem with a core of inert heartwood, which may comprise a considerable proportion of the tree's total biomass. For a better comparison between woody and herbaceous species, it may be helpful to distinguish between dead and living tissue. In Pretzsch (2002), functions for the estimation of biomass and sapwood area, and a stereometric model for distinguishing stem sapwood from dead heartwood are developed for European beech,

Norway spruce, Scots pine, and Sessile oak. With $\bar{w}'$ representing living and not total biomass, the allometry $\bar{w}' \propto N^{\beta'}$ provided values of $\beta' = -1.396, -1.365, -1.447$, and -1.369, respectively (Fig. 10.17b). The heartwood elimination yields a less biased slope β' and improves the comparability between the scaling rules for woody and herbaceous plants.

10.4.3 Link Between Individual Tree and Stand Allometry

Allometry at the individual plant level (Sect. 10.2) describes the internal allocation of growth resources and the resulting development of proportions of organs and shapes for individual plants. Of particular interest is the allometry between the leaf biomass w_L, i.e. the investment into assimilating area, and total body weight $w_B : w_L \propto w_B^{\alpha}$. Allometry at the stand level (Sects. 10.4.1–10.4.2) relates the average plant size to plant number per area, e.g. plant weight $\bar{w}_B$ to plant number N per hectare, $\bar{w}_B \propto N^{\beta}$ (according to Yoda's rule $\beta = -3/2$; cf. Sect. 10.4.2 of this chapter).

Now, we link the physiologically important allometry between individual tree leaf biomass and tree biomass, and apply Yoda's rule to relate average biomass to tree number per area at the stand level. For the individual tree allometry,

$$w_L \propto w_B^{\alpha}. \tag{10.37}$$

we assume that leaf biomass is proportional to leaf area (la), and regard it as a surrogate variable for the resource (r) or area (s) demand of the tree:

$$w_L \propto la \propto r \propto s. \tag{10.38}$$

Simple geometrical scaling between the two-dimensional area demand (surface) and the three-dimensional volume-related tree biomass then yields

$$s \propto w_B^{2/3}, \tag{10.39}$$

and with $w_L \propto s$ (10.38), the exponent α results as 2/3.

For stand allometry, Yoda's rule (Yoda et al. 1963) gives us

$$\bar{w}_B \propto N^{\beta} \text{ with } \beta = -3/2. \tag{10.40}$$

Since the average growing area $\bar{s}$ in the stand can be calculated by dividing the hectare by the tree number per hectare, $\bar{s} = 10{,}000/N$, we can set

$$\bar{s} \propto N^{-1} \tag{10.41}$$

and (10.41) can be rewritten as

$$\bar{s} \propto \bar{w}_B^{2/3}. \tag{10.42}$$

The apparent similarity between (10.39) and (10.42) leads to the following simple relationship between the individual tree leaf biomass and plant weight allometry (α), and Yoda's self-thinning rule (β):

$$\alpha = -1/\beta. \tag{10.43}$$

Yet, the simplicity, and significance of this link between individual plant physiology (internal allocation key) and production ecology (biomass per hectare) is deceptive. Investigations show that, generally, self-thinning is weaker than individual tree allometry would suggest, i.e. more individuals remain alive than predicted by the individual plant investment into leaf biomass: $\alpha > |1/\beta|$. Pretzsch and Mette (2008) attributed the discrepancy mainly to a decreasing average specific leaf area with age ((10.38) does not hold). Furthermore, crown shyness, or mechanical abrasion (Fish et al. 2006; Putz et al. 1984; Rudnicki et al. 2003), may decouple at least temporarily the proportionality between leaf biomass and space demand (also violating (10.38)).

Moreover, the individual-plant allometric exponent α cannot be generalised in the stand, but depends on tree size, competition and crown ratio (=crown length/tree height). Mäkelä and Valentine (2006) find a clear increase in α from suppressed to dominant trees within the stand, and a decrease in α from young to old trees during stand development. When the size distribution changes during the stand growth, e.g. due to mortality and competition processes, the number of trees with short crowns and low α values gradually increases. Therefore, the fact that stand allometry is based on a changing individual tree-collective must be taken into account. Unfortunately, such changes in size distributions are not always considered. Individual tree allometry is transferred thoughtlessly to stand allometry (Weller 1987, 1990; White 1981), or the connection between them is not explained (Enquist et al. 1998). The attempts of Mäkelä and Valentine (2006), and Pretzsch and Mette (2008) to overcome this gap were addressed repeatedly in various empirical investigations (Matthew et al. 1995; Sackville Hamilton et al. 1995; Pretzsch 2006a).

This link between the two hierarchical levels may enable conclusions to drawn, which an analysis of each individual does not permit. For instance, we can try to explain why, despite the strong variation in the leaf biomass allometry with size, age and competition, the self-thinning lines frequently result in comparably similar slopes, even between species. Apparently, at the higher, aggregated stand level, self-thinning only occurs within relatively narrow boundaries that are optimal or necessary for inter- and intraspecific competition for resources. This infers that, in terms of evolution, optimisation develops and is more evident at the stand than the individual plant level.

10.4.4 Allometric Scaling as General Rule

Because of their ecophysiological significance, allometric exponents have been discussed profusely ever since. Often, it was proposed that volume or mass-related allometric functions be scaled by exponents of 1/3 due to the volume dimensionality

(Bertalanffy 1951; Yoda et al. 1963, 1965; Gorham 1979). More recently, West et al. (1997, 1999), Enquist et al. (1998, 1999) and Enquist and Niklas (2001) presented a model for a general explanation of allometric scaling with 1/4 exponents, based on fractal networks of transportation systems in organisms.

Empirical investigations both at the individual and at the stand level allometry, show that allometry is a function of tree species (Pretzsch 2005c, 2006a; Pretzsch and Biber 2005), site conditions (von Gadow 1986) and stand history (Río et al. 2001). It is therefore not surprising that generalised comprehensive allometric rules such as Yoda's self-thinning rule have been assessed variously as universally valid through to complete uselessness (Yoda: Harper 1977, p. 183; Long and Smith 1984, p. 195; Weller 1987, 1990; Sackville Hamilton et al. 1995; Reineke: Pretzsch and Biber 2005; von Gadow 1986; Río et al. 2001; WBE: Whitfield 2001; Kozlowski and Konarzewski 2004; Reich et al. 2006). In this chapter, we have shown that (10.1) size relations may not necessarily be optimally represented by the general allometric formula, (10.2) it may be advisable to distinguish between living and dead biomass, and (10.3) application of allometric equations to some distributions may overlook the effect of a changing collective of individuals.

The author therefore agrees with Zeide's (1987, p. 532) conclusion with respect to Yoda's rule: "unlike the fixed value of −3/2, the actual slopes convey valuable information about species… that should not be cast away". To obtain a better understanding of competitive mechanisms in forest stands, further research should clarify scaling rules for individual species rather than continuing to search for *"the ultimate law"*, which may be like hunting for a phantom.

Last, but not least, it should be noted that differences also may arise when investigations into allometry are based on different statistical methods (OLS-Regression, PCA, RMA-regression etc.). The use of these different methods produces considerable variations in the results (Sackville Hamilton et al. 1995; Matthew et al. 1995). To take these methodological differences into account, various methods should be applied to the dataset in question: e.g. OLS-regression analysis using the model $\ln(y) = \ln(a) - \alpha \times \ln(x)$, or sub-sections of the allometric relation $\alpha_i = \ln(y_{i+1}/y_i)/\ln(x_{i+1}/x_i)$. Neither approach necessarily will produce exactly the same results unless the $\ln(y) - \ln(x)$-pairs form a perfectly straight line.

10.5 Stand Density and Growth

A question that has intrigued forestry science from its beginning is whether stand volume production is at a maximum in untreated self-thinning stands, or whether it can be raised by silvicultural thinning. Figure 10.18 graphically depicts the two hypotheses: density-growth curve 1 is asymptotic as maximum growth occurs in untreated (maximum stocked) stands, whereas the density-growth curve 2 is a unimodal or optimum curve where maximum growth is reached at below-maximum densities. Rousseau's philosophy that "nature" is synonymous with "rationality"

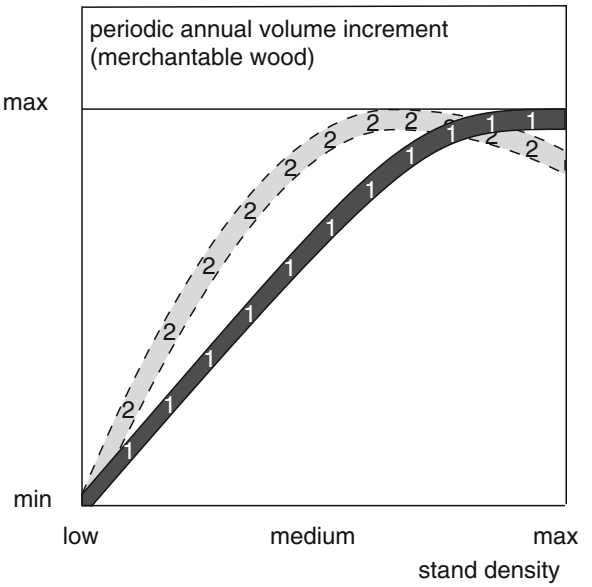

Fig. 10.18 Hypotheses of the relationship between stand density and production of merchantable wood presentation schematically: asymptotic increase towards a maximum growth at maximum stand densities (*curve* 1) vs a unimodal optimum curve with a maximum growth at suboptimum densities (*curve* 2)

(Rousseau 1762), and his credo, that things develop best when left to the hands of the creator and everything inevitably degenerates in the hands of man, explains the prevailing view during the "Age of Enlightenment", that untreated stands produce maximum volume, while any reduction in density would cause growth losses (Fig. 10.18, curve 1). In contrast, Hartig (1795, p. 17) and Cotta (1828, p. 103) were convinced that a periodic removal of suppressed trees would increase volume production. This view strongly contradicted those above. Reventlow (1879, pp. 79–81) still considered the thinning promoted by the founding fathers of forest science, Hartig and Cotta, to be too light. As the pioneer of heavy thinning, he was convinced of the validity of an optimum relationship (Fig. 10.18, curve 2) between density and growth. While Hartig, Cotta, and Reventlow founded their opinions about optimal density mainly on personal experience, Schwappach (1908, 1911) provided the first evidence of a growth increase through thinning from experiments. Numerous long-term experiments followed, some of them confirming, others refuting the existence of an optimum curve (Assmann 1970; Kramer 1988; Langsaeter 1941; Pardé 1979; Schober 1967, 1979, 1980). After reviewing the results of new experiments, Curtis et al. (1997) doubt the occurrence of an optimum relation between density and growth. In view of this return to the opinion prevailing before Hartig and Cotta, Zeide (2001, p. 21) fears a never-ending story in the attempts to understand the density–growth relationship.

10.5.1 Assmann's Concept of Maximum, Optimum and Critical Stand Density

In his analysis of long-term thinning experiments in stands of the dominant species in Southern Germany, Assmann (1961a) found that stands at maximal stand density do not achieve maximum volume growth at all, especially not young or early mature stands. As a measure for stand density, he invented the mean stand basal area (mBA) in a given growth or survey period (cf. Sect. 7.4.3). He found that volume growth increases with a reduction in stand density up to a certain optimum, and then decreases with a further reduction in density. In Fig. 10.19, we apply the relative mean basal area (mBA_{rel} in %, maximum (untreated) = 100%) instead of the absolute basal area values (m^2ha^{-1}).

Assmann describes the relationship between stand density (mBA_{rel}) and volume growth (PAI_{rel} in %, untreated variant = 100%) by the following three density levels (from right to left in Fig. 10.19). Maximum stand density (black filled circle) is achieved in unthinned stands. It can either be given as absolute value for the maximum basal area in square metres per hectare, or as the relative mean basal area as in Fig. 10.19. Assmann defines the optimum stand density as the stand density at which the annual volume increment is at a maximum (up-right square in Fig. 10.19).

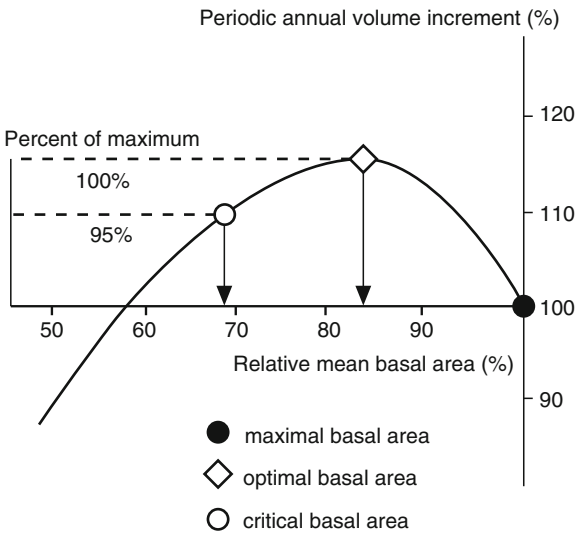

Fig. 10.19 Principles of optimum and minimum basal area in schematic array (according to Assmann 1961a). At first, stands respond with increased increment to a reduction of maximum stand density (100%). Maximum increments are achieved at medium stand densities (optimum basal area). A further reduction of basal area leads to increment losses. The density still providing 95% of the maximum increment is called the critical basal area

Finally the critical basal area corresponds to the mean stand basal area, where still 95% of maximal volume growth is reached (white filled circle in Fig. 10.19). When basal area is reduced even further, volume growth declines almost linearly (see left branch of the dose–response-curve in Fig. 10.19). Assmann established a species- and site-specific maximum, and optimum and critical basal area values for quantitative silvicultural prescriptions (Chap. 5).

Assmann (1961a) observed an optimum relationship between density and growth, especially when removals are concentrated on co-dominant and suppressed trees, which are rather inefficient in terms of water and nutrient use (Chap. 2, Sect. 2.7). He considered that the capacity of a stand to compensate or overcompensate for thinning removals depends on tree species, age and site conditions (Fig. 10.20). The high flexibility of European beech and Norway spruce is reflected in the low critical stand densities of 60 and 70%. The flexibility of Sessile oak, and Scots pine is lower with critical stand densities of 75, and 80% respectively. This means in European beech stands 20–40%, and, in Scots pine stands only 10–20% of maximal basal area can be removed without risking volume growth losses of more than 5% of the maximum growth (cf. Fig. 10.20a).

The capacity to buffer, or even overcompensate for a density reduction declines with increasing age. Consequently, optimum and critical stand density of younger stands is lower than in older stands, where maximum growth requires almost maximum density (cf. Fig. 10.20b).

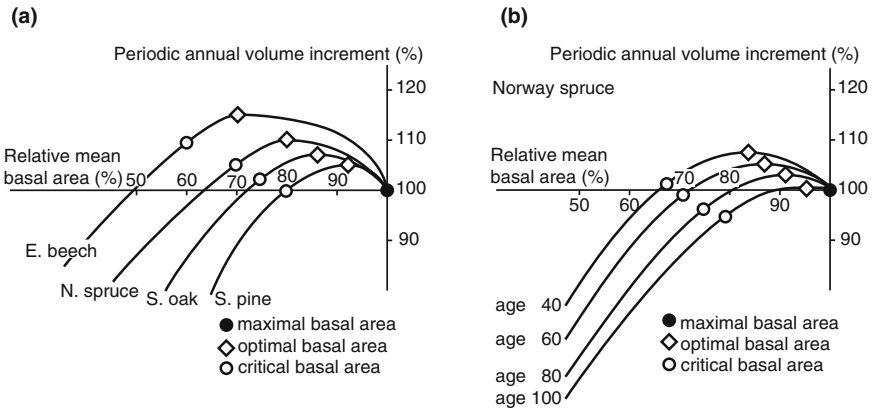

Fig. 10.20 Growth response to stand density in relation to (**a**) tree species and (**b**) stand age. *Black, filled circles* mark maximum basal area, *upright squares* optimum basal area, and *white, filled circles* critical basal area according to Assmann (1961a) (**a**) relative periodic annual volume growth of early mature stands of European beech, Norway spruce, Sessile oak and Scots pine in relation to mean basal area; (**b**) stand density–growth relationship for Norway spruce stands at age 40, 60, 80 and 100 years; site index 40, and medium subdivided special yield levels according to Assmann and Franz (1963)

10.5.2 Biometric Formulation of the Unimodal Optimum Curve of Volume Growth in Relation to Stand Density and Mean Tree Size

Positive thinning effects in terms of growth acceleration can be realised only to a limited extent, as size growth acceleration is accompanies by physiological aging and the lowering of responsiveness and efficiency. When the stand has been thinned already, and, as a result, growth acceleration has occurred repeatedly, its capacity to respond to thinning declines. This shows that growth acceleration after thinning is rather a function of the size trees has achieved already (i.e. the physiological age) than of the true stand age (Chap. 1, Sect. 1.1). A stand's capacity to respond to thinning with additional growth depends on the previous silvicultural treatment rather than on the physical stand age. In the following model, we compare the growth response using mean diameter (as a surrogate variable for physiological age or development phase) rather than true physical age.

On the basis of 9 Norway spruce, and 10 European beech thinning experiments in Germany for which both residual and removed volume have been recorded since 1870, we look at how moderate and heavy thinning from below (B and C grade) affects the production of merchantable volume compared to light thinning (A grade) (Pretzsch 2005b). Stand density was derived from Reineke's (1933) stand density index (SDI) with species- and site-specific slopes (Sect. 10.4.1). Growth was quantified by periodic annual volume increment (PAI), and yield by cumulative total volume yield (Y).

Compared to the A grade, the cumulative merchantable volume yield (Y) of the B grade and C grade amounts to 103–107% in juvenile and 97–102% in mature Norway spruce stands on average respectively. The corresponding findings for European beech are 101–106% and 94–102%. Between the individual stands, Y varies between 89 and 130% for Norway spruce, and 73 and 155% for European beech (Y of A grade = 100%). The relationship between stand density (SDI) and periodic annual increment (PAI) substantiates these findings. On the B and C grade plots of Norway spruce and European beech, the SDI was reduced to 41–91% and 31–83% of the A grade respectively. In young stands, the density–growth relationship follows a unimodal curve. The PAI of Norway spruce culminates at 109% if SDI is reduced to 59%, and for European beech at 123% for a 50% reduction of in SDI. Whereas Norway spruce responds most positively to thinning under poor site conditions, and, on favourable sites, with a growth reduction, the reverse applies to European beech. With increasing age, the culmination point of the unimodal density–growth relationship moves to the right, i.e. to maximum density, until in older stands, the density–growth relationship assumes a more asymptotic form.

10.5.2.1 Modelling the PAI in Relation to Stand Density and Diameter

The following model (10.44) unifies apparently contradictory patterns of stand density–growth responses by integrating relative stand density, average tree size and

site fertility effects, and makes the findings applicable for forest management:

$$\mathrm{RPAI} = \mathrm{e}^{(\mathrm{d}+\mathrm{e}\times\ln(\mathrm{SSDI})+\mathrm{f}\times\mathrm{SSDI}+\mathrm{g}\times\ln(\mathrm{d_q})\times\ln(\mathrm{SSDI})+\mathrm{h}\times\ln(\mathrm{SI})\times\ln(\mathrm{SSDI}))}, \qquad (10.44)$$

and, in logarithmic transformation:

$$\begin{aligned}\ln(\mathrm{RPAI}) = {} & \mathrm{d}+\mathrm{e}\times\ln(\mathrm{SSDI})+\mathrm{f}\times\mathrm{SSDI}+\mathrm{g}\times\ln(\mathrm{d_q})\times\ln(\mathrm{SSDI}) \\ & +\mathrm{h}\times\ln(\mathrm{SI})\times\ln(\mathrm{SSDI}), \end{aligned} \qquad (10.45)$$

where RPAI is the relative periodic annual increment of merchantable wood, SSDI the standardised stand density index at the beginning of a given survey period (setting $\mathrm{SDI_{max}} = 1$), SI the mean height (m) at age 100 as an indicator of site fertility, and $\mathrm{d_q}$ is mean diameter (cm) at the beginning of a given survey period. The model is sufficiently flexible to represent both an asymptotic, as well as a unimodal density–growth curve for SSDI ≤ 1.0 (Fig. 10.21). Apart from the direct influence of SSDI on RPAI, the model considers the interaction terms $\ln(\mathrm{d_q})\times\ln(\mathrm{SSDI})$ and $\ln(\mathrm{SI})\times\ln(\mathrm{SSDI})$, which represent the modification of the density–growth relationship by further stand properties.

Figure 10.21 displays the model behaviour for stands of different mean diameters $\mathrm{d_q}$ (above) and site fertility SI (below). Whereas the species density–growth response is strongest in the juvenile phase (=at low diameters), and weakens with increasing tree size (above), stands react differently on different site conditions (below). The better the site conditions, the narrower the density–growth curve of Norway spruce. While on moderate and unfavourable sites, young stands respond with a 10% increase of RPAI to moderate and heavy thinnings (SSDI = 0.7–0.8), on favourable sites such treatments would cause a 5–10% loss of increment. European beech responds in the opposite manner; the better the site conditions are, the higher the level of density–growth curve and the benefit of RPAI after thinning. For European beech, a decrease in site fertility weakens the density–growth response; this means stands are less able to buffer, or even overcompensate for a lowering of stand density.

Since the underlying experiments cover a wide spectrum of development stages and sites, the model presented (10.44) enables one to differentiate response patterns on a continuum, which so far have been studied only either in stands of different ages (Nelson 1961), or in stands of different site fertility (Assmann 1970). So, in principle, the density–growth relationship follows a unimodal curve, but depending on the observed range of densities, stand development phases, and site fertility, we may perceive only a particular – apparently asymptotic – portion of the curve.

The model reflects the apparently paradoxical fact (Zeide 2004) that a thinning, which keeps a stand at maximum periodic increment RPAI permanently, does not guarantee a maximum cumulative merchantable volume CV. Supposing a young beech stand ($\mathrm{d_q} = 10\,\mathrm{cm}$, $\mathrm{SI} = 32\,\mathrm{m}$) is thinned heavily by reducing SSDI to 0.50, so that PAI is accelerated to 123%. Due to the increased stand growth of $\mathrm{d_q}$ (=faster physiological aging), the growth acceleration potential induced by a thinning tapers

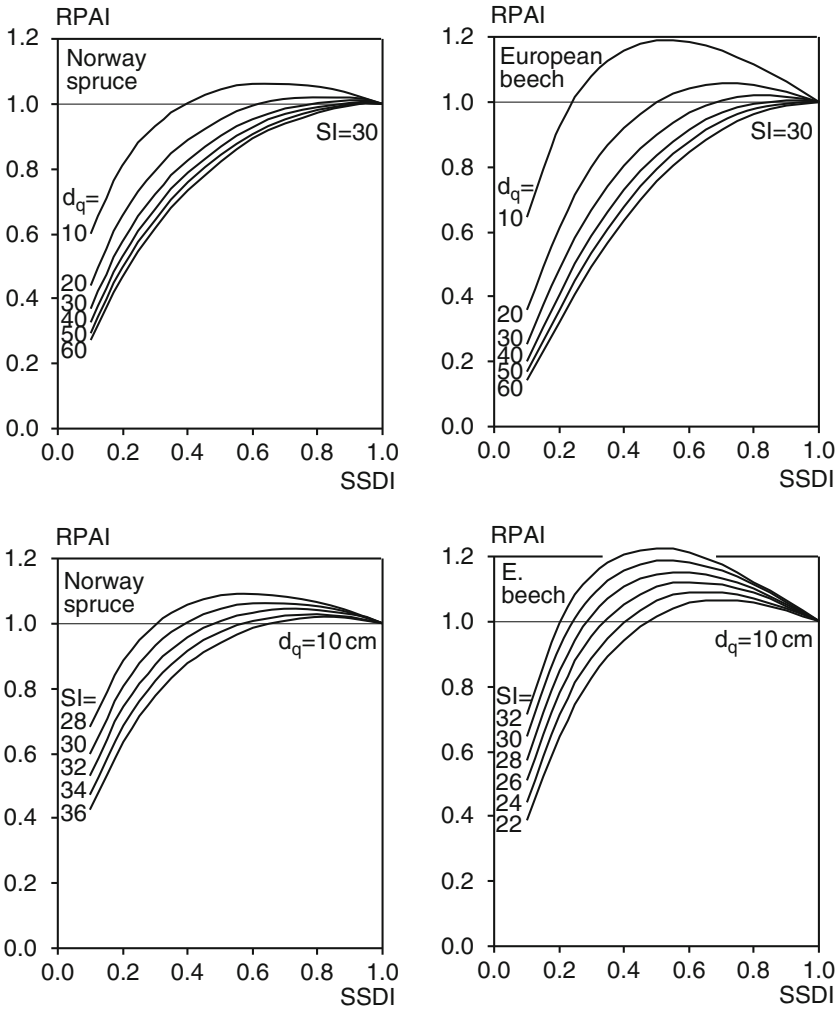

Fig. 10.21 Relationship between standardised stand density SSDI and diameter increment RPAI for Norway spruce (left) and European beech (right) stands of different mean diameter d_q and site index SI: effect of diameter d_q (10…60 cm) for SI = 30 m (*above*); effect of SI (22…36) for d_q = 10 cm (*below*); RPAI relative periodic annual increment of merchantable volume; SSDI standardised Stand Density Index; d_q quadratic mean diameter at the beginning of the relevant growth period; SI mean height at age 100 years; Models for Norway spruce and European beech: $\ln(\text{RPAI}) = 0.85 - 2.64 \times \ln(\text{SSDI}) - 0.85 \times \text{SSDI} + 0.19 \times \ln(d_q) \times \ln(\text{SSDI}) + 0.81 \times \ln(\text{SI}) \times \ln(\text{SSDI})$ and $\ln(\text{RPAI}) = 1.33 - 2.31 \times \ln(\text{SSDI}) - 1.33 \times \text{SSDI} + 0.37 \times \ln(d_q) \times \ln(\text{SSDI}) + 0.72 \times \ln(\text{SI}) \times \ln(\text{SSDI})$

off earlier. This response pattern explains why the CVs of older B and C grade plots differ little in the end, although PAI can be increased considerably by B and C grade thinning. This feedback between growth and density is revealed better by d_q than by stand age.

10.5.2.2 Causal Explanations of the Optimum Curve

The response pattern revealed, in particular the transgressive growth of moderate, compared to lightly thinned stands calls for a causal explanation (Zeide 2001). Assmann (1970) and Mar-Möller (1945) assume that light deficiency makes suppressed trees less efficient than dominant trees at using water and nutrients for the fixation and retention of carbon. Assmann (1970, p. 233) suggests that dominant trees use the resources made available when suppressed trees are removed more efficiently to boost their growth. Furthermore, competition processes may cause reduced growth due to the increased formation of secondary metabolic substances. Perhaps a tree under stress of competition invests more into its defence against parasites or pathogens (growth–differentiation-balance theory from Herms and Mattson (1992)). Growth loss under increasing competitive pressure may be attributable to increased energy consumption in the attempt to produce allelopathic or toxic effects on neighbours (Tubbs 1973). Kesselmeier and Staudt (1999) found that stress-related emission of hydrocarbons can vary from a few thousandths of a percent up to 10, 20 or even 50% of the assimilated carbon.

10.5.2.3 Stand Density and Growth Under Changing Environmental Conditions and Resource Supply

Recent analyses of long-term experiments in Southern Bavarian showed that maximal stand density and growth increased in the past decades. Figure 10.22 shows the

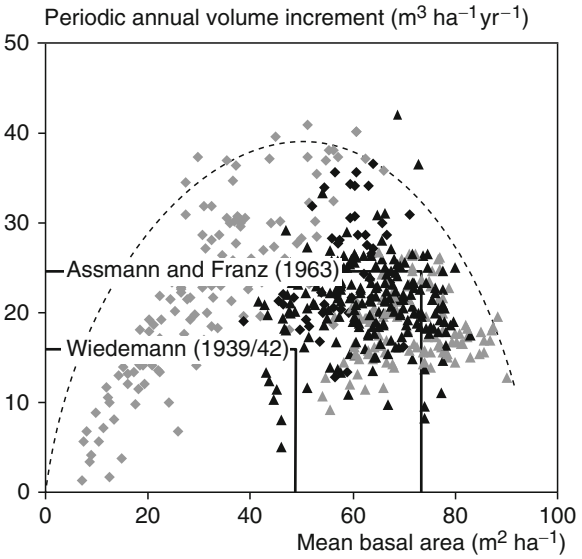

Fig. 10.22 Relationship between basal area and volume increment on permanent plots of Norway spruce (*Picea abies* (L.) Karst.) in Southern Bavaria (according to Pretzsch 2000): *black symbols* represent increment data prior to 1960, *grey symbols* increment data after 1960

extent of those changes based on 22 Norway spruce thinning trial plots in South-West Bavaria near Kempten, Kaufbeuren, Illertissen, Schwabmünchen, Schongau, Zusmarshausen, and Laugna.

The oldest of these plots have been under observation since 1882. Each of the more than 100 data points in Fig. 10.22 represents a stand density–growth measurement on the thinning plots, which range from A grade thinning to very heavy thinning from above and almost solitary treatment. The findings are classified according to the represented time period. Value pairs of basal area and growth from observations prior to 1960 are plotted with black symbols, and those after 1960 with grey symbols. If we imagine an upper boundary line around the point cloud, a characteristic unimodal optimum curve becomes visible (broken line). As can be seen, this curve exceeds the frames given in the yield tables from Wiedemann (1936/42), and Assmann and Franz (1963) (black rectangles). In general, for a given density value, we can anticipate much higher volume growth nowadays. Conversely, basal area can be reduced substantially, and the stand still grows more than the yield tables predict.

10.6 Dealing with Biological Variability

Due to biological variability, measurements of target response variables are scattered around a mean value, e.g. tree diameters around the stand mean diameter, volume increment of certain variants around the mean volume increment of all repetitions. This scattering is caused by uncontrollable or uncontrolled influences of site, weather, climate, competition situation, genetics, etc. Especially ontogenetic and phylogenetic factors (e.g. method of stand initiation, intermediate thinning, provenance) can overshadow cause–effect-relationships at the tree, stand and ecosystem level. For these reasons, experiments might yield different growth responses despite equal tending, and apparent ceteris paribus conditions. The consequences for experimental planning, which results from the historical development of biological systems, are that observed variants need to be repeated in sufficient number to account for the lack of knowledge of trial object's pre-history. In contrast, variability in the measurements of non-living objects, as it is the case in classical physics or chemistry is caused almost exclusively by errors in the measurement and realisation of experiments, and not by the individual history of the objects of the investigation. Here, variability is more a question of instrument precision than an object characteristic.

When forest growth is recorded, analysed and modelled, processes and structures are broken down into increasingly smaller units of time and space (cf. Chaps. 1 and 15). On these scales, the variability of biological processes and structures is very obvious. Rougher statistical observation methods, such as for the generation of yield tables, describe the average behaviour of a large number of single findings, and also effects by aggregating measures, for example the development of mean height. Here, the mean of present state, and increment measures of groups (e.g. stand mean measures) or time periods (e.g. periodical increments) smoothes and

eliminates biological variation. To reproduce biological variability of processes and structures in models as well, variation needs to be quantified and integrated into models as a stochastic component.

10.6.1 Quantifying Variability

The most important statistical measure for condensing a sample of single values $x_1, x_2, \ldots, x_n$ is their mean value

$$\bar{x} = \frac{(x_1 + x_2 + x_3 + \cdots + x_n)}{n} = \frac{\sum_{i=1}^{n} x_i}{n}. \tag{10.46}$$

The mean value is also an important reference value for biological variability although the most simple measure of variability, the variation range

$$VR = x_{max} - x_{min} \tag{10.47}$$

results from the difference between highest and lowest single value of the sample variables $x_1, x_2 \ldots x_n$. The variation range VR, among other things, is used to quantify scattering, to quantify the repetitions needed in trial plot planning. A much better measure for characterising statistical scattering is the variance:

$$s_x^2 = \frac{\sum_{i=1}^{n} (x_i - \bar{x})^2}{n-1} = \frac{\sum_{i=1}^{n} x_i^2 - \frac{\left(\sum_{i=1}^{n} x_i\right)^2}{n}}{n-1}, \tag{10.48}$$

which quantifies the mean square deviation of measured values from their mean value. The square root of the variance is the standard deviation, or the scattering about the mean value:

$$s_x = \sqrt{s_x^2}. \tag{10.49}$$

A typical example of the standard deviation is a scattering about the stand mean height of, e.g. $s_x = \pm 50\,\text{cm}$, or about the arithmetic mean diameter of, e.g. $s_x = \pm 5\,\text{cm}$. If the measured values are normally distributed (see below), we can assume that 68.3% fall into an interval of $\bar{x} \pm 1 \times s_x$, 95.5% into an interval of $\bar{x} \pm 2 \times s_x$, and 99.7% into an interval of $\bar{x} \pm 3 \times s_x$. The variation coefficient V relates the standard deviation s_x to the mean value $\bar{x}$:

$$V = s_x\% = \frac{s_x \times 100}{\bar{x}}. \tag{10.50}$$

Through such a transformation, the variation coefficient has no absolute dimension as the physical dimensions cancel out, and measurement results with very different origins and physical dimensions become comparable with respect to their variation.

In the following, it will be important to distinguish between statistical parameters of a measured random sample and the commonly unknown distribution measures of the entire population. Accordingly, we will label the population mean and standard deviation (mostly theoretical) μ and σ, respectively. The actual, measured mean and standard deviation of a random sample is denoted $\bar{x}$ and s_x, respectively.

Not only single values $x_1, x_2, \ldots, x_n$ display scattering but also mean values of random samples $\bar{x}_1, \bar{x}_2, \ldots, \bar{x}_3$. If, from a statistical population, different sets of sample values are selected, and the mean values $\bar{x}_1, \bar{x}_2, \ldots, \bar{x}_n$ are calculated for each set, then the scatter of those mean values will be pronounced more or less around the real (unknown) mean μ. The scattering of the mean is termed standard error of the mean, and can be estimated from a single sample by dividing the standard deviation of the single value $\sqrt{n}$:

$$s_{\bar{x}} = \sqrt{\frac{s_x^2}{n}} = \frac{s_x}{\sqrt{n}}. \tag{10.51}$$

Similar to the variation coefficient, the division of the standard error $s_{\bar{x}}$ by $\bar{x}$ gives the relative standard error of the mean (in %):

$$s_{\bar{x}}\% = \frac{s_x \times 100}{\bar{x}}. \tag{10.52}$$

The standard error $s_{\bar{x}}$ is, e.g. used to calculate the confidential intervals, which contain the true mean with a certain level of probability. Since, in (10.51), the sample size appears in the denominator as $\sqrt{n}$, the standard error decreases with increasing sample size, i.e. the estimation gains in accuracy.

A measured value x can deviate more or less from mean value $\bar{x}$. As small deviations from the mean value are more frequent than large ones, the histogram of the error distribution (=probability function) often follows a Gaussian distribution. The frequency y (or marginal probability) of a certain deviation from the mean $\bar{x}$ is given by

$$y = f(x) = \frac{1}{\sigma \times \sqrt{2 \times \pi}} \times e^{-\frac{1}{2} \times \left(\frac{x-\mu}{\sigma}\right)^2}. \tag{10.53}$$

The Gaussian distribution is bell-shaped with the maximum at the mean value μ. Beneath the curve, 68.3% of the area occurs between $\mu \pm 1 \times \sigma$, 95.5% between $\mu \pm 2 \times \sigma$, and 99.7% between $\mu \pm 3 \times \sigma$. A normal distribution with the parameters μ and σ is represented by $N(\mu, \sigma)$. The N(0,1)-distribution is called standardised normal distribution with the mean $\mu = 0$ and $\sigma = 1$:

$$y = f(z) = \frac{1}{\sqrt{2 \times \pi}} \times e^{-\frac{z^2}{2}}. \tag{10.54}$$

It can be obtained from the normal distribution $N(\mu, \sigma)$ by standardisation:

$$\frac{x - \mu}{\sigma} = z. \tag{10.55}$$

In this operation, all measured values $x_1, x_2 \ldots$ are adjusted to a mean value and related to the standard deviation. From this standardisation, the term standardised normal distribution results.

10.6.2 Reproduction of Variability

Methods for the model reproduction of variability are used, for instance, in the generation of stem number–diameter distributions, tree spacings, modelling mortality, or for integrating natural scattering in model equations parameterised by regression analysis (Chap. 11). All these applications are based on the notion of understanding and quantifying the natural variation in processes and structures, and of introducing natural variability into models with the aim of obtaining realistic confidence intervals for simulations as well.

The $N(0,1)$ distribution (10.54) introduced in the preceding paragraph is very important for reconstructing biological variability. The standardised normal distribution $N(0,1)$ is helpful, since the probability–density function of any (assumed) $N(\mu,\sigma)$ distributed variable x (with known $\bar{x}$ and s_x) can be derived from z in a linear transformation (cf. (10.56)):

$$x = z \times s_x + \bar{x}. \tag{10.56}$$

So, how can we obtain the standard normally distributed measures z, and, if required, the random numbers from exponential, gamma, or lognormal distributions? In the following the procedure is outlined using $N(0,1)$ distributed random numbers by way of example. In this case, we start with random numbers distributed uniformly in the interval [0,1], which can be calculated according to the multiplicative congruence method, or read from random number tables (Bratley et al. 1983). This series of random numbers $r_1, r_2, \ldots, r_n$, which generates values between 0 and 1 with equal probability, is transformed now in such a way that its probability–density function approaches the standardised normal distribution. It makes sense to assign the value of $r = 0.5$ to the mean, i.e. $z = 0$. Correspondingly, r-values between $0.16 < r < 0.84$ (68% of the r-values) lie between $-1 < z < 1$. The simplest way of carrying out this transformation is with the inverse integral of the standardised normal distribution $N(0,1)$ (Fig. 10.23). For the generation of almost standard normally distributed values z, for example, the following simplified algorithm stood the test: for each uniformly distributed random number $r_i = r_1, r_2, \ldots, r_n$ in the interval [0,1] ($n \geq 12$), the random number z can be calculated. e.g. as

$$z = \frac{\sum_{i=1}^{n} r_i - \frac{n}{2}}{\sqrt{\frac{n}{12}}}. \tag{10.57}$$

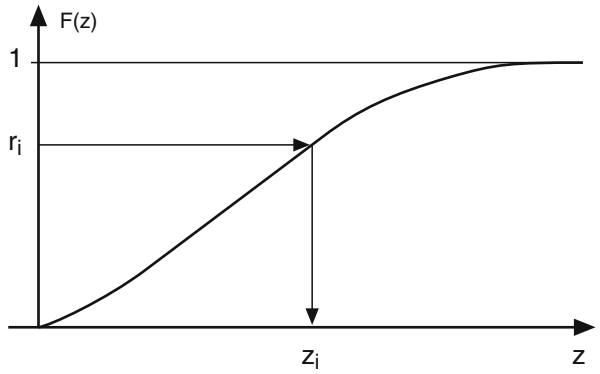

Fig. 10.23 The inversion method starts with random numbers r_i uniformly distributed on the interval [0, 1], and calculates the transformed random numbers $z_i = F^{-1}(r_i)$ via an inverse function of $F(z)$. Starting with a random number r_i on the ordinate axis, the corresponding z_i can be read off the distribution function $F(z)$ on the abscissa (according to Bauknecht et al. 1976)

Other methods for the generation of uniformly distributed random numbers, and for their transformation into non-uniformly distributed random number can be taken a.o. from Bauknecht et al. (1976) and Bratley et al. (1983). After transforming uniformly distributed random numbers into standardised normally distributed numbers, the linear transformation (10.55) supplies the $N(\bar{x}, s_x)$ distributed x-values needed for further processing.

Similar to the reproduction of scattering about a mean, the scattering about a regression line also can be reproduced. This makes it possible to model not only the scattering given by a functional relationship (explained variance), e.g. between height and diameter $h = f(d_{1.3})$, but also the residual scattering due to genetics and stand history. In that case, the height h assigned to a certain diameter $d_{1.3}$ does not have the same value always, but scatters within a certain range.

The simplest case of integrating residual scattering into a prognosis is by calculating the mean $\bar{x}$ and standard deviation s_x of the residuals (whereby in an undistorted parameter estimation the mean of the residuals should equal zero, i.e. homoscedasticity). Then, the prognosis can be completed by adding the residual scattering from normally distributed random numbers. If the residues are not normally distributed with a mean of zero over the predicted regression values (i.e. heteroscedasticity), it is wiser to calculate a mean value function of residuals in relation to the predicted values, and thereby make the distribution of the standard deviation dependent on the predicted values.

If, for example, the point cloud from Fig. 10.24a is fitted by regression analysis with the regression line $y = f(x)$, the variability of y is expressed by the scattering of measurement values about this regression line. If not only the regression line $y = f(x)$, but also the scattering about the line is to be reconstructed, this can be done by the method of random numbers described above. Since the standard deviation of the residuals about the mean increases with increasing y_{pred} (Fig. 10.24b), and the mean value of the residuals partially deviates from zero, the mean m and standard

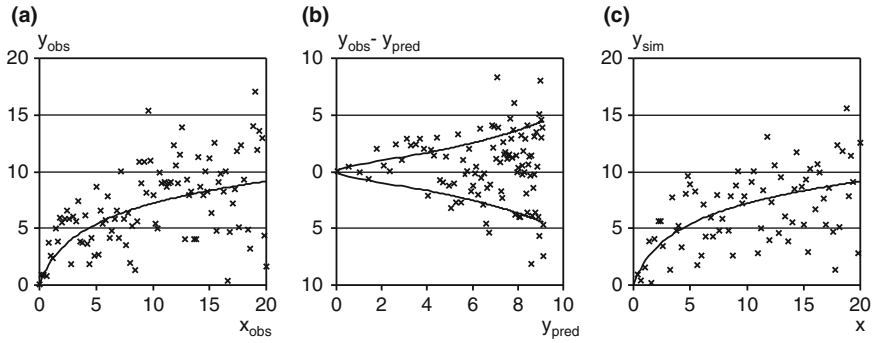

Fig. 10.24 Consideration of random effects in model equations of growth simulator SILVA 2.2 depicted in schematic array (obs observed values, pred predicted values). (**a**) Regression-analytical fitting of the x, y-pairs: $y = f(x)$; residues y_{obs}–y_{pred}, plotted over y_{pred}. (**b**) Mean value m and standard deviation s of the residues are modelled as a function of y_{pred} with $m = f(y_{pred})$, and $s = f(y_{pred})$ respectively. (**c**) for y_{sim}, residual values $m(y_{pred}) + s(y_{pred})$ are added to the estimation value y_{pred}

deviation s of residuals are modelled as a function of y_{pred} : $m = f(y_{pred})$ alias $s = f(y_{pred})$. After calculating the residuals from the transformation of the uniform z-values to normally distributed z-values (10.57), the y_{pred}-dependency of the residuals is accounted for by the function $m(y_{pred}) + s(y_{pred})$ and added to the z-value. These new z-values are then transformed to the actual y-values using (10.56). This way, the simulated relation between x and y_{sim} in Fig. 10.24c is constructed from its determinative component (black continuous regression line) and a stochastic component (deviation of crosses from regression line).

Summary

In forest ecosystems, biological variability makes it difficult to reveal strict functional laws as in physics or mathematics. We must be content with stochastic relationships, which we call biological relationships or rules. The growth relationships at the individual-tree and stand level, and the biological variability of these relationships, are of particular interest in forest growth and yield science. This chapter introduces a number of established growth relationships, and shows how to separate deterministic components from stochastic components of growth, which is important when simulating the growth behaviour of biological systems in models.

(1) The growth response of an organism follows a unimodal dose-effect-curve when the dose of a particular growth factor is increased under ceteris paribus conditions. In this curve, growth commences above a certain threshold value (minimum), increases up to an optimum, and at some point in time decreases until it becomes zero again at a certain maximum value.

(2) Allometry is concerned with the description and causality of deterministic size relations in and between organisms. As size and shape relations reflect the result of the phylo- and ontogenetic evolution towards a functional optimisation, the study of allometry seeks to understand the adaptations of living organisms to their environment.
(3) Allometry at the individual plant level relates the relative growth rate dy/y of one organ to the relative growth rate dx/x of another organ, or entire body ($dy/y/dx/x = \alpha$). α determines the ratio of relative growth rates of y and x, and is called the allometric exponent as integration of the above equation results in $y = a \times x^{\alpha}$. The allometric exponent α can be understood as the distribution key of the growth resources: when x increases by 1%, y increases by α%.
(4) Allometry at the individual plant level is regarded as the result of a distribution process, in which the growth resources of the entire organism are distributed between the organs according to a certain distribution key. Examples are height-diameter allometry and crown width-tree height allometry. Environmental changes can lead to deviations in allometric development, i.e. abrupt changes in the allometric exponent α.
(5) Despite the complexity of the processes involved, growth and yield at the scale of the individual organism often exhibit astonishing regularity, which can be described with relatively simple growth and yield functions. We introduce Bertalanffy's (1951) function as an example for a growth function, which is deduced theoretically by combining ecophysiological reasoning and the allometric relationships introduced in the previous section.
(6) Established growth and yield functions are introduced (yield function results from the integration of the growth function, growth function from the first derivative of the yield function) that try to quantify the principles of tree growth at the macro level: functions by Hossfeld, Gompertz, Bertalanffy, Chapman-Richards, Levakovic, Korf, as well as the logistic function and the monomolecular function. These functions describe changes in tree diameter, height or volume over time, and define growth as balance of increase and loss effects.
(7) Allometry at the stand level describes how the number of plants N per unit area decreases if resources are no longer sufficient for all individuals and self-thinning commences. For the relationship between tree number N and quadratic mean diameter d_q in fully stocked, evenaged forest stands, Reineke (1933) defined the "stand density rule" $N = b \times d_q^{-1.605}$.
(8) With no knowledge of the stand density rule by Reineke (1933), Kira et al. (1953) and Yoda et al. (1963) discovered the $-3/2$ power rule of self-thinning, initiating probably the most prominent controversial discussion of a scaling rule. It describes the relationship between the average shoot weight $\bar{w}$ and the plant number N per unit area in evenaged and fully stocked monospecific plant populations as: $\bar{w} \propto N^{-3/2}$ with the species invariant scaling exponent $\beta_Y = -3/2$.

(9) Empirical investigations both at tree and stand level allometry show that allometry is a function of tree species, site conditions and stand history. It is therefore not surprising that the validity of generalised allometric rules such as Yoda's or Reineke's self-thinning rule or Enquist's fractal scaling rule have been discussed controversially.

(10) Assmann's concept of maximum, optimum and critical stand density assumes that volume growth increases with a reduction in stand density up to a certain optimum, and then decreases with a further reduction in density. The capacity of the remaining stand to buffer, or even overcompensate the lost growth potential of the removed trees declines with increasing age.

(11) In principle, the density-growth relationship follows a unimodal curve, but depending on the observed range of densities, stand development phases, and site fertility, we may perceive only a particular – apparently asymptotic – portion of the curve. Growth acceleration after thinning is rather a function of the size that the trees have achieved already (i.e. the physiological age) than of their true physical age. This way, a stand's capacity to respond to thinning with increased growth should also be viewed as a function of the reached size (which depends on the previous silvicultural treatment) rather than on the true physical stand age.

(12) Due to biological variability, measurements of target response variables are scattered around a mean value, e.g. tree diameters around the stand mean diameter, volume increment of certain variants around the mean volume increment of all repetitions. This scattering is caused by uncontrollable or uncontrolled influences of site, weather, climate, competition situation, genetics, etc. Biometrical formulation of, e.g., growth functions, dose-response curves or stand density-growth relationships eliminates such variation. In order to reproduce this biological variability of processes and structures, variation needs to be quantified and integrated into models as a stochastic component.

Chapter 11
Forest Growth Models

The earliest abstractions and models of forests are maps. Displaying the availability and localisation of resources like forest stands, forest pasturage, hunting grounds, or beehives, they reflect the concept of multiple use (cf. Fig. 11.1 for illustration). The subsequent history of forest models is not a continuum of better models constantly superseding earlier, inferior ones. Instead, different model types with diverse objectives and conceptions were developed simultaneously. The objectives and structure of models reflect the state of the art of the particular research area at the time, and document the contemporary approaches to forest growth prediction. In this sense, the history of forest growth modelling also provides a record of the expanding knowledge about forest functions and structures, as well as the increasingly sophisticated methods of long-term forest growth forecasts.

Beginning with yield tables for large regions, the basic unit for taxation and planning, model development progressed to sub-regional and site-specific yield tables and culminates in the construction of growth simulators for the evaluation of stand development under different management schemes. From the 1960s to 1980s, Vuokila (1966), Fries (1974) and Dudek and Ek (1980) summarised the state of forest growth modelling. Since then forest growth modelling has developed rapidly, benefiting greatly from the expansion in computer capacity (e.g. Franc et al. 2000; Pretzsch 1992a; Sterba 1989a; Wenk et al. 1990). Vanclay (1994) provides an overview of growth and yield management models and their application to mixed tropical forests. The 1960s brought about a new trend with the development of ecophysiological models, which establish complex causal relationships to predict forest growth processes in relation to ecological conditions. These models followed a biocentric view aimed at supporting a sustainable management of the carbon and nutrient balance. Initially, ecophysiological models, which did not take spatial structure into account, were later combined with yield simulators or complemented with explicit tree dimensional modelling (for overviews see Battaglia and Sands 1998; Mäkelä et al. 2000; Le Roux et al. 2001). With increasing computer power, physiologically based models were applied on a landscape scale to serve ecoregional management. Recent models actually consider horizontal flows of energy or matter

H. Pretzsch, *Forest Dynamics, Growth and Yield: From Measurement to Model*,
DOI: 10.1007/978-3-540-88307-4_11,

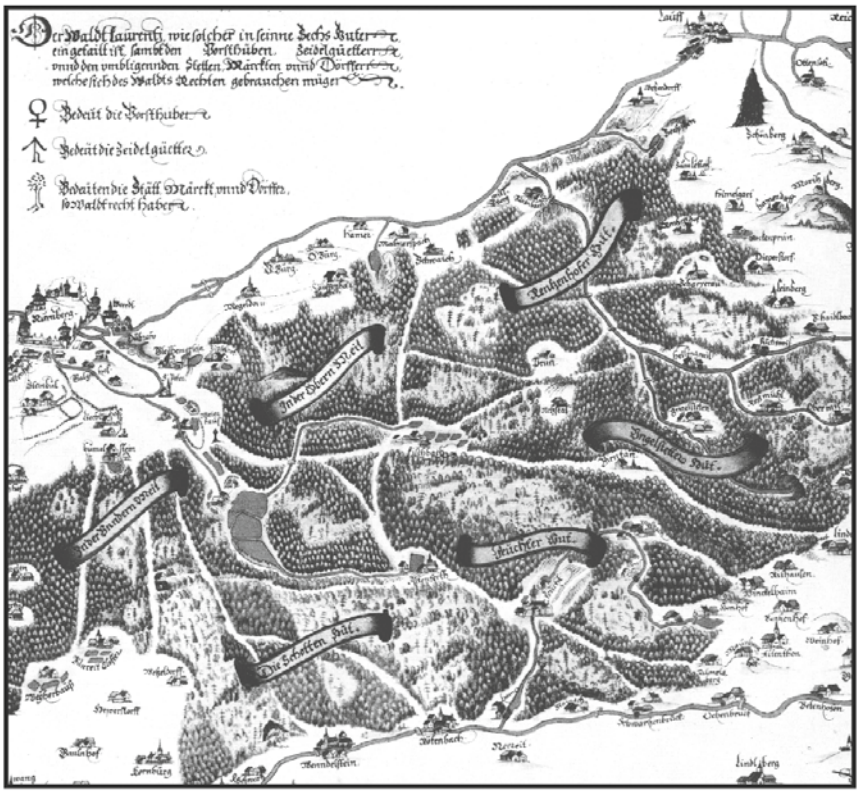

Fig. 11.1 Map from the "Lorenzer Wald" near Nürnberg, Germany as an example of a simple model for forest ecosystem management. By locating forest resources like hunting grounds, beehives, and mature forests ready for harvest, this map from Paulus Pfinzing illustrates the multiple use paradigm in the sixteenth century (Hilf 1938, pp. 184–185). Legend: Mitternacht. Der Wald Laurentz, wie solcher in seinne sechs Huten eingetailt ist, sambt den Forsthüben, Zeidelgüettern, unnd den umbligennden Stetten, Märckten unnd Dörffern, welche sich des Waldts Rechten gebrauchen mügen. Bedeüt die Forsthuber. Bedeüt die Zeidelgüetter. Bedeüten die Stätt, Märckt, and Dörffer, so Waldrecht haben. Inscription: The Laurentz forest has being divided into its six forest districts with their the ranger stations, and shows the customary rights of forest use of the beekeepers, and the people living in towns, market towns, and villages. The symbols in the legend indicate the stations of rangers, apiarists, towns, market towns, and villages, which have proper rights of use of the forest

between sites. These landscape approaches are still in their infancy. At the same time, progress is also made with graphical representations at a both site and landscape scale, enabling visual planning aspects such as landscape aesthetics to be taken into account. This chapter is intended to give the reader an overview of the different modelling approaches at the tree, stand and ecosystem levels.

11.1 Scales of Observation, Statistical and Mechanistic Approaches to Stand Dynamics

11.1.1 Scales of Forest Growth and Yield Research and Models

The complexity of forest processes and structures increases with the temporal and spatial level of integration from seconds to thousands of years, and from molecules to landscape units, respectively. At the same time our knowledge of processes, which range from physiological to chemical processes at the molecule and cell level to evolution and succession processes at the ecosystem and regional level, declines because the processes and structures at higher levels of aggregation are much more difficult to access experimentally (Leuschner and Scherer 1989). The grey window in Fig. 11.2 shows the spatial–temporal scale of observation in forest growth research and modelling. The spatial scale ranges from tree parts (e.g. crown shape analyses) to regions (e.g. regional growth and yield predictions). The time scale ranges from days (e.g. electronic dendrometer measurements) to decades and centuries (e.g. repeated surveys in thinning trials). Thus, forest growth research is concerned rather with the slower processes occurring on a moderate to large spatial scale.

As in any biological system, the processes at a certain level of integration are more than the mere sum of the subordinate process components in the system hierarchy (cf. Fig. 1.11). The feedback mechanisms between processes in the same or different hierarchies shape the complex behaviour of biological systems. This behaviour cannot be deduced from the isolated process components alone. For

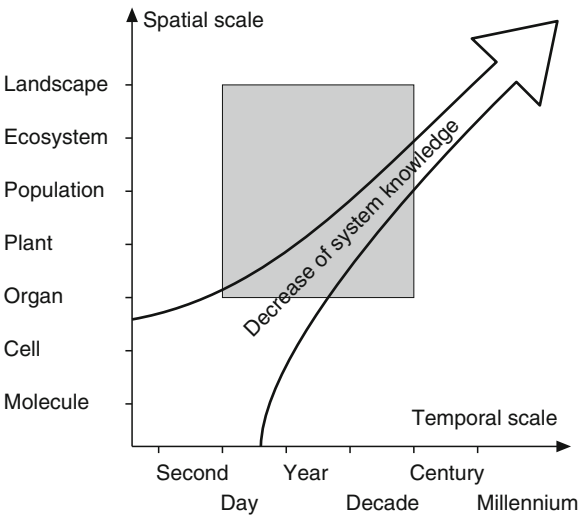

Fig. 11.2 The spatial–temporal range in observation for forest growth research and modelling (*area shaded grey*) reveals a high degree of system complexity that is difficult to approach experimentally

example, research and modelling approaches for forest health that merely focus on soil processes or plant physiology would lead almost certainly to the prediction of far-reaching destabilisation and stand break up. The extent to which specific stressors affect stand growth would be overestimated, and the buffering capacity of stabilising cross-scale feedback loops would be underestimated. Thus, the dieback scenarios predicted by high-resolution process models have rarely come true. Despite all experimental accuracy, knowledge of soil chemical, biochemical or physiological process components with high spatial and temporal resolutions cannot replace the highly integrated data from forest growth and yield research such as those carried out on long-term trial plots. In particular, the information available from the historical time series data from study sites is essential for a comprehensive understanding of systems and model evaluation.

11.1.2 From the Classical Black-Box to White-Box Approaches

Until today, forest growth research in various countries has generated an impressive empirical database. Based on records of the resource supply, environmental conditions (causes) on experimental plots and the growth responses of individual trees and whole stands as determined from measurements of diameter, height and crown growth (effects), forest growth research reveals stochastic relationships between cause and effect, and draws conclusions about the behaviour of the system. Especially early model approaches did not really consider the underlying processes (e.g. photosynthesis, respiration, transpiration, nutrient uptake, allocation, senescence, and mortality) in these relationships.

Such approaches are described as black-box approaches since we remain in the dark, to a large extent, about the inner structure of the system and the underlying causal relationships. Only the systems behaviour is explained statistically, not the structure and function of the system. The description of the relationship determined by regression analysis between the amount of nitrogen inputs in a forest stand and the wood production provides an example (Fig. 11.3). When the modelling approach includes the system elements and their interactions, we speak of a white-box approach. Here, the effect of the nitrogen on photosynthesis, allocation and decomposition processes would be described so that the stemwood production would be obtained from the underlying ecophysiological processes (Fig. 11.4).

Early forest growth research pursues the traditional black-box approach with the aim of merely predicting the behaviour of the system. Its main interest is to describe, analyse and predict accurately the overall behaviour of biological systems, be it tree growth, stand development, or age class rotation at the forest estate level. In the past, the accurate and rapid forest growth predictions from these approaches have supported well the demands of decision makers in forestry and environmental politics for realistic information based on an empirical database.

From the perspective of a plant physiologist, the purely statistical link between input and output parameters presented in Fig. 11.3 would be regarded as a black-box

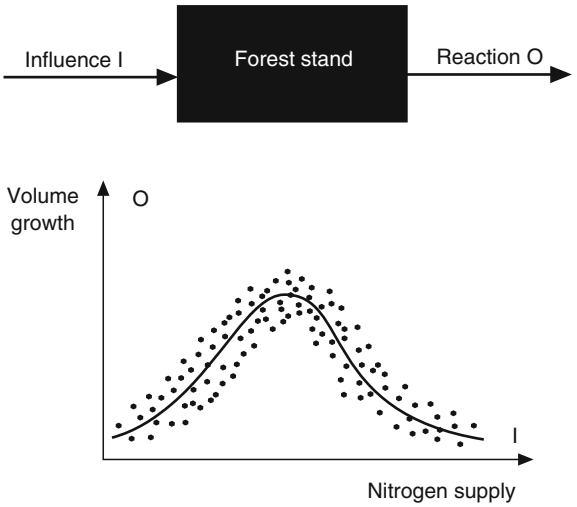

Fig. 11.3 In black-box approaches, statistical correlations between cause and effect variables, for example nitrogen input and growth response, are used to describe and reproduce the system behaviour. Individual processes and structures of the system are not resolved

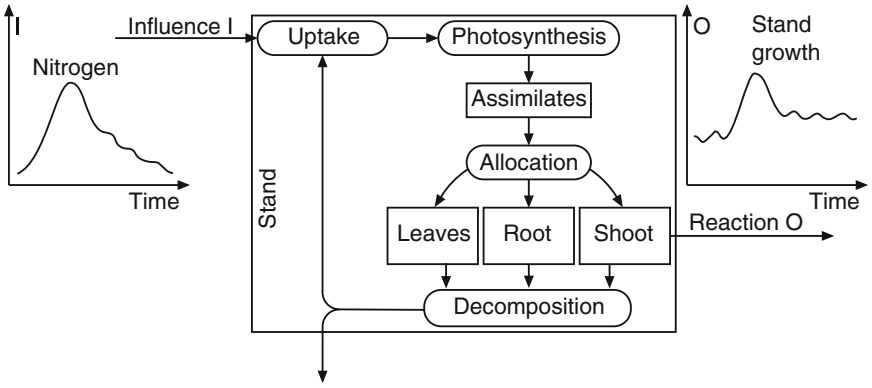

Fig. 11.4 If, for example, the response of a forest stand to nitrogen input in separate individual processes and structures is determined to understand a system, one speaks of a grey-box or white-box system depending on the degree of resolution

method. However, from the viewpoint of a forest manager or geobotanist, who is used to thinking on the scale of age classes, an entire forest enterprise, or larger vegetation units, stand-based relationships between nitrogen availability and growth represent a rather high resolution, detailed white-box approach. Whether an approach is regarded as a black-box approach that describes the system behaviour, or as a white-box approach, that explains and reflects the structure of the system, is therefore relative, and essentially depends on the perspective of the observer and the level at which they work within the system (Berg and Kuhlmann 1993). Forest

growth processes, structures and growth relationships certainly are observed and analysed at a broad range of different levels.

In stable ecosystems, macro-structures and slow processes determine the processes at higher levels of resolution (cf. Chap. 1). However, the relationships statistically derived for stable systems cannot be transferred directly to other ecological conditions. If one assumes that the physiological response to environmental changes is rapid and consistent, the establishment of short-term experiments possibly may be sufficient to forecast long-term growth responses. In the view of an increasing instability in forest growth due to atmospheric pollution, increased NO_x deposition, atmospheric CO_2 concentrations, and climate change, forest growth research cannot restricted itself to statistical links between system variables at high levels of aggregation, but must understand and predict the responses of forest ecosystems. Hence, the development of ecophysiological process models has gained momentum as they model forest growth on the basis of physiological cause–effect chains and interactions between the system processes even though little or nothing is known about their impacts in the long-term.

In such models, processes need to be included at a higher temporal and spatial resolution to gain an understanding of systems behaviour and to make realistic predictions. Often, black-box approaches are modified to grey-box or white-box approaches when they are supported by a deeper knowledge of structure and processes. The transition in terminology from black–grey–white reflects how processes and structures not yet understood or considered, are gradually resolved and included in the system model. The statistical relationships then are replaced by process knowledge from subordinate levels in the hierarchy, and explained in biological terms.

11.1.3 Top–Down Approach vs Bottom–Up Approach

This cautious advance from lower to higher resolution and complexity and from the upper to the lower levels in the process hierarchy (Figs. 1.11 and 1.12) is called the "top–down" approach. It commences with the observation and reproduction of macro-structures and processes; the "black-box", defined at first statistically, is gradually filled with more systems understanding.

Alternatively, the system may be developed using a "bottom–up" approach where the systems understanding builds upon the integration of all known process components and their interactions from the bottom to the top. This does not necessarily produce a more realistic prediction and a better understanding of the overall behaviour of the system (Landsberg 1986). However, neither approach is right or wrong. Rather, they are more or less suitable for a given purpose and state of knowledge.

For example, the first descriptions of the relationship between site fertility and growth performance were based on standing volume or tree height as an indicator of site conditions (Baur 1876; Perthuis de Laillevault 1803). The descriptive approach merges with the site index system used today, which forms the backbone of the pure

stand yield tables (cf. also Assmann 1961a; Eichhorn 1902; Gehrhardt 1909). The description of growth performance based on ground vegetation as in Scandinavia (Cajander 1926; Keller 1978) or on the basis of site variables on a nominal or ordinal scale (Kahn 1994; Moosmayer and Schöpfer 1972; Wykoff et al. 1982) approximates the actual processes more closely. A higher resolution of the processes and structures of biological systems is gained from the description of stand growth on the basis of ecophysiological processes such as photosynthesis, respiration, transpiration and nutrient uptake (Bossel 1994; Grote and Erhard 1999; Mäkelä and Hari 1986; Mohren 1987). Even this approach may appear crude and simplistic from the viewpoint of a geneticist or microbiologist. But, as the interest in detail increases, it is important to maintain the links between the individual system elements, and to ensure that the importance of the single elements for the whole is understood. This must include an understanding of structures and processes across the various hierarchical levels.

11.2 Model Objectives, Degree of System Abstraction, Database

We speak of a model when a real system, for example a forest stand, has been abstracted and reproduced biometrically. The model, or system model, collects, organises and aggregates reliable knowledge bases in a system algorithm. When a system model is converted into a useful computer program, one creates a forest growth simulator that, with the help of the computer, can reproduce the behaviour of the system and perform scenario and prediction computations. Through the organisation, synthesis and utilisation of forest growth knowledge, forest models and growth simulators can expand both the basic and applied knowledge required in forest management and forest science equally. Thus, model development and system simulation are of paramount importance for forest growth research.

The aim and purpose of a model, as well as the state of knowledge about the system considered, determines the degree of complexity necessary, or possible, and the temporal and spatial resolution of the model. The temporal scale may range from seconds to thousands of years, the spatial scale from the cell and mineral surfaces up to the vegetation zone, resulting in ecophysiological process models, individual-tree models, yield tables, gap models, landscape and biome shift models (Fig. 1.17).

Just as a hiking map with the scale 1:1 is too detailed for a hiker, a spatial and temporal degree of complexity describing processes and structures in second or minute time-step and at the cell or plant organ level may overlook the information needed by forest practice for decisions at the stand level. However, if the system to be managed and the effects and performance expected of it are very complex and should include diverse environmental effects and management options, then highly detailed systems knowledge also is required to permit a high spatial–temporal resolution and reliable simulation results.

11.2.1 Growth Models as Nested Hypotheses About Systems Behaviour

Forest growth models and their realisation in simulators are simplified purpose-oriented representations of reality. Therefore, object-specific characteristics of forest systems, such as longevity, historical factors, openness and structural features (cf. Chap. 1) should guide the conceptualisation and development of models. The systems model with its underlying elements, links, and, in particular, the cause–effect chains may be regarded as a series of network hypotheses about the structure and behaviour of the real system. The evaluation of a model, and testing of its aggregated hypotheses in form of system elements and causal relationships is carried out via simulation runs, whereby simulation is defined here as the reproduction of system behaviour with the aid of a computer (Berg and Kuhlmann 1993; De Wit 1982). Simulation models, and their corresponding simulation runs, are an important tool for testing hypotheses and acquiring knowledge in forest growth research (Chap. 15).

Hypotheses about single aspects of forest growth, for example whether diameter growth of unpruned and pruned trees differs, can be tested with statistical standard methods, e.g. by variance analysis. However, the evaluation of growth models, which comprise a network of hypotheses about structures, processes, and cause–effect relationships, is more complex. This is carried out through simulation runs. The underlying model assumptions are tested by comparing simulation results with experimental data.

11.2.2 Growth Models as a Decision Tool for Forest Management

Growth models and forest growth simulations play an important role in forest management due to the longevity of trees and forest stands. In contrast, the growth and treatment of new varieties of agricultural crops such as sunflowers, rape or corn can be tested experimentally in a matter of days or months prior to large-scale cultivation. This is generally possible for organisms with a life expectancy of one or several orders of magnitude lower than that of humans. Due to the longevity of forest stands, new silvicultural regimes simply cannot be tested experimentally; upon completion of such a test after several years to decades, the previously acute question may long be outdated.

Therefore, forest growth research derives tree growth relationships from already established experimental plots and aggregates the results in forest growth models. These models enable forest stand growth for the desired silvicultural regime to be modelled in time-lapse. The yield-related, financial and ecological consequences of new management regimes or disturbances can be predicted without establishing new experiment.

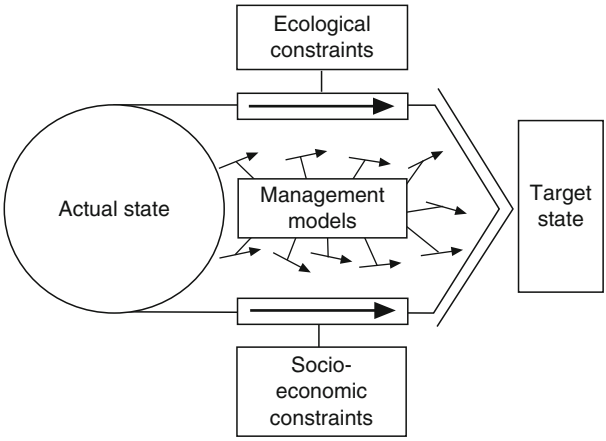

Fig. 11.5 Management models support decisions within a given range of possibilities (*framed arrows*) by predicting the long-term consequences of treatment variants (*mobile arrows*). The different treatment options can be analysed with mechanistic model approaches on stand and landscape level

By using them as a research tool, growth models can replace experiments to a certain degree. Within defined limits, models can predict forest developments under changed site conditions, variations in silvicultural concepts, or changes in the intensity and frequency of disturbances. This is not possible in practical experiments. Ecophysiological process models, on the other hand, facilitate the determination of a range of options, or a framework of forest management strategies for a given site. They assist the definition of boundaries within which forest management practices do not endanger the stability of the system (Fig. 11.5).

The transition from management models such as yield tables, diameter distribution models or position-dependent individual-tree models, to more complex models such as succession models or ecophysiological process models, promotes the need for a more complex database for model generation and parameterisation. The following series of models, commencing with experience tables and yield tables as a prototype of descriptive stand growth models, progressing to mechanistic ecophysiological process models, simultaneously describes the fundamental change in the understanding of forestry systems, as well as changes in the information supply and demand in forest management. They should not be regarded as a chronological sequence in which poorer models are succeeded by better models each time. Rather the best model is the one that fulfils its purpose best. Thus, yield tables may be the best approach for forest management in countries where available forest growth data are incomplete, or where volume production is given priority. For the sustainable management of pure and mixed forest stands with detailed structural information, site sensitive individual-tree models may be more appropriate in some circumstances.

11.3 Growth Models Based on Stand Level Mean and Cumulative Values

The idea of modelling stand growth by the age development of mean and cumulative stand variables such as height, standing volume or volume growth for use in the assessment, planning and implementation of forestry operations has a history of more than 200 years. Beginning with the first "experience tables" at the end of the eighteenth century, the generation of stand growth models has become an important field of research in forest science. The principle of representing stand development in tabular form remains largely unchanged (cf. Tables 11.1–11.4). However, the underlying databases and the methods of modelling have undergone major changes. The following introduction to the broad spectrum of growth models will commence with the yield tables, which are particularly important as a reference in central Europe.

11.3.1 Principles of Yield Table Construction

11.3.1.1 Three Basic Relationships for Determining Total Volume Production

The following three relationships form the foundation of the yield tables commonly used. They are statistically derived from a large empirical data set (monitoring data, long-term experimental plots, permanent inventory plots), and allow site-dependent estimations of total volume production.

The first relationship:

$$\text{Height} = f_1(\text{age}) \tag{11.1}$$

states that forest stands at a given site follow a particular height development with age. The stand age–stand height scatter plot obtained from the monitoring plot data is divided into a number of height curves, which form the basis for the yield table construction. These height curves divide the data range into defined height growth pathways into, e.g. five site index classes. As the height curves are used for assigning stands to site quality classes we also call this first relationship (11.1) the site index assigning relationship.

Since the total volume yield for a given age, not mid-height is primarily of interest, but, a second relationship underlying the yield tables states that

$$\text{Total volume yield} = f_2(\text{height}) \tag{11.2}$$

which Assmann (1961a) described as an intermediate relationship since, if the relationship determining site index is known, this relation is merely an intermediate, though essential, step to the total volume yield–age relation.

The resulting third and final relationship is

$$\text{Total volume yield} = f_3(\text{age}). \tag{11.3}$$

Depending on the database available, the relationships (11.1)–(11.3) may be parameterised directly by fitting curves to the stand age, height and total volume yield data from given experimental plots. In Chap. 10, Sect. 10.3, we introduced a set of growth and yield curves, appropriate for this first step of model building. In a second step, the age development of total volume yield, and also for mean height, mean diameter, stem number, basal area is broken down into the remaining and removed stand (top down approach). The growth curve is obtained by differentiating the total volume yield curve in time.

Alternatively, the tables are generated from the development of volume by age with variables determining stand volume; i.e. mean height, basal area, form factor and stem number. In this approach, the primary relationships (11.1)–(11.3) are obtained by aggregating the individual relationships (bottom up approach). In both cases the mean site index curves of the different stand parameters are derived from graphs or by regression analysis and compiled in a table for the total, remaining and removed stand (Tables 11.1–11.4).

11.3.1.2 From Site Class Determinations by Volume to Determinations by Top Height

Despite some resistance in the beginning, the use of stand age and height for the estimation of stand productivity (11.1) has become so prevalent that the concepts site index and yield class are rarely distinguished from one another today. The approach of using plant production itself to define a site quality system dates back to the eighteenth century. At this time, sites were still classified directly by the standing volume (Fig. 11.6a).

This site classification by standing volume was only valid at the times when light and moderate thinning was common. With the transition to more intensive thinning concepts in the nineteenth century, the thinned-out fraction of total volume production increased so that the remaining volume increasingly lost its meaning as an indicator of site productivity. Because stand mean height is less dependent on stand density and thinning, it provided an alternative (Fig. 11.6b). With intensification of thinning from below, which significantly influenced the mean height in the mid-twentieth century, the reference height measure was switched to top height as an indicator of site quality (Fig. 11.6c). Yet we see that the basic idea of using stand volume or height growth as a “phytometer” for site productivity continues to the present day. However, again, this approach is being questioned as thinning from above and structurally diverse mixed stands are of increasing importance today. The more a stand deviates from an evenaged, single-layered structure, the greater the influence of the level of competition on tree height growth becomes. Thus, top height also loses its significance as an indicator of site fertility in highly structured mixed stands.

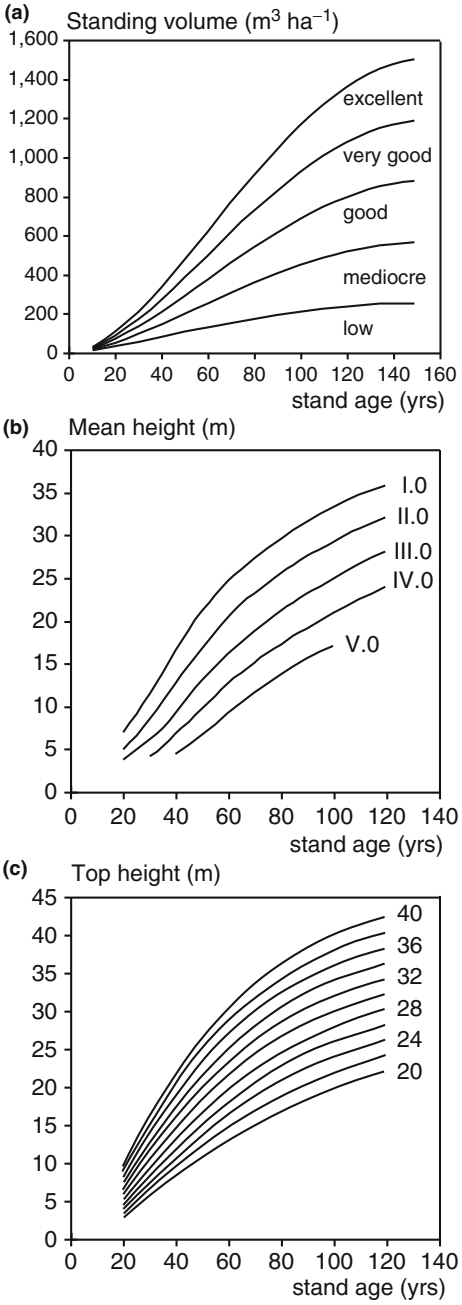

Fig. 11.6 From the determination of site class by volume to the determination by top height exemplified by Norway spruce. (**a**) The determination of site class by volume for "normal closed stands" from Pressler's (1877) tables. (**b**) Mean height site indices for moderately thinned stands from Wiedemann's (1936/1942) tables for moderate thinning from below. (**c**) Top height site indices from yield tables by Assmann and Franz (1963) for graduated thinning

11.3.1.3 From Eichhorn's Rule to Assmann's Sub-Divided Special Yield Levels

With improvements in the database from experimental plots, and in the knowledge of the principles of tree growth at the stand level, the intermediate relationship (11.2), which defines total volume production for a given height, has become more precise. In the beginning, the Eichhorn's rule (1902), which identified the statistical relationship between stand mean height and standing volume, was valid for more or less untreated stands (Fig. 11.7a). Gehrhardt (1909, 1923, 1930) refined Eichhorn's

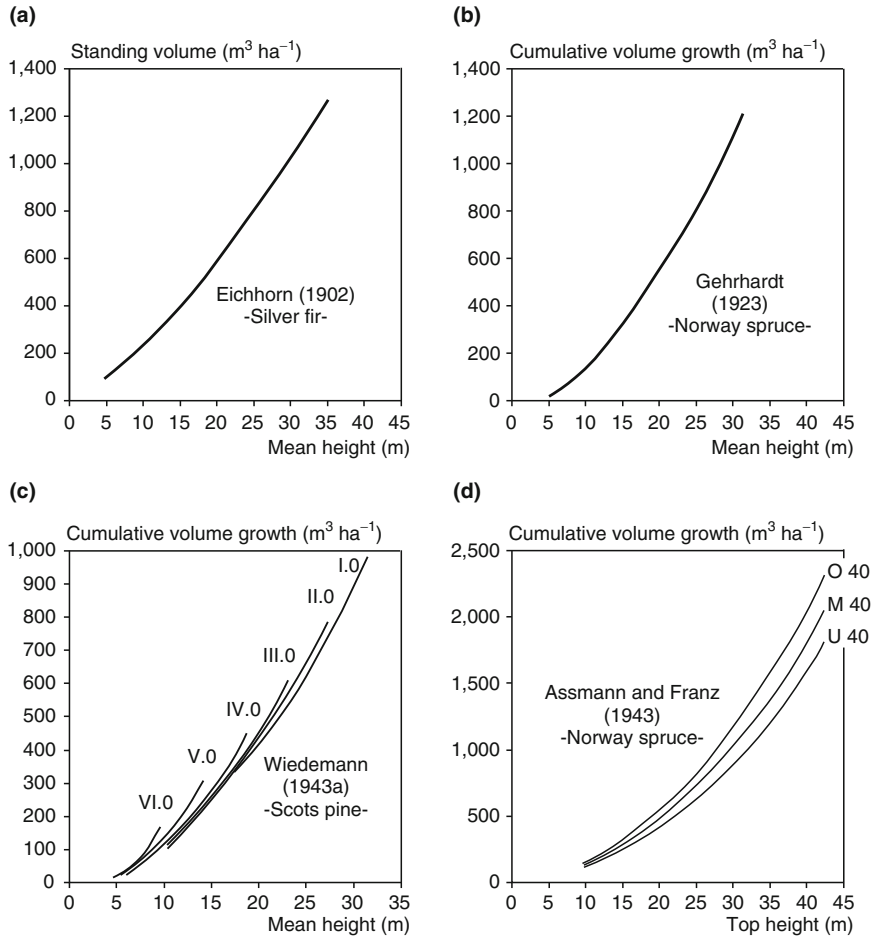

Fig. 11.7 From Eichhorn's rule to the sub-divided special yield levels by Assmann. (**a**) Eichhorn's rule (1902) Silver fir stands with moderate thinning. (**b**) Common yield levels from the Norway spruce yield tables for medium strong thinning from Gehrhardt (1923). (**c**) Special yield levels from the Scots pine yield tables for moderate thinning from Wiedemann (1943a). (**d**) Sub-divided special yield levels in the Norway spruce yield tables for graduated thinning and top height site index 40 from Assmann and Franz (1963)

rule twice based on the extended database from experimental plots. First, he found that total volume production was also closely related to mean height. Then he refined this relationship by specifying mean height–total volume relationships for each site index (Fig. 11.7b). In the first variation of Eichhorn's rule, Gehrhardt describes a site-independent height–volume relationship, later referred to as the common yield level by Assmann (1961a). The second variation is a site-dependent height–volume relationship, termed the "special" yield level by Assmann (1961a). It was used, for instance, in the Scots pine yield tables of Wiedemann (1943a, 1948) (Fig. 11.7c). In his evaluation of Norway spruce experimental plots in Southern Germany, Assmann found that the total volume yield of forest stands, even with the same age and mean height, may still vary by about $\pm 15\%$ depending on site conditions. Thus, Assmann and Franz (1963) sub-divided their Norway spruce yield tables into three subdivided special yield levels (low, medium and high, Fig. 11.7d). The development from the Eichhorn's rule to the estimation of total production in relation to age, height and yield classes reveals the increasing precision of the intermediate relationship (11.2) which, in turn, allows for a more realistic estimation of total volume production in relation to age [final relationship see (11.3)]

11.3.1.4 Strip and Indicator Methods

In the strip method introduced by Perthuis de Laillevault (1803) and applied by Baur (1876), important stand parameters such as mean height or stand volume were plotted against age based on a single cross-sectional survey of age on as many study sites as possible. Curves defining the upper and lower limits of the scatter plot are then added. The area between these limits is then divided into five strips by adding curves at equal distances apart at 120 years of age. Commencing at age zero, the five strips spread out proportionally up to the age of 120 years, and divided the age–size pair of measurements into five site index classes. The centre lines of the five strips delimit the average development of, e.g. height and stand volume. Strip method results only prove useful when the stands surveyed represent an actual growth series; that is their true height growth actually matches the constructed height curves of the age-cross-sectional survey.

As the congruency between the true growth behaviour of the experimental stands and the cross-sectional site index curves is not certain, R. Hartig (1868) used the indicator method to construct yield tables for Norway spruce in the Harz Mountain ranges in Northern–Central Germany. In addition to the traditional stand parameters, he also analysed individual tree growth by stem analysis on his study sites. Knowing the height growth over time from stem analysis, he was able to test whether growth at certain study sites corresponded to the determined growth series. One limitation of the indicator method is that stand level data, such as stand volume, mean height or top height develop differently from the corresponding values of sample trees. That is because mortality and tree removal leads to a shift in the tree collective used to calculate stand mean and cumulative values data while the individual tree dimensions remain unaffected.

If repeated survey data are available from study sites, the yield tables stratify and determine site index curves from the true mean height growth over time. Thus, on long-term monitoring plots, the true stand development over time can serve as an indicator of site index rather than the indicator method based on stem analyses, which is prone to error.

11.3.2 From Experience Tables to Stand Simulators

With a history of more than 200 years, yield tables for pure stands may be considered the oldest models in forestry science and forest management. They reflect stand growth over defined rotation periods, and are based on long-term measurements of diameter, height, biomass, etc. Early experience tables applied standing volume for the estimation of site fertility and volume growth; later, yield tables applied mean height and stand age as surrogate variables for estimations of site fertility and growth (Batho and Garcia 2006).

11.3.2.1 Experience Tables from Early Yield Table Research

The first instructions for the construction of yield tables originate from Réaumur in 1721 (cf. Schwappach 1903, p. 165). The period from 1787, when Paulsen developed the first German yield tables (Paulsen 1795), to the establishment of uniform principles for the construction of yield tables by the Association of German Forest Research Stations at the end of the nineteenth century (notably at the conferences in Eisenach in 1874 and Ulm in 1888) may be regarded as the initial phase of yield table research. The yield tables developed during this period represent the first generation of stand growth models. The contributions from Paulsen (1795) and Öttelt (1765) to the construction of yield tables triggered numerous subsequent investigations including those from Hennert (1791), Hartig (1795) and Cotta (1821). Further development of these initial approaches in the nineteenth century are closely linked to Hartig (1868), Hartig (1847), Heyer (1852), Hundeshagen (1823–1845), Judeich (1871), König (1842), Pfeil (1860), Pressler (1865, 1870, 1877) and Smalian (1837). This first generation of stand growth models and production tables was characterised by unsatisfactory databases, regional limitations, or restrictions to their validity, and the limited comparability of the methods due to the different methods used to construct the tables. By regarding these yield tables as experience tables, their descriptive and empirical character is emphasised, as is their immediate relevance for the requirements of the local forest management where the tables were developed.

Tables 11.1 and 11.2 present excerpts from the “experience tables for the yield that is to be expected from the most common tree species in Germany in closed stands under continuous management at different ages on different sites”

(Cotta 1821, pp. 33–34). The table for the determination of the site quality from Cotta (1821, p. 17) is based on standing volume at the age of 100 years (Table 11.1). The two numbers in each cell provide the upper and lower values for the stand volume at age 100 years in relation to tree species (columns) and site class (rows). To convert these values to today's standard of cubic meters per hectare, the stand volumes in Tables 11.1 and 11.2 must be multiplied by 0.04, since 1 ft $\hat{=}$ 0.28 m and 1 acre $\hat{=}$ 0.55 ha (Jordan 1877). The production-oriented site classes established in this way provide the input parameters used in tables for mean stand volume vs age (Table 11.2). In contrast to today's practice of classifying stands from the highest to lowest growth as I. to V. respectively, these experience tables classify the stands with highest standing volume as X. and the lowest as I.

Table 11.1 Class tables for determining the site quality in relation to stand volume from H. Cotta (1821, p. 17). The two numbers in each cell give the upper and lower ranges in stand volume at an age of 100 years in cubic feet per acre (1 ft $\hat{=}$ 0.28 m, 1 acre $\hat{=}$ 0.55 ha, 1 ft^3 acre^{-1} $\hat{=}$ 0.04 m^3 ha^{-1}). Translation of the legend: Klassentafel zur Bestimmung der Standortgüte = Table for the determination of the site quality; Klassen für die Güte der Standorte = Classes of site quality; Wenn ein Standort von der Beschaffenheit ist, daß auf einem Sächsischen Acker in 100 Jahren, bei einer regelmäßigen Bewirtschaftung, so viel Kubikfuß Holzmasse erwartet werden kann, wie hier unten angegeben ist; so gehört derselbe in vorstehende Klasse. = If the standing volume at the age of 100 years amounts to the number of Saxon cubic feet shown in the table below, it can be assigned to the corresponding site quality class

Klaffentafel zur Beftimmung der Standortsgüte.

Klaffen für die Güte der Stand- orte.	Wenn ein Standort von der Beschaffenheit ift, daß auf einem Sächf. Acker in 100 Jahren, bei einer regelmäßigen Bewirtfchaftung, fo viel Kubikfuß Holzmaffe erwartet werden kann, wie hier unten angegeben ift; fo gehört derfelbe in vorftehende Klaffe.								
	Fich- ten.	Tan- nen.	Kie- fern	Ler- chen.	Ahor- ne ꝛc.	Ei- chen.	Bu- chen.	Erlen ꝛc.	Bir- ken.
I.	1832 3692	2139 3983	2046 3846	3212 4852	1860 3276	2187 3115	1595 2633	1218 2662	944 2072
II.	3692 5551	3983 5827	3846 5647	4852 6492	3276 4691	3115 4042	2633 3672	2662 4106	2072 3204
III.	5551 7411	5827 7070	5647 7447	6492 8132	4691 6106	4042 4970	3672 4710	4106 5552	3204 4334
IV.	7411 9271	7070 9512	7447 9247	8132 9771	6106 7522	4970 5898	4710 5749	5552 6996	4334 5466
V.	9271 11131	9512 11356	9247 11048	9771 11411	7522 8937	5898 6825	5749 6787	6996 8440	5466 6596
VI.	11131 12990	11356 13199	11048 12848	11411 13051	8937 10352	6825 7753	6787 7825	8440 9884	6596 7728
VII.	12990 14850	13199 15043	12848 14648	13051 14691	10352 11767	7753 8681	7825 8864	9884 11328	7728 8858
VIII.	14850 16710	15043 16886	14648 16449	14691 16330	11767 13182	8681 9609	8864 9902	11328 12774	8858 9990
IX.	16710 18570	16886 18729	16449 18249	16330 17970	13182 14598	9609 10536	9902 10941	12774 14218	9990 11120
X.	18570 20430	18729 20571	18249 20050	17970 19610	14598 16013	10536 11464	10941 11979	14218 15662	11120 12252

Table 11.2 Experience tables showing the yield per acre expected for different tree species in closed stands treated regularly at different ages, and at different sites (from Cotta, 1821, p. 34). Excerpts from tables showing the mean stand volume of Norway spruce stands in cubic feet per acre ($1.0\,\mathrm{ft}^3\,\mathrm{acre}^{-1} \triangleq 0.04\,\mathrm{m}^3\,\mathrm{ha}^{-1}$) by age, from the poorest to best growth (site quality classes I.–X.). Translation of the legend: Tafel V. = Table V.; A. Norway spruce; Jahre = years

Tafel V. A. Fichten.

Jahre.	I.	II.	III.	IV.	V.	VI.	VII.	VIII.	IX.	X.
20	269	450	632	813	994	1175	1356	1538	1719	1900
21	290	485	680	875	1071	1266	1461	1656	1851	2047
22	311	520	730	939	1149	1358	1568	1777	1987	2196
23	333	557	781	1005	1229	1453	1677	1901	2124	2349
24	355	593	832	1071	1310	1549	1788	2026	2265	2504
25	377	631	885	1139	1393	1646	1900	2154	2408	2662
26	400	669	939	1208	1477	1747	2016	2285	2555	2824
27	423	708	993	1278	1563	1848	2133	2418	2703	2989
28	447	748	1049	1350	1651	1952	2233	2554	2855	3156
29	471	788	1106	1423	1740	2057	2375	2692	3009	3327
30	495	830	1163	1497	1831	2165	2499	2832	3166	3500
31	520	871	1222	1573	1923	2274	2625	2975	3326	3677
32	546	914	1282	1649	2017	2385	2753	3120	3488	3856
33	572	957	1342	1728	2113	2498	2883	3268	3653	4039
34	598	1001	1404	1807	2210	2613	3015	3418	3821	4224
35	625	1046	1467	1887	2308	2729	3150	3571	3992	4413
36	652	1091	1530	1969	2408	2848	3287	3726	4165	4604
37	679	1137	1595	2053	2510	2968	3426	3883	4341	4799
38	707	1183	1660	2137	2613	3089	3566	4042	4519	4995
39	735	1231	1726	2222	2717	3213	3709	4205	4701	5197
40	764	1279	1793	2308	2822	3338	3853	4369	4884	5400
41	794	1328	1861	2395	2928	3464	4000	4534	5070	5606
42	823	1377	1929	2481	3035	3590	4145	4701	5256	5812
43	853	1426	1998	2570	3143	3718	4295	4870	5445	6020
44	882	1475	2067	2660	3252	3847	4443	5038	5633	6229
45	912	1525	2137	2750	3362	3977	4593	5208	5824	6438
46	942	1575	2207	2840	3472	4107	4743	5378	6013	6649
47	972	1625	2277	2930	3583	4239	4894	5549	6205	6860
48	1002	1675	2358	3021	3695	4370	5046	5721	6397	7073
49	1032	1726	2420	3113	3807	4502	5198	5894	6590	7286
50	1062	1777	2491	3205	3920	4636	5352	6068	6785	7500
51	1093	1828	2563	3297	4034	4770	5507	6244	6981	7717
52	1123	1880	2636	3392	4149	4906	5664	6421	7179	7936
53	1156	1934	2711	3488	4266	5044	5823	6602	7380	8159
54	1188	1987	2786	3584	4384	5184	5984	6785	7584	8384
55	1220	2041	2862	3682	4504	5325	6147	6970	7791	8613
56	1253	2096	2939	3781	4625	5468	6313	7157	8001	8844
57	1286	2152	3017	3881	4747	5613	6480	7347	8213	9079
58	1320	2208	3096	3983	4871	5760	6649	7539	8427	9316
59	1354	2265	3175	4086	4997	5909	6821	7734	8645	9557

The insufficient database is a major weakness of these old tables. Consequently, they were quickly superseded once experimental centres responded to the obvious lack of data by expanding the network of study sites, and thereby broadening and updating the information base.

11.3.2.2 Standardised Yield Tables

At the end of the nineteenth century the Association of German Research Stations responded to the often uncoordinated yield table investigations by outlining a work plan for the future construction of yield tables (Ganghofer 1881). This laid the foundation for the development of a new uniform series of yield tables for all commercially important species. The development of these second generation stand growth models, largely owing to Weise (1880), continued into the first half of the twentieth century. They present, in tabular form, the most important stand characteristics (stem number, mean height, mean diameter, basal area, form factor, mean periodic growth, total volume production, and mean annual growth) according to established silvicultural prescriptions in homogeneous evenaged managed "normal" stands, usually every 5 years (Table 11.3). As the tables are constructed uniformly for this normal case, that is for stands with homogeneous structures, disturbed only by the defined thinning regimes, they enable better comparability and easy applicability. The Anglo-American "normal yield tables" describe stand development in unthinned stands. Contrary to the Central European practice, the adjective normal implies unthinned.

The tables from the Schwappach, Wiedemann and Schober school (cf. also Schwappach 1902; Wiedemann 1932, 1936/42, 1949; Schober 1975) stand out from other important yield tables of this generation developed in the first half of the twentieth century, for example by Guttenberg (1915), Gehrhardt (1909, 1923), Zimmerle (1952), Vanselow (1951), Krenn (1946) and Grundner (1913), because of the uniform conceptual basis, which, despite the need to update them at times, has been adhered to.

The yield tables developed in the 1920s and 1930s by Gehrhardt (1923, 1930) may be regarded as prototypes of a third generation of stand growth models, which were developed in the 1960s and 1970s with the transition to biometric growth models. Gehrhardt based his first yield tables for the most important European tree species on mathematically formulated tree growth relationships, which he

Table 11.3 Yield table from Schwappach (1890) for Norway spruce *Picea abies* (L.) Karst. in South Germany, a precursor of the Norway spruce Picea abies (L.) Karst. yield table commonly used today from Wiedemann (1936/1942). Presented is a section of the table for site quality class I.0 (Schwappach 1890, pp. 56–57). Translation of the terms in the table legend in the in order of their appearance: Hauptbestand = main stand; Periodischer Abgang = removed stand; Hauptbestand und periodischer Abgang; main stand and removed stand; Massenzuwachs = volume growth; Alter = age; Jahre = years; Stammzahl = stem number; Stammgrundfläche = basal area; Mittelhöhe = mean height; laufender jährlicher Zuwachs der Mittelhöhe = current annual increment of mean height; durchschnittlicher jährlicher Zuwachs der Mittelhöhe = mean annual increment of mean height; Mittlerer Durchmesser = mean diameter; Masse = volume; Derbholz = merchantable stem volume; Reisholz = volume of brushwood; Derb- und Reisholz = total above ground volume; Formzahl = form factor; Derbholz = merchantable stem volume > 7 cm at the smaller end; Baumholz = above ground tree volume; Summe der Vorerträge = sum of volume removed; Gesamtmasse = total volume; Per. Abgang in % der Gesamtmasse = removed volume in percentage of total volume production; durchschnittl. jährlicher Massenzuwachs = mean annual volume growth; laufendjährlicher Massenzuwachs = current annual volume growth; des Hauptbestand = of the remaining stand; der Gesamtmasse = of the total stand

Alter	Hauptbestand										Periodischer Abgang						Hauptbestand und periodischer Abgang				Massenzuwachs								Alter
	Stamm-Zahl	Stamm-grund-fläche	Mittel-höhe	Jährlicher Zuwachs der Mittelhöhe		Mittlerer Durch-messer	Masse			Formzahl		Stamm-zahl	Stamm-grund-fläche	Masse			Summe der Vorerträge		Gesamtmasse		Per. Abgang in % der Gesamtmasse		durchschnittl. jährlicher				laufendjährlicher				
				laufender	durchschnittlicher		Derbholz	Reisholz	Derb- und Reisholz	Derbholz	Baum			Derbholz	Reisholz	Derb- und Reisholz	Derbholz	Derb- und Reisholz	Derbholz	Derb- und Reisholz	Derbholz	Derb- und Reisholz	des Hauptbestandes		der Gesamtmasse		der Gesamtmasse				
																							Derbholz	Derb- und Reisholz	Derbholz	Derb- und Reisholz	Derbholz		Derb- und Reisholz		
Jahre		qm	m	m		cm	fm						qm	fm					fm		%		fm				fm	%	fm	%	Jahre
10	---	---	2,6	0,29	0,26	---	---	90	90	---	---	---	---	---	---	---	---	---	---	90	---	---	---	9,0	---	9,0	---	---	---	---	10
15	---	18,1	4,6	0,41	0,30	---	---	142	142	---	1,705	---	---	---	---	---	---	---	---	142	---	---	---	9,5	---	9,5	---	---	11,0	7,6	15
20	6720	25,6	6,7	0,44	0,33	7,0	4,8	152	200	280	1,166	---	---	---	---	---	---	---	48	200	---	---	2,4	10,0	2,4	10,0	---	---	13,9	6,6	20
25	5100	32,1	9,0	0,48	0,36	9,0	127	141	268	440	0,928	1620	2,19	---	13	13	---	13	127	281	---	4,6	5,1	10,7	5,1	11,2	17,7	13,0	17,9	6,2	25
30	3900	37,6	11,5	0,52	0,38	11,1	219	126	345	507	798	1200	3,06	6	15	21	6	34	225	379	2,6	9,0	7,3	11,5	7,5	12,6	20,5	8,9	20,0	5,2	30
35	3020	42,0	14,2	0,53	0,40	13,3	314	116	430	526	721	880	3,64	12	15	27	18	61	332	491	5,4	12,4	8,7	12,3	9,2	14,0	22,1	6,6	23,0	4,6	35
40	2380	45,8	16,8	0,50	0,42	15,6	410	107	517	533	672	640	3,96	18	13	31	36	92	446	609	8,1	15,1	10,3	12,9	11,2	15,2	22,7	4,6	23,2	3,9	40
45	1920	49,1	19,2	0,46	0,43	18,0	499	98	597	539	633	460	4,11	24	10	34	60	126	559	723	10,7	17,4	11,1	13,3	12,4	16,1	21,8	3,9	22,1	3,1	45
50	1590	52,0	21,4	0,42	0,43	20,4	576	93	669	511	593	330	4,18	28	7	35	88	161	664	830	13,3	19,4	11,5	13,4	13,5	16,6	19,7	3,0	20,3	2,5	50
55	1350	54,4	23,4	0,38	0,42	22,7	638	91	729	501	573	240	4,04	30	6	36	118	197	756	926	15,6	21,3	11,6	13,3	13,8	16,8	17,6	2,3	18,3	2,0	55
60	1170	56,4	25,2	0,34	0,42	24,8	691	89	780	486	542	180	3,74	31	5	36	149	233	840	1013	17,7	23,0	11,5	13,0	14,0	16,9	16,1	1,9	16,8	1,7	60
65	1030	58,1	26,8	0,30	0,41	26,8	738	89	827	474	531	140	3,38	30	4	34	179	267	917	1094	19,5	24,4	11,3	12,7	14,1	16,8	15,0	1,6	15,8	1,4	65
70	920	59,6	28,2	0,26	0,40	28,7	782	90	872	465	520	110	3,07	29	3	32	108	299	990	1171	21,0	25,5	11,2	12,4	14,1	16,7	14,3	1,4	15,0	1,2	70
75	830	61,0	29,4	0,23	0,39	30,6	824	91	915	459	510	90	2,86	28	2	30	236	329	1060	1244	22,2	26,4	11,0	12,2	14,1	16,6	13,7	1,3	14,3	1,1	75
80	755	62,3	30,5	0,22	0,38	32,5	864	92	956	454	503	75	2,69	27	2	29	263	258	1127	1314	23,3	27,2	10,8	11,9	14,1	16,4	13,1	1,2	13,7	1,0	80
85	690	63,5	31,6	0,21	0,37	34,3	902	93	995	449	496	65	2,54	26	2	28	289	286	1191	1381	24,3	28,0	10,6	11,7	14,0	16,2	12,5	1,1	13,1	0,9	85
90	635	64,6	32,6	0,20	0,36	36,0	938	94	1032	444	490	55	2,40	25	2	27	314	413	1252	1445	25,1	28,6	10,4	11,5	13,9	16,0	11,8	1,0	12,4	0,9	90
95	590	65,6	33,6	0,19	0,35	37,6	972	95	1067	441	484	45	2,25	23	2	25	337	438	1309	1505	25,7	29,1	10,2	11,2	13,8	15,8	11,1	0,9	11,6	0,8	95
100	555	66,5	34,5	0,17	0,34	39,1	1004	96	1100	438	479	35	2,09	22	1	23	359	461	1363	1561	26,4	29,5	10,0	11,0	13,6	15,6	10,5	0,8	10,9	0,7	100
105	525	67,4	35,3	0,15	0,34	40,4	1034	97	1131	434	476	30	1,93	21	1	22	380	483	1414	1614	26,9	29,9	9,9	10,8	13,4	15,3	9,9	0,7	10,4	0,6	105
110	500	68,2	36,0	0,13	0,33	41,6	1062	99	1161	432	473	25	1,78	20	1	21	400	504	1462	1665	27,4	30,3	9,7	10,6	13,2	15,1	9,5	0,7	10,1	0,6	110
115	480	69,0	36,6	0,11	0,32	42,7	1089	101	1190	431	471	20	1,65	20	1	21	420	525	1509	1715	27,8	30,6	9,5	10,3	13,0	14,9	9,2	0,6	9,8	0,6	115
120	465	69,7	37,1	0,10	0,31	43,7	1115	103	1218	431	471	15	1,55	19	1	20	439	545	1554	1763	28,2	30,9	9,3	10,1	12,9	14,7	9,0	0,6	9,5	0,5	120

B. Süddeutschland.

I. Bonität.

derived almost exclusively from data already available from earlier yield tables (Gehrhardt 1930). Although the tables from Gehrhardt were less popular than those from Schwappach and Wiedemann, his contribution to model research cannot be estimated highly enough as he went beyond Schwappach's and Wiedemann's purely empirical approaches and introduced theoretical considerations as well as biometrical and statistical methods into the development of yield models, giving model research an important new impulse.

11.3.2.3 Computer-Supported Yield Table Models

In the 1950s and 1960s, a third generation of stand growth models evolved with the transition to EDP-supported growth models. Protagonists in the development of these models included Assmann and Franz (1963), Bradley, Christie and Johnston (1966), Décourt (1965, 1966), Faber (1966), Fries (1964, 1966), Hamilton and Christie (1973), Myers (1966), Rehàk (1966) and Vuokila (1966).

The core element of these tables consisted of a biometric model in the form of a flexible system of mathematical equations. These equations were based on approved tree and stand growth relationships as much as possible, and were usually parameterised statistically using data from study sites. Normally, the biometric models were transferred to computer programmes and predict the stand development in relation to a specified management regime, site index and yield level. Excerpts of the preliminary Norway spruce yield tables for Bavaria from Assmann and Franz (1963), presented in Table 11.4, show the characteristics of a modern, computerised third generation yield table. The table was constructed by processing data from an existing comprehensive database by means of modern statistical methods. The yield table model is built on important tree growth

Table 11.4 Excerpts from the preliminary Norway spruce yield table for Bavaria from Assmann and Franz (1963). Taken from the tables for Norway spruce stands of the mean subdivided special yield level, top height site index 40. Translation of the terms in the table legend in the in order of their appearance: Vorläufige Fichten-Ertragstafel für Bayern = preliminary yield table for Norway spruce in Bavaria; Mittleres Ertragsniveau = medium yield level; Oberhöhenbonität 40 = top height 40 m; verbleibender Bestand = remaining stand; ausscheidender Bestand = removed stand; Gesamtbestand = total stand; Reduzierte Tafelwerte = volume and volume growth harvested, without bark; Alter = age; Oberhöhe = top height; Mittelhöhe = mean height; Stammzahl = tree number; mittlerer Durchmesser = mean diameter; optimale Grundfläche = optimal basal area; kritische Grundfläche = critical basal area; mittlere Schaftformzahl = mean form factor of stem wood; Schaftholzvorrat = volume total stem wood; Derbholzvorrat = volume merchantable stem wood >7 cm at the smaller end; Schaftholzmasse = volume total stem wood; Summe der Durchforstung = sum of removed volume; Vornutzung-Anteil Schaftholz = portion of removed volume; Gesamtleistung Schaftholz = total growth of stem volume; lfd. jährl. Schaftholzzuwachs = current annual growth of stem volume; durchschn. Gesamtzuwachs Schaftholz = mean annual growth of stem volume; Derbholzmasse des verbl. Best. = merchantable volume of remaining stand; Derbholzmasse des aussch. Bestandes = merchantable volume of removal stand, Gesamtleistung Derbholz = cumulative growth of merchantable stem volume; lfd. jährl. Derbholzzuwachs = current annual growth of merchantable stem volume; dGz Derbholz = mean annual growth of merchantable stem volume

Vorläufige Fichten-Ertragstafel für Bayern
Mittleres Ertragsniveau — ASSMANN-FRANZ 1963

Oberhöhenbonität 40 **Oberhöhenbonität 40**

Alter	Oberhöhe	verbleibender Bestand								ausscheidender Bestand				Gesamtbestand			Reduzierte Tafelwerte					Alter
		Mittelhöhe	Stammzahl	mittlerer Durchmesser	optimale Grundfläche	kritische Grundfläche	mittlere Schaftformzahl	Schaftholzvorrat	Derbholzvorrat	Stammzahl	Schaftholzmasse	Summe der Durchforstung	Vornutzung-Anteil Schaftholz	Gesamtleistung Schaftholz	lfd. jährl. Schaftholzzuwachs	durchschn. Gesamtzuwachs Schaftholz	Derbholzmasse des verbl. Best.	Derbholzmasse des aussch. Bestandes	Gesamtleistung Derbholz	lfd. jährl. Derbholzzuwachs	dGz Derbholz	
A	h_o	h_m	N	d_m	Gopt.	Gkrit.	F_S	V_S	V_D	N	V_S	V_S	VN%	GWL_{VS}	Lz_{VS}	d_{GZ}	Efm o. R.	Efm o. R.	Efm o. R.	Efm o. R.	Efm o.R.	A
20	9.6	7.6	4100	8.6	23.6	—	0567	101	80	1101	30	18	15.3	119	18.0	5.9	65	16	65	13.9	3.3	20
25	12.8	10.6	2999	11.0	28.3	—	0.539	160	146	680	40	48	23.0	208	23.1	8.3	118	29	134	17.0	5.4	25
30	16.0	13.5	2319	13.4	32.4	—	0.521	226	216	446	46	88	28.0	314	23.4	10.5	175	35	219	18.8	7.3	30
35	18.9	16.2	1873	15.7	36.2	—	0.508	297	288	308	49	134	31.1	431	24.6	12.3	233	39	314	19.8	9.0	35
40	21.6	18.8	1565	18.0	39.7	34.6	0.497	370	362	225	40	183	33.2	553	24.9	13.8	293	39	412	20.1	10.3	40
45	24.1	21.3	1340	20.3	43.0	37.5	0.488	445	438	170	49	233	34.5	678	24.8	15.1	355	39	513	20.0	11.4	45
50	26.3	23.5	1170	22.5	46.2	40.0	0.480	519	513	134	48	282	35.3	801	24.3	16.0	416	38	613	19.6	12.3	50
55	28.4	25.5	1036	24.6	49.1	42.7	0.474	592	587	109	46	330	35.8	922	23.5	16.8	476	37	711	19.0	12.9	55
60	30.3	27.4	927	26.7	51.9	45.2	0.469	664	659	91	44	376	36.2	1040	22.6	17.3	534	36	806	18.2	13.4	60
65	32.0	29.1	836	28.8	54.4	47.5	0.464	732	727	77	43	420	36.5	1152	21.5	17.7	589	35	897	17.4	13.8	65
70	33.5	30.6	759	30.9	56.7	49.2	0.460	797	792	66	42	463	36.8	1260	20.5	18.0	642	34	984	16.5	14.1	70
75	34.9	32.1	693	32.9	58.7	51.1	0.456	857	852	58	41	505	37.1	1362	19.4	18.2	690	33	1066	15.6	14.2	75
80	36.2	33.3	635	34.9	60.5	52.8	0.453	912	908	52	40	546	37.5	1458	18.3	18.2	736	33	1145	14.8	14.3	80
85	37.3	34.5	583	36.9	62.1	54.0	0.450	963	959	45	40	586	37.9	1549	17.2	18.2	777	32	1218	13.9	14.3	85
90	38.3	35.6	538	38.8	63.5	55.3	0.448	1009	1005	41	40	626	38.4	1635	16.2	18.2	814	32	1288	13.1	14.3	90
95	39.2	36.5	497	40.8	64.7	56.4	0.445	1050	1046	37	39	666	38.9	1716	15.2	18.1	847	32	1353	12.3	14.3	95
100	40.0	37.4	460	42.7	65.8	57.4	0.443	1087	1083	33	39	705	39.4	1792	14.3	17.9	877	32	1415	11.5	14.2	100
105	40.8	38.1	427	44.6	66.6	57.9	0.441	1119	1115	30	39	744	40.0	1863	13.4	17.7	903	32	1472	10.8	14.0	105
110	41.4	38.8	397	46.5	67.4	58.6	0.439	1147	1143	28	39	783	40.6	1930	12.6	17.5	926	31	1527	10.2	13.9	110
115	42.0	39.5	369	48.4	68.0	59.2	0.437	1170	1167	25	39	822	41.3	1992	11.8	17.3	945	31	1577	9.5	13.7	115
120	42.5	40.0	344	50.3	68.4	59.6	0.436	1190	1187	—	—	861	42.0	2051	—	17.1	961	—	1625	—	13.5	120

relationships derived by Assmann, which continued to influence the construction of tables thereafter. Many of the tables developed since the 1970s, for example by Bergel (1985), Braastad (1975), Curtis et al. (1981), Curtis (1982), Halaj et al. (1987), Lembcke, Knapp and Dittmar, (1975), Nagel (1985) and Wenk, Römisch and Gerold (1982) were in many aspects based on the first tables of this generation. This applies equally to the newly created interregional and regional yield tables, to local yield tables and to site productivity tables. For example, Assmann's finding that total volume yield between Norway spruce stands of the same site index may still vary considerably (Fig. 11.7d), was confirmed for other tree species as well. Accordingly, also the tables from Bergel (1985), Bradley, Christie and Johnston, (1966) and Lembcke, Knapp and Dittmar, (1975) distinguish subdivided special yield levels in addition to the site index.

11.3.2.4 Stand Growth Simulators

Since the 1960s a fourth generation of stand growth models was developed; the modern stand growth simulators. The impetus for the development of these simulators came from Franz (1968), Hoyer (1975), Hradetzky (1972), Bruce et al. (1977), Curtis et al. (1981) and Curtis (1982), among others.

Stand growth simulators predict stand development under different site conditions for different initial stem numbers and management regimes in a computer programme. A defined system of functions and algorithms, which forms the core of the growth simulator, is responsible for the simulation of the stand development in relation to growth conditions. Stand growth simulators aggregate the forest growth data into a multi-layered biometrical model that simulates the expected stand development for a broad spectrum of potential management alternatives, and collates the results in a table similar to the yield tables. In contrast to the yield tables of the previous generations where the table actually is the model, a yield table produced by the simulator represents only one of many possible stand growth processes that can be simulated.

In the last decades, with the advances in computer capacity, the size of the database available for model construction, and the increased information demand in forestry, growth models focussed on stand level data have gradually been replaced by stand growth models that predict stem number frequencies and individual-tree growth models, especially in Anglo-American forest services. As for the importance of yield tables in the context of forest growth science and forestry, in general, Prodan (1965, p. 605) recognised "it is doubtless that the construction of yield tables has been the greatest achievement of forest science until now. This fact is not diminished by the fact that yield tables will be rather of comparative value in the future".

11.4 Growth Models Based on Tree Number Frequencies

The transition towards new intensive thinning concepts changed the information demand in forestry. As a consequence, the emphasis shifted towards size class distributions instead of average stand values. This resulted in the development of growth models predicting not only stand mean values but also frequency distributions of individual tree dimensions. Stem number frequencies in diameter classes are needed, for example, to predict log grades and potential revenue from entire forest stands or, more accurately, selected tree cohorts in the stands. Depending on their concept and structure, stand-oriented growth models analysing stem number frequency can be assigned to differential equation models, distribution progression models, and stochastic evolution models.

Given the initial diameter–frequency distribution of a stand in the year t_0, these models reproduce the changes in the diameter–frequency distribution from the time t_0 to a rotation age of t_n in relation to growth, removal and mortality. The commonality of all models in this group is that the stand development results from a shift in the stem number–diameter distribution along the time axis.

11.4.1 Representing Stand Development by Systems of Differential Equations

In the 1960s and 1970s, Buckman (1962) Clutter (1963), Leary 1970), Moser and Hall (1969), Moser (1972, 1974), and Pienaar and Turnbull (1973) advanced the development of stand growth models based on systems of differential equations.

Like many other natural processes, the change in tree number, basal area or volume distribution in diameter classes can be expressed as a function of the actual stand characteristics, and is formulated in differential equations. The development of yield components over time is derived by integration, although sometimes a numerical derivation only is possible.

The first set of differential equations (base functions) describes the changes in the parameter y (stem number, basal area, or volume), $\Delta y_i/\Delta t$ in the diameter class i as a function of the rates of ingrowth from lower diameter classes, the exit rates of upgrowth to higher diameter classes, and mortality and removals within each diameter class. They make a balance of the filling of the size classes after each time step:

$$\frac{\Delta y_i}{\Delta t} = \frac{\Delta y_{entry}}{\Delta t} - \frac{\Delta y_{exit}}{\Delta t} - \frac{\Delta y_{mortality+removal}}{\Delta t}. \tag{11.4}$$

The ingrowth, upgrowth and mortality+removal rates are reproduced for each diameter classes in a second set of differential equations (control functions). The control functions model the movement of tree numbers, basal area or tree volume through the diameter classes in relation to site index, stand density, volume in upper and lower diameter classes etc. The parameters for these control functions can be derived from repeated surveys on study sites or inventory plots.

The distributions of stem number, basal area and the volume at time t_0 taken from inventories provide initial values for the prognosis run. The stem number, basal area and volume in the different diameter classes from t_0 to t_n is obtained by stepwise numerical integration of differential equations over the time intervals t_0–t_1, t_1–$t_2, \ldots, t_{n-1}$–t_n, applying numerical methods by Euler, Heun or Runge-Kutta (e.g., Metzler 1987, pp. 46–50). The control functions estimate the further development of the stand attributes in each size class (remain, transition, loss in dependence on site quality and stand structure) in each time step. The base functions balance each size class after each time step. The results of the balance for each size class are used as input variables for the control functions in the subsequent time step. The prognosis output includes the stem number, basal area and volume distributions in each diameter class and the period t_0–t_n (Fig. 11.8), which provide more differentiated and, hence, more valuable information for the forester or forestry enterprise.

11.4.2 Growth Models Based on Progressing Distributions

In the mid-1960s, Clutter and Bennett (1965) developed another approach for modelling stand development with frequency distributions. They characterised the stand by its diameter and height distributions, and modelled the stand development as a periodic progression of these frequency distributions. The accuracy of such models is primarily determined by the flexibility of the underlying type of distribution. The suitability of different types of distributions, for instance the *beta*, *gamma*, *log normal*, Weibull or Johnston distributions must be tested first before their use. The Weibull distribution has proven the most useful distribution due to its adaptability to different diameter and height distributions (Wenk et al. 1990):

$$F(x) = 1 - e^{-((x-a)/b)^c}, \tag{11.5}$$

where the distribution parameters are a (location parameter), b (scaling parameter), and c (shape parameter), under the condition, $x, b, c > 0$ (Fig. 11.9). By changing the parameters a, b, and c, the diameter distribution of a model stand fitted by the Weibull function can be shifted along the time axis, and the form of the distribution also can be adjusted over time (Figs. 11.10 and 11.11). Functions that control the diameter distribution parameters in relation to age, initial stem number, the management regime and the site index are integral elements of these models:

$$\text{Distribution parameters} = f(\text{age, initial stem number, treatment, site index}). \tag{11.6}$$

For the Weibull function, these distribution parameters are a, b, and c (11.5). So, in these models, stand development is not modelled from the stand variables directly, but from the parameters of the underlying frequency distribution. Models of this type were first produced by Clutter and Bennett (1965) for North American pine

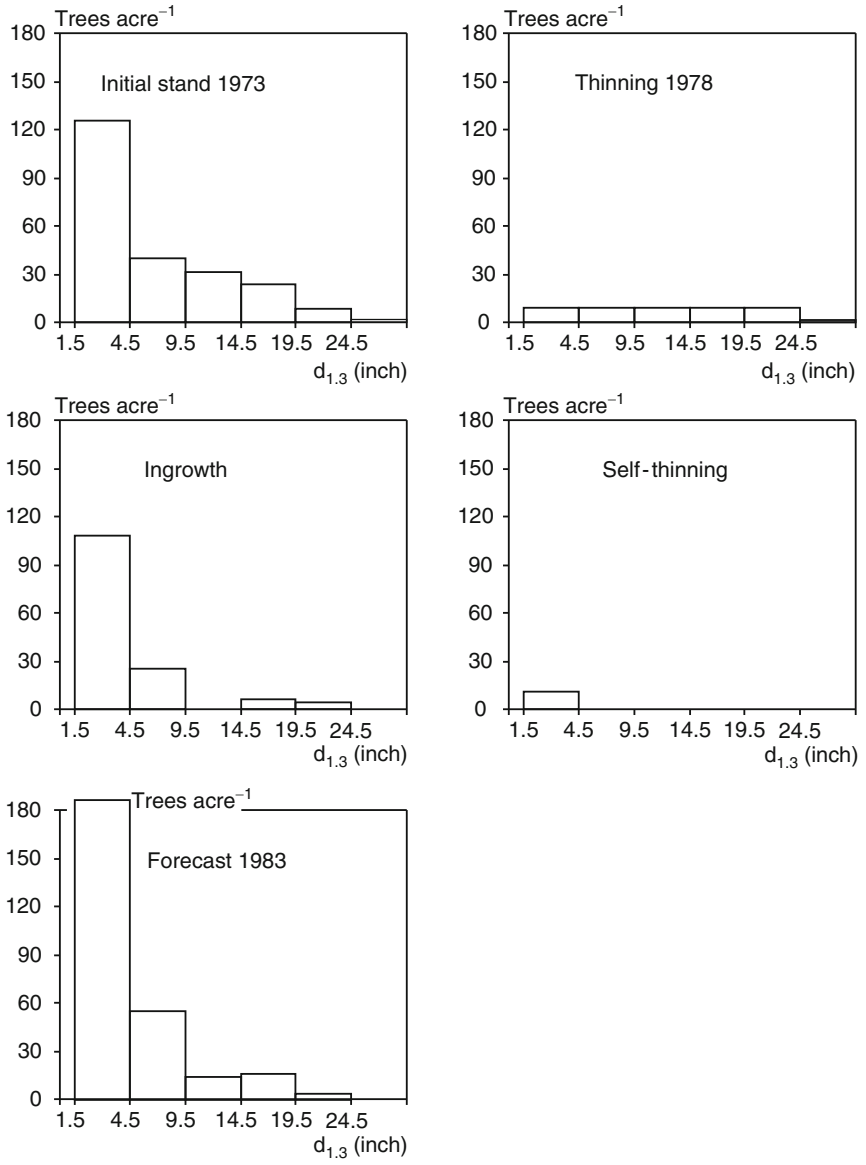

Fig. 11.8 Prognosis run for sugar maple stands (*Acer saccharum* Marsh.) with the diameter class-model from Moser (1974). Here, the diameter–frequency distributions (tree number per acre) for the initial stand in 1973, for the trees that were removed, died naturally or regenerated between 1973 and 1983, and the predicted diameter–frequency distribution for 1983 are shown (according to Moser 1974, p. 287)

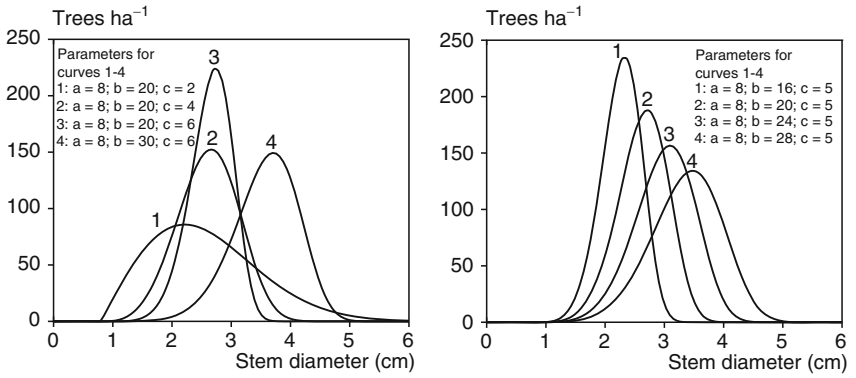

Fig. 11.9 Curve behaviour of the Weibull-function in relation to the parameters a, b and c (according to Gadow 1987, p. 43)

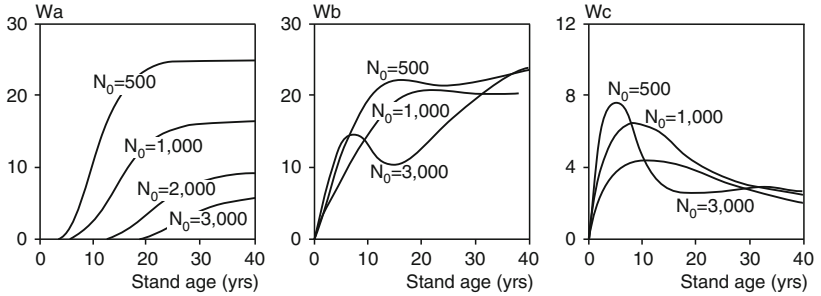

Fig. 11.10 Modelling South African pine and Eucalyptus stands (*Pinus sp. and Eucalyptus sp.* respectively) by periodically updating the diameter frequency distribution. Development of the location parameter Wa, the scaling parameter Wb and the shape parameter Wc of the Weibull-distribution for the diameter–frequency distribution of pine stands (*Pinus radiata D. Don.*) of different initial stem number densities (according to v. Gadow 1987)

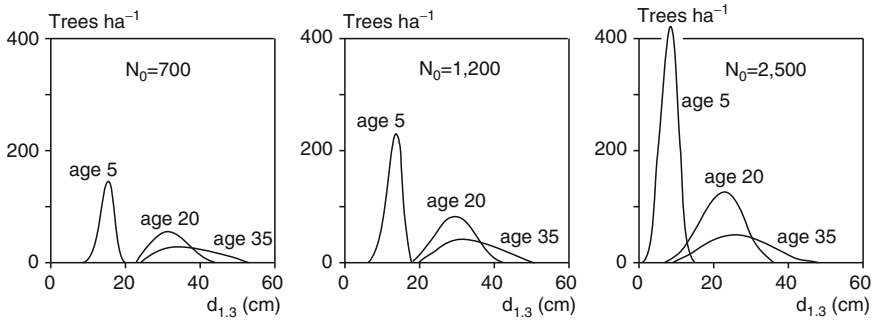

Fig. 11.11 Modelling of South African pine and Eucalyptus stands (*Pinus sp.* and *Eucalyptus sp.* respectively) by periodically updating the diameter frequency distribution. Simulated development of the diameter frequency distribution of pine stands (*Pinus radiata D. Don.*) after 5, 20 and 35 years with initial stem numbers of $N_0 = 700, N_0 = 1,200$, and $N_0 = 2,500$ (according to Gadow 1987)

stands and further developed by McGee and Della-Bianca (1967), Bailey (1973), Bailey and Dell (1973), Bennett, (1968), Feduccia et al. (1979), Zutter et al. (1986) and v. Gadow (1987) among others.

11.4.3 Stand Evolution Models – Stand Growth as a Stochastic Process

The term evolution model derives from the notion that stand development evolves stochastically from initial diameter distributions. Stochastic growth models were introduced to forestry by Suzuki and his team in Japan at the end of the 1960s and beginning of the 1970s (Suzuki 1971, 1983). After a thorough examination of Suzuki's original works, Sloboda (1976) introduced his work to the German speaking forest science community. Since the mid-1970s Sloboda and his team have continued to develop Suzuki's growth model further, primarily by adapting the principles of the model, which was designed for Japanese forestry purposes, to questions concerning European forestry research. They validated the model using the database from permanent sample plots.

The following introduction merely outlines the basic principle of stand evolution models; for further reading see Sloboda (1976, 1988). From an initial stand diameter–frequency distribution in the year t_0, the diameter frequency distribution for the following year t_1 is determined by the transition probability $p_{0,1}$, determining the rate at which trees pass into the next diameter classes during the time interval t_0–t_1. The stand diameter frequency distribution for the year t_1 results from the application of the transition probability $p_{0,1}$ to all trees in the initial (t_0) distribution. Next, the procedure is carried out for the t_1-distribution for the transition from t_1 to t_2 based on the transition probability $p_{1,2}$. If the transition probability p is known for the whole lifespan of the stand then the initial distribution $\varphi(t_0, x_0)$ at time t_0 can be extrapolated while taking into account intermediate removal of trees and mortality, to obtain the distribution $\varphi(\tau, x_\tau)$ at time τ (Fig. 11.12). In general, the expression $p(t_0, x_0; \tau, x_\tau)$ describes the probability with which a tree of the diameter x at time t_0 will achieve a diameter x_τ by time τ. Thus, we call $p(t_0, x_0; \tau, x_\tau)$ the transfer function of diameter distribution φ. The transfer function $p(t_0, x_0; \tau, x_\tau)$ is obtained by combining a drift function, diffusion function and mortality rate.

The drift function $\beta(\tau, \gamma) = b \times k \times e^{-k \times \tau}$ defines the direction of the age–diameter development and constitutes the deterministic component in the otherwise stochastic model. The diffusion function $\alpha^2(\tau, x_\tau) = 4 \times a^2 \times k \times e^{-2 \times k \times \tau}$ represents the stochastic component of the transition function, and determines the extent of variation in individual-tree values about the mean direction of diameter development. The function $\alpha^2(\tau, x_\tau)$ is termed the diffusion function because it determines the movement of trees along the ranks of the diameter distribution. Consequently, it influences the changes in social dominance between individual trees. The mortality rate $\gamma(\tau, x_\tau)$ indicates the portion of trees in diameter class y that drop out by time τ In the simplest case, it is kept constant for the entire growth period ($\gamma = c = \text{constant}$).

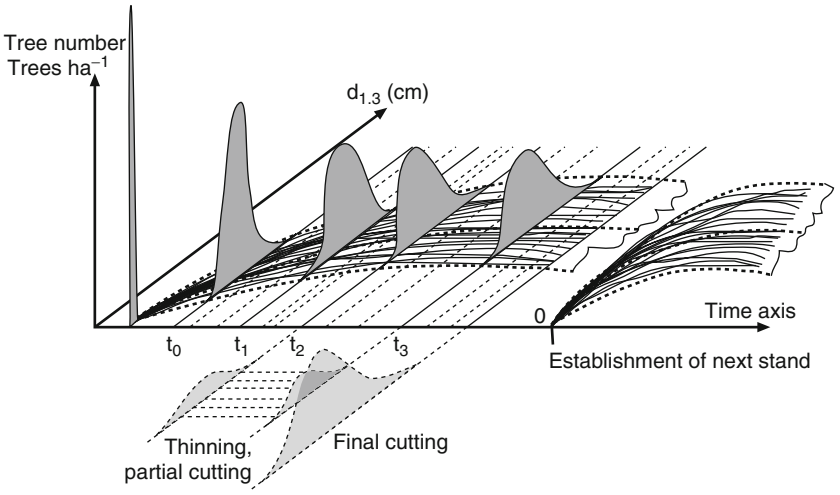

Fig. 11.12 Frequency models abstract stand dynamics as shifts in the diameter frequency distribution along the time axis from time t_0 until the rotation age (from Sloboda 1976, p. 158)

With the transfer function

$$p(t_0, x; \tau, x_\tau) = f(\text{Drift } \beta,\ \text{Diffusion } \alpha^2,\ \text{mortality rate } \gamma) \tag{11.7}$$

the distribution $\varphi\ (\tau,\ x_\tau)$ expected at time τ can be obtained from any given initial distribution $\varphi\ (t_0, x_0)$. The functions $\beta(\tau, x_\tau), \alpha^2(\tau, x_\tau)$ and $\gamma(\tau, x_\tau)$ beyond the transition function, provide the framework for the periodic progression of individual trees on the time axis. The parameters a, b and k can be derived from a regression analysis of the age–diameter curve $d_{1.3} = f_1(\text{age})$, and the diameter differential diagram $d_{1.3}(t+1) = f_1(d_{1.3}(t))$ of the mean stem for the stand to be modelled. Parameter c for the mortality rate of the stand in question is determined empirically. Thus, the transition function comprises underlying predictions of diameter development, the changes in social dominance and the mortality processes in the stand.

Growth models based on stochastic processes have also been developed for pure stands by Bruner and Moser (1973) and Rudra (1968), for mixed stands by Stephens and Waggoner (1970), and for age class stand management systems at the enterprise level by Kouba (1977, 1989).

11.5 Individual Tree Growth and Yield Models

Individual-tree growth and yield models break a stand up into a mosaic of individual trees, and reproduce their interconnectedness in the computer as a spatial–temporal system. In contrast to models that simulate stand development using stand level data, or frequency distributions, in individual-tree models, the descriptive level and

the level of biological observation are identical: the individual tree, which is the basic unit of the stand, also forms the information unit in the model. Individual-tree models have a higher resolution than yield tables and distribution models, but, by compiling and aggregating the individual tree sizes and their changes, information can be derived at the lower resolutions, such as mean tree development or frequency distributions, as well.

The core element of all individual-tree models is a system of equations that models the growth behaviour of the individual trees in relation to their growing conditions. When transferred to a biometric model and computer program, individual-tree models simulate stand dynamics in a growing period tree by tree. As the entire prediction process is based on individual trees and their spatial arrangement, there is an inherent flexibility in the model that permits the modelling of any combination of species mixture and stand structures, management regimes and regeneration methods. Thus, individual-tree models provide an appropriate tool for predicting growth and yield in structurally diverse pure and mixed stands. Individual-tree models have been developed as computer programmes that allow the user either to interactively control the simulation for the development of a special stand, or to predict stand development for a large number of stands in batch mode. In the interactive mode, the user is able to follow the stand development throughout the simulation run and specify thinning measures or the impact of disturbance factors, for example, at any time during the simulation run (Chap. 13, Fig. 13.1).

11.5.1 Overview of the Underlying Principles of Individual-Tree Models

Individual-tree models represent a much higher level of resolution in terms of system abstraction and modelling than stand models (Newnham 1964; Ek and Monserud 1974; Nagel 1996; Pretzsch et al. 2002a; Wykoff et al. 1982). As individual-tree models consider feedback loops between stand structure and individual tree growth (Chap. 13, Fig. 13.2), they need to be more complex, yet they are also more flexible. We distinguish between position-dependent and position-independent individual-tree models as two approaches which represent competition either with or without accounting for the spatial distribution pattern respectively (stem coordinates, distances between tree pairs, crown parameters). In Chap. 8, some of the most relevant approaches for the compilation of competition indices are reviewed. These indices form the core of such models, and control the growth of individual trees. Stand level data for forestry management are provided by aggregation of the individual tree results (Pukkala 1987; Sterba et al. 1995).

Figure 11.13 shows the most important steps in the prediction process of individual-tree growth and yield models. The model is initialised with start up values for a simulation run of a sample plot. These include the stand level attributes and the characteristics of all individual trees at the beginning of the prediction period. The tree list should contain data about tree species, stem size, crown dimension

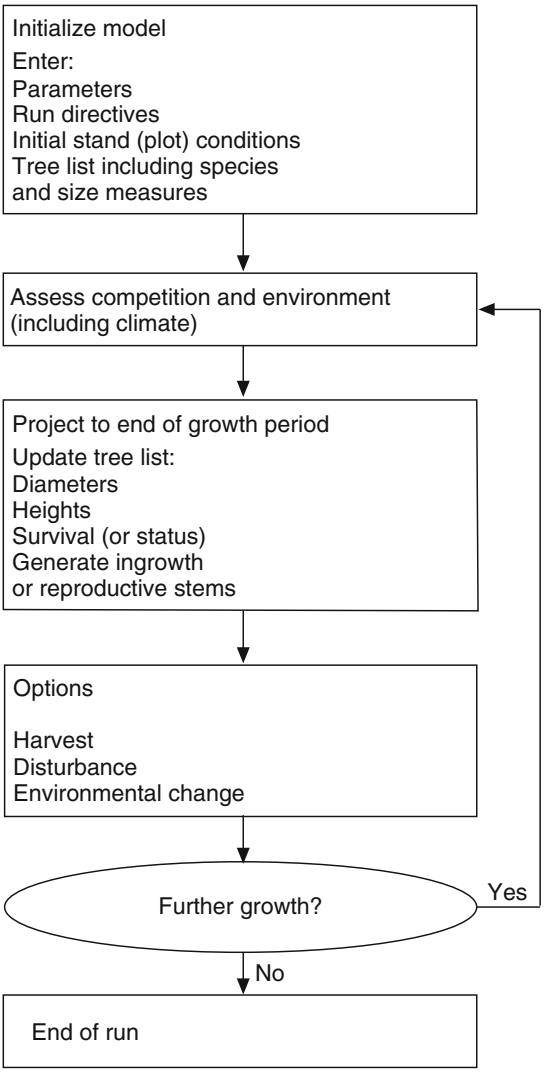

Fig. 11.13 Schematic representation of the simulation process in individual-tree models according to Ek and Dudek (1980)

and stem position for all trees. The data usually have been collected in individual tree-based surveys of sample plots in the course of forest management, or in forest inventories or experimental observations. In several individual-tree growth models, the start up values for individual tree attributes may also be artificially generated (Pretzsch 1995, 1997, 2001). From these values, the development of all trees in the stand (e.g. diameter, height, and crown development or mortality) is predicted in relation to their individual growing conditions using appropriate estimation functions.

Once the entire tree list of the first growth period, e.g. 5 years, has been processed, changes in the competitive status of trees, for example, due to thinning or disturbance, can be specified before simulating the next growth period. The updated values at the end of the first period become the start up values for the second simulation cycle. In each simulation cycle, the development of all individual trees is estimated and provided as an interim result. The simulation runs continue period by period until the entire specified prediction period is completed. The time intervals are usually set to 5 years, sometimes 1 or 2 years. To model silvicultural interventions, for example, the time at which trees should be removed from the sample plots can be defined either interactively or by means of predefined silvicultural thinning concepts (cf. Chap. 5). The spatial arrangement of the residual trees in the modelled stand changes as a result of these removals, as does their growth behaviour in subsequent growth periods. The growth response of the stand to thinning is thereby explained through the individual tree responses to this intervention.

11.5.2 Growth Functions as the Core Element of Individual-Tree Models

Two approaches have proven useful for controlling individual tree growth, the *direct* estimation of growth by regression analysis, and the *indirect* control over growth with the potential modification method.

11.5.2.1 Direct Estimation of Individual Tree Growth

The first approach involves a regression analytical estimation of the size, and increment of individual trees in relation to tree and stand parameters, and surrogate variables, which reflect the site conditions. The STAND PROGNOSIS MODEL, the distance-independent model from Wykoff et al. (1982), used widely in the North American Forest Services, adopts this approach, estimating the annual basal area increment i_{ba} of a tree in relation to regional and local site factors, stand characteristics, individual-tree characteristics, and disturbance factors:

$$i_{ba} = f(\text{forest community, ecoregion, elevation, aspect, slope, crown competition and stand density, tree basal area at 1.3 m, crown length, competition index, etc}). \quad (11.8)$$

In a regression analysis, i_{ba} is related to four sets of variables. The first set consists of regional site factors such as forest community and growth region as well as the local site factors aspect, slope and elevation. The second set encompasses stand level characteristics like crown competition, and stand density. The third set comprises individual-tree parameters describing the tree's size, morphology and competitive

status in the stand. The fourth set adds scaling factors and multipliers for the effects of growth promoting and inhibiting disturbances, e.g. fertilisation and CO_2 increase as well as insect infestation and atmospheric pollution.

11.5.2.2 Potential Modifier Method

In the potential modifier method, an assumed potential annual or periodical annual increment of a tree i_{pot} is used to estimate growth. The potential growth i_{pot} can be derived from potential height–age or diameter–age curves, which represent the upper boundary line on a given site (Fig. 11.14). Such potential curves may be determined, e.g. from stem analysis of open grown trees, or from dominant trees on long-term experiment plots. The predicted growth i_{pred} of an individual tree is obtained by multiplying the potential growth expected in the absence of competition, i_{pot}, by a modifier mod, which has a value between 0 and 1.0:

$$i_{pred} = i_{pot} \times \text{mod}. \tag{11.9}$$

The modifier mod is essentially dependent on the individual competitive situation of a tree, expressed by its competition index CI (cf. Chap. 8). Competition indices use diameter, height, crown dimensions and neighbouring species to quantify the competitive status of individual trees and the effect on their growth. The CI value for solitary trees is $CI = 0$, and increases with increasing competition. Height and diameter increment are influenced differently by competition. For many tree species, maximum height increment already occurs under moderate competition while maximum diameter increment is only reached in the absence of competition. The curves $\text{mod}_h = f(CI)$ and $\text{mod}_d = f(CI)$ in Fig. 11.15 reflect this relationship. We refer to position-dependent or position-independent competition indices when the distances to the stand neighbours are considered in the calculation of competition indices or

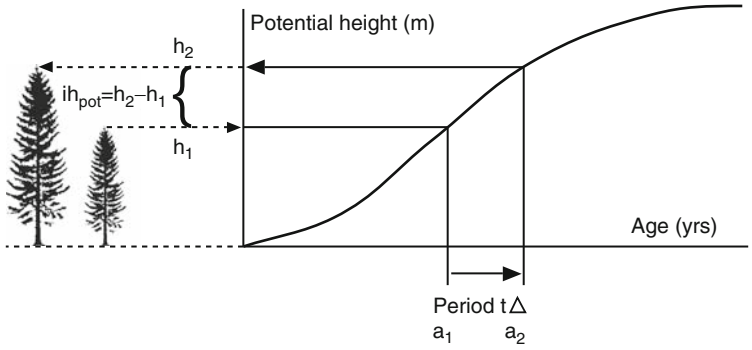

Fig. 11.14 Determination of potential height growth ih_{pot} from the potential age–height curve by the following principle: read off the (virtual) age a_1 for a desired height h_1, add e.g. 5 years (a_2), and read off h_2; the resulting potential height growth is $ih_{pot} = h_2 – h_1$

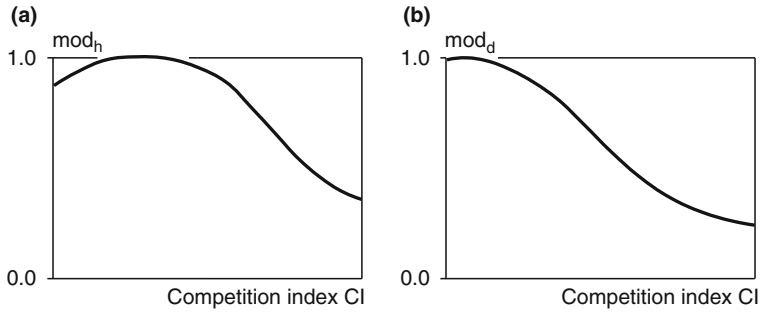

Fig. 11.15 Relationship between competition (measured by the competition index CI) and (**a**) the reduction factor mod_h for height increment and (**b**) mod_d for diameter increment (from Ek and Monserud 1974, p. 71)

ignored respectively. The influence of site conditions can be modelled by methods of direct estimation (11.8) that require the input of appropriate regression parameters, or by indirect estimation methods which make use of predefined site dependent potential curves (11.9).

11.5.3 Overview of Model Types

The first individual-tree model was developed in 1963 by Newnham for pure Douglas fir stands (Newnham 1964). Thereafter, Arney (1972), Bella (1971), Lee (1967), Lin (1970) and Mitchell (1969, 1975) introduced other individual-tree models for pure stands. In the mid-1970s Ek and Monserud transferred the principles of constructing individual-tree growth models for pure stands to unevenaged pure and mixed stands (Ek and Monserud 1974; Monserud 1975). Munro (1974) differentiated position-dependent from position-independent individual-tree models according to whether they included stem positions and distances to model individual-tree growth or not. In the FOREST model, Ek and Monserud (1974) elaborated a particularly brilliant position-dependent individual-tree model for pure and mixed stands for all age relationships. The STAND PROGNOSIS MODEL from Wykoff et al. (1982), used widely in North American Forest Service, serves as a prime example of a position-independent individual-tree model. The bibliography compiled by Dudek and Ek (1980) reviews individual-tree models world-wide, identifying more than 40 different individual-tree models which can be divided more or less evenly into position-dependent and position-independent models. Since the 1980s individual-tree models, many of which refer to the methodological principles of the forerunners, have been developed by Biber (1996), Burkhart et al. (1987), Deusen and Biging (1985), Eckmüllner and Fleck, (1989), Hasenauer (1994), Kahn and Pretzsch (1997), Kolström (1993), Krumland (1982), Larson (1986), Nagel (1996, 1999), Pretzsch (1992a, 2001), Pukkala, (1987), Schneider and

Kreysa (1981), Sterba et al. (1983, 1985, 1989a, 1995), Wensel and Daugherty (1984) and Wensel and Koehler (1985). Owing to the continued development of the user interface in modern computers, they are considerably more user friendly than the older individual-tree models.

In Europe these kinds of models are applied in forestry practice for management planning in pure and mixed stand (Pukkala 1987; Kolström 1993; Sterba 1995; Nagel 1996; Pretzsch et al. 2008). The site sensitivity of these models is derived from basic ecophysiological knowledge as well as a wealth of growth and yield data. Version 2.2 of SILVA, a model developed in Germany for pure and mixed stands (Pretzsch 1992a; Pretzsch and Kahn 1996; Kahn and Pretzsch 1997; Pretzsch et al. 2002a), is discussed in detail in Chaps. 12 and 13 as an example for this category.

11.6 Gap and Hybrid Models

According to the mosaic cycle theory, many large-scale ecosystems can be abstracted as a mosaic of individual patches in different successional phases (Aubreville 1938; Müller-Dombois 1983). However, the successional development on these patches does not represent a linear progression towards a permanent and large-scale climax stadium, but rather constitutes an asynchronous spatial–temporal patchwork with a constant turnover (Bormann and Likens 1979a, b). The spatial–temporal dynamics of the mosaic cycle depend primarily on the lifespan of the species, the occurrence of disturbances and the interspecific competition strategies (cf. Chap. 12).

Watt (1925, 1947), Bray (1956), Curtis (1959), Bormann and Likens (1979a, b) and Shugart (1984) transferred the view, that large-scale systems can be regarded as a mosaic of gaps or patches which, when investigated, contribute to description, understanding and modelling of the forest ecosystem as a whole. This laid the foundation for the concept of gap models described below. According to this view, a forest ecosystem is an aggregation of small areas, or gaps, the size of which is defined as the space occupied by a mature tree or a biological group. The tree group in the gap space forms the actual observation and information unit of gap models. Values for stands or larger units are obtained by adding or averaging the gap values, which may occur in different stages of development.

Small-area or gap models reproduce the growth of individual trees in forest patches (e.g. 100 m^2 areas) in relation to the prevailing mean growth conditions at the site (Botkin et al. 1972; Shugart 1984; Leemans and Prentice 1989). Growth is predicted in relation to a combination of surrogate variables and primary factors using pre-defined regression procedures. Explanatory parameters include numeric (e.g. annual precipitation, mean temperature, slope, exposition), nominal (e.g. levels of nutrition supply, levels of water supply), and ordinal (e.g. ecoregion, degree of disturbance of topsoil by harvest machines) variables. Gap and hybrid models have intermediate position between statistically based and ecophysiologically based

matter balance models (see also Bugmann 2001). They are relevant primarily in the development of competition and succession in close-to-nature forests. Thinning algorithms are considered rarely, with few exceptions such as the SORTIE model (Pacala et al. 1993; Menard et al. 2002).

11.6.1 Development Cycle in Gaps

Gap models assume that natural forest development in gaps proceeds according to the cycle presented in Fig. 11.16. Harvesting, or mortality of mature trees in the dominant stand layer creates a gap. Afterwards, the growing conditions improve for the trees in the lower canopy and the natural regeneration. Regrowth closes the gap gradually, and, through the process of self-thinning, finally forms a new overstorey. Severe losses in the dominant stand layer reinitiate the cycle. Such events are reflected clearly in the biomass production over time (Fig. 11.16, centre). The biomass minimum occurs after the loss of the dominant tree layer. It increases exponentially thereafter with the regrowth of natural regeneration in gaps. With increasing age, the quantity of accumulated biomass approaches an upper site-specific

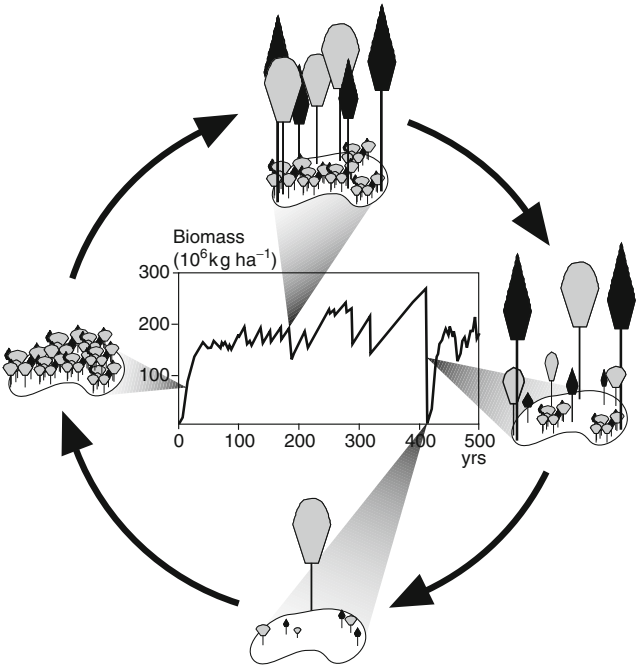

Fig. 11.16 Gap models assume the following characteristic cycle. Death or removal of a dominant mature tree improves the growth conditions in gaps. The regrowth closes the gap created in the stand. Through self-thinning the number of dominant trees in the gap decreases gradually, closing the cycle. This cycle is reflected in the age curve for biomass production (from Shugart 1984)

ceiling biomass. The sawtooth biomass curve up to 400 years of age is caused by the reduction in biomass following occasional stem losses, which are then compensated for by the growth of the remaining stand. With the loss of an entire mature stand through senescence or a natural disaster, the biomass approaches zero once again, closing the cycle.

Gap models are largely used for investigating competition and succession in near natural forests stands, e.g. in the old growth coastal conifer forests in Western, and the boreal forests in Eastern Canada. They model the growth of individual trees in gaps in relation to the prevailing growth conditions within the gap, and thereby approximate position-dependent individual-tree models (Sect. 11.5). Gap models, like position-dependent individual-tree models, also can provide output data relevant to forest management, for example the diameter, height and volume development of individual trees or stands. However, the input and output variables are less suited to forest management information demands than position-dependent individual-tree models, since gap, or succession models are designed primarily to predict long-term succession patterns in unmanaged forest stands, and to enhance the ecological understanding of biomass production under the changing growing conditions during the succession.

11.6.2 JABOWA – Prototype Model from Botkin et al. (1972)

As a part of the Hubbard Brook ecosystem study, Botkin, Janak and Wallis (1972) developed the small area simulation model JABOWA, a prototype for models of this generation. Kimmin's (1997, p. 488) review of the evolution of gap models based on the original JABOWA model identified more than 40 subsequent models, some differing only slightly from the original approach. JABOWA models individual-tree growth in small areas ($100\,m^2$) in relation to average radiation, climate, soil conditions and also water availability in the gap. Diameter at breast height was the main parameter for progressing individual-tree development. All other size parameters, for example height and leaf area of individual trees, are estimated in relation to tree diameter measurements. To predict individual-tree diameter development, Botkin et al. (1972) and Shugart (1984) take the initial diameter values of all trees in a gap and determine the actual diameter increment id in a growth period for each tree by reducing its potential diameter increment id_{pot}. The potential diameter increment id_{pot} is obtained from a function between relative growth rate of diameter and initial diameter. Under suboptimal growing conditions, the potential diameter increment id_{pot} is reduced by the factors r, t, s and w, representing the effects of radiation, temperature, soil conditions and water supply respectively according to

$$id_{pred} = id_{pot} \times r \times t \times s \times w. \tag{11.10}$$

In contrast to individual-tree models, gap models calculate individual-tree or mean tree growth from mean growing conditions in the gap, not from the specific growing

conditions of the individual trees. The reduction factors r, t, s and w assume values between 0.0 (growth not possible) and 1.0 (maximum growth) depending on whether the growing conditions in the gap are favourable or unfavourable for a tree, thereby reducing the potential growth to the actual diameter growth value. The advantage of this approach is that newly acquired knowledge about the factors influencing growth simply can be incorporated into the model as multipliers (between 0.0 and 1.0) without having to adjust the entire structure of the model.

Botkin et al. (1972) calculated the factor r, which quantifies the reduction in the potential increment id_{pot} due to radiation (11.10), as a function of the incoming radiation I_0, the leaf area index LAI, species specific crown transparency and the tree height layer. If the resulting radiation supply I_x of a tree is known, then the reduction factor r is derived from a species-specific radiation–photosynthesis response curves $r = f(I_x)$. This explains how, in terms of the degree of mechanistic explanation, gap models fall between individual-tree management models and ecophysiological process models.

As the radiation above the crown space I_0 passes through the canopy it is reflected, scattered and absorbed by the needles, or leaves, and the branches, so that radiation decreases as it passes deeper into the crown. To determine the amount of radiation that can be used in biomass assimilation at a given height x, gap models apply the Lambert–Beer rule (Monsi and Saeki 1953) in most cases:

$$I_x = I_0 \times e^{(-k \times LAI_x)}, \tag{11.11}$$

where I is radiation intensity in crown space at height x, I_0 is radiation intensity above the crown space, LAI is leaf area index resulting from leaves above height x, and k represents the extinction coefficient.

This rule says that the incoming radiation intensity of I_0 at the crown top declines within the canopy in relation to the LAI, which is modelled as a function of the height x. For given coordinates (longitude/latitude) of a given stand, radiation climate models deliver the radiation intensity I_0 at the temporal resolution desired. The extinction coefficient k scales the decline in radiation as it penetrates the needles, or leaves; high k means rapid decline. The factor k is a medium-specific coefficient, and is available for the main tree species. The greater the leaf area LAI_x is above a given height x, the lower is the radiation intensity penetrating through to the middle and lower canopy. The total leaf area or leaf area index is estimated mostly in relation to stand basal area of the trees in the gap and the heights of these trees. From (11.11), the radiation intensity can be determined at any point within the stand. In gap models the radiation-height profile is assumed uniform within a gap. For the assumed radiation intensity I_x at a given height x, the reduction factor r can be read off the radiation–photosynthesis response curve, and entered into (11.10) for the reduction of the potential diameter increment. The response curves $r = f(I_x)$ are species-specific; for instance, a low radiation intensity produces higher r values for shade tolerant tree species than for light demanding tree species.

To derive the factors t, s, and w, which describe the effect of temperature, soil and water availability respectively, different methods are recommended depending

on the data available. Temperature within the gaps is modelled in relation to meteorological data, and the effect of the soil from simple parameters obtained from site quality maps. The effect of water availability w is derived from precipitation data, evapotranspiration, soil characteristics as well as the ratio of actual to potential stocking density as an indicator of root competition. The multiplication of these factors r, t, s and w neglects possible compensatory or enhancing interaction between them. Kahn and Pretzsch (1997) attempt to incorporate these interactions in their site production model by introducing flexible aggregation operators.

In the JABOWA model, regeneration and mortality processes are superimposed with a random component, leading to different results for each simulation run, even for the same starting values. The mean expected growth behaviour of these stands can only be obtained by averaging the results for an entire series of repeated simulation runs. The results from the $100\,m^2$ areas are projected to hectare values. Succession processes, biomass development, and the effects of disturbances in stands and larger forest areas can be predicted with this type of model. Stands and larger forest units comprise a mosaic of small areas, and the boundaries and interactions between adjacent areas are dealt with in the model by the stochastic variation of area-specific growth parameters.

Gap models developed for the investigation of long-term natural forest development under given site conditions are also implemented on climate research questions. This is reflected in research by Kellomäki et al. (1993), Kienast and Kräuchi (1991), Leemans and Prentice (1989), Lindner (1998), Pastor and Post (1985) and Prentice and Leemans (1990). Gap models allow the calculation of scenarios for natural tree species composition under given site conditions and of changes in growth brought about by changed environmental conditions.

The transfer of specific ecophysiological process knowledge to stand, gap, or individual tree models, calibrated with long-term growth measurements, results in so called hybrid growth models, e.g. FORCYTE and FORECAST (Kimmins 1993, 1997). The aim of these models is to predict plausible responses in net primary production to different (combinations of) environmental conditions to derive reliable estimates of growth and matter balance suitable for forest planning and management. Tree or stand productivity (e.g. in terms of net primary production assessed or measured at the given site) and growing conditions (e.g. nutrient supply in leaves) are applied to estimate site-specific coefficients of photosynthetic efficiency. Such efficiency coefficients are used to estimate net primary production in different scenarios for management, stand structures and disturbances (Fig. 11.17). Because of the species-specific relationships to site conditions, they can be applied equally to pure and mixed stands. In Europe, only few developments in this direction have been undertaken (e.g. Hauhs et al. 1995); neither gap models nor hybrid models have been found reliable enough to become practical management tools. In other countries, however, hybrid models are used more commonly in the analysis of impacts of forest management on ecosystem structure and function (Kimmins et al. 1999; Seely et al. 2002, Welham et al. 2002), and for calculating growth and

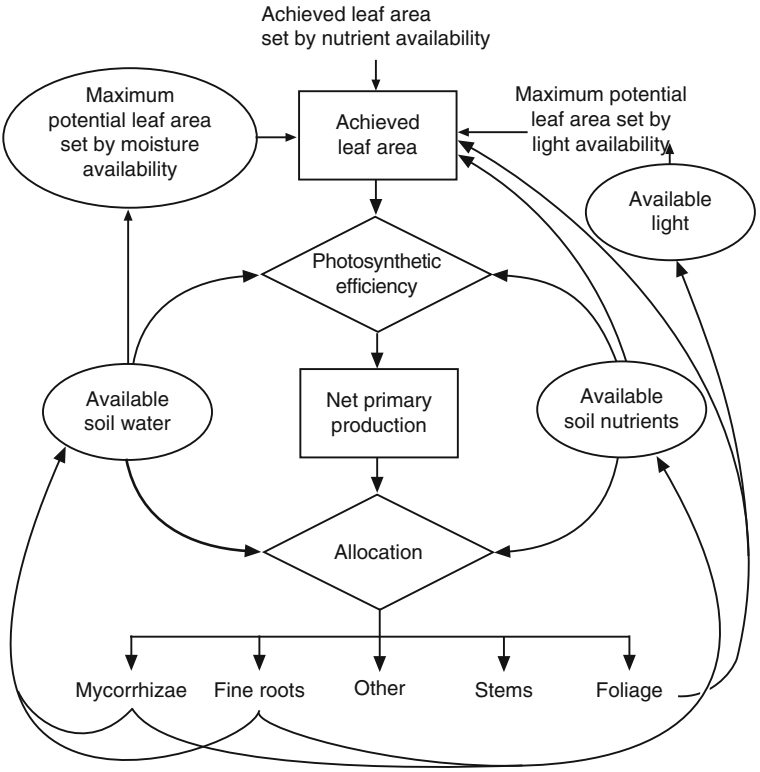

Fig. 11.17 Principle of using photosynthetic efficiency in hybrid models for estimating net primary production, which is then allocated to different biomass components after Kimmins (1993, p. 12) (by courtesy of Hamish Kimmins)

matter balance in plantations (e.g. Baldwin et al. 2001; Schwalm and Ek 2004). In tropical forest management, the gap type models FORMIX and FORMIND (Huth et al. 1998; Köhler and Huth 1998) have been used to address sustainability and nature conservation issues.

Growth models based on stand level data, frequency distributions, individual-tree dimensions and gaps (Sects. 11.3–11.6, respectively) represent different approaches in describing the actual stand development. None of these approaches can be replaced entirely by another; each model provides specific knowledge about forest growth, yield, stand structure and biogeochemistry. Hybrid models combine statistical stand, or individual-tree models, described in the previous sections, with mechanistic biogeochemical-based matter balance models, which is the subject of the following section.

11.7 Matter Balance Models

Compared with growth and yield models, mass or matter balance models focus on the description of carbon, and, in some cases, also of nitrogen balances as components of biogeochemical processes. Therefore, they are also known as biogeochemical or process-based models. All these models consider vegetation development primarily as a change in matter in different compartments, that is as a balance between uptake (e.g. photosynthesis) and loss (e.g. senescence) processes that in turn depend on environmental conditions (e.g. temperature or water availability). This category includes models that were developed for a wide range of scales and purposes.

11.7.1 Increasing Structural and Functional Accordance of Models with Reality

In the construction of ecophysiological models, the focus no longer lies in the derivation of statistical relationships to produce an accurate prognosis of volume growth or gap dynamics, but rather on an accurate process-oriented modelling of the system's structure and function. The differences lie mainly in the manner in which the effects of different environmental factors on life processes are considered. For example, in yield tables the diameter growth of the mean stem is modelled by the diameter–age curve and its dependence on the site index. Also, individual-tree models represent diameter growth individually in relation to stand, individual-tree and site characteristics (e.g. stand density, competition index, site index). In contrast, in ecophysiological models, growth is calculated on the basis of photosynthesis, respiration and allocation, i.e. from processes and nutrient flows occurring in the leaves, stem, branches and roots, and between these tree parts and the environment.

The reproduction of stand growth may be implemented at different temporal or spatial resolutions. In a first approach, a stand may be broken down roughly into its leaf area, living and dead biomass, etc. The basic physiological processes, such as assimilation and respiration, are calculated separately for these compartments. This way, the gross and net photosynthesis of the stand can be estimated in 1–5 year intervals, and the synthesised biomass can be divided between the organs and individuals according to defined allocation patterns. In another approach, the model may reproduce the stand dynamic starting from a high resolution. Structures and processes are modelled, first, at the organ or individual-tree level, and the stand dynamics result from the three dimensional structural organisation and process resolutions in the order of minutes. Stand parameters (e.g. net primary production per hectare, average tree weight or stem volume) are calculated as cumulative or mean values of all individuals in the stand.

In ecophysiologically based matter balance models, combined effects of resource supply and environmental conditions on tree and stand growth can be simulated

although the understanding of cause–effect relationships between growth conditions and growth response from long-term experiments is at best fragmentary. If we assume that the physiological characteristics of plants do not change, short-term experiments may be used to predict long-term growth responses.

To illustrate the approach and range of results from ecophysiological models, we present the model TREEDYN3 from Bossel (1994) in more detail. In this model, stand development is abstracted by the mean tree development, i.e. a medium spatial resolution. The growth of the mean tree is determined in relation to radiation, temperature and nutrient supply, as well as the effect of intervening factors by analysing the carbon allocation in leaves, fine roots, fruit and wood (Fig. 11.18). Figure 11.19a shows the typical decrease in tree number per hectare arising from mortality and thinning in a Norway spruce forest in the first site class with a moderate thinning regime. The periodic removal of trees produces fluctuations in the standing wood biomass. From the age of 50–60 years, after the intensive thinning and self-thinning phase, the standing wood biomass increases markedly, and diameter and height growth slows down as stand density increases. Figure 11.19b shows the development of standard growth and yield characteristics. The sawtooth curve obtained for stand basal area reflects the thinning actions. The management operations also produce oscillations in the leaf and fine root volume (Fig. 11.19c). After the thinning operations, the leaf and fine root volume remain at an upper limit determined by the site conditions. Whereas, after a rapid increase in the early growth years, the amount of assimilates maintains approximately the same level throughout the total growth period, the nature of assimilate distribution changes. In the first decades, assimilates are used primarily in the formation of wood. Thereafter, more and more assimilates are be invested into the maintenance metabolism of the growing tree body. Thinning operations and natural tree losses increase the carbon supply in the litter layer, yet it hardly affects the carbon pool in the soil humus layer (Fig. 11.19d). The initial, high availability of nitrogen decreases with stand age as it is incorporated into the organic material. Yet nitrogen availability at a given site remains optimal at 1.0 throughout the entire growth period.

As, in addition to predicting wood yield from trees and stands, ecophysiological matter balance models also make predictions about carbon, nitrogen and water cycles, they offer decision support for comprehensive ecosystem management. However, this type of model requires relatively detailed stand, site and climatic data to initialise the programme, which, currently, are rarely available for practical use. Thus, ecophysiological models are not yet feasible for routine predictions for forest management, but rather serve as a research tool to gain a better understanding of cause–effect relationships between site parameters, disturbance factors and stand development. The increasing disturbance of forest ecosystems from damaging agents such as air pollution, the increase in atmospheric CO_2 concentrations, climatic change together with the desire to understand and better predict the response of forest ecosystems has provided a new stimulus for the development of ecophysiological process models. These model best represent the effects and interactions of the factors essential for growth, for which hardly any statistical relationships exist.

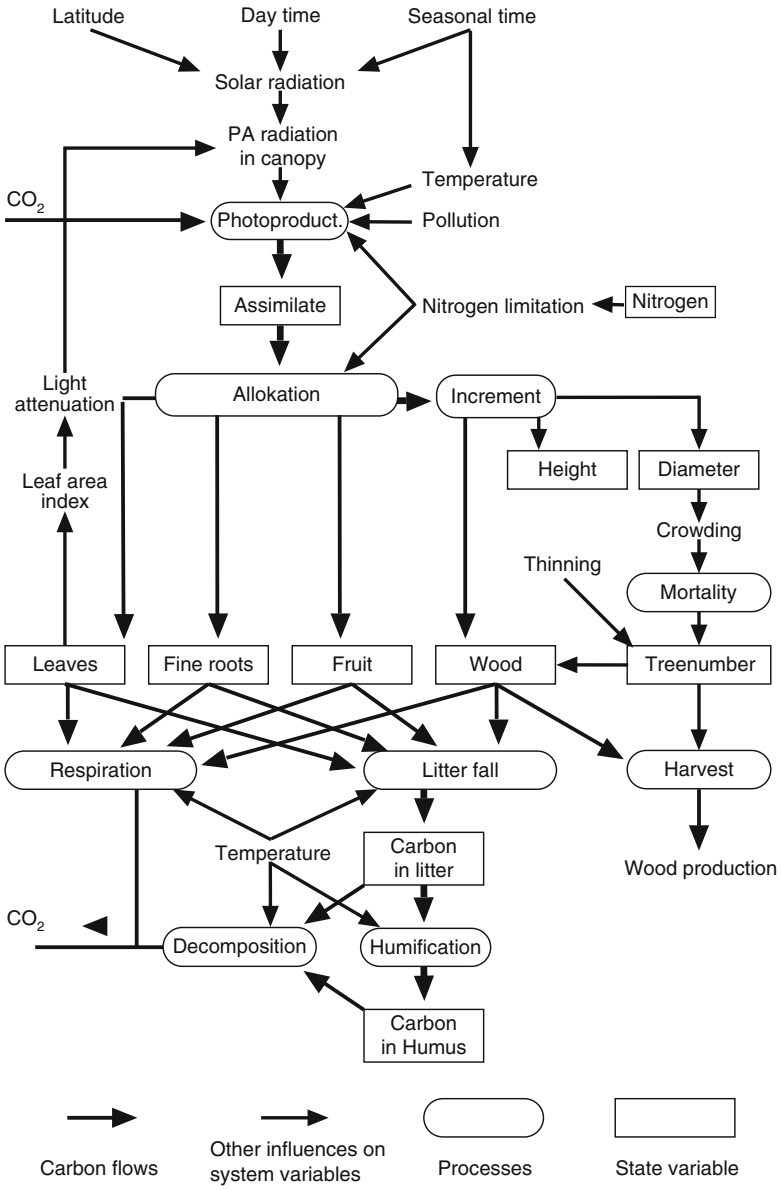

Fig. 11.18 A systems diagram of the model TREEDYN3 from Bossel (1994, p. 10) with the major carbon flows: variables are indicated by *boxes*, and processes by *ovals*. The *bold arrows* represent carbon flux, *narrow arrows* represent other influences on system variables. Photosynthesis depends primarily on radiation, temperature, nutrient supply and the deposition of toxic substances. The carbon assimilates produced are allocated in the leaves, roots, fruits and wood growth. Depending on the competitive status of a tree, modelled as a function of stand density, either height growth or diameter growth dominates. A feedback loop exists between the leaf, or needle, biomass produced and PA radiation available in the canopy. Carbon loss occurs through respiration, leaf and branch death, and wood harvesting. Decay processes absorb carbon in the humus or release it as CO_2 (by courtesy of Hartmut Bossel)

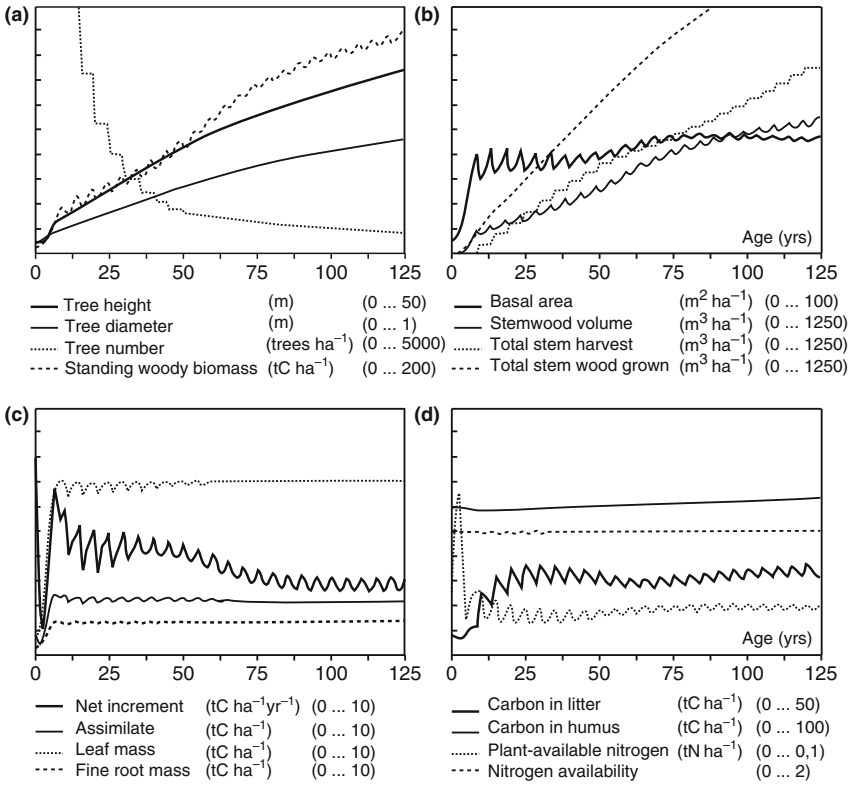

Fig. 11.19 Growth simulation of Norway spruce stands with site conditions corresponding to the site quality class I.0, and under moderate thinning according to Wiedemann (1936/1942), with TREEDYN3 (from Bossel 1994, p. 100). The time series for stand yield and soil variables are presented up to the age 125 years

11.7.2 Modelling of the Basic Processes in Matter Balance Models

11.7.2.1 Overview: The Basic Physical, Biochemical and Physiological Processes

Among the basic processes incorporated in most matter balance models are radiation absorption, interception of precipitation, evapotranspiration, nutrient uptake, photosynthesis, respiration, allocation, senescence and mortality. They are processed at different levels in most ecophysiological process models. The details are explained in steps number (1) to (8) in the simplified systems diagram in Fig. 11.20.

(1) Stand structure is reproduced from the initial stand values, e.g. diameter, height, crown size and positions of all individual trees. It is possible to abstract crown space as a homogeneous medium, to differentiate various layers of different

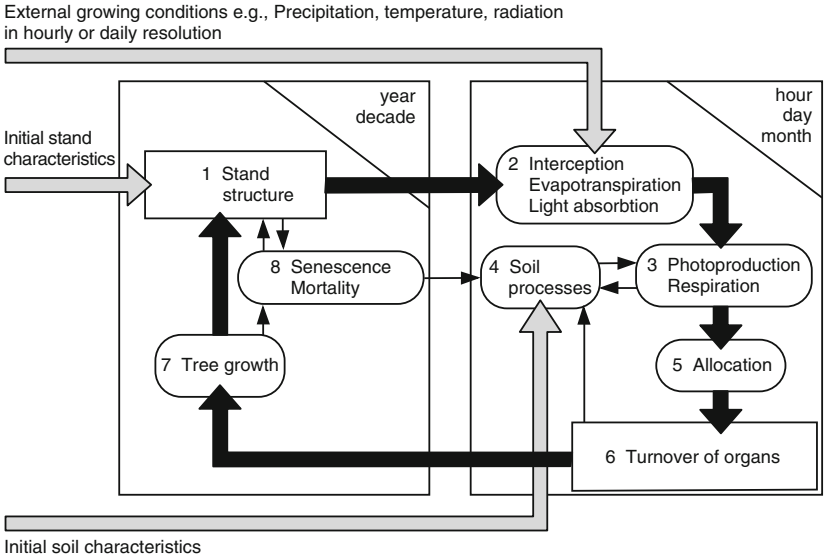

Fig. 11.20 Basic processes in ecophysiological process models (*ovals*) calculated at an annual (*left box*), and daily (*right box*) resolution respectively from Bellmann et al. (1992). The closed feedback loop, stand structure → photosynthesis → respiration → allocation → tree growth → stand structure, and the calculation procedure (1) to (8), described in the text in greater detail, are highlighted

needle or leaf densities, or to use an explicit three-dimensional spatial model in which the spatial arrangement is taken into account for each tree in the stand.

(2) Based on the resulting spatial occupation pattern of the leaf area, interception, evapotranspiration and light absorption within the crown space, the canopy layer or the individual trees are modelled in hourly, daily or monthly time intervals.

(3) Modelling of photosynthesis and respiration at the stand, individual tree or organ level requires time series data about the resource supply and environmental conditions above- and belowground.

(4) Soil process sub-models deliver, among other variables, water and nutrient supply of the roots.

(5) The allocation model reflects the distribution of assimilates to different organs with respect to growth (roots, wood, fruit and leaves or needles) and defence (resistance, parasitic defence, healing of wounds).

(6) Turnover by litter fall, loss of reproductive organs, fruits, death of plant organs are essential variables for the calculation of the tree net growth as for the entire matter balance.

(7) Net tree growth is modelled on the basis of the estimated net primary production minus the turnover. Net growth of biomass is typically calculated at sub-annual, annual or 5-year resolution. This is done by modelling an average tree, representatives of particular diameter classes, or by the explicit reproduction of the spatial structure of all trees in the stand.

(8) Finally, all tree or stand parameters (diameter, height, leaf area etc.) and stand structures (average LAI, LAI for different height layers, leaf area for individual trees etc.) are updated after subtracting the organ and tree loss (turnover). The updated structure provides the framework for the physical and ecophysiological processes in the next period (→ 1).

While the changes in spatial structure are updated typically in time steps of 1 year or 1 decade, the physical and ecophysiological processes are resolved at much higher resolutions, in hourly, daily or monthly time step, so that even the consequences of short-term events (drought, frost, atmospheric pollution) can be modelled. That stand structure is updated every hour or day is justifiable since changes in stand structure, and the processes determining individual tree growth occur more slowly. The sequence of prognosis steps represents a feedback loop, shown in Fig. 11.20 by the thick black arrows, that makes it possible to model the combined impact on the system due to tree removal during thinning operations, insect infestation browsing, changes in root–shoot ratio arising from nitrogen input or an increase in the atmospheric CO_2 concentrations. These slow changes in the macro structure define the framework and parameter limits for the spatially and temporally higher resolved processes.

11.7.2.2 Light Interception

Being the most relevant of the basic ecophysiological processes, we will first discuss the role of the resources radiation and water in the estimation of gross photosynthesis, and quantify the respiration spent in maintenance metabolism. Because photosynthesis is a light dependent process, the modelling of radiation relationships, e.g. with the Lambert–Beer rule (Monsi and Saeki 1953), is of particular importance (cf. (11.11) and Fig. 11.21):

$$\text{Radiation intensity at height x in the crown space} = \text{f(radiation intensity above the crown, shading leaf area above height x, light extinction coefficient)} \quad (11.12)$$

11.7.2.3 Interception and Evapotranspiration of Water

Most of the precipitation forests receive reaches the ground and is available for plant growth. Yet a considerable part (10–30%) is intercepted in the canopy, and evaporates without replenishing the soil water reservoir. The interception is calculated in relation to the following variables:

$$\text{Interception of water} = \text{f(precipitation, stand density, leaf area index, evaporation).} \quad (11.13)$$

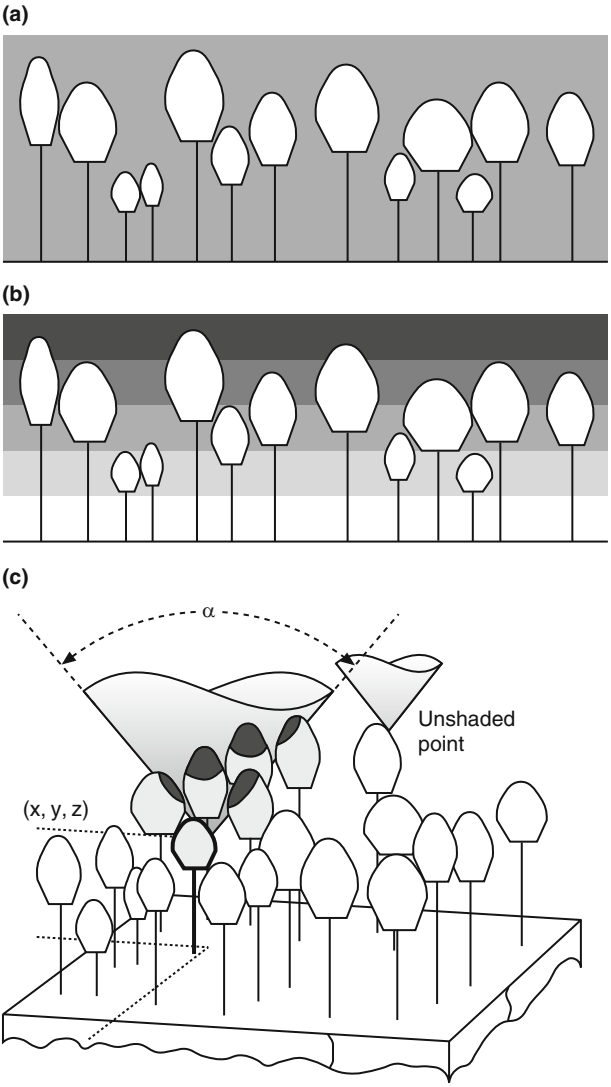

Fig. 11.21 The incoming radiation model abstracts the crown space (**a**) as a medium with homogeneous leaf density, (**b**) as different crown space layers with different needle or leaf densities or by (**c**) explicitly modelling the three-dimensional stand structure. For the latter approach Sloboda and Pfreundt (1989) introduced the light cone method, where the apex of an imaginary cone, with a width defined by the opening angle α placed at the point (x, y, z). The needle or leaf volume falling within the cone determines the radiation intensity at the point (x, y, z)

Common approaches, e.g. Gash (1979), Navar and Bryan (1994), or, more generally, Rutter et al. (1975), take the amount of precipitation and subtract two components: the throughfall, as that part of the precipitation that directly reaches the forest ground through canopy gaps, is estimated with respect to stand density (e.g. degree

of canopy cover, stand density index); the interception that temporarily remains on the leaves, but drips off to the ground is estimated in relation to leaf area index and the evaporation rate (interception evaporation). These two components determine the amount of precipitation that replenishes the soil water reservoir and are ultimately available for plant growth.

To determine the evapotranspiration components (interception, soil surface, tree and undergrowth transpiration, etc.), most ecophysiological process models apply the formula from Penman–Monteith (Monteith 1965; Penman and Long 1960). It calculates the various evapotranspiration components from a broad set of variables:

$$\text{Evapotranspiration} = \text{f(relative humidity, radiation, density and specific heat of air, vapour pressure deficit, air resistance, psychrometric constant, surface resistance).} \quad (11.14)$$

Simplifications are possible if not all the bioclimatic variables are used in the model (Makkink 1957; Mohren et al. 1993; Running and Coughlan 1988). For a given precipitation, interception and evapotranspiration, the plant water supply and possible drought stress can be determined using the following method: the lower the ratio of actual to potential transpiration (or evapotranspiration) drops below 1.0, the more likely the plants respond by reducing their stomatal opening, i.e. by increasing the stomatal resistance, which leads to a reduced photosynthetic capacity.

11.7.2.4 Photosynthesis

For the calculation of the photosynthesis, many different approaches are available, ranging from empirical light response curves to the explicit description of biochemical reactions that integrate light, temperature and nutrient effects (see overview in Farquhar et al. 2001). Moreover, the degree of detail and abstraction varies strongly. The biochemical approach (Farquhar et al. 1980):

$$\text{Gross photosynthesis} = \text{f(rate of carboxylation, regeneration rate of the enzyme RuBisCo)} \quad (11.15)$$

explains the assimilation through biological processes at the cell level. The rate of carboxylation in turn depends on the maximum activity of the enzyme RuBisCO, the internal CO_2- and O_2-partial pressure, the CO_2-partial pressure at the light compensation point, the reaction constant of the CO_2-assimilation and the reaction constant of the O_2-binding. The regeneration rate of the enzyme RuBisCO is dependent on the photosynthetic active radiation, on the fraction of absorbed radiation, the internal CO_2- and O_2-partial pressure, the reaction constant of the CO_2-assimilation and the reaction constant of the O_2-binding.

In models based on the light response curve, the gross photosynthesis is described as a direct function of radiation without considering the biochemical relationships, e.g. (Monsi and Saeki 1953):

$$\text{Gross photosynthesis} = \text{f(maximal photosynthetic rate, photosynthetically active radiation, leaf area).} \quad (11.16)$$

In the most common models, influences such as CO_2 concentration, nutrient supply, temperature and stomatal resistance, which can affect the photosynthesis rate in very different ways, are usually incorporated by modifying the maximal photosynthetic rate. This approach is similar to forest growth models with higher degrees of aggregation, such as the individual-tree and succession models. Here, the actual production rate from the stand or individual trees is determined by reducing a potential curve in relation to specific influence factors (see (11.9) and (11.10)).

11.7.2.5 Respiration

Respiration is usually divided into three different types of CO_2-releasing processes: dark respiration of the photosynthetically active tissue is only considered explicitly in models with below-day temporal resolutions. Growth respiration, where energy is invested in the formation of new tissue, usually is modelled by strictly linear reductions in primary production or in growth of plant organs. Maintenance respiration is described as a function of temperature and nutrient supply:

$$\text{Maintenance respiration} = \text{f(biomass, temperature, nutrient supply).} \quad (11.17)$$

It is caused by the sum of the metabolism in the living organs. It is of particular relevance for the trees that are comparatively long-lived with a large biomass. Models of higher complexity only differentiate a larger number of biomass fractions. This deficit in self-regulating capacity has been recognised as a bias in physiologically-based simulations (Thornley and Cannell 2000).

11.7.2.6 Resource Allocation

The modelling of tree or forest carbon allocation into compartments with slow and fast turnover is a crucial element of growth simulations (Poorter and Nagel 2000; Barton 2001). Existing rules for this process are still very simplistic (see overview in Lacointe 2000). Many approaches have been suggested reaching from empirical partitioning coefficients, functional balance and optimisation principles, to models focussing on resistance mass-flow and source-sink (see Le Roux et al. 2001). However, essential points, like the control of environmental effects and the distribution of carbon into regenerative compartments, defence, exudates and mycorrhiza are far from being understood yet.

The majority of tree and stand models describe the allocation of assimilated carbon within the tree at annually using (1) constant partitioning coefficients, e.g., allometric proportions, (2) purpose-oriented distribution as part or result of an evolutionary process, or (3) distribution in relation to transport resistance.

(1) Constant partitioning coefficients: the assimilates may be distributed between the plant organs so that a certain allometric proportion is maintained within the tree. Expressed in the so-called allometric formula, the allometric exponent α an be regarded as the distribution coefficient. α may be constant, dependent on age, or dependent on the competitive status of a tree (Pretzsch and Schütze (2005). Supposing x and y quantify the size of plant organs or a total plant, the allometric formula (Huxley 1932; Huxley and Teissier 1936) is

$$y = a \times x^{\alpha}. \tag{11.18}$$

The differential representation,

$$dy/y/dx/x = \alpha \tag{11.19}$$

shows that the allometric exponent α describes the ratio between the relative growth rates of x and y, what Bertalanffy (1951, p. 313) called the relative growth rate relationship ("Verhältnis der relativen Wachstumsgeschwindigkeiten"). An allometric exponent of α means, when x increases by 1%, y increases by α%. According to the allometric formula, an organism allocates his resources to organs x and y in such a proportion, that α remains constant (cf. Chap. 10, Sect. 10.2).

Since different resource supply and environmental conditions lead to different or changing distribution patterns among trees and forests, approaches with constant partitioning coefficients do not satisfy long-term growth simulations (McMurtrie and Wolf 1983). Therefore, new models try to provide for variation in the allocation proportions or allocation coefficients in relation to tree size (Mohren et al. 1993), resource supply and environmental conditions (King 1996; Mäkelä and Hari 1986; Running and Gower 1991; Weinstein et al. 1991), or a combination of both (Arp and Oja 1997).

(2) Purpose-oriented distribution: a purely purpose-oriented distribution is also referred to as the principle of teleonomy. Teleonomy emphasises the purposefulness of the genetically determined form and function of biological systems. The assimilates are distributed according to a predefined optimum pattern following a hierarchical priority list, which represents a rule-based allocation system (Eckersten 1994; Waring and Schlesinger 1985). The functional balance method assures that all organs can carry out their functions to the best possible extent. Davidson (1969) introduced the principle that the uptake of nutrient minerals is proportional to the amount of assimilated carbon:

$$\sigma_N \times W_r = \rho \times \sigma_C \times W_f \tag{11.20}$$

with W_r, W_f root and shoots dry weight, σ_N, σ_C nitrogen and carbon assimilation rates, and ρ = ratio of mineral gain/carbon gain in the tissue. The proportionality factor ρ may be assumed constant (Mäkelä 1990), or be adapted to fulfil certain criteria, e.g. a constant nitrogen concentration (Reynolds and Thornley 1982).

The functional balance method was originally developed from grassland vegetation (Davidson 1969), where plant biomass is composed mainly of living, metabolically active leaf and root biomass. To transfer this method to tree and stem growth, it is necessary to introduce an additional allocation factor for the woody biomass. Mäkelä and Hari (1986) proposed the use of the "pipe-model" theory (Shinozaki et al. 1964), which assumes a linear relationship between stem sapwood area (at crown base) A_s and total foliage biomass W_f (Fig. 11.22):

$$A_s = \eta_s \times W_f, \tag{11.21}$$

where η_s is a species-specific parameter, which depends on the xylem conductivity and the hydrological conditions of a given site.

This way, the stem attributes (conductive cross-sectional area of the transport units) are related to the leaf biomass, inherently assuming that a certain sap wood area is necessary to supply a certain leaf mass. The stem increment (primarily the stem cross-section, via auxiliary variables also the entire stem volume) can be estimated in relation to the produced leaf area, determined from formula (11.21). So far, this method has been applied successfully to the modelling of boreal forests (Mäkelä 1990, pp. 81–95), yet a larger comparison

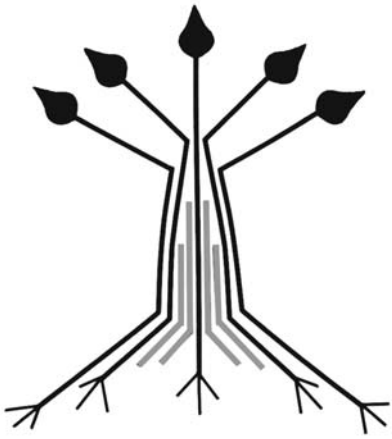

Fig. 11.22 Pipe-model theory provides a link between leaf biomass W_f and stem sapwood area A_s. Active pipes represent the connection between leaves and feeder roots and form the sapwood (*black modular units*). Inactive pipes no longer are connected to leaves or feeder roots. They represent the non-conducting xylem or heartwood (*grey* modular units). The stem sapwood area at the crown base is assumed to be a linearly correlated to the total leaf biomass $A_s = \eta_s \times W_f$ (by courtesy of Harry Valentine)

of morphological investigations over all of Europe shows that the relationship between the cross-sectional area of the conductive xylem tissue and the leaf biomass supplied is not constant, but varies under different environmental conditions.

(3) Distribution in relation to transport resistance: an alternative method from Thornley (1991) models the allocation in relation transport resistance:

$$\text{Transport rate of assimilates and nutrients} = \text{f(conductive resistance, assimilate or nutrient concentrations in plant parts i or j).} \quad (11.22)$$

The carbon and nitrogen distribution in the tree is determined by the demand of the individual plant organs or compartments. The specific supply and distribution is obtained from the concentration gradient between plant parts i (source) and j (sink) and the conductive resistances between them. Tree size is a direct result of nutrient availability from the substrate and the physiologically based constants for the conductance of assimilates. Due to the effort required in the determination of parameters for approaches of this type, and to the existing uncertainty about the variability in conductive resistances, this method did not develop a niche for itself in forest growth modelling.

11.7.2.7 Mortality Processes

In most ecophysiologically based tree or stand models, mortality processes of individual organs are modelled by defining an assumed lifespan, which is reduced under stress. Stress factors may include temperature (Thornley 1991), water availability (Zhang et al. 1994) or the impact of pollutants (Bellmann et al. 1992; Mohren and Bartelink 1990). In models with differentiated vertical allocation of the assimilated biomass, efficiency values also can be used as senescence criteria. In this case, leaves, or needles, are shed, or not renewed when a given limit in the ratio of assimilate gain to respiration loss is not reached (Nikinmaa and Hari 1990). The description of senescence is closely linked to allocation modelling. Thus, in models with a comparably inflexible allocation algorithm, a temporal increase in senescence due to adverse environmental conditions generally leads to greater structural changes than in models with flexible allocation algorithms with adaptable allocation strategies.

A mechanistic approach to modelling mortality of entire trees in ecophysiological models is based on the ratio between the anabolic and catabolic processes of an individual tree. The relationship between net photosynthesis and maintenance respiration for a given time period provides a measure of the tree's production balance from which vitality can be estimated and mortality controlled.

Alternatively, the tree number loss of entire stands also can be deduced from the $-3/2$-power rule derived by Yoda et al. (1963) for self-thinning in herbaceous plant communities:

$$\ln \bar{w} = \ln a - 3/2 \times \ln N. \quad (11.23)$$

Plotting the logarithm of the mean biomass $\bar{w}$ the logarithm of the plant number N per unit area results in the so-called self-thinning line (11.23) with the site-specific parameter a, and the slope $-3/2$, which is a good first approximate for many species and site conditions. Under maximum density conditions, the level of the self-thinning line, expressed by $\ln(a)$ can be fixed according to the observed or published maximum density for the species in question. The transformation of this equation indicates the plant number N per unit area:

$$N = e^{\left[\frac{\ln \bar{w} - \ln a}{-3/2}\right]} \tag{11.24}$$

in relation to the mean biomass $\bar{w}$, a key variable in ecophysiological models. From this relationship, the actual stem number expected after self-thinning can be calculated. The stem number reduction is carried out by removing the trees exposed to the greatest competition from the stand. Yoda's rule can be transferred from herbaceous to woody plants, and therefore is related to Reineke's (1933) rule for evenaged forest stands (Pretzsch 2000, 2006a) (cf. Chap. 10, Sect. 10.4).

11.7.2.8 Derivation of Stand Structure and Tree Size

Many ecophysiological models, e.g. Running and Coughlan (1988), McMurtrie (1991), Liu et al. (1992), Comins and McMurtie (1993), Kellomäki (1993), Zhang et al. (1994), Eckersten (1994), Arp and Oja (1997), Landsberg and Waring (1997) and Cropper (2000), only specify the biomass development per area, but not the forest structures or stem dimensions, important for the scientific interpretation of the simulation outcome. Other models (e.g. Hauhs et al. 1995; Sloboda and Pfreundt 1989) include modules that allow the derivation of plausible stand structures and stem dimensions, and the documentation during the simulation runs.

A realistic description of the light absorption and resource uptake from the soil requires model-like reproductions of the crown structure and root space. The explicit allocation of the woody biomass is rather trivial, as its effect on the light climate within the crown space is minimal, it can be regarded as a compartment with no fixed spatial reference. The simplest assumption for the structure of the assimilating (leaf) biomass, or the fine root biomass is a uniform distribution within a defined volume, the so-called "big-leaf approach" (Arp and Oja 1997; Running and Coughlan 1988; Thornley 1991). Some models also simulate an additional undergrowth vegetation layer in the forest (Friend et al. 1997; Vertessy et al. 1996). The homogeneity of the assimilating compartments, however, does not exclude a differentiated treatment of different needle age classes in the case of conifers (Eckersten 1994).

For a better estimation of the true absorption of radiation, especially in structured pure and mixed stands, which may deviate significantly from the assumed homogeneity, the crown space is often divided into two (Hoffmann 1995), four (Meng and Arp 1994) or a variable number of layers (Aber et al. 1995; Bossel and Schäfer 1989), which possess different shares of leaf biomass and leaf area. Some

models even account for an uneven light penetration of an irregularly horizontal leaf area distribution (Mohren et al. 1993), while others divide each horizontal layer into cohorts of different tree species or classes (Kellomäki and Väisänen 1995). Principally, the same approaches can be transferred to the structure and processes in the root space (cf. Timilin and Pachepsky 1997).

The real macrostructure of stands may be approximated further by modelling each tree by its individual position, and shoot and root dimensions. This requires a three-dimensional representation of the stand, which, due to its processing intensity, has been realised so far only in few physiologically based forest growth models (Grote and Pretzsch 2002; Hauhs et al. 1995; Rötzer et al. 2008; Sloboda and Pfreundt 1989).

In models that resolve stand structure, or even individual-tree dimensions, the weight of carbon w_C that has accumulated in the compartment stem is used to calculate the diameter at breast height and tree height at the end of each simulation cycle, e.g. after a 1- or 5-year period. Once these dendrometric parameters are known, other stand structural parameters can be updated (cf. Fig. 11.20). Tree volume,

$$v = w_C/(k \times R) \tag{11.25}$$

is obtained from the amount of accumulated carbon w_C, k = carbon content/dry biomass, which is usually set to 0.5, and the species-specific wood density R (cf. Chap. 2, Table 2.8). The tree diameter,

$$d = \sqrt{(v \times 4)/(f_{1.3} \times \pi \times h)} \tag{11.26}$$

can then be calculated from the accumulated stem wood volume v, the predefined stem form factor $f_{1.3}$ and tree height h. In many ecophysiological growth models, beyond tree height development, the causality is still not explained completely (Hauhs et al. 1995; Mäkelä and Hari 1986; Pfreundt 1988; Sloboda and Pfreundt 1989). Instead, tree height is derived from a potential age–height curve as in individual-tree models, or calculated assuming a constant form factor and h/d value ($q_{h/d} = h/d$). The stem volume ($v = f_{1.3} \times \pi/4 \times d^2 \times h$) becomes ($v = f_{1.3} \times \pi/4 \times d^3 \times q_{h/d}$) and the stem diameter is

$$d = \sqrt[3]{\frac{v \times 4}{f_{1.3} \times \pi \times q_{h/d}}}. \tag{11.27}$$

Despite the disadvantage that the h/d-value is neither constant for an entire tree collective nor over larger simulation periods, the formulae provide a first mechanistic derivation of the tree dimensions from the estimated carbon assimilation. Such models include forest yield and economically relevant parameters as supplementary information derived from a top to bottom distribution of the carbon assimilates.

To overcome the disadvantage of constant h/d-values, these can be modified in relation to stand density. In the models TREEDYN3 (Bossel 1994) and FORSANA (Grote et al. 1996, 1997), the increase in biomass is added directly onto the

existing stem. Whether height or diameter growth are promoted equally (constant h/d-value), or one is favoured over the other, may be controlled in relation to the nature of competition in the crown space.

According to the assumptions of the pipe-model theory (11.21), the increase in leaf biomass is correlated directly with the increase in the conducting basal area, and hence with the stem diameter. This connection makes it possible to derive stem diameter from leaf biomass, even when the latter is calculated in a different way (Nikinmaa 1992). Height growth then results as a secondary parameter from specific h/d relationship, or from generalised, regionally calibrated stand height curves.

11.7.3 Overview of Matter Balance Model Approaches

Ecophysiological models were developed for a wide range of scales and purposes that can be roughly differentiated into four categories according to their stand structural resolution.

The first category is models that only provide stand scale biomass development in one or over a few years, such as the PnET family (Aber and Federer 1992; Aber et al. 1995, 2002; Li et al. 2000) or BIOMASS (Bergh et al. 2003), which usually provide detailed carbon and nitrogen balances, and thus primarily address ecological issues such as carbon sequestration and nutrient sustainability.

The second category is forest growth models that include parameters relevant to forestry, such as height and stem volume, at the stand level, usually run over one generation, such as EFIMOD (Komarow et al. 2003), TREEDYN3 (Bossel 1996), FORGRO (Mohren et al. 1987, 1995), FINNFOR (Kellomäki and Väisänen 1997; Matala et al. 2003), or 3-PG (Landsberg et al. 2001, 2003). This type of model aims to provide forest yield estimations in response to environmental impacts, including climate change.

The third category is individual-tree or tree-cohort models that are designed primarily to simulate forest development over several generations, such as 4C (Bugmann et al. 1997; Lasch et al. 2005), or PICUS (Lexer and Hönninger 2001), and feature several similarities with conventional gap models, yet differ by their explicit consideration of a closed carbon balance. They are particularly useful for forest services for defining long-term forest management strategies (e.g. species selection to ensure sustainable yield or sufficient protection from erosion).

The fourth category is structural–functional individual tree models, such as LIGNUM (Perttunen et al. 1998; Lo et al. 2001) or EMILION (Bosc 2000), which are only capable of simulating a rather limited number of trees as yet. However, a few models, such as BALANCE (Grote and Pretzsch 2002; Rötzer et al. 2005), use a relatively simple structure, yet, still represent the individual development of separate crown parts. With such models, small stands of mature trees have already been represented, indicating that this type of model could be used eventually to aid individual tree management in mixed forests, and still consider various site conditions dynamically.

It should be noted that the given examples of each type by no means represent the full spectrum of available models in this field. Furthermore, during the past decades, some models have shifted their primary purpose. Examples include the EFM (Thornley 1991) and BGC models (Running and Gower 1991; White et al. 2000), which were developed to simulate carbon and nitrogen balances, and were later modified to produce standard stand characteristics for management purpose (Korol et al. 1996; Thornley and Cannell 2000; Petritsch et al. 2007). Another approach is to modularise existing models to couple them with soil process or gap models (e.g. Peng et al. 2002; Wallman et al. 2005). In general, aided by increasing computational capabilities, we can observe a trend towards more complex models in each of the fields outlined above. This trend reflects a desire to consider a larger number of processes, impacts and feedbacks within the forest system.

11.7.3.1 Processes Take Place and Generate Structure on all Temporal and Spatial Scales

The description of ecophysiological stand models as process models is misleading in that, of course, all forest models describe processes. The transition from yield table models to evolution and succession models and subsequently to ecophysiological matter balance models accompanies a refinement of the temporal and spatial resolution of the modelling processes (cf. Chap. 1, Fig. 1.17). The increase in the structural resolution and mechanistics of the system abstraction does not necessarily make the simulation results more realistic. The ecophysiological growth models of this type developed to date still contain many untested hypotheses regarding, for example, root growth or the distribution of assimilates to leaves or needles, branches, and stem and roots, and rely on statistically parameterised functions. Good intentions to create *the* complete model tend to lead to unwieldy models that become loaded with more and more system details and, finally, contain so many, often hypothetical parameters, that the increase in complexity results in a loss of transparency and robustness. Kimmins (1997, pp. 491–492) refers to this tendency as “dinosaurism” in modelling.

The growth modelling on the basis of photosynthesis and allocation of the assimilates to plant organs reveals a relatively high level of mechanistic functionality compared to other forest growth models discussed. On the other hand, from the perspective of molecular biology, which looks at the cell level, even this type of approach may appear rather general and oversimplified. In the end, all explanation approaches merely provide an approximation of the fundamental processes of biological systems and their structures. Whether a model approach is perceived as descriptive or explanatory, statistical or mechanistic is relative, and depends on the observer’s perspective and the systems level of the particular investigation (Berg and Kuhlmann 1993).

11.8 Landscape Models

Landscape models deal with area units with much smaller scales than the stand level resolution, i.e. a few up to thousands of hectares. Principally, landscape models capture an entire region through a grid of cells, e.g. with a $50 \times 50\,m^2$ side length. Within each of the cells, stand development is simulated in 1- to 5-year periods (Fig. 11.23, thin black arrows indicate feedback within cells).

Depending on the model purpose, the stand dynamics at the cell level can be reproduced from statistical, mechanistic or hybrid models. Thus far, they are not different from those models already discussed. The innovation arises in the existence of interactions between the cells (Fig. 11.23, thick black arrows indicate feedback between cells). On the one hand, regional growth conditions and disturbance factors that affect forest growth within a certain cell can be modified by attributes of neighbouring and further distant cells (e.g. relief, wind speed and direction). On the other hand, the growth and mortality processes in a certain cell equally influence the conditions in its neighbouring or more distant cells. Whereas the within-cell processes are updated in 1- to 5-year periods (inner feedback loop), the processes between the cells (i.e. the landscape level) are updated at a coarser resolution, e.g. 10-year-periods (outer feedback loop).

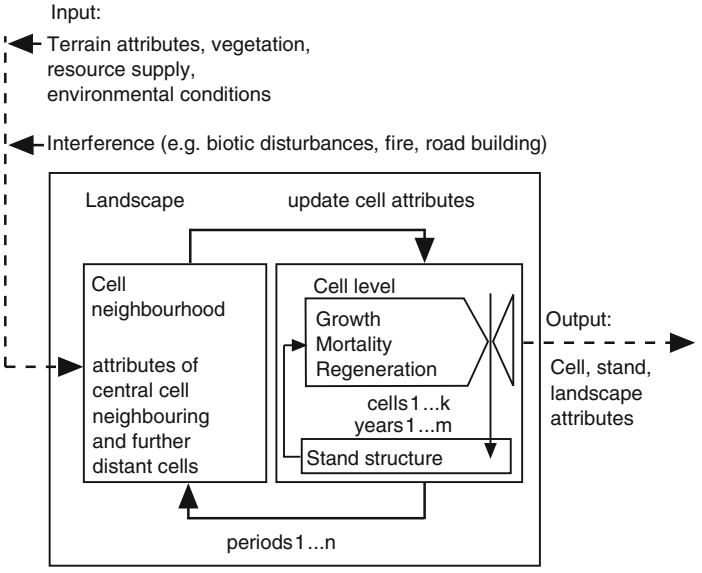

Fig. 11.23 After model initialisation by specifying terrain attributes, vegetation type and site conditions for each cell, and the defining of climate time series as well as expected disturbances, the landscape dynamics are modelled through two interacting feedback loops: The vegetation development of each cell is modelled with a high temporal resolution (feedback loop symbolised by *thin arrows* on cell level). The resulting development of the entire landscape is updated in coarser time steps and affects the modelling of the vegetation development on the cell level (feedback loop symbolised by *bold arrows* between cell and cell neighbourhood level)

The model is initialised by specifying site conditions, vegetation composition, biomass stocks, etc. for each cell. Furthermore, the climate scenario, disturbance factors and management strategies are defined at the landscape level. The development within the cells then depends on the cell-specific state variables (vegetation, site conditions, etc.) as well as the influence of neighbouring cells (wind exposition, fire events, flooding, etc.). The model output comprises cumulative landscape information (percent forest cover, water balance, tree species diversity) as well as spatially explicit representations in the mosaic of cells (bark beetle expansion, fire dynamics, storm damages).

Landscape models themselves may combine models for forest, grasslands, agricultural fields, etc. among which direct lateral interactions exist (e.g. mass movements), and indirect ones through atmospheric or hydrospheric exchange processes (Fig. 11.24). Such integrated system models are inevitable for interdisciplinary cooperation in the investigation of climate change consequences, biodiversity or natural risk assessments. For instance, the likelihood of flood, fire or drought occurrences, and the damage they cause, can be estimated only by integrating forest, agricultural and hydrological system components.

The role of landscape models is to assess potential effects of environmental change (climate, deposition, land-use changes) on regional-scale sustainability of forest functions (resources, protection, socio-economics). In addition, they reveal the consequences of certain natural disturbances (storm, fire, barkbeetle attacks), forest management activities (selective thinning, clearcut), or construction projects (forest roads, dams, river engineering) for the landscape as a whole. This knowledge is important; on the one hand, it provides decision makers with information about how to minimise adverse effects of environmental changes (mitigation), and, on the other hand, it identifies management strategies to ensure sustainable ecosystem functioning, even under changed environmental conditions (adaptation).

The first important area for the use of landscape models is in the analysis of the relationship between landscape structural forest arrangement and regional risks.

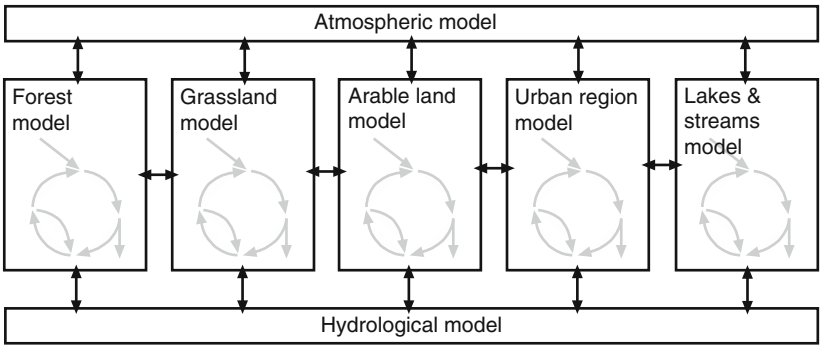

Fig. 11.24 Landscape models can combine models for forests, agriculture, grasslands, and aquatic and urban systems. The subsystems are interrelated through direct lateral exchange processes (e.g. by erosion, seed rain) or indirect ones via the atmosphere or hydrosphere

Examples include fire risks (He et al. 2004; Mouillot et al. (2001, 2002), windthrow risks (Ancelin et al. 2004; Cucchi et al. 2005), insect diseases (Lexer and Hönninger 1998; Sturtevant et al. 2004), mass movements (Kulakowski et al. 2006), air quality (Parra et al. 2004; Schaab et al. 2000), water availability (Strasser and Etchevers 2005) and water quality (Matjicek et al. 2003). While it is increasingly recognised that the long-term development of regional risks in response to environmental changes needs to take ecosystem properties into account, which, in themselves, are inevitably linked to those changes, landscape models that include integrative feedback cycles from disturbance regimes to ecosystem dynamics and vice versa are still scarce. The applications of gap models in combination with regional assessments of fire risk are examples of such developments (Laurence et al. 2001; Weinstein et al. 2005; Schumacher et al. 2006).

Assessments of regional-scale matter fluxes, e.g. water, carbon, and nutrients, represent the second application of landscape models. While this does not necessarily require the particular design of a new model, generally it is carried out with site-specific (matter balance) models in combination with GIS information on a regional scale. Examples of this type of application typically include the development of specific ecosystem properties such as forest growth (e.g. Lasch et al. 2002; Nuutinen et al. 2006), species change (e.g. Hickler et al. 2004), carbon budgets (e.g. Song et al. 2003), or changes in the water balance of catchments (e.g. Baron et al. 2000; Wattenbach et al. 2005). Other investigations have been concerned with more specific applications, such as soil acidification (Alveteg 2004) or nitrogen flux (Kesik et al. 2005, 2006). These analyses reveal a number of shortcomings because the applied models do not always account for the interactive dynamics of matter flux and forest structure. Important variables such as canopy coverage and leaf area index are often assumed to be constant in water, and nutrient balance studies although they are closely linked to species composition and tree size distribution that change continuously. On the other hand, site conditions, especially water and nutrient availability, are often assumed to be constant in forest growth studies although they change with changes in climate, deposition, or soil weathering. The simplified assumptions of a more or less constant forest structure, or equilibrium conditions for matter balance, restrict the regional application of such models to rather short periods.

The importance of an integrated coupling between vegetation dynamics and the dynamics of matter fluxes is most obvious for water, where the distinction between evapotranspiration into the atmosphere (that affects regional cloud distribution and precipitation) and runoff/percolation into ground and surface water (that determines water availability and flood occurrences downstream) depends on the vegetation type and successional, or developmental phase. Examples of coupled terrestrial/hydrological models include studies on water availability (e.g. Cui et al. 2005; Walko et al. 2000), and climate effects (Lu et al. 2001). Coupled terrestrial/hydrological models can also serve to determine the impact of forest dynamics and silvicultural management on nitrate concentration in surface and groundwater. Promising approaches in this direction have been developed in Sweden (Arheimer et al. 2005), the Netherlands (Wolf et al. 2005) and the US (Hartman et al. 2006;

Hong et al. 2006). Another important area, where long-term effects of climate change can be estimated only with coupled terrestrial/climate models, are air pollution issues such as ozone concentration, which depends on the emission of biogenic carbohydrates in rural areas. The particular importance in ozone episodes has already been shown (e.g. Derognat et al. 2003; Solmon et al. 2004).

11.8.1 Application of Landscape Model LandClim

As an example for the application of landscape models, we introduce LandClim, which analyses the effects of topography, climate and land use on forest structure and dynamics. A particular focus is on large-scale natural disturbances like fire (Schumacher et al. 2004, 2006; Schumacher and Bugmann 2006). LandClim abstracts the landscape as a grid of cells. The state of the forest in each grid cell is represented by the number and biomass of trees in cohorts (individuals of the same age and species). Processes at the stand-scale, i.e. growth and mortality, operate in annual time steps, whereas landscape-scale processes, i.e. fire, wind, harvesting and seed dispersal, are simulated with time steps in decades. The input into grid cells includes the initial conditions (stocking, forest floor vegetation, soil conditions, altitude etc.), the definition of management-regimes (type of forest use, tree species selection, regeneration etc.) and as climate scenarios (constant climate conditions, warming etc.). Then, the processes within the cells are modelled in annual resolution. Growth and regeneration of individual trees or tree cohorts are based on physiological processes, and linked to the water and nutrient balances of the particular sites. Such models are sensitive to environmental changes as well as to different kinds of disturbances, and can be used for short and long-term forest management planning. In particular, variables that have an effect beyond the grid cell level, e.g. seed dispersal, fire propagation and erosion, also are included in the model. Such variables are updated at smaller resolutions (e.g. 10- or 20-year intervals). They influence the development on the neighbouring cells via rules. For instance, the spread of fires depends on climate and topography; but it is independent of tree species composition. Fire effects, i.e. tree mortality, however, are species-specific. LandClim operates over long time scales (hundreds to thousands of years), and on large areas (>100 ha) with relatively fine grid cells of $25 \times 25\,m^2$.

Figure 11.25 illustrates the impact of direct (via increased species pool) and indirect (via altered fire regime) effects of climate change on forest biomass and species diversity in the Dischma valley near Davos (Grisons) in the eastern part of the Swiss Alps. The goal is to obtain a differentiated analysis of the above-mentioned effects with respect to elevation and exposition. The valley covers an area of $16.7\,km^2$, with an altitudinal range of 1,550–2,800 m; mean annual temperature is 3.2°C, and mean annual precipitation is approximately 900 mm. The first (reference) scenario for the current climatic conditions uses data from the climate station Davos–Platz (elevation 1,560 m a.s.l.). The second climate warming scenario with mean annual temperature of 6.2°C and mean annual precipitation of 700 mm corresponds to predictions based on the SRES A2 transient greenhouse gas scenario

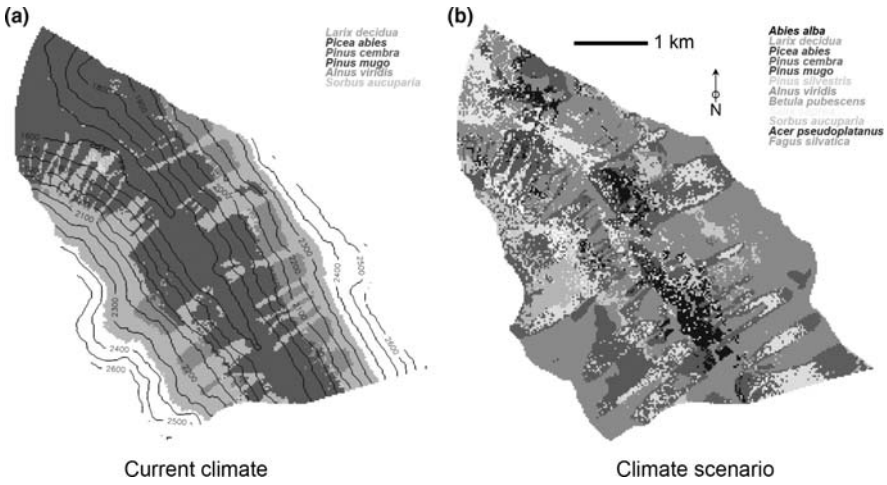

Fig. 11.25 Distributions of dominant tree species in the Dischma valley simulated with LandClim under (**a**) current climate conditions (3.2 °C mean annual temperature, 900 m mean annual precipitation) and (**b**) a climate warming scenario (6.2 °C mean annual temperature, 700 mm mean annual precipitation)

(Schar et al. 2004). Simulations commence with the current forest cover, and run for a period of 300 years. Twenty-five repetitions were performed for each scenario. The results show that, on a landscape scale, the diversity of (potential natural) forest types after 300 years is higher in the climate change scenario compared to current climatic conditions (Fig. 11.25a, b). In the valley bottom, stands dominated by Norway spruce are replaced by Scots pine, Sycamore maple, and Silver fir. There is an overall upward migration in tree species, and the upper treeline formed by *Pinus cembra* increases from 2,250 to elevations of 2,650 m a.s.l.

Long-term simulations with landscape models aim to achieve a better understanding of the intricate relationship between landscape structure and dynamics. They reveal long-term consequences of possible management alternatives by translating the scenarios, formulated in terms of land-use and climate change, into changes in the forest landscape structure. Visualisation tools like L-VIS may assist the visual interpretation of model results (see Sect. 11.9).

11.9 Visualisation of Forest Stands and Wooded Landscapes

In the models introduced so far, the results of simulation runs for standing volume ($m^3\,ha^{-1}$), net primary production ($t\ ha^{-1}\,yr^{-1}$), or potential annual cut ($m^3\,ha^{-1}\,yr^{-1}$) are meaningful for forest scientists and practitioners, but hardly for non-foresters involved in forest planning and decision processes. The easiest way to explain the results of scenario based simulations at the stand and landscape level to non-specialised stakeholders is by means of visualisation (Pretzsch

and Seifert 1999; Seifert 2006, 2008). Illustrations and photographs were among the first media to describe forest stands, landscapes and the availability of forest resources (Fig. 11.1). Realistic illustrations make use of the intuitive human potential for pattern recognition and imagination (Paivio 1971). Computer technology can provide a three-dimensional visualisation of forest stands and landscapes. The provision of easy to use tools, which enable the user to choose the perspective arbitrarily and interactively, represents substantial progress in this field. The opportunity to combine visualisation tools with simulation runs from forest growth models to show forest stand or forest landscape development over decades or even centuries is equally important. This affords the opportunity to look at scenario results from different angels, compare them visually, and paves the way for the integration of aesthetic aspects in long-term planning and decision making.

We consider four main criteria for an effective forest stand and landscape visualisation tool. First, visualisation needs to cover the temporal scales suited to both the level of human perception and tree growth and forest stand development. This necessity arises from the fact that people's perceptions of landscapes are rather short-term compared to forest regeneration cycles. People are not aware of slow changes occurring over long time periods, yet they are able to detect fast changes easily (Meitner 2005). The representation of long periods in small time steps, however, represents a challenge to any visualisation tool.

Second, visualisation should be based on solid data (e.g. Sheppard and Harshaw 2001). Any planning purpose should therefore remember Sir Arthur Conan Doyle's opinion that it is a capital error to visualise a scenario before one has facts. Immediately, one begins to twist facts to suit perception instead of allowing fact to inform perception. However, it seems to be a common feature that the primacy of sound data over artistic licence in the visualisation process has not been acknowledged fully (Wang et al. 2006).

Third, visualisation must keep to realism. To support the intuitive recognition pattern of the human brain, it is essential to display plants and landscapes as realistic as possible (Meitner 2005). This implies for instance that visualisation of forests needs to be based on individual-trees to account for structural differentiation which is an important element of forest recognition.

Finally, visualisation must allow free choice of perspective. A single static view is insufficient for an adequate impression of a forest stand or landscape. Different viewpoints and perspectives are required for an assessment of aesthetic value for decision making. The free choice of the bird eye view or the human perspective from the forest floor is equally important to experience the properties and aesthetics of a landscape (Bell 2001). The technical reproduction of a fast and smooth "immersion" into the forest is therefore a crucial aspect of visualisation. It helps to create a three-dimensional impression, and provides the user with a feeling of proportion.

Bishop (2005) emphasises the usefulness of real-time visualisation as a tool for public participation in decision making processes. This goes even further than merely providing different views of the landscape. Real-time visualisation enables the user to interactively switch between different scenarios, and manipulate the boundary conditions for simulations to see the results of changes instantly through changes in the visualised image.

To support long-term planning, many different approaches for the visualisation of trees and stands (e.g. Gilet et al. 2005) and forest landscapes (Deussen et al. 2002; Decaudin and Nayret 2004) were developed recently. The technical solutions stretch from point-based rendering to full ray tracing. However, software packages for stand and landscape visualisation are not yet very common. There are "all-purpose landscape visualisation" systems, which use certain object arrangements to display different ecosystems and do not allow for any interactive movement in the image. One of the most common systems of this kind is the Visual Nature Studio [VNS] (3D Nature, Vancouver, Canada), which assembles object arrangements, called "ecotypes", with single objects representing, for example, solitary trees. Within the ecotypes, the objects contained are arranged randomly according to prescribed density parameters. The coupling with simulation tools is achieved with GIS systems. Tools such as VNS are very useful if the specific forest structure is not very important. However, they require considerable computing resources, and are not capable of producing images in real-time. The Envision program (McGaughey 2006) applies similar methods, and was explicitly developed for forest management purposes. Thus, the data exchange with forest inventory databases has been optimised, and it is possible to retrieve numeric information about stands directly through the visualisation system.

Compared with these ecotype approaches, which, in most cases, display only abstracted tree objects or images, programmes like Lenné3D (Werner et al. 2005) and the software system AMAP (Blaise et al. 2002) visualise individual plants with detailed geometrical resolution, including even branches and leaves. Here, plant objects are very realistic, even from a viewing point within stand, or near the canopy. Furthermore, Lenné3D is able to display interactive animations of the image in real-time.

The third group of software solutions concentrates on the visualisation of forest landscapes and on the opportunity for the user to gain an impression from a walk or flight through the image. Examples of this group are ViewScape3D (ViewScape3D Inc.), Lenné3D (only for small areas) and L-VIS (Seifert 2006, 2008). These visualisation models make a direct link to statistical or mechanistic stand simulation systems possible, which is an important feature for displaying dynamic changes in the landscape. It is important to provide an interactive display as well as the opportunity to move back and forth in time to understand the processes of landscape change. L-VIS (Seifert 2006) meets both needs through a tight coupling with a simulation model for long-term tree, stand or landscape development.

11.9.1 Visualisation Tools TREEVIEW and L-VIS

As an example of a visualisation tool, we present TREEVIEW, a software optimised for fast, spatially explicit interactive visualisation of forest stands, and L-VIS, the forest landscape visualisation software (Pretzsch et al. 2008; Seifert 2008).

Fig. 11.26 TREEVIEW enables the interactive elimination of trees for promoting selected future crop trees

TREEVIEW is designed for realistic and thematic forest visualisation at the stand level. It is a data-driven, interactive visualisation tool. One design goal was to display directly the outputs of spatially explicit statistical or mechanistic individual tree models, while staying on the same level of resolution as simulation models, i.e. the individual tree and tree compartment level. With TREEVIEW it is possible to display interactively the simulation results of individual-tree models, perform a virtual flight through the stands, and manually select future trees or trees for interactive thinning by mouse click (Fig. 11.26). It is possible to visualise a given stand structure, or to disseminate simulation results of stand level forest growth models for teaching purposes. The software also supports thematic visualisation like the false colouring of crowns, e.g. to display the biomass density distribution calculated by ecophysiological models (Fig. 11.27). TREEVIEW displays geometrically modelled trees with the same geometry as the virtual objects in the individual-tree simulation models. To create a more realistic appearance, species-specific textures are applied to the tree models.

The landscape visualisation system L-VIS (Seifert 2006, 2008) was developed to create realistic views of forest landscapes up to an area of $5 \times 5\,\mathrm{km}^2$. It uses the simulation results of individual tree simulators, such as SILVA 2.0, BWIN, or MOSES (Pretzsch et al. 2008), to visualise changes in a landscapes, e.g. according to defined management or climate scenarios. It can be used in participatory planning, and the dissemination of scientific results on expected landscape changes to the public. Examples of applications are the visualisation of impacts of insect outbreaks, power plants or motorways (Fig. 11.28).

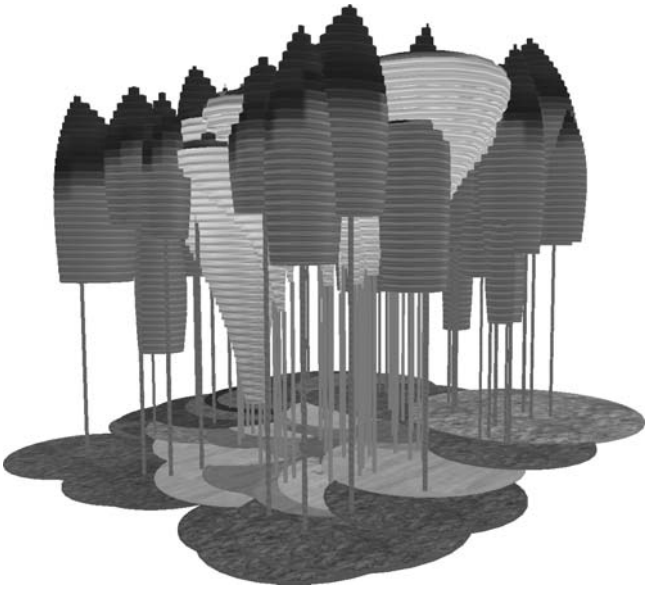

Fig. 11.27 TREEVIEW can visualise the output of ecophysiological models (e.g. nutrient content in different organs, water content, leaf area density). In this example leaf area density in a mixed stand of Norway spruce and European beech is indicated by colour tone (the darker the shade, the higher the leaf area density)

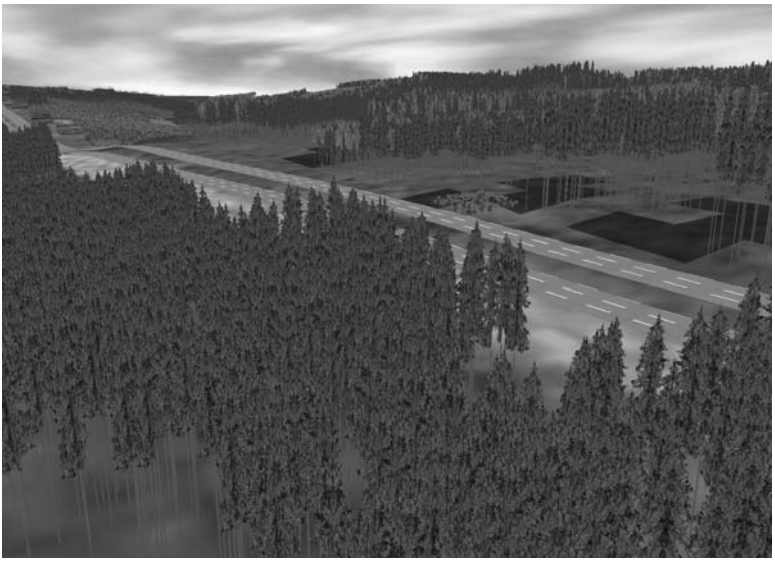

Fig. 11.28 Example of the use of L-VIS for displaying landscape changes in a motorway planning project. Area with high risk of wind-throw are shaded in *light grey*

One goal in the design of L-VIS is to preserve the individual tree as the structural element in forest landscapes. In central Europe, with its long tradition in continuous cover forestry and selective thinning, features like species mixture, individual tree distances, tree group spacing, or variation of tree sizes are crucial silvicultural specifications. At the same time these features strongly determine the visual impression of a forest landscape. For this reason, L-VIS uses the individual-tree dimensions, tree positions and distribution of regeneration from the simulation results of individual-tree models. These individual-tree models perform actual simulations of the long-term forest development at the stand, estate and landscape level based on inventory data, and provide the data for landscape scale visualisation. The area surrounding inventory sample points are represented according to the exact simulation results of individual tree models, using inventory data as initialisation and calibration data. The forest dynamics among the sample points is completed by structural interpolation routines.

To display individual trees, species-specific textures from photographs are scaled to the individual-tree dimensions. Additional methods for providing high visual realism of the images are incorporated into the visualisation system directly. These methods generate additional tree properties like crown radius variation and stem declination.

The user may obtain an visual impression of the scenario displayed not only from an interactive walk through the forest, but also may track virtual change in the forest over time. This is achieved with the help of pre-generated time slices from individual-tree model results. Figure 11.29 shows a section of the "Bürgerwald" in Traunstein. Initially, the stand comprises a 25-year-old mixed stand of Norway spruce and European beech. This stand, with an area of about 5 ha, is displayed firstly in its existing condition by the visualisation program L-VIS (Fig. 11.29, upper line). The growth simulator SILVA is used to simulate the stand development from 25 to 125 years in 5-year time steps. Three management alternatives are compared in three corresponding simulation runs: (1) development with no silvicultural management, (2) moderate promotion of beech by thinning from above, and (3) strong promotion of beech by thinning from above. The results of these alternatives are visualised with L-VIS (Fig. 11.29, left, middle and right column, respectively). With no silvicultural intervention, a homogeneous pure Norway spruce stand evolves (left column). Beech cannot compete against Norway spruce, and is lost almost completely by the age of 125 years due to self-thinning. With moderate promotion, European beeches account for 20% of the basal area at the end of the simulation period, with strong promotion, 50%.

The individual tree model not only provides the tree dimensions at the beginning and end of the simulation period. Tree growth, regeneration and tree loss are resolved in one to 5-year time steps, and make possible a four dimensional virtual flight through the simulated scenario to visualise not only spatial but also temporal changes of the landscape. The level of abstraction in the model is identical to the level of biological observation. Visualisation may evolve into an effective tool in participatory planning and decision-making processes by assisting forest managers and stakeholders to make decisions about which what forest management strategies to adopt.

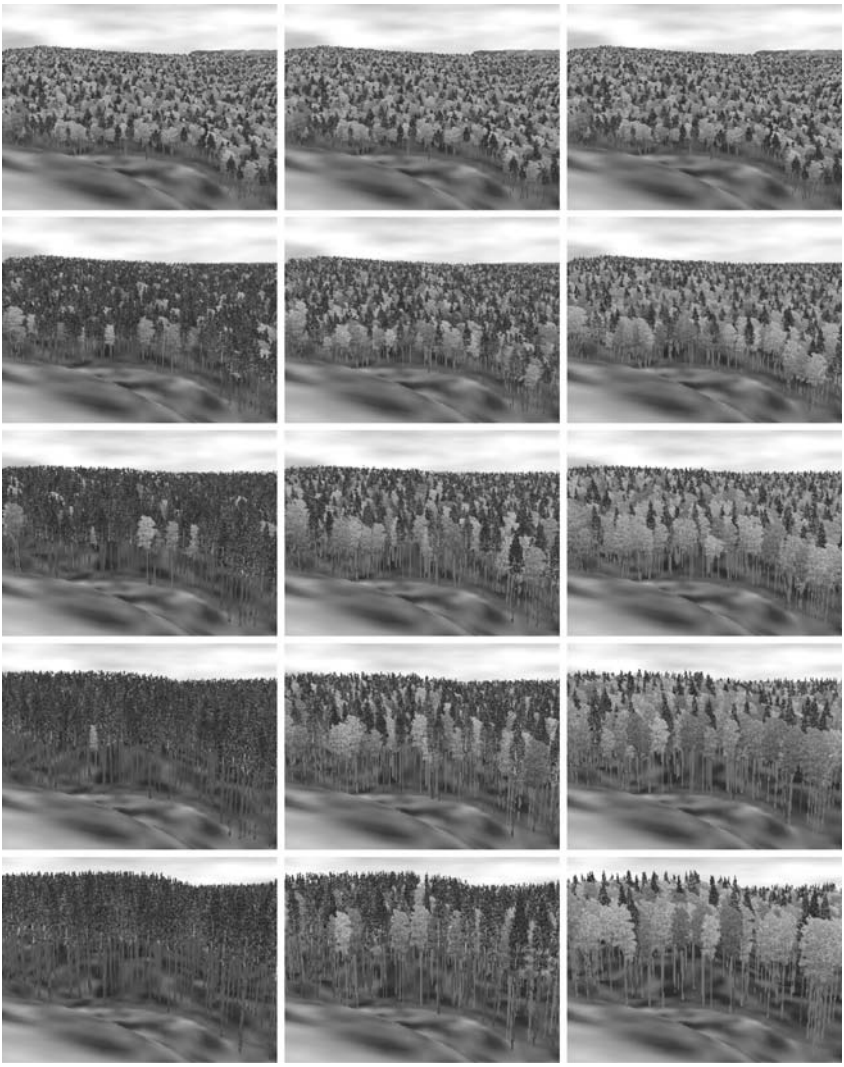

Fig. 11.29 Visualisation at the landscape level by L-VIS (Seifert 2006, 2008). Development of Norway spruce–European beech mixed stands in the Traunstein forest estate, Germany, from age 25 to 125 (*from top to bottom*). Without management (*left column*), moderate promotion of beech through thinning from above (*middle column*) and strong promotion of European beech (*right column*)

11.10 Perspective

The overview of the different kinds of models and current research aims reveals two general types of models. The first type includes models with rather generalised input requirements (e.g. age and site index), and thematically restricted output variables,

typically including accurate predictions for wood-production. These models are mostly built on regressions deduced from measurements of the required response variables from long-term trials or sample plots. Since the same variables required for model construction are produced in the output, they are generally classified as "empirical" (Constable and Friend 2000).

On the other hand, models have been introduced that explain various forest developments from underlying physiological and ecological principles. Although the biometrical description of these principles may also be derived from sample measurements, the inherent linkage between two or more levels, and the implementation of cause–effect chains led to the classification of this approach as "mechanistic" or "process-based" (Constable and Friend 2000; Mäkelä et al. 2000). Since several important processes at the physiological and individual level influence the developments of the stand, these models require a more extensive set of input variables. As these are often unavailable, or need to be estimated roughly, and since process knowledge is incomplete, mechanistic models are often comparably unreliable with respect to growth and yield prediction and management decisions.

An innovative option are hybrid model approaches that have been pointed out as one of the most promising developments for future ecosystem management decision support (Battaglia and Sands 1998; Landsberg 2003; Monserud 2003). These aim at an estimation of stand primary production considering the dependencies of physiological processes on environmental conditions, in combination with statistically determined allocation patterns of the produced biomass to individual trees. Especially, the second aspect requires expertise from growth and yield research. Hybrid models comprise above and below ground processes and provide an extensive list of output variables. However, the information about the vegetation and soil processes such as net carbon gain, allocation and turnover is generally derived from only a small number of extensive long-term experimental plots.

The current challenge of forest ecosystem management in Europe is the integration of system knowledge from different temporal and spatial scales and from various disciplines. For Europe, where ecosystem management is oriented at integrative concepts, models are needed that consider and provide ecological, economical and social aspects alike. Planning and decision making in European forests requires the evaluation of long-term scenarios of different treatment options (such as thinning, species selection, regeneration techniques) and environmental change assumptions with respect to various forest functions as well the trade-off between them (e.g. growth and yield, water supply, wood quality, recreation, or esthetical value). For this purpose, a toolbox principle can be realised in form of an independent platform that controls a set of models with different focuses that can be selected according to particular needs (e.g. matter balance, habitats, visualisation). This seems more promising than the development of a single giant model, that covers ecological, production, and landscape issues equally well.

Summary

The progression from prototypes of stand oriented growth models, the yield tables for pure stands from Schwappach and Wiedemann, to stand growth simulators for defined management strategies followed by ecophysiological process models as research tools and landscape and visualisation models for ecosystem management reflect the changes in the aims of modelling, the advance in forest ecosystems knowledge and the continuous development of forest growth theory.

(1) A model is an abstraction of a real system. Forest growth models abstract the structures and processes occurring in forest stands to meet a specific aim and purpose.
(2) When a model is translated into a computer programme a simulator is created, which models the behaviour of the system with the assistance of the computer.
(3) As a model describes the most important elements of a system, system interrelations and, in particular, cause-effects chains, it can be regarded as a hypothesis of the structure and behaviour of the real system. The model, and hence the aggregated hypotheses it contains, is validated on the basis of the results of the simulation runs. Models promote the advance of knowledge.
(4) As long as the model is not falsified it is regarded as a representation of the real system. It may be used to carry out experiments, prognosis and scenario runs, which is particularly useful in forest growth research where the long observation periods and the intensive field experiments prevent the experiments from being carried out in reality. Approved models can be applied for research, practice and education.
(5) Models support the decision process in practice by simulating stand growth in time-lapse. The scenario calculations allow analysing the effects of silvicultural treatments, changes in the site conditions, or disturbances on stand, enterprise and regional levels.
(6) The yield tables that were first introduced at the end of the nineteenth century can be regarded as the first stand models. Being constructed for pure stands under different thinning intensities, the stand development was modelled from stand level data. The yield tables listed the important stand characteristics (tree number, mean height, mean diameter, basal area, form factor, annual increment, total volume production, and mean annual increment) in 5-year intervals in tabular form. The way from the earlier experience tables to the first standardised yield tables and later to computer supported yield table models has generated a fundamental information base for sustainable wood production.
(7) In the 1960s, a second generation of models arose, which, in addition to stand level data, also produced stem number frequencies and diameter classes to enable better predictions of assortment yield, timber quality and financial yield. Differential equation models, distribution extrapolation models and stochastic evolution models served this purpose. They abstracted the development dynamics of even-aged homogeneous pure stands by shifting the stem number-diameter distribution along the time axis.

(8) Individual-tree models achieve a much higher level of resolution in the system abstraction and modelling. They divide the stand into a mosaic of individual trees and model their interactions as a spatial-temporal system in the computer. Since the individual tree is the basic information unit, the level of description is identical to the level of biological observation. Averaging and summarising the individual tree data produces the stand level data required in forest management.

(9) Small area or gap models reproduce the growth of individual trees in forest patches (e.g. $100\,m^2$ areas) in relation to the prevailing mean growth conditions at the site. They are used to investigate competition and succession processes in near natural forest stands.

(10) Matter balance models reproduce tree and stand development from fundamental ecophysiological processes such as radiation absorption, interception of precipitation, evapotranspiration, nutrient uptake, photosynthesis, respiration, carbon allocation, senescence and mortality. In addition to predicting the wood yield from trees and stands these models also provide information about carbon, nitrogen and water cycles, thereby supporting a comprehensive understanding and management of ecosystems.

(11) Due to the large data demand for initialisation and parameterisation, long-time forest growth surveys and detailed climate and soil time series, the ecophysiologically based process models have primarily served as research tools to date. However, in future they will become increasingly relevant in forestry practice. The increasing demand for information about the reaction of forest ecosystems to changing conditions requires a flexibility inherent only in ecophysiological process models.

(12) Landscape models can combine models for forests, agricultural, grassland, aquatic and urban model systems. They link these subsystems through exchange processes via atmosphere and hydrosphere. By visualising scenario outcomes on stand or landscape level, the long-term consequences of different species compositions, thinning strategies or regeneration systems with respect to forest esthetics, recreation value and scenic beauty can be conveyed to decision makers at the round table.

(13) A "toolbox" of models with different focuses seems more promising than developing one single complex model that covers ecological, production, and landscape issues equally well. Improving networks of meteorological conditions, detection of pollutants, terrestrial and airborne inventories of forest stands, site conditions, etc. can be more and more integrated in models as they deliver increasingly suitable data for parameterisation, calibration or initialisation of different model types. This way, information for modelling and simulation can be induced from the inventory data itself, while former approaches deduced system behaviour from general models.

Chapter 12
Evaluation and Standard Description of Growth Models

This chapter refers to forest growth models and growth simulators that serve the following purposes: make predictions for short-term and medium-term planning, long-term scenario calculations for the development of stand management strategies and provide information on growth responses to stand treatment and disturbances. The presented criteria for model description, model evaluation and ongoing development, when applied cautiously and reasonably, may also be transferred to other models of a different type, e.g. models based on ecophysiological processes.

For a better understanding, the following strict difference is made between the concepts of forest growth modelling and growth simulation. The biometric and mathematical representation of growth processes results in a growth model. The conversion of this growth model into a practicable computer program for prediction and scenario calculations results in the development of a growth simulator. Therefore a model must exist before a simulator can be developed, yet the development of a model need not necessarily result in a simulator.

The evaluation of growth models should look at the suitability of the model selected, the validity of the biometric model developed, and the suitability of the software used to translate the biometric model. Thus the evaluation of a biometric model not only involves testing its accuracy (Gertner and Guan 1992; Vanclay and Skovsgaard 1997). First, the terms evaluation, validation and verification need to be clarified.

By evaluation we mean the "[...] analysis and assessment of a case, primarily an accompaniment to an investigation. In this case, evaluation means checking the efficiency and success of a model being tested. [...]" (Brockhaus 1994, vol. 6, p. 716).

Validation is one aspect of evaluation (Brockhaus 1994, vol. 23, p. 42): "[...] The validation indicates the degree of accuracy to which a method measures what it purports to measure [...]. The determination of the validity (validation) occurs 1) on the basis of the agreement of the test results with a criterion, obtained outside the test values [...] (criterion validity), 2) on the basis of whether a

H. Pretzsch, *Forest Dynamics, Growth and Yield: From Measurement to Model*,
DOI: 10.1007/978-3-540-88307-4_12,

prediction is correct (predictive validity), 3) on the basis of the plausibility of the logic and content (content validity), or 4) on the basis of the whether the context of the theory and methods are verifiable (construct validity) [...]".

The terms validation and verification often are used incorrectly as synonyms. A growth model cannot be verified, since, verification involves "[...] in general, the proof of the truth of statements [...]. According to the theory of Critical Rationalism (esp. K. R. Popper), the conclusive verification of general empirical statements (hypotheses, laws) is not possible, yet conclusive falsification is [...]" (Brockhaus 1994, vol. 23, p. 213; Popper 1984).

In the following discussion, we adopt the individual tree simulator SILVA 2.2 to explain evaluation and validation. However, the methods can be transferred readily to other models, such as BWIN, PROGNAUS and MOSES, which are used widely in German speaking regions (Nagel 1996; Sterba et al. 1995; Sterba 1999; Hasenauer 1994, 1999). Several sections of this chapter are based on the "Recommendations for the Introduction and Further Development of Forest Growth Simulators" from the Growth and Yield Science Section of the German Union of Forest Research Organisations (Deutscher Verband Forstlicher Forschungsanstalten 2000; Pretzsch et al. 2002b), prepared with the aim of standardising model descriptions, model evaluation and software structure.

The processes of testing model approaches, validating biometric models, and evaluating software are not one-off steps. Rather, they accompany the development of the model, and also are dependent on the state of technology. Consequently, model development is an iterative process (cf. Chap. 15, Fig. 15.1).

12.1 Approaches for Evaluation of Growth Models and Simulators

12.1.1 Suitability for a Given Purpose

When assessing the suitability of a model, one questions whether it serves its intended purpose. The following criteria are important in the assessment: model integration into the forestry information flow; the extent to which the existing knowledge and database is used; and the degree of complexity of system abstraction.

12.1.1.1 Integration of the Model into the Forestry Information Flow

In this aspect of evaluation, the model is examined to determine whether the initial, and control parameters required are compatible with the information available to the user. The model should use the information available about site conditions and stand structures to the greatest extent possible for predictions. Furthermore, it should have

the flexibility to use, as input data, the individual tree data with or without tree coordinates, mean stand data, sample data from permanent sample plots, angle count samples, or full inventories. The output variables produced by the model also should meet the user's information needs. When the user is interested in testing new silvicultural prescriptions for improving the quality and stability of a stand to increase the value of, and minimise the risk to growing stock, then the output variables from yield tables or diameter distribution models do not meet the information needs. Instead, the user expects if–then statements from a model indicating the implications of treatment scenarios for the assortments produced, for wood quality and individual tree and stand stability.

12.1.1.2 Use of Current Knowledge and Data to the Full Extent

A model should be able to use the available data and existing biological knowledge to the greatest extent possible to fulfil its purpose. Whereas primary data once entailed cumulative and mean stand values, individual-tree dimensions gradually have become more important in surveys of long-term sample plots and in forest inventories since about the 1960s. Thus, in recent decades, a considerable body of information has been collected about the dimensions, neighbourhood structure and growth behaviour of individual trees within the stand.

At the same time, data for site factors and disturbance factors from more detailed surveys of long-term sample plots and inventory plots have improved. The measurement of tree coordinates, crown radius projection, stem analysis, measurements retracing shoot length growth, branch measurements, and qualitative assessments of standing and fallen trees are almost an essential feature of standard inventories conducted on experimental plots. Data from such detailed inventories of sample plots have enabled a series of growth relationships to be developed at the individual-tree level in recent years, for example, the relationship between competitive status and stress of individual trees and their growth rates, or the relationships between competition and stem shape and stem stability.

Forest models and growth simulators that intend to manage the transition from evenaged to unevenaged stands with forest management practices such as "structural thinning" and "target diameter harvesting", and to establish and care for mixed stands, should make use of such relationships as they envisage the stand as mosaic of individual, interacting trees.

12.1.1.3 Degree of Complexity of System Abstraction

The degree of complexity selected for system abstraction should be tested continually. Modelling should be carried out at a spatial and temporal scale compatible with the explanatory variables available for parameterising and validating the model, and with the output variables the user expects from the model. Whereas, for example, statements about branch and leaf growth separated into crown layers in either

daily or yearly time-step are expected from an ecophysiological process model for research purposes, such output parameters would produce unnecessary, excessive information for users of management models.

Whether or not a model serves its purpose can be tested best through participatory model development, such as outlined in the following example for the simulator SILVA 2.2. Since the growth model SILVA 2.2 was developed at the outset in close cooperation with different model users, including forest scientists, forest planners, lecturers, freelance experts, consultants and advisers for state, private and communal forests, the test of suitability of the model was not an independent step. On the contrary, model development and suitability testing was an iterative development process (cf. Chap. 15, Fig. 15.1).

At the suggestion of these users, the approach for determining the site–growth relationship, which was based on age–height-curves dependent on site index in the first version, was replaced by a more flexible approach. In version SILVA 3.0, site conditions can be accounted for by site index (Pretzsch 1992a), site variables from site mapping surveys (Kahn 1994), or by potential age–height curves estimated from inventory data (Ďurský 2000; Klemmt 2007).

To use forest inventory data as initialisation data for prognosis runs, algorithms were developed to generate forest structures. These algorithms produced plausible data for initialising simulation runs at the stand level from data collected in sample inventories of different intensities (Pretzsch 1993, 1997). A stand structure generator provides a flexible interface between inventory data of variable resolution and spatially explicit individual tree simulators.

The users from forestry management and forestry schools also requested the expansion of the original output parameters, almost exclusively relevant to wood production, to include economic and ecological variables, and a more realistic visualisation of the stand structures modelled (Pretzsch et al. 2008; Seifert 2006).

In addition to the interactive version of the model, which is suitable for processing scenarios for individual stands, an automated batch-mode also was developed to facilitate the use of the simulator at the enterprise, regional or state level. To achieve this, stand data from forest planning inventory databases and site mapping databases were read into the model sequentially so that an unlimited number of predictions can be run continuously to completion through the control data files (Pretzsch et al. 2005a,b, 2008).

12.1.2 Validation of the Biometric Model

The most critical element of validating growth models lies in quantitative comparisons of model simulations to actual growth behaviour. Measures of bias $\bar{e}$, precision s_e and accuracy m_x need to be determined here (Akça 1997; Freese 1960).

Figure 12.1 illustrates the concepts of bias and precision with target shooting, where the shots diverge from the bulls-eye (inner circle) in different patterns. Independent of whether the shots hit the bulls-eye, or systematically land next to it,

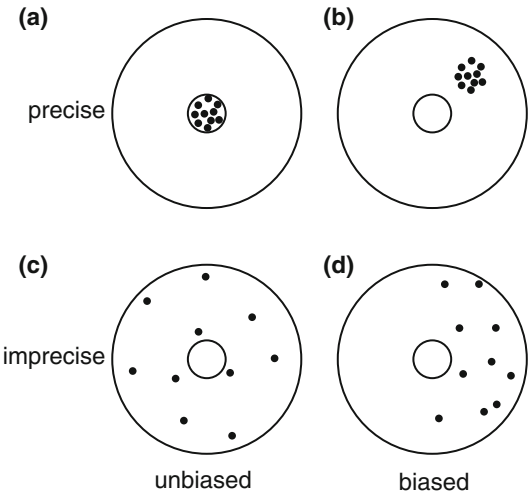

Fig. 12.1 Bias and precision as the two components of accuracy: (**a**) highest accuracy because repeated attempts (*dots*) are neither scattered nor deviate systematically from the bulls-eye as on targets (**b**), (**c**) and (**d**) (after Gadow and Hui 1999)

the precision indicates how close repeated shots are to one another. In Fig. 12.1a,b, the precision is high, in Fig. 12.1c,d precision is low. The bias quantifies the degree of systematic deviation of the shots from the centre. For example, the shots in Fig. 12.1b have a high precision, yet they deviate systematically from the centre. Only a precise and unbiased estimation provides a high accuracy, as can be seen on the target presented in Fig. 12.1a (Gadow and Hui 1999).

12.1.2.1 Bias

If we compare the results of the simulation runs ($x_{i,i=1\ldots n}$) for each of $i = 1\ldots n$ stands with the actual development of these n stands ($X_{i,i=1\ldots n}$), we obtain the differences $e_i = x_i - X_i$. The mean difference between simulation and observation,

$$\bar{e} = \frac{\sum_{i=1}^{n} e_i}{n} = \frac{\sum_{i=1}^{n} (x_i - X_i)}{n}, \tag{12.1}$$

corresponds to the bias in the simulation for the estimated stand characteristic x. Reliable statements about bias are only possible by comparing a large number of simulated and actual developments. In the schematic diagram in Fig. 12.2a, the simulated and the observed age-diameter growth of forest stands have been drawn wide apart deliberately so that the large bias is apparent. The systematic deviation between predicted and observed values can also be expressed as a percentage of the mean observed value $\bar{X}$:

$$\bar{e}_{\%} = \frac{\bar{e}}{\bar{X}} \times 100. \tag{12.2}$$

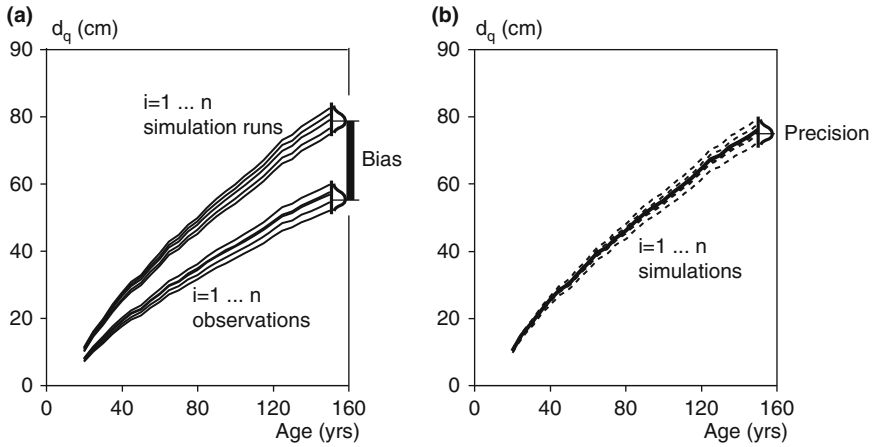

Fig. 12.2 Diagram of bias and precision of model predictions. (**a**) Bias (*solid bold line*) obtained from the mean difference of i = 1…n comparisons between observed and predicted developments. (**b**) Precision expressed by the degree of concentration of the i = 1…n predictions (*dashed lines*) around the mean (*solid bold line*)

12.1.2.2 Precision

The precision s_e indicates the amassing or concentration of simulation values around the arithmetic mean of the predictions. It is calculated from the deviation of the simulation values ($x_{i,i=1...n}$) from the observed values $X_{i,i=1...n}$, once the simulated values have been cleared of bias. If we replace the differences $x_i - X_i$ by e_i (cf. (12.1)), then the precision is represented as the standard deviation of the bias:

$$s_e = \sqrt{\frac{\sum_{i=1}^{n} (x_i - \bar{e} - X_i)^2}{n-1}} = \sqrt{\frac{\sum_{i=1}^{n} (e_i - \bar{e})^2}{n-1}}. \tag{12.3}$$

Often precision is given as a percentage of the mean observed value:

$$s_{e\%} = \frac{s_e}{\bar{X}} \times 100. \tag{12.4}$$

In Fig. 12.2b, the precision of the simulation is apparent by the width of spread of the dashed lines. The bold solid line represents the mean value of many simulations; the dashed lines show the degree of concentration of i = 1… n simulations about the line representing the mean. When the arithmetic mean of the simulation values clearly deviates from the actual development, as shown in Fig. 12.2a, bias in the simulation has prevented the actual value from being obtained. The precision of the simulation values is high in this case, yet their accuracy is low due to bias.

12.1.2.3 Accuracy

If we want to subject a model to a broad test of accuracy, then simulation calculations would be carried out for n stands. The accuracy m_x is calculated from the $i = 1 \ldots n$ differences between the predicted and observed values, $x_{i,i=1\ldots n}$ and $X_{i,i=1\ldots n}$:

$$m_x = \sqrt{\frac{\sum_{i=1}^{n} (x_i - X_i)^2}{n-1}}. \tag{12.5}$$

The accuracy m_x of the model in relation to the parameter x is obtained from the precision s_e and the bias $\bar{e}$:

$$m_x = \sqrt{s_e^2 + \bar{e}^2}. \tag{12.6}$$

The relative accuracy is obtained from

$$m_{x\%} = \frac{m_x}{\bar{X}} \times 100 \tag{12.7}$$

and expresses the accuracy as a percentage of the actual mean $\bar{X}$. The accuracy represents the degree to which the estimation approximates the reality. It can be unsatisfactory when bias $\bar{e}$ occurs. Furthermore, poor accuracy may arise from a low precision s_e. The greatest accuracy m_x occurs when there is no bias, $\bar{e} = 0$, and precision is high. In such cases, the accuracy m_x takes on small values and approaches s_e because, in equation (12.6), $\bar{e}^2 = 0.0$.

12.1.3 Suitability of the Software

We have developed a growth model once we have a biometric reproduction of stand growth. For it to be useful for predictions and scenario calculations in forest practice and forest science, it is converted into a forest growth simulator by a computer program. The acceptance, distribution, and opportunities to expand the program depend on whether the program is user friendly, whether it can be applied to meet a broad range of information needs, whether the interfaces included permit switching to and from other programs and databases, and whether the software is well-documented (van Steenis 1992). The following questions are of interest to the user.

Is the Forest Growth Simulator User-Friendly?

The qualities of the software that translates the biometric growth model are critical for the acceptance of the model. The user-friendliness of a program is an essential aspect, and it is achieved best when the user interface is based on a known, standard software design. User-friendly programs are predominantly self-explanatory, and can be mastered quickly.

Are the Simulator and Its Components Flexible in Their Application?

The biometric model should be programmed in a language that is not specific to a particular platform. A modular structure for the program core ensures that individual calculation routines are interchangeable between different working groups, and can be developed further independently.

Can the Forest Growth Simulator be Integrated into the Forestry Information Flow?

Both the definition of interfaces for the user's input data, and the definition of data formats for coupling the simulator to other programs and output of results are crucial for the practical application of the simulator. An interactive model is the best option for training and further education, and for the development of tending regimes from silvicultural scenario calculations.

Alternatively, simulators for growth predictions at the enterprise level, which could assist utilisation planning, are run in batch-mode. In this case many individual stands are simulated over long time periods without user interaction. For this purpose, the program is controlled with external data files in which, for example, the type of tending operations, regeneration measures and harvest times are stipulated.

Is the Forest Growth Simulator Adequately Documented?

In addition to the standard descriptions recommended in Table 12.1, a handbook outlining the model structure, the operating instructions for the simulator, examples of model calculations, and opportunities and limitations of the growth model must also accompany a growth model designed for use in teaching, research and practice. The handbook should provide a reference list of the most important sources, outlining the database for the parameterisation of the model, the model parameters and functions, model evaluation and the technical requirements for installing the model.

12.1.4 Customising Models and Simulators for End-Users

The following discussion about the identification of end-users, model transfer to users, and model application is based mainly on experience with the SILVA 2.2 and 3.0 simulation models (Chap. 13), but is probably partially transferable to other models. The best way to ensure that the application of the model is flexible is to tailor the simulation model user-interface as much as possible to the requirements of the end-user, who may be a practitioner, researcher or a lecturer. Thus, we can distinguish completely different user-groups; a clear separation between the graphical user-interface and the model itself makes customising the model easier.

Table 12.1 List of criteria for the standardised description of growth simulators. The criteria model approach, range of application, calibration specifications, etc., with up to 11 model properties each, should be described in concise form, with references to the relevant literature

Criterion		Model properties
1 Model approach	1.1	Spatial resolution (competition, regeneration, treatment)
	1.2	Age dependency
	1.3	Principle of growth model (e.g., potential/reduction, direct estimation, growth equations using site factors or site indices site-specific growth potential)
	1.4	Deterministic and stochastic model components
	1.5	Flow chart
2 Range of application	2.1	Silvicultural scenario studies
	2.2	Updating of forest stands
	2.3	Updating of larger assessment units
	2.4	Instruction, professional training, research
3 Calibration specifications	3.1	Specifications with regard to region
	3.2	Site specifications
	3.3	Types of mixtures and stand structure
	3.4	Integrated treatment variants
	3.5	Integrated tree species
	3.5	Tree dimensions covered
4 Input	4.1	Area shape and size
	4.2	Minimum input data requirements
	4.3	Additional input data to be possibly processed
	4.4	Automatic generation of missing information
	4.5	Database interface
	4.6	Maximum number of trees per calculated area
5 Software control	5.1	Use (interactive, batch-mode)
	5.2	Possibilities of program control (visual, algorithmic)
	5.3	Interactive changing of equations
	5.4	Interactive changing of coefficients
	5.5	Saving of interim results with continuation
6 Output	6.1	Tree lists
	6.2	Stand characteristics
	6.3	Yield characteristics at forest enterprise level
	6.4	Structural characteristics at stand and forest enterprise level
	6.5	Economic measures
	6.6	Biomass components
	6.7	Visualization methods (spatial representation, diagrams)
	6.8	Interfaces with other programs
7 Sub-models of the growth simulator (concise description)	7.1	Database
	7.2	Increment model (model principles)
	7.3	Representation of liberation felling effects
	7.4	Crown model (dynamic, static)
	7.5	Mortality model
	7.6	Ingrowth model
	7.7	Stochastic components of sub-models
	7.8	Derivation of coefficients
8 Additional algorithms	8.1	Statistical timber grading
	8.2	Thinning algorithms
	8.3	Determination of ingrowth co-ordinates
	8.4	Biomass equations

(continued)

Table 12.1 (continued)

Criterion		Model properties
	8.5	Inventory interface
	8.6	Prediction loops for forestry enterprises
	8.7	Abort criteria and data complementation
	8.8	Three-dimensional stand visualization
	8.9	Consideration of edge effects
	8.10	Quantification of spatial structure
	8.11	Continuous updating
9 Model validation	9.1	Precision
	9.2	Bias
	9.3	Accuracy
	9.4	Sensitivity analysis
10 Software and hardware	10.1	Operating system
	10.2	Hardware requirements
	10.3	Current version giving year and date
	10.4	Programming language
	10.5	Program approach (structured, object-oriented)

A client–server solution is preferred, where the user interface is developed in close contact with the end-user running the model. All other essential elements, such as algorithms for estimating growth, mortality, thinning reactions and regeneration, are non-specific, and are run on a server, and therefore they can be combined with different user-interfaces. By means of the user-interface, initialisation data for a model run, the output of the simulation results and the steps in the prediction process can be specified sequentially for different modules in the model.

At least three groups of end-users can be distinguished. The first user group, comprising scientists, experts and consultants, presents few problems. They apply simulation models in an interactive mode for a rather limited number of cases, e.g. for the analysis of silvicultural operations, providing expert opinion in legal matters, or the economic valuation of forests. Simulations at the stand, enterprise, regional, national or even international level rarely require standard user-friendly applications. This user group familiarises itself conscientiously with new, demanding tools, readily adapts existing software for their particular purpose and requires the least computer customisation, introduction and training.

The user group comprising forest managers and planners, who are responsible for state, municipal, private or communal forests is very labour-intensive. They apply models for the development of silvicultural guidelines, preparation of forest management plans, timber volume predictions and the assessment of sustainable annual cut. They use stand models mainly in batch mode for some 1,000–10,000 inventory plots to calculate several thinning options per plot or stratum, and repeat each run 5–20 times to obtain means and standard errors. This user-group requires the development of transparent and easy user-interfaces with enterprise-specific algorithms integrated permanently as special optional modules, e.g. modules for stratifying inventory data, thinning options, assortment rules, or harvesting

techniques. In this user group, in particular, models meet with general scepticism or ignorance about software applications in forestry. For some, models appear to threaten their silvicultural expertise as they question the monopolisation of knowledge by state forest headquarters. This uncertainty might be resolved through training courses, model application in teams, provision of technical support for scenario analysis. In addition, those working in the enterprise should be involved in deciding how the results should affect management. Educating students in the application of models would help to promote open-mindedness about models. Finally, as in other management sectors, demographic shifts will pave the way for modern decision support tools.

A large group of lecturers, trainers, teachers, and private and communal forestry consultants apply models for education, teaching and advisory services. Like private asset consultants, these users use software to perform calculations and quantitative analyses of different options as a basis for their advice. For this purpose, they use interactive model versions to simulate growth of a few stands under a few different silvicultural options to provide a striking and simple illustration of the effect of different decisions.

12.2 Examples of Model Validation

12.2.1 Validation on the Basis of Long-Term Sample Plots and Inventory Data

12.2.1.1 Use of Data from Long-Term Experimental Plots

Data from the survey of long-term growth and yield experiments in Bavaria in the period 1870–1995, which were not used to parameterise the growth functions, were used in the following determinations of the bias, precision and accuracy of the growth model SILVA 2.2. For each of the pure and mixed stands included, comprising Norway spruce, Scots pine, European beech and Sessile oak, the quadratic mean diameter d_q, height of the mean basal area tree h_q, stand basal area BA, and site quality information were entered into the growth model SILVA. Then, SILVA can predict, e.g. the site-dependent height growth, tree number–diameter distributions, and determine horizontal tree distribution patterns as initialisation values. Once the initial stand structure is generated, growth is projected over 5 years without thinning operations. This process is repeated 10 times for each stand. Then, the predicted periodic annual volume increment from the 10 repetitions is compared to the observed stand volume increment.

Figure 12.3 shows the distribution and distribution parameters for the percentage differences between the observed and predicted annual volume increment (PAI_{obs} and PAI_{pred}) for the (a) Norway spruce, (b) European beech, (c) Sessile oak and (d) Scots pine stands. The differences correspond to the difference $e_i = x_i - X_i$ in

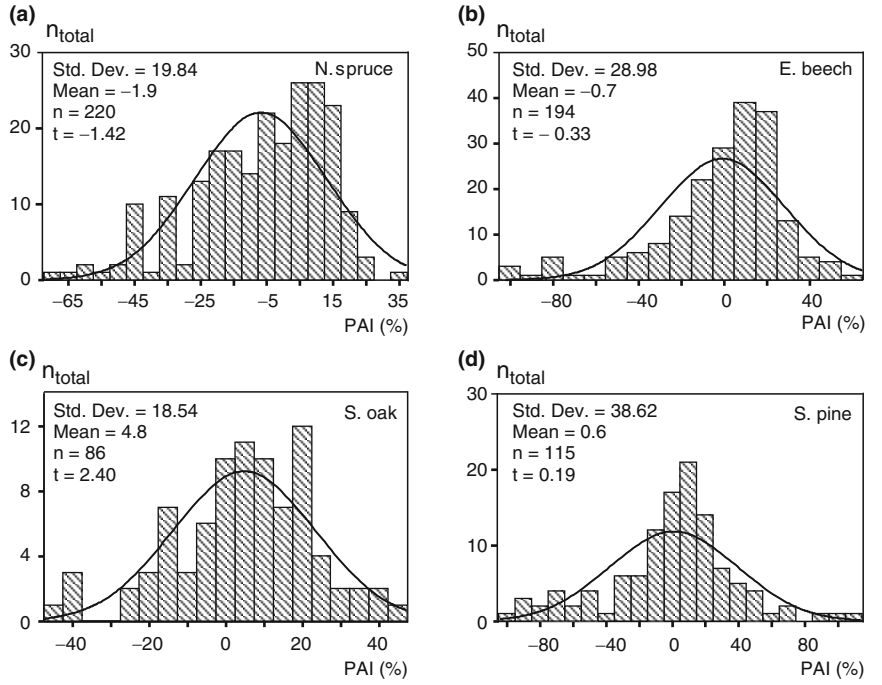

Fig. 12.3 Frequency distributions and measures of the percentage differences between observed and predicted volume growth for the tree species (**a**) Norway spruce, (**b**) European beech, (**c**) Sessile oak and (**d**) Scots pine. The mean value of distributions indicates the bias and the standard deviation the accuracy of volume growth predictions with the growth simulator SILVA 2.2

(12.1) expressed as a percentage of the observed value PAI_{obs}. Therefore, the mean difference indicates the accuracy of the model's prediction of percentage volume increment in relation to the bias (12.2) and relative accuracy (12.7).

The database for this analysis of Norway spruce and European beech, for example, comprises data from 220 and 194 inventory periods respectively. The distribution of the percentage deviation from observation has resulted in a bias in the growth prediction of $\bar{e}_{\%} = -1.9\%$, and -0.7%, with a relative accuracy of the volume growth prediction of $m_{\%} = 19.84\%$ and $m_{\%} = 28.98\%$ for Norway spruce and European beech respectively. This means that, for a normal distribution, 68% of the volume growth predictions do not deviate by more than $\pm 19.84\%$, and $\pm 28.98\%$ from the observed volume growth, respectively. The calculation of bias in the periodic annual volume increment for Norway spruce, European beech, Sessile oak and Scots pine produces values between $\bar{e}_{\%} = -0.7\%$ and 4.8%. Accuracies calculated with (12.7) of $m_{\%} = 18.54\%$ and 38.62% were obtained.

Compared to the mean bias of up to 120% and the corresponding low accuracy, which, according to Reimeier (2001), results from volume growth estimates using the yield tables from Assmann and Franz (1963) and Schober (1967), formerly used in South Germany for Norway spruce and European beech stands respectively, the

bias and accuracy achieved with the simulator SILVA are much more favourable. The accuracy of the simulator $m_{\%}$ varies between 5% and 40% at the stand level depending on the yield parameter estimated and treatment regime. The accuracy of the predicted mean diameter and height values is about $m_{x\%} = 5$–10%. The accuracy of tree number, basal area and the volume of growing stock, which are directly influenced by thinning and mortality, ranges from $m_{\%} = 10$–20%, and of periodic annual volume increment from $m_{\%} = 20$–40%.

Ďurský (1999) scrutinised the bias and accuracy of the diameter growth model in SILVA by using 2,254 trees on a total of 30 long-term mensuration sample plots. The test of validity of Norway spruce predictions was conducted in selection forests, forests in conversion from pure to mixed stands, and spacing and thinning trials that were not included in the model parameterisation data set, and which covered a broad range of stand structures and treatment regimes. The (a) mean bias, and (b) accuracy of the 5-year quadratic mean diameter increments id simulated for all stands is presented in Fig. 12.4. In individual stands, and for individual inventories, the deviations in predicted and observed growth, largely weather related, may lie between -30% and 70%. On average, there is no significant systematic bias in diameter increment. The accuracy of the diameter growth predictions for individual trees fluctuated between 16.8% in poorly structured stands and 48.9% in highly structured and very dense stands. In most stands, the accuracy ranges from 30% to 35% (Fig. 12.4b).

Long-term survey data also can be used for the validation of the simulator at the individual tree level. In Fig. 12.5, the observed and simulated mean annual diameter increment in the period 1987S–1996s and 1992S–1996a are compared for the Norway spruce sample plots, Weißenburg 613/2 and Fürstenfeldbruck 612/12. At Weißenburg 613/2, shown in Fig. 12.5a, the observed and predicted diameter growth correspond well, and bias is only $\bar{e} = -0.13$ cm in the growth period considered. The accuracy is $m_x = \pm 27\%$, which means that in 68% of the simulation runs, the diameter growth calculated does not deviate from the observed values by more than $\pm 27\%$.

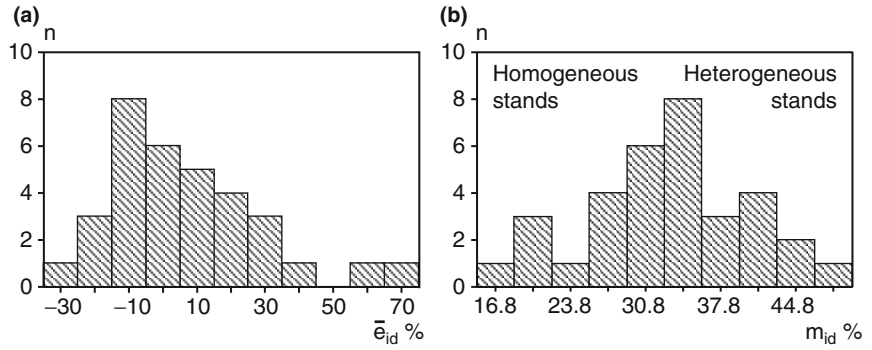

Fig. 12.4 Relative bias $\bar{e}_{\%}$ and accuracy $m_{x\%}$ of quadratic mean diameter growth (id) predictions in Norway spruce stands. The frequency of (**a**) bias ranges from -30% to 70%, and of (**b**) accuracy from 16.8% to 48.8% in the structurally poor and rich Norway spruce stands investigated

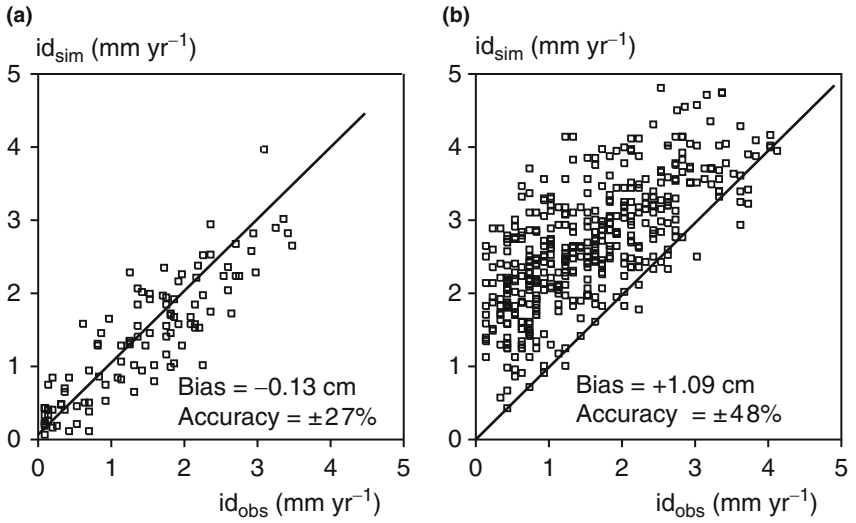

Fig. 12.5 Validation of the model with individual-tree diameter increments from the long-term Norway spruce sample plots (**a**) Weißenburg 613/2 and (**b**) Fürstenfeldbruck 612/12

The relationships at Fürstenfeldbruck 612/12, shown in Fig. 12.5b, differ. Here, diameter growth is overestimated by $\bar{e} = 1.09$ cm on average, and the accuracy is about $m_x = \pm 48\%$ of the actual diameter growth. This inaccuracy in growth predictions arises because a short, climatically unrepresentative growth period was used in the validation. The superimposition of extreme weather or biotic calamities on long-term growth makes it difficult to compare simulations with observation. If the growing conditions in the growth period selected for modelling validation change, then a bias in the predictions will result if these changes are not considered in the model. This problem can be overcome by applying longer time periods with average weather conditions for the validation, or by incorporating known weather events or climate trends in site-sensitive models.

12.2.1.2 Validation with Inventory Data

The mensuration data collected in forest planning inventories also presents an option for validating and calibrating the growth model (cf. Chap. 1, Sect. 1.3) at the regional level. To validate the height growth model in SILVA 2.2, we use the forest planning inventory height data from the growth regions 11.03 Bavarian Forest, 15.05 central Bavarian limestone mountains, 12.08 Upper Bavarian Tertiary hillside and 8.03 Fichtel mountains by way of example. Several thousands of entries for height data are available from forest inventory planning in these regions. To compare the predicted and observed height development, one site unit each from the upper and lower site productivity range is selected in each forest district. At these site units,

representative stands are identified and their forest mensuration data recorded at a stand age of 30 years. These representative stands are simulated assuming a heavy selection thinning over 100 years. The mean height and mean diameter development resulting indicates good correspondence between the simulated and observed heights and diameters for most growth regions, even though the model version tested was parameterised with data from the less representative long-term experimental plots, and not with inventory data.

Figure 12.6 shows good correspondence between prediction and observation in the growth regions 11.03 Bavarian Forest and 15.05 central Bavarian limestone mountains. This is evident from the position of the inventory data between the height growth curves for the upper and lower productivity ranges, which represent the upper and lower limits of the scattered points. The systematic deviation between prediction and observation in the growth districts 12.08 Upper Bavarian Tertiary hillside and 8.03 Fichtel mountains (Fig. 12.6c,d) are most likely due to the particularly high nitrogen inputs in the Upper Bavarian Tertiary hillside, and the prevalent, familiar major crown damage in the Fichtel mountains (Pretzsch and Utschig 2000).

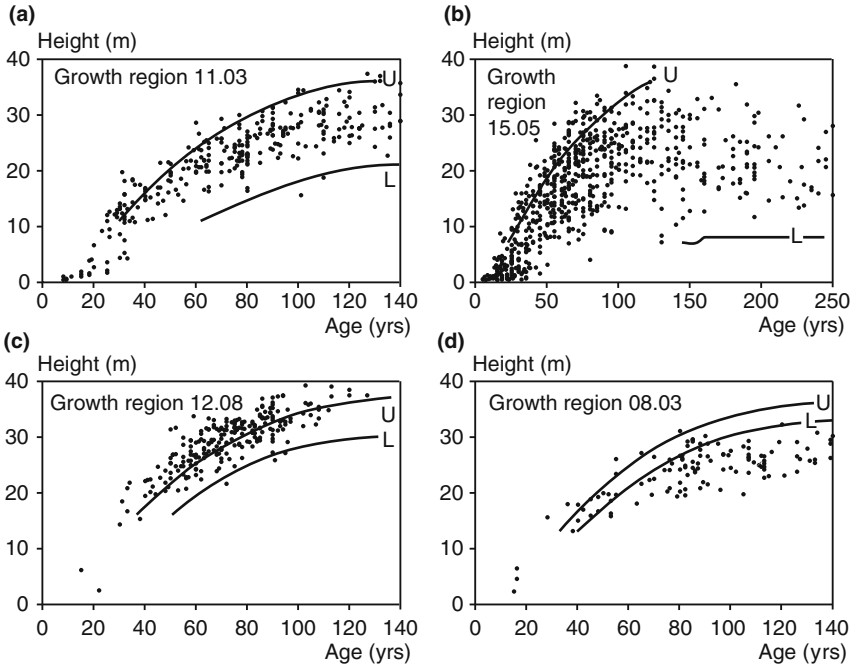

Fig. 12.6 Validation of the height growth model in the simulator SILVA 2.2 by comparing predicted height growth development in selected growth regions with those from sample data collected in forest planning inventories. The development of mean height of a more productive stand (*upper solid black line*, U), and a less productive stand (*lower black solid line*, L) for the growth regions (**a**) 11.03 Bavarian forest, (**b**) 15.05 central Bavarian limestone mountains, (**c**) 12.08 Upper Bavarian Tertiary hillside, and (**d**) 8.03 Fichtel mountains

In this way, conclusions can be drawn about the accuracy of the model, and the need to re-parameterise the most important yield variables for each specific region.

12.2.2 Comparison with Growth Relationships

To test whether the model conforms to the growth relationships, we return to two rules discussed in Chap. 10. Sect. 10.4 showed how, independent of their initial density, Norway spruce stands approach an upper limit between tree number N per hectare and quadratic mean diameter d_q, after which, in accordance with Reineke's (1933) rule, the tree number begins to decline with a slope of about $\beta = -1.605$ (Fig. 12.7).

Now we test whether the system of functions in the individual-tree simulator SILVA 2.2 adheres to this rule. To do so, the development of large numbers of pure Norway spruce stands on fertile soils in South Bavaria is simulated. Figure 12.7b shows that the simulated $\ln(N) - \ln(d_q)$ development runs below the self-thinning line at first, approaching an upper limit, and then declining along a line with an approximate gradient of $\beta = -1.746$. The tendency of the model to conform to the known growth relationships in this case supports the individual-tree based mortality model from Ďurský (1997) implemented by the simulator. The conformity is particularly remarkable because mortality is modelled at the individual-tree level and not the stand level (Pretzsch 2002a). We find a deviation from Reineke's generalised slope $\beta = -1.605$, but a remarkable approximation to the steeper slope of $\beta = -1.773$ derived theoretically by Pretzsch (2000) from Reineke's (1933)

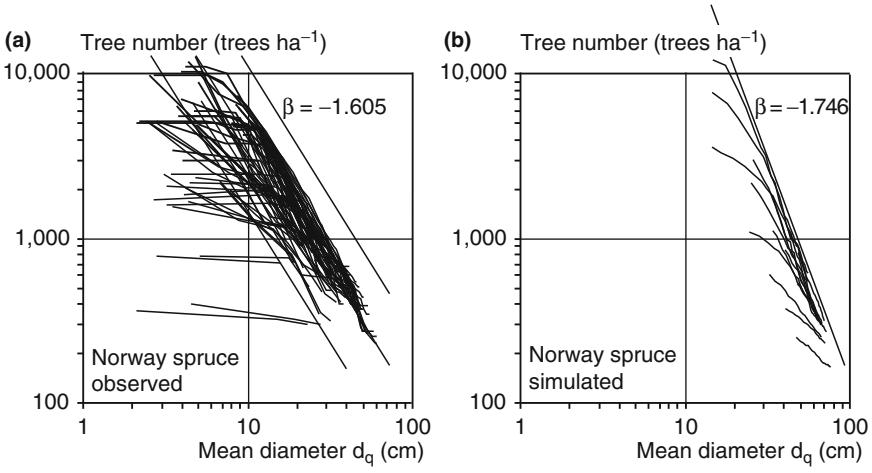

Fig. 12.7 Test of model's agreement with Reineke's (1933) stand density rule. (**a**) Comparison of the observed stem number–mean diameter trajectories in Norway spruce stands in Bavaria with the self-thinning line ($\beta = -1.605$) generalised by Reineke (1933). (**b**) Simulation results from SILVA 2.2 for unthinned Norway spruce stands

stand density rule and the self-thinning rule from Yoda et al. (1963). Furthermore, the value obtained from the simulation runs corresponds closely with the slope of $\beta = -1.737$ found by Sterba (1987) for Norway spruce stands.

The concept of critical and optimal mean basal area levels from Assmann (1961a) describes the relationship between degrees of stocking and volume growth with a unimodal optimum curve (Chap. 10, Sect. 10.5). Maximum growth is obtained with moderate density reduction. The optimal mean basal area is dependent on age and site. In addition, this relationship is species-specific (Chap. 10, Sect. 10.5). To validate the growth model in relation to Assmann's concept, a series of simulation runs are needed for stands with defined age and site conditions. For these stands, the volume growth was calculated first for maximum basal area, and thereafter for subsequent reductions in basal area by 10%. The pair of values obtained, volume growth and basal area level, represent the relationship between stand density and volume growth assumed in the growth model. If we were to repeat these predictions for stands of different ages and different site indices, we would see whether the relationship modelled between basal area level and volume growth corresponded to the growth relationships found by Assmann (1961a).

In Fig. 12.8a,b, for example, it can be seen that, in accordance with Assmann's rule, volume growth declines slowly with decreasing stand density at first, and then falls quickly once the basal area drops below the 50–60% level. This decline in volume growth with a reduction in basal area is – again in accordance with Assmann's rule – less marked at a stand age of 40 years than at 80 years. Similarly, the reduction in growth conforms to the rule if we calculate it for different site classes. On mediocre and fertile soils, the relationship between stand density and volume growth is optimal at basal area levels of 100–80%; reductions in basal area beyond this level reveal linear reductions in volume increment. The quite plausible growth response in the latter figures results from the interaction of the diameter, height, crown, and mortality models in SILVA 2.2.

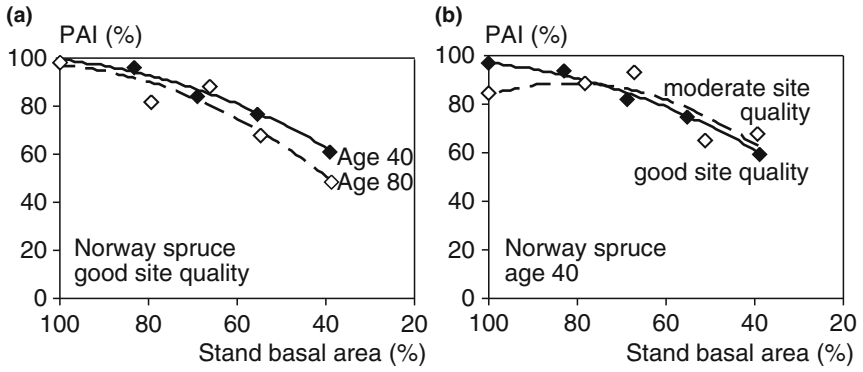

Fig. 12.8 Test of model's agreement with Assmann's (1961a) concept of optimal and critical basal area levels. The periodic annual volume increment in relation to basal area of pure Norway spruce projected with SILVA 2.2 for stands in growth region 13.4, Vorallgäu foothills: (**a**) on fertile sites at different stand ages, and (**b**) at age 40 under different site conditions

12.2.3 Comparison with Knowledge from Experience

Investigations by Kennel (1965), v. Lüpke and Spellmann (1997), Magin (1959), Mitscherlich (1970) and Spellmann and Nagel (1996), among others, have shown that the inferior tree species in a mixed stand delay the culmination of growth (rhythm shift), and reduce absolute growth levels (amplitude restricting) with age (Chap. 7, Sect. 7.1.1). To test the plausibility of the simulator SILVA 2.2, the stand development expected at a site with average water and nutrient availability is modelled for the growth region 12.7 central Swabian "Schotterriedelland and Hügelland", where Norway spruce growth has been found to be superior to that of European beech. Hence, we test the consistency of the representation from SILVA 2.2 with this observation.

In the Norway spruce–European beech mixed stands represented at 30 years of age (Chap. 7, Fig. 7.3), the values for cumulative and mean stand variables are similar, as are the individual-tree size frequencies; only the structural mixtures differ. Norway spruce and European beech occur singly in the stand depicted in Fig. 7.3a, yet, in Fig. 7.3b, these tree species are present in groups and clumps. When all else is equal, these initial structural differences alone have major effect on stand development up to the age of 150 years. Norway spruce's initial height superiority of 4.1 m is enhanced in the single-tree mixtures in subsequent years such that the percentage of European beech in the mixture drops from an initial 36% down to 25% at the age of 150 years. The inferiority of European beech in single-tree mixtures leads to Norway spruce becoming dominant over entire areas because it can increase its growth at the expense of European beech. In contrast, the slower growing European beech faces less competition from Norway spruce in clumps or patches, and is capable of increasing its percentage in the mixture to 48% at the age of 150 years at the expense of the Norway spruce, contributing about 50% to the total volume growth of the stand.

These response patterns modelled by the simulator correspond with the findings of the authors mentioned above, whereby, under the given inter-specific competition on moist and acid sites, Norway spruce can continue to consolidate its superiority over European beech as long as European beech is not favoured by silvicultural operations or group mixtures.

12.3 Standards for Describing Models and Simulators

A standardised description of models has been recommended to assist users in the selection of a model or simulator, the interpretation of predictions, and the evaluation of the accuracy and limitations of the selected model. The list of criteria in Table 12.1 provides a guide that developers may use when describing a model. In the overview, the most important features of each criterion listed are noted. Developers should give a brief, standardised description of each feature together with the source

of information (Deutscher Verband Forstlicher Forschungsanstalten 2000; Pretzsch 2002b).

(1) Model approach
The approach for the description of cumulative and mean stand values, frequency distributions, or individual trees with or without consideration of position, determines the input and output data generated. Whether, and in what manner, site variables, inventory data, or treatment alternatives are processed by the model, determines its flexibility, and the required input and parameterisation data. A system diagram helps users understand the model conceptualisation based on some essential model components, and the calculation process for predictions.

(2) Range of application
The range of application needs to be defined in relation to the spatial scale (individual tree, stand, enterprise, regional, large-scale), and the time scale (short-term predictions for the development of tending regimes, generation of comprehensive simulations for succession and climate research).

(3) Parameterisation and calibration specifications
To characterise the model validity, calibration data should be specified for geographical region, site conditions, tree species composition, stand structure, stand treatment, range of tree sizes and stand variables. The user also needs to be aware of any limitations in parameterisation or calibration data.

(4) Input
The following information is essential for the user: what initial values need to be taken into account; what initial information and initial tree data are needed for predictions; and to what extent can missing initial values (e.g. crown parameters, stem co-ordinates) be supplemented realistically by the model.

(5) Program control
The control of prediction runs may comprise, for example, the silvicultural treatment regime, changing site conditions and the formation of artificial or natural regeneration. An indication of whether the program is controlled only interactively, or also in batch-mode with control files should also be given.

(6) Output
A complete overview of the stand variables and individual tree data predicted by the simulator, the process used for the evaluation of results, and possible interfaces for subsequent databases are all important for making the simulator an integral part of the information flow in forestry practice.

(7) Growth model
The database, model equations, model parameters and parameter estimation methods for the simulation of the development of stem, crown, regeneration and mortality should be given.

(8) Additional algorithms
Additional model components that allow the user to, e.g. generate initial structures, quantify assortment yield and financial performance, visualise results or compensate for edge effects should be accompanied by a description of the

model equations, model parameters and data required. Information about the model and/or simulator's potential to update predictions continually as new inventory data, or other relevant information become available also should be included.

(9) Model validation
Conventional statistical information on the precision and accuracy of model equations and predictions may prove helpful in assessing whether a simulator is suitable for a specific purpose. Characteristics of statistic validation procedures (e.g. Mayer and Butler 1993; Pretzsch and Ďurský 2001; Reynolds et al. 1981; Sterba and Monserud 1996; Vanclay and Skovsgaard 1997) as well as a statement characterising the validation material may help users decide which simulator to use. If the forest growth simulator described contains random variables, the results of prediction runs may vary even when all other conditions are equal. Therefore, information about the model components with random control effects should be provided. If results of a sensitivity analysis are available, these should be provided as well.

(10) Software and hardware
For the current version of any growth simulator, the software and hardware requirements, programming languages and memory capacity requirements of the computer should be given in detail to enable potential users to assess its suitability for specific purposes. Upon completion of a model description standardised in accordance with the criteria shown above, the references referred to in the description provided for the ten criteria are listed. Yet, this list does not serve in place of precise information.

Summary

Several European states introduced uneven-aged forest management methods, such as "structural thinning" and "target diameter harvesting", and promoted the establishment and tending of mixed stands. During the past two decades this development has been supported by (and at the same time enhanced) the development of forest growth simulators that rely less and less on conventional yield tables for pure stands. With the objective of overcoming the limited applicability of yield tables, a multitude of new model approaches and growth simulators of confusing variety has being created. In contrast to yield tables, they lack, to date, any form of standardisation that could serve as a guide for users and developers. Efforts to develop such guidelines have been undertaken by the Division of Forest Yield Science in the German Union of Forest Research Organisations.

(1) The evaluation of models should look at the suitability of the model approach selected for given objectives and purposes, the validity and logic of the biometric model developed and the suitability of the software developed from the biometric model.

(2) To evaluate the model's suitability for user's objectives and purposes, the following questions need to be addressed: Does the model approach make full use of existing information from forestry practice to meet the user's needs? Does the model approach fulfil the user's information requirements? Does the model approach make the best possible use of existing data and the state of biological knowledge to solve user problems? Does the degree of complexity selected correspond to the model objectives?
(3) An evaluation of the software addresses the questions: Is the growth simulator designed for easy use? Is the simulator, and its components, flexible in use? Is it possible to integrate the growth simulator into the information flow in forestry practice? Has the growth simulator been adequately documented?
(4) One aspect of evaluation is validation. Validation defines the degree of accuracy with which a process measures what it claims to measure.
(5) The validation of the growth model scrutinises the accuracy of model predictions compared to reality. Does the model performance correspond to the mathematical relationships and to general biological experience? Do prediction results correspond to those from other models?
(6) For example, the individual tree simulator SILVA is validated in several ways. We compare simulation results with data from long-term sample plots and inventory data. We assess whether model behaviour accords with the rule of self-thinning, and the relationship between stand density and growth. Finally, we compare the simulation results with practical experience.
(7) A growth model cannot be verified, since, verification requires proof of the truth of statements. According to the theory of Critical Rationalism (K.R. Popper), the conclusive verification of general empirical statements is not possible, yet conclusive falsification is (Popper 1984).
(8) Standards for the description and evaluation of growth models and growth simulators can give users of growth simulators confidence in the transition to modern prediction systems, and increase the level of acceptance of new information technologies. Table 12.1 comprises the 10 most important criteria together with the model and simulator properties, which are helpful for both model users and developers.
(9) For users, a standardised model description is designed to help them in their choice of the simulator, interpretation of prediction results, assessment of precision and accuracy and of the limitations of the model of their choice.
(10) For developers, the list of criteria serves as an organisation guide for model description. The list presents information about the model approach, range of application, parameterisation and calibration specifications, input, program control, output, growth model, additional algorithms, model validation, software and hardware.

Chapter 13
Application of Forest Simulation Models for Decision Support in Practice

With the growth model SILVA 2.2 as an example, this chapter shows how forest growth simulators can facilitate forecasting and analysis of forest development in inventory plots, whole stands, forest enterprises or large forest areas to provide the information needed by forest practice. Model application for integration of knowledge and testing of hypotheses for scientific purpose will be sketched in the Chap. 15. The simulator SILVA (current versions SILVA 2.2 in Delphi Pascal and SILVA 3.0 in C^{++}) has been developed at the Munich Chair for Forest Growth and Yield Science since the late 1980s (Pretzsch 1992a; Pretzsch and Kahn 1996; Pretzsch and Ďurský 2001; Pretzsch et al. 2002a; Pretzsch et al. 2008). This simulator, with its various modules for stand generation and economic and ecological predictions, is capable of scenario analyses for single inventory plots, entire stands, forestry enterprises and large regions. For a detailed description of the applied functions, species-specific model parameters, model evaluation and a demonstration version on CD see Pretzsch (2001).

The fields of application for the simulator SILVA range from the simple analysis of the effect of a certain thinning regime on forest growth (Deegen et al. 2000; Knoke 1998) to the development of mitigation concepts of climate change consequences (Ďurský 2000). SILVA 2.2 is already applied routinely in the development of silvicultural guidelines (Kahn and Pretzsch 1997; Moshammer 2006; Utschig 1999), and of management strategies at the forest district level (Duschl and Suda 2002; Hanewinkel and Pretzsch 2000; Pretzsch and Kahn 1996). At the regional and national level, the model was used for timber supply prognosis (Pretzsch et al. 2005a,b), the estimation of carbon sequestration in forests (Rötzer et al. 2008), and the evaluation of nutrient exports through modern silvicultural treatments and wood harvesting techniques (Seifert et al. 2006). The interface with the visualisation software (TREEVIEW and L-VIS) facilitates virtual training in silvicultural practise (Seifert 2006), and landscape visualisation for forest district planning and management (Pretzsch et al. 2008).

H. Pretzsch, *Forest Dynamics, Growth and Yield: From Measurement to Model*,
DOI: 10.1007/978-3-540-88307-4_13,

13.1 Model Objective and Prediction Algorithm

13.1.1 Model Objective

SILVA 2.2 has been developed as a hybrid prediction and explanation model specifically for use in forestry practice, research and teaching. It predicts growth in pure and mixed stands of any age composition, and can be used to develop and optimise silvicultural management strategies at the stand level. At the enterprise level, it is particularly suitable for short-term and long-term scenario analysis, and provides decision support for management plans. At the regional and state level, it is useful for predicting the development of the wood resources, growth and yield both under steady-state conditions and for disturbances like, for example, climate change.

An inventory interface serves for entering information on stand structure and site conditions from practical forest management. Incomplete information can be supplemented by the model (e.g. derivation of environmental variables from rough site information, generation of tree data from trial plot information). Additional output routines for timber grading, and calculating harvesting costs and sales returns are available. With these features, the simulator SILVA 2.2 is applied widely for various forest management purposes by several German forest services and private forest owners, as well as in research and as an instrument for educating forestry students and managers. A detailed description of SILVA 2.2, including tree representation, input and output routines, core module equations of growth and mortality, and references parameters can be found in Pretzsch et al. (2002a).

As start up and control parameters, SILVA 2.2 requires: initial stand parameters, site variables, and selected silvicultural prescriptions (Chap. 5). The results from SILVA 2.2 scenario calculations include estimates of timber yields as well as of ecological and socio-economic indicators.

13.1.2 Prediction Algorithm

Growth models, which are based on individual trees, break stands down into a mosaic of individual trees and simulate the individual tree interactions in a space–time system (Fig. 13.1). The growth model SILVA 2.2 is run with only a few start and control parameters, which characterise a stand and its site conditions, and then models the stand dynamics in 5-year cycles from the time of stand establishment through to the regeneration phase.

To begin, data for the dimensions and positions of the individual trees and site conditions are needed (Fig. 13.2). The site growth model is then adapted to the given site conditions. Data, generated realistically, are used to supplement any missing data (Pretzsch 1997). Once the start up and control parameters have been compiled, the simulation run can proceed. The actual growth prognosis is carried out in 5-year-cycles. The user may determine the number of cycles, i.e. the length of

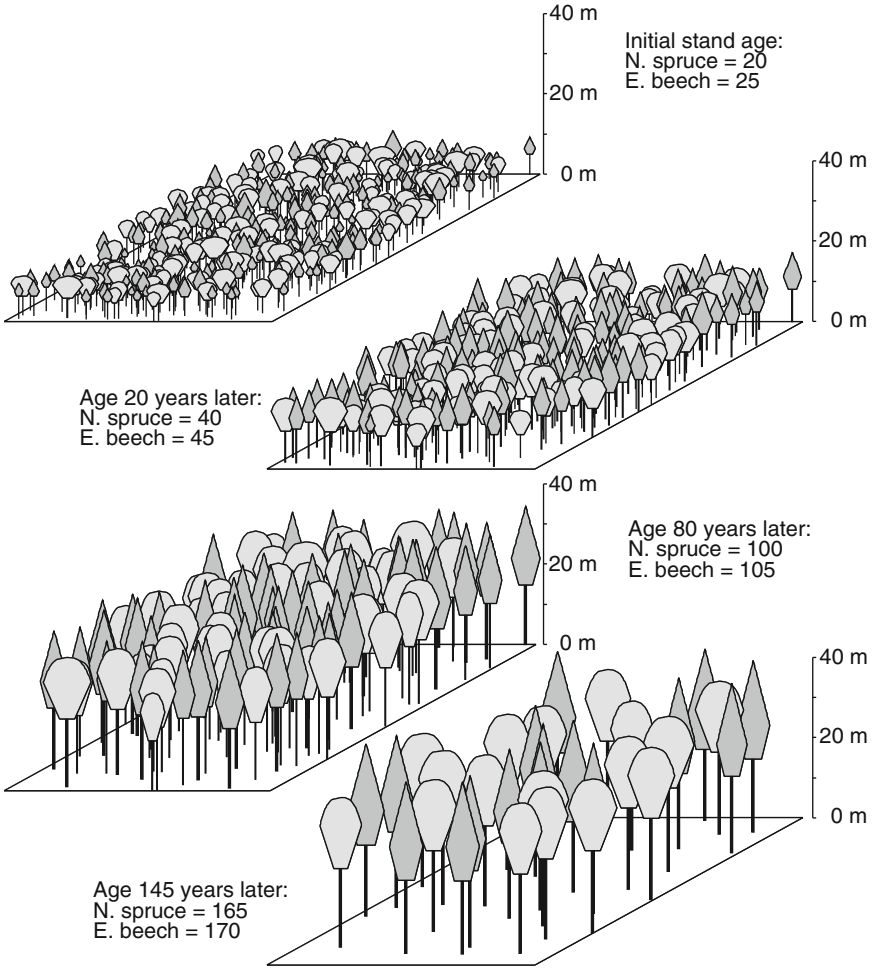

Fig. 13.1 The growth simulator SILVA 2.2 models the development of pure and mixed stands in 5 year steps: a Norway spruce–European beech mixed stand in the growth region Oberbayerisches Tertiärhügelland in South Bavaria is simulated from 20 to 165 years of age; the top height site index of Norway spruce is about 34 m after Assmann and Franz (1965), and European beech falls to site class II.0 after Schober (1967), with moderate thinning; a heavy selection thinning has been conducted in the stands

the simulation period, used. Each cycle comprises four steps. The first step is to quantify the three-dimensional growth arrangement for each individual tree via a competition index. In a second step, the trees to be removed are identified according to the thinning regime defined by the user. Then, the competition index determined previously is used to control the changes in the size of all trees in the stand. The fourth step involves the use of a mortality model to determine which trees did not survive due to competition effects. Steps 1–4 are repeated until the entire prediction period has been covered.

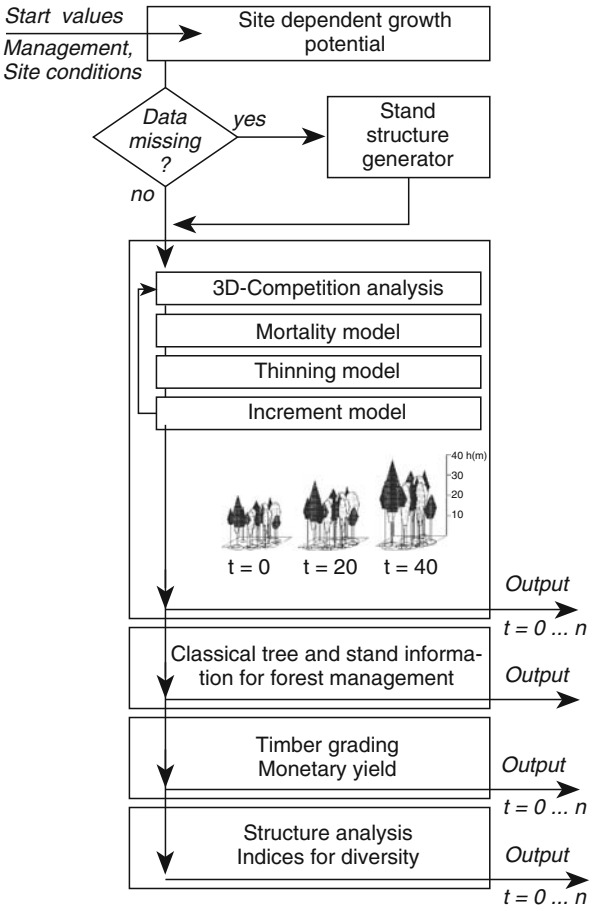

Fig. 13.2 Overview of the prediction algorithm in the growth simulator SILVA 2.2. Variable t denotes the simulation time in years, running from 0 to n

Prediction results cover a range of yield related, economical and ecological parameters, and are available in the form of tables, diagrams or stand images for each simulation period. Stand structure can be resolved by the classical mean and cumulative growth and yield characteristics, frequency distributions, and at the individual tree level. Furthermore, each tree may be classified into timber grades according to user-defined specifications, since the stem dimensions are known. The economic development of a stand and individual trees can be followed, because wood prices and harvesting costs are taken into account. For the ecological evaluation, spatial stand structure at different scales is characterised by ecological standard indices and pair correlation functions (Chap. 7). Moreover, results on the total biomass production of trees (separated for stem, branches, leaves/needles, thin and thick roots), carbon and nitrogen fixation are included.

Apart the numerical data, the visualisation module provides vivid impressions of the three-dimensional forest structure at stand and landscape level (cf. Chap. 11, Sect. 11.9).

13.1.3 Database

The simulator owes its flexibility at the stand level to the spatially explicit model approach and parameter estimation, which is based on long-term experimental plots in pure and mixed stands. Some of the time series included data back to 1870. The Bavarian network of long-term growth and yield experimental plots, maintained by the Chair for Forest Growth and Yield Science provides the main data for parameterisation of model functions. The data were gathered on about 400 long-term experiments and cover mainly survey periods from the 1950s to the present day. Over all experiments, plots and surveys some 350,000 tree observations were available for model development. Around 40% of these data points were used for parameterisation. All these observations covered trees from a broad range of diameters at breast height and stand structures respectively (cf. Pretzsch et al. 2002a). Repeated upgrades of the parameterisation were carried out with an extended database of mixed stands that also covered site-specific interactions between the species. Additionally, data from the Forestry Research Station of Lower Saxony and the Swiss Research Station for Forest, Snow and Landscape in Switzerland were used for the development of the site-related potential height growth model (cf. Kahn 1994).

In many aspects, SILVA 2.2 anticipates other forest growth simulators, by containing a quasi-mechanistic site–growth-model, a forest structure generator for the generation of realistic initial structures, and by controlling the individual tree dynamics in relation to the spatial growth arrangement (stand structure, species mixture, thinning regime). Since these features are fundamental for the model application, we will discuss them in more detail in the following.

13.2 Site–Growth Model

By estimating the forest growth behaviour from site parameters (variables that describe the environmental conditions and the resource supply), SILVA 2.2 chooses an intermediate path between empirical and mechanical model approaches, and can be regarded as a hybrid model (cf. Chaps. 1 and 11). To adapt the model flexibly to the data and information base of the required application, SILVA provides the following options for the input of the site conditions: a detailed list of known local site conditions, and average site conditions from the growth region in question. In both cases, the internal site–growth module calculates the site-specific potential

height and diameter growth curve. Alternatively, especially if information on site conditions is missing, the potential height and diameter curve can also be derived directly from inventory data.

13.2.1 The Principles of Controlling Individual Tree Growth by Means of Site Factors

The model for height increment is used to explain the principle of how the site growth model controls the size development of individual trees. The expected height increment ih_{exp} in any given 5-year period is estimated from the potential height increment ih_{pot} of the tree and the multiplier Mod, which expresses the increment-reducing effects of competition, vitality and site (Fig. 13.3, top). The potential height increment ih_{pot} in this case is deduced from the potential age–height curve. Based on the actual height of a given tree, its physiological age is read off the x-axis of the potential age–height curve. The potential height 5 years later, i.e. one simulation period (Δt), can similarly easily be read off the y-axis, and the potential height increment ih_{pot} is obtained from the difference between the current height and the potential height after 5 years (Fig. 13.3, centre).

Kahn (1994) developed and parameterised a system of functions from which the potential age–height curves for any type of site unit may be estimated from the following nine site variables: soil nutrient supply (NUT), NO_x-content of the air (NO_x), atmospheric CO_2 (CO_2), duration of growing season (DT_V), annual temperature amplitude (T_{VAR}), mean temperature during growing season (T_V), aridity index according to de Martonne (M_V), total precipitation in the growing season (P_V) and degree of soil moisture (Moist) (Fig. 13.3, bottom).

13.2.2 Modelling the Potential Age–Height Curve in Dependence on Site Conditions

The site-dependent modelling of the age–height curve uses the function by Richards (1959):

$$h_{100} = A \times (1 - e^{-k \times t})^p, \tag{13.1}$$

where h_{100} represents stand top height in m, A the asymptote in m, k, p the parameters for slope and shape, and t stand age in years. To determine this age–height curve for any given site, the height curve A and the time at which increment culmination t_{culm} is reached are estimated in relation to nine site variables. By using A and t_{culm} in auxiliary equations, the site-specific parameters k and p of the age–height curve may also be calculated. The potential height curve h_{pot} for individual trees is obtained from stand top height h_{100} by multiplying the stand top heights of Norway spruce, Silver fir, Scots pine, European beech and Sessile oak with the factors

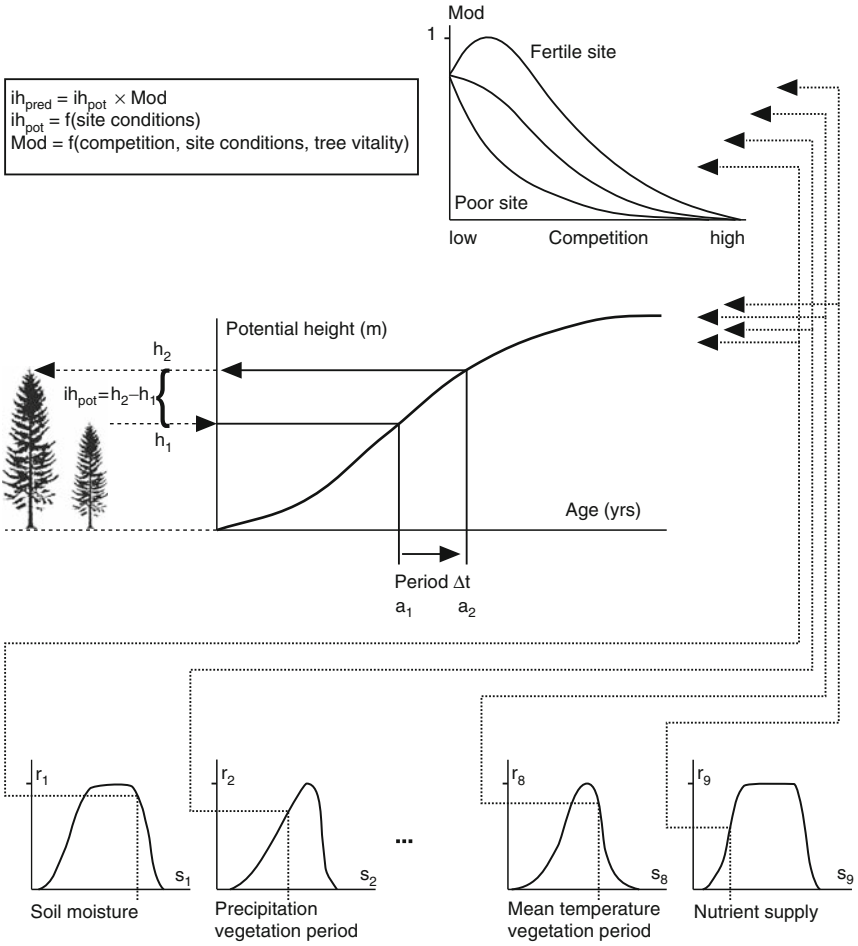

Fig. 13.3 Derivation of the periodic annual height increment ih_{exp} in the growth model SILVA 2.2. The expected height increment results from the site-dependent potential age–height curve and a tree's competitive status. Variable ih_{pot} represents the potential height increment, s_1–s_9 are site variables and Mod modifies the potential growth to the expected height growth

1.138, 1.138, 1.189, 1.132, and 1.184, respectively. These factors have been derived by Pretzsch and Kahn (1998) from the height–frequency distributions of long-term experimental plots. This way, the estimation of the potential height increment ih_{pot} becomes a function of the site variables as shown in Fig. 13.3. This enables the growth model SILVA 2.2 to simulate stand development for a wide range of site conditions. The problem of determining the quality (i.e. the site index) of mixed stands is avoided if height and diameter increment potential are considered in relation to site factors. The parameterisation of the relationship between site characteristics and the variables A and t_{culm} is based on a total of 330 long-term experimental plots.

The asymptote of the height curve A and the age t_{culm} at which height increment culminates are modelled in relation to the above-mentioned site conditions. The following provides a more detailed description of these $n = 1....9$ site variables s:

s_1 = Soil nutrient supply NUT (relative values between 0 and 1, i.e. upper and lower boundaries of the ecological amplitude)
s_2 = Atmospheric NO_x (ppb)
s_3 = Atmospheric CO_2 (ppm)
s_4 = Duration of growing season DT_V (number of days with temperatures over 10°C)
s_5 = Annual temperature amplitude T_{VAR} (°C)
s_6 = Mean temperature in the growing season T_V (°C)
s_7 = Aridity index according to de Martonne M_V ($mm\,°C^{-1}$)
s_8 = Total precipitation in the growing season P_V (mm in vegetation period)
s_9 = Degree of soil moisture Moist (relative values between 0 and 1, i.e. upper and lower boundaries of the ecological amplitude)

The variables s_n express the factors that characterise a site. Soil nutrient supply and degree of soil moisture are given on an ordinal scale. A fuzzy-set theoretical approach for linguistic variables, which follows the approximation system by Chen and Hwang (1992), converts them to a metric scale. The required information on climate can be deduced from the growth region to which a specific site belongs. Atmospheric NO_x and CO_2 are regional and/or global variables. All variables are transformed by unimodal dose response functions $f(s_n)$ in the interval [0;1]:

$$r_n = f(s_n),\ n = 1...9 \quad \text{and} \quad r_n \in [0;1]. \tag{13.2}$$

The response factors r_n describe the effect of the factor s_n on potential height growth of a tree species, and hence proves context-sensitive for tree species. Figure 13.4 shows the dose–response functions for Norway spruce and European beech, and gives an example of the effect of the nine site variables on the potential height increment under the dominating site conditions (the site type with the most frequent occurrence) in the growth region 12.8 Oberbayerisches Tertiärhügelland (Southern Bavarian pre-alpine uplands) (vertical beam). The response factors r_n are being aggregated to form complex ecological factors. We start off by aggregating the response factors r_1–r_3, r_4–r_6 and r_7–r_9 into the three ecological factors nutrient supply KF_1, thermal supply KF_2 and water supply KF_3, respectively:

$$KF_1 = \left(\prod_{i=1}^{3} r_i\right)^{1-\gamma_3} \times \left(1 - \prod_{i=1}^{3}(1-r_i)\right)^{\gamma_3} \tag{13.3}$$

$$KF_2 = \left(\prod_{i=4}^{6} r_i\right)^{1-\gamma_4} \times \left(1 - \prod_{i=4}^{6}(1-r_i)\right)^{\gamma_4} \tag{13.4}$$

$$KF_3 = \left(\prod_{i=7}^{9} r_i\right)^{1-\gamma_5} \times \left(1 - \prod_{i=7}^{9}(1-r_i)\right)^{\gamma_5} \tag{13.5}$$

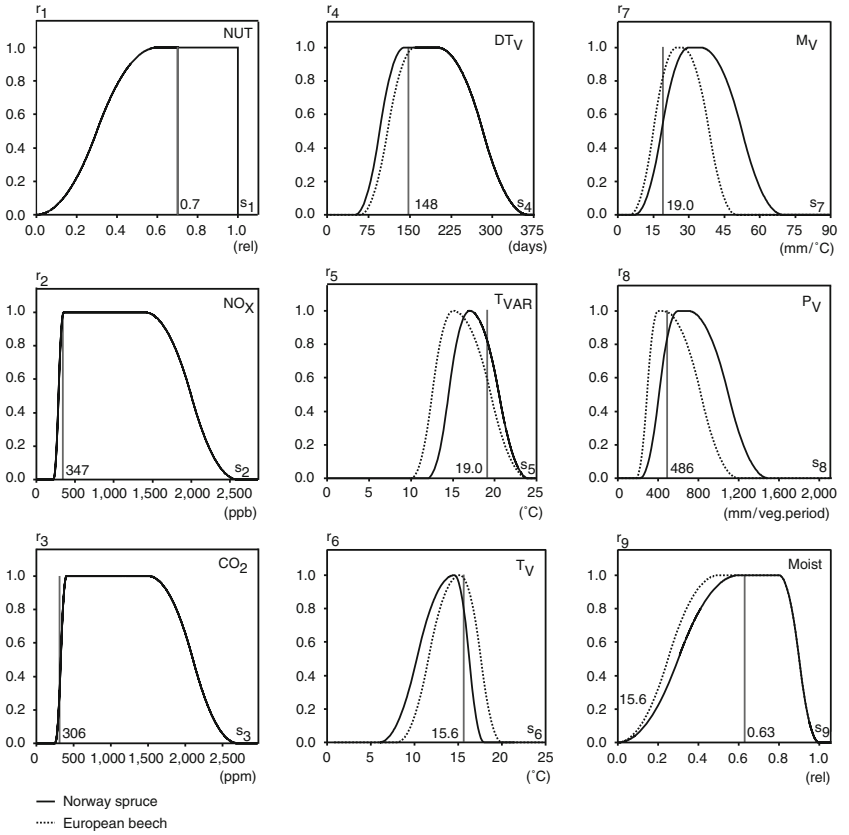

Fig. 13.4 Site variables s_1–s_9 soil nutrient supply (NUT), atmospheric NO_x (NO_x), atmospheric carbon dioxide concentration (CO_2), duration of growing season (DT_V), annual temperature amplitude (T_{VAR}), mean temperature during the growing season (T_V), aridity index according to De Martonne (M_V), total precipitation during the growing season (P_V) and soil moisture (Moist), and relative response factors r_1–r_9 on potential height increment of Norway spruce (*full line*) and European beech (*dotted line*). The dotted line perpendicular to the x-axis represents the site conditions for representative stands in the growth region 12.8 Oberbayerisches Tertiärhügelland in the South Bavarian tertiary uplands

In a second step, these three ecological factors are combined, and then used to estimate the asymptote of the height curve A and the time of culmination t_{culm}:

$$A = A_0 + A_1 \times \left(\prod_{j=1}^{3} KF_j\right)^{1-\gamma_1} \times \left(1 - \prod_{j=1}^{3} (1 - KF_j)\right)^{\gamma_1} \tag{13.6}$$

and

$$t_{culm} = t_0 + t_1 \times \left(\prod_{j=1}^{3} KF_j\right)^{1-\gamma_2} \times \left(1 - \prod_{j=1}^{3} (1 - KF_j)\right)^{\gamma_2} \tag{13.7}$$

with A asymptote in m, A_0 minimum asymptote in m, A_1 maximum asymptote minus A_0 in m, t_{culm} age of stand at which height increment culmination is reached (in years), t_0 minimum value for t_{culm} (in years), KF = complex ecological factor, γ_1–γ_5 aggregation operators, and j index for the ecological factors. In all equations (13.3)–(13.7), the γ aggregation operation from Zimmermann and Zysno (1980) is used, and γ_1–γ_5 are estimated from the regression analysis of the data of long-term experimental plots.

This gives us parameter A for the Richards function (13.1). To determine the parameters k and p of the same function, an auxiliary equation is used. This equation calculates the tree height h_{tculm} as a function of the time of increment culmination t_{culm} as follows:

$$h_{tculm} = B \times (1 - e^{c \times t_{culm}}). \tag{13.8}$$

The parameters B and c are estimated using the data from long-term experimental plots. This permits the derivation of the tree height h_{tculm} at the time of increment culmination. It is related to the asymptote A and the parameter p as follows:

$$h_{tculm} = A \times (1 - \frac{1}{p})^p. \tag{13.9}$$

An algorithm is used to solve this equation to derive p, which together with t_{culm} helps to determine the slope parameter k:

$$k = \frac{-\ln(\frac{1}{p})}{t_{culm}}. \tag{13.10}$$

Figure 13.5 gives an example of the height growth potential, and the change in competitive conditions in favour of European beech if precipitation in the growing season were to decrease from 700 to 300 mm, and soil moisture from 0.6 to 0.2

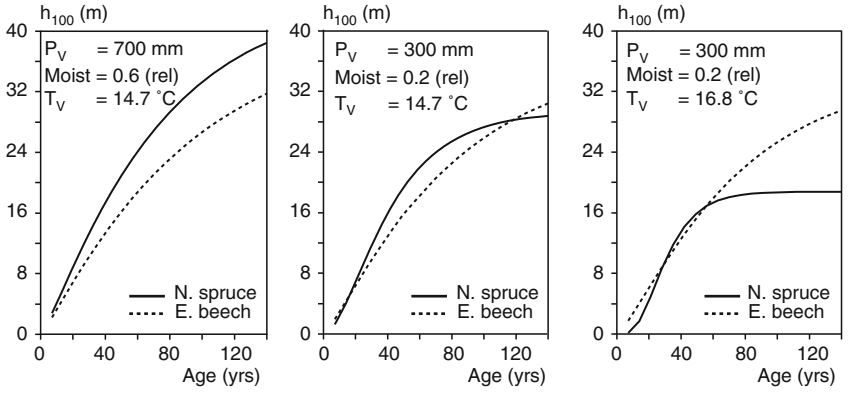

Fig. 13.5 Depending on the site factors s_1–s_9, the site–growth-model provides height growth relationships for Norway spruce and European beech, which may range from inferior growth of European beech, to similar growth of both species, to superior growth of European beech in the mixed Norway spruce–European beech stand. P_V is given in mm yr^{-1}, Moist in a relative scale from 0 to 1.0 and T_V in °C

(centre). The site is located in the Upper Bavarian tertiary uplands ($P_V = 700$ mm, Moist $= 0.6$ and $T_V = 14.7$) and characterised further in Fig. 13.5. The right hand side of the figure shows what height development could be expected if the temperature during the growing season were to rise also from $T_V = 14.7$ to 16.8°C.

13.3 Generation of Initial Values for Simulation Runs

The initial forest structure determines stand development to a large extent. With the flexible structure generation outlined below, position-dependent individual-tree models make the best possible use of the available data, and can be applied to various types of data sources. By basing structure generation on initial values, a prediction can be based largely on measured tree positions and sizes, and, if necessary, these datasets can be supplemented (Fig. 13.6).

To initialise position-dependent individual-tree models, values for diameter, height, crown base height and stem coordinates of all trees are required; a database that only exists for long-term growth and yield experiments. Therefore SILVA 2.2 is provided with algorithms for calculating realistically any missing tree dimensions or tree positions prior to a simulation run. If spatially explicit data are available as initial values for a simulation run, then only missing tree heights, and perhaps crown dimensions are needed to supplement the existing database. If the prediction is based on sample data from incomplete surveys of circular sample plots or angle-count sampling, then realistic diameter, height, crown base height and tree position values need to be calculated to supplement the existing dataset so that whole stands may be reproduced and simulated. The proportion of realistic to supplementary information increases when a prediction is constructed only from the cumulative and mean stand data, such as stand basal area, mean diameter, and mean height, and from qualitative descriptions of stand structure, such as clumped or group mixtures.

Assuming minimal information about the range in diameter and stand basal area, a stem-diameter distribution is produced using an algorithm from Nagel and Biging (1995). The diameter values produced in this way are assigned corresponding height values from the standard diameter-height curves, and individual crown sizes from

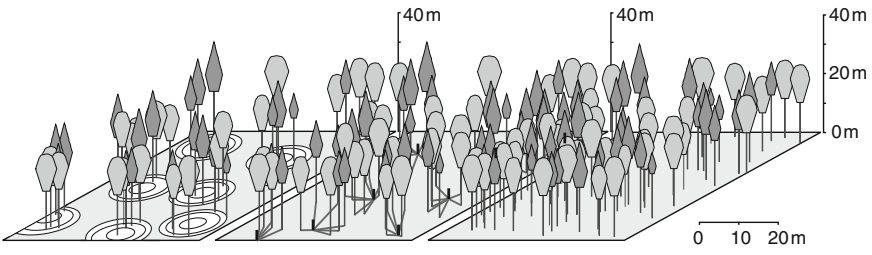

Fig. 13.6 Where information on individual trees in a stand is limited to samples from permanent test plots (*left*) or angle counts (*centre*), data for the missing stand elements is supplemented (*right*) by the structure generator STRUGEN

species-specific crown base and crown diameter functions. The given number of trees is then placed in the stand in a Poisson process that generates realistic distances between trees. A second algorithm converts the qualitative description of the type of species mixture, i.e. the degree of clustering, into the macro structure of the stand. These processes are carried out by the structure generation module STRUGEN, which is explained in more detail below.

13.3.1 Stand Structure Generator STRUGEN

A simulation run requires the stem coordinates of all trees at the initial point at time t_0. If these are unavailable, then all the coordinates are produced with the structure generator STRUGEN (Pretzsch 1993, 1997). The algorithm for structure generation, constructed from the tree list or the stem number-diameter distribution of the stand, is illustrated by way of example in Fig. 13.7 for the construction of a group mixture comprising two tree species. To position a tree in the stand to be generated, the area is covered with random, uniformly distributed x- and y-coordinates as a shower of points across the stand. To produce the macro structures of the stand, for example the type of mixture or gap placement in a selection for-

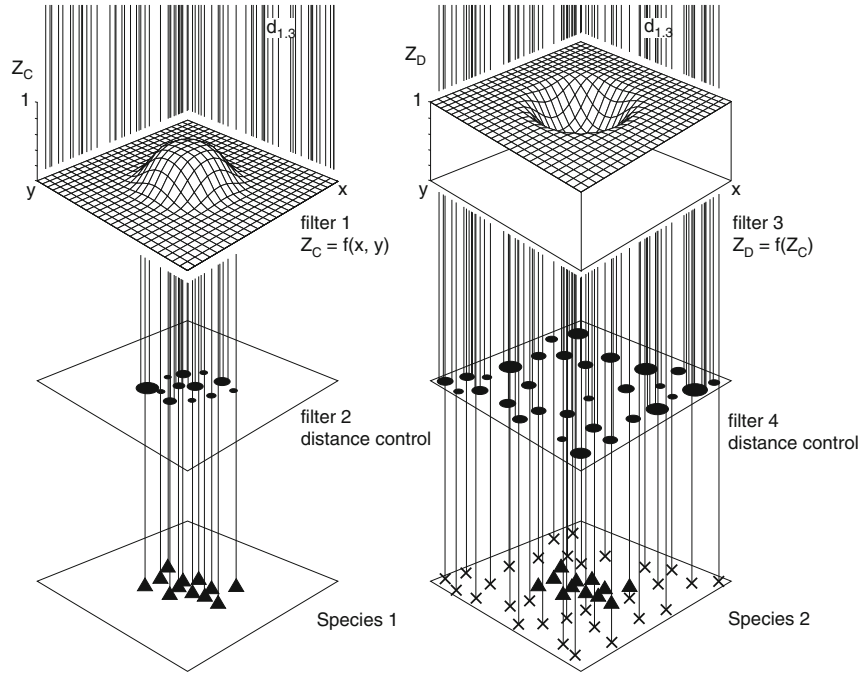

Fig. 13.7 Overview of the principle of structure generation by STRUGEN (after Pretzsch 1997)

est, the dots are accepted with different levels of probability, which are controlled by the function $Z_C(x, y)$ for a cluster mixture (Fig. 13.7). In essence, the points must pass through the first of a series of filters, which regulates the macro structure, for example a group mixture, by allowing the random points through with different position-dependent probabilities. Of the points that have passed through the first filter, only those are accepted that have a stipulated distance to neighbouring trees already present; that is, ultimately a point is accepted only if its distance is plausible. The process is repeated until the entire diameter distribution of the first tree species has been completed. Subsequently, a second process is carried out to introduce the second species (Fig. 13.7). A third filter is applied, where the function $Z_D(x, y)$ controls the intermingling of the two species, and a fourth filter regulates the distances between neighbouring trees (Pretzsch 1993, 1997).

This supplementation of missing values, and the generation of initial structures can deliver realistic initialisation data for the simulation for a wide spectrum of stand structural configurations (cf. Fig. 13.8). Agreement between the actual and generated initial structures in this case does not mean that a particular tree in the actual and generated stand must be situated at the same position, but rather that the qualities that characterise the structure correspond in the real and generated stand in terms of species mixture, the vertical structure and the horizontal distribution patterns. For the estimation of the further stand development, the spatial growth arrangement is quantified for each individual tree of the generated initial structure (cf. Fig. 13.8a–d) as described in the following.

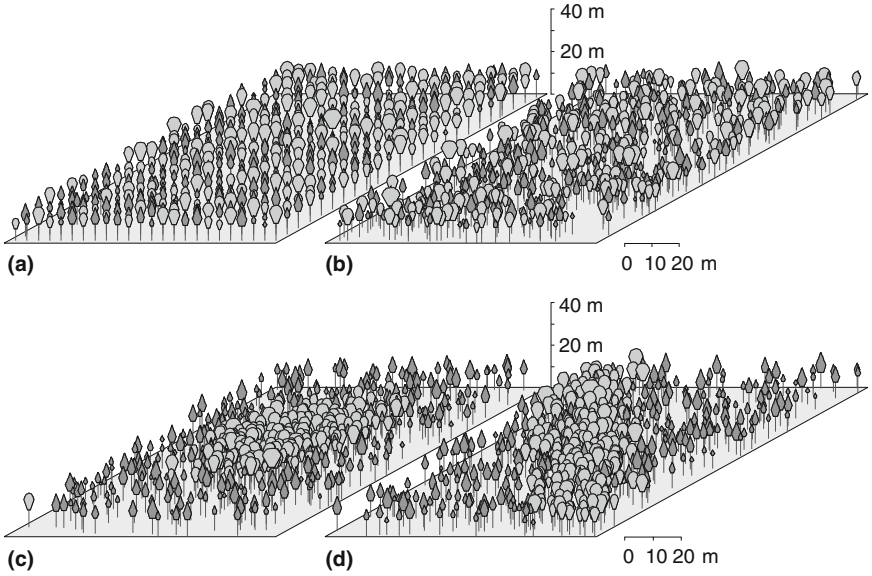

Fig. 13.8 Generation of initial stand structure of Norway spruce–European beech mixed stands by the structure generator STRUGEN with (**a**) single mixtures at plant spacing 4 m × 4 m, (**b**) single mixtures with random distribution, (**c**) mixture in patches with diameter 60 m and (**d**) in strips with strip width 30 m

13.4 Spatially Explicit Modelling of the Growth Arrangement of the Individual Trees

In SILVA 2.2, the influence of the neighbouring trees on the growth of the tree in question (=central tree) is described in three indices.

13.4.1 Index KKL as the Indicator of the Crown Competition

The KKL value indicates the social position and size of the central tree in relation to its neighbours. The meaning and calculation of the KKL have been introduced previously in Chap. 8.2.1 (cf. Fig. 8.1–8.3). By determining the KKL before and after the removal of competing neighbours, the effect of release can be modelled from $\Delta KKL = KKL_{b.th.} - KKL_{a.th.}$.

13.4.2 Index NDIST as the Indicator for Competition Asymmetry

A certain deficit of the competition index KKL arises from neglecting the influence of the competition direction. Moderate yet surrounding competition, and strong yet one-sided competition may yield the same KKL value. This symmetry or asymmetry of a tree's competitive situation is quantified in accordance with Pukkala (1989) by the distance between the coordinate of the stem basis of the central tree and the competition centre (KS) of the surrounding neighbours. This distance is calculated in four steps: first, the Cartesian x, y-coordinates of all competitor trees, already determined for the derivation of the KKL, are recorded, averaged and weighted by their respective KKL, i.e. by the competitive strength:

$$\bar{x}_j = \frac{\sum_{\substack{i=1 \\ i \neq j}}^{n} x_i \times KKL_{ij}}{\sum_{\substack{i=1 \\ i \neq j}}^{n} KKL_{ij}} \quad \text{and} \quad \bar{y}_j = \frac{\sum_{\substack{i=1 \\ i \neq j}}^{n} y_i \times KKL_{ij}}{\sum_{\substack{i=1 \\ i \neq j}}^{n} KKL_{ij}}. \tag{13.11}$$

The distance measure $DIST_j$:

$$DIST_j = \sqrt{(x_j - \bar{x}_j)^2 + (y_j - \bar{y}_j)^2} \tag{13.12}$$

where x_j, y_j are the coordinates of the stem basis of central tree j (SF) in (m), and $\bar{x}_j$, $\bar{y}_j$ the coordinate of the competition centre (KS) in (m). The resulting

$DIST_j$ quantifies the horizontal distance between stem basis SF of the central tree j and competition centre KS. If SF and KS are equal ($DIST_j = 0$), the competition is symmetrical. The greater values $DIST_j$ assumes, the more uni-directional (=asymmetric) the competition exerted by the neighbours becomes. To eliminate the absolute dimensionality (m), $DIST_j$ is set into relation to the average distance r_j that would result if all trees inside the search cone used to derive KKL were randomly distributed:

$$r_j = \frac{1}{2 \times \sqrt{\frac{M_j}{A_j}}}. \tag{13.13}$$

The variable A_j represents the projection area of the light search cone of central tree j, and M_j for the number of trees inside the area A_j. Based on the stem positions of all regarded competitors i and the central tree j, the average tree distance within the given tree group is used in the "normalisation" of the absolute distance measure $DIST_j$:

$$NDIST_j = \frac{DIST_j}{\frac{1}{2 \times \sqrt{\frac{M_j}{A_j}}}}. \tag{13.14}$$

This way, NDIST provides a normalised measure of the symmetry/asymmetry of the competition situation of each tree inside the stand.

13.4.3 Index KMA for the Species Mixture in the Neighbourhood of Individual Trees

The KMA quantifies the proportion of conifers in the neighbourhood of the central tree j by relating the cumulative crown surface area of the conifers to the crown surface area of all trees. Then the model can reproduce species-specific mixture effects as documented for Norway spruce–European beech stands by Kennel (1965a), Petri (1966), Pretzsch (1992a), Rothe (1997) and Wiedemann (1942), among others. In this case, the neighbourhood is defined by circle around the central tree's stem base with a radius corresponding to double the crown radius. To include a sufficiently large area in young stands as well, the minimum radius is set to 10 m. All trees within this area, possibly also trees not included as competitors for the KKL, are considered in the calculation of the KMA:

$$KMA_j = \left(\sum_{\substack{i=1 \\ i \in c}}^{n} KM_i\right) / \left(\sum_{i=1}^{n} KM_i\right), \tag{13.15}$$

where KMA_j quantifies the proportion of the conifer crown surface area in the neighbourhood of central tree j, KM_i the crown surface area of all trees $i = 1 \ldots n\,(m^2)$, where in the numerator $i \in c$ restricts the index to the conifers.

As KKL, NDIST and KMA enable one to differentiate the effect of different types of competition on height and diameter growth, it is possible to reproduce a wide spectrum of stand configurations from even- to uneven-aged, from pure to mixed, and from single- to multi-layered stands. For example, the variable NDIST for the asymmetry of spatial competition is important for a realistic prediction of tree growth in heterogeneous forests and at stand boundaries. The variable KMA accounts for the effect of growth enhancement or reduction through species-specific interactions.

13.5 Application for Scenario Analysis at the Stand Level: A Pure Norway Spruce Stand vs a Norway Spruce – European Beech Mixed Stand

The following comparison of a pure Norway spruce stand and a Norway spruce–European beech mixed stand illustrates the use of the growth model SILVA 2.2 at the stand level. The model is initialised to develop Norway spruce and European beech on a moderately moist site with poor nutrient status in the growth region "Oberbayerisches Tertiärhügelland". The Norway spruce site index is about 34 m at age 100 years after Assmann and Franz (1965), and European beech falls in site class II. by moderate thinning after Schober (1967). Initially the pure stand comprised 1,400 planted Norway spruce trees per hectare (Norway spruce aged 20 years) whereas the mixed stand consisted of 1,000 planted Norway spruce trees and 600 naturally regenerated European beech trees per hectare (Norway spruce aged 20 years; European beech aged 25 years; cf. Fig. 13.1). A moderate selection thinning was carried out in both stands controlled by the relevant species-specific tree number–tree height-curve (Chap. 5).

In the following we highlight some key information from the extensive range of available output variables, which includes performance of growth and yield at the tree and stand level, crown development, stem quality, assortment structures, carbon and nutrient contents, nutrients export due to harvest, harvesting costs, value development of the stand and individual trees, net return, stability, structural stand diversity, and scenic value.

13.5.1 Growth and Yield at the Stand Level

Simulations cover a period of 145 years and Fig. 13.9 provides an example of the development of basal area and mean periodic annual volume increment. Thinning is repeated several times in the first half of the prediction period because the volume growth of Norway spruce at this stage of stand development is high. Basal area increases from 2.8 $m^2 ha^{-1}$ in the pure Norway spruce stand, and 2.9 $m^2 ha^{-1}$ in the mixed Norway spruce–European beech stand (35% mixture portion of European beech) to a maximum of 67 and 58 $m^2 ha^{-1}$ respectively, at age 130, and declines

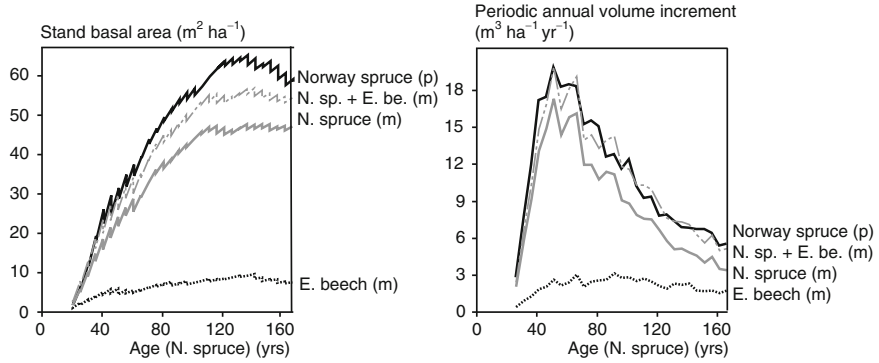

Fig. 13.9 Results of the variant study on pure Norway spruce stand vs mixed Norway spruce–European beech stand. This shows the basal areas of the stands (*left*) and the mean periodic annual volume increment (*right*) for the 145 year prediction period

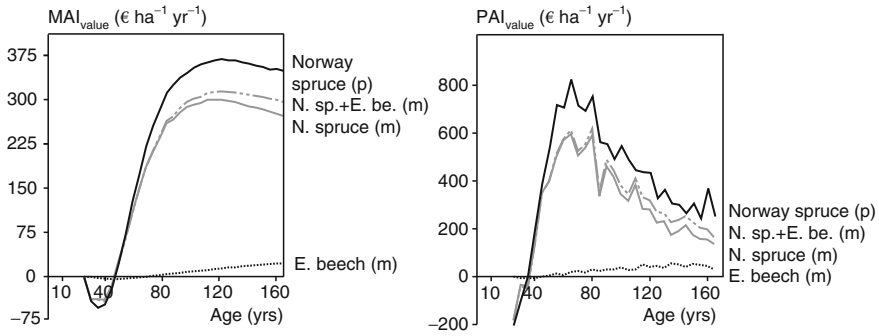

Fig. 13.10 Results of the variant study on a pure Norway spruce stand vs mixed Norway spruce–European beech stand. This shows the development of the mean annual value increment MAI_{value} (*left*), and of the mean periodic annual value increment PAI_{value} (*right*) for the 145 year prediction period

progressively with age. Figure 13.9 (right) shows that the annual volume increment at young stand age rises quicker in the pure (full black line) than in the mixed stand (grey dotted line). The admixture of European beech causes a slight decrease in culmination height, and a retardation in the time required for the culmination of the mean periodic annual volume increment due to the competitive strength of European beech. With advancing age European beech may even cause the volume increment of the mixed stand to repeatedly exceed that of the pure stand, despite the later culmination age of European beech.

For the assessment of financial yield, the mean annual value increment MAI_{value} (Fig. 13.10 left) is considered as the most appropriate characteristic (i.e. financial yield at respective age plus accumulated intermediate financial yield, divided by stand age). In contrast, the mean periodic annual value increment PAI_{value} (Fig. 13.10 right) corresponds to the difference between the total value achieved in two consecutive periods, divided by the duration of these periods.

The pure Norway spruce stand in this example produces a better result in the mean annual value increment than the mixed stand (Fig. 13.10 left). If these results are transferred to corresponding management blocks, the Norway spruce stand at age 120 years sustainably yields € 365 $ha^{-1}\,yr^{-1}$ at the time of MAI_{value} culmination on the basis of given costs and prices. To simplify matters, prices and costs are assumed constant and any risks of damage to the stands are ignored. The MAI_{value} in the Norway spruce–European beech stand peaks at age 120 with a sustainable MAI_{value} of € 310 $ha^{-1}\,yr^{-1}$ (Fig. 13.10 left). Thus the difference to the pure Norway spruce stand is characterised by opportunity costs of € 55 $ha^{-1}\,yr^{-1}$ (=365 €–310 €). However, if a rotation time of 80 years is envisaged for the Norway spruce stand, the MAI_{value} would be reduced to € 300 $ha^{-1}\,yr^{-1}$. In practice this may be advisable due to root rot, air pollution, storms and ice-breakage, or insect calamities in pure Norway spruce stands. In this case the balance results in € 10 $ha^{-1}\,yr^{-1}$ in favour of the mixed stand. The steep rise in the MAI_{value} prior to the culmination point, and the fact that it only recedes slowly beyond this point, gives the manager a greater latitude in extending rather than reducing the rotation time. This also explains the development of the PAI_{value} (Fig. 13.10 right), which achieves peak values of € 600 – € 820 $ha^{-1}\,yr^{-1}$ at stand ages ranging from 50 to 80 years.

13.5.2 Growth and Yield on Tree Level

The simulator SILVA 2.2 models the stand as a mosaic of individual trees, and calculates the PAI_{value} and MAI_{value} at the tree level analogous to the stand level (Fig. 13.11). In the mixed stand, the MAI_{value} of the remaining Norway spruce with diameters of 50–60 cm culminates with MAI_{value} of € 0.75–2.0 yr^{-1} per tree while European beech, at € 0.5–0.75 yr^{-1} per tree, is still on an upward trajectory. That is, in view of its suitability for analysing and optimising modern harvesting scenarios based on the promotion of individual trees, the model presents a planning tool, which facilitates the calculation of growth and yield characteristics at both the tree and stand level, and analyses of the trade-off between both approaches.

13.5.3 Modelling Structural Diversity

As SILVA 2.2 models the stand in 5-year time-steps as a spatial–temporal system of individual trees (cf. Fig. 13.1), the structural indices, which provide indicator values for habitat and species diversity (Chap. 7), can be calculated at any stage of the simulation run. The R Index from Clark and Evans (1954) for the horizontal tree distribution pattern, the A Index from Pretzsch (1998) for the vertical species profile, and S Index from Pielou (1977) for species intermingling all show how stand structures in a pure Norway spruce stand and a Norway spruce–European beech mixed stand (Fig. 13.12) are modified by age and thinning.

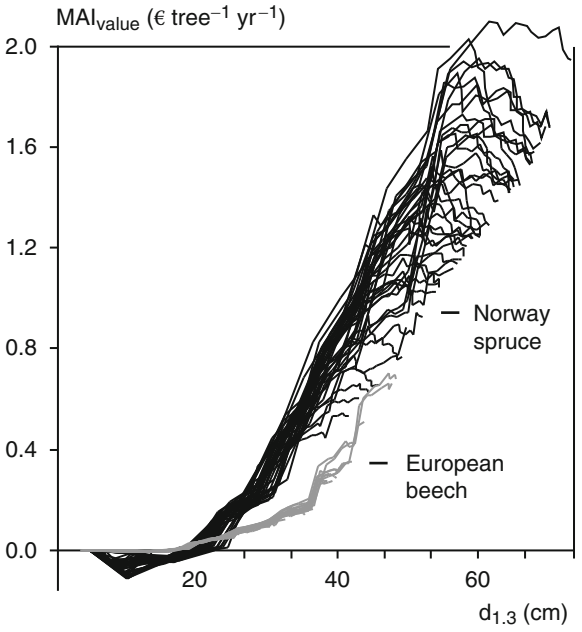

Fig. 13.11 Development of the mean annual value increment MAI_{value} for individual Norway spruce (*black solid line*) and European beech (*grey solid line*) trees in the mixed stand

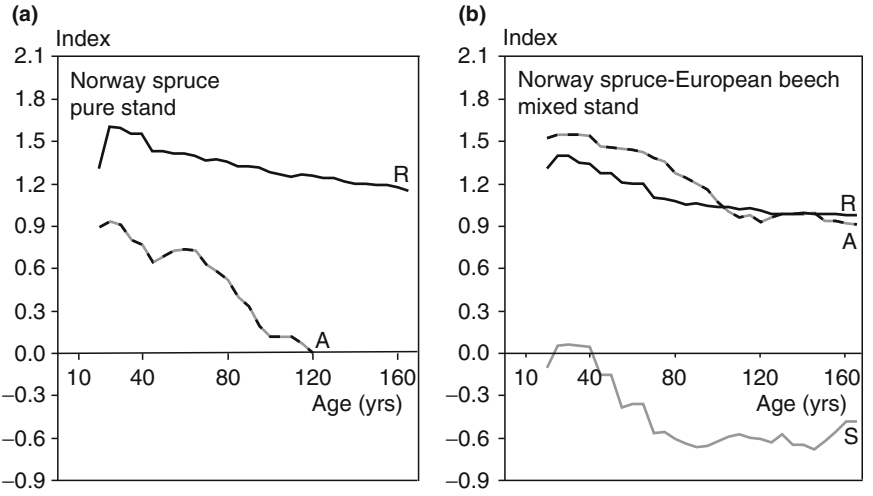

Fig. 13.12 Changes in structure in the (**a**) pure Norway spruce stand and (**b**) Norway spruce–European beech mixed stand over the 145-year simulation period, expressed by the structure parameter R from Clark and Evans (1954), A from Pretzsch (1998), and S from Pielou (1977)

The R Index may assume values between 0 (greatest clumping) and 2.1491 (strictly regular distribution); R values around 1.0 indicate random tree distribution (Chap. 7). In pure and mixed stands, the selection thinning converts the initially more regular distribution (R = 1.1–1.4) into a random to clumped one (R = 0.9–1.0) by maintaining the lower and middle stand, and, occasionally leaving the good growing stock in groups, and thereby promotes heterogeneity.

The A Index characterises the vertical structure of stands by quantifying the extent to which the stand structure deviates from that of a single-layered pure stand (A = 0.0). The more heterogeneous the vertical profile, the higher A becomes (Chap. 7). As expected, the selection thinning of the pure Norway spruce stand, which is still highly structured in the pole phase, reduces the vertical structure with increasing age. The A Index declines almost linearly. In mixed stands, the A Index values develop very differently (Fig. 13.12b). When the prediction commences A is already about 1.5 and decreases only to 0.9 during the life of the stand. This is due to the species mixture present at the beginning as well as to the selection thinning, which enables European beech to survive in the lower and intermediate stand.

The S Index values lie between −1.0 and +1.0. Values below 0.0 indicate a rather intensive intermingling, whereas values above 0.0 indicate the separate occurrence of species (Chap. 7). Thus an intensive single-tree mixture develops in the mixed stand over the prediction period (Fig. 13.12b) as a result of the tending measures in the pole- and sapling stages, and ensures a continuous heterogeneous mosaic of interspecific and intra-specific competition between Norway spruce and European beech until the stand reaches maturity.

13.5.4 Multi-Criteria Considerations

A summary of the results (Fig. 13.13) assists comparisons and the weighing up of different treatment variants by further analyses. In addition to the structural indices S, A and R, the summary presents the h_q/d_q value, an indicator of stability, the maximal MAI_{value} and MAI values for the treatment variants in question. The structural indices, and the h_q/d_q value indicate the structure of a stand with a top height of 30 m; similar profiles can be produced at any time during the simulation run. The MAI of volume and MAI_{value} of the pure Norway spruce stand on the site selected appears to be superior to that of the Norway spruce–European beech mixed stand for the thinning regime modelled, and for the assumptions made about harvesting costs, wood prices and risks. Yet the structure and stability characteristics indicate the pure stand is inferior. So, already this simple example shows how the ranking of different treatment variants changes as soon as we go beyond a more limited growth and yield approach to include elements of stability, resilience and structural diversity.

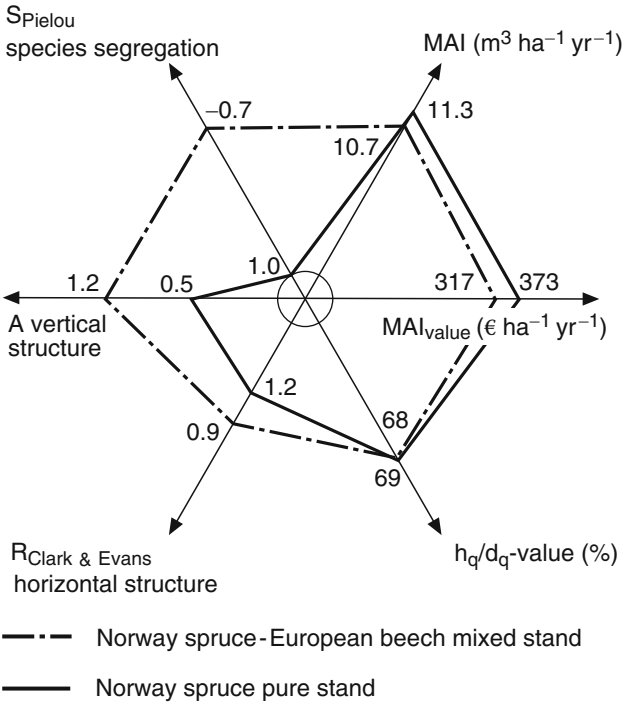

Fig. 13.13 Profile of the most important output parameters for pure and mixed stands (structural indices S, A, R, h_q/d_q-values, maximal MAI_{value} and maximal MAI) facilitate weighing up and optimisation of ecological and economic aspects of stand management

13.6 Growth Models for Dynamic Enterprise Planning

Unlike the interactive use via a menu dialogue as in the previous example, at the enterprise, regional or national level, the simulator is applied semi-automatically in the batch-mode. The starting values for the prediction runs (inter alia forest inventory site classification data) go back to the input provided by forest inventory databases, while the control variables (inter alia treatment regimes, wood prices, wood harvesting costs) are downloaded to special files so that any number of subsequent forecasts may be performed (Ďurský 2000). At the enterprise, regional or national level the overall consequences of individual forest management decisions presented by way of example in the last section, become obvious. Thus, undesirable developments, such as future liquidity problems, or long-term losses of growing stock or annual cut, may be rectified by re-considering and adjusting treatment programmes at strata or stand level.

13.6.1 Simulation at the Enterprise Level for Long-Term Strategic Planning

Enterprise simulations enable a planner to test and evaluate different management alternatives (e.g. tending strategies, final cutting rates, changing tree species composition) and their long-term consequences for forest development at the enterprise level. If possible, besides the classical variables of timber production, simulation scenarios should also include indicators of ecological, economical and socio-economical relevance. In this case, planning alternatives can be evaluated (simultaneously at stand, stratum or forestry enterprise level) according to how they fulfill the desired set of criteria.

Figure 13.14 outlines the use of indicators $[I_1, \ldots, I_n]$ for strategic planning and decision-making: beginning with the initial state of a given site unit at time t_0 (black circles), three management alternatives (A, B, and C) are simulated: (A) continuation of the present evenaged forest, (B) conversion of pure Norway spruce stands into mixed stands of Norway spruce and European beech, (C) increasing plantations of Douglas fir. The analysis of these scenarios reveals the consequences of management alternatives in the long run. After an assessment of all criteria in our example scenario, (C) remains close to a fixed target value, whereas scenarios (A) and (B) are sub-optimal. Scenario simulations are an important prerequisite for a multi-criteria evaluation of management alternatives.

The routine application of the simulator SILVA for long-term enterprise management planning typically should include, in addition to the standard scenarios, scenarios of more extensive and intensive harvest. In this way, the forest enterprise can consider and compare the consequences of alternative treatment options.

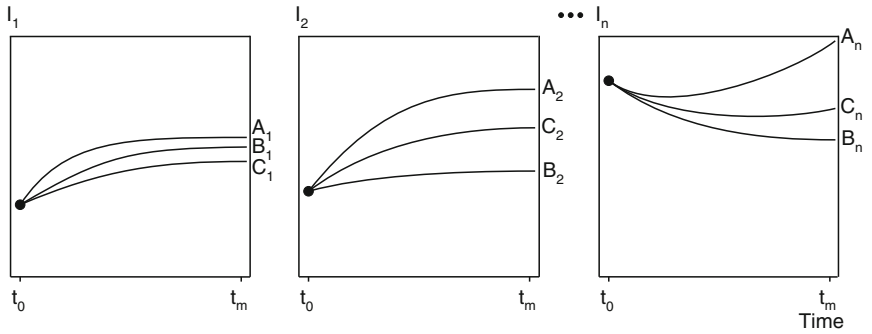

Fig. 13.14 Application of the indicators $I_1, \ldots, I_n$ (e.g. standing volume, annual cut, biodiversity) for strategic forest management planning. Trajectories A_i, B_i and C_i show the simulated dynamics of $I_1, \ldots, I_n$ in the time span $t_0, \ldots, t_m$ as a result of alternative management regimes (e.g. various regimes of thinning, tending, stand establishment, final cut)

13.6.2 Application of Models for Decision Support

This section demonstrates how to apply simulations at forest enterprise level on the base of inventory data. It involves the following six steps (Fig. 13.15).

13.6.2.1 Access to the Inventory Database

The inventory database contains the essential information about forest structure at the time of the last inventory along with important site characteristics. For the majority of the central European forest enterprises, such data are available in form of temporary or permanent (sometimes already repeated) grid sample inventories, long-term growth and yield experiments, or, at least, indicator plots and detailed

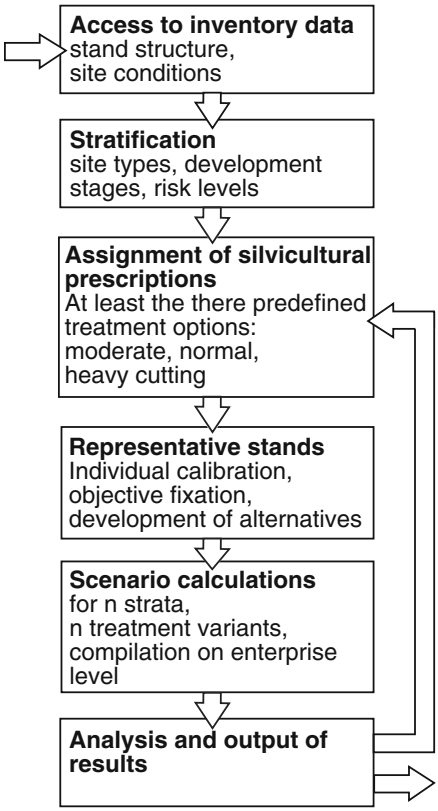

Fig. 13.15 Concept for the application of growth models for recursive strategic planning at the enterprise level. Simulation helps understanding the long-term effects of alternative silvicultural treatments on the development of the whole enterprise. Simulation models enable recursive testing of different combinations of treatment options and their effect on enterprise level. This way, the option that approximates the overall planning objective best can be selected and stipulated in the management plan

maps of the site conditions. Such precise information, acquired at a high cost, has, until now, rarely been exploited in the application of models for forest management planning.

13.6.2.2 Stratification

All inventory sampling points are allocated to certain strata in a cross-classification process; these strata may refer to site-types, stand development stages or a combination of both. This procedure represents a compromise between a rough, and therefore statistically insignificant stratification, and a too detailed stratification where the number of strata is equal to the number of stands.

Stratification serves to reduce the complexity arising from a diversity of sites, tree species mixtures, development stages, etc. to a number of manageable planning units. The criteria tree species composition, development stages, or site conditions may be used in stratification. Under relatively homogeneous site conditions in Southern Bavaria, we can use tree species composition and stand development stage to stratify the forest area. The strata for tree species composition may, e.g. be (1) Norway spruce, (2) Norway spruce/hardwood species, and (3) hardwood species. The stand development stages may be (1) juvenile stage (stands with mean diameter at breast height below 7 cm), (2) growth stage 1 (stands with mean diameter at breast height above 7 cm, with increasing volume increment, up to 35-years-old), (3) growth stage 2 (stands with mean diameter at breast height above 7 cm, with increasing volume increment, over 35-years-old), (4) mature stage (stands with mean diameter at breast height above 7 cm, abating volume increment, no natural regeneration with development potential), (5) regeneration stage (stands with adequate natural regeneration); and (6) selection stage (stands with at least three layers, with adequate natural regeneration). So, $3 \times 6 = 18$ strata are distinguished, and all inventory plots are assigned to one of these 18 strata, which form the basic prognosis unit.

13.6.2.3 Assignment of Silvicultural Prescriptions

A specific silvicultural treatment scenario (e.g. selective or schematic thinning, target diameter or crop tree thinning, thinning from below) is assigned to each stratum. To analyse the long-term effects of different silvicultural prescriptions, standard applications include the assignment of three silvicultural prescriptions to each stratum: a standard variant, a more conservative and low harvest treatment, and a more exploitive management.

SILVA 2.2 provides a whole set of predefined treatment programmes embracing standard programmes widely distributed in forestry practice, as well as more conservative and progressive forestry concepts. These treatment programmes are stored in a database. They define, for every stage, from the seedling stage through to the regeneration stage, the kind, severity and intensity of treatment. In Chapter 5 (Fig. 5.14) we give an example of the silvicultural prescriptions for Norway spruce stands in Bavaria.

13.6.2.4 Representative Stands

For dominant strata, or for all strata, representative stands can be chosen as examples for inspection, discussion and calibration, and as the basis for the development and allocation of silvicultural prescriptions. The representative stands can be visited by the stakeholders involved in the planning process to demonstrate the silvicultural procedures planned, and to substantiate negotiations of treatment alternatives. They further serve as a reference and trainings aid for the assigned silvicultural prescriptions.

13.6.2.5 Scenario Calculations

For the simulation, a representative stand of each stratum is generated on the basis of the inventory points for each respective stratum. The prognosis over several decades is then carried out strata-wise and for selected treatment alternatives. This makes it possible to analyse the consequences of stand or strata-related treatment on the long-term development of the enterprise as a whole. To prevent undesirable developments at the enterprise level, the treatment regimes applied to a strata may be modified if required. So, a feedback loop between the allocation of silvicultural prescriptions and the analysis of how they affect whole enterprise development enables what Speidel (1972) calls a recursive procedure of forest planning.

13.6.2.6 Analysis and Compilation of the Results

Important results for planning practice include site-related yield tables with gross felling budgets and maps of the natural, economic and ecological variables for the selected treatment regimes. The results extend from the initial forest state to the state of the forest at the end of the forecasting period, and describe the development of indicators on single plots, stands, strata, and within the enterprise as a whole. The scope of results was mentioned in the last section (Sect. 13.5.4) in the discussion of simulation results at the stand level.

The advantage of enterprise simulation runs performed by growth models lies in its improved planning flexibility: undesired dynamics at the enterprise level can be identified and corrected by changes in the silvicultural planning at the stand or enterprise level. Without the help of a simulator, the recursive procedure Speidel (1972, p. 162) strives for – “corrections are repeated as long as a convenient adjustment between singular and total planning is attained” – has proven to be very elaborate, and barely feasible within the planning of sustainable timber production, even in evenaged forests. In unevenaged forests with a wider range of management models and sustainable development criteria, a recursive procedure is simply impossible without the support of simulation models.

13.6.3 Application of the Munich Forestry Enterprise Forest Management Plan

13.6.3.1 Short Characteristic of the Forest Enterprise District Munich

The Munich forestry enterprise, with a total area of approximately 18,000 ha, is located 10–20 km south of Munich in the gravel plains and moraine landscape shaped by the last ice age (growth regions Münchner Schotterebene, Oberbayerische Jungmoräne and Molassevorberge). On the mainly moist and eutrophic sites, conifers dominate with 68% (mainly Norway spruce, minor portions of Scots pine, European larch and Silver fir) while broadleaved species hold 32% (mainly European beech and Sessile oak). According to the last forest inventory in 2003, mean standing volume amounts to 291 $m^3 ha^{-1}$ (v. t. h = volume of timber harvested).

The Munich forest enterprise is a special case, in that the disproportionately high volume is concentrated in the older age classes III, IV and V; nearly 80% of the annual cut falls to final cuts. About 65% of the standing volume consists of trees with dbh 30–60 cm (Fig. 13.16). Thus, the growing stock is predominantly mature, often

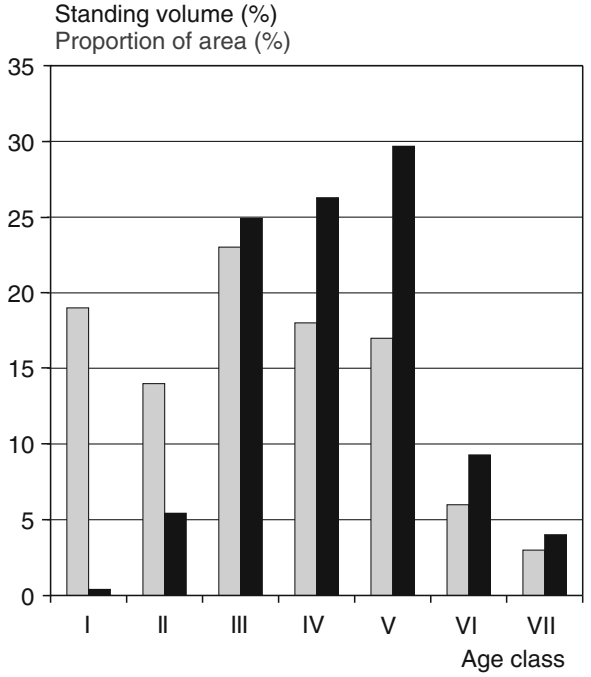

Fig. 13.16 Frequency distribution of the enterprise area (*white bars*) and the standing volume (*black bars*) within the age classes for the Munich forest enterprise: age class I = 0–19 years, age class II = 20–39 years …. age class VII = 120–139 years

unstable, and due to be cut. The SILVA 2.2 model was used to analyse how a light, moderate, and heavy thinning, and final cut would affect the long-term development of growing stock and growth.

The key question in long-term forest enterprise management planning is how the intended thinning variants, final cut, regeneration or conversion of pure to mixed stands might affect the long-term development of standing volume, annual volume growth, and the annual cut quota. Even if other multiple functions (e.g. protection, recreation) are considered in planning, the greatest emphasis usually rests with ensuring a sustainable and continuous wood production. Only in this way can gaps in the wood supply be avoided, continuity in financial liquidity and staff employment be guaranteed, and supply to the wood industry remain reliable. In the following, we outline the way in which a growth model can be used for scenario analyses for sustainable wood production at the enterprise level.

13.6.3.2 Set up of Simulation Runs

We used the data from the last forest inventory as initial values for simulation runs over 30 years. About 6,000 plots (each 500 m^2 in size) were assigned to 220 different strata with a minimum of 5 and a maximum of 300 plots per stratum. The criteria for the stratification were stand development stage, site conditions, species composition, and risk factor (susceptibility to wind throw, ice-breakage, bark-beetle attack).

Once the plots were assigned, we generated a representative stand for each stratum, and used it for the first simulations with SILVA 2.2. In addition, we assigned three silvicultural prescriptions to each stratum. The standard variant in the simulation represents the conventional tending, thinning and final harvest measures used in practice ("business as usual"). The moderate and heavy thinning regimes are similar in the kind and intensity of silvicultural treatments, yet the severity of harvest differs: the moderate thinning regime thins about 15–30% less volume than the standard variant, whereas the heavy thinning exploits 15–30% more. The applied silvicultural prescriptions are developed together with the planning team, discussed on the basis of the real stands representing the identified strata, quantified numerically (cf. Chap. 5, Sect. 5.4) and saved in a database for external control of the simulation runs.

13.6.3.3 Results

Of the broad spectrum of results, we focussed on the development of growing stock (Fig. 13.17a), annual volume growth (Fig. 13.17b), and annual cut (Fig. 13.17c) in the next 30 years. The management plan prescribes silvicultural measures only until 2016 (10 years), but, at the same time, must consider the sustainability of the forest development long after.

The continuation of the silvicultural practice as usual would lastingly reduce the growing stock to 250–270 $m^3 ha^{-1}$ (volume timber harvested = v. t. h.), the

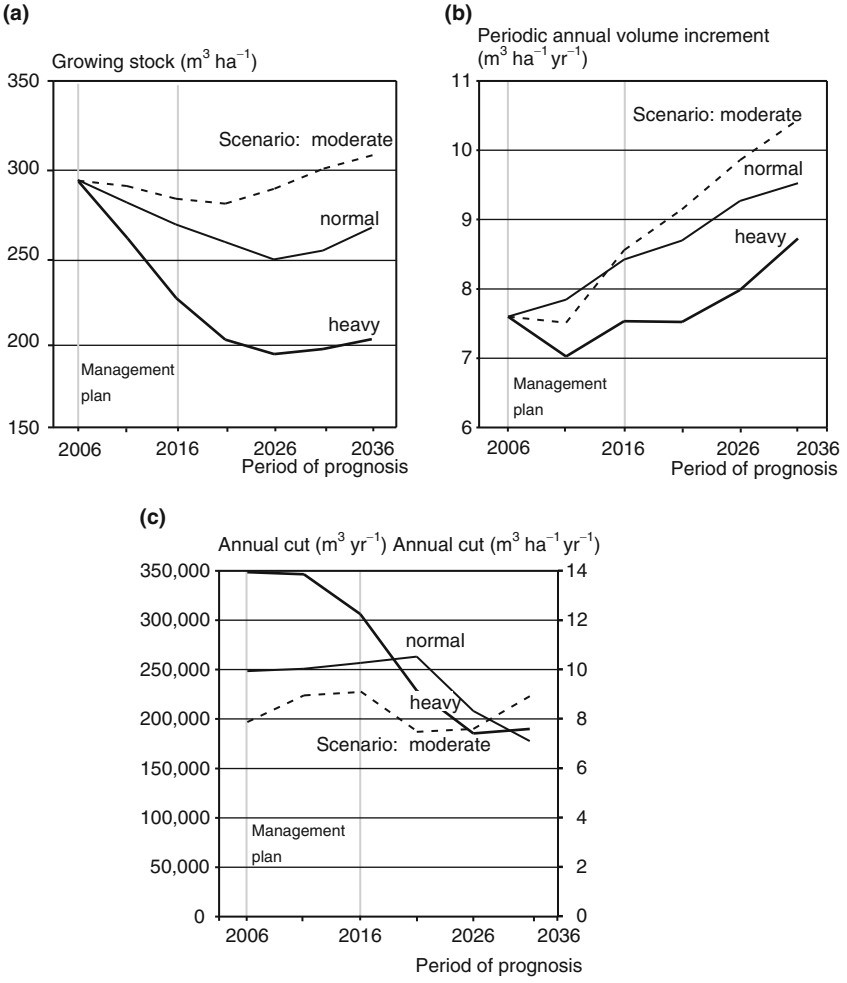

Fig. 13.17 Results of scenario analyses for (**a**) volume of growing stock, (**b**) periodic annual volume growth, and (**c**) annual cut for the Munich forest enterprise (in volume timber harvested m^3 v. t. h.). The scenario analyses start with the inventory data 2006, and simulate different treatment scenarios for the long-term management planning until 2036: moderate harvest (*dashed line*), normal harvest (*thin solid line*) and heavy cutting (*thick solid line*). The management plan defines the forest management activities up to 2016, but, at the same time, considers the long term sustainability of the forest development

annual volume growth would increase from 7.5 to $9.5\,m^3\,ha^{-1}\,yr^{-1}$, and the annual cut would decrease from 10 to $7.5\,m^3\,ha^{-1}\,yr^{-1}$. This is mainly due to the disproportional age distribution: the older high volume stands are due to be harvested soon, shifting the age spectrum to the faster growing younger stands with less volume.

Before the simulations, the original plan foresaw a heavy thinning scenario, which would have increased the annual cut for a short period of time, but depleted the growing stock even more than in the previous business as usual scenario, and, in the long run, the annual cut would have to be reduced again. As thinning continues, the stand basal area and consequently the annual volume growth will decline. We see that the heavy thinning scenario enhances the disproportionality of the age spectrum, leading to strong fluctuations in growing stock and wood production in future.

In view of the continuity and sustainability of the annual cut and growing stock, a more moderate silvicultural concept appears preferable. It might foresee lower harvests for the current 10 year period (planning interval) in the order of 100,000–150,000 m^3 less than the standard or heavy cutting scenario (Fig. 13.17c), yet, in the long run, the growing stock is kept constant, and the annual volume growth is raised from 7 to 10 $m^3\,ha^{-1}\,yr^{-1}$ (v. t. h.).

In the end the management plan fixed the annual cut to 9.7 $m^3\,ha^{-1}\,yr^{-1}$, slightly lower than in the standard variant. In the long run, this value will lead to a more balanced age spectrum, and ensure a more or less constant growing stock and volume growth, thereby avoiding temporary deficiencies in the wood supply. The simulation helped to predict the long-term consequences of the thinning variants considered, and altered the original decision in favour of a more moderate felling budget. Although a higher annual cut of, e.g. 12–14 $m^3\,ha^{-1}\,yr^{-1}$ might have increased wood supply and revenue for a short time, this would be at the expense of decreased productivity, and fluctuations in wood supply and revenue from the next generation onwards (Fig. 13.17c).

13.7 Estimation of Growth and Yield Responses to Climate Change

The research conducted by Kauppi et al. (1992), Kenk et al. (1991), Lindner et al. 2002), Myneni et al. (1997), Pretzsch (1999), Röhle (1994, (1997), Spiecker et al. (1996) and Utschig (1989) quantifies the extent to which the growth of the main tree species in Europe has changed at the local, regional and global level in recent decades. While site conditions have always changed gradually, the current changes in the climate and anthropogenic emissions of NO_x, NH_3, CO_2, SO_2 etc. are rather abrupt and drastic. It is clear that constant site conditions can no longer be assumed, and forest management and planning, silvicultural prescriptions, and recommendations for choice and cultivation of tree species must take into account the consequences for forest growth behaviour. The site–growth module in the growth model SILVA 2.2 permits the input of altered climate and site conditions and therefore also the estimation of their effects on forest growth (Fig. 13.3). This facilitates the diagnosis of sensitivity and vulnerability of forests to climate changes, and the development of adaptation and mitigation measures.

13.7.1 Dependence of Response Patterns on Site and Tree Species

As an example, the growth of Norway spruce and European beech is projected under present and changed climatic conditions in growth region 12 selected by Wolff et al. (1998), comprising forests in Bavaria, the Upper Palatinate, Franken, Thüringen and in the Erz Mountains. First, we first show how a temperature increase of 1 or 3 °C can affect the growth of a representative stand in this region. The example uses a dose–response function, simplified for purposes of clarity, in the growth simulator SILVA 2.2 (Fig. 13.18). Given a current mean temperature in the growing season of 13.3 °C, the MAI_{100} (mean annual volume increment at age 100 $m^3\,ha^{-1}\,yr^{-1}$) of the stand is set to 100%, and we observe the percentage change in MAI_{100} as a result of climate change. Figure 13.18 shows that the current mean temperature in the growing season for (a) Norway spruce and (b) European beech investigated in growth region 12 is not optimal, and a rise in temperature of 1 °C would cause an increase in MAI_{100} of about 5.9% for Norway spruce, and about 11.7% for European beech. In contrast, a rise in temperature of 3 °C places Norway spruce in a worse temperature environment, as MAI_{100} drops by 8.9% to 91.1%. The situation differs for European beech, as its optimum temperature is higher than that of Norway spruce. The growth of European beech therefore would respond still favourably to the same change in temperature, as shown by the predicted 5.9% rise in MAI_{100} to 105.9%.

This outcome clearly shows that the growth response to climate change is largely dependent on tree species, the given initial site conditions and the given change. Whether a positive or negative growth response to climate change occurs depends on the actual position of, and the shift in the site conditions with respect to the species ecological amplitude. Depending on whether a site lies on the increasing or decreasing branch of the unimodal optimum curve, and on its distance from the optimum, the effects on growth and yield may be either positive or negative (Chap. 10). That

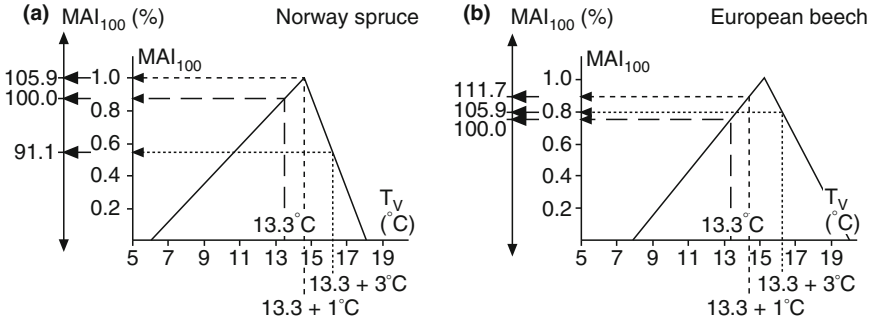

Fig. 13.18 Effect of a rise in mean temperature during the growing season of 1 or 3 °C on mean annual volume growth at age 100 (MAI_{100} in $m^3\,ha^{-1}\,yr^{-1}$) of (**a**) Norway spruce and (**b**) European beech. The response of representative stands in growth region 12, encompassing areas of Bayerischer Wald, Oberpfälzer Wald, Frankenwald, Thüringer Wald and Erzgebirge is shown

Norway spruce responds dramatically to changes in temperature during the growing season has already been shown by Thomasius (1990). He found that Norway spruce tolerated only a quite narrow temperature range between 5 and 8 °C annual mean temperature. In many regions in central Europe, the annual mean temperature is only about 7.0–7.5 °C. Therefore a slight rise of 1–2 °C in temperature would place Norway spruce at the upper edge of its ecological amplitude.

13.7.2 Sensitivity Analysis at the Regional Level

13.7.2.1 Methods

As an example for the growth response at the regional level, the growth of Norway spruce is projected under present and changed climatic conditions across all growth regions in Bavaria. The analysis is based on the site type that occurs most frequently in any given growth region, so that the site growth model (Sect. 13.2) predicts one potential growth curve for each region. Each scenario comprises the development of Norway spruce stands from age 30 up to age 120 years (90 year period). Therefore, as a first step, 30-year-old forest stands representative of the most frequent site type in each growth region are identified from the Bavarian State Forestry forest inventory database. These sample plot data (points in a 200 m × 200 m grid) are used to determine the start, control and site parameters for the simulations.

Next, the yield-related parameters of the selected forest stands (mean height, mean diameter and basal area of the stand per hectare at age 30) are calculated. These serve to reproduce the missing stand structure data needed for the growth simulations (Nagel and Biging 1995; Pretzsch 2001). The scenario calculations are based on thinning from above at the young stage, and, from age 50 years onwards, on thinning from below.

The simulation under changed climatic conditions is performed in the same manner as the simulation of the stand dynamic for current climatic conditions above. Growth responses to the following climate scenario (2050–2100) were tested: a 2 °C rise in temperature and a 10% decrease in the precipitation during the growing season together with a prolongation of the growing season by 10 days (Bayerischer Klimaforschungsverbund 1999; Fabian 1991). Thus, based on the present and assumed future climatic conditions, the characteristic values for natural production, economy and ecology were calculated for each growth region, and the results of these scenario calculations compared to one another. Before proceeding to the calculation results, we should mention that the climate–growth relationship in SILVA 2.2 is static, that is it does not reflect the effect of continually changing climatic conditions, but predicts what growth would be like under future climate steady-state conditions.

13.7.2.2 Thematic Mapping of Response Patterns

Figure 13.19a shows the top heights at age 100 for the representative stands in the growth regions covered. These values may be used directly to determine site quality (= site index). The top heights were highest in the growth regions 13.4, 14.4, 12.9, 5.3, 5.2, 5.1 and 2.2. Growth region 2.2 has been included in this peak group because in the Buntsandsteinspessart (mottled sandstone hills in the Spessart) Norway spruce will grow on only a few exceptionally favourable sites. We see that Norway spruce is capable of reaching top heights of 35–40 m in many growth regions. The bottom end on this scale contains Norway spruce stands on sites in lowlands with limited supplies of water and nutrients, which typically comprise growth regions where Scots pine is the dominant tree species.

Under the selected climate scenario, the top heights of the study sites did not exceed 40 m at age 100 years. In areas with limited water supply, e.g. in growth region 13.2 Münchner Schotterebene (Munich gravel plateau) there is a distinct decrease in top height. In the growth regions 4.1, 4.2, 5.5 and 5.6, the top height at age 100 years only amounts to 22–25 m. Here, growth conditions for Norway spruce clearly have deteriorated. By contrast, in some regions of North and East Bavaria, the assumed changes in climate will result in optimum top height development.

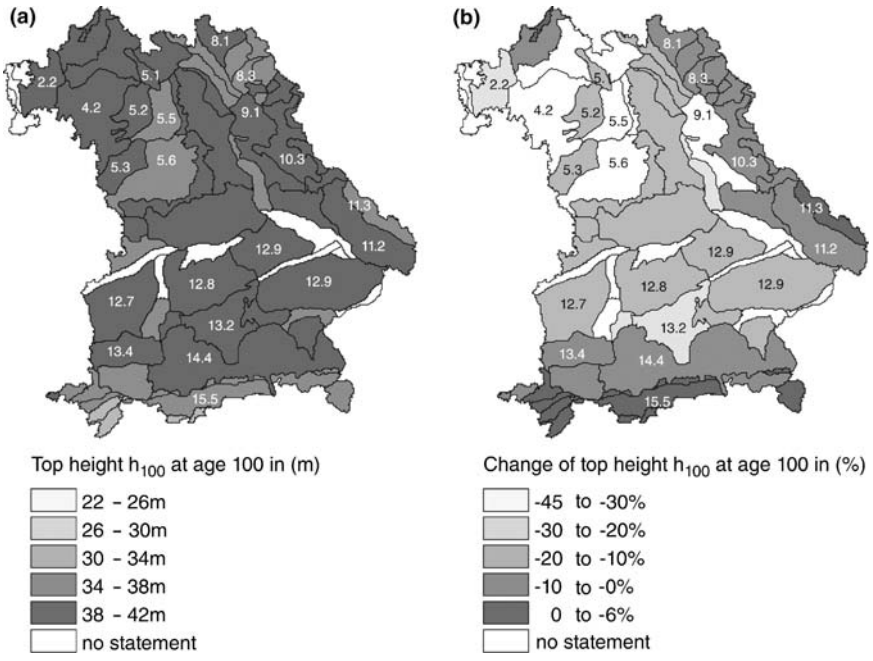

Fig. 13.19 Top height h_{100} in representative Norway spruce stands in the Bavarian growth regions at age 100 years (**a**) under current climatic conditions and (**b**) assuming a temperature rise of 2 °C, reduction in precipitation by 10% during the growing season, and an extension of the growing season by 10 days

In the alpine foothills, Norway spruce is expected to continue to show good height growth performance as well. Figure 13.19b shows the expected change in top height at age 100 years in relative terms. Areas shaded in the lightest colour tone predict a 30–40% decrease in top height at age 100 for some regions mainly in Northeast Bavaria compared to the present growth. For most growth regions, top height is expected to decrease between 10 and 20% at age 100 years. In the alpine foothills, and in the eastern mountain ranges, the decrease remains below 10%. In some growth regions of the Alps and the Bayerischer Wald (Bavarian forest), the scenario analyses show an increase in top height of 6%. However, this growth enhancement of top height through climatic changes is noted for only very few sites.

This region-specific response pattern of top height growth is reflected in the MAI_{100} values of the representative Norway spruce stands in the growth regions. Figure 13.20 shows, for example, above-average growth at the South Bavarian sites with MAI_{100} values between 17 and 20 $m^3\,ha^{-1}\,yr^{-1}$. In growth region 15 in the Bavarian Alps, MAI_{100} values of 14–15 $m^3\,ha^{-1}\,yr^{-1}$ are found. The North and East Bavarian central mountains, with MAI_{100} values between 10 and 12 $m^3\,ha^{-1}\,yr^{-1}$, lie at the lower end of the productivity scale. The good height growth in the growth districts 5.1, 5.2 and 5.3 in the Keuper mountain region is not reflected in the MAI_{100}

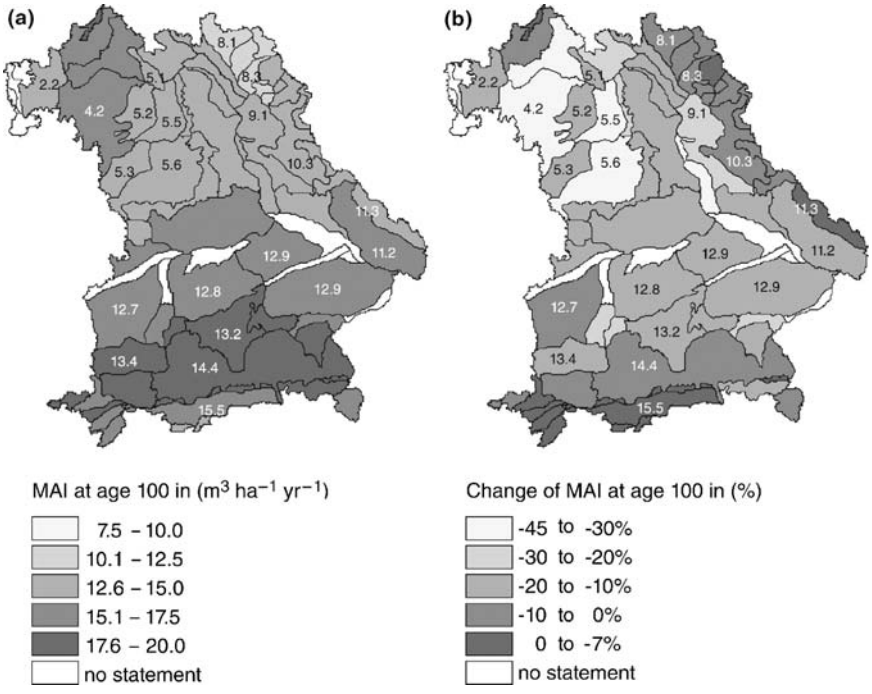

Fig. 13.20 Mean annual volume increment MAI_{100} ($m^3\,ha^{-1}\,yr^{-1}$) of representative Norway spruce stands in Bavarian growth regions at age 100 years (**a**) under current climatic conditions and (**b**) assuming a temperature rise of 2 °C, reduction in precipitation by 10% during the growing season, and an extension of the growing season by 10 days

values. Here, the low basal area levels in the older stands negatively affect the MAI_{100} values. Stand structure often is disturbed by wind-throw in this region. With the exception of growth region 6.2 and 11.2, all other regions North of the Danube River have MAI_{100} values of between 10 and 15 $m^3\,ha^{-1}\,yr^{-1}$.

Under the changed climatic conditions (rise in temperature in the growing season by 2 °C, drop in precipitation in the growing season by 10%, lengthening of the growing season by 10 days) only a few growth districts reach MAI_{100} values above 17 $m^3\,ha^{-1}\,yr^{-1}$. In particular, in the growth districts that currently have a warm, dry climate, the scenario calculations predict a decline in the MAI_{100} to 8–10 $m^3\,ha^{-1}\,yr^{-1}$. To identify the regional response patterns more easily, Fig. 13.20b shows the percentage change in MAI_{100} compared to undisturbed conditions as reference values. However, severe reductions in stand growth would be found in growth region 4, in the Franconian lowlands, and in the growth districts 5.5 and 5.6 in the Keuper Hills. The reduction in growth would be 30–45% of the MAI_{100} values reached to date. For large areas in Bavaria, decreases in the MAI_{100} values of 10–20% are expected. In contrast, the sub-regions 12.7 and 14.4 in the foothills of the Alps continue to be highly productive sites for Norway spruce under the assumed climate changes. The Alps and the central mountain range show either only a slight decline in MAI_{100}, or a slight increase.

13.7.3 Development of Silvicultural Measures for Mitigation and Adaptation to Climate Change

The scenario calculations performed by the model SILVA 2.2 assist the development of concepts for silvicultural counter-measures against growth losses arising from climate change. First, we investigate how MAI in the pure Norway spruce stand in the Upper Bavarian Tertiary hillside (site unit 203, moderately moist to moist loam) develops under current climatic conditions with moderate selective thinning (Pretzsch 1999). Figure 13.21a shows that MAI (bold black line) rises above 20 $m^3\,ha^{-1}\,yr^{-1}$ at a stand age of 90–140 years, and subsequently decreases. This course of Norway spruce stand growth under current climatic conditions is given in Fig. 13.21b (bold black line) as a reference (100% line) to compare the change in Norway spruce stand growth due to climate change (black dotted line). The climate change scenario models a temperature rise in the growing season of 2 °C, a drop in the precipitation in the growing season of 10%, and a lengthening of the growing season by 10 days. Under this scenario, we see that the MAI in pure Norway spruce stands drops below the reference line by about 10%.

Next, it was tested whether, and to what extent, the growth loss could be counteracted by admixing 30–70% European beech (Fig. 13.21b, black dashes). Calculations from SILVA 2.2 indicate that an admixture of 30% European beech, which grows better under the assumed climatic conditions, would more than compensate for the growth losses in Norway spruce arising from the climate change for a rotation

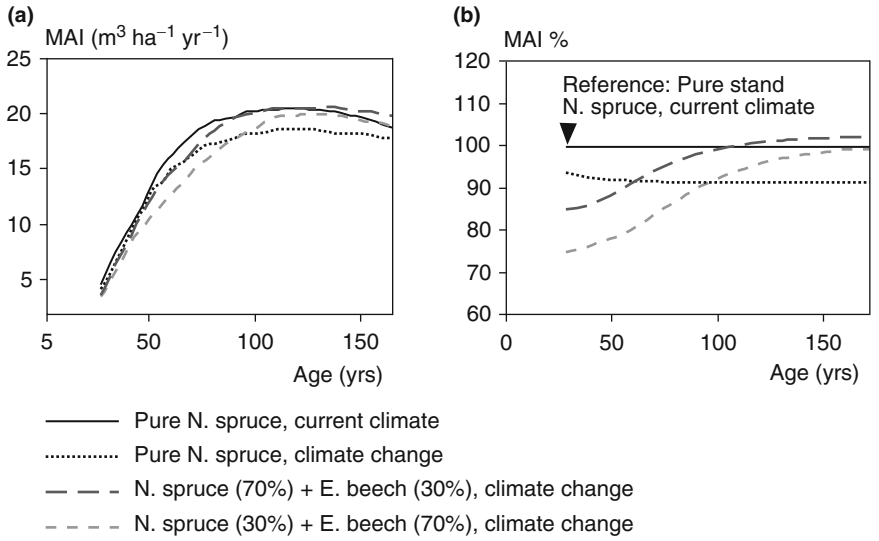

Fig. 13.21 Volume growth of pure and mixed stands of Norway spruce and European beech under current (solid line), and changed (dashed line) climatic conditions. (**a**) MAI curve and (**b**) MAI of different scenario calculations in relation to stand growth of Norway spruce under present climate conditions. Scenario runs with SILVA 2.2 for sites in the growth region Oberbayerisches Tertiärhügelland, site unit 203; moderately moist to moist loam; climate scenario: 2 °C rise in temperature during the growing season; 10% drop in precipitation during growing season; 10-day extension of growing season

of 100–150 years. An admixture of 70% European beech (grey dashed line) can compensate for the climate-related growth losses of Norway spruce only once stand age reaches 150 years.

Although changes in climate and site conditions are often thought to enhance the growth rates, such scenarios show that greater climate changes can result in severe reductions in growth, and shifts the competitive relationships between the species. Furthermore, the site-related growth losses in the Upper Bavarian Tertiary hillside can be compensated for by converting the forest stands to better-adapted species mixtures. Such scenario analyses with site-sensitive individual-tree models provide quantitative information to support the development of silvicultural options and management decisions, even under climate change.

Summary

This chapter illustrates the application of growth models in forestry practice. As an example the forest growth simulator SILVA is used which was already applied on a wide range of problems from analyses of local silvicultural treatments to regional and national growing stock assessments. Central challenge in European forestry is

the management of heterogeneously structured pure and mixed stands, which requests silvicultural concepts that explicitly promote certain collectives, the conversion of homogeneous pure stands to structured mixed stands, natural regeneration and the mitigation of adverse effects due to climate change. Position-dependent and climate-sensitive individual tree based growth models which can be employed on pure and mixed stands cover those demands best, and increasingly substitute the yield tables used in the past. The examples of practical application therefore refer to this kind of model.

(1) Models allow predicting long-term consequences of silvicultural treatment alternatives in time lapse. If different treatments or growth conditions are tested comparatively, this is referred to as a scenario analysis. Such scenario analyses deliver if-then statements and thereby provide a decision support in practice concerning the choice of the silvicultural treatment model, amount of the annual cut, natural regeneration methods, etc. Models do not produce the "perfect" treatment variant, but allow choosing among a set of considered variants the ones that match the desired objective best.
(2) Models only become an efficient tool and decision support if the available initial and control parameters (inventory data, site conditions, silvicultural treatment programmes, etc.) are utilised to the maximum possible extent in the scenario analyses. Only then can models actually meet the mostly site-specific and treatment-differentiated information required by the user.
(3) The limit of most models (yield tables, diameter distribution models, distance-independent pure stand models) mainly consists in the assumption of constant site conditions, exclusive applicability to pure stands and the emphasis on stand-related growth parameters (stocking volume, mid stem, basal area). However, the reconstruction of common treatment programmes like crop-tree thinning, selective thinning, or selection forests, requires position-dependent model approaches. The reproduction of the trees' growth reaction to changed site conditions can only be realised with climate-sensitive growth models. And last but not least, the analysis of conversion scenarios from homogeneous pure stands to structurally heterogeneous pure and mixed stands with natural regeneration needs spatially explicit models.
(4) Models designed for decision support are expected to cover a whole spectrum of output variables including stand and individual tree information on the natural production, ecological and economic key parameters as well as specific characteristics of habitat quality and recreational value.
(5) Modern silvicultural treatment programmes, methods of the conversion of pure to mixed stands and natural regeneration techniques cannot be tested experimentally before their transfer into practice due to the long period of time of a forest's development. Models make it possible to reproduce, optimise and modify new treatment variants (silvicultural prescriptions) with the help of a simulator, and evaluate the predicted economic, ecological and socio-economic consequences.

(6) Another important application of forest growth models is the use in long-term planning on the enterprise level. Silvicultural management strategies that appear attractive at the stand scale might not necessarily be the best concept for an entire forest enterprise. To ensure sustainability of the natural productivity and the ecological, economic and socio-economic value of the forest, growth simulators can predict the forest development for decades on the basis of former forest inventories. By testing different treatment options on stratified representative stands, it can be evaluated how the considered silvicultural concepts match the long-term objectives of the forest enterprise. Repeated refinement of variants, a quasi recursive procedure, allows optimising both the short-term management plan, e.g. the 10-year felling-budget, and at the same time the long-term development (sustainable timber supply, stocking volume, etc.).

(7) In many regions in central Europe the forest is made up of tree species that would not dominate under natural conditions. Historical forest exploitation (deforestation, site degradation, litter usage, reparation cuts) led to large scale reforestation and conversion favouring Norway spruce and Scots pine in often unsuitable lowland plains. The ongoing and future climate changes will derogate the distribution, susceptibility and growth potential, especially where trees occur at the limit of their ecological amplitude. Here, the climate-sensitivity of the growth model SILVA 2.2 was utilised to analyse the growth of Norway spruce under the current and predicted climate conditions.

(8) Growth models can also support the development of silvicultural concepts to mitigate adverse effects of climate change like disturbance susceptibility, increment losses or stand deterioration. For a selected stand in the pre-alpine region, scenario simulations with SILVA 2.2 show that growth losses expected for pure spruce stands can be compensated by admixing beech.

(9) For the exemplary testing of treatment variants on stand scale or for educational reasons, an interactive mode provides the user with the options to vary initial data, site conditions and treatment. For applications with real data on enterprise, regional or national level, an automated batch version is required. The provision of the input files in the form of (stratified) inventory data, assignment of treatment programmes and handling of the results must also be easy to realise for a non-expert.

(10) Very important for a causal argumentation when introducing the long-term consequences of certain planning options to the participating public is the visualisation of the management alternatives. Position-dependent, individual-tree oriented models deliver the necessary input for such visualisations on stand and landscape levels. They make the scenario-analyses that were based on natural production, and ecological and economic considerations, approachable for the non-expert in form of dynamic landscape simulations.

Chapter 14
Diagnosis of Growth Disturbances

The growth of trees and whole forest stands increasingly is being impaired by disturbance factors. These disturbances may be locally or temporally restricted, such as the lowering of the groundwater table, road construction, and industrial and agricultural pollution, or of global and long-term character, such as changes in atmospheric carbon dioxide and ozone concentrations and global climate change. In forests, these disturbance factors can result in specific response patterns, such as changes in the carbon allocation, the tree allometry, the branching behaviour, the foliage density, height or diameter growth trends or the composition of forest communities. Typically, several process levels are affected (Chap. 1, Sect. 1.1). All these response patterns can be used to analyse the system behaviour, and to diagnose possible disturbances. Yet the analysis of long-term growth trends of diameter, height or volume of trees or stands is probably the most important and accessible tool.

The growth trend is a highly aggregated, and therefore reliable and robust indicator of system behaviour in comparison to findings of a biochemical, ecophysiological, or branching-morphological nature. So, whenever the long-term growth of individual trees or entire forest stands is affected, the growth disturbance must be very profound. Conversely, apparently normal growth behaviour does not necessarily indicate undisturbed system behaviour because disturbances at sub-ordinate process levels can be buffered to a certain extent. The higher the resolution of an observed process, the greater the uncertainty associated with extrapolating disturbances of this sub-processes to the whole system because the number of intermediate regulatory feedback loops also increases.

For the evaluation of present growth trends we can refer to long-term increment measurements from experimental plots, which date back far as far as the nineteenth century. Such long time series do not exist for any other state forest ecosystems. As increments also can be determined retrospectively via increment cores or stem analyses, growth trend analysis is an immensely important indicator, e.g. for climate or catastrophic events in the past.

For practical reasons (measuring technique, sampling procedure, forest ecological significance etc.), most diagnoses are carried out on basis of stem diameter increment and tree height measurements, needle loss estimates, and mortality records.

H. Pretzsch, *Forest Dynamics, Growth and Yield: From Measurement to Model*,
DOI: 10.1007/978-3-540-88307-4_14,

More refined information is available from whole-stem analyses, crown structure analyses and increment analyses of roots. However, this is usually infeasible on the large scale.

One has to be aware that growth disturbance at the individual tree level does not necessarily affect the stand level in terms of stand productivity loss. The regulatory feedback loop, growing condition of individual tree → individual tree growth → stand structure → growing condition of individual tree, results in a feedback between affected, and less, or unaffected individuals (Fig. 7.2). The vigorous trees may make up, or even overcompensate for the growth loss from the disturbed or dying trees. Therefore, the quantities used as indicators of growth disturbances, such as needle loss, increment, and seed production should be regarded at both the individual tree and stand level.

This chapter introduces methods for long-term growth analyses, which are based on the available datasets from inventories, temporary and long-term research plots, increment cores and stem analyses. The methods are summarised in Table 14.1, and ordered in four groups according to the type of reference used. The reference represents the supposedly "normal" growth behaviour against which the supposedly disturbed growth behaviour is compared. The comparison between disturbed and reference growth behaviour makes it possible to determine the beginning, duration and strength of the growth response, and may help to identify the sources of disturbance. The type of reference depends on the type of presumed disturbance, its temporal and spatial dimension, and the available database, e.g. the growth curve, climate parameters, and groundwater regime or pollutants measurements. The field of application varies from ecological monitoring or the verification of cause-and-effect models to regional planning or provision of evidence in legal disputes. The main differences between the methods lie in the degree to which a certain method can eliminate the initial difference between the "normal" and "disturbed" samples, and separate the effect of the disturbance factor from general local climate or other site-specific effects. The choice of one or the other method may lead to small differences in the precision of the results and associated costs. In practise, it is advisable to apply different methods to the one problem to take advantage of the strengths of each method.

Finally, it should be noted that, while all the methods mentioned may reveal apparent cause-and-effect chains, these rarely could be taken as proof. Field conditions hardly ever accommodate the ceteris paribus conditions required for a direct link between cause and effect, and one must accept an uncontrollable multitude of factors, each with greater or less influence on growth. On the other hand, the lack of a direct proof between disturbance factor and growth responses does not lead necessarily to a reduction in the importance of these methods for diagnostic increment analyses. In the end, it is a question of epistemic character, whether, when testing a hypothesis, the aim is to obtain direct experimental proof, or an evidence-based result. Particularly the analysis of large-scale, long-term growth disturbances will rely on evidence, as the experimental design to trace directly the cause-and-effect chain can be realised at best only temporarily on few sites.

Table 14.1 Methods for the diagnosis of growth disturbances for trees and whole forest stands and their fields of application. According to the applied reference, which presents "normal" undisturbed growth, four approaches can be distinguished

Method	Data pool	Reference	Fields of application	Example	Section
Growth models as reference					
Comparison with yield table	Data of individual trees and forest stands which were collected on small- to large-scale basis	Growth models	Scrutiny of models for planning, trend analyses	Röhle (1997)	14.1.1
Reality-scenario-comparison				Hari et al. (1984)	14.1.2
Synthetical reference curves	Stem analyses	Tending programmes	Trend analyses	Gerecke (1986)	14.1.3
Undisturbed trees or stands as reference					
Increment trend method pair-wise comparison	Increment time series from coring, stem analyses and successive surveys which were collected on small- to large-scale basis	Increment time series from undamaged individual trees, tree groups, forest stands	Impact research, proceedings for the preservation of evidence	Pretzsch and Utschig (1988)	14.2.1
Reference plot comparison via covariance analysis				Sterba (1984)	14.2.2
Reference plot comparison via indexing				Franz and Pretzsch (1988)	14.2.3
				Vinš (1961)	14.2.4
Regression-analytical increment diagnosis		Regression models		Dong and Kramer (1987)	14.2.5
Growth in other calendar periods as reference					
Comparison with previous periods	Coring, stem analyses	Increment of previous period	Trend and sensitivity analyses	Röhle (1987)	14.3.1
Diagnosis of abrupt increment events				Schweingruber et al. (1983)	14.3.1
Method of constant age	Increment measurements for a wide age spectrum	Historic ring width of individual trees	Bio-indicators, trend analyses	Mielikäinen and Timonen (1996)	14.3.2
Generation comparison	Permanent plots	Historic stand growth recordings		Wiedemann (1923)	14.3.3
Comparison of succeeding periods	Large-scale successive surveys	Level of annual increment of past inventories		Kauppi et al. (1992)	14.3.4
Dendro-chronological time series analysis					
Analysis of dendro-ecological time series	Coring, stem analyses, Climatic time series	Response function	Impact research proceedings for the preservation of evidence	Fritts (1976) Cook and Kairiukstis (1992)	14.4

Compared with the formation of new buds, leaves, shoots, and fine roots, carbon allocation in stem wood is relatively low priority (Waring and Schlesinger 1985). Due to the low allocation priority attributed to diameter increment, diameter increment at breast height is a particularly sensitive, even though unspecific, indicator of tree resource availability. Assuming equal tree size, a high diameter increment indicates a reasonable balance in carbon allocation, whereas a low increment indicates a shortage of building material, where limited carbohydrates are allocated to storage or defence (Waring and Schlesinger 1985). Kramer (1986), Pretzsch (1985b) and Sterba (1996) show that Norway spruce, Scots pine and Silver fir growth declines during stress particularly in the lower third of the stem. Although the crowns of Silver fir, Scots pine and Norway spruce did not show definite stress symptoms always, Elling (1993), Pretzsch (1985b) and Schweingruber et al. (1983) detected, by means of year ring analysis, up to 20 missing tree rings at diameter at breast height. Clearly, increment at stem base is appropriate for early detection of stress and vitality decline. However, a decline in increment at stem base is not representative for the whole stem, least of all for the whole tree. Under stress, tree rings in the lower part of the stem can be missing or rather narrow (Elling 1993; Pollanschütz 1975, 1980; Pretzsch 1985b; Rubner 1910), whereas rings in the upper stem and branches are still normal, i.e. trees become more top-heavy. Therefore, conclusions extrapolating a particular decline in increment at breast height to the whole stem, or even the whole tree, would result in an overestimation of the growth decline.

14.1 Growth Models as Reference

14.1.1 Comparison with Yield Table

A comparison with yield tables relates the growth of a given forest stand to the values from forest yield tables. Large deviations between real growth behaviour and that expected from the yield tables would bring into question the suitability of the yield tables for the planning of stand management and annual cut. Thus, the detection of such differences is important for strategic decisions in forestry.

It is important to understand that yield tables reflect an average stand development within a certain region and time, derived from a network of research plots. Given the spatial distribution of the plots, the yield tables essentially incorporate a heterogeneous database in terms of site conditions, age structure, provenance and stand treatment. Therefore the value of yield table comparison is only of limited significance, but this increases when a larger number of stands is included.

When using a yield table as a reference, one needs to be aware of the background of the data, and the way it is compiled (range and quality of data material, choice of growth functions, statistical adjustments etc.; cf. Chap. 10, Sect. 10.3). An inadequate choice of the reference yield table may mistake an actual growth increase for a growth reduction, and vice versa (Sterba 1989b). Therefore, one must ensure that the correct growth table is chosen for the task in question. Differences

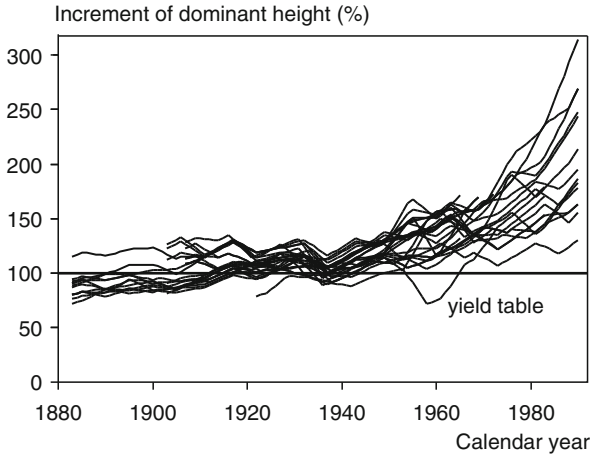

Fig. 14.1 Comparison of actual height increment and increment according to yield tables (100%-reference line) by Röhle (1997). Increment of dominant height at 27 long-term experimental plots with Norway spruce in the forest districts Denklingen, Egelharting, Ottobeuren and Sachsenried in South Bavaria from 1882 to 1990 in comparison with the yield table from Assmann and Franz (1963)

in the stocking may be overcome by density–increment relationships (Assmann and Franz 1965). Röhle (1997) gives an example for the diagnosis of long-term growth trends of Norway spruce stands in South Bavaria via the comparison with yield tables. The database encompasses 27 research plots (in four different forest districts) with more than 100 years of continual observation. The yield tables from Assmann and Franz (1963), partly based on the stands under consideration, were chosen as the reference. The results in Fig. 14.1 indicate that, from 1882 until the 1950s, the height growth of the dominant trees forms a narrow band that slightly increases from 90% to 110%. Thereafter, the height growth increase is much stronger, and, in 1990, the former narrow band has spread out into a wide range of values between 129% and 314%. Being given the identity between the examined stands and the applied reference basis excludes stand treatment and provenance as possible causes for the growth increase. This leaves climatic changes, for example a prolonged growing season or increased atmospheric nitrogen, or carbon fertilisation as the most likely explanation.

14.1.2 Dynamic Growth Models as Reference

Dynamic growth models represent a valuable reference for the analysis and assessment of assumed growth trends (Hari et al. 1984; Mielikäinen and Timonen 1996). One major advantage is that dynamic growth models offer far more differentiated growth conditions than the yield tables. This is especially true for site, and treatment

sensitive individual-tree models, parameterised from a large, heterogeneous spectrum of long-term research plots. Within this spectrum, the model can be easily adjusted to the given stand structure and site conditions, and can be assumed to reproduce correctly "normal" growth behaviour. The use of a dynamic growth model for analysing growth disturbances is demonstrated for the Norway spruce long-term research plot Denklingen 05 (A grade) in South Bavaria. This plot was included in the comparison with yield tables in the previous section, indicating a much greater increase in height growth since the 1950s (cf. Fig. 14.1). The reference for the comparison was generated with the growth simulator SILVA 2.2 (Pretzsch 2001, 2002). SILVA 2.2 predicts the growth of pure and mixed stands in relation to site factors, competition, thinning activity, and disturbance factors (cf. Chap. 13). The application of SILVA 2.2 as reference for detecting growth disturbances is illustrated by the four different model scenarios shown in Fig. 14.2. For this purpose, the actual height growth of the dominant height was set as the 100% line (which is normally given by the reference). Scenarios 1–4 were initialised for the true stand structure in 1882, and identical thinning regimes were employed. However, each of the model runs was carried out under different growing conditions as follows.

Regarding scenarios 1 and 2 (Fig. 14.2, left), in scenario 1, the constant growing conditions prevailing at the end of the nineteenth century were assumed for the whole growing period. With this parameter set, the growth model SILVA 2.2 reconstructs the real height growth until age 110 ($\sim$1960) with surprising accuracy. For the last 40 years, from 1960 to 2000, however, the simulation increasingly underestimates the true height growth, at last by as much as 4%. In scenario 2, growing conditions were fixed to the situation in the 1980s and 1990s. The more favourable climate and increased nutrient supply result in an overestimation of height growth. Maximum height growth of 106% is reached in 1960; thereafter the simulated height

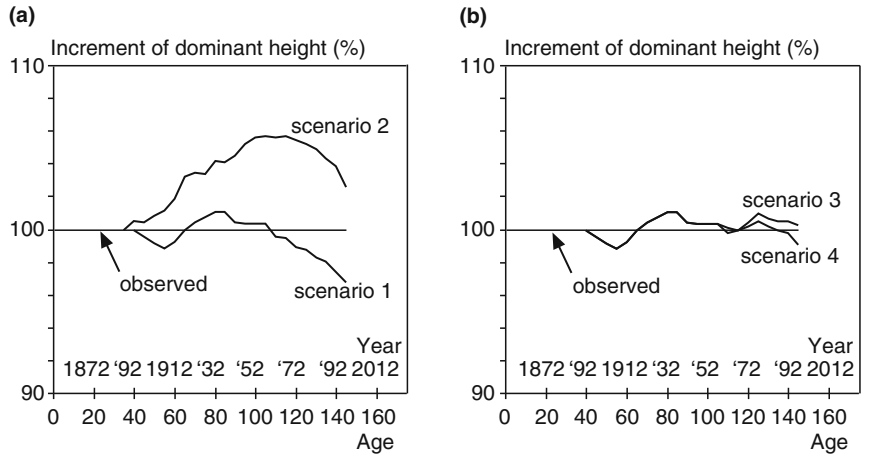

Fig. 14.2 Analysis of dominant height growth on the experimental plot Denklingen 05 (A grade) by means of the growth simulator SILVA 2.2. **(a)** Scenarios 1 and 2 imply constant site conditions for the complete growth period. **(b)** An accurate simulation of the observed dominant height growth can only be achieved via a change of nutrient supply as implemented in scenarios 3 and 4

growth approximates the true growth once again. These two, and all scenarios indicate that the last third of the growing period requires changes to the site conditions.

Regarding scenarios 3 and 4 (Fig. 14.2, right), while variation in temperature and precipitation do not bring about much difference in height growth, an increase in the nutrient supply leads to the desired convergence of the curves. The results are displayed in Fig. 14.2b, where for scenario 3 and 4 the nutrient supply was raised from 0.2 in 1880–1960 to 0.5 and 0.3, respectively, in 1960–2000 (NUT, scale from 0–1).

The example shows the advantage of the flexibility of a growth simulator. Stand structure and management for growth references could be adapted precisely to the real situation, and were thereby eliminated as possible reasons for the enhanced height growth in the last decades. This way, the reasons for this observation could be narrowed down to the profound changes in site conditions since ∼1960, whereby an enhanced nutrient supply was isolated as the most probable cause. Conclusions from such comparisons between models and reality are more reliable, the broader the validation of the model beforehand.

14.1.3 Synthetic Reference Curves

Abetz (1985) developed so-called synthetic reference curves for the increment prognosis of stands of Norway spruce, Silver fir, Douglas fir and Scots pine, managed under the future crop tree concept. These curves plot the expected radial increment at 1.3 m height vs the age, and distinguish three different levels of site fertility. The curves for MAI = 9, 12, and 15 represent site conditions where the mean annual volume increment amounts to 9, 12, and 15 $m^3\,ha^{-1}\,yr^{-1}$ on average respectively (MAI_{100} for Norway spruce, Silver fir and Scots pine, MAI_{60} for Douglas fir; MAI_{100} = mean annual volume increment till stand age 100).

The term "synthetic reference curves" refers to the normative character of their derivation. Rather than using an experimental basis as reference, Abetz defines the growth of the reference tree from certain forest economic production aims and programs (Gerecke 1986). This means the reference reflect a desired ideal path of radial increment and h/d development under a defined thinning prescription. Potential increment anomalies of certain trees are detected when comparing their actual relative radial increment to the predicted one from the corresponding reference curve (Fig. 14.3). For the radial increment development of the displayed Norway spruce tree in the upper mountainous region of the Black Forest, the synthetic reference curves (100% line) are capable of eliminating site quality and age effects. Periods of enhanced growth (e.g. 1960–1970, (+) in Fig. 14.4), and of decreased growth (e.g. 1970–1980, (−) in Fig. 14.4) are clearly pronounced.

Due to the normative character of the synthetic reference curves, the use of these curves is restricted essentially to stands managed according to the future crop tree concept, and within these stands exclusively to the radial increment of selected final crop trees. This is a major limitation of this method, especially as guidelines for forestry practise are subject to constant changes. Whether the radial increment after

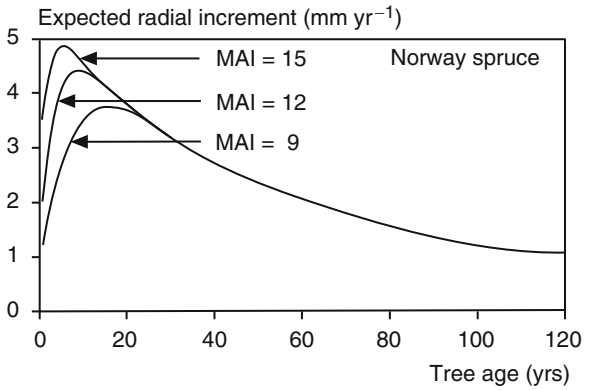

Fig. 14.3 Synthetic reference curves for predominant Norway spruce in the mean annual increment-classes MAI = 9, 12, and 15 ($m^3\,ha^{-1}\,yr^{-1}$). The expected radial growth of future crop trees at 1.3 m tree height is plotted against tree age (Abetz 1985)

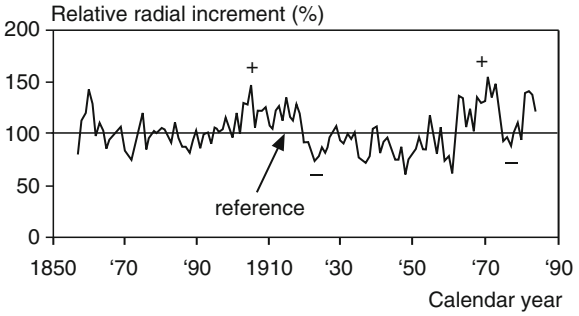

Fig. 14.4 Radial increment (in percent) of Norway spruce in the high altitudes of the Black Forest plotted against the synthetic reference increment of MAI-class 9 $m^3\,ha^{-1}\,yr^{-1}$, which was set as 100%-line. This elimination of natural age trends, clearly emphasises the phases of increment depression during the 1920s and 1970s (−), as well as phases of higher increment (+) at the beginning of the twentieth century and in the 1960s (Abetz 1985)

age 40 actually is independent of site quality which seems to contradict common empirical knowledge, should be checked carefully.

14.2 Undisturbed Trees or Stands as a Reference

14.2.1 Increment Trend Method

The increment trend method was developed to estimate increment losses of Norway spruce and Scots pine trees on long-term research plots that were affected by the forest dieback phenomenon in the 1980s (Pretzsch and Utschig 1988; Röhle 1987).

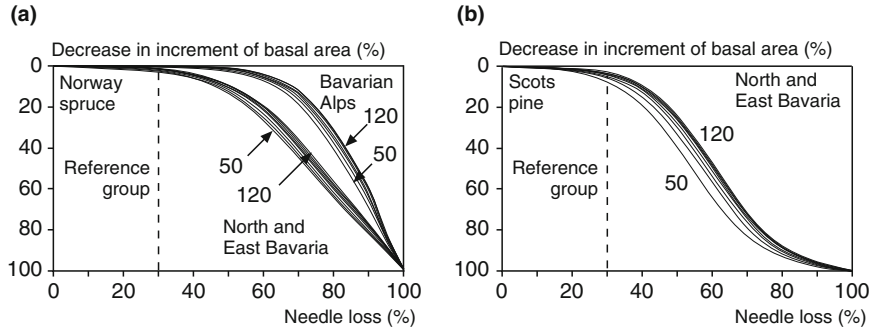

Fig. 14.5 Relationship between needle loss (in percent) and decrease in individual tree basal area increment of (**a**) Norway spruce in the regions North and East Bavaria and Bavarian Alps and (**b**) Scots pine in North and East Bavaria (Utschig 1989)

The damaged trees, identified by their degree of defoliation, were compared to healthy trees on the same plots. Hence, this method uses healthy individuals in the same stand as a reference. This has the advantage that similar site fertility can be assumed for reference and disturbed trees. Nevertheless one must ensure that the social position of the trees is comparable to avoid effects of competition in the comparison. The increment trend method has become a powerful method, and conforms to the recommendations of the Forest and Yield Science Section of the German Union of Forest Research Organisations (Deutscher Verband Forstlicher Forschungsanstalten 1988) for increment diagnoses in damaged forest stands.

Results of the application of this method are given in Fig. 14.5, showing the percentage needle loss against percentage decrease in annual basal area increment for Norway spruce and Scots pine trees. To ensure homogeneity within the sampling material, only pre-dominant and dominant trees between 50 and 120 years were considered. Needle loss was estimated in 10% steps, and increment recorded from increment cores. Norway spruce was assigned to two main growing regions, North and East Bavaria, and the Bavarian Alps (240 plots), Scots Pine to only one (North and East Bavaria, 54 plots). Clearly, below 30% needle loss, neither Norway spruce nor Scots pine reduce their basal area increment significantly (Norway spruce in the Alps up to 60%). It seems that the remaining needles can compensate for the loss in needle area through an increased efficiency of the remaining needles. Higher needle losses reduce the basal area increment and follow a dose–response function. Due to the negligible reduction in increment for needle losses up to 30%, it appears justifiable to include these trees in the reference group. Narrower defoliation limits, e.g. 10% or 20%, would leave natural variations in the defoliation due to climate, season etc. unaccounted for.

The following paragraphs explain the individual steps and calculations in the method in detail. Figure 14.6 helps through graphical visualisation. In the first step, the reference tree collectives (denoted $R_1 \ldots R_n$) and disturbed trees (denoted $A_1 \ldots A_n$) are selected, carefully watching for a similar social position. The disturbed collective may be split further into classes of different degrees of damage.

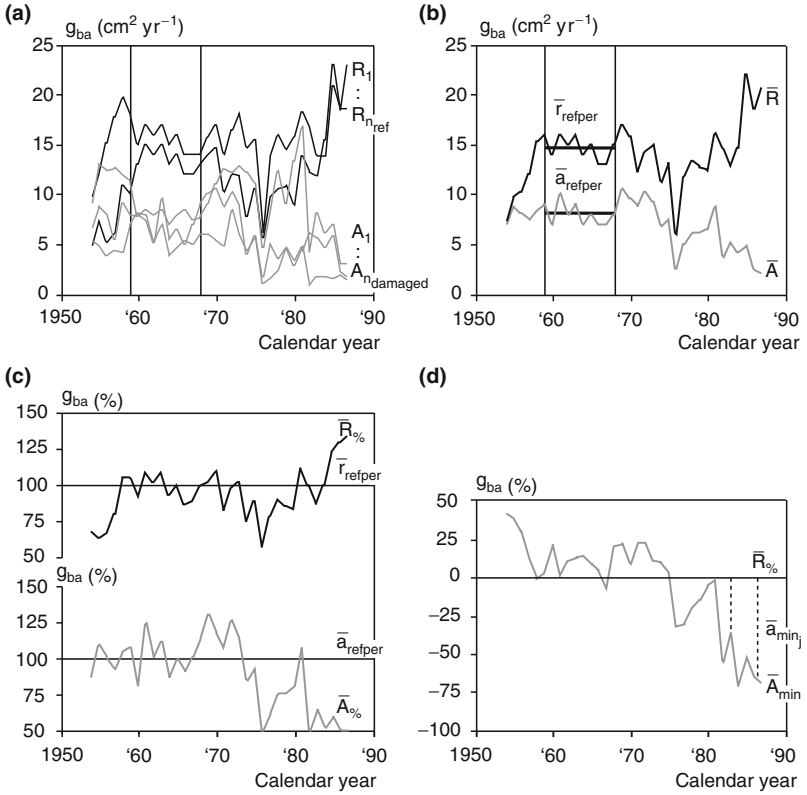

Fig. 14.6 Methodological basis of the increment trend method. (**a**) Annual basal area growth (g_{ba}) of undisturbed reference trees $R_{i,\,i=1\ldots n_{ref}}$ and supposedly damaged trees $A_{i,\,i=1\ldots n_{damaged}}$. (**b**) Calculation of mean basal area growth development $\overline{R}$ and $\overline{A}$ for the reference and damaged trees. Determination of reference period and mean growth levels $\bar{r}_{refper}$ and $\bar{a}_{refper}$ in this period. (**c**) First percentaging by setting the basal area growth development $\overline{R}$ and $\overline{A}$ in relation to $\bar{r}_{refper}$ and $\bar{a}_{refper}$, respectively. So, a priori existing differences between the collectives are eliminated. (**d**) Second percentaging by setting $\bar{A}_{\%}$ in relation to $\bar{R}_{\%}$. In this way growth losses $\bar{a}_{min\,j}$, caused by disturbance are quantified

The mean basal area growth $\bar{r}_j$ and $\bar{a}_j$ are calculated for the R and A collectives for each year j as follows (Fig. 14.6a and b):

$$\bar{r}_j = \frac{\sum_{i=1}^{n_{reference}} g_{baij}}{n_{reference}}, \tag{14.1}$$

$$\bar{a}_j = \frac{\sum_{i=1}^{n_{damaged}} g_{baij}}{n_{damaged}}. \tag{14.2}$$

The capital letters (e.g., $R_1, A_1, \bar{R}_{\%}$) represent the whole time series and small letters (e.g., $\bar{r}_j$, $\bar{a}_j$, $\bar{r}_{\%}$) the annual increment, as follows:

i	tree index within sub-group of reference trees ($i = 1 \ldots n_{reference}$) and disturbed trees ($i = 1 \ldots n_{damaged}$)
j	year index from start to end of the observation period $j = 1 \ldots m$
$\bar{r}_j$	mean basal area increment of reference trees in year j
$\bar{a}_j$	mean basal area increment of trees to be assessed in year j
g_{baij}	basal area increment of tree i in year j
$n_{reference}$	number of reference trees
$n_{damaged}$	number of damaged trees

The first step results in the two mean curves $\bar{R}$ for the reference collective and $\bar{A}$ for the trees to be assessed (Fig. 14.6b). Based on those curves, the second step compensates for differences in the increment level that might already have existed before the onset of the disturbance. The onset of the disturbance can be determined as the point where the mean increment curves $\bar{R}$ and $\bar{A}$ are no longer parallel. The preceding "reference period" serves to determine a "mean reference increment" $\bar{r}_{refper}$ and $\bar{a}_{refper}$ for both collectives (14.3). This mean increment in the reference period is then set to 100% (first percentaging), thereby overcoming the offset between both collectives (Fig. 14.4b and c). Then the whole increment curve is related to $\bar{r}_{refper}$ and $\bar{a}_{refper}$, resulting in the percentaged curves $\bar{R}_{\%}$ and $\bar{A}_{\%}$ ((14.5) and (14.6)). The mean reference increments $\bar{r}_{refper}$ and $\bar{a}_{refper}$, and the percentaged $\bar{r}_{\%}$ and $\bar{a}_{\%}$ are calculated as follows:

$$\bar{r}_{refper} = \frac{\sum_{i=1}^{n_{reference}} \sum_{j=b}^{f} g_{ba\,ij}}{per \times n_{reference}}, \tag{14.3}$$

$$\bar{a}_{refper} = \frac{\sum_{i=1}^{n_{damaged}} \sum_{j=b}^{f} g_{ba\,ij}}{per \times n_{damaged}} \tag{14.4}$$

with:

$\bar{r}_{refper}$	mean basal area increment of reference trees during reference period b…f
$\bar{a}_{refper}$	mean basal area increment of the trees to be assessed during reference period b…f
b, f	beginning and final year of reference period
per	duration of preference period in years.

$$\bar{r}_{\%\,j} = \frac{\bar{r}_j}{\bar{r}_{refper}} \times 100, \tag{14.5}$$

$$\bar{a}_{\%\,j} = \frac{\bar{a}_j}{\bar{a}_{refper}} \times 100 \tag{14.6}$$

with:

$\bar{r}_{\%j}$ increment deviation (in percent) of reference trees in year j from group-specific reference level in period b … f

$\bar{a}_{\%j}$ increment deviation (in percent) of trees to be assessed in year j from group-specific reference level in period b…f

In the third and last step, the percentaged basal area increment curves $\bar{R}_{\%}$ and $\bar{A}_{\%}$ are compared to each other (second percentaging). $\bar{R}_{\%}$ is set as the reference line at 0% (Fig. 14.6d), and the relationship of $\bar{r}_{\%j}$ and $\bar{a}_{\%j}$, denoted $\bar{a}_{minj}$, quantifies the deviation of the disturbed basal area increment from the reference (normal) increment: the deviation between the both curves $\bar{R}_{\%}$ and $\bar{A}_{min}$ shows the relative increment loss of the damaged trees:

$$\bar{a}_{minj} = \left(1 - \frac{\bar{a}_{\%j}}{\bar{r}_{\%j}}\right) \times 100 \tag{14.7}$$

with:

$\bar{a}_{minj}$ mean increment decrease of trees to be assessed in year j compared to the reference curve (0%-reference line) in percent.

The principle of the two percentaging steps is related to the reference plot method from Pollanschütz (1966) and Vinš (1961,1966) (cf. Sect. 14.2.4). The difference is that the first percentaging is made relative to a mean value while the reference plot method uses a growth function of, e.g. polynomial, exponential or hyperbolic form. The increment trend method makes use of the fact that, in most damaged stands, still some vigorous individuals can be found from which the normal, i.e. reference growth behaviour can be derived. The method implies that the differences in the increment levels during the undisturbed reference period can be assumed equally for the disturbed period of investigation. Therefore the choice of the reference period has some influence on the final result if the offset between the mean values varies.

Utschig (1989) applied this method to 960 Norway spruce trees on 48 research plots in North and East Bavaria to evaluate the increment losses due to the forest dieback in that region (Fig. 14.7). In accordance with the above-mentioned study, the results reveal no increment loss up to 39% needle loss, whereas higher needle losses lead to a increasing reduction in the basal area increment.

Note, that at the individual tree level, the increment trend method may not always prove an increment decrease. Some trees with moderate needle losses may still reach the same or even exceed the average increment of trees classified as healthy. In general, the method is well suited to detecting the onset of a disturbance, its effect over time, and the degree of increment loss in relation to the damage class. Since this method only uses relative numbers, not absolute values, it is not affected by an overall improvement or deterioration in growth conditions (Deutscher Verband Forstlicher Forschungsanstalten 1988). So, it takes into consideration Sterba's notion (1995, 1996) that an overall increase in growth may enhance competition-induced self-thinning and needle loss. Natural self-differentiation of

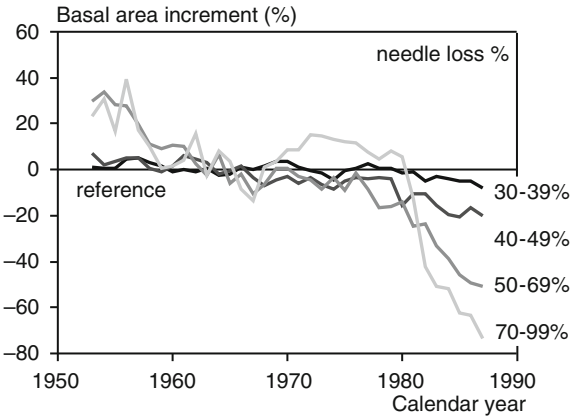

Fig. 14.7 Basal area increment diagnosis on basis of the increment trend method for individual Norway spruce trees on experimental plots in North and East Bavaria (Utschig 1989). The decrease in basal area increment is plotted for trees of defoliation levels with 30–99% needle loss

a stand, which has been described mainly for undisturbed stands, also results in a certain canopy transparency. However, this transparency should not affect the method, since the reference limit is set to 30%. Only when the healthy trees, which serve as a reference, comprise less than 25% of the stand, should the reference curve be derived from a comparable stand with better vitality.

14.2.2 Pair-Wise Comparison

The pair-wise comparison is applied to a tree of normal growth (plus-tree) and a tree of supposedly disturbed growth (minus-tree) to examine any growth response as a result of assumed disturbance factors. Minus trees can be selected explicitly on basis of visible damage (leaf shedding, crown transparency, stagnation of height increment etc.), or on basis of their proximity to disturbance sources (roadside, water withdrawals, industrial plant pollution etc.). Before damage occurs, plus and minus trees should be similar in as many attributes as possible (locality, climate, soil, age, stem and crown dimension, social position within the stand, competition pressure), except in the disturbance factor under investigation. Strictly speaking, the plus–minus tree pair should be selected before the disturbance, since it is difficult to estimate whether growth of the damaged tree would be similar to the undamaged tree in reality.

Without sufficient repetition, pair-wise comparisons are not sufficient for making statistically reliable statements about the increment response due to the disturbance. Rather, they should be regarded as a sounding board for more profound studies. The exemplary character, however, allows for more refined analyses of roots, stem and foliage that could not be carried out at large scales. Increment losses can be

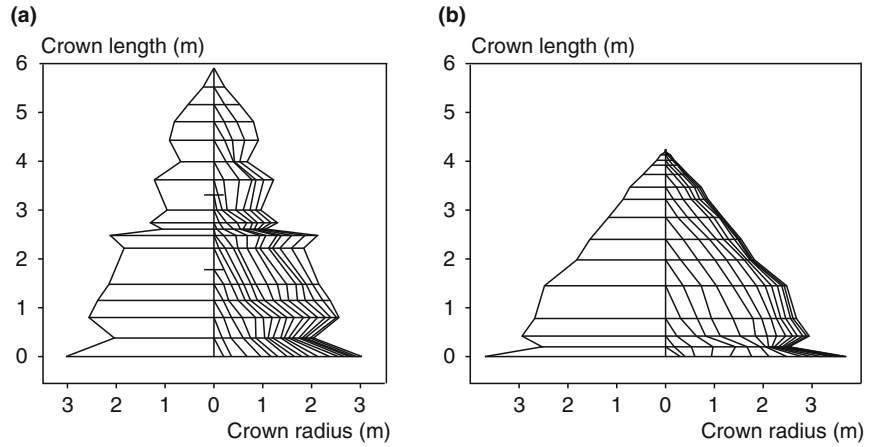

Fig. 14.8 Diagnosis of crown damages of Scots pine by pair-wise comparison (Pretzsch 1989a) in the forestry district Bodenwöhr in East Bavaria. Crown profiles are plotted for (**a**) an undamaged Scots pine and (**b**) a Scots pine growing on the same site but with stagnating shoot growth

calculated similarly to the increment trend method (Sect. 14.2.1). If only one pair of trees is chosen, $n_{reference}$ and $n_{damaged}$ in (14.1) to (14.4) simplify become 1.0.

The growth and yield analyses of forest damage from Franz (1983), Pretzsch (1989a,b), Röhle (1987) and Sterba (1984, 1989b) made use of pair-wise comparisons in the initial phase. This method proved equally useful for the variables investigated, including missing year rings, stem form, crown morphology, or foliage mass. Figure 14.8 shows results from the pair-wise comparison of crown-damaged Scots pine trees in the forest district Bodenwöhr, East Bavaria. Each horizontal line in the crown corresponds to the shoot growth of 1 year (including the short ones). The vertical diagonal lines indicate the horizontal growth of the branches per year. Clearly, both the shoot and branch growth in the disturbed tree in Fig. 14.8b stalls for 5–6 years as a result of calcium-chlorosis.

14.2.3 Reference Plot Comparison

In the reference plot comparisons, supposed disturbed stands are compared to neighbouring supposedly undisturbed reference stands. This method does not differ essentially from the two previous methods, except that whole stands are investigated instead of single trees. An investigation of the increment loss of Scots pine stands in the vicinity of the brown coal power plant Schwandorf in East Bavaria (Franz and Pretzsch 1988) provides an example. As in the previous two methods, also in the reference plot comparison, one needs to ensure that tree species composition, stand age, site fertility and silvicultural treatment are comparable in reference and disturbed stands.

To investigate the effects of location of the stands (factor 1) and time (factor 2) on the growth behaviour of Scots pine stands in the vicinity of a brown coal power plant 103 sample plots were established (Franz and Pretzsch 1988; Pretzsch 1989b). Emitting 20–40 tons of SO_2 per hour this power plant was among the most severe air pollution sources in Bavaria throughout the period 1960s–1980s. By arranging the study plots in concentric circles of 5, 15 and 30 km around the power plant, the effect of location (factor 1) on growth in the surrounding Scots pine stands could be tested. On the inner circle (5 km radius), 23 sample plots are located. On the middle (15 km) and outer (30 km) circles, there were 33 and 47 plots respectively (Fig. 14.9).

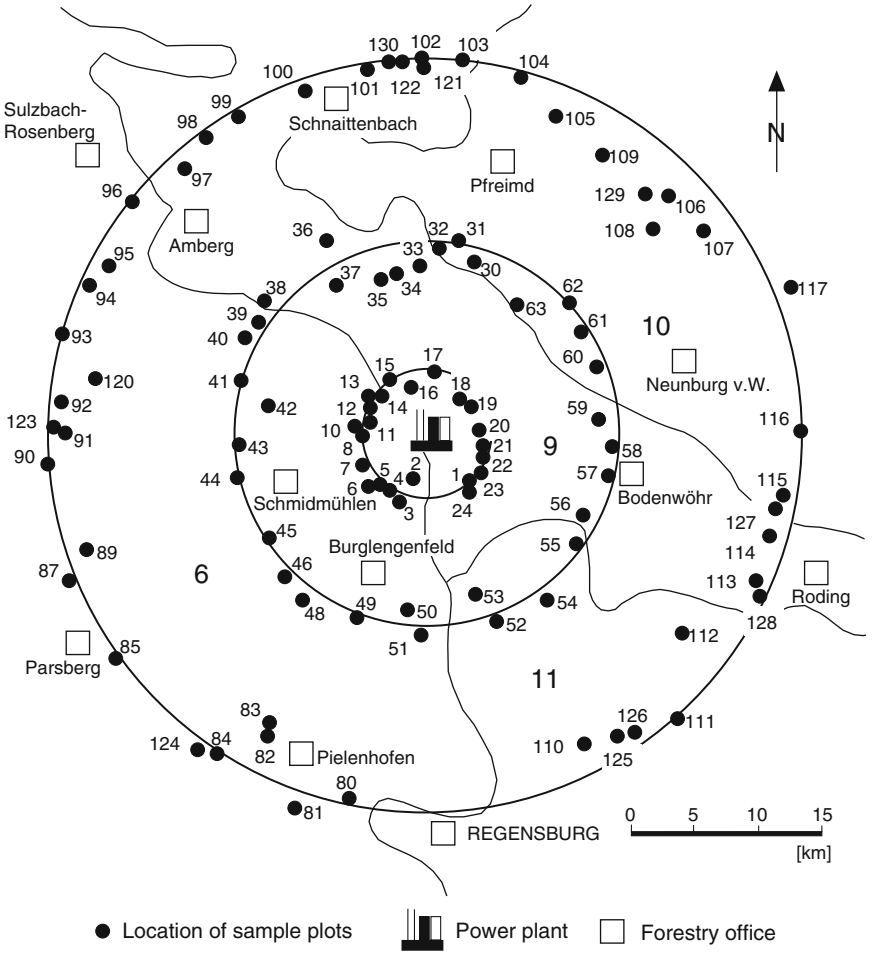

Fig. 14.9 Establishment of Scots pine sample plots in the vicinity of a brown coal power plant at Schwandorf (Pretzsch 1989b). A total of 103 sample plots are located on three concentric rings in a distance of 5, 15, and 30 km around the power station. In addition, the area was divided in four quadrants representing the directions N, E, S and W; the plots were assign to those quadrants. Increment cores dating back at least 40 years were taken from 20 dominant trees per plot

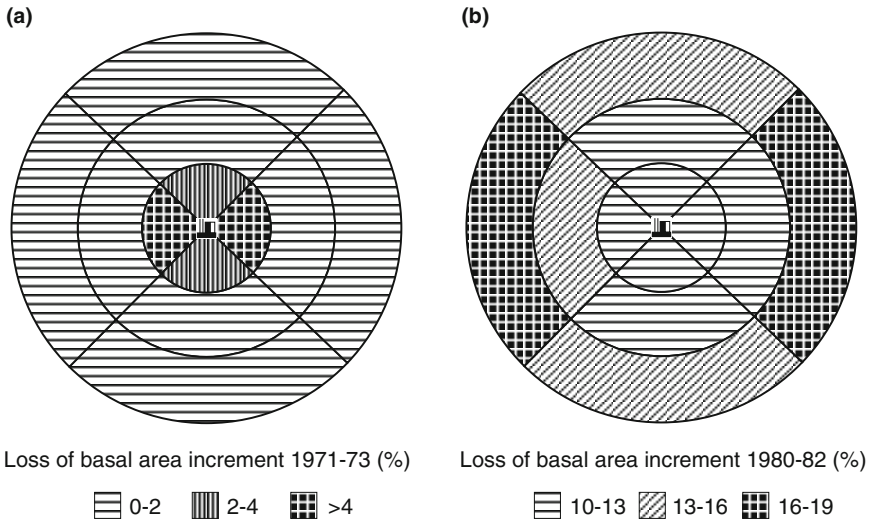

Fig. 14.10 Spatial–temporal patterns of losses in stand basal area growth (%) in the Scots pine stands around the power plant before (**a**) and after (**b**) the conversion to 235 m high chimneys. The synchronous occurrence of the impact of pollutants from the power plant and the growth of Scots pine enable conclusions to be drawn about the cause and extent of damage (Pretzsch 1989b)

To test the influence of typical emissions development over time (factor 2) on growth behaviour increment cores dating back at least 40 years were taken from 20 dominant trees per plot. All sample plots are set up in normally stocked early mature Scots pine stands with moderate site fertility. For each sample plot, statements about the continuous annual increment of the stand in the previous 40-year-period can be obtained.

In a first statistical analysis, the sample plots were grouped according to their distance from the power plant and direction. All plots were assigned to 3 distances levels (5, 10, 15 km) and 4 directions (N, E, S and W), producing 12 groups: distance 5 km, 1st quadrant, distance 5 km, 2nd quadrant... distance 30 km, 4th quadrant (cf. Figs. 14.9 and 14.10). The periodic annual stand basal area increment was modelled by a simple linear relation:

$$g_{ij} = \mu + \alpha_j + \varepsilon_{ij} \tag{14.8}$$

with:

g_{ij} periodical annual stand basal area growth ($m^2\ ha^{-1}\ yr^{-1}$) in sample stand i in location j
μ mean basal area growth ($m^2\ ha^{-1}\ yr^{-1}$) of all sample plots
α_j deviation of plot i from total mean, caused by the location j of the plot
ε_{ij} error term

The univariate analysis of variance can be applied for testing the null hypothesis H_0 that the growth is the same in all k = 12 location groups, i.e. $\alpha_1 = \alpha_2 = \ldots = \alpha_k$, vs H_1, which means that at least two groups differ in growth. For a closer analysis of the group differences, multiple mean value comparisons of Scheffé (1953) and Tukey (1977) can be applied. The univariate ANOVA provides statistically significant results about whether possible growth disturbances can be attributed to the proximity of the pollution source.

If there are a priori differences between the sampled stands, e.g. in terms of stand density or site fertility, these must be eliminated from the analysis. The covariance analysis is an appropriate tool. To take such a priori effects into consideration we can extend (14.9) as follows:

$$g_{ij} = \mu_g + \alpha_j + \beta_j \times \left(x_{ij} - \mu_x\right) + \varepsilon_{ij} \tag{14.9}$$

with:

μ_g mean stand basal area growth ($m^2\ ha^{-1}\ yr^{-1}$) of all sample stands
β_j regression coefficient, which quantifies the effect of covariable x on growth at location j
x_{ij} value of covariable for plot i at location j
μ_x overall mean of covariable

By using a covariable x, a priori differences between the mean class values are eliminated (Bortz 1993; Pruscha 1989). Possible covariables include stem number, basal area, stem volume, site index or stand age. Especially in larger investigations, these stand parameters are rarely equal for all plots, and hence must be considered in the analysis.

To analyse both the spatial and temporal effects of pollution from the power plant on the growth of the Scots pine stands in the vicinity, two factors can be integrated in the model: the factor location with 12 factor levels, as in (14.7), and the factor time. For this purpose, we divided the period of time covered by the increment boring into 3 year periods. Thus, the factor time is represented by the levels 1980–1982, 1977–1979 etc. The model is extended as follows:

$$g_{ijk} = \mu + \alpha_j + \gamma_k + \omega_{jk} + \varepsilon_{ijk} \tag{14.10}$$

with:

g_{ijk} periodical annual basal area growth ($m^2\ ha^{-1}\ yr^{-1}$) in sample stand i in location j in time period k
μ mean basal area growth ($m^2\ ha^{-1}\ yr^{-1}$) of all sample plots over all periods
α_j effect of location j on growth
γ_k effect of period of time on growth
ω_{jk} interaction between spatial and temporal effects
ε_{ijk} error term

The two factorial analysis of variance checks, first of all, whether all α and all γ are zero, or whether at least one α or γ is not equal to zero. Moreover, the test shows whether interactions between location and period of time ω_{jk} are equal to zero for all j and k, or whether at least one ω_{jk} is not equal to zero. By means of this analysis, temporal and spatial patterns of increment reactions are revealed which can become important evidence for effect of a point air pollution source on a surrounding forest area.

In our example, the two-factorial analysis of variance for the evaluation of the impact of the brown coal power plant Schwandorf on the stand basal area growth of Scots Pine stands leads to the following results (Franz and Pretzsch 1988): during the 40-year-period analysed, the increment is significantly lower in Western and Eastern direction than in the Southern and Northern direction of the plant, which corresponds to the main wind directions. At the beginning of the investigation period, the chimney was lower, and the contamination, and hence, the increment loss was highest in the immediate vicinity (cf. Fig. 14.10a). After 10–15 years, after raising the chimney, the increment behaviour was reversed. Then the increment losses indicated a higher contamination further away from the power plant (Fig. 14.10b). This close correlation in time and space between the SO_2 pollution and the increment behaviour provides evidence in support of the assumption that the brown coal plant is responsible for the Scots pine increment loss.

Finally, for more background on the statistical methodology, the textbooks of Bortz (1993), Rasch et al. (1973) and Weber (1980) are recommended, for multiple mean value comparisons see also Scheffé (1953) and Tukey (1977). The data processing and statistical analysis is facilitated by statistics software packages such as R, BMDP, SAS, SPSS or SYSDAT. Examples of the successful application of this method are found in the diagnosis of increment losses due to the lowering of the groundwater table through water withdrawals, straightening of riverbeds or canal constructions (Altherr and Zundel 1966; Altherr 1969, 1972; Pretzsch and Kölbel 1988; Preuhsler 1990), the verification of growth responses to stand opening up for road construction (Preuhsler 1987), and the analysis of increment losses in the vicinity of a point-source of contamination (Franz and Pretzsch 1988).

14.2.4 Reference Plot Comparison by Indexing

The methodology of the reference plot comparison by indexing is similar to the increment trend method. However, instead of laying mean values through the basal area growth curve a growth function is applied. This makes the method more flexible, and permits the inclusion of more heterogeneous collective of trees with individual growth patterns. The reference plot comparison by indexing was developed by Vinš (1961) to quantify increment decreases in the vicinity of point sources of pollution in former Czechoslovakia. It was applied successfully, and refined further by Vinš (1961, 1966), Vinš and Mrkva (1972), Pollanschütz (1966, 1967, 1980) and Neumann and Schieler (1981). This method was recommended in the presence of

undisturbed reference plots, a clearly defined disturbance period of 5–15 years, a previous 40 year reference period without disturbance.

The experimental design is also very similar to the methods discussed previously. A sufficient number of undisturbed and disturbed stands is chosen in the vicinity of the pollution source for which the basal area increment is calculated on the basis of increment core samples. The samples should originate from the predominant and dominant tree layer to exclude growth suppression caused by competition. However, unlike the former methods, the stands included may differ in age or site fertility. Figure 14.11a shows courses of radial increment from two stands, from undisturbed reference plots above, and disturbed plots below. The next step is to determine the specific growth behaviour for each stand via a regression with certain growth equations. Vinš (1961) and Pollanschütz (1967) recommended a set of four growth equations:

$$g_t = a_0 \times t^{a_1}, \tag{14.11}$$

$$g_t = a_0 \times t^{a_1} \times a_2^t, \tag{14.12}$$

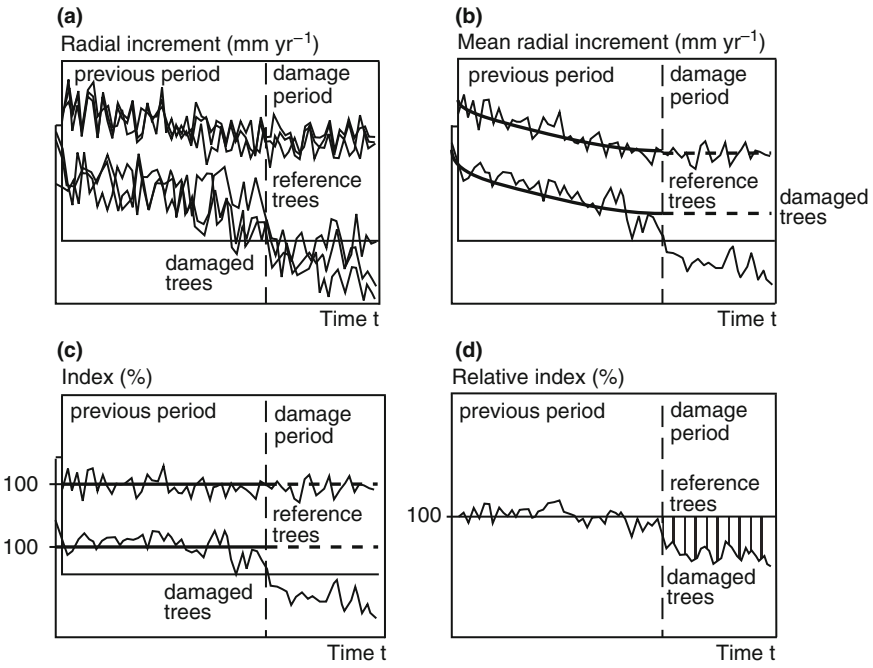

Fig. 14.11 Overview of the reference plot comparison by indexing. **(a)** Radial increment of individual trees is collected from undisturbed reference plots and one or more disturbed stands. **(b)** Radial increment development is averaged stand-wise, and the records from the previous period without damages are modelled by a regression function. **(c)** Deviations of the observed mean radial increment from the regression function, which is set to 100%. **(d)** Calculation of the loss in percentage radial increment in by relating the indexed radial increment of the disturbed stands to the one of the reference plots (100%-reference line)

$$g_t = a_0 + a_1 \times \frac{1}{t}, \tag{14.13}$$

$$g_t = a_0 + a_1 \times t + a_2 \times \frac{1}{t} \tag{14.14}$$

where g_t = radial growth in year t, t = time, and a_0, a_1, a_2 = regression coefficients.

The flexibility of the growth equations, instead of the fixed mean value, that makes this method adaptable to the differences in the growth behaviour in various age classes and site fertilities. To avoid effects arising from the disturbance investigated, only the undisturbed reference period is used to fit the curve (Fig. 14.11b, solid line). Then, a first percentaging is carried out. The actual increment is scaled relative to the growth function, which represents 100% (Fig. 14.11c). At this point, the deviations can be averaged for a certain collective of trees in the stands. Finally, the relative differences between reference and disturbed trees are calculated for the whole stand. Here, the reference is set to 100%, and, except for the effect of the disturbance to be assessed, the periodic deviations caused by climate and other variations are eliminated (Fig. 14.11d).

Although the method can include different stand ages and site fertilities, attention has to be paid to the thinning cycles. Yet, different treatments, especially strong thinnings to boost the increment, are not only difficult to adapt with a growth function, but, more problematic, they introduce a second "disturbance" factor apart from the one investigated. In this way, if one is not wary, the assessment may lead to the opposite conclusion. Here, the method was only shown for two stands in Fig. 14.11, comprising one reference and one disturbed stand. In the study by Vinš (1961, 1966), Vinš and Mrkva (1972) and others, more disturbance classes were differentiated using the distance to the pollution source as a grouping criterion. The example in Fig. 14.12 shows the growth reduction of Scots pine in the vicinity of a fertiliser factory. Beginning in the mid 1960s the basal area increment was reduced by as much as 70% for the stands closest to the factory.

Pollanschütz (1975) completes the method with a test of statistical significance for the increment differences between the reference and the disturbed trees. Depending on the strength of the radial increment loss, different methods should be used for the determination of tree- and area-based decreases in basal area and volume increment (Pollanschütz 1966). Neumann and Schieler (1981) modify the procedure by employing the growth regression based on the tree, and not the stand average. They conclude that both the original (Vinš 1961) and modified procedure achieve similar and stable results given that the disturbance period can be dated clearly, the disturbed period is not too long (10 years), the reference period is long enough for a reliable regression (at least 40 years), and the collectives are represented by a sufficient number of increment core analyses.

14.2.5 Regression–Analytical Estimation of Increment Decrease

A priori differences between disturbed and reference trees or stands in the increment trend method, pair-wise comparison and reference plot comparisons were

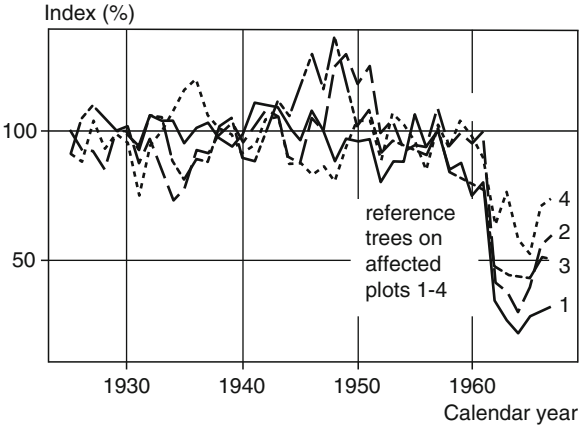

Fig. 14.12 Mean year ring index curves of trees from an undisturbed experimental plot (reference plot) and trees from plots with different levels of disturbance. Experimental plots 1, 2, 3, 4, and the reference plot are located at 500, 750, 1,250, 2,050 and 5,000 m distance from a pollution point source (a fertiliser factory). In comparison with the undisturbed reference plot (100%-reference line), the radial growth in the factory's close vicinity decreased to 30% of the normal increment (Vinš and Mrkva 1972)

eliminated via percentaging and/or indexing. In a regressions–analysis, these differences are excluded with the help of covariables, which are unrelated to the disturbance (Kramer and Dong 1985; Kramer et al. 1985). Three such methods are introduced in this chapter.

14.2.5.1 Crown Surface as Covariable

This approach was applied by Kramer (1986) and Dong and Kramer (1987) to quantify the effect of needle loss on the annual volume growth (g_v) of Norway spruce in the coastal region of Lower Saxony, and in the Harz mountains in Northern Germany. Since a broad spectrum of undisturbed and disturbed trees was included, it was necessary to consider natural increment differences due to age and crown size. For age, the collective was stratified into age classes, the crown size was accounted for by employing a regression model of the following form:

$$g_v/\text{crown surface area} = a_0 + a_1 \times \text{needle loss}, \tag{14.15}$$

$$g_v = b_0 + b_1 \times \text{needle loss} + b_2 \times \text{crown surface area}, \tag{14.16}$$

where a and b represent regression coefficients. Figure 14.13a shows the regression–analytical relationship between volume growth per crown surface and needle loss for the five age classes employed (Dong and Kramer 1987). The effect of crown size on volume increment is taken into consideration by scaling volume increment relative

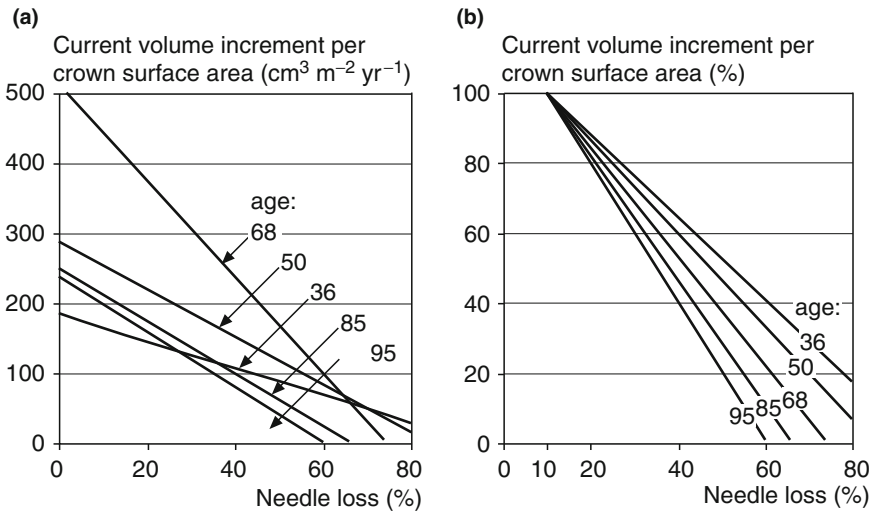

Fig. 14.13 Regression–analytical estimation of increment decrease in damaged Norway spruce stands in the coastal region of Lower Saxony and the Harz mountains (Northern Germany). **(a)** Relationship between current annual volume increment (cm^3 per m^2 crown surface area and year according to (14.15)) and needle loss in percent. **(b)** Calculated relationship between relative volume loss in relation to needle loss (Dong and Kramer 1987)

to crown surface. Then, to facilitate the comparison of the age classes, the absolute increment values are converted to relative increments by setting the growth of the collective with 10% needle loss to 100% (Fig. 14.13b).

One constraint of this method is the fact that crown surface is only one of several factors determining volume increment. Therefore, Dong et al. (1989) recommend including further tree and stand parameters in the regression model ((14.15) and (14.16)). Further criticisms of the this regression–analytical approach include the low reference level at 10% needle loss (Spelsberg 1987), a sometimes poor fit of the regression (Kramer 1986), indications of a rather sigmoidal relationship between needle loss and increment reduction (Pretzsch 1989a; Utschig 1989), and the difficulty in measuring and calculating the exact crown surface.

14.2.5.2 Increment in Previous Period as Covariable

Using the increment in a previous, undisturbed period as a covariable was originally applied by Sterba (1970, 1973, 1978) and Krapfenbauer et al. (1975) for the statistical analysis of fertilisation experiments, yet it is equally applicable for the analysis of growth disturbances with negative impacts on stand and tree growth. As displayed in Fig. 14.14, the growth (gd) in a presumed damage period is presented against the growth (gp) in a certain preceding period. Next, a linear regression is carried out for

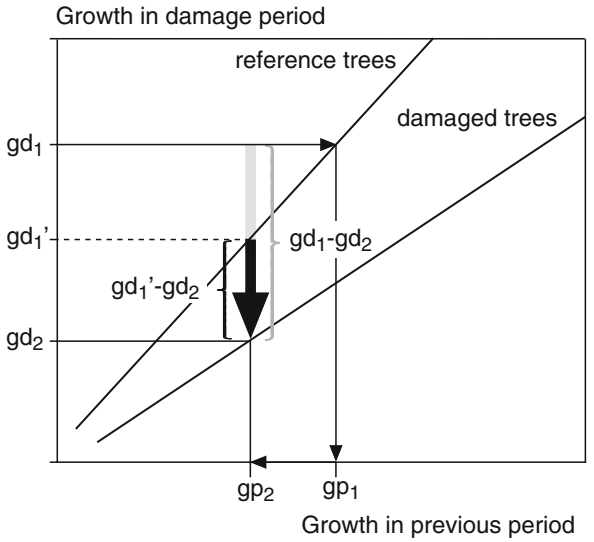

Fig. 14.14 Adjustment of growth differences between undamaged and damaged trees by taking into account size and growth differences already existing in the previous period (Sterba 1970). Straight lines (*grey*) represent the relationship between growth in the damage, and previous period for both the group of reference and damaged trees. By applying gd_1' rather than gd_1 as a reference for undisturbed growth, the method eliminates a priori existing superiority of tree 1 in the previous period. Unadjusted (*grey arrow*) and adjusted (*black arrow*) difference in the growth between the undamaged tree 1 and the damaged tree 2

the undisturbed trees (reference) and the disturbed tree collective. Then, the vertical offset between the two regressions indicates the average difference in increment in the investigation period as a function of the increment in the previous period. A direct comparison between the increment of an undamaged tree gd_1 and a damaged tree gd_2 would attribute the total difference in increment gd_1–gd_2 (Fig. 14.14, long grey vertical arrow) to the disturbance. This ignores that fact that the undamaged tree 1 was growing faster than tree 2 already in the previous period before the damage occurred. The true difference is approximated as the distance gd_1' – gd_2 (Fig. 14.14, short black vertical arrow). This difference takes into account the superiority of tree 1 over tree 2 already in the pervious period. This superiority is eliminated by applying gd_1' as a more appropriate reference, and reading the loss due to damage as gd_1' – gd_2 above gp_2 off the abscissa.

14.2.5.3 Multiple Tree and Stand Attributes as Covariables

An elegant mathematical method for the estimation of increment decreases was developed by Ďurský (1993, 1994), Ďurský (1994) and Šmelko et al. (1996). They include a number of factors influencing growth, such as the disturbance in a multiple regression, and thereby separate the impact of each factor. In the first step, the

relative growth $g_{rel\,obs}$ of each tree is calculated as the quotient between growth in a disturbed, and an undisturbed reference period:

$$g_{rel\,obs} = \frac{g_{damaged}}{g_{ref}} \tag{14.17}$$

In a second step, the trees sampled are stratified according to their social position (predominant or dominant trees). Then, for each stratum, a functional relation between the relative increment $g_{rel\,obs}$ and a defined set of growth determining factors (crown length, tree diameter, competition, needle loss) is formulated. Ďurský (1993, 1994), who based his study on the periodical basal area increment, employed the following model:

$$g_{rel\,pred} = a_0 + (a_1 + a_2 \times CL) \times NL + a_3 \times NL^2 + a_4 \times (NL/CL) + a_5 \times DBH + a_6 \times CS + \varepsilon \tag{14.18}$$

where CL = crown length, NL = needle loss, DBH = diameter at breast height, CS = competition, $a_0 \ldots a_6$ = regression coefficients, and ε = error.

In the third and final step, the observed increment $g_{rel\,obs}$ is compared to the undisturbed increment $g_{rel\,pred}$ predicted by the model. This is done by estimating the growth of trees with the same crown length, diameter and competition index as the investigated ones, but with only 20% needle loss. The resulting relative increment loss is then

$$\text{increment loss} = 1 - \frac{g_{rel\,obs}}{g_{rel\,pred}} \tag{14.19}$$

Compared to the regression–analytical approach from Dong and Kramer (1987), which only uses crown surface as a covariable, this method can account for differences in the tree collective in a much more detailed way.

14.3 Growth Behaviour in Other Calendar Periods as Reference

14.3.1 Individual Growth in Previous Period as Reference

In this method, a certain (typically early) part of the total observed growth period of a tree or a stand serves as the reference period for the diagnosis and quantification of increment changes in other (typically successive) periods. Röhle (1987) analysed increment changes of Norway spruce stands in Bavaria in the period 1959–1983 due to needle loss. He chose the years 1959–1968 as the reference period for which he assumed a "normal and undisturbed" increment (Fig. 14.15). Then, he expressed the volume growth after 1968 as a percentage of the reference period's mean increment. This way he diagnosed an increment decrease up to 75% of the reference increment in a 120-year-old Norway spruce stand with 35% needle loss. As his results are strongly dependent on the choice of the reference period, and as the natural dependency of the increment on age is not considered, at best this method may serve

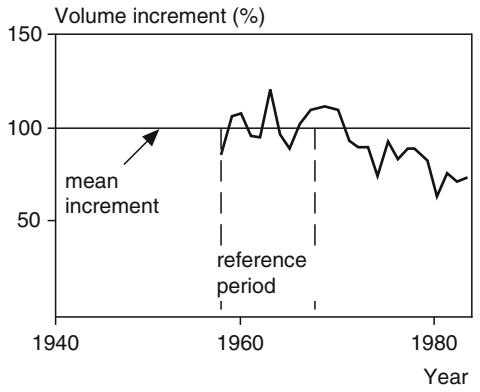

Fig. 14.15 Quantification of increment decreases in a 120-year-old Norway spruce stand in the Fichtel mountains (Northeast Bavaria) with a mean needle loss of 35%. Volume increment after 1968 is related to the mean increment within the reference period from 1959–1968 (Röhle 1987, p. 50)

as a first indication of increment changes arising from a given disturbance. If the reference period covers, for instance, a favourable climate period or the age-related phase of increment culmination, increment decreases would be overestimated considerably.

It seems that the comparison of increment between a previous (reference) and a subsequent period is better suited to uncovering abrupt increment changes (Bachmann 1988; Schweingruber et al. 1983, 1986; Utschig 1989). For the diagnosis of such abrupt increment reduction or regeneration, a time frame of 10 years is shifted along the time series of increment records in the observation period. The increment of the first 5 years of the time frame $t-5 \ldots t-1$ is now set as the reference for the increment in the subsequent 5-year-period $t \ldots t+4$:

$$p_t = \frac{g_t + g_{t+1} + \ldots + g_{t+4}}{g_{t-5} + g_{t-4} + \ldots + g_{t-1}} \times 100, \tag{14.20}$$

where p_t quantifies (in percent) the average change in increment in a given 5-year-period relative to the previous 5-year-period.

Next, a lower and upper threshold is chosen for the definition of an abrupt increment reduction and regeneration. Kontic et al. (1986), for example, distinguish between an abrupt loss of increment in year t when $p_t < 60\%$ (increment loss of 40%), and assume an abrupt increase or regeneration when $p_t > 166\%$ (increment acceleration of 66%). Of course, one can further distinguish different levels of growth reduction or regeneration, by defining various thresholds, or identifying specific patterns of reduction and regeneration years (Fig. 14.16).

Using this method, Bachmann (1988) found that the number of abrupt increment reductions increased dramatically from the mid-1970s compared to the previous decades (Fig. 14.17). He implemented a time frame of 8 years, and thresholds of

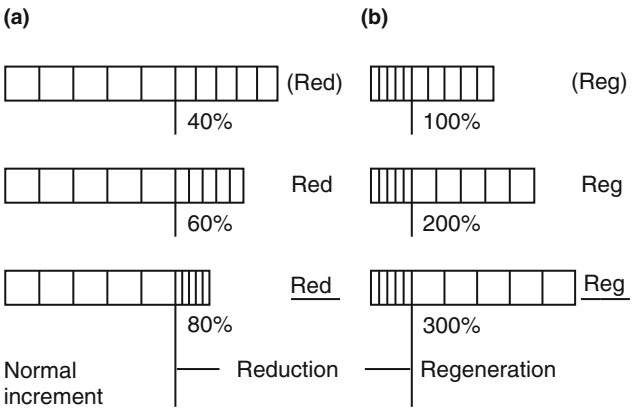

Fig. 14.16 Tree ring patterns in schematic representation with **(a)** abrupt increment reductions of 40, 60 and 80%, and **(b)** regeneration coupled with an increment increase of 100, 200 and 300% (Kontic et al. 1986)

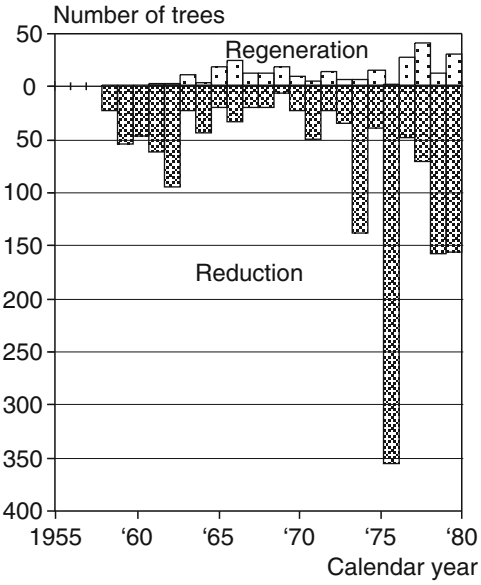

Fig. 14.17 Abrupt increment changes on Norway spruce experimental plots in Bavaria according to Bachmann (1988). In the period from 1958 to 1980, 32% of a total of 3,433 sample trees show abrupt increment reduction (*grey bars*) or regeneration (*white bars*)

60% and 150% for the detection of losses and regeneration, respectively. By studying the annual ring pattern from 1958 to 1980 of altogether 3,433 Norway spruce trees in Bavaria, he found abrupt increment changes in 1,093 individuals (32%), the majority of which occurred after the 1970s. This increase indicates an increasing oscillation in growth curves since the 1970s.

14.3.2 Long-Term, Age-Specific Tree Growth as Reference (Constant Age Method)

This method quantifies changes in the age-specific growth behaviour in a certain calendar period. It was applied, e.g. by Bert and Becker (1990), Mielikäinen and Timonen (1996), and Mielikäinen and Nöjd (1996).

The example introduced here (Pretzsch and Utschig 2000) is based on Norway spruce data from Southern Bavaria between 1902 and 1995 (Fig. 14.18a). The dataset was divided into four age classes (20–29, 30–39, 40–49, and 50–59 years) in calendar years (Fig. 14.18b), and the diameter increment of each age class was plotted against the calendar year (Fig. 14.18c). In this way, changes in growth behaviour can be dated, quantified and differentiated according to age classes.

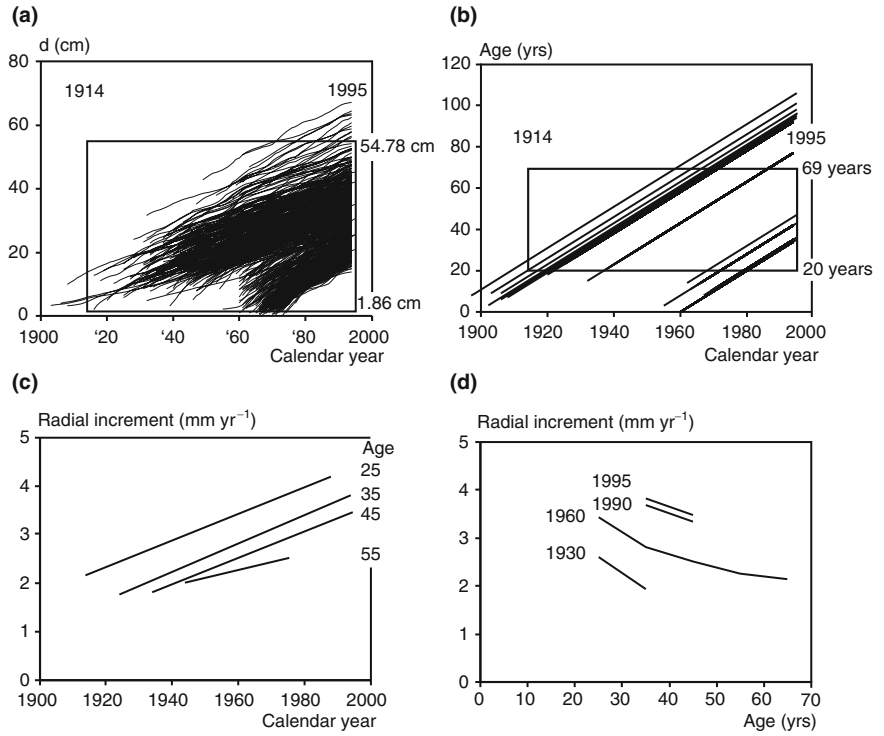

Fig. 14.18 Constant age method applied for diameter growth of Norway spruce on the experimental trial plot Freising 813/1–6. **(a)** The window inside the plot shows the diameter range and the calendar years, which were included in the trend analysis. The analysis includes increment values from the calendar years 1914–1995 and stem diameters from 1.86 to 54.78 cm. **(b)** For this growth period, the stands range in age from 20 to 69 years, which is divided four age classes of 10 years each. **(c)** Radial increment of the four age classes plotted on a calendar axis. In younger stands the increment increase is more pronounced than in older stands. **(d)** Radial increment for selected calendar years. For the time period 1930–1995 we observe a considerable increase and shift of the radial increment

Again, the evaluation was based on the diameter growth at breast height, which can be obtained from increment cores or stem disks. Since diameter growth depends on site conditions and stand density, and is very sensitive to competition, similar site conditions and management strategies are needed, and only dominant trees should be included in the analysis. Further more, it is important that the age classes are represented by sufficiently large, balanced tree collectives in each period. This means, the mean age within an age class should be equal in the different calendar periods.

The result of linear regression in Fig. 14.18c shows a steady increase in the diameter growth of each age class from the beginning of the observation period till the present. For example, while in 1920, 25-year-old Norway spruce trees grew on average $2.2\,\mathrm{mm\,yr^{-1}}$ in diameter, in 1995 they grew $4\,\mathrm{mm\,yr^{-1}}$. Plotted on an age axis, Fig. 14.18d shows the rise in increment between 1930 and 1995. In the light of both the strength and persistence of the growth increase, it is unlikely that this growth is caused by stand establishment or treatment, particularly as the observed stands have been treated conservatively until today. Rather the cause of the growth increase may be found in the rising temperature, nitrogen input and atmospheric CO_2 concentration.

14.3.3 Growth Comparison of Previous and Subsequent Generation at the Same Site

A growth comparison between previous and subsequent stands at the same site can diagnose long-term changes in the growth behaviour over two stand generations (Kenk et al. 1991; Röhle 1994, 1997; Wiedemann 1923). It is clear that the analysis over such a large time span requires an exceptionally large database with consistent surveys of the present and previous generation, which might easily date back 200 years. Few long-term experimental plots provide such valuable databases. The comparison can be carried out for diameter, height, basal area and volume, of which height is especially useful as it remains almost unaffected by stand silvicultural treatment.

In an early study, Wiedemann (1923) detected an impeded height growth of Norway spruce in Saxony (Germany), which he attributed to unsustainable forest management and climatic effects. Comparing the height growth behaviour between stands established in 1700–1730 with the subsequent generation established in 1825–1845, he proved a degradation in the site fertility by two levels of Schwappachs's (1890) yield tables for Norway spruce (Fig. 14.19).

More recently, Kenk et al. (1991) detected a growth improvement of up to seven site index levels of the Assmann and Franz yield tables (1963) for Norway spruce for stands with poor to medium site fertility in Baden-Württemberg (Fig. 14.20). The time span between the establishment of the previous stands (1820) and the subsequent stands (1950) was – similar to Wiedemann (1923) – approximately 130 years.

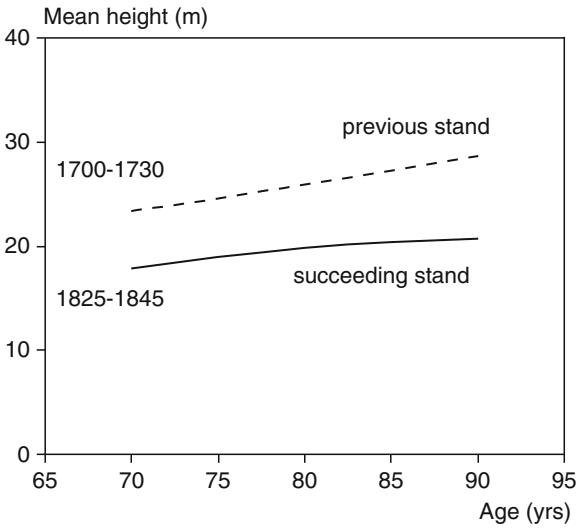

Fig. 14.19 Detection of static growth of Norway spruce in the Forest near Tharandt (East Germany) by comparison of previous and subsequent forest stands (Wiedemann 1923, p. 157, Tab. 1). Mean height of forest stands established between 1700–1730 (*dashed line*) and the subsequent stands between 1825–1845 (*continuous line*)

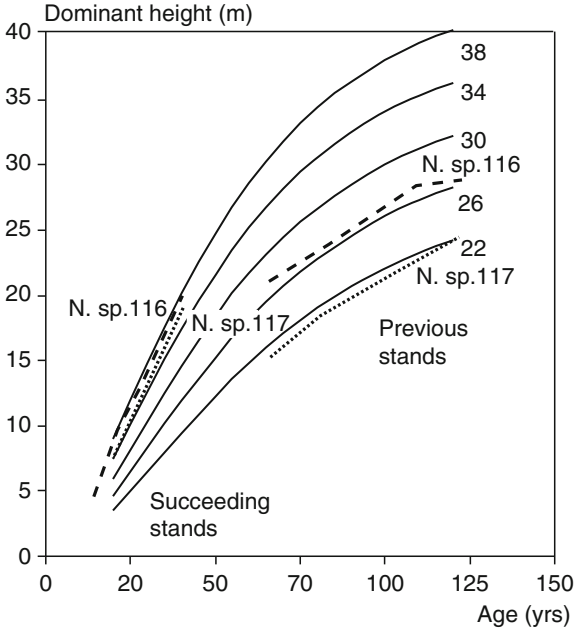

Fig. 14.20 Comparison of height development of previous and subsequent generation on the Norway spruce (N. sp.) experimental trial plots N. sp. 116 and N. sp. 117 in the Black Forest (Kenk et al. 1991, p. 30, Fig. 14). The comparison reveals a growth improvement of several site classes (from $h_{100} = 22–26$ m to $h_{100} = 34–38$ m) according to the yield table from Assmann and Franz (1963)

The growth comparison of two successive generations on the same site can prove the existence of a disturbance, and the time and strength of its effect. Although the underlying causes are not determined this way, uncertainties about site comparability, present in the reference plot comparison, for instance, can be excluded. Furthermore, provided the stand treatment (e.g. A, B, or C grade thinning), and the genetic composition (establishment through natural regeneration or by sowing seeds of the previous stands) is similar, then effects due to treatment and genetics can be assumed negligible. In a strict sense, though, the seed from the previous stand used for establishment of the subsequent stand originate from the collective of the individuals that survived self-differentiation, thinning and calamities, and therefore the subsequent stands represent only a fraction of the previous stand's gene pool.

14.3.4 Diagnosis of Growth Trends from Succeeding Inventories

In contrast to the methods presented so far, repeated forest inventories at national, state or enterprise level provide statistically reliable information by area for volume growth and yield. With their long tradition of forest inventories, Scandinavian countries have access to the large database necessary for the analysis of long-term growth trends. Kauppi et al. (1992) has diagnosed pronounced changes in standing volume and volume growth in Scandinavia and other European countries since the 1950s (Fig. 14.21). However, such time series need to deal with several difficulties, primarily changes in inventory methods and definitions between the countries over time. Also, conclusions based on standing volume and volume growth are ambiguous if changes in forest area, species and age composition, and silvicultural treatment

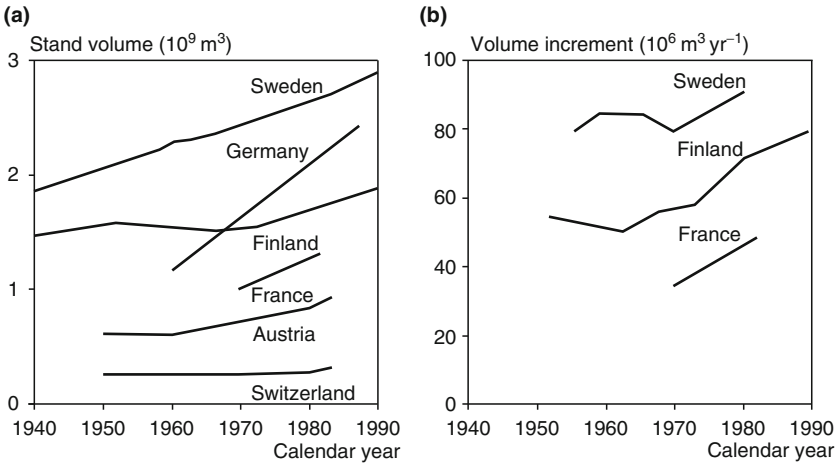

Fig. 14.21 Long-term development of (**a**) standing volume and (**b**) volume growth in European countries according to the results of national inventories (Kauppi et al. 1992)

programs are not taken into account. A stratification of the data pool in terms of species, site, age, silvicultural treatment is indispensable before proceeding with the calculation of standing volume and volume growth. By stratifying their data pool, Arovaara et al. (1984) and Elfving and Tegnhammar (1996) confirmed the increment trends revealed by Kauppi et al. (1992) for Finland and Sweden (Fig. 14.21).

In the former West Germany (nation until 1990), the first national inventory with consistent sampling procedures (Bundeswaldinventur I, short BWI^1) was carried out in 1987 and repeated for the unified Germany in 2002 (BWI^2). In Bavaria, the state inventory from 1970/71 (GRI 1970/71) also can be compared to the two BWI-inventories. Table 14.2 shows standing volume and volume growth development from 1971 to 2002, in the Bavarian state forest. Except for Sessile oak, all species show a considerable increase in standing volume ($m^3\,ha^{-1}$); on average standing volume accumulated to 126% compared to the initial level. Even more noticeable is the increase in volume growth ($m^3\,ha^{-1}\,yr^{-1}$). While common yield tables predicted a species-dependent 4.5–9.6 $m^3\,ha^{-1}\,yr^{-1}$ in 1971, volume growth ranges from 4.2 to 12.6 $m^3\,ha^{-1}\,yr^{-1}$ from 1971 to 1987, and from 8.7 to 15.0 $m^3\,ha^{-1}\,yr^{-1}$ in the period 1987–2002. On average, the annual volume growth increases from 7.6 $m^3\,ha^{-1}\,yr^{-1}$ expected by the yield tables to 10.1 $m^3\,ha^{-1}\,yr^{-1}$ in 1971–1987, and 12.4 $m^3\,ha^{-1}\,yr^{-1}$ in 1987–2002. In other words, depending on the species, growth increased by 56–93%, and by 63% on average.

Table 14.2 Development of standing volume ($m^3\,ha^{-1}$) and volume growth ($m^3\,ha^{-1}\,yr^{-1}$) of forest stands in Bavaria from 1971 to 2002 (merchantable volume over bark >7 cm at the smaller end). Results from the Bavarian state forest inventory of 1970/71, and the national forest inventories BWI^1 in 1987 and BWI^2 in 2002. The analysis was carried out for species groups, however, all groups are dominated by the first-mentioned species as Norway spruce, Scots pine, European beech and Sessile oak.

Species	Standing volume ($m^3\,ha^{-1}$)			Volume growth ($m^3\,ha^{-1}\,yr^{-1}$) according to yield table[c]	Volume growth ($m^3\,ha^{-1}\,yr^{-1}$)	
	1971[a]	1987[a]	2002[b]	1971–1987[a]	1971–1987[a]	1987–2002[b]
Norway spruce/ Silver fir/Douglas fir	344	406	439	9.6 (100%)	12.6 (131%)	15.0 (156%)
Scots pine/ European larch	240	269	307	5.9 (100%)	8.5 (144%)	9.4 (159%)
Sessile oak/ Common oak	278	276	278	4.5 (100%)	4.2 (93%)	8.7 (193%)
European beech/ other decidious spec.	232	264	307	5.7 (100%)	6.4 (112%)	10.9 (191%)
Total	296	343	374	7.6 (100%)	10.1 (133%)	12.4 (163%)

[a]According to Foerster et al. (1993, 1995); [b]According to Bundesministerium für Ernährung, Landwirtschaft und Verbraucherschutz (2005); [c]Applied were the yield tables for moderate thinning for Norway spruce, Scots pine, European beech and Sessile oak by Wiedemann (1936/42), Wiedemann (1943b), Wiedemann (1932), and Jüttner (1955), respectively

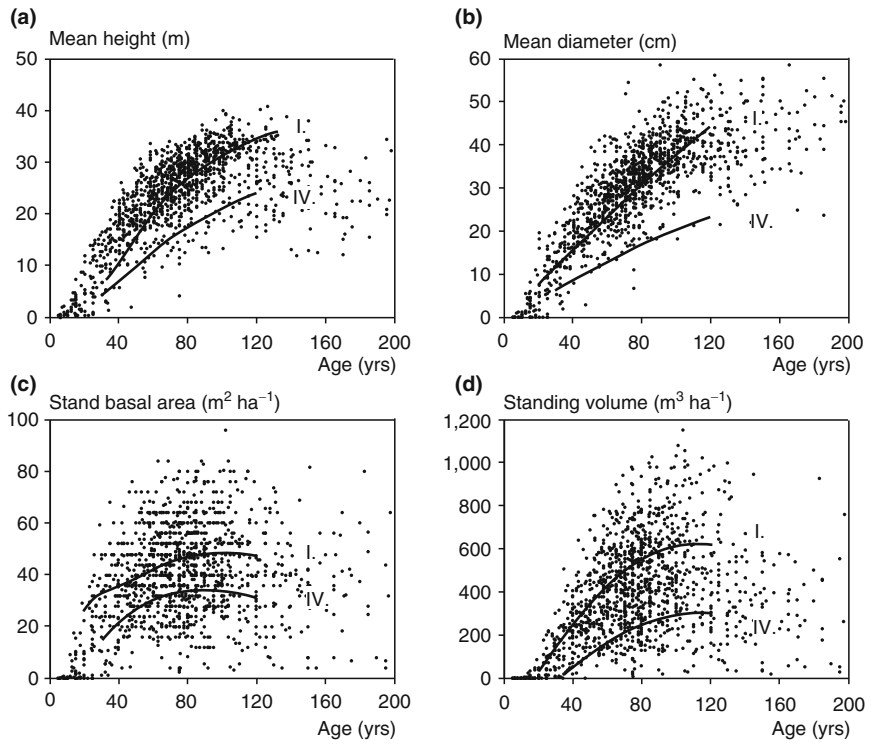

Fig. 14.22 Application of inventory data for compiling an artificial time series and analysing growth trends. Stand characteristics of Norway spruce in Bavaria in comparison to the yield table from Wiedemann (1936/42), moderate thinning. The following results from permanent state forest inventories on estate level are plotted over stand age (**a**) mean height, (**b**) diameter at breast height, (**c**) stand basal area, and (**d**) standing volume

When real time series from successive inventories are not available, artificial time series can be compiled from a single inventory, and used to analyse growth trends. This way, Pott (1997) proved the above-mentioned discrepancy between yield tables and present forest growth based on 24,648 plot surveys of the permanent Bavarian state forest inventory. Figure 14.22 shows the mean height (m), mean quadratic diameter (cm), stand basal area ($m^2\,ha^{-1}$) and standing volume ($m^3\,ha^{-1}$) for Norway spruce stands plotted over stand age. For clarity, only a random sample of 5% of all data points is displayed. The span of the Wiedemann yield tables (1936/1942) from yield class I. to IV. is depicted by the two reference lines. Obviously, more than 50% of all stands younger than 100 years exceed the height bounds of the yield tables. Only the older stands, especially those older that 120 years, still fall within the yield table range. The same applies for diameter, and, to a lesser extent, also for stand basal area and standing volume. The small numbers of stands between 50–70 $m^2\,ha^{-1}$ stand basal area, or 600–1,200 $m^3\,ha^{-1}$ standing volume is an argument in itself for boosting stand growth in the twentieth century. A stratification of the data pool by site conditions can lead to the responsible factors (Pott 1997).

14.4 Dendro-Chronological Time Series Analysis

This method provides evidence, date and strength of a disturbance in an increment and climate time series. A part or the whole growth curve is used to derive a reference curve, which reflects the age and long-term climate and management trends. Deviations from this reference curve can be interpreted with respect to possible disturbance influences beyond age, management and climate effects (Cook and Kairiukstis 1992; Fritts 1976; Kiessling and Sterba 1992; Schweingruber 1983).

The dendro-chronological time series analysis is based on the assumption that a growth time series G_t consists of a smooth (reference) component S_t, and an oscillating (deviating) component O_t (Fig. 14.23). The smooth component includes age, and long-term management and climate effects, and is estimated for a reference (or calibration) period. The oscillating component reflects short-term climate or weather effects or other disturbances (including statistical noise):

$$G_t = \text{smooth component } S_t + \text{oscillating component } O_t \tag{14.21}$$

When the parameters of both the smoothed reference function and the climate-dependent short-term deviations are determined from the reference period, they can be used to detect changed growth behaviour in the test period. The following paragraphs summarise the procedure in four consecutive steps.

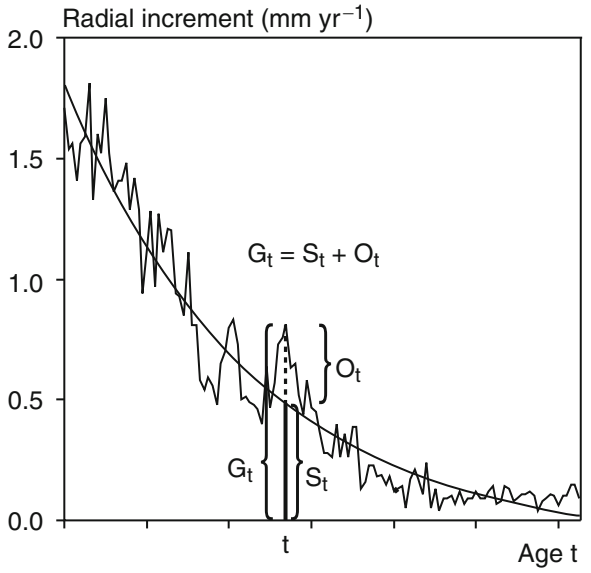

Fig. 14.23 The dendro-chronological time series analysis splits the course of annual growth G_t into a smooth component S_t, which describes the age and long-term climate and management-related effects, and an oscillating component O_t, i.e. the deviations from the smooth component ($G_t = S_t + O_t$)

14.4.1 Elimination of the Smooth Component

The smooth component of the dendro-chronological time series originates from the natural age trend, but also may contain long-term management and climate effects. To model these trends, typically a simple exponential function is sufficient:

$$S_t = a_0 + a_1 \times e^{-a_2 \times t}. \tag{14.22}$$

Complete age series from an early to old age, can be modelled using the Hugershoff (14.23) or double-logarithmic function (14.24):

$$S_t = a_0 \times t^{a_1} \times e^{-a_2 \times t}, \tag{14.23}$$

$$\ln(S_t) = a_0 + a_1 \times \ln(t) + a_2 \times \ln^2(t). \tag{14.24}$$

Polynomials of higher degrees additionally eliminates intermediate effects that might result from particular silvicultural measures:

$$S_t = a_0 + a_1 \times t + a_2 \times t^2 + \ldots + a_n \times t^n. \tag{14.25}$$

The spline functions (Späth 1983; Riemer 1994), and the moving average (Schlittgen and Streitberg 1997) are two more smoothing methods.

Figure 14.24 depicts the radial increments of the Norway spruce trees No. 335 and No. 510 and the Silver fir No. 105 from an experimental series in the Bavarian Alps near Garmisch-Partenkirchen. Different regressions were used to model the smooth component of the radial growth. Two aspects are very important in the modelling of the smooth component. First, one needs to choose an appropriate function for describing the smooth component. If short-term deviations are to be analysed, e.g. growth reaction due to variations in annual precipitation, a moving average might be best suited to eliminating age, climate and management trends. If long-term growth deviations need to be detected, a growth curve that excludes supposed growth anomalies should be adapted to the growth reference period. Otherwise the increment boost in Silver fir No. 105 after 1970, or the increment peak for Norway spruce 510 between 1885 and 1905, distort the growth curve (Fig. 14.24). Secondly, a representative number of sample trees should be included in the analysis. Growth responses at the stand level can only be evaluated if tree-specific growth responses, e.g. due to shading, are avoided. In Fig. 14.25, it might make sense to ignore the last 10 years of Silver fir No. 442, which was already dying, and omit Silver fir No. 451 whose increment culminates much later than its neighbours.

One must be aware that the reference function might always smooth out long-term climate or management effects. Becker (1989) eliminated the smooth component by basing his reference function on a well-distributed cross-section of age classes and calendar periods. This curve represents the mean growth behaviour during the calendar period, and thereby avoids climate and management trends in the data.

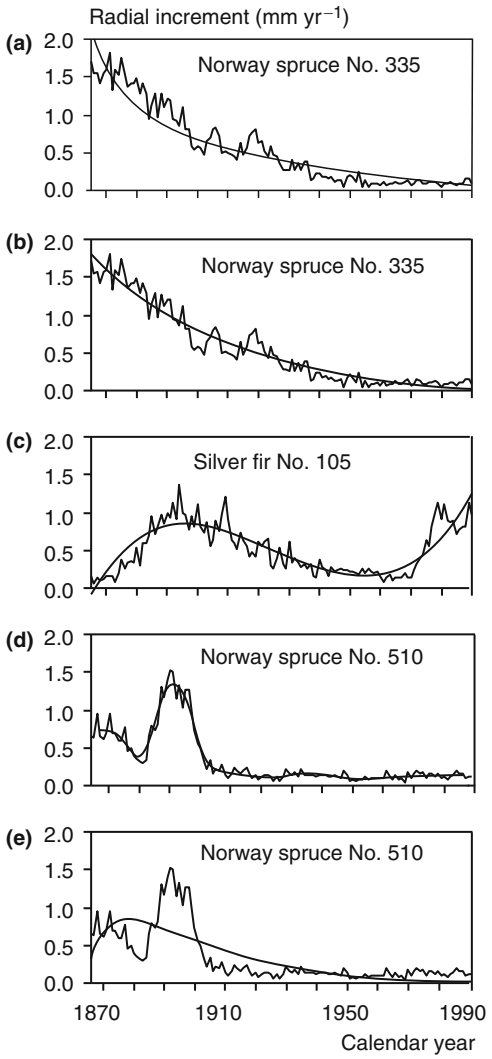

Fig. 14.24 Modelling the smooth component of growth time series via regression–analytically adapted functions and calculation of moving average. The following approaches were used to model the smooth component: **(a)** $G_t = a_0 - a_1 \times \ln(t)$, **(b)** $G_t = b_0 + b_1 \times e^{-b_2 \times t}$, **(c)** $G_t = c_0 + c_1 \times t + c_2 \times t^2 + c_3 \times t^3$, **(d)** $G_t = (z_{t-3} + z_{t-2} + z_{t-1} + z_t + z_{t+1} + z_{t+2} + z_{t+3})/7$, **(e)** $G_t = d_0 \times t^{d_1} \times e^{-d_2 \times t}$

14.4.2 Indexing

In a second step, the measured growth is related to the reference curve. The resulting index curve I_t is free of age and long-term climate and management trends:

$$I_t = \frac{G_t}{S_t}. \tag{14.26}$$

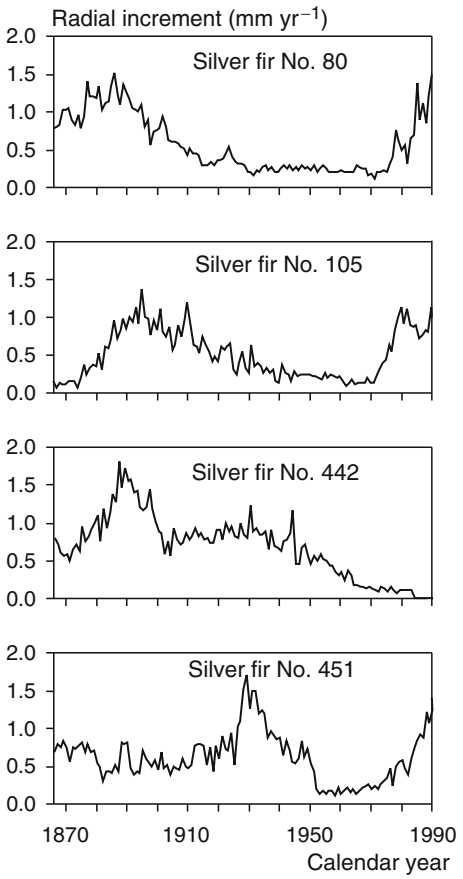

Fig. 14.25 Annual radial growth of the four neighbouring Silver fir trees in a mixed mountain forest show remarkable differences in their individual development, but also similarities in their present increment trend

14.4.3 Response Function

In a third step, unique to this method, the deviations in the index function are explained by the climate series data. The resulting response function is parameterised by regression–analysis. Auto-correlation between the current annual increments should be considered:

$$\hat{I}_t = f\,(\text{climate}, \text{increment at time } t-1, t-2\ldots). \qquad (14.27)$$

As a rule, the parameterisation of this function does not rely on the whole observation period, but only on the data for the reference period (here: calibration period), which is supposedly free of disturbances.

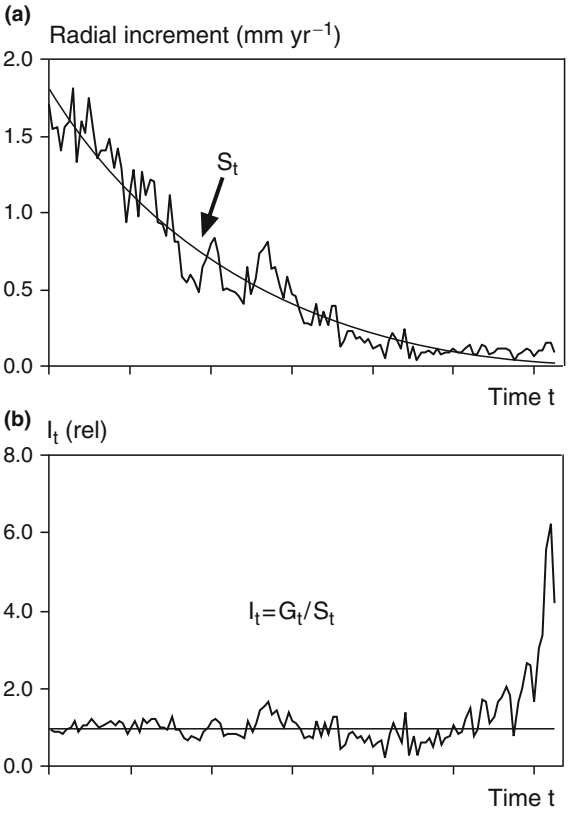

Fig. 14.26 The index curve I_t is derived by relating the annual growth G_t to the smooth component S_t. The resulting oscillating pattern of index I_t is free from age and long-term climate and management-related effects. **(a)** Original radial growth and smooth component S_t. **(b)** Indexed radial growth ($I_t = G_t / S_t$) and detection of growth acceleration for the last decade

14.4.4 Quantification of Increment Losses

In the fourth and last step, the model (14.27) is applied to the analysis period, and the expected increment is calculated by multiplying the reference and response function:

$$\hat{G}_t = \hat{S}_t \times \hat{I}_t. \tag{14.28}$$

In this expected growth $\hat{G}_t$, age, long-term management trends and climate effects are accounted for. Therefore, deviations from the expected increment must be attributed to other sources of disturbance, and the results can be used as evidence for the effect, e.g. of groundwater table lowering, air pollutants or fertilisation. Figure 14.27 shows the results of a dendro-chronological time series analysis from Eckstein (1981) on the increment behaviour of 253 roadside trees under different degrees of traffic intensity. He proved that the increment loss increases with traffic intensity, and attributed the losses mainly to the increased use of thawing salt.

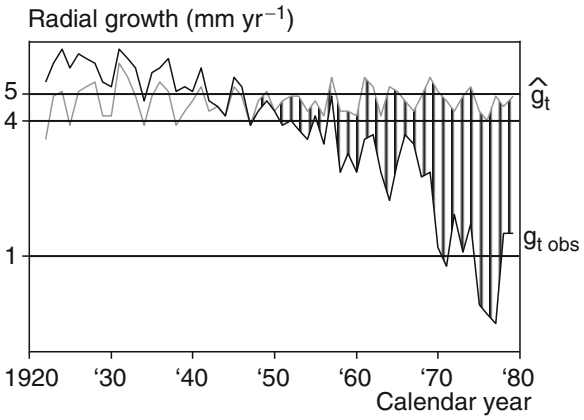

Fig. 14.27 Diagnosis of increment disturbances of roadside trees via dendro-chronological time series analysis (Eckstein et al. 1981): expected (*grey*) and real (*black*) development of annual ring widths of Sycamore maple trees under high traffic intensity. The comparison between expected ($\hat{g}_t$) and observed increment ($g_{t\,obs}$) provides a dating and quantification of increment decreases due to disturbances (growth loss $= \hat{g}_t - g_{t\,obs}$)

Summary

This chapter introduces methods for long-term growth analyses which are oriented at the available data pool from inventories, temporary and long-term research plots, increment cores and stem analyses. They can be ordered in four groups according to the type of reference used. Due to its low priority in the allocation hierarchy, stem increment in breast height (radial, diameter or basal area increment) is particularly sensitive – even though unspecific – to disturbances and suitable for diagnosis of disturbances. The comparison between disturbed and reference growth behaviour makes it possible to determine the beginning, duration and strength of the growth reaction, and may help to find the disturbance sources.

(1) For the diagnosis of growth disturbances, the growth of supposedly disturbed individual trees or stands is compared with a reference development, which reflects the development expected under unimpaired "normal" conditions.
(2) The comparison between the to-be-assessed growth and the reference allows the dating and quantification of growth reactions. Even though it can provide evidence for disturbance causes, it is no direct proof of a cause-and-effect chain.
(3) In the first group of methods, the reference is derived from growth models. The comparison between observed growth behaviour with those from yield tables, scenario calculations with dynamic growth models and synthetic reference curves give information on deviations between model and reality. Generally speaking, the comparison with models is suited for the diagnosis of long-term and large-scale deviations with empirically derived model ideas from past time periods.

(4) In a second group, the increment trend method, the pair-wise comparison, the comparison with reference plots, the comparison via indexing and the regression-analytical increment estimation, the reference is deduced from undisturbed neighbouring trees or stands. This method group is well-adapted to the diagnosis of disturbance factors restricted in time and space, and also suited for the raising of juridical evidence.
(5) In the case of using preceding periods for reference, the method of constant age, the comparison of preceding and succeeding generations and the analysis of successive inventories, the to-be-assessed growth behaviour is compared with the growth behaviour in previous times. Methods of this fourth group can detect abrupt growth changes as well as growth changes due to long-term and large-scale effects.
(6) The dendro-chronological time series analysis diagnoses and quantifies disturbances by statistically analysing the increment of supposedly disturbed trees or stands. By eliminating the age trend, indexing and developing a response function, it is possible to date and quantify disturbance influences. The reference curve for diagnosis and damage quantification is deduced from the very material itself. This method makes a differentiated diagnosis of local and regional growth disturbances possible, however asks also for long-term time series of the most important site factors (temperature, precipitation, etc.).
(7) When approaching a problem, it is recommended to apply methods of different procedure groups whenever possible, in order to combine the specific strengths of each one. Evidence on the degree and cause of damages becomes safer if methods with different forms of reference derivation come to similar results.

Chapter 15
Pathways to System Understanding and Management

Some chapters in the book deal with separate knowledge acquired in forest growth research. For example, in the Chapters 9 and 14 the effects of species mixture and disturbances of tree growth are discussed. The aim of other sections of the book, for example the Chapters 10 and 11 is to integrate the isolated knowledge into models, and to reveal rules, growth relationships and derive theories. Both approaches, which include both the individual investigations for revealing empirical principles and the synthesis and development of the theory of forest dynamics, are essentially indispensable since, in the forest growth research, the process of acquiring knowledge occurs in a feedback process between theory development and separate empirical investigations. This is shown in the first section of this chapter (Fig. 15.1).

Science inquires into nature. The questions asked are heavily influenced by the Zeitgeist of society. Currently, forest growth research in central Europe is concerned about the relationships between tree species diversity and productivity, the responses of tree species to climate changes or the carbon storage capacity of forests. Thirty years ago, research was focussed on the maximisation of volume production in pure stands, the effect of air pollution on forest growth, and increasing stand productivity by fertilisation. The actual research questions reflect, to a certain extent, the actual problems, themes and values of society, and hence also forestry practices. Researchers' questions also are determined largely by the questions posed by foresters or society. Thus, with a change in the cultural Zeitgeist, the research questions also change.

Society and foresters expect quick and simple answers to their questions relevant to the decisions that need to be made. Suppose practice reacts to current topics and questions relevant to forestry practice by establishing new experiments first, and waiting for results from these experimental plots. Forest growth research would provide answers decades afterwards due to the long lifespan of forest stands, and the consequent duration of experiments. In the second part of this chapter, a discussion of how knowledge about forest ecosystems can be used to regulate and manage

H. Pretzsch, *Forest Dynamics, Growth and Yield: From Measurement to Model*,
DOI: 10.1007/978-3-540-88307-4_15,

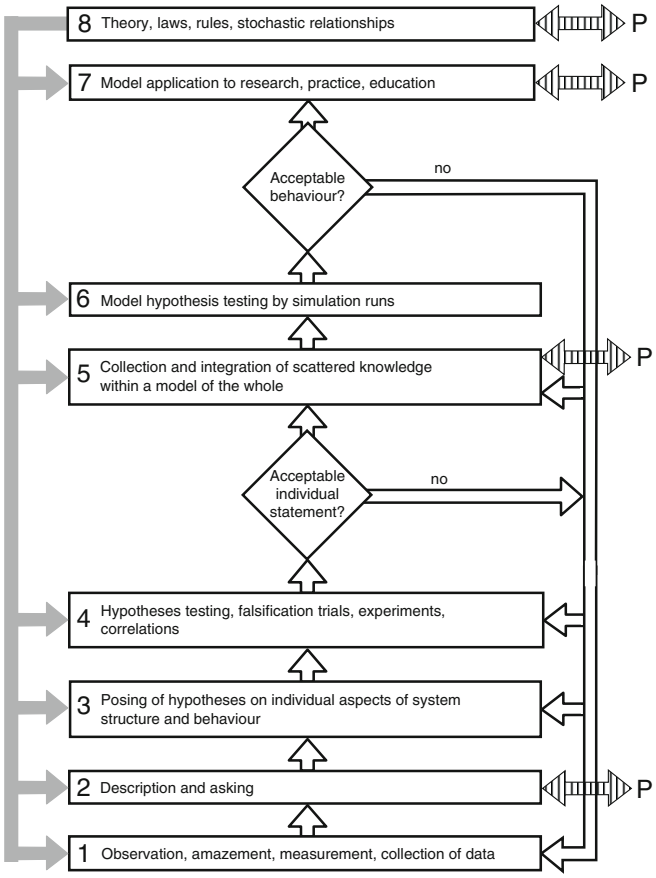

Fig. 15.1 Overview of the process of acquiring knowledge in forest growth research

forest ecosystems sustainably is presented (Fig. 15.8). The opportunities, tools and also the narrow limits of information exchange between science and society, theory and practice are outlined.

15.1 Overview of Knowledge Pathways in Forest Growth and Yield Research

Currently, in most areas of forest science, an extraordinary amount of detailed knowledge is being accumulated about structures and processes at a high level of temporal and spatial detail (min, sec; mm, µm, nm). Yet, at the same time there is a lack of theoretical development for compiling this knowledge, synthesising it into a big picture to understand the whole, and the importance of its

components. Advances in knowledge currently touch on the feedback processes between separate, empirical investigations on the one hand, and the development of overarching explanations and theories on the other.

These important feedback processes are highlighted in Fig. 15.1 where observation, measurement, description, hypothesis testing, model development etc. (white solid arrow in the middle; from bottom to top) ultimately feed into general ideas, stochastic relationships, rules and theories. Conversely, theories, models and the desire to synthesise knowledge advances empirical research (grey arrow left; from top to bottom) because the overarching theories, laws and stochastic relationships disclose gaps in knowledge, suggesting new questions and the need for new, detailed investigations.

The exchange between the practical living world (P) and the process of acquiring knowledge occurs at different levels, extending from observation through hypothesis testing to the use of models and determination of general growth relationships. Forestry practice formulates questions, for example, about the stability of trees, the relationship between species diversity and productivity, and expected growth models for sustainable planning at the enterprise level. It depends on information, which can be generalised, and reliable growth relationships, e.g. relationships between stand density and stand growth, imparted during further education training and so on. This feedback between science and practical application is symbolised by the hatched arrows in Fig. 15.1 (right side).

The entire path from the observation and measurement of data to models, the derivation of laws, and the feedback between theory and individual investigations is directed certainly more by scientific intuition and inventiveness than by the methodological schematism outlined in Fig. 15.1. However, the basic knowledge about the process of cognition and systematic research, as it is conveyed in the following, is indispensable to those involved in forest science and research. Perhaps the diagram helps to perceive one's own approach and scientific work as a part of the overall pathway to system understanding and management. The eight essential steps outlined in Fig. 15.1 are: (1) observation, measurement, and collection of data; (2) description; (3) formulation of hypotheses for elements of system structure or behaviour; (4) test of hypotheses, trials of falsification by experiments and correlation; (5) synthesis of relevant knowledge into a system model; (6) test of model hypotheses by simulation; (7) application of the model in research, practice and education; and (8) development of theories, laws, rules and stochastic relationships. These steps are elements of an iterative feedback process, not milestones in a linear, uni-directional procedure. In Sects.15.1.1–15.1.8 below, steps (1)–(8) are discussed in sequence.

15.1.1 Observation, Measurement, and Collection of Data

In each realm of science, the acquisition of knowledge commences with observation, amazement at structures and processes in the real world, collection of data, and compilation of objective facts to gather an empirical information base. The traditional

sources of growth and yield data have been monitoring plots or experimental plots, where the development of individual trees or stands is recorded (Franz 1972; Ganghofer 1877; Spellmann et al. 1996). On early long-term experimental plots, which have been established since 1860, and some of which are surveyed still today, stem diameter and tree height were measured to obtain the stand cumulative and mean values for calculating expected stand yield. The network of experimental plots includes study sites with no evidence of human influence, and others showing the long-term effects of management alternatives, and sample plots established to investigate disturbance factors (Pretzsch 2002). In recent decades, retrospective growth analysis of single trees and stands, and of inventory data have also become important (Spiecker et al. 1996): successive measurements of, e.g. crown projection, crown height, or crown length, have transformed former stand-based experiments, to individual tree-based, spatially explicit experiments. Stem analysis and biomass measurements of selected trees on these plots highlight the shift from stand to individual tree research. Investigations carried out by forest ecosystem research centres, which are placed only selectively yet go into considerable depth, provide additional new sources of objective information relevant to forest growth science that have only just begun to be tapped (Matyssek et al. 2005). In addition to the structural variables measured to date, completely different variables were considered, e.g. physiological and physical rates of assimilation, respiration, transpiration, water and sap flow in the stem, radiation and light absorption in the canopy, or the flow of water and nutrient solution in plant and soil.

Observation and measurement form the basis of forest growth research, which places Galileo's principle – "measure what there is to measure, and make measurable what can be made measurable" – at the centre of their efforts (Assmann 1961b). That quantitative information about forest growth from measurement, modelling and prediction provides an essential basis for forest management decisions, rather than presenting a threat to the creativity and inspiration of the silviculturalist, is not questioned seriously any longer.

In all quantitative sciences, the recording of raw data and testing its plausibility, followed by its organisation, standard analysis and permanent storage forms the basis of empirical knowledge. Due to the prolonged observation period, which extends back to the 1860s and 1870s for many forest growth research sites, the organisation and standardised analysis of data is of particular importance in the generation of knowledge in forest growth science. Monitoring sites often provide meaningful results about forest growth only after having been surveyed over decades and measured 10–20 times. Forest growth research has access to valuable time series data for the entire life of the tree or stand only when data from previous surveys are available. These time series are essential to understand, not only the temporary effects of management practices, e.g. thinning, species mixing, fertilisation, or soil treatments, but also the long-term effects of management practices that influence the stand throughout its rotation, or even thereafter.

In addition, in the regulation of long-term experiments with quantitative silvicultural prescriptions, especial attention needs to be paid to the organisation of data and standardisation of analysis because data about the present status of the plots

and their development in each preceding period are required at any given time. Thus the data recorded must be tested immediately for plausibility, and aggregated in a standardised analysis to make it available for regulating the experiment in the subsequent period (e.g. by removal the amount of standing volume that exceeds a prescribed target curve) (Johann 1993).

15.1.2 Description

The description of tree and stand dynamics represents an important step in the process of understanding forest growth. It provides, on the one hand, quantitative information about the forest stand investigated that is relevant for forest practice and, on the other hand, an important foundation for the formulation of hypotheses for thorough scientific analyses. We define description as the representation of one or more attributes of the tree or stand investigated using descriptive statistics, such as tables, graphs, mean values, frequency distributions, and measures of dispersion. It is confined to the reproduction of objective facts, or "that-is-so" statements. Forest growth research describes, for example, crown structure, diameter increment over time, or stem form changes of individual trees. At the stand level, it describes basal area and volume development, volume increment over time and structural development of the natural regeneration.

Despite the importance of "that-is-so" statements, forest growth research always should be governed by the formulation of hypotheses, the development of models, relationships and theories. Efficient research, and the provision of up-to-date information for decision makers in forestry and environmental politics demands a balanced relationship between the systematic collection and description of facts, and the usefulness of these in the derivation of causal relationships, general principles, rules, laws, and models. Comprehensive forest ecosystem management is not possible without a deep understanding of the effects of factors such as site conditions, disturbance factors and anthropological influences on the behaviour of the system so that general "if-then" statements can be formulated about the effects of these factors.

15.1.3 Formulation of Hypotheses for Elements of Individual System Elements

We define hypothesis as an assumption, not yet proven in practice, which is set up as methodological principle for, and an aid to generate scientific knowledge. Hypotheses differ from pure speculation in that they have undergone some preliminary testing of their validity through, for example, discussions among the scientific community or literature review. Hypotheses may focus on single causal relationships or sequences of causal relationships. The formulation of hypotheses about the behaviour of entire systems leads to the construction of models.

Hypotheses can, on the one hand, directly result from observations or measurements: for example, a hypothesis at the tree level might be that crowns in mixed stands are longer than in pure stands. At the stand level one could postulate, on the basis of study site surveys, that the productivity of forest stands with the retained number of tree species, that is species diversity, increases. Alternatively, hypotheses can be derived from theories. The test of hypotheses derived in this way can contribute to the evaluation, or possibly the confirmation or expansion of the theory. The self-thinning theory developed by Yoda et al. (1963) in herbaceous plant communities provides one example. It describes the reduction in the number of individuals per area in relation to the mean size of the individuals. Given this existing theory developed for evenaged herbaceous stands, the hypotheses that this theory also applies to woody plants in pure and mixed stands can be put forward. To propose hypotheses from broader theories, a further example is presented: from the island theory (MacArthur and Wilson 1967) and the mosaic cycle theory (Aubreville 1938; Müller-Dombois 1983), one could conclude that the natural forests and forest nature reserves, as they are presently delineated, are not nearly large enough to conserve the forest and fauna communities currently present (cf. Sect. 1.8). Hypotheses can be derived from still more general theories developed in biological sciences. This happens, for example, when the inner or outer structures of trees are quantified according to their fractal dimension (Zeide 1998), and by assuming self-similar fractal structures when modelling them (Kurth 1999). Thus the principles of fractal geometry and the chaos theory are transferred to trees and forests (Mandelbrot 1977; Nicolis and Prigogine 1987; Seifritz 1987).

Science inquires into nature by formulating hypotheses. From the wealth of possible questions, those with good prospects of supplying an answer are selected. Hypotheses cannot be derived in a purely logical fashion. Rather, the formulation of a hypothesis requires scientific intuition, imagination and a wealth of ideas, and is consequently very much influenced by the personality of the scientist. The selection of questions is also strongly influenced by the intellectual climate at the research institution, the scientific viewpoint, and sometimes also by the Zeitgeist of society. There is an element of danger in the latter that the hypotheses postulated are influenced in all probability by the Zeitgeist. In very militaristic societies, hypotheses are marked by the aims and values of the military, and serve to kill. In a society whose principles of conduct are power and wealth, the goal is to maximise profit. In communities striving for long-term stability, questions, hypotheses and technologies that serve the sustainable development of life and the resources required can thrive. But even in the latter, questionable hypotheses can flourish, become fashionable, and just as quickly abate. Many examples can be found in the hypotheses proposed for investigations into forest decline during the 1970s and 1980s, which were tendentious, and hence short-lived, about the existence, process and causes of forest damage.

Although hypotheses may be founded irrationally, testing hypotheses for internal consistency and congruency with known facts and principles can be conducted strictly rationally, and processed virtually schematically.

15.1.4 Test of Hypotheses

Hypotheses and modelling approaches should be scrutinised in four ways (Popper 1984). First, a check for inner contradictions needs to be carried out. One way of doing this is to compare the logical consequences of the hypotheses. Second, the hypotheses and modelling approaches, which may be perceived as a bundle of hypotheses, are examined for their logical form and their character as hypotheses. Here, one needs to analyse whether the hypotheses are tautological, whether they can be falsified or cannot be tested. Third, a deductive examination is undertaken, comparing the hypotheses with already proven relationships, principles and theories. In forest growth science, hypotheses, usually focus on macro processes and structures, are tested also to determine whether a posed hypothesis can be derived from the known facts about processes and structures at the next subordinate system level. Fourth, a hypothesis needs to be tested to determine whether it is realistic by comparing it to observation data. This empirical examination should be undertaken especially for hypotheses about the existence of a typical system condition and pattern, or about development trends and chains of causal relationships. It demands a solid empirical database, from which hypotheses may be tested by description, experiment or correlation analysis. Systematic screening (i.e. identification of counter-examples for the falsification of a hypothesis), as is common in the field of biology or medicine, is rarely used as a means of hypothesis testing in forest yield science.

The four tests can be recommended for systematic tests of falsification, the principle of modern biological science. The falsity of a hypothesis is tested again and again. If the hypothesis holds up consistently after these four tests, then one can be more certain of its general validity. Yet new data, collected systematically or unsystematically, continues to be used to test the validity of hypotheses and models anew. The stand yield tables from the 1940s and 1950s, to cite an example, were regarded as a proven model for decades. This changed once unstable growth conditions and growth trends were identified in the 1970s (Röhle 1994). Moreover, once yield tables were not upheld in more recent falsification tests (Chapters 1, 11, 14), a conversion to more flexible approaches for modelling growth in relation to resource supply and environmental conditions appeared advisable.

15.1.4.1 Data for Testing Hypotheses

Raw data and facts from two different sources essentially form the basis for testing hypotheses in forest growth research. The first source of data comprises precise facts collected intensively from growth analyses and long-term study sites. These data are only valid locally or for certain locations as a rule but data back a long time. A network of long-term study sites investigating a broad spectrum of experimental factors (including tree species, provenances, site conditions, species mixes, treatments) is an ideal source of data for formulating and testing forest growth hypotheses.

Inventories and forest planning provide the second source of information. These record extensive yet representative data for the area. Both sources of data are valuable for testing hypotheses.

15.1.4.2 Hypothesis Testing by Experiment

Ideally, hypotheses about individual aspects of forest growth are tested in experiments. In an experiment, all factors of influence, except the one under investigation, are kept constant. The factor being investigated is changed in a defined way, and its effect on the development of trees or stands investigated. In this way, experiments can provide strong evidence for cause–effect relationships (Fig. 15.2). In multi-factorial experiments, the effects of multiple factors on forest growth, e.g. different initial stocking, thinning and fertilisation intensity, are investigated by establishing a whole series of research sites to test different levels defined for these factors.

Experiments with trees or entire forest stands as the unit of information consume considerable areas elevating the danger of inhomogeneity in site conditions. Forest sites, per se, are more inhomogeneous than agricultural sites, and therefore hamper the establishment of strict ceteris paribus conditions. The variation in site conditions and forest stand history warrants a larger number of repetitions, which, therefore, are technically and financially more resource intensive. To experimentally test the effects of three factor levels for planting patterns, thinning and fertilisation, for example, $3 \times 3 \times 3 = 27$ trial plots would be necessary. Therefore, with a 3-fold repetition of an experiment, already the number of plots required would reach 81. For a typical plot size of 0.25 ha, a total area of 20 ha would be required, yet a homogeneous site of this size can be found only rarely.

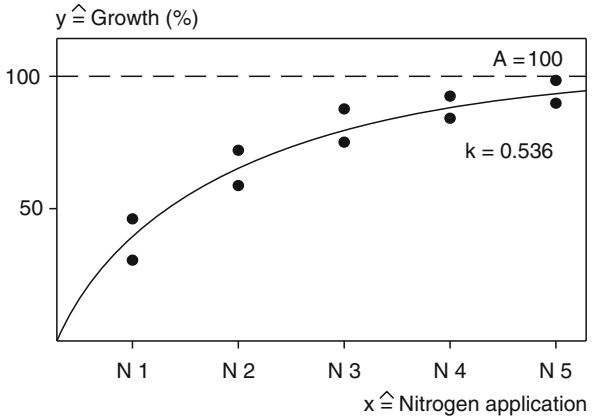

Fig. 15.2 Results of a nitrogen increment experiment with five treatment categories and two repetitions. The experiment facilitated testing and quantifying the causal relationships between nitrogen added and growth

In field experiments, one can analyse only the effect of explicit factors because they can be controlled without too much time and effort. These factors might include stocking density in thinning experiments, nutrient supply in fertilisation experiments or crown length in pruning experiments. However, the regulation of the majority of factors influencing forest growth, such as temperature, water supply, carbon dioxide concentration, is extremely complex in open-air conditions. Therefore, the opportunities for obtaining meaningful data for such factors from multi-factorial field experiments are relatively low. As an alternative, planting individual trees in phytotrons is associated with the danger of creating artefacts, and, at best, provides results about growth responses of individual juvenile trees, which, however, cannot be extrapolated to infer long-term stand dynamics.

15.1.4.3 Hypothesis Testing by Correlation

Relationships, for example, between temperature in the growing season and height growth of a certain tree species, virtually impossible to investigate exactly in field experiments, can be developed from cross-sectional or longitudinal section studies with correlation analysis. The analysis of scattered experiments, for which the ceteris paribus condition does not apply, may identify correlations (Fig. 15.3a). Clearly, these do not have the accuracy of cause–effect findings from experiments, but they can contribute to hypothesis testing. Correlations should not be used thoughtlessly to draw conclusions about causal relationships, as shown in Fig. 15.3b.

In view of the limited experimental opportunities in forest ecosystems, the long time horizon for the observation of growth responses and the interest in multiple criteria, a network of long-term trial sites affords a versatile database for testing hypotheses by correlation. Study sites that span a broad spectrum of sites and

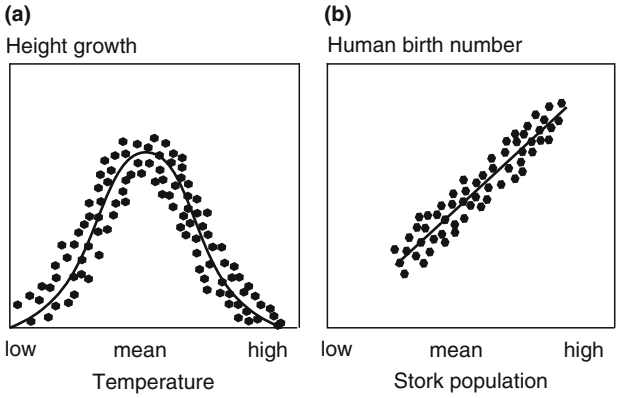

Fig. 15.3 Correlation analysis to deduce relationships rarely accessible experimentally from scattered experimental and inventory data. A correlation, which can be proven, between (**a**) growth and temperature data, or (**b**) human birth numbers and stork occurrence does not permit conclusions about causal relationships to be made

undergo a defined treatment for a long period of time are particularly valuable. A well-documented network of long-term study sites also puts forest growth research in a position to test new hypotheses about forest responses to forest management, growth trends following nutrient inputs or growth responses to climate change without having to establish new special study sites each time a new question or hypothesis arises.

15.1.5 Models as a Chain of Hypotheses

The development and use of models to enhance knowledge is explained below using stand models. The discussion applies analogously to models used at different organisational levels, for example, at the plant component, individual tree or landscape level.

Growth models compile reliable knowledge about single aspects of forest growth, forming a picture of the whole system, of the stand in our case. To develop a model for a real system, for example a forest stand, a simplified quantitative systems model is developed by abstraction. The degree of abstraction, or degree of complexity, of the systems model depends on the existing knowledge about the structure and behaviour of the real system, and also on the reason for developing the model. The systems model, with its underlying system elements and chains of cause and effect, may be regarded as a hypothesis about the structure and behaviour of the entire system. The systems model can be expressed in mathematical equations and transferred to a computer programme, creating a simulation model that allows systems behaviour to be reproduced with the computer. These computer programmes are described as stand simulators. In this context, we define simulation as the reproduction of systems behaviour with the aid of a computer.

Once developed, models can be used to test hypotheses at study sites for which the initial conditions, environmental factors, resource availability etc. as well as the stand dynamics are known. Clearly the stand data should not be used in model construction beforehand. A test is conducted to determine whether the model is suitable for reproducing the system behaviour observed. If the simulation results agree with the reality, it enhances the reliability of the underlying chain of hypotheses in the model. In this case, the model is the hypothesis. In falsification, the observations and model behaviour are compared. We do not want the model to recreate exactly an historical sample, but rather to exhibit the kind of behaviour found in the real system (Forrester 2007). As long as a model reflects reality again and again, it provides us with a valid representation of the system or parts of the system it describes. Each new comparison between simulation and reality represents a test of falsification. If a deviation between the behaviour of the model and the reality is found, then the model has been falsified, i.e. the model assumptions about the structures and processes clearly are not accurate. Other hypotheses are then introduced to obtain a better, more realistic description of the behaviour (feedback between step 6 and steps 1–5, Fig. 15.1). Here, one should concentrate less on the exact reproduction

of the observed, historical path of development, and rather more on the agreement of characteristic system behaviour. An exact match of an historical time series is a weak indicator of model usefulness because, if the real system could be rerun with a different random environment, the data curves would be different even though the system and its essential dynamic character are the same.

Ideally, the development of a model, designed either for the purpose of explanation or prediction, commences when planning the investigation and not after data collection. The development of a model of the system to be investigated may assist in structuring the information already available, identifying the information lacking and the observation and measurement data required, and achieving a balance between accuracy and resolution in the analysis of different system elements. The model concept is developed first into a mathematical model, often calibrated with biometric methods, and ultimately to a simulation model. In interdisciplinary projects in particular, the model concept should be developed cooperatively. This ensures that any differences in time and spatial scales of the information participating scientists contribute will fit together. Model designs based on a well-worked concept at the outset ensure that the investigation is well structured, efficient, and goal-oriented from the measurement phase through to the output phase.

15.1.6 Test of Model Hypothesis by Simulation

Simulation provides a powerful tool for hypothesis testing in forest yield science. It mirrors hypotheses about a system's behaviour, and can be compared to system behaviour observed in the real world. To test a hypothesis about individual aspects of forest growth, such as the question whether growth of pruned trees differs from that of non-pruned trees, approved methods are at hand, such as variance analysis, t-test or χ^2-test. In contrast, testing or evaluating growth models, which, by nature, are a network of hypotheses about structures, processes and causal chains, is vastly more complicated.

Validation indicates the degree of accuracy with which a method measures what it is supposed to. Validity is established when: the test results are found to be in agreement with a criterion established independently of the test results (criterion-validation); a prediction is found to be accurate (predictive validation); the content logic is plausible (content validation); or the context of the theories and approaches can be verified (construct validation). The terms validation and verification are often incorrectly believed to be synonymous. A growth model ultimately cannot be verified because verification requires the general proof of the truth of premises. According to the theory of critical rationalism (Popper 1984), general empirical statements (hypotheses, laws) cannot be verified conclusively, although a conclusive falsification is possible.

The validation of a stand model, and the inherent aggregated hypotheses about system elements and causal relationships, is based largely on the results

of simulation runs. Tree and stand models, and the computer runs carried out with them, provide a "tool" for testing hypotheses in forest growth research. The simulation runs reflect the behaviour of the model under defined limiting conditions, and can be compared to the behaviour of the real system. However, accordance in model behaviour and reality does not signify that hypotheses about structures and processes fit real structures and processes. Trust in validity of the assumed chain of hypotheses grows only when tests of model behaviour with a wide range of data reveal no falsification (Vanclay and Skovsgaard 1997; Pretzsch et al. 2000). Conversely, deviations in individual cases are insufficient to falsify a model when the model reveals largely similar behaviour to the real system.

The first version of the system model only rarely leads to an expedient representation of reality; more often, repeated changes, improvements and extensions of system models would need to be carried out before they can be approved. This iterative process requires a highly aggregated approach to modelling from the beginning that permits a stepwise development towards an increasingly suitable model (top–down approach). The advantage of a simple, highly aggregated model is that invalid hypotheses can be found more easily than in models with a high resolution from the outset (Landsberg 1986). Thus model evaluation is an iterative process (depicted in Fig. 15.1 by the feedback from step 6 to steps 1–5), which incorporates new data, newly derived growth relationships, knowledge gained from practical experience, technical innovations and changes in information demands over time.

15.1.7 Application of the Model in Research, Practice, and Education

If the model is validated sufficiently for acceptance as a useful representation of reality, it is regarded as representative of the real system. Thereafter, it can be used to carry out experiments, prognoses and scenario runs. This is particularly useful in forest growth research where the long observation periods and intensive field experiments prevent experiments from being carried out in reality. Approved models can be applied in research, practice and education (cf. Chapters 12 and 13).

15.1.8 Relationships, Rules, Laws, and Theories

Models, in particular computer simulation models, present a very effective connection between theory and empiricism (Sterman 2007) because the entire bundle of cause–effect relationships in a theory can be integrated and quantified in simulation models. Simulation runs produce development processes that can be compared with reality. In this way, theories can be examined, tightened and further developed.

Deviations in model scenarios from the expected behaviour, or from reality may initiate new experiments, hypotheses, or chains of hypotheses (feedback from step 8 to steps 1–7, Fig. 15.1). Alternatively, the empirical findings can be integrated and brought together to a whole. Only then is it possible to determine the characteristics of a system, which cannot be derived from the isolated consideration of findings obtained separately. Yet, often, it only becomes apparent that critical information is lacking when attempting to summarise individual findings into a model for the entire system. Thus model development and simulation becomes an important link between theory and empiricism (Pool 1992).

15.1.8.1 Stochastic Relationships

Laws, or rules of biological systems, are better referred to as relationships, or stochastic relationships because they can be superimposed onto an overwhelming multitude of influence factors, which are difficult to isolate. We define such relationships as experimentally deduced quantitative connections, which lie somewhere between descriptions and explanations, the two extremes of a phenomenon. Examples for approved relationships include Assmann's unimodal optimum curve for the relationship between stand density and forest stand growth (Assmann 1961a), the self-thinning rules from Yoda et al. (1963) and Reineke (1931), or the allometric scaling rules at the individual plant level posed by Enquist et al. (1998, 1999).

15.1.8.2 Biological and Ecological Theories

We define a theory as a systematically structured volume of findings about laws of a given field of reality, such as forest ecosystems. One can contribute to a theory about the growth of trees and forests via collection, systematic arrangement and linking of approved hypotheses, principles, laws and experiences. In performing this task, growth models become instruments and tools of theory generation and testing. An aggregation of facts from a given field of knowledge for the formation and testing of theories is virtually unthinkable without resorting to mathematical models, which can be transformed to simulation programs.

Theories may apply to different levels of biological organisation: the organism, populations, flora and fauna communities and ecosystems. We present a few important examples below.

Growth–differentiation balance theory, relevant at the individual plant level, states that there is a physiological trade-off between growth and secondary metabolism. And it predicts that nutrient (or water) availability will have a parabolic effect on secondary metabolite concentration, resulting in a unimodal optimum curve with a maximum of secondary metabolites at low–medium nutrient availability. In source-limited plants, a positive correlation is predicted between growth and secondary metabolism. In sink limited plants the correlation is predicted to be

negative: carbohydrates are invested more and more in growth and less in constitutive secondary metabolism when nutrient availability rises.

Island-theory describes processes and patterns on isolated parts of a landscape (MacArthur and Wilson 1967). It describes the dynamic, balanced state of populations on real islands, or near-natural habitats similar to islands in the cultural landscape. It describes the dynamic relationship between immigration and extinction in relation to the size of the island, the degree of isolation of the island and characteristics of the taxonomic groups under consideration (Klötzli 1993, pp. 261–266).

The mosaic cycle theory (Aubreville 1938; Müller-Dombois 1983) describes the structure of large ecosystems as a mosaic of different phases of the climax community in different successional stages. The spatial–temporal dynamic, among other things, is driven by the lifespan of the species, by catastrophes and interspecific competition strategies (Remmert 1992). There is no linear path to a permanent, large and characteristically stable climax stadium. Rather, a constantly changing patchwork develops from the asynchronous, spatial–temporal dynamic of the various phases present (Bormann and Likens 1979a). A balance only exists when all species, phases and stages occur over large areas in the long term with a probability specific for the ecosystem. The extrapolation of conclusions from one mosaic to the whole system, e.g. from a stadium of decline to the stability, diversity and productivity of the entire system (as often occurs) is misleading (Müller-Dombois 1987).

According to Darwin's theory of natural selection, the fitness of the individual is maximised by survival and seed development so that the number of progeny is higher than any of its competing neighbours. The abundance of a genotype is maximised, not the productivity of a stand or a species. Anything that assists its reproduction success helps a tree in a stand, e.g. sit-and-wait, inhibition or poisoning a neighbour; rapid growth and production is not the only strategy. Even if the individual does not increase the number of its progeny, its fitness is increased when it causes a reduction in that of its neighbour, as its relative fitness is then higher.

The anthropogenic view that the tree utilising the resources in a stand works for the common good of the population with the aim of maximising production is unfounded biologically. Rather the individual develops the decisive unit and level of the maximisation of fitness, and that explains the distribution and success of models that unravel a stand or a population commencing with the individual.

15.1.8.3 Chaos Theory: Basics and Consequences for Research in Forest Stand Dynamics

Higher theories in mathematics and physics have also influenced the research direction, investigations and explanations in forest growth research. The theory of relativity and the quantum theory have influenced the approaches to research in forests little because, at the spatial and temporal scales of forest growth, the consequences of these theories appear to be minimal. We do not include the use

of GPS to record forest structures when error would result from ignoring the relativity of time and space.

In contrast, the concepts of the chaos theory are highly relevant to forest research. It says that most natural systems, by virtue of their non-linearity, are too complex to model, or to predict their behaviour. This applies to meteorological and astronomical systems (e.g. forecasts about weather or planet orbits) as well as to biological, social or economic systems (e.g. forecasts of insect infestation, population development, share prices).

Such systems can exist in three different states. Before the chaos theory, the focus was upon the first state, the stable state. In this state, the system responds to small disturbances in a predictable way. Here the same causes also have the same effects (weak causality) (Fig. 15.4a), and similar causes also have similar effects (strong causality) (Fig. 15.4b). Strong causality includes weak causality, and forms the basis of all experimental sciences as, in experiments, one assumes that repetition will produce a similar result even if small changes in conditions occur.

A second system state can be described as a transition from order to chaos; here processes are carried out, and structures that are neither stable nor chaotic are created. Depending on the initial conditions and parameters, the system jumps backwards and forwards between very different system states (attractors). For example,

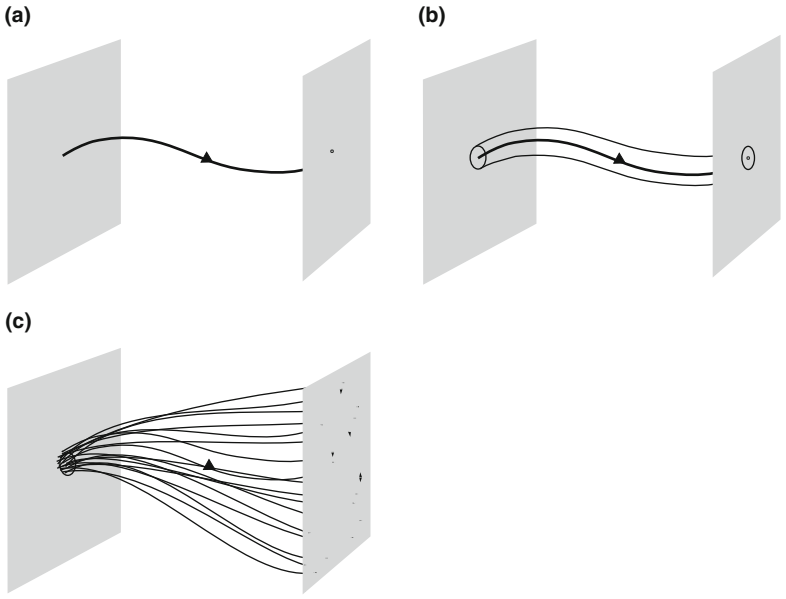

Fig. 15.4 Limits of determinism and causality: graphic illustration of (**a**) the weak causality principle, (**b**) the strong causality principle and (**c**) chaotic system behaviour. Chaotic system behaviour rules out the strong causality principle in that even small changes in the initial conditions can lead to entirely different effects (adapted from Seifritz 1987)

due to the feedback between resources and population size, ladybirds and other insects are prolific every few years, and then the size of their populations declines.

A third system state is the chaotic state. Here responses to small changes in the initial conditions or disturbances are unpredictable (strange attractors). In such system states, the so-called butterfly effect occurs, meaning that the beat of a butterfly's wings in Vancouver may cause a hurricane in Munich a few months later. In this case weak causality, not strong causality, applies with the consequence that similar causes lead to similar effects (Fig. 15.4c).

Ecosystems, in particular, are open, and their initial conditions and influence cannot be identified as accurately as desired through external factors. Consequently, the chaos theory questions the predictability of an effect brought about by a cause. Conversely, completely different values for the causes can lead to the same result or pattern (attractor) (Fig. 15.5). This means different causes may be behind a certain response; in this way, patterns become non-specific indicators of a deviation from stability or normality.

Overall, chaotic system behaviour appears to be very widespread in nature. Stability through attractors and weak causality represent special cases in the continuum between stability and chaos. These special cases include those that have been focussed on to date, and have obstructed the viewing of unstable states with limited predictability. The chaos theory shows that unstable systems in a state of transition from stability to chaos develop fractal behavioural patterns and self-similar geometric forms, so-called fractal structures (fractal tree structures, crystal structures etc.). Fractals are objects that exist, not in an entire dimension but in a broken dimension. Thus, for example, a fractal is a form between a line and an area (e.g. tightly packed pipes in the xylem), or between an area and a body (e.g. screwed up piece of paper, tree crown). The behavioural and structural patterns that we see, measure, and have described quantitatively in this book exhibit more common fractal dimensions (e.g. packed water courses in the stem with a fractal dimension between line and level; foliage of the tree crown with a fractal dimension between area and volume) and self-similar patterns (e.g. twig, branch, tree) as simple one-, two- or three-dimensional structures.

For example, tree crowns have fractal dimensions between 2 and 3, i.e. they have shapes somewhere between areas (two-dimensional) and bodies

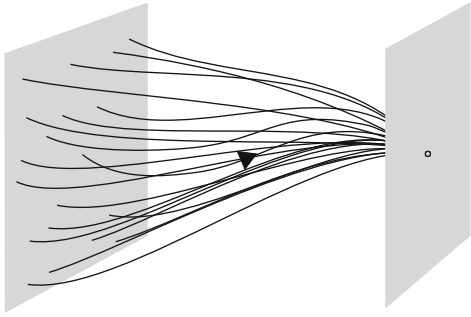

Fig. 15.5 In systems in a state between stability and chaos, any values for causes selected can produce to the same effect (*attractor*)

(three-dimensional). Furthermore, they belong to such fractal forms with self-similarities (twig, branch, tree). This combination of fractal dimension and self-similarity often enables a space to be filled optimally with area (tree crown and leaf surface for light uptake, lungs and cell surfaces for oxygen uptake), or with line-like pathways (xylem for water distribution, phloem for sap flow).

Mandelbrot (1977) and Wolfram's (2002) work shows that, behind the highly complex structures such as we find in nature (flowers, leaves, snowflakes, etc.), the rules of generation are mostly extremely simple. Research should be concerned with recognising and interpreting observed behavioural and structural patterns that have self-similar fractal images, and understanding they are the result of system behaviour. It would need to explain how fractal structures (e.g. from tree crowns, roots, mycorrhiza) arise from non-linear processes at the boundary between stability and chaos. Perhaps fractal behavioural and structural patterns represent proven archetypes in transition from chaotic systems (maximum disorder, maximum entropy) to stable, predictable ones (maximum order, minimum entropy). When Wolfram (2002) used cellular machines with very simple rules to produce the incredibly complex structures such as, e.g. tree fine branching patterns, leaf forms etc. (Fig. 15.6), he created a new approach for seeing, analysing and modelling.

15.1.8.4 Predictions Despite Supposed Unpredictability

Chaotic system behaviour and fractal structures can be created by feedback or iteration with relatively simple mathematical or geometric models. Biological systems such as forest stands consist of organisms, which have acquired the trait adaptability in their development history (phylogenesis), and, therefore, can respond to changes in external factors by switching genes on and off initiating such adaptation. Moreover, biological systems are equipped with an entire network of stabilising feedback loops. With this network, initial effects and external influences can be buffered to a certain extent, and the development of the system can be kept on a certain path. This stabilisation is certainly in effect when, despite unpredictable, or chaotic behaviour at subordinate process levels, the dynamic at the tree and stand level is still driven largely by causality. Light, or heavy thinning in the juvenile phase typically results, e.g. in small, or large tree diameters in the mature stand respectively, even though 100 years and numerous external influences have occurred in between.

From this viewpoint, we understand the chaos theory and its consequences as a warning not to place too much trust in determinism and causality. From it, we gain new insights into the creation of nature and structural formation, and develop new research questions. We have learned that the consideration of the initial conditions (e.g. stand structure) and external influences (events and trends) is possible only to a limited extent, yet has a profound effect on the results. However, the chaos theory does not prevent us from making combined deterministic–stochastic reproductions and predictions of the development of ecosystems for which there is no alternative to date.

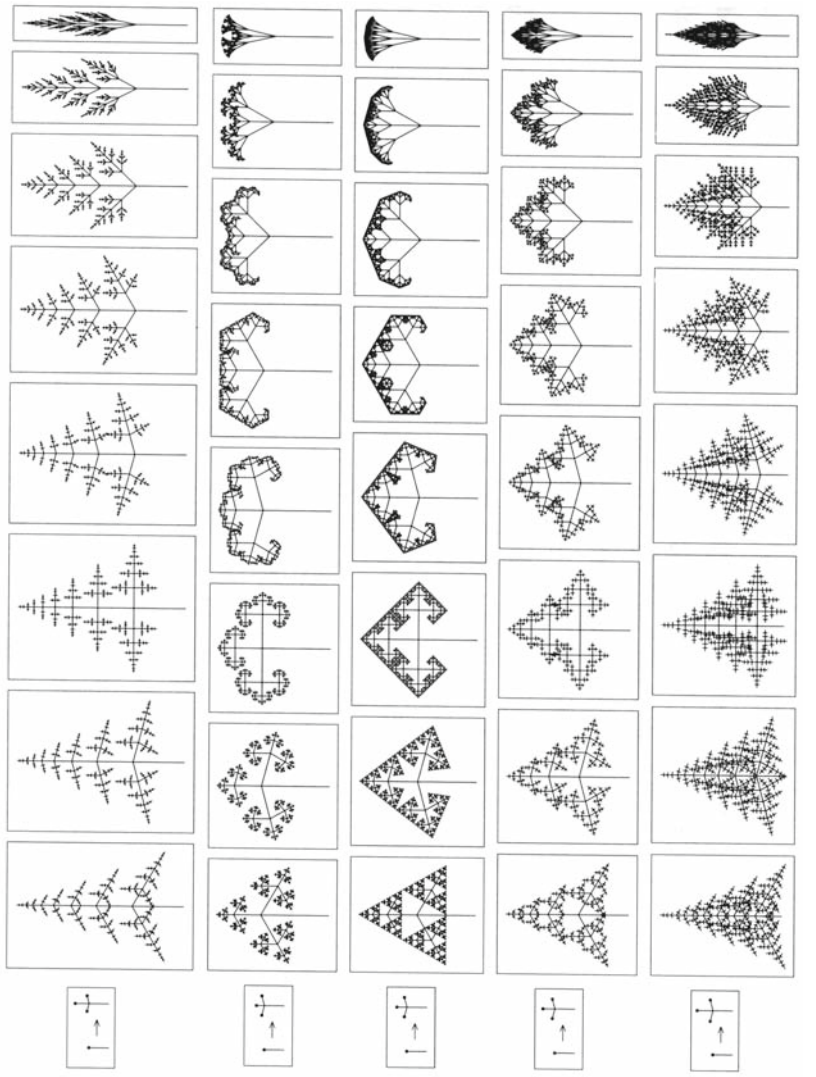

Fig. 15.6 Generation of complex patterns of plant growth by simple substitution systems and simple rules after Wolfram (2002, p. 402) (by courtesy of Stephen Wolfram.

15.2 Transfer of Knowledge from Science to Practice

15.2.1 Concept of Forest Ecosystem Management

A concept of forest and ecosystem management is outlined (Fig. 15.7) to illustrate the potential for putting knowledge transfer into practice. If we assume a particular actual state of a forest, e.g. a pure Norway spruce stand, then forest ecosystem management involves the development of a target state for the system, and the transformation of the actual, into the target state. The development of a target state, in our example a mixed Norway spruce and European beech stand, results from negotiations among the people concerned, e.g. forest owners and stakeholders. In the figure, the negotiation process is symbolised by the round table. The negotiations tend to be dominated by normative values of the society rather than by scientific knowledge. Vague arguments such as "European beech forests are good as they are attractive and natural" whereas "Norway spruce forests are bad as they are un-ecological and artificial" are often much more decisive in this negotiation process than arguments based on scientific knowledge. However, forest science should instil as much system knowledge as possible into the negotiation and decision making process. If the target state is defined clearly and formulated quantitatively, practical rules can be developed as guidelines for the realisation of the target transformation (feedback loop in the middle of Fig. 15.7).

The concept presented in Fig. 15.7 reveals the two most promising gateways for introducing scientific knowledge into forest ecosystem management. The first part is the supply of *target knowledge* for the development of objectives, e.g. deciding which species mixture to optimise the expected forest functions in a municipal forest

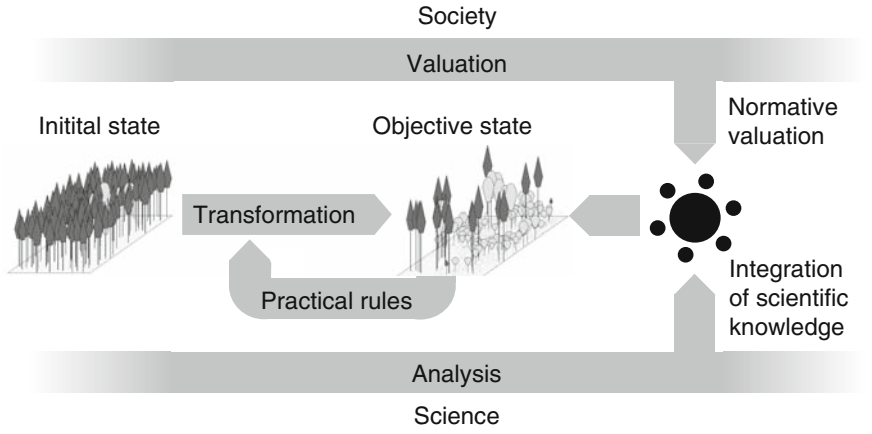

Fig. 15.7 Concept for forest ecosystem management, and the role of knowledge and models: given an initial state (forest stand, landscape unit), the aim of forest management is to transform a system into a target state. The normative values of society and scientific knowledge contribute to the development and achievement of the objective

of recreation, identifying the economic expectations and demand for stand stability in the face of storms given its vicinity to houses. The second part is the supply of *transformation knowledge*, and follows after establishing further development objectives; e.g. which practice to use to transform a pure stand into a mixed stand, which stand thinning regime to use so that a maximum number of trees with a prescribed threshold diameter can be harvested, or which stand treatments should be implemented to maximise stability against wind-throw.

Of course, once developed, target states for forests are not static, but change dynamically. Objectives of forest management are mainly the result of changing environment, societal preferences and economy. We identify five paradigms of forest ecosystem management (Pretzsch 2006; Yaffee 1999). They range from anthropocentric to bio-centric and ecocentric approaches in dealing with forest ecosystems: multiple use, dominant use, environmentally sensitive multiple use, the ecosystem approach, and the ecoregional management paradigm. The next paragraph gives a brief overview of the development of these paradigms in Europe.

The first, very early phase that persisted in Europe until the seventeenth century is characterised by *multiple use* forestry: hunting, beekeeping, grazing in forests, forest assortments, wood harvesting and timber use. The market demand in the seventeenth century (need of daily firewood, wood for furnaces, salt works, the demand of construction timber for rebuilding after 30 years of war) resulted in the second phase, the *dominant use* paradigm. As the forests were heavily exploited, C. von Carlowitz (1645–1714) wrote his "Silvicultura Oeconomica" with the aim of ensuring a sustainable wood supply (Carlowitz 1713). Later, the *environmentally sensitive multiple use* paradigm developed to assure the supply of other goods and services from the forests (supply of high quality fresh water, high recreation value, or biodiversity). The utilisation of timber was concentrated in specific regions, but was limited or restricted in areas where other services had high priorities. The three approaches, *multiple use, dominant use,* and *environmentally sensitive multiple use,* adopt an anthropocentric perspective and seek to foster human use. The *ecosystem approach*, however, takes a biocentric perspective. It originates from the perception that ecosystems are vulnerable, and threatened by exploitation, acid rain, climate change, etc. Sustainable use and conservation have a primary ethical value of their own. This approach furthered system understanding and holistic approaches. Finally, *ecoregional management* shifted the focus away from the biota and species composition of a particular forest towards the regional perspective, including the interaction between different land coverage types such as forests, grassland, arable land, or limnological systems. These five paradigms do not follow one another in a strict chronological order, but rather reflect particular state values within a continuum. Forest ecosystem management moves back and forth within this continuum; e.g. the current neo-liberalism in central Europe drives forestry backwards from the ecosystem approach to the sensitive use, or even to the dominant use paradigm. In contrast, currently, countries in Asia, South America, and Africa are moving gradually from dominant use to an environmentally sensitive use paradigm.

15.2.2 Long-Term Experiments and Models for Decision Support

The training plots and simulation models are the two most helpful support tools for the incorporating system knowledge into the process of developing target states and transformation guidelines. Both provide "if–then" information: how will a stand with a given initial state develop with respect to system variables if different treatments are applied? Experiments with differently treated plots show the consequences of a number of treatment options in nature; that is in the real world. If suitable data is available for model parameterisation and calibration, models deliver different scenarios, i.e. they present the long-term consequences of different options in a virtual reality.

Models provide tools for argumentation and decision at the round table in a range of contexts (Fig. 15.7): in the private forest company, in the state forest service, or in a municipal forest. The strength of models in forest research and management is that they display the consequences of management options "in quick motion". In contrast to many other branches of natural sciences, scenario analyses and models are extremely important in forest research because the lifespan of trees is greater than other organisms, e.g. herbaceous plants. In forests we cannot commence experiments each time we have a new management idea or question and await the results.

The main benefit of models lies in the scenario calculations, which display how a stand with a given initial state will develop with respect to system variables ($i_1 \ldots i_n$) if treatment A, B, C, or D were applied (Fig. 15.8). In our example, we distinguish

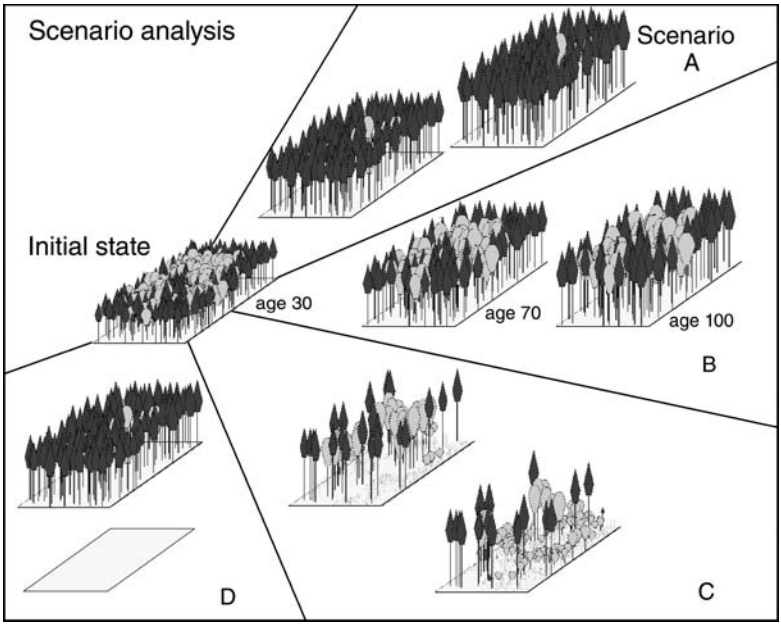

Fig. 15.8 Scenario analysis with forest stand models: given an initial state of an ecosystem, models display the long-term consequences of the different management options A, B, C, and D for achieving different objectives and target states

four scenarios (A) no management, i.e. self-thinning, (B) moderate thinning, (C) threshold diameter thinning, and (D) the classical clear-cut system. How do these alternative treatments affect a given vector of indicator variables? For each scenario considered, advanced models deliver information about the achievement of objectives, such as carbon stock, stability, growth and yield, biodiversity, protective value, and potential forest recreation uses. The scenario calculations can be repeated for different land use options. Given a certain weighting of the different indicator variables, the total value of each option can be assessed, compared with other scenarios, and ranked. In addition, an optimal treatment can be revealed by heuristic optimisation methods (Hanewinkel 2001).

The most important applications of stand models in forestry are for strategic silvicultural planning and continual recording of inventory data and management models. In addition, ecosystem analyses increasingly are being carried out with ecophysiological process models. Stand models pave the way for simulation calculations of entire enterprises, regions or large-scale regions (von Gadow 1996; Lemm 1991; Pretzsch et al. 1998). Here, the long-term effects of controlling measures such as thinning, fertilisation and tree species mixture on forestry also can be predicted.

15.2.2.1 The European Perspective

Whereas in other parts of the world plantations for intensive wood production are separated from forests for conservation of biodiversity or recreation, European forests integrate a multitude of different functions in the one area. Forest ecosystem management in Europe must be sustainable, participatory and transparent. Thus, ecological, economic, and social functions of forests should be considered together, tradeoffs ought to be analysed and decisions

Table 15.1 Pan-European criteria 1–6 and examples for corresponding indicators for sustainable forest development (adapted from MCPFE 1993)

Criteria	Indicators (examples)
1. Forest resources	Forest area, carbon storage, age and volume structure, …
2. Forest ecosystem health and vitality	Chemical soil state, defoliation, deposition of nutrients, pollutants, …
3. Productive functions	Growth, felling budget, non-wood products, …
4. Biological diversity	Tree species's diversity, orientation by nature, share of dead wood, landscape diversity, …
5. Protective functions	Share of forest area for protection of climate, soil, water, …
6. Socio-economic functions	Net financial yield, number of employees, natural scenery, …

made to achieve multipurpose objectives. The principle of integration requires greater knowledge, more negotiation and compromise than does segregation, which is equivalent to a spatial or temporal uncoupling of different forest functions (Spellmann et al. 2001). The more diverse the demands on a forest, the more demanding inventory, planning, and decision-making becomes. However, this highlights the need for appropriate system knowledge, innovative planning methods, efficient knowledge transfer from science to practice, and a clear identification of research demands from the end users of scientific knowledge.

The conferences in Rio 1992, Helsinki 1993, Lisbon 1998, and Vienna 2003 emphasise the demand for quantitative criteria and indicators for steering, controlling and certifying sustainable management. The European countries agreed to a list of criteria and indicators for quantifying ecological, economic and social sustainability (Table 15.1). These criteria reflect the scope of European ecosystem managers' thinking, and are not merely an empty political exercise. Models can apply these variables to ensure that forest managers understand the simulation results and that the most relevant variables for support of decision-making are provided.

Summary

In forest growth research, as in other natural sciences, knowledge is gained in a feedback process between theory development and empirical experimentation. Eight steps are identified in the pathway to systems understanding: (1) observation, measurement and collection of data; (2) description; (3) formulation of hypotheses for elements of system structure or behaviour; (4) test of hypotheses, falsification of trials, experiments and correlation; (5) synthesis into the growth model of all relevant knowledge; (6) test of model hypotheses by simulation; (7) application of the model in research, practice and education; and (8) development of theory, laws, rules and stochastic relationships. These steps are elements of an iterative feedback process, not milestones in a linear, unidirectional process. The way in which reliable knowledge acquired about forest ecosystems can be used successfully for the regulation and sustainable management of these ecosystems is outlined.

(1) The acquisition of knowledge commences with the observation of structures and processes in the real world, and the collection of data. In forest growth research, this database comprises time series obtained from long-term studies that provide information about the entire life of a tree or stand.
(2) The description of tree and stand dynamics represents an important step in the process of understanding, and results in "that-is-so" statements. By description we mean the representation of one or more attributes of the investigated object with descriptive statistics, such as tables, graphs, mean values, frequency distributions, and measures of dispersion.
(3) The formulation of hypotheses is based on the findings from data collected and facts described. Hypotheses are unproven assumptions, set up as methodological principles to help acquire scientific knowledge. A hypothesis differs from

speculation in that it has been tested formally. Hypotheses may address causal relationships, whole chains of causal relationships or sections of the system.

(4) Hypotheses are tested in the following four different ways: for inner contradictions; for logical form, tautology and capacity to disprove; deductively by comparing them with existing hypotheses, relationships, principles or theories; and in a comparison with reality using observation data (experiments, correlation).

(5) Growth models compile reliable knowledge about single aspects of forest growth, forming a picture of the whole system. The systems model with its underlying systems elements and chains of cause and effect may be regarded as a series of hypotheses about the structure and behaviour of the entire system.

(6) The validation of a stand model and the inherent aggregated hypotheses about system elements and causal relationships is based largely on the results of simulation runs. For forest growth research, tree and stand models, and the simulations carried out with them, provide a "tool" for testing hypotheses. Trust in the validity of the assumed chain of hypotheses grows only when tests of model behaviour with a wide range of data cannot be falsified.

(7) As long as the model is not falsified, it is considered to be representative of the real system. Thereafter it can be used to carry out experiments, prognosis and scenario runs. This is particularly useful in forest growth research as long observation periods and intensive field experiments prevent experiments from being carried out in reality. Approved models can be applied in research, practice and education.

(8) Theories, general relationships and stochastic relationships are fundamental to gaining scientific knowledge. They form the basis of new distinct questions. Empirical investigations lead to their development. Models, in particular simulation models, provide a very effective link between theory and empiricism. With the theory of natural selection, the mosaic cycle theory and chaos theory as examples, the role of models in the cognitive process is shown.

(9) To explain the potential for transferring knowledge into practice, we outline a concept for forest and ecosystem management. Forest ecosystem management means the development of a target system state, and the transformation of the system from its actual, state to this target state. The supply of knowledge for the development of the target state, and for transferring the system to the target state is the starting point for applying scientific knowledge to forest ecosystem management.

(10) The development of a target state results from negotiations among the people involved, e.g., forest owners and stakeholders. The negotiations are often dominated by normative values of society rather than by scientific knowledge. However, forest science should instil as much system knowledge as possible into the negotiation and decision-making process.

(11) Training plots and simulation models are the two most helpful tools to support the use of system knowledge to achieve target states and for preparing guidelines for the transfer to this state. Both provide "if-then" scenarios; they display the long-term consequences of management options in time-lapse.

(12) Whereas, in other parts of the world, plantations for intensive wood production are separated from forests designated for conservation of biodiversity or recreation, European forests integrate a multitude of different functions. Ecological, economic, and social functions of forests are considered together, trade-offs need to be analysed and decisions must try to achieve multipurpose objectives as far as possible. This concept requires models that quantify the ecological, economic, and social consequences of selected treatment options to general silvicultural strategies.

References

Aber JD, Federer CA (1992) A generalized, lumped parameter model of photosynthesis, evaporation and net primary production in temperate and boreal forest ecosystems. Oecologia 92: 463–474

Aber JD, Ollinger SV, Federer CA, Reich PB, Goulden ML, Kicklighter DW, Melillo JM, Lathrop RG Jr (1995) Predicting the effects of climate change on water yield and forest production in the northeastern United States. Climate Research 5: 207–222

Aber JD, Ollinger SV, Driscoll CT, Likens GE, Holmes RT, Freuder RJ, Goodale CL (2002) Inorganic nitrogen losses from a forested ecosystem in response to physical, chemical, biotic,and climatic perturbations. Ecosystems 5: 648–658

Abetz P (1974) Zur Standraumregulierung in Mischbeständen und Auswahl von Zukunftsbäumen. Allgemeine Forstzeitschrift 29 (41): 871–873

Abetz P (1975) Entscheidungshilfen für die Durchforstung von Fichtenbeständen (Durchforstungshilfe Fi 1975). Merkbl Forstl Versuchs- u Forschungsanstalten, Bad-Württ 13, Freiburg, 9 pp

Abetz P (1985) Ein Vorschlag zur Durchführung von Wachstumsanalysen im Rahmen der Ursachenerforschung von Waldschäden in Südwestdeutschland. Allgemeine Forst- und Jagdzeitung 156 (9/10): 177–187

Abetz P, Mitscherlich G (1969) Überlegungen zur Planung von Bestandesbehandlungsversuchen. Allgemeine Forst- und Jagdzeitung 140: 175–178

Abetz P, Merkel O, Schaurer E (1964) Düngungsversuche in Fichtenbeständen Südbadens. Allgemeine Forst- und Jagdzeitung 135: 247–262

Akça A (1997) Waldinventur. Cuvillier, Göttingen, 140 pp

Alemdag IS (1978) Evaluation of some competition indexes for the prediction of diameter increment in planted white spruce. Can For Serv, For Mngt Inst, Ottawa, Canada, Inf Rep FMR-X-108, 39 pp

Altenkirch W (1982) Ökologische Vielfalt – ein Mittel natürlichen Waldschutzes? Forst- u Holzwirt 37 (8): 211–217

Altherr E (1969) Das Karlsruher Wasserwerk “Hardtwald” aus forstlicher Sicht. Teil 2. Allgemeine Forst- und Jagdzeitung 140: 213–226

Altherr E (1972) Das Karlsruher Wasserwerk “Hardtwald” aus forstlicher Sicht. Teile 3, 4. Allgemeine Forst- und Jagdzeitung 143: 109–117, 245–253

Altherr E, Zundel R (1966) Das Karlsruher Wasserwerk “Hardtwald” aus forstlicher Sicht. Teil 1. Allgemeine Forst- und Jagdzeitung 137: 237–261

Alveteg M (2004) Projecting regional patterns of future soil chemistry status in Swedish forests using SAFE. Water, Air, and Soil Pollution, Focus 4: 49–59

Ammer U, Schubert H (1999) Arten-, Prozeß- und Ressourcenschutz vor dem Hintergrund faunistischer Untersuchungen im Kronenraum des Waldes. Forstw Cbl (118): 70–87

Ammer U, Detsch R, Schulz U (1995) Konzepte der Landnutzung. Forstw Cbl 114: 107–125

Ancelin P, Courbaud B, Fourcaud TY (2004) Development of an individual tree-based mechanical model to predict wind damage within forest stands. Forest Ecosystem Management 203: 101–121

Anderson MC (1964) Studies of the woodland light climate. Journal of Ecology 52: 27–41

Arheimer B, Andreasson J, Fogelberg S, Johnsson H, Pers BC, Persson K (2005) Climate change impact on water quality: model results from southern Sweden. Ambio 34: 559–566

Arney JD (1972) Computer simulation of Douglas-fir tree and stand growth. PhD thesis, Oregon State University, OR, USA, 79 pp

Arovaara H, Hari P, Kuusela K (1984) Possible effect of changes in atmospheric composition and acid rain on tree growth. An analysis based on the results of Finnish National Forest Inventories. Com Inst Forestalis Fenniae 122, Helsinki, 16 pp

Arp PA, Oja T (1997) A forest soil vegetation atmosphere model (ForSVA), I: Concepts. Ecological Modelling 95: 211–224

Assmann E (1943) Untersuchungen über die Höhenkurven von Fichtenbeständen. Allgemeine Forst- und Jagdzeitung 119: 77–88, 105–123, 133–151

Assmann E (1953/1954) Die Standraumfrage und die Methodik von Mischbestandsuntersuchungen. Allgemeine Forst- und Jagdzeitung 125 (5): 149–153

Assmann E (1961a) Waldertragskunde. Organische Produktion, Struktur, Zuwachs und Ertrag von Waldbeständen. BLV Verlagsgesellschaft, München, Bonn, Wien, 490 pp

Assmann E (1961b) Wald und Zahl. Allgemeine Forstzeitschrift 16 (36): 509–511

Assmann E (1970) The principles of forest yield study. Pergamon, Oxford, New York, 506 pp

Assmann E, Franz F (1963) Vorläufige Fichten-Ertragstafel für Bayern. Forstl Forschungsanstalten München, Inst Ertragskd, 104 pp

Assmann E, Franz F (1965) Vorläufige Fichten-Ertragstafel für Bayern. Forstw Cbl 84 (1): 13–43

Aubreville A (1938) La forêt colonial: les forêts de l'Afrique occidentale Française. Annals of Academy of Science: Paris 9: 1–245

Avery TE, Burkhardt HE (1975) Forest measurements, 3rd edn. McGraw-Hill, New York, 331 pp

Bachmann M (1988) Zuwachsreaktionen geschädigter Fichten, erfaßt nach der Methode von Schweingruber. Diploma thesis, Forest Yield Science, LMU München, MWW-DA 63, 66 pp

Bachmann M (1998) Indizes zur Erfassung der Konkurrenz von Einzelbäumen. Methodische Untersuchung in Bergmischwäldern. Forstl Forschungsber München 171, 261 pp

Bachmann M, Nickel M, Peters A, Schütze G, Seifert T, Steinacker L, Utschig H (2001) Lehrstuhlinterne Zusammenstellung für die Vorgehensweise bei der Anlage und Aufnahme von Versuchsflächen. Unpubl manuscript, Forest Yield Science, TU München, Freising, 40 pp

Badoux E (1946) Krone und Zuwachs. Mitt Schweiz Anst Forstl Versuchswesen 24 (2): 405–513

Bailey RL (1973) Development of unthinned stands of *Pinus radiata* in New Zealand. PhD thesis, Univ Georgia, Athens, GA, 67 pp

Bailey RL, Dell TR (1973) Quantifying diameter distributions with the Weibull function. Forest Science 19: 97–104

Baldwin VC Jr, Burkhart HE, Westfall JA, Peterson KD (2001) Linking growth and yield and process models to estimate impact of environmental changes on growth of Loblolly pine. Forest Science 47: 77–82

Baron JS, Hartman M, Band LE, Lammer R (2000) Sensitivity of a high-elevation Rocky Mountain watershed to altered climate and CO_2. Water Resources Research 36: 89–100

Bartelink HH, Olsthoorn AFM (1999) Mixed forest in western Europe. In: Olsthoorn AFM, Bartelink HH, Gardiner JJ, Pretzsch H, Hekhuis HJ, Franc A (eds) Management of mixed-species forest: Silviculture and economics. IBN Scientific Contributions 15: 9–16

Barton C (2001) The role of allocation in modelling NEE. In: Kirschbaum MUF, Mueller R (eds) CRC-Workshop Proceedings on Net ecosystem exchange. Coop Research Centre Greenhouse Acc, Canberra, Australia, 18-4-0001: 43–49

Batho A, Garcia O (2006) De Perthuis and the origins of site index: a historical note. Forest Biometry, Modelling and Information Sciences (1): 1–10

Battaglia M, Sands PJ (1998) Process-based forest productivity models and their application in forest management. Forest Ecology and Management 102: 13–32

Bätz G, Dörfel H, Eenderlein G, Grimm H, Herrendörfer G, Körschens M, Rasch D, Specht G, Thomas E, Trommer R, Wiegand H (1972) Biometrische Versuchsplanung. VEB Deutscher Landwirtschaftsverlag, Berlin, 355 pp

Bauhus J, Khanna PK, Menden N (2000) Aboveground and belowground interactions in mixed plantations of *Eucalyptus globulus and Acacia mearnsii*. Canadian Journal of Forest Research 30: 1886–1894

Bauknecht K, Kohlas J, Zehnder CA (1976) Simulationstechnik, Entwurf und Simulation von Systemen auf digitalen Rechenautomaten. Springer, Berlin, 218 pp

Baur von F (1876) Die Fichte in Bezug auf Ertrag, Zuwachs und Form. Springer, Berlin, 58 pp

Bayerischer Klimaforschungsverbund (1999) Klimaänderungen in Bayern und ihre Auswirkungen. Abschlussber, München, 90 pp

Becker M (1989) The role of climate on present and past vitality of Silver fir forests in the Vosges mountains of northeastern France. Canadian Journal of Forest Research 19 (9): 1110–1117

Becking JH (1953) Einige Gesichtspunkte für die Durchführung von vergleichenden Durchforstungsversuchen in gleichaltrigen Beständen. Proc 11th IUFRO Congress 1953, Rome, pp 580–582

Bégin E, Bégin J, Bélanger L, Rivest L-P, Tremblay S (2001) Balsam fir self-thinning relationship and its constancy among different ecological regions. Canadian Journal of Forest Research 31: 950–959

Begon ME, Harper JL, Townsend CR (1998) Ökologie. Spektrum Akademischer Verlag, Heidelberg

Bell S (2001) Can a fresh look at the psychology of perception and the philosophy of aesthetics contribute to a better management of forest landscapes. In: Sheppard SRJ, Harshaw HW (eds) Forests and landscapes: linking ecology, sustainability and aesthetics. CABI, New York

Bella IE (1971) A new competition model for individual trees. Forest Science 17 (3): 364–372

Bellmann K, Lasch P, Schulz H, Suckow F (1992) The PEMU forest decline model. In: Nilsson S, Salinas O, Duinker, PN (eds) Future forest resources of western and eastern Europe. International Institute of Applied System Analysis (IIASA), Austria, and Swedish University of Agricultural Science, Sweden, 496 pp

Bennett FA, Clutter JL (1968) Multiple-product yield estimates for unthinned slash pine plantations-pulpwood, sawtimber, gum. USDA Southeast Forest Exp Station, Asheville, NC, Research Paper SE-35, 21 pp

Berg E, Kuhlmann F (1993) Systemanalyse und Simulation für Agrarwissenschaftler und Biologen. Verlag Eugen Ulmer, Stuttgart, 344 pp

Bergel D (1985) Douglasien-Ertragstafel für Nordwestdeutschland. Niedersächs Forstl Versuchsanst, Abt Waldwachstum, 72 pp

Bergh J, Freeman M, Sigurdsson BD, Kellomäki S, Laitinen K, Niinistö S, Peltola H, Linder S (2003) Modelling the short-term effects of climate change on the productivity of selected tree species in Nordic countries. Forest Ecology and Management 183: 327–340

Bert GD, Becker HM (1990) Present and past vitality of Silver fir (Abies alba Mill.) in the Jura mountains. A dendroecological study. Annals of Forest Science 47: 395–412

Bertalanffy von L (1951) Theoretische Biologie: II. Band, Stoffwechsel, Wachstum, 2nd edn. A Francke AG, Bern, 418 pp

Bertalanffy von L (1968) General system theory, foundations, development, applications. George Braziller, New York, 295 pp

Besag JE (1977) In: Ripley BD (1977) Modelling spatial patterns (with discussion). Journal of Royal Statistical Society, Series B 39 (2): 172–212

Biber P (1996) Konstruktion eines einzelbaumorientierten Wachstumssimulators für Fichten-Buchen-Mischbestände im Solling. Ber Forschungszentrum Waldökosysteme, Univ Göttingen, Reihe A, vol 142, 252 pp

Biber P (1997) Analyse verschiedener Strukturaspekte von Waldbeständen mit dem Wachstumssimulator SILVA 2. Berichte der Jahrestagung des Deutschen Verbandes Forstlicher, Sektion Ertragskunde, in Grünberg, pp 100–120

Biber P (1999) Ein Verfahren zum Ausgleich von Randeffekten bei der Berechnung von Konkurrenzindizes. Berichte der Jahrestagung des Deutschen Verbandes Forstlicher, Sektion Ertragskunde, in Volpriehausen, pp 189–202

Biging GS, Dobbertin M (1992) A comparison of distance-dependent competition measures for height and basal area growth of individual conifer trees. Forest Science 38 (3): 695–720

Biging GS, Dobbertin M (1995) Evaluation of competition indices in individual tree growth models. Forest Science 41: 360–377

Bishop ID (2005) Visualization for participation: The advantages of real-time? In: Buhmann E, Paar P, Bishop ID, Lange E (eds) Trends in real-time landscape visualization and participation. Wichmann, Berlin

Bitterlich W (1952) Die Winkelzählprobe. Forstw Cbl 71: 215–225

Blaise F, Saint-André L, Leban JM, Gégout JC, Hervé JC (2002) Connection between forest inventory data and geographic information systems for assessing timber value at the stand level. Proc 4th Workshop IUFRO S5.01.04, Canada, pp 1–12

Böckmann T, Saborowski J, Dam S, Nagel J, Spellmann H (1998) Die Weiterentwicklung der Betriebsinventur in Niedersachsen. Forst u Holz 53: 219–226

Bolte A, Villanueva I (2006) Interspecific competition impacts on the morphology and distribution of fine roots in European beech (*Fagus sylvatica* L.) and Norway spruce (*Picea abies* (L.) Karst.). European Journal of Forest Research 125 (1): 15–26

Bonnemann A (1939) Der gleichaltrige Mischbestand von Kiefer und Buche. Mitt Forstwirtsch u Forstwiss 10: (4), 45 pp

Borggreve B (1891) Die Holzzucht. Ein Grundriß für Unterricht und Wirtschaft, 2nd edn. Paul Parey, Berlin, 363 pp (without appendix)

Bormann FH, Likens GE (1979a) Pattern and process in a forested ecosystem. Springer, New York, 253 pp

Bormann FH, Likens GE (1979b) Catastrophic disturbance and the steady state in northern hardwood forests. American Scientist 67: 660–669

Bortz J (1993) Statistik für Sozialwissenschaftler, 4th edn. Springer, Berlin, 753 pp

Bosc A (2000) EMILION, a tree functional-structural model: presentation and first application to the analysis of branch carbon balance. Annals of Forest Science 57: 555–569

Bossel H (1992) Modellbildung und Simulation: Konzepte, Verfahren und Modelle zum Verhalten dynamischer Systeme. Vieweg, Braunschweig, Wiesbaden, 400 pp

Bossel H (1994) TREEDYN3 Forest simulation model. Ber Forschungszentrum Waldökosysteme, Univ Göttingen, Reihe B, vol 35, 118 pp

Bossel H (1996) TREEDYN3 forest simulation model. Ecological Modelling 90: 187–227

Bossel H, Schäfer H (1989) Generic simulation model of forest growth, carbon and nitrogen dynamics, and application to tropical acacia and European spruce. Ecological Modelling 48: 221–265

Botkin DB, Janak JF, Wallis JR (1972) Some ecological consequences of a computer model of forest growth. Journal of Ecology 60: 849–872

Boysen-Jensen P (1932) Die Stoffproduktion der Planzen, Verlag Gustav Fischer, Jena

Braastad H (1975) Produksjonstabeller og tilvekstmodeller for gran (Yield tables and growth model for Picea abies). Meddelelser fra Norsk Institutt for Skogforskning, No. 31 (9), Ås, Norway, 537 pp

Bradley RT, Christie JM, Johnston DR (1966) Forest management tables. Her Majesty's Stationery Office, London, Forest Comm Booklet 16, 212 pp

Bratley P, Bennett LF, Schrage LE (1983) A guide to simulation. Springer, New York, Berlin, Heidelberg, Tokio, 383 pp

Bristow M, Vanclay JK, Brooks L, and Hunt H (2006) Growth and species interactions of Eucalyptus pellita in a mixed and monoculture plantation in the humid tropics of north Queensland. Forest Ecology and Management 233 (2–3): 285–294

Brockhaus (1994) Die Enzyklopädie: in 24 Bänden, 20th edn. Brockhaus, Leipzig, Mannheim

Brodlie KW, Carpenter LA, Earnshaw RA, Gallop JR, Hubbold RJ, Mumford AM, Osland CD, Quarendon P (1992) Scientific visualization, techniques and applications. Springer, Berlin, 284 pp

Brown GS (1965) Point density in stems per acre. New Zealand Forest Research Note 38, Wellington, New Zealand, 12 pp

Brown S (1997) Estimating biomass and biomass change of tropical forests: a primer (English). FAO Forestry Paper 134, FAO Rome, Italy, 65 pp

Bruce D, Schumacher FX (1950) Forest mensuration, 3rd edn. The American Forestry Series, McGraw-Hill, New York, Toronto, London, 483 pp

Bruce D, de Mars DJ, Reukema DC (1977) Douglas-fir managed yield simulator: DFIT user's guide. USDA Forest and Range Exp Station, Portland, OR, General Technical Report PNW-57, 26 pp

Bruner HD, Moser JW (1973) A Markov chain approach to the prediction of diameter distributions in uneven-aged forest stands. Canadian Journal of Forest Research 3: 409–417

Brünig EF (1971) Forstliche Produktionslehre. Europ Hochschulschr, Reihe XXV, Verlag Herbert Lang, Bern und Peter Lang, Frankfurt, 318 pp

Buckman RE (1962) Growth and yield of Red pine in Minnesota. USDA Lake States Forest Exp Station, St Paul, MN, USA, Techn Bull 1272, 50 pp

Bues C-T (1984) Radiodensitometrische Untersuchung der Variation von Jahrringbreite und Holzdichte in südafrikanischen *Pinus-radiata*-Beständen unter dem Einfluß des Klimas und verschiedener Durchforstungsmaßnahmen. Forstl Forschungsber München 59, 153 pp

Bugmann H (2001) A review of forest gap models. Climatic Change 51: 259–305

Bugmann H, Grote R, Lasch P, Lindner M, Suckow F (1997) A new forest gap model to study the effects of environmental change on forest structure and functioning. In: Mohren GMJ, Kramer K, Sabaté S (eds) Impacts of global change on tree physiology and forest ecosystems. Forestry sciences. Kluwer, Wageningen, The Netherlands, pp 255–261

Bülow von G (1962) Die Sudwälder von Reichenhall. Mitt Staatsforstverwaltung Bayerns 33, München, 316 pp

Bundesministerium für Ernährung, Landwirtschaft und Verbraucherschutz (2005) Die zweite Bundeswaldinventur – BWI2, Der Inventurbericht. Bundesministerium für Ernährung, Landwirtschaft und Verbraucherschutz, Bonn, 231 pp

Burger H (1939) Holz, Blattmenge und Zuwachs. Mitt Schweiz Anst Forstl Versuchswesen 1939–1953, vol 15–29

Burger H (1941) Beitrag zur Frage der reinen oder gemischten Bestände. Mitt Schweiz Anst Forstl Versuchswesen 22, pp 164–203

Burkhart HE, Farrar KD, Amateis RL, Daniels RF (1987) Simulation of individual tree growth and stand development in loblolly pine plantations on cutover, site-prepared areas. Polytechn Inst, Virginia State Univ, Petersburg, VA, FWS-1–87, 47 pp

Burschel P, Huss J (1987) Grundriß des Waldbaus. Pareys Studientexte 49, Hamburg, Berlin, 352 pp

Burschel P, Kürsten E, Larson BC (1993) Die Rolle von Wald und Forstwirtschaft im Kohlenstoffhaushalt, Forstl Forschungsber München 126, 135 pp

Cajander AK (1926) The theory of forest types. Acta forestalia fennica 29, 108 pp

Carlowitz von HC (1713) Sylvicultura Oekonomica oder Haußwirthliche Nachricht und Naturmäßige Anweisung zur wilden Baum-Zucht. JF Braun, Leipzig

Caspersen JP, Pacala SW (2001) Successional diversity and forest ecosystem function. Ecological Research 16: 895–903

Chen SJ, Hwang CL (1992) Fuzzy multiple attribute decision making, methods and applications. In cooperation with Hwang FP. Lectures notes in economics and mathematical systems 375, Springer, Berlin, New York, 536 pp

Clapham AR (1936) Over-dispersion in grassland communities and the use of statistical methods in plant ecology. Journal of Ecology 24: 232–251

Clark PJ, Evans FC (1954) Distance to nearest neighbour as a measure of spatial relationships in populations. Ecology 35 (4): 445–453

Clutter JL (1963) Compatible growth and yield models for Loblolly pine. Forest Science 9: 354–371

Clutter JL, Bennett FA (1965) Diameter distributions in old-field slash pine plantations, Georgia.USDA Southeastern Forest Exp Station, Asheville, NC, Forest Research Council Rep 13, 9 pp

Cochran WG, Cox GM (1957) Experimental designs. Wiley, New York, 611 pp

Comeau PG, Kimmins JP (1986) The relationship between net primary production and foliage nitrogen content, and its application in the modelling of forest ecosystems: a study of Lodgepole pine (*Pinus contorta*). Fujimori T, Whitehead D (eds) Crown and canopy structure in relation to productivity. Forestry and Forest Products Research Institute, Ibaraki, Japan, pp 202–223

Comeau PG, Kimmins JP (1989) Above- and below-ground biomass and production of Lodgepole pine on sites with differing soil moisture regimes. Canadian Journal of Forest Research (19): 447–454

Comins HN, McMurtie RE (1993) Long-term biotic response of nutrient-limited forest ecosystems to CO_2-enrichment: equilibrium behavior of integrated plant-soil modesles. Ecological Applications 3: 666–681

Constable JVH, Friend AL (2000) Suitability of process-based tree-growth models for adressing tree response to climate change. Environmental Pollution 110: 47–59

Constanza R, D'Arge R, De Groot R, Farber S, Grasso M, Hannon B, Limburg K, Naeem Sh, O'Neil R. V, Paruelo J, Raskin R. G, Sutton P, Belt M. van der (1997) The value of the world's ecosystem services and natural capital. Nature 387: 253–260

Cook ER, Kairiukstis LA (eds) (1992) Methods of dendrochronology: Applications in the enviromental sciences. Kluwer, Dordrecht, 394 pp

Cotta von H (1821) Hülfstafeln für Forstwirte und Forsttaxatoren. Arnoldische Buchhandlung, Dresden, 80 pp

Cotta von H (1828) Anweisung zum Waldbau. Arnoldische Buchhandlung, Dresden, Leipzig

Cox F (1971) Dichtebestimmung und Strukturanalyse von Pflanzenpopulationen mit Hilfe von Abstandsmessungen. Mitt Bundesforschungsanstantan Forst- u Holzwirtschaft 87, Reinbek (Hamburg), 184 pp

Cropper WPJ (2000) SPM2: A simulation model for Slash pine (*Pinus elliottii*) forests. Forest Ecology and Management 126: 201–212

Cucchi V, Meredieu C, Stokes A, de Coligny F, Suarez J, Gardiner BA (2005) Modelling the windthrow risk for simulated forest stands of Maritime pine (*Pinus pinaster* Ait.). Forest Ecology and Management 213: 184–196

Cui J, Li C, Sun G, Trettin C (2005) Linkage of MIKE SHE to Wetland-DNDC for carbon budgeting and anaerobic biogeochemistry simulation. Biochemistry 42: 147–167

Curtis, RO (1982) A simple index of stand density of Douglas fir. Forest Science 28: 92–94

Curtis RO, Clendenen GW, de Mars DJ (1981) A new stand simulator for coast Douglas-fir: user's guide. USDA Forest and Range Exp Station, Portland, OR, General Technical Report PNW-128, 79 pp

Curtis RO, Marshall DD, Bell JF (1997) LOGS. A pioneering example of silvicultural research in coast Douglas-fir. Journal of Forestry 95: 19–25

Dale VH, Doyle TW, Shugart HH (1985) A comparison of tree growth models. Ecological Modelling 29: 145–169

David FN, Moore PG (1954) Notes on contagious distributions in plant populations. Annals of Botany of London 18: 47–53

Davidson RL (1969) Effect of root/leaf temperature differentials on root/shoot ratios in some passture grasses and clover. Annals of Botany 33: 561–569

De Wit CT (1982) Simulation of living systems. In: Penning de Vries FWT, Laar HH van (eds) Simulation of plant growth and crop production. Pudoc, Wageningen, pp 3–8 (308 pp)

DeBell DS, Whitesell CD, Schubert TH (1989) Using N2-fixing *Albizia* to increase growth of *Eucalyptus plantations* in Hawai. Forest Science 35: 64–75

Decaudin P, Nayret F (2004) Rendering forest scenes in real-time. In: Hansmann W, Purgathofer W, Sillion F (eds) Eurographics Symposium on Rendering 2004, Aire-la-Ville, Switzerland, pp 93–102

Décourt, N (1965) Les tables de production pour le pin silvestre et le pin laricio de Corse en Sologne. Rev Forestière Francaise 17 (12): 818–831

Décourt N (1966) Die Ertragstafeln in Frankreich. Wiss Zeitschr TU Dresden 15: 359–363

Deegen P, Stümer W, Villa W, Pretzsch H (2000) Zur finanziellen Analyse der Waldpflegeentscheidung bei Berücksichtigung der Biodiversität, dargestellt am Beispiel der Fichte in Sachsen. Forstw Cbl 119: 226–244

Derognat C, Beekmann M, Baeumle M, Martin D, Schmidt H (2003) Effect of biogenic volatile organic compound emissions on tropospheric chemistry during the Atmospheric Pollution Over the Paris Area (ESQUIF) campaign in the Ile-de-France region. Journal of Geophysical Research 108 (D17), 8560

Deusen van PC, Biging GS (1985) STAG a stand generator for mixed species stands, version 2.0. Northern California Forest Yield Cooperative, Department of Forest and Research Management, University of California, Research Note 11, 25 pp

Deussen O, Colditz C, Stamminger M, Drettakis G (2002) Interactive visualization of complex plant ecosystems. In: Moorhead R, Gross M, Joy KI (eds) Proc IEEE Visualization 2002, Boston, MA, pp 219–226

Deutscher Verband Forstlicher Forschungsanstalten (1986a) Empfehlungen für ertragskundliche Versuche zur Beobachtung der Reaktion von Bäumen auf unterschiedliche Freistellung. Allgemeine Forst- und Jagdzeitung 157 (3/4): 78–79

Deutscher Verband Forstlicher Forschungsanstalten (1986b) Empfehlungen für Freistellungsversuche. Versuchsprogramm Fichte mit Z-Baum-Freistellung 1983. Allgemeine Forst- und Jagdzeitung 157 (3/4): 79–82

Deutscher Verband Forstlicher Forschungsanstalten (1988) Empfehlungen zur ertragskundlichen Aufnahme- und Auswertungsmethodik für den Themenkomplex "Waldschäden und Zuwachs". Allgemeine Forst- und Jagdzeitung 159 (7): 115–116

Deutscher Verband Forstlicher Forschungsanstalten (2000) Empfehlungen zur Einführung und Weiterentwicklung von Waldwachstumssimulatoren. Allgemeine Forst- und Jagdzeitung 171 (3): 52–57

Dietrich V (1927) Über den Einbau des Nadelholzes in Laubholgebieten. Forstl Wochenschr Silva 15: 285–291, 295–297

Dietrich. V (1928) Untersuchungen in Mischbeständen. Mitt Württ Forstl Versuchsanst 1: 25–34

Dittmar O, Knapp E, Zehler H (1986) Die langfristige Versuchsfläche Tornau im StFB Dübener Heide, ein Beispiel für den Weg vom Kiefernreinbestand zum Buchennaturverjüngungsbetrieb. Soz Forstw 36: 344–348

Donnelly K (1978) Simulation to determine the variance and edge-effect of total nearest neighbour distance. In: Hodder I (ed) Simulation studies in archaeology. Cambridge University Press, London, pp 91–95 (139 pp)

Dong PH, Kramer H (1987) Zuwachsverlust in erkrankten Fichtenbeständen. Allgemeine Forst- und Jagdzeitung 158 (7/8): 122–125

Dong PH, Laar van A, Kramer H (1989) Ein Modellansatz für die Waldschadensforschung. Allgemeine Forst- und Jagdzeitung 160 (2/3): 28–32

Douglas JB (1975) Clustering and aggregation. Sankhya, Series B 37: 398–417

Droste Hülshoff, von zu B (1969) Struktur und Biomasse eines Fichtenbestandes auf Grund einer Dimensionsanalyse an oberirdischen Baumorganen. PhD thesis, LMU München, 209 pp

Ducey MJ, Larson BC (1999) Accounting for bias and uncertainty in nonlinear stand density indices. Forest Science 45 (3): 452–457

Dudek A, Ek AR (1980) A bibliography of worldwide literature on individual tree based stand growth models. Dep Forest Resources, Univ of Minnesota, Staff Paper Series, 33 pp

Ďurský J (1993) Kvantifikácia prírastkových zmien smreka v porastoch poškodzovaných imisiami (Quantifizierung von Zuwachsänderungen in immissionsgeschädigten Wälder). KDP, Zvolen, 131 pp

Ďurský J (1994) Kvantifikácia prírastkových zmien jednotlivých stromov v oblasti horná Orava (The Quantification of Increment Changes of The Trees in Horná Orava Area). Zpravodaj Beskydy 6: 205–208

Ďurský J (1997) Modellierung der Absterbeprozesse in Rein- und Mischbeständen aus Fichte und Buche. Allgemeine Forst- und Jagdzeitung 168 (6/7): 131–134

Ďurský J (2000) Einsatz von Waldwachstumssimulatoren für Bestand, Betrieb und Großregion. Habil, Forstwiss Fak, TU München, Freising, 223 pp

Ďurský J, Šmelko Š (1994) Kvantifikácia prírastkových zmien smreka v oblasti horná Orava (Quantification of Increment Changes of Norway Spruce in the Area of Horná Orava). Lesnictví-Forestry 40 (1/2): 42–47

Duschl C, Suda M (2002) Simulation of management strategies in the forest estate model "Germany". Forstw Cbl 121 (Suppl 1): 89–107

Eberhardt LL (1967) Some developments in "distance sampling". Biometrics 23: 207–216

Eckersten H (1994) Modelling daily growth and nitrogen turnover for a short-rotation forest over several years. Forest Ecology and Management 69: 57–72

Eckmüllner O, Fleck W (1989) Begleitdokumentation zum Wachstumssimulationsprogramm WASIM Version 1.0. Inst Forstl Ertragslehre, Univ für Bodenkultur, Wien, 30 pp

Eckstein D, Breyne A, Aniol RW, Liese W (1981) Dendroklimatologische Untersuchungen zur Entwicklung von Straßenbäumen. Forstw Cbl 100: 381–396

Ehrenspiel G (1970) Auswertung des Einzelbaumdüngungsversuches. Berichte der Jahrestagung des Deutschen Verbandes Forstlicher, Sektion Ertragskunde, in Mainz, pp 28–30

Eichhorn F (1902) Ertragstafeln für die Weißtanne. Verlag Julius Springer, Berlin, 81 p

Eid T, Tuhus E (2001) Models for individual tree mortality in Norway. Forest Ecology and Management 154: 69–84

Ek AR, Dudek A (1980) Development of individual tree based stand growth simulators: progress and applications. Department of Forest Resources, University of Minnesota, Staff Paper 20, 25 pp

Ek AR, Monserud RA (1974) Trials with program FOREST: growth and reproduction simulation for mixed species even- or uneven-aged forest stands. In: Fries J (ed.) Growth models for tree and stand simulation. Royal College of Forestry, Stockholm, Sweden, Research Notes 30, pp 56–73 (379 pp)

Elfving B, Tegnhammar L (1996) Trends of tree growth in Swedish forests 1953–1992: an analysis based on sample trees from the national forest inventory. Scandinavian Journal of Forest Research 11: 26–37

Ellenberg H (1963) Vegetation Mitteleuropas mit den Alpen: In kausaler, dynamischer und historischer Sicht. Verlag Eugen Ulmer, Stuttgart

Ellenberg H, Einem von M, Hudeczek H, Lade HJ, Schumacher HU, Schweingruber M, Wittekindt H (1985) Über Vögel in Wäldern und die Vogelwelt des Sachsenwaldes. Hamb Avifaun Beitr 20, pp 1–50

Ellenberg H, Mayer R, Schauermann, J (1986) Ökosystemforschung – Ergebnisse des Sollingprojektes. Verlag Eugen Ulmer, Stuttgart, 507 pp

Elling W (1993) Immissionen im Ursachenkomplex von Tannenschädigung und Tannensterben. Allgemeine Forst- und Jagdzeitung 48 (2): 87–95

Enquist BJ, Niklas KJ (2001) Invariant scaling relations across tree-dominated communities. Nature 410: 655–660

Enquist BJ, Brown JH, West GB (1998) Allometric scaling of plant energetics and population density. Nature 395: 163–165

Enquist BJ, West GB, Charnov EL, Brown JH (1999) Allometric scaling of production and life-history variation in vascular plants. Nature 401: 907–911

Faber PJ (1966) The growth of the Red oak in the Netherlands. Ned Bosbouw Tijdschr 38: 357–374

Faber PJ (1981) Die Standflächenschätzung über den Distanzfaktor. Berichte der Jahrestagung des Deutschen Verbandes Forstlicher, Sektion Ertragskunde, in Soest, pp 87–95

Faber PJ (1983) Concurrentie en groei van de bomen binnen een opstand (Konkurrenz und Wachstum der Bäume in einem Waldbestand). Pijksinstituut voor onderzoek in de bos- en landschapsbouw "De Dorschkamp". Uitvoerig verslag, Wageningen, vol 18 (1), 116 pp
Fabian P (1991) Klima und Wald – Perspektiven für die Zukunft. Forstw Cbl 110: 286–304
FAO (2001) Global Forest Resources Assessment 2000. FAO, Rome, Italy
FAO (2005) Global Forest Resources Assessment 2005. FAO, Rome, Italy
Farquhar GD, Caemmerer von S, Berry JA (1980) A biochemical model of photosynthetic CO2 assimilation in leaves of C3-species. Planta 149: 78–90
Farquhar GD, Caemmerer von S, Berry JA (2001) Models of photosynthesis. Plant Physiology 125: 42–45
Feduccia DP, Dell TR, Mann WF, Polmer BH (1979) Yields of unthinned Loblolly pine plantations on cutover sites in the West Gulf region. USDA Southern Forest Exp Station, New Orleans, LA, Research Paper SO-148, 88 pp
Fink A (1969) Planzenernährung in Stichworten. Verlag Ferdinand Hirt, Zug, 200 pp
Fish H, Lieffers VJ, Silins U, Hall RJ (2006) Crown shyness in Lodgepole pine stands of varying stand height, density, and site index in the upper foothills of Alberta. Canadian Journal of Forest Research 36 (9): 2104–2111
Flury Ph (1926) Über Zuwachs und Ertrag reiner und gemischter Bestände. Schweiz Z Forstw 77: 337–342
Flury P (1931) Untersuchungen über Zuwachs, Massen- und Geldertrag reiner und gemischter Bestände. Mitt Schweiz Anst Forstl Versuchswesen 16, pp 452–472
Foerster W (1990) Zusammenfassende ertragskundliche Auswertung der Kiefern-Düngungsversuchsflächen in Bayern. Forstl Forschungsber München 105, pp 1–328 pp
Foerster W (1993) Der Buchen-Durchforstungsversuch Mittelsinn 025. Allgemeine Forstzeitschrift 48: 268–270
Fogel R (1983) Root turnover and productivity of coniferous forests. Plant and Soil 71: 75–85
Forrester, JW (2007) System dynamics – the next fifty years. System Dynamics Review 23 (2/3): 359–370
Franc A, Gourlet-Fleury S, Picard N (2000) Une introduction à la modélisation des forêts hétérogènes. ENGREF, Nancy, 312 pp
Franz F (1965) Ermittlung von Schätzwerten der natürlichen Grundfläche mit Hilfe ertragskundlicher Bestimmungsgrößen des verbleibenden Bestandes. Forstw Cbl 84: 357–386
Franz F (1967a) Düngungsversuche und ihre ertragskundliche Interpretation. Sonderdruck Kolloquiums für Forstdüngung in Jyväskylä/Finnland, Internat Kali-Inst, Bern, Schweiz, pp 91–110
Franz F (1967b) Ertragsniveau-Schätzverfahren für die Fichte anhand einmalig erhobener Bestandesgrößen. Forstw Cbl 86 (2): 98–125
Franz F (1968) Das EDV-Programm STAOET – zur Herleitung mehrgliedriger Standort-Leistungstafeln. Unpublished manuscript, München
Franz F (1972) Gedanken zur Weiterführung der langfristigen ertragskundlichen Versuchsarbeit. Forstarchiv 43 (11): 230–233
Franz F (1981) Entwurf eines Konzeptes für zeitvariable reaktionskinetische Untersuchungen an ausgewählten Probestämmen (Zentralbaum-Konzept). Berichte der Jahrestagung des Deutschen Verbandes Forstlicher, Sektion Ertragskunde, in Soest, pp 133–142
Franz F (1983) Auswirkungen der Walderkrankungen auf Struktur und Wuchsleistung von Fichtenbeständen. Forstw Cbl 102: 186–200
Franz F, Pretzsch H (1988) Zuwachsverhalten und Gesundheitszustand der Waldbestände im Bereich des Braunkohlekraftwerkes Schwandorf. Forstl Forschungsber München 92, 169 pp
Franz F. Bachler J, Deckelmann B, Kennel E, Kennel R, Schmidt A, Wotschikowsky U (1973) Bayerische Waldinventur 1970/71, Inventurabschnitt I: Großrauminventur Aufnahme- und Auswertungsverfahren. Forstl Forschungsber München 11, 143 pp
Fraser AR (1977) Triangle Based Probability Polygons for Forest Sampling. Forest Science 23 (1): 111–121
Freese F (1960) Testing accuracy. Forest Science 6 (2): 139–145

Freese F (1964) Linear regression methods for forest research. US Forest Service Research Paper, Forest Products Laboratory, Washington, 137 pp
Friend AD, Stevens AK, Knox RG, Cannell MGR (1997) A process-based, terrestrial biosphere model of ecosystem dynamics (Hybrid v3.0). Ecological Modelling 95: 249–287
Fries J (1964) Vartbjörkens produktion in Svealand oach södra Norrland. Studia Forestalia Suecica 14, 303 pp
Fries J (1966) Mathematisch-statistische Probleme bei der Konstruktion von Ertragstafeln. Tagungsber Internation Ertragskundetagung 1966, Wien, 77 pp
Fries J (ed) (1974) Growth models for tree and stand simulation. Royal College of Forestry, Stockholm, Sweden, Research Notes 30, 379 pp
Fritts HC (1976) Tree rings and climate. Academic, London, 567 pp
Frivold LH, Frank J (2002) Growth of mixed birch-coniferous stands in relation to pure coniferous stands at similar sites in South-eastern Norway. Scandinavian Journal of Forest Research 17: 139–149
Frivold LH, Kolström T (1999) Yield and treatment of mixed stands of boreal tree species in Fennoscandia. In: Olsthoorn AFM, Bartelink HH, Gardiner JJ, Pretzsch H, Hekhuis HJ, Franc A (eds) Management of mixed-species forest: Silviculture and economics. IBN Scientific Contributions 15, pp 37–45
Füldner K (1995) Strukturbeschreibung von Buchen-Edellaubholz-Mischwäldern. PhD thesis Forstl Fak Göttingen, Cuvillier Verlag, Göttingen: 146 + annex
Füldner K (1996) Die "Strukturelle Vierergruppe" – ein Stichprobenverfahren zur Erfassung von Strukturparametern in Wäldern. In: Beitr zur Waldinventur. Festschrift on the 60th anniversary of Prof. Dr. Alparslan Akça. Cuvillier, Göttingen, 139 pp
Gadow von K (1986) Observation on self-thinning in pine plantations. South African Journal of Science 82: 364–368
Gadow von K (1987) Untersuchungen zur Konstruktion von Wuchsmodellen für schnellwüchsige Plantagenbaumarten. Forstl Forschungsber München 77, 147 pp
Gadow von K (1993) Zur Bestandesbeschreibung in der Forsteinrichtung. Forst u Holz 48 (21): 602–606
Gadow von K (2005) Forsteinrichtung. Analyse und Entwurf der Waldentwicklung. Univ-Verlag Göttingen, Göttingen, 342 pp
Gadow von K, Hui GY (1999) Modelling forest development. Kluwer, Dordrecht, 213 pp
Ganghofer von A (1877) Das forstliche Versuchswesen. Selfpubl by editor, vol 1(1), München, 176 pp
Ganghofer von A (1881) Das Forstliche Versuchswesen, Band I. Augsburg, 1881, 505 pp
Garber SM, Maguire DA (2004) Stand productivity and development in two mixed-species spacing trials in the central Oregon Cascades. Forest Science 50 (1): 92–10
Gash JHC (1979) An analytical model of rain fall interception by forests. Quarterly Journal of Royal Meteorological Society 105: 43–55
Gayer K (1886) Der gemischte Wald, seine Begründung und Pflege, insbesondere durch Horst- und Gruppenwirtschaft. Paul Parey, Berlin
Gehrhardt E (1909) Ueber Bestandes-Wachstumsgesetze und ihre Anwendung zur Aufstellung von Ertragstafeln. Allgemeine Forst- und Jagdzeitung 85: 117–128
Gehrhardt E (1923) Ertragstafeln für Eiche, Buche, Tanne, Fichte und Kiefer. Springer, Berlin, 46 pp
Gehrhardt E (1930) Ertragstafeln für reine und gleichartige Hochwaldbestände von Eiche, Buche, Tanne, Fichte, Kiefer, grüner Douglasie und Lärche. Springer, Berlin, 73 pp
Gerecke KL (1986) Zuwachsuntersuchungen an vorherrschenden Tannen aus Baden-Württemberg. Allgemeine Forst- und Jagdzeitung 157 (3/4): 59–68
Gertner G, Guan BT (1992) Using an error budget to evaluate the importance of component models within a large-scale simulation model. In: Franke J, Röder A (eds) Mathematical Modelling of Forest Ecosystems. Workshop Proc Forstl Versuchsanst Rheinland-Pfalz and Zentr für Prakt Math, JD Sauerländer's Verlag, Frankfurt am Main, pp 62–74 (174 pp)

Gilet G, Meyer A, Neyret F (2005) Point-based rendering of trees. Galin E, Poulin P (eds) Proc Eurographics Workshop on Natural Phenomena 2005, Dublin, Ireland, pp 67–72 DOI: 10.2312/NPH/NPH05/067-072
Gompertz B (1825) On the nature of the function expressive of the law of human mortality, and on a new mode of determining the value of life contingencies. Philosophical Transactions of Royal Society (London) 115: 513–585
Gorham E (1979) Shoot height, weight and standing crop in relation to density of monospecific plant stands. Nature 279: 148–150
Grier CC, Logan RS (1977) Old-growth Pseudotsuga menziesii communities of a western Oregon watershed: Biomass distribution and production budgets. Ecological Monographs 47: 373–400
Grote R, Erhard M (1999) Simulation of tree and stand development under different environmental conditions with a physiologically based model. Forest Ecology and Management 120: 59–76
Grote R, Pretzsch H (2002) A model for individual tree development based on physiological processes. Plant Biology 4: 167–180
Grote R, Suckow F, Bellmann K (1996) A physiology-based growth model for simulations under changing conditions of climate, nitrogen availability, air pollution and ground cover competition. Conf Effects of Environmental Factors on Tree and Stand Growth in Berggießhübel, TU Dresden, Germany, pp 68–77
Grote R, Bellmann K, Erhard M, Suckow F (1997) Evaluation of the forest growth model FORSANA. Potsdam Institute of Climate Impact Research, Potsdam, Rep 32, 64 pp
Grundner F (1913) Normalertragstafeln für Fichtenbestände. Springer, Berlin, 24 pp
Grundner F, Schappach A (1952) Massentafeln zur Bestimmung des Holzgehaltes stehender Waldbäume und Bestände. Paul Parey, Berlin
Guttenberg von A (1915) Wachstum und Ertrag der Fichte im Hochgebirge. Deuticke, Wien, Leipzig, 153 pp
Haber W (1982) Was erwarten Naturschutz und Landschaftspflege von der Waldwirtschaft? Schr Dt Rates für Landespflege 40: 962–965
Halaj J, Grek J, Panek F, Petras R, Rehak J (1987) Rastove tabulky hlavnych drevin CSSR (Die Ertragstafeln der Hauptbaumarten in der CSSR). Priroda, 361 pp
Hamilton GJ, Christie JM (1973) Construction and application of stand yield tables. British Forest Commission Research and Development, London, Paper 96, 14 pp
Hampel R (1955) Forstliche Ertragselemente. Mitt Forstl Bundesversuchsanst Wien 51, 187 pp
Hanewinkel M (2001) Neuausrichtung der Forsteinrichtung als strategisches Management instrument. Allgemeine Forst- und Jagdzeitung 172: 203–211
Hanewinkel M, Pretzsch H (2000) Modelling the conversion from even-aged stands of Norway spruce (*Picea abies* L. Karst.) with a distance-dependent growth simulator, Forest Ecology and Management 134: 55–70
Hari, P (1985) Theoretical aspects of eco-physiolocigal research. In: Tigerstedt PMA, Puttonen P, Koski V (eds) Crop physiology of forest trees. Helsinki University Press, pp 21–30 (336 pp)
Hari P, Arovaara H, Rauemaa T, Hautojärvi A (1984) Forest growth and effects of energy production: a method for detecting trends in the growth potential of trees. Canadian Journal of Forest Research 14: 437–440
Harper JL (1977) Population Biology of Plants. Academic Press, London, New York
Hart HMJ (1928) Stamtal en dunning: een oriënteerend onderzoek naar de beste plantwijdte en dunningswijze voor den djati. Mededeelingen van het Proefstation voor het Boschwezen 21, Veenman and Zonen, Wageningen, 219 pp
Hartig GL (1791) Anweisung zur Holzzucht für Förster. Neue Akademische Buchhandlung, Marburg
Hartig GL (1795) Anweisung zu Taxation der Forsten oder zur Bestimmung des Holzertrages der Wälder. Heyer, Gießen, 166 pp
Hartig GL (1804) Anweisung zur Taxation und Beschreibung der Forste. Gießen und Darmstadt, bey Georg Friedrich Heyer
Hartig R (1868) Die Rentabilität der Fichtennutzholz- und Buchenbrennholzwirtschaft im Harze und im Wesergebirge. Cotta, Stuttgart, 199 pp

Hartig T (1847) Vergleichende Untersuchungen über den Ertrag der Rotbuche. Förstner Verlag, Berlin, 148 pp

Hartman MD, Baron JS, Ojima DS (2006) Application of a coupled ecosystem-chemical equilibrium model, DayCent-Chem, to stream and soil chemistry in a Rocky Mountain watershed. Ecological Modelling 200: 493–510

Hasenauer H (1994) Ein Einzelbaumwachstumssimulator für ungleichaltrige Kiefern- und Buchen-Fichtenmischbestände. Forstl Schr Univ Bodenkultur Wien, 152 pp

Hasenauer H (1999) Methodische Aspekte bei der Evaluierung von Baummodellen, Berichte der Jahrestagung des Deutschen Verbandes Forstlicher, Sektion Ertragskunde, in Volpriehausen, pp 45–53

Hasenauer H, Amateis RL (1998) Crown efficiency in a Loblolly pine (Pinus taeda) spacing experiment. Canadian Journal of Forest Research 28 (9): 1344–1351

Hattemer HH (1994) Die genetische Variation und ihre Bedeutung für Wald und Waldbäume. J Forestier Suisse 145 (12): 953–975

Hauhs M, Kastner-Maresch A, Rost-Siebert K (1995) A model relating forest growth to ecosystem-scale budgets of energy and nutrients. Ecological Modelling 83: 229–243

Hausser K, Assmann E, Franz F, Gussone HA, Kennel R, Mitscherlich G, Seibt G, Ulrich B, Weihe J (1969) Empfehlungen für das Planen, Anlegen, Behandeln und Auswerten forstlicher Düngungsversuche. Allgemeine Forst- und Jagdzeitung 140 (6): 121–132

He HS, Shang BZ, Crow TR, Gustafson EJ, Shifley SR (2004) Simulating forest fuel and fire risk dynamics across landscapes – LANDIS fuel module design. Ecological Modelling 180: 135–151

Hector A, Schmid B, Beierkuhnlein C, Caldeira MC, Diemer M, Dimitrakopoulus PG, Finn JA, Freitas H, Giller PS, Good J, Harris R, Högberg P, Huss-Danell K, Joshi J, Jumpponen A, Körner C, Leadley PW, Loreau M, Minns A, Mulder CPH, O'Donovan G, Otway SJ, Pereira JS, Prinz A, Read DJ, Scherer-Lorenzen M, Schulze ED, Siamantziouras ASD, Spehan EM, Terry AC, Troumbis AY, Woodward FI, Yachi S, Lawton JH (1999) Plant diversity and productivity experiments in European grasslands. Science 286: 1123–1127

Hegyi F (1974) A simulation model for managing Jack-pine stands. In: FRIES J (ed) Growth models for tree and stand simulation. Royal College of Forest, Stockholm, Sweden, pp 74–90 (379 pp)

Helms JA (1998) The dictionary of forestry. The Society of American Foresters, Bethesda, MD

Hennert CW (1791) Anweisung zur Taxation der Forsten; nach der hierueber ergangenen und bereits bey vielen Forsten in Ausuebung gebrachten Koenigl. Preuss. Verordnungen. Theil 1. Nicholai, Berlin, Stettin, 297 pp

Herms DA, Mattson WJ (1992) The dilemma of plants: To grow or defend. Quarterly Reviews of Biology 67: 283–335

Heyer G (1845) Wedekinds Neue Jahrb. 30: 1–127

Heyer G (1852) Über die Ermittlung der Masse, des Alters und des Zuwachses der Holzbestände. Verlag Katz, Dessau, 150 pp

Hickler T, Smith B, Sykes MT, Davis MB, Sugita S, Walker K (2004) Using a generalized vegetation model to simulate vegetation dynamics in northeastern USA. Ecology 85: 519–530

Hilf RB (1938) Der Wald in Geschichte und Gegenwart, Wald und Weidwerk. Akad Verlagsges Athenaion, Potsdam, 290 pp

Hoel PG (1943) On indices of dispersion. Annals of Mathematical Statistics 14: 155–162

Hoffmann F (1995) FAGUS, a model for growth and development of beech. Ecological Modelling 83: 327–348

Hofmann F (1923) Mischungen aus Buchen mit Nadelholz, insbesondere mit der Fichte und Tanne. Allgemeine Forst- und Jagdzeitung 99: 273–281

Hong B, Swaney DP, Weinstein DA (2006) Simulating spatial nitrogen dynamics in a forested reference watershed, Hubbard Brook Watershed 6, New Hampshire, USA. Landscape Ecology 21: 195–211

Hopkins P (1954) A new method for determining the type of distribution of plant individuals. Annals of Botany 18: 213–227

Hoyer G. E (1975) Measuring and interpreting Douglas-fir management practices. Washington State Department of Natural Resources, Olympia, WA, Rep 26, 80 pp

Hradetzky J (1972) Modell eines integrierten Ertragstafel-Systems in modularer Form. PhD thesis, Univ Freiburg, 172 pp

Hundeshagen JC (1823–45) Beiträge zur gesamten Forstwirtschaft, Verlag Laupp, Tübingen, vol 1 (1) (1824), 191 pp; vol 1 (2) (1825), 206 pp; vol 1 (3) (1823–24), 161 pp; vol 2 (1) (1825), 136 pp; vol 2 (2) (1827), 247 pp; vol 2 (3) (1829), 180 pp; vol 3a (1) (1833), 222 pp; vol 3b (2) (1845), 190 pp

Huston M, DeAngelis D, Post W (1988) New computer models unify ecological theory. Bio Science 38 (10): 682–691

Huth A, Ditzer Th, Bossel H (1998) The Rain Forest Growth Model FORMIX3: model description and analysis of forest growth and logging scenarios for the Deramakot Forest Reserve (Malaysia). In: Seifert HSH, Vlek PLG, Weidelt H-J (eds) Series: Göttinger Beiträge zur Land- und Forstwirtschaft in den Tropen und Subtropen 124. Verlag Erich Goltze, Göttingen, 182 pp

Huxley JS (1932) Problems of relative growth. Lincoln Mac Veagh, The Dial, New York

Huxley JS, Teissier G (1936) Terminology of relative growth. Nature 137: 780–781

IPCC (2000) Land Use, Land-Use Change and Forestry. 6th Conference of the Parties to the United Nations Framework Convention on Climate Change in The Hague, The Netherlands

IPCC (2001) Climate Change: The Scientific Basis. Cambridge Univ Press, Cambridge

IUFRO (1993) IUFRO Centennial, Organisationskomitee "100 Jahre IUFRO". 100- Anniversary Proc, Berlin, Eberswalde, 544 pp

Jack WH (1968) Single trees sampling in evenaged plantations for survey and experimentation. 14th IUFRO Congress, München, pp 379–403

Jacobsen C, Rademacher P, Meesenburg H, Meiwes KJ (2003) Gehalte chemischer Elemente in Baumkompartimenten. Literaturstudie und Datensammlung. Ber Forschungszentrum Waldökosysteme, Univ Göttingen, Reihe B, vol 69, 81 pp

Jeffers JNR (1960) Experimental design and analysis in forest research. Almqvist and Woksell, Stockholm, 172 pp

Jensen AM (1983) Growth of Silver fir (*Abies alba* Mill.) compared with the growth of Norway spruce (*Picea abies* (L) Karst.) in pure and mixed stands on sandy soils in the western parts of Denmark. Department of Forestry, Royal Veterinary and Agricultural University, London, Rep 14, 498 pp

Johann K (1976) Ein integriertes Konzept für die Aufnahme und Auswertung ertragskundlicher Dauerversuche, Berichte der Jahrestagung des Deutschen Verbandes Forstlicher, Sektion Ertragskunde, in Paderborn, 12 pp

Johann K (1982) Der "A-Wert"– ein objektiver Parameter zur Bestimmung der Freistellungsstärke von Zentralbäumen. Berichte der Jahrestagung des Deutschen Verbandes Forstlicher, Sektion Ertragskunde, in Weibersbrunn, pp 146–158

Johann K (1983) Beispiele "A-Wert"-gesteuerter Z-Baum-Freistellung. Anwendungen im Versuchswesen und in der Praxis, Berichte der Jahrestagung des Deutschen Verbandes Forstlicher, Sektion Ertragskunde, in Neuhaus/Solling, pp 3/1–3/14

Johann K (1990) Adjustierung von Bestandeshöhenkurvenscharen nach der Methode des Koeffizientenausgleichs. Meth Proposal Working Group "Auswertemethodik bei langfristigen Versuchen" der Sek Ertragskd Dt Verb Forstl Forschungsanstalten, München, 2 pp

Johann K (1993) DESER-Norm 1993. Normen der Sektion Ertragskunde im Deutschen Verband Forstlicher Forschungsanstalten zur Aufbereitung von waldwachstumskundlichen Dauerversuchen. Berichte der Jahrestagung des Deutschen Verbandes Forstlicher, Sektion Ertragskunde, in Unterreichenbach-Kapfenhardt, pp 96–104

Jordan W (1877) Handbuch der Vermessungskunde. Verlag JB Metzler'schen Buchhandlung, Stuttgart, 717 pp

Jørgensen U, Schelde K (2001) Energy crop water and nutrient use efficiency. Prepared for the International Energy Agency IEA Bioenergy Task 17, Short Rotation Crops. Danish Institute of Agricultural Sciences (DIAS), Department of Crop Physiology and Soil Science, Research Centre Foulum, Tjele, Denmark, 11 pp

Judeich F (1871) Die Forsteinrichtung. Schönfeld Verlag, Dresden, 388 pp
Jüttner O (1955) Eichenertragstafeln. In: Schober R (ed) (1971) Ertragstafeln der wichtigsten Baumarten. JD Sauerländer's Verlag, Frankfurt am Main, pp 12–25, 134–138
Kahn M (1994) Modellierung der Höhenentwicklung ausgewählter Baumarten in Abhängigkeit vom Standort. Forstl Forschungsber München 141, 221 pp
Kahn M, Pretzsch, H (1997) Das Wuchsmodell SILVA 2.1 – Parametrisierung für Rein- und Mischbestände aus Fichte und Buche. Allgemeine Forst- und Jagdzeitung 168 (6/7): 115–123
Kathirgamatamby N (1953) Note on the Poisson index of dispersion. Biometrika 40: 225–228
Kató F (1979) Qualitative Gruppendurchforstung zur Rationalisierung der Buchenwirtschaft. Allgemeine Forstzeitschrift 34 (8): 173–177
Kató F (1987) Wirtschaftliche Bewertung der "Qualitativen Gruppendurchforstung" nach 20-jähriger Beobachtung. Forst- u Holzwirt 42 (14): 371–373
Kató F, Müldner D (1978) Über die soziologische und qualitative Zusammensetzung gleichaltriger Buchenbestände. Schr Forstl Fak Univ Göttingen u Niedersächs Forst Versuchsanst, JD Sauerländer's Verlag, Frankfurt am Main, vol 51, 110 pp
Kauppi PE, Mielikäinen K, Kuusela K (1992) Biomass and carbon budget of European forests, 1971 to 1990. Science 256: 70–74
Keller W (1978) Einfacher ertragskundlicher Bonitätsschlüssel für Waldbestände in der Schweiz. Mitt Eidg Forschungsanstalten Wald Schnee Landschaft 54 (1): 3–98
Keller W (1995) Zur Oberhöhenberechnung in Mischbeständen aus standortkundlicher Sicht. Berichte der Jahrestagung des Deutschen Verbandes Forstlicher, Sektion Ertragskunde, in Joachimsthal, pp 52–60
Kellomäki S, Väisänen H (1995) Model computations on the impact of changing climate on natural regeneration of Scots pine in Finland. Canadian Journal of Forest Research 25: 929–942
Kellomäki S, Väisänen H (1997) Modelling the dynamics of the forest ecosystem for climate change studies in the boreal conditions. Ecological Modelling 97: 121–140
Kellomäki S, Väisänen H, Strandman H (1993) FinnFor: a model for calculating the response of boreal forest ecosytems to climate change. University of Joensuu, Joensuu, Finland, Research Notes 6, 120 pp
Kelty MJ (1992) Comparative productivity of monocultures and mixed stands. In: Kelty MJ, Larson BC, Oliver CD (eds) The ecology and silviculture of mixed-species forests. Kluwer, Dordrecht, pp 125–141
Kelty MJ, Cameron IR (1995) Plot design for the analysis of species interactions in mixed stands. Commonwealth Forestry Review 74: 322–332
Kenk G, Spiecker H, Diener G (1991) Referenzdaten zum Waldwachstum. Kernforschungszentrum Karlsruhe, KfK-PEF 82, 59 pp
Kennel R (1965a) Untersuchungen über die Leistung von Fichte und Buche im Rein- und Mischbestand. Allgemeine Forst- und Jagdzeitung 136: 149–161, 173–189
Kennel R (1965b) Die Herleitung verbesserter Formzahltafeln am Beispiel der Fichte. Berichte der Jahrestagung des Deutschen Verbandes Forstlicher, Sektion Ertragskunde, in Gießen, pp 51–57
Kennel R (1969) Formzahl- und Volumentafeln für Buche und Fichte. Selfpubl Inst Ertragskd, Forstl Forschungsanstalten München, München, 55 pp
Kesik M, Ambus P, Baritz R, Brüggemann N, Butterbach-Bahl K, Damm M, Duyzer J, Horvath L, Kiese R, Kitzler B, Leip A, Li C, Pihlatie M, Pilegaard K, Seufert G, Simpson D, Skiba U, Smiatek G, Vesala T, Zechmeister-Boltenstern S (2005) Inventories of N2O and NO emissions from European forest soils. Biogeosciences 2: 353–375
Kesselmeier J, Staudt M (1999) Biogenic volatile organic compounds (VOC): an overview on emission, physiology and ecology. Journal of Atmosphere Chemistry 33: 23–88
Keyes MR, Grier CC (1981) Above-and below-ground net production in 40-years-old Douglas-fir stands on low and high productivity sites. Canadian Journal of Forest Research 11: 599–605
Kienast F, Kräuchi N,(1991) Simulated successional characteristics of managed and unmanaged low-elevation forests in central Europe. Forest Ecology and Management 42: 49–61

Kiessling KB, Sterba H (1992) Dendrochronologische und dendroklimatologische Untersuchungen im Zusammenhang mit den großräumig auftretenden Eichenerkrankungen. Cbl für das ges Forstwesen 109: 145–161

Killian H (1974) Die Geschichte der Forstlichen Bundesversuchsanstalt und ihrer Institute. Mitt Forstl Bundes-Versuchsanst Wien 106, 79 pp

Kimmins JP (1985) Future shock in forest yield forecasting: the need for a new approach. The Forestry Chronicle 61: 503–513

Kimmins JP (1993) Scientific foundations for the simulation of ecosystem function and management in FORCYTE-11. Forestry Canada, Northern Forestry Centre, Edmonton, Alberta, Inf Rep NOR-X-328, 88 pp

Kimmins JP (1997) Forest ecology. A foundation for sustainable management, 2nd edn. Prentice Hall, Upper Saddle River, NJ, 596 pp

Kimmins JP Mailly D, Seely B (1999) Modelling forest ecosystem net primary production: The hybrid simulation approach used in FORECAST. Ecological Modelling 122: 195–224

King DA (1996) A model to evaluate factors controlling growth in Eucalyptus plantations of southeastern Australia. Ecological Modelling 87: 181–203

Kira T, Shidei T (1967) Primary production and turnover of organic matter in different forest ecosystems of the western Pacific. Journal of Japan Ecology 17: 70–87

Kira T, Ogawa H and Sakazaki N (1953) Intraspecific competition among higher plants, I. Competition-yield-density interrelationship in regularly dispersed populations. Journal of the Institute of Polytechnics, Osaka City Univ Series D, pp 1–16

Kiviste AK (1988) Mathematical functions of forest growth. Estonian Agricultural Academy, Tartu, 108 pp

Klemmt H-J (2007) Anwendung von Entscheidungsbaumverfahren und Regressionsanalysen zur semiautomatischen Feinkalibrierung des Wuchsmodells SILVA mit Hilfe von Forstinventurdaten. PhD thesis, Forest Yield Science, TU München, Freising, 228 pp

Klötzli FA (1993) Ökosysteme. Series UTB für Wissenschaft, Gustav Fischer, Stuttgart, Jena, 447 pp

Knigge W, Schulz H (1966) Grundriss der Forstbenutzung. Verlag Paul Parey, Hamburg, Berlin, 584 pp

Knoke T (1998) Analyse und Optimierung der Holzproduktion in einem Plenterwald- zur Forstbetriebsplanung in ungleichaltrigen Wäldern. Forstl Forschungsber München 170, 198 pp

Knoke T, Stimm B, Ammer C, Moog M (2005) Mixed forests reconsidered: A forest economics contribution on an ecological concept. Forest Ecology and Management 213: 102–116

Köhl M (1991) Anzahl Wiederholungen bei der Versuchsplanung, Forstw Cbl 110: 95–103

Köhler P, Huth A (1998) The effects of tree species grouping in tropical rainforest modelling: Simulations with the individual-based model FORMIND. Ecological Modelling 109: 301–321

Komarov A, Chertov O, Zudin S, Nadporozhskaya M, Mikhailov A, Bykhovets S, Zudina E, Zoubkova E (2003) EFIMOD2 – a model of growth and cycling of elements in boreal forest ecosystems. Ecological Modelling 170: 373–392

König G (1842) Gehalt und Wertschätzung aufbereiteter Hölzer, stehender Bäume und ganzer Waldbestände. Becker Verlag, Gotha, 135 pp

Konnert M (1992) Genetische Untersuchungen in geschädigten Weistannenbeständen (Abies alba Mill.) Südwestdeutschlands. PhD thesis, Forstl Fak, Univ Göttingen, pp 26–30

Kontic R, Niederer M, Nippel C, Winkler-Seifert A (1986) Jahrringanalysen an Nadelbäumen zur Darstellung und Interpretation von Waldschäden (Wallis, Schweiz). Ber Eidg Anst Forstwesen 283, 46 pp

Korf V (1939) Prispevek k matematicke definici vzrustoveho zakona lesnich porostu. Lesnicka prace 18: 339–356

Körner C (2002) Ökologie. In: Sitte P, Weiler EW, Kadereit JW, Bresinsky A, Körner C (eds) Strasburger Lehrbuch für Botanik, 35th edn. Spektrum Akademischer Verlag, Heidelberg, Berlin, pp 886–1043

Korol RL, Milner KS, Running SW (1996) Testing a mechanistic model for predicting stand and tree growth. Forest Science 42: 139–153

Korsun H (1935) Zivot normalniho porostu ve vzoroich (Das Leben des normalen Waldes in Formeln). Lesnicka prace 14: 289–300
Köstler JN (1953) Waldpflege. Paul Parey, Hamburg Berlin, 200 pp
Kouba J (1977) Markov chains and modelling the long-term development of the age structure and production of forests. Proposal of a new theory of the normal forest. Scientia Agriculturae Bohemoslovaca 26 (9): 179–193
Kouba J (1989) Control of the conversion process towards the stochastically defined normal forest by the linear and stochastic programming. Lesnictvi 35: 1025–1040
Kozlowski J, Konarzewski M (2004) Is West, Brown and Enquist's model of allometric scaling mathematically correct and biologically relevant? Functional Ecology 18: 283–289
Kozovits AR, Matyssek R, Winkler JB, Göttlein A, Blaschke H, Grams T (2005) Above-ground space sequestration determines competitive success in juvenile beech and spruce trees. New Phytologist 167: 181–196
Kraft G (1884) Beiträge zur Lehre von den Durchforstungen, Schlagstellungen und Lichtungshieben. Klindworth's Verlag, Hannover, 147 pp
Kramer H (1978) Der Bowmont-Durchforstungsversuch. Forstw Cbl 97: 131–141
Kramer H (1986) Beziehungen zwischen Kronenschadbild und Volumenzuwachs bei erkrankten Fichten. Allgemeine Forst- und Jagdzeitung 157 (2): 22–27
Kramer H (1988) Waldwachstumslehre. Paul Parey, Hamburg, Berlin
Kramer H, Akça A (1995) Leitfaden zur Waldmeßlehre. JD Sauerländer's Verlag, Frankfurt am Main, 266 pp
Kramer H, Dong PH (1985) Kronenanalyse für Zuwachsuntersuchungen in immissionsgeschädigten Nadelholzbeständen. Forst- u Holzwirt 40: 115–118
Kramer H, Dong PH, Saborowski HJ (1987) Auswirkungen von Waldschäden auf den Zuwachs von Fichten. Forstarchiv 59 (4): 154–155
Krapfenbauer A, Sterba H, Glatzel G, Hager H (1975) Ergebnisse von der Auswertung eines Einzelstammdüngungsversuches zu Kiefer. Cbl für das ges Forstwesen 92 (4): 237–243
Krenn, K (1946) Ertragstafeln für Fichte (1945) für Süddeutschland und Österreich. Schr Forstl Versuchsanst Bad-Württ 3, Freiburg, 30 pp
Kulakowski D, Rixen C, Bebi P (2006) Changes in forest structure and in the relative importance of climatic stress as a result of suppression of avalanche disturbances. Forest Ecology and Management 223: 66–74
Kurth W (1999) Die Simulation der Baumarchitektur mit Wachstumsgrammatiken. Wissenschaftlicher Verlag, Berlin, 327 pp
Landsberg JJ (1986) Physiological Ecology of Forest Production. Academic, London, 198 pp
Landsberg JJ (2003) Modelling forest ecosystems: state of the art, challenges, and future directions. Canadian Journal of Forest Research 33: 385–397
Landsberg JJ, Waring RH (1997) A generalised model of forest productivity using simplified concepts of radiation-use efficiency, carbon balance and partitioning. Forest Ecology and Management 95: 209–228
Landsberg J, Johnsen K, Albaugh T, Allen H, McKeand S (2001) Applying 3-PG, a simple process-based model designed to produce practical results to data from loblolly pine experiments. Forest Science 47: 43–51
Landsberg JJ, Waring RH, Coops NC (2003) Performance of the forest productivity model 3-PG applied to a wide range of forest types. Forest Ecology and Management 172: 199–214
Langsaeter A (1941) Om tynning i enaldret gran- og furuskog Maddel. Det Norske Skogforoksvesen 8: 131–216
Larcher W (1994) Ökophysiologie der Pflanzen, 5th edn. Verlag Eugen Ulmer, Stuttgart, 394 pp
Larcher W (2003) Physiological plant ecology, 4th edn. Springer, Berlin
Lasch P, Lindner M, Erhard M, Suckow F, Wenzel A (2002) Regional impact assessment on forest structure and functions under climate change – the Brandenburg case study. Forest Ecology and Management 162: 73–86
Lasch P, Badeck F-W, Suckow F, Lindner M, Mohr P (2005) Model-based analysis of management alternatives at stand and regional level in Brandenburg (Germany). Forest Ecology and Management 207: 59–74

Laurence JA, Retzlaf WA, Kern JS, Lee EH, Hogsett WE, Weinstein DA (2001) Predicting the regional impact of ozone and precipitation on the growth of loblolly pine and yellow-poplar using linked TREGRO and ZELIG models. Forest Ecology and Management 146: 247–263

Le Roux X, Lacointe A, Escobar-Gutierrez A, Le Dizes S (2001) Carbon-based models of individual tree growth: A critical appraisal. Annals of Forest Science 58: 469–506

Le Tacon, F, Oswald, R, Tomassone, R (1970) Der Einzelbaum-Düngungsversuch "Clefmont". Berichte der Jahrestagung des Deutschen Verbandes Forstlicher, Sektion Ertragskunde, in Mainz, pp 30–33

Leary RA (1970) System identification principles in studies of forest dynamics. USDA North Central Forest Exp Station, St Paul, MN, Research Pap NC-45, 38 pp

Lee Y (1967) Stand models for lodgepole pine and limits to their application. PhD thesis, Forestry Fac, Univ of BC, Vancouver, Canada, 333 pp

Leemans R, Prentice IC (1989) FORSKA, a general forest succession model. Inst Ecol Bot, Univ Uppsala, Uppsala, Sweden, Meddelanden fran Växtbiologiska Institutionen 2, pp 1–45

Lembcke G, Knapp E, Dittmar O (1975) Die neue DDR-Kiefernertragstafel 1975. Beitr für die Forstwirtschaft 15 (2): 55–64

Lemm R (1991) Ein dynamisches Forstbetriebs-Simulationsmodell. Prognosen von betriebsspezifischen Waldentwicklungen, Waldschäden und deren monetäre Bewertung unter variablen Einflussgrößen. PhD thesis No 9369, Eidg TH Zürich, Dep Forsteinrichtung und Waldwachstum, 235 pp

Letcher BH, Priddy JA, Walters JR, Crowder LB (1998) An individual-based, spatially-explicit simulation model of the population dynamics of the endangered red-cockaded woodpecker, *Picoides borealis*. Biological Conservation 86: 1–14

Leuschner C, Scherer B (1989) Fundamentals of an applied ecosystem research project in the Wadden Sea of Schleswig-Holstein. Helgoländer Meeresuntersuchungen 43: 565–574

Levakovic A (1935) Analytical form of growth laws. Glasnik za sumske pokuse (Zagreb) 4: 189–282

Lexer MJ, Hönninger K (1998) Simulated effects of bark beetle infestations on stand dynamics in *Picea abies*s stands: Coupling a patch model an a stand risk model. In: Beniston M, Innes JL (eds) The Impacts of Climate Change on Forests. Lecture Notes in Earth Sciences, Springer, Berlin, pp 289–308

Lexer MJ, Hönninger K (2001) A modified 3D-patch model for spatially explicit simulation of vegetation composition in heterogeneous landscapes. Forest Ecology and Management 144: 43–65

Li C, Aber J, Stange F, Butterbach-Bahl K, Papen H (2000) A process-oriented model of N2O and NO emissions from forest soils: 1, Model development. Journal of Geophysical Research 105: 4369–4384

Lin JY (1970) Growing space index and stand simulation of young western hemlock in Oregon. PhD thesis, Duke University, Durham, NC, 182 pp

Linder A (1951) Statistische Methoden für Naturwissenschaftler, Mediziner und Ingenieure, 2nd edn. Verlag Birkhäuser, Basel, 238 pp

Linder A (1953) Planen und Auswerten von Versuchen. Eine Einführung für Naturwissenschaftler, Mediziner und Ingenieure. Verlag Birkhäuser, Basel, Stuttgart, 182 pp

Lindner M (1998) Wirkung von Klimaveränderungen in Mitteleuropäischen Wirtschaftswäldern. PhD thesis, Potsdam Inst Klimafolgenforschung, Abt globaler Wandel und natürliche Systeme, 98 pp

Lindner M, Cramer W (2002) German forest sector under global change. An interdisciplinary impact assessment. In: Pretzsch H, Lindner M, Suda M (eds) German Forest Sector under Global Change. German Journal of Forest Science 121 (1): 3–17

Liu S, Munson R, Johnson DW (1992) The nutrient cycling model (NuCM). In: Johnson DW, Lindberg SE (eds) Atmospheric deposition and forest nutrient cycling. Ecological Studies. Springer, New York, pp 583–609

Lo E, Wang ZM, Lechowicz M, Messier C, Nikinmaa E, Perttunen J, Sievänen (2001) Adaptation of the LIGNUM model for simulation of growth and light response in Jack pine. Forest Ecology and Management 150: 279–291

Loetsch F (1973) Prüfung der Verteilungsart und Dichte mit Hilfe des Nullflächendiagramms. Forstarchiv 44: 77–83

Loetsch F, Haller KE (1964) Forest Inventory, Volume 1: Statistics of Forest Inventory and Information from Aerial Photographs. BLV Verlagsgesellschaft München, Basel, Wien, 436 pp

Loetsch F, Zöhrer F, Haller KE (1973) Forest inventory, vol 2: Inventory data collected by terrestrial measurements and observations, data processing in forest inventory. The sample plot, plotless sampling and regenerations survey. List sampling with unequal probabilities and planning, performance and field checking of forest inventories. BLV-Verlagsgesellschaft, München, Bern, Wien, 469 pp

Lohmann J (1992) Die Xylemleitquerschnitte von Fichten (Picea abies [L.] Karst.) unterschiedlicher Vitalitätsgrade und Altersklassen. Ber Forschungszentrum Waldökosysteme, Univ Göttingen, Reihe A, vol 88, 123 pp

Long JN (1985) A practical approach to density management. For Chron 61: 23–27

Long JN, Smith FW (1984) Relation between size and density in developing stands: a description and possible mechanisms. Forest Ecology and Management 7: 191–206

Loreau M, Naeem S, Inchausti P, Bengtsson J, Grimr JP, Hector A, Hooper DU, Huston MA, Raffaelli D, Schmid B, Tilman D, Wardle DA (2001) Biodiversity and ecosystem functioning: Current knowledge and future challenges. Science 294: 804–808

Lorey T (1878) Die mittlere Bestandeshöhe. Allgemeine Forst- und Jagdzeitung 54: 149–155

Lorimer CG (1983) Tests of age-independent competition indices for individual trees in natural hardwood stands. Forest Ecology and Management 6: 343–360

Lu L, Pielke RA Sr, Liston GE, Parton WJ, Ojima DS, Hartman M (2001) Implementation of a two-way interactive atmospheric and ecological model and its application to the Central United States. Journal of Climate 14: 900–919

Lüpke von B, Spellmann H (1997) Aspekte der Stabilität und des Wachstums von Mischbeständen aus Fichte und Buche als Grundlage für waldbauliche Entscheidungen. Forstarchiv 68: 167–179

Lüpke von B, Spellmann H (1999) Aspects of stability, growth and natural regen.eration in mixed Norway spruce-beech stands as a basis of silvicultural decisions. In: Olsthoorn AFM, Bartelink HH, Gardiner JJ, Pretzsch H, Hekhuis HJ, Franc A (eds) Management of mixed-species forest: silviculture and economics. IBN Scientific Contributions 15, pp 245–267

Lyr H, Polster H, Fiedler HJ (1967) Gehölzphysiologie. VEB Gustav Fischer Verlag, Jena, 337 pp

MacArthur RH, Wilson EO (1967) The theory of island biogeography. Princeton University Press, Princeton, NJ

Magin R (1959) Struktur und Leistung mehrschichtiger Mischwälder in den bayerischen Alpen. Mitt Staatsforstverwaltung Bayerns 30, 161 pp

Mäkelä A (1990) Modeling structural-functional relationships in whole-tree growth: Resource allocation. In: Dixon RK, Meldahl RS, Ruarki GA, Warren WG (eds) Process modeling of forest growth responses to environmental stress. Timber, Portland, OR, pp 81–95

Mäkelä A, Hari P (1986) Stand growth model based on carbon uptake and allocation in individual trees. Ecological Modelling 33: 205–229

Mäkelä A, Valentine HT (2006) Crown ratio influences allometric scaling in trees. Ecology 87 (12): 2967–2972

Mäkelä A, Landsberg J, Ek AR, Burk TE, Ter-Mikaelian M, Ågren GI, Oliver CD, Puttonen P (2000) Process-based models for forest ecosystem management: current state of the art and challenges for practical implementation. Tree Physiology 20: 289–298

Makkink GF (1957) Testing the Penman formula by means of lysimeters. Journal of Institute of Water Engineering 11: 277–288

Mandelbrot B (1977) Form, Chance, Dimension. Freeman, San Francisco 1977, dt. Ausgabe: Die fraktale Geometrie der Natur. Birkhäuser, Basel 1986

Mang K (1955) Die Fohrenüberhaltsbetriebe im FA Lindau i.B. PhD thesis, LMU München, 76 p

Mar-Möller C (1945) Untersuchungen über Laubmenge, Stoffverlust und Stoffproduktion des Waldes. Verlag Kandrup und Wunsch, Kopenhagen, 287 pp
Martin GL, Ek AR (1984) A comparison of competition measures and growth models for predicting plantation Red pine diameter and heigt growth. Forest Science 30 (3): 731–743
Martin GL, Ek AR, Monserud RA (1977) Control of plot edge bias in forest stand growth simulation models. Canadian Journal of Forest Research 3 (1): 100–105
Matala J, Hynynen J, Miina J, Ojansuu R, Peltola H, Sievänen R, Väisänen H, Kellomäki S (2003) Comparison of a physiological model and a statistical model for prediction of growth and yield in boreal forests. Ecological Modelling 161: 95–116
Matjicek L, Benesova L, Tonika J (2003) Ecological modelling of nitrate pollution in small river basins by spreadsheets and GIS. Ecological Modelling 170: 245–263
Matthew C, Lemaire G, Sackville Hamilton NR, Hernandez-Garay A (1995) A modified self-thinning equation to describe size/density relationships for defoliated swards. Annals of Botany 76: 579–587
Matyssek R, Agerer R, Ernst D, Munch JC, Oßwald W, Pretzsch H, Priesack E, Schnyder H, Treutter D (2005) The plant's capacity in regulating resource demand. Plant Biology 7: 560–580
Mayer FJ (1999) Beziehungen zwischen der Belaubungsdichte der Waldbäume und Standortsparametern. PhD thesis, Forstwiss Fak, LMU München, Freising, 183 pp
Mayer H (1984) Waldbau auf soziologisch-ökologischer Grundlage. Gustav Fischer Verlag, Stuttgart, New York, 514 pp
Mayer DG, Butler DG (1993) Statistical validation. Ecological Modelling 68: 21–32
McGaughey RJ (2006) EnVision – Environmental Visualization System. University of Washington, WA, http://forsys.cfr.washington.edu/envision.html
McGee CE, Della-Bianca L (1967) Diameter distributions in natural Yellow-poplar stands. USDA Southeastern Forest Exp Station, Asheville, NC, SE-25, 7 pp
Mckelvey K, Noon BR, Lamberson RH (1993) Conservation planning for species occupying fragmented landscapes: the case of the northern spotted owl. In: Kareiva PM, Kingsolver JG, Huey RB (eds) Biotic interactions and global change. Sinauer, Sunderland, MA, pp 424–450 (480 pp)
McMurtrie RE (1991) Relationship of forest productivity to nutrient and carbon supply – a modelling analysis. Tree Physiology 9: 87–100
McMurtrie RE, Wolf L (1983) Above- and below-ground growth of forest stands: A carbon budget model. Annals of Botany 52: 437–448
MCPFE (1993) Resolution H1: General guidelines for the sustainable management of forests in Europe. Proc 2nd Ministerial Conference on the Protection of Forests in Europe, Helsinki, Finland, pp 5
Meitner MJ, Gandy R, Sheppard SRJ (2005) Reviewing the role of visualization in communicating and understanding forest complexity. Proc 9th Internat Conf Information Visualisation (IV'05), pp 121–128
Menard A, Dube P, Bouchard A, Canham CD, Marceau DJ (2002) Evaluating the potential of the SORTIE forest succession model for spatio-temporal analysis of small-scale disturbances. Ecological Modelling 153: 81–96
Meng FR, Arp PA (1994) Modelling photosynthetic responses of a spruce canopy to SO2 exposure. Forest Ecology and Management 67: 69–85
Meng SX, Rudnicki M, Lieffers VJ, Reid DEB, Silins U (2006) Preventing crown collisions increases the crown cover and leaf area maturing lodgepole pine. Journal of Ecology 94 (3): 681–686
Menzel L, Rötzer T (2007) SWAT – Modelle und deren Anwendung. Forum für Hydrologie und Wasserbewirtschaftung (21.07.2007), pp 113–146
Mettin C (1985) Betriebswirtschaftliche und ökologische Zusammenhänge zwischen Standortskraft und Leistung in Fichtenreinbeständen und Fichten/Buchen-Mischbeständen. Allgemeine Forstzeitschrift 40: 803–810
Metzler W (1987) Dynamische Systeme in der Ökologie. Studienbücher Mathematik, BG Teubner, Stuttgart, 210 pp

Meyer HA (1953) Forest mensuration. Penns. Valley, State College, Pennsylvania, 357 pp
Michailoff I (1943) Zahlenmäßiges Verfahren für die Ausführung der Bestandeshöhenkurven, Forstw Cbl 6: 273–279
Mielikäinen K (1980) Mänty-koivusekametsiköiden rakenne ja kehitys. Summary: structure and development of mixed pine and birch stands. Com Inst Forestalis Fenniae 99: 1–8
Mielikäinen K (1985) Koivusekoituksen Vaikutus Kuusikon Rakenteeseeen ja kehitykseen, Effect of an admixture of birch on the structure and development of Norway Spruce Stands. Comm Inst Forestalis Fenniae 133: 1–79
Mielikäinen K, Nöjd P (1996) Growth trends in the Finnish forest: results and methodological considerations. Proc Conf of Effects of Environmental Factors on Tree and Stand Growth, TU Dresden, pp 164–174
Mielikäinen K, Timonen M (1996) Growth trends of Scots pine (Pinus sylvestris, L.) in unmanaged and regularly managed stands in southern and central Finland. In: Spiecker H, Mielikäinen K, Köhl M, Skovsgaard JP (eds) Growth trends in European forests. European Forest Institute, Research Report 5, Springer, Heidelberg, pp 41–59 (372 pp)
Mitchell KJ (1969) Simulation of the growth of even-aged stands of white spruce. Yale University, School of Forestry, Bulletin 75, 48 pp
Mitchell KJ (1975) Dynamics and simulated yield of Douglas-fir. Forest Science Monographs 17, 39 pp
Mitscherlich EA (1948) Die Ertragsgesetze. Deutsche Akademie der Wissenschaften zu Berlin, Vorträge und Schriften 31, Akademie, Berlin, 42 pp
Mitscherlich G (1970) Wald, Wachstum und Umwelt. 1. Band, Form und Wachstum von Baum und Bestand. JD Sauerländer's Verlag, Frankfurt am Main
Mohren GM. J (1987) Simulation of forest growth, applied to Douglas fir stands in the Netherlands. PhD thesis, Agricultural Univ Wageningen, The Netherlands, 183 pp
Mohren GMJ, Bartelink HH (1990) Modelling the effects of needle mortality rate and needle area distribution on dry matter production of Douglas fir. Netherlands Journal of Agricultural Science 38: 53–66
Mohren GMJ, Van de Veen JR (1995) Forest growth in relation to site conditions. Application of the model FORGRO to the Solling spruce site. Ecological Modelling 83: 173–183
Mohren GMJ, Bartelink HH, Jorritsma ITM, Kramer K (1993) A process-based growth model (FORGRO) for analysis of forest dynamics in relation to environmental factors. In: Brokemeijer M, Vos W, Koop HGJM (eds) European Forest Reserves. Proc European Forest Reserves Workshop in Wageningen, The Netherlands, 6–8 May 1992, Pudoc, Wageningen, pp 273–280
Möller A (1922) Der Dauerwaldgedanke. Sein Sinn und seine Bedeutung. Verlag Julius Springer, Berlin
Monserud RA (1975) Methodology for simulating Wisconsin northern hardwood stand dynamics. Univ Wisconsin-Madison, PhD thesis Abstracts 36, No 11, 156 pp
Monserud RA (2003) Evaluating forest models in a sustainable forest management context. Forest Biometry, Modelling and Information Sciences 1: 35–47
Monserud RA, Ek AR (1974) Plot Edge Bias in Forest Stand Growth Simulation Models. Canadian Journal of Forest Research 4 (4): 419–423
Monsi M, Saeki T (1953) Über den Lichtfaktor in den Pflanzengesellschaften und seine Bedeutung für die Stoffproduktion. Japan Journal of Botany 14: 22–52
Monteith JL (1965) Evaporation and environment. In: Fogg, GE (ed) The state and movement of water in living organisms. Symp Soc Exp Biol. Academic, London, pp 205–234
Moore PG (1954) Spacing in plant populations. Ecology 35: 222–227
Moosmayer HU, Schöpfer W (1972) Beziehungen zwischen Standortsfaktoren und Wuchsleistung der Fichte. Allgemeine Forst- und Jagdzeitung 143 (10): 203–215
Morisita M (1959) Measuring of the Dispersion of Individuals and Analysis of the Distributional Patterns. Mem Fac Sci Kyushu Univ, Series E (Biology) 2 (4): 215–235
Moser JW (1972) Dynamics of an uneven-aged forest stand. Forest Science 18: 184–191

Moser JW (1974) A system of equations for the components of forest growth. In: Fries J (ed) Growth models for tree and stand simulation. Royal College of Forestry, Stockholm, Sweden, Research Notes 30, pp 260–287 (397 pp)
Moser JW, Hall OF (1969) Deriving growth and yield functions for uneven-aged forest stands. Forest Science 15: 183–188
Moshammer R (2006) Vom Inventurpunkt zum Forstbetrieb. Allgemeine Forstzeitschrift 61: 1164–1165
Mouillot F, Rambal S, Lavorel S (2001) A generic process-based SImulator for meditERRanean landscApes (SIERRA): Design and validation exercises. Forest Ecology and Management 147: 75–97
Mouillot F, Rambal S, Joffre R (2002) Simulating climate change impacts on fire frequency and vegetation dynamics in a Mediterranean-type ecosystem. Global Change Biology 8: 423–437
Mudra A (1958) Statistische Methoden für landwirtschaftliche Versuche. Verlag Paul Parey, Berlin, Hamburg, 336 pp
Müller HJ (1991) Ökologie. Gustav Fischer Verlag, Jena, 415 pp
Müller F (1992) Hierarchical approaches to ecosystem theory. Ecological Modelling 63: 215–242
Müller-Dombois D (1983) Population death in Hawaiian plant communities: a causal theory and its successional significance. Tuexenia 3: 117–130
Müller-Dombois D (1987) Natural dieback in forests. Bioscience 37: 575–583
Munro DD (1974) Forest growth models – a prognosis. In: Fries, J (ed) Growth models for tree and stand simulation. Royal College of Forestry, Stockholm, Sweden, Research Notes 30, pp 7–21 (397 pp)
Munzert M (1992) Einführung in das pflanzenbauliche Versuchswesen. Pareys Studientexte 71, Verlag Paul Parey, Berlin, Hamburg, 163 pp
Myers CA (1966) Yield tables for managed stands with special reference to the Black Hills. USDA Rocky Mtn Forest and Range Exp Station, Research Paper RM-21, 20 pp
Myneni RB, Keeling CD, Tucker CJ, Asrar G, Nemani RR (1997) Increased plant growth in the northern high latitudes from 1981 to 1991. Nature 386: 698–702
Nagel J (1985) Wachstumsmodell für Bergahorn in Schleswig-Holstein. PhD thesis, Univ Göttingen, 124 pp
Nagel J (1996) Anwendungsprogramm zur Bestandesbewertung und zur Prognose der Bestandesentwicklung. Forst u Holz 51 (3): 76–78
Nagel J (1999) Konzeptionelle Überlegungen zum schrittweisen Aufbau eines waldwachstumskundlichen Simulationssystems für Nordwestdeutschland. Schr Forstl Fak Univ Göttingen u Niedersächs Forstl Versuchsanst 128, JD Sauerländer's Verlag, Frankfurt am Main, 122 pp
Nagel J, Biging GS (1995) Schätzung der Parameter der Weibullfunktion zur Generierung von Durchmesserverteilungen, Allgemeine Forst- und Jagdzeitung 166 (9/10): 185–189
Nagel J, Wagner S, Biber P, Guericke M (1996) Vergleich von Strahlungswerten aus Fisheye-Fotos und Modellrechnungen. Berichte der Jahrestagung des Deutschen Verbandes Forstlicher, Sektion Ertragskunde, in Neresheim, pp 306–313
Navar J, Bryan RB (1994) Fitting the analytical model of rainfall interception of Gash to individual shrubs of semi-arid vegetation in northeastern Mexico. Agricultural and Forest Meteorology 68: 133–143
Nelder JA (1962) New kinds of systematic designs for spacing experiments. Biometrics 18 (3): 283–307
Nelson TC (1961) Loblolly pine growth as related to site, age, and stand density. Proc Soc of American Foresters 1960, pp 12–14
Neumann M, Schieler K (1981) Vergleich spezieller Methoden zuwachskundlicher Schadensabschätzung. Mitt Forstl Bundesversuchsanst Wien 139, pp 49–66
Newnham RM (1964) The development of a stand model for Douglas-fir. PhD thesis, Forestry Fac, University of British Columbia, Vancouver, Canada, 201 pp
Newton PF (1997) Stand density management diagrams: review of their development and utility in stand-level management planning. Forest Ecology and Management 98: 251–265
Nicolis G, Prigogine I (1987) Die Erforschung des Komplexen. Piper, München

Nikinmaa E (1992) Analysis of the growth of Scots pine matching structure with function. Acta Forestalia Fennica 235: 1–68

Nikinmaa E, Hari P (1990) A simplified carbon partitioning model for Scots pine to address the effects of altered needle longevity and nutritient uptake on stand development. In: Dixon RK, Meldahl RS, Ruark GA, Warren WG (eds) Process modeling of forest growth responses to environmental stress. Timber, Portland, OR, pp 263–270

Niklas KJ (1994) Plant Allometry. Univ Chicago Press, Chicago, IL

Nuutinen T, Matala J, Hirvelä H, Härkönen K, Peltola H, Väisänen H, Kellomäki S (2006) Regionally optimized forest management under changing climate. Climatic Change 79: 315–333

Oliveira A (1980) Untersuchungen zur Wuchsdynamik junger Kiefernbestände. PhD thesis, LMU München

Oliver CD, Larson B (1996) Forest Stand Dynamics. John Wiley & Sons Inc, New York, Chichester, Brisbane, Toronto, Singapore, 520 pp

Olsson L, Carlsson K, Grip H, Perttu K (1982) Evaluation of forest-canopy photographs with diode-array scanner OSIRIS. Canadian Journal of Forest Research 12: 822–828

Öttelt KC (1765) Practischer Beweis, dass die Mathesis bey dem Forstwesen unentbehrliche Dienste thue. Grießbach, Eisennach, 127 pp

Pacala SW, Canham CD, Silander JA Jr (1993) Forest models defined by field measurements: 1. The design of a northeastern forest simulator. Canadian Journal of Forest Research 23: 1980–1988

Paivio A (1971) Imagery and verbal processes. Holt, Rinehart and Winston, New York, 592 pp

Pardé J (1979) Entwicklung, Stand und Zukunft der Forschungen über die Durchforstung in Frankreich. Forstw Cbl 98: 110–119

Parra R, Gasso S, Baldasano JM (2004) Estimating the biogenic emissions of non-methane volatile organic compounds from the North Western Mediterranean vegetation of Catalonia, Spain. Science of the Total Environment 329: 241–259

Pastor J, Post WM (1985) Development of a linked forest productivity-soil process model. Oak Ridge National Laboratory for the US Department of Energy, Environmental Sciences Div 2455, Oak Ridge, TN, 161 pp

Paulsen JC (1795) Kurze praktische Anleitung zum Forstwesen. Verfaßt von einem Forstmanne. Detmold, 152 pp

Payandeh B (1974) Spatial pattern of trees in the mayor forest types of Northern Ontario. Canadian Journal of Forest Research 4: 8–14

Peck AK (2004) Hydrometeorologische und mikroklimatische Kennzeichen von Buchenwäldern. Ber Meteorolog Inst 10, Univ Freiburg

Pelt van R (2001) Forest giants of the Pacific coast. University of Washington Press, Seattle, London, 200 pp

Pelz DR (1978) Estimating individual tree growth with tree polygons. School of Forestry and Wildlife Res, Blacksburg, VA, FWS-1-78, pp 172–178

Peng C, Liu J, Dang Q, Apps MJ, Jiang H (2002) TRIPLEX: a generic hybrid model for predicting forest growth and carbon and nitrogen dynamics. Ecological Modelling 153: 109–130

Penman HL, Long IF (1960) Weather in wheat: an essay in mirometeorology. Quarterly Journal of Royal Meteorological Society 86: 16–50

Perthuis de Laillevault de R (1803) Traité de l'aménagement et de la restauration des bois et forêts de la France, Madame Huzard, Paris, 384 pp

Perttunen J, Sievänen R, Nikinmaa E (1998) LIGNUM: a model combining the structure and the functioning of trees. Ecological Modelling 108: 189–198

Petri H (1966) Versuch einer standortgerechten, waldbaulichen und wirtschaftlichen Standraumregelung von Buchen-Fichten-Mischbeständen. Mitt Landesforstverwaltung Rheinland-Pfalz 13, 145 pp

Petritsch R, Hasenauer H, Pietsch SA (2007) Incorporating forest growth response to thinning within biome-BGC. Forest Ecology and Management 242: 324–336

Petterson H (1955) Die Massenproduktion des Nadelwaldes. Mitt Schwed Forstl Forschungsanstalten, Stockholm, vol 45 (IB), 391 pp

Pfeil W (1860) Die deutsche Holzzucht. Verlag Baumgartner, Leipzig, 551 pp
Pfisterer AB, Schmid B (2002) Diversity-dependent production can decrease the stability of ecosystem functioning. Nature 416: 84–86
Pfreundt J (1988) Modellierung der räumlichen Verteilung von Strahlung, Photo-synthesekapazität und Produktion in einem Fichtenbestand und ihre Beziehung zur Bestandesstruktur. PhD thesis, Univ Göttingen, 163 pp
Pielou EC (1959) The use of point-to-plant distances in the study of the pattern of plant population. Journal of Ecology 47: 607–613
Pielou EC (1975) Ecological diversity. Wiley, New York, 165 pp
Pielou EC (1977) Mathematical Ecology. Wiley, New York, 385 pp
Pienaar LV, Turnbull KJ (1973) The Chapman-Richards generalization of von Bertalanffy's growth model for basal area growth and yield in even-aged stands. Forest Science 19 (2): 2–22
Piotto D (2007) A meta-analysis comparing tree growth in monocultures and mixed plantations. Forest Ecology and Management 255: 781–786
Pollanschütz J (1966) Verfahren zur objektiven "Abschätzung" (Messung) verminderter Zuwachsleistung von Einzelbäumen und Beständen. Mitt Forstl Bundesversuchsanst Wien 73, pp 129–144
Pollanschütz J (1967) Objektive Ermittlung der Auswirkung äußerer Einflüsse auf die Zuwachsleistung. Mitt Forstl Bundesversuchsanst Wien 77 (1): 277–296
Pollanschütz J (1974) Erste ertragskundliche und wirtschaftliche Ergebnisse des Fichten-Pflanzweiteversuches "Hauersteig". In: Egger, J (ed) 100 Jahre Forstliche Bundesversuchsanst Wien. Eigenverlag Forstl Bundesversuchsanst Wien, pp 99–171 (379 pp)
Pollanschütz J (1975) Zuwachsuntersuchungen als Hilfsmittel der Diagnose und Beweissicherung bei Forstschäden durch Luftverunreinigungen. Allgemeine Forstzeitschrift 86 (6): 187–192
Pollanschütz J (1980) Jahrringmessung und Referenzprüfung: Ein Beitrag zur Frage der Zuverlässigkeit bestimmter Verfahren der Zuwachsermittlung. Mitt Forstl Bundesversuchsanst Wien 130: 263–285
Pool R (1992) The third branch of science debuts. Science 256: 44–47
Poorter H, Nagel O (2000) The role of biomass allocation in the growth response of plants to different levels of light, CO_2, nutrients and water: a quantitative review. Australian Journal of Plant Physiology 27: 595–607
Popper KR (1984) Logik der Forschung. Verlag JCB Mohr (Paul Siebeck), Tübingen, 477 pp
Pott M (1997) Wachstum der Fichte in Bayern: Auswertung von Daten der Forsteinrichtungsdatenbank der Bayerischen Staatsforstverwaltung. Dipl thesis Forest Yield Science, LMU München, Freising, MWW-DA 117, 95 pp
Prentice IC, Leemans R (1990) Pattern and process and the dynamics of forest structure: a simulation approach. Journal of Ecology 78: 340–355
Pressler M (1865) Das Gesetz der Stammformbildung. Verlag Arnold, Leipzig, 153 pp
Pressler M (1870) Forstliche Ertrags- und Bonitierungstafeln nach Cubicmeter pro ha. Verlag Baumgartner, Leipzig
Pressler M (1877) Forstliche Zuwachs-, Ertrags- und Bonitierungs-Tafeln mit Regeln und Beispielen. 2nd edn. Selfpubl, Tharandt, 72 pp
Pretzsch H (1985a) Die Fichten-Tannen-Buchen-Plenterwaldversuche in den ostbayerischen Forstämtern Freyung und Bodenmais. Forstarchiv 56 (1): 3–9
Pretzsch H (1985b) Wachstumsmerkmale süddeutscher Kiefernbestände in den letzten 25 Jahren. Forstl Forschungsber München 65, 183 pp
Pretzsch H (1989a) Untersuchungen an kronengeschädigten Kiefern (Pinus sylvestris L.) in Nordost-Bayern. Forstarchiv 60 (2): 62–69
Pretzsch H (1989b) Zur Zuwachsreaktionskinetik der Waldbestände im Bereich des Braunkohlekraftwerkes Schwandorf in der Oberpfalz. Allgemeine Forst- und Jagdzeitung 160 (2/3): 43–54
Pretzsch H (1992a) Konzeption und Konstruktion von Wuchsmodellen für Rein- und Mischbestände. Forstl Forschungsber München 115, 358 pp

Pretzsch H (1992b) Modellierung der Kronenkonkurrenz von Fichte und Buche in Rein- und Mischbeständen. Allgemeine Forst- und Jagdzeitung 163 (11/12): 203–213
Pretzsch H (1992c) Zur Analyse der räumlichen Bestandesstruktur und der Wuchskonstellation von Einzelbäumen. Forst u Holz, 47 (14): 408–418
Pretzsch H (1993) Analyse und Reproduktion räumlicher Bestandesstrukturen. Versuche mit dem Strukturgenerator STRUGEN. Schr Forstl Fak Univ Göttingen u Niedersächs Forstl Versuchsanst 114, JD Sauerländer's Verlag, Frankfurt am Main, 87 pp
Pretzsch H (1995) Zum Einfluß des Baumverteilungsmusters auf den Bestandeszuwachs. Allgemeine Forst- und Jagdzeitung 166 (9/10): 190–201
Pretzsch H (1996a) Konzept für die Erfassung der Wuchsdynamik bayerischer Mischbestände aus Fichte/Buche, Kiefer/Buche, Eiche/Buche und Fichte/Tanne/Buche über ein Netz von Wuchsreihen, Anweisung zu Anlage und Aufnahme der Parzellen von Wuchsreihen. Unpubl manuscript, Chair for Forest Yield Science, TU München, Freising, 17 pp
Pretzsch H (1996b) Zum Einfluß waldbaulicher Maßnahmen auf die räumliche Bestandesstruktur. Simulationsstudie über Fichten-Buchen-Mischbestände in Bayern. In: Müller-Starck G (ed) Biodiversität und nachhaltige Forstwirtschaft. Ecomed Verlagsgesellschaft, Landsberg, pp 177–199 (360 pp)
Pretzsch H (1997) Analysis and modeling of spatial stand structures. Methodological considerations based on mixed beech-larch stands in Lower Saxony, Forest Ecology and Management 97: 237–253
Pretzsch H (1998) Structural diversity as a result of silvicultural operations. Lesnictví-Forestry 44 (10): 429–439
Pretzsch H (1999) Waldwachstum im Wandel, Konsequenzen für Forstwissenschaft und Forstwirtschaft. Forstw Cbl 118: 228–250
Pretzsch H (2000) Die Regeln von Reineke, Yoda und das Gesetz der räumlichen Allometrie. Allgemeine Forst- und Jagdzeitung 171 (11): 205–210
Pretzsch H (2001) Modellierung des Waldwachstums. Blackwell Wissenschafts-Verlag, Berlin, Wien, 336 pp
Pretzsch H (2002) Grundlagen der Waldwachstumsforschung. Blackwell Wissenschafts-Verlag, Berlin, Wien, 414 pp
Pretzsch H (2005a) Diversity and productivity in forests. In: Scherer-Lorenzen M, Körner C, Schulze E-D (eds) Forest diversity and function. Ecological Studies 176, Springer, Berlin, pp 41–64
Pretzsch H (2005b) Stand density and growth of Norway spruce (Picea abies (L.) Karst.) and European beech (*Fagus sylvatica* L.). Evidence from long-term experimental plots. European Journal of Forest Research 124: 193–205
Pretzsch H (2005c) Link between the self-thinning rules for herbaceous and woody plants, Scientia Agriculturae Bohemica 36 (3): 98–107
Pretzsch H (2006a) Species-specific allometric scaling under self-thinning. Evidence from longtern plots in forest stands. Oecologia 146: 572–583
Pretzsch H (2006b) Von der Standfächeneffizienz der Bäume zur Dichte-Zuwachs-Beziehung des Bestandes. Beitrag zur Integration von Baum- und Bestandesebene, Allgemeine Forst- und Jagdzeitung 177: 188–199
Pretzsch H (2008) Wirkung von Stress auf die Allometrie von Baumkronen. Berichte der Jahrestagung des Deutschen Verbandes Forstlicher, Sektion Ertragskunde in Trippstadt, 5–21
Pretzsch H, Biber P (2005) A re-evaluation of Reineke's rule and Stand Density Index. Forest Science 51: 304–320
Pretzsch H, Ďurský J (2001) Evaluierung von Waldwachstumssimulatoren auf Baum- und Bestandesebene. Allgemeine Forst- und Jagdzeitung 172 (8/9): 146–150
Pretzsch H, Kahn M (1998) Wuchsmodelle für die Unterstützung der Wirtschaftsplanung im Forstbetrieb, Anwendungsbeispiel: Variantenstudie Fichtenreinbestand versus Fichten/Buchen-Mischbestand. Allgemeine Forstzeitschrift 51: 1414–1419

Pretzsch H, Kölbel M (1988) Einfluß von Grundwasserabsenkungen auf das Wuchsverhalten der Kiefernbestände im Gebiet des Nürnberger Hafens. Ergebnisse ertragskundlicher Untersuchungen auf der Weiserflächenreihe Nürnberg 317. Forstarchiv 59 (3): 89–96
Pretzsch H, Mette T (2008) Linking stand-level self-thinning allometry to the tree-level leaf biomass allometry. Trees 22: 611–622
Pretzsch H, Schütze G (2005) Crown allometry and growing space efficiency of Norway spruce (*Picea abies* (L.) Karst.) and European beech (*Fagus sylvatica* L.) in pure and mixed stands. Plant Biology 7: 628–639
Pretzsch H, Schütze G (2009) Trangressive overyielding in mixed compared with pure stands of Norway spruce and European beech in Central Europe: Evidence on stand level and explanation on individual tree level. European Journal of Forest Research 128: 183–204
Pretzsch H, Seifert S (1999) Wissenschaftliche Visualisierung des Waldwachstums. Allgemeine Forstzeitschrift 54 (18): 960–962
Pretzsch H, Utschig H (1989) Das "Zuwachstrend-Verfahren" für die Abschätzung krankheitsbedingter Zuwachsverluste auf den Fichten- und Kiefern-Weiserflächen in den bayerischen Schadgebieten. Forstarchiv 60 (5): 188–193
Pretzsch H, Utschig H (2000) Wachstumstrends der Fichte in Bayern. Mitt Bayer Staatsforstverwalt 49, Bayer StMin Ernährung, Landwirtschaft u Forsten, München, 170 pp
Pretzsch H, Biber P, Ďurský J (2002a) The single tree based stand simulator SILVA. Construction, application and evaluation. Forest Ecology and Management 162: 3–21
Pretzsch H, Biber P, Ďurský J, Gadow von K, Hasenauer H, Kändler G, Kenk G, Kublin E, Nagel J, Pukkala T, Skovsgaard JP, Sodtke R, Sterba H (2002b) Recommendations for Standardized Documentation and Further Development of Forest Growth Simulators. Forstw Cbl 121: 138–151
Pretzsch H, Biber P, Moshammer R (2005a) Prognose der Waldentwicklung auf Landesebene, Allgemeine Forstzeitschrift 60 (4): 200–203
Pretzsch H, Biber P, Moshammer R (2005b) Das Aufkommen von Fichtenstarkholz im bayerischen Staatswald. Allgemeine Forstzeitschrift 60 (4): 204–208
Pretzsch H, Grote R, Reineking B, Rötzer T, Seifert S (2008) Models for forest ecosystem management: A European perspective. Annals of Botany 101: 1065–1087
Preuhsler T (1979) Ertragskundliche Merkmale oberbayerischer Bergmischwald-Verjüngungsbestände auf kalkalpinen Standorten im Forstamt Kreuth. Forstl Forschungsber München 45, 372 pp
Preuhsler T (1987) Wachstumsreaktionen nach Trassenaufhieb in Kiefernbeständen. Forstl Forschungsber München 81, 210 pp
Preuhsler T (1989) Die Entwicklung von Oberstand und Naturverjüngung in Bergmischwald-Verjüngungsbeständen des Forstamtes Kreuth, Centralbl für das ges Forstwesen 106 (1): 23–54
Preuhsler T (1990) Einfluß von Grundwasserentnahmen auf die Entwicklung der Waldbestände im Raum Genderkingen bei Donauwörth. Forstl Forschungsber München 101, 95 pp
Prodan M (1951) Messung der Waldbestände. JD Sauerländer's Verlag, Frankfurt am Main, 260 pp
Prodan M (1961) Forstliche Biometrie. BLV Verlagsgesellschaft, München, Bonn, Wien, 432 pp
Prodan M (1965) Holzmeßlehre. JD Sauerländer's Verlag, Frankfurt am Main, 644 pp
Prodan M (1968) Einzelbaum, Stichprobe und Versuchsfläche. Allgemeine Forst- und Jagdzeitung 139 (11): 239–248
Prodan M (1973) Spatiale Variation und Punktstichproben. Allgemeine Forst- und Jagdzeitung 144: 229–236
Pruscha H (1989) Angewandte Methoden der Mathematischen Statistik. Teubner Skripten zur Math Stat, Verlag BG Teubner, Stuttgart, 391 pp
Puettmann KJ, Hibbs DE, Hann DW (1992) The dynamics of mixed stands of *Alnus rubra* and *Pseudotsuga menziesii*: Extension of size-density analysis to species mixtures. Journal of Ecology 80 (3): 449–458
Puettmann KJ, Hann DW, Hibbs DE (1993) Evaluation of the size-density relationship for pure red elder and Douglas-fir stands. Forest Science 37: 574–592

Pukkala T (1987) Simulation model for natural regeneration of pinus sylvestris, picea abies, betula pendula and betula pubescens. Silva Fennica 21: 37–53
Pukkala T (1989) Methods to describe the competition process in a tree stand. Scandinavian Journal of Forest Research 4: 187–202
Pukkala T, Kolström T (1987) Competition indices and the prediction of radial growth in scots pine. Silva Fennica 21 (1): 55–67
Putz FE, Parker GG, Archibald RM (1984) Mechanical abrasion and intercrown spacing. American Midland Naturalist 113 (1): 24–28
Radtke PJ, Burkhart HE (1998) A comparison of methods for edge-bias compensation. Canadian Journal of Forest Research 28: 942–945
Rasch D (1987) Einführung in die Biostatistik, 2nd edn. Verlag Harri Deutsch, Frankfurt am Main, 276 pp
Rasch D, Enderlein G, Herrendörfer G (1973) Biometrie. Verfahren, Tabellen, Angewandte Statistik. VEB Deutscher Landwirtschaftsverlag, Berlin, 390 pp
Rasch D, Griar V, Nürnberg G (1992) Statistische Versuchsplanung, Einführung in die Methoden und Anwendung des Dialogsystems CADEMO. Gustav Fischer Verlag, Stuttgart, Jena, New York, 386 pp
Rehàk J (1966) Beitrag zur Aufstellungsmethodik der Ertragstafeln. Vedecke Prace 33: 183–210
Rehfuess KE (1981) Waldböden Entwicklung, Eigenschaften und Nutzung, Pareys Studientexte 29, Parey Verlag, Hamburg, Berlin, 193 pp
Reich PB, Tjoelker MG, Machado J-L,Oleksyn J (2006) Universal scaling of respiratory metabolism, size and nitrogen in plants. Nature 439: 457–461
Reimeier S (2001) Analyse der Zuwachsveränderungen von Waldbeständen und Möglichkeiten der Prognose aus permanenten Stichprobeninventuren. Forstl Forschungsber München 183, pp 1–141
Reineke LH (1933) Perfecting a stand-density index for even-aged forests. Journal of Agricultural Research 46: 627–638
Reiter IM, Häberle K-H, Nunn AJ, Heerdt C, Reitmayer H, Grote R, Matyssek R (2005) Competitive strategies in adult beech and spruce: Space-related foliar carbon investment versus carbon gain. Oecologia 146: 337–349
Remmert H (1992) Ökologie. Springer, Berlin
Reventlow CDF (1879) Forslag til en forbedret Skovdrift grundet, paa Undersogelser over Traeernes Vegetation i Danmarks og Slesvigs Skove. P Hauberg and Co, Kjøbenhavn, Denmark (English version (1960) A treatise on forestry. Forest History Society, Hørsholm, Denmark)
Reynolds M, Burkhart H, Daniels R (1981) Procedures for statistical validation of stochastic simulation models. Forest Science 27 (2): 349–364
Reynolds T (1982) A shoot: root partitioning model. Annals of Botany 43: 401–404
Richards FJ (1959) A flexible growth function for empirical use. Journal of Experimental Botany 10: 290–300
Riemer T (1994) Über die Varianz von Jahrringbreiten. Statistische Methoden für die Auswertung der jährlichen Dickenzuwächse von Bäumen unter sich ändernden Lebensbedingungen. Ber Forschungszentrum Waldökosysteme, Reihe A, vol 121, 375 pp
Río del M, Montero G, Bravo F (2001) Analysis of diameter-density relationships and self-thinning in non-thinned even-aged Scots pine stands. For Ecol Mngt 142: 79–87
Ripley BD (1977) Modelling spatial patterns (with discussion). Journal of Royal Statistical Society, Series B, 39 (2): 172–212
Ripley BD (1981) Spatial statistics. Wiley, New York, 252 pp
Röhle H (1986) Vergleichende Untersuchungen zur Ermittlung der Genauigkeit bei der Ablotung von Kronenradien mit dem Dachlot und durch senkrechtes Anvisieren des Kronenrandes (Hochblick-Methode). Forstarchiv 57 (1): 67–71
Röhle H (1987) Entwicklung von Vitalität, Zuwachs und Biomassenstruktur der Fichte in verschiedenen bayerischen Untersuchungsgebieten unter dem Einfluß der neuartigen Walderkrankungen. Forstl Forschungsber München 83, 122 pp

Röhle H (1994) Zum Wachstum der Fichte auf Hochleistungsstandorten in Südbayern. Ertragskundliche Auswertung langfristig beobachteter Versuchsreihen unter besonderer Berücksichtigung von Trendänderungen im Wuchsverhalten. Habil Forstwiss Fak, LMU München, 249 pp

Röhle H (1997) Änderung von Bonität und Ertragsniveau in südbayerischen Fichtenbeständen. Allgemeine Forst- und Jagdzeitung 168 (6/7): 110–114

Röhle H (1999) Datenbank gestützte Modellierung von Bestandeshöhenkurven. Cbl für das ges Forstwesen 116 (1/2): 35–46

Röhle H, Huber W (1985) Untersuchungen zur Methode der Ablotung von Kronenradien und der Berechnung von Kronengrundflächen. Forstarchiv 56 (6): 238–243

Roloff A (1989) Kronenentwicklung und Vitalitätsbeurteilung ausgewählter Baumarten der gemäßigten Breiten. Schr Forstl Fak Univ Göttingen u Niedersächs Forstl Versuchsanstalt 93, 258 pp

Rothe A (1997) Einfluß des Baumartenanteils auf Durchwurzelung, Wasserhaushalt, Stoffhaushalt und Zuwachsleistung eines Fichten-Buchen-Mischbestandes am Standort Höglwald. Forstl Forschungsber München 163, 174 pp

Rothe A, Binkley D (2001) Nutritional interactions in mixed species forests: a synthesis. Canadian Journal of Forest Research 31: 1855–1870

Rötzer T, Häckel H, Würländer R (1997) Agrar- und Umweltklimatologischer Atlas von Bayern. Selbstverlag Deutscher Wetterdienst, Weihenstephan, Zolling

Rötzer T, Grote R, Pretzsch H (2005) Effects of environmental changes on the vitality of forest stands. European Journal of Forest Research 124: 349–362

Rötzer T, Seifert T, Pretzsch H (2009) Modelling above and below ground carbon dynamics in a mixed beech and spruce stand influenced by climate. European Journal of Forest Research 128: 171–182

Rousseau J-J (1762) Du Contract Social. German Ed (1977) Gesellschaftsvertrag. Reclam, Stuttgart

Rubner K (1910) Das Hungern des Cambiums und das Aussetzen der Jahrringe. Naturwiss Zeitschr Forst- u Landwirtschaft 8: 212–262

Rubner M (1931) Die Gesetze des Energieverbrauchs bei der Ernährung. Proc preuß Akad Wiss Physik-Math Kl 16/18, Berlin, Wien, 1902 pp

Rudnicki M, Lieffers VJ, Silins U (2003) Stand structure governs the crown collisions of Lodgepole pine. Canadian Journal of Forest Research 33 (7): 1238–1244

Rudra AB (1968) A stochastic model for the prediction of diameter distribution of even-aged forest stands. OPSEARCH. Journal of Operational Society of India 5 (2): 59–73

Runge M (1973) Energieumsätze in den Biozönosen terrestrischer Ökosysteme. Erich Goltze KG, Göttingen, Scripta Geobotany 4: 123–141

Running SW, Coughlan JC (1988) A general model of forest ecosystem processes for regional applications. I. Hydrologic balance, canopy gas exchange and primary production processes. Ecological Modelling 42: 125–154

Running SW, Gower ST (1991) FOREST-BGC, a general model of forest ecosystem processes for regional applications. II. Dynamic carbon allocation and nitrogen budgets. Tree Physiology 9: 147–160

Rutter AJ, Morton AJ, Robins PC (1975) A predictive model of rainfall interception in forests. II. Generalisations of the model and comparisons with observations in some coniferous and hardwood stands. Journal of Applied Ecology 12: 367–380

Sackville Hamilton NR, Matthew C, Lemaire G (1995) In defence of the –3/2 boundary rule. Annals of Botany 76: 569–577

Samuelson PA, Nordhaus WD (1998) Volkswirtschaftslehre. Ueberreuter Verlag, Wien, Heidelberg, 927 pp

Santantonio D, Hermann RK, Overton WS (1977) Root biomass studies in forest ecosystems. Pedobiologia 17: 1–31

Schaab G, Steinbrecher R, Lacaze B, Lenz R (2000) Assessment of long-term vegetation changes on potential isoprenoid emission for a Mediterranean-type ecosystem in France. Journal of Geophysical Research 105: 28863–28876
Schadauer K (1999) Verfahren zur Ergänzung fehlender Baumhöhen bei Wiederholungsmessungen. Cbl für das ges Forstwesen 116 (1/2): 67–80
Schädelin W (1942) Die Auslesedurchforstung als Erziehungsbetrieb höchster Wertleistung, 3rd edn. Verlag Paul Haupt, Bern, Leipzig, 147 pp
Scheffé H (1953) A method of judging all contrasts in the analysis of variance. Biometrika 40: 87–104
Scherer-Lorenzen M, Körner C, Schulze E-D (2005) Forest diversity and function. Ecological Studies 176, Springer, Berlin, Heidelberg, 399 pp
Schlittgen R, Streitberg BHJ (1997) Zeitreihenanalyse, 7th edn. Oldenburg Verlag, München, Wien, 574 pp
Schmidt A (1967) Der rechnerische Ausgleich von Bestandeshöhenkurven. Forstw Cbl 86: 370–382
Schmidt A (1969) Der Verlauf des Höhenwachstums von Kiefern auf einigen Standorten der Oberpfalz. Forstw Cbl 88: 33–40
Schmidt A (1971) Wachstum und Ertrag der Kiefer auf wirtschaftlich wichtigen Standorteinheiten der Oberpfalz. Forstl Forschungsber München 1, 187 pp
Schmid I (2002) The influence of soil type and interspecific competition on the fine root system of Norway spruce and European beech. Basic Applied Ecology 3 (4): 339–355
Schmid I, Kazda M (2002) Root distribution of Norway spruce in monospecific and mixed stands on different soils. Forest Ecology and Management 159: 37–47
Schober R (1950/1951) Zum jahreszeitlichen Ablauf des sekundären Dickenwachstums. Allgemeine Forst- und Jagdzeitung 122: 81–96
Schober R (1961) Zweckbestimmung, Methodik und Vorbereitung von Provenienzversuchen. Allgemeine Forst- und Jagdzeitung 132 (2): 29–38
Schober R (1967) Buchen-Ertragstafel für mäßige und starke Durchforstung, In: Schober R (1972) Die Rotbuche 1971. Schr Forstl Fak Univ Göttingen u Niedersächs Forstl Versuchsanst 43/44, JD Sauerländer's Verlag, Frankfurt am Main, 333 pp
Schober R (1975) Ertragstafeln wichtiger Baumarten. JD Sauerländer's Verlag, Frankfurt am Main
Schober R (1979) Massen-, Sorten- und Wertertrag der Fichte bei verschiedener Durchforstung. Teil 1. Allgemeine Forst- und Jagdzeitung 150: 129–152
Schober R (1980) Massen-, Sorten- und Wertertrag der Fichte bei verschiedener Durchforstung. Teil 2. Allgemeine Forst- und Jagdzeitung 151: 1–21
Schober R (1988a) Von der Niederdurchforstung zu Auslesedurchforstungen im Herrschenden. Allgemeine Forst- und Jagdzeitung 159 (9/10): 208–213
Schober R (1988b) Von Zukunfts- und Elitebäumen. Allgemeine Forst- und Jagdzeitung 159 (11/12): 239–249
Schöpfer W, Hradetzky J (1983) Zielsetzungen, Methoden und Probleme der terrestrischen Waldzustandsinventur in Baden-Württemberg 1983. Mitt Forstl Versuchs- u Forschungsanstalten Bad-Württ 106, Freiburg, 26 pp
Schöpfer W, Hradetzky J (1988) Vergleich von Kronenkennwerten für Fichte und Tanne. Forst u Holz 43 (6): 132–137
Schulze, E-D, Beck E, Müller-Hohenstein K (2002) Plant Ecology. Springer, Berlin
Schumacher S, Bugmann H (2006) The relative importance of climatic effects, wildfires and management for future forest landscape dynamics in the Swiss Alps. Global Change Biology 12: 1435–1450
Schumacher S, Bugmann H, Mladenoff DJ (2004) Improving the formulation of tree growth and succession in a spatially explicit landscape model. Ecological Modelling 180: 175–194
Schumacher S, Reineking B, Sibold J, Bugmann H (2006) Modeling the impact of climate and vegetation on fire regimes in mountain landscapes. Landscape Ecology 21: 539–554
Schütz JP (1989) Zum Problem der Konkurrenz in Mischbeständen. Schweiz Zeitschr Forstwesen 140 (12): 1069–1083

Schütz JP (1997) Sylviculture 2. La gestion des forˆets irrégulières et mélangées. Presses Polytechniques et Universitaires Romandes, Lausanne, 178 pp
Schwalm CR, Ek AR (2004) A process-based model of forest ecosystems driven by meteorology. Ecological Modelling 179: 317–348
Schwappach A (1889) Wachsthum und Ertrag normaler Kiefernbestände in der norddeutschen Tiefebene. Verlag Julius Springer, Berlin, 72 pp
Schwappach A (1890) Wachstum und Ertrag normaler Fichtenbestände. Verlag Julius Springer, Berlin, 100 pp
Schwappach A (1893) Wachstum und Ertrag normaler Rotbuchenbestände. Verlag Julius Springer, Berlin, 104 pp
Schwappach A (1902) Wachstum und Ertrag normaler Fichtenbestände in Preussen unter besonderer Berücksichtigung des Einflusses verschiedener wirtschaftlicher Behandlungsweisen. Mitt Forstl Versuchswesen Preussens, Verlag J Neumann, Neudamm, pp 44–119
Schwappach A (1903) Leitfaden der Holzmeßkunde, 2nd edn. Verlag Julius Springer, 173 pp
Schwappach A (1908) Die Kiefer. Wirtschaftliche und statische Untersuchungen der forstlichen Abteilung der Hauptstation des forstlichen Versuchswesens in Eberswalde. Verlag J Neumann, Neudamm,180 pp
Schwappach A (1909) Untersuchungen in Mischbeständen. Zeitschr Forst- u Jagdwesen 41: 313–332
Schwappach A (1911) Die Rotbuche. Wirtschaftliche und statische Untersuchungen der forstlichen Abteilung der Hauptstation des forstlichen Versuchswesens in Eberswalde. Verlag J Neumann, Neudamm
Schwappach A (1912) Ertragstafeln der wichtigeren Holzarten in tabellarischer und graphischer Form. Verlag J Neumann, Neudamm
Schweingruber FH, Kontic R, Winkler-Seifert A (1983) Eine jahrringanalytische Studie zum Nadelbaumsterben in der Schweiz. Ber Eidg Anst forstl Versuchswesen 253, 29 pp
Schweingruber FH, Albrecht H, Beck M, Hessel J, Joos K, Keller D, Kontic R, Lange K, Niederer M, Nippel C, Spang S, Spinnler A, Steiner B, Winkler-Seifert A (1986) Abrupte Zuwachsschwankungen in Jahrringabfolgen als ökologische Indikatoren. Ber Eidg Anst forstl Versuchswesen, pp 125–179
Seely B, Welham C, Kimmins H (2002) Carbon sequestration in a boreal forest ecosystem: results from the ecosystem simulation model, FORECAST. Forest Ecology and Management 169: 123–135
Seibt G (1972) Aufgaben und Probleme der Ertragskunde im forstlichen Versuchswesen. Forstarchiv 43 (11): 227–230
Seibt G, Wittich W (1965) Ergebnisse langfristiger Düngungsversuche im Gebiet des nordwestdeutschen Diluviums und ihre Folgerungen für die Praxis. Schr Forstl Fak Univ Göttingen 27/28, JD Sauerländer's Verlag, Frankfurt am Main, 156 pp
Seifert S (1998) Dreidimensionale Visualisierung des Waldwachstums. Dipl thesis, Dep Informatik, FH München in cooperation with Department of Forest Yield Science, LMU München, MWW-DA 124, 133 pp
Seifert S (2006) Visualisierung von Waldlandschaften. Allgemeine Forstzeitschrift 61: 1170–1171
Seifert S (2008) Modellierung und Visualisierung des Waldwachstums auf Landschaftsebene. PhD thesis, Univ Göttingen, Dep Ökoinformatik, Biometrie und Waldwachstum, Göttingen, 120 pp
Seifert T, Müller-Starck G (2009) Impacts of fructification on biomass production and correlated genetic effects in Norway spruce (*Picea abies* [L.] Karst.). European Journal of Forest Research 128: 155–169
Seifert T, Schuck J, Block J, Pretzsch H (2006) Simulation von Biomasse- und Nährstoffgehalt von Waldbäumen mit dem Waldwachstumssimulator SILVA. Berichte der Jahrestagung des Deutschen Verbandes Forstlicher, Sektion Ertragskunde, in Staufen, pp 208–223
Seifritz W (1987) Wachstum, Rückkopplung und Chaos. Hanser Verlag, München, Wien
Senge PM (1994) The fifth discipline. Currency/Doubleday, New York, London, Toronto Sydney, Auckland, 423 pp

Shannon CE (1948) The mathematical theory of communication. In: Shannon CE, Weaver W (eds) The mathematical theory of communication. Urbana, University of Illinois Press, pp 3–91
Sheppard SRJ, Harshaw HW (2001) Forests and Landscapes: Linking ecology, sustainability and aesthetics. CABI. IUFRO Research Series, 294 pp
Shinozaki K, Yoda K, Hozumi K, Kira T (1964) A quantitative analysis of plant form – the pipe model theory, I. Basic analyses. Japanese Journal of Ecology 14: 97–105
Shugart HH (1984) A theory of forest dynamics. The ecological implications of forest succession models. Springer, New York, Berlin, Heidelberg, Tokyo, 278 pp
Simpson WT (1993) Specific gravity, moisture content, and density relationship for wood. USDA, Gen Techn Rep FPL-GTR-76, 13 pp
Sloboda B (1976) Mathematische und stochastische Modelle zur Beschreibung der Statik und Dynamik von Bäumen und Beständen – insbesondere das bestandesspezifische Wachstum als stochastischer Prozess. Habil, Univ Freiburg, 310 pp
Sloboda B (1988) Representation and projection of diameter distribution in regarding change of rank in indicative experimental plots. In: Sloboda B (ed) Biometrische Modelle und Simulationstechniken bei Prozessen in forstlicher Forschung und Praxis. Schr Forstl Fak Univ Göttingen u Niedersächs Forstl Versuchsanst 90, pp 6–21
Sloboda B, Pfreundt J (1989) Baum- und Bestandeswachstum. Ein systemanalytischer, räumlicher Ansatz mit Versuchsplanungskonsequenzen für die Durchforstung und Einzelbaumentwicklung, Berichte der Jahrestagung des Deutschen Verbandes Forstlicher, Sektion Ertragskunde, in Attendorn, pp 17/1–17/25
Smalian HL (1837) Beitrag zur Holzmeßkunst. Verlag Löffler, Stralsund, 87 pp
Smaltschinski T (1981) Bestandesdichte und Verteilungsstruktur. PhD thesis, Forstwiss Fak Univ Freiburg, 127 pp
Šmelko Š, Scheer L, Ďurský J (1996) Poznatky z monitorovania zdravotného a produkaného stavu lesa v imisnej oblasti horná Orava (Die Erkentnisse aus der Waldzustandserhebung im immisionsgeschädigten Gebiet Horná Orava). Vedecke studie, Technická Univerzita vo Zvolene, vol 16, 142 p, including summary in German
Solmon F, Sarrat C, Serca D, Tulet P, Rosset R (2004) Isoprene and monoterpenes biogenic emissions in France: modeling and impact during a regional pollution episode. Atmospheric Environment 38: 3853–3865
Song C, Woodcock CE (2003) A regional forest ecosystem carbon budget model: impacts of forest age structure and landuse history. Ecological Modelling 164: 33–47
Späth H (1983) Spline Algorithmen. Verlag Oldenbourg, München, Wien, 134 pp
Speidel G (1972) Planung im Forstbetrieb. Verlag Paul Parey, Hamburg, Berlin, 267 pp
Spellmann H (1991) Beiträge der Forsteinrichtung und Ertragskunde für ein forstliches Informationssystem. Forst u Holz 46: 57–65
Spellmann H (1996) Leistung und Windstabilität von Fichten-Buchen-Mischbeständen. Berichte der Jahrestagung des Deutschen Verbandes Forstlicher, Sektion Ertragskunde, in Neresheim, pp 46–56
Spellmann H, Wagner S, Nagel J, Guericke M, Griese F (1996) In der Tradition stehend, neue Wege beschreitend. Forst u Holz 51 (11): 363–368
Spellmann H, Hillebrand K, Cornelius P (2001) Konzept zur Erfassung und Sicherung der Nachhaltigkeit in multifunktional genutzten Wäldern. Forst u Holz 56: 469–473
Spelsberg G (1987) Zum Problem der Beurteilung des Zuwachses in geschädigten Beständen. Allgemeine Forst- und Jagdzeitung 158 (11/12): 205–211
Spencer H (1864) The principles of biology, vol. 1. Williams and Norgate, London
Spiecker H, Mielikäinen K, Köhl M, Skovsgaard JP eds (1996) Growth trends in european forests. Europ For Inst, Research Report 5, Springer, Heidelberg, 372 pp
Sprugel DG, Ryna MG, Brooks J, Vogt KA, Martin TA (1995) Respiration from the organ level to the stand. In: Smith WK, Hinkley TM (eds) Resource physiology of conifers. Acquisition, allocation, and utilization. Academic, New York, pp 255–299

Steenis van H (1992) Informationssysteme – Wie man sie plant, entwickelt und nutzt. Ein Leitfaden für effiziente und benutzerfreundliche Informationssysteme. Verlag Carl Hanser, München, Wien, 271 pp
Stephano C, Libalto J (1598) XV Bücher von dem Feldbau und recht volkommener Wolbestellung eines bekömmlichen Landsitzes. Bernhart Jobins, Straßburg, 763 pp
Stephens GR, Waggoner PE (1970) The forests anticipated from 40 years of natural transitions in mixed hardwoods. Connecticut Agricultural Experiment Station, New Haven, CT, Bull 707, 58 pp
Sterba H (1970) Untersuchungen zur Frage der Anlage und Auswertung von Einzelstammdüngungsversuchen. Cbl für das ges Forstwesen 87 (3): 166–189
Sterba H (1973) Auswertung eines Bestandesdüngungsversuches auf Terra Fusca. Cbl für das ges Forstwesen 90: 34–45
Sterba H (1975) Assmanns Theorie der Grundflächenhaltung und die "Competition-Density-Rule" der Japaner Kira, Ando und Tadaki. Cbl für das ges Forstwesen 92 (1): 46–62
Sterba H (1978) Methodische Erfahrungen bei Einzelstammdüngungsversuchen. Allgemeine Forst- und Jagdzeitung 149: 35–40
Sterba H (1981) Natürlicher Bestockungsgrad und Reinekes SDI. Cbl für das ges Forstwesen 98: 101–116
Sterba H (1984) Pärchenuntersuchungen in Österreich. Berichte der Jahrestagung des Deutschen Verbandes Forstlicher, Sektion Ertragskunde, in Neustadt a d Weinstraße, pp 8/1–8/10
Sterba H (1987) Estimating potential density from thinning experiments and inventory data. Forest Science 33 (4): 1022–1034
Sterba H (1989a) Concepts and techniques for forest growth models. Proc IUFRO Meeting, Vienna, Austria, 18–22.09.1989, Univ für Bodenkultur Wien, pp 14–20
Sterba H (1989b) Waldschäden und Zuwachs. In: Ulrich B (ed) Wissensstand und Perspektiven. Internationaler Kongreß Waldschadensforschung, 2–6.10.1989, Friedrichshafen, pp 61–80
Sterba H (1991) Forstliche Ertragslehre 4. Lecture at the Univ Bodenkulturl, Wien, 160 pp
Sterba H (1996) Forest decline and growth trends in central Europe. In: Spiecker H, Mielilkäinen K, Köhl M, Skovsgaard JP (eds) Growth trends in European forests. Springer, Berlin, pp 149–165
Sterba H (1999) Genauere Höhenmessungen-Bedeutung des Höhenzuwachses in der Waldwachstumstheorie. Cbl für das ges Forstwesen 116 (1/2): 141–153
Sterba H, Monserud RA (1993) The maximum density concept appled to uneven-aged mixed stands. Forest Science 39: 432–452
Sterba H, Moser M, Monserud RA (1995) Prognaus – Ein Waldwachstumssimulator für Rein- und Mischbestände. Österreich Forstzeitg 5: 19–20
Sterman JD (2007) Exploring the next great frontier: System dynamics at fifty. System Dynamics Review 23 (2/3): 89–93
Stoyan D, Stoyan H (1992) Fraktale Formen und Punktfelder: Methoden der Geometrie-Statistik. Akademie Verlag, Berlin, 394 pp
Strasser U, Etchevers P (2005) Simulation of daily discharges for the upper Durance catchment (French Alps) using subgrid parameterization for topography and a forest canopy climate model. Hydrological Processes 19: 2361–2373
Sturtevant BR, Gustafson EJ, Li W, He HS (2004) Modeling biological disturbances in LANDIS: a module description and demonstration using spruce budworm. Ecological Modelling 180: 153–174
Suzuki T (1971) Forest transition as a stochastic process. Mitt Forstl Bundesversuchsanst Wien 91, pp 69–86
Suzuki T (1983) Übergang des Waldbestandes als ein stochastischer Prozess. In: Beitr zur biometrischen Modellbildung in der Forstwirtschaft, Schr Forstl Fak Univ Göttingen u Niedersächs Forst Versuchsanst, JD Sauerländer's Verlag, Frankfurt am Main, vol 76, pp 23–58
Teissier G (1934) Dysharmonies et discontinuités dans la Croissance. Act Sci et Industr 95 (Exposés de Biometrie, 1), Hermann, Paris

Thomasius H (1990) Waldbau 1, Allgemeine Grundlagen des Waldbaus. Hochschulstudium Forstingenieurwesen, Karl-Marx-Univ Leipzig, Agrarwiss Fak (ed), Leipzig, 180 pp

Thompson DW (1917) On growth and form. Cambridge Univ Press, Cambridge

Thompson HR (1956) Distribution of distance to n^{th} nearest neighbour in a population of randomly distributed individuals. Ecology 37: 391–394

Thornley JHM (1991) A transport-resistance model of forest growth and partitioning. Annals of Botany 68: 211–226

Thornley JHM, Cannell MGR (2000) Modelling the components of plant respiration: Representation and realism. Annals of Botany 85: 55–67

Timilin DJ, Pachepsky Y (1997) A modular soil and root process simulator. Ecological Modelling 94: 67–80

Tomé M, Burkhart HE (1989) Distance-dependent competition measures for predicting growth of individual trees. Forest Science 35 (3): 816–831

Trendelenburg R, Mayer-Wegelin H (1955) Das Holz als Rohstoff. Hanser Verlag, München, 541 pp

Tubbs CH (1973) Allelopathic relationship between Yellow birch and Sugar maple seedlings. Forest Science 19: 139–145

Tukey JW (1977) Exploratory Data Analysis. Addison Wesley, Reading, MA, 688 pp

Überla, K (1968) Faktorenanalyse. Springer, Berlin, 399 pp

Ulrich B (1993) Prozeßhierarchie in Waldökosystemen. Ein integrierender ökosystemtheoretischer Ansatz. Biologie in unserer Zeit 23 (5): 322–329

Ulrich B (1999) Entwicklungsprognosen für Waldökosysteme aus der Sicht der Hierarchietätstheorie. Forstw Cbl 118: 118–126

Upton GJG, Fingleton B (1985) Spatial data analysis by example: Volume I: Point pattern and quantitative data. Wiley, New York, 410 pp

Upton GJG, Fingleton B (1989) Spatial data analysis by example: Volume II: Categorical and directional data. Wiley, New York, 416 pp

Utschig H (1989) Waldwachstumskundliche Untersuchungen im Zusammenhang mit Waldschäden. Auswertung der Zuwachstrendanalyseflächen des Lehrstuhles für Waldwachstumskunde für die Fichte (*Picea abies* (L.) Karst.) in Bayern. Forstl Forschungsber München 97, 198 pp

Utschig H (1999) Reconversion of pure spruce stands into mixed forests: an ecological and economic valuation. In: Olsthoorn AFM, Bartelink HH, Gardiner JJ, Pretzsch H, Hekhuis HJ, Franc A (eds) Management of mixed-species forest: Silviculture and economics. IBN Scientific Contributions 15: 319–330

Valentine HT (1990) A carbon-balance model of tree growth with a pipe-model framework. In: Dixon RK, Meldahl RS, Ruarki GA, Warren WG (eds) Process Modeling of Forest Growth Responses to Environmental Stress. Timber, Portland, OR, pp 33–40

Vanclay JK (1994) Modelling forest growth and yield. Applications to mixed tropical stands. CAB International, Wallingford, UK, 312 pp

Vanclay JK, Skovsgaard JP (1997) Evaluating forest growth models. Ecological Modelling 98: 1–12

Vanselow K (1951) Fichtenertragstafel für Südbayern. Forstw Cbl 70: 409–445

Verein Deutscher Forstlicher Versuchsanstalten (1873) Anleitung für Durchforstungsversuche. In: Ganghofer von A ed (1884) Das Forstliche Versuchswesen. Schmid'sche Buchhandlung, Augsburg, vol 2, pp 247–253

Verein Deutscher Forstlicher Versuchsanstalten (1902) Beratungen der vom Vereine Deutscher Forstlicher Versuchsanstalten eingesetzten Kommission zur Feststellung des neuen Arbeitsplanes für Durchforstungs- und Lichtungsversuche. Allgemeine Forst- und Jagdzeitung 78: 180–184

Vertessy RA, Hatton TJ, Benyon RG, Dawes WR (1996) Long-term growth and water balance predictions for a mountain ash (*Eucalyptus regnans*) forest catchment subject to clear-felling and regeneration. Tree Phys 16: 221–232

Vinš B (1961) Störungen der Jahresringbildung durch Rauchschäden. Die Naturwissenschaften 48 (13): 484–485
Vinš B (1966) Die Jahrringbreite im gleichaltrigen Fichtenreinbestand und ihre Veränderungen. Wissensch Zeitschr TU Dresden 15 (2): 419–424
Vinš B, Mrkva R (1972) Zuwachsuntersuchungen in Kiefernbeständen in der Umgebung einer Düngerfabrik. Mitt Forstl Bundesversuchsanst 97: 173–192
Vötter D (2005) Splintholzerkennung mittels Computertomographie und Färbeverfahren an Fichte und Buche. Ein Methodenvergleich. Diploma thesis, TU München, MWW-DA 146, 151 pp
Vries de PG (1986) Sampling theory for forest inventory. Springer, Berlin, 399 pp
Vuokila Y (1966) Functions for variable density yield tables of pine based on temporary sample plots. Com Inst Forestalis Fenniae 60 (4), 86 pp
Wagner S (1994) Strahlungsschätzung in Wäldern durch hemisphärische Fotos: Methode und Anwendung. PhD thesis, Univ Göttingen, 166 pp
Walko RL, Band LE, Baron J, Kittel TGF, Lammers R, Lee TJ, Qjima D, Pielke RA Sr, Taylor C, Tague C, Tremback CJ, Vidale PL (2000) Coupled atmosphere–biophysics–hydrology models for environmental modeling. Journal of Applied Meteorology 39: 931–944
Wallman P, Svensson MGE, Sverdrup H, Belyazid S (2005) ForSAFE – an integrated process-oriented forest model for long-term sustainability assessments. Forest Ecology and Management 207: 19–36
Wang X, Song B, Chen J, Crow TR, LaCroix JJ (2006) Challenges in Visualizing Forests and Landscapes. Journal of Forestry 104: 316–319
Wattenbach M, Hattermann F, Wenig R, Wechsung F, Krysanova V, Badeck F (2005) A simplified approach to implement forest eco-hydrological properties in regional hydrological modelling. Ecological Modelling 187: 40–59
Weber E (1980) Grundriß der biologischen Statistik. Gustav Fischer Verlag, Stuttgart, 652 pp
Webster CR, Lorimer CG (2003) Comparative growing space efficiency of four tree species in mixed confer-hardwood forests, Forest Ecology and Management 177: 361–377
Weck J (1955) Forstliche Zuwachs- und Ertragskunde. Neumann Verlag, Radebeul, Berlin
Weetman G (2005) Partial cutting in the boreal: some concerns, its history and its place in management, Lecture on workshop "Partial cutting in the eastern boreal forest: current knowledge and perspectives". Univ of Quebéc at Temiskaming UQAT, Rouyn-Noranda, revised and updated Jan/05, UBC Vancouver, 29 pp
Weihe J (1968) Der Einzelbaumdüngversuch. Berichte der Jahrestagung des Deutschen Verbandes Forstlicher, Sektion Ertragskunde, in Münster, pp 25–29
Weihe J (1970) Die Praxis des Einzelbaumdüngungsversuches. Berichte der Jahrestagung des Deutschen Verbandes Forstlicher, Sektion Ertragskunde, in Mainz, pp 25–28
Weihe J (1979) Arbeit und Zusammenarbeit in der Sektion Ertragskunde. Berichte der Jahrestagung des Deutschen Verbandes Forstlicher, Sektion Ertragskunde, in Mehring, pp 1–10
Weinstein DA, Beloin RM, Yanai RD (1991) Modeling changes in red spruce carbon balance and allocation in response to interacting ozone and nutrient stresses. Tree Physiology 9: 127–146
Weinstein DA, Laurence JA, Retzlaff WA, Kern JS, Lee EH, Hogsett WE, Weber J (2005) Predicting the effects of tropospheric ozone on regional productivity of Ponderosa pine and White fir. Forest Ecology and Management 205: 73–89
Weise W (1880) Ertragstafeln für die Kiefer. Springer, Berlin, 156 pp
Welham C, Seely B, Kimmins H (2002) The utility of the two-pass harvesting system: an analysis using the ecosystem simulation model FORECAST. Canadian Journal of Forest Research 32: 1071–1079
Weller DE (1987) A reevaluation of the -3/2 power rule of plant self-thinning. Ecological Monographs 57: 23–43
Weller DE (1990) Will the real self-thinning rule please stand up? A reply to Osawa and Sugita. Ecology 71: 1204–1207
Wenk G, Römisch K, Gerold D (1982) Die Grundbeziehungen der neuen Fichtenertragstafel für das Mittelgebirge der DDR. Wiss Zeitschr TU Dresden 31: 267–271

Wenk G, Antanaitis V, Šmelko Š (1990) Waldertragslehre. VEB Deutscher Landwirtschaftsverlag, Berlin, 448 pp
Werner A, Deussen O, Döllner J, Hege HC, Paar P, Rekitte J (2005) Lenné3D – Walking through Landscape Plans. In: Buhmann E, Paar P, Bishop ID, Lange E (eds). Trends in real-time landscape visualization and participation.Wichmann, Berlin
West GB, Brown JH, Enquist BJ (1997) A general model for the origin of allometric scaling laws in biology. Science 276: 122–126
West GB, Brown JH, Enquist BJ (1999) A general model for the structure and allometry of plant vascular systems. Nature 400: 664–667
White J (1981) The allometric interpretation of the self-thinning rule. Journal of Theoretical Biology 89: 475–500
White MA, Thornton PE, Running SW, Nemani RR (2000) Parameterization and sensitivity analysis of the BIOME–BGC Terrestrial ecosystem model: net primary production controls. Earth Interactions 4 (3): 1–85
Whitfield J (2001) All creatures great and small. Nature 413: 342–344
Whittaker RH, Likens GE (1973) Carbon in the biota. In: Woodwell GW, Pecan EV (eds) Carbon and the Biosphere. US Atomic Energy Commission, Washington DC
Wiedemann E (1923) Zuwachsrückgang und Wuchsstockungen der Fichte in den mittleren und unteren Höhenlagen der sächsischen Staatsforsten. Kommissionsverlag W Laux, Tharandt, 181 pp
Wiedemann E (1928) Zukunftsfragen des Preußischen Versuchswesens. Zeitschr Forst- u Jagdwesen 60 (5): 257–272
Wiedemann E (1931) Anweisung für die Aufnahme und Bearbeitung der Versuchsflächen der Preußischen Forstlichen Versuchsanstalt. Verlag J Neumann, Neudamm, 47 pp
Wiedemann E (1932) Die Rotbuche 1931. Mitt Forstwirtsch u Forstwiss 3 (1): 189
Wiedemann E (1936/1942) Die Fichte 1936. Verlag M & H Schaper, Hannover, 248 pp
Wiedemann E (1942) Der gleichaltrige Fichten-Buchen-Mischbestand. Mitt Forstwirtsch u Forstwiss 13: 1–88
Wiedemann E (1943a) Kiefern-Ertragstafel für mäßige Durchforstung, starke Durchforstung und Lichtung, In: Wiedemann E (1948) Die Kiefer 1948. Verlag M & H Schaper, Hannover, 337 pp
Wiedemann E (1943b) Der Vergleich der Massenleistung des Mischbestandes mit dem Reinbestand. Allgemeine Forst- und Jagdzeitung 119: 123–132
Wiedemann E (1948) Über die Arbeitsmethoden des forstlichen Versuchswesens. Beitr Agrarwiss, Landbuch-Verlag, Hannover 4: 1–24
Wiedemann E (1949) Ertragstafeln der wichtigen Holzarten bei verschiedener Durchforstung. Verlag M & H Schaper, Hannover
Wiedemann E (1951) Ertragskundliche und waldbauliche Grundlagen der Forstwirtschaft. JD Sauerländer‘s Verlag, Frankfurt am Main
Wiegand T (1998) Die zeitlich-räumliche Populationsdynamik von Braunbären. Habil, Forstwiss Fak, LMU München, 202 pp
Wimmenauer K (1914) Zur Frage der Mischbestände. Allgemeine Forst- und Jagdzeitung 90: 90–93
Windhager M (1997) Die Berechnung des Ek und Monserud (1974) Konkurrenzindex für Randbäume nach unterschiedlichen Berechnungsmethoden. Berichte der Jahrestagung des Deutschen Verbandes Forstlicher, Sektion Ertragskunde, in Grünberg, pp 74–86
Wirth C, Schumacher J, Schulze E-D (2004) Generic biomass functions for Norway spruce in Central Europe – a meta-analysis approach toward prediction and uncertainty estimation. Tree Physiology 24: 121–139
Wohlrab B, Ernstberger H, Meuser A, Sokollek V (1992) Landschaftswasserhaushalt. Verlag Paul Parey, Hamburg
Wolf J, Hack-ten Broeke MJD, Rötter R (2005) Simulation of nitrogen leaching in sandy soils in The Netherlands with the ANIMO model and the integrated modelling system STONE. Agriculture and Forest Meteorology 105: 523–540
Wolfram ST (2002) A new kind of science. Wolfram media Inc, Champaign, IL

Wuketits FM (1981) Biologie und Kausalität, Biologische Ansätze zur Kausalität, Determination und Freiheit. Verlag Paul Parey, Hamburg, 165 pp
Wykoff WR, Monserud RA (1988) Representing site quality in increment models: A comparison of methods. In: Ek AR, Shifley SR, Burk TE (eds) Proc IUFRO conference, Aug 1987, Gen Tech Rep NC-120, Minneapolis, MN, pp 184–191
Wykoff WR, Crookston NL, Stage AR (1982) User's guide to the stand prognosis model. US Forest Serv, Gen Techn Rep INT-133, Ogden, UT, 112 pp
Yachi S, Loreau M (1999) Biodiversity and ecosystem productivity in a fluctuating environment: The insurance hypothesis. Proc Nat Acad Sci 96: 1463–1488
Yaffee SL (1999) Three faces of ecosystem management. Conservation Biology 13: 713–725
Yoda KT, Kira T, Ogawa H, Hozumi K (1963) Self-thinning in overcrowded pure stands under cultivated and natural conditions. Journal of Institute of Polytechnic, Osaka Univ D 14: 107–129
Yoda KT, Shinozaki K, Ogawa J, Hozumi K, Kira T (1965) Estimation of the total amount of respiration in woody organs of trees and forest forest communities. Journal of Biology Osaka City University (16): 15–26
Zeide B (1972) On the mathematical description of the aging process of trees. In: Kocharov GE, Dergachov VA, Bitvinskas TT (eds) Dendroclimatochronology and radiouglerod. Institut botaniki Academii Nauk Litovskoi SSR, Kaunas, pp 169–174 (325 pp)
Zeide B (1985) Tolerance and self-tolerance of trees. Forest Ecology and Management 13: 149–166
Zeide B (1987) Analysis of the 3/2 power law of self-thinning. Forest Science 33: 517–537
Zeide B (1989) Accuracy of equations describing diameter growth. Canadian Journal of Forest Research 19: 1283–1286
Zeide B (1993) Analyses of growth equations. Forest Science 39 (3): 594–616
Zeide B (2001a) Natural thinning and environmental change: An ecological process model. Forest Ecology and Management 154: 165–177
Zeide B (2001b) Thinning and growth: a full turnaround. Journal of Forestry 99: 20–25
Zeide B (2002) Density and the growth of even-aged stands. Forest Science 48: 743–754
Zeide B (2003) The U-approach to forest modeling. Canadian Journal of Forest Research 33: 480–489
Zeide B (2004) How to measure density. Trees 19: 1–14
Zeide B (2005) Increasing forst productivity by optimizing stand density and diversifying land use. Unpubl paper, School of Forest Resources, University of Arkansas, Monticello, 19 pp
Zhang Y, Reesd DD, Cattelino PJ, Gale MR, Jones EA, Liechty HO, Mroz GD (1994) A process-based growth model for young red pine. Forest Ecology and Management 69: 21–40
Ziegler F (1991) Die Bedeutung des organischen Kohlenstoffes im Unterboden-Vorratsberechnungen an Waldböden. Zeitschr Umweltchemie, Ökotoxologie 3 (5): 276–277
Zimmerle H (1949) Zur Mischbestandsfrage. Allgemeine Forst- und Jagdzeitung 121: 20–29
Zimmerle H (1952) Ertragszahlen für Grüne Douglasie, Japaner Lärche und Roteiche in Baden-Württemberg. Mitt Forstl Versuchsanst Württ 9(2), Verlag Eugen Ulmer, Stuttgart, 44 pp
Zimmermann H-J, Zysno P (1980) Latent connectives in human decision making. Fuzzy Sets and Systems 4: 37–51
Zöhrer F (1969) Bestandeszuwachs und Leistungsvergleich montan, subalpiner Lärchen-Fichten-Mischbestand. Forstw Cbl 88 (1): 41–63
Zutter BR, Oderwald RG, Murphy PA, Farrar JRRM (1986) Charakterizing diameter distributions with modified data types and forms of the Weibull distribution. Forest Science 31 (1): 37–48

Index